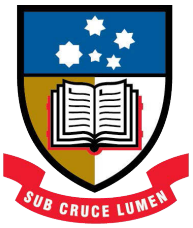

THE UNIVERSITY
of ADELAIDE

AXIAL COMPRESSIVE BEHAVIOR OF ACTIVELY CONFINED AND FRP-CONFINED CONCRETES

Jian Chin Lim
BEng (Civil & Structural) Hons

Thesis submitted to The University of Adelaide
School of Civil, Environmental and Mining Engineering
in fulfilment of the requirements
for the degree of Doctor of Philosophy

THIS PAGE HAS BEEN LEFT INTENTIONALLY BLANK

CONTENTS

ABSTRACT

Since the 1920s, a significant research effort has been dedicated to the understanding of the improved compressive behavior of concrete under lateral confinement. Upon the introduction of fiber-reinforced polymer (FRP) composites to the construction industry, the use of FRP as confinement material has received much attention. To that end, a great number of studies have been conducted in the past two decades on the axial compressive behavior of unconfined, actively confined and FRP-confined concretes, resulting in the development of over 110 stress-strain models. These models are classified into four broad categories, namely design-oriented, analysis-oriented, evolutionary algorithm, and finite element models. In the present study, existing models in each category were carefully reviewed and assessed using comprehensive experimental test databases assembled through an extensive review of the literature. The databases cover more than 7000 test results of unconfined, actively confined, and FRP-confined concrete specimens from 500 studies. A close examination of the assessment results has led to a number of important findings on factors influencing the performances of existing models. For each model category possible areas for further improvement were identified and new models were proposed.

First, an empirical model in simple closed-form expressions that are suitable for engineering design purpose was developed using the database of FRP-confined concrete. The distinct feature of this design-oriented model includes its applicability to normal- and high-strength concretes with cross-sections ranging from circular to rectangular. The model also considers the observed dependency of the hoop rupture stain of the confining jacket on the material properties of the concrete and FRP. In addition, a novel concept, referred to as the confinement stiffness threshold condition, was incorporated into this model to allow for an accurate prediction of post-peak strain softening behavior of FRP-confined concrete.

Following this, using the combined database, a unified analysis-oriented model that is capable of predicting the complete stress-strain and dilation behaviors of unconfined, actively confined, and FRP-confined concretes was developed. It was found that, at a given axial strain, lateral strains of actively confined and FRP-confined concretes of the same concrete strength correspond when they are subjected to the same lateral confining pressure. However, under the same condition, concrete confined by FRP exhibits a lower strength enhancement compared to that seen in companion actively confined concrete. On the basis of this observation, a novel approach that incorporates the confining pressure gradient between the two confinement systems was established and a unified stress-strain model was developed. Other distinct features of this highly versatile model are its applicability to concretes ranging from light- to normal-weight and low- to high-strength. In addition, it is also applicable to specimens with various sizes and slenderness.

To improve the capability of handling complex databases with a large number of independent variables, a third category of model that uses evolutionary algorithm and soft computing techniques was considered. In this study, a genetic programming approach that is capable of gradually refining the solution while maintaining the versatility of the model in closed-form expressions was used to develop an evolutionary algorithm model for FRP-confined concrete.

Lastly, the finite element modeling approach was investigated. A review of the existing literature revealed that the failure criterion and flow rule considered by existing FE models for confined concretes are based on limited test results and they are not very sensitive to the variations in unconfined concrete strength and confining pressure. Based on the comprehensive experimental databases assembled, a concrete strength-sensitive finite element model applicable to concrete subjected to various confining pressure levels was developed.

Comparison with experimental test results show that the predictions of all of the proposed models are in good agreement with the test results, and the models provide improved accuracy compared to the existing models. Comparison of models in different categories indicates that model accuracy generally improves with the size of database and the complexity of modeling framework; however, the choice of models depends mainly on the suitability of their end use.

STATEMENT OF ORIGINALITY

I certify that this work contains no material which has been accepted for the award of any other degree or diploma in my name, in any university or other tertiary institution and, to the best of my knowledge and belief, contains no material previously published or written by another person, except where due reference has been made in the text. In addition, I certify that no part of this work will, in the future, be used in a submission in my name, for any other degree or diploma in any university or other tertiary institution without the prior approval of the University of Adelaide and where applicable, any partner institution responsible for the joint-award of this degree.

I give consent to this copy of my thesis when deposited in the University Library, being made available for loan and photocopying, subject to the provisions of the Copyright Act 1968.

The author acknowledges that copyright of published works contained within this thesis resides with the copyright holder(s) of those works.

I also give permission for the digital version of my thesis to be made available on the web, via the University's digital research repository, the Library Search and also through web search engines, unless permission has been granted by the University to restrict access for a period of time.

19/05/2015

_____ _____

Signature Date

ACKNOWLEDGEMENTS

Firstly, I would like to acknowledge the support of my supervisors, Dr. Togay Ozbakkaloglu and Dr. Alex Ching-Tai Ng, for their supervision, support and encouragement over the course of my PhD candidature. I would particularly like to thank Dr. Togay Ozbakkaloglu for his continual enthusiasm, vision, and determination for my research to succeed. I am also grateful to Dr. Alex Ching-Tai Ng for his constant motivation and scientific insight into my research.

I would also like to take this opportunity to express my gratitude to all academics and technical staffs who have helped me with this thesis in their fields of expertise. In particular, I thank Mr. Adam Ryntjes who provided technical assistance throughout the experimental program and Barbara Brougham who provided technical reviews to most of the publications presented in this thesis.

I am very grateful to my fellow PhD students Mr. Thomas Vincent, Butje Alfonsius Louk Fanaggi, Tianyu Xie, Yongjian Chen, and Ms. Yunita Idris for their friendship, encouragement, and help. Many thanks also to other PhD students in the School of Civil, Environmental and Mining Engineering who have helped me throughout the course.

I would also like to thank my wife, Eva Hooi Ying Beh, for her unwavering support and motivation.

Finally, and most importantly, I thank God, who put me on this journey, which has been challenging but in the end very rewarding.

INTRODUCTION

An important application of fiber reinforced polymer (FRP) composites is as a confining material for concrete, in both the seismic retrofit of existing reinforced concrete columns and in the construction of concrete-filled FRP tubes as earthquake-resistant columns in new construction. Reliable design of these structural members necessitates clear understanding and accurate modeling of the stress-strain relationship of confined concrete.

Research objectives

This research aims to improve the understanding of the compressive behavior of actively confined and FRP-confined concrete. To this end, three large databases of experimental test results of unconfined, actively confined, and FRP-confined specimens, covering more than 7000 test results from 500 studies published between the 1920s to 2014, were assembled and presented in a series of publications as a united framework for future reference. The combined database covers specimens tested under axial compression with unconfined concrete strengths ranging from 6 to 170 MPa. It consists of a wide range of test parameters, thereby allowing detailed observations of the important factors influencing the unconfined and confined behaviors of concrete. Gaps identified from the parameters of these databases were covered through new tests conducted at the University of Adelaide in a series of experimental programs. A great number of existing models developed for the predictions of the axial compressive behavior of unconfined, actively confined and FRP-confined concretes were then carefully reviewed and assessed using the experimental databases. These models are classified into four broad categories, namely design-oriented, analysis-oriented, evolutionary algorithm, and finite element models. A close examination of the assessment results and modeling techniques of these models has led to a number of important findings on factors influencing the performances of the existing models, including the size of database, test parameters considered, ability to handle uncertainties, dependency on theoretical assumptions, and architecture of their modeling frameworks. Following this, improved models in each category were developed on the basis of the up-to-date experimental databases.

Thesis overview

This thesis is structured into 14 chapters. Each of these chapters is a manuscript that had been submitted for publication as a journal article throughout the course of this study [1-14]. Table 1 outlines the areas focused by each of these manuscripts, the experimental test databases used, and the parameters investigated. Table 2 outlines the type of models proposed in these publications, together with their application ranges and the conditions considered. As summarized in Table 1, the three main databases of unconfined, actively confined, and FRP-confined concretes were presented in a series of publications [2, 3, 6, 7, 10] and were used in most of the analyses in this study. Gaps identified from the parameters of these databases were covered with new tests

presented in another series of publications [4, 5, 8, 9]. In Refs. [1-3, 6, 7, 10, 12, 13], a great number of existing models developed for unconfined, actively confined, and FRP-confined concrete were reviewed and their performances were assessed using the test results of the databases. Based on a close examination of the model performances and a detailed study of the database results, important parameters affecting the axial compressive behavior of confined concrete, as outlined in Table 1, have been investigated in this study. These parameters include:

1. Hoop rupture strain of FRP jacket – the hoop rupture strain of recorded on FRP jacket is often lower than the ultimate tensile strain measured from material tests. In this study, the observed influences of unconfined concrete strength and elastic modulus of fiber on the reduction in the hoop rupture strain of FRP jackets have been statistically quantified using the test database results [3] and validated using independent test results [8].
2. Confinement threshold – the threshold condition occurs when the amount of FRP confinement supplied to concrete results in a stress-strain curve that has a horizontal second branch. An amount of FRP confinement lesser than this threshold will result in a descending second branch, and vice versa. In this study, the threshold was observed to increase significantly with an increase in the unconfined concrete strength. A novel approach has been established to quantify the threshold condition using the experimental test database results [3].
3. Cross sectional shape – shape factors are commonly used to account for the reduction in confinement efficiency of FRP jacket confining concrete in square or rectangular cross-section. In this study, the shape factors have been related to the aforementioned threshold condition to distinguish the ascending and descending types of stress-strain curves of FRP-confined concrete in square and rectangular sections [6].
4. Silica fume content – it was observed that the stress-strain relationship, dilation behavior, and ultimate condition of FRP-confined concrete change with the presence of and the increase in silica fume content in concrete [4].
5. Age of concrete – the stress-strain relationship, dilation behavior, and ultimate condition of FRP-confined concrete was also observed to change with an increase in concrete age [5].
6. Specimen size and slenderness – the influence of specimen size and slenderness at the peak and post-peak conditions of unconfined and confined concretes has been statistically quantified using the comprehensive experimental databases that cover various test parameters [10, 11].
7. Confining pressure gradient – it was observed that, under the same confining pressure, concrete confined by FRP exhibits a lower strength enhancement compared to that seen in companion actively confined concrete [9]. To account for the axial stress difference between FRP-confined and actively confined concretes, a novel concept has been established to quantify the confining pressure gradient between the two confinement systems [12].

The four main types of models that have been developed and presented in a series of publications include the design-oriented model [2, 3, 6], analysis-oriented model [10-12], evolutionary algorithm model [13], and finite element model [14]. As summarized in Table 2, each category of these models has its own application domains. Comparisons with experimental test results show that the predictions of the proposed models are in good agreement with the test results, and the models provide improved predictions compared to the existing models reviewed in this study. Comparison of models in different categories indicates that model accuracy generally improves with the size of the database they were based on and the complexity of modeling framework; however, the choice of models depends mainly on the suitability of their end use.

Table 1. Summary of publications, experimental databases used, and test parameters investigated

Publication	Research area focused	Experimental database used/presented						Parameter investigated						
		Unconfined concrete	Actively confined concrete	FRP-confined NSC in circular cross-section	FRP-confined HSC in circular cross-section	FRP-confined concrete in square and rectangular cross-section	New experimental test results reported	Hoop rupture strain of FRP jacket	Confinement threshold	Cross-sectional shape	Silica fume content	Age of Concrete	Specimen size and slenderness	Confining pressure gradient
Ozbakkaloglu et al. [1]	Review of existing FRP-confined concrete models	-	-	Used	-	-	-	-	-	-	-	-	-	-
Ozbakkaloglu and Lim [2]	FRP-confined normal strength concrete	-	-	Presented and used	-	-	-	Yes	-	-	-	-	-	-
Lim and Ozbakkaloglu [3]	FRP-confined high strength concrete	-	-	Used	Presented and used	-	-	Yes	Yes	-	-	-	-	-
Lim and Ozbakkaloglu [4]	Influence of silica fume on FRP-confined concrete	-	-	-	-	-	Yes	-	-	-	Yes	-	-	-
Lim and Ozbakkaloglu [5]	Influence of concrete age on FRP-confined concrete	-	-	Used	Used	-	Yes	Yes	-	-	-	Yes	-	-
Lim and Ozbakkaloglu [6]	FRP-confined concrete in square and rectangular cross-sections	-	-	Used	Used	Presented and used	-	Yes	Yes	Yes	-	-	-	-
Lim and Ozbakkaloglu [7]	Dilation behavior of confined concrete	Used	Presented and used	Used	Used	-	-	Yes	-	-	-	-	-	-
Lim and Ozbakkaloglu [8]	Factors influencing hoop rupture strain of FRP jacket	-	-	-	-	-	Yes	Yes	-	-	-	-	-	-
Lim and Ozbakkaloglu [9]	Axial stress difference between actively confined and FRP-confined concretes	-	Used	Used	Used	-	Yes	-	-	-	-	-	-	Yes
Lim and Ozbakkaloglu [10]	Light-weight and normal-weight concretes	Presented and used	Used	-	-	-	-	-	-	-	-	-	Yes	-
Lim and Ozbakkaloglu [11]	Size and slenderness effect on confined concrete	Used	Used	-	-	-	-	-	-	-	-	-	Yes	-
Lim and Ozbakkaloglu [12]	Unified modeling approach of confined concrete	Used	Used	Used	Used	-	-	Yes	-	-	-	-	-	Yes
Lim et al. [13]	Genetic programming approach	-	-	Used	-	-	-	Yes	-	-	-	-	-	-
Lim et al. [14]	Finite element modeling approach	Used	Used	-	-	-	-	-	-	Yes	-	-	Yes	-

Table 2. Summary of types and details of model proposed

Publication	Type of model proposed	Application range of proposed model							Stress-strain curve modeled			
		Confinement type	Light-weight concrete	Normal-weight concrete	Normal-strength concrete	High-strength concrete	Circular cross-section	Square and rectangular cross-section	Shape of curve	Peak condition of actively confined concrete	Residual condition of actively confined concrete	Ultimate condition of FRP-confined concrete
Ozbakkaloglu et al. [1]	-	-	-	-	-	-	-	-	-	-	-	-
Ozbakkaloglu and Lim [2]	Design-oriented	FRP	-	Yes	Yes	-	Yes	-	Ascending	-	-	Yes
Lim and Ozbakkaloglu [3]	Design-oriented	FRP	-	Yes	Yes	Yes	Yes	-	Ascending, descending	-	-	Yes
Lim and Ozbakkaloglu [4]	-	-	-	-	-	-	-	-	-	-	-	-
Lim and Ozbakkaloglu [5]	-	-	-	-	-	-	-	-	-	-	-	-
Lim and Ozbakkaloglu [6]	Design-oriented	FRP	-	Yes	Yes	Yes	Yes	Yes	Ascending, descending	-	-	Yes
Lim and Ozbakkaloglu [7]	Analysis-oriented	Active, FRP	-	Yes	Yes	Yes	Yes	-	-	-	-	-
Lim and Ozbakkaloglu [8]	-	-	-	-	-	-	-	-	-	-	-	-
Lim and Ozbakkaloglu [9]	-	-	-	-	-	-	-	-	-	-	-	-
Lim and Ozbakkaloglu [10]	Analysis-oriented	Active	Yes	Yes	Yes	Yes	Yes	-	Ascending, descending	Yes	Yes	-
Lim and Ozbakkaloglu [11]	Analysis-oriented	Active	Yes	Yes	Yes	Yes	Yes	-	Descending	Yes	Yes	-
Lim and Ozbakkaloglu [12]	Analysis-oriented	Active, FRP	-	Yes	Yes	Yes	Yes	-	Ascending, descending	Yes	Yes	Yes
Lim et al. [13]	Soft computing	FRP	-	Yes	Yes	-	Yes	-	Ascending	-	-	Yes
Lim et al. [14]	Finite element	Biaxial, Triaxial	-	Yes	Yes	Yes	Yes	Yes	Ascending, descending	Yes	Yes	-

REFERENCES

[1] Ozbakkaloglu T, Lim JC, Vincent T. FRP-confined concrete in circular sections: Review and assessment of stress–strain models. Engineering Structures. 2013;49:1068–88.

[2] Ozbakkaloglu T, Lim JC. Axial compressive behavior of FRP-confined concrete: Experimental test database and a new design-oriented model. Composites Part B. 2013;55:607-34.

[3] Lim JC, Ozbakkaloglu T. Confinement model for FRP-confined high-strength concrete. Journal of Composites for Construction, ASCE. 2014;18(4):04013058.

[4] Lim JC, Ozbakkaloglu T. Influence of silica fume on stress-strain behavior of FRP-confined HSC. Construction and Building Materials. 2014;63:11-24.

[5] Lim JC, Ozbakkaloglu T. Influence of concrete age on stress–strain behavior of FRP-confined normal- and high-strength concrete. Construction and Building Materials. 2014; (Accepted).

[6] Lim JC, Ozbakkaloglu T. Design model for FRP-confined normal- and high-strength concrete square and rectangular columns. Magazine of Concrete Research. 2014;66(20):1020-35.

[7] Lim JC, Ozbakkaloglu T. Lateral strain-to-axial strain relationship of confined concrete. Journal of Structural Engineering, ASCE. 2014;Doi: 10.1061/(ASCE)ST.1943-541X.0001094.

[8] Lim JC, Ozbakkaloglu T. Hoop strains in FRP-confined concrete columns: Experimental observations. Materials and Structures. 2014;Doi: 10.1617/s11527-014-0358-8.

[9] Lim JC, Ozbakkaloglu T. Investigation of the Influence of Application Path of Confining Pressure: Tests on Actively Confined and FRP-Confined Concretes. Journal of Structural Engineering, ASCE. 2014;Doi: 10.1061/(ASCE)ST.1943-541X.0001177.

[10] Lim JC, Ozbakkaloglu T. Stress-strain model for normal- and light-weight concretes under uniaxial and triaxial compression. Construction and Building Materials. 2014;71:492-509.

[11] Lim JC, Ozbakkaloglu T. Influence of size and slenderness on compressive strain softening of confined and unconfined concrete. Journal of Materials in Civil Engineering. 2014; (Submitted).

[12] Lim JC, Ozbakkaloglu T. Unified stress-strain model for FRP and actively confined normal-strength and high-strength concrete. Journal of Composites for Construction. 2014;Doi: 10.1061/(ASCE)CC.1943-5614.0000536.

[13] Lim JC, Karakus M, Ozbakkaloglu T. Evaluation of ultimate conditions of FRP-confined concrete columns using genetic programming. Computers and Structures. 2014; (Submitted).

[14] Lim JC, Sadeghi R, Bennett T, Ozbakkaloglu T. Finite element modeling of normal- and high-strength concrete under uni-, bi-, and triaxial Compression International Journal of Plasticity. 2014; (To be submitted).

PUBLICATIONS

THIS PAGE HAS BEEN LEFT INTENTIONALLY BLANK

Statement of Authorship

Title of Paper	FRP-Confined Concrete in Circular Sections: Review and Assessment of Stress-Strain Models
Publication Status	(•) Published ( ) Accepted for Publication ( ) Submitted for Publication ( ) Publication Style
Publication Details	Engineering Structures, Volume 49, Pages 1068–1088, Year 2013

Author Contributions

By signing the Statement of Authorship, each author certifies that their stated contribution to the publication is accurate and that permission is granted for the publication to be included in the candidate's thesis.

Name of Principal Author	Dr. Togay Ozbakkaloglu		
Contribution to the Paper	Research supervision and review of manuscript		
Signature		Date	23/02/2015

Name of Co-Author (Candidate)	Mr. Jian Chin Lim		
Contribution to the Paper	Review of literature, assessment of existing models, and preparation of manuscript		
Signature		Date	23/02/2015

Name of Co-Author	Mr. Thomas Vincent		
Contribution to the Paper	Preparation of manuscript		
Signature		Date	23/02/2015

THIS PAGE HAS BEEN LEFT INTENTIONALLY BLANK

FRP-CONFINED CONCRETE IN CIRCULAR SECTIONS: REVIEW AND ASSESMENT OF STRESS-STRAIN MODELS

Togay Ozbakkaloglu, Jian C. Lim and, Thomas Vincent

ABSTRACT

An important application of FRP composites is as a confining material for concrete, in both the seismic retrofit of existing reinforced concrete columns and in the construction of concrete-filled FRP tubes as earthquake-resistant columns in new construction. Reliable design of these structural members necessitates clear understanding and accurate modeling of the stress-strain behavior of FRP-confined concrete. To that end, a great number of studies have been conducted in the past two decades, which has led to the development of a large number of models to predict the stress-strain behavior of FRP-confined concrete under axial compression. This paper presents a comprehensive review of 88 models developed to predict the axial stress-strain behavior of FRP-confined concrete in circular sections. Each of the reviewed models and their theoretical bases are summarized and the models are classified into two broad categories, namely design-oriented and analysis-oriented models. This review summarizes the current published literature until the end of 2011, and presents a unified framework for future reference. To provide a comprehensive assessment of the performances of the reviewed models, a large and reliable test database containing the test results of 730 FRP-confined concrete cylinders tested under monotonic axial compression is first established. The performance of each existing stress-strain model is then assessed using this database, and the results of this assessment are presented through selected statistical indicators. In the final part of the paper, a critical discussion is presented on the important factors that influenced the overall performances of the models. A close examination of results of the model assessment has led to a number of important conclusions on the strengths and weaknesses of the existing stress–strain models, which are clearly summarized. Based on these observations, a number of recommendations regarding future research directions are also outlined.

KEYWORDS: Concrete; Fiber reinforced polymer; Confinement; Axial stress; Axial strain; Stress-strain models; Strength models.

1. INTRODUCTION

It is now clearly understood that lateral confinement of concrete can enhance its strength and ductility significantly. Upon the introduction of fiber-reinforced polymer (FRP) composites to the construction industry, the use of FRP as confinement material has received much attention. Over the last two decades, a great number of experimental and analytical studies have been conducted to understand and model the compressive behavior of FRP-confined concrete. These studies have lead to the development of 88 axial stress-axial strain models, which are referred to herein as stress-strain models.

Early models proposed for FRP-confined concrete [1-3] directly adopted the stress-strain models developed for actively confined or steel-confined concrete (e.g. [4-6]). The disadvantages of this approach became obvious in following studies, when differences in the stress-strain behavior of FRP-confined and steel-confined concrete were recognized and reported by a number of research groups [7-11]. Subsequent research efforts have led to the development of a large number of analytical stress-strain models that are specific for FRP-confined concrete. However, many of these models
were based on limited experimental test data, which were often obtained only from the tests performed by the originators of the model. As have previously been illustrated in Lam and Teng [12], De Lorenzis and Tepfers [13] and Bisby et al. [14], performances of these models degrade considerably when the models are assessed against larger databases covering wider parametric ranges. Given the magnitude of research conducted on FRP-confined concrete in the past two decades, a comprehensive review of the literature, where existing models are categorized into groups based on their similarities and differences, has become essential to gain a clearer view of the existing research efforts within the field. Furthermore, the development of a unified approach for the analysis and design of FRP-confined concrete columns necessitates a systematic assessment of these models to establish their strengths and weaknesses.

This paper is aimed at providing an all-encompassing review and assessment of the existing models that have been proposed to predict the compressive behavior of FRP-confined concrete in circular sections. To this end, a total of 88 models are first reviewed and classified into sub categories. The performance of these models is then assessed using a reliable test database that was carefully assembled by the authors through an extensive review of the literature that covered 2038 test results from 202 experimental studies published between 1991 and the end of 2011. In the final part of the paper, a critical discussion is presented on the important factors that influence the overall performance of the models.

2. MECHANISM OF CONFINEMENT

In FRP-confined circular concrete sections, the lateral confining pressure (f_l) provided by the FRP shell can be assumed to be uniformly distributed around the circumference (Figure 1). The confinement action exerted by the FRP shell on the concrete core is of the passive type; that is, this pressure arises as a result of the lateral expansion of concrete under axial compression. As the FRP shell is subjected to tension along its hoop direction, the confining pressure (f_l) increases proportionally with the lateral expansion until the eventual failure of

the system when the FRP shell ruptures. Based on the deformation compatibility between the confining shell and the concrete surface, the lateral confining pressure applied to concrete by the FRP shell at ultimate (f_{lu}) can be theoretically calculated from Eq. 1 as a function of the ultimate tensile strain of fibers (ε_f). However, it has been reported in a number of previous studies that the ultimate strain measured on the FRP shell at the time of FRP hoop rupture ($\varepsilon_{h,rup}$) is lower than the ultimate tensile strain of the fibers (ε_f) or FRP material (ε_{frp}) [12, 13, 15-21]. To establish the relationship between the hoop rupture strain of the FRP shell ($\varepsilon_{h,rup}$) to the ultimate tensile strain of the material (ε_f), a strain reduction factor (k_ε) was introduced by Pessiki et al. [15] (Eq. 2). Lam and Teng [12] then defined a term actual confining pressure ($f_{lu,a}$) (Eq. 3), by replacing material ultimate tensile strain (ε_f) with the hoop rupture strain of the FRP shell ($\varepsilon_{h,rup}$) in Eq. 1.

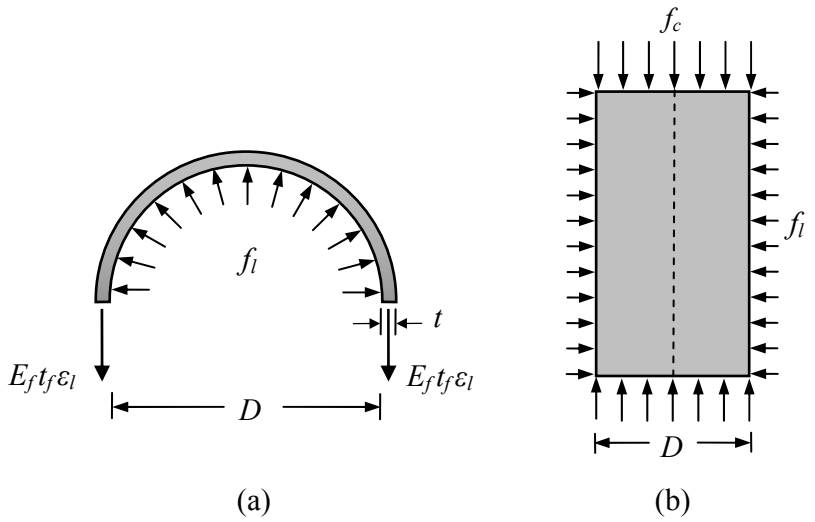

Figure 1. Confining action of FRP shell on concrete core: (a) FRP shell; (b) Concrete core

$$f_{lu} = \frac{2E_f t_f \varepsilon_f}{D} \tag{1}$$

$$\varepsilon_{h,rup} = k_\varepsilon \varepsilon_f \tag{2}$$

$$f_{lu,a} = \frac{2E_f t_f \varepsilon_{h,rup}}{D} \tag{3}$$

Throughout this paper a clear distinction is made between the nominal confinement ratio (f_{lu}/f'_{co}) and the actual confinement ratio ($f_{lu,a}/f'_{co}$), as illustrated in the expressions given in Tables 1 and 2. Furthermore, information regarding the consideration of the strain reduction factor by each model is provided in the final columns of Tables 1 and 2. In these columns, 'Yes' indicates that the model employed the strain reduction factor (k_ε) or it called for the experimentally recorded hoop rupture strain ($\varepsilon_{h,rup}$) data to establish the actual confining pressures ($f_{lu,a}$), whereas 'No' indicates that strain reduction factor (k_ε) was not taken into consideration and the model directly employed the ultimate tensile strain of fibers (ε_f) or FRP composites (ε_{frp}) to determine the lateral confining pressures (f_{lu}).

Table 1. Summary of existing design-oriented models of FRP-confined concrete

Year	Model	Axial stress-strain curve expression	Type of curve	Consideration of strength and strain enhancements at first peak	Ultimate condition expressions		Consideration of FRP hoop strain reduction by the model
					Strength	Strain	
1982	Fardis and Khalili [1]	$f_c = \frac{E_c \varepsilon_c}{1+\varepsilon_c\left(\frac{E_c}{f_{lu}}-\frac{1}{\varepsilon_{cu}}\right)}$	I	N/A	Adopted from Richart et al. [4] $\frac{f'_{cc}}{f'_{co}} = 1+4.1\left(\frac{f_{lu}}{f'_{co}}\right)$ Adopted from Newman and Newman [109] $\frac{f'_{cc}}{f'_{co}} = 1+3.7\left(\frac{f_{lu}}{f'_{co}}\right)^{0.86}$	$\varepsilon_{cu} = 0.002 + 0.001\left(\frac{E_f t_f}{D f'_{co}}\right)$	No
1991	Ahmad et al. [2]	Modified from Sargin [51] (Eq . 10) as $f_c = \left[\frac{A_i\left(\frac{\varepsilon_c}{\varepsilon_{co,i}}\right)+(D_i-1)\left(\frac{\varepsilon_c}{\varepsilon_{co,i}}\right)^2}{1+(A_i-2)\left(\frac{\varepsilon_c}{\varepsilon_{co,i}}\right)+D_i\left(\frac{\varepsilon_c}{\varepsilon_{co,i}}\right)^2}\right] f'_{cc}$ $\varepsilon_{co,i} = 0.001648 + 1.65\times10^{-5}\left(f'_{co}\right)$	I	N/A	N/A	N/A	N/A
1994	Demers and Neale [36]	A bi-linear curve with the first linear line terminating at f'_{co} and ε_{co}, followed by the second branch defined by the below expression $f_c = f'_{co} + (\varepsilon_c - \varepsilon_{cu}) g\left(\frac{E_f t_f}{f'_{co}}\right)$	II	No	N/A	N/A	N/A
1994	Saadatmanesh et al. [3]	Popovics [34] (Eq . 17), with ultimate condition of FRP-confined concrete assumed to correspond to the peak condition of actively-confined concrete	I	N/A	Mander et al. [6] $f'_{cc} = f'_{co}\left(2.254\sqrt{1+7.94\frac{f_{lu}}{f'_{co}}}-2\frac{f_{lu}}{f'_{co}}-1.254\right)$	Richart et al. [4] $\varepsilon_{cu} = \varepsilon_{co}\left[1+5\left(\frac{f'_{cc}}{f'_{co}}-1\right)\right]$	No
1996	Mirmiran [113]	N/A	N/A	N/A	$f'_{cc} = f'_{co} + 4.269\left(f_{lu}\right)^{0.587}$	N/A	No
1997	Karbhari and Gao [39]	$f'_{c1} = f'_{co} + 4.1 f'_{co} v_c\left(\frac{2E_{frp}t_{frp}}{DE_c}\right)$ $\varepsilon_{c1} = \frac{f'_{c1}}{E^{eff}}$	II	Yes	$f'_{cc} = f'_{co} + 3.1 f'_{co} v_c\left(\frac{2E_{frp}t_{frp}}{DE_c}\right) + f_{lu}$ $f'_{cc} = f'_{co}\left[1+2.1\left(\frac{f_{lu}}{f'_{co}}\right)^{0.87}\right]$	$\varepsilon_{cu} = \varepsilon_{co} + 0.01\left(\frac{f_{lu}}{f'_{co}}\right)$	No
1997	Miyauchi et al. [9]	Hognestad's Parabola [40] (Eq. 4) for the first branch, followed by a straight line that extends until the ultimate condition	IIIa	No	$f'_{cc} = f'_{co} + k_{e1} 4.1 f_{lu}$ if $f'_{co} \le 50MPa$ $k_{e1} = 0.85$	$\varepsilon_{cu} = \varepsilon_{co}\left[1+10.6\left(\frac{f_{lu}}{f'_{co}}\right)^{0.373}\right]$ for $f'_{co} = 30MPa$ $\varepsilon_{cu} = \varepsilon_{co}\left[1+10.5\left(\frac{f_{lu}}{f'_{co}}\right)^{0.525}\right]$ for $f'_{co} = 50MPa$	No
1998	Jolly and Lillistone [42]	$f_c = 0.67\frac{f'_{co}}{\gamma_m}\left[2\frac{\varepsilon_c}{0.002}-\left(\frac{\varepsilon_c}{0.002}\right)^2\right] + E_p\varepsilon_c$ if $0 < \varepsilon_c \le 0.002$ $f_c = 0.67\frac{f'_{co}}{\gamma_m} + E_p\varepsilon_c$ if $0.002 < \varepsilon_c < \varepsilon_{cu}$	IIIa	No	$\frac{f'_{cc}}{f'_{co}} = 1+3.594\left(\frac{2t_{frp}}{D}\right)\left(\frac{E_{frp}\varepsilon_{lu}}{f'_{co}}\right)$ $\varepsilon_{lu} = 0.0117 + 0.0321\left(\frac{2t_{frp}}{D}\right)\frac{E_{frp}}{E_c}$	N/A	No

1998	Kono et al. [61]	N/A	N/A	N/A	$\frac{f'_{cc}}{f'_{co}} = 1 + 0.0286\left(\frac{4t_f}{D}\right)f_f$ if $30 \le f'_{co} \le 40 MPa$, $220 \le E_f \le 350\,GPa$, and $1280 \le f_f \le 3820\ MPa$ for CFRP sheets	$\frac{\varepsilon_{cu}}{\varepsilon_{co}} = 1 + 0.140\left(\frac{4t_f}{D}\right)f_f$ if $30 \le f'_{co} \le 40 MPa$, $220 \le E_f \le 350\,GPa$, and $1280 \le f_f \le 3820 MPa$ for CFRP sheets	No
1998	Samaan et al. [8]	Modified from Richard and Abbott [44] (Eq. 7) $f_o = 0.872 f'_{co} + 0.371 f_{lu} + 6.258 \quad n$=1.5 $E_{c1} = 3950\ \sqrt{f'_{co}}$ $E_{c2} = 245.61 f'^{\,0.2}_{co} + 1.3456\left(\frac{E_{frp} t_{frp}}{D}\right)$	IIIb	Yes	$f'_{cc} = f'_{co} + 6.0\left(f_{lu}\right)^{0.7}$	$\varepsilon_{cu} = \frac{f'_{cc} - f_o}{E_{c2}}$	No
1999	Miyauchi et al. [41]	Stress-stain curve exhibiting strain-hardening behavior: Hognestad's Parabola [40] (Eq. 4) for the first branch, until the transition strain at $\varepsilon_{c,\lambda}$, followed by the ascending second straight line defined by the below expression $f_c = f'_{cc} - \lambda(\varepsilon_{cu} - \varepsilon_c)$ if $\varepsilon_{c,\lambda} \le \varepsilon_c \le \varepsilon_{cu}$ $\quad \varepsilon_{c,\lambda} = \varepsilon_{co} - \frac{\lambda\,\varepsilon_{co}^{\,2}}{2 f'_{co}}$ $\lambda = \frac{\left[-2f'_{co}(\varepsilon_{cu} - \varepsilon_{co}) + \sqrt{4f'_{co}\left(f'_{co}\varepsilon_{cu}^{\,2} - 2f'_{co}\varepsilon_{co}\varepsilon_{cu} + f'_{cc}\varepsilon_{co}^{\,2}\right)}\right]}{\varepsilon_{co}^{\,2}}$ Stress-strain curve exhibiting strain-softening behavior: Hognestad's Parabola [40] (Eq. 4) for the first branch, until the unconfined concrete peak strain at ε_{co}, followed by the descending second straight line defined by the below expression $f_c = f'_{co} + \frac{(\varepsilon_c - \varepsilon_{co})(f'_{cc} - f'_{co})}{(\varepsilon_{cu} - \varepsilon_{co})}$ if $\varepsilon_{co} \le \varepsilon_c \le \varepsilon_{cu}$	IIIa	Yes	$f'_{cc} = f'_{co} + 2.98\, f_{lu}$	$\varepsilon_{cu} = \varepsilon_{co} + \varepsilon_{co}(15.87 - 0.093\, f'_{co}) \times \left(\frac{f_{lu}}{f'_{co}}\right)^{(0.246 + 0.0064 f'_{co})}$	No
1999	Saafi et al. [10]	Modified from Sargin [51] (Eq. 10) into Eq. 11, with: $f'_{c1} = f'_{co}\left[1 + 0.0213\left(\frac{t_{frp} E_{frp}}{D f'_{co}}\right)^{0.84}\right]$ $\varepsilon_{c1} = \varepsilon_{co}\left[1 + 0.0783\left(\frac{t_{frp} E_{frp}}{D f'_{co}}\right)^{0.84}\right]$ $E_{c1} = 10200\ (f'_{co})^{\frac{1}{3}} \qquad E'_{c2} = 0.272\left(\frac{f'_{co}}{\varepsilon_{co}}\right)$	IIIc	Yes	$f'_{cc} = f'_{co} + k_1 f_{lu}$ $k_1 = 2.2\left(\frac{f_{lu}}{f'_{co}}\right)^{-0.16}$ for FRP tube-encased concrete	$\varepsilon_{cu} = \varepsilon_{co}\left[1 + k_2\left(\frac{f'_{cc}}{f'_{co}} - 1\right)\right]$ $k_2 = 537\,\varepsilon_{lu} + 2.6$	No
1999	Spoelstra and Monti [11] 'approximate'	N/A	N/A	N/A	$f'_{cc} = f'_{co}\left[0.2 + 3\left(\frac{f_{lu}}{f'_{co}}\right)^{0.5}\right]$	$\varepsilon_{cu} = \varepsilon_{co}\left[2 + 1.25\left(\frac{E_c}{f'_{co}}\right)\left(\frac{f_{lu}}{f'_{co}}\right)^{0.5}\varepsilon_{lu}\right]$	No
1999	Toutanji [52]	Modified from Sargin [51] (Eq. 10) into Eq. 11, with: $f'_{c1} = f'_{co}\left[1 + 0.0178\left(\frac{E_l}{f'_{co}}\right)^{0.85}\right]$ $\varepsilon_{c1} = \varepsilon_{co}\left[1 + 0.0448\left(\frac{E_l}{f'_{co}}\right)^{0.85}\right]$ $E_{c1} = 10200\left(f'_{co}\right)^{\frac{1}{3}} \qquad E'_{c2} = 0.3075\left(\frac{f'_{co}}{\varepsilon_{co}}\right)$	IIIc	Yes	$f'_{cc} = f'_{co} + k_1 f_{lu}$ $k_1 = 3.5\left(\frac{f_{lu}}{f'_{co}}\right)^{-0.15}$ for FRP-wrapped concrete	$\varepsilon_{cu} = \varepsilon_{co}\left[1 + k_2\left(\frac{f'_{cc}}{f'_{co}} - 1\right)\right]$ $k_2 = 310.57\,\varepsilon_{lu} + 1.9$	No
2000	Jolly and Lillistone [43]	Same as Jolly and Lillistone [42] $E_p = 1.282\, E_l$ for $E_l \ge 1000$	IIIa	No	$\frac{f'_{cc}}{f'_{co}} = 0.83 + 0.05\left(\frac{E_l}{f'_{co}}\right)$	N/A	No

2000	Thériault and Neale [114]	N/A	N/A	N/A	$f'_{cc} = f'_{co}\left(1 + 2\frac{f_{lu}}{f'_{co}}\right)$	N/A	No
2000	Xiao and Wu [16]	A bi-linear curve with the first linear line defined by the below expression and terminating at $1.1 f'_{co}$ $f_c = E_c \varepsilon_c + 2 v_c f_l$ $v_c = 0.18$ followed by the second straight line defined by the below expression that terminates at ultimate condition $\frac{f_c}{f'_{co}} = 1.1 + k_1 \frac{f_l}{f'_{co}}$	II	Yes	$\frac{f'_{cc}}{f'_{co}} = 1.1 + k_1 \frac{f_{lu,a}}{f'_{co}}$ for CFRP-wrapped concrete $k_1 = 4.1 - 0.75\left(\frac{E_l}{f'^{2}_{co}}\right)^{-1.0}$	$\varepsilon_{cu} = \frac{\varepsilon_{h,rup} + \varepsilon_o}{\mu_{tu}}$ for CFRP-wrapped concrete $\mu_{tu} = 7\left(\frac{E_l}{f'_{co}}\right)^{-0.8}$ $\varepsilon_o = -0.0005$	Yes, experimentally determined value of $k_\varepsilon = 0.5$ for CFRP
2001	Lin and Chen [111]	N/A	N/A	N/A	$f'_{cc} = f'_{co} + 2 f_{lu}$	N/A	No
2002	Ilki et al. [100]	N/A	N/A	N/A	$\frac{f'_{cc}}{f'_{co}} = 1 + 2.227\left(\frac{f_{lu}}{f'_{co}}\right)$ for CFRP-wrapped concrete	$\frac{\varepsilon_{cu}}{\varepsilon_{co}} = 1 + 15.156\left(\frac{f_{lu}}{f'_{co}}\right)^{0.735}$ for CFRP-wrapped concrete	No
2002	Lam and Teng [115]	N/A	N/A	N/A	$\frac{f'_{cc}}{f'_{co}} = 1 + 2\frac{f_{lu}}{f'_{co}}$	N/A	No
2002	Moran and Pantelides [78]	Adopted the analysis-oriented model by Moran and Pantelides [45]	IIIb	Yes	$\frac{f'_{cc}}{f'_{co}} = 1 + k_1 \frac{f_{lu}}{f'_{co}}$ average $k_1 \approx 4.14$ for bonded FRP shell average $k_1 \approx 2.33$ for unbonded FRP shell	$\frac{\varepsilon_{cu}}{\varepsilon_{co}} = 1 + k_2 \frac{f_{lu}}{f'_{co}}$ $k_2 \approx \frac{1}{9.27\times10^{-3}\left(\frac{E_l}{f'_{co}}\right)^{\frac{1}{3}}} \approx \frac{1}{\varepsilon_{co}\mu_{tu}\left(\frac{E_l}{f'_{co}}\right)}$ $\mu_{tu} \approx 4.635\left(\frac{E_l}{f'_{co}}\right)^{-\frac{2}{3}}$	No
2002	Shehata et al. [116]	N/A	N/A	N/A	$\frac{f'_{cc}}{f'_{co}} = 1 + 2\frac{f_{lu}}{f'_{co}}$	$\frac{\varepsilon_{cu}}{\varepsilon_{co}} = 1 + 632\left(\frac{f_{lu}}{f'_{co}}\frac{f'_{cc}}{E_f}\right)^{0.5}$	No
2003	De Lorenzis and Tepfers [52]	N/A	N/A	N/A	Nominated the ultimate strength expressions by Samaan et al. [8], Toutanji [52], and Spoelstra and Monti ('approximate' model) [11].	$\frac{\varepsilon_{cu}}{\varepsilon_{co}} = 1 + 26.2\left(\frac{f_{lu}}{f'_{co}}\right)^{0.8} E_l^{-0.148}$ for FRP-wrapped concrete $\frac{\varepsilon_{cu}}{\varepsilon_{co}} = 1 + 26.2\left(\frac{f_{lu}}{f'_{co}}\right)^{0.68} E_l^{-0.127}$ for FRP tube-encased concrete	No
2003	Lam and Teng [12]	Modified from Richard and Abbott [44] (Eq. 7) $f_c = E_{c1}\varepsilon_c - \frac{(E_{c1} - E_{c2})^2}{4 f_o}\varepsilon_c^{\,2}$ if $0 \le \varepsilon_c \le \varepsilon_{c1}$ $f_o = f'_{co} \quad f_c = f'_{co} + E_{c2}\varepsilon_c$ if $\varepsilon_{c1} \le \varepsilon_c \le \varepsilon_{cu}$ $\varepsilon_{c1} = \frac{2 f'_{co}}{(E_{c1} - E_{c2})} \qquad E_{c2} = \frac{f'_{cc} - f'_{co}}{\varepsilon_{cu}}$	IIIb	Yes	$\frac{f'_{cc}}{f'_{co}} = 1 + 3.3\frac{f_{lu,a}}{f'_{co}}$	$\frac{\varepsilon_{cu}}{\varepsilon_{co}} = 1.75 + 12\left(\frac{f_{lu,a}}{f'_{co}}\right)\left(\frac{\varepsilon_{h,rup}}{\varepsilon_{co}}\right)^{0.45}$ for FRP-wrapped concrete $\frac{\varepsilon_{cu}}{\varepsilon_{co}} = 1.75 + 5.53\left(\frac{f_{lu,a}}{f'_{co}}\right)\left(\frac{\varepsilon_{frp}}{\varepsilon_{co}}\right)^{0.45}$ for CFRP-wrapped concrete	Yes, experimentally determined values of $k_\varepsilon = 0.586$ for CFRP, 0.788 for HM CFRP, 0.851 for AFRP, and 0.624 for GFRP
2003	Li et al. [35]	<u>Stress-strain curve exhibiting strain-hardening behavior:</u> Modified from Hognestad's Parabola [40] $f_c = f'_{cc}\left[2\left(\frac{\varepsilon_c}{\varepsilon_{cu}}\right) - \left(\frac{\varepsilon_c}{\varepsilon_{cu}}\right)^2\right]$ if $0 \le \varepsilon_c \le \varepsilon_{cc}$ <u>Stress-strain curve exhibiting strain-softening behavior:</u> the stress-strain curve as defined above followed by a descending line defined by the below expression $f_c = f'_{cc} + E_{des}(\varepsilon_c - \varepsilon_{cc})$ if $\varepsilon_{cc} \le \varepsilon_c \le \varepsilon_u$	I	N/A	$f'_{cc} = f'_{co} + f_{lu,a}\tan^2\left(45° + \frac{\phi}{2}\right)$ $\phi = 36° + 1°\left(\frac{f'_{co}}{35}\right) \le 45°$ for CFRP-confined concrete	<u>Stress-strain curve exhibiting strain-hardening behavior:</u> $\varepsilon_{cc} = \varepsilon_{co}\left[1 + 2.24\tan^2\left(45° + \frac{\phi}{2}\right)\frac{f_{lu,a}}{f'_{co}}\right]$ for CFRP-confined concrete <u>Stress-strain curve exhibiting strain-softening behavior:</u> $\varepsilon_u = \varepsilon_{cc} + \frac{f'_{cc}}{2E_{des}}$ for CFRP-confined concrete	Yes, k_ε was defined as thickness reduction factor of CFRP

2003	Xiao and Wu [54]	Modified from Richard and Abbott [44] (Eq. 7) $E_{c1} = 4733\sqrt{f'_{co}}$ $E_{c2} = k_1 E_l \mu_{tu}$ $f_o = (1 + 4.8\times10^{-4} E_l) f'_{co}$ n=2	IIIb	Yes	Similar to Xiao and Wu [16] with $k_1 = 4.1 - 0.45\left(\frac{E_l}{f'^{2}_{co}}\right)^{-1.4}$	Similar to Xiao and Wu [16] with $\mu_{tu} = 10\left(\frac{E_l}{f'_{co}}\right)^{-0.9}$ $\varepsilon_o = -0.00047$	Yes, experimentally determined value of k_ε = 0.5 ~ 0.8 for CFRP and GFRP
2004	Ilki et al. [53]	Richard and Abbott [44] (Eq. 7)	IIIb	No	$\frac{f'_{cc}}{f'_{co}} = 1 + 2.4\left(\frac{f_{lu,a}}{f'_{co}}\right)^{1.2}$ for CFRP-wrapped concrete	$\frac{\varepsilon_{cu}}{\varepsilon_{co}} = 1 + 20\left(\frac{f_{lu,a}}{f'_{co}}\right)^{0.5}$ for CFRP-wrapped concrete	Yes, experimentally determined value of k_ε = 0.7 for CFRP
2005	Bisby et al. [14]	N/A	N/A	N/A	$f'_{cc} = f'_{co}\left(1 + 2.425\,\frac{f_{lu}}{f'_{co}}\right)$ $f'_{cc} = f'_{co}\left[1 + 2.217\left(\frac{f_{lu}}{f'_{co}}\right)^{0.911}\right]$ $f'_{cc} = f'_{co} + 3.587\, f_{lu}^{0.840}$	$\varepsilon_{cu} = \varepsilon_{co} + k_2\left(\frac{f_{lu}}{f'_{co}}\right)$ $k_2 = 0.0240$ for CFRP-confinement $k_2 = 0.0137$ for GFRP-confinement $k_2 = 0.0536$ for AFRP-confinement	No
2005	Mandal et al. [117]	N/A	N/A	N/A	$\frac{f'_{cc}}{f'_{co}} = 0.0017\left(E_l\frac{f_{lu}}{f'_{co}}\right)^2 + 0.0232\left(E_l\frac{f_{lu}}{f'_{co}}\right) + 1$	$\frac{\varepsilon_{cu}}{\varepsilon_{co}} = 0.0136\left(E_l\frac{f_{lu}}{f'_{co}}\right)^2 + 0.0842\left(E_l\frac{f_{lu}}{f'_{co}}\right) + 1$	No
2005	Saiidi et al. [56]	A bi-linear curve with the first linear line terminating at the first peak stress defined by the below expressions $f'_{c1} = f'_{co} + 0.003\frac{2E_f t_f}{D}$ $\varepsilon_{c1} = 0.002$ followed by the second straight line that extends until the ultimate condition	II	Yes	$f'_{cc} = f'_{co} + 6.2 f_{lu,a}^{0.7}$ for CFRP-confined concrete	$\varepsilon_{cu} = \frac{\varepsilon_{h,rup}}{0.1 - 0.25\ln\left(\frac{f_{lu,a}}{f'_{co}}\right)}$ for CFRP-confined concrete	Yes, recommended value of k_ε = 0.5 for CFRP
2006	Berthet et al. [55]	Modified from Sargin [51] (Eq. 10) into Eq. 11, with: $E_{c1} = E_c\frac{E_c + (1 - v_c)E_l}{E_c + (1 - v_c - 2v_c^2)E_l}$ $f'_{c1} = f'_{cc} - E_{\theta 2}(\varepsilon_{h,rup} - \varepsilon_{l1})$ $E_{\theta 2} = 2.73E_l - 163$ $\varepsilon_{l1} = 0.002$ $\varepsilon_{c1} = \varepsilon_{co} + \frac{\varepsilon_{l1} - v_c\varepsilon_{co}}{\mu_{tu}}$	IIIc	Yes	$f'_{cc} = f'_{co} + k_1 f_{lu,a}$ $k_1 = 3.45$ if $20\,MPa \le f'_{co} \le 50\,MPa$ $k_1 = \frac{9.5}{(f'_{co})^{\frac{1}{4}}}$ if $50\,MPa < f'_{co} \le 200\,MPa$	$\varepsilon_{cu} = \varepsilon_{co} + \frac{\varepsilon_{h,rup} - v_c\varepsilon_{co}}{\mu_{tu}}$ $\mu_{tu} = \frac{1}{\sqrt{2}}\left(\frac{E_l}{f'^{2}_{co}}\right)^{\frac{2}{3}}$	Yes
2006	Guralnick and Gunawan [102]	N/A	N/A	N/A	$\frac{f'_{cc}}{f'_{co}} = 1 + 2.2\left(\frac{f_{lu,a}}{f'_{co}}\right)^{0.828}$ 'empirical model' $\frac{f'_{cc}}{f'_{co}} = 0.616 + \frac{f_{lu,a}}{f'_{co}} + 1.57\left(\frac{f_{lu,a}}{f'_{co}} + 0.06\right)^{0.5}$ 'analytical model' for $20.7\,MPa \le f'_{co} \le 55.1\,MPa$	N/A	Yes
2006	Jiang and Teng [46]	Same as Lam and Teng [12]	IIIb	Yes	$\frac{f'_{cc}}{f'_{co}} = 1 + 3.5\left(\frac{E_l}{(f'_{co}/\varepsilon_{co})} - 0.01\right)\left(\frac{\varepsilon_{h,rup}}{\varepsilon_{co}}\right)$ if $\frac{E_l}{(f'_{co}/\varepsilon_{co})} \ge 0.01$, $\frac{f'_{cc}}{f'_{co}} = 1$ if $\frac{E_l}{(f'_{co}/\varepsilon_{co})} < 0.01$	$\frac{\varepsilon_{cu}}{\varepsilon_{co}} = 1.65 + 6.5\left(\frac{E_l}{(f'_{co}/\varepsilon_{co})}\right)^{0.8}\left(\frac{\varepsilon_{h,rup}}{\varepsilon_{co}}\right)^{1.45}$	Yes, recommended values of k_ε = 0.5 for CFRP, 0.7 for GFRP
2006	Matthys et al. [118]	Hognestad's Parabola [40] (Eq. 4) for first branch, followed by the proposed strength expression	IIIa	No	$f'_{cc} = f'_{co}\left[1 + 3.5\left(\frac{f_{lu,a}}{f'_{co}}\right)^{0.85}\right]$	Same as Toutanji [52]	Yes, recommended value of k_ε = 0.6 for CFRP and GFRP
2006	Tamuzs et al. [79, 80]	N/A	N/A	N/A	$\frac{f'_{cc}}{f'_{co}} = 1 + 4.2\frac{f_{lu,a}}{f'_{co}}$	$\varepsilon_{cu} = \varepsilon_{co} + \frac{\varepsilon_{h,rup} - v_c\varepsilon_{co}}{\mu_{tu}}$ $\mu_{tu} = 5.9\left(\frac{E_l}{f'_{co}}\right)^{-0.65}$	Yes, experimentally determined value of k_ε = 0.6 for CFRP

2006	Wu et al. [59]	N/A	N/A	N/A	Stress-strain curve exhibiting strain-hardening behavior: $\frac{f'_{cc}}{f'_{co}} = 0.745 + 3.357\frac{f_{lu}}{f'_{co}} - 1.053\left(\frac{f_{lu}}{f'_{co}}\right)^2$ or $\frac{f'_{cc}}{f'_{co}} = 1 + 2.0\frac{f_{lu}}{f'_{co}}$ for common CFRP wraps with coupon test properties with $f_{lu}/f'_{co} \geq 0.13$ $\frac{f'_{cc}}{f'_{co}} = 1.0 + 2.755\frac{f_{lu}}{f'_{co}} - 0.6\left(\frac{f_{lu}}{f'_{co}}\right)^2$ or $\frac{f'_{cc}}{f'_{co}} = 1 + 2.4\frac{f_{lu}}{f'_{co}}$ for high modulus CFRP wraps with coupon test properties with $f_{lu}/f'_{co} \geq 0.13\sqrt{250/E_{frp}}$ $\frac{f'_{cc}}{f'_{co}} = 1.316 + 2.098\frac{f_{lu}}{f'_{co}} - 0.317\left(\frac{f_{lu}}{f'_{co}}\right)^2$ or $\frac{f'_{cc}}{f'_{co}} = 1 + 2.5\frac{f_{lu}}{f'_{co}}$ for FRP tubes with coupon test properties with $f_{lu}/f'_{co} \geq 0.1$ $\frac{f'_{cc}}{f'_{co}} = 0.408 + 6.157\frac{f_{lu}}{f'_{co}} - 3.25\left(\frac{f_{lu}}{f'_{co}}\right)^2$ or $\frac{f'_{cc}}{f'_{co}} = 1 + 3.0\frac{f_{lu}}{f'_{co}}$ for FRP wraps with manufacturer specified properties Stress-strain curve exhibiting strain-softening behavior: $\frac{f'_{cu}}{f'_{co}} = 0.75 + 2.5\frac{f_{lu}}{f'_{co}}$	Stress-strain curve exhibiting strain-hardening behavior: $\varepsilon_{cu} = \frac{\varepsilon_{frp}}{\mu_{su}}$ $\mu_{su} = 0.56k_4\left(\frac{f_{lu}}{f'_{co}}\right)^{-0.66}$ for CFRP-wrapped concrete $k_4 = 1$ if $E_{frp} \leq 250\,GPa$ $k_4 = \sqrt{\frac{250}{E_{frp}}}$ if $E_{frp} > 250\,GPa$ where E_{frp} is in GPa unit $\mu_{su} = 0.33\left(\frac{f_{lu}}{f'_{co}}\right)^{-0.35}$ for CFRP and GFRP tube-encased concrete Stress-strain curve exhibiting strain-softening behavior: $\frac{\varepsilon_{cu}}{\varepsilon_{co,u}} = 1.3 + 6.3\frac{f_{lu}}{f'_{co}}$ where $\varepsilon_{co,u} = 0.0038$	No
2007	Al-Tersawy et al. [119]	N/A	N/A	N/A	$\frac{f'_{cc}}{f'_{co}} = 1 + 1.96\left(\frac{f_{lu,a}}{f'_{co}}\right)^{0.81}$	$\frac{\varepsilon_{cu}}{\varepsilon_{co}} = 1 + 8.16\left(\frac{f_{lu,a}}{f'_{co}}\right)^{0.34}$	Yes
2007	Ciupala et al. [101]	N/A	N/A	N/A	$\frac{f'_{cc}}{f'_{co}} = 1 + 1.7\left(\frac{2f_{lu}}{f'_{co}}\right)^{0.8}$ for CFRP- and GFRP-confined concrete	$\frac{\varepsilon_{cu}}{\varepsilon_{co}} = 1 + 6.7\left(\frac{f'_{cc}}{f'_{co}} - 1\right)^{\frac{2}{3}}$ for CFRP- and GFRP-confined concrete	No
2007	Shehata et al. [110]	N/A	N/A	N/A	$\frac{f'_{cc}}{f'_{co}} = 1 + 2.4\frac{f_{lu}}{f'_{co}}$	Same as Shehata et al. [116]	No
2007	Tabbara and Karam [120]	N/A	N/A	N/A	$\frac{f'_{cc}}{f'_{co}} = 0.598\frac{f'^{*}_{cc}}{f'_{co}}$ for FRP-confined concrete $\frac{f'^{*}_{cc}}{f'_{co}} = \sqrt{10.59\frac{f^{*}_{l}}{f'_{co}} + 1.10} + \frac{f^{*}_{l}}{f'_{co}}$ for actively confined concrete	N/A	No
2007	Vintzileou and Panagiotidou [105]	N/A	N/A	N/A	$f'_{cc} = f'_{co}\left(1 + 2.8\frac{f_{lu,a}}{f'_{co}}\right)$	$\varepsilon_{cu} = \gamma_{frp}\left[0.003\left(\frac{f'_{cc}}{f'_{co}}\right)^2\right]$ $\gamma_{frp} = 1.15$ for CFRP-confined concrete $\gamma_{frp} = 1.95$ for CFRP-confined concrete	N/A

2007	Yan and Pantelides [47]	<u>Stress-strain curve exhibiting strain-hardening behavior:</u> Richard and Abbott [44] (Eq. 7) with $E_{c1} = 5500\sqrt{f'_{co}} \qquad f'_{c1} = \frac{E_{c1}\varepsilon_{c1}}{1+2\beta_1\varepsilon_{c1}} \qquad \varepsilon_{c1} = 0.004$ <u>Stress-strain curve exhibiting strain-softening behavior:</u> Same as the above except Richard and Abbott [44] expression was modified for descending second branch with $E_{c2} = \frac{f'_{cu} - f'_{c1}}{\varepsilon_{cu} - \varepsilon_{c1}} \qquad \varepsilon_{c1} = \frac{f'_{cc}}{E_{c1} - \beta_1 f'_{cc}}$ $f_o = f'_{cu} - E_{c2}\varepsilon_{cu}$ $\frac{f'_{c1}}{f'_{co}} = \max\left[\frac{f'_{cc}}{f'_{cu}}, 1\right]$ if $\frac{f_{lu,a}}{f'_{co}} < 0.2$	IIIb	Yes	<u>Stress-strain curve exhibiting strain-hardening behavior:</u> $\frac{f'_{cc}}{f'_{co}} = 4.721\sqrt{4.193\frac{f_{lu,a}}{f'_{co}} + 1} - 2\frac{f_{lu,a}}{f'_{co}} - 4.322$ if $\frac{f_{lu,a}}{f'_{co}} \geq 0.2$ <u>Stress-strain curve exhibiting strain-softening behavior:</u> $\frac{f'_{cu}}{f'_{co}} = 0.0768\ln\left(\frac{f_{lu,a}}{f'_{co}}\right) + 1.122$ if $\frac{f_{lu,a}}{f'_{co}} < 0.2$	<u>Stress-strain curve exhibiting strain-hardening behavior:</u> $\varepsilon_{cc} = \frac{f'_{cc}\left(1 + 2\beta_1\varepsilon_{h,rup}\right)}{E_{c1}}$ $\beta_1 = 190\left(\frac{f_{lu,a}}{f'_{co}}\right)^{-0.8}$ <u>Stress-strain curve exhibiting strain-softening behavior:</u> $\varepsilon_{cu} = \frac{f'_{cu}\left(1+2\beta_1\varepsilon_{h,rup}\right)}{E_{c1}}$	Yes
2007	Youssef et al. [27]	$f_c = E_c\varepsilon_c\left[1 - \frac{1}{m}\left(\frac{\varepsilon_c}{\varepsilon_{c1}}\right)^{m-1}\right]$ if $0 \leq \varepsilon_c \leq \varepsilon_{c1}$ $m = \frac{E_c\varepsilon_{c1}}{E_c\varepsilon_{c1} - f'_{c1}}$ $f_c = f'_{c1} + E'_{c2}\left(\varepsilon_c - \varepsilon_{c1}\right)$ if $\varepsilon_c > \varepsilon_{c1}$ $\frac{f'_{c1}}{f'_{co}} = 1 + 3\left(\frac{4t_{frp}E_{frp}\varepsilon_{l1}}{Df'_{co}}\right)^{\frac{5}{4}}$ $\varepsilon_{c1} = 0.002748 + 0.1169\left(\frac{4t_{frp}E_{frp}\varepsilon_{l1}}{f'_{co}}\right)^{\frac{6}{7}}\left(\frac{f_{frp}}{E_{frp}}\right)^{\frac{1}{2}}$ $\varepsilon_{l1} = 0.002$	IIIa	Yes	$\frac{f'_{cc}}{f'_{co}} = 1 + 2.25\left(\frac{f_{lu}}{f'_{co}}\right)^{\frac{5}{4}}$	$\varepsilon_{cu} = 0.003368 + 0.2590\left(\frac{f_{lu}}{f'_{co}}\right)\left(\frac{f_{frp}}{E_{frp}}\right)^{\frac{1}{2}}$	No
2008	Binici [60]	A bi-linear curve with the first straight line terminating at f'_{co} and ε_{co}, followed by the second straight line that extends until the ultimate condition	II	No	<u>Stress-strain curve exhibiting strain-hardening behavior:</u> $\frac{f'_{cc}}{f'_{co}} = 1 + 2.6\left(\left(\frac{f_{lu,a}}{f'_{co}}\right) - 0.14\right)^{0.17}$ if $\left(\frac{f_{lu,a}}{f'_{co}}\right) \geq 0.14$ <u>Stress-strain curve exhibiting strain-softening behavior:</u> $\frac{f'_{cc}}{f'_{co}} = 1.8\left(\frac{f_{lu,a}}{f'_{co}}\right)^{0.3}$ if $\left(\frac{f_{lu,a}}{f'_{co}}\right) < 0.14$	Adopted from Lam and Teng [12] $\frac{\varepsilon_{cu}}{\varepsilon_{co}} = 1.75 + 12\left(\frac{f_{lu,a}}{f'_{co}}\right)\left(\frac{\varepsilon_{h,rup}}{\varepsilon_{co}}\right)^{0.45}$	Yes
2009	Al-Salloum and Siddiqui [121]	N/A	N/A	N/A	$\frac{f'_{cc}}{f'_{co}} = 1 + 2.312\frac{f_{lu}}{f'_{co}}$	N/A	No
2009	Girgin et al. [106]	N/A	N/A	N/A	$f'_{cc} = f_{lu} + \sqrt{f'^{2}_{co} + k_5 f'_{co} f_{lu}}$ $k_5 = 2.9$ if $f'_{co} = 7$ to $18\,MPa$ $k_5 = 6.34 - 0.076\,f'_{co}$ if $f'_{co} = 20$ to $82\,MPa$ $k_5 = 0.1$ if $f'_{co} = 82$ to $108MPa$	N/A	N/A
2009	Teng et al. [48]	Same as Lam and Teng [12] for the first branch Modified from Lam and Teng [12] for the second branch as $f_c = f'_{co} + E_{c2}\varepsilon_c$ if $\frac{E_l}{\left(f'_{co}/\varepsilon_{co}\right)} \geq 0.01$ and $\varepsilon_{c1} < \varepsilon_c \leq \varepsilon_{cu}$ $f_c = f'_{co} - \frac{f'_{co} - f'_{cu}}{\varepsilon_{cu} - \varepsilon_{co}}\left(\varepsilon_c - \varepsilon_{co}\right)$ if $\frac{E_l}{\left(f'_{co}/\varepsilon_{co}\right)} < 0.01$ and $\varepsilon_{c1} < \varepsilon_c \leq \varepsilon_{cu}$	IIIb	Yes	Same as Jiang and Teng [46]	$\frac{\varepsilon_{cu}}{\varepsilon_{co}} = 1.75 + 6.5\left(\frac{E_l}{\left(f'_{co}/\varepsilon_{co}\right)}\right)^{0.8}\left(\frac{\varepsilon_{h,rup}}{\varepsilon_{co}}\right)^{1.45}$	Yes

2009	Wu and Wang [63]	N/A	N/A	N/A	$\frac{f'_{cc}}{f'_{co}} = 1 + 2.23\left(\frac{f_{lu}}{f'_{co}}\right)^{0.96}$	N/A	No
2009	Wu et al. [57]	Modified from Richard and Abbott [44] (Eq. 7) with $E_{c1} = 3320\sqrt{f'_{co}} + 6900$ (ACI 363R-84 [122]) $E_{c2} = \frac{f'_{cc} - f'_{co}}{\varepsilon_{cu}}$ n=2.5 $f_o = 0.872 f'_{co} + 0.371 f_{lu} + 6.258$	IIIb	Yes	$\frac{f'_{cc}}{f'_{co}} = 1 + 3.2\left(\frac{f_{lu}}{f'_{co}}\right)$ for AFRP-confined concrete	$\frac{\varepsilon_{cu}}{\varepsilon_{co}} = 1 + 9.5\left(\frac{f_{lu}}{f'_{co}}\right)$ for AFRP-confined concrete	No
2010	Benzaid et al. [123]	N/A	N/A	N/A	$\frac{f'_{cc}}{f'_{co}} = 1 + 2.2\frac{f_{lu,a}}{f'_{co}}$	$\frac{\varepsilon_{cu}}{\varepsilon_{co}} = 2 + 7.6\frac{f_{lu,a}}{f'_{co}}$	Yes, k_ε=0.73 for CFRP
2010	Fahmy and Wu [49]	Expression modified from Lam and Teng [12] with $E_{c2} = m_2\left(245.61 f'^{\,m_1}_{co} + 0.6728 E_l\right)$ modified from Samaan et al. [8] with $m_1 = 0.5$, $m_2 = 0.83$ if $f'_{co} \le 40\,MPa$ $m_1 = 0.2$, $m_2 = 1.73$ if $f'_{co} > 40MPa$	IIIb	Yes	$f'_{cc} = f'_{co} + k_1 f_{lu}$ $k_1 = 4.5 f_{lu}^{-0.3}$ if $f'_{co} \le 40MPa$ $k_1 = 3.75 f_{lu}^{-0.3}$ if $f'_{co} > 40MPa$	$\varepsilon_{cu} = \frac{f'_{cc} - f'_{co}}{E_{c2}}$	No
2010	Mohamed and Masmoudi [103]	N/A	N/A	N/A	$f'_{cc} = f'_{co}\left[0.7 + 2.7\left(\frac{f_{lu,a}}{f'_{co}}\right)^{0.7}\right]$ for FRP tube-encased concrete with $25 \le f'_{co} \le 60\,MPa$	N/A	Yes, recommended value of k_ε = 0.55
2010	Wu and Wang [58]	Same as Wu et al. [57]	IIIb	Yes	$\frac{f'_{cc}}{f'_{co}} = 1 + 3.4\left(\frac{f_{lu}}{f'_{co}}\right)$ for AFRP-confined concrete	Same as Wu et al. [57]	No
2010	Wu and Zhou [124]	N/A	N/A	N/A	$\frac{f'_{cc}}{f'_{co}} = \frac{f_{lu}}{f'_{co}} + \sqrt{\left(\frac{16.7}{f'^{\,0.42}_{co}} - \frac{f'^{\,0.42}_{co}}{16.7}\right)\frac{f_{lu}}{f'_{co}} + 1}$	N/A	No.
2011	Cevik [125]	N/A	N/A	N/A	$f'_{cc} = (f_{lu})^{1.5} + [\ln(f'_{co})]^3 + 2\ln(f_{lu}) - 13.65\left(\frac{f_{lu}}{f'_{co}}\right) + \left(\frac{f_{lu}}{f'_{co}}\right)^{1.5}$ $f'_{cc} = -93.53 + 2.44(f_{lu}) + 40.11\ln(f'_{co}) - 27.03\left(\frac{f_{lu}}{f'_{co}}\right)$	N/A	No
2011	Park et al. [126]	N/A	N/A	N/A	$\frac{f'_{cc}}{f'_{co}} = 0.7 + 3.7\frac{f_{lu}}{f'_{co}}$	N/A	No
2011	Realfonso and Napoli [127]	N/A	N/A	N/A	$\frac{f'_{cc}}{f'_{co}} = 1 + 3.49\left(\frac{f_{lu,a}}{f'_{co}}\right)^{0.86}$ $\frac{f'_{cc}}{f'_{co}} = 1 + 3.57\left(\frac{f_{lu,a}}{f'_{co}}\right)$	N/A	Yes
2011	Wang and Wu [128]	$f'_{c1} = \frac{\left(1.2 + 3.85\frac{f_{lu}}{f'_{co}}\right)f'_{co}}{\sqrt{1 + \frac{(H-D)}{545}}}$	N/A	Yes	$f'_{cc} = \frac{\left(1.0 + 5.54\frac{f_{lu}}{f'_{co}}\right)f'_{co}}{\sqrt{1 + \frac{(H-D)}{353}\left(1 - 1.49\frac{f_{lu}}{f'_{co}}\right)}}$	N/A	No
2011	Yu and Teng [129]	Same as Lam and Teng [12]	IIIb	Yes	$f'_{cc} = f'_{co} + 3.5E_l\left(1 - 6.5\frac{f'_{co}}{E_l}\right)\varepsilon_{h,rup}$ for FRP tube-encased concrete	$\varepsilon_{cu} = 0.0033 + 0.6\left(\frac{E_l}{f'_{co}}\right)^{0.8}(\varepsilon_{h,rup})^{1.45}$ for FRP tube-encased concrete	Yes

Table 2. Summary of existing analysis-oriented models of FRP-confined concrete

Year	Model	Stress-strain equation of the base curve	Peak point expressions for the base curves		Dilation expression	Consideration of concrete dilation behavior in model	Consideration of FRP hoop strain reduction in model
			Stress	Strain			
1997	Mirmiran and Shahawy [107, 130]	Popovics [34] (Eq. 17)	Mander et al. [6] (Eq. 19)	Richart et al. [4] (Eq. 20)	$\mu_t = \dfrac{v_c - 2v_c\left(\dfrac{\varepsilon_c}{\varepsilon_{co}}\right) + \mu_{tu}\left(\dfrac{\mu_{t,\max} - v_c}{\mu_{t,\max} - \mu_{t,asym}}\right)\left(\dfrac{\varepsilon_c}{\varepsilon_{co}}\right)^2}{1 - 2\left(\dfrac{\varepsilon_c}{\varepsilon_{co}}\right) + \left(\dfrac{\mu_{t,\max} - v_c}{\mu_{t,\max} - \mu_{t,asym}}\right)\left(\dfrac{\varepsilon_c}{\varepsilon_{co}}\right)^2}$ $\mu_{t,\max} = -0.7611 \ln\left(\dfrac{E_l}{f'_{co}}\right) + 4.0167$ $\mu_{t.asym} = -0.1375 \ln\left(\dfrac{E_l}{f'_{co}}\right) + 0.8646$	Explicitly derived from FRP-confined concrete test results	N/A
1999	Spoelstra and Monti [11] 'exact'	Popovics [34] (Eq. 17) with $E_c = 5700\sqrt{f'_{co}}$	Mander et al. [6] (Eq. 19)	Richart et al. [4] (Eq. 20)	Modified from Pantazopoulou and Mills [108] $\varepsilon_l = \dfrac{E_c\varepsilon_c - f_c}{2\alpha f_c}$ $\alpha = \dfrac{5700}{\sqrt{f'_{co}}} - 500$	Implicitly adopted from an actively confined concrete model	No
2001	Fam and Rizkalla [67]	Popovics [34] (Eq. 17) with $E_c = 5000\sqrt{f'_{co}}$	Mander et al. [6] (Eq. 19)	Richart et al. [4] (Eq. 20)	Developed based on the results reported in Gardner [131] from triaxial concrete tests of concrete $\dfrac{\mu_s}{v_c} = \left(1.914\ \dfrac{f_l}{f'_{co}} + 0.719\right)\dfrac{\varepsilon_c}{\varepsilon_{cu}} + 1$	Implicitly derived from actively confined concrete test results	No
2002	Chun and Park [68]	Popovics [34] (Eq. 17)	Mander et al. [6] (Eq. 19)	Richart et al. [4] (Eq. 20)	Adopted from Elwi and Murray [75] $\mu_s = v_c\left[1.0 + 1.3763\left(\dfrac{\varepsilon_c}{\varepsilon_{cc}}\right) + 5.36\left(\dfrac{\varepsilon_c}{\varepsilon_{cc}}\right)^2 + 8.586\left(\dfrac{\varepsilon_c}{\varepsilon_{cc}}\right)^3\right]$ if $\mu_s \le \mu_{su}$ $\mu_{su} = -0.2305\ln\left(\dfrac{f_{lu}}{f'_{co}}\right) + 0.087$ for CFRP-wrapped concrete	Implicitly adopted from an actively confined concrete model	No
2002	Harries and Kharel [72]	Modified from Popovics [34] (Eq. 17) as $\dfrac{f_c}{f'_{co}} = \dfrac{\varepsilon_c}{\varepsilon_{co}}\left(\dfrac{r}{r - 1 + \left(\varepsilon_c/\varepsilon_{co}\right)^{rk}}\right)$ $k = 1$ if $\dfrac{\varepsilon_c}{\varepsilon_{cc}} \le 1$ $k = \left(0.67 + \dfrac{f'_{co}}{62}\right)\dfrac{f'_{co}}{f'_{cc}}$ if $\dfrac{\varepsilon_c}{\varepsilon_{cc}} \le 1$ $E_c = \left(3300\sqrt{f'_{co}} + 6900\right)\left(\dfrac{\gamma_c}{2300}\right)^{1.5}$	Mirmiran [113] $f'_{cc} = f'_{co} + 4.269\left(f_{lu,a}\right)^{0.587}$	Richart et al. [4] (Eq. 20)	$\mu_s = v_c$ if $\varepsilon_c < 0.6\varepsilon_{co}$ $\mu_s = \left(\dfrac{\mu_{su} - v_c}{1.4\varepsilon_{co}}\right)(\varepsilon_c - 0.6\varepsilon_{co}) + v_c$ if $0.6\varepsilon_{co} < \varepsilon_c < 2\varepsilon_{co}$ $\mu_s = \mu_{su}$ if $\varepsilon_c \ge 2\varepsilon_{co}$ $\mu_{su} = -0.99\ln(n_{frp}E_{frp}) + 12$ for E-GFRP-confined concrete $\mu_{su} = -0.66\ln(n_{frp}E_{frp}) + 8$ for CFRP-confined concrete	Explicitly derived from FRP-confined concrete test results	Yes
2002	Moran and Pantelides [45]	Modified from Richard and Abbott [44] (Eq. 7) and Popovics [34] as $f_c = \left(E_{c,ch} + E_{c,cs}\right)\varepsilon_c$			Same as Moran and Pantelides [78] $\mu_{tu} \approx 4.635\left(\dfrac{E_l}{f'_{co}}\right)^{-\frac{2}{3}}$	Explicitly derived from FRP-confined concrete test results	Yes

2004	Marques et al. [69]	Popovics [34] (Eq. 17) with $E_c = 3320\sqrt{f'_{co}} + 6900$ (ACI 363R-84)	Razvi and Saatcioglu [112] $f'^{*}_{cc} = f'_{co} + k_1 f^{*}_{l}$ $k_1 = 6.7 f^{*-0.17}_{l}$	Razvi and Saatcioglu [112] $\varepsilon^{*}_{cc} = \varepsilon_{co}\left(1 + 5k_1k_3\frac{f^{*}_{l}}{f'_{co}}\right)$ $k_3 = \frac{40}{f'_{co}} \le 1$	Adopted from Pantazopoulou and Mills [108] $\varepsilon_l = v_c\varepsilon_c$ for $\varepsilon_c \le \varepsilon_{c,cr}$ $\varepsilon_l = v_c\varepsilon_c + \frac{1-2v_c}{2}\varepsilon_{c,vo}\left(\frac{\varepsilon_c - \varepsilon_{c,cr}}{\varepsilon_{c,vo} - \varepsilon_{c,cr}}\right)^2$ for $\varepsilon_{c,cr} \le \varepsilon_c \le \varepsilon_{c,vo}$ with additional expressions below proposed by the researchers for $\varepsilon_c > \varepsilon_{c,vo}$ $\varepsilon_l = \frac{1}{2}\left(\frac{E_c\varepsilon_c}{\alpha f_c} - \frac{1}{\alpha}\right)^{\frac{1}{\psi}}$ $\psi = \frac{1}{2}\frac{E_c\varepsilon_{co}}{E_c\varepsilon_{co} - f'_{co}}\frac{(\varepsilon_{co} - \varepsilon_{c,cr})}{[(1-v_c)\varepsilon_{co} - v_c\varepsilon_{c,cr}]}$ $\alpha = \frac{E_c\varepsilon_{co} - f'_{co}}{f'_{co}}(\varepsilon_{co})^{-\psi}$	Implicitly adopted from an actively confined concrete model	No
2005	Binici [73]	Modified from Popovics [34] (Eq. 17) as $f_c = E_c\varepsilon_c$ $E_c = 4750\sqrt{f'_{co}}$ for $\varepsilon_c \le \varepsilon_{c,e}$ $f_c = f_{c,e} + (f'^{*}_{cc} - f_{c,e})\left(\frac{\varepsilon_c - \varepsilon_{c,e}}{\varepsilon^{*}_{cc} - \varepsilon_{c,e}}\right) \times \frac{r}{r - 1 + \left(\frac{\varepsilon_c - \varepsilon_{c,e}}{\varepsilon^{*}_{cc} - \varepsilon_{c,e}}\right)^r}$ for $\varepsilon_{c,e} \le \varepsilon_c < \varepsilon_{c1}$ $f_c = f_{c,res} + (f'^{*}_{cc} - f_{c,res}) \times \exp\left[-\left(\frac{\varepsilon_c - \varepsilon^{*}_{cc}}{\alpha_1}\right)^2\right]$ for $\varepsilon_{c1} < \varepsilon_c$	$f'^{*}_{cc} = f'_{co}\left[\sqrt{1 + 9.9\left(\frac{f_{lu,a}}{f'_{co}}\right)} + \frac{f_{lu,a}}{f'_{co}}\right]$	Richart et al. [4] (Eq. 20)	$\mu_{su} = \mu_{s,\max} - (\mu_{s,\max} - v_c)\exp\left[-\left(\frac{\varepsilon_c - \varepsilon_{c,cr}}{\Delta}\right)^2\right]$ $\mu_{s,\max} = \mu_{s1} + \frac{1}{\left(\frac{f_{lu}}{f'_{co}} + 0.85\right)^4}$ $\Delta = \frac{\varepsilon_{c1} - \varepsilon_{c,cr}}{\sqrt{-\ln\beta_2}}$ $\beta_2 = \frac{\mu_{s,\max} - \mu_{s1}}{\mu_{s,\max} - v_c}$ $\mu_{s1} = 0.5$	Implicitly derived from actively confined concrete test results	Yes, recommended value of $k_\varepsilon = 0.65$
2007	Albanesi et al. [77]	N/A	$\frac{f'_{cu}}{f'_{co}} \cong 1 + 3.609\frac{f_{lu}}{f'_{co}}$ for $\frac{f_{lu}}{f'_{co}} \le 0.7$	$\frac{\varepsilon_{cu}}{\varepsilon_{co}} \cong 1 + 18.045\frac{f_{lu}}{f'_{co}}$ for $\frac{f_{lu}}{f'_{co}} \le 0.7$	Modified from Fam and Rizkalla [67] as $\frac{\mu_s}{v_c} \cong \left[\frac{1.914\left(\frac{f_l}{f'_{co}}\right) + 0.719}{1 + 18.045\left(\frac{f_l}{f'_{co}}\right)}\right]\frac{\varepsilon_c}{\varepsilon_{co}} + 1$	Modified from a model that was implicitly derived from actively confined concrete test results.	No
2007	Teng et al. [62]	Popovics [34] (Eq. 17)	$\frac{f'^{*}_{cc}}{f'_{co}} = 1 + 3.5\frac{f^{*}_{l}}{f'_{co}}$	Richart et al. [4] (Eq. 20)	$\frac{\varepsilon_c}{\varepsilon_{co}} = 0.85\left(1 + 8\frac{f_l}{f'_{co}}\right) \times \left\{\left[1 + 0.75\left(\frac{\varepsilon_l}{\varepsilon_{co}}\right)\right]^{0.7} - \exp\left[-7\left(\frac{\varepsilon_l}{\varepsilon_{co}}\right)\right]\right\}$	Explicitly derived from FRP-confined and actively confined concrete test results	Yes
2007	Jiang and Teng [66]	Popovics [34] (Eq. 17)	Same as Teng et al. [62]	$\frac{\varepsilon^{*}_{cc}}{\varepsilon_{co}} = 1 + 17.5\left(\frac{f^{*}_{l}}{f'_{co}}\right)^{1.2}$	Same as Teng et al. [62]	Explicitly derived from FRP-confined and actively confined concrete test results	Yes
2010	Aire et al. [70]	Popovics [34] (Eq. 17) with $E_c = 3320\sqrt{f'_{co}} + 6900$	Mander et al. [6] (Eq. 19)	Razvi and Saatcioglu [112] $\varepsilon^{*}_{cc} = \varepsilon_{co}\left(1 + 5k_1k_3\frac{f^{*}_{l}}{f'_{co}}\right)$ $k_3 = \frac{40}{f'_{co}} \le 1$ $k_1 = 6.7(f_l)^{-0.17}$	Modified from Marques et al. [69] with $\varepsilon_l = \frac{1}{2}\left(\frac{E_c\varepsilon_c}{f_c} - \frac{1}{\alpha}\right)^{\frac{1}{\psi}}$ $\psi = \frac{1}{4 - 6v_c}\left(1 + \frac{f'_{co}}{E_c\varepsilon_{co} - f'_{co}}\right)$	Implicitly adopted from an actively confined concrete model	No
2010	Xiao et al. [64]	Popovics [34] (Eq. 17) with $E_c = 4700\sqrt{f'_{co}}$	$\frac{f'^{*}_{cc}}{f'_{co}} = 1 + 3.24\left(\frac{f^{*}_{l}}{f'_{co}}\right)^{0.80}$	$\frac{\varepsilon^{*}_{cc}}{\varepsilon_{co}} = 1 + 17.4\left(\frac{f^{*}_{l}}{f'_{co}}\right)^{1.06}$	Same as Teng et al. [62]	Same as Teng et al. [62]	Yes

3. STRESS-STRAIN MODELS FOR FRP-CONFINED CONCRETE

A comprehensive review of the existing literature has revealed 88 stress-strain models developed for FRP-confined concrete in circular sections. The majority of the existing models can be classified into two broad categories using the category names previously suggested by Teng and Lam [12], namely the design-oriented and analysis-oriented models. Of the reviewed models, 59 fell into the design-oriented model category, and the details of these models are presented in Table 1. Most of these models consist of closed-form equations that were developed through regression analyses and were calibrated from axial compression test results of FRP-confined concrete. Therefore, the accuracy of these models depends greatly on the size and reliability of the test database as well as the parametric range of the test data used in the model development. The remaining 29 models consist of 13 models classified as analysis-oriented models, with their details summarized in Table 2*,* and 16 models classified as models based on other approaches as discussed in Section 3.3. Most of the analysis-oriented models capture the interaction between the FRP confining device and concrete core through force equilibrium and strain compatibility of each element as defined by Eq. 1 or Eq. 3 and illustrated in Figure 1.

In the following sections, the existing models of FRP-confined concrete are categorized and reviewed and their theoretical bases are discussed. Although this paper is concerned with the models developed for FRP-confined concrete, throughout the paper constant references have been made to the models developed for actively confined and steel-confined concrete due to the intimate connections that exist between the latter and former and the vital role the latter played in the development of the former. It should be noted that all of the expressions given in this paper are in SI units. This review is limited to models or parts of models that are developed for FRP-confined concrete in circular sections. The effect of specimen size on the stress-strain response is recognized by a few studies (e.g. [22-24]), this review includes all existing models independent of application to specimen size. Some models may consist of features making them applicable to non-circular sections (e.g. [25-27]), cyclically loaded specimens (e.g. [28-30]) or sections with internal steel-reinforcement (e.g.[31-33]). Such integrated features are beyond the scope of the review reported herein.

3.1 Design-oriented models

3.1.1 Types of stress-strain curves used by design-oriented models

The progression of research on FRP-confined concrete has seen a large quantity and wide variety of proposed axial stress-strain relationships. In this paper, the design-oriented models are classified into three broad categories based on the geometric form of the curves (i.e. parabolic, bilinear, or combination of both) they proposed, namely as Type I, II and III. Models based on Type III curves are then further divided into three sub-categories according to the approach they adopted in the development of their proposed curves, namely as Type IIIa, IIIb and IIIc. The important aspects of these curves are discussed in this section.

3.1.1.1 Type I curves

In early studies of FRP-confinement, the models developed for actively confined or steel-confined concrete [5, 34] were applied to describe the stress-strain behavior of FRP-confined

concrete (e.g. [1-3, 35]). Hence, the stress-strain curves given by these early models feature parabolic curves similar to that of steel or actively confined concrete (Figure 2). This type of curve is classified as Type I in this paper. As to be expected, these stress-strain models do not accurately capture the typical bilinear shape of the stress-strain curves of FRP-confined concrete.

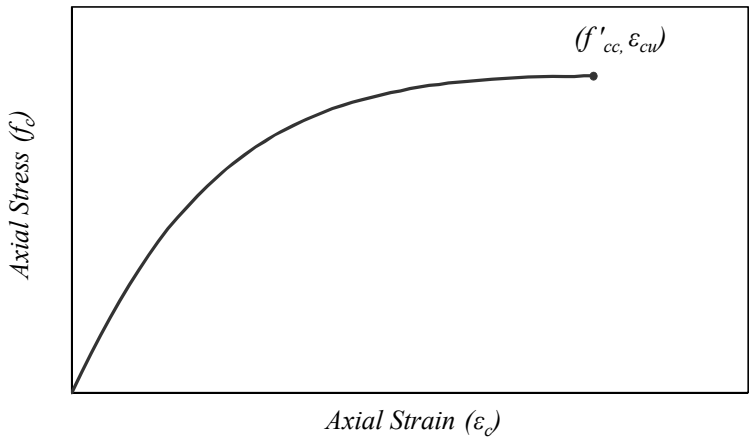

Figure 2. Stress-strain curve of FRP-confined concrete based on steel or actively confined concrete models – Type I

3.1.1.2 Type II curves

The bilinear stress-strain curves appeared more frequently in the subsequent studies on FRP-confined concrete (e.g. [16, 36-39]). These early studies recognized that FRP-confined concrete developed significantly different stress-strain response than steel or actively confined concrete. Behavior of FRP-confined concrete was simply represented by a bilinear curve defined by a transition point (f'_{c1}, ε_{c1}) near the location of the unconfined concrete peak stress and a final point (f'_{cc}, ε_{cu}) at the ultimate condition as shown in Figure 3. As marked in Table 1 some of the models did not consider the strength enhancement due to confinement at the transition point and defined the transition point using the corresponding stress (f'_{co}) and strain (ε_{co}) of unconfined concrete.

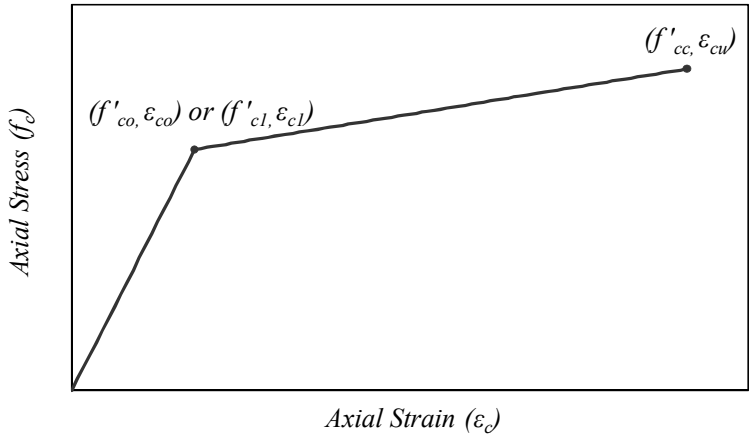

Figure 3. Bilinear stress-strain curve of FRP-confined concrete – Type II

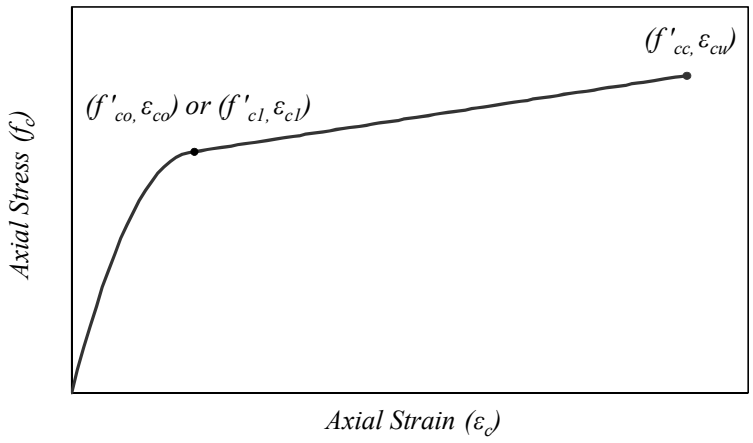

(a)

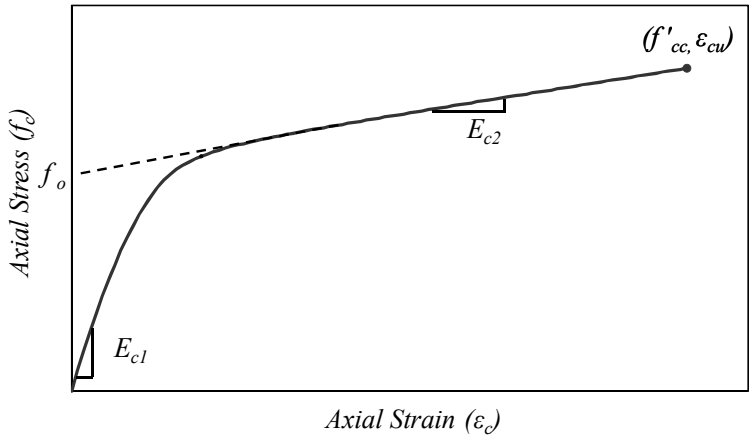

(b)

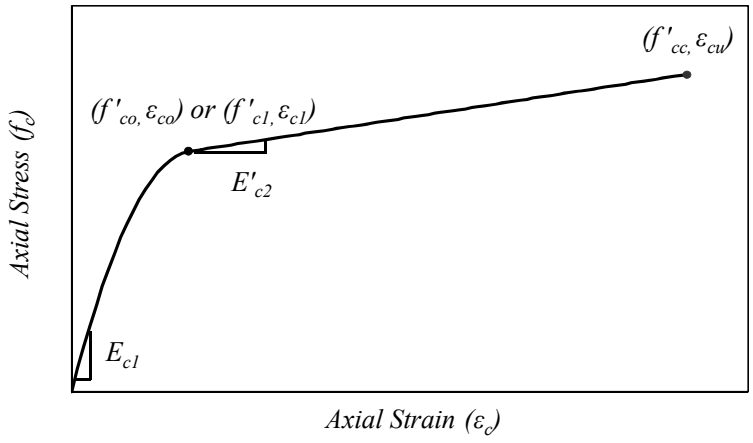

(c)

Figure 4. Stress-strain curves of FRP-confined concrete with parabolic initial ascending branch and linear or quasi-linear second branch: (a) type IIIa; (b) type IIIb; (c) type IIIc

3.1.1.3 Type III curves

In most of the later studies, the stress-strain models of FRP-confined concrete were further improved by more accurate modeling of the initial ascending portion of the stress-strain curves. These models described the initial ascending region as a parabola, which was

followed by a second region that was approximately linear (Figures 4(a) to (c)). As noted previously, several different approaches have been used to establish the Type III stress-strain curves, which are further classified herein as Types IIIa, IIIb and IIIc curves.

Type IIIa curves: Hognestad's parabola [40] has been used by several researchers to model the initial ascending portion of the stress-strain curve of FRP-confined concrete [9, 22, 27, 41-43]. The second branch of the stress-strain curve was obtained by connecting the initial peak with the ultimate condition (f'_{cc}, ε_{cu}) through a straight line defined by Eq 5. In Table 1, this type of curve is classified as Type IIIa. The shape of the curve and the relevant notations are illustrated in Figure 4(a).

$$f_c = f'_{c1}\left[2\left(\frac{\varepsilon_c}{\varepsilon_{c1}}\right)-\left(\frac{\varepsilon_c}{\varepsilon_{c1}}\right)^2\right] \text{ for } \varepsilon_c \le \varepsilon_{c1} \tag{4}$$

$$f_c = f'_{c1} + E_{c2}(\varepsilon_c - \varepsilon_{c1}) \text{ for } \varepsilon_c > \varepsilon_{c1} \tag{5}$$

$$\text{where } E_{c2} = \frac{f'_{cc} - f'_{c1}}{\varepsilon_{cu} - \varepsilon_{c1}} \tag{6}$$

Type IIIb curves: The four-parameter curve proposed by Richard and Abbott [44] (Type IIIb – Figure 4(b)) (Eq. 7) has been used widely in modeling the stress-strain relationship of FRP-confined concrete (refer to Table 1 for a complete list of models). In some of the studies, the original version of the stress-strain relationship was modified in establishing the final form of the new model expressions [8, 12, 45-49]. The modified parts of these model expressions that differ from the original version are presented in Table 1. In the original model, the stress-strain behavior of FRP-confined concrete was described by two slopes, namely the slope of the elastic portion of the initial ascending branch (E_{c1}) and the post-peak second branch (E_{c2}) (Figure 4(b)), in the form given in Eq. 7. In these curves, a polynomial constant (n) (Eq. 9) was used to fit a smooth transition curve between the two segments. The expression given by ACI 318-95 [50] for the elastic modulus of concrete $E_c = 4730\sqrt{f'_{co}}$ was used by most of the reviewed models to determine the slope of the initial ascending branch (E_{c1}). For the models that recommended different expressions for the determination of E_{c1}, these expressions are given in Table 1.

$$f_c = \frac{(E_{c1} - E_{c2})\varepsilon_c}{\left\{1+\left[\frac{(E_{c1} - E_{c2})\varepsilon_c}{f_o}\right]^n\right\}^{\frac{1}{n}}} + E_{c2}\varepsilon_c \tag{7}$$

$$f_o = f'_{cc} - E_{c2}\varepsilon_{cu} \tag{8}$$

$$n = 1 + \frac{1}{\frac{E_{c1}}{E_{c2}} - 1} \tag{9}$$

Type IIIc curves: Based on the general expression developed by Sargin [51] (Eq. 10), Ahmad and Shah [5] proposed a stress-strain model for concrete confined by steel spirals. Ahmad and Shah's model [5] was then modified by Toutanji [52] for FRP-confined concrete into the form given in Eq. 11, which was subsequently adopted by a number of models to describe the stress-strain relationship of FRP-confined concrete (Type IIIc – Figure 4(c)). These models use the slopes of the initial ascending branch (E_{c1}) and the post-peak second branch (E'_{c2}) to describe the stress-strain curve. It should be noted that in these models the slope of the second branch (E'_{c2}) refers to the tangential slope of the stress-strain curve taken immediately after the initial peak stress (f'_{c1}) is reached (Figure 4(c)).

$$\frac{f_c}{f'_{co}} = \frac{A_i\left(\frac{\varepsilon_c}{\varepsilon_{co}}\right) + (D_i - 1)\left(\frac{\varepsilon_c}{\varepsilon_{co}}\right)^2}{1 + (A_i - 2)\left(\frac{\varepsilon_c}{\varepsilon_{co}}\right) + D_i\left(\frac{\varepsilon_c}{\varepsilon_{co}}\right)^2} \tag{10}$$

$$f_c = \frac{A_j \varepsilon_c}{1 + C_j \varepsilon_c + D_j \varepsilon_c^{\,2}} \tag{11}$$

where $A_j = E_{c1}$ (12)

$$C_j = \frac{E_{c1}}{f'_{c1}} - \frac{2}{\varepsilon_{c1}} + \frac{E_{c1} E'_{c2} \varepsilon_{c1}}{f'^{\,2}_{c1}} \tag{13}$$

$$D_j = \frac{1}{\varepsilon_{c1}^{\,2}} - \frac{E_{c1} E'_{c2}}{f'^{\,2}_{c1}} \tag{14}$$

3.1.2 Important aspects of the stress-strain curves

Typical axial stress-strain curves of FRP-confined concrete are shown in Figure 5. In some of the models reviewed in this paper, the behavior of FRP-confined concrete at the initial ascending portion of the stress-strain relationship was assumed to be similar to that of unconfined concrete (Figure 5(a)) (e.g. [9, 22, 42, 43, 53]). This was based on the assumption that confinement provided by the FRP shell was insignificant along the initial branch because the lateral strain of confined concrete and the resulting lateral confinement pressure were low during that stage. Consequently, initial axial strength and strain enhancement were considered negligible by these models. There were also a number of models that considered the strengthening effect of FRP confinement on the initial ascending portion of the stress-strain curve as illustrated in Figure 5(b) [8, 10, 12, 16, 27, 41, 46-48, 52, 54-58]. Information regarding this aspect of the models were provided in the fifth column of Table 1, where 'Yes' indicates that the initial strength and strain enhancement effects were considered by the model.

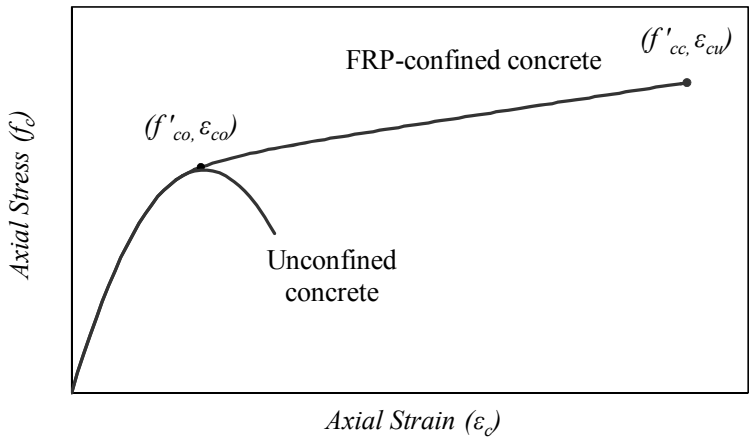

(a)

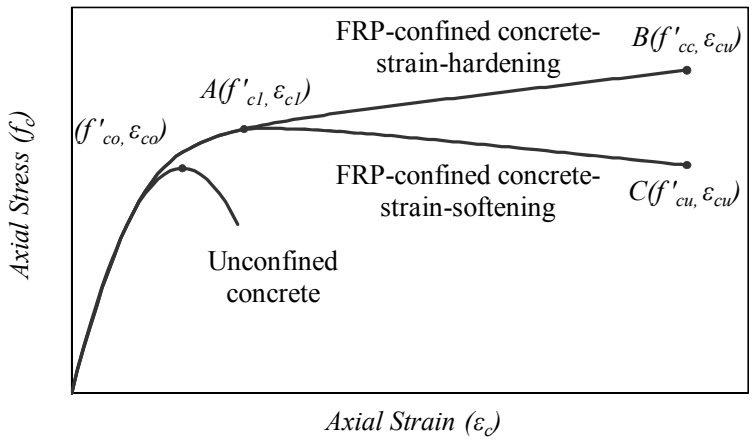

(b)

Figure 5. Stress-strain curves of FRP-confined concrete: (a) with the first peak corresponding to that of unconfined concrete; (b) with consideration of strengthening effect of confinement at the first peak

After the transition zone that starts towards the end of the ascending branch, the cracked concrete dilates rapidly and the lateral expansion triggers the passive confinement mechanism of the FRP shell. In return, the lateral confining pressure (f_l) generated by the FRP shell counteracts degradation of the axial stiffness of the concrete core and prevents the core from losing its integrity. This confinement mechanism often leads to a ductile plateau in the axial stress-strain curve after the initial ascending branch, which is often referred as the second branch. If the level of confinement provided by the FRP shell is greater than the threshold confinement level, the second branch of the stress-strain curve demonstrates a post-peak ascending behavior, known as strain-hardening (Line *A-B* in Figure 5(b)). Conversely, if the level of confinement is lower than the threshold value, a post-peak descending behavior known as strain-softening is observed (Line *A-C* in Figure 5(b)). Except for the models proposed by Miyauchi et al. [41], Li et al. [35], Jiang and Teng [46], Wu et al. [59], Yan and Pantelides [47], Binici [60], and Teng et al. [48], the design-oriented models reviewed in this paper did not provide expressions for predictions of the strain softening behavior of FRP-confined concrete.

3.1.3 Ultimate condition models

Of the reviewed models, 25 consisted only of expressions given to determine the ultimate condition (i.e. ultimate strength (f'_{cc}) and corresponding strain (ε_{cu})) of FRP-confined concrete. The complete stress-strain relationship was not described in these models, and some of the models gave an expression only for the ultimate strength not including one for the ultimate strain. These details all highlighted in Table 1, where the ultimate condition models were marked as 'N/A' in the 'type of curve' column of the table. The majority of these models were based on the general form of the expressions proposed by Richart et al. [4] for the calculation of the compressive strength ($f'_{cc}{}^{*}$) and corresponding strain ($\varepsilon_{cc}{}^{*}$) of actively confined concrete. The general form of these ultimate condition models is described by EqS. 15 and 16.

$$\frac{f'_{cc}}{f'_{co}} = c_1 + k_1 \frac{k_\varepsilon f_{lu}}{f'_{co}} \tag{15}$$

$$\frac{\varepsilon_{cu}}{\varepsilon_{co}} = c_2 + k_2 \frac{k_\varepsilon f_{lu}}{f'_{co}} \tag{16}$$

where c_1 and c_2 are calibration constants, and k_1 and k_2 are strength and strain enhancement coefficients for FRP-confined concrete, respectively.

These models were calibrated using recorded stress and strain data of test specimens at failure. As the ultimate condition expressions were developed empirically, their accuracy depends on the size and reliability of the database used in their calibration. Some of these models were developed based on rather limited test data, often only from tests performed by the originators of the model (e.g. [1, 9, 10, 52, 61]). Several researchers, on the other hand, developed their ultimate condition expressions using larger test databases they assembled from the published literature (e.g. [12, 13, 62-64]).

3.2 Analysis-oriented models

Analysis-oriented models consider the interaction between the external confining shell and internal concrete core. Incremental iterative numerical procedures have been often used to solve the force equilibrium and strain compatibility between the two elements. These models are capable of providing a unified treatment of both well-confined concrete with a continuously ascending stress-strain curve and weakly confined concrete with a stress-strain curve featuring a descending branch. These models also have the potential to predict the behavior of concrete confined with different materials provided that appropriate constitutive relationships are used for the confining material. As stated by Teng et al. [62], these features make analysis-oriented models more versatile and powerful than design-oriented models. On the other hand, most of the analysis-oriented models are built on the assumption of stress path independence, which assumes that the axial stress and axial strain of FRP-confined concrete at a given lateral strain are the same as those of the same concrete actively confined with a constant confining pressure equal to that supplied by the FRP shell [62]. Based on the

observations of their investigations on FRP-confined high-strength concrete (HSC), Xiao et al. [64] recently stated that the assumption of stress path independence was incorrect for confined HSC, and suggested that confinement effectiveness of FRP-confined HSC might be lower than that of actively confined HSC. Xiao et al. [64] further concluded that the stress path independence assumption deviated from the actual behavior more significantly when the confining FRP shell was softer and/or when the unconfined concrete strength was higher. These observations are supported by the results of the recently conducted tests on FRP-confined HSC by the first author's research group at the University of Adelaide [65]. Although the effect of path dependence was easier to recognize in confined HSC due to the inherently high confinement demand of the HSC, this should not be interpreted as this effect is limited to HSC, and for confined normal-strength concretes with low nominal confinement ratios (f_{lu}/f'_{co}) deviations may also be significant. Therefore, alongside the previously mentioned advantages of the analysis-oriented models the abovementioned limitations of the models should also be recognized. Only a brief summary of the analysis-oriented models is presented in this paper as a detailed review of majority of these models was previously presented by Jiang and Teng [66].

In the development of analysis-oriented models for FRP-confined concrete, the stress-strain curves of actively confined concrete are employed as the base curves (Figure 6(a)). The axial stress-strain curve of FRP-confined concrete is then obtained through an incremental approach, with the resulting curve crossing a family of stress-strain curves for the same concrete under different levels of active confinement pressure (Figure 6(a)). This approach requires the lateral-to-axial strain (i.e. dilation relationship (μ)) of FRP-confined concrete as an input. The iterative process involved in the determination of the stress-strain curves of FRP-confined concrete can be summarized as follows. If the lateral-to-axial strain relationship is known, for a given axial strain ($\varepsilon_{c,A}$), then the corresponding lateral strain ($\varepsilon_{l,A}$) can be determined as illustrated in Figure 6(b). The confining pressure in FRP can then be calculated using this strain. The actively confined concrete stress-strain curve corresponding to this confining pressure can then be selected from the family of curves, such as *Curve A* in Figure 6(a), and can be used to determine the axial stress of FRP-confined concrete ($f_{c,A}$) for the given axial strain ($\varepsilon_{c,A}$). The confining pressure in FRP-confined concrete varies continuously with the axial strain, therefore the above steps should be repeated to generate the entire stress-strain curve. Finally, the stress-strain curve of FRP-confined concrete terminates at the point where the lateral strain reaches the hoop rupture strain of the FRP ($\varepsilon_{h,rup}$).

It should be clear from the above summary that the accuracy of analysis-oriented models is very sensitive to both the active confinement base curves and the lateral-to-axial strain relationships used in the models. In the following section, a brief summary of these key relationships are presented. Table 2 summarizes the expressions used by each analysis-oriented model to establish the actively confined concrete base curves and model the lateral-to-axial strain relationship of FRP-confined concrete.

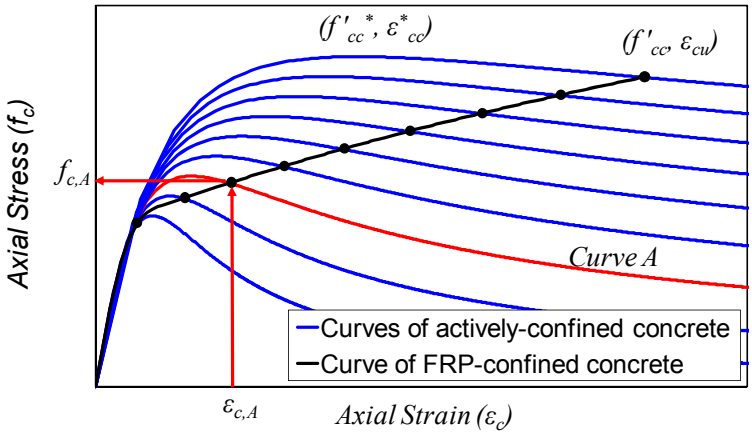

(a)

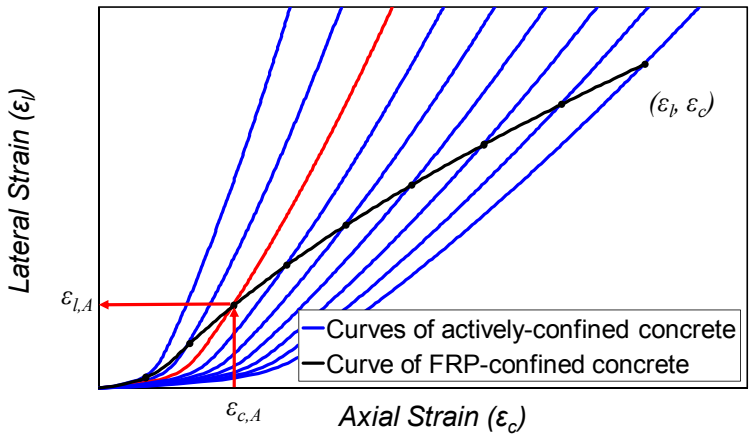

(b)

Figure 6. Determination of stress-strain curves of FRP-confined concrete by analysis-oriented models: (a) axial stress-strain curves; (b) lateral strain-axial strain curves

3.2.1 *Axial stress-strain curves for actively confined concrete*

The prediction of stress-strain curves of actively confined concrete requires a stress-strain equation together with a set of equations to predict the peak stress (f'^{*}_{cc}) and the corresponding strain (ε^{*}_{cc}) of confined concrete. The majority of the existing analysis-oriented models adopted the stress-strain model proposed by Popovics [34] (Eq. 17), to determine the shape of the actively confined concrete base curves [3, 7, 11, 62, 64, 66-70]. Popovics' [34] model describes the stress-strain curve of concrete through an energy balance approach as:

$$f_c = \frac{f'^{*}_{cc}\left(\varepsilon_c / \varepsilon^{*}_{cc}\right) r}{r - 1 + \left(\varepsilon_c / \varepsilon^{*}_{cc}\right)^{r}} \tag{17}$$

where the constant r accounts for the brittleness of concrete and was originally given in the model as $r = 0.0004 f'^{*}_{cc} + 1$. All the models reviewed in this study that adopted the original or modified version of Popovics' [34] model determined this constant by an expression given by Carreira and Chu [71] as:

$$r = \frac{E_c}{E_c - f'^{*}_{cc} / \varepsilon^{*}_{cc}} \tag{18}$$

For the models that modified the original version of Popovics' [34] stress-strain curve [72, 73], the modified parts of the model expressions are presented in Table 2. It should be noted that the expression for E_c, given by ACI 318-95 [50] as $E_c = 4730\sqrt{f'_{co}}$, was used by most of the reviewed models to determine the initial elastic modulus of concrete. For the models that recommended different expressions for the determination of E_c, these expressions are given in Table 2.

3.2.2 *Peak stress and strain expressions for actively confined concrete*

The expressions used by each analysis oriented model to determine the peak stress and corresponding strain on the stress-strain curve of actively confined concrete are shown in Table 2. The most commonly used peak stress (f'^{*}_{cc}) expression was the one given by Mander at al. [6] (Eq. 19). This expression was based on the general expression proposed by Willam and Warnke [74] and was calibrated using the test results of hydrostatically confined concrete specimens tested by Elwi and Murray [75].

$$f'^{*}_{cc} = f'_{co}\left(2.254\sqrt{1+\frac{7.94 f^{*}_{l}}{f'_{co}}} - 2\frac{f^{*}_{l}}{f'_{co}} - 1.254\right) \tag{19}$$

The most commonly used expression for the prediction of the axial strain (ε^{*}_{cc}) at peak stress was the one originally proposed by Richart et al. [4]:

$$\varepsilon^{*}_{cc} = 5\varepsilon_{co}\left(\frac{f'^{*}_{cc}}{f'_{co}} - 0.8\right) \tag{20}$$

3.2.3 *Dilation behavior of FRP-confined concrete*

In analysis-oriented models, the lateral-to-axial strain relationship (i.e. dilation behavior) of FRP-confined concrete provides the essential link between the response of the concrete core and the passive confinement of the FRP shell. The existing analysis-oriented models either used explicitly derived relationships (i.e.[45, 62, 72, 76]) or they gave them implicitly (i.e. [11, 64, 67-70, 73, 77]), in majority of the models, through the modification of the expressions originally given by actively confined concrete models. Most of the explicit models are capable of accurately capturing the dilation behavior of FRP-confined concrete in the final stage of the behavior, where the rapid expansion of concrete is stabilized by the FRP confinement, and lateral-to-axial strain ratio asymptotically approaches to a constant value. Accurate prediction of the dilation behavior within this region is highly important for the overall accuracy of the dilation model. The majority of the implicit models, on the other hand, are unable to capture the dilation behavior in this region, as they often predict a dilation behavior that resembles the ones observed in actively confined or steel-confined concrete, where the concrete dilation continues at an increasing rate until the eventual failure. Different expressions proposed for the dilation behavior of FRP-confined concrete are summarized in

Table 2. It may be worthwhile to note that in addition to the analysis-oriented models discussed in this section, some of the design-oriented models also gave expressions for the prediction of the dilation ratio of FRP-confined concrete at ultimate [16, 54, 55, 78-80]. These expressions are included in Table 1.

3.3 Models based on other approaches

In addition to the design- and analysis-oriented models reviewed in this paper, a few other FRP-confined concrete models were developed using a number of different approaches. For completeness, these models are summarized briefly in this section. The model developed by Harmon et al. [81] was based on the concept of crack slip and separation in the concrete. In this model, the relationship between lateral strain and axial strain was not given explicitly but defined as a function of the crack slip-separation path. The analytical models developed by Karabinis and Rousakis [82] and Rousakis et al. [83] were based on plasticity approach, which involved numerical integration. In these models, concrete is assumed to behave as an elastoplastic material following the Drucker-Prager yield criterion. The Drucker-Prager criterion was also employed by models proposed by Eid et al. [84] and Eid and Paultre [85]. Becque et al. [86] modified Gerstle's [87, 88] octahedral stress-strain models by adopting Samaan's [8] expression for ultimate strength to define the failure surface of FRP-confined concrete. The damage-based model developed by Moran and Pantelides [89] was based on the extent of internal damage in the confined concrete core. In addition, a number of finite element-based models were developed such as those proposed by Rochette and Labossiére [90], Mirmiran et al. [91], Parent and Labossiére [92], Yu et al. [93, 94], Cho and Kwon [95], Csuka and Kollár [96], Dandapat et al. [97] and Jiang et al. [98].

4. EXPERIMENTAL TEST DATABASE USED IN THE MODEL ASSESSMENT

In this paper a carefully prepared test database of FRP-confined concrete cylinders tested under monotonic axial compression is used for model assessment. The database was assembled through an extensive review of the literature that covered 2038 test results from 202 experimental studies. The suitability of these results for the database was then assessed using a set of carefully established selection criteria to ensure the reliability and consistency of the database. Only monotonically loaded circular specimens with unidirectional fibers orientated in the hoop direction and an aspect ratio (H/D) less than 3 were included in the assessment database. Specimens containing internal steel reinforcement, partial FRP confinement or specimens with unconfined concrete compressive strengths greater than 55 MPa were not included. This resulted in a final database size of 730 datasets collected from 92 experimental studies published between 1992 and the end of 2011.

The database used in the model assessment was sorted into eight groups based on two main confinement parameters; that is, confinement technique (wraps or tubes) and type of FRP material (Carbon FRP (CFRP), S- or E-Glass FRP (GFRP), Aramid FRP (AFRP), or High-modulus Carbon FRP (HM CFRP)). 653 specimens in the database were FRP-wrapped, whereas 77 specimens were confined by FRP tubes. 422 of the specimens were confined by CFRP, 198 by GFRP, 58 by AFRP and 52 by HM CFRP. The diameters of the specimens (D) included in the test database varied between 47 and 600 mm, with the majority of the

specimens having a diameter of 150 mm. The unconfined concrete strength (f'_{co}) and strain (ε_{co}), as obtained from concrete cylinder tests, varied from 6.2 to 55.2 MPa and 0.14% to 0.63%, respectively. The actual confinement ratio, defined as the ratio of the actual ultimate confining pressure to the unconfined concrete strength ($f_{lu,a}/f'_{co}$), varied from 0.02 to 4.86. It should be noted that not all the datasets included in the database contained all the relevant details required for model assessment. As a result, out of the 730 datasets, 705 were used in the assessment of the strength enhancement ratios and 527 in the assessment of the strain enhancement ratios.

5. ASSESSMENT OF FRP-CONFINED CONCRETE STRESS-STRAIN MODELS

5.1. Summary of the assessed models

The experimental test database, described in Section 4, was used in the performance assessment of the stress-strain models reviewed in the Sections 3.1 and 3.2. The list of the design- and analysis-oriented models included in the assessment is given in Tables 3 and 4, respectively, together with the results of the statistical analysis conducted to assess the performance of these models. Additional details of each of these models can be found in Tables 1 and 2. As mentioned previously, 59 of the reviewed models were classified as design-oriented models, 13 as analysis-oriented models, and the remaining 16 as 'models based on other approaches'. All of the design-oriented and analysis-oriented models that had sufficiently defined parameters to allow numerical calculations were used in the assessment. This led to an assessment study that consisted of 68 of the 88 reviewed models.

5.2. Procedures used in model assessment

In this section the key assumptions made and approaches used in the assessment of the models are briefly discussed. In the present study, the model performances are evaluated based on their predictions of the strength enhancement ratios $(f'_{cc}/f'_{co})_{model}$ and strain enhancement ratios $(\varepsilon_{cu}/\varepsilon_{co})_{model}$. Each model was assessed against all the test results included in the database, unless the model specified specific limitations for certain test parameters. In which case, the specimens that satisfied the criteria given by the model were used in the assessment of the corresponding model. The number of specimens used in the assessment of each model is reported in Tables 3 and 4. Details of the limitations and defined parametric ranges of the models are further discussed in Section 5.3.3. It is worthwhile to note that some of the specimen details that were required by the models were not always provided in the publications that reported the results included in the database. These omitted details included the unconfined concrete strain at peak stress (ε_{co}), elastic modulus of concrete (E_c), and hoop rupture strain of FRP shell ($\varepsilon_{h,rup}$). If such details were not provided in the source document, in the present study they were predicted using the approaches outlined in the following sections.

5.2.1. Properties of unconfined concrete

The unconfined concrete strengths (f'_{co}) given in the database were obtained from cylinder test results reported in the original studies, and they were employed directly in the model assessment. On the other hand, it was not possible to directly use the strains corresponding to the strength of unconfined concrete (ε_{co}) in the model assessment, due to problems with availability and/or reliability of these results. Reported values of ε_{co} varied significantly from one study to another even for the same unconfined concrete strengths, pointing to potential difficulties experienced with experimental determination of these values. To ensure uniformity and consistency among the test results used in the model assessment, in the present study unconfined concrete strains (ε_{co}) used in the model assessment were calculated by Eq. 21 proposed by Tasdemir et al. [99].

$$\varepsilon_{co} = \left(-0.067 f'^{2}_{co} + 29.9 f'_{co} + 1053\right) \times 10^{-6} \tag{21}$$

If an expression was not specified in the original publication, the elastic modulus of the unconfined concrete (E_c) was computed based on the expression given by ACI 318-95 [50] (Eq. 22).

$$E_c = 4730\sqrt{f'_{co}} \tag{22}$$

5.2.2. FRP confinement pressure

Of the 68 assessed models, 45 of them employed the nominal ultimate confining pressure (f_{lu}) in their predictions of the ultimate conditions of FRP-confined concrete. However, as explained previously in Section 2 it is now well understood that a strain reduction factor k_ε is required to accurately determine the actual confining pressure at ultimate ($f_{lu,a.}$). The average fiber strain reduction factor ($k_{\varepsilon,f}$) and FRP strain reduction factor ($k_{\varepsilon,frp}$) were calculated as 0.641 and 0.685 from the experimental test database, respectively. In the model assessment, for the datasets that did not include $\varepsilon_{h,rup}$ data or contained k_ε values that differed significantly from the rest of the results, average k_ε values of 0.641 or 0.685 were used to calculate the corresponding hoop rupture strain ($\varepsilon_{h,rup}$) of the FRP shell, based either on the ultimate tensile strain of the fibers (ε_f) or the FRP (ε_{frp}), respectively. When both fiber and FRP properties were available, unless otherwise specified by the model, the fiber properties were used for the determination of the actual confinement pressures ($f_{lu,a}$). It should be noted that, as shown in the last columns of Tables 1 and 2, some of the assessed models recommended certain k_ε values to be used in the absence of experimentally recorded $\varepsilon_{h,rup}$ data. In the present study, the k_ε values recommended by these models were not employed in the model assessment, and the average k_ε values determined from the database were used for all the models in predicting the ultimate conditions of the datasets for which $\varepsilon_{h,rup}$ values were not reported.

Table 3. Design-oriented model predictions of ultimate conditions of FRP-confined concrete

No.	Model	Prediction of f'_{cc}/f'_{co}					Prediction of $\varepsilon_{cu}/\varepsilon_{co}$				
		Number of test data	Mean Square Error	Average Absolute Error	Linear Trend Slope	Standard Deviation	Number of test data	Mean Square Error	Average Absolute Error	Linear Trend Slope	Standard Deviation
1	Fardis and Khalili 1 [1]	705	1.530	0.412	1.465	0.268	527	35.872	0.514	0.850	1.031
	Fardis and Khalili 2 [1]	705	1.033	0.417	1.392	0.234					
2	Saadatmanesh et al. [3]	705	0.474	0.327	1.126	0.243	527	17.873	0.411	0.794	0.565
3	Mirmiran [113]	705	0.499	0.200	0.731	0.187	-	-	-	-	-
4	Karbhari and Gao 1 [39]	705	0.618	0.244	0.675	0.154	527	48.217	0.575	0.342	0.183
	Karbhari and Gao 2 [39]	705	0.220	0.145	0.843	0.155					
5	Miyauchi et al. [9]	637	0.830	0.292	1.312	0.230	480	20.472	0.350	0.695	0.508
6	Jolly and Lillistone [42]	705	0.927	0.241	1.195	0.384	-	-	-	-	-
7	Kono et al. [61]	91	0.094	0.106	0.939	0.137	74	13.477	0.340	0.607	0.188
8	Samaan et al. [8]	705	0.160	0.168	1.037	0.189	527	48.202	1.082	1.229	1.022
9	Miyauchi et al. [41]	705	0.373	0.208	1.176	0.199	527	15.523	0.439	0.841	0.597
10	Saafi et al. [10]	76	0.180	0.202	1.055	0.224	55	113.064	0.827	1.805	0.515
11	Spoelstra and Monti 1 [11]	705	0.157	0.150	0.990	0.178	527	101.283	1.194	1.694	1.057
12	Toutanji [52]	629	0.789	0.367	1.334	0.214	472	67.923	0.844	1.520	0.845
13	Jolly and Lillistone [43]	705	0.609	0.210	1.127	0.337	-	-	-	-	-
14	Thériault and Neale [132]	705	0.137	0.129	0.924	0.159	-	-	-	-	-
15	Xiao and Wu [16]	407	0.169	0.109	1.052	0.144	288	17.040	0.386	1.187	0.494
16	Lin and Chen [111]	705	0.137	0.129	0.924	0.159	-	-	-	-	-
17	Ilki et al. [100]	383	0.101	0.105	0.899	0.133	266	12.607	0.380	0.962	0.477
18	Lam and Teng [115]	705	0.137	0.129	0.924	0.159	-	-	-	-	-
19	Moran and Pantelides [45]	705	1.415	0.385	1.430	0.274	527	87.024	1.186	1.727	0.853
20	Shehata et al. [116]	705	0.137	0.129	0.924	0.159	527	49.257	0.731	1.127	1.006
21	De Lorenzis and Tepfers [13]	Nominated the ultimate strength expressions by Samaan et al. [8], Toutanji [52], and Spoelstra and Monti [11]					527	23.569	0.336	0.580	0.377
22	Lam and Teng [12]	705	0.118	0.127	0.975	0.162	472	13.508	0.376	1.064	0.501
23	Li et al. [35]	407	0.171	0.140	1.088	0.153	288	35.967	0.500	0.406	0.189
24	Xiao and Wu [54]	705	0.201	0.147	1.056	0.190	527	18.428	0.388	1.141	0.509
25	Ilki et al. [53]	383	0.380	0.209	0.771	0.119	266	23.284	0.688	1.113	0.640
26	Bisby et al. 1 [14]	705	0.151	0.142	1.034	0.173	480	28.173	0.416	0.689	0.464
	Bisby et al. 2 [14]	705	0.123	0.138	0.991	0.170					
	Bisby et al. 3 [14]	705	0.120	0.134	0.979	0.169					
27	Saiidi et al. [56]	407	0.180	0.135	0.892	0.164	286	58.112	0.791	1.513	0.769
28	Berthet et al. [55]	670	0.118	0.132	0.993	0.166	517	11.984	0.294	0.756	0.379
29	Guralnick and Gunawan [102]	657	0.201	0.145	0.849	0.166	-	-	-	-	-
30	Jiang and Teng [46]	705	0.141	0.129	0.920	0.141	527	10.835	0.358	0.982	0.491
31	Matthys et al. [22]	705	0.158	0.176	1.069	0.181	-	-	-	-	-
32	Tamuzs et al. [79]	705	0.260	0.179	1.129	0.185	-	-	-	-	-
	Tamuzs et al. [80]	-	-	-	-	-	527	9.470	0.318	0.872	0.442
33	Wu et al. [59]	574	0.365	0.184	1.104	0.237	322	59.232	0.541	0.987	0.823
34	Al-Tersawy et al. [119]	705	0.339	0.164	0.789	0.169	527	30.522	0.369	0.541	0.481
35	Ciupala et al. [101]	605	0.429	0.297	1.211	0.208	439	14.790	0.442	0.885	0.544
36	Shehata et al. [110]	705	0.146	0.140	1.027	0.172	527	55.145	0.775	1.183	1.040

37	Tabbara and Karam [120]	705	0.280	0.175	0.802	0.136	-	-	-	-	-
38	Vintzileou and Panagiotidou [105]	705	0.156	0.133	0.889	0.154	439	18.960	0.326	0.955	0.392
39	Yan and Pantelides [47]	705	0.226	0.202	0.972	0.237	-	-	-	-	-
40	Youssef et al. [27]	705	0.229	0.145	0.973	0.171	527	13.719	0.345	1.071	0.465
41	Binici [60]	705	0.652	0.379	1.116	0.382	Same as Lam and Teng [12]				
42	Al-Salloum and Siddiqui [121]	705	0.134	0.134	1.005	0.169	-	-	-	-	-
43	Girgin et al. [106]	696	0.119	0.132	0.981	0.167	-	-	-	-	-
44	Teng et al. [48]	Same as Jiang and Teng [46]					527	10.981	0.367	0.990	0.497
45	Wu and Wang [63]	705	0.124	0.133	0.988	0.167	-	-	-	-	-
46	Wu et al. [57]	53	0.347	0.152	1.182	0.161	41	38.467	0.342	0.516	0.312
47	Benzaid et al. [123]	705	0.311	0.174	0.787	0.150	527	40.187	0.434	0.410	0.279
48	Fahmy and Wu [49]	705	0.217	0.149	0.866	0.179	527	16.770	0.353	0.732	0.472
49	Mohamed and Masmoudi [103]	74	0.141	0.145	0.915	0.188	-	-	-	-	-
50	Wu and Wang [58]	53	0.475	0.177	1.230	0.171	Same as Wu et al. [57]				
51	Wu and Zhou [124]	705	0.122	0.132	0.993	0.167	-	-	-	-	-
52	Cevik 1 [125]	705	4.225	0.564	1.671	0.474	-	-	-	-	-
	Cevik 2 [125]	705	2.452	0.233	0.767	0.387	-	-	-	-	-
53	Park et al. [126]	705	0.682	0.216	1.239	0.247	-	-	-	-	-
54	Realfonso and Napoli 1 [127]	705	0.152	0.171	1.063	0.179	-	-	-	-	-
	Realfonso and Napoli 2 [127]	705	0.132	0.136	1.021	0.168	-	-	-	-	-
55	Wang and Wu [128]	51	1.096	0.371	1.436	0.315	-	-	-	-	-
56	Yu and Teng [129]	76	0.147	0.135	0.897	0.161	55	6.493	0.233	0.836	0.356
	Average values of all design-oriented models	-	0.337	0.186	1.020	0.189	-	34.704	0.530	0.964	0.571

Table 4. Analysis-oriented model predictions of ultimate conditions of FRP-confined concrete

No.	Model	Prediction of f'_{cc}/f'_{co}					Prediction of $\varepsilon_{cu}/\varepsilon_{co}$				
		Number of test data	Mean Square Error	Average Absolute Error	Linear Trend Slope	Standard Deviation	Number of test data	Mean Square Error	Average Absolute Error	Linear Trend Slope	Standard Deviation
1	Mirmiran and Shahawy [107]	705	0.216	0.203	0.992	0.224	527	37.430	0.501	0.469	0.232
2	Spoelstra and Monti 2 [11]	705	0.356	0.252	1.055	0.220	527	336.266	2.104	2.390	1.623
3	Fam and Rizkalla [67]	705	0.305	0.212	1.055	0.204	527	367.224	2.877	1.937	2.935
4	Chun and Park [68]	371	0.245	0.217	1.027	0.208	260	2685.72	3.322	4.647	3.305
5	Harries and Kharel [72]	705	0.703	0.242	0.663	0.185	439	2079.67	0.822	0.708	5.464
6	Marques et al. [69]	705	0.980	0.332	1.364	0.236	527	244.999	1.916	2.003	1.730
7	Binici [73]	705	0.163	0.184	1.060	0.184	527	16.405	0.322	0.714	0.423
8	Albanesi et al. [77]	582	0.297	0.272	1.217	0.207	449	9.394	0.372	0.866	0.517
9	Jiang and Teng [66]	705	0.130	0.129	0.962	0.154	Same as Teng et al. [62]				
10	Teng et al. [62]	705	0.116	0.121	0.987	0.154	527	11.689	0.368	1.030	0.499
11	Aire et al. [70]	705	0.401	0.288	1.102	0.220	527	16.185	0.370	0.842	0.535
12	Xiao et al. [64]	705	0.469	0.209	0.721	0.140	Same as Teng et al. [62]				
	Average values of all analysis-oriented models	-	0.365	0.222	1.017	0.195	-	580.499	1.297	1.561	1.726

5.2.3. Models with limited applicability

Some of the reviewed models were specified to be applicable only within certain parametric ranges. These parameters include: method of confinement (i.e. wraps or tubes), type of FRP material (i.e. CFRP, GFRP, AFRP, or HM CFRP), and unconfined concrete strength (f'_{co}). In the present study, wherever applicable, the parametric ranges of the models were clearly established and the model assessment was performed giving due consideration to these model specifications. The applicability limitations and parametric ranges of each assessed model are specified in Tables 1 and 2. As shown in these tables some models are only applicable to certain types of FRP materials or confinement techniques (e.g. [10, 16, 35, 52, 53, 56-58, 61, 68, 100, 101]), to certain unconfined concrete strength ranges (f'_{co}) (e.g. [9, 61, 102, 103]), and/or to certain confinement ratio ranges ($f_{lu,a}/f'_{co}$) (e.g. [77]). There were also a group of models that specified certain parametric coefficients to account for the differences in the types of FRP material, concrete strength and/or confinement techniques (e.g. [14, 45, 49, 55, 59, 104-106]). Specified limitations of the models resulted in a reduction in the number of datasets available for the assessment of some of the models. The number of the datasets used in the assessment of each model is reported in the Tables 3 and 4.

5.2.4. Confinement models for actively confined concrete

The analysis-oriented models used in the model assessment typically supplied strength and strain enhancement ratios to determine the peak stress point (ε^*_{cc} and f'^*_{cc}) on the stress-strain curve of actively confined concrete, as discussed in detail in Section 3.2. The assessment of the models used to determine these points was not within the scope of the study reported herein. Only those analysis-oriented models that supplied adequate information to allow determination of the ultimate condition of FRP-confined concrete (ε_{cu} and f'_{cc}) were included in this assessment. This information was provided by the models in the form of: expressions for ε^*_{cc} and f'^*_{cc}, a stress-strain relationship for actively confined concrete, and a dilation relationship for FRP-confined concrete that is applicable at ultimate conditions. The analysis-oriented model by Moran and Pantelides [45] did not provide sufficient information to allow determination of the ultimate axial strength and strain of FRP-confined concrete, hence, it was not included in the model assessment.

6. PERFORMANCE OF EXISTING DESIGN- AND ANALYSIS-ORIENTED MODELS

In the present study, the model performances, established in terms of accuracy and consistency were quantified using four statistical indicators: the mean square error (*MSE*), the average absolute error (*AAE*), the linear trend slope (*LTS*) and the standard deviation (*SD*). The two statistical indicators used to establish overall model accuracy were the mean square error (*MSE*) and average absolute error (*AAE*), defined by Eqs. 23 and 24 respectively. The linear trend slope (*LTS*), determined by a regression analysis, was used to describe the associated average overestimation or underestimation of the model, where an overestimation is represented by a linear trend slope greater than 1. The standard deviation (*SD*), determined by Eq. 25*,* is used to establish the magnitude of the associated scatter for each model. Tables 3 and 4 present the statistical summary of design-oriented and analysis-oriented model performances, respectively.

$$AAE = \frac{\sum_{i=1}^{n} \left| \frac{\text{mod}_i - \text{exp}_i}{\text{exp}_i} \right|}{N} \tag{23}$$

$$MSE = \frac{\sum_{i=1}^{n} (\text{mod}_i - \text{exp}_i)^2}{N} \tag{24}$$

$$SD = \sqrt{\frac{\sum_{i=1}^{n} \left(\frac{\text{mod}_i}{\text{exp}_i} - \frac{\text{mod}_{avg}}{\text{exp}_{avg}} \right)^2}{N-1}} \tag{25}$$

where *mod* is the model prediction, *exp* is the experimental value, *N* is the total number of datasets and *avg* is the sample average.

The reliability of model predictions depends on the size and completeness of the database used in model development. The statistical summaries of model performances presented in Tables 3 and 4 illustrate that the ultimate condition expressions of the design-oriented models that were calibrated from relatively small test databases of FRP-confined concrete (e.g. [1, 9, 52]) and those that were based on active/steel-confined concrete (e.g. [3, 11, 68]) performed relatively poorly in comparison to the rest of the assessed models. The results further indicate that the analysis-oriented models that were based on implicitly derived dilation behaviors (e.g. [11, 67, 68]) performed significantly worse than those that were based on explicitly derived dilation relationships of FRP-confined concrete (e.g. [62, 78, 107]).

Among all of the assessed models in Tables 3 and 4, the best performing models were determined among the models that were capable of being applied to the complete dataset in terms of their *MSE* and *AAE* values. Considering these factors, the top performing strength enhancement models were found to be those proposed by Lam and Teng [12], Bisby et al. 3 [14] and Teng et al. [62], for each of which *MSE* and *AAE* values were less than 0.120 and 0.134, respectively. The best performing strain enhancement models were determined to be the ones proposed by Tamuzs et al. [80], Jiang and Teng [46] and Teng et al. [48], which each had *MSE* and *AAE* values below 10.981 and 0.367 respectively. Among the aforementioned models, the model proposed by Teng et al. [62] is an analysis-oriented model, whereas the remaining models are design-oriented ones.

7. IMPORTANT FACTORS INFLUENCING MODEL PERFORMANCE

7.1. The type of model

As evident from the average values of the statistical indicators given in Tables 3 and 4, among the two model categories, the design-oriented models generally performed better than the analysis-oriented models in predicting the ultimate strength enhancement and strain enhancement ratios. The average values of *MSE* and *AAE* for the design oriented models were found to be lower, with the difference becoming more significant in the prediction of the strain enhancement ratios. The better performance of the design-oriented models can be

explained by the fact that most of these design-oriented models were calibrated from test databases of FRP-confined concrete that enabled them to directly interpret the important parametric influences on the behavior of FRP-confined concrete. On the other hand, the analysis-oriented models often adopted expressions from other models, such as active/steel-confined concrete models to describe the dilation behavior of FRP-confined concrete. The results of the model assessment indicate that these implicitly adopted expressions do not accurately describe the behavior of FRP-confined concrete. A similar observation was reported previously by Jiang and Teng [62]. It should be noted, however, that the analysis-oriented models that used explicitly derived dilation relationships for FRP-confined concrete (e.g. [62, 107]) performed much better than their aforementioned counterparts, with model performances rivaling the best performing design-oriented models.

7.2. The forms of model expressions

The model expressions proposed for the ultimate strength enhancement (f'_{cc}/f'_{co}) and strain enhancement ($\varepsilon_{cu}/\varepsilon_{co}$) ratios were given either as a linear (e.g. [4, 41, 42]) or a nonlinear function (e.g. [6, 8, 109]) of the nominal or actual confinement ratios (i.e. f_{lu}/f'_{co} or f_{lua}/f'_{co}). The results of the model assessment indicate that some of the better performing ultimate strength enhancement expressions had linear forms (e.g. [12, 46, 110]). On the other hand, as indicated by the results of the model assessment, almost all of the better performing ultimate strain enhancement expressions had non-linear forms (e.g. [46, 55, 80]). This is due to the dependency of the ultimate strain enhancement ratio ($\varepsilon_{cu}/\varepsilon_{co}$) to the ultimate tensile strain of the FRP material (ε_{frp}) in addition to the confinement ratio (f_{lu}/f'_{co}), as was pointed out in a number of previous studies (e.g. [12, 20, 39, 111]). Furthermore, the results indicate that the models that make use of the hoop rupture strains ($\varepsilon_{h,rup}$) (e.g. [46, 47, 79]), in general, perform better than the models that directly use the ultimate tensile strain of fibers (ε_f) (e.g. [9, 11, 61]). This performance difference becomes particularly significant in the prediction of the ultimate strain enhancement ratios, with most of the better performing models employing strain efficiency factors (k_ε) implicitly or explicitly in their expressions.

8. CONCLUSIONS

In the past two decades, a great deal of research effort has been devoted to the understanding of the axial compressive behavior of FRP-confined concrete. As a result, 88 models have been developed to predict the behavior of FRP-confined concrete in circular sections. This paper has presented a comprehensive review and systematic assessment of the existing models, where the models have been reviewed and classified into appropriate categories. Each model's key features have been summarized, its theoretical basis has been discussed and any relationship between the model and other models are identified.

A systematic performance assessment for the 68 reviewed models is then presented. Based on this study, the following observations and conclusions can be drawn:

1. In the predictions of ultimate conditions, in general, the design-oriented models perform better than analysis-oriented models. Furthermore, in general, the performance of the design-oriented models increase with the size of the database used in their

development and the analysis-oriented models with explicitly derived dilation relationships perform better than those with implicitly adopted dilation relationships.

2. Of the 68 FRP-confined concrete stress-strain models assessed, those by Lam and Teng [12] and Tamuzs et al. [80] are the most accurate for the predictions of the ultimate strength and strain enhancement ratios, respectively. Both models are design-oriented.
3. The common modeling issues that compromises model accuracies include: the use of relatively small test databases in the development of design-oriented models (e.g. [1, 9, 52]) and the use of implicitly determined dilation relationships in the development of analysis-oriented models (e.g. [11, 67, 68]).
4. Accuracy of the models that make use of the hoop rupture strains ($\varepsilon_{h,rup}$) are, in general, significantly higher than the models that directly use the ultimate tensile strain of fibers (ε_f). The performance difference between these models is particularly in the prediction of the ultimate strain enhancement ratios, and most of the better performing models employ rupture strain efficiency factors (k_ε) in their expressions.
5. Through the analysis of the results in the database, the average values of the hoop strain reduction factors based on fiber and FRP properties ($k_{\varepsilon,f}$ and $k_{\varepsilon,frp}$) are determined as 0.641 and 0.685, respectively. The observed variation of the average k_ε values with fiber type points to the possible influence of the type of fibers on the strain reduction factor.
6. The model prediction errors associated with the prediction of ultimate axial strains (ε_{cu}) are significantly larger than those of ultimate strengths (f'_{cu}). These higher prediction errors are partly caused by the sensitivity of the ultimate strains to the type of FRP used as confinement, and the inability of the majority of the models to accurately predict this influence.

There is no doubt that the great number of studies conducted in the past two decades has led to a good understanding of the behavior of FRP-confined normal-strength concrete in circular sections. However, there are still a number of areas where further research is required. One such area involves the study of the influence of the type of FRP on the ultimate conditions of FRP-confined concrete and on the strain reduction factor (k_ε) of the FRP jacket.

The model assessment that has been presented herein clearly indicates the important influence of the size and reliability of the test databases used in the model development on the overall performance of the models, especially for the design-oriented models. Therefore, it is recommended that a carefully chosen selection criteria is applied in the future database development efforts. Although the analysis-oriented models with explicitly derived dilation relationships (e.g. [62, 107]) perform reasonably well, in the future, accuracies of these models can be further improved through better modeling of the lateral-to-axial strain behavior of FRP-confined concrete. Furthermore, in future analysis-oriented model development efforts, due attention should be given to the implications of the path dependency assumption discussed in detail in Section 3.2.

NOMENCLATURE

AAE Average Absolute Error
A_i Parameter in model proposed by Sargin [51]
A_j Parameter in model proposed by Toutanji [52]
c_1 Constant in the strength enhancement expression (Eq.15)
c_2 Constant in the strain enhancement expression (Eq.16)
C_j Parameter in model proposed by Toutanji [52]
D Diameter of concrete core (*mm*)
D_i Parameter in model proposed by Sargin [51]
D_j Parameter in model proposed by Toutanji [52]
E'_{c2} Tangent slope of the second branch of axial stress-strain curve at f'_{c1} (*MPa*)
E_c Elastic modulus of unconfined concrete (*MPa*)
E_{c1} Initial slope of axial stress-strain curve of FRP-confined concrete (*MPa*)
E_{c2} Slope of the second branch of axial stress-strain curve of FRP-confined concrete (*MPa*)
E_{co} Secant elastic modulus of unconfined concrete at f'_{co} (*MPa*)
$E_{c,ch}$ Variable strain-hardening secant modulus in model proposed by Moran and Pantelides [45]
$E_{c,cs}$ Variable strain-softening secant modulus in model proposed by Moran and Pantelides [45]
E_{des} Deterioration rate of FRP-confined concrete in model proposed by Li et al. [35]
E^{eff} Effective modulus of composite in model proposed by Karbhari and Gao [39]
E_f Elastic modulus of fibers (*MPa*)
E_{frp} Elastic modulus of FRP material (*MPa*)
E_l Lateral confinement stiffness (*MPa*); $E_l = 2E_f t_f/D$ or $2\,E_{frp}t_{frp}/D$
E_p Second branch slope of axial stress-strain curve of FRP-confined concrete in Jolly and Lillistone [42]
$E_{\theta 2}$ Second branch slope of axial stress-lateral strain curve of FRP-confined concrete in Berthet et al. [55]
f'_{c1} Axial compressive stress of FRP-confined concrete at first peak (*MPa*)
f'_{cc} Peak axial compressive stress of FRP-confined concrete (*MPa*)
f'^{*}_{cc} Peak axial compressive stress of actively confined concrete (*MPa*)
f'_{co} Peak axial compressive stress of unconfined concrete (*MPa*)
f'_{cu} Axial compressive stress of FRP-confined concrete at ε_{cu} (*MPa*)
f_c Axial compressive stress of concrete (*MPa*)
$f_{c,e}$ Axial compressive stress at elastic limit in model proposed by Binici [73] (*MPa*)
$f_{c,res}$ Residual stress in model proposed by Binici [73] (*MPa*)
f_f Ultimate tensile strength of fibers; $f_f = E_f\varepsilon_f$ (*MPa*)
f_{frp} Ultimate tensile strength of FRP material; $f_{frp} = E_{frp}\varepsilon_{frp}$ (*MPa*)
$f_{c,A}$ Axial compressive stress of concrete at $\varepsilon_{c,A}$ (*MPa*)
f_l Lateral confining pressure (*MPa*)
f_{l^*} Lateral confining pressure of actively confined concrete (*MPa*)
f_{lu} Nominal lateral confining pressure at ultimate; $f_{lu} = E_l\varepsilon_f$ or $f_{lu} = E_l\varepsilon_{frp}$ (*MPa*)
$f_{lu,a}$ Actual lateral confining pressure at ultimate; $f_{lu,a} = E_l\varepsilon_{h,rup}$ (*MPa*)

f_o Intercept stress at the stress axis of axial stress-strain curve (*MPa*)
g Parameter in model proposed by Demers and Neale [36]
H FRP confined concrete specimen height (mm)
k Parameter in model proposed by Harries and Kharel [72]
k_1 Axial strength enhancement coefficient
k_2 Axial strain enhancement coefficient
k_3 Parameter in model proposed by Razvi and Saatcioglu [112]
k_4 Parameter in model proposed by Wu et al. [59]
k_5 Parameter in model proposed by Girgin [106]
k_ε Hoop strain reduction factor
$k_{\varepsilon,f}$ Hoop strain reduction factor of fibers
$k_{\varepsilon,frp}$ Hoop strain reduction factor of FRP material
k_{e1} FRP effectiveness factor in model proposed by Miyauchi [9]
LTS Linear Trend Slope
M Sample mean
MSE Mean Square Error
m Parameter in model proposed by Youssef et al. [27]
m_1 parameter in model proposed by Fahmy and Wu [49]
m_2 parameter in model proposed by Fahmy and Wu [49]
N Number of data in sample
n Constant in model proposed by Richard and Abbott [44]
n_{frp} Number of fiber sheets in FRP shell
r Concrete brittleness constant in model proposed by Popovics [34]
SD Standard deviation
t_f Total nominal thickness fibers (*mm*)
t_{frp} Total thickness of FRP material (*mm*)
α Reciprocal of secant axial modulus softening rate; $\alpha = 1/\beta$
α_1 Parameter in model proposed by Binici [73]
β Secant axial modulus softening rate
β_1 Parameter in model proposed by Yan and Pantelides [47]
β_2 Parameter in model proposed by Binici [73]
γ_{frp} Parameter in model proposed by Vintzileou and Panagiotidou [105]
γ_m Material strength reduction factor in model proposed by Jolly and Lillistone [42]
ε^*_{cc} Axial strain of actively confined concrete at f'^*_{cc}
ε_c Axial strain of concrete
$\varepsilon_{c,A}$ Axial strain of concrete at $\varepsilon_{l,A}$
$\varepsilon_{c,cr}$ Axial strain of concrete at concrete cracking
$\varepsilon_{c,e}$ Axial strain at elastic limit in model proposed by Binici [73]
$\varepsilon_{c,vo}$ Axial strain of concrete at zero volumetric strain
ε_{c1} Axial strain of FRP-confined concrete at f'_{c1}
$\varepsilon_{c,\lambda}$ Axial strain of FRP-confined concrete at the first peak in model proposed by Miyauchi et al. [41]
ε_{co} Axial strain of unconfined concrete at f'_{co}
$\varepsilon_{co,i}$ Axial strain of unconfined concrete in model proposed by Ahmad et al. [2]

$\varepsilon_{co,u}$ Ultimate axial strain of unconfined concrete in model proposed by Wu et al. [59]

ε_{cu} Ultimate axial strain of FRP-confined concrete

ε_f Ultimate tensile strain of fibers

ε_{frp} Ultimate tensile strain of FRP material

$\varepsilon_{h,rup}$ Hoop rupture strain of FRP shell

ε_l Lateral strain of concrete

ε_{lo} Lateral strain of concrete at axial strain ε_{co}

$\varepsilon_{l,A}$ Lateral strain of concrete at axial strain $\varepsilon_{c,A}$

$\varepsilon_{l,vo}$ Lateral strain of concrete at zero volumetric strain

ε_{l1} Lateral strain of concrete at f'_{c1}

ε_o Intercept strain of the axial strain axis of axial strain-lateral strain curve in Xiao and Wu [16, 54]

ε_u Axial strain in the post-peak descending branch of stress-strain curve of FRP-confined concrete corresponding to 50% of the peak strength, in model proposed by Li et al. [35]

γ_c Density of concrete

λ Parameter in model proposed by Miyauchi et al. [41]

μ Lateral-to-axial strain ratio or dilation ratio of concrete

μ_s Secant dilation ratio of confined-concrete

μ_{s1} Secant dilation ratio of confined-concrete at f'_{c1} in model proposed by Binici [73]

$\mu_{s,max}$ Maximum secant dilation ratio of confined-concrete in model proposed by Binici [73]

μ_{su} Secant dilation ratio of confined-concrete at ε_{cu}

μ_t Tangent dilation rate of confined-concrete

$\mu_{t,asym}$ Asymptotic tangent dilation rate of FRP-confined concrete in Mirmiran and Shahawy [107]

$\mu_{t,max}$ Maximum tangent dilation rate of FRP-confined concrete in Mirmiran and Shahawy [107]

μ_{tu} Average tangent dilation rate of confined-concrete at ε_{cu}

ν_c Initial Poisson's ratio of concrete

ψ Material factor in models proposed by Marques et al. [69] and Aire et al. [70]

ϕ Internal friction angle of concrete

Δ Parameter in model proposed by Binici [73]

REFERENCES

1. Fardis, M.N., and Khalili, H., *FRP-encased concrete as a structural material.* Mag. Concr. Res., 1982. 34(122): p. 1991-202.
2. Ahmad, S.M., Khaloo, A. R., and Irshaid, A., *Behaviour of concrete spirally confined by fiberglass filaments.* Mag. Concr. Res., 1991. 43(56): p. 143-148.
3. Saadatmanesh, H., Ehsani, M. R., and Li, M. W., *Strength and ductility of concrete columns externally reinforced with fiber composite straps.* ACI Struct. J., 1994. 91(4): p. 434-447.
4. Richart, F.E., Brandtzaeg, A., and Brown, R. L., *A study of the failure of concrete under combined compressive stresses.*, in *Bulletin no. 185*. 1928, Univ. of Illinois, Engineering Experimental Station: Champaign, Ill.
5. Ahmad, S.H., and Shah, S. P., *Complete triaxial stress-strain curves for concrete.* ASCE J. Struct. Div., 1982. 108(4): p. 728-742.
6. Mander, J.B., Priestley, M. J. N., and Park, R., *Theoretical stress-strain model for confined concrete.* ASCE J. Struct. Eng., 1988. 114(8): p. 1804-1826.
7. Mirmiran, A., Kargahi, M., Samaan, M. S., and Shahawy, M. . *Composite FRP-concrete column with bi-directional external reinforcement.* in *Proc. 1st Int. Conf. Composites in Infrastructure*. 1996. Tucson, Arizona: Univ. of Arizona.
8. Samaan, M., Mirmiran, A., and Shahawy, M., *Model of concrete confined by fiber composites.* ASCE J. Struct. Eng., 1998. 124(9): p. 1025-1031.
9. Miyauchi, K., Nishibayashi, S., and Inoue, S. . *Estimation of strengthening effects with carbon fiber sheet for concrete column.* in *3rd Int. Symp. Of Non-Metallic Reinforcement for Concrete Structures*. 1997.
10. Saafi, M., Toutanji, H. A., and Li, Z., *Behavior of concrete columns confined with fiber reinforced Polymer tubes.* ACI Struct. J., 1999. 96(5): p. 500-509.
11. Spoelstra, M.R., and Monti, G., *FRP-confined concrete model.* ASCE J. Compos. Constr., 1999. 3(3): p. 143-150.
12. Lam, L., and Teng, J. G., *Design-oriented stress-strain model for FRP-confined concrete.* Constr. Build. Mater., 2003. 17(6&7): p. 471-489.
13. De Lorenzis, L., and Tepfers, R., *Comparative study of models on confinement of concrete cylinders with fiber reinforced polymer Composites.* ASCE J. Compos. Constr., 2003. 7(3): p. 219-237.
14. Bisby, L.A., Dent, A. J. S., Green, M. F., *Comparison of confinement models for fiber-reinforced polymer-wrapped concrete.* ACI Struct. J., 2005. 102(1): p. 62-72.
15. Pessiki, S., Harries, K. A., Kestner, J., Sause, R., and Ricles, J. M., *The axial behavior of concrete confined with fiber reinforced composite jackets.* ASCE J. Compos. Constr., 2001. 5(4): p. 237-245.
16. Xiao, Y., and Wu, H., *Compressive behavior of concrete confined by carbon fiber composite jackets.* J. Mater. Civ. Eng., 2000. 12(2): p. 139-146.
17. Mirmiran, A., Shahawy, M., Samaan, M., El Echary, H., Mastrapa, J. C., and Pico, O., *Effect of Column Parameters on FRP-confined Concrete.* ASCE J. Compos. Constr., 1998. 2(4): p. 175-185.

18. Matthys, S., Taerwe, L., and Audenaert, K. . *Tests on axially loaded concrete columns confined by fiber reinforced polymer sheet wrapping.* in *Proc. 4th Int. Symp. On Fiber Reinforced Polymer Reinforcement for Reinforced Concrete Structures*. 1999. Detroit.
19. Harries, K.A., and Carey, A., *Shape and 'gap' effects on the behavior of variably confined concrete.* Cem. Concr. Res., 2002. 33(6): p. 873-880.
20. Lam, L., and Teng, J. G., *Ultimate condition of FRP-confined concrete.* ASCE J. Compos. Constr., 2004. 8(6): p. 539-548.
21. Ozbakkaloglu, T. and D.J. Oehlers, *Manufacture and testing of a novel FRP tube confinement system.* Engineering Structures, 2008. 30: p. 2448-2459.
22. Matthys, S., Toutanji. H., and Taerwe, L., *Stress-strain behavior of large-scale circular columns confined with FRP composites.* ASCE J. Struct. Eng., 2006. 132(1): p. 123-133.
23. Thériault, M., Neale, K. W., M. ASCE, and Claude, S., *Fiber reinforced polymer-confined circular concrete columns: investigation of size and slenderness effects.* ASCE J. Compos. Constr., 2004. 8(4): p. 323-331.
24. Carey, S.A., and Harries, K. A., *Axial behavior and modeling of confined small, medium, and large scale circular sections with carbon fiber-reinforced polymer jackets.* ACI Struct. J., 2005. 102(4): p. 596-604.
25. Wu, Y.F. and Y.Y. Wei, *Effect of cross-sectional aspect ratio on the strength of CFRP-confined rectangular concrete columns.* Engineering Structures, 2010. 32(1): p. 32-45.
26. Zhang, D.J., Y.F. Wang, and Y.S. Ma, *Compressive behaviour of FRP-confined square concrete columns after creep.* Engineering Structures, 2010. 32(8): p. 1957-1963.
27. Youssef, M.N., Feng, M. Q., and Mosallam, A. S., *Stress-strain model for concrete confined by FRP composites.* Composites Part B: Engineering., 2007. 38(5-6): p. 614-628.
28. Abbasnia, R. and H. Ziaadiny, *Behavior of concrete prisms confined with FRP composites under axial cyclic compression.* Engineering Structures, 2010. 32(3): p. 648-655.
29. Lam, L. and J.G. Teng, *Stress-strain model for FRP-confined concrete under cyclic axial compression.* Engineering Structures, 2009. 31(2): p. 308-321.
30. Rousakis, T.C., A.I. Karabinis, and P.D. Kiousis, *FRP-confined concrete members: Axial compression experiments and plasticity modelling.* Engineering Structures, 2007. 29(7): p. 1343-1353.
31. Campione, G. and G. Minafo, *Compressive behavior of short high-strength concrete columns.* Engineering Structures, 2010. 32(9): p. 2755-2766.
32. Chastre, C. and M.A.G. Silva, *Monotonic axial behavior and modelling of RC circular columns confined with CFRP.* Engineering Structures, 2010. 32(8): p. 2268-2277.
33. Eid, R. and A.N. Dancygier, *Confinement effectiveness in circular concrete columns.* Engineering Structures, 2006. 28(13): p. 1885-1896.
34. Popovics, S., *A numerical approach to the complete stress-strain curves for concrete.* Cem. Concr. Res., 1973. 3(5): p. 583-599.
35. Li, Y.F., Lin, C. T., and Sung, Y. Y., *A constitutive model for concrete confined with carbon fiber reinforced plastics.* Mech. Mater., 2003. 35(3-6): p. 603-619.

36. Demers, M., and Neale, K. W. . *Strengthening of concrete columns with unidirectional composite sheets.* in *Proc. Developments in Short and Medium Span Bridge Engineering*. 1994. Montreal, Que.: Canadian Society for Civil Engineering.
37. Howie, I., and Karbhari, V. M. . *Effect of materials architecture on strengthening: efficiency of composite wraps for deteriorating columns in the North-East*. in *Proc. 3rd Materials Engineering Conference*. 1994. San Diego.
38. Nanni, A., and Bradford, N. M., *FRP jacketed concrete under uniaxial compression.* Constr. Build. Mater., 1995. 9(2): p. 115-124.
39. Karbhari, V.M., and Gao, Y., *Composite jacketed concrete under uniaxial compression-verification of simple design equations.* J. Mater. Civ. Eng., 1997. 9(4): p. 185-193.
40. Hognestad, E., *A study of combined bending and axial load in reinforced concrete members.* Bulletin no. 399, Univ. of Illinois, Engineering Experimental Station, Champaign., 1951.
41. Miyauchi, K., Inoue, S., Kuroda, T., and Kobayashi, A. . *Strengthening effects with carbon fiber sheet for concrete column.* in *Japan Concr. Inst.* 1999.
42. Jolly, C.K., and Lilistone, D. . *The stress-strain behavior of concrete confined by advanced fibre composites.* in *Proc. 8th BCA Conference Higher Education and the Concrete Industry*. 1998. Southampton.
43. Jolly, C.K., and Lilistone, D., *An innovative form of reinforcement for concrete columns using advanced composites.* Structural Engineer, 2000. 78(23-24): p. 20-28.
44. Richard, R.M., and Abbottt, B. J., *Versatile elastic-plastic stress-strain formula.* ASCE J. Eng. Mech. Div., 1975. 101(4): p. 511-515.
45. Moran, D.A., and Pantelides, C. P., *Stress-strain model for fiber reinforced polymer-confined concrete.* ASCE J. Compos. Constr., 2002. 6(4): p. 233-240.
46. Jiang, T., and Teng, J. G. . *Strengthening of short circular RC columns with FRP jackets: a design proposal.* in *Proc. 3rd Int. Conf. on FRP Composites in Civil Engineering*. 2006. Miami, Florida, USA.
47. Yan, Z., and Pantelides, C. P. . *Design-oriented model for concrete columns confined with bonded FRP jackets or post-tensioned FRP shells*. in *Proc. 8th Int. Symp. On Fiber Reinforced Polymer Reinforcement for Concrete Structures*. 2007. Patras, Greece: Univ. of Patras.
48. Teng, J.G., Jiang, T., Lam, L. and Luo, Y., *Refinement of a Design-Oriented Stress-Strain Model for FRP-Confined Concrete.* ASCE J. Compos. Constr., 2009. 13(4): p. 269-278.
49. Fahmy, M., and Wu, Z., *Evaluating and proposing models of circular concrete columns confined with different FRP composites.* Composites Part B: Engineering., 2010. 41(3): p. 199-213.
50. ACI, *Building Code Requirement for Structural Concrete (ACI 318-95) and Commentary (318R-95)*, in *ACI Committee 318* 1995, American Concrete Institute: Farmington Hills, Michigan.
51. Sargin, M., *Stress-strain relationship for concrete and the analysis of structural concrete section.* 1971, Univ. of Waterloo: Ontario, Canada.

52. Toutanji, H.A., *Stress-strain characteristics of concrete columns externally confined with advanced fiber composite sheets.* ACI Mater. J., 1999. 96(3): p. 397-404.
53. Ilki, A., Kumbasar, N., and Koc, V., *Low strength concrete members externally confined with FRP sheets.* Struct. Eng. Mech, 2004. 18(2): p. 167-194.
54. Xiao, Y., and Wu, H., *Compressive behavior of concrete confined by various types of FRP composites jackets.* J. Reinf. Plas. Compos., 2003. 22(13): p. 1187-1202.
55. Berthet, J.F., Ferrier, E., and Hamelin, P., *Compressive behavior of concrete externally confined by composite jackets. Part B: modeling.* Constr. Build. Mater., 2006. 20(5): p. 338-347.
56. Saiidi, M.S., Sureshkumar, K., and Pulido, C., *Simple carbon-fiber-reinforced-plastic-confined concrete model for moment-curvature analysis.* ASCE J. Compos. Constr., 2005. 9(1): p. 101-104.
57. Wu, H., Wang, Y., Yu, L. and Li, X., *Experimental and Computational Studies on High-Strength Concrete Circular Columns Confined by Aramid Fiber-Reinforced Polymer Sheets.* ASCE J. Compos. Constr., 2009. 13(2): p. 125-134.
58. Wu, H., and Wang, Y., *Experimental study on high-strength concrete short columns confined with AFRP sheets.* Steel Compos. Struct., 2010. 10(6): p. 501-516.
59. Wu, G., Lu, Z. T., and Wu, Z. S., *Strength and ductility of concrete cylinders confined with FRP composites.* Constr. Build. Mater., 2006. 20(3): p. 134-148.
60. Binici, B., *Design of FRPs in circular bridge column retrofits for ductility enhancement.* Eng. Struct., 2008. 30(3): p. 766-776.
61. Kono, S., Inazuni, M., and Kaku, T. . *Evaluation of confining effects of CFRP sheets on reinforced concrete members.* in *Proc. 2nd Int. Conf. on Composites in Infrastructures*. 1998.
62. Teng, J.G., Huang, Y. L., Lam, L., and Ye, L., *Theoretical model for fiber reinforced polymer-confined concrete.* ASCE J. Compos. Constr., 2007. 11(2): p. 201-210.
63. Wu, Y.F., and Wang, L., *Unified Strength Model for Square and Circular Concrete Columns Confined by External Jacket.* ASCE J. Struct. Eng., 2009. 135(3): p. 253-261.
64. Xiao, Q., Teng, J. G., and Yu, T., *Behavior and Modeling of Confined High-Strength Concrete.* ASCE J. Compos. Constr., 2010. 14(3): p. 249-259.
65. Li, D., *Stress-strain relationship of concrete confined by FRP tubes.*, in *The School of Civil, Environmental and Mining Engineering*. 2011, University of Adelaide: Adelaide.
66. Jiang, T., and Teng, J. G., *Analysis-oriented stress-strain models for FRP-confined concrete.* ASCE J. Eng. Struct., 2007. 29(11): p. 2968-2986.
67. Fam, A.Z., and Rizkalla, S. H., *Confinement model for axially loaded concrete confined by circular fiber-reinforced polymer tubes.* ACI Struct. J., 2001. 98(4): p. 451-461.
68. Chun, S.S., and Park, H. C. . *Load carrying capacity and ductility of RC columns confined by carbon fiber reinforced polymer.* in *Proc. 3rd Int. Conf. on Composites in Infrastructure.* 2002.
69. Marques, S.P.C., Marques, D. C. S. C., da Silva, J. L., and Cavalcante, M. A. A., *Model for analysis of short columns of concrete confined by fiber reinforced polymer.* ASCE J. Compos. Constr., 2004. 8(4): p. 332-340.

70. Aire, C., Gettu, Casas, J., Marques, S. and Marques, D., *Concrete laterally confined with fibre-reinforced polymers (FRP): experimental study and theoretical model.* Materiales de Construcción, 2010. 60: p. 297.
71. Carreira, D.J., and Chu, K. H., *Stress-strain relationship for plain concrete in compression.* ACI Journal, 1985. 82(6): p. 797-804.
72. Harries, K.A., and Kharel, G., *Behavior and modeling of concrete subject to variable confining pressure.* ACI Mater. J., 2002. 99(2): p. 180-189.
73. Binici, B., *An analytical model for stress-strain behavior of confined concrete.* Eng. Struct., 2005. 27(7): p. 1040-1051.
74. Willam, K.J., and Warnke, E. P. . *Constitutive model for the triaxial behaviour of concrete.* in *Proc. Int. Association for Bridge and Structural Engineering*. 1975.
75. Elwi, A.A., and Murray, D. W., *A 3D hypoelastic concrete constitutive relationship.* ASCE J. Eng. Mech. Div., 1979. 105(4): p. 623-641.
76. Mirmiran, A., *FRP-concrete composite column and pile jacket splicing-Phase 2*, in *Contract no. B-9895*. 1997, Florida Department of Transportation: Tallahassee, FL.
77. Albanesi, T., Nuti, C., and Vanzi, I., *Closed form constitutive relationship for concrete filled FRP tubes under compression.* Construction and Building Materials, 2007. 21(2): p. 409-427.
78. Moran, D.A., and Pantelides, C. P., *Variable strain ductility ratio for fiber reinforced polymer-confined concrete.* ASCE J. Compos. Constr., 2002. 6(4): p. 224-232.
79. Tamuzs, V., Tepfers, R., and Sparnins, E., *Behavior of concrete cylinders confined by carbon composite II: prediction of strength.* Mech. Compos. Mater., 2006. 42(2): p. 109-118.
80. Tamuzs, V., Tepfers., R, Zile, E., and Ladnova, O., *Behavior of concrete cylinders confined by a carbon composite III: deformability and the ultimate axial strain.* Mech. Compos. Mater., 2006. 42(4): p. 303-314.
81. Harmon, T.G., Ramakrishnan, S., and Wang, E. H., *Confined concrete subjected to uniaxial monotonic loading.* ASCE J. Eng. Mech. Div., 1998. 124(12): p. 1303-1309.
82. Karabinis, A.I., and Rousakis, T. C., *Concrete confined by FRP material: a plasticity approach.* ASCE J. Eng. Struct., 2002. 24(7): p. 923-932.
83. Rousakis, T., Karabinis, A., Kiousis, P. and Tepfers, R., *Analytical modeling of plastic behavior of uniformly FRP confined concrete members.* Composites Part B: Engineering., 2008. 39(7-8): p. 1104-1113.
84. Eid, R., Dancygier, M., and Paultre, P., *Elastoplastic Confinement Model for Circular Concrete Columns.* ASCE J. Struct. Eng., 2007. 133(12): p. 1821 - 1831.
85. Eid, R., and Paultre, P., *Plasticity-based model for circular concrete conlumns confined with fibre-composite sheets.* Eng. Struct., 2007. 29(12): p. 3301-3311.
86. Becque, J., Patnaik, A. K., and Rizkalla, S. H., *Analytical models for concrete confined with FRP tubes.* ASCE J. Compos. Constr., 2003. 7(1): p. 31-38.
87. Gerstle, K.H., *Simple formulation of biaxial concrete behavior.* ACI J., 1981. 78(1): p. 62-68.
88. Gerstle, K.H., *Simple formulation of triaxial concrete behavior.* ACI J., 1981. 78(5): p. 382-387.

89. Moran, D.A., and Pantelides, C. P., *Damage-based stress-strain model for fiber reinforced polymer-confined concrete.* ACI Struct. J., 2005. 102(1): p. 54-61.
90. Rochette, P., and Labossiére, P. . *A plasticity approach for concrete columns confined with composite materials.* in *Proc., 2nd Int. Conf. on Advanced Compos. Mat. in Bridges and Struct.* 1996. Montreal, Canada: Canadian Society for Civil Engineering.
91. Mirmiran, A., Zagers, K., and Yuan, W., *Nonlinear finite element modeling of concrete confined by fiber composites.* Finite Element in Analysis and Design, 2000. 35: p. 79-96.
92. Parent, P., and Labossiere, P., *Finite element analysis of reinforced concrete columns confined with composite materials.* Can. J. Ci. Eng., 2000. 27(3): p. 400-411.
93. Yu, T., Teng, J. G., Wong, Y. L., and Dong, S. L., *Finite element modeling of confined concrete-I: Drucker-Prager type plasticity model.* ASCE J. Eng. Struct., 2010. 32(3): p. 665-679.
94. Yu, T., Teng, J. G., Wong, Y. L., and Dong, S. L., *Finite element modeling of confined concrete-II: Plastic-damage model.* ASCE J. Eng. Struct., 2010. 32(3): p. 680-691.
95. Cho, C.G., and Kwon, M. H., *Nonlinear failure prediction of concrete composite columns by a mixed finite element formulation.* J. Eng. Failure Analysis, 2011. 18: p. 1723-1734.
96. Csuka, B., and Kollár, L. P., *Analysis of FRP confined columns under eccentric loading.* J. Compos. Struct., 2011. 94: p. 1106-1116.
97. Dandapat, R., Deb, A., and Bhattacharyya, S. K., *Failure modes for FRP wrapped cylindrical concrete columns.* J. Reinf. Plas. Compos., 2011. 30(7): p. 561-579.
98. Jiang, J.F., Wu, Y. F, and Zhao, X. M., *Application of Drucker-Prager plasticity model for stress-strain modeling of FRP confined concrete columns.* J. Procedia Eng., 2011. 14: p. 687-694.
99. Tasdemir, M.A., Tasdemir, C., Jefferson, A. D., Lydon, F. D., and Barr, B. I. G., *Evaluation of strains at peak stresses in concrete: a three-phase composite model approach.* Cem. Concr. Res., 1998. 20(4): p. 301-318.
100. Ilki, A., Kumbasar, N., and Koc, V. . *Strength and deformability of low strength concrete confined by carbon fibre composite sheets*. in *Proc. 15th Engineering Mechanics Conference*. 2002. New York, NY.: Columbia Univ.
101. Ciupala, M.A., Pilakoutas, K., and Mortazavi, A. A. . *Effectiveness of FRP composites in confined concrete.* in *Proc. 8th Int. Symp. On Fiber Reinforced Polymer Reinforcement for Concrete Structures,* . 2007. Patras, Greece University of Patras.
102. Guralnick, S.A., and Gunawan, L., M., *Strengthening of Reinforced Concrete Bridge Columns with FRP Wrap.* Practice Periodical on Structural Design and Construction, ASCE, 2006. 11(4): p. 218-228.
103. Mohamed, H., and Masmoudi R., *Axial Load Capacity of Concrete-Filled FRP Tube Columns: Experimental versus Predictions.* ASCE J. Compos. Constr., 2010. 14(2): p. 231-243.
104. Harries, K.A., and Kharel, G., *Experimental investigation of the behavior of variably confined concrete.* Cem. Concr. Res., 2003. 33(6): p. 873-880.

105. Vintzileou, E., and Panagiotidou, E. . *An empirical model for predicting the mechanical properties of FRP-confined concrete.* in *Proc. 8th Int. Symp. On Fiber Reinforced Polymer Reinforcement for Concrete Structures*. 2007. Patras, Greece: Univ. of Patras.
106. Girgin, Z., *Modified Failure Criterion to Predict Ultimate Strength of Circular Columns Confined by Different Materials.* ACI Struct. J., 2009. 106(6): p. 800-809.
107. Mirmiran, A., and Shahawy, M., *Dilation characteristics of confined concrete.* Mechanics of Cohesive-Frictional Materials, 1997. 2(3): p. 237-249.
108. Pantazopoulou, S.J., and Mills, R. H., *Microstructural aspects mechanical response of plain concrete.* ACI Mater. J., 1995. 92(6): p. 605-616.
109. Newman, K., and Newman, J. B. . *Failure theories and design criteria for plain concrete.* in *Proc. Int. Civil Engineering Materials Conference on Structure*. 1969. New York: Wiley Interscience.
110. Shehata, I.A.E.M., Carneiro, L. A. V., and Shehata, L. C. D. . *Strength of confined short concrete columns.* in *Proc. 8th Int. Symp. On Fiber Reinforced Polymer Reinforcement for Concrete Structures*. 2007. Patras, Greece: Univ. of Patras.
111. Lin, H.J., and Chen, C. T., *Strength of concrete cylinder confined by composite materials.* J. Reinf. Plas. Compos., 2001. 20(18): p. 1577-1600.
112. Razvi, S., and Saatcioglu, M., *Confinement model for high-strength concrete.* ASCE J. Struct. Eng., 1999. 125(3): p. 281-289.
113. Mirmiran, A., *Analytical and experimental investigation of reinforced concrete columns encased in fibre glass tubular jackets and use of fiber jacket for pile splicing.*, in *Contract no. B-9135*. 1996, Florida Department of Transport: Tallahassee, FL.
114. Thériault, M., and Neale, K. W., *Design equations for axially loaded reinforced concrete columns strengthened with FRP wraps.* Can. J. Ci. Eng., 2009. 27(5): p. 1011 - 1020.
115. Lam, L., and Teng, J. G., *Strength models for fiber-reinforced plastic-confined concrete.* ASCE J. Struct. Eng., 2002. 128(5): p. 612-623.
116. Shehata, I.A.E.M., Carneiro, L. A. V., and Shehata, L. C. D., *Strength of short concrete columns confined with CFRP sheets.* Mater. and Struct., 2002. 35: p. 50-58.
117. Mandal, S., Hoskin, A., and Fam, A., *Influence of concrete strength on confinement effectiveness of fiber-reinforced polymer circular jackets.* ACI Struct. J., 2005. 102(3): p. 383-392.
118. Matthys, S., Toutanji. H., Audenaert, K., and Taerwe, L., *Axial load behavior of large-scale columns confined with fiber-reinforced polymer composites.* ACI Struct. J., 2005. 102(2): p. 258-267.
119. Al-Tersawy, S.H., Hodhod, O. A., and Hefnawy, A. A. . *Reliability and code calibration of RC short columns confined with CFRP wraps.* in *Proc. 8th Int. Symp. On Fiber Reinforced Polymer Reinforcement for Concrete Structures*. 2007. Patras, Greece: Univ. of Patras.
120. Tabbara, M., and Karam, G. . *Modeling the strength of concrete cylinders with FRP wraps using the Hoek-Brown strength criterion.* in *Proc. 8th Int. Symp. On Fiber Reinforced Polymer Reinforcement for Concrete Structures*. 2007. Patras, Greece: Univ. of Patras.

121. Al-Salloum, Y., and Siddiqui, N. . *Compressive Strength Prediction Model for FRP-Confined Concrete.* in *Proc. 9th Int. Symp. On Fiber Reinforced Polymer Reinforcement for Concrete Structures*. 2009. Sydney, Australia. : University of Adelaide.
122. ACI, *State of the art report on high strength concrete (ACI 363R-84).* in *ACI Committee 363*. 1984, American Concrete Institute: Detroit, Michigan.
123. Benzaid, R., Mesbah, H., and Chikh, N., *FRP-confined Concrete Cylinders: Axial Compression Experiments and Strength Model.* J. Reinf. Plas. Compos., 2010. 29(16): p. 2469-2488.
124. Wu, Y.F., and Zhou, Y., *Unified Strength Model Based on Hoek-Brown Failure Criterion for Circular and Square Concrete Columns Confined by FRP.* ASCE J. Compos. Constr., 2010. 14(2): p. 175-184.
125. Cevik, A., *Modeling strength enhancement of FRP confined concrete cylinders using soft computing.* Expert Systems with Applications, 2011. 38: p. 5662-5673
126. Park, J.H., Jo, B. W., Yoon, S. J., and Park, S. K., *Experimental investigation on the structural behavior of concrete filled FRP tubes with/without steel re-bar.* KSCE J. Civ. Eng., 2011. 15(2): p. 337-345.
127. Realfonzo, R.a.N., A., *Concrete confined by FRP systems: Confinement efficiency and design strength models.* Composites Part B: Engineering, 2011. 42: p. 736-755.
128. Wang, Y.F., and Wu, H. L, *Size effect of concrete short columns confined with aramid FRP jackets.* ASCE J. Compos. Constr., 2011. 15(4): p. 535-544.
129. Yu, T., and Teng, J. G., *Design of concrete-filled FRP tubular columns: Provisions in the Chinese Technical Code for infrastructure application of FRP composites.* ASCE J. Compos. Constr., 2011. 15(3): p. 451-461.
130. Mirmiran, A., and Shahawy, M., *Behavior of concrete columns confined by fiber composites.* ASCE J. Struct. Eng., 1997. 123(5): p. 583-590.
131. Gardner, N.J., *Triaxial Behavior of Concrete.* ACI L., 1969. 66(2): p. 136-146.
132. Thériault, M., and Neale, K. W., *Design equations for axially loaded reinforced concrete columns strengthened with FRP wraps.* Can. J. Ci. Eng., 2000. 27(5): p. 1011-1020.

Statement of Authorship

Title of Paper	Axial Compressive Behavior of FRP-Confined Concrete: Experimental Test Database and a New Design-Oriented Model
Publication Status	(•) Published ( ) Accepted for Publication ( ) Submitted for Publication ( ) Publication Style
Publication Details	Composites Part B: Engineering, Volume 55, Pages 607-634, Year 2013

Author Contributions

By signing the Statement of Authorship, each author certifies that their stated contribution to the publication is accurate and that permission is granted for the publication to be included in the candidate's thesis.

Name of Principal Author	Dr. Togay Ozbakkaloglu		
Contribution to the Paper	Research supervision and review of manuscript		
Signature		Date	23/02/2015

Name of Co-Author (Candidate)	Mr. Jian Chin Lim		
Contribution to the Paper	Preparation of experimental database, development of model, and preparation of manuscript		
Signature		Date	23/02/2015

THIS PAGE HAS BEEN LEFT INTENTIONALLY BLANK

AXIAL COMPRESSIVE BEHAVIOR OF FRP-CONFINED CONCRETE: EXPERIMENTAL TEST DATABASE AND A NEW DESIGN-ORIENTED MODEL

Togay Ozbakkaloglu and Jian C. Lim

ABSTRACT

A large number of experimental studies have been conducted over the last two decades to understand the behavior of FRP-confined concrete columns. This paper presents a comprehensive test database constructed from the results of axial compression tests on 832 circular FRP-confined concrete specimens published in the literature. The database was assembled through an extensive review of the literature that covered 3042 test results from 253 experimental studies published between 1991 and the middle of 2013. The suitability of the results for the database was determined using carefully chosen selection criteria to ensure a reliable database. This database brings reliable test results of FRP-confined concrete together to form a unified framework for future reference. Close examination of the test results reported in the database led to a number of important observations on the influence of important parameters on the behavior of FRP-confined concrete. A new design-oriented model that was developed to quantify these observations is presented in the final part of the paper. It is shown that the predictions of the proposed model are in close agreement with the test results and the model provides improved predictions of the ultimate conditions of FRP-confined concrete compared to any of the existing models.

KEYWORDS: FRP-confined concrete; Fibers; Plastic deformation; Strength; Mechanical testing

1. INTRODUCTION

Axial compressive behavior of FRP-confined concrete has received significant attention over the last two decades, and it is now well understood that the confinement of concrete with fiber reinforced polymer (FRP) composites can substantially enhance concrete strength and deformability. A large number of experimental studies have produced over 3000 test results on FRP-confined concrete and resulted in the development of over 90 axial stress-axial strain models, 88 of which were recently reviewed and assessed in Ozbakkaloglu et al. [1]. It became evident from the results of the assessment reported in Ozbakkaloglu et al. [1] the performances of a large proportion of the existing models were compromised when assessed against a large test database with a parametric range that is much wider than the databases used in the development of these models. These observations clearly revealed the need for an extensive and reliable experimental test database of FRP-confined concrete for the development of models of higher accuracy.

In this paper, a carefully prepared database of circular FRP-confined concrete specimens tested under monotonic uniaxial compression is presented. The database was assembled through an extensive review of the literature that cataloged 3042 test results from 253 experimental studies published between 1991 and the middle of 2013. These results were then assessed according to criteria that had been critically determined to establish a reliable database. Assessment using these criteria resulted in a final database of 832 test results from 99 different sources. This database serves as a valuable reference document for: i) future model development and verification; ii) assessment of existing models; and iii) future database establishment. The important factors that influence the overall behavior of FRP-confined concrete, as identified from the results reported in the comprehensive database, are then discussed. In the final part of the paper, a new design-oriented model developed using the database to predict the ultimate condition of FRP-confined concrete is presented.

2. CONSTRUCTION OF EXPERIMENTAL TEST DATABASE

2.1 Previous databases

Due to the inherent complexity of the behavior of FRP-confined concrete, test databases serve as a vital verification tool in assessing the performance of a model. Recognition of the importance of systematically collecting and categorizing the existing test results has led to a number of previous attempts to develop test databases for FRP-confined concrete. All relevant details of these previous databases are summarized in Table 1. The earlier databases reported by Lam and Teng [2, 3], De Lorenzis and Tepfers [4] and Bisby et al. [5] are extensive and include the majority of the experimental data with sufficient detail that were available at the time the databases were published. More recently, Turgay et al. [6] compiled a database of carbon FRP-confined concrete specimens and Realfonzo and Napoli [7] reported a fairly large database of carbon and glass FRP-wrapped specimens. However, a comprehensive review of the literature indicated that a large number of the currently available test results summarized in Table 2 were not included in any of the existing databases.

Table 1. Summary of existing databases of axial compression tests on circular FRP-confined concrete specimens

Paper	Number of studies covered	Number of test data	Confinement technique	Fiber type	Unconfined concrete strength range, f'_{co} (MPa)	Nominal confinement ratio range, f_{lu}/f_{co}	Specimen Diameter range, D (mm)	Specimen Height range, H (mm)
Lam and Teng [2, 3]	30	275	Tube and wrap	CFRP, GFRP, AFRP, and HM CFRP	18.0 - 62.4	0.03 - 2.30	51 - 200	102 - 788
De Lorenzis and Tepfers [4]	17	180	Tube and wrap	CFRP, GFRP, and AFRP	19.4 - 82.1	0.06 - 2.31	51 - 219	102 - 438
Bisby et al. [5]	23	197	Wrap	CFRP, GFRP, and AFRP	15 - 103	-	50 - 300	-
Turgay et al. [6]	20	127	Tube and wrap	CFRP	17.4 - 171.0	0.032 - 0.95	51 - 200	102 - 610
Realfonzo and Napoli [7]	63	465	Wrap	CFRP, GFRP	15.2 - 169.7	0.002 - 2.22	51 - 406	102 - 1824

Table 2. Summary of test results included in the database

Paper	Total number of datasets	Confinement technique	Fiber type	Diameter, D (mm)	Height, H (mm)	Unconfined concrete strength range, f'_{co} (MPa)	Strength enhancement ratio range, f'_{cc}/f'_{co}	Strain enhancement ratio range, $\varepsilon_{cu}/\varepsilon_{co}$	Actual confinement ratio range, $f_{lu,a}/f'_{co}$	Number of identical specimens per entry in the database	Lateral strain measurement method (see notes)	Axial strain measurement method (see notes)
Abdollahi et al. [54]	5	Wrap	GFRP	150	300	14.8 - 41.7	1.24 - 3.32	1.54 - 12.04	0.06 - 0.43	2	N/A	AFL
Ahmad et al. [55]	2	Wrap	GFRP	102	203	39.0 - 50.5	2.68 - 2.96	-	0.55 - 0.73	Single	N/A	N/A
Aire et al. [56]	6	Wrap	CFRP, GFRP	150	300	42.0	0.97 - 2.57	3.33 - 13.17	0.09 - 0.71	3	HS	AFL
Akogbe et al. [57]	12	Wrap	CFRP	100 - 300	200 - 600	21.7 - 26.5	2.38 - 3.19	7.03 - 12.68	0.26 - 0.32	Single	HS	AML
Almusallam [58]	4	Wrap	GFRP	150	300	47.7 - 50.8	1.09 - 2.10	-	0.14 - 0.46	3	HL	N/A
Al-Salloum [45]	2	Wrap	CFRP	150	300	32.4 - 36.2	2.35 - 2.57	15.77	0.30 - 0.33	Single	HS	AML
Au and Buyukozturk [59]	1	Wrap	GFRP	150	375	24.2	1.81	6.19	0.26	3	HL	AML
Benzaid et al. [60]	4	Wrap	CFRP	160	320	25.9 - 49.5	1.07 - 2.55	1.48 - 5.57	0.09 - 0.59	Single	HL	AML
Berthet et al. [61]	42	Wrap	CFRP, GFRP	160	320	25.0 - 52.0	1.12 - 4.15	2.18 - 13.50	0.07 - 0.95	Single	HL	AML
Bisby et al. [62]	3	Wrap	CFRP	150	300	34.4	1.25 - 1.28	2.42 - 2.73	0.10 - 0.13	Single	N/A	N/A
Bisby et al. [63]	3	Wrap	CFRP	100	200	28.0	1.89 - 2.25	4.24 - 5.28	0.20 - 0.22	Single	N/A	N/A
Bullo [64]	12	Wrap	GFRP, HM CFRP	150	300	32.5	1.62 - 4.17	3.36 - 19.53	0.11 - 0.60	Single	HL	AFL
Campione et al. [65]	1	Wrap	CFRP	100	200	20.1	2.47	12.32	0.36	N/A	N/A	N/A
Carey and Harries [66]	2	Wrap	CFRP	152 - 254	305 - 762	33.5 - 38.9	1.40 - 1.41	3.47 - 4.04	0.15 - 0.17	≥ 2	HL	AML
Comert et al. [67]	2	Wrap	GFRP	150	300	39.0	1.56 - 1.64	9.92 - 10.86	0.23	Single	HS	AFL
Cui and Sheikh [68]	24	Wrap	CFRP, GFRP, HM CFRP	152	305	45.6 - 48.1	1.21 - 3.38	4.24 - 13.92	0.07 - 0.48	Single	HS	AML
Dai et al. [40]	9	Wrap	AFRP	152	305	39.2	1.42 - 3.01	9.75 - 22.52	0.09 - 0.39			
Demers and Neale [69]	8	Wrap	CFRP, GFRP	152	305	32.2 - 43.7	0.96 - 1.72	4.35 - 10.48	0.07 - 0.24	Single	HS	AFL
Elsanadedy et al. [70]	6	Wrap	CFRP	50 - 150	100 - 300	41.1 - 53.8	1.86 - 3.51	2.61 - 4.54	0.20 - 0.59	2 to 5	N/A	AML
Erdil et al. [71]	2	Wrap	CFRP	150	300	11.1 - 20.8	2.28 - 2.96	11.67 - 14.00	0.23 - 0.44	3	HS	AML
Evans et al. [72]	1	Wrap	CFRP	150	300	37.3	1.73	6.31	0.28	Single	HS	AFL
Green et al. [73]	3	Wrap	CFRP, GFRP	152	305	46.0 - 54.0	1.15 - 1.28	-	0.05 - 0.10	Single	HS	N/A
Harmon and Slattery [74]	4	Wrap	CFRP	51	102	41.0	2.10 - 5.88	5.08 - 15.70	0.19 - 1.42	Single	HS	AFL
Harries and Carey [8]	4	Wrap, unbonded wrap	GFRP	152	305	31.8	1.06 - 1.52	2.32	0.08 - 0.21	≥ 5	HL	AML
Harries and Kharel [75]	10	Wrap	CFRP, GFRP	152	305	32.1	1.02 - 1.87	1.43 - 4.93	0.02 - 0.33	≥ 5	HL	AML
Hong and Kim [13]	2	Tube	CFRP	300	600	17.5	4.32 - 4.58	14.33 - 18.51	1.11	Single	HS	AML
Hosotani et al. [76]	2	Wrap	CFRP, HM CFRP	200	600	41.7	2.16 - 2.23	4.41 - 6.18	0.23 - 0.25	Single	N/A	N/A
Howie and Karbhari [77]	12	Wrap	CFRP	152	305	38.6	1.09 - 2.33	-	0.06 - 0.40	Single	HL	N/A
Ilki et al. [78]	5	Wrap	CFRP	150	300	32.0	1.48 - 3.37	7.20 - 24.80	0.12 - 0.79	Single	HS	AFL
Ilki et al. [79]	12	Wrap	CFRP	150	300	6.2	3.13 - 17.47	13.00 - 52.00	0.55 - 4.74	Single	HS	AFL
Issa [80]	3	Wrap	CFRP	150	300	23.6 - 23.9	1.66 - 1.77	-	0.17 - 0.18	Single	HL	N/A
Issa and Karam [81]	9	Wrap	CFRP	150	300	30.5	1.17 - 2.48	-	0.14 - 0.41	Single	HL	N/A
Jiang and Teng [32]	23	Wrap	CFRP, GFRP	152	305	33.1 - 47.6	0.88 - 4.24	2.66 - 17.05	0.06 - 0.99	Single	HS	AML
Karabinis and Rousakis [82]	16	Wrap	CFRP	200	320	35.7 - 38.5	1.08 - 1.89	1.26 - 8.99	0.07 - 0.23	Single	N/A	AML
Karam and Tabbara [83]	2	Wrap	CFRP	150	300	12.8	1.39 - 2.48	2.91 - 5.91	0.29 - 0.59	2	HL	AML
Karantzikis et al. [84]	2	Wrap, unbonded wrap	CFRP	200	350	12.1	1.78 - 2.42	5.27 - 8.73	0.22	3	N/A	AML

Karbhari and Gao [37]	3	Wrap	CFRP	152	305	38.4	1.56 - 2.33	6.18 - 11.42	0.25 - 0.41	≥ 3	HL	AFL
Kono et al. [85]	15	Wrap	CFRP	100	200	32.3 - 34.8	1.46 - 3.16	3.93 - 12.37	0.14 - 0.62	Single	N/A	N/A
Lam and Teng [18]	18	Wrap	CFRP, GFRP	152	305	34.3 - 38.5	1.31 - 2.84	5.44 - 13.38	0.13 - 0.42	Single	HS	AML
Lam et al. [29]	6	Wrap	CFRP	152 - 152.5	304 - 305	38.9 - 41.1	1.28 - 2.03	3.52 - 8.32	0.11 - 0.31	Single	HS	AML
Lee et al. [86]	5	Wrap	CFRP	150	300	36.2	1.15 - 2.88	4.17 - 12.92	0.11 - 0.56	Single	HL	AML
Li et al. [87]	1	Wrap	GFRP	152.4	305	45.6	1.08	-	0.24	3	N/A	N/A
Li et al. [88]	2	Tube	GFRP	150	300	47.5	1.07 - 1.80	2.25 - 5.25	0.09 - 0.15	N/A	N/A	N/A
Liang et al. [89]	12	Wrap	CFRP	100	200	22.7 - 25.9	2.4 - 3.04	7.78 - 12.27	0.29 - 0.44	Single	HL	AFL
Lin and Chen [38]	10	Wrap	GFRP, HM CFRP	120	240	32.7	1.52 - 3.20	-	0.10 - 0.55	Single	N/A	N/A
Lin and Li [90]	27	Wrap	CFRP	100 - 150	200 - 300	17.7 - 25.9	1.92 - 5.23	-	0.19 - 1.23	3	HS	N/A
Lin and Liao [91]	6	Wrap	CFRP	100	200	23.9	2.57 - 3.91	-	0.51 - 0.96	Single	N/A	N/A
Mandal et al. [92]	9	Wrap	CFRP, GFRP	102 - 105	200	30.7 - 54.5	1.17 - 2.58	1.33 - 11.41	0.16 - 0.74	3	N/A	AML
Mastrapa [10]	13	Wrap, unbonded wrap	GFRP	152.5	305	29.8 - 37.2	0.90 - 3.10	7.96 - 32.54	0.19 - 1.03	Single	HS	AFL
Matthys et al. [11]	4	Wrap, unbonded wrap	CFRP, UHM CFRP	150	300	34.9	1.17 - 1.27	1.71 - 4.22	0.10 - 0.12	Single	HS	AS
Micelli et al. [93]	2	Wrap	CFRP, GFRP	102	204	32.0 - 37.0	1.61 - 1.62	4.93 - 8.93	0.19 - 0.23	N/A	N/A	N/A
Mirmiran et al. [9]	26	Wrap, unbonded wrap	GFRP	152.5	305	29.8 - 31.2	1.04 - 3.24	5.31 - 32.80	0.15 - 0.78	Single	HS	AFL
Miyauchi et al. [94]	10	Wrap	CFRP	100 - 150	200 - 300	31.2 - 51.9	1.31 - 3.26	4.32 - 10.32	0.07 - 0.42	2	N/A	AS
Miyauchi et al. [95]	6	Wrap	CFRP	100 - 150	200 - 300	23.6 - 26.3	1.55 - 3.23	8.83 - 13.24	0.14 - 0.55	N/A	N/A	N/A
Modarelli et al. [96]	3	Wrap	CFRP, GFRP	150	300	28.4 - 38.2	1.64 - 1.95	2.37 - 4.49	0.13 - 0.26	3	HS	AFL
Nanni and Bradford [97]	17	Wrap	GFRP, AFRP	150	300	35.6 - 36.3	1.13 - 5.40	9.21 - 47.37	0.18 - 1.66	Single	N/A	AFL
Ongpeng [98]	2	Wrap	CFRP	180	500	27.0	1.38 - 1.90	-	0.12 - 0.25	Single	N/A	N/A
Owen [99]	8	Wrap	CFRP	102 - 152	203 - 305	47.9 - 53.0	1.33 - 4.89	3.86 - 17.02	0.15 - 1.66	1 to 4	N/A	N/A
Ozbakkaloglu and Akin [39]	4	Wrap	AFRP	152	305	39.0	1.72 - 2.25	10.95 - 14.80	0.25 - 0.45	Single	HS	AFL
Ozbakkaloglu and Vincent [14]	24	Tube	CFRP, AFRP, UHM CFRP	74 - 302	152 - 600	34.0 – 55.0	1.06 - 2.47	3.29 - 15.97	0.05 - 0.38	Single	HS	AFL
Park et al. [100]	12	Tube	GFRP	150	300 - 450	32.0 - 54.0	1.69 - 3.82	7.73 - 15.69	0.11 - 0.58	Single	N/A	AFL
Picher et al. [101]	1	Wrap	CFRP	152	304	39.7	1.41	5.01	0.21	3	HL	AFL
Piekarczyk et al. [102]	2	Wrap	CFRP	47	112	55.0	2.18 - 3.44	2.86 - 4.00	0.52 - 0.86	Single	N/A	N/A
Pon et al. [103]	8	Wrap	CFRP	150 - 600	300 - 1200	7.1 - 9.6	1.73 - 4.68	-	0.28 - 1.30	N/A	N/A	N/A
Rochette and Labossiére [104]	7	Wrap	CFRP, AFRP	100 - 150	200 - 300	42.0 - 43.0	1.10 - 1.75	5.01 - 7.86	0.08 - 0.26		HL	AFL
Rousakis [105]	20	Wrap	HM CFRP	150	300	25.2 - 51.8	1.36 - 2.67	2.22 - 7.88	0.07 - 0.46	Single	HS	AFL
Rousakis et al. [26]	6	Wrap	CFRP	150	300	20.4 - 49.2	1.61 - 3.09	2.06 - 5.46	0.13 - 0.95	Single	HS	AML
Saafi et al. [12]	6	Tube	GFRP, HM CFRP	152	435	35.0	1.51 - 2.77	4.00 - 12.00	0.07 - 0.40	3	HS	AFL
Saenz and Pantelides [106]	4	Wrap	CFRP	152	304	40.3 - 47.5	1.72 - 2.68	3.79 - 9.49	0.22 - 0.59	3	HS	AML
Santarosa et al. [107]	3	Wrap	CFRP	150	300	15.3 - 28.1	1.37 - 3.05	3.01 - 8.70	0.11 - 0.42	2	HS	AS
Shahawy et al. [16]	9	Wrap	CFRP	152.5	305	19.4 - 49.0	1.21 - 4.13	2.14 - 10.79	0.30 – 4.00	5	HS	AML
Shao et al. [108]	2	Wrap	GFRP	152	305	40.2	1.23 - 1.78	-	0.18 - 0.37	Single	HS	N/A
Shehata et al. [109]	4	Wrap	CFRP	150	300	25.6 - 29.8	1.71 - 2.42	5.86 - 8.29	0.19 - 0.41	9	N/A	N/A
Shehata et al. [110]	4	Wrap	CFRP	150 - 225	300 - 450	34.0	1.29 - 2.41	3.10 - 5.50	0.10 - 0.29	9	N/A	N/A
Silva and Rodrigues [111]	7	Wrap	GFRP	150 - 250	300 - 750	29.6 - 31.2	1.79 - 3.03	4.54 - 11.33	0.20 - 0.58	Single	HS	N/A
Smith et al. [36]	4	Wrap	CFRP	250	500	35.0	1.43 - 1.69	-	0.11 - 0.17	Single	HS	N/A
Song et al. [112]	12	Wrap	CFRP	100 - 150	300 - 450	22.4	1.40 - 5.30	4.01 - 19.61	0.12 - 0.88	2	HS	AFL
Stanton and Owen [30]	5	Wrap	CFRP	152.5	305	49.0	1.41 - 5.63	4.24 - 19.51	0.11 - 0.90	N/A	N/A	N/A
Suter and Pinzelli [113]	16	Wrap	CFRP, GFRP, AFRP, UHM CFRP	150	300	33.3 - 54.0	1.14 - 3.12	1.16 - 8.92	0.09 - 0.46	≥ 1	N/A	N/A
Tamuzs et al. [114]	4	Wrap	CFRP	150	300	20.8 - 48.8	1.48 - 2.03	3.21 - 5.48	0.25 - 0.62	Single	HS	AS

Teng et al. [115]	6	Wrap	GFRP	152.5	305	39.6	0.94 - 1.66	3.14 - 9.73	0.07 - 0.26	Single	HS	AML
Thériault et al. [116]	5	Wrap	CFRP, GFRP	51 - 304	102 - 608	18.0 - 37.0	1.73 - 3.89	-	0.25 - 1.15	3	N/A	N/A
Valdmanis et al. [27]	6	Wrap	CFRP	150	300	40.0 - 44.3	1.65 - 2.60	3.18 - 8.00	0.09 - 0.28	Single	HS	AML
Vincent and Ozbakkaloglu [117]	6	Wrap	CFRP	152	305	35.5 – 38.0	1.21 - 1.74	3.79 – 7.88	0.11 - 0.23	Single	HS	AFL
Vincent and Ozbakkaloglu [118]	12	Wrap, tube	AFRP	152	305	49.4	2.09 - 2.24	12.59 - 15.76	0.30 - 0.42	Single	HS	AFL
Wang and Wu [33]	12	Wrap	CFRP	150	300	30.9 - 52.1	1.28 - 2.85	-	0.09 - 0.43	Single	HS	N/A
Wang and Wu [119]	18	Wrap	AFRP	70 - 194	210 - 582	24.0 - 51.6	0.98 - 3.37	1.36 - 5.68	0.04 - 0.35	N/A	N/A	N/A
Wang and Zhang [120]	2	Wrap	AFRP	150	450	47.3 - 51.1	1.73 - 1.78	6.01 - 6.99	0.20 - 0.22	Single	N/A	AS
Watanabe et al. [28]	9	Wrap	CFRP, AFRP, UHM CFRP	100	200	30.2	1.29 - 3.46	2.48 - 24.13	0.14 - 0.79	N/A	N/A	N/A
Wong et al. [34]	4	Wrap	GFRP	152.5	305	36.5 - 46.7	1.24 - 1.73	5.58 - 8.40	0.14 - 0.27	Single	HS	AML
Wu and Jiang [121]	4	Wrap	CFRP	150	300	28.7 - 30.1	1.91 - 3.00	-	0.17 – 0.32	Single	N/A	AML
Wu and Jiang [24]	34	Wrap	CFRP	150	300	20.6 - 36.7	1.69 - 6.83	-	0.15 – 1.31	Single	HS	AML
Wu et al. [31]	4	Wrap	CFRP, AFRP, HM CFRP, GFRP	150	300	23.0	1.96 - 2.30	-	0.15 - 0.23	Single	HS	N/A
Wu et al. [35]	10	Wrap	CFRP, GFRP, AFRP, UHM CFRP	150	300	23.1	1.94 - 3.55	4.49 - 14.04	0.15 - 0.42	Single	HS	AFL
Wu et al. [122]	2	Wrap	AFRP	100	300	46.4	1.69 - 2.77	3.54 - 7.37	0.17 - 0.34	Single	N/A	AML
Xiao and Wu [15]	27	Wrap	CFRP	152	305	33.7 - 55.2	1.05 - 2.83	1.66 - 15.27	0.06 - 0.51	Single	HS	AS
Yan et al. [123]	1	Wrap	CFRP	305	610	15.2	2.49	5.50	0.39	Single	HS	AML
Youssef et al. [53]	40	Wrap	CFRP, GFRP	152.4 - 406.4	304.8 - 812.8	29.4 - 44.6	1.44 - 4.31	2.56 - 14.24	0.10 - 0.88	Single	HS	AML
Zhang et al. [124]	1	Wrap	CFRP	150	300	34.3	1.73	10.50	0.30	5	N/A	AFL

Specimen instrumentation notes:
HS denotes hoop strains were measured by strain gauges attached on the surface of specimens
HL denotes hoop strains were measured by lateral LVDTs, extensometers, or dial gauges mounted on specimens
AS denotes axial strains were measured by strain gauges attached on the surface of specimens
AFL denotes axial strains were determined from LVDTs or dial gauges mounted on loading platens to measure deformations along the full height of specimens
AML denotes axial strains were determined from LVDTs, extensometers, or dial gauges mounted on specimens to measure deformations within a gauge length along the height of specimens
N/A denotes information that was either not applicable to the dataset or not available in the source document

2.2 Selection criteria for the new database

The suitability of the results for the database was assessed using carefully established selection criteria to ensure both the reliability and consistency of the test data. This resulted in a final database of 832 datasets, which makes it by far the most comprehensive database reported in the literature. The test results included in this database, summarized in Table 2 and presented in Tables 3 to 7 in Appendix, met the following requirements:

1) Only the specimens with unidirectional fibers orientated in the hoop direction were included in the database.
2) Specimens with transverse and/or longitudinal steel or internal FRP reinforcement were excluded.
3) Only the specimens that were confined with continuous FRP jackets were included. Specimens with partial wrapping (i.e., FRP strips) were excluded.
4) Specimens with a height-to-diameter *(H/D)* ratio greater than three were excluded from the database to eliminate the influence of specimen slenderness.
5) Specimens with unconfined concrete compressive strengths greater than 55 MPa were excluded to limit the database to only normal-strength concrete.
6) Only the specimens that failed due to FRP rupture at the ultimate condition were included. Specimens that failed prematurely due to other types of failure, such as FRP shell debonding or premature failure due to excessive eccentricity were excluded.
7) Specimens for which the ultimate conditions were not recorded accurately due to inadequate testing equipment or instrumentation errors were excluded.
8) Specimens reported with insufficient details in regards to material and geometric properties were excluded.

The specimens that satisfied the above conditions, and hence were included in the test database, were then subjected to an additional set of conditions to establish their suitability for their inclusion in the assessment of the existing models and development of the new model. The specimens with compressive strengths (f'_{cc}) and ultimate axial strains (ε_{cu}) that deviated significantly from the global trends of relevant strength and strain enhancement ratios (i.e. by limiting the variation of a given dataset from the trendline to maximum 40% for f'_{cc}/f'_{co} and 70% for $\varepsilon_{cu}/\varepsilon_{co}$) were excluded in the model assessment and development. The specimens that were excluded from the calculations of the strength and strain enhancement ratios (f'_{cc}/f'_{co} and $\varepsilon_{cu}/\varepsilon_{co}$) are marked respectively with the superscripts '*s*' and '*a*' in Tables 3 to 7. Furthermore, the specimens with hoop rupture strain reduction factors (k_ε) that deviated significantly from the average values of the corresponding material (i.e. more than ±20% of average k_ε) are marked with the superscript '^' in Tables 3 to 7, and they were excluded in the development of the expression for the hoop rupture strain reduction factor (k_ε). In addition to these, datasets from specimens exhibiting a stress-strain curve with a descending second branch (marked with superscript '*d*' in database tables) and ones from specimens having tubes that were fabricated using an automated manufacturing method (marked with superscript '*fm*' in database tables) were also excluded in the model development and assessment to limit the investigation to specimens with ascending second branches and manually manufactured FRP jackets.

3. NEW TEST DATABASE

The complete test database assembled in the present study is displayed in Tables 3 to 7 in Appendix. The database consists of the following information for each specimen: confinement technique (wrapped or tube-encased concrete); specimen geometric properties (diameter D and height H); unconfined concrete strength (f'_{co}) and strain (ε_{co}); material properties of the FRP shell (elastic modulus E_{frp}, tensile strength f_{frp}, total thickness t_{frp}); material properties of the fibers used in the FRP shell (elastic modulus E_f, tensile strength f_f, total thickness t_f); compressive strength (f'_{cc}) and ultimate axial strain (ε_{cu}) of confined concrete, and average FRP hoop strain at rupture ($\varepsilon_{h,rup}$); and hoop rupture strain reduction factor based on fiber properties ($k_{\varepsilon,f}$) and FRP material properties ($k_{\varepsilon,frp}$).

The test data presented in the database were sorted into eight groups based on two main confinement parameters: confinement technique (wraps or tubes) and type of FRP material [carbon FRP (CFRP); S- or E-glass FRP (GFRP); aramid FRP (AFRP); high-modulus carbon FRP (HM CFRP); or ultra-high-modulus carbon FRP (UHM CFRP)]. 755 specimens in the database were FRP-wrapped, whereas 77 specimens were confined by FRP tubes. 495 of the specimens were confined by CFRP; 206 by GFRP; 79 by AFRP; 40 by HM CFRP; and 12 by UHM CFRP.

The results of FRP-wrapped specimens are presented in Tables 3 to 6, categorized according to fiber type, and the results of all FRP tube-encased specimens are given in Table 7. It is worthwhile noting that for some of the datasets, a single entry in Tables 3 to 7 may represent the average results of more than one nominally identical specimen, as reported in the original study. These datasets are clearly marked in Table 2. In addition, a group of unbonded-wrapped specimens tested by Harries and Carey [8], Mirmiran et al. [9], Mastrapa [10] and Matthys et al. [11] were grouped under the category of tube-encased specimens in the database. Furthermore, except for the datasets from Saafi et al. [12], Hong and Kim [13] and Ozbakkaloglu and Vincent [14], all the datasets included in the database tables were obtained from specimens that were confined by FRP shells (wraps or tubes) manufactured using a manual hand lay-up technique. The specimens of Ozbakkaloglu and Vincent [14] and Hong and Kim [13], on the other hand, were confined by FRP tubes that were manufactured using an automated filament winding technique; and the specimens of Saafi et al. [12] were confined with FRP tubes supplied by a manufacturer, with no specific manufacturing method reported in the source document. These datasets are marked with a superscript *'fm'* in Table 7 to highlight the fact that the FRP shells of these specimens were manufactured using an automated manufacturing method rather than a manual one.

The diameters of the specimens (D) included in the test database varied between 47 and 600 mm, with the majority of the specimens having a diameter of 150 mm. The unconfined concrete strength (f'_{co}) and strain (ε_{co}), as obtained from concrete cylinder tests, varied from 6.2 to 55.2 MPa and 0.14% to 0.70%, respectively. The actual confinement ratio, defined as the ratio of the actual ultimate confining pressure to the unconfined concrete strength ($f_{lu,a}/f'_{co}$), varied from 0.02 to 4.74. The FRP material properties reported in the database were obtained either from the material test results (i.e., coupon or ring splitting tests) reported in

the original study or the specifications provided by the manufacturers. The specimens with FRP properties that differed significantly from the reference properties of the corresponding material were marked with the superscript '*m*' in Tables 3 to 7, to point to potential errors in these properties.

3.1 Material properties of fibers and FRP composites reported in the database

In FRP-confined circular concrete sections, the lateral confining pressure (f_l) provided by the FRP shell can be assumed to be uniformly distributed around the circumference (Figure 1). The confinement exerted by the FRP shell on the concrete core is passive; that is, this pressure arises as a result of the lateral expansion of the concrete under axial compression. As the FRP shell is subjected to tension along its hoop direction, the confining pressure (f_l) increases proportionally with the lateral expansion until the eventual failure of the system when the FRP shell ruptures. Based on the deformation compatibility between the confining shell and the concrete surface and assumption of a uniform confining pressure distribution, the lateral confining pressure applied to the concrete by the FRP shell at ultimate (f_{lu}) can be theoretically calculated from Eq. 1 as a function of the ultimate tensile strain of the fibers (ε_f).

$$f_{lu} = \frac{2E_f t_f \varepsilon_f}{D} \tag{1}$$

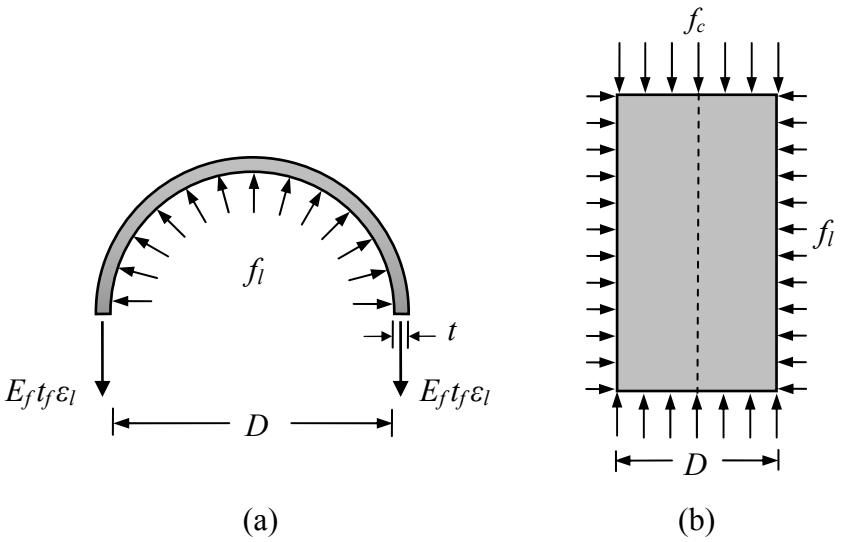

Figure 1. Confining action of FRP shell on concrete core: (a) FRP shell; (b) Concrete core

However, it has been well documented that the ultimate strain measured on the FRP shell at the time of FRP hoop rupture ($\varepsilon_{h,rup}$) is often lower than the ultimate tensile strain of the fibers (ε_f) or FRP material (ε_{frp}) (e.g. [3, 4, 8, 9, 11, 15-25]). Several causes have been given for the observed differences between hoop rupture strains and material ultimate tensile strains, including: (i) the quality of workmanship; (ii) overlaps of fiber sheets in the FRP shell; (iii) manufacturing imperfections (e.g., misalignment of fibers); (iv) shrinkage of the concrete (for FRP tube-encased concrete); (v) localized or non-uniform effects caused by imperfections in FRP shells and/or heterogeneity of cracked concrete; (vi) load eccentricities

caused by specimen imperfections and/or test setup imprecisions; (vii) multiaxial stress condition generated on the FRP shell; and (viii) effect of the curvature of the FRP shell.

To establish the relationship of the hoop rupture strain of the FRP shell ($\varepsilon_{h,rup}$) and the ultimate tensile strain of the material (ε_f or ε_{frp}) , a strain reduction factor (k_ε) was defined by Pessiki et al. [17] (Eq. 2). Lam and Teng [3] then defined a term called the actual confining pressure ($f_{lu,a}$) (Eq. 3), by replacing the ultimate tensile strain (ε_f or ε_{frp}) of the material with the hoop rupture strain of the FRP shell ($\varepsilon_{h,rup}$) in Eq. 1.

$$\varepsilon_{h,rup} = k_{\varepsilon,f}\varepsilon_f \text{ or } \varepsilon_{h,rup} = k_{\varepsilon,frp}\varepsilon_{frp} \tag{2}$$

$$f_{lu,a} = \frac{2E_f t_f \varepsilon_{h,rup}}{D} \tag{3}$$

In Eq. 2, due attention should be given to ensure that the strain reduction factors ($k_{\varepsilon,f}$ or $k_{\varepsilon,frp}$) are used consistently with the corresponding ultimate material tensile strain (ε_f or ε_{frp}). In the studies examined, the properties of the FRP confinement systems were reported in several different ways. The reported details included: (i) the manufacturer specified properties of fibers; (ii) the manufacturer specified properties of FRP (iii) FRP properties as determined from flat coupon tests based on measured coupon thickness; (iv) FRP properties as determined from flat coupon tests based on nominal fiber sheet thickness; and (v) FRP properties as determined from ring-splitting tests. Only a small number of studies [10, 26, 27] reported the FRP properties obtained from ring-splitting tests, and the majority of the studies provided the properties obtained from flat coupon tests or supplied by manufacturers. As for the FRP properties obtained from flat coupon tests, in some of the studies [18, 28-36] the elastic moduli (E_{frp}) and tensile stresses (f_{frp}) were calculated based on nominal fiber thickness instead of the measured thickness of flat FRP coupons. The datasets from these studies are marked with the superscript '*t*' in Tables 3 to 7.

In the database provided in Tables 3 to 7, due attention was given to establish a clear distinction between the fiber and FRP properties in the reported values of the elastic modulus (E_f or E_{frp}), tensile strength (f_f or f_{frp}), and total thickness (t_f or t_{frp}) of the confining material. In the model assessment and development, if a dataset included both fiber and FRP properties, the model predictions were based on the fiber properties, unless the fiber properties were marked with the superscript '*f*' indicating they were either incomplete or established to be inaccurate based on the analysis of the database.

3.2 FRP confinement technique

A potentially important distinction, often recognized by the models assessed in the present study, is the one that is made between FRP-wrapped and FRP tube-encased specimens. Previously, both Mirmiran et al. [9] and Lam and Teng [2] reported that there was no significant difference between the behaviors of FRP-wrapped and FRP tube-encased concrete specimens. On the other hand, Saafi et al. [12] concluded that the ultimate condition of FRP-confined concrete was influenced by the adopted confinement technique.

In the present study, the test database was sorted into two categories and the results of the FRP-wrapped and FRP tube-encased specimens are presented in separate tables. Tables 3 to 6 show the results for FRP-wrapped concrete, whereas Table 7 reports the results for FRP tube-encased specimens. Comparison of the trends of the strength and strain enhancement ratios of FRP-wrapped specimens with those of FRP tube-encased specimens (Figures 2 and 3) indicate that there are noticeable differences between the ultimate conditions of these two groups of specimens. However, it is not possible to draw a definitive conclusion based on these observations, as in the database the FRP-wrapped specimens significantly outnumber the FRP tube-encased specimens. It is possible that observed differences might have been caused partly or entirely by the differences in the data ranges and specimen distributions between the two sets of test results.

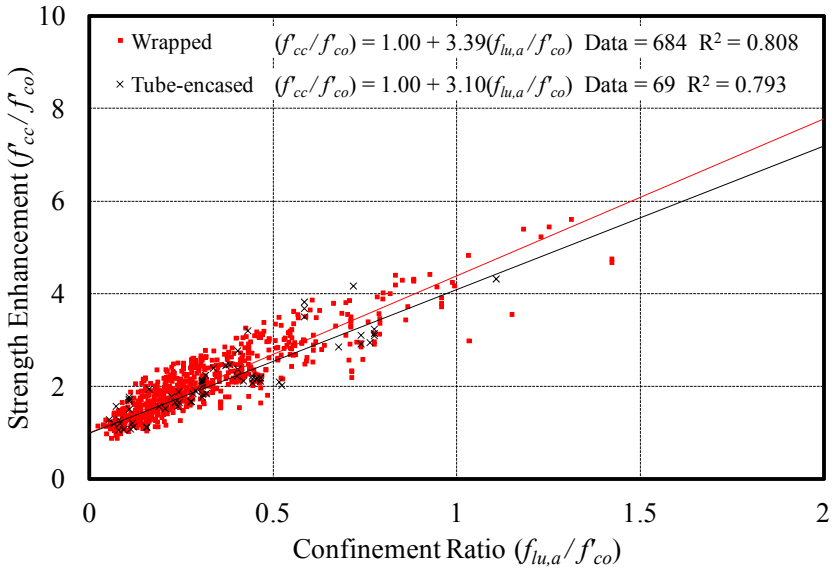

Figure 2. Variation of strength enhancement ratio with confinement ratio

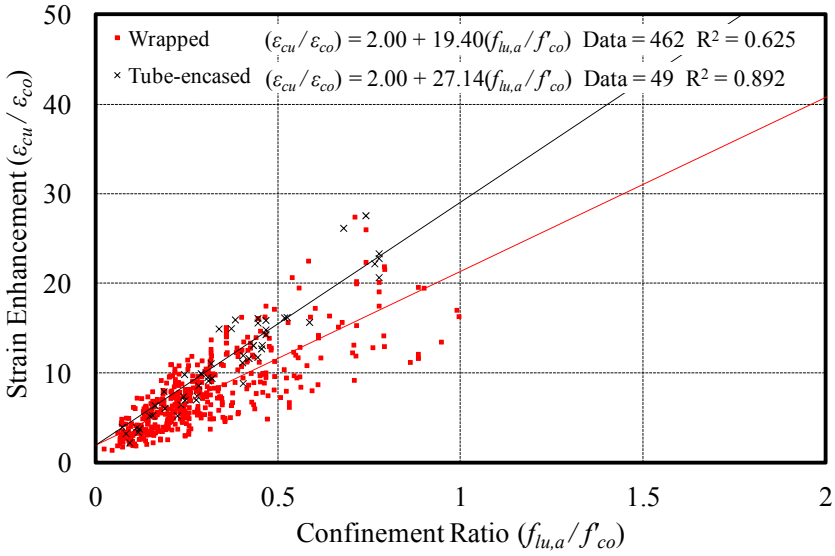

Figure 3. Variation of strain enhancement ratio with confinement ratio

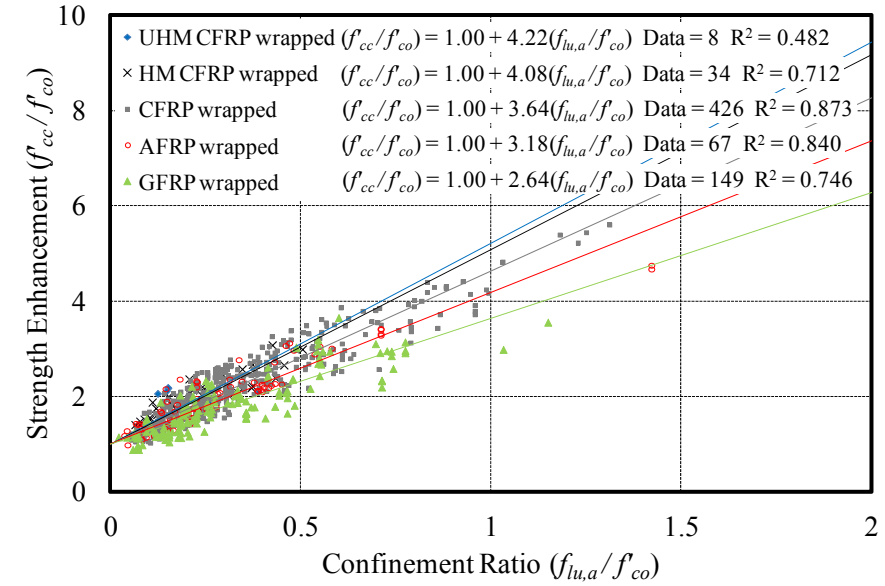

(a)

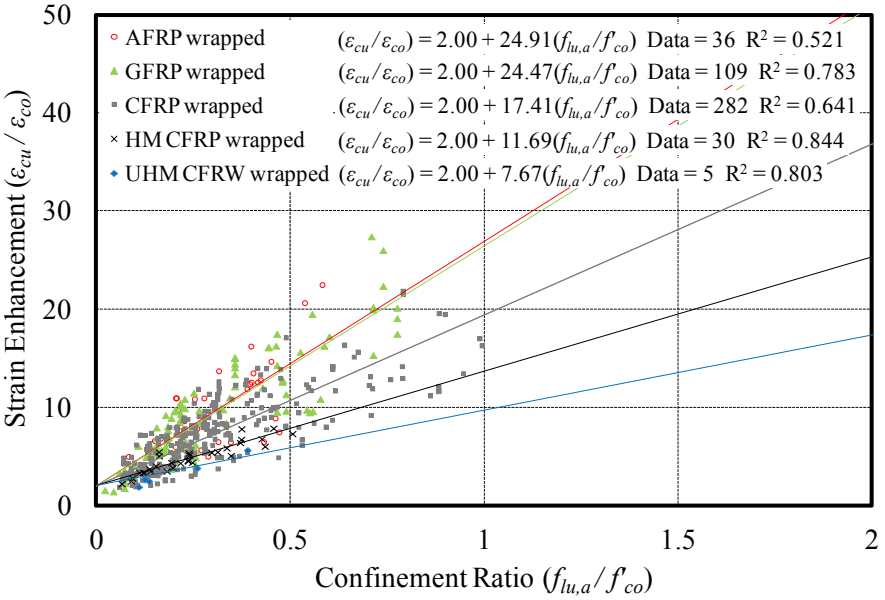

(b)

Figure 4. Influence of FRP type on ultimate conditions of FRP-confined concrete: (a) compressive strength; (b) ultimate axial strain

3.3 Type of FRP material

Several previous studies have focused on the influence of the types of FRP materials on the behavior of FRP-confined concrete (e.g., [3, 18, 37, 38]). Most of these studies reported that, for a given confinement ratio ($f_{lu,a}/f'_{co}$), the compressive strength (f'_{cc}) of FRP-confined concrete is influenced only marginally by the type of FRP material; whereas, it was found that the ultimate strain of FRP-confined concrete (ε_{cu}) is highly sensitive to the material properties of the confining FRP. It is now understood that, for a given confinement ratio

($f_{lu,a}/f'_{co}$), the ultimate axial strain of the FRP-confined concrete increases with the increased ultimate tensile strain (ε_f or ε_{frp}) of the materials used in confining it. This understanding is supported by the trends of the test results reported in the database of the present study [Figures 4 (a) and (b)]. It is evident from these figures that the trend lines of the strain enhancement ratios are sensitive to the type of FRP, whereas the strength enhancement ratio is not highly influenced by changes in the type of FRP.

Given its direct influence on the actual confinement ratio ($f_{lu,a}/f'_{co}$) and therefore the ultimate condition of FRP-confined concrete, it is obvious that the accurate determination of hoop rupture strains plays an instrumental role in the prediction of the ultimate condition of FRP-confined concrete. The average values of the strain reduction factors determined from the database reported in the present study (Table 8), point to the influence of the fiber type on the strain reduction factor ($k_{\varepsilon,f}$) and hence on the hoop rupture strains. This influence, which was also reported previously in Ozbakkaloglu and Akin [39] and Dai et al. [40], is discussed further later in the paper.

3.4 Instrumentation details of specimens reported in the database

The ultimate axial strains (ε_{cu}) and FRP hoop rupture strains ($\varepsilon_{h,rup}$) in the database are the average values obtained by strain gauges or deformation measuring devices. In the previous studies, a number of measurement methods were used to record the ultimate axial strains, including: (i) strain gauges attached to the surface of FRP shells (AS); (ii) deformation measuring devices, such as linear variable deformation transducers (LVDTs), extensometers or dial gauges mounted between each platen of the axial compression test machine (AFL); and (iii) measuring devices mounted within a certain gauge length along the height of the specimens (AML).

Similarly, different measuring methods have been used in measuring the hoop strains, including methods (i) and (iii) noted above, with strain gauges or measuring devices oriented in the hoop direction. Information regarding the specific methods in the measurement of both of these strains is reported in the final column of Table 2 for each study included in the database. For the specimens where multiple hoop strain gauges were used, such as the specimens tested by Lam and Teng [18], Smith et al. [36], and Wu and Jiang [24], the average values of the strain gauge measurements have been recorded in the database. In the calculations of the average values, due attention was given to the exclusion of inconsistent strain gauge readings, such as those coming from the overlap regions of FRP sheets.

3.5 Test database size and scatter

Test databases inherently produce a scatter of test results. Bisby et al. [5] reported that the scatter of test results caused an average absolute error (*AAE*) of no less than 13% for the strength enhancement ratio (f'_{cc}/f'_{co}) and 35% *AAE* for the strain enhancement ratio ($\varepsilon_{cu}/\varepsilon_{co}$) in their database of approximately 200 datasets. The natural scatter of the database reported in the present study was lower than these thresholds, with *AAE* values of 11% and 23% for strength and strain enhancement ratios respectively, even though the size of the database was

significantly larger with 832 datasets. The relatively low scatter of this database was achieved through the use of carefully chosen selection criteria in the collection of the test data, as outlined previously, to ensure consistency and reliability.

As was reported previously in De Lorenzis and Tepfers [4], variability in material properties of the test specimens, such as the stiffness of the FRP confining shell, the type and size of aggregates used in the concrete mix, and the mix proportions and moisture content of the concrete, contribute to the scatter found in test databases. As discussed in Section 3.4, the differences in the instrumentation of the specimens and the setups used in testing them also contribute significantly to scatter. In particular, the two key ultimate condition properties, the ultimate axial strain (ε_{cu}) and hoop rupture strain ($\varepsilon_{h,rup}$), are highly sensitive to the instrumentation arrangement used in specimen testing. Figure 5 shows the variation of the strain enhancement ratios ($\varepsilon_{cu}/\varepsilon_{co}$) with the actual confinement ratios ($f_{lu,a}/f'_{co}$), as obtained using different axial strain measurement methods. Only CFRP-wrapped specimens, which formed the largest sub-group in the database, were included in Figure 5 in order to eliminate the additional influences caused by differences in the type of FRP and the method of confinement. Differences in the trendlines shown in Figure 5 suggest that the recorded ultimate axial strains may be influenced by the measurement method used in their determination.

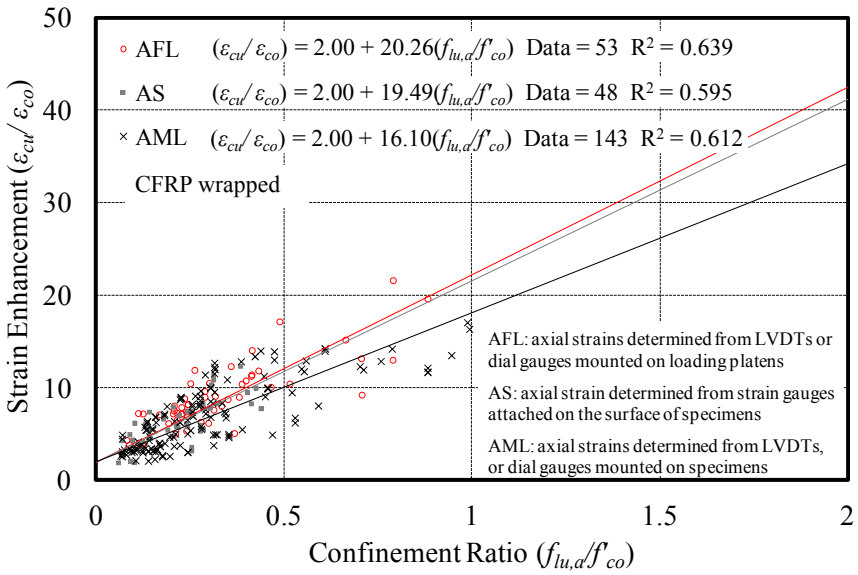

Figure 5. Influence of measurement method on ultimate strain of CFRP-wrapped concrete

Similarly, it should be expected that the average recorded hoop rupture strains ($\varepsilon_{h,rup}$) will be influenced by the number and placement of strain gauges used in the measurement of these strains. As reported originally in Lam and Teng [3], hoop strains measured within the overlap regions of the FRP jackets are known to be lower than those measured elsewhere around the perimeter of the same FRP jacket. It follows, therefore, that the differences in the hoop strain gauge arrangements of the specimens included in the database are one of the main reasons for the inherent scatter in the hoop rupture strain data reported in the database.

4. A NEW DESIGN-ORIENTED MODEL

This section presents a new design-oriented model to predict the ultimate condition of FRP-confined concrete. The model contains closed-form expressions that were developed using the test database presented in Tables 3 to 7. Not all the datasets included in the database contained all the relevant details required for the development of all the components of the model. Furthermore, as discussed previously, the results that failed to satisfy the criteria outlined in Section 2.2 were excluded from model development. The total number of datasets that were used in the calibration of the hoop strain reduction factor (k_ε), strength enhancement coefficient (k_1), and strain enhancement coefficient (k_2) are given in Tables 8 to 10, respectively.

Table 8. Average hoop rupture strain reduction factor (k_ε) with FRP type and confinement technique

Specimens	$k_{\varepsilon,f}$			$k_{\varepsilon,frp}$		
	Number	SD	Average	Number	SD	Average
All	201	0.135	0.675	150	0.125	0.709
All wrapped	186	0.134	0.675	146	0.126	0.707
CFRP wrapped	131	0.115	0.680	116	0.127	0.682
GFRP wrapped	25	0.084	0.793	23	0.059	0.803
AFRP wrapped	8	0.087	0.732	7	0.066	0.809
HM CFRP wrapped	22	0.115	0.493	-	-	-
UHM CFRP wrapped	-	-	-	-	-	-
All tube-encased	15	0.157	0.675	4	0.047	0.775
CFRP tube-encased	4	0.033	0.690	-	-	-
GFRP tube-encased	5	0.094	0.723	4	0.047	0.775
AFRP tube-encased	4	0.055	0.775	-	-	-
HM CFRP tube-encased	-	-	-	-	-	-
UHM CFRP tube-encased	2	0.051	0.326	-	-	-

4.1 Hoop rupture strain of FRP-confined concrete

Table 8 provides the values of the strain reduction factors ($k_{\varepsilon,f}$ and $k_{\varepsilon,frp}$) determined from the database presented in this paper. Using these values together with the ones obtained from the tests of over 250 FRP-confined high-strength concrete specimens reported in Lim and Ozbakkaloglu [41], the key parameters that influence the strain reduction factor were indentified. It was found that the increase in either the compressive strength of concrete (f'_{co}) or elastic modulus of confining fibers (E_f) result in a decrease in the recorded hoop rupture strains ($\varepsilon_{h,rup}$) and hence in the strain reduction factors ($k_{\varepsilon,f}$ and $k_{\varepsilon,frp}$). The former influence was first reported in Ozbakkaloglu and Akin [39] and it can be attributed to the increased concrete brittleness with increasing concrete strength, which alters the concrete crack patterns from heterogenic microcracks to localized macrocracks. The observed dependence of the strain reduction factor to the type of confining fibers was previously noted in Ozbakkaloglu and Akin [39] and Dai et al. [40]. Further observations from the comprehensive database reported in this study on the relationship between the elastic modulus of confining fibers (E_f) and recorded hoop rupture strains ($\varepsilon_{h,rup}$) indicate that the influence of the fiber brittleness on the strain reduction factor resembles the aforementioned influence of the concrete brittleness on the same factor. The statistical quantification of the influences of these two parameters

resulted in the expression given in Eq. 4 for the calculation of the hoop rupture strain reduction factor of fibers ($k_{\varepsilon,f}$) . The expression is capable of predicting the $k_{\varepsilon,f}$ for FRP-confined concrete with an unconfined concrete strength up to 120 MPa, and confined by any of GFRP, AFRP, CFRP, HM FRP or UHM CFRP.

$$k_{\varepsilon,f} = 0.9 - 2.3 f'_{co} \times 10^{-3} - 0.75 E_f \times 10^{-6} \tag{4}$$

where f'_{co} and E_f are in MPa.

4.2 Compressive strength of FRP-confined concrete

The proposed compressive strength expression (Eq. 5) incorporates several important parameters which were previously identified in Ozbakkaloglu et al. [1]. The strength enhancement effect at the first peak stress (f'_{c1}) of the stress-strain response is captured using Eq. 6 as a function of the confinement stiffness of the FRP shell (K_l). In order for the FRP-confined concrete to achieve a strain-hardening response after the first peak stress (f'_{c1}), the stiffness of the FRP reinforcing shell (K_l) has to exceed a minimum threshold value. The confining pressure at the corresponding condition is defined as the threshold confining pressure (Eq. 7) and can be estimated based on the corresponding hoop strain (ε_{l1}) (Eq. 8) in the FRP shell. As the proposed strength expression (Eq. 5) is only applicable to specimens that achieves strength enhancement after the first peak stress (f'_{c1}), the expression satisfies the confinement stiffness threshold requirement as given in Eq. 9. The prediction of the strength enhancement effect after the first peak stress (f'_{c1}) is based on the net confining pressure, that is, the reduced actual confining pressure ($f_{lu,a}$) after subtraction of the threshold confining pressure (f_{lo}). The strength enhancement effect generated by the net confining pressure is quantified using the coefficient of strength enhancement (k_1) in Eq. 5. It was found that establishing the compressive strength expression based on the net confining pressure yields an improved model prediction especially for specimens with higher unconfined concrete strengths (f'_{co}).

$$f'_{cc} = c_1 f'_{co} + k_1 \left(f_{lu,a} - f_{lo} \right) \tag{5}$$

$$c_1 = \frac{f'_{c1}}{f'_{co}} = 1 + 0.0058 \frac{K_l}{f'_{co}} \tag{6}$$

$$f_{lo} = K_l \varepsilon_{l1} \tag{7}$$

$$\varepsilon_{l1} = \left(0.43 + 0.009 \frac{K_l}{f'_{co}} \right) \varepsilon_{co} \tag{8}$$

$$K_l = \frac{2 E_f t_f}{D} \text{ and } K_l \geq f'^{1.65}_{co} \tag{9}$$

where K_l and f'_{co} are in unit MPa. It should be noted that the expression given in Eq. 5 is intended for FRP-confined concrete exhibiting a stress-strain curve with an ascending second branch. To this end, a statistically established condition equation, which is based on the

observed influence of the confinement stiffness (K_l) and concrete strength (f'_{co}) on the trend of the second branch, is given in Eq. 9 as part of the proposed expression.

Table 9 summarizes the values of the strength enhancement coefficient (k_1) calibrated from the database for different types of FRP materials and confinement methods. It should be noted that the k_1 values of the UHM CFRP-wrapped and HM and UHM CFRP tube-encased specimens are not presented in the table due to unreliability of the results caused by very limited number of available datasets. Additional experimental results are required to be able to determine reliable k_1 values for these specific subgroups. In the absence of these results, the average value of k_1 established from the database (i.e. k_1 = 3.2) can be used for conservative estimates of these specimens.

Table 9. Variation of strength enhancement coefficients (k_1) with FRP type and confinement technique

Specimens	k_1		
	Number	R^2	*Average*
All	753	0.799	3.22
All wrapped	684	0.806	3.26
CFRP wrapped	426	0.870	3.67
GFRP wrapped	149	0.759	2.49
AFRP wrapped	67	0.889	3.30
HM CFRP wrapped	34	0.772	4.96
UHM CFRP wrapped	8	-	-
All tube-encased	69	0.759	2.94
CFRP tube-encased	14	0.907	2.87
GFRP tube-encased	36	0.731	2.92
AFRP tube-encased	12	0.811	2.95
HM CFRP tube-encased	3	-	-
UHM CFRP tube-encased	4	-	-

4.3 Ultimate axial strain of FRP-confined concrete

As reported in Ozbakkaloglu et al. [1] almost all of the better performing ultimate strain enhancement expressions proposed in the literature have non-linear forms in their predictions of the strain enhancement ratio ($\varepsilon_{cu}/\varepsilon_{co}$) as a function of confinement ratios ($f_{lu,a}/f'_{co}$) (e.g. [42, 43]). This is due to the dependency of the strain enhancement ratio ($\varepsilon_{cu}/\varepsilon_{co}$) to the ultimate tensile strain of the material (ε_f or ε_{frp}), in addition to the confinement ratio ($f_{lu,a}/f'_{co}$), as was pointed out in a number of previous studies [3, 18, 37, 39]. To develop unified strain enhancement expressions for different types of FRP materials in model presented in this paper, the axial strain (ε_{cu}) was quantified as a non-linear function of the confinement stiffness (K_l), hoop rupture strain ($\varepsilon_{h,rup}$), and unconfined concrete strength (f'_{co}), as given in Eq. 10. In the equation, k_2 is the coefficient of strain enhancement and c_2 (Eq. 11) is the concrete strength factor, which is incorporated into the proposed expression to allow for the change in the shape of the stress-strain curve of unconfined concrete with the variation of concrete strength (f'_{co}). In Eq. 10, the axial strain corresponding to the unconfined concrete peak strength (ε_{co}) is determined by the expression given by Tasdemir et al. [44] (Eq. 12).

Table 10. Variation of strain enhancement coefficients (k_2) with FRP type and confinement technique

Specimens	All, k_2			AS, k_2			AFL, k_2			AML, k_2		
	Number	R^2	*Average*	Number	R^2	*Average*	Number	R^2	*Average*	Number	R^2	*Average*
All	511	0.786	0.271	53	0.583	0.270	179	0.831	0.297	215	0.723	0.261
All wrapped	462	0.753	0.266	50	0.564	0.271	134	0.809	0.296	215	0.723	0.261
CFRP wrapped	282	0.682	0.267	48	0.546	0.269	53	0.677	0.296	143	0.660	0.259
GFRP wrapped	109	0.820	0.262	-	-	-	40	0.719	0.281	60	0.765	0.249
AFRP wrapped	36	0.613	0.265	2	1.000	0.339	15	0.847	0.355	8	0.981	0.334
HM CFRP wrapped	30	0.688	0.320	-	-	-	26	0.714	0.320	4	0.863	0.321
UHM CFRP wrapped	5	-	-	-	-	-	-	-	-	-	-	-
All tube-encased	49	0.883	0.298	3	0.433	0.258	45	0.870	0.299	-	-	-
CFRP tube-encased	12	0.959	0.268	-	-	-	11	0.965	0.272	-	-	-
GFRP tube-encased	22	0.862	0.298	3	0.433	0.258	19	0.797	0.300	-	-	-
AFRP tube-encased	12	0.351	0.302	-	-	-	12	0.351	0.302	-	-	-
HM CFRP tube-encased	3	-	-	-	-	-	3	-	-	-	-	-
UHM CFRP tube-encased	-	-	-	-	-	-	-	-	-	-	-	-

Specimen instrumentation notes:

AS denotes axial strains were determined from axial axial strain gauges mounted on the surface of the specimens at mid-height of specimens

AFL denotes axial strains were determined from LVDTs or dial gauges mounted on loading platens to measure deformations along the full height of specimens

AML denotes axial strains were determined from LVDTs or dial gauges mounted on the specimens to measure deformations within a gauge length along the height of specimens

$$\varepsilon_{cu} = c_2\varepsilon_{co} + k_2\left(\frac{K_l}{f'_{co}}\right)^{0.9}\varepsilon_{h,rup}^{1.35} \quad (10)$$

$$c_2 = 2 - \frac{(f'_{co} - 20)}{100} \text{ and } c_2 \geq 1 \quad (11)$$

$$\varepsilon_{co} = \left(-0.067 f'^{2}_{co} + 29.9 f'_{co} + 1053\right) \times 10^{-6} \quad (12)$$

In Eqs. 11 and 12, f'_{co} is in MPa.

Table 10 summarizes the values of the strain enhancement coefficient (k_2) values calibrated from the database for different types of FRP materials, confinement methods and axial strain measurement methods. As discussed previously in Section 3.5, the magnitude of the recorded ultimate axial strains may be influenced by the methods used in the measurement of the strains. In Table 10, in addition to the average values of the strain enhancement coefficients (k_2), its specific values obtained from each of the three aforementioned axial strain measurement methods are also given. As can be seen in Table 10, k_2 is not sensitive to FRP type and hence it is recommended that an average value of k_2 = 0.27 can be used in Eq.10 independent of FRP material type.

4.4 Comparison with test data

Figure 6 shows comparisons of the strength and strain enhancement (f'_{cc}/f'_{co} and $\varepsilon_{cu}/\varepsilon_{co}$) predictions of the proposed model with results from the database presented in this paper. These comparisons indicate that the model predictions are in close agreement with the test results, which are quantified through the use of statistical indicators: average absolute error (*AAE*) to establish overall model accuracy; mean (*M*) to establish average overestimation or underestimation of the model; and standard deviation (*SD*) to establish the magnitude of the associated scatter. The details of the assessment procedure can be found in Ozbakkaloglu et al. [1].

To establish the relative performance of the proposed model, its prediction statistics were compared with those of a group of selected models, which were identified as the best performing models [3-5, 7, 32, 42, 43, 45-53] among over 80 existing models reviewed in Ozbakkaloglu et al. [1] and a few additional models proposed in 2012 and 2013. The lists of the 10 most accurate strength and strain models are given in Tables 11 and 12, respectively, together with their prediction statistics for strength and strain enhancement ratios (f'_{cc}/f'_{co} and $\varepsilon_{cu}/\varepsilon_{co}$). Figures 7(a) and 7(b), respectively, show the average absolute errors (*AAE*) of the strength and strain enhancement ratio predictions of these models. The comparisons of the model prediction statistics shown in Figure 7 and Tables 11 and 12 demonstrate the improved accuracy of the proposed model over the best performing existing models. The improvement on the prediction of the ultimate strain enhancement ratio ($\varepsilon_{cu}/\varepsilon_{co}$) is particularly significant, which is achieved through the use of an expression (Eq.10) that accurately captures the relative influences of the key parameters. It might be worth noting that in the evaluation of

the models, the experimentally recorded hoop rupture strains ($\varepsilon_{h,rup}$) were used rather than the values or expressions recommended by the original models for the calculation of $\varepsilon_{h,rup}$. In the absence of the experimental values, $\varepsilon_{h,rup}$ was established using the average value of $k_{\varepsilon,f}$ or $k_{\varepsilon,frp}$ reported in Table 8 in the assessment of the existing models, and it was calculated from Eq.4 in the assessment of the proposed model. It might be worth noting that the proposed model would have outperformed the existing models even more significantly if the hoop rupture strains were established using the original model expressions.

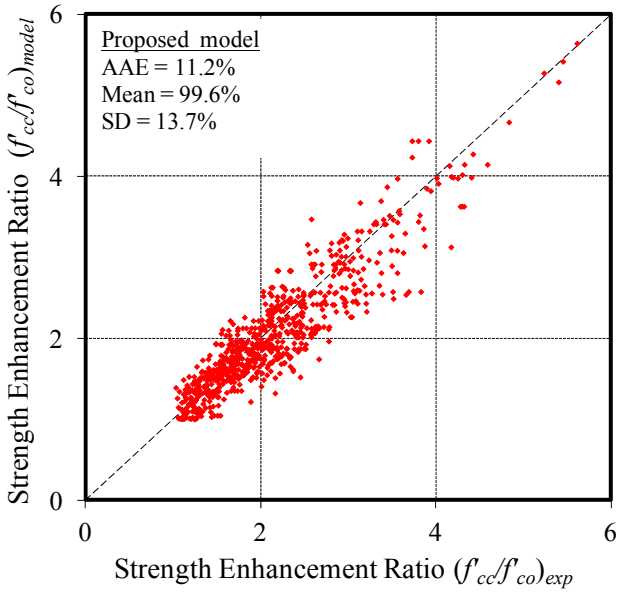

(a)

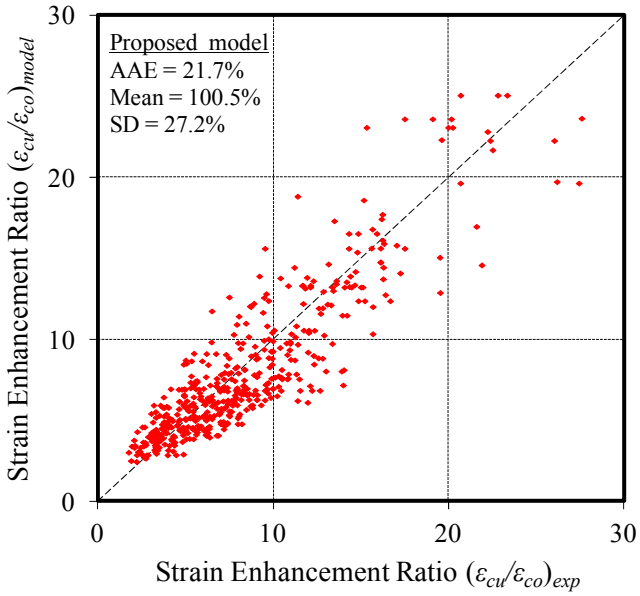

(b)

Figure 6. Comparison of model predictions of: (a) strength enhancement ratios (f'_{cc}/f'_{co}) and (b) strain enhancement ratios ($\varepsilon_{cu}/\varepsilon_{co}$) with experimental data

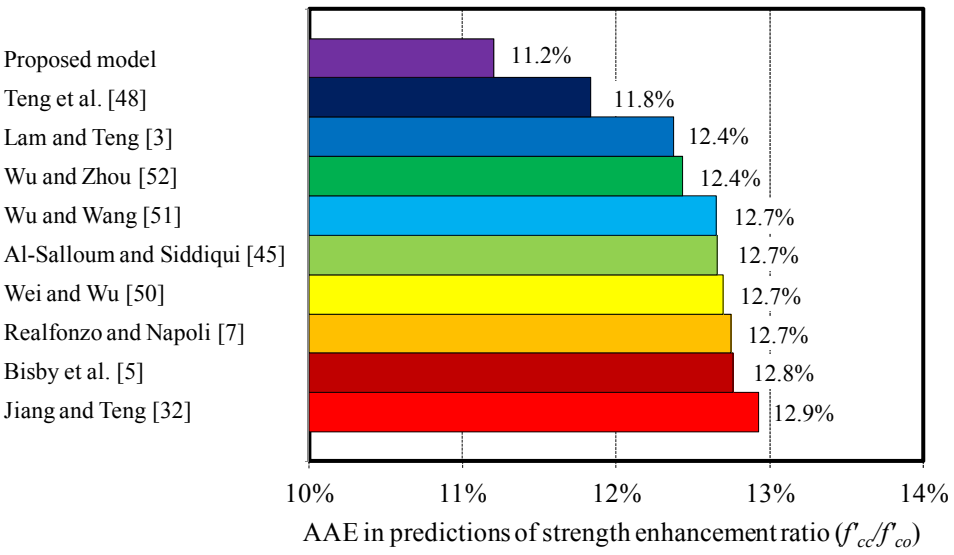

(a)

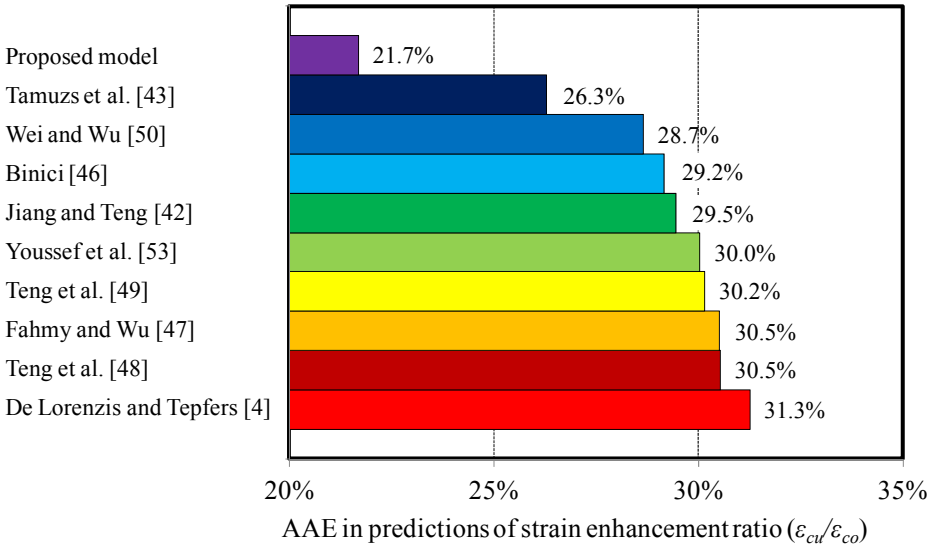

(b)

Figure 7. Average absolute error in model predictions of: (a) strength enhancement ratios (f'_{cc}/f'_{co}), (b) strain enhancement ratios ($\varepsilon_{cu}/\varepsilon_{co}$)

Table 11. Statistics of strength enhancement ratio (f'_{cc}/f'_{co}) predictions of best performing models

Model	Prediction of f'_{cc}/f'_{co}			
	Test data	Average Absolute Error (%)	Mean (%)	Standard Deviation (%)
Proposed model	753	11.2	99.6	13.7
Teng et al. [48]	753	11.8	98.8	14.5
Lam and Teng [3]	753	12.4	99.4	15.3
Wu and Zhou [52]	753	12.4	102.1	15.5
Wu and Wang [51]	753	12.7	101.4	15.7
Wei and Wu [50]	753	12.7	101.5	15.7
Al-Salloum and Siddiqui [45]	753	12.7	101.7	15.8
Realfonzo and Napoli [7]	753	12.7	103.2	15.8
Bisby et al. [5]	753	12.8	101.9	15.8
Jiang and Teng [32]	753	12.9	93.9	14.6

Table 12. Statistics of strain enhancement ratio ($\varepsilon_{cu}/\varepsilon_{co}$) predictions of best performing models

Model	Prediction of $\varepsilon_{cu}/\varepsilon_{co}$			
	Test data	Average Absolute Error (%)	Mean (%)	Standard Deviation (%)
Proposed model	511	21.7	100.5	27.2
Tamuzs et al. [43]	511	26.3	108.4	35.0
Wei and Wu [50]	511	28.7	98.0	35.8
Binici [46]	511	29.2	92.3	34.8
Jiang and Teng [42]	511	29.5	116.1	38.5
Youssef et al. [53]	511	30.0	112.5	39.0
Teng et al. [49]	511	30.2	117.6	39.0
Fahmy and Wu [47]	511	30.5	99.5	38.9
Teng et al. [48]	511	30.5	117.0	39.3
De Lorenzis and Tepfers [4]	511	31.3	77.9	27.9

5. CONCLUSIONS AND RECOMMENDATIONS

This paper has presented a comprehensive test database of 832 datasets that was assembled by the authors through an extensive review of the literature that covered 253 experimental studies published on the compressive behavior of FRP-confined concrete. Initially, 3042 test results were collected from the published literature. The suitability of these results for the database was then assessed using carefully composed selection criteria to ensure the reliability and consistency of the database. Using the criteria to refine the contents of the database resulted in a final database size of 832 datasets collected from 99 experimental studies published between 1992 and the middle of 2013. Key features of each study included in the database, including the range of the key test parameters and the specimen instrumentation information, have been summarized and important observations regarding these studies have been marked on the database tables. The database that has been presented

in this paper will serve as a valuable reference document for future model development efforts. In the final part of the paper, a design-oriented model for predicting the ultimate conditions of FRP-confined concrete is presented. The proposed model provides improved predictions of the compressive strength and ultimate axial strain of FRP-confined concrete compared to the existing models.

Based on the observations made during the compilation of the experimental database, the following conclusions can be drawn:

1. Analysis of the results reported in the database indicate that the average values of the hoop strain reduction factors based on fiber and FRP properties ($k_{\varepsilon,f}$ and $k_{\varepsilon,frp}$) are equal to 0.675 and 0.709, respectively. The observed variation of the average k_{ε} values according to fiber type points to the possible influence of the type of fibers on the strain reduction factor.
2. Two key ultimate condition properties, namely ultimate axial strain (ε_{cu}) and hoop rupture strain ($\varepsilon_{h,rup}$), are both highly sensitive to the instrumentation arrangement used in specimen testing. Therefore, the variability in the instrumentation arrangements used in different studies contributes to scatter in the database.
3. There are differences between the strength and strain enhancement ratios of FRP-wrapped and FRP-tube encased specimens included in the database of the present study. However, due to the differences between the number and parametric ranges of FRP-wrapped and FRP tube-encased specimens, it is not possible to draw a definitive conclusion based on these observations.

As noted previously, it was not possible to include all the test results published in the literature in the database presented in this paper, due to a lack of information in regards to the material properties, geometric properties or ultimate conditions of these specimens. Therefore, in future studies, effort should be made to ensure that the results of the experiments are presented with a complete set of information, providing as much relevant information as possible about the material and geometric properties of the specimens, test setup and instrumentation, recorded capacities of the specimens and their failure modes. Furthermore, in future experimental studies due consideration should be given to the instrumentation of the specimens for the accurate measurement of ultimate axial strains and hoop rupture strains.

NOMENCLATURE

AAE	Average absolute error
c_1	Parameter in ultimate strength expression
c_2	Parameter in ultimate strain expression
D	Diameter of concrete core (mm)
E_f	Elastic modulus of fibers (MPa)
E_{frp}	Elastic modulus of FRP material (MPa)
f'_{cc}	Ultimate axial compressive stress of FRP-confined concrete (MPa)
f'_{co}	Peak axial compressive stress of unconfined concrete (MPa)
f'_{c1}	Axial compressive stress of FRP-confined concrete at first peak (MPa)
f_f	Ultimate tensile strength of fibers; $f_f = E_f\varepsilon_f$ (MPa)
f_{frp}	Ultimate tensile strength of FRP material; $f_{frp} = E_{frp}\,\varepsilon_{frp}$ (MPa)
f_l	Confining pressure (MPa)
f_{lo}	Threshold confining pressure (MPa)
f_{lu}	Nominal lateral confining pressure at ultimate; $f_{lu} = K_l\varepsilon_f$ or $f_{lu} = K_l\varepsilon_{frp}$ (MPa)
$f_{lu,a}$	Actual lateral confining pressure at ultimate; $f_{lu,a} = K_l\,\varepsilon_{h,rup}$ (MPa)
H	FRP confined concrete specimen height (mm)
K_l	Lateral confinement stiffness (MPa); $K_l = 2\,E_f t_f/D$ or $2\,E_{frp}t_{frp}/D$
k_1	Axial strength enhancement coefficient
k_2	Axial strain enhancement coefficient
k_ε	Hoop strain reduction factor
$k_{\varepsilon,f}$	Hoop strain reduction factor of fibers
$k_{\varepsilon,frp}$	Hoop strain reduction factor of FRP material
M	Mean
SD	Standard deviation
t_f	Total nominal thickness of fibers (mm)
t_{frp}	Total thickness of FRP material (mm)
ε_{co}	Axial strain of unconfined concrete at f'_{co}
ε_{c1}	Axial strain of FRP-confined concrete at f'_{c1}
ε_{cu}	Ultimate axial strain of FRP-confined concrete
ε_f	Ultimate tensile strain of fibers
ε_{frp}	Ultimate tensile strain of FRP material
$\varepsilon_{h,rup}$	Hoop rupture strain of FRP shell
ε_{11}	Hoop strain of FRP-confined concrete at f'_{c1}

REFERENCES

1. Ozbakkaloglu, T., Lim, J. C, and Vincent, T., (2013). "FRP-confined concrete in circular sections: Review and assessment of stress–strain models." *Eng. Struct.,* 49, p. 1068–1088.
2. Lam, L., and Teng, J. G., (2002). "Strength models for fiber-reinforced plastic-confined concrete." *ASCE J. Struct. Eng.,* 128(5), p. 612-623.
3. Lam, L., and Teng, J. G., (2003). "Design-oriented stress-strain model for FRP-confined concrete." *Constr. Build. Mater.,* 17(6-7), p. 471-489.
4. De Lorenzis, L., and Tepfers, R., (2003). "Comparative study of models on confinement of concrete cylinders with fiber reinforced polymer Composites." *ASCE J. Compos. Constr.,* 7(3), p. 219-237.
5. Bisby, L.A., Dent, A. J. S., Green, M. F., (2005). "Comparison of confinement models for fiber-reinforced polymer-wrapped concrete." *ACI Struct. J.,* 102(1), p. 62-72.
6. Turgay, T., Köksal, H. O., Polat, Z., and Karakoc, C., (2009). "Stress-strain model for concrete confined with CFRP jackets." *Materials and Design,* 30(8), p. 3243-3251.
7. Realfonzo, R. and Napoli, A., (2011). "Concrete confined by FRP systems: Confinement efficiency and design strength models." *Composites Part B: Engineering,* 42, p. 736-755.
8. Harries, K.A., and Carey, A., (2002). "Shape and 'gap' effects on the behavior of variably confined concrete." *Cem. Concr. Res.,* 33(6), p. 873-880.
9. Mirmiran, A., Shahawy, M., Samaan, M., El Echary, H., Mastrapa, J. C., and Pico, O., (1998). "Effect of Column Parameters on FRP-confined Concrete." *ASCE J. Compos. Constr.,* 2(4), p. 175-185.
10. Mastrapa, J.C., (1997). "Effect of construction bond on confinement with fiber composites." Masters, University of Central Florida, Orlando, Fla.
11. Matthys, S., Taerwe, L., and Audenaert, K., (1999). "Tests on axially loaded concrete columns confined by fiber reinforced polymer sheet wrapping." *Proc. 4th Int. Symp. On Fiber Reinforced Polymer Reinforcement for Reinforced Concrete Structures*, Detroit.
12. Saafi, M., Toutanji, H. A., and Li, Z., (1999). "Behavior of concrete columns confined with fiber reinforced Polymer tubes." *ACI Struct. J.,* 96(5), p. 500-509.
13. Hong, W.K., and Kim, H. C., (2004). "Behavior of concrete columns confined by carbon composite tubes." *Can. J. Ci. Eng.,* 31(2), p. 178-188.
14. Ozbakkaloglu, T. and Vincent, T., (2013). "Axial compressive behavior of high- and ultra high-strength concrete-filled FRP tubes." *J. Compos. Constr.,* (Submitted).
15. Xiao, Y., and Wu, H., (2000). "Compressive behavior of concrete confined by carbon fiber composite jackets." *J. Mater. Civ. Eng.,* 12(2), p. 139-146.
16. Shahawy, M., Mirmiran, A., and Beitelman, T., (2000). "Tests and modeling of carbon-wrapped concrete columns." *Composites Part B: Engineering.,* 31(471 - 480).
17. Pessiki, S., Harries, K. A., Kestner, J., Sause, R., and Ricles, J. M., (2001). "The axial behavior of concrete confined with fiber reinforced composite jackets." *ASCE J. Compos. Constr.,* 5(4), p. 237-245.
18. Lam, L., and Teng, J. G., (2004). "Ultimate condition of FRP-confined concrete." *ASCE J. Compos. Constr.,* 8(6), p. 539-548.

19. Ozbakkaloglu, T., and Oehlers, D. J., (2008). "Concrete-filled Square and Rectangular FRP Tubes under Axial Compression." *ASCE J. Compos. Constr.,* 12(4), p. 469-477.
20. Ozbakkaloglu, T., and Oehlers, D. J., (2008). "Manufacture and testing of a novel FRP tube confinement system." *Eng. Struct.,* 30, p. 2448-2459.
21. Cui, C., and Sheikh, A., (2009). "Behaviour of normal and high strength concrete confined with fibre reinforced polymers (FRP)." Masters, Univ. of Toronto.
22. Ozbakkaloglu, T., (2012). "Concrete-filled FRP Tubes: Manufacture and Testing of New Forms Designed for Improved Performance." *ASCE J. Compos. Constr.,* 17(2), p. 280 -291.
23. Ozbakkaloglu, T., (2012). "Axial Compressive Behavior of Square and Rectangular High-Strength Concrete-Filled FRP Tubes." *ASCE J. Compos. Constr.,* 17(1), p. 151-161.
24. Wu, Y.-F. and Jiang, J.-F., (2013). "Effective strain of FRP for confined circular concrete columns." *Composite Structures,* 95, p. 479–491.
25. Ozbakkaloglu, T., (2013). "Compressive behavior of concrete-filled FRP tube columns: Assessment of critical column parameters." *Engineering Structures,* 51, p. 188-199.
26. Rousakis, T., You, C., De Lorenzis, L., and Tamuzs, V., (2003). "Concrete Cylinders Confined by Carbon FRP Sheets Subjected to Monotonic and Cyclic Axial Compressive Loads." *Proc. 6th Int. Symp. On FRP Reinforcement for Concrete Structures.*
27. Valdmanis, V., De Lorenzis, L., Rousakis, T., and Tepfers, R., (2007). "Behaviour and capacity of CFRP-confined concrete cylinders subjected to monotonic and cyclic axial compressive load." *Structural Concrete,* 8(4), p. 187-190.
28. Watanabe, K., Nakamura, R., Honda, Y., Toyoshima, M., Iso, M., Fujimaki, T., Kaneto, M., and Shirai, N., (1997). "Confinement effect of FRP sheet on strength and ductility of concrete cylinders under uniaxial compression." *Proc. Non-metallic Reinforcement for Concrete Structures*.
29. Lam, L., Teng, J. G., Cheung, C. H., and Xiao, Y., (2006). "FRP-confined concrete under cyclic axial compression." *Cem. Concr. Compos.,* 28(10), p. 948-958.
30. Stanton, J.F., and Owen, L. M., (2006). "The Influence of Concrete Strength and Confinement Type on the Response of FRP-Confined Concrete Cylinders." *ACI Special Publication October 2006,* 238, p. 347-362.
31. Wu, G., Lu, Z. T., and Wu, Z. S., (2006). "Strength and ductility of concrete cylinders confined with FRP composites." *Constr. Build. Mater.,* 20(3), p. 134-148.
32. Jiang, T., and Teng, J. G., (2007). "Analysis-oriented stress-strain models for FRP-confined concrete." *ASCE J. Eng. Struct.,* 29(11), p. 2968-2986.
33. Wang, L.M., and Wu, Y. F., (2008). "Effect of Corner Radius on the Performance of CFRP-Confined Square Concrete Columns: Test." *Eng. Struct.,* 30(2), p. 493-505.
34. Wong, Y.L., Yu, T., Teng, J. G., and Dong, S. L., (2008). "Behavior of FRP-confined concrete in annual section columns." *Composites Part B: Engineering.,* 39, p. 451-466.
35. Wu, G., Wu, Z. S., Lu, Z. T., and Ando Y. B., (2008). "Structural Performance of Concrete Confined with Hybrid FRP Composites." *J. Reinf. Plas. Compos.,* 27(12), p. 1323-1348.

36. Smith, S.T., Kim, S. J. and Zhang, H., (2010). "Behavior and Effectiveness of FRP Wrap in the Confinement of Large Concrete Cylinders." *ASCE J. Compos. Constr.,* 14, p. 573-582.
37. Karbhari, V.M., and Gao, Y., (1997). "Composite jacketed concrete under uniaxial compression-verification of simple design equations." *J. Mater. Civ. Eng.,* 9(4), p. 185-193.
38. Lin, H.J., and Chen, C. T., (2001). "Strength of concrete cylinder confined by composite materials." *J. Reinf. Plas. Compos.,* 20(18), p. 1577-1600.
39. Ozbakkaloglu, T., and Akin, E., (2011). "Behavior of FRP-confined normal- and high-strength concrete under cyclic axial compression." *ASCE J. Compos. Constr.,* 16(4), p. 451–463.
40. Dai, J.G., Bai, Y. L., and Teng, J. G., (2011). "Behavior and modeling of concrete confined with FRP composites of large deformability." *ASCE J. Compos. Constr.,* 15(6), p. 963–973.
41. Lim, J.C. and Ozbakkaloglu, T., (2013). "Confinement model for FRP-confined high-strength concrete." *J. Compos. Constr.,* 18(4), 04013058.
42. Jiang, T., and Teng, J. G., (2006). "Strengthening of short circular RC columns with FRP jackets: a design proposal." *Proc. 3rd Int. Conf. on FRP Composites in Civil Engineering*, Miami, Florida, USA.
43. Tamuzs, V., Tepfers., R, Zile, E., and Ladnova, O., (2006). "Behavior of concrete cylinders confined by a carbon composite III: deformability and the ultimate axial strain." *Mech. Compos. Mater.,* 42(4), p. 303-314.
44. Tasdemir, M.A., Tasdemir, C., Jefferson, A.D., Lydon, F.D., and Barr, B.I.G., (1998). "Evaluation of strains at peak stresses in concrete: A three-phase composite model approach." *Cement and Concrete Research,* 20(4), p. 301-318.
45. Al-Salloum, Y., and Siddiqui, N., (2009). "Compressive Strength Prediction Model for FRP-Confined Concrete." *Proc. 9th Int. Symp. On Fiber Reinforced Polymer Reinforcement for Concrete Structures*, Sydney, Australia. .
46. Binici, B., (2005). "An analytical model for stress-strain behavior of confined concrete." *Eng. Struct.,* 27(7), p. 1040-1051.
47. Fahmy, M., and Wu, Z., (2010). "Evaluating and proposing models of circular concrete columns confined with different FRP composites." *Composites Part B: Engineering.,* 41(3), p. 199-213.
48. Teng, J.G., Huang, Y. L., Lam, L., and Ye, L., (2007). "Theoretical model for fiber reinforced polymer-confined concrete." *ASCE J. Compos. Constr.,* 11(2), p. 201-210.
49. Teng, J.G., Jiang, T., Lam, L. and Luo, Y., (2009). "Refinement of a Design-Oriented Stress-Strain Model for FRP-Confined Concrete." *ASCE J. Compos. Constr.,* 13(4), p. 269-278.
50. Wei, Y.Y. and Wu, Y.F., (2012). "Unified stress-strain model of concrete for FRP-confined columns." *Construction and Building Materials,* 26(1), p. 381-392.
51. Wu, Y.F. and Wang, L.M., (2009). "Unified strength model for square and circular concrete columns confined by external jacket." *Journal of Structural Engineering,* 135(3), p. 253-261.

52. Wu, Y.F., and Zhou, Y., (2010). "Unified Strength Model Based on Hoek-Brown Failure Criterion for Circular and Square Concrete Columns Confined by FRP." *ASCE J. Compos. Constr.,* 14(2), p. 175-184.
53. Youssef, M.N., Feng, M. Q., and Mosallam, A. S., (2007). "Stress-strain model for concrete confined by FRP composites." *Composites Part B: Engineering.,* 38(5-6), p. 614-628.
54. Abdollahi, B., Bakhshi, M., Motavalli, M., and Shekarchi, M., (2007). "Experimental modeling of GFRP confined concrete cylinders subjected to axial loads." *Proc. The 8th Int. Symp. on Fiber Reinforced Polymer Reinforcement for Concrete Structures*, Patras, Greece.
55. Ahmad, S.M., Khaloo, A. R., and Irshaid, A., (1991). "Behaviour of concrete spirally confined by fiberglass filaments." *Mag. Concr. Res.,* 43(56), p. 143-148.
56. Aire, C., Gettu, Casas, J., Marques, S. and Marques, D., (2010). "Concrete laterally confined with fibre-reinforced polymers (FRP): experimental study and theoretical model." *Materiales de Construcción,* 60, p. 297.
57. Akogbe, R.K., M. Liang, and Wu, Z. M, (2011). "Size effect of axial compressive strength of CFRP confined concrete cylinders." *Int. J. Conc. Struct. Mater.,* 5(1), p. 49-55.
58. Almusallam, T.H., (2007). "Behaviour of normal and high-strength concrete cylinders confined with E-glass/epoxy composite laminates." *Composites Part B: Engineering.,* 38, p. 629-639.
59. Au, C., and Buyukozturk, O., (2005). "Effect of fiber orientation and ply mix on fiber reinforced polymer-confined concrete." *ASCE J. Compos. Constr.,* 9(5), p. 397-407.
60. Benzaid, R., Mesbah, H., and Chikh, N., (2010). "FRP-confined Concrete Cylinders: Axial Compression Experiments and Strength Model." *J. Reinf. Plas. Compos.,* 29(16), p. 2469-2488.
61. Berthet, J.F., Ferrier. E., and Hamelin. P., (2005). "Compressive behavior of concrete externally confined by composite jackets. Part A: experimental study." *Constr. Build. Mater., ,* 19(3), p. 223-232.
62. Bisby, L., Take, W. A., and Caspary, A., (2007). "Quantifying strain variation FRP confined using digital image correlation: proof-of-concept and initial results." *Asia-Pacific Conference on FRP in Structures*.
63. Bisby, L.A., Chen, J. F., Li, S. Q., Stratford, T. J., Cueva, N., and Crossling, K., (2011). "Strengthening fire-damaged concrete by confinement with fibre-reinforced polymer wraps." *Eng. Struct,* 33, p. 3381-3391.
64. Bullo, S., (2003). "Experimental study of the effects of the ultimate strain of fiber reinforced plastic jackets on the behavior of confined concrete." *Proc. of the Int. Conf. Compos. in Constr.*, Cosenza, Italy.
65. Campione, G., Miraglia, N., and Scibilia, N., (2001). "Compressive behaviour of RC members strengthened with carbon fibre reinforced plastic layers." *Advances in Earthquake Engineering,* 9, p. 397-406.
66. Carey, S.A., and Harries, K. A., (2005). "Axial behavior and modeling of confined small, medium, and large scale circular sections with carbon fiber-reinforced polymer jackets." *ACI Struct. J.,* 102(4), p. 596-604.

67. Comert, M., Goksu, C., and Ilki, A., (2009). "Towards a tailored stress-strain behavior for FRP confined low strength concrete." *Proc. 9th Int. Symp. On Fiber Reinforced Polymer Reinforcement for Concrete Structures*, Sydney, Australia.
68. Cui, C., and Sheikh, A., (2010). "Experimental Study of Normal- and High-Strength Concrete Confined with Fiber-Reinforced Polymers." *ASCE J. Compos. Constr.,* 14(5), p. 553-561.
69. Demers, M., and Neale, K. W., (1994). "Strengthening of concrete columns with unidirectional composite sheets." *Proc. Developments in Short and Medium Span Bridge Engineering*, Montreal, Que.
70. Elsanadedy, H.M., Al-Salloum, Y.A., Alsayed, S.H., and Iqbal, R.A., (2012). "Experimental and numerical investigation of size effects in FRP-wrapped concrete columns." *Construction and Building Materials,* 29, p. 56–72.
71. Erdil, B., Akyuz, U., and Yaman, I. O., (2011). "Mechanical behavior of CFRP confined low strength concretes subjected to simultaneous heating-cooling cycles and sustained loading." *Mater. Struct.,* (223-233).
72. Evans, J., Kocman, M. and Kretschmer, T., (2008). "Hybrid FRP Confined Concrete Columns." Honours, *The School of Civil, Environmental and Mining Engineering*, Univ. of Adelaide., Adelaide, Australia.
73. Green, M.F., Bisby, L. A., Fam, A. Z., and Kodur, V. K. R., (2006). "FRP confined concrete columns: behaviour under extreme conditions." *Cem. Concr. Res.,* 28(10), p. 928-993.
74. Harmon, T.G., and Slattery, K. T., (1992). "Advanced composite confinement of concrete." *Proc. Advanced Composite Materials for Bridges and Structures I*, Montreal, Canada.
75. Harries, K.A., and Kharel, G., (2002). "Behavior and modeling of concrete subject to variable confining pressure." *ACI Mater. J.,* 99(2), p. 180-189.
76. Hosotani, K., Kawashima, K., and Hoshikuma, J., (1997). "A model for confinement effect for concrete cylinders confined by carbon fiber sheets." *NCEER-INCEDE Workshop on Earthquake Engineering Frontiers of Transportation Facilities*, State Univ. of New York, Buffalo, NY.
77. Howie, I., and Karbhari, V. M., (1994). "Effect of materials architecture on strengthening: efficiency of composite wraps for deteriorating columns in the North-East." *Proc. 3rd Materials Engineering Conference*, San Diego.
78. Ilki, A., Kumbasar, N., and Koc, V., (2002). "Strength and deformability of low strength concrete confined by carbon fibre composite sheets." *Proc. 15th Engineering Mechanics Conference*, New York, NY.
79. Ilki, A., Kumbasar, N., and Koc, V., (2004). "Low strength concrete members externally confined with FRP sheets." *Struct. Eng. Mech,* 18(2), p. 167-194.
80. Issa, C.A., (2007). "The effect of elevated temperatures on CFRP wrapped concrete cylinders." *Proc. 8th Int. Symp. On Fiber Reinforced Polymer Reinforcement for Concrete Structures*, Patras, Greece.
81. Issa, C.A., and Karam, G. N., (2004). "Compressive strength of concrete cylinders with variable widths CFRP wraps." *Proc. 4th Int. Conf. on Advanced Composite Materials in Bridges and Structures*, Calgary, Alberta, Canada.

82. Karabinis, A.I., and Rousakis, T. C., (2002). "Concrete confined by FRP material: a plasticity approach." *ASCE J. Eng. Struct.,* 24(7), p. 923-932.
83. Karam, G.N., and Tabbara, M., (2004). "Corner effects in CFRP wrapped square columns." *Mag. Concr. Res.,* 56(8), p. 461-464.
84. Karantzikis, M., Papanicolaou, C. G. Antonopoulos, C. P., and Triantafillou, T. C., (2005). "Experimental investigation of nonconventional confinement for concrete using FRP." *ASCE J. Compos. Constr.,* 9(6), p. 480-487.
85. Kono, S., Inazuni, M., and Kaku, T., (1998). "Evaluation of confining effects of CFRP sheets on reinforced concrete members." *Proc. 2nd Int. Conf. on Composites in Infrastructures*.
86. Lee, J., Yi C., Jeong, H., Kim, S., and Kim, J., (2009). "Compressive Response of Concrete Confined with Steel Spirals and FRP Composites." *J. Compos. Materials.,* 44(4), p. 481-504.
87. Li, G., Maricherla, D., Singh, K., Pang, S. S., and John, M., (2006). "Effect of fiber orientation on the structural behavior of FRP wrapped concrete cylinders." *J. Compos. Struct.,* 74(4), p. 475-483.
88. Li, Y., and Ou, (2007). "Compressive behavior and nonlinear analysis of selfsensing concrete-filled frp tubes and frp-steel composite tubes." *Proc. 8th Int. Symp. On Fiber Reinforced Polymer Reinforcement for Concrete Structures*, Patras, Greece.
89. Liang, M., Wu, Z.-M., Ueda, T., Zheng, J.-J., and Akogbe1, R., (2012). "Experiment and modeling on axial behavior of carbon fiber reinforced polymer confined concrete cylinders with different sizes." *Journal of Reinforced Plastics and Composites,* 31(6), p. 389–403.
90. Lin, C., and Li, Y., (2003). "An Effective Peak Stress Formula for Concrete Confined with Carbon Fibre Reinforced Plastics." *J. Civ. Eng.,,* 30, p. 882-889.
91. Lin, H.J., and Liao, C. I., (2004). "Compressive strength of reinforced concrete column confined by composite material." *J. Compos. Struct.,* 65(239 - 250).
92. Mandal, S., Hoskin, A., and Fam, A., (2005). "Influence of concrete strength on confinement effectiveness of fiber-reinforced polymer circular jackets." *ACI Struct. J.,* 102(3), p. 383-392.
93. Micelli, F., Myers, J. J., and Murthy, S., (2001). "Effect of environmental cycles on concrete cylinders confined with FRP." *Proc. Int. Conf. on Composites in Construction*, Porto, Portugal.
94. Miyauchi, K., Nishibayashi, S., and Inoue, S., (1997). "Estimation of strengthening effects with carbon fiber sheet for concrete column." *3rd Int. Symp. Of Non-Metallic Reinforcement for Concrete Structures*.
95. Miyauchi, K., Inoue, S., Kuroda, T., and Kobayashi, A., (1999). "Strengthening effects with carbon fiber sheet for concrete column." *Japan Concr. Inst.*
96. Modarelli, R., Micelli, F., and Manni, O., (2005). "FRP-confinement of hollow concrete cylinders and prisms." *Proc. 7th Int. Symp. On Fiber Reinforced Polymer Reinforcement of Reinforced Concrete Structures*.
97. Nanni, A., and Bradford, N. M., (1995). "FRP jacketed concrete under uniaxial compression." *Constr. Build. Mater.,* 9(2), p. 115-124.

98. Ongpeng, J.M.C., (2006). "Retrofitting RC circular columns using CFRP sheets as confinement." *Symp. On Infrastructure Development and the Environment*, Diliman, Quezon City.
99. Owen, L.M., (1998). "Stress-strain behavior of concrete confined by carbon fiber jacketing." Masters, Univ. of Washington, Seattle.
100. Park, J.H., Jo, B. W., Yoon, S. J., and Park, S. K., (2011). "Experimental investigation on the structural behavior of concrete filled FRP tubes with/without steel re-bar." *KSCE J. Civ. Eng.,* 15(2), p. 337-345.
101. Picher, F., Rochette, P., and Labossiére, P., (1996). "Confinement of concrete cylinders with CFRP." *Proc. 1st Int. Conf. on Composites in Infrastructure*, Tucson, Arizona.
102. Piekarczyk, J., Piekarczyk, W., and Blazewicz, S., (2011). "Compression strength of concrete cylinders reinforced with carbon fiber laminate." *Constr. Build. Mater.,* 25(2365-2369).
103. Pon, T.H., Li, Y. F., Shih, B. J., Han, M. S., Chu, G. D., Chiu, Y. J., Lin, J. C., and Cheng, Y. S., (1998). "Experiments of scale effects on the strength of FRP reinforced concrete." *Proc. 4th National Conference on Structural Engineering*, Taipei, Taiwan.
104. Rochette, P., and Labossiére, P., (2000). "Axial testing of rectangular column models confined with composites." *ASCE J. Compos. Constr.,* 4(3), p. 129-136.
105. Rousakis, T., (2001). "Experimental investigation of concrete cylinders confined by carbon FRP sheets under monotonic and cyclic axial compressive load." *Research Report*, Chalmers Univ. of Technology, Göteborg, Sweden.
106. Saenz, N., and Pantelides, C. P., (2006). "Short and medium term durability evaluation of FRP-confined circular concrete." *ASCE J. Compos. Constr.,* 10(3), p. 244-253.
107. Santarosa, D., Filho, A. C., Beber, A. J., and Campagnolo, J. L., (2001). "Concrete columns confined with CFRP sheets." *Proc. Int. Conf. of FRP Composites in Civil Engineering*, Hong Kong.
108. Shao, Y., Zhu, Z., and Mirmiran, A., (2006). "Cyclic modeling of FRP-confined concrete with improved ductility." *Cem. Concr. Res.,* 28(10), p. 959-968.
109. Shehata, I.A.E.M., Carneiro, L. A. V., and Shehata, L. C. D., (2002). "Strength of short concrete columns confined with CFRP sheets." *Mater. and Struct.,* 35, p. 50-58.
110. Shehata, I.A.E.M., Carneiro, L. A. V., and Shehata, L. C. D., (2007). "Strength of confined short concrete columns." *Proc. 8th Int. Symp. On Fiber Reinforced Polymer Reinforcement for Concrete Structures*, Patras, Greece.
111. Silva, M.A.G., and Rodrigues, C. C., (2006). "Size and relative stiffness effects on compressive failure of concrete columns wrapped with glass FRP." *ASCE J. Mater. Civ. Eng.,* 18(3), p. 334-342.
112. Song, X., Gu, X., Li, Y., Chen, T., and Zhang, W., (2013). "Mechanical Behavior of FRP-Strengthened Concrete Columns Subjected to Concentric and Eccentric Compression Loading." *Journal of Composites for Construction,* 17(3), p. 336-346.
113. Suter, R., and Pinzelli, R., (2001). "Confinement of concrete columns with FRP sheets." *Proc. 5th Symp. On Fibre Reinforced Plastic Reinforcement for Concrete Structures*, London.

114. Tamuzs, V., Valdmanis, V., Tepfers, R. & Gylltoft, K., (2008). "Stability analysis of CFRP-wrapped concrete columns strengthened with external longitudinal CFRP sheets." *Mech. Compos. Mater.,* 44, p. 199-208.
115. Teng, J.G., Yu, T., Wong, Y. L., and Dong, S. L., (2007). "Hybrid FRP-concrete-steel tubular columns: concept and behaviour." *Constr. Build. Mater.,* 21(4), p. 846-854.
116. Thériault, M., Neale, K. W., M. ASCE, and Claude, S., (2004). "Fiber reinforced polymer-confined circular concrete columns: investigation of size and slenderness effects." *ASCE J. Compos. Constr.,* 8(4), p. 323-331.
117. Vincent, T. and Ozbakkaloglu, T., (2013). "Influence of concrete strength and confinement method on axial compressive behavior of FRP-confined high- and ultra high-strength concrete." *Composites Part B,* 50, p. 413–428.
118. Vincent, T. and Ozbakkaloglu, T., (2013). "Influence of fiber orientation and specimen end condition on axial compressive behavior of FRP-confined concrete." *Constr. Build. Mater.,* 47, 814-826.
119. Wang, Y.F., and Wu, H. L, (2011). "Size effect of concrete short columns confined with aramid FRP jackets." *ASCE J. Compos. Constr.,* 15(4), p. 535-544.
120. Wang, Y., and Zhang, D., (2009). "Creep-Effect on Mechanical Behaviour of Concrete Confined by FRP under Axial Compression." *ASCE J. Eng. Mech. Div.,* 135(11), p. 1315-1322.
121. Wu, Y.-F. and Jiang, C., (2013). "Effect of load eccentricity on the stress–strain relationship of FRP-confined concrete columns." *Composite Structures,* 98, p. 228–241.
122. Wu, H., Wang, Y., Yu, L. and Li, X., (2009). "Experimental and Computational Studies on High-Strength Concrete Circular Columns Confined by Aramid Fiber-Reinforced Polymer Sheets." *ASCE J. Compos. Constr.,* 13(2), p. 125-134.
123. Yan, Z., Pantelides, C. P., Reaveley, D., (2006). "Fiber-reinforced polymer jacketed and shape-modified compression members: I-Experimental Behavior." *ACI Struct. J.,* 6, p. 885-893.
124. Zhang, S., Ye, L., and Mai, Y. W., (2000). "Study on polymer composite strengthening systems for concrete columns." *Applied Compos. Mater.,* 7(2), p. 125-138.

APPENDIX

Table 3. Test database of CFRP-wrapped concrete specimens

Paper	Specimen Dimensions		Concrete Properties		FRP Properties			Fiber Properties			Measured Ultimate Conditions			Hoop Rupture Strain Reduction Factors	
	D (mm)	H (mm)	f'_{co} (MPa)	ε_{co} (%)	E_{frp} (GPa)	f_{frp} (MPa)	t_{frp} (mm)	E_f (GPa)	f_f (MPa)	t_f (mm)	f'_{cc} (MPa)	ε_{cu} (%)	$\varepsilon_{h,rup}$ (%)	$k_{\varepsilon,frp}$	$k_{\varepsilon,f}$
Aire et al. [56]	150	300	42	0.24				240	3900	0.117	46	0.92	0.38		0.234^
Aire et al. [56]	150	300	42	0.24				240	3900	0.351	77	2.12	0.88		0.542
Aire et al. [56]	150	300	42	0.24				240	3900	0.702	108	3.16	1.32		0.812
Akogbe et al. [57]	100	200	26.5	0.31				242	3248	0.167	64.3	2.55			
Akogbe et al. [57]	100	200	26.5	0.31				242	3248	0.167	63.0	2.18			
Akogbe et al. [57]	100	200	26.5	0.31				242	3248	0.167	66.4	2.29			
Akogbe et al. [57]	100	200	26.5	0.31				242	3248	0.167	64.8	2.48			
Akogbe et al. [57]	200	400	21.7	0.22				242	3248	0.334	64.3[s]	2.79			
Akogbe et al. [57]	200	400	21.7	0.22				242	3248	0.334	69.1[s]	2.69			
Akogbe et al. [57]	200	400	21.7	0.22				242	3248	0.334	60.1	2.10			
Akogbe et al. [57]	200	400	21.7	0.22				242	3248	0.334	66.3[s]	2.54			
Akogbe et al. [57]	300	600	24.5	0.22				242	3248	0.501	58.8	1.80			
Akogbe et al. [57]	300	600	24.5	0.22				242	3248	0.501	59.4	2.00			
Akogbe et al. [57]	300	600	24.5	0.22				242	3248	0.501	63.0	1.90			
Akogbe et al. [57]	300	600	24.5	0.22				242	3248	0.501	60.6	2.00			
Al-Salloum [45]	150	300	32.4	0.205	75.1	935	1.2				83.16	3.233[a]			
Al-Salloum [45]	150	300	36.2	0.205	75.1	935	1.2				85.04	3.233[a]			
Benzaid et al. [60]	160	320	25.9	0.273				238	4300	0.13	39.63	1.28	1.31		0.725
Benzaid et al. [60]	160	320	25.9	0.273				238	4300	0.39	66.14	1.52[a]	1.32		0.731
Benzaid et al. [60]	160	320	49.5	0.169				238	4300	0.13	52.75	0.25[a]	0.29		0.161^
Benzaid et al. [60]	160	320	49.5	0.169				238	4300	0.39	82.91	0.73[a]	1.32		0.731
Berthet et al. [61]	160	320	25.0	0.233				230	3200	0.165	42.8	1.633	0.957		0.688
Berthet et al. [61]	160	320	25.0	0.233				230	3200	0.165	37.8	0.932	0.964		0.693
Berthet et al. [61]	160	320	25.0	0.233				230	3200	0.165	45.8	1.674	0.960		0.690
Berthet et al. [61]	160	320	25.0	0.233				230	3200	0.330	56.7	1.725	0.899		0.646
Berthet et al. [61]	160	320	25.0	0.233				230	3200	0.330	55.2	1.577	0.911		0.655
Berthet et al. [61]	160	320	25.0	0.233				230	3200	0.330	56.1	1.680	0.908		0.653
Berthet et al. [61]	160	320	40.1	0.200				230	3200	0.110	49.8	0.554	1.015		0.730
Berthet et al. [61]	160	320	40.1	0.200				230	3200	0.110	50.8	0.663	0.952		0.684
Berthet et al. [61]	160	320	40.1	0.200				230	3200	0.110	48.8	0.608	1.203		0.865^
Berthet et al. [61]	160	320	40.1	0.200				230	3200	0.165	53.7	0.660	0.880		0.633
Berthet et al. [61]	160	320	40.1	0.200				230	3200	0.165	54.7	0.619	0.853		0.613
Berthet et al. [61]	160	320	40.1	0.200				230	3200	0.165	51.8	0.639	1.042		0.749
Berthet et al. [61]	160	320	40.1	0.200				230	3200	0.220	59.7	0.599	0.788		0.566
Berthet et al. [61]	160	320	40.1	0.200				230	3200	0.220	60.7	0.693	0.830		0.597
Berthet et al. [61]	160	320	40.1	0.200				230	3200	0.220	60.2	0.730	0.809		0.581
Berthet et al. [61]	160	320	40.1	0.200				230	3200	0.440	91.6	1.443	0.924		0.664
Berthet et al. [61]	160	320	40.1	0.200				230	3200	0.440	89.6	1.364	0.967		0.695
Berthet et al. [61]	160	320	40.1	0.200				230	3200	0.440	86.6	1.166	0.885		0.636
Berthet et al. [61]	160	320	40.1	0.200				230	3200	0.990	142.4	2.461	0.989		0.711
Berthet et al. [61]	160	320	40.1	0.200				230	3200	0.990	140.4	2.389	1.002		0.720
Berthet et al. [61]	160	320	40.1	0.200				230	3200	1.320	166.3	2.700	0.999		0.718
Berthet et al. [61]	160	320	52.0	0.227				230	3200	0.330	82.6	0.832	0.934		0.671
Berthet et al. [61]	160	320	52.0	0.227				230	3200	0.330	82.8	0.699	0.865		0.622
Berthet et al. [61]	160	320	52.0	0.227				230	3200	0.330	82.3	0.765	0.891		0.640
Berthet et al. [61]	160	320	52.0	0.227				230	3200	0.660	108.1	1.141	0.667		0.479^
Berthet et al. [61]	160	320	52.0	0.227				230	3200	0.660	112.0	1.124	0.871		0.626
Berthet et al. [61]	160	320	52.0	0.227				230	3200	0.660	107.9	1.121	0.882		0.634

Paper	D (mm)	H (mm)	f'_{co} (MPa)	ε_{co} (%)	E_{frp} (GPa)	f_{frp} (MPa)	t_{frp} (mm)	E_f (GPa)	f_f (MPa)	t_f (mm)	f'_{cc} (MPa)	ε_{cu} (%)	$\varepsilon_{h,rup}$ (%)	$k_{\varepsilon,frp}$	$k_{\varepsilon,f}$
Bisby et al. [62]	150	300	34.4	0.33				231	4100	0.12	44.1	0.80	0.93		
Bisby et al. [62]	150	300	34.4	0.33				231	4100	0.12	44.1	0.87	1.10		
Bisby et al. [62]	150	300	34.4	0.33				231	4100	0.12	43.0	0.90	1.21		
Bisby et al. [63]	100	200	28.0	0.25				231	4100	0.12	63.0				
Bisby et al. [63]	100	200	28.0	0.25				231	4100	0.12	61.0	1.32	1.02		
Bisby et al. [63]	100	200	28.0	0.25				231	4100	0.12	53.0	1.06	1.00		
Campione et al. [65]	100	200	20.1	0.207				230	3430	0.165	49.6	2.55			
Carey and Harries [66]	254	762	38.9	0.30				72.5[p]	875[p]	1.0	54.8	1.04	1.00		0.829
Carey and Harries [66]	152	305	33.5	0.23				25[p]	350[p]	1.7	46.8	0.93	1.48		1.057^
Cui and Sheikh [68]	152	305	48.1	0.222	85	816	1				86.6	1.53	1.124	1.171^	
Cui and Sheikh [68]	152	305	48.1	0.222	85	816	2				109.4	2.01	0.968	1.008^	
Cui and Sheikh [68]	152	305	48.1	0.222	85	816	2				126.7	2.66	1.212	1.263^	
Cui and Sheikh [68]	152	305	48.1	0.222	85	816	3				162.7	3.09	1.158	1.206^	
Cui and Sheikh [68]	152	305	48.1	0.222	85	816	3				153.6	2.89	1.035	1.078^	
Cui and Sheikh [68]	152	305	45.6	0.247				241	3639	0.11	57.7	1.21	1.678		1.111^
Cui and Sheikh [68]	152	305	45.6	0.247				241	3639	0.11	55.4	1.31[a]	1.599		1.059^
Cui and Sheikh [68]	152	305	45.6	0.247				241	3639	0.22	78.0	1.97[a]	1.616		1.070^
Cui and Sheikh [68]	152	305	45.6	0.247				241	3639	0.22	86.8	2.14[a]	1.801		1.193^
Cui and Sheikh [68]	152	305	45.6	0.247				241	3639	0.33	106.5	2.90[a]	1.786		1.183^
Cui and Sheikh [68]	152	305	45.6	0.247				241	3639	0.33	106.0	2.83[a]	1.798		1.191^
Cui and Sheikh [68]	152	305	48.1	0.222	85	816	1				80.9	1.51	1.052	1.096^	
Demers and Neale [69]	152	305	32.2		25[p]	380[p]	1				41.1	1.41			
Demers and Neale [69]	152	305	43.7		25[p]	380[p]	1				48.4	0.97			
Demers and Neale [69]	152	305	43.7		25[p]	380[p]	3				75.2	1.83			
Demers and Neale [69]	152	305	43.7		25[p]	380[p]	3				73.4	1.83			
Elsanadedy et al. [70]	50	100	53.8	0.344	77.3	846	1				146.2	1.563[a]			
Elsanadedy et al. [70]	100	200	49.1	0.361	77.3	846	1				94.5	1.091			
Elsanadedy et al. [70]	100	200	49.1	0.361	77.3	846	2				146.0	1.541[a]			
Elsanadedy et al. [70]	150	300	41.1	0.362	77.3	846	1				76.4	0.945			
Elsanadedy et al. [70]	150	300	41.1	0.362	77.3	846	2				111.5	1.335[a]			
Elsanadedy et al. [70]	150	300	41.1	0.362	77.3	846	3				144.2	1.485[a]			
Erdil et al. [71]	150	300	11.1	0.3				230	3430	0.165	32.9	4.2			
Erdil et al. [71]	150	300	20.8	0.3				230	3430	0.165	47.5	3.5[a]			
Evans et al. [72]	152	305	37.3					240	3800	0.234	64.4	1.31	1.39		0.878^
Green et al. [73]	152	305	46.0		22.4[p]	237[p]	1				53				
Green et al. [73]	152	305	46.0		22.4[p]	237[p]	2				59				
Harmon and Slattery [74]	51	102	41					235	3500	0.09	86				
Harmon and Slattery [74]	51	102	41					235	3500	0.179	117	1.1			
Harmon and Slattery [74]	51	102	41					235	3500	0.344	158	2.0			
Harmon and Slattery [74]	51	102	41					235	3500	0.690	241[s]	3.4[a]			
Harries and Kharel [75]	152	305	32.1	0.28	15.7	174	1	25[p]	350[p]	1	32.9	0.60	1.03	0.929^	0.736
Harries and Kharel [75]	152	305	32.1	0.28	15.7	174	2	25[p]	350[p]	2	41.0	0.86	1.19	1.074^	0.850
Harries and Kharel [75]	152	305	32.1	0.28	15.7	174	3	25[p]	350[p]	3	52.2	1.38	1.55	1.399^	1.107^
Hosotani et al. [76]	200	600	41.7	0.34	243	4227	0.44	230	3481	0.444	93.0	2.1			
Howie and Karbhari [77]	152	305	38.6		73.3	755	0.305				45.5				
Howie and Karbhari [77]	152	305	38.6		73.3	755	0.305				41.9				
Howie and Karbhari [77]	152	305	38.6		73.3	755	0.305				47.2				
Howie and Karbhari [77]	152	305	38.6		70.6	1047	0.61				56.5				
Howie and Karbhari [77]	152	305	38.6		70.6	1047	0.61				60.6				
Howie and Karbhari [77]	152	305	38.6		70.6	1047	0.61				61.9				
Howie and Karbhari [77]	152	305	38.6		77.5	1105	0.92				80.9				
Howie and Karbhari [77]	152	305	38.6		77.5	1105	0.92				76.4				
Howie and Karbhari [77]	152	305	38.6		77.5	1105	0.92				75.8				
Howie and Karbhari [77]	152	305	38.6		95.7	1352	1.22				89.5				
Howie and Karbhari [77]	152	305	38.6		95.7	1352	1.22				89.9				
Howie and Karbhari [77]	152	305	38.6		95.7	1352	1.22				89.0				

Paper	D (mm)	H (mm)	f'_{co} (MPa)	ε_{co} (%)	E_{frp} (GPa)	f_{frp} (MPa)	t_{frp} (mm)	E_f (GPa)	f_f (MPa)	t_f (mm)	f'_{cc} (MPa)	ε_{cu} (%)	$\varepsilon_{h,rup}$ (%)	$k_{\varepsilon,frp}$	$k_{\varepsilon,f}$
Ilki et al. [78]	150	300	32	0.2				230	3430	0.165	47.2	1.44	0.79		0.530
Ilki et al. [78]	150	300	32	0.2				230	3430	0.495	83.8	3.43	1.03		0.691
Ilki et al. [78]	150	300	32	0.2				230	3430	0.495	91.0	3.92[a]	1.08		0.724
Ilki et al. [78]	150	300	32	0.2				230	3430	0.825	107.1	4.96[a]	0.64		0.429^
Ilki et al. [78]	150	300	32	0.2				230	3430	0.825	107.7	4.32	1.00		0.671
Ilki et al. [79]	150	300	6.2	0.2				230	3430	0.165	25.3[s]	3.9[a]	0.67		0.449^
Ilki et al. [79]	150	300	6.2	0.2				230	3430	0.165	19.4	2.6			
Ilki et al. [79]	150	300	6.2	0.2				230	3430	0.330	41.9	5.9	1.30		0.872
Ilki et al. [79]	150	300	6.2	0.2				230	3430	0.330	40.0	5.9			
Ilki et al. [79]	150	300	6.2	0.2				230	3430	0.495	52.2	6.9			
Ilki et al. [79]	150	300	6.2	0.2				230	3430	0.495	56.9	7.5	1.10		0.738
Ilki et al. [79]	150	300	6.2	0.2				230	3430	0.660	76.6	8.8			
Ilki et al. [79]	150	300	6.2	0.2				230	3430	0.660	69.7	7.6			
Ilki et al. [79]	150	300	6.2	0.2				230	3430	0.825	87.7	9.1			
Ilki et al. [79]	150	300	6.2	0.2				230	3430	0.825	82.7	9.4			
Ilki et al. [79]	150	300	6.2	0.2				230	3430	0.990	108.3	10.4			
Ilki et al. [79]	150	300	6.2	0.2				230	3430	0.990	103.3	9.6			
Issa [80]	150	300	23.7					231	4100	0.12	39.34				
Issa [80]	150	300	23.9					231	4100	0.12	39.83				
Issa [80]	150	300	23.6					231	4100	0.12	41.79				
Issa and Karam [81]	150	300	30.5					230	4100	0.122	35.8				
Issa and Karam [81]	150	300	30.5					230	4100	0.122	37.6				
Issa and Karam [81]	150	300	30.5					230	4100	0.122	42.0				
Issa and Karam [81]	150	300	30.5					230	4100	0.244	48.7				
Issa and Karam [81]	150	300	30.5					230	4100	0.244	50.0				
Issa and Karam [81]	150	300	30.5					230	4100	0.244	64.5				
Issa and Karam [81]	150	300	30.5					230	4100	0.244	50.0				
Issa and Karam [81]	150	300	30.5					230	4100	0.244	64.5				
Issa and Karam [81]	150	300	30.5					230	4100	0.366	68.7				
Issa and Karam [81]	150	300	30.5					230	4100	0.366	64.6				
Issa and Karam [81]	150	300	30.5					230	4100	0.366	75.6				
Jiang and Teng [32]	152	305	38.0	0.217	240.7[t]					0.68	110.1	2.551	0.977		
Jiang and Teng [32]	152	305	38.0	0.217	240.7[t]					0.68	107.4	2.613	0.965		
Jiang and Teng [32]	152	305	38.0	0.217	240.7[t]					1.02	129.0	2.794	0.892		
Jiang and Teng [32]	152	305	38.0	0.217	240.7[t]					1.02	135.7	3.082	0.927		
Jiang and Teng [32]	152	305	38.0	0.217	240.7[t]					1.36	161.3	3.700	0.872		
Jiang and Teng [32]	152	305	38.0	0.217	240.7[t]					1.36	158.5	3.544	0.877		
Jiang and Teng [32]	152	305	37.7	0.275	260[t]					0.11	48.5	0.895	0.935		
Jiang and Teng [32]	152	305	37.7	0.275	260[t]					0.11	50.3	0.914	1.092		
Jiang and Teng [32]	152	305	42.2	0.260	260[t]					0.11	48.1	0.691	0.734		
Jiang and Teng [32]	152	305	42.2	0.260	260[t]					0.11	51.1	0.888	0.969		
Jiang and Teng [32]	152	305	42.2	0.260	260[t]					0.22	65.7	1.304	1.184		
Jiang and Teng [32]	152	305	42.2	0.260	260[t]					0.22	62.9	1.025	0.938		
Jiang and Teng [32]	152	305	47.6	0.279	250.5[t]					0.33	82.7	1.304	0.902		
Jiang and Teng [32]	152	305	47.6	0.279	250.5[t]					0.33	85.5	1.936	1.130		
Jiang and Teng [32]	152	305	47.6	0.279	250.5[t]					0.33	85.5	1.821	1.064		
Karabinis and Rousakis [82]	200	320	38.5	0.276				240	3720	0.117	43.0	0.796			
Karabinis and Rousakis [82]	200	320	38.5	0.276				240	3720	0.117	41.6	0.714			
Karabinis and Rousakis [82]	200	320	38.5	0.276				240	3720	0.117	46.0	0.349[a]			
Karabinis and Rousakis [82]	200	320	38.5	0.276				240	3720	0.234	51.5	0.877			
Karabinis and Rousakis [82]	200	320	38.5	0.276				240	3720	0.234	50.0	0.577			
Karabinis and Rousakis [82]	200	320	38.5	0.276				240	3720	0.234	55.0	0.860			
Karabinis and Rousakis [82]	200	320	38.5	0.276				240	3720	0.351	67.0	1.760			
Karabinis and Rousakis [82]	200	320	38.5	0.276				240	3720	0.117	42.5	0.859			
Karabinis and Rousakis [82]	200	320	38.5	0.276				240	3720	0.117	42.0	1.238			
Karabinis and Rousakis [82]	200	320	35.7	0.191				240	3720	0.117	41.0	0.296[a]			
Karabinis and Rousakis [82]	200	320	35.7	0.191				240	3720	0.234	50.0	0.604			
Karabinis and Rousakis [82]	200	320	35.7	0.191				240	3720	0.234	48.5	1.040			

Paper	D (mm)	H (mm)	f'_{co} (MPa)	ε_{co} (%)	E_{frp} (GPa)	f_{frp} (MPa)	t_{frp} (mm)	E_f (GPa)	f_f (MPa)	t_f (mm)	f'_{cc} (MPa)	ε_{cu} (%)	$\varepsilon_{h,rup}$ (%)	$k_{\varepsilon,frp}$	$k_{\varepsilon,f}$
Karabinis and Rousakis [82]	200	320	35.7	0.191				240	3720	0.234	50.0	1.072			
Karabinis and Rousakis [82]	200	320	35.7	0.191				240	3720	0.351	63.0	1.718			
Karabinis and Rousakis [82]	200	320	35.7	0.191				240	3720	0.351	67.5	1.705			
Karabinis and Rousakis [82]	200	320	35.7	0.191				240	3720	0.351	65.5	1.686			
Karam and Tabbara [83]	150	300	12.8	0.47				231	3650	0.12	17.8[s]	1.37[a]			
Karam and Tabbara [83]	150	300	12.8	0.47				231	3650	0.24	31.8	2.78[a]			
Karantzikis et al. [84]	200	350	12.1	0.22				230	3500	0.12	29.25	1.92			
Karbhari and Gao [37]	152	305	38.4		138.1	1047	0.66	227	3500		59.7	1.3			
Karbhari and Gao [37]	152	305	38.4		77.39	1105	0.99	227	3500		77.7	2.2			
Karbhari and Gao [37]	152	305	38.4		95.7	1352	1.32	227	3500		89.5	2.4			
Kono et al. [85]	100	200	34.3					235	3820	0.167	57.4	0.785	0.84		0.517
Kono et al. [85]	100	200	34.3					235	3820	0.167	64.9	1.11	0.92		0.566
Kono et al. [85]	100	200	32.3					235	3820	0.167	58.2				
Kono et al. [85]	100	200	32.3					235	3820	0.167	61.8	1.07	0.96		0.591
Kono et al. [85]	100	200	32.3					235	3820	0.167	57.7	1.07	0.63		0.388^
Kono et al. [85]	100	200	32.3					235	3820	0.334	80.2	1.75	0.89		0.548
Kono et al. [85]	100	200	32.3					235	3820	0.501	86.9	1.65	0.77		0.474^
Kono et al. [85]	100	200	32.3					235	3820	0.501	90.1	1.59	0.67		0.412^
Kono et al. [85]	100	200	34.8					235	3820	0.167	57.8	0.935	0.91		0.560
Kono et al. [85]	100	200	34.8					235	3820	0.167	55.6	1.05	0.89		0.548
Kono et al. [85]	100	200	34.8					235	3820	0.167	50.7	0.982	0.61		0.375^
Kono et al. [85]	100	200	34.8					235	3820	0.334	82.7	2.06	0.66		0.406^
Kono et al. [85]	100	200	34.8					235	3820	0.334	81.4		0.88		0.541
Kono et al. [85]	100	200	34.8					235	3820	0.501	103.3	2.36	0.91		0.560
Kono et al. [85]	100	200	34.8					235	3820	0.501	110.1	2.49	0.8		0.492
Lam and Teng [18]	152	305	35.9	0.203	250.5[t]	3795[t]		230	3420	0.165	50.4	1.273	1.147	0.757	0.771
Lam and Teng [18]	152	305	35.9	0.203	250.5[t]	3795[t]		230	3420	0.165	47.2	1.106	0.969	0.640	0.652
Lam and Teng [18]	152	305	35.9	0.203	250.5[t]	3795[t]		230	3420	0.165	53.2	1.292	0.981	0.648	0.660
Lam and Teng [18]	152	305	35.9	0.203	250.5[t]	3795[t]		230	3420	0.330	68.7	1.683	0.988	0.652	0.664
Lam and Teng [18]	152	305	35.9	0.203	250.5[t]	3795[t]		230	3420	0.330	69.9	1.962	1.001	0.661	0.673
Lam and Teng [18]	152	305	35.9	0.203	250.5[t]	3795[t]		230	3420	0.330	71.6	1.850	0.949	0.626	0.638
Lam and Teng [18]	152	305	34.3	0.188	250.5[t]	3795[t]		230	3420	0.495	82.6	2.046	0.799	0.527	0.537
Lam and Teng [18]	152	305	34.3	0.188	250.5[t]	3795[t]		230	3420	0.495	90.4	2.413	0.884	0.584	0.595
Lam and Teng [18]	152	305	34.3	0.188	250.5[t]	3795[t]		230	3420	0.495	97.3	2.516	0.968	0.639	0.651
Lam and Teng [18]	152	305	34.3	0.188	250.5[t]	3795[t]		230	3420	0.165	50.3	1.022	0.908	0.599	0.611
Lam and Teng [18]	152	305	34.3	0.188	250.5[t]	3795[t]		230	3420	0.165	50.0	1.082	0.890	0.587	0.599
Lam and Teng [18]	152	305	34.3	0.188	250.5[t]	3795[t]		230	3420	0.165	56.7	1.168	0.927	0.612	0.623
Lam et al. [29]	152.5	305	41.1	0.256	250.5[t]	3795[t]				0.165	52.6	0.90	0.81	0.533	
Lam et al. [29]	152.5	305	41.1	0.256	250.5[t]	3795[t]				0.165	57.0	1.21	1.08	0.711	
Lam et al. [29]	152.5	305	41.1	0.256	250.5[t]	3795[t]				0.165	55.4	1.11	1.07	0.704	
Lam et al. [29]	152.5	305	38.9	0.250	250.5[t]	3795[t]				0.330	76.8	1.91	1.06	0.697	
Lam et al. [29]	152.5	305	38.9	0.250	250.5[t]	3795[t]				0.330	79.1	2.08	1.13	0.744	
Lam et al. [29]	152.5	305	38.9	0.250	250.5[t]	3795[t]				0.330	65.80[s]	1.25[a]	0.79		
Lee et al. [86]	150	300	36.2	0.24				250	4510	0.11	41.7	1.0			
Lee et al. [86]	150	300	36.2	0.24				250	4510	0.22	57.8	1.5			
Lee et al. [86]	150	300	36.2	0.24				250	4510	0.33	69.1	2.0			
Lee et al. [86]	150	300	36.2	0.24				250	4510	0.44	85.4	2.7			
Lee et al. [86]	150	300	36.2	0.24				250	4510	0.55	104.3	3.1			
Lin and Li [90]	150	300	18.3					232	4170	0.138	38.62				
Lin and Li [90]	120	240	17.7					232	4170	0.138	43.62				
Lin and Li [90]	100	200	17.9					232	4170	0.138	46.08				
Lin and Li [90]	150	300	18.3					232	4170	0.275	55.74				
Lin and Li [90]	120	240	17.7					232	4170	0.275	63.47				
Lin and Li [90]	100	200	17.9					232	4170	0.275	71.46				
Lin and Li [90]	150	300	18.3					232	4170	0.413	73.57				
Lin and Li [90]	120	240	17.7					232	4170	0.413	85.61				

Paper	D (mm)	H (mm)	f'_{co} (MPa)	ε_{co} (%)	E_{frp} (GPa)	f_{frp} (MPa)	t_{frp} (mm)	E_f (GPa)	f_f (MPa)	t_f (mm)	f'_{cc} (MPa)	ε_{cu} (%)	$\varepsilon_{h,rup}$ (%)	$k_{\varepsilon,frp}$	$k_{\varepsilon,f}$
Lin and Li [90]	100	200	17.9					232	4170	0.413	93.33				
Lin and Li [90]	150	300	23.2					232	4170	0.138	45.41				
Lin and Li [90]	120	240	23.2					232	4170	0.138	49.11				
Lin and Li [90]	100	200	23.5					232	4170	0.138	57.37				
Lin and Li [90]	150	300	23.2					232	4170	0.275	61.98				
Lin and Li [90]	120	240	23.2					232	4170	0.275	76.90				
Lin and Li [90]	100	200	23.5					232	4170	0.275	81.91				
Lin and Li [90]	150	300	23.2					232	4170	0.413	84.46				
Lin and Li [90]	120	240	23.2					232	4170	0.413	91.17				
Lin and Li [90]	100	200	23.5					232	4170	0.413	103.77				
Lin and Li [90]	150	300	25.5					232	4170	0.138	49.02				
Lin and Li [90]	120	240	25.9					232	4170	0.138	56.40				
Lin and Li [90]	100	200	25.5					232	4170	0.138	62.26				
Lin and Li [90]	150	300	25.5					232	4170	0.275	69.82				
Lin and Li [90]	120	240	25.9					232	4170	0.275	81.29				
Lin and Li [90]	100	200	25.5					232	4170	0.275	90.54				
Lin and Li [90]	150	300	25.5					232	4170	0.413	88.73				
Lin and Li [90]	120	240	25.9					232	4170	0.413	98.73				
Lin and Li [90]	100	200	25.5					232	4170	0.413	109.48				
Liang et al. [89]	100	200	25.9	0.24	245	3248	0.167	242	3591	0.167	64.3	2.31	1.48	1.116^	0.997^
Liang et al. [89]	100	200	25.9	0.24	245	3248	0.167	242	3591	0.167	63.0	1.93	1.07	0.807	0.721
Liang et al. [89]	100	200	25.9	0.24	245	3248	0.167	242	3591	0.167	66.4	2.16	1.39	1.048^	0.937^
Liang et al. [89]	100	200	25.9	0.24	245	3248	0.167	242	3591	0.167	64.8	2.16	1.22	0.920	0.822
Liang et al. [89]	200	400	22.7	0.22	245	3248	0.334	242	3591	0.334	64.3	2.29	1.09	0.822	0.735
Liang et al. [89]	200	400	22.7	0.22	245	3248	0.334	242	3591	0.334	69.1	2.37	1.12	0.845	0.755
Liang et al. [89]	200	400	22.7	0.22	245	3248	0.334	242	3591	0.334	60.1	2.00	0.89	0.671	0.600
Liang et al. [89]	200	400	22.7	0.22	245	3248	0.334	242	3591	0.334	66.3	2.48	1.16	0.875	0.782
Liang et al. [89]	300	600	24.5	0.22	245	3248	0.501	242	3591	0.501	58.8	1.84	0.98	0.739	0.660
Liang et al. [89]	300	600	24.5	0.22	245	3248	0.501	242	3591	0.501	59.4	1.71	1.33	1.003^	0.896^
Liang et al. [89]	300	600	24.5	0.22	245	3248	0.501	242	3591	0.501	63.0	2.27	1.70	1.282^	1.146^
Liang et al. [89]	300	600	24.5	0.22	245	3248	0.501	242	3591	0.501	60.6	2.09	1.22	0.920	0.822
Lin and Liao [91]	100	200	23.9		23.83	455.4	1.84				62.42				
Lin and Liao [91]	100	200	23.9		23.83	455.4	1.84				62.06				
Lin and Liao [91]	100	200	23.9		23.83	455.4	1.84				61.45				
Lin and Liao [91]	100	200	23.9		22.46	403.1	3.89				93.56				
Lin and Liao [91]	100	200	23.9		22.46	403.1	3.89				90.69				
Lin and Liao [91]	100	200	23.9		22.46	403.1	3.89				88.98				
Mandal et al. [92]	102	200	30.7	0.27	47	784	0.8				73.8	3.08			
Mandal et al. [92]	102	200	46.3	0.23	47	784	0.8				77.1	1.84			
Mandal et al. [92]	102	200	54.5	0.24	47	784	0.8				72.1	0.80			
Matthys et al. [11]	150	300	34.9		198	2600		240	3900	0.117	44.3	0.85	1.15	0.876^	0.708
Micelli et al. [93]	102	204	37.0					227	3790	0.16	60	1.02	1.2		0.719
Miyauchi et al. [94]	150	300	31.2	0.195				230.5	3481	0.11	52.4	1.213			
Miyauchi et al. [94]	150	300	31.2	0.195				230.5	3481	0.22	67.4	1.554			
Miyauchi et al. [94]	150	300	31.2	0.195				230.5	3481	0.33	81.7	2.013			
Miyauchi et al. [94]	100	200	33.7	0.190				230.5	3481	0.11	69.6	1.406			
Miyauchi et al. [94]	100	200	33.7	0.190				230.5	3481	0.22	88.0	1.488			
Miyauchi et al. [94]	100	200	33.7	0.190				230.5	3481	0.33	109.9	1.900			
Miyauchi et al. [94]	150	300	45.2	0.219				230.5	3481	0.11	59.4	0.945			
Miyauchi et al. [94]	150	300	45.2	0.219				230.5	3481	0.22	79.4	1.245			
Miyauchi et al. [94]	100	200	51.9	0.192				230.5	3481	0.11	75.2	0.956			
Miyauchi et al. [94]	100	200	51.9	0.192				230.5	3481	0.22	104.6	1.275			
Miyauchi et al. [95]	150	300	23.6	0.18				230.5	3481	0.11	36.5	1.589[a]			
Miyauchi et al. [95]	150	300	23.6	0.18				230.5	3481	0.22	50.8	2.384[a]			
Miyauchi et al. [95]	150	300	23.6	0.18				230.5	3481	0.33	64.3				
Miyauchi et al. [95]	100	200	26.3	0.193				230.5	3481	0.11	50.7	1.991[a]			

Paper	D (mm)	H (mm)	f'_{co} (MPa)	ε_{co} (%)	E_{frp} (GPa)	f_{frp} (MPa)	t_{frp} (mm)	E_f (GPa)	f_f (MPa)	t_f (mm)	f'_{cc} (MPa)	ε_{cu} (%)	$\varepsilon_{h,rup}$ (%)	$k_{\varepsilon,frp}$	$k_{\varepsilon,f}$
Miyauchi et al. [95]	100	200	26.3	0.193				230.5	3481	0.22	70.9	2.356[a]			
Miyauchi et al. [95]	100	200	26.3	0.193				230.5	3481	0.33	84.9				
Modarelli et al. [96]	150	300	28.4	0.490	221	3070	0.165	230	3430	0.165	55.25	2.20	1.53		0.890^
Modarelli et al. [96]	150	300	38.2	0.630	221	3070	0.165	230	3430	0.165	62.73	1.49	1.32		0.768
Ongpeng [98]	180	500	27.0					231	3650	0.13	37.23				
Ongpeng [98]	180	500	27.0					231	3650	0.26	51.18				
Owen [99]	102	203	53		238	4200	0.165	262	4200	0.165	70.5	1	1.23	0.697	0.767
Owen [99]	102	203	53		238	4200	0.33	262	4200	0.33	108.8	1.82	1.53	0.867^	0.954^
Owen [99]	102	203	53		238	4200	0.66	262	4200	0.66	149.0[s]	2.32[a]	1.33	0.754	0.830
Owen [99]	102	203	53		238	4200	0.99	262	4200	0.99	197.4[s]	3.3[a]	1.23	0.697	0.767
Owen [99]	102	203	53		238	4200	1.32	262	4200	1.32	259.0[s]	4.17[a]	1.3	0.737	0.811
Owen [99]	152	305	47.9		238	4200	1.32	262	4200	0.165	65.4	0.9	1.28	0.725	0.798
Owen [99]	152	305	47.9		238	4200	1.32	262	4200	0.33	96.2	1.69	1.4	0.793	0.873
Owen [99]	152	305	47.9		238	4200	1.32	262	4200	0.66	121.1	2.04	1.28	0.725	0.798
Picher et al. [101]	152	304	39.7		83	1266	0.9	230	3400	0.33	56	1.07	0.84	0.551	0.568
Piekarczyk et al. [102]	47	112	55	0.7	113	1420	0.82	240	4810		189	2.8			
Piekarczyk et al. [102]	47	112	55	0.7	110	1150	0.51	240	4810		120	2.0			
Pon et al. [103]	450	900	7.1						4410	0.22	15.5				
Pon et al. [103]	450	900	7.1						4410	0.33	21.2				
Pon et al. [103]	300	600	7.2						4410	0.22	21.1				
Pon et al. [103]	300	600	7.2						4410	0.33	26.8				
Pon et al. [103]	600	1200	7.4						4410	0.22	12.8				
Pon et al. [103]	600	1200	7.4						4410	0.33	16.7				
Pon et al. [103]	150	300	9.6						4410	0.22	34.1[s]				
Pon et al. [103]	150	300	9.6						4410	0.33	44.9[s]				
Rochette and Labossiére [104]	100	200	42		82.7	1265	0.6	230	3400	0.22	73.5	1.60	0.89	0.582	0.602
Rochette and Labossiére [104]	100	200	42		82.7	1265	0.6	230	3400	0.22	73.5	1.57	0.95	0.621	0.643
Rochette and Labossiére [104]	100	200	42		82.7	1265	0.6	230	3400	0.22	67.6	1.35	0.80	0.523	0.541
Rousakis et al. [26]	150	300	20.4	0.26				234	4493	0.17	41.3	0.96			0.417^
Rousakis et al. [26]	150	300	20.4	0.26				234	4493	0.34	57.2	1.42[a]			0.333^
Rousakis et al. [26]	150	300	20.4	0.26				234	4493	0.51	63.1[s]	1.42[a]			0.302^
Rousakis et al. [26]	150	300	49.2	0.17				234	4493	0.17	79.0	0.39[a]			0.229^
Rousakis et al. [26]	150	300	49.2	0.17				234	4493	0.34	83.9	0.35[a]			0.135^
Rousakis et al. [26]	150	300	49.2	0.17				234	4493	0.51	100.6	0.62[a]			0.250^
Saenz and Pantelides [106]	152	304	41.8		86.8[p]	1220[p]	1				83.7	1.18	0.92	0.655	
Saenz and Pantelides [106]	152	304	47.5		86.8[p]	1220[p]	1				81.5	0.88	0.93	0.662	
Saenz and Pantelides [106]	152	304	40.3		86.8[p]	1220[p]	2				108.1	2.04	0.92	0.655	
Saenz and Pantelides [106]	152	304	41.7		86.8[p]	1220[p]	2				109.5	1.76	1.08	0.768	
Santarosa et al. [107]	150	300	28.1					230	3400	0.11	38.6				
Santarosa et al. [107]	150	300	15.3					230	3400	0.11	33.6	0.45[a]			
Santarosa et al. [107]	150	300	15.3					230	3400	0.22	46.7	1.30			
Shahawy et al. [16]	152.5	305	19.4	0.33	82.7	2275	0.36	207	3654	0.5	33.8[s]	1.59[a]			
Shahawy et al. [16]	152.5	305	19.4	0.33	82.7	2275	0.58	207	3654	1	46.4[s]	2.21[a]			
Shahawy et al. [16]	152.5	305	19.4	0.33	82.7	2275	0.81	207	3654	1.5	62.6[s]	2.58[a]			
Shahawy et al. [16]	152.5	305	19.4	0.33	82.7	2275	1.03	207	3654	2	75.7[s]	3.56[a]			
Shahawy et al. [16]	152.5	305	19.4	0.33	82.7	2275	1.25	207	3654	2.5	80.2[s]	3.42[a]			
Shahawy et al. [16]	152.5	305	49	0.29	82.7	2275	0.36	207	3654	0.5	59.1[s]	0.62[a]			
Shahawy et al. [16]	152.5	305	49	0.29	82.7	2275	0.58	207	3654	1	76.5[s]	0.97[a]			
Shahawy et al. [16]	152.5	305	49	0.29	82.7	2275	0.81	207	3654	1.5	98.8[s]	1.26[a]			
Shahawy et al. [16]	152.5	305	49	0.29	82.7	2275	1.03	207	3654	2	112.7[s]	1.90[a]			
Shehata et al. [109]	150	300	29.8	0.21				235	3550	0.165	57.0	1.23	1.23		0.814
Shehata et al. [109]	150	300	29.8	0.21				235	3550	0.330	72.1	1.74	1.19		0.788
Shehata et al. [109]	150	300	25.6					235	3550	0.165	43.9				
Shehata et al. [109]	150	300	25.6					235	3550	0.330	59.6				
Shehata et al. [110]	225	450	34	0.2				235	3550	0.165	43.7	0.62			
Shehata et al. [110]	225	450	34	0.2				235	3550	0.330	62.9	1.09			

Paper	D (mm)	H (mm)	f'_{co} (MPa)	ε_{co} (%)	E_{frp} (GPa)	f_{frp} (MPa)	t_{frp} (mm)	E_f (GPa)	f_f (MPa)	t_f (mm)	f'_{cc} (MPa)	ε_{cu} (%)	$\varepsilon_{h,rup}$ (%)	$k_{\varepsilon,frp}$	$k_{\varepsilon,f}$
Shehata et al. [110]	150	300	34	0.2				235	3550	0.165	61.2	0.91			
Shehata et al. [110]	150	300	34	0.2				235	3550	0.330	82.1	1.10			
Smith et al. [36]	250	500	35		210.52[t]	3182[t]				0.262	50		0.893	0.591	
Smith et al. [36]	250	500	35		210.52[t]	3182[t]				0.262	57		1.218	0.806	
Smith et al. [36]	250	500	35		210.52[t]	3182[t]				0.262	59		1.311	0.867^	
Smith et al. [36]	250	500	35		210.52[t]	3182[t]				0.262	56		1.149	0.760	
Song et al. [112]	100	300	22.4					237	4073	0.13	56.2	0.903	0.874		0.509
Song et al. [112]	100	300	22.4					237	4073	0.26	78.2	1.762	0.937		0.545
Song et al. [112]	100	300	22.4					237	4073	0.39	118.7[s]	3.313	1.070		0.623
Song et al. [112]	150	450	22.4					237	4073	0.13	45.7	1.217	1.117		0.650
Song et al. [112]	150	450	22.4					237	4073	0.26	65.4	2.000	1.179		0.686
Song et al. [112]	150	450	22.4					237	4073	0.39	85.0	2.564	1.207		0.702
Song et al. [112]	100	300	40.9					237	4073	0.13	71.1	1.984[a]	0.920		0.535
Song et al. [112]	100	300	40.9					237	4073	0.26	97.6	1.646	1.039		0.605
Song et al. [112]	100	300	40.9					237	4073	0.39	125.0	2.180	1.030		0.599
Song et al. [112]	150	450	40.9					237	4073	0.13	57.1	0.868	1.238		0.720
Song et al. [112]	150	450	40.9					237	4073	0.26	78.4	1.415	1.074		0.625
Song et al. [112]	150	450	40.9					237	4073	0.39	100.4	1.894	1.164		0.677
Stanton and Owen [30]	152.5	305	49.0		262[t]	4200[t]		238	4200	0.165	68.97	1.0			
Stanton and Owen [30]	152.5	305	49.0		262[t]	4200[t]		238	4200	0.330	103.45	1.8			
Stanton and Owen [30]	152.5	305	49.0		262[t]	4200[t]		238	4200	0.660	151.72	2.3			
Stanton and Owen [30]	152.5	305	49.0		262[t]	4200[t]		238	4200	0.990	213.79[s]	3.7			
Stanton and Owen [30]	152.5	305	49.0		262[t]	4200[t]		238	4200	1.320	275.86[s]	4.6			
Suter and Pinzelli [113]	150	300	44.7					240	3800	0.234	68.31	0.856			
Tamuzs et al. [114]	150	300	20.8	0.241	231	2390		234	4500	0.34	37.49[s]	1.076[a]	0.316	0.305^	0.164^
Tamuzs et al. [114]	150	300	20.8	0.241	231	2390		234	4500	0.34	42.26[s]	1.321[a]	0.551	0.533	0.287^
Tamuzs et al. [114]	150	300	48.8	0.251	231	2390		234	4500	0.34	72.08	0.806	0.449	0.434^	0.233^
Tamuzs et al. [114]	150	300	48.8	0.251	231	2390		234	4500	0.34	72.55	0.902	0.373	0.361^	0.194^
Thériault et al. [116]	51	102	18			549		230	3481	0.165	70				
Thériault et al. [116]	152	304	37			549		230	3481	0.330	64				
Thériault et al. [116]	304	608	37			549		230	3481	0.660	66				
Valdmanis et al. [27]	150	300	40.0	0.17	200.5	1906	0.17	234	4500	0.17	66.0	0.63	0.89	0.936^	0.463^
Valdmanis et al. [27]	150	300	40.0	0.17	231.0	2389	0.34	234	4500	0.34	87.2	1.07	0.84	0.812	0.437^
Valdmanis et al. [27]	150	300	40.0	0.17	236.0	2661	0.51	234	4500	0.51	96.0	1.36	0.69	0.612	0.359^
Valdmanis et al. [27]	150	300	44.3	0.17	200.5	1906	0.17	234	4500	0.17	73.3	0.58	0.74	0.778	0.385^
Valdmanis et al. [27]	150	300	44.3	0.17	231.0	2389	0.34	234	4500	0.34	82.6	0.54[a]	0.43	0.416^	0.224^
Valdmanis et al. [27]	150	300	44.3	0.17	236.0	2661	0.51	234	4500	0.51	115.1	0.94	0.78	0.692	0.406^
Vincent and Ozbakkaloglu [117]	152	305	35.5					240	3800	0.117	44.0	0.77	1.20		0.758
Vincent and Ozbakkaloglu [117]	152	305	35.5					240	3800	0.117	43.9	0.82	1.10		0.695
Vincent and Ozbakkaloglu [117]	152	305	35.5					240	3800	0.117	43.1	0.82	1.10		0.695
Vincent and Ozbakkaloglu [117]	152	305	38.0					240	3800	0.234	63.5	1.51	1.17		0.739
Vincent and Ozbakkaloglu [117]	152	305	38.0					240	3800	0.234	66.1	1.65	1.17		0.739
Vincent and Ozbakkaloglu [117]	152	305	36.1					240	3800	0.234	58.6	1.27	1.11		0.701
Wang and Wu [33]	150	300	30.9	0.24	219[t]	4364[t]		230.5	3482	0.165	53.8		1.24	0.622	0.821
Wang and Wu [33]	150	300	30.9	0.24	219[t]	4364[t]		230.5	3482	0.165	61.2		1.24	0.622	0.821
Wang and Wu [33]	150	300	30.9	0.24	219[t]	4364[t]		230.5	3482	0.165	52.3		1.24	0.622	0.821
Wang and Wu [33]	150	300	30.9	0.24	219[t]	4364[t]		230.5	3482	0.330	88.2		1.32	0.662	0.874
Wang and Wu [33]	150	300	30.9	0.24	219[t]	4364[t]		230.5	3482	0.330	85.6		1.32	0.662	0.874
Wang and Wu [33]	150	300	30.9	0.24	219[t]	4364[t]		230.5	3482	0.330	80.6		1.32	0.662	0.874
Wang and Wu [33]	150	300	52.1	0.27	225.7[t]	3788[t]		230	3500	0.165	68.0		1.57	0.935^	1.032^
Wang and Wu [33]	150	300	52.1	0.27	225.7[t]	3788[t]		230	3500	0.165	69.2		1.57	0.935^	1.032^
Wang and Wu [33]	150	300	52.1	0.27	225.7[t]	3788[t]		230	3500	0.165	66.5		1.57	0.935^	1.032^
Wang and Wu [33]	150	300	52.1	0.27	225.7[t]	3788[t]		230	3500	0.330	100.0		1.56	0.929^	1.025^
Wang and Wu [33]	150	300	52.1	0.27	225.7[t]	3788[t]		230	3500	0.330	94.9		1.56	0.929^	1.025^
Wang and Wu [33]	150	300	52.1	0.27	225.7[t]	3788[t]		230	3500	0.330	103		1.56	0.929^	1.025^
Watanabe et al. [28]	100	200	30.2		224.6[t]	2716[t]		235	3432	0.167	46.6	1.51	0.94	0.777	0.644

Paper	D (mm)	H (mm)	f'_{co} (MPa)	ε_{co} (%)	E_{frp} (GPa)	f_{frp} (MPa)	t_{frp} (mm)	E_f (GPa)	f_f (MPa)	t_f (mm)	f'_{cc} (MPa)	ε_{cu} (%)	$\varepsilon_{h,rup}$ (%)	$k_{\varepsilon,frp}$	$k_{\varepsilon,f}$
Watanabe et al. [28]	100	200	30.2		224.6[t]	2873[t]		235	3432	0.501	87.2	3.11	0.82	0.641	0.561
Watanabe et al. [28]	100	200	30.2		224.6[t]	2658[t]		235	3432	0.668	104.6	4.15	0.76	0.642	0.520
Wu and Jiang [121]	150	300	28.7		254	4192	0.167	230	3400	0.167	59.34	2.534[a]			
Wu and Jiang [121]	150	300	28.7		254	4192	0.167	230	3400	0.167	54.82	2.140[a]			
Wu and Jiang [121]	150	300	30.1		254	4192	0.334	230	3400	0.334	88.14[s]	3.887[a]			
Wu and Jiang [121]	150	300	30.1		254	4192	0.334	230	3400	0.334	90.40[s]	3.798[a]			
Wu and Jiang [24]	150	300	20.6		242	4441	0.167	242	4059	0.167	50.35		1.41	0.768	0.841
Wu and Jiang [24]	150	300	20.6		242	4441	0.167	242	4059	0.167	52.95		1.56	0.850^	0.930^
Wu and Jiang [24]	150	300	20.6		242	4441	0.167	242	4059	0.167	53.23		1.43	0.779	0.853
Wu and Jiang [24]	150	300	20.6		242	4441	0.334	242	4059	0.334	83.72[s]		1.84	1.003^	1.097^
Wu and Jiang [24]	150	300	20.6		242	4441	0.334	242	4059	0.334	86.55[s]		1.86	1.014^	1.109^
Wu and Jiang [24]	150	300	20.6		242	4441	0.334	242	4059	0.334	88.76[s]		2.26	1.232^	1.347^
Wu and Jiang [24]	150	300	20.6		242	4441	0.501	242	4059	0.501	110.20[s]		1.79	0.975^	1.067^
Wu and Jiang [24]	150	300	20.6		242	4441	0.501	242	4059	0.501	108.11[s]		1.37	0.747	0.817
Wu and Jiang [24]	150	300	20.6		242	4441	0.501	242	4059	0.501	109.97[s]		1.73	0.943^	1.031^
Wu and Jiang [24]	150	300	20.6		242	4441	0.668	242	4059	0.668	127.74[s]		1.92	1.046^	1.145^
Wu and Jiang [24]	150	300	20.6		242	4441	0.668	242	4059	0.668	132.54[s]		1.85	1.008^	1.103^
Wu and Jiang [24]	150	300	20.6		242	4441	0.668	242	4059	0.668	140.58[s]		1.71	0.932^	1.020^
Wu and Jiang [24]	150	300	24.8		242	4441	0.167	242	4059	0.167	61.66		1.81	0.986^	1.079^
Wu and Jiang [24]	150	300	24.8		242	4441	0.167	242	4059	0.167	56.68		1.56	0.850	0.930^
Wu and Jiang [24]	150	300	24.8		242	4441	0.167	242	4059	0.167	56.91		2.04	1.112^	1.216^
Wu and Jiang [24]	150	300	24.8		242	4441	0.334	242	4059	0.334	87.23[s]		1.87	1.019^	1.115^
Wu and Jiang [24]	150	300	24.8		242	4441	0.334	242	4059	0.334	87.80[s]		1.71	0.932^	1.020^
Wu and Jiang [24]	150	300	24.8		242	4441	0.334	242	4059	0.334	88.25[s]		1.65	0.899^	0.984^
Wu and Jiang [24]	150	300	24.8		242	4441	0.501	242	4059	0.501	118.63[s]		1.73	0.943^	1.031^
Wu and Jiang [24]	150	300	24.8		242	4441	0.501	242	4059	0.501	114.67[s]		1.75	0.954^	1.043^
Wu and Jiang [24]	150	300	24.8		242	4441	0.501	242	4059	0.501	114.55[s]		2	1.090^	1.192^
Wu and Jiang [24]	150	300	24.8		242	4441	0.668	242	4059	0.668	133.79		1.36	0.741	0.811
Wu and Jiang [24]	150	300	24.8		242	4441	0.668	242	4059	0.668	135.03		1.44	0.785	0.859
Wu and Jiang [24]	150	300	24.8		242	4441	0.668	242	4059	0.668	139.05		1.51	0.823	0.900^
Wu and Jiang [24]	150	300	36.7		242	4441	0.167	242	4059	0.167	61.89		1.52	0.828	0.906^
Wu and Jiang [24]	150	300	36.7		242	4441	0.167	242	4059	0.167	71.56		1.91	1.041^	1.139^
Wu and Jiang [24]	150	300	36.7		242	4441	0.167	242	4059	0.167	65.51		1.6	0.872	0.954^
Wu and Jiang [24]	150	300	36.7		242	4441	0.334	242	4059	0.334	92.38		1.6	0.872	0.954^
Wu and Jiang [24]	150	300	36.7		242	4441	0.334	242	4059	0.334	97.64		1.68	0.915^	1.002^
Wu and Jiang [24]	150	300	36.7		242	4441	0.334	242	4059	0.334	95.66		1.71	0.932^	1.020^
Wu and Jiang [24]	150	300	36.7		242	4441	0.501	242	4059	0.501	121.23		1.52	0.828	0.906^
Wu and Jiang [24]	150	300	36.7		242	4441	0.501	242	4059	0.501	128.64[s]		1.54	0.839	0.918^
Wu and Jiang [24]	150	300	36.7		242	4441	0.501	242	4059	0.501	116.53		1.7	0.926^	1.014^
Wu and Jiang [24]	150	300	36.7		242	4441	0.668	242	4059	0.668	141.77		1.62	0.883	0.966^
Wu et al. [31]	150	300	23.0		243[t]	4234[t]		230	3400	0.167	45.0				
Wu et al. [35]	150	300	23.1	0.260	243[t]	4234[t]		230	3400	0.167	44.9	2.01			
Wu et al. [35]	150	300	23.1	0.267	243[t]	4234[t]		230	3400	0.167	45.9	2.15			
Wu et al. [35]	150	300	23.1	0.267	243[t]	4234[t]		230	3400	0.334	82.0[s]	3.75			
Xiao and Wu [15]	152	305	33.7		105	1577	0.381				47.9	1.20	0.84	0.559	
Xiao and Wu [15]	152	305	33.7		105	1577	0.381				49.7	1.40	1.15	0.766	
Xiao and Wu [15]	152	305	33.7		105	1577	0.381				49.4	1.24	0.87	0.579	
Xiao and Wu [15]	152	305	33.7		105	1577	0.762				64.6	1.65	0.91	0.606	
Xiao and Wu [15]	152	305	33.7		105	1577	0.762				75.2	2.25	1.00	0.666	
Xiao and Wu [15]	152	305	33.7		105	1577	0.762				71.8	2.16	1.00	0.666	
Xiao and Wu [15]	152	305	33.7		105	1577	1.143				82.9	2.45	0.82	0.546	
Xiao and Wu [15]	152	305	33.7		105	1577	1.143				86.2	3.03[a]	0.90	0.599	
Xiao and Wu [15]	152	305	33.7		105	1577	1.143				95.4				
Xiao and Wu [15]	152	305	43.8		105	1577	0.381				54.7	0.98	0.81	0.539	
Xiao and Wu [15]	152	305	43.8		105	1577	0.381				52.1	0.47	0.76	0.506	
Xiao and Wu [15]	152	305	43.8		105	1577	0.381				48.7	0.37[a]	0.28	0.186^	

Paper	D (mm)	H (mm)	f'_{co} (MPa)	ε_{co} (%)	E_{frp} (GPa)	f_{frp} (MPa)	t_{frp} (mm)	E_f (GPa)	f_f (MPa)	t_f (mm)	f'_{cc} (MPa)	ε_{cu} (%)	$\varepsilon_{h,rup}$ (%)	$k_{\varepsilon,frp}$	$k_{\varepsilon,f}$
Xiao and Wu [15]	152	305	43.8		105	1577	0.762				84.0	1.57	0.92	0.613	
Xiao and Wu [15]	152	305	43.8		105	1577	0.762				79.2	1.37	1.00	0.666	
Xiao and Wu [15]	152	305	43.8		105	1577	0.762				85.0	1.66	1.01	0.672	
Xiao and Wu [15]	152	305	43.8		105	1577	1.143				96.5	1.74	0.79	0.526	
Xiao and Wu [15]	152	305	43.8		105	1577	1.143				92.6	1.68	0.71	0.473^	
Xiao and Wu [15]	152	305	43.8		105	1577	1.143				94.0	1.75	0.84	0.559	
Xiao and Wu [15]	152	305	55.2		105	1577	0.381				57.9	0.69	0.70	0.466^	
Xiao and Wu [15]	152	305	55.2		105	1577	0.381				62.9	0.48	0.62	0.413^	
Xiao and Wu [15]	152	305	55.2		105	1577	0.381				58.1	0.49	0.19	0.127^	
Xiao and Wu [15]	152	305	55.2		105	1577	0.762				74.6	1.21	0.74	0.493	
Xiao and Wu [15]	152	305	55.2		105	1577	0.762				77.6	0.81	0.83	0.553	
Xiao and Wu [15]	152	305	55.2		105	1577	0.762				77.0				
Xiao and Wu [15]	152	305	55.2		105	1577	1.143				106.5	1.43	0.76	0.506	
Xiao and Wu [15]	152	305	55.2		105	1577	1.143				108.0	1.45	0.85	0.566	
Xiao and Wu [15]	152	305	55.2		105	1577	1.143				103.3	1.18	0.70	0.466^	
Yan et al. [123]	305	610	15.0	0.200	86.9	1220	1				37.8	1.1			
Youssef et al. [53]	406.4	812.8	29.4	0.24	103.84	1246	5.840				125.80	2.813			
Youssef et al. [53]	406.4	812.8	29.4	0.24	103.84	1246	5.840				126.39	2.914			
Youssef et al. [53]	406.4	812.8	29.4	0.24	103.84	1246	5.840				127.01	2.801			
Youssef et al. [53]	406.4	812.8	29.4	0.24	103.84	1246	3.504				83.05	1.492			
Youssef et al. [53]	406.4	812.8	29.4	0.24	103.84	1246	3.504				88.68	1.621			
Youssef et al. [53]	406.4	812.8	29.4	0.24	103.84	1246	2.336				64.78	1.155			
Youssef et al. [53]	406.4	812.8	29.4	0.24	103.84	1246	2.336				62.09	1.112			
Youssef et al. [53]	406.4	812.8	29.4	0.24	103.84	1246	2.336				67.47	1.199			
Youssef et al. [53]	406.4	812.8	29.4	0.24	103.84	1246	1.168				45.95	0.647			
Youssef et al. [53]	406.4	812.8	29.4	0.24	103.84	1246	1.168				45.78	0.615			
Youssef et al. [53]	152.4	304.8	44.6	0.20	103.84	1246	2.336				124.08	2.847			
Youssef et al. [53]	152.4	304.8	44.6	0.20	103.84	1246	2.336				129.17	2.792			
Youssef et al. [53]	152.4	304.8	44.6	0.20	103.84	1246	2.336				138.72	2.844			
Youssef et al. [53]	152.4	304.8	44.6	0.20	103.84	1246	1.752				94.24	1.996			
Youssef et al. [53]	152.4	304.8	44.6	0.20	103.84	1246	1.752				95.02	1.999			
Youssef et al. [53]	152.4	304.8	44.6	0.20	103.84	1246	1.752				100.52	1.979			
Youssef et al. [53]	152.4	304.8	44.6	0.20	103.84	1246	1.168				85.96	1.706			
Youssef et al. [53]	152.4	304.8	44.6	0.20	103.84	1246	1.168				88.14	2.003			
Youssef et al. [53]	152.4	304.8	44.6	0.20	103.84	1246	1.168				84.23	1.996			
Zhang et al. [124]	150	300	34.3		91[p,m]	753[p,m]	1	240	3800	0.33	59.4	2.1			

p denotes fiber tensile strength and elastic modulus are given in N/mm-ply
t denotes FRP properties calculated based on total nominal ply thickness of fiber sheet
m denotes FRP material properties that differ significantly from the reference properties of the corresponding material
d denotes ultimate axial stress values that are lower than the unconfined concrete strength
s denotes inconsistent axial stress when compared with overall trend in the database
a denotes inconsistent axial strain when compared with overall trend in the database
^ denotes inconsistent k_ε values when compared with overall trend in the database

Table 4. Test database of GFRP-wrapped concrete specimens

Paper	Specimen Dimensions		Concrete Properties		FRP Properties			Fiber Properties			Measured Ultimate Conditions			Hoop Rupture Strain Reduction Factors	
	D (mm)	H (mm)	f'_{co} (MPa)	ε_{co} (%)	E_{frp} (GPa)	f_{frp} (MPa)	t_{frp} (mm)	E_f (GPa)	f_f (MPa)	t_f (mm)	f'_{cc} (MPa)	ε_{cu} (%)	$\varepsilon_{h,rup}$ (%)	$k_{\varepsilon,frp}$	$k_{\varepsilon,f}$
Aire et al. [56]	150	300	42					65	3000	0.149	41[s]	0.73[a]	0.55		0.119^
Aire et al. [56]	150	300	42					65	3000	0.447	61[s]	1.74[a]	1.3		0.282^
Aire et al. [56]	150	300	42					65	3000	0.894	85[s]	2.5[a]	1.1		0.238^
Abdollahi et al. [54]	150	300	14.8	0.24	26.49	537	0.508	24.59	504		30.0	1.85			
Abdollahi et al. [54]	150	300	25.1	0.23	26.49	537	0.508	24.59	504		34.2	1.40			
Abdollahi et al. [54]	150	300	41.7	0.28	26.49	537	0.508	24.59	504		51.9	0.43[a]			
Abdollahi et al. [54]	150	300	25.1	0.23	26.49	537	1.016	24.59	504		55.5	1.96			
Abdollahi et al. [54]	150	300	25.1	0.23	26.49	537	2.032	24.59	504		83.3[s]	2.77			
Ahmad et al. [55]	102	203	39.0		48.3	2070	0.88				115.3				
Ahmad et al. [55]	102	203	50.5		48.3	2070	0.88				135.1				
Almusallam [58]	150	300	47.7	0.308	27	540	1.3				56.7	1.485	0.849	0.425^	
Almusallam [58]	150	300	47.7	0.308	27	540	3.9				100.1	2.723	0.800	0.400^	
Almusallam [58]	150	300	50.8	0.294	27	540	1.3				55.5	0.970	1.007	0.504	
Almusallam [58]	150	300	50.8	0.294	27	540	3.9				90.8	0.970	0.802	0.401^	
Au and Buyukozturk [59]	150	375	24.2	0.360	26.1	575	1.2				43.8	2.230	1.480	0.672	
Berthet et al. [61]	160	320	25					74	2500	0.330	42.8	1.698	1.655		0.490^
Berthet et al. [61]	160	320	25					74	2500	0.330	42.3	1.687	1.643		0.486^
Berthet et al. [61]	160	320	25					74	2500	0.330	43.1	1.711	1.671		0.495^
Berthet et al. [61]	160	320	40					74	2500	0.220	44.8	0.526	1.369		0.405^
Berthet et al. [61]	160	320	40					74	2500	0.220	46.3	0.467[a]	1.246		0.369^
Berthet et al. [61]	160	320	40					74	2500	0.220	49.8	0.496[a]	1.075		0.318^
Berthet et al. [61]	160	320	40					74	2500	0.330	50.8	0.632[a]	0.900		0.266^
Berthet et al. [61]	160	320	40					74	2500	0.330	50.8	0.582[a]	1.281		0.379^
Berthet et al. [61]	160	320	40					74	2500	0.330	51.8	0.635[a]	1.197		0.354^
Berthet et al. [61]	160	320	40					74	2500	0.550	66.7	1.050	1.546		0.458^
Berthet et al. [61]	160	320	40					74	2500	0.550	68.2	1.240	1.817		0.538
Berthet et al. [61]	160	320	40					74	2500	0.550	67.7	1.168	1.582		0.468^
Berthet et al. [61]	160	320	52					74	2500	0.495	64.7	0.529[a]	1.190		0.352^
Berthet et al. [61]	160	320	52					74	2500	0.495	75.1	1.132	1.265		0.374^
Berthet et al. [61]	160	320	52					74	2500	0.495	76.1	1.132	1.274		0.377^
Bullo [64]	150	300	32.54	0.248				65	1700	0.46	72.43	3.727[a]	2.145		0.820
Bullo [64]	150	300	32.54	0.248				65	1700	0.46	73.56	3.928[a]	2.171		0.830
Bullo [64]	150	300	32.54	0.248				65	1700	0.46	75.83	2.853	2.048		0.783
Bullo [64]	150	300	32.54	0.248				65	1700	1.15	118.84	4.280	1.961		0.750
Bullo [64]	150	300	32.54	0.248				65	1700	1.15	130.15[s]	4.038	1.918		0.733
Bullo [64]	150	300	32.54	0.248				65	1700	1.15	135.81[s]	4.844	1.816		0.694
Comert et al. [67]	150	300	39					65	1700	0.56	64	2.3			
Comert et al. [67]	150	300	39					65	1700	0.56	61	2.1			
Cui and Sheikh [68]	152	305	47.8	0.222	22	508.2	1.25				59.1	1.35	2.020	0.874^	
Cui and Sheikh [68]	152	305	47.8	0.222	22	508.2	1.25				59.8	1.15	2.143	0.928^	
Cui and Sheikh [68]	152	305	47.8	0.222	22	508.2	2.5				88.9	2.21	2.032	0.880^	
Cui and Sheikh [68]	152	305	47.8	0.222	22	508.2	2.5				88.0	2.21	2.114	0.915^	
Cui and Sheikh [68]	152	305	47.8	0.222	22	508.2	3.75				113.2	2.85	2.112	0.914^	
Cui and Sheikh [68]	152	305	47.8	0.222	22	508.2	3.75				112.5	2.80	2.110	0.913^	
Demers and Neale [69]	152	305	32.2		10.5[p]	220[p]	1				31.0[d]				
Demers and Neale [69]	152	305	32.2		10.5[p]	220[p]	1				30.8[d]				
Demers and Neale [69]	152	305	32.2		10.5[p]	220[p]	3				48.3	2.04			
Demers and Neale [69]	152	305	32.2		10.5[p]	220[p]	3				48.3	1.97			
Green et al. [73]	152	305	54.0					8.8[p]	182[p]	2	62				
Harries and Carey [8]	152	305	31.8	0.28	4.9[p]	75[p]	3	10.3[p]	154[p]		37.3	0.65	1.216	0.794	0.813
Harries and Carey [8]	152	305	31.8	0.28	4.9[p]	75[p]	9	10.3[p]	154[p]		53.2[S]	0.95[a]	1.438	0.939^	0.962^

Paper	D (mm)	H (mm)	f'_{co} (MPa)	ε_{co} (%)	E_{frp} (GPa)	f_{frp} (MPa)	t_{frp} (mm)	E_f (GPa)	f_f (MPa)	t_f (mm)	f'_{cc} (MPa)	ε_{cu} (%)	$\varepsilon_{h,rup}$ (%)	$k_{\varepsilon,frp}$	$k_{\varepsilon,f}$
Harries and Kharel [75]	152	305	32.1	0.28	4.9[p]	75[p]	1	10.3[p]	154[p]		36.8	0.44			
Harries and Kharel [75]	152	305	32.1	0.28	4.9[p]	75[p]	2	10.3[p]	154[p]		36.6	0.40			
Harries and Kharel [75]	152	305	32.1	0.28	4.9[p]	75[p]	3	10.3[p]	154[p]		36.6	0.50	1.20	0.784	0.803
Harries and Kharel [75]	152	305	32.1	0.28	4.9[p]	75[p]	6	10.3[p]	154[p]		37.6	0.57[a]	1.03	0.673	0.689
Harries and Kharel [75]	152	305	32.1	0.28	4.9[p]	75[p]	9	10.3[p]	154[p]		46.7	0.68[a]	1.11	0.725	0.742
Harries and Kharel [75]	152	305	32.1	0.28	4.9[p]	75[p]	12	10.3[p]	154[p]		50.2	0.82[a]	1.09	0.712	0.729
Harries and Kharel [75]	152	305	32.1	0.28	4.9[p]	75[p]	15	10.3[p]	154[p]		60	0.87[a]	1.11	0.725	0.742
Jiang and Teng [32]	152	305	33.1	0.309	80.1[t]	1826[t]				0.17	42.4	1.303	2.08	0.912^	
Jiang and Teng [32]	152	305	33.1	0.309	80.1[t]	1826[t]				0.17	41.6	1.268	1.758	0.771	
Jiang and Teng [32]	152	305	45.9	0.243	80.1[t]	1826[t]				0.17	40.5	0.813	1.523	0.668	
Jiang and Teng [32]	152	305	45.9	0.243	80.1[t]	1826[t]				0.17	40.5	1.063	1.915	0.84	
Jiang and Teng [32]	152	305	45.9	0.243	80.1[t]	1826[t]				0.34	52.8	1.203	1.639	0.719	
Jiang and Teng [32]	152	305	45.9	0.243	80.1[t]	1826[t]				0.34	55.2	1.254	1.799	0.789	
Jiang and Teng [32]	152	305	45.9	0.243	80.1[t]	1826[t]				0.51	64.6	1.554	1.594	0.699	
Jiang and Teng [32]	152	305	45.9	0.243	80.1[t]	1826[t]				0.51	65.9	1.904	1.940	0.851	
Lam and Teng [18]	152	305	38.5	0.223	21.8[t]	506.9[t]		22.46	450	1.27	56.2		1.849	0.795	0.923^
Lam and Teng [18]	152	305	38.5	0.223	21.8[t]	506.9[t]		22.46	450	1.27	51.9	1.315	1.442	0.62	0.72
Lam and Teng [18]	152	305	38.5	0.223	21.8[t]	506.9[t]		22.46	450	1.27	58.3	1.459	1.885	0.811	0.941^
Lam and Teng [18]	152	305	38.5	0.223	21.8[t]	506.9[t]		22.46	450	2.54	75.7	2.457	1.762	0.758	0.879^
Lam and Teng [18]	152	305	38.5	0.223	21.8[t]	506.9[t]		22.46	450	2.54	77.3	2.188	1.674	0.72	0.836
Lam and Teng [18]	152	305	38.5	0.223	21.8[t]	506.9[t]		22.46	450	2.54	75.2		1.772	0.762	0.884^
Li et al. [87]	152.4	305	45.6		15.1	320.2	0.738	70	3000	0.4	49.4[s]				
Lin and Chen [38]	120	240	32.7		32.9	743.9	0.9				62.2				
Lin and Chen [38]	120	240	32.7		32.9	743.9	0.9				61.4				
Lin and Chen [38]	120	240	32.7		32.9	743.9	0.9				66.3				
Lin and Chen [38]	120	240	32.7		32.9	743.9	1.8				101.3				
Lin and Chen [38]	120	240	32.7		32.9	743.9	1.8				88.0				
Lin and Chen [38]	120	240	32.7		32.9	743.9	1.8				104.5				
Mandal et al. [92]	103	200	30.7	0.270	26.1	575	1.3				54.5	1.54[a]			
Mandal et al. [92]	105	200	30.7	0.270	26.1	575	2.6				79.3	2.75[a]			
Mandal et al. [92]	103	200	46.3	0.230	26.1	575	1.3				58.5	0.90[a]			
Mandal et al. [92]	105	200	46.3	0.230	26.1	575	2.6				83.8	1.48			
Mandal et al. [92]	103	200	54.5	0.240	26.1	575	1.3				63.5	0.32[a]			
Mandal et al. [92]	105	200	54.5	0.240	26.1	575	2.6				84.1	0.80[a]			
Mastrapa [10]	152.5	305	29.8		19.19	565	0.61	55.85	1800	0.330	33.7				
Mastrapa [10]	152.5	305	31.2		19.19	565	1.84	55.85	1800	0.991	67.5	3.01	2.26	0.767	0.701
Mastrapa [10]	152.5	305	31.2		19.19	565	1.84	55.85	1800	0.991	64.67	3.13	1.99	0.676	0.617
Mastrapa [10]	152.5	305	31.2		19.19	565	3.07	55.85	1800	1.651	91.01	5.27	1.83	0.621^	0.568^
Mastrapa [10]	152.5	305	31.2		19.19	565	3.07	55.85	1800	1.651	96.87	6.25[a]	1.80	0.611^	0.559^
Mastrapa [10]	152.5	305	37.2		19.19	586	4.06	55.85	1800	2.311	111.0				
Micelli et al. [93]	102	204	32.0	0.14				72	1520	0.35	51.6	1.25	1.25		0.592^
Mirmiran et al. [9]	152.5	305	29.8					55.85	1800	0.275	31.03	1.0			
Mirmiran et al. [9]	152.5	305	29.8					55.85	1800	0.275	34.06	1.3			
Mirmiran et al. [9]	152.5	305	29.8					55.85	1800	0.275	35.58	1.5			
Mirmiran et al. [9]	152.5	305	29.8					55.85	1800	0.826	63.02	2.7			
Mirmiran et al. [9]	152.5	305	29.8					55.85	1800	0.826	49.02	1.8			
Mirmiran et al. [9]	152.5	305	29.8					55.85	1800	0.826	58.68	3.3			
Mirmiran et al. [9]	152.5	305	29.8					55.85	1800	1.376	86.81	3.3			
Mirmiran et al. [9]	152.5	305	29.8					55.85	1800	1.376	88.32	3.6			
Mirmiran et al. [9]	152.5	305	29.8					55.85	1800	1.376	93.63	3.8			
Mirmiran et al. [9]	152.5	305	31.2					55.85	1800	0.826	63.09	3.1			
Mirmiran et al. [9]	152.5	305	31.2					55.85	1800	0.826	65.43	3.1			
Mirmiran et al. [9]	152.5	305	31.2					55.85	1800	1.376	91.91	4.3			
Mirmiran et al. [9]	152.5	305	31.2					55.85	1800	1.376	89.01	5.0			
Modarelli et al. [96]	150	300	28.35	0.49	86	1957	0.23	65	1700	0.23	53.27	1.9[a]			
Nanni and Bradford [97]	150	300	36.3		52	583[m]	0.3	72.59	3240	0.215	46.00	2.292[a]			

Paper	D (mm)	H (mm)	f'_{co} (MPa)	ε_{co} (%)	E_{frp} (GPa)	f_{frp} (MPa)	t_{frp} (mm)	E_f (GPa)	f_f (MPa)	t_f (mm)	f'_{cc} (MPa)	ε_{cu} (%)	$\varepsilon_{h,rup}$ (%)	$k_{\varepsilon,frp}$	$k_{\varepsilon,f}$
Nanni and Bradford [97]	150	300	36.3		52	583[m]	0.3	72.59	3240	0.215	41.20	1.889			
Nanni and Bradford [97]	150	300	36.3		52	583[m]	0.6	72.59	3240	0.43	60.52	3.079			
Nanni and Bradford [97]	150	300	36.3		52	583[m]	0.6	72.59	3240	0.43	59.23	3.405[a]			
Nanni and Bradford [97]	150	300	36.3		52	583[m]	0.6	72.59	3240	0.43	59.77	2.744			
Nanni and Bradford [97]	150	300	36.3		52	583[m]	0.6	72.59	3240	0.43	60.16	2.887			
Nanni and Bradford [97]	150	300	36.3		52	583[m]	0.6	72.59	3240	0.43	69.02	3.100			
Nanni and Bradford [97]	150	300	36.3		52	583[m]	0.6	72.59	3240	0.43	55.75	2.489			
Nanni and Bradford [97]	150	300	36.3		52	583[m]	0.6	72.59	3240	0.43	56.41	2.968			
Nanni and Bradford [97]	150	300	36.3		52	583[m]	1.2	72.59	3240	0.86	84.88	3.145			
Nanni and Bradford [97]	150	300	36.3		52	583[m]	1.2	72.59	3240	0.86	84.33	4.150			
Nanni and Bradford [97]	150	300	36.3		52	583[m]	1.2	72.59	3240	0.86	79.64	4.100			
Nanni and Bradford [97]	150	300	36.3		52	583[m]	1.2	72.59	3240	1.72	106.87[s]	5.242[a]			
Nanni and Bradford [97]	150	300	36.3		52	583[m]	1.2	72.59	3240	1.72	104.94[s]	5.453[a]			
Nanni and Bradford [97]	150	300	36.3		52	583[m]	1.2	72.59	3240	1.72	107.91[s]	4.509[a]			
Shao et al. [108]	152	305	40.2		26.13	610	1.02	72.4	2275	0.358	49.6				
Shao et al. [108]	152	305	40.2		26.13	610	2.03	72.4	2275	0.716	71.4				
Silva and Rodrigues [111]	150	300	31.1	0.240	21.3	464.3	2.54	26.1	575	2.6	91.6	2.61	1.985	0.911	0.901
Silva and Rodrigues [111]	150	300	29.6	0.240	21.3	464.3	2.54	26.1	575	2.6	89.4	2.72			
Silva and Rodrigues [111]	150	300	31.1	0.240	21.3	464.3	2.54	26.1	575	2.6	87.5	2.28	1.890	0.867	0.858
Silva and Rodrigues [111]	150	450	31.1	0.240	21.3	464.3	2.54	26.1	575	2.6	91.9	2.34	1.865	0.856	0.847
Silva and Rodrigues [111]	150	450	29.6	0.240	21.3	464.3	2.54	26.1	575	2.6	89.8	2.32			
Silva and Rodrigues [111]	150	450	31.2	0.240	21.3	464.3	2.54	26.1	575	2.6	91.9	2.31	1.925	0.883	0.874
Silva and Rodrigues [111]	250	750	31.2	0.240	21.3	464.3	2.54	26.1	575	2.6	55.8	1.09	1.160	0.532^	0.527^
Suter and Pinzelli [113]	150	300	44.7					73	2300	0.308	52.69	0.232[a]			
Teng et al. [115]	152.5	305	39.6	0.263	80.1[t]	1826[t]				0.17	37.2[d]	0.942	1.609	0.706	
Teng et al. [115]	152.5	305	39.6	0.263	80.1[t]	1826[t]				0.17	38.8[d]	0.825	1.869	0.820	
Teng et al. [115]	152.5	305	39.6	0.263	80.1[t]	1826[t]				0.34	54.6	2.130	2.040	0.895^	
Teng et al. [115]	152.5	305	39.6	0.263	80.1[t]	1826[t]				0.34	56.3	1.825	2.061	0.904^	
Teng et al. [115]	152.5	305	39.6	0.263	80.1[t]	1826[t]				0.51	65.7	2.558	1.955	0.858	
Teng et al. [115]	152.5	305	39.6	0.263	80.1[t]	1826[t]				0.51	60.9	1.792	1.667	0.731	
Thériault et al. [116]	152	304	37			642		27.6	552	3.9	90				
Thériault et al. [116]	51	102	18			642		27.6	552	1.3	64				
Wong et al. [34]	152.5	305	46.7	0.287	80.1[t]	1826[t]				0.34	58.0	1.77			
Wong et al. [34]	152.5	305	36.7	0.274	80.1[t]	1826[t]				0.34	53.1	1.53			
Wong et al. [34]	152.5	305	36.5	0.256	80.1[t]	1826[t]				0.34	53.8	1.54			
Wong et al. [34]	152.5	305	36.5	0.256	80.1[t]	1826[t]				0.51	63.1	2.15			
Wu et al. [31]	150	300	23.0		80.5[t]	1794[t]		73	1500	0.354	45.0				
Wu et al. [35]	150	300	23.1	0.267	80.5[t]	1794[t]		73	1500	0.354	46.4	2.49			
Wu et al. [35]	150	300	23.1	0.267	80.5[t]	1794[t]		73	1500	0.354	45.0	2.36			
Youssef et al. [53]	406.4	812.8	29.4	0.24	18.47	424.7	7.267				70.77	1.527[a]			
Youssef et al. [53]	406.4	812.8	29.4	0.24	18.47	424.7	7.267				71.78	1.445[a]			
Youssef et al. [53]	406.4	812.8	29.4	0.24	18.47	424.7	7.267				76.78	1.387[a]			
Youssef et al. [53]	406.4	812.8	29.4	0.24	18.47	424.7	4.472				49.53	1.345			
Youssef et al. [53]	406.4	812.8	29.4	0.24	18.47	424.7	4.472				54.90	1.003			
Youssef et al. [53]	406.4	812.8	29.4	0.24	18.47	424.7	4.472				61.19	1.189			
Youssef et al. [53]	406.4	812.8	29.4	0.24	18.47	424.7	3.354				49.30	0.971			
Youssef et al. [53]	406.4	812.8	29.4	0.24	18.47	424.7	3.354				51.19	0.897			
Youssef et al. [53]	406.4	812.8	29.4	0.24	18.47	424.7	3.354				47.88	0.912			
Youssef et al. [53]	406.4	812.8	29.4	0.24	18.47	424.7	1.677				44.14	0.781			
Youssef et al. [53]	406.4	812.8	29.4	0.24	18.47	424.7	1.677				42.96	0.695			
Youssef et al. [53]	406.4	812.8	29.4	0.24	18.47	424.7	1.677				45.11	0.715			
Youssef et al. [53]	152.4	304.8	44.1	0.24	18.47	424.7	3.354				94.10	2.013			
Youssef et al. [53]	152.4	304.8	44.1	0.24	18.47	424.7	3.354				91.87	2.014			
Youssef et al. [53]	152.4	304.8	44.1	0.24	18.47	424.7	3.354				89.29	2.011			
Youssef et al. [53]	152.4	304.8	44.1	0.24	18.47	424.7	2.236				80.39	1.518			
Youssef et al. [53]	152.4	304.8	44.1	0.24	18.47	424.7	2.236				80.04	1.488			

Paper	D (mm)	H (mm)	f'_{co} (MPa)	ε_{co} (%)	E_{frp} (GPa)	f_{frp} (MPa)	t_{frp} (mm)	E_f (GPa)	f_f (MPa)	t_f (mm)	f'_{cc} (MPa)	ε_{cu} (%)	$\varepsilon_{h,rup}$ (%)	$k_{\varepsilon,frp}$	$k_{\varepsilon,f}$
Youssef et al. [53]	152.4	304.8	44.1	0.24	18.47	424.7	2.236				81.13	1.530			
Youssef et al. [53]	152.4	304.8	44.1	0.24	18.47	424.7	1.677				66.20	1.298			
Youssef et al. [53]	152.4	304.8	44.1	0.24	18.47	424.7	1.677				66.60	1.357			
Youssef et al. [53]	152.4	304.8	44.1	0.240	18.47	424.7	1.677				63.62	1.295			

p *denotes fiber tensile strength and elastic modulus are given in N/mm-ply*
t *denotes FRP properties calculated based on total nominal ply thickness of fiber sheet*
m *denotes FRP material properties that differ significantly from the reference properties of the corresponding material*
d *denotes ultimate axial stress values that are lower than the unconfined concrete strength*
a *denotes inconsistent axial strain when compared with overall trend in the database*
^ *denotes inconsistent k_ε values when compared with overall trend in the database*

Table 5. Test database of AFRP -wrapped concrete specimens

Paper	Specimen Dimensions		Concrete Properties		FRP Properties			Fiber Properties			Measured Ultimate Conditions			Hoop Rupture Strain Reduction Factors	
	D (mm)	H (mm)	f'_{co} (MPa)	ε_{co} (%)	E_{frp} (GPa)	f_{frp} (MPa)	t_{frp} (mm)	E_f (GPa)	f_f (MPa)	t_f (mm)	f'_{cc} (MPa)	ε_{cu} (%)	$\varepsilon_{h,rup}$ (%)	$k_{c,frp}$	$k_{\varepsilon,f}$
Dai et al. [40]	152	305	39.2		115.2[t]	3732[t]		78[f]	2400[f]	0.169	61.4	2.33	3.16	0.975	1.053^
Dai et al. [40]	152	305	39.2		115.2[t]	3732[t]		78[f]	2400[f]	0.169	62.7	2.33	3.13	0.966	1.043^
Dai et al. [40]	152	305	39.2		115.2[t]	3732[t]		78[f]	2400[f]	0.169	55.8	2.07	3.21	0.991	1.070^
Dai et al. [40]	152	305	39.2		115.2[t]	3732[t]		78[f]	2400[f]	0.338	90.1	3.80[a]	2.89	0.892	0.963
Dai et al. [40]	152	305	39.2		115.2[t]	3732[t]		78[f]	2400[f]	0.338	88.3	3.45	3.05	0.941	1.017^
Dai et al. [40]	152	305	39.2		115.2[t]	3732[t]		78[f]	2400[f]	0.338	83.3	3.68[a]	2.96	0.914	0.987
Dai et al. [40]	152	305	39.2		115.2[t]	3732[t]		78[f]	2400[f]	0.507	113.2	4.39	2.74	0.846	0.913
Dai et al. [40]	152	305	39.2		115.2[t]	3732[t]		78[f]	2400[f]	0.507	116.3	4.6[a]	2.46	0.759	0.820
Dai et al. [40]	152	305	39.2		115.2[t]	3732[t]		78[f]	2400[f]	0.507	118	4.78	2.97	0.917	0.990
Nanni and Bradford [97]	150	300	35.6		62.2	1150	3.8	127.5	2640	2.16	192.21[s]	9.628[a]			
Nanni and Bradford [97]	150	300	35.6		62.2	1150	3.8	127.5	2640	2.16	186.35[s]	6.778[a]			
Ozbakkaloglu and Akin [39]	152	305	39					120	2900	0.4	69.2	2.32	1.71		0.684
Ozbakkaloglu and Akin [39]	152	305	39					120	2900	0.4	67.1	2.30	1.56		0.624
Ozbakkaloglu and Akin [39]	152	305	39					120	2900	0.6	87.6	3.11	1.84		0.736
Ozbakkaloglu and Akin [39]	152	305	39					120	2900	0.6	85.0	2.86	1.66		0.664
Rochette and Labossiére [104]	150	300	43		13.6	230	1.27				47.3	1.11	1.55	0.917	
Rochette and Labossiére [104]	150	300	43		13.6	230	2.56				58.9	1.47	1.39	0.822	
Rochette and Labossiére [104]	150	300	43		13.6	230	3.86				71.0	1.69	1.33	0.786	
Rochette and Labossiére [104]	150	300	43		13.6	230	5.21				74.4	1.74	1.18	0.698	
Suter and Pinzelli [113]	150	300	44.7		31.2	602.2	0.7	120	2900	0.193	52.23	0.238[a]			
Suter and Pinzelli [113]	150	300	44.7		31.2	602.2	1.4	120	2900	0.386	76.85	1.136			
Suter and Pinzelli [113]	150	300	44.7		31.2	602.2	2.1	120	2900	0.579	103.45	1.300			
Suter and Pinzelli [113]	150	300	44.7		31.2	602.2	2.8	120	2900	0.772	136.89	1.784			
Suter and Pinzelli [113]	150	300	36.2		31.2	602.2	0.7	120	2900	0.193	48.15	0.664			
Suter and Pinzelli [113]	150	300	36.2		31.2	602.2	1.4	120	2900	0.386	75.30	1.006			
Suter and Pinzelli [113]	150	300	36.2		31.2	602.2	2.1	120	2900	0.579	98.46	1.304			
Suter and Pinzelli [113]	150	300	33.3		31.2	602.2	0.7	120	2900	0.193	50.28	0.790			
Suter and Pinzelli [113]	150	300	33.3		31.2	602.2	1.4	120	2900	0.386	78.59	1.302			
Suter and Pinzelli [113]	150	300	33.3		31.2	602.2	2.1	120	2900	0.579	103.90	1.502			
Suter and Pinzelli [113]	150	300	54		31.2	602.2	0.7	120	2900	0.193	61.56	0.342[a]			
Suter and Pinzelli [113]	150	300	54		31.2	602.2	1.4	120	2900	0.386	84.24	0.638[a]			
Suter and Pinzelli [113]	150	300	54		31.2	602.2	2.1	120	2900	0.579	111.24	0.816[a]			
Vincent and Ozbakkaloglu [118]	152	305	49.4					120	2900	0.6	109.0	3.73	2.54		1.016^
Vincent and Ozbakkaloglu [118]	152	305	49.4					120	2900	0.6	103.4	3.40	2.10		0.839
Vincent and Ozbakkaloglu [118]	152	305	49.4					120	2900	0.6	105.3	3.37	2.08		0.831
Vincent and Ozbakkaloglu [118]	152	305	49.4					120	2900	0.6	107.7	3.41	2.18		0.873
Vincent and Ozbakkaloglu [118]	152	305	49.4					120	2900	0.6	104.0	3.22	2.12		0.848
Vincent and Ozbakkaloglu [118]	152	305	49.4					120	2900	0.6	110.1	3.48	2.22		0.888
Wang and Wu [119]	70	210	51.63	0.248				118	2060	0.057	65.97	0.403[a]			
Wang and Wu [119]	70	210	51.63	0.248				118	2060	0.095	72.63	0.530[a]			
Wang and Wu [119]	70	210	51.63	0.248				118	2060	0.191	111.43	0.567[a]			
Wang and Wu [119]	105	315	50.64	0.244				118	2060	0.072	59.48	0.331[a]			
Wang and Wu [119]	105	315	50.64	0.244				118	2060	0.143	62.69	0.387[a]			
Wang and Wu [119]	105	315	50.64	0.244				118	2060	0.286	96.02	0.423[a]			
Wang and Wu [119]	194	582	44.92	0.260				118	2060	0.143	44.00	0.358[a]			
Wang and Wu [119]	194	582	44.92	0.260				118	2060	0.286	58.75	0.387[a]			
Wang and Wu [119]	194	582	44.92	0.260				118	2060	0.572	106.03	0.460[a]			
Wang and Wu [119]	70	210	29.37	0.203				118	2060	0.095	49.64	0.537[a]			
Wang and Wu [119]	70	210	29.37	0.203				118	2060	0.057	41.80	0.360[a]			
Wang and Wu [119]	70	210	29.37	0.203				118	2060	0.191	86.07[s]	0.953[a]			
Wang and Wu [119]	105	315	28.79	0.202				118	2060	0.072	41.20	0.363[a]			

Paper	D (mm)	H (mm)	f'_{co} (MPa)	ε_{co} (%)	E_{frp} (GPa)	f_{frp} (MPa)	t_{frp} (mm)	E_f (GPa)	f_f (MPa)	t_f (mm)	f'_{cc} (MPa)	ε_{cu} (%)	$\varepsilon_{h,rup}$ (%)	$k_{\varepsilon,frp}$	$k_{\varepsilon,f}$
Wang and Wu [119]	105	315	28.79	0.202				118	2060	0.143	47.77	0.583[a]			
Wang and Wu [119]	105	315	28.79	0.202				118	2060	0.286	87.42[s]	1.147			
Wang and Wu [119]	194	582	23.98	0.207				118	2060	0.143	33.84	0.383[a]			
Wang and Wu [119]	194	582	23.98	0.207				118	2060	0.286	43.90	0.513[a]			
Wang and Wu [119]	194	582	23.98	0.207				118	2060	0.572	80.86[s]	0.933[a]			
Wang and Zhang [120]	150	450	47.3					118	2060	0.572	84.30	1.619			
Wang and Zhang [120]	150	450	51.1					118	2060	0.572	88.65	1.446			
Watanabe et al. [28]	100	200	30.2	0.23	97.1[t]	2589[t]		73	3432	0.145	39.0	1.58	2.36	0.885	0.502^
Watanabe et al. [28]	100	200	30.2	0.23	87.3[t]	2707[t]		73	3432	0.290	68.5	4.74[a]	3.09	0.997	0.657
Watanabe et al. [28]	100	200	30.2	0.23	87.3[t]	2667[t]		73	3432	0.430	92.1	5.55[a]	2.65	0.867	0.564
Wu et al. [31]	150	300	23.0		115[t]	2324[t]		120	2000	0.286	53.0				
Wu et al. [35]	150	300	23.1	0.267	115[t]	2324[t]		120	2000	0.286	45.2	2.31			
Wu et al. [35]	150	300	23.1	0.267	115[t]	2324[t]		120	2000	0.286	50.7	3.03[a]			
Wu et al. [35]	150	300	23.1	0.267	115[t]	2324[t]		120	2000	0.286	53.7	3.29[a]			
Wu et al. [122]	100	300	46.4	0.255				118	2060	0.286	78.26	0.903			
Wu et al. [122]	100	300	46.4	0.255				118	2060	0.572	128.49	1.879			

t *denotes FRP properties calculated based on total nominal ply thickness of fiber sheet*
f *denotes fiber properties established to be inaccurate based on the analysis of the database*
a *denotes inconsistent axial strain when compared with overall trend in the database*
^ *denotes inconsistent k_ε values when compared with overall trend in the database*

Table 6. Test database of HM and UHM CFRP-wrapped concrete specimens

Paper	Specimen Dimensions		Concrete Properties		FRP Properties			Fiber Properties			Measured Ultimate Conditions			Hoop Rupture Strain Reduction Factors	
	D (mm)	H (mm)	f'_{co} (MPa)	ε_{co} (%)	E_{frp} (GPa)	f_{frp} (MPa)	t_{frp} (mm)	E_f (GPa)	f_f (MPa)	t_f (mm)	f'_{cc} (MPa)	ε_{cu} (%)	$\varepsilon_{h,rup}$ (%)	$k_{\varepsilon,frp}$	$k_{\varepsilon,f}$
Bullo [64]	150	300	32.54	0.248				390	3000	0.165	52.63	0.833	0.467		0.607
Bullo [64]	150	300	32.54	0.248				390	3000	0.165	56.59	0.928	0.52		0.676
Bullo [64]	150	300	32.54	0.248				390	3000	0.165	61.11	0.833	0.421		0.547
Bullo [64]	150	300	32.54	0.248				390	3000	0.495	97.33	1.817	0.639		0.831^
Bullo [64]	150	300	32.54	0.248				390	3000	0.495	83.75	1.265	0.439		0.571
Bullo [64]	150	300	32.54	0.248				390	3000	0.495	100.16	1.687	0.539		0.701
Cui and Sheikh [68]	152	305	45.7	0.243				436	3314	0.16	67.5	1.11[a]	0.789		1.038^
Cui and Sheikh [68]	152	305	45.7	0.243				436	3314	0.16	64.1	1.03[a]	0.769		1.012^
Cui and Sheikh [68]	152	305	45.7	0.243				436	3314	0.33	84.2	1.33	0.642		0.845^
Cui and Sheikh [68]	152	305	45.7	0.243				436	3314	0.33	83.1	1.23	0.634		0.834^
Cui and Sheikh [68]	152	305	45.7	0.243				436	3314	0.49	99.7	1.56	0.603		0.793^
Cui and Sheikh [68]	152	305	45.7	0.243				436	3314	0.49	94.9	1.43	0.546		0.718^
Hosotani et al. [76]	200	600	41.7	0.34	439	3972	0.676	392	2943	0.652	90	1.5			
Lin and Chen [38]	120	240	32.7		157.54	770	0.5				51.0				
Lin and Chen [38]	120	240	32.7		157.54	770	0.5				49.6				
Lin and Chen [38]	120	240	32.7		157.54	770	1.0				77.3				
Lin and Chen [38]	120	240	32.7		157.54	770	1.0				68.9				
Rousakis [105]	150	300	25.2	0.311				377	4410	0.17	41.6	1.437	0.695		0.594
Rousakis [105]	150	300	25.2	0.311				377	4410	0.17	38.8	1.206	0.581		0.497
Rousakis [105]	150	300	25.2	0.311				377	4410	0.34	60.1	1.881	0.641		0.548
Rousakis [105]	150	300	25.2	0.311				377	4410	0.34	55.9	2.097	0.551		0.471
Rousakis [105]	150	300	25.2	0.311				377	4410	0.51	67.0	2.452	0.449		0.384
Rousakis [105]	150	300	25.2	0.311				377	4410	0.51	67.3	2.432	0.368		0.315
Rousakis [105]	150	300	47.4	0.308				377	4410	0.17	72.3	1.085	0.772		0.660
Rousakis [105]	150	300	47.4	0.308				377	4410	0.17	64.4	0.866	0.513		0.439
Rousakis [105]	150	300	47.4	0.308				377	4410	0.34	82.4	1.399	0.656		0.561
Rousakis [105]	150	300	47.4	0.308				377	4410	0.34	82.4	1.350	0.537		0.459
Rousakis [105]	150	300	47.4	0.308				377	4410	0.51	96.3	1.585	0.443		0.379
Rousakis [105]	150	300	47.4	0.308				377	4410	0.51	95.2	1.687	0.578		0.494
Rousakis [105]	150	300	51.8	0.298				377	4410	0.17	78.7	0.748	0.543		0.464
Rousakis [105]	150	300	51.8	0.298				377	4410	0.17	72.8	0.663	0.398		0.340
Rousakis [105]	150	300	51.8	0.298				377	4410	0.34	95.4	1.047	0.551		0.471
Rousakis [105]	150	300	51.8	0.298				377	4410	0.34	90.7	1.001	0.364		0.311
Rousakis [105]	150	300	51.8	0.298				377	4410	0.51	110.5	1.292	0.438		0.374
Rousakis [105]	150	300	51.8	0.298				377	4410	0.51	103.6	1.203	0.310		0.265^
Rousakis [105]	150	300	51.8	0.298				377	4410	0.85	112.7	1.593	0.289		0.247^
Rousakis [105]	150	300	51.8	0.298				377	4410	0.85	126.7	1.612	0.360		0.308
Matthys et al. [11]	150	300	34.9	0.21	480	1100		640	2650	0.235	41.3[s]	0.40	0.19	0.829^	0.459
Suter and Pinzelli [113]	150	300	44.7					640	2650	0.38	91.98	0.534			
Watanabe et al. [28]	100	200	30.2	0.23	628[t]	1579[t]		637	2452	0.14	41.7	0.57	0.23	0.916^	0.598
Watanabe et al. [28]	100	200	30.2	0.23	629[t]	1824[t]		637	2452	0.28	56.0	0.88	0.22	0.759^	0.572
Watanabe et al. [28]	100	200	30.2	0.23	576[t]	1285[t]		637	2452	0.42	63.3	1.30	0.22	0.987^	0.572
Wu et al. [31]	150	300	23.0		563[t]	2544[t]		540	1900	0.286	50.0				
Wu et al. [35]	150	300	23.1	0.267	563[t]	2544[t]		540	1900	0.286	50.5	1.27[a]			
Wu et al. [35]	150	300	23.1	0.267	563[t]	2544[t]		540	1900	0.286	48.9	1.20[a]			

t *denotes FRP properties calculated based on total nominal ply thickness of fiber sheet*
^ *denotes inconsistent k_ε values when compared with overall trend in the database*

Table 7. Test database of unbonded-wrap or tube encased concrete specimens

Paper	FRP type	Specimen Dimensions		Concrete Properties		FRP Properties			Fiber Properties			Measured Ultimate Conditions			Hoop Rupture Strain Reduction Factors	
		D (mm)	H (mm)	f'_{co} (MPa)	ε_{co} (%)	E_{frp} (GPa)	f_{frp} (MPa)	t_{frp} (mm)	E_f (GPa)	f_f (MPa)	t_f (mm)	f'_{cc} (MPa)	ε_{cu} (%)	$\varepsilon_{h,rup}$ (%)	$k_{\varepsilon,frp}$	$k_{\varepsilon,f}$
Hong and Kim [13]	CFRP[fm]	300	600	17.5		137	2058	2	235	3920		75.6	2.88[a]			
Hong and Kim [13]	CFRP[fm]	300	600	17.5		137	2058	3	235	3920		80.2[s]	2.23[a]			
Karantzikis et al. [84]	CFRP[ub]	200	350	12.1	0.22				230	3500	0.12	21.54	1.16			
Matthys et al. [11]	CFRP[ub]	150	300	34.9	0.21	200	2600	0.117	240	3900	0.117	42.2	0.72	1.08	0.831	0.665
Ozbakkaloglu and Vincent [14]	CFRP	74	152	43.0					240	3800	0.117	67.4	1.35	1.07		0.676
Ozbakkaloglu and Vincent [14]	CFRP	74	152	43.0					240	3800	0.117	71.0	1.44	1.32		0.834
Ozbakkaloglu and Vincent [14]	CFRP	74	152	43.0					240	3800	0.117	61.1	0.92	0.91		0.575
Ozbakkaloglu and Vincent [14]	CFRP	74	152	47.8					240	3800	0.117	60.9	0.84	0.83		0.524^
Ozbakkaloglu and Vincent [14]	CFRP	74	152	55.0					240	3800	0.117	56.5[d]	0.80	0.72		0.455^
Ozbakkaloglu and Vincent [14]	CFRP	74	152	55.0					240	3800	0.234	96.0	1.43	1.13		0.714
Ozbakkaloglu and Vincent [14]	CFRP	74	152	50.3					240	3800	0.234	98.1	1.71	0.95		0.600
Ozbakkaloglu and Vincent [14]	CFRP	74	152	52.0					240	3800	0.234	105.7	2.41	1.07		0.675
Ozbakkaloglu and Vincent [14]	CFRP	152	305	37.3					240	3800	0.117	42.0	0.79	1.20		0.758
Ozbakkaloglu and Vincent [14]	CFRP	152	305	34.6					240	3800	0.117	41.6	0.66	0.77		0.486^
Ozbakkaloglu and Vincent [14]	CFRP	152	305	35.5					240	3800	0.234	59.1	1.43	1.32		0.834
Ozbakkaloglu and Vincent [14]	CFRP	152	305	36.3					240	3800	0.234	60.9	1.53	1.36		0.859
Ozbakkaloglu and Vincent [14]	CFRP	152	305	37.3					240	3800	0.234	61.7	1.45	1.23		0.777
Ozbakkaloglu and Vincent [14]	CFRP	302	600	36.3					240	3800	0.234	38.6	0.80	1.08		0.682
Ozbakkaloglu and Vincent [14]	CFRP	302	600	36.3					240	3800	0.468	57.0	1.52	1.17		0.739
Harries and Carey [8]	GFRP[ub]	152	305	31.8	0.28	4.9[p]	75[p]	3	10.3[p]	154[p]		33.6		1.29	0.843	0.863^
Harries and Carey [8]	GFRP[ub]	152	305	31.8	0.28	4.9[p]	75[p]	9	10.3[p]	154[p]		48.4		1.13	0.738	0.756
Li et al. [88]	GFRP	150	300	47.5	0.4				73	1800	0.3	50.9	0.9	1.5		0.608
Li et al. [88]	GFRP	150	300	47.5	0.4				73	1800	0.3	85.7[s]	2.1	2.4		0.973^
Mastrapa [10]	GFRP[ub]	152.5	305	37.2		19.19	586	4.06	55.85	1800	2.311	112[s]				
Mastrapa [10]	GFRP[ub]	152.5	305	37.2		19.19	586	4.06	55.85	1800	2.311	110[s]				
Mastrapa [10]	GFRP[ub]	152.5	305	29.8		19.19	565	0.61	55.85	1800	0.330	26.68[d]	1.50	1.10	0.374^	0.341^
Mastrapa [10]	GFRP[ub]	152.5	305	31.2		19.19	565	1.84	55.85	1800	0.991	63.09	3.12	2.25	0.764	0.698
Mastrapa [10]	GFRP[ub]	152.5	305	31.2		19.19	565	1.84	55.85	1800	0.991	65.43	3.11	2.22	0.754	0.689
Mastrapa [10]	GFRP[ub]	152.5	305	31.2		19.19	565	3.07	55.85	1800	1.651	91.91	4.27	1.97	0.669	0.611
Mastrapa [10]	GFRP[ub]	152.5	305	31.2		19.19	565	3.07	55.85	1800	1.651	89.01	5.03	1.75	0.594	0.543
Mirmiran et al. [9]	GFRP[ub]	152.5	305	29.8					55.85	1800	0.275	33.65	1.0			
Mirmiran et al. [9]	GFRP[ub]	152.5	305	29.8					55.85	1800	0.275	33.16	2.3[a]			
Mirmiran et al. [9]	GFRP[ub]	152.5	305	29.8					55.85	1800	0.275	33.23	2.0[a]			
Mirmiran et al. [9]	GFRP[ub]	152.5	305	29.8					55.85	1800	0.826	63.02	2.7			
Mirmiran et al. [9]	GFRP[ub]	152.5	305	29.8					55.85	1800	0.826	65.16	3.0			
Mirmiran et al. [9]	GFRP[ub]	152.5	305	29.8					55.85	1800	0.826	65.23	2.8			
Mirmiran et al. [9]	GFRP[ub]	152.5	305	29.8					55.85	1800	1.376	93.70	4.3			
Mirmiran et al. [9]	GFRP[ub]	152.5	305	29.8					55.85	1800	1.376	92.26	3.9			
Mirmiran et al. [9]	GFRP[ub]	152.5	305	29.8					55.85	1800	1.376	96.46	4.4			
Mirmiran et al. [9]	GFRP[ub]	152.5	305	31.2					55.85	1800	0.826	67.50	3.0			
Mirmiran et al. [9]	GFRP[ub]	152.5	305	31.2					55.85	1800	0.826	64.68	3.1			
Mirmiran et al. [9]	GFRP[ub]	152.5	305	31.2					55.85	1800	1.376	91.01	5.3			
Mirmiran et al. [9]	GFRP[ub]	152.5	305	31.2					55.85	1800	1.376	96.87	6.3[a]			
Park et al. [100]	GFRP	150	300	32		39.59	321	1				54.2	1.50[a]			
Park et al. [100]	GFRP	150	300	32		39.59	321	1				55.3				
Park et al. [100]	GFRP	150	300	32		39.59	321	1				56.7	1.70[a]			
Park et al. [100]	GFRP	150	300	54		56.12	530	3				95.5				
Park et al. [100]	GFRP	150	300	54		56.12	530	3				114.7	2.36			
Park et al. [100]	GFRP	150	300	54		56.12	530	3				111.7				
Park et al. [100]	GFRP	150	300	54		56.99	607	5				206.4	3.88			
Park et al. [100]	GFRP	150	300	54		56.99	607	5				198.9				
Park et al. [100]	GFRP	150	300	54		56.99	607	5				189.1				
Park et al. [100]	GFRP	150	450	54		56.12	530	3				115.3	3.14[a]			
Park et al. [100]	GFRP	150	450	54		56.12	530	3				113.4	3.42[a]			
Park et al. [100]	GFRP	150	450	54		56.12	530	3				108.5	3.64[a]			

Paper	D (mm)	H (mm)	f'_{co} (MPa)	ε_{co} (%)	E_{frp} (GPa)	f_{frp} (MPa)	t_{frp} (mm)	E_f (GPa)	f_f (MPa)	t_f (mm)	f'_{cc} (MPa)	ε_{cu} (%)	$\varepsilon_{h,rup}$ (%)	$k_{\varepsilon,frp}$	$k_{\varepsilon,f}$	Paper
Saafi et al. [12]	GFRP[fs]	152	435	35	0.25	32	450	0.8				52.8	1.90[a]			
Saafi et al. [12]	GFRP[fs]	152	435	35	0.25	34	505	1.6				66.0	2.47			
Saafi et al. [12]	GFRP[fs]	152	435	35	0.25	36	560	2.4				83.0	3.00			
Ozbakkaloglu and Vincent [14]	AFRP	100	200	37					120	2900	0.2	70.6	2.06	2.22		0.888
Ozbakkaloglu and Vincent [14]	AFRP	100	200	35.5					120	2900	0.2	65.5	1.75	2.08		0.832
Ozbakkaloglu and Vincent [14]	AFRP	100	200	34					120	2900	0.2	62.8	1.88	2.25		0.900
Ozbakkaloglu and Vincent [14]	AFRP[fm]	100	200	37.2					99	2930	0.3	89.1	3.10	2.11		0.713
Ozbakkaloglu and Vincent [14]	AFRP[fm]	100	200	37.2					99	2930	0.3	91.9	3.31	2.39		0.808
Ozbakkaloglu and Vincent [14]	AFRP[fm]	100	200	35.4					99	2930	0.3	86.7	3.04	2.21		0.747
Vincent and Ozbakkaloglu [118]	AFRP	152	305	49.4					120	2900	0.6	104.6	3.15	2.19		0.876
Vincent and Ozbakkaloglu [118]	AFRP	152	305	49.4					120	2900	0.6	107.9	3.55	2.42		0.968
Vincent and Ozbakkaloglu [118]	AFRP	152	305	49.4					120	2900	0.6	106.3	3.47	2.38		0.952
Vincent and Ozbakkaloglu [118]	AFRP	152	305	49.4					120	2900	0.6	109.9	3.01	2.11		0.843
Vincent and Ozbakkaloglu [118]	AFRP	152	305	49.4					120	2900	0.6	109.9	3.18	2.33		0.930
Vincent and Ozbakkaloglu [118]	AFRP	152	305	49.4					120	2900	0.6	110.7	2.98	2.80		1.120^
Saafi et al. [12]	HM CFRP	152	435	35.0	0.25	367	3300[t]	0.11[t]				55	1.0			
Saafi et al. [12]	HM CFRP	152	435	35.0	0.25	390	3550[t]	0.23[t]				68	1.6			
Saafi et al. [12]	HM CFRP	152	435	35.0	0.25	415	3700[t]	0.55[t]				97	2.2			
Ozbakkaloglu and Vincent [14]	UHM CFRP	152	305	36.3					640	2650	0.190	46.4	0.28[a]	0.12		0.290
Ozbakkaloglu and Vincent [14]	UHM CFRP	152	305	36.3					640	2650	0.190	46.0	0.30[a]	0.11		0.266
Ozbakkaloglu and Vincent [14]	UHM CFRP	152	305	36.3					640	2650	0.190	43.3	0.25[a]	0.18		0.435
Matthys et al. [11]	UHM CFRP[ub]	150	300	34.9	0.21	420	1100[m]	0.235	640	2650	0.235	40.7[s]	0.36[a]	0.18	0.687	0.435

p *denotes fiber tensile strength and elastic modulus are given in N/mm-ply*
t *denotes FRP properties calculated based on total nominal ply thickness of fiber sheet*
m *denotes FRP material properties that differ significantly from the reference properties of the corresponding material*
d *denotes ultimate axial stress values that are lower than the unconfined concrete strength*
s *denotes inconsistent axial stress when compared with overall trend in the database*
a *denotes inconsistent axial strain when compared with overall trend in the database*
^ *denotes inconsistent k_ε values when compared with overall trend in the database*
fm *denotes tubes fabricated using automated manufacturing method*
fs *denotes tubes suppiled by manufacturer*
ub *denotes unbonded-wrap specimen*

Statement of Authorship

Title of Paper	Confinement Model for FRP-Confined High-Strength Concrete
Publication Status	(•) Published ( ) Accepted for Publication ( ) Submitted for Publication ( ) Publication Style
Publication Details	Journal of Composites for Construction, Volume 18, Issue 4, Pages 1-19, Year 2013

Author Contributions

By signing the Statement of Authorship, each author certifies that their stated contribution to the publication is accurate and that permission is granted for the publication to be included in the candidate's thesis.

Name of Principal Author (Candidate)	Mr. Jian Chin Lim		
Contribution to the Paper	Preparation of experimental database, development of model, and preparation of manuscript		
Signature		Date	23/02/2015

Name of Co-Author	Dr. Togay Ozbakkaloglu		
Contribution to the Paper	Research supervision and review of manuscript		
Signature		Date	23/02/2015

THIS PAGE HAS BEEN LEFT INTENTIONALLY BLANK

CONFINEMENT MODEL FOR FRP-CONFINED HIGH-STRENGTH CONCRETE

Jian C. Lim, and Togay Ozbakkaloglu

ABSTRACT

It is well understood that the confinement of concrete with fiber reinforced polymer (FRP) composites can significantly enhance its strength and deformability. However, the confinement demands of concrete increase exponentially with its strength and resulted in substantially higher confinement requirement for HSC. This paper reports on a study on the axial compressive behavior of FRP-confined high-strength concrete (HSC). A large experimental test database that consists of 237 axial compression tests results of FRP-confined HSC was assembled from the published literature and presented in this paper. The database was augmented with another database of FRP-confined normal-strength concrete (NSC) that consists of 832 test results. The combined database of 1063 test results that covers the specimens with unconfined concrete strengths ranging from 6.2 to 169.7 MPa was used to investigate and quantify the factors that influence the compressive behavior of FRP-confined HSC. Analysis of the test results reported in the database indicates that the confinement requirement increases significantly with an increase in concrete strength, which in turn adversely affects the observed strength enhancement through confinement. In addition, it was also observed that the hoop rupture strain of the FRP shell decreases as the concrete strength increases. A number of existing stress-strain models developed for FRP-confined concrete are assessed using the HSC database. A close examination of the results of the model assessment has led to a number of important conclusions regarding the strengths and weaknesses of existing stress-strain models. Finally, a novel design-oriented model for FRP-confined concrete that was developed on the basis of the database summarized in the paper is presented. It is shown that the proposed model performs significantly better than any of the existing stress-strain models of FRP-confined concrete in predicting the ultimate conditions of FRP-confined HSC.

KEYWORDS: Fiber reinforced polymer (FRP); Confinement; High-strength concrete (HSC); Concrete; Axial stress; Axial strain; Stress-strain models.

1. INTRODUCTION

The use of HSC in column construction has received increasing attention in the last two decades due to the advantages the higher strength concrete offers over normal-strength concrete (NSC) in terms of engineering properties. However, the brittleness of the concrete, which increases as the strength increases, poses a major concern in its structural applications in seismically active regions. In an effort to prevent such brittle failure, research into the use of FRP composite shells as external confinement reinforcement for concrete has received a significant amount of attentions (Ozbakkaloglu et al. 2013).

It is widely accepted that HSC generally behaves differently from NSC (Setunge et al. 1993; Attard and Setunge 1996). Although the behavior of FRP-confined concrete has been extensively investigated for NSC range, the behavior of FRP-confined HSC is much less understood. Furthermore, the availability of models applicable to FRP-confined HSC is extremely limited. Out of the 88 FRP-confined concrete models reviewed in Ozbakkaloglu et al. (2013), only five models were directly applicable to FRP-confined HSC (Miyauchi et al. 1999; Mandal et al. 2005; Berthet et al. 2006; Cui and Sheikh 2010a; Xiao et al. 2010). In addition, these FRP-confined HSC models were developed based on limited experimental test data, which were often obtained only from the tests performed by the originators of the models.

To address this gap in the research, the authors have undertaken extensive experimental and analytical investigation on the stress-strain behavior of FRP-confined concrete, particularly for HSC. In the current study, a database summarizing 231 test results of FRP-confined HSC cylinders ranging from 56.7 to 169.7 MPa in unconfined concrete strengths (f'_{co}) is collated and presented. The database is augmented with a database of FRP-confined NSC (f'_{co} ranging from 6.2 to 55.2 MPa) constructed at the University of Adelaide, which consists of 832 test results (Ozbakkaloglu and Lim 2013). This combined database of over 1000 test results, which makes it by far the most comprehensive database of FRP-confined concrete tests reported in the literature, was used to develop a better understanding on the influence of unconfined concrete strength on the behavior of FRP-confined concrete. The parameter space of the combined database is continuous, consistent and greatly extended in ranges, which allows clear observations to be made on the influences of the important factors. A new design-oriented model that was developed on the basis of the combined database is then presented. The model is applicable to both NSC and HSC of strengths up to 120 MPa, and it incorporates the important factors identified from the close examination of the results reported in the database and assessment of previous models. The comparison of the proposed model with previous models demonstrates that the proposed model provides a significant improvement over the existing models in the prediction of the ultimate condition of FRP-confined HSC.

Table 1. Summary of test results included in the HSC database

Number	Researcher	Number of test data	Identical specimens per test data	Confinement technique	Fiber type	Diameter	Height	Unconfined concrete strength	Strength enhancement ratio	Strain enhancement ratio	Actual confinement ratio	Lateral strain recording method (see notes)	Axial strain recording method (see notes)
-	-	N	n	-	-	D (mm)	H (mm)	f'_{co} (MPa)	f'_{cu}/f'_{co}	$\varepsilon_{cu}/\varepsilon_{co}$	$f_{lu,a}/f'_{co}$	-	-
1	Ahmad et al. (1991)	1	3	Wrap	GFRP	102	203	64.2	2.27	-	0.38	N/A	N/A
2	Aire et al. (2001)	5	3	Wrap	GFRP	150	300	69.0	1.14 - 2.46	1.96 - 5.92	0.06 - 0.70	N/A	AFL
3	Aire et al. (2010)	5	3	Wrap	CFRP	150	300	69.0	1.36 - 3.14	3.25 - 9.96	0.05 - 0.56	N/A	AFL
4	Almusallam (2007)	8	3	Wrap	GFRP	150	300	60.0 - 107.8	1.04 - 1.66	1.01 - 5.36	0.06 - 0.33	HL	AML
5	Benzaid et al. (2009)	3	1	Wrap	GFRP	160	320	56.7	1.31 - 1.68	4.67 - 7.83	0.03 - 0.12	HL	AML
6	Benzaid et al. (2010)	2	1	Wrap	CFRP	160	320	61.8	1.51	3.71	0.07 - 0.24	HL	AML
7	Berthet et al. (2005)	6	1	Wrap	CFRP	70	140	112.6 - 169.7	1.10 - 1.75	1.94 - 3.13	0.06 - 0.36	HL	AML
8	Cheek et al. (2011)	3	1	Tube	AFRP	153	305	109.8	1.38 - 1.60	5.33 - 6.55	0.24 - 0.29	HS	AFL
9	Chikh et al. (2012)	2	1	Wrap	CFRP	160	320	61.8	1.01 - 1.51	1.15 - 3.71	0.07 - 0.20	HL	AML
10	Cui and Sheikh (2010b)	40	1	Wrap	CFRP, GFRP, HM CFRP	152	305	79.9 - 111.8	0.75 - 2.28	1.20 - 6.14	0.03 - 0.27	HS	AML
11	Green et al. (2007)	2	1	Wrap	CFRP, GFRP	152	305	59.0	1.19 - 1.24	-	0.14 - 0.26	HS	AS
12	Harmon and Slattery (1992)	3	1	Wrap	CFRP	51	102	103.0	1.27 - 2.95	3.21 - 9.94	0.13 - 0.35	N/A	AFL
13	Mandal and Fam (2004)	18	1	Wrap	CFRP, GFRP	100	200	67.0 - 80.6	1.19 - 1.46	-	0.10 - 0.31	N/A	AML
14	Miyauchi et al. (1999)	2	1	Wrap	CFRP	100	200	109.5	1.00 - 1.01	1.48 - 1.92	0.04 - 0.08	N/A	AS
15	Owen (1998)	3	2-4	Wrap	CFRP	298	610	58.1	1.03 - 2.59	2.96 - 11.27	0.05 - 0.26	N/A	N/A
16	Ozbakkaloglu and Akin (2012)	4	1	Wrap	AFRP	152	305	100 - 106	1.16 - 1.46	3.79 - 4.86	0.15 - 0.20	HS	AFL
17	Ozbakkaloglu and Vincent (2013)	69	1	Tube	CFRP, HM CFRP	74 - 152	152 - 305	59.0 - 110.1	0.98 - 2.03	1.82 - 9.93	0.05 - 0.36	HS	AFL
18	Rousakis (2001)	14	1	Wrap	HM CFRP	150	300	56.9 - 82.1	0.99 - 1.51	1.40 - 3.67	0.03 - 0.17	HS	AML
19	Shehata et al. (2007)	2	1	Wrap	CFRP	150	300	61.7	1.24 - 1.58	3.33 - 4.83	0.08 - 0.15	HS	AS
20	Valdmanis et al. (2007)	3	1	Wrap	CFRP	150	300	61.6	1.31 - 1.70	1.50 - 2.00	0.10 - 0.30	HS	AML
21	Vincent and Ozbakkaloglu (2013a)	18	1	Wrap, Tube	CFRP	152	305	59.0 - 102.5	1.06 - 1.38	1.52 - 5.96	0.03 - 0.25	HS	AFL
22	Wu et al. (2009)	6	1	Wrap	AFRP	100	300	78.5 - 101.2	1.22 - 2.37	1.38 - 3.57	0.07 - 0.29	N/A	AML
23	Xiao et al. (2010)	12	1	Wrap	CFRP	152	305	70.8 - 111.6	1.20 - 2.79	2.21 - 7.28	0.11 - 0.50	HS	AML

Specimen instrumentation notes:
HS denotes hoop strains were measured by strain gauges
HL denotes hoop strains were measured by lateral LVDTs,extensometers, or dial gauges
AS denotes axial strains were measured by strain gauges
AFL denotes axial strains were determined from LVDTs or dial gauges mounted on loading platens to measure deformations along the full height of the specimens
AML denotes axial strains were determined from LVDTs, extensometers, or dial gauges mounted on the specimens to measure deformations within a gauge length along the height of specimens
N/A denotes information that was either not applicable to the dataset or not available in the source document

2. THE EXPERIMENTAL DATABASES

2.1 Construction of the Database of FRP-Confined HSC

The database was assembled through an extensive review of the literature that catalogued 2038 test results from 202 experimental studies published between 1991 and the middle of 2013. The results included in the database were chosen using a set of carefully considered selection criteria to ensure reliability and consistency of the database. This required the use of a total of 9 selection criteria listed in this section in the order of importance (as measured by number of dataset exclusions resulted by a given criterion). Assessment using these criteria resulted in a final database of FRP-confined HSC of 231 datasets from 23 sources. It is worthwhile noting that 94 of these test results were sourced from the experimental studies conducted at the University of Adelaide (Ozbakkaloglu and Akin 2012; Ozbakkaloglu and Vincent 2013; Vincent and Ozbakkaloglu 2013a). All of the test results included in this database, summarized in Table 1 and presented in Tables 2 to 5 in Appendix, met the following requirements :

1) Specimens with unconfined concrete compressive strengths lower than 55 MPa were excluded.
2) Only the specimens with unidirectional fibers orientated in the hoop direction were included in the database.
3) Specimens with transverse and/or longitudinal steel or internal FRP reinforcement were excluded.
4) Only the specimens that were confined with continuous FRP jackets were included. Specimens with partial wrapping (i.e., FRP strips) were excluded.
5) Specimens with height-to-diameter (*H/D*) ratio greater than three were excluded from the database to eliminate the influence of specimen slenderness.
6) Only those specimens failed due to FRP rupture at the ultimate condition were included. Specimens that failed prematurely due to other types of failure, such as FRP shell debonding or premature failure due to excessive eccentricity were excluded.
7) Specimens for which the ultimate conditions were not recorded accurately due to inadequate testing equipment or instrumentation errors were excluded.
8) Specimens reported with insufficient details in regards to material and geometric properties were excluded.

The specimens that satisfied the above conditions, and hence were included in the test database, were then subjected to an additional set of conditions to establish their suitability for their inclusion in the assessment of the existing models and development of the new model. The specimens with compressive strengths (f'_{cc}) and ultimate axial strains (ε_{cu}) that deviated significantly from the global trends of relevant strength and strain enhancement ratios (i.e. by limiting the variation of a given dataset from the trendline to maximum 40% for f'_{cc}/f'_{co} and 70% for $\varepsilon_{cu}/\varepsilon_{co}$) were excluded in the model assessment and development. The specimens that were excluded from the calculations of the strength and strain enhancement ratios (f'_{cc}/f'_{co} and $\varepsilon_{cu}/\varepsilon_{co}$) are marked respectively with the superscripts '*s*' and '*a*' in Tables 2 to 5. Furthermore, the specimens with hoop rupture strain reduction factors (k_ε) that deviated significantly from the reference values of the corresponding materials (i.e. more than ±20%

of average k_ε) are marked with the superscript '^' in Tables 2 to 5, and they were excluded in the development of the expression for the hoop rupture strain reduction factor (k_ε). In addition to these, datasets from specimens exhibiting a stress-strain curve with a descending second branch (marked with superscript '*d*' in database tables) and ones from specimens having tubes that were fabricated using an automated manufacturing method (marked with superscript '*fm*' in database tables) were also excluded in the model development and assessment to limit the investigation to specimens with ascending second branches and manually manufactured FRP jackets.

2.2 Details of the Database of FRP-Confined HSC

The database consists of the following information for each specimen: the specimen confinement methods (wrapped or tube-encased concrete); the geometric properties (diameter D and height H); the unconfined concrete strength (f'_{co}) and strain (ε_{co}); material properties of the FRP shell [elastic modulus (E_{frp}), tensile stress (f_{frp}), total thickness (t_{frp}), and rupture strain reduction factor ($k_{\varepsilon,frp}$)]; material properties of the fibers [elastic modulus (E_f), tensile stress (f_f), total thickness (t_f), and rupture strain reduction factor ($k_{\varepsilon,f}$)]; the compressive strength at initial peak of the stress-strain curve (f'_{c1}) and the corresponding axial strain at initial peak (ε_{c1}) of confined concrete; the ultimate axial stress (f'_{cu}) and strain (ε_{cu}) of confined concrete; and the average FRP hoop strain at rupture ($\varepsilon_{h,rup}$).

The test data in the database were sorted into seven groups based on two main confinement parameters: confinement technique (wraps or tubes) and type of FRP material [carbon FRP (CFRP); S- or E-Glass FRP (GFRP); aramid FRP (AFRP); high-modulus carbon FRP (HM CFRP); or ultra-high-modulus carbon FRP (UHM CFRP)]. 155 specimens in the database were FRP wrapped, whereas 76 specimens were confined by FRP tubes. 124 of the specimens were confined by CFRP, 40 by GFRP, 37 by AFRP, 24 by HM CFRP, and 6 by UHM CFRP.

The results of the FRP-wrapped and FRP tube-encased specimens are presented in Tables 2 to 5 in Appendix, categorized according to the fiber type. It is worthwhile noting that for some of the datasets, a single entry in Tables 2 to 5 may represent the average results of more than one nominally identical specimen, as reported by the researchers of the original study. These datasets are clearly noted in Table 1. It should also be noted that, except for the datasets from Ozbakkaloglu and Vincent (2013), all the datasets included in the database tables were obtained from specimens that were confined by FRP shells (i.e. wraps or tubes) manufactured using a manual hand lay-up technique. The specimens of Ozbakkaloglu and Vincent (2013) were confined by FRP tubes that were manufactured using an automated filament winding technique, and these datasets are marked in Table 4 with a superscript '*fm*'.

As summarized in Table 1, the diameters of the specimens (D) included in the test database varied between 51 and 298 mm, with the majority of the specimens having a diameter of 150 mm. The unconfined concrete strength (f'_{co}), as obtained from concrete cylinder tests, varied from 56.7 to 169.7 MPa. The actual confinement ratio, defined as the ratio of the actual confining pressure to the unconfined concrete strength ($f_{lu,a}/f'_{co}$), varied from 0.02 to 0.39.

The ultimate axial strains (ε_{cu}) and FRP hoop rupture strains ($\varepsilon_{h,rup}$) in the database are the average values obtained by strain gauges or deformation measuring devices. Several measurement methods have been used in different studies to record the ultimate axial strains reported in the database tables. The methods include: (i) strain gauges (e.g. unidirectional strain gauges or bi-directional rosettes) attached to the external surface of the FRP shells; (ii) deformation measuring devices (e.g. linear variable deformation transducers (LVDTs) or extensometers or dial gauges) mounted within the loading platens of the axial compression test machine; or (iii) measuring devices mounted within a certain gauge length along the height of the specimens. Different measuring methods have also been used in measuring the hoop strains, including methods (i) and (iii) outlined above with strain gauges or measuring devices oriented in the hoop direction. The specific methods used in each study for the measurement of both of these strains are reported in the final two columns of Table 1.

Care has been taken to distinguish the results from specimens exhibiting stress-strain curves with a post-peak strain-softening (i.e., descending second branch: $f'_{cu} < f'_{c1}$) or -hardening behavior (i.e., ascending second branch: $f'_{cu} > f'_{c1}$). The specimens exhibiting a strain-softening behavior were marked with superscript '*d*' in Tables 2 to 5. Specimens with only a single compressive strength value available from the original publication were assigned with either f'_{c1} or f'_{cu} based on the observed shape of their stress-strain curves, or otherwise based on the authors' best knowledge.

2.3 Details of the Database of FRP-Confined NSC

The test results that satisfied the aforementioned criteria used in the construction of the database of FRP-confined HSC, with Criterion 1 adjusted to only include the specimens with unconfined concrete strength (f'_{co}) of 55.2 MPa or lower, were collated to form the database of FRP-confined NSC (Ozbakkaloglu and Lim 2013). The NSC database consisted of 755 FRP-wrapped and 77 specimens FRP tube-encased specimens, in which 495 of the specimens were confined by CFRP; 206 by GFRP; 79 by AFRP; 40 by HM CFRP; and 12 by UHM CFRP. The unconfined concrete strength (f'_{co}) in the database varied from 6.2 to 55.2 MPa.

3. A NEW MODEL FOR FRP-CONFINED HSC

This section presents a new design-oriented model to predict the ultimate condition of FRP-confined concrete with unconfined concrete strengths up to 120 MPa. The model contains simple closed-form expressions and it was developed using both the test databases of FRP-confined HSC and NSC. Not all the datasets included in the database contained all the relevant details required for the development of all the components of the model. Furthermore, as discussed previously, the results that failed to satisfy the selection criteria were excluded from model development. The total number of datasets that were used in the calibration of the hoop strain reduction factor (k_ε), strength enhancement coefficient (k_1), and strain enhancement coefficient (k_2) are given in Tables 6 to 8, respectively.

3.1 FRP hoop rupture strain

The accuracy in determination of the hoop rupture strains plays an instrumental role in predicting the ultimate conditions of FRP-confined concrete. As discussed in a number of studies previously (Mirmiran et al. 1998; Matthys et al. 1999; Xiao and Wu 2000; Fam and Rizkalla 2001; Pessiki et al. 2001; De Lorenzis and Tepfers 2003; Harries and Carey 2003; Lam and Teng 2003b,2004; Ozbakkaloglu and Oehlers 2008a; Ozbakkaloglu and Oehlers 2008b; Zinno et al. 2010; Ozbakkaloglu 2013a,b), the ultimate hoop strain ($\varepsilon_{h,rup}$) reached in the FRP shell is often smaller than the ultimate tensile strain of the fibers (ε_f) or the FRP materials (ε_{frp}). This necessitates the use of a hoop rupture strain reduction factor ($k_{\varepsilon,f}$ or $k_{\varepsilon,frp}$) for calculating the actual confining pressures at ultimate ($f_{lu,a}$) (Eq. 1).

$$f_{lu,a} = \frac{2E_f t_f \varepsilon_{h,rup}}{D} \tag{1}$$

$$\varepsilon_{h,rup} = k_{\varepsilon,f}\varepsilon_f \quad \text{or} \quad \varepsilon_{h,rup} = k_{\varepsilon,frp}\varepsilon_{frp} \tag{2}$$

It is worthwhile noting that the results presented in Table 6 and Figures 1 and 2, and the findings presented in this section are based on fiber properties specified by the manufacturers, as the datasets consisted of FRP properties determined from flat coupon tests were insufficient to perform a complete statistical analysis. In the analysis, due attention was given to the influence of the unconfined concrete strength, type of FRP material, and fabrication method of the FRP shells on the hoop strain reduction factor ($k_{\varepsilon,f}$).

As previously reported in Ozbakkaloglu and Akin (2012), an increase in the compressive strength of concrete has an adverse influence on the hoop rupture strain of the FRP shell. As evident in Figures 1(a) to 1(e), the $k_{\varepsilon,f}$ values decrease with the increase in unconfined concrete strength (f'_{co}). The variation in FRP rupture strain with concrete strength can be explained by the increase in concrete brittleness (from NSC to HSC), which alters the concrete crack patterns from heterogenic microcracks to localized macrocracks. The average values of $k_{\varepsilon,f}$ for FRP-confined concretes, as given in Table 6, decrease from 0.693 to 0.521 as the unconfined concrete strength (f'_{co}) increases from the strength range of 0 - 40 MPa to 100 - 120 MPa. Furthermore, as evident from Figure 2, an increase in the elastic modulus of fibers (E_f) also results in a decrease in the recorded hoop strain reduction factor ($k_{\varepsilon,f}$). It should be noted, however, that this trend is clear for the fiber elastic modulus range of 100,000 to 640,000 MPa that covers AFRP, CFRP, HM CFRP and UHM CFRP. For fibers with elastic modulus (E_f) lower than 100,000 MPa, no further increase in the hoop strain reduction factor ($k_{\varepsilon,f}$) is observed, as evident from the comparison of the GFRP and AFRP-confined specimens in Figures 1(a) and 1(b).

Table 6. Variation of hoop strain reduction factor ($k_{\varepsilon,f}$) with unconfined concrete strength, FRP type and confinement technique

f'_{co} ranges	0 - 40MPa			40 - 60MPa			60 - 80MPa			80 - 100MPa			100 - 120MPa		
Specimens	$k_{\varepsilon,f}$	*S.D.*	*No.*	$k_{\varepsilon,f}$	*S.D.*	*No.*	$k_{\varepsilon,f}$	*S.D.*	*No.*	$k_{\varepsilon,f}$	*S.D.*	*No.*	$k_{\varepsilon,f}$	*S.D.*	*No.*
All	0.693	0.122	155	0.624	0.153	92	0.576	0.131	29	0.526	0.124	44	0.521	0.128	37
All wrapped	0.688	0.119	132	0.629	0.144	64	0.574	0.124	22	0.477	0.094	18	0.449	0.111	21
CFRP wrapped	0.686	0.110	84	0.655	0.098	42	0.634	0.078	16	0.540	0.051	6	0.497	0.084	13
GFRP wrapped	0.761	0.113	29	0.642	0.133	5	-	-	-	0.424	0.016	2	-	-	-
AFRP wrapped	0.673	0.041	5	0.856	0.024	5	-	-	-	-	-	-	0.464	0.039	4
HM CFRP wrapped	0.560	0.094	10	0.438	0.104	12	0.414	0.065	6	0.450	0.106	10	0.276	0.042	4
UHM CFRP wrapped	0.550	0.062	4	-	-	-	-	-	-	-	-	-	-	-	-
All tube-encased	0.718	0.137	23	0.611	0.173	28	0.582	0.160	7	0.535	0.119	26	0.579	0.086	16
CFRP tube-encased	0.732	0.112	9	0.622	0.107	20	0.467	0.058	4	0.506	0.076	21	0.535	0.046	4
GFRP tube-encased	0.693	0.111	6	0.791	0.258	2	-	-	-	-	-	-	-	-	-
AFRP tube-encased	0.815	0.075	6	0.859	0.023	2	0.734	0.106	3	0.712	0.045	5	0.594	0.093	12
HM CFRP tube-encased	-	-	-	-	-	-	-	-	-	-	-	-	-	-	-
UHM CFRP tube-encased	0.435	0.000	2	0.344	0.131	4	-	-	-	-	-	-	-	-	-

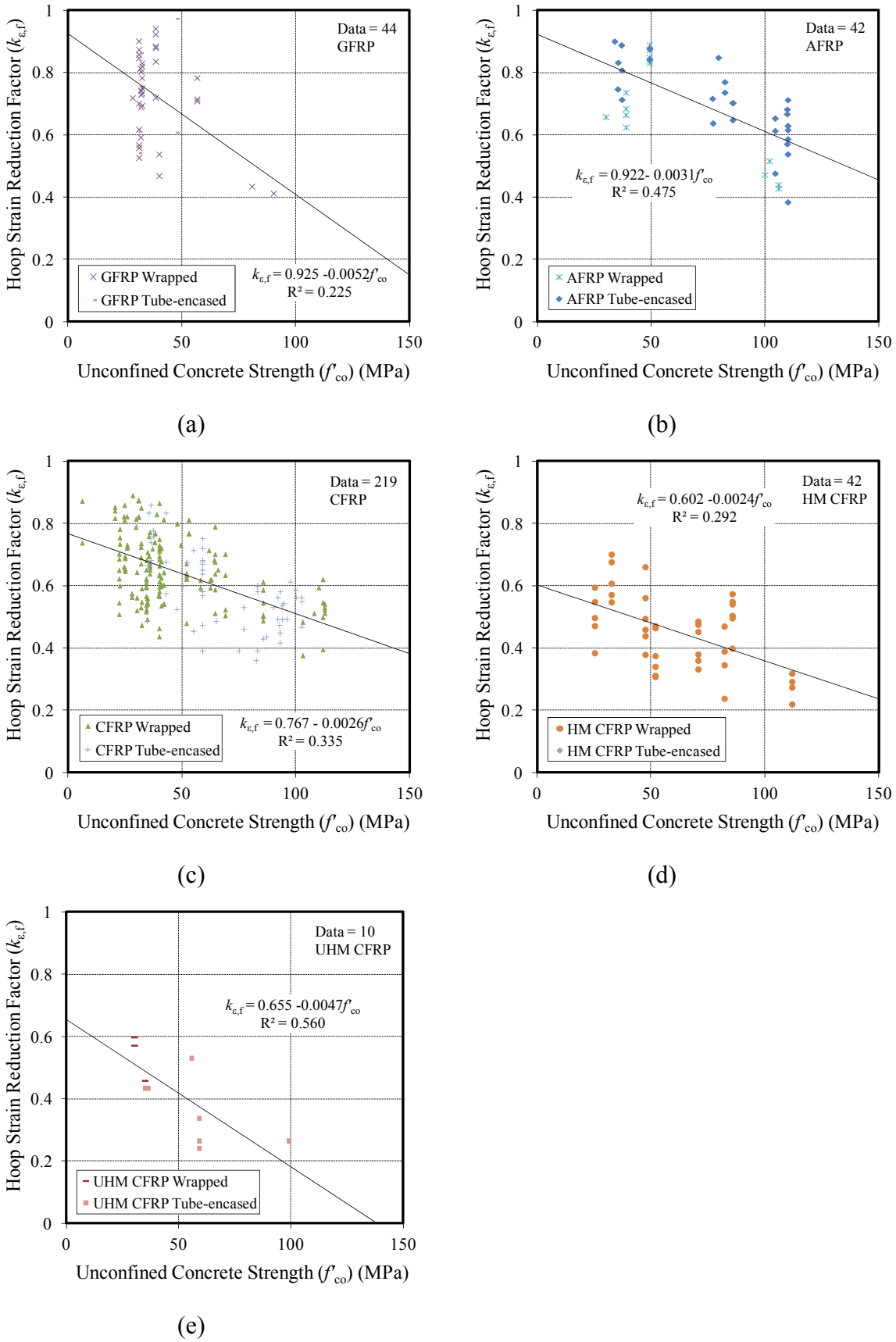

Figure 1. Variation of hoop strain reduction factors ($k_{\varepsilon,f}$) of different type of fibers with unconfined concrete strength: (a) GFRP; (b) AFRP; (c) CFRP; (d) HM CFRP; and (e) UHM CFRP

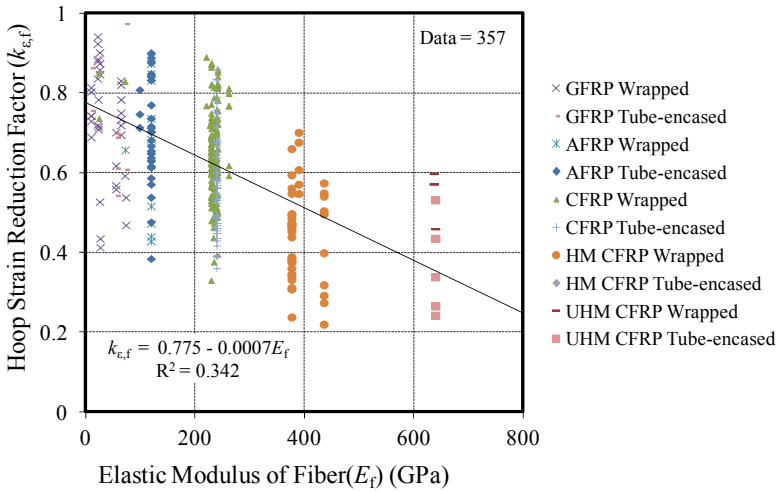

Figure 2. Variation of hoop strain reduction factors ($k_{\varepsilon,f}$) with elastic modulus of fibers (E_f)

The aforementioned influences of unconfined concrete strength (f'_{co}) and elastic modulus of fiber (E_f) were statistically quantified through multivariable regression analysis, which resulted in the expression given in Eq. 3. The expression is able to predict the hoop strain reduction factor ($k_{\varepsilon,f}$) of FRP-confined concrete with an unconfined concrete strength up to 120 MPa, and confined by any of GFRP, AFRP, CFRP, HM CFRP or UHM CFRP. For the reasons discussed previously, the expression specifies a minimum value for E_f (i.e. 100,000 MPa) thereby not allowing a further increase in the hoop strain reduction factor ($k_{\varepsilon,f}$) for fibers with elastic modulus below 100,000 MPa. It should also be noted that current experimental results on GFRP-confined specimens are limited and the available results do not always come with reliable material properties. In the present study, the GFRP-confined specimens reported with fiber elastic modulus (E_f) lower than 60,000 MPa or ultimate material tensile strains (ε_f) greater than 4.0% were excluded from the development of Eq. 3. Additional experimental studies are required to be able to determine the material specific variations of the $k_{\varepsilon,f}$ for GFRP-confined concrete with increased accuracy.

$$k_{\varepsilon,f} = 0.9 - 2.3f'_{co} \times 10^{-3} - 0.75E_f \times 10^{-6} \quad (3)$$

where $100{,}000\text{MPa} \leq E_f \leq 640{,}000\text{MPa}$

where f'_{co} and E_f are in MPa.

3.2 Compressive Strength

As illustrated in Figure 3, the axial stress-strain curves of FRP-confined concrete consist of an ascending portion that is followed by a second branch. Depending on the confinement parameters, the stress-strain curve may demonstrate a full strain-hardening behavior (i.e. Specimen C36 in Figure 3) or it may consist of a second branch that exhibits an initial strain softening region (i.e. Specimens C54 and C94 in Figure 3), which may or may not be subsequently recovered. The important coordinates that correspond to the axial stress, axial strain and lateral strain at the initial peak (f'_{c1}, ε_{c1}, ε_{l1}), second transition point (f'_{c2}, ε_{c2}, ε_{l2}),

and the ultimate condition (f'_{cu}, ε_{cu}, $\varepsilon_{h,rup}$) are marked in Figure 3. The model presented in this paper is intended for specimens demonstrating an overall ascending second branch (with or without initial strain softening) (i.e. $f'_{cu} > f'_{c1}$), for which the ultimate axial stress (f'_{cu}) is equal to the compressive strength (f'_{cc}). In order for FRP-confined concrete to exhibit a full strain-hardening response with no initial strain softening, the stiffness of the FRP reinforcing shell (K_l) (Eq. 4) has to exceed a minimum threshold (K_{lo}). As reported previously in Ozbakkaloglu (2013a), due to the increased confinement demand of the higher strength concretes, the accurate determination of the threshold level of FRP confinement is of vital importance for the design of FRP-confined HSC. Figure 3 shows the variation of the stress-strain responses of the specimens having comparable normalized confinement stiffness ($K_l/f'_{co} \approx 19$) and different unconfined concrete strengths (f'_{co} = 36, 54, 91 MPa). As evident from the reduction of the strength enhancement ratios (f'_{cc}/f'_{co}) from 1.68 to 1.26 as the unconfined concrete strength (f'_{co}) rises from 36 to 91 MPa, confinement stiffness thresholds change in response to changes in unconfined concrete strength. Therefore, if this relationship between the confinement stiffness threshold and variations in unconfined concrete strength is not taken into design consideration, the compressive strength of FRP-confined HSC is likely to be overestimated. Based on this understanding, the exponential increment of the threshold confinement stiffness (K_{lo}) with the unconfined concrete strength (f'_{co}) was closely examined in the present study. This resulted in the development of an expression for K_{lo} as a function of concrete strength (Eq. 5) on the basis of the observed relationships illustrated in Figure 4.

$$K_l = \frac{2E_f t_f}{D} \tag{4}$$

$$K_{lo} = f'^{\,1.65}_{co} \tag{5}$$

where K_{lo} and f'_{co} are in MPa

In addition, it is found that a recovery from strain-softening behavior to hardening behavior, as illustrated in the stress-strain curves of Specimens C54 and C91 in Figure 3, is often experienced by FRP-confined HSC. This behavior is defined as softening recovery in the present paper. In order to distinguish FRP-confined concretes that exhibit a full strain-hardening, full strain-softening, or softening recovery behaviors, 114 specimens tested at the University of Adelaide (Cheek et al. 2011; Ozbakkaloglu and Akin 2012; Ozbakkaloglu and Vincent 2013; Vincent and Ozbakkaloglu 2013a,b) were closely examined. 64 of these specimens exhibited a full strain-hardening behavior. As shown in Figure 4(a) the confinement stiffness of all of these specimens fell above the boundary line that represents the threshold stiffness (K_{lo}). These specimens were then used to define the initial peak stress (f'_{c1}) as a function of confinement stiffness (K_l) and unconfined concrete strength (f'_{co}). The remaining 50 specimens experienced strain-softening behavior and their confinement stiffness remained below the boundary line as shown in Figure 4(b). 32 of these specimens experienced a softening recovery, and they were subsequently used to identify the stress corresponding to the second transition point (f'_{c2}) in the stress-strain relationship.

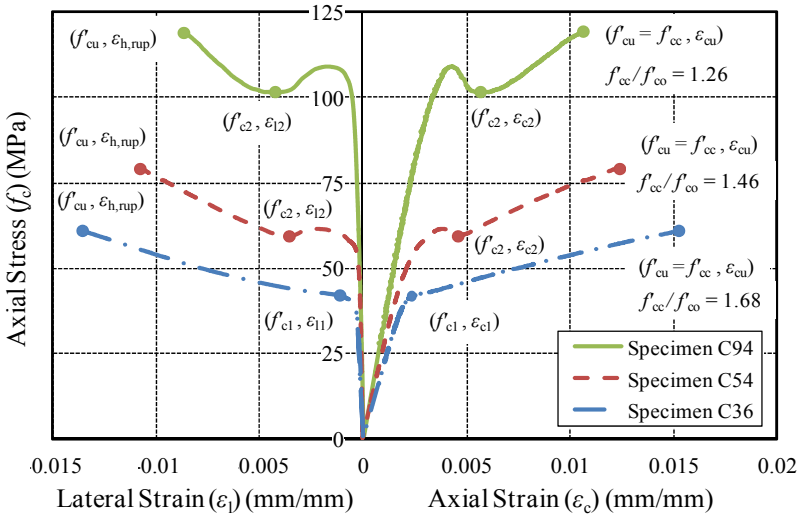

Figure 3. Stress-strain relationships of FRP-confined concrete with unconfined concrete strengths of 36, 54, and 91MPa

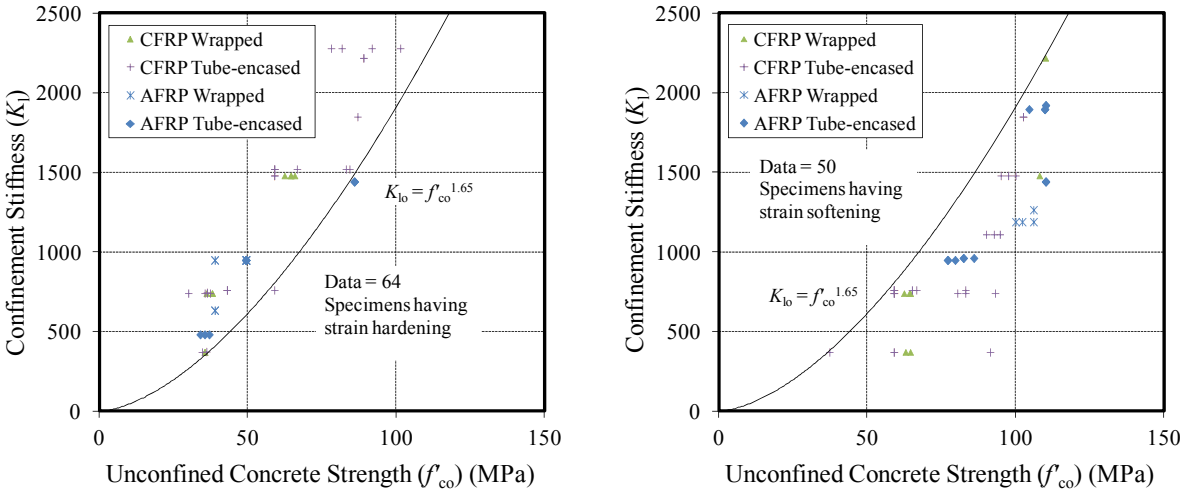

(a) (b)

Figure 4. Threshold confinement stiffness separating specimens having: (a) post-peak strain hardening behavior; (b) strain softening behavior

As discussed previously, determination of the threshold confining pressure (f_{lo}) that occurs at the initial peak stress (f'_{c1}) or the second transition stress (f'_{c2}) of the stress-strain curve plays an important role in the prediction of the post-peak behavior of the FRP-confined concrete that exhibit either a strain-hardening or softening recovery behavior. When the confinement stiffness (K_l) is greater than the threshold stiffness (K_{lo}), a full strain hardening response similar to that of the 36 MPa specimen shown in Figure 3 is expected. The confining pressure that corresponds to the initial peak stress (f'_{c1}) is defined as the threshold confining pressure (f_{lo}) and is calculated based on the corresponding hoop strain in the FRP shell (ε_{l1}) (Eq. 8). When the confinement stiffness (K_l) is lower than the threshold stiffness (K_{lo}), but the actual confining pressure ($f_{lu,a}$) at the ultimate condition is greater than the threshold confining pressure (f_{lo}), a softening recovery response similar to that of the 54 and 91 MPa specimens

shown in Figure 3 is expected. The stress corresponding to the second transition point (f'_{c2}) that marks the initiation of softening recovery is given in Eq. 9 and the corresponding threshold confining pressure (f_{lo}) is given in Eq. 10. The influence confinement stiffness first captured in the literature in this study is integrated into the proposed strength expression (Eq. 6) presented in this paper. The prediction of the strength enhancement effect in the ascending second branch is based on the net confining pressure ($f_{lu,a}$ - f_{lo}), which is calculated by subtracting the threshold confining pressure (f_{lo}) from the actual confining pressure ($f_{lu,a}$). The strength enhancement effect generated by the net confining pressure is then quantified using the coefficient of strength enhancement (k_1). During the development of the model, it was observed that basing the form of strength enhancement expression on the net confining pressure yields an improved model prediction especially for specimens with higher concrete strengths. It should be noted that a negative value of the net confining pressure ($f_{lu,a}$ - f_{lo}) implies a full softening response with $f'_{cu} < f'_{c1}$, and the proposed expression (Eq. 6) is not intended to predict the ultimate axial stress (f'_{cu}) of these specimens.

$$f'_{cc} = c_1 f'_{co} + k_1 (f_{lu,a} - f_{lo}) \tag{6}$$

$$\text{if } K_l \geq K_{lo}, \qquad c_1 = \frac{f'_{c1}}{f'_{co}} = 1 + 0.0058 \frac{K_l}{f'_{co}} \tag{7}$$

$$f_{lo} = f_{l1} = K_l \varepsilon_{l1}, \qquad \varepsilon_{l1} = \left(0.43 + 0.009 \frac{K_l}{f'_{co}}\right) \varepsilon_{co} \tag{8}$$

$$\text{if } K_l < K_{lo}, \qquad c_1 = \frac{f'_{c2}}{f'_{co}} = \left(\frac{K_l}{f'^{\,1.6}_{co}}\right)^{0.2} \tag{9}$$

$$f_{lo} = f_{l2} = K_l \varepsilon_{l2}, \qquad \varepsilon_{l2} = 24 \left(\frac{f'_{co}}{K_l^{1.6}}\right)^{0.4} \varepsilon_{co} \quad \text{where} \quad f_{lu,a} \geq f_{lo} \tag{10}$$

where $f'_{co}, f_{lu,a}, f_{lo}, K_l$, and K_{lo} are in MPa.

In Eqs. 8 and 10, the peak axial strain of unconfined concrete (ε_{co}) is to be determined using the expression proposed by Tasdemir et al. (1998) (Eq. 11).

$$\varepsilon_{co} = \left(-0.067 f'^{\,2}_{co} + 29.9 f'_{co} + 1053\right) \times 10^{-6} \tag{11}$$

Table 7. Variation of strength enhancement coefficient (k_1) with FRP type and confinement technique

Specimens	k_1	R^2	*No.*
All	3.17	0.861	896
All wrapped	3.24	0.862	775
CFRP wrapped	3.64	0.898	482
GFRP wrapped	2.47	0.822	161
AFRP wrapped	3.44	0.865	77
HM CFRP wrapped	4.50	0.768	47
UHM CFRP wrapped	-	-	8
All tube-encased	2.81	0.850	121
CFRP tube-encased	2.16	0.899	47
GFRP tube-encased	2.97	0.711	38
AFRP tube-encased	3.08	0.936	29
HM CFRP tube-encased	-	-	3
UHM CFRP tube-encased	-	-	4

Figure 5 shows the model prediction of the strength enhancement ratios (f'_{cc}/f'_{co}) of the specimens in the test databases of both FRP-confined NSC and HSC. The strength enhancement coefficients (k_1) in Eq. 6 are calculated from the combined database as 3.24 and 2.81 for FRP-wrapped and FRP tube-encased concretes, respectively. Table 7 summarizes the individual k_1 values calibrated for each FRP material and confinement method. It is recommended that an average value of k_1 = 3.2 can be used in Eq.6. It should be noted that the k_1 values of the UHM CFRP-wrapped and HM and UHM CFRP tube-encased specimens are not presented in the table due to unreliability of the results caused by very limited number of available datasets. Additional experimental results are required to be able to determine reliable k_1 values for these specific subgroups. In the absence of these results, the recommended k_1 value of 3.2 should provide conservative estimates for these specimens.

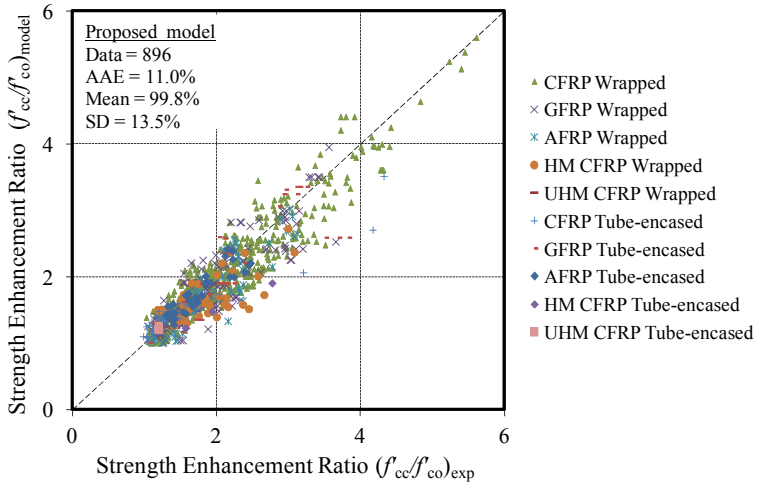

Figure 5. Comparison of model predictions of strength enhancement ratios (f'_{cc}/f'_{co}) with experimental data

3.3 Ultimate Axial Strain

As reported in Ozbakkaloglu et al. (2013) almost all of the better performing existing ultimate strain enhancement expressions proposed non-linear forms to predict the strain enhancement ratio ($\varepsilon_{cu}/\varepsilon_{co}$) as a function of confinement ratios ($f_{lu,a}/f'_{co}$) [e.g. (Berthet et al. 2006; Jiang and Teng 2006; Tamuzs et al. 2006b)]. This is due to the dependency of the strain enhancement ratio ($\varepsilon_{cu}/\varepsilon_{co}$) to the ultimate tensile strain of the FRP materials (ε_{frp}), in addition to the confinement ratio (f_{lu}/f'_{co}), as was also pointed out in a number of previous studies (Karbhari and Gao 1997; Lam and Teng 2003a). In the present study, in order to develop a unified strain enhancement expression for different types of FRP materials, the axial strain (ε_{cu}) was quantified as a non-linear function of the confinement stiffness (K_l), hoop rupture strain ($\varepsilon_{h,rup}$), and unconfined concrete strength (f'_{co}), as given in Eq. 12. To allow for the change in the shape of the stress-strain curve of the unconfined concrete with the variation in its strength (f'_{co}), a new factor c_2 (Eq. 13) was incorporated into the proposed expression. In Eq. 12, the hoop rupture strain ($\varepsilon_{h,rup}$) is to be calculated from Eq. 3, and the peak axial strain of unconfined concrete (ε_{co}) is to be determined using Eq. 11.

$$\varepsilon_{cu} = c_2\varepsilon_{co} + k_2\left(\frac{K_l}{f'_{co}}\right)^{0.9}\varepsilon_{h,rup}{}^{1.35} \tag{12}$$

$$c_2 = 2 - \left(\frac{f'_{co} - 20}{100}\right) \text{ and } c_2 \geq 1 \tag{13}$$

Table 8. Variation of strain enhancement coefficients (k_2) with FRP type and confinement technique

Specimens	k_2	R^2	*No.*
All	0.271	0.814	655
All wrapped	0.265	0.781	555
CFRP wrapped	0.266	0.715	339
GFRP wrapped	0.257	0.822	115
AFRP wrapped	0.274	0.739	48
HM CFRP wrapped	0.322	0.820	48
UHM CFRP wrapped	-	-	5
All tube-encased	0.303	0.926	100
CFRP tube-encased	0.282	0.901	50
GFRP tube-encased	0.298	0.862	22
AFRP tube-encased	0.324	0.527	25
HM CFRP tube-encased	-	-	3
UHM CFRP tube-encased	-	-	-

Figure 6 shows the model prediction of the strain enhancement ratios ($\varepsilon_{cu}/\varepsilon_{co}$) for the specimens included in the combined database of FRP-confined NSC and HSC. The strain enhancement coefficients (k_2) in Eq. 11 are calculated from the combined database as 0.271 and 0.303 for FRP-wrapped and FRP tube-encased concretes, respectively. Table 8 summarizes the individual k_2 values established for each FRP material and confinement method. As can be seen in the table that k_2 is not sensitive to FRP type, and hence it is recommended that an average value of k_2 = 0.27 can be used in Eq.10 independent of FRP material type.

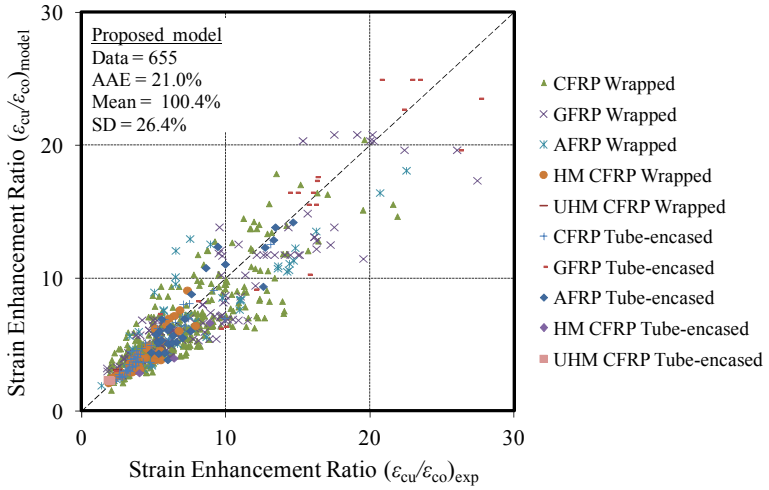

Figure 6. Comparison of model predictions of strain enhancement ratios ($\varepsilon_{cu}/\varepsilon_{co}$) with experimental data

4. COMPARISON WITH TEST DATA

Out of the five FRP-confined HSC models identified from the review of literature (Miyauchi et al. 1999; Mandal et al. 2005; Berthet et al. 2006; Cui and Sheikh 2010a; Xiao et al. 2010), four models that had sufficiently defined parameters to allow numerical calculations were used in the assessment. The performances of these four models (i.e., (Miyauchi et al. 1999; Berthet et al. 2005; Mandal et al. 2005; Xiao et al. 2010) and the model presented in this paper were compared using the FRP-confined HSC database presented in Tables 2 to 5 (in Appendix). Figures 7 and 8 graphically illustrate the model performances through the plots that compare model predictions to experimental values, with the 45° line corresponding to perfect agreement between the predictions and the test results. A trend that spans above the 45° reference line represents overestimation of the experimental results by model predictions, whereas a trend that spans below the reference line indicates an underestimation of the test results. Table 9 reports the statistical summary of the model performances. Average absolute error (*AAE*) is used to establish overall model accuracy. The standard deviation (*SD*) is used to establish the magnitude of the associated scatter for each model. The mean (*M*) is used to describe the associated average overestimation or underestimation of the model, where an overestimation is represented by a mean value greater than 1.

Table 9. Statistics on performances of HSC models in predicting ultimate conditions of FRP-confined HSC

No.	Model	Consideration of $\varepsilon_{h,rup}$	Prediction of f'_{cc}/f'_{co}					Prediction of $\varepsilon_{cu}/\varepsilon_{co}$				
			Test data	Average absolute error (%)	Mean (%)	Standard deviation (%)	Coeficient of variation (%)	Test data	Average absolute error (%)	Mean (%)	Standard deviation (%)	Coeficient of variation (%)
1	Miyauchi et al. (1999)	*No*	168	34.8	133.8	22.4	16.7	144	32.3	115.4	41.5	36.0
2	Mandal et al. (2005)	*No*	168	71.8	170.7	91.7	53.7	144	211.6	305.8	337.0	110.2
3	Berthet et al. (2006)	*No*	168	15.2	110.8	15.5	14.0	144	30.9	73.5	21.9	29.8
4	Xiao et al. (2010)	*Yes*	168	25.4	123.1	18.7	15.2	144	37.5	134.4	37.0	27.5
5	Proposed	*Yes*	168	10.5	101.4	13.1	12.9	144	15.8	100.2	21.2	21.2

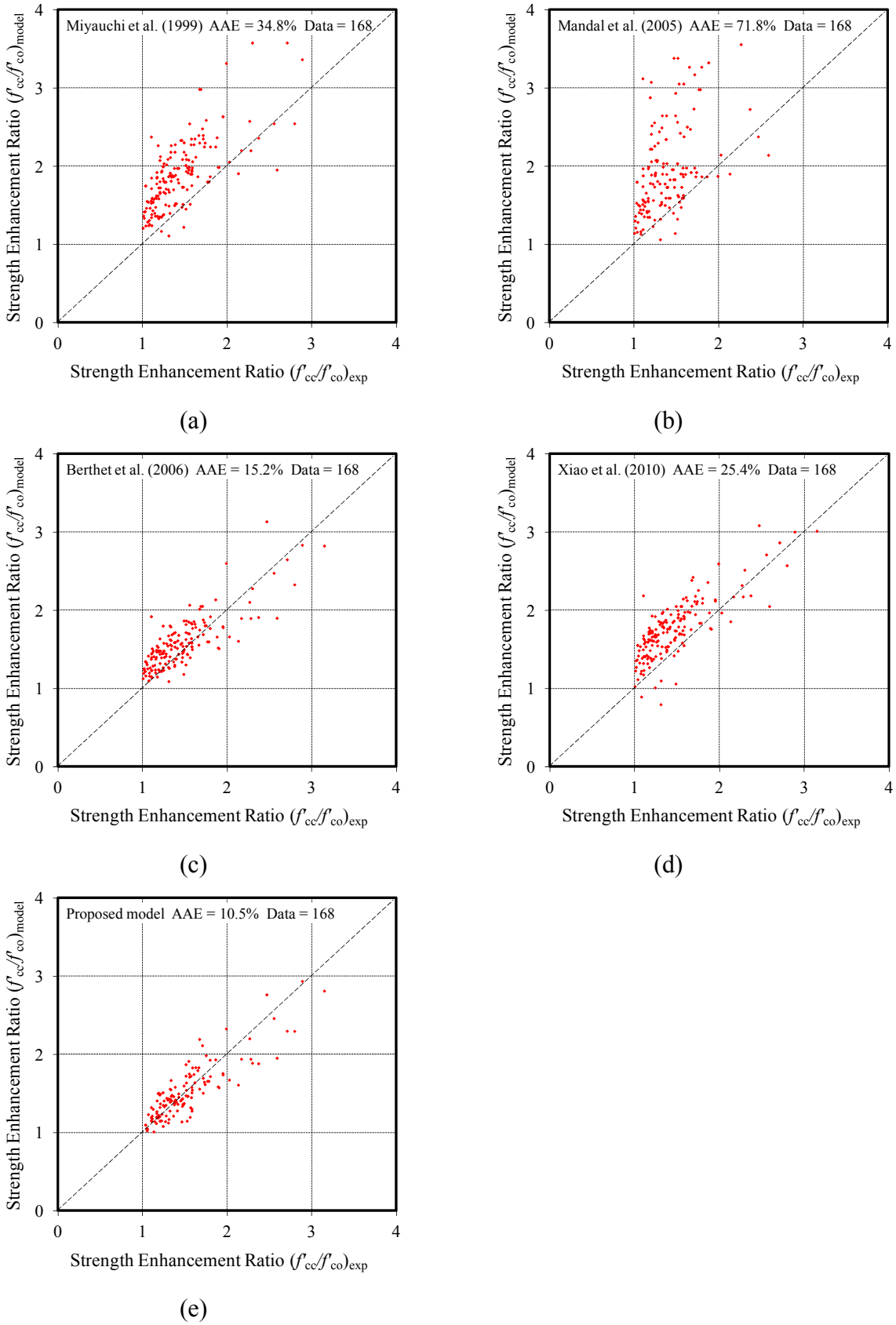

Figure 7. Comparison of strength enhancement predictions (f'_{cc}/f'_{co}) of FRP-confined HSC models with experimental data

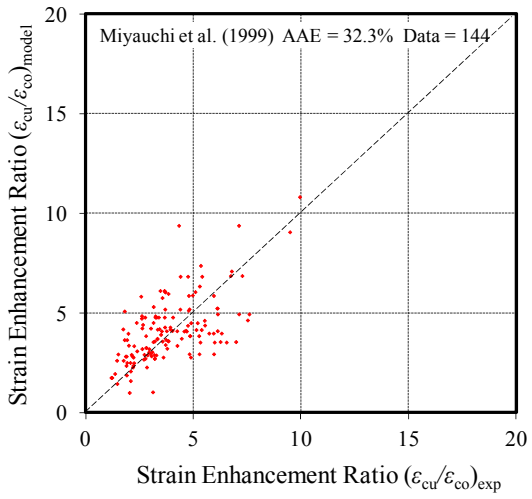

(a)

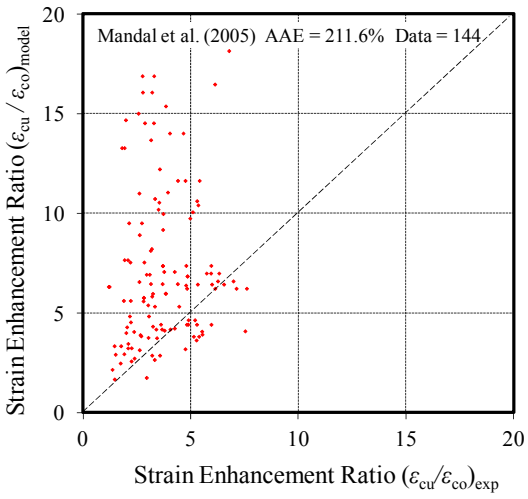

(b)

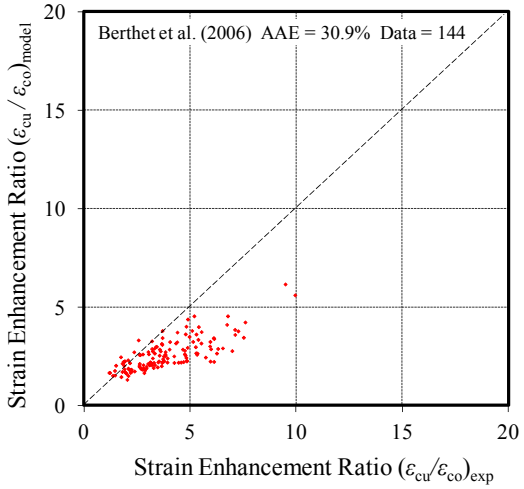

(c)

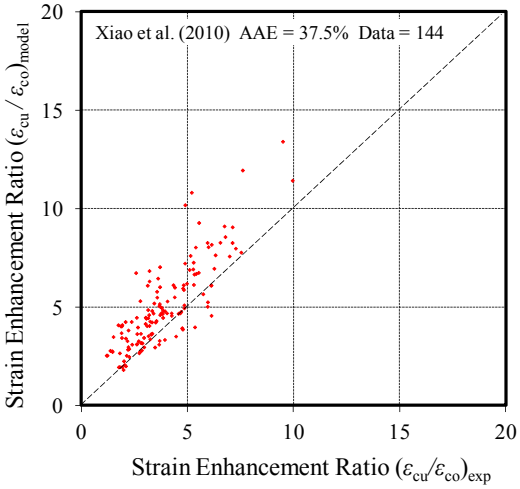

(d)

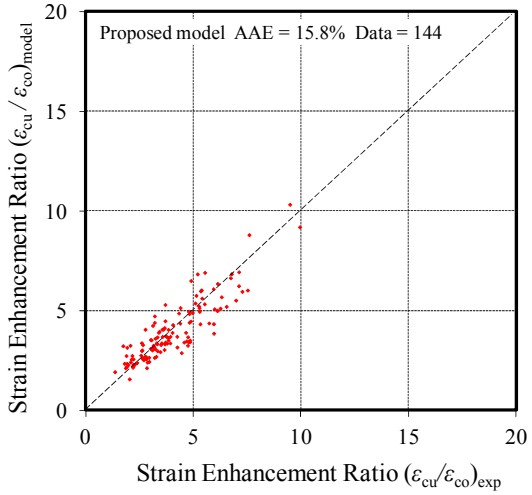

(e)

Figure 8. Comparison of strain enhancement predictions ($\varepsilon_{cu}/\varepsilon_{co}$) of FRP-confined HSC models with experimental data

Except for the model by Berthet et al. (2006), which underestimates the strain enhancement ratio, all of the existing models overestimate the strength and strain enhancement ratios of FRP-confined HSC. These observed overestimations reinforce the need for a reliable model that is applicable to FRP-confined HSC. Common modeling issues that compromise model accuracy include the use of relatively small test databases in the development of the FRP-confined HSC models and the failure of the models to accurately capture the influence of important factors, such as the unconfined concrete strength and type of FRP material. The comparison of the predictions of the proposed model with the results in the database shows a good correlation, with AAEs of 10.5% and 15.8% in the predictions of the strength enhancement ratio (f'_{cc}/f'_{co}) and the strain enhancement ratio ($\varepsilon_{cu}/\varepsilon_{co}$), respectively.

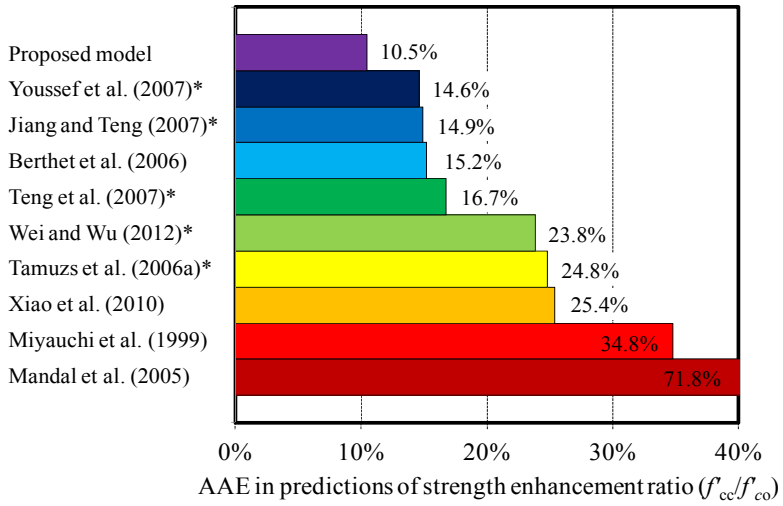

(a)

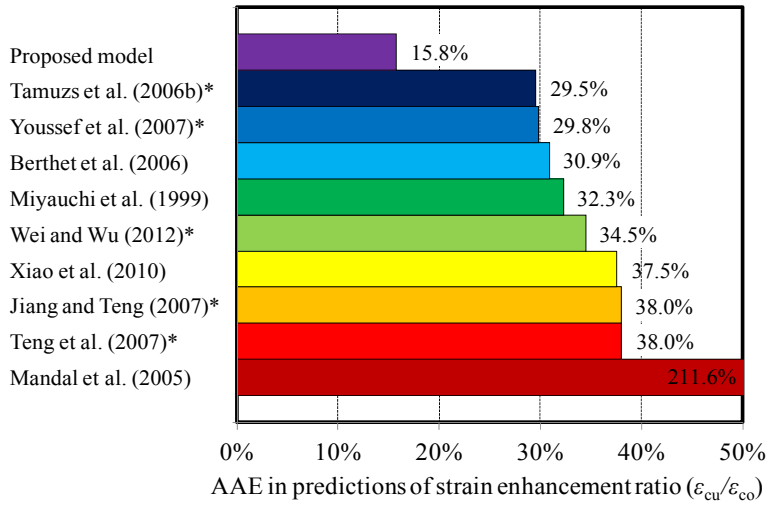

(b)

Figure 9. Average absolute error in model predictions of ultimate conditions of FRP-confined HSC: (a) strength enhancement ratios; (b) strain enhancement ratios

For the completeness of the model comparison, in addition to the models applicable to HSC, five of the top performing models (i.e., (Binici 2005; Tamuzs et al. 2006a; Tamuzs et al. 2006b; Jiang and Teng 2007; Teng et al. 2007; Youssef et al. 2007) out of the 88 NSC

models reviewed in Ozbakkaloglu et al. (2013) (marked with '*') are also included in the performance comparison given in Figure 9. These models were selected on the basis of their performances in the predictions of the strength and strain enhancement ratios of the entire specimens included in the FRP-confined NSC database. As evident from Figures 9(a) and 9(b), the proposed model performs significantly better in predicting the ultimate conditions of FRP-confined HSC than the other top performing models. It should be noted that in the evaluation of the models, the experimentally recorded hoop rupture strains ($\varepsilon_{h,rup}$) were used rather than the values or expressions recommended by the original models for the calculation of $\varepsilon_{h,rup}$. In the absence of the experimental values, $\varepsilon_{h,rup}$ was established using the average value of $k_{\varepsilon,f}$ or $k_{\varepsilon,frp}$ from the database (i.e., 0.625 or 0.710, respectively) in the assessment of the existing models, and it was calculated from Eq.3 in the assessment of the proposed model. It might be worth noting that the proposed model would have outperformed the existing models even more significantly if the hoop rupture strains were established using the original model expressions.

5. CONCLUSIONS

This paper has presented the results of an investigation on the axial compressive behavior of FRP-confined HSC. A large experimental test database that consisted of with 231 test results of FRP-confined HSC has been presented in this paper. The database was augmented with another database of FRP-confined NSC to create a combined database that includes 1063 axial compression tests results of FRP-confined concrete specimens with unconfined concrete strengths ranging from 6.2 to 169.7 MPa. The combined database provides a significantly extended parameter space, thereby allowing clearer observations to be made on the important factors that influence the behavior of FRP-confined concrete. A new design-oriented model, which was developed on the basis of the database, has been presented in the second half of the paper. The model is applicable to both NSC and HSC of strengths up to 120 MPa, and it incorporates the important factors identified from the close examination of the results reported in the database and assessment of previous models. The model comparisons have demonstrated that the proposed model provides significantly improved predictions of the ultimate conditions of FRP-confined HSC compared to any of the existing models.

Based on the observations made during the compilation of the experimental database and the development of the model, the following conclusions are drawn:

1) The hoop rupture strain reduction factor ($k_{\varepsilon,f}$) of FRP shells decreases with an increase in the unconfined concrete strength (f'_{co}) and elastic modulus of fiber material (E_f).
2) The confinement stiffness threshold (K_{lo}) increases with an increase in the unconfined concrete strength (f'_{co}). This results in a reduced strength enhancement ratio (f'_{cc}/f'_{co}) in higher strength concrete, even when the amount of confinement is increased as a linear function of concrete strength.
3) As expected, the ultimate axial strain (ε_{cu}) decreases with the increase in the unconfined concrete strength (f'_{co}). However, if the amount of confinement is increased linearly with the unconfined concrete strength (f'_{co}), the reduction in the ultimate axial strain (ε_{cu}) with increased unconfined concrete strength (f'_{co}) is not very significant.

NOMENCLATURE

AAE	Average absolute error
c_1	Parameter in the compressive strength expression
c_2	Parameter in the ultimate strain expression
D	Diameter of concrete core (mm)
E_f	Elastic modulus of fibers (MPa)
E_{frp}	Elastic modulus of FRP material (MPa)
f'_{cc}	Peak axial compressive stress of FRP-confined concrete (MPa)
f'_{cu}	Ultimate axial compressive stress of FRP-confined concrete (MPa)
f'_{co}	Peak axial compressive stress of unconfined concrete (MPa)
f'_{c1}	Axial compressive stress of FRP-confined concrete at first peak (MPa)
f'_{c2}	Axial compressive stress of FRP-confined concrete at second transition (MPa)
f_f	Ultimate tensile strength of fibers; $f_f = E_f\varepsilon_f$ (MPa)
f_{frp}	Ultimate tensile strength of FRP material; $f_{frp} = E_{frp}\varepsilon_{frp}$ (MPa)
f_l	Confining pressure (MPa)
f_{l1}	Confining pressure at f'_{c1} (MPa)
f_{l2}	Confining pressure at f'_{c2} (MPa)
f_{lo}	Threshold confining pressure (MPa)
f_{lu}	Nominal lateral confining pressure at ultimate; $f_{lu} = K_l\varepsilon_f$ or $f_{lu} = K_l\varepsilon_{frp}$ (MPa)
$f_{lu,a}$	Actual lateral confining pressure at ultimate; $f_{lu,a} = K_l\varepsilon_{h,rup}$ (MPa)
H	FRP confined concrete specimen height (mm)
K_l	Lateral confinement stiffness; $K_l = 2E_f t_f/D$ or $2E_{frp}t_{frp}/D$ (MPa)
k_1	Axial strength enhancement coefficient
k_2	Axial strain enhancement coefficient
k_ε	Hoop strain reduction factor
$k_{\varepsilon,f}$	Hoop strain reduction factor of fibers
$k_{\varepsilon,frp}$	Hoop strain reduction factor of FRP material
M	Mean
SD	Standard deviation
t_f	Total nominal thickness of fibers (mm)
t_{frp}	Total thickness of FRP material (mm)
ε_{co}	Axial strain of unconfined concrete at f'_{co}
ε_{c1}	Axial strain of FRP-confined concrete at f'_{c1}
ε_{c2}	Axial strain of FRP-confined concrete at f'_{c2}
ε_{cu}	Ultimate axial strain of FRP-confined concrete
ε_f	Ultimate tensile strain of fibers
ε_{frp}	Ultimate tensile strain of FRP material
$\varepsilon_{h,rup}$	Hoop rupture strain of FRP shell
ε_{11}	Hoop strain of FRP-confined concrete at f'_{c1}
ε_{12}	Hoop strain of FRP-confined concrete at f'_{c2}

REFERENCES

Ahmad, S. M., Khaloo, A. R. and Irshaid, A. (1991). "Behaviour of concrete spirally confined by fiberglass filaments." *Magazine of Concrete Research*, 43(56), 143-148.

Aire, C., Gettu, R. and Casas, J. R. (2001). "Study of the compressive behavior of concrete confined by fiber reinforced composites." *Composites in Construction*.

Aire, C., Gettu, R., Casas, J. R., Marques, S. and Marques, D. (2010). "Concrete laterally confined with fibre-reinforced polymers (FRP): experimental study and theoretical model." *Materiales De Construccion*, 60(297), 19-31.

Almusallam, T. H. (2007). "Behavior of normal and high-strength concrete cylinders confined with E-glass/epoxy composite laminates." *Composites Part B-Engineering*, 38(5-6), 629-639.

Attard, M. M. and Setunge, S. (1996). "Stress-strain relationship of confined and unconfined concrete." *ACI Materials Journal*, 93(5), 432-442.

Benzaid, R., Chikh, N. E. and Mesbah, H. (2009). "Study of the Compressive Behavior of Short Concrete Columns Confined by Fiber Reinforced Composite." *Arabian Journal for Science and Engineering*, 34(1B), 15-26.

Benzaid, R., Mesbah, H. and Chikh, N. E. (2010). "FRP-confined Concrete Cylinders: Axial Compression Experiments and Strength Model." *Journal of Reinforced Plastics and Composites*, 29(16), 2469-2488.

Berthet, J. F., Ferrier, E. and Hamelin, P. (2005). "Compressive behavior of concrete externally confined by composite jackets. Part A: experimental study." *Construction and Building Materials*, 19(3), 223-232.

Berthet, J. F., Ferrier, E. and Hamelin, P. (2006). "Compressive behavior of concrete externally confined by composite jackets - Part B: modeling." *Construction and Building Materials*, 20(5), 338-347.

Binici, B. (2005). "An analytical model for stress-strain behavior of confined concrete." *Engineering Structures*, 27(7), 1040-1051.

Cheek, J., Formichella, N., Graetz, D. and Varasteh, S. (2011). "The behaviour of ultra high strength concrete in FRP confined concrete systems under axial compression." Honours Bachelor's thesis, *The School of Civil, Environmental and Mining Engineering*, The University of Adelaide, Adelaide.

Chikh, N., Gahmous, M. and Benzaid, R. (2012). "Structural Performance of High Strength Concrete Columns Confined with CFRP Sheets." *Proceedings of the World Congress on Engineering*, London, U.K.

Cui, C. and Sheikh, S. A. (2010a). "Analytical Model for Circular Normal- and High-Strength Concrete Columns Confined with FRP." *Journal of Composites for Construction*, 14(5), 562-572.

Cui, C. and Sheikh, S. A. (2010b). "Experimental Study of Normal- and High-Strength Concrete Confined with Fiber-Reinforced Polymers." *Journal of Composites for Construction*, 14(5), 553-561.

De Lorenzis, L. and Tepfers, R. (2003). "Comparative study of models on confinement of concrete cylinders with fiber-reinforced polymer composites." *Journal of Composites for Construction*, 7(3), 219-237.

Fam, A. Z. and Rizkalla, S. H. (2001). "Confinement model for axially loaded concrete confined by circular fiber-reinforced polymer tubes." *ACI Structural Journal*, 98(4), 451-461.

Green, M. F. (2007). "FRP repair of concrete structures: performance in cold regions." *International Journal of Materials & Product Technology*, 28(1-2), 160-177.

Harmon, T. G. and Slattery, K. T. (1992). "Advanced composite confinement of concrete." *Proceedings of the First International Conference on Advanced Composite Materials in Bridges and Structures*, Quebec, Canada, 299-306.

Harries, K. A. and Carey, S. A. (2003). "Shape and "gap" effects on the behavior of variably confined concrete." *Cement and Concrete Research*, 33(6), 881-890.

Jiang, T. and Teng, J. G. (2006). "Strengthening of short circular RC columns with FRP jackets: a design proposal." *Proceedings of the 3rd International Conference on FRP Composites in Civil Engineering*, Miami, Florida, USA.

Jiang, T. and Teng, J. G. (2007). "Analysis-oriented stress-strain models for FRP-confined concrete." *Engineering Structures*, 29(11), 2968-2986.

Karbhari, V. M. and Gao, Y. Q. (1997). "Composite jacketed concrete under uniaxial compression - Verification of simple design equations." *Journal of Materials in Civil Engineering*, 9(4), 185-193.

Lam, L. and Teng, J. G. (2003a). "Design-oriented stress-strain model for FRP-confined concrete." *Construction and Building Materials*, 17(6-7), 471-489.

Lam, L. and Teng, J. G. (2003b). "Hoop rupture strains of FRP jackets in FRP confined concrete." *Proceedings of the 6th Intermational Symposium of Fibre-Reinforcement Polymer Reinforcement for Concrete Structures*, 1, 601-612.

Lam, L. and Teng, J. G. (2004). "Ultimate condition of fiber reinforced polymer-confined concrete." *Journal of Composites for Construction, ASCE*, 8(6), 539-548.

Mandal, S. and Fam, A. (2004). "Axial loading tests on FRP confined concrete of different compressive strengths." *Proceedings of the 4th International Conference of Advanced Composite Materials in Bridges and Structures*, Calgary, Alberta, 20-23.

Mandal, S., Hoskin, A. and Fam, A. (2005). "Influence of concrete strength on confinement effectiveness of fiber-reinforced polymer circular jackets." *ACI Structural Journal*, 102(3), 383-392.

Matthys, S., Taerwe, L. and Audenaert, K. (1999). "Tests on axially loaded concrete columns confined by fiber reinforced polymer sheet wrapping." *ACI Special Publications 188*, 217-228.

Mirmiran, A., Shahawy, M., Samaan, M., El Echary, H., Mastrapa, J. C. and Pico, O. (1998). "Effect of column parameters on FRP-confined concrete." *Journal of Composites for Construction*, 2(4), 175-185.

Miyauchi, K., Inoue, S., Kuroda, T. and Kobayashi, A. (1999). "Strengthening effects with carbon fiber sheet for concrete column." *Proceedings of Japan Concrete Institution*, 21(3), 1453-1458.

Owen, L. M. (1998). "Stress-strain behavior of concrete confined by carbon fiber jacketing." Masters, University of Washington, Seattle.

Ozbakkaloglu, T. (2013a). "Axial compressive behavior of square and rectangular high-strength concrete-filled FRP tubes." *Journal of Composites for Construction*, 17(1), 151-161.

Ozbakkaloglu, T. (2013b). "Concrete-filled FRP Tubes: Manufacture and testing of new forms designed for improved performance." *Journal of Composites for Construction*, 17(2), 280-291.

Ozbakkaloglu, T. and Akin, E. (2012). "Behavior of FRP-Confined Normal- and High-Strength Concrete under Cyclic Axial Compression." *Journal of Composites for Construction*, 16(4), 451-463.

Ozbakkaloglu, T. and Lim, J. C. (2013). "Axial compressive behavior of FRP-confined concrete: Experimental test database and a new design-oriented model." *Composites Part B: Engineering*, 55, 607-634.

Ozbakkaloglu, T., Lim, J. C. and Vincent, T. (2013). "FRP-confined concrete in circular sections: Review and assessment of stress–strain models." *Engineering Structures*, 49, 1068–1088.

Ozbakkaloglu, T. and Oehlers, D. J. (2008a). "Concrete-filled square and rectangular FRP tubes under axial compression." *Journal of Composites for Construction*, 12(4), 469-477.

Ozbakkaloglu, T. and Oehlers, D. J. (2008b). "Manufacture and testing of a novel FRP tube confinement system." *Engineering Structures*, 30, 2448-2459.

Ozbakkaloglu, T. and Vincent, T. (2013). "Axial compressive behavior of circular high-strength concrete-filled FRP tubes." *Journal of Composites for Construction, ASCE*, 18(2), 04013037.

Pessiki, S., Harries, K. A., Kestner, J. T., Sause, R. and Ricles, J. M. (2001). "Axial behavior of reinforced concrete columns confined with FRP jackets." *Journal of Composites for Construction*, 5(4), 237-245.

Rousakis, T. (2001). "Experimental investigation of concrete cylinders confined by carbon FRP sheets under monotonic and cyclic axial compressive load." Masters, *Department of Civil Engineering*, Demokritus University of Thrace, Greece.

Setunge, S., Attard, M. M. and Darvall, P. L. (1993). "Ultimate strength of confined very high-strength concretes." *ACI Structural Journal*, 90(6), 632-641.

Shehata, I. A. E. M., Carneiro, L. A. V. and Shehata, L. C. D. (2007). "Strength of confined short concrete columns." *Proceedings of the 8th International Symposium on Fiber Reinforced Polymer Reinforcement for Concrete Structures*, University of Patras, Patras, Greece.

Tamuzs, V., Tepfers, R. and Sparnins, E. (2006a). "Behavior of concrete cylinders confined by carbon composite - 2. Prediction of strength." *Mechanics of Composite Materials*, 42(2), 109-118.

Tamuzs, V., Tepfers, R., Zile, E. and Ladnova, O. (2006b). "Behavior of concrete cylinders confined by a carbon composite - 3. Deformability and the ultimate axial strain." *Mechanics of Composite Materials*, 42(4), 303-314.

Tasdemir, M. A., Tasdemir, C., Jefferson, A. D., Lydon, F. D. and Barr, B. I. G. (1998). "Evaluation of strains at peak stresses in concrete: A three-phase composite model approach." *Cement and Concrete Research*, 20(4), 301-318.

Teng, J. G., Huang, Y. L., Lam, L. and Ye, L. P. (2007). "Theoretical model for fiber-reinforced polymer-confined concrete." *Journal of Composites for Construction, ASCE*, 11(2), 201-210.

Valdmanis, V., De Lorenzis, L., Rousakis, T. and Tepfers, R. (2007). "Behaviour and capacity of CFRP-confined concrete cylinders subjected to monotonic and cyclic axial compressive load." *Structural Concrete*, 8(4), 187-200.

Vincent, T. and Ozbakkaloglu, T. (2013a). "Influence of concrete strength and confinement method on axial compressive behavior of FRP-confined high- and ultra high-strength concrete." *Composites Part B*, 50, 413–428.

Vincent, T. and Ozbakkaloglu, T. (2013b). "Influence of fiber orientation and specimen end condition on axial compressive behavior of FRP-confined concrete." *Construction and Building Materials*, 47, 814-826.

Wu, H. L., Wang, Y. F., Yu, L. and Li, X. R. (2009). "Experimental and Computational Studies on High-Strength Concrete Circular Columns Confined by Aramid Fiber-Reinforced Polymer Sheets." *Journal of Composites for Construction*, 13(2), 125-134.

Xiao, Q. G., Teng, J. G. and Yu, T. (2010). "Behavior and Modeling of Confined High-Strength Concrete." *Journal of Composites for Construction, ASCE*, 14(3), 249-259.

Xiao, Y. and Wu, H. (2000). "Compressive behavior of concrete confined by carbon fiber composite jackets." *Journal of Materials in Civil Engineering*, 12(2), 139-146.

Youssef, M. N., Feng, M. Q. and Mosallam, A. S. (2007). "Stress-strain model for concrete confined by FRP composites." *Composites Part B-Engineering*, 38(5-6), 614-628.

Zinno, A., Lignola, G. P., Prota, A., Manfredi, G. and Cosenza, E. (2010). "Influence of free edge stress concentration on effectiveness of FRP confinement." *Composites Part B-Engineering*, 41(7), 523-532.

APPENDIX

Table 2. Test database of CFRP-confined HSC specimens

Paper	Specimen Dimensions		Concrete Properties		FRP Properties			Fiber Properties			Measured Initial Peak Conditions		Measured Ultimate Conditions			Hoop Strain Reduction Factors	
	D (mm)	H (mm)	f'_{co} (MPa)	ε_{co} (%)	E_{frp} (GPa)	f_{frp} (MPa)	t_{frp} (mm)	E_f (GPa)	f_f (MPa)	t_f (mm)	f'_{c1} (MPa)	ε_{c1} (%)	f'_{cu} (MPa)	ε_{cu} (%)	$\varepsilon_{h,rup}$ (%)	$k_{\varepsilon,frp}$	$k_{\varepsilon,f}$
CFRP-wrapped specimens																	
Aire et al. (2010)	150	300	69	0.24				240	3900	0.117	94	0.27			0.09		0.055^
Aire et al. (2010)	150	300	69	0.24				240	3900	0.351			98	0.78	0.82		0.505
Aire et al. (2010)	150	300	69	0.24				240	3900	0.702			156	1.63	1.03		0.634
Aire et al. (2010)	150	300	69	0.24				240	3900	1.053			199	2.28	1.14		0.702
Aire et al. (2010)	150	300	69	0.24				240	3900	1.404			217	2.39	0.85		0.523
Benzaid et al. (2010)	160	320	61.81	0.284				238	4300	0.13	62.68	0.327			0.246		0.136^
Benzaid et al. (2010)	160	320	61.81	0.284				238	4300	0.39			93.19	1.054	1.289		0.713
Berthet et al. (2005)	70	140	112.6	0.233				230	3200	0.33			141.1	0.451	0.712		0.512
Berthet et al. (2005)	70	140	112.6	0.233				230	3200	0.33			143.1	0.487	0.738		0.530
Berthet et al. (2005)	70	140	112.6	0.233				230	3200	0.82			189.5	0.723[a]	0.754		0.542
Berthet et al. (2005)	70	140	112.6	0.233				230	3200	0.82			187.9	0.701[a]	0.728		0.523
Berthet et al. (2005)	70	140	169.7	0.324				230	3200	0.33			186.4	0.665	0.459		0.330
Berthet et al. (2005)	70	140	169.7	0.324				230	3200	0.99			296.4	1.015	0.799		0.574^
Chikh et al. (2012)	160	320	61.8	0.284				238	4300	0.13			62.68	0.327[a]			
Chikh et al. (2012)	160	320	61.8	0.284				238	4300	0.39			93.19	1.054			
Cui and Sheikh (2010b)	152	305	79.9	0.241	85	816	1.0				94.8	0.332	90.9	0.525	1.097	1.143^	
Cui and Sheikh (2010b)	152	305	79.9	0.241	85	816	1.0						105.3	0.739	0.917	0.955^	
Cui and Sheikh (2010b)	152	305	79.9	0.241	85	816	2.0						142.1	1.125	0.985	1.026^	
Cui and Sheikh (2010b)	152	305	79.9	0.241	85	816	2.0						140.8	0.974	1.099	1.145^	
Cui and Sheikh (2010b)	152	305	79.9	0.241	85	816	3.0						172.9	1.479	0.975	1.016^	
Cui and Sheikh (2010b)	152	305	79.9	0.241	85	816	3.0						181.8	1.474	1.113	1.159^	
Cui and Sheikh (2010b)	152	305	110.6	0.262	85	816	1.0				146.6	0.352	107.3[d]	0.518	1.029	1.072^	
Cui and Sheikh (2010b)	152	305	110.6	0.262	85	816	1.0				149.2	0.342	116.6	0.551	0.855	0.891^	
Cui and Sheikh (2010b)	152	305	110.6	0.262	85	816	3.0				176.4	0.431	198.4	0.843	0.867	0.903^	
Cui and Sheikh (2010b)	152	305	110.6	0.262	85	816	3.0				164.5	0.379	182.3	0.730	0.746	0.777^	
Cui and Sheikh (2010b)	152	305	85.6	0.258				241	3639	0.11	95.4	0.281	64.4[d]	0.443	0.823		0.545
Cui and Sheikh (2010b)	152	305	85.6	0.258				241	3639	0.11	89.8	0.285	66.6[d]	0.436	0.758		0.502
Cui and Sheikh (2010b)	152	305	85.6	0.258				241	3639	0.22	96.0	0.312	78.9[d]	0.560	0.736		0.487
Cui and Sheikh (2010b)	152	305	85.6	0.258				241	3639	0.22	94.5	0.301	86.1	0.582	0.763		0.505
Cui and Sheikh (2010b)	152	305	85.6	0.258				241	3639	0.44	100.8	0.368	125.4	0.995	0.886		0.587
Cui and Sheikh (2010b)	152	305	85.6	0.258				241	3639	0.44	100.1	0.395	126.5	0.991	0.924		0.612
Cui and Sheikh (2010b)	152	305	111.8	0.261				241	3639	0.22	134.1	0.301	101.1[d]	0.324[a]	0.937		0.621
Cui and Sheikh (2010b)	152	305	111.8	0.261				241	3639	0.22	135.7	0.303	94.3[d]	0.481	0.825		0.546
Cui and Sheikh (2010b)	152	305	111.8	0.261				241	3639	0.55	145.5	0.334	152.1	0.496	0.753		0.499
Cui and Sheikh (2010b)	152	305	111.8	0.261				241	3639	0.55	153.3	0.365	145.3	0.580	0.597		0.395
Green et al. (2007)	152	305	59		70.3	881	1[p]						70				
Harmon and Slattery (1992)	51	102	103					235	3500	0.179			131.1	1.1	0.02		0.013^
Harmon and Slattery (1992)	51	102	103					235	3500	0.344			193.2	2.1	0.72		0.483
Harmon and Slattery (1992)	51	102	103					235	3500	0.689			303.6[s]	3.4[a]	0.56		0.376
Mandal and Fam (2004)	100	200	80.6	0.223				47[m]	784	0.8	96.4	0.31					
Mandal and Fam (2004)	100	200	80.6	0.223				47[m]	784	0.8	104.6	0.35					
Mandal and Fam (2004)	100	200	80.6	0.223				47[m]	784	0.8	100.4	0.33					

Paper	D (mm)	H (mm)	f'_{co} (MPa)	ε_{co} (%)	E_{frp} (GPa)	f_{frp} (MPa)	t_{frp} (mm)	E_f (GPa)	f_f (MPa)	t_f (mm)	f'_{c1} (MPa)	ε_{c1} (%)	f'_{cu} (MPa)	ε_{cu} (%)	$\varepsilon_{h,rup}$ (%)	$k_{\varepsilon,frp}$	$k_{\varepsilon,f}$
Mandal and Fam (2004)	100	200	67.03	0.217				47[m]	784	0.8	90.5	0.34					
Mandal and Fam (2004)	100	200	67.03	0.217				47[m]	784	0.8	85.9	0.30					
Mandal and Fam (2004)	100	200	67.03	0.217				47[m]	784	0.8	93.6	0.32					
Miyauchi et al. (1999)	100	200	109.5	0.287				230.5	3481	0.11	117.3	0.346	109.5	0.424			
Miyauchi et al. (1999)	100	200	109.5	0.287				230.5	3481	0.22	122.5	0.325	110.8	0.551			
Owen (1998)	298	610	58.1		238	4200	1.32	262	4200	0.165			60.0	0.76	0.95	0.538	0.593
Owen (1998)	298	610	58.1		238	4200	1.32	262	4200	0.33			84.8	1.22	0.99	0.561	0.618
Owen (1998)	298	610	58.1		238	4200	1.32	262	4200	0.66			150.2	2.89[a]	1.31	0.742	0.817^
Ozbakkaloglu and Vincent (2013)	152	305	64.5					240	3800	0.117	65.6	0.29	46.7[d]	0.59	0.93		0.600
Ozbakkaloglu and Vincent (2013)	152	305	64.5					240	3800	0.117	68.7	0.29	48.6[d]	0.57	0.81		0.523
Ozbakkaloglu and Vincent (2013)	152	305	62.9					240	3800	0.117	66.3	0.29	50.4[d]	0.65	0.98		0.630
Ozbakkaloglu and Vincent (2013)	152	305	64.5					240	3800	0.234			72.3	0.93	1.25		0.806
Ozbakkaloglu and Vincent (2013)	152	305	62.4					240	3800	0.234			68.4	0.71	0.94		0.606
Ozbakkaloglu and Vincent (2013)	152	305	64.2					240	3800	0.234			68.2	0.82	1.08		0.697
Ozbakkaloglu and Vincent (2013)	152	305	64.5					240	3800	0.351			85.9	1.19	1.07		0.688
Ozbakkaloglu and Vincent (2013)	152	305	64.5					240	3800	0.351			80.3	1.00	1.01		0.653
Ozbakkaloglu and Vincent (2013)	152	305	64.5					240	3800	0.468			99.4	1.38	1.11		0.715
Ozbakkaloglu and Vincent (2013)	152	305	62.4					240	3800	0.468			101.3	1.41	0.98		0.630
Ozbakkaloglu and Vincent (2013)	152	305	65.8					240	3800	0.468			104.3	1.36	1.03		0.663
Ozbakkaloglu and Vincent (2013)	152	305	108.0					240	3800	0.468	103.3	0.36	117.4	0.96	0.81		0.525
Ozbakkaloglu and Vincent (2013)	152	305	112.0					240	3800	0.585	119.6	0.41	121.2	1.09	0.80		0.515
Ozbakkaloglu and Vincent (2013)	152	305	110.0					240	3800	0.702			122.3[s]	1.13	0.94		0.605
Shehata et al. (2007)	150	300	61.7	0.18				235	3550	0.165			76.4	0.60			
Shehata et al. (2007)	150	300	61.7	0.18				235	3550	0.330			97.3	0.87			
Valdmanis et al. (2007)	150	300	61.6	0.18	200.5	1906	0.17	234	4500	0.17			80.5	0.27[a]	0.18	0.189^	0.094^
Valdmanis et al. (2007)	150	300	61.6	0.18	231	2389	0.34	234	4500	0.34			95.3	0.32[a]	0.16	0.155^	0.083^
Valdmanis et al. (2007)	150	300	61.6	0.18	236	2661	0.51	234	4500	0.51			104.9	0.36[a]	0.32	0.284^	0.166^
Xiao et al. (2010)	152	305	70.8	0.32	237.8[t]	2738[t]	0.34						104.2	1.07	1.10	0.955^	
Xiao et al. (2010)	152	305	70.8	0.32	237.8[t]	2738[t]	0.34						110.3	1.43	1.21	1.051^	
Xiao et al. (2010)	152	305	70.8	0.32	237.8[t]	2738[t]	1.02						180.5	2.16	1.00	0.869^	
Xiao et al. (2010)	152	305	70.8	0.32	237.8[t]	2738[t]	1.02						197.7	2.33	0.90	0.782	
Xiao et al. (2010)	152	305	70.8	0.32	237.8[t]	2738[t]	1.7						191.5	2.28	0.67	0.582	
Xiao et al. (2010)	152	305	70.8	0.32	237.8[t]	2738[t]	1.7						162.4	1.39	0.52	0.452	
Xiao et al. (2010)	152	305	111.6	0.34	237.8[t]	2738[t]	0.68						141.2	0.97	0.57	0.495	
Xiao et al. (2010)	152	305	111.6	0.34	237.8[t]	2738[t]	0.68						134.0	0.75	0.58	0.504	
Xiao et al. (2010)	152	305	111.6	0.34	237.8[t]	2738[t]	1.02						170.4	0.98	0.52	0.452	
Xiao et al. (2010)	152	305	111.6	0.34	237.8[t]	2738[t]	1.02						176.6	1.12	0.60	0.521	
Xiao et al. (2010)	152	305	111.6	0.34	237.8[t]	2738[t]	1.7						217.3	1.56	0.56	0.486	
Xiao et al. (2010)	152	305	111.6	0.34	237.8[t]	2738[t]	1.7						217.1	1.60	0.57	0.495	
CFRP tube-encased specimens																	
Ozbakkaloglu and Vincent (2013)	74	152	62.0					240	3800	0.117			69.9	0.63	0.50		0.320
Ozbakkaloglu and Vincent (2013)	74	152	66.6					240	3800	0.117	71.5		70.1	0.57	0.36		0.230^
Ozbakkaloglu and Vincent (2013)	74	152	62.0					240	3800	0.117			69.9	0.63	0.50		0.321^
Ozbakkaloglu and Vincent (2013)	74	152	66.6					240	3800	0.117	71.5		70.1	0.57	0.36		0.232^
Ozbakkaloglu and Vincent (2013)	74	152	75.0					240	3800	0.117			86.2	0.66	0.62		0.401
Ozbakkaloglu and Vincent (2013)	74	152	77.0					240	3800	0.117			83.4	0.78	0.83		0.535
Ozbakkaloglu and Vincent (2013)	74	152	83.1					240	3800	0.117	84.5		78.4[d]	0.70	0.62		0.397

Paper	D (mm)	H (mm)	f'_{co} (MPa)	ε_{co} (%)	E_{frp} (GPa)	f_{frp} (MPa)	t_{frp} (mm)	E_f (GPa)	f_f (MPa)	t_f (mm)	f'_{c1} (MPa)	ε_{c1} (%)	f'_{cu} (MPa)	ε_{cu} (%)	$\varepsilon_{h,rup}$ (%)	$k_{\varepsilon,frp}$	$k_{\varepsilon,f}$
Ozbakkaloglu and Vincent (2013)	74	152	83.1					240	3800	0.234	104.4		96.9	1.31	0.95		0.613
Ozbakkaloglu and Vincent (2013)	74	152	83.1					240	3800	0.234			111.2	1.16	0.95		0.613
Ozbakkaloglu and Vincent (2013)	74	152	93.8					240	3800	0.351			141.4	1.29	0.85		0.547
Ozbakkaloglu and Vincent (2013)	74	152	99.9					240	3800	0.351	121.2		119.8	1.26	0.93		0.599
Ozbakkaloglu and Vincent (2013)	74	152	77.0					240	3800	0.351			131.8	1.14	0.73		0.468
Ozbakkaloglu and Vincent (2013)	74	152	82.5					240	3800	0.351			122.6	0.97	0.57		0.370
Ozbakkaloglu and Vincent (2013)	152	305	59.0					240	3800	0.468			78.4	1.14	0.92		0.592
Ozbakkaloglu and Vincent (2013)	152	305	59.0					240	3800	0.468			88.0	1.36	0.98		0.632
Ozbakkaloglu and Vincent (2013)	152	305	59.0					240	3800	0.468			81.3	1.23	0.62		0.402
Ozbakkaloglu and Vincent (2013)	152	305	92.7					240	3800	0.351	101.5	0.36	84.8[d]	0.81	0.75		0.481
Ozbakkaloglu and Vincent (2013)	152	305	94.7					240	3800	0.351	103.7	0.34	99.2	0.89	0.86		0.555
Ozbakkaloglu and Vincent (2013)	152	305	90.1					240	3800	0.351	96.0	0.34	86.7[d]	0.82	0.84		0.543
Ozbakkaloglu and Vincent (2013)	152	305	93.0					240	3800	0.468	97.9	0.51	95.8	0.92	0.71		0.458
Ozbakkaloglu and Vincent (2013)	152	305	100.0					240	3800	0.468	107.9	0.34	98.9[d]	0.96	0.88		0.570
Ozbakkaloglu and Vincent (2013)	152	305	97.5					240	3800	0.468			107.2	1.01	0.97		0.626
Ozbakkaloglu and Vincent (2013)	152	305	102.5					240	3800	0.702			131.1	1.27	0.89		0.574
Ozbakkaloglu and Vincent (2013)	152	305	96.0					240	3800	0.702			124.2	1.16	0.78		0.501
Ozbakkaloglu and Vincent (2013)	152	305	93.0					240	3800	0.702			112.1	1.09	0.66		0.426
Vincent and Ozbakkaloglu (2013a)	152	305	59.0					240	3800	0.117	58.8		45.2[d]	0.72	0.89		0.574
Vincent and Ozbakkaloglu (2013a)	152	305	59.0					240	3800	0.117	60.1		39.0[d]	0.56	1.08		0.697
Vincent and Ozbakkaloglu (2013a)	152	305	59.0					240	3800	0.117	57.3		43.3[d]	0.61	1.03		0.665
Vincent and Ozbakkaloglu (2013a)	152	305	59.0					240	3800	0.234			68.4	0.95	1.14		0.735
Vincent and Ozbakkaloglu (2013a)	152	305	59.0					240	3800	0.234			65.4	1.05	1.19		0.768
Vincent and Ozbakkaloglu (2013a)	152	305	62.0					240	3800	0.234			66.8	0.84	1.03		0.665
Vincent and Ozbakkaloglu (2013a)	152	305	59.0					240	3800	0.351			79.2	1.24	1.07		0.692
Vincent and Ozbakkaloglu (2013a)	152	305	65.0					240	3800	0.351			78.0	1.30	0.77		0.498
Vincent and Ozbakkaloglu (2013a)	152	305	59.0					240	3800	0.351			81.6	1.54	0.92		0.595
Vincent and Ozbakkaloglu (2013a)	152	305	92.0					240	3800	0.117	96.7	0.33	67.6[d]	0.60	0.78		0.503
Vincent and Ozbakkaloglu (2013a)	152	305	85.6					240	3800	0.117	91.0	0.32	81.3[d]	0.45	0.68		0.439
Vincent and Ozbakkaloglu (2013a)	152	305	92.0					240	3800	0.117	97.6	0.33	97.6[d]				
Vincent and Ozbakkaloglu (2013a)	152	305	93.1					240	3800	0.234	97.9	0.33	68.1[d]	0.75	0.92		0.592
Vincent and Ozbakkaloglu (2013a)	152	305	83.1					240	3800	0.234	95.6	0.44	67.1[d]	0.79	0.92		0.595
Vincent and Ozbakkaloglu (2013a)	152	305	80.4					240	3800	0.234			89.7	0.46	0.50		0.323^
Vincent and Ozbakkaloglu (2013a)	152	305	87.0					240	3800	0.585	110.8	0.43	107.8	0.83	0.69		0.445
Vincent and Ozbakkaloglu (2013a)	152	305	102.5					240	3800	0.585			119.2	1.06	0.87		0.561
Vincent and Ozbakkaloglu (2013a)	152	305	102.5					240	3800	0.585			112.8	1.01	0.74		0.475

p *denotes fiber tensile strength and elastic modulus are given in N/mm-ply*
t *denotes FRP properties calculated based on total nominal ply thickness of fiber sheet*
s *denotes inconsistent ultimate axial stress when compared with overall trend in database*
a *denotes inconsistent ultimate axial strain when compared with overall trend in database*
d *denotes ultimate axial stress values that are lower than the unconfined concrete strength*
^ *denotes inconsistent k_ε values when compared with overall trend of the database*

Table 3. Test database of GFRP-confined HSC specimens

Paper	Specimen Dimensions		Concrete Properties		FRP Properties			Fiber Properties			Measured Initial Peak Conditions		Measured Ultimate Conditions			Hoop Strain Reduction Factors	
	D (mm)	H (mm)	f'_{co} (MPa)	ε_{co} (%)	E_{frp} (GPa)	f_{frp} (MPa)	t_{frp} (mm)	E_f (GPa)	f_f (MPa)	t_f (mm)	f'_{c1} (MPa)	ε_{c1} (%)	f'_{cu} (MPa)	ε_{cu} (%)	$\varepsilon_{h,rup}$ (%)	$k_{\varepsilon,frp}$	$k_{\varepsilon,f}$
GFRP-wrapped specimens																	
Ahmad et al. (1991)	102	203	64.2	0.27				48.3	2070	0.88	145.6	1.23					
Aire et al. (2001)	150	300	69	0.24				65	3000	0.149	79	0.24		0.47[a]	0.62		0.134^
Aire et al. (2001)	150	300	69	0.24				65	3000	0.447	81	0.26		0.78[a]	0.74		0.160^
Aire et al. (2001)	150	300	69	0.24				65	3000	0.894			107	1.24[a]	1.1		0.238^
Aire et al. (2001)	150	300	69	0.24				65	3000	1.341			137	1.42[a]	1.05		0.228^
Aire et al. (2001)	150	300	69	0.24				65	3000	1.788			170	1.42[a]	1.11		0.241^
Almusallam (2007)	150	300	60.0	0.298				27	540	1.3			62.4	0.522	0.491		0.246^
Almusallam (2007)	150	300	60.0	0.298				27	540	3.9			99.6	1.597	0.698		0.349^
Almusallam (2007)	150	300	80.8	0.265				27	540	1.3			88.9	0.369[a]	0.239		0.120^
Almusallam (2007)	150	300	80.8	0.265				27	540	3.9			100.9	0.694	0.869		0.435
Almusallam (2007)	150	300	90.3	0.320				27	540	1.3			97.0	0.324[a]	0.253		0.127^
Almusallam (2007)	150	300	90.3	0.320				27	540	3.9			110.0	0.900	0.825		0.413
Almusallam (2007)	150	300	107.8	0.261				27	540	1.3			116.0	0.276[a]	0.31		0.155^
Almusallam (2007)	150	300	107.8	0.261				27	540	3.9			125.2	0.324[a]	0.307		0.154^
Benzaid et al. (2009)	160	320	56.7	0.24				23.8	383	0.44			74	1.12[a]	1.14		0.708
Benzaid et al. (2009)	160	320	56.7	0.24				23.8	383	0.88			84	1.28[a]	1.15		0.715
Benzaid et al. (2009)	160	320	56.7	0.24				23.8	383	1.76			95.5[s]	1.88[a]	1.26		0.783
Cui and Sheikh (2010b)	152	305	79.9	0.241	22	508.2	1.25				85.4	0.255	66.7[d]	0.758	2.018	0.874	
Cui and Sheikh (2010b)	152	305	79.9	0.241	22	508.2	1.25				89	0.249	74.7[d]	0.878	2.418	1.047^	
Cui and Sheikh (2010b)	152	305	79.9	0.241	22	508.2	2.5				91.5	0.262	92.5	0.863	1.389	0.601	
Cui and Sheikh (2010b)	152	305	79.9	0.241	22	508.2	2.50				92.3	0.269	94.1	0.775	1.694	0.733	
Cui and Sheikh (2010b)	152	305	79.9	0.241	22	508.2	3.75						120.8	1.255	2.008	0.869	
Cui and Sheikh (2010b)	152	305	79.9	0.241	22	508.2	3.75						126.1	1.182	1.916	0.829	
Cui and Sheikh (2010b)	152	305	110.6	0.262	22	508.2	2.50				144.3	0.322	106.3[d]	0.665	1.192	0.516	
Cui and Sheikh (2010b)	152	305	110.6	0.262	22	508.2	2.50				143.5	0.321	100.3[d]	0.459	1.080	0.468	
Cui and Sheikh (2010b)	152	305	110.6	0.262	22	508.2	5.00				157.7	0.351	174.6	0.949	1.398	0.605	
Cui and Sheikh (2010b)	152	305	110.6	0.262	22	508.2	5.00				158.5	0.382	172.9	1.282	1.538	0.666	
Green et al. (2007)	152	305	59		33.8	748	2[p]						73				
Mandal and Fam (2004)	100	200	80.6	0.223				26.1	575	1.3	100.4	0.44					
Mandal and Fam (2004)	100	200	80.6	0.223				26.1	575	1.3	96.3	0.30					
Mandal and Fam (2004)	100	200	80.6	0.223				26.1	575	1.3	111.5	0.37					
Mandal and Fam (2004)	100	200	67.03	0.217				26.1	575	1.3	86.7	0.31					
Mandal and Fam (2004)	100	200	67.03	0.217				26.1	575	1.3	81.3	0.29					
Mandal and Fam (2004)	100	200	67.03	0.217				26.1	575	1.3	92.4	0.34					
Mandal and Fam (2004)	100	200	80.6	0.223				26.1	575	2.6	98.3	0.36					
Mandal and Fam (2004)	100	200	80.6	0.223				26.1	575	2.6	95.8	0.37					
Mandal and Fam (2004)	100	200	80.6	0.223				26.1	575	2.6	101	0.32					
Mandal and Fam (2004)	100	200	67.03	0.217				26.1	575	2.6	97.5	0.32					
Mandal and Fam (2004)	100	200	67.03	0.217				26.1	575	2.6	97.6	0.36					
Mandal and Fam (2004)	100	200	67.03	0.217				26.1	575	2.6	89.9	0.45					

p *denotes fiber tensile strength and elastic modulus are given in N/mm-ply*
s *denotes inconsistent ultimate axial stress when compared with overall trend in database*
a *denotes inconsistent ultimate axial strain when compared with overall trend in database*
d *denotes ultimate axial stress values that are lower than the unconfined concrete strength*
^ *denotes inconsistent k_ε values when compared with overall trend of the database*

Table 4. Test database of AFRP-confined HSC specimens

Paper	Specimen Dimensions		Concrete Properties		FRP Properties			Fiber Properties			Measured Initial Peak Conditions		Measured Ultimate Conditions			Hoop Strain Reduction Factors	
	D (mm)	H (mm)	f'_{co} (MPa)	ε_{co} (%)	E_{frp} (GPa)	f_{frp} (MPa)	t_{frp} (mm)	E_f (GPa)	f_f (MPa)	t_f (mm)	f'_{c1} (MPa)	ε_{c1} (%)	f'_{cu} (MPa)	ε_{cu} (%)	$\varepsilon_{h,rup}$ (%)	$k_{\varepsilon,frp}$	$k_{\varepsilon,f}$
AFRP-wrapped specimens																	
Ozbakkaloglu and Akin (2012)	152	305	102.0					120	2900	0.8	112.9	0.36	118.7	1.29	1.29		0.516
Ozbakkaloglu and Akin (2012)	152	305	100.0					120	2900	0.8	110.6	0.36	122.3	1.45	1.18		0.472
Ozbakkaloglu and Akin (2012)	152	305	106.0					120	2900	1.2	121.2	0.43	153.2	1.70	1.07		0.428
Ozbakkaloglu and Akin (2012)	152	305	106.0					120	2900	1.2	120.0	0.45	154.7	1.70	1.10		0.440
Wu et al. (2009)	100	300	78.5	0.451				118	2060	0.286			118.3	1.082			
Wu et al. (2009)	100	300	78.5	0.451				118	2060	0.572			167.1	1.424			
Wu et al. (2009)	100	300	78.5	0.451				118	2060	0.858			185.8	1.611			
Wu et al. (2009)	100	300	101.2	0.456				118	2060	0.286			123.3	0.627			
Wu et al. (2009)	100	300	101.2	0.456				118	2060	0.572			154.0	1.016			
Wu et al. (2009)	100	300	101.2	0.456				118	2060	0.858			204.5	1.437			
AFRP tube-encased specimens																	
Cheek et al. (2011)	153	305	109.8					120	2900	1.2	121.4	0.48	175.9	2.31	1.70		0.682
Cheek et al. (2011)	153	305	109.8					120	2900	1.2	120.6	0.48	151.6	1.88	1.43		0.571
Cheek et al. (2011)	153	305	109.8					120	2900	1.2	121.8	0.53	172.2	2.12	1.67		0.667
Ozbakkaloglu and Vincent (2013)	100	200	85.9					120	2900	0.4			121.3	1.65	1.76		0.702
Ozbakkaloglu and Vincent (2013)	100	200	82.4					120	2900	0.4			107.3	1.58	1.84		0.736
Ozbakkaloglu and Vincent (2013)	100	200	82.4					120	2900	0.4			112.3	1.65	1.92		0.770
Ozbakkaloglu and Vincent (2013)	100	200	85.9					120	2900	0.6			148.2	1.92	1.62		0.648
Ozbakkaloglu and Vincent (2013)	100	200	85.9					120	2900	0.6			154.3	2.23	1.76		0.703
Ozbakkaloglu and Vincent (2013)	100	200	85.9					120	2900	0.6			159.7	2.38	2.17		0.870^
Ozbakkaloglu and Vincent (2013)	100	200	110.1					120	2900	0.6	122.2	0.5	154.8	2.11	1.35		0.538
Ozbakkaloglu and Vincent (2013)	100	200	110.1					120	2900	0.6			150.9	1.71	1.54		0.616
Ozbakkaloglu and Vincent (2013)	100	200	110.1					120	2900	0.6			156.6	1.87	1.78		0.712
Ozbakkaloglu and Vincent (2013)	100	200	110.1					120	2900	0.8			183.8	2.21	1.47		0.586
Ozbakkaloglu and Vincent (2013)	100	200	110.1					120	2900	0.8			190.9	2.47	1.57		0.629
Ozbakkaloglu and Vincent (2013)	100	200	110.1					120	2900	0.8			198.8[s]				
Ozbakkaloglu and Vincent (2013)	152	305	79.6					120	2900	0.6			105.0	1.67	2.12		0.848
Ozbakkaloglu and Vincent (2013)	152	305	77.2					120	2900	0.6	85.5	0.47	102.0	1.64	1.59		0.637
Ozbakkaloglu and Vincent (2013)	152	305	77.0					120	2900	0.6			118.0	2.23	1.79		0.716
Ozbakkaloglu and Vincent (2013)	152	305	104.5					120	2900	1.2			164.3	1.98	1.19		0.472
Ozbakkaloglu and Vincent (2013)	152	305	104.5					120	2900	1.2			168.7	2.18	1.53		0.613
Ozbakkaloglu and Vincent (2013)	152	305	104.5					120	2900	1.2			178.9	2.05	1.63		0.653
Ozbakkaloglu and Vincent (2013)	100	200	85.9					99[fm]	2930[fm]	0.4			176.2[s]	2.89	2.36		0.797
Ozbakkaloglu and Vincent (2013)	100	200	83.0					99[fm]	2930[fm]	0.4			154.9[s]	2.53	1.74		0.589
Ozbakkaloglu and Vincent (2013)	100	200	85.9					99[fm]	2930[fm]	0.4			176.6[s]	2.89	2.42		0.818
Ozbakkaloglu and Vincent (2013)	100	200	110.1					99[fm]	2930[fm]	0.6			232.4[s]	3.22	2.01		0.679
Ozbakkaloglu and Vincent (2013)	100	200	110.1					99[fm]	2930[fm]	0.6			224.1[s]	2.81	2.11		0.713
Ozbakkaloglu and Vincent (2013)	100	200	110.1					99[fm]	2930[fm]	0.6			244.6[s]	3.48	2.26		0.764

s *denotes inconsistent ultimate axial stress when compared with overall trend in database*
a *denotes inconsistent ultimate axial strain when compared with overall trend in database*
^ *denotes inconsistent k_ε values when compared with overall trend of the database*
fm *denotes tubes fabricated using automated manufacturing method*

Table 5. Test database of HM and UHM CFRP-confined HSC specimens

Paper	Specimen Dimensions		Concrete Properties		FRP Properties			Fiber Properties			Measured Initial Peak Conditions		Measured Ultimate Conditions			Hoop Strain Reduction Factors	
	D (mm)	H (mm)	f'_{co} (MPa)	ε_{co} (%)	E_{frp} (GPa)	f_{frp} (MPa)	t_{frp} (mm)	E_f (GPa)	f_f (MPa)	t_f (mm)	f'_{c1} (MPa)	ε_{c1} (%)	f'_{cu} (MPa)	ε_{cu} (%)	$\varepsilon_{h,rup}$ (%)	$k_{\varepsilon,frp}$	$k_{\varepsilon,f}$
HM CFRP-wrapped specimens																	
Cui and Sheikh (2010b)	152	305	85.6	0.258				436	3314	0.16	97.1	0.335	91.5	0.421[a]	0.303		0.399
Cui and Sheikh (2010b)	152	305	85.6	0.258				436	3314	0.16	99.7	0.360	94.5	0.543	0.417		0.549
Cui and Sheikh (2010b)	152	305	85.6	0.258				436	3314	0.33			117.7	0.706	0.436		0.574
Cui and Sheikh (2010b)	152	305	85.6	0.258				436	3314	0.33			117.5	0.553	0.411		0.541
Cui and Sheikh (2010b)	152	305	85.6	0.258				436	3314	0.65			161.6	1.017	0.383		0.504
Cui and Sheikh (2010b)	152	305	85.6	0.258				436	3314	0.65			162.6	0.953	0.377		0.496
Cui and Sheikh (2010b)	152	305	111.8	0.261				436	3314	0.33	151.7	0.364	139.1	0.323	0.222		0.292
Cui and Sheikh (2010b)	152	305	111.8	0.261				436	3314	0.33	148.9	0.326	123.3	0.314	0.167		0.220
Cui and Sheikh (2010b)	152	305	111.8	0.261				436	3314	0.82	183.2	0.470	176.4	0.488	0.242		0.318
Cui and Sheikh (2010b)	152	305	111.8	0.261				436	3314	0.82	178.3	0.461	172.5	0.499	0.208		0.274
Rousakis (2001)	150	300	56.9	0.298				377	4410	0.17			79.3				
Rousakis (2001)	150	300	56.9	0.298				377	4410	0.17			78.7				
Rousakis (2001)	150	300	70.6	0.35				377	4410	0.17			72.4	0.705	0.556		0.475
Rousakis (2001)	150	300	70.6	0.35				377	4410	0.17			70.1[d]	0.651	0.529		0.452
Rousakis (2001)	150	300	70.6	0.35				377	4410	0.34			70.6[d]	0.804	0.388		0.332
Rousakis (2001)	150	300	70.6	0.35				377	4410	0.34			87.3	0.917	0.568		0.486
Rousakis (2001)	150	300	70.6	0.35				377	4410	0.51			83.2	1.285	0.444		0.380
Rousakis (2001)	150	300	70.6	0.35				377	4410	0.51			94.1	1.218	0.421		0.360
Rousakis (2001)	150	300	82.1	0.315				377	4410	0.17			94.1	0.462	0.278		0.238
Rousakis (2001)	150	300	82.1	0.315				377	4410	0.17			96.0	0.558	0.455		0.389
Rousakis (2001)	150	300	82.1	0.315				377	4410	0.34			97.4	0.517[a]	0.156		0.133^
Rousakis (2001)	150	300	82.1	0.315				377	4410	0.34			98.9	0.441[a]	0.14		0.120
Rousakis (2001)	150	300	82.1	0.315				377	4410	0.51			124.2	1.042	0.549		0.469
Rousakis (2001)	150	300	82.1	0.315				377	4410	0.51			120.4	0.873	0.404		0.345
UHM CFRP tube-encased specimens																	
Ozbakkaloglu and Vincent (2013)	152	305	59.0					640	2650	0.19			70.0	0.50	0.26		0.638^
Ozbakkaloglu and Vincent (2013)	152	305	55.6					640	2650	0.19			66.6	0.50	0.22		0.553
Ozbakkaloglu and Vincent (2013)	152	305	59.0					640	2650	0.19			69.9	0.47	0.26		0.638^
Ozbakkaloglu and Vincent (2013)	152	305	59.0					640	2650	0.38			70.8	0.47	0.11		0.283
Ozbakkaloglu and Vincent (2013)	152	305	59.0					640	2650	0.38			77.3	0.45	0.14		0.350
Ozbakkaloglu and Vincent (2013)	152	305	59.0					640	2650	0.38			73.5	0.40	0.10		0.250

s *denotes inconsistent ultimate axial stress when compared with overall trend in database*
a *denotes inconsistent ultimate axial strain when compared with overall trend in database*
^ *denotes inconsistent k_ε values when compared with overall trend of the database*

Statement of Authorship

Title of Paper	Influence of Silica Fume on Stress-Strain Behavior of FRP-Confined HSC
Publication Status	(•) Published ( ) Accepted for Publication ( ) Submitted for Publication ( ) Publication Style
Publication Details	Magazine of Concrete Research, Volume 63, Pages 11-24, Year 2014

Author Contributions

By signing the Statement of Authorship, each author certifies that their stated contribution to the publication is accurate and that permission is granted for the publication to be included in the candidate's thesis.

Name of Principal Author (Candidate)	Mr. Jian Chin Lim		
Contribution to the Paper	Preparation of experiment, analysis of test results, and preparation of manuscript		
Signature		Date	23/02/2015

Name of Co-Author	Dr. Togay Ozbakkaloglu		
Contribution to the Paper	Research supervision and review of manuscript		
Signature		Date	23/02/2015

THIS PAGE HAS BEEN LEFT INTENTIONALLY BLANK

INFLUENCE OF SILICA FUME ON STRESS-STRAIN BEHAVIOR OF FRP-CONFINED HSC

Jian C. Lim, and Togay Ozbakkaloglu

ABSTRACT

Confinement of high-strength concrete (HSC) columns with fiber reinforced polymer (FRP) composites has been receiving increasing research attention due to the advantageous engineering properties offered by the composite system. The use of silica fume as a concrete additive is a widely accepted practice in producing HSC. However, the influence of the presence and amount of silica fume on the efficiency of FRP confinement is not clearly understood. This paper presents the results of an experimental study on the influence of silica fume on the compressive behavior of FRP-confined HSC. 30 FRP-confined and 30 unconfined concrete cylinders containing different amounts of silica fume were tested under axial compression in two phases. In the first phase of the study, specimens with a constant water-cementitious binder ratio were tested. The results of this phase indicate that for a given water-cementitious binder ratio, the compressive strength of unconfined concrete increases with an increase in the amount of silica fume. It is found that this increase in strength leads to an increased concrete brittleness, which adversely affects the effectiveness of FRP confinement. In the second phase, water-cementitious binder ratios of the specimens were adjusted to attain a constant unconfined concrete strength for specimens containing different amounts of silica fume. The results of these tests indicate that for a given unconfined concrete strength, strength enhancement ratios of FRP-confined HSC specimens are not influenced by the silica fume content of the concrete mix. On the other hand, it is found that the silica fume content influences the axial strain enhancement ratios of these specimens. In addition, the transition zones of the stress-strain curves of FRP-confined HSC are observed to be sensitive to the amount of silica fume used in the mix.

KEYWORDS: High-strength concrete (HSC); Fiber reinforced polymer (FRP); Confinement; Compression; Silica fume; Stress-strain relations.

1. INTRODUCTION

The popularity of higher strength concretes in the construction industry has been on a steady incline during the last two decades due to the superior performance and economy offered by high-strength concrete (HSC) over normal-strength concrete (NSC) in a large number of structural engineering applications. The use of FRP for confinement of HSC leads to high-performance columns that exhibit very ductile behavior as was demonstrated in Ozbakkaloglu and Saatcioglu [1, 2] and Idris and Ozbakkaloglu [3]. It has been reported in a number of studies that the efficiency of FRP confinement reduces with an increase in concrete strength [4, 5]. However, the main contributors to this adverse effect of higher concrete strength have not been fully identified. Silica fume is one of the most popular pozzolans used to increase concrete strength [6-9], and it is known to have a significant effect on the compressive behavior of confined concrete [10-12]. Although several studies have reported that silica fume alters the brittleness of confined concrete [10, 12, 13], its influence on the behavior of confined concrete has been difficult to quantify due to the limited results and controversial experimental observations found from existing triaxial compression tests of HSC [10, 12, 14-18].

In FRP-confined HSC, the influence of silica fume is even less understood. Silica fume has been used in the existing experimental studies [4, 5, 19-27] to produce desirable concrete strengths. However, none of these studies attempted to establish the influence of silica fume on the behavior of confined concrete. This paper presents the results of the first-ever experimental study undertaken to address this gap, where the changes in the axial stress-strain behavior and ultimate conditions of FRP-confined HSC with silica fume were investigated.

2. EXPERIMENTAL PROGRAM

2.1 Test Specimens and Materials

30 FRP-confined and 30 unconfined control concrete cylinders were manufactured and tested under monotonic axial compression. All of the specimens were 152.5 mm in diameter and 305 mm in height. The influence of silica fume on the mechanical properties of the confined and unconfined specimens was investigated using 10 separate batches of concrete mixes containing different percentage replacements of cement with silica fume and water-cementitious binder (*w/c*) ratios. The cementitious binder materials used were ordinary Portland cement and silica fume. Their chemical compositions and physical properties are given in Table 1. Detail of the mix proportions of each batch of concrete is given in Table 2. Crushed bluestone gravel of 7 mm maximum size and graded sand were used as the aggregates. Carboxylic ether polymer based superplasticiser was used in all batches. The superplasticiser contained 80% water by weight. The test results of the unconfined specimens are given in Table 3.

Table 1. Chemical composition and physical properties of cementitious materials

Item	Cementitious materials (%)	
	Ordinary Portland cement	Silica fume
SiO_2	21.46	92.5
$ZrO_2 + HfO_2$	-	5.5
Al_2O_3	5.55	0.35
Fe_2O_3	3.46	0.4
P_2O_5	-	0.3
CaO	63.95	0.02
MgO	1.86	-
SO_3	1.42	0.9
K_2O	0.54	0.02
Na_20	0.26	0.02
	Compounds	
C_3S	50.96	-
C_2S	23.10	-
C_3A	8.85	-
C_4AF	10.53	-
	Fineness	
Surface area (m^2/kg)	330	18,000

The experimental program consisted of two phases. The first phase consisted of specimens fabricated from four different concrete batches containing different amounts of silica fume at designated *w/c* ratios. In Batches 1, 2A, and 3 that contain a fixed *w/c* ratio of 0.27, the percentages of silica fume that replaced cement were 0%, 8%, and 16% by weight. The *w/c* ratio was reduced to 0.24 in Batch 2B that contain 8% silica fume. As shown from Table 3, the unconfined concrete strengths (f'_{co}) of specimens in this phase varied with the silica fume content and *w/c* ratios.

The aim of Phase II of the experimental program was to attain a same unconfined strength among each specimen group having 0%, 8%, and 16% silica fume. The specimen groups in this phase were manufactured using two different concrete grades (i.e. a higher grade HSC with an average strength of 84.7 MPa in Batches 4 to 6 and a lower grade HSC with an average strength of 54.6 MPa in Batches 7 to 9). To establish the final *w/c* ratios used in Batches 4 to 9, a large number of trial batches were manufactured and tested.

Table 2. Mix proportions of concrete containing different levels of silica fume

Experimental Program	Phase I				Phase II					
	AFRP-wrapped HSC				GFRP tube-encased higher grade HSC			GFRP tube-encased lower grade HSC		
Batch	1	2A	2B	3	4	5	6	7	8	9
Cement (kg/m^3)	550	506	506	462	550	506	462	450	414	378
Silica fume (kg/m^3)	0.0	44	44	88	0	44	88	0	36	72
Sand (kg/m^3)	700	700	700	700	710	710	710	710	710	710
Gravel (kg/m^3)	1050	1050	1050	1050	1065	1065	1065	1065	1065	1065
Water (kg/m^3)	124	124	108	124	130	155	170	205	223	235
Superplasticiser (kg/m^3)	30	30	30	30	20	20	14	2	3	1.5
Water-cementitious binder ratio	0.270	0.270	0.240	0.270	0.265	0.310	0.330	0.460	0.500	0.525
Superplasticiser-binder ratio	0.055	0.055	0.055	0.055	0.036	0.036	0.025	0.004	0.007	0.003
Silica fume-binder ratio	0.000	0.080	0.080	0.160	0.000	0.080	0.160	0.000	0.080	0.160
Slump height (m)	0.240	0.215	0.130	0.220	>0.250	>0.250	>0.250	0.230	0.250	0.095

Table 3. Compression test results of unconfined specimens

Phase	Specimen	Concrete batch	Silica fume percentage (%)	*w/c* ratio (%)	Average f'_{co} (MPa)	Average ε_{co} (%)
I	B1-SF0-WC27-A0	1	0	0.27	85.7	0.24
	B2A-SF8-WC27-A0	2A	8	0.27	112.4	0.27
	B2B-SF8-WC24-A0	2B	8	0.24	120.9	0.26
	B3-SF16-WC27-A0	3	16	0.27	113.5	0.26
II	B4-SF0-WC27-G0	4	0	0.27	84.7	0.28[P]
	B5-SF8-WC31-G0	5	8	0.31	84.8	0.28[P]
	B6-SF16-WC33-G0	6	16	0.33	84.5	0.28[P]
	B7-SF0-WC46-G0	7	0	0.46	57.3	0.26[P]
	B8-SF8-WC50-G0	8	8	0.50	52.1	0.25[P]
	B9-SF16-WC53-G0	9	16	0.53	54.4	0.25[P]

P: Axial strains were not recorded experimentally. Theoretical values determined using expression given by Popovics [29].

A total of 30 confined specimens was fabricated and tested in the two-phase experimental program. In Phase I, 12 specimens wrapped with Aramid FRP (AFRP) were prepared using a manual wet lay-up process by wrapping epoxy resin impregnated unidirectional fiber sheets around precast concrete cylinders in the hoop direction. The 18 specimens in Phase II were manufactured as tube-encased specimens using S-glass FRP (GFRP) tubes. The GFRP tubes were also prepared using the manual wet lay-up process, with the resin impregnated fiber sheets wrapped around precision-cut high-density Styrafoam templates, which were removed prior to concrete casting. The specimens tested in Phase I and the higher grade HSC specimens in Phase II had six layers of FRP, whereas the lower grade HSC specimens in Phase II had four layers of FRP. The specimens with four layers of FRP were wrapped with one continuous sheet with a single 150-mm long overlap zone, whereas the specimens with six layers were wrapped with two sheets creating two overlap zones of 150 mm terminating at the same location.

Table 4. Material properties of fibers and FRP composites

Type	Nominal thickness t_f (mm/ply)	Provided by manufacturers			Obtained from flat FRP coupon tests		
		Tensile strength f_f (MPa)	Ultimate tensile strain ε_f (%)	Elastic modulus E_f GPa)	Tensile strength f_{frp} (MPa)	Ultimate tensile strain ε_{frp} (%)	Elastic modulus E_{frp} (GPa)
Aramid	0.200	2600	2.20	118.2	2390	1.86	128.5
S-Glass	0.200	3040	3.50	86.9	3055	3.21	95.3

The FRP epoxy adhesive used consisted of two parts: epoxy resin binder (MBrace Saturant) and thixotropic epoxy adhesive (MBrace Laminate Adhesive), which were mixed in the ratio of 3:1. The material properties of the unidirectional fiber sheets used to manufacture the FRP tubes and jackets are provided in Table 4. The table reports both the manufacturer-supplied fiber properties and the tensile tested FRP composite properties. The tensile properties of the

FRP made from these fiber sheets and epoxy resin were determined from flat coupon tests undertaken in accordance with ASTM D3039 [28].

Three flat coupon specimens were made using the wet layout technique in a high-precision mould with 1 mm thickness and 25 mm width for each type of fiber. The coupons had a 138 mm clear span with each end bonded with two 0.5 mm by 85 mm aluminum tabs for stress transfer during tensile tests. Each coupon was instrumented with two 20 mm strain gauges at mid-height, with one on each side, for the measurement of the longitudinal strains. The coupons were allowed to cure in the laboratory environment for at least seven days prior to testing. The tensile test specimens were tested using a screw-driven tensile test machine that had a peak capacity of 200 kN. The load was applied at a constant cross-head movement rate of 0.03 mm per second. The test results from the flat coupon specimens, calculated using nominal fiber thicknesses and actual coupon widths, are reported in Table 4. As evident from Table 4, the average rupture strains obtained from the tensile coupon tests were slightly lower than those reported by the manufacturer.

Three nominally identical specimens were tested for each unique specimen configuration. The FRP-confined specimens were tested on the same day with their companion unconfined specimens, through which the test day unconfined concrete strengths (f'_{co}) reported in Table 3 were established.

2.2 Specimen Designation

The specimens in Tables 3 and 5 were labeled as follows: letters B, SF, WC, A or G, and W or T were used to represent the test parameters, namely the concrete batch, silica fume percentage, *w/c* ratio, type of FRP (i.e. AFRP or GFRP), followed by the number of layers and the confinement technique (i.e. wrapped or tube-encased), respectively. Each letter was followed by a number that was used to represent the value of that particular parameter for a given specimen. Finally, the last number in the specimen designation (i.e., 1, 2 or 3) was used to make the distinction between three nominally identical specimens.

2.3 Instrumentation and Testing

The specimens were tested under axial compression using a 5000-kN capacity universal testing machine. During the initial elastic stage of the behavior, the loading was applied with the load control set at 5 kN per second, whereas displacement control operated at 0.004 mm per second beyond the initiation of transition region until specimen failure. Prior to testing, all specimens were ground at both ends to ensure uniform distribution of the applied pressure, and load was applied directly to the concrete core using precision-cut high-strength steel plates.

The hoop strains of the specimens were measured using a minimum of three unidirectional strain gauges placed at the mid-height around the circumference of specimens outside the overlap region. As illustrated in Figure 1, the axial strains of the confined specimens were measured using three different methods: (i) four linear variable displacement transformers (LVDTs) mounted at each corner of the steel loading platens with a gauge length of 305 mm; (ii) four LVDTs placed at the mid-height at a gauge length of 175 mm at 90° spacing along

the circumference of specimens; (iii) three axial strain gauges with a gauge length of 20 mm placed at the mid-height at 120° spacing along the circumference of specimens.

3. TEST RESULTS AND DISCUSSION

3.1 Failure mode

The typical failure modes the unconfined HSC specimens tested in Phase I are illustrated in Fig. 2. As can be seen in Fig. 2(a), the formation of microcracks and the surface spalling of concrete were observed in the unconfined specimens containing 0% silica fume at failure. On the other hand, Figs. 2(b) to 2(d) show that the unconfined specimens containing 8% and 16% silica fume failed due to concrete crushing after the formation of major macrocracks. The observed variations in the failure mode pattern suggest that the brittleness of the concrete increases with its strength in the presence of and with an increase in the amount of silica fume.

Figure 3 shows typical failure modes of the confined HSC specimens tested in Phase I. As can be seen from the figure, all of the AFRP-wrapped specimens of Phase I failed by the rupture of the FRP jackets. As evident from Figs. 3(a) to 3(c), the location of the rupture of the specimens containing 0% and 8% silica fume occurred at mid-height, with the height of the ruptures increasing with an increase in silica fume content. Full height ruptures, as illustrated in Fig. 3(d), were observed in two out of three nominally identical AFRP-wrapped specimens containing 16% silica fume. Figures 3(b) and 3(c) show specimens containing the same amount of silica fume of 8% but different *w/c* ratios of 0.27 and 0.24. Comparison of the figures shows that the specimen with the lower *w/c* ratio had a larger rupture region height.

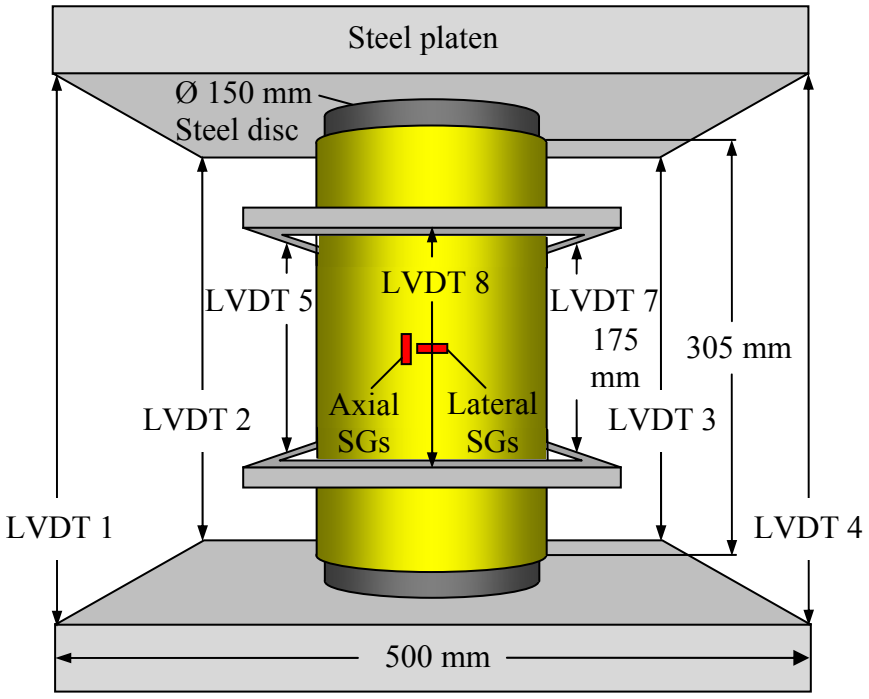

Figure 1. Test setup and instrumentation

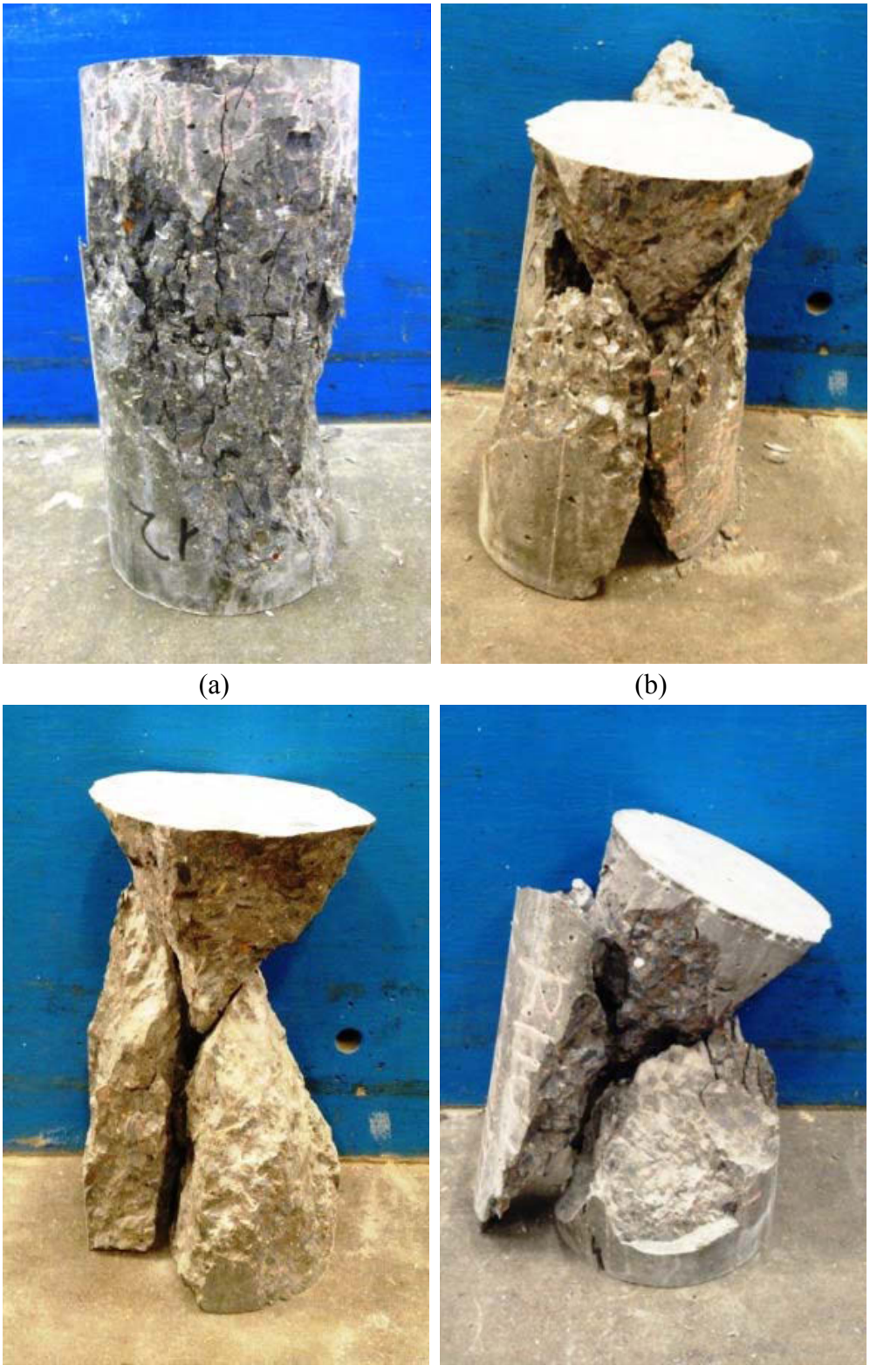

(a) (b)

(c) (d)

Figure 2. Failure modes of unconfined HSC specimens: a) 0% silica fume and 0.27 *w/c* ratio; b) 8% silica fume and 0.27 *w/c* ratio; c) 8% silica fume and 0.24 *w/c* ratio; d) 16% silica fume and 0.27 *w/c* ratio

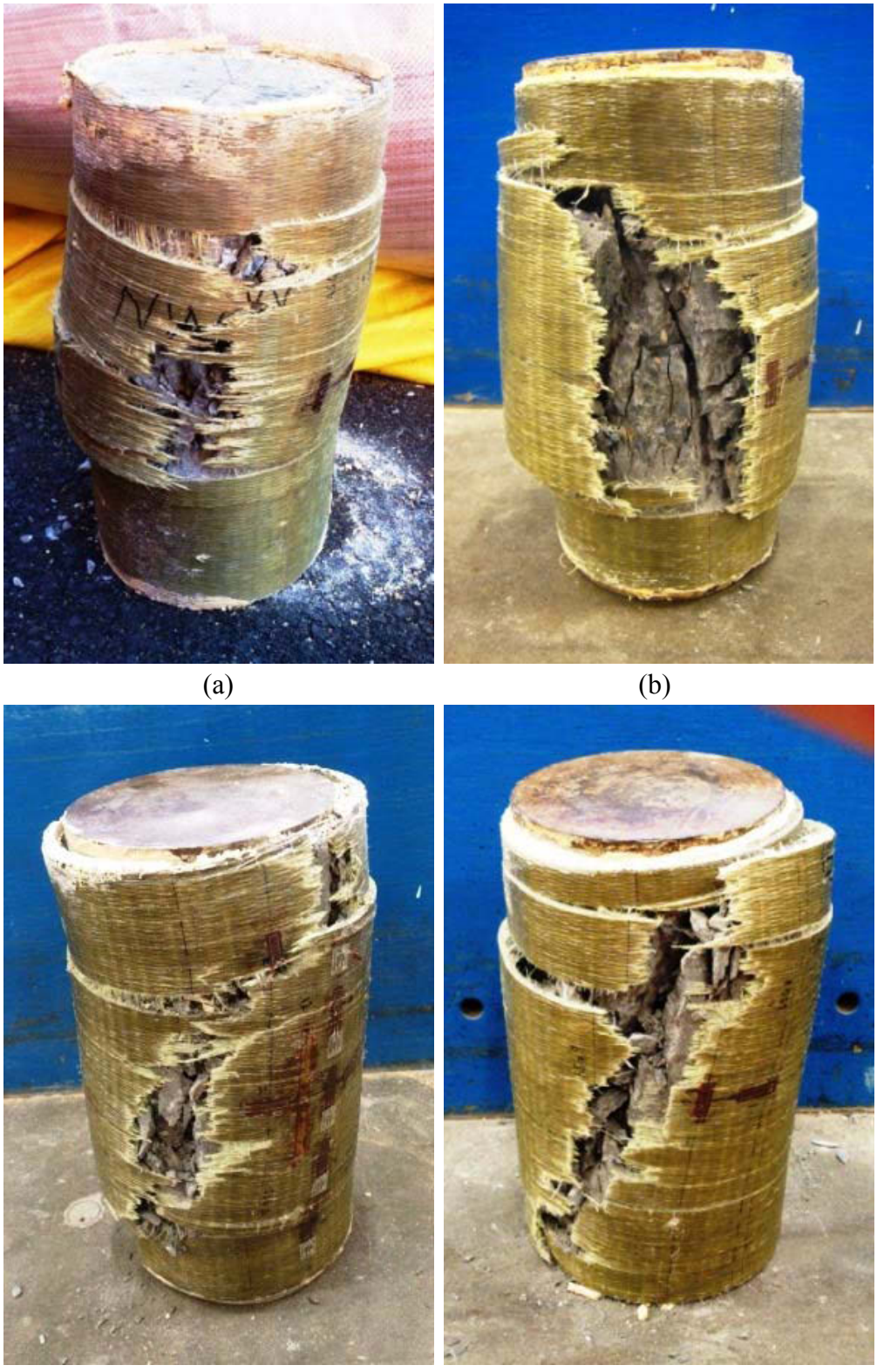

(a) (b)

(c) (d)

Figure 3. Failure modes of AFRP-wrapped HSC specimens: a) 0% silica fume and 0.27 *w/c* ratio; b) 8% silica fume and 0.27 *w/c* ratio; c) 8% silica fume and 0.24 *w/c* ratio; d) 16% silica fume and 0.27 *w/c* ratio

(a) (b)

(c)

Figure 4. Failure modes of GFRP tube-encased high-grade HSC specimens: a) 0% silica fume and 0.27 *w/c* ratio; b) 8% silica fume and 0.31 *w/c* ratio; and c) 16% silica fume and 0.33 *w/c* ratio

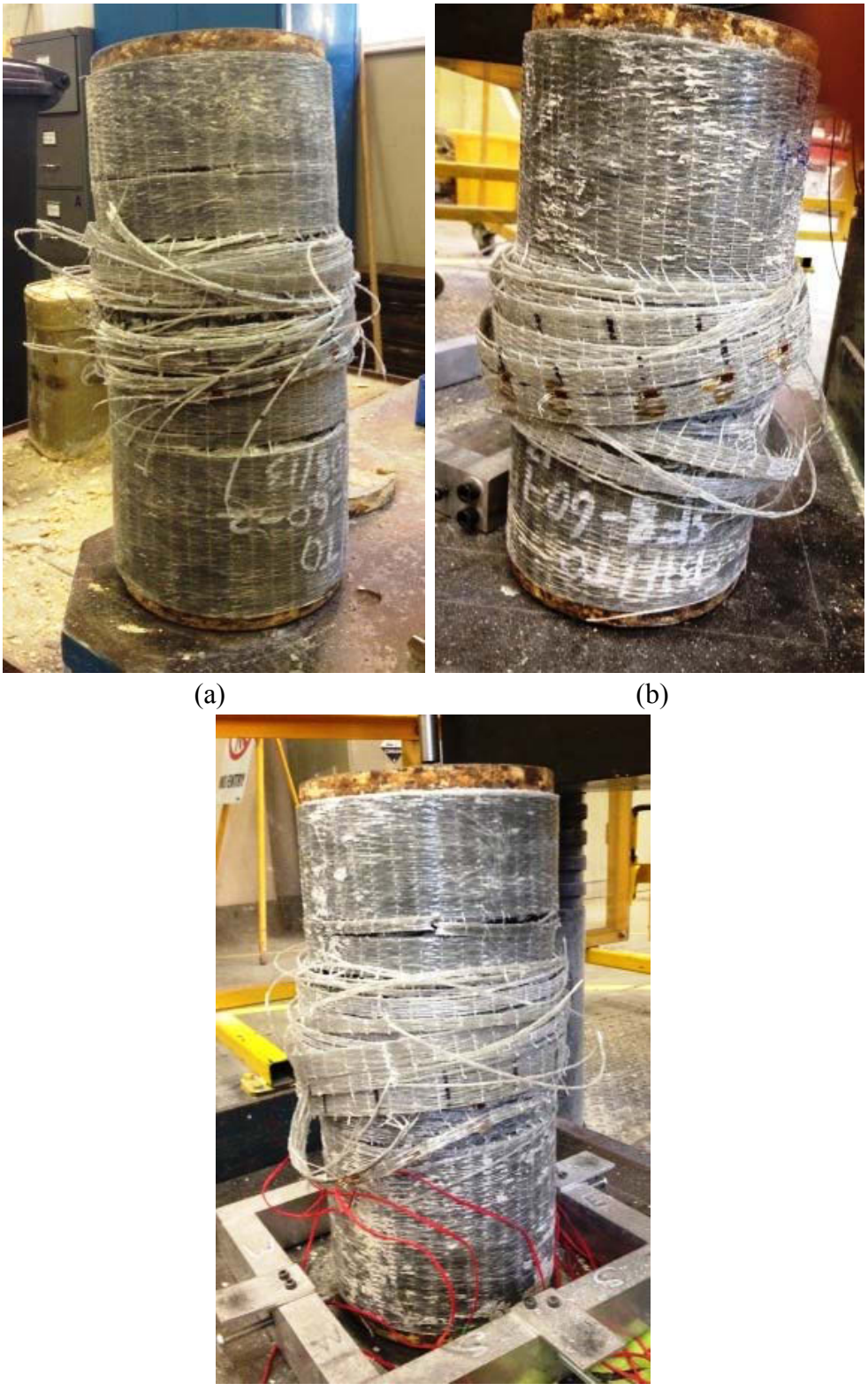

(a) (b)

(c)

Figure 5. Failure modes of GFRP tube-encased low-grade HSC specimens: a) 0% silica fume and 0.46 *w/c* ratio; b) 8% silica fume and 0.50 *w/c* ratio; and c) 16% silica fume and 0.53 *w/c* ratio

Figures 4 and 5 show the typical failures of the GFRP tube-encased specimens tested in Phase II, which were composed of two different grades of HSC. As illustrated in Figs. 4 and 5, all of these specimens failed due to the rupture of the FRP tubes. As evident from Figs. 4 and 5, the heights of the rupture regions of the specimens were not significantly affected by the change in the silica fume content. Similar failure modes observed in specimens containing varying amounts of silica fume indicates that the influence of silica fume on the failure mode of FRP-confined concrete is minor, when the unconfined concrete strength remains constant. Further discussions on the influence of silica fume on the compressive behavior of FRP-confined HSC are presented in the following sections.

3.2 Ultimate conditions

The ultimate condition of FRP-confined concrete is often characterized as the ultimate axial stress and strain of concrete recorded at the rupture of the FRP jacket. This makes the relationship between the ultimate axial stress (f'_{cu}), ultimate axial strain (ε_{cu}) and hoop rupture strain ($\varepsilon_{h,rup}$) an important one. The test results of the confined specimens are given in Table 5, which include: the silica fume percentage, compressive strength and ultimate axial strain of the specimens (f'_{cc} and ε_{cu}); hoop rupture strain ($\varepsilon_{h,rup}$); strength and strain enhancement ratios (f'_{cc}/f'_{co} and $\varepsilon_{cu}/\varepsilon_{co}$); and hoop strain reduction factor ($k_{\varepsilon,f}$). The hoop strain reduction factor ($k_{\varepsilon,f}$) of the confined specimens was calculated as the ratio of the hoop rupture strain ($\varepsilon_{h,rup}$) to ultimate tensile strain of the fiber (ε_f).

The summary of the test results of the companion unconfined specimens are shown in Table 3, which include the unconfined peak stress (f'_{co}) and the corresponding axial strain (ε_{co}). The unconfined concrete strain (ε_{co}) and ultimate axial strain of confined concrete (ε_{cu}) were averaged from the four steel platen mounted LVDTs. It should be noted that the unconfined concrete strains (ε_{co}) of specimens in Batches 4 to 9 were not recorded during the compression tests. The ε_{co} values for these specimens, reported in Table 3, were calculated using the expression given by Popovics [29].

3.2.1 Strength enhancement ratio

As shown in Table 3, the unconfined concrete strengths (f'_{co}) of specimens tested in Phase I increased from 85.7 MPa to 112.4 MPa with an increase in silica fume content from 0% to 8% for a constant *w/c* ratio of 0.27 (Batches 1 and 2A). Only a slight improvement in strength from 112.4 MPa to 113.5 MPa was observed with a further increase in silica fume content from 8% to 16% (Batches 2A and 3). These observations indicate that for a given *w/c* ratio, the presence of silica fume increases the unconfined concrete strength (f'_{co}), and this increase is not directly proportional to the amount of silica fume.

Table 5. Compression test results of confined specimens containing different levels of silica fume

Phase	Specimen	Silica fume percentage (%)	f'_{cc} (MPa)	ε_{cu} (%)	$\varepsilon_{h,rup}$ (%)	f'_{cc}/f'_{co}	Average f'_{cc}/f'_{co}	$\varepsilon_{cu}/\varepsilon_{co}$	Average $\varepsilon_{cu}/\varepsilon_{co}$	$k_{\varepsilon,f}$	Average $k_{\varepsilon,f}$
I	B1-SF0-WC27-A6W-1	0	166.2	2.02	1.50	1.94	1.94	8.25	8.56	0.68	0.67
	B1-SF0-WC27-A6W-2		168.0	2.18	1.48	1.96		8.89		0.67	
	B1-SF0-WC27-A6W-3		165.2	2.09	1.45	1.93		8.54		0.66	
	B2A-SF8-WC27-A6W-1	8	165.5	1.97	1.37	1.47	1.47	7.38	6.97	0.62	0.66
	B2A-SF8-WC27-A6W-2		168.4	1.74	1.48	1.50		6.51		0.68	
	B2A-SF8-WC27-A6W-3		163.1	1.87	1.47	1.45		7.01		0.67	
	B2B-SF8-WC24-A6W-1	8	167.1	1.77	1.14	1.38	1.40	6.72	6.72	0.52	0.58
	B2B-SF8-WC24-A6W-2		172.1	1.76	1.39	1.42		6.68		0.63	
	B2B-SF8-WC24-A6W-3		168.4	1.78	1.33	1.39		6.76		0.60	
	B3-SF16-WC27-A6W-1	16	186.5	2.04	1.50	1.64	1.57	7.89	7.38	0.68	0.63
	B3-SF16-WC27-A6W-2		170.7	1.75	1.19	1.50		6.77		0.54	
	B3-SF16-WC27-A6W-3		178.5	1.94	1.45	1.57		7.47		0.66	

Table 5. (continued)

Phase	Specimen	Silica fume percentage (%)	f'cc (MPa)	εcu (%)	εh,rup (%)	f'cc/f'co	Average f'cc/f'co	εcu/εco	Average εcu/εco	kε,f	Average kε,f
II	B4-SF0-WC27-G6T-1	0	184.1	2.91	2.24	2.17	2.14	10.24	9.99	0.64	0.61
	B4-SF0-WC27-G6T-2		182.0	2.71	1.99	2.15		9.53		0.57	
	B4-SF0-WC27-G6T-3		178.4	2.90	2.18	2.11		10.20		0.62	
	B5-SF8-WC31-G6T-1	8	187.9	2.83	1.96	2.22	2.14	9.95	9.68	0.56	0.61
	B5-SF8-WC31-G6T-2		180.4	2.78	2.46	2.13		9.78		0.70	
	B5-SF8-WC31-G6T-3		176.3	2.65	1.94	2.08		9.32		0.55	
	B6-SF16-WC33-G6T-1	16	188.6	3.61	2.38	2.23	2.11	12.71	11.28	0.68	0.64
	B6-SF16-WC33-G6T-2		181.7	3.26	2.35	2.15		11.48		0.67	
	B6-SF16-WC33-G6T-3		164.3	2.74	1.99	1.94		9.64		0.57	
	B7-SF0-WC46-G4T-1	0	125.7	3.54	2.48	2.19	2.23	13.73	14.16	0.71	0.73
	B7-SF0-WC46-G4T-2		127.2	3.61	2.67	2.22		14.00		0.76	
	B7-SF0-WC46-G4T-3		131.2	3.80	2.50	2.29		14.74		0.71	
	B8-SF8-WC50-G4T-1	8	119.4	2.81	2.56	2.29	2.38	11.16	12.78	0.73	0.74
	B8-SF8-WC50-G4T-2		126.8	3.48	2.60	2.43		13.82		0.74	
	B8-SF8-WC50-G4T-3		125.3	3.36	2.58	2.40		13.35		0.74	
	B9-SF16-WC53-G4T-1	16	109.2	3.44	2.30	2.01	2.20	13.52	16.06	0.66	0.69
	B9-SF16-WC53-G4T-2		123.5	4.28	2.39	2.27		16.82		0.68	
	B9-SF16-WC53-G4T-3		126.5	4.54	2.57	2.33		17.84		0.73	

To illustrate the influence of silica fume on the behavior of confined concrete, Figure 6 shows the variation of strength enhancement ratios (f'_{cc}/f'_{co}) of the specimens with silica fume-cementitious binder ratio (*sf/c*). As shown by the trendline of the specimens in Phase I in Fig. 6 and the results in Table 5, the strength enhancement ratio (f'_{cc}/f'_{co}) reduced from 1.94 to 1.47 when the silica fume content was increased from 0% to 8% (Batches 1 and 2A). The reduction is a result of the significant improvement of unconfined concrete strength (f'_{co}) from 85.7 MPa to 112.4 MPa due to the silica fume addition. When the silica fume addition from 8% to 16% (Batches 2A and 3) resulted only a marginal improvement to the unconfined concrete strength (f'_{co}) from 112.4 MPa to 113.5 MPa, a minimal change in the strength enhancement ratio (f'_{cc}/f'_{co}) from 1.47 to 1.57 was observed. These observations indicate that the reduction in the strength enhancement ratio (f'_{cc}/f'_{co}) is primarily caused by the increase in the unconfined concrete strength (f'_{co}). This accords with the findings reported in Lim and Ozbakkaloglu [30] that the strength enhancement ratio (f'_{cc}/f'_{co}) decreases with an increase in the unconfined concrete strength (f'_{co}).

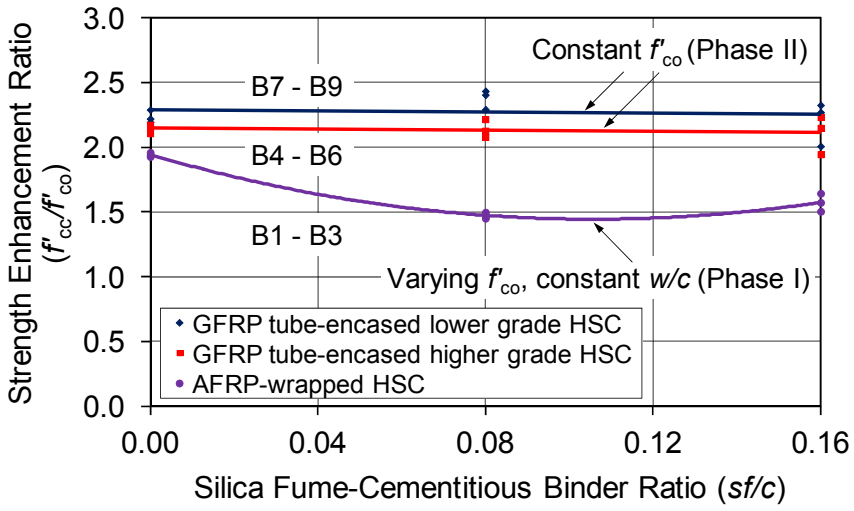

Figure 6. Variation of strength enhancement ratio (f'_{cc}/f'_{co}) with silica fume- cementitious binder ratio (*sf/c*)

Comparison of the results from specimen groups of Phase I containing 8% silica fume and different *w/c* ratios in Table 3 indicates that the unconfined concrete strength (f'_{co}) increased from 112.4 MPa to 120.9 MPa with a reduction in *w/c* ratio from 0.27 to 0.24 (Batches 2A and 2B). As illustrated in Table 5, the increased concrete strength (f'_{co}) resulted in a reduction in the strength enhancement ratios (f'_{cc}/f'_{co}) of the confined specimens from 1.47 to 1.40. This observation indicates that an increase in the unconfined concrete strength (f'_{co}) resulting from a reduction in the *w/c* ratio leads to a decrease in the strength enhancement ratio (f'_{cc}/f'_{co}), similar to that reported due to an increase in the silica fume content.

To isolate the discrete influence of silica fume from the effects of concrete strength (f'_{co}), the GFRP tube-encased specimens tested in Phase II (Batches 4 to 9) were prepared to attain the same unconfined concrete strengths (f'_{co}) with different silica fume percentages. As shown by the trendlines of the higher grade (Batches 4 to 6) and the lower grade HSC specimens

(Batches 7 to 9) in Fig. 6, for a given unconfined concrete strength, a change in silica fume content from 0% to 16% had no significant influence on the strength enhancement ratios (f'_{cc}/f'_{co}) of companion specimens of Phase II. The slightly higher f'_{cc}/f'_{co} ratio of the specimen group with a silica fume content of 8% (Batch 8) can be attributed to the lower f'_{co} of this group compared to the companion groups with 0% and 16% silica fume contents. These observations indicate that silica fume content has no influence on the strength enhancement ratio (f'_{cc}/f'_{co}) provided that the unconfined strength of the concrete remains constant. These observations support the supposition that the change in the strength enhancement ratios (f'_{cc}/f'_{co}) of the specimens of Phase I was primarily caused by the change in their unconfined concrete strengths (f'_{co}).

3.2.2 Strain enhancement ratio

Figure 7 shows the variation of the strain enhancement ratio ($\varepsilon_{cu}/\varepsilon_{co}$) of the FRP-confined specimens with silica fume-cementitious binder ratio (*sf/c*). As shown by the trendline of specimens in Phase I in Fig. 7 and results in Table 5, the increase in the concrete strength (f'_{co}) due to silica fume addition from 0% to 8% (Batches 1 and 2A) resulted in a reduction in the strain enhancement ratio ($\varepsilon_{cu}/\varepsilon_{co}$) from 8.56 to 6.97. The additional increase in silica fume content from 8% to 16% (Batches 2A and 3), which resulted in only a marginal increase in the unconfined concrete strength, led to a slight increase in the strain enhancement ratio ($\varepsilon_{cu}/\varepsilon_{co}$) from 6.97 to 7.38 was observed. Comparison of the specimens with 8% silica fume and different *w/c* ratios of 0.27 and 0.24 (Batches 2A and 2B) in Table 5 indicates that the increase in unconfined strength (f'_{co}) as a result of the *w/c* ratio reduction decreased the strain enhancement ratio ($\varepsilon_{cu}/\varepsilon_{co}$) from 6.97 to 6.72. These observations indicate that an increase in unconfined concrete strength resulting from either the silica fume addition or *w/c* ratio reduction also leads to a reduction in the strain enhancement ratio ($\varepsilon_{cu}/\varepsilon_{co}$).

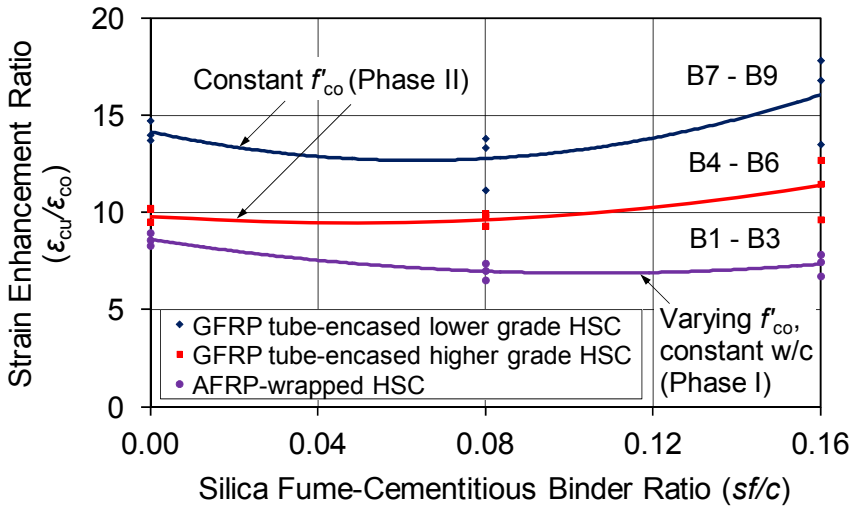

Figure 7. Variation of strain enhancement ratio ($\varepsilon_{cu}/\varepsilon_{co}$) with silica fume-cementitious binder ratio (*sf/c*)

As illustrated by the trendline of higher grade HSC specimens of Phase II in Fig. 7, an increase in the silica fume content from 0% to 8% resulted in a slight reduction in the strain enhancement ratio ($\varepsilon_{cu}/\varepsilon_{co}$) from 9.99 to 9.68 (Batches 4 and 5). A further increase in the silica fume content from 8% to 16%, however, resulted in an increase in the strain enhancement ratio from 9.68 to 11.28 (Batches 5 and 6). Similarly, the lower grade HSC specimens of Phase II exhibited a reduction in strain enhancement ratio ($\varepsilon_{cu}/\varepsilon_{co}$) from 14.16 to 12.78 with an increase in silica fume content from 0% to 8% (Batches 7 and 8), which is followed by an increase in strain enhancement ratio ($\varepsilon_{cu}/\varepsilon_{co}$) from 12.78 to 16.06 with an increase in silica fume content from 8% to 16% (Batches 8 and 9). These observations suggest that specimens with silica fume content above a certain threshold exhibits a higher strain enhancement ratio ($\varepsilon_{cu}/\varepsilon_{co}$) than the companion specimens with the same unconfined strength (f'_{co}) and lower or no silica fume content. Additional studies are required to gain further insight into this interesting influence.

3.2.3 Hoop strain reduction factor

It has been discussed previously in a number of studies [5, 31-36] that the ultimate hoop strain ($\varepsilon_{h,rup}$) reached in the FRP jacket is often smaller than the ultimate tensile strain of the fibers (ε_f), which necessitates the use of a strain reduction factor ($k_{\varepsilon,f}$) in the determination of the actual confining pressures. The recorded hoop rupture strains ($\varepsilon_{h,rup}$) and calculated strain reduction factors ($k_{\varepsilon,f} = \varepsilon_{h,rup}/\varepsilon_f$) of the specimens in the present study are provided in Table 5. The results reveal that the $k_{\varepsilon,f}$ values recorded in Phase I decrease slightly with an increase in unconfined concrete strength (f'_{co}), resulting from either an increase in silica fume content or a reduction in *w/c* ratio. The influence of the concrete strength on the strain reduction factor was previously reported in Lim and Ozbakkaloglu [30] and findings of the present study are in agreement with those observations. On the other hand, no clear influence of silica fume on the strain reduction factor ($k_{\varepsilon,f}$) can be observed from the results of specimen groups in Phase II within a given concrete strength grade. These observations indicate that amount of silica fume does not have direct influence on the strain reduction factor ($k_{\varepsilon,f}$).

3.3 Axial stress-strain behavior

Figures 8 and 9, respectively, illustrate the different stages observed on a typical axial stress-strain curve and the corresponding lateral strain-axial strain curve of the specimens exhibiting stress-strain behaviors with and without post-peak strength softening regions. The different stages marked on these curves were established based on the observed changes in the concrete expansion behavior, which is indicated by different tangential slopes of the corresponding regions shown in Figs. 8(b) and 9(b), namely: linear elastic region, rapid expansion region, and the stabilized dilation region.

The axial stress-strain and lateral strain-axial strain curves of the specimens of Phase I are shown in Figures 10 and 11, respectively. Those of the specimens of Phase II are shown in Figures 12 to 15. In Figs. 10 to 15, the curves of the three companion specimens in each group are represented through the use of three different line styles. As evident from the axial stress-strain curves in Figs. 10, 12 and 14, FRP-confined HSC can exhibit highly ductile compressive behavior. It is well established that sufficiently confined concrete exhibits a

monotonically ascending curve, which consists of a parabolic first ascending branch and a nearly straight-line second branch (e.g., Specimen B1-SF0-WC27-A6W in Fig. 10(a) and specimens in Figs. 12 and 14). On the other hand, when the confinement level is below a certain threshold, the first ascending branch is followed by a second branch that exhibits a post-peak strength softening region [37, 38] (e.g., Specimens B2A-SF8-WC27-A6W, B2B-SF8-WC24-A6W and B3-SF16-WC27-A6W in Figs. 10(b) to 10(d)). The confinement requirements and the threshold conditions for distinguishing the curves with or without post-peak strength softening are discussed in detail in Lim and Ozbakkaloglu [30]. This section of the present study presents a discussion on the influence of silica fume on the transition region that connects the first ascending branch to the second branch of the stress-strain curves of FRP-confined concrete.

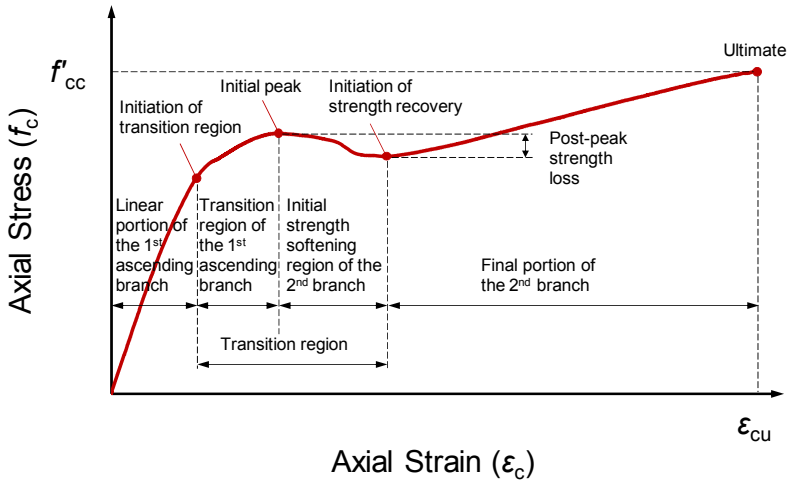

(a)

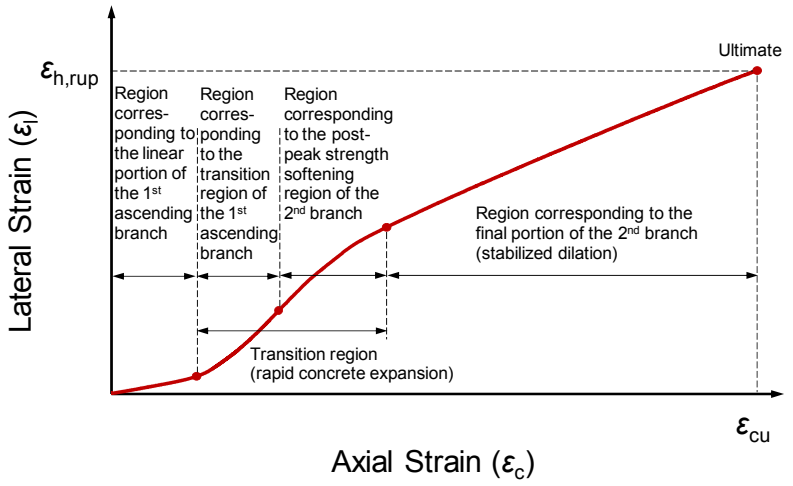

(b)

Figure 8. Illustration of different stages of: (a) axial stress-strain; and (b) lateral strain-axial strain curves of specimen with initial strength softening behavior

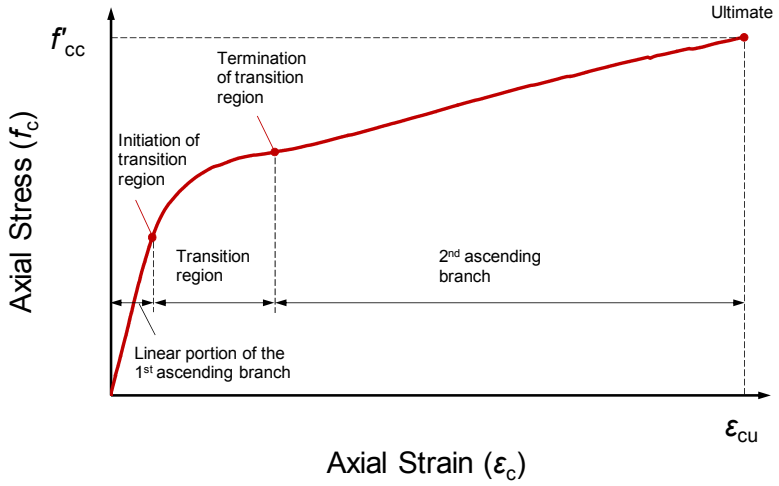

(a)

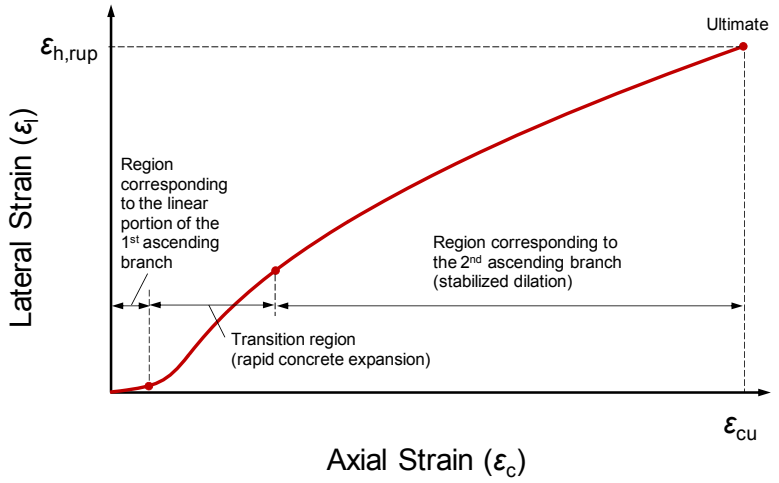

(b)

Figure 9. Illustration of different stages of: (a) axial stress-strain; and (b) lateral strain-axial strain curves of specimen without initial strength softening behavior

The specimens with 8% and 16% silica fume shown in Figs. 10(b) to 10(d) experienced a sudden drop in strength starting at the initial peak of their stress-strain curves. This post-peak strength softening phenomenon can be attributed to the increased concrete brittleness with increasing concrete strength, which alters the concrete crack patterns from heterogenic microcracks to localized macrocracks [25]. The failure modes of the unconfined specimens shown in Fig. 2 illustrates the larger crack formations observed in the specimens with 8% and 16% silica fume contents compared to those of the specimens containing no silica fume.

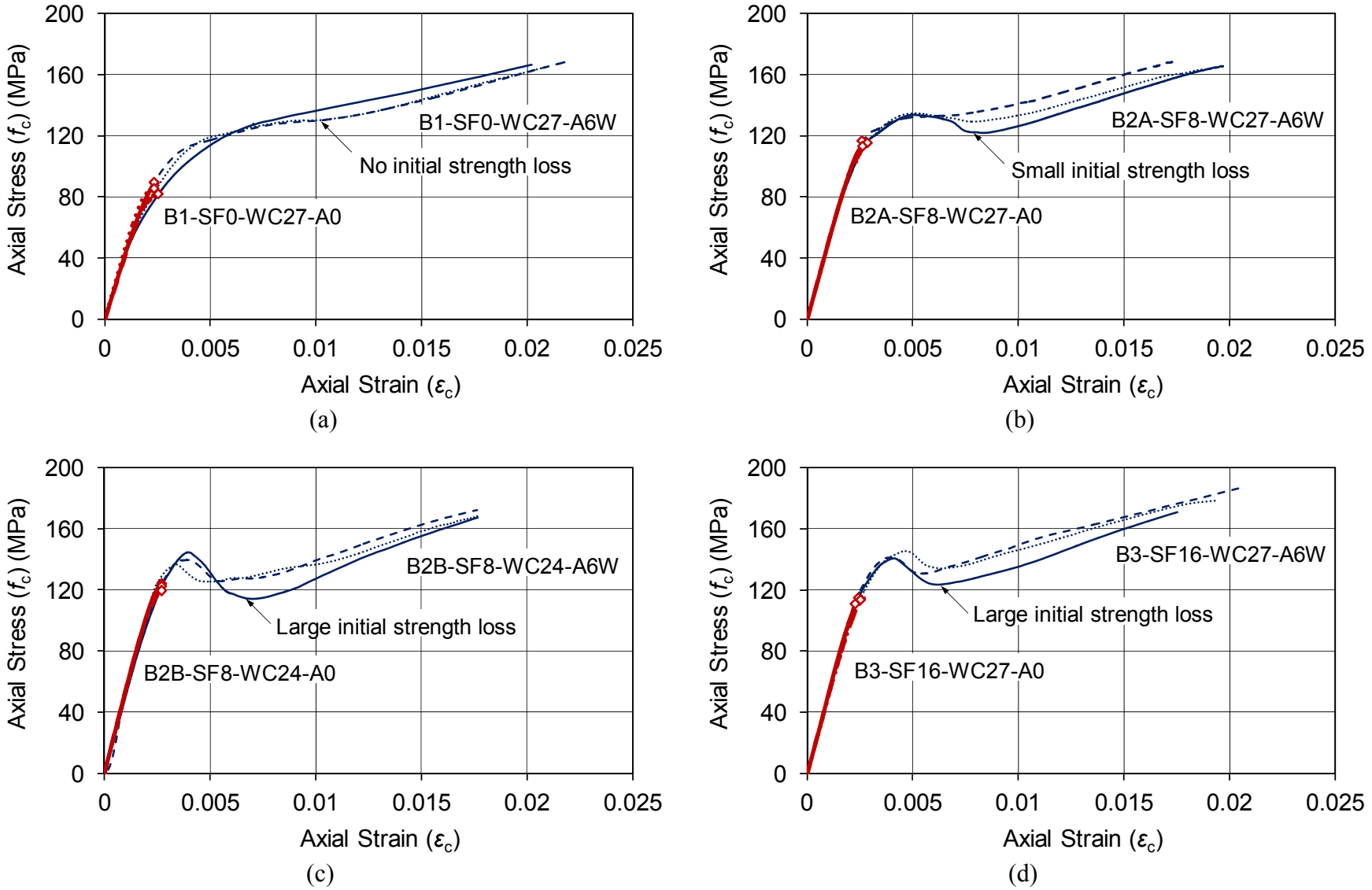

Figure 10. Axial stress-strain curves of: AFRP-wrapped HSC specimens with: a) 0% silica fume and 0.27 *w/c* ratio; b) 8% silica fume and 0.27 *w/c* ratio; c) 8% silica fume and 0.24 *w/c* ratio; d) 16% silica fume and 0.27 *w/c* ratio

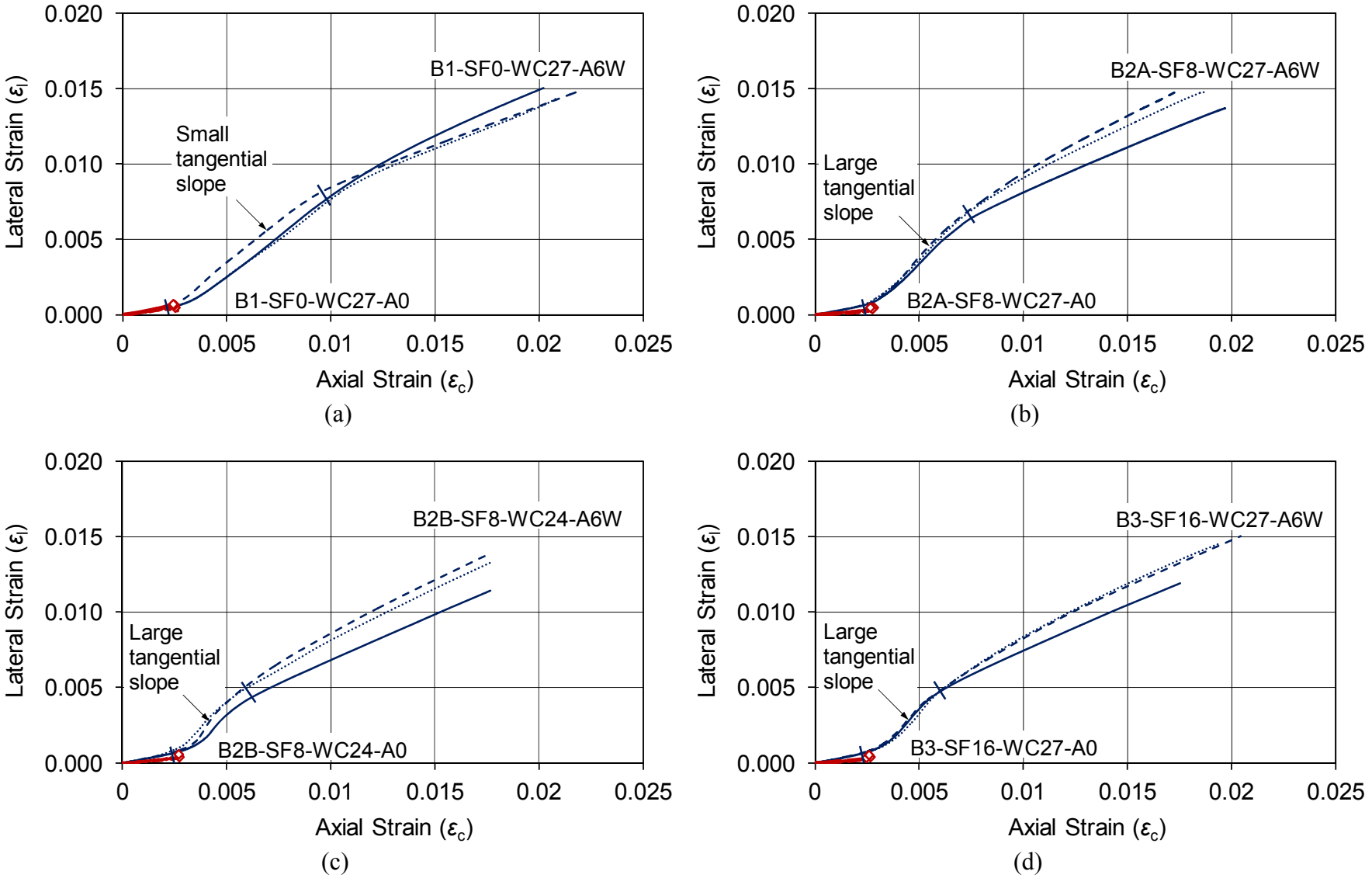

Figure 11. Lateral strain-axial strain curves of: AFRP-wrapped HSC specimens with: a) 0% silica fume and 0.27 *w/c* ratio; b) 8% silica fume and 0.27 *w/c* ratio; c) 8% silica fume and 0.24 *w/c* ratio; d) 16% silica fume and 0.27 *w/c* ratio

As illustrated by the lateral strain-axial strain curves shown in Fig. 11, the rate of lateral expansion of concrete (i.e. dilation rate) along the post-peak strength softening region was larger for specimens with 8% and 16% silica fume contents compared to that of the specimens containing no silica fume. The more rapid lateral expansion of the former specimens results in their sustaining a significant amount of damage before the full activation of the confinement mechanism that marks the initiation of strength recovery shown in Fig. 8(a). This is evident from Figs. 10(a) to 10(d), which illustrate that the magnitude of the strength loss observed along the post-peak strength softening region was more significant for the specimens with higher unconfined strengths resulting from either an addition of silica fume or a reduction in *w/c* ratio.

Figures 12 and 14 show the stress-strain curves of the specimens of Phase II, which all exhibited monotonically ascending curves. Figures 13 and 15 show the corresponding lateral strain-axial strain curves of these specimens. Although no post-peak strength loss was observed from the stress-strain curve of specimens in Phase II, the changes in their transition radii and second branches are nevertheless evident in the comparisons of Figs. 12(a) to 12 (c) and 14(a) to 14(c). The transition radii are the radii of the curved segments that form the transition regions marked in Figs. 12 and 14, which connect the first and second branches of the axial stress-strain curves. Smaller transition radii and longer second branches of the axial stress-strain curves of specimens containing 16% silica fume shown are evident in Figs. 12 and 14, when compared to those of their companions with 0% and 8% silica fume content. These changes can be attributed to the differences in the dilation behavior of these specimens, as illustrated by their lateral strain-axial strain curves shown in Figs. 13 and 15. To enable an easier observation of these differences, the segments corresponding to the transition regions on the axial stress-strain curves are also marked on the companion lateral strain-axial strain curves in Figs. 13 and 15. As evident from these figures, the lateral strain-axial strain curves of the specimens with 16% silica fume content exhibit lower tangential slopes along the marked segments and stabilized dilation regions of the second branch, compared to those of their counterparts containing 0% and 8% silica fume. The lower tangential slopes observed along the second branches of the specimens with 16% silica fume content led to longer second branches on the axial stress-strain curves of these specimens, resulting in higher ultimate axial strains. Comparison of the specimens of Phase I with similar unconfined concrete strengths (i.e. Specimen groups B2A-SF8-WC27-A6W and B3-SF16-WC27-A6W) further supports this observation, with the specimens containing 16% silica fume exhibiting longer second branches compared to those of the specimens with 8% silica fume content as shown in Fig. 10. These observations indicate that the addition of silica fume above a certain threshold increases the axial deformation capacity of confined concrete by reducing its dilation rate along the second branch of the stress-strain relationship.

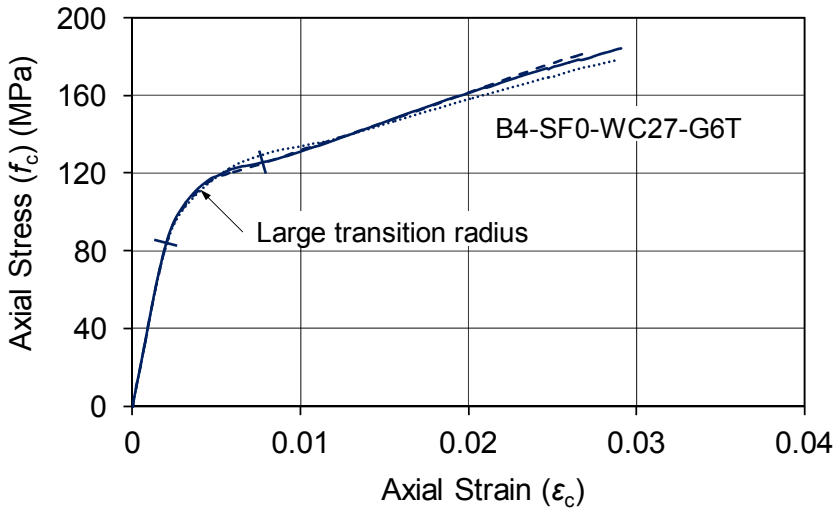

(a)

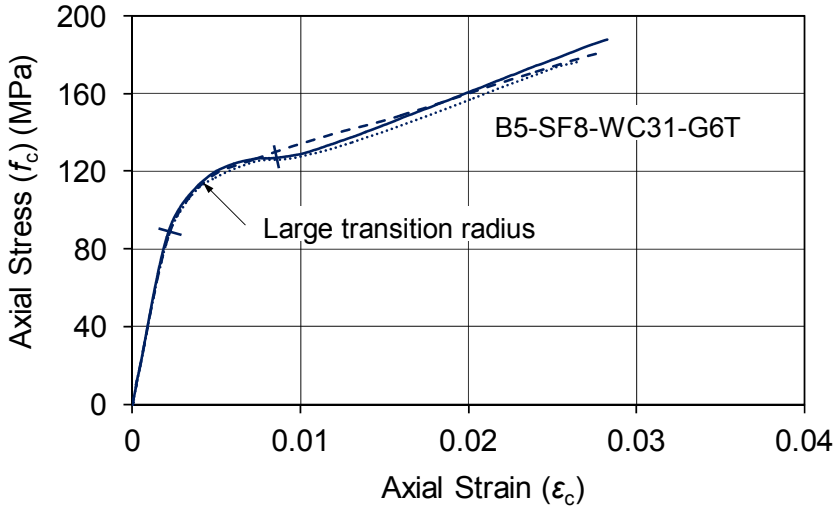

(b)

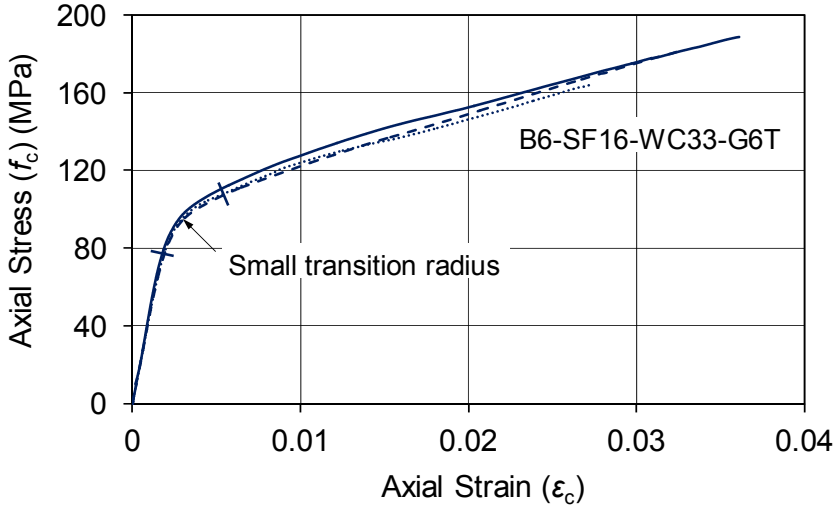

(c)

Figure 12. Axial stress-strain curves of GFRP tube-encased high-grade HSC specimens with: a) 0% silica fume and 0.27 *w/c* ratio; b) 8% silica fume and 0.31 *w/c* ratio; c) 16% silica fume and 0.33 *w/c* ratio

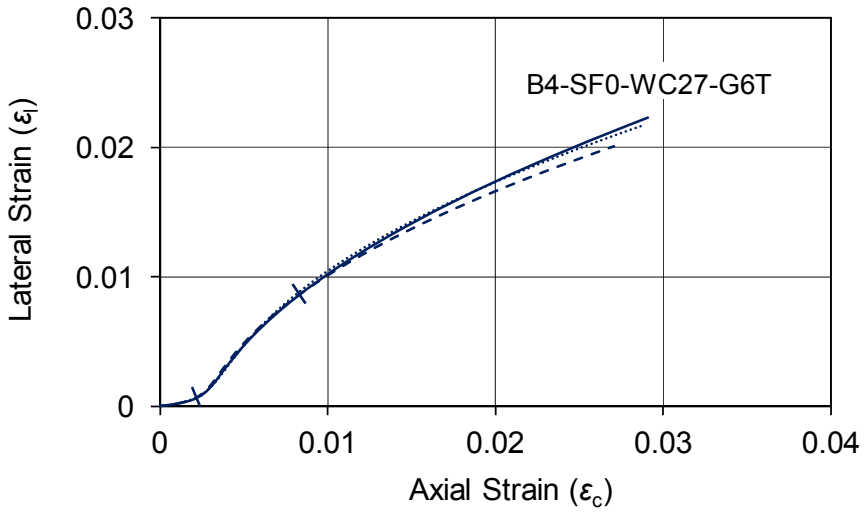

(a)

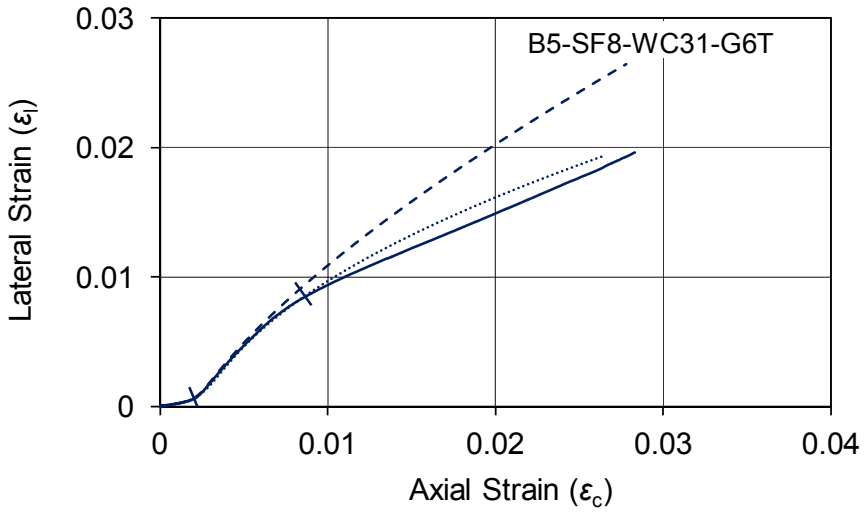

(b)

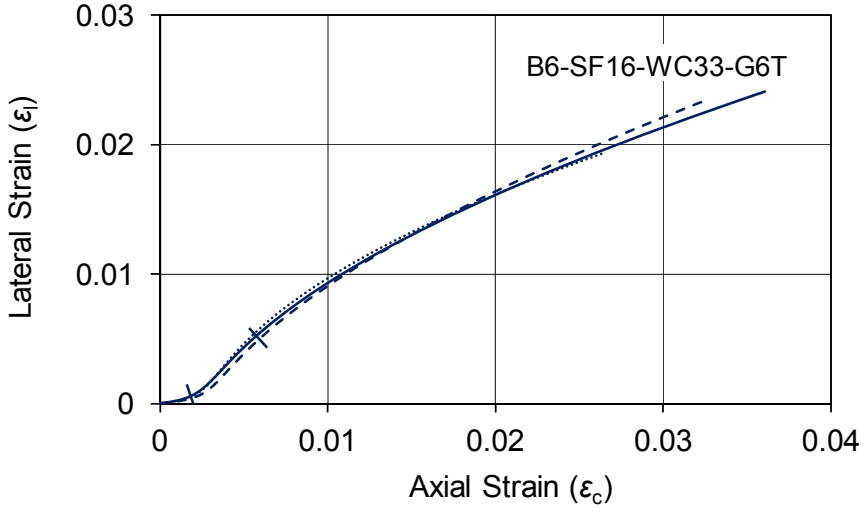

(c)

Figure 13. Lateral strain-axial strain curves of GFRP tube-encased high-grade HSC specimens with: a) 0% silica fume and 0.27 *w/c* ratio; b) 8% silica fume and 0.31 *w/c* ratio; c) 16% silica fume and 0.33 *w/c* ratio

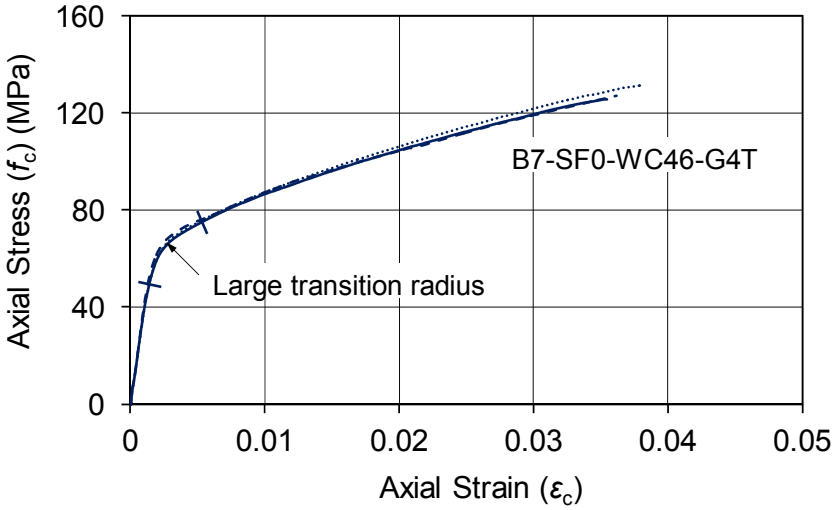

(a)

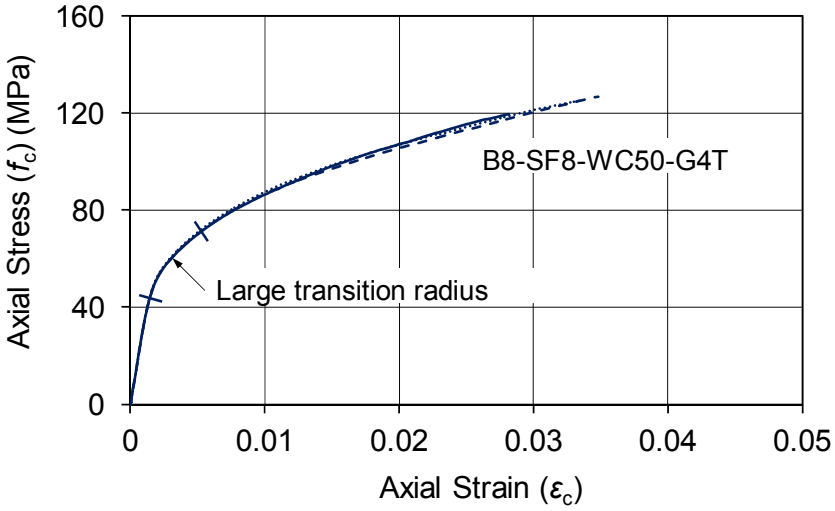

(b)

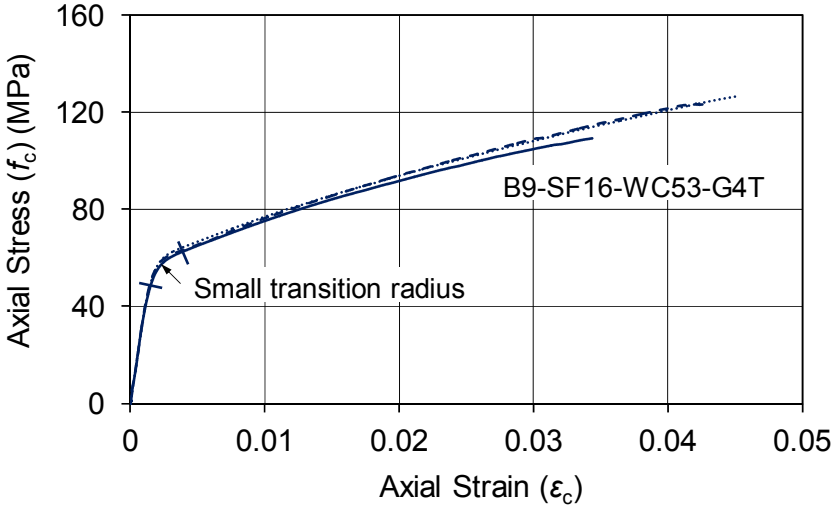

(c)

Figure 14. Axial stress-strain curves of GFRP tube-encased low-grade HSC specimens with: a) 0% silica fume and 0.46 *w/c* ratio; b) 8% silica fume and 0.50 *w/c* ratio; c) 16% silica fume and 0.53 *w/c* ratio

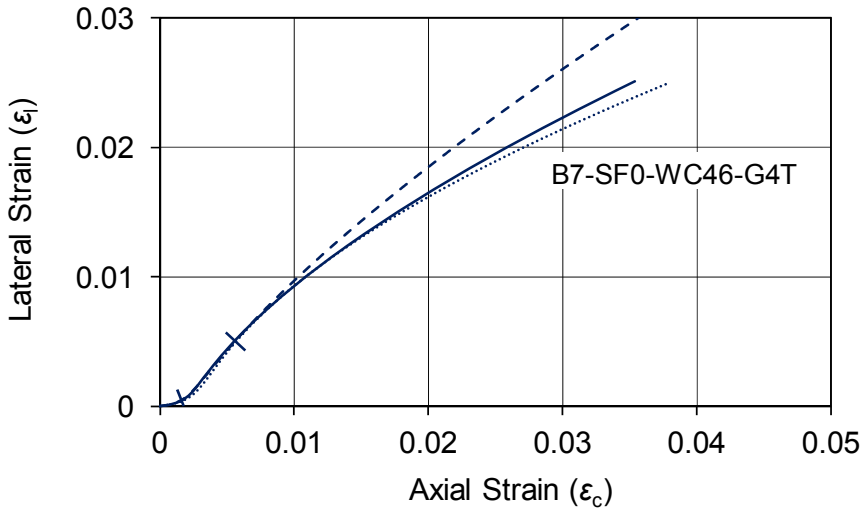

(a)

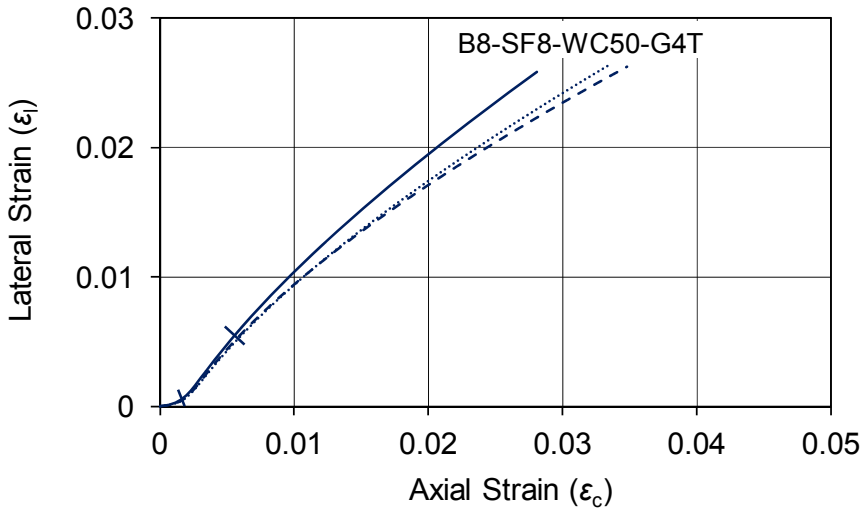

(b)

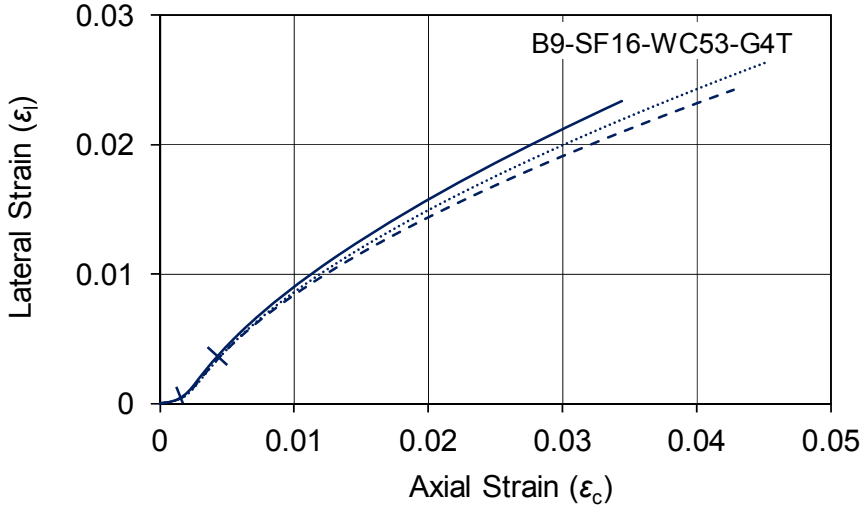

(c)

Figure 15. Lateral strain-axial strain curves of GFRP tube-encased low-grade HSC specimens with: a) 0% silica fume and 0.46 *w/c* ratio; b) 8% silica fume and 0.50 *w/c* ratio; c) 16% silica fume and 0.53 *w/c* ratio

3.3.1. Influence of axial strain measurement method

As was previously discussed in Ozbakkaloglu and Lim [36], the recorded ultimate axial strains (ε_{cu}) are highly sensitive to the type of instrumentation used in their measurement. Based on a large database of experimental results, it was shown that LVDTs mounted along the entire height of the specimens gave higher axial strains than those measured by LVDTs mounted at mid-height of the specimens and by axial strain gauges [36].

In the present study, factors causing discrepancies between the axial strains obtained from these three instrumentation arrangements were experimentally investigated. An example comparison is shown in Figure 16, which illustrates the stress-strain curves of one of the test specimens obtained using the three different measurement methods. As evident from the figure, significant differences exist among the axial strains measured by these methods beyond the initial peak of the stress-strain curves. Table 6 presents the comparison of ultimate axial strains (ε_{cu}) of all specimens recorded using the three different measurement methods, including the ultimate axial strains recorded by the axial strain gauges (ASG), the LVDTs mounted at the mid-height of the specimens (AML), and the LVDTs mounted along the entire height of the specimens (AFL). Figure 17 shows the comparison of the difference between AML and AFL, defined by the ratios of AML/AFL, with a change in unconfined concrete strength (f'_{co}). This accords with the observation reported in Ozbakkaloglu and Lim [36] that the difference in axial strain recorded by AML and AFL increases with an increase in unconfined concrete strength (f'_{co}). The increased discrepancies between AML and AFL were attributed to the change in the concrete cracking pattern from microcracks to macrocracks as a result of the increased concrete brittleness with an increase in concrete strength [36].

Table 6. Comparison of axial strains measured by different methods

Specimen	Average f'_{co} (MPa)	Average ε_{cu} (%)			Differences	
		AFL	AML	ASG	AML/ AFL	ASG/ AFL
B1-SF0-WC27-A6W	85.7	2.10	1.19	1.02	0.57	0.49
B2A-SF8-WC27-A6W	112.4	1.86	0.97	0.86	0.52	0.46
B2B-SF8-WC24-A6W	120.9	1.77	0.80	0.61	0.45	0.35
B3-SF16-WC27-A6W	113.5	1.91	1.00	0.89	0.52	0.47
B4-SF0-WC27-G6T	84.70	2.84	1.27	-	0.45	-
B5-SF8-WC31-G6T	84.80	2.75	1.53	-	0.56	-
B6-SF16-WC33-G6T	84.50	3.20	2.07	-	0.65	-
B7-SF0-WC46-G4T	57.30	3.65	2.88	-	0.79	-
B8-SF8-WC50-G4T	52.10	3.22	2.61	-	0.81	-
B9-SF16-WC53-G4T	54.40	4.09	3.74	-	0.91	-

AFL: axial strains determined from LVDTs mounted along the entire height of the specimens
AML: axial strains determined from LVDTs mounted at the mid-height of the specimens
ASG: axial strains determined from strain gauges attached on the surface of specimens

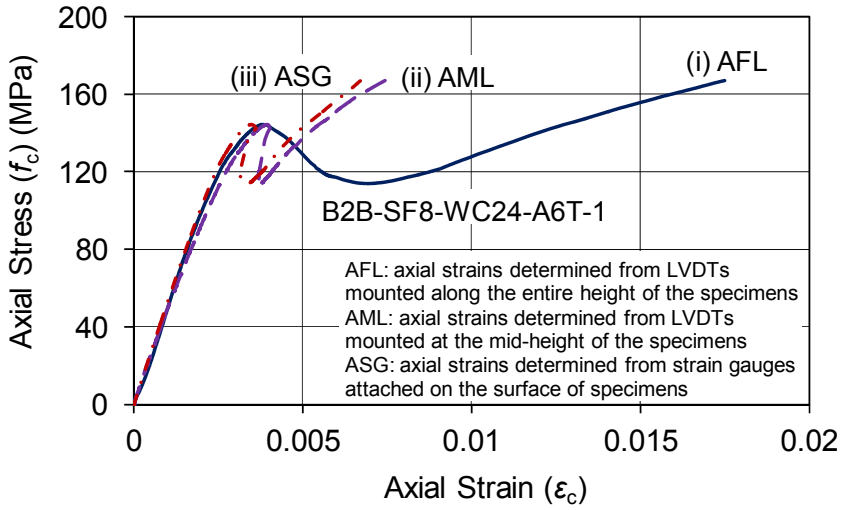

Figure 16. Influence of instrumentation arrangement on axial stress-strain curves

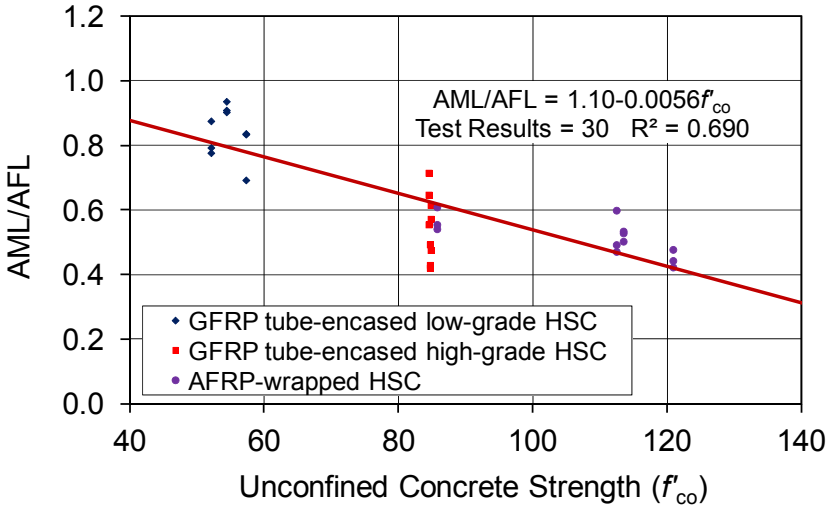

Figure 17. Variation of AML/AFL ratio with unconfined concrete strength (f'_{co})

Closer investigation of the result of the present study indicates that, for a given concrete strength, the difference between AML and AFL becomes less significant with an increase in the silica fume content. This is evident from the comparison of the AML/AFL ratios of specimens in Batches 4 to 6 and Batches 7 to 9 in Table 6. As discussed previously, the reduced discrepancy between AML and AFL can be attributed to the smaller concrete crack size. These observations, therefore, indicate that, for a given unconfined concrete strength, FRP-confined concrete specimens with higher silica fume content develop smaller cracks than their counterparts with a lower or no silica fume content. This in turn leads to a more favorable dilation behavior and, as was noted previously, results in higher axial deformation capacities of specimens with higher silica fume content.

Based on the significant differences observed in the axial strains obtained from different measurement methods as outlined herein, it is recommended that in future studies due consideration be given to the influence of instrumentation method in the interpretation of the results of FRP-confined HSC specimens, with or without silica fume.

4. CONCLUSIONS

This paper has presented the results of an experimental study on the influence of silica fume on the axial compressive behavior of FRP-confined HSC. Based on the results and discussions presented in the paper, the following conclusions can be drawn:

1. Sufficiently confined HSC with and without silica fume can exhibit highly ductile compressive behavior.
2. An increase in the unconfined concrete strength resulting from a reduction in the *w/c* ratio or an increase in silica fume content leads to reductions in the strength and strain enhancement ratios.
3. For a given unconfined concrete strength, the presence and change in silica fume content do not significantly alter the strength enhancement effect of FRP confinement.
4. For a given unconfined concrete strength, specimens with silica fume content above a certain threshold exhibits a higher strain enhancement than the companion specimens with lower or no silica fume content.
5. FRP-confined concrete can exhibit a monotonically ascending stress-strain curve or a curve with a post-peak strength loss at the transition region. Due to the resulting increase in concrete strength and its associated brittleness, the silica fume addition or *w/c* ratio reduction in the concrete mix leads to a more significant post-peak strength loss on the stress-strain relationships.
6. Transition regions of stress-strain curves of FRP-confined concrete are observed to be sensitive to the silica fume content of the concrete mix, with mixes having higher silica fume content exhibiting curves with smaller transition radii.
7. The hoop strain reduction factor ($k_{\varepsilon,f}$) is observed to decrease slightly with an increase in concrete strength (f'_{co}) resulting from the addition of silica fume to the mix or reduction of *w/c* ratio of the mix.
8. The discrepancy between the axial strains measured using LVDTs mounted on FRP-confined HSC specimens at their mid-height (AML) and LVDTs mounted along the full-height of specimens (AFL) increases with an increase in the concrete strength (f'_{co}). However the discrepancy reduces with an increase in silica fume content at a given concrete strength.

NOMENCLATURE

E_f Elastic modulus of fibers (MPa)
E_{frp} Elastic modulus of FRP material (MPa)
f'_{cc} Peak axial compressive stress of FRP-confined concrete (MPa)
f'_{co} Peak axial compressive stress of unconfined concrete (MPa)
$k_{\varepsilon,f}$ Hoop strain reduction factor of fibers
sf/c Silica fume-cementitious binder ratio
t_f Total nominal thickness of fibers (mm)
w/c Water-to-cementitious binder ratio
ε_{co} Axial strain at peak axial compressive stress of unconfined concrete
ε_{cu} Ultimate axial strain of FRP-confined concrete
ε_f Ultimate tensile strain of fibers
ε_{frp} Ultimate tensile strain of FRP material
$\varepsilon_{h,rup}$ Hoop rupture strain of FRP shell

REFERENCES

1. Ozbakkaloglu, T. and Saatcioglu, M., (2006). "Seismic behavior of high-strength concrete columns confined by fiber-reinforced polymer tubes." *Journal of Composites for Construction, ASCE,* 10(6), p. 538-549.
2. Ozbakkaloglu, T. and Saatcioglu, M., (2007). "Seismic performance of square high-strength concrete columns in FRP stay-in-place formwork." *Journal of Structural Engineering,* 133(1), p. 44-56.
3. Idris, Y. and Ozbakkaloglu, T., (2013). "Seismic behavior of high-strength concrete-filled FRP tube columns." *Journal of Composites for Construction, ASCE,* 17(6), p. 04013013.
4. Berthet, J.F., Ferrier, E., and Hamelin, P., (2005). "Compressive behavior of concrete externally confined by composite jackets. Part A: experimental study." *Construction and Building Materials,* 19(3), p. 223-232.
5. Vincent, T. and Ozbakkaloglu, T., (2013). "Influence of concrete strength and confinement method on axial compressive behavior of FRP-confined high- and ultra high-strength concrete." *Composites Part B,* 50, p. 413–428.
6. Toutanji, H.A. and El-Korchi, T., (1995). "The influence of silica fume on the compressive strength of cement paste and mortar." *Cement and Concrete Research,* 25(7), p. 1591-1602.
7. Tasdemir, C., Tasdemir, M.A., Lydon, F.D., and Barr, B.I.G., (1996). "Effects of silica fume and aggregate size on the brittleness of concrete." *Cement and Concrete Research,* 26, p. 63-68.
8. Duval, R. and Kadri, E.H., (1998). "Influence of silica fume on the workability and the compressive strength of high-performance concretes." *Cement and Concrete Research,* 28(4), p. 533-547.
9. Mazloom, M., Ramezanianpour, A.A., and Brooks, J.J., (2004). "Effect of silica fume on mechanical properties of high-strength concrete." *Cement and Concrete Composites,* 26(4), p. 347-357.
10. Setunge, S., Attard, M.M., and Darvall, P.L., (1993). "Ultimate strength of confined very high-strength concretes." *ACI Structural Journal,* 90(6), p. 632-641.
11. Jansen, D.C., Shah, S., and Rossow, E., C., (1995). "Stress-strain results of concrete from circumferential strain feedback control testing." *ACI Material journal,* 92(4), p. 419-428.
12. Samani, A.K. and Attard, M.M., (2012). "A stress-strain model for uniaxial and confined concrete under compression." *Engineering Structures,* 41, p. 335-349.
13. Xiao, Q.G., Teng, J.G., and Yu, T., (2010). "Behavior and Modeling of Confined High-Strength Concrete." *Journal of Composites for Construction, ASCE,* 14(3), p. 249-259.
14. Lahlou, K., Aitcin, P.C., and Chaallal, O., (1992). "Behaviour of High-strength Concrete Under Confined Stresses." *Cement and Concrete Composites,* 14(3), p. 185-193.
15. Hammons, M.I. and Neeley, B.D., (1993). "Triaxial characterization of high-strength Portland cement concrete." *Transportation Research Record,* (1382), p. 73-77.
16. Xie, J., Elwi, A.E., and Macgregor, J.G., (1995). "Mechanical-properties of high-strength concretes containing silica fume." *ACI Materials Journal,* 92(2), p. 135-145.
17. Attard, M.M. and Setunge, S., (1996). "Stress-strain relationship of confined and unconfined concrete." *ACI Materials Journal,* 93(5), p. 432-442.

18. Ansari, F. and Li, Q.B., (1998). "High-strength concrete subjected to triaxial compression." *ACI Materials Journal,* 95(6), p. 747-755.
19. Aire, C., Gettu, R., and Casas, J.R., (2001). "Study of the compressive behavior of concrete confined by fiber reinforced composites." *Composites in Construction*, ed. J. Figueiras, L. Juvanders, and R. Faria. 239-243.
20. Rousakis, T., (2001). "Experimental investigation of concrete cylinders confined by carbon FRP sheets under monotonic and cyclic axial compressive load." *Research Report*, Chalmers University of Technology, Göteborg, Sweden.
21. Mandal, S., Hoskin, A., and Fam, A., (2005). "Influence of concrete strength on confinement effectiveness of fiber-reinforced polymer circular jackets." *ACI Structural Journal,* 102(3), p. 383-392.
22. Almusallam, T.H., (2007). "Behavior of normal and high-strength concrete cylinders confined with E-glass/epoxy composite laminates." *Composites Part B-Engineering,* 38(5-6), p. 629-639.
23. Valdmanis, V., De Lorenzis, L., Rousakis, T., and Tepfers, R., (2007). "Behaviour and capacity of CFRP-confined concrete cylinders subjected to monotonic and cyclic axial compressive load." *Structural Concrete,* 8(4), p. 187-200.
24. Aire, C., Gettu, R., Casas, J.R., Marques, S., and Marques, D., (2010). "Concrete laterally confined with fibre-reinforced polymers (FRP): experimental study and theoretical model." *Materiales De Construccion,* 60(297), p. 19-31.
25. Ozbakkaloglu, T. and Akin, E., (2012). "Behavior of FRP-confined normal- and high-strength concrete under cyclic axial compression." *Journal of Composites for Construction, ASCE,* 16(4), p. 451-463.
26. Ozbakkaloglu, T. and Vincent, T., (2013). "Axial compressive behavior of circular high-strength concrete-filled FRP tubes." *Journal of Composites for Construction, ASCE,* 18(2), p. 04013037.
27. Vincent, T. and Ozbakkaloglu, T., (2013). "Influence of fiber orientation and specimen end condition on axial compressive behavior of FRP-confined concrete." *Construction and Building Materials,* 47, p. 814-826.
28. ASTM-D3039, (2008). "Standard test method for tensile properties of polymer matrix composite materials." *D3039/D3039M-08*, West Conshohocken, PA.
29. Popovics, S., (1973). "A numerical approach to the complete stress-strain curves for concrete." *Cement and Concrete Research,* 3(5), p. 583-599.
30. Lim, J.C. and Ozbakkaloglu, T., (2013). "Confinement model for FRP-confined high-strength concrete." *Journal of Composites for Construction,* 18(4), 04013058.
31. Harries, K.A. and Carey, S.A., (2003). "Shape and "gap" effects on the behavior of variably confined concrete." *Cement and Concrete Research,* 33(6), p. 881-890.
32. De Lorenzis, L. and Tepfers, R., (2003). "Comparative study of models on confinement of concrete cylinders with fiber-reinforced polymer composites." *Journal of Composites for Construction,* 7(3), p. 219-237.
33. Lam, L. and Teng, J.G., (2004). "Ultimate condition of fiber reinforced polymer-confined concrete." *Journal of Composites for Construction, ASCE,* 8(6), p. 539-548.

34. Ozbakkaloglu, T. and Oehlers, D.J., (2008). "Concrete-filled square and rectangular FRP tubes under axial compression." *Journal of Composites for Construction,* 12(4), p. 469-477.
35. Ozbakkaloglu, T. and Oehlers, D.J., (2008). "Manufacture and testing of a novel FRP tube confinement system." *Engineering Structures,* 30, p. 2448-2459.
36. Ozbakkaloglu, T. and Lim, J.C., (2013). "Axial compressive behavior of FRP-confined concrete: Experimental test database and a new design-oriented model." *Composites Part B: Engineering,* 55, p. 607-634.
37. Ozbakkaloglu, T., (2013). "Axial compressive behavior of square and rectangular high-strength concrete-filled FRP tubes." *Journal of Composites for Construction,* 17(1), p. 151-161.
38. Ozbakkaloglu, T., (2013). "Behavior of square and rectangular ultra high-strength concrete-filled FRP tubes under axial compression." *Composites Part B: Engineering.,* 54, p. 97-111.

THIS PAGE HAS BEEN LEFT INTENTIONALLY BLANK

Statement of Authorship

Title of Paper	Influence of Concrete Age on Stress-Strain Behavior of FRP-Confined Normal- and High-Strength Concrete
Publication Status	(•) Published ( ) Accepted for Publication ( ) Submitted for Publication ( ) Publication Style
Publication Details	Construction and Building Materials, Doi: 10.1016/j.conbuildmat.2015.02.020, Year 2015

Author Contributions

By signing the Statement of Authorship, each author certifies that their stated contribution to the publication is accurate and that permission is granted for the publication to be included in the candidate's thesis.

Name of Principal Author (Candidate)	Mr. Jian Chin Lim		
Contribution to the Paper	Preparation of experiment, analysis of test results, and preparation of manuscript		
Signature		Date	23/02/2015

Name of Co-Author	Dr. Togay Ozbakkaloglu		
Contribution to the Paper	Research supervision and review of manuscript		
Signature		Date	23/02/2015

THIS PAGE HAS BEEN LEFT INTENTIONALLY BLANK

INFLUENCE OF CONCRETE AGE ON STRESS-STRAIN BEHAVIOR OF FRP-CONFINED NORMAL- AND HIGH-STRENGTH CONCRETE

Jian C. Lim and Togay Ozbakkaloglu

ABSTRACT

The potential applications of fiber reinforced polymer (FRP) composites as concrete confinement in retrofitting existing concrete columns and in the construction of new high-performance composite columns have received significant research attention. In practical applications, the ages of concrete in retrofitted columns are significantly different from those of newly constructed columns. Without a full understanding on the influence of concrete age on their compressive behaviors, the validity of existing experimental findings, which are based the age of concrete at the time of testing, remains ambiguous when the design application lapses in time. This paper presents the results of an experimental study on the influence of concrete age on the compressive behavior of FRP-confined normal-strength (NSC) and high-strength concrete (HSC). The first part of the paper presents the results of 18 FRP-confined and 18 unconfined concrete specimens tested at 7 and 28 days. To extend the investigation with specimens with concrete ages up to 900 days, existing test results of FRP-confined concrete was assembled from the review of the literature. Based on observations from both short- and long-term influences of concrete age on compressive behavior of FRP-confined concrete, a number of important findings were drawn and are presented in the second part of the paper. It was observed that, at a same level of FRP confinement and unconfined concrete strength, the stress-strain behavior of FRP-confined concrete changes with concrete age. This difference is particularly pronounced at the transition zone of the stress-strain curves. It is found that, in the short-term, the ultimate condition of FRP-confined concrete is not significantly affected by the age of concrete. However, in the long-term, slight decreases in the compressive strength and the ultimate axial strain are observed with an increase in concrete age.

KEYWORDS: Concrete; High-strength concrete (HSC); Fiber reinforced polymer (FRP); Confinement; Compression; Age; Stress-strain relations.

1. INTRODUCTION

Understanding the influence of concrete age on the compressive behavior of FRP-confined concrete in newly constructed and retrofitted existing columns is of vital importance. A number of existing studies have investigated time-related issues affecting the compressive behavior of FRP-confined concrete under various environmental exposures [1-6] and sustained loading [7-12] . However, none of these studies directly investigated the influence of concrete age on the stress-strain behavior of FRP-confined concrete. To gain an insight into the possible changes in the behavior of FRP-confined concrete members throughout their service lives, influence of concrete age on the stress-strain behavior of FRP-confined concrete needs to be understood. To this end, the experimental program reported in the present study investigated the axial compressive behaviors of 18 FRP-confined and 18 unconfined NSC and HSC specimens tested at 7 or 28 days of concrete age. The specimens were prepared such that concretes at different ages attained the same unconfined strength at the day of testing and they were confined with the same amount of FRP. To extend the observation range of concrete age up to 900 days, the results of the present study were analyzed together with those from several groups of specimens assembled from the published literature.

2. EXPERIMENTAL PROGRAM

2.1 Test Specimens and Materials

18 FRP-confined and 18 unconfined concrete cylinders were prepared. All of the specimens were 152.5 mm in diameter and 305 mm in height. The influence of concrete age on the mechanical properties of the confined and unconfined specimens was investigated using six separate batches of concrete mixes. Detail of the mix proportions of each batch of concrete is given in Table 1. Crushed bluestone gravel of 7 mm maximum size and graded sand were used as the aggregates. The specimens were manufactured using two different concrete mixes, including a HSC and a NSC mix. The HSC specimens in Batches 1 to 4 had an average strength of 73.0 MPa and the NSC specimens in Batches 5 and 6 had an average strength of 33.9 MPa. To establish the final *w/c* ratios used in Batches 1 to 6, a large number of trial batches were prepared and tested. The summary of the axial compression test results of the unconfined specimens are given in Table 2, which provides the peak stress (f'_{co}) and corresponding axial strain (ε_{co}) of the specimens. The axial strain corresponding to the peak stress of unconfined concrete (ε_{co}) was not recorded during the compression tests, and values reported in Table 2 were calculated using the expression proposed by Lim and Ozbakkaloglu [13].

$$\varepsilon_{co} = \frac{f'^{\,0.225k_d}_{co}}{1000} k_s k_a \quad (1)$$

where, f'_{co} is in MPa, and k_d, k_s, and k_a, respectively, are the coefficients to allow for concrete density, specimens size and specimen aspect ratio. Each of these coefficients becomes unity for a specimen with concrete density of 2400 kg/m^3, diameter of 152 mm and height of 305 mm, as was the case for the control cylinders of the present study.

Table 1. Mix proportions of concrete specimens tested at different ages

Designated Study	AFRP tube-encased HSC		GFRP tube-encased HSC		GFRP tube-encased NSC	
Batch	B1	B2	B3	B4	B5	B6
Cement (kg/m^3)	550	520	550	520	380	380
Sand (kg/m^3)	710	710	710	710	710	710
Gravel (kg/m^3)	1065	1065	1065	1065	1065	1065
Water (kg/m^3)	133	137	133	137	213	243
Superplasticiser (kg/m^3)	20	20	20	20	0	0
Water-cementitious binder ratio	0.270	0.294	0.270	0.294	0.560	0.640
Slump height (m)	>0.250	>0.250	>0.250	>0.250	0.065	0.190
Concrete age at testing (day)	7	28	7	28	7	28

Table 2. Compression test results of unconfined specimens

Specimen	Concrete batch	Age (day)	w/c ratio (%)	Avg. f'_{co} (MPa)	Avg. ε_{co}* (%)
A0-U73-D7	B1	7	0.27	72.0	0.26
A0-U73-D28	B2	28	0.29	74.9	0.26
G0-U73-D7	B3	7	0.27	70.8	0.26
G0-U73-D28	B4	28	0.29	74.1	0.26
G0-U34-D7	B5	7	0.56	33.0	0.22
G0-U34-D28	B6	28	0.64	34.7	0.22

* Axial strains were not recorded experimentally. Values determined using expression given by Lim and Ozbakkaloglu [13].

Table 3. Material properties of fibers and FRP composites

Type	Nominal thickness t_f (mm/ply)	Provided by manufacturers			Obtained from flat FRP coupon tests		
		Tensile strength f_f (MPa)	Ultimate tensile strain ε_f (%)	Elastic modulus E_f (GPa)	Tensile strength f_{frp} (MPa)	Ultimate tensile strain ε_{frp} (%)	Elastic modulus E_{frp} (GPa)
Aramid	0.200	2600	2.20	118.2	2390	1.86	128.5
S-glass	0.200	3040	3.50	86.9	3055	3.21	95.3

A total of 18 FRP tubes were prepared using a manual wet lay-up process by wrapping epoxy resin impregnated unidirectional fiber sheets around precision-cut high-density Styrafoam templates, which were removed prior to concrete casting. The FRP tubes were prepared using a single continuous fiber sheet and had a single 150-mm long overlap region. The material properties of the aramid and S-glass fiber sheets used to manufacture the FRP tubes are provided in Table 3. The table reports both the manufacturer-supplied fiber properties and the tensile tested FRP composite properties. The tensile properties of the FRP made from these fiber sheets were determined from flat coupon tests, where the loading was applied in accordance with ASTM D3039 [14].

The FRP tubes of the 12 specimens were manufactured using S-glass FRP (GFRP), and the tubes of the remaining six specimens were manufactured with aramid FRP (AFRP). The specimens with AFRP tubes and six of the specimens with GFRP tubes were cast with HSC, whereas the remaining six GFRP tube encased specimens were manufactures using NSC. The tubes of NSC and HSC specimens had two and four layers of FRP, respectively. These FRP layer arrangements were determined based on the understanding that the confinement demand of concrete increases with its strength [15-18]. Three nominally identical specimens were tested for each unique specimen configuration. The FRP-confined specimens were tested on the same day with their companion unconfined specimens, through which the test day unconfined concrete strengths (f'_{co}) reported in Table 2 were established.

2.2 Specimen Designation

The specimens in Tables 2 and 4 were labeled as follows: the first letter A, G or C represents the type of FRP (i.e., AFRP, GFRP or CFRP) and it is followed by the number of FRP layer; the second letter U is followed by the unconfined concrete strength in MPa; and the third letter D is followed by the age of concrete in days at the day of testing. Finally, the last number in the specimen designation (i.e., 1, 2 or 3) was used to make the distinction between three nominally identical specimens. For instance, A4-C73-D7-2 represents the second of the three nominally identical specimens, which were tested at 7 days of concrete age were and cast from a concrete mix with a 73 MPa unconfined concrete strength in an FRP tube manufactured with 4 layers of aramid fibers.

2.3 Instrumentation and Testing

T The specimens were tested under axial compression using a 5000-kN capacity universal testing machine. During the initial elastic stage of the behavior, the loading was applied with the load control set at 5 kN per second, whereas displacement control operated at 0.004 mm per second beyond the initiation of transition region until specimen failure. Prior to testing, all specimens were ground at both ends to ensure uniform distribution of the applied pressure, and load was applied directly to the concrete core using precision-cut high-strength steel plates with a 150 mm diameter.

The hoop strains of the specimens were measured using 12 unidirectional strain gauges placed at the mid-height around the circumference of specimens outside the overlap region. As illustrated in Figure 1, the axial strains of the confined specimens were measured using two

different methods: (i) four linear variable displacement transformers (LVDTs) mounted at each corner of the steel loading platens with a gauge length of 305 mm; and (ii) four LVDTs placed at the mid-height at a gauge length of 175 mm at 90° spacing along the circumference of specimens. The readings from the mid-height LVDTs were used to correct the full-height LVDT measurements at the early stages of loading, where additional displacements due to closure of the gaps in the setup were also recorded by the full-height LVDTs.

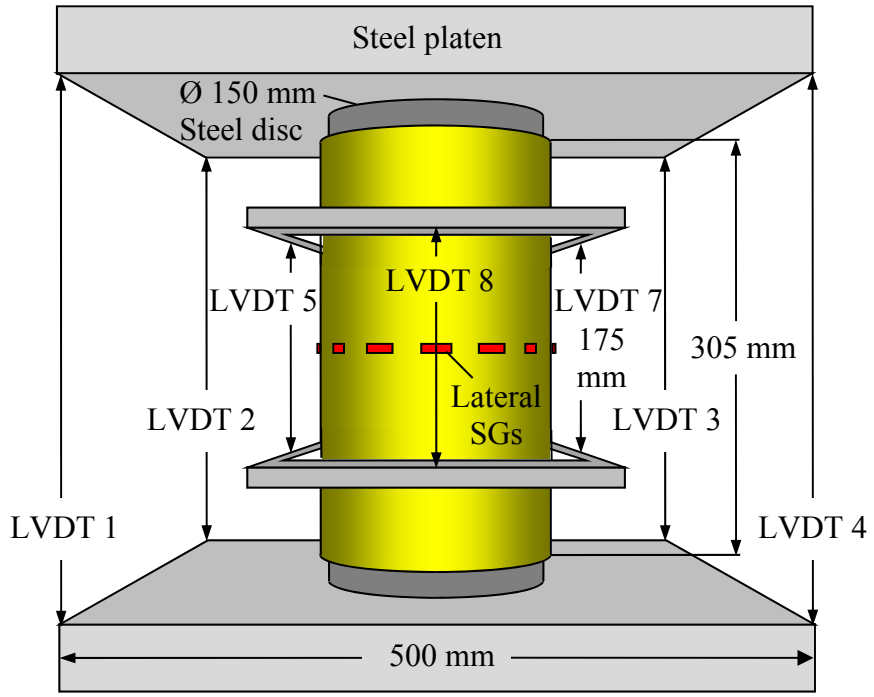

Figure 1. Test setup and instrumentation

3. TEST RESULTS AND DISCUSSION

3.1 Failure mode

The typical failure modes of the FRP-confined specimens tested at 7 and 28 days are illustrated in Figures 2 to 4. As can be seen from the photos, all of the specimens failed by the rupture of the FRP jackets. As illustrated in Figures 2(a) and 3(a), heterogenic microcrack formations were observed in the concretes of the 7-day old AFRP- and GFRP-confined HSC specimens at failure. On the other hand, as evident from Figures 2(b) and 3(b), the concrete in the companion 28-day old specimens exhibited larger cracks that were more localized. In the GFRP-confined NSC specimens shown in Figures 4(a) and (b), the change in the concrete cracking pattern from microcrack to marcocrack with an increase in concrete age are also evident, however the change is not as pronounced as those seen in the HSC specimens. The observed variations in the cracking patterns of concretes of same compressive strength suggest that the concrete brittleness increases with its age. This change in concrete brittleness with concrete age is more pronounced in higher strength concrete.

(a) (b)

Figure 2. Failure modes of AFRP-confined HSC specimens tested at: a) 7 days; and b) 28 days

(a) (b)

Figure 3. Failure modes of GFRP-confined HSC specimens tested at: a) 7 days; and b) 28 days

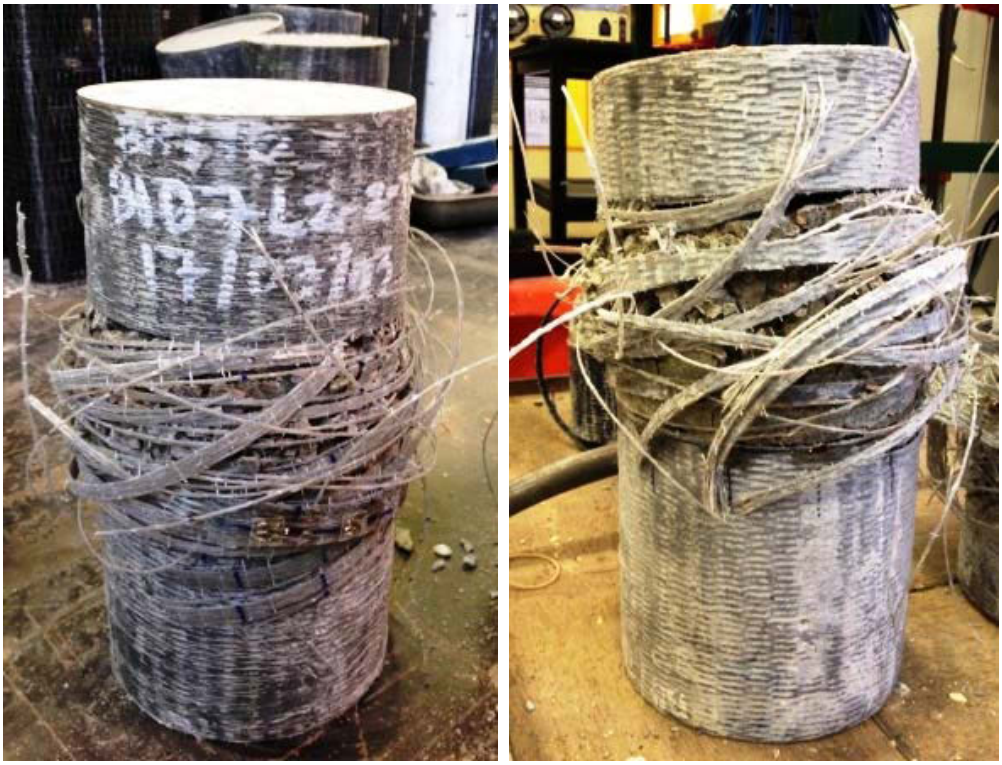

(a) (b)

Figure 4. Failure modes of GFRP-confined NSC specimens tested at: a) 7 days; and b) 28 days

3.2 Axial stress-strain and lateral strain-axial strain relationships

Figures 5(a) and 5(b) illustrate the different stages observed on a typical axial stress-strain curve and the corresponding lateral strain-axial strain curve of the specimens. The different stages marked on these curves were established based on the observed changes in the concrete expansion behavior, which is indicated by different tangential slopes of the corresponding regions shown in Figure 5(b), namely: linear elastic region, rapid expansion region, and stabilized dilation region. These regions matches the three different portions of the axial stress-strain curves shown in Figure 5(a), namely: first ascending portion, transition region, and second ascending branch.

The axial stress-strain curves of the AFRP-confined HSC, GFRP-confined HSC, and GFRP-confined NSC specimens are shown in Figures 6 to 8, respectively. As illustrated in the figures, the shape of stress-strain curves of both the 7-day and 28-day old specimens initiated with an ascending branch that was followed by a transition region, which connected the initial branch to a nearly straight-line second branch. As evident from the curved segments marked in Figures 6 to 8, there were significant differences in the radii of the transition regions of the 7-day and 28-day old specimens. Comparisons of Figures 6(a) and 6(b) and Figures 7(a) and 7(b) indicate that the transition radii of the 7-day old HSC specimens were larger than those of their 28-day old counterparts. For the NSC specimens, the change in the transition radii with concrete age was less pronounced but can still be seen from the comparison of Figure 8(a) and 8(b). The reduction in the transition radius with concrete age can be attributed to the change in the concrete cracking pattern from microcracks to macrocracks, as illustrated earlier in Figures 2 to 4.

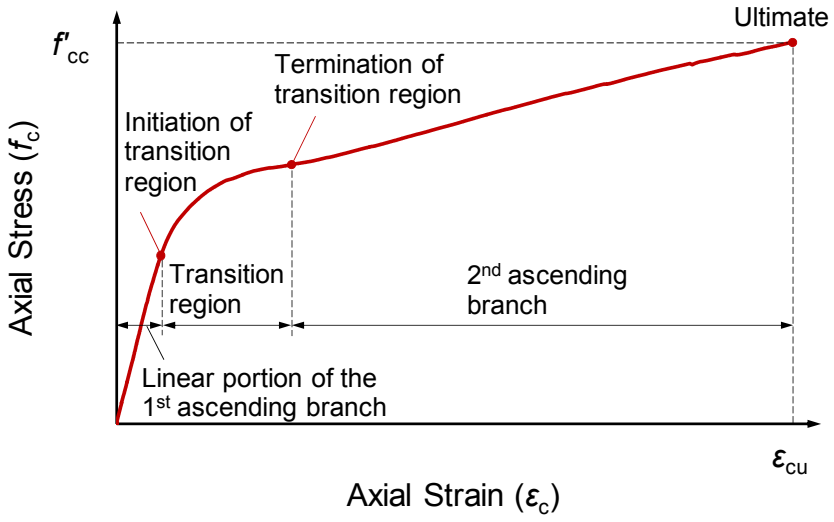

(a)

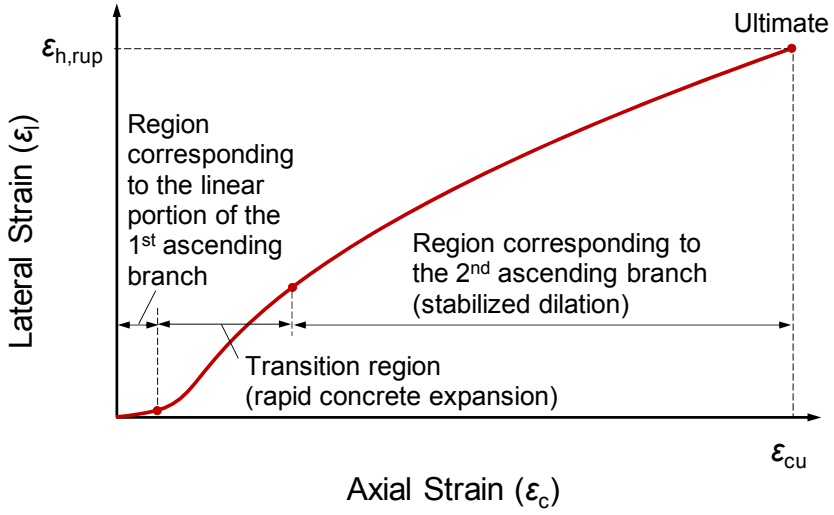

(b)

Figure 5. Illustration of different stages of: (a) axial stress-strain; and (b) lateral strain-axial strain curves of specimen

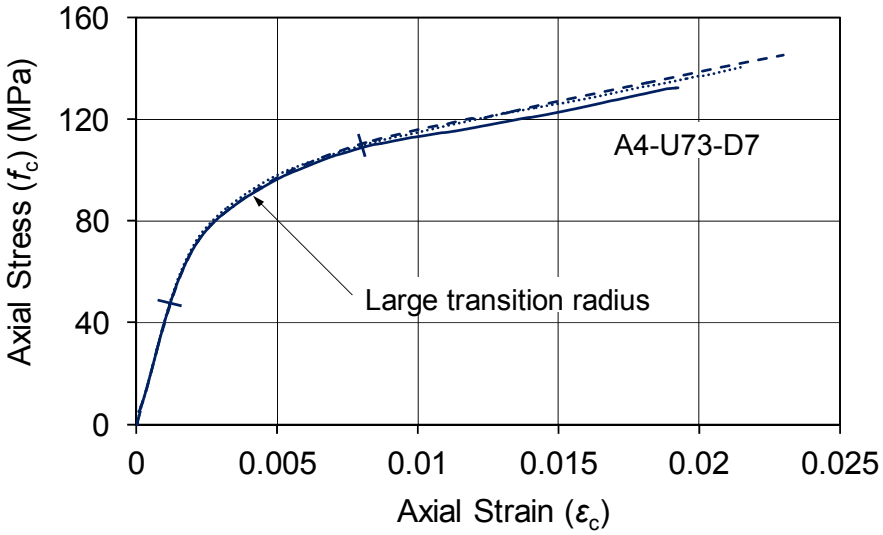

(a)

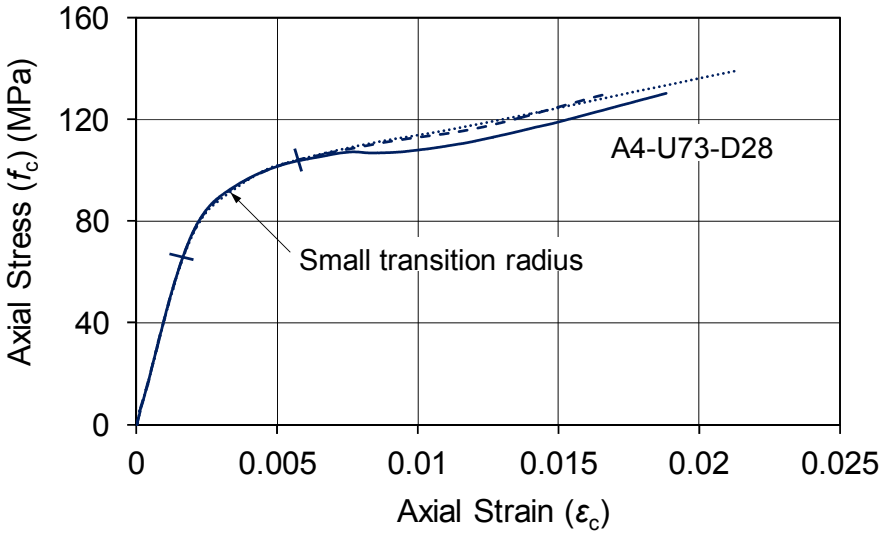

(b)

Figure 6. Axial stress-strain curves of AFRP-confined HSC specimens tested at: a) 7 days; and b) 28 days

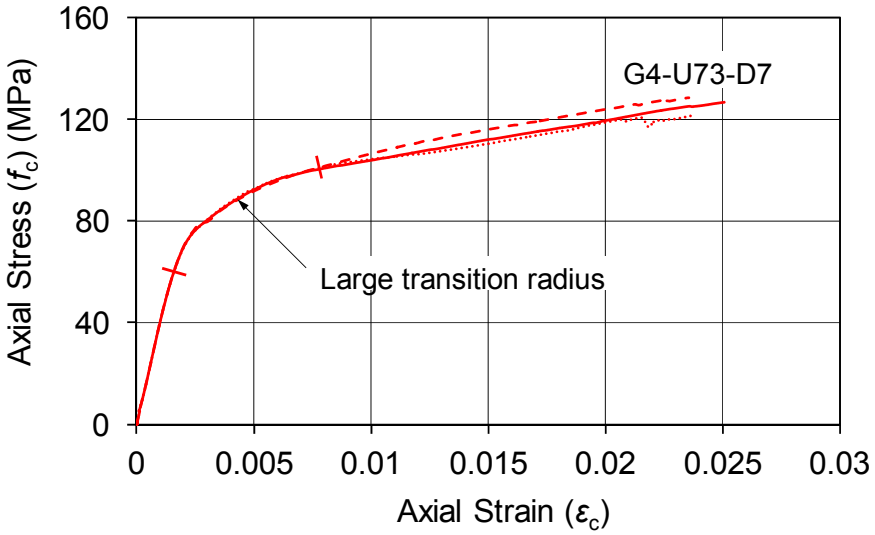

(a)

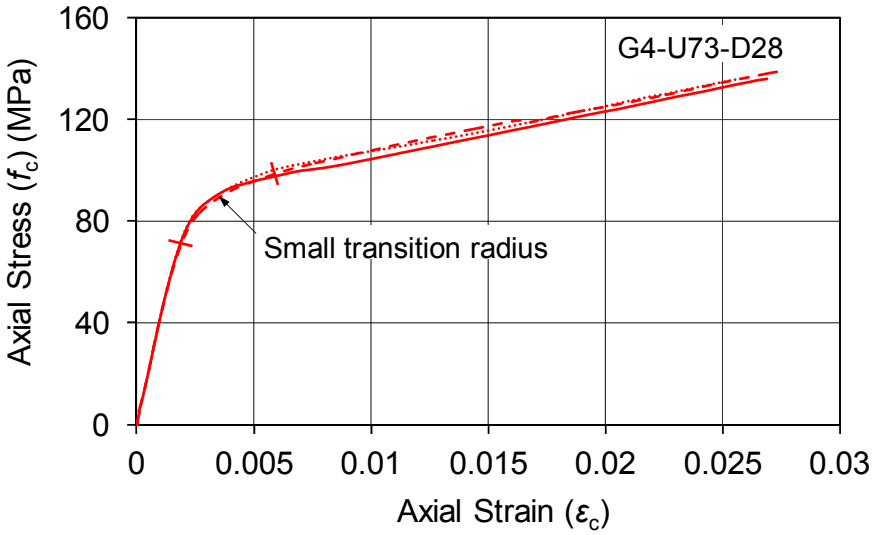

(b)

Figure 7. Axial stress-strain curves of GFRP-confined HSC specimens tested at: a) 7 days; and b) 28 days

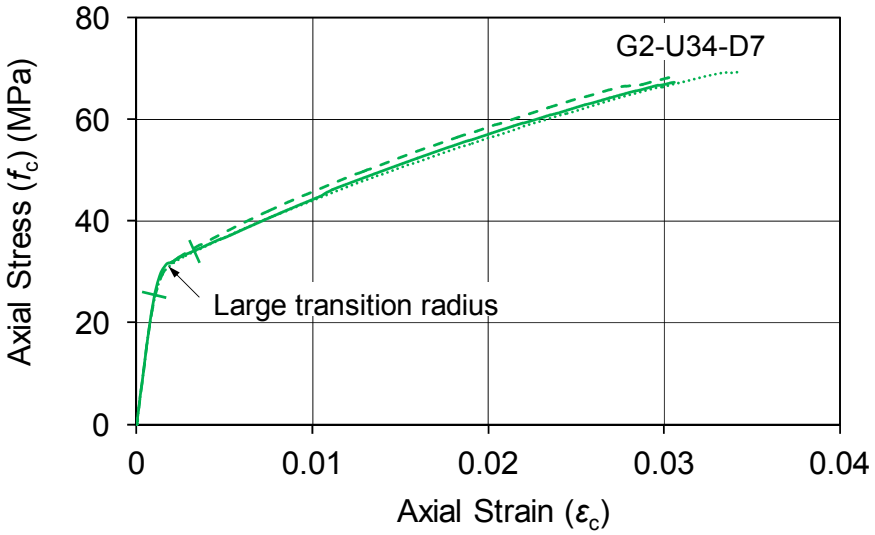

(a)

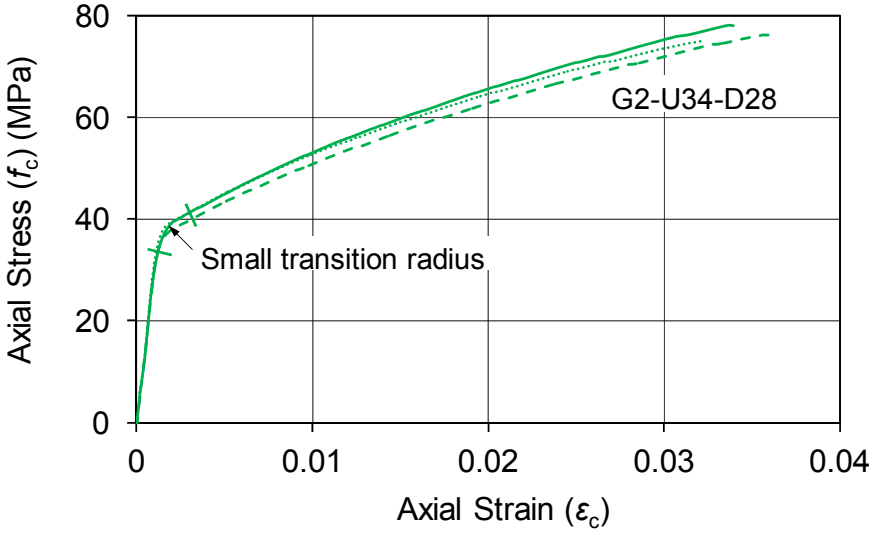

(b)

Figure 8. Axial stress-strain curves of GFRP-confined NSC specimens tested at: a) 7 days; and b) 28 days

The resulting influence of the change in concrete cracking pattern on the dilation behavior of concrete can be seen in the lateral strain-axial strain relationships shown in Figures 9 to 11. To enable an easier observation of these differences, the segments corresponding to the transition regions on the axial stress-strain curves are also marked on the companion lateral strain-axial strain curves in Figures 9 to 11. In addition, the average slope of the marked segment in each figure is indicated by the dash-dotted line. As evident from Figures 9 to 11, the curves of the 28-day old specimens exhibited higher tangential slopes within the marked segments compared to the curves of the 7-day old specimens. The increased tangential slope indicates that the concrete dilation rates of the 28-day old specimens are higher at the transition region as a result of the more rapid concrete expansion. This rapid concrete expansion can be attributed to the increased concrete crack size due to the change in cracking pattern from microcrack to macrocrack formation, as seen earlier from the failure modes of

the specimens in Figures 2 to 4. It can also be seen from Figures 9(b) to 11(b) that the 28-day old specimens experienced higher concrete dilation rates as a result of the change in concrete cracking pattern. This increased concrete dilation rates in turn resulted in smaller transition radii of the axial stress-strain curves shown earlier in Figures 6(b) to 8(b). The observations from Figures 6 to 11 indicate that, for concretes with the same strength, an increase in concrete age alters the cracking pattern and dilation rate of concrete, which in turn reduces the transition radius of the stress-strain curves.

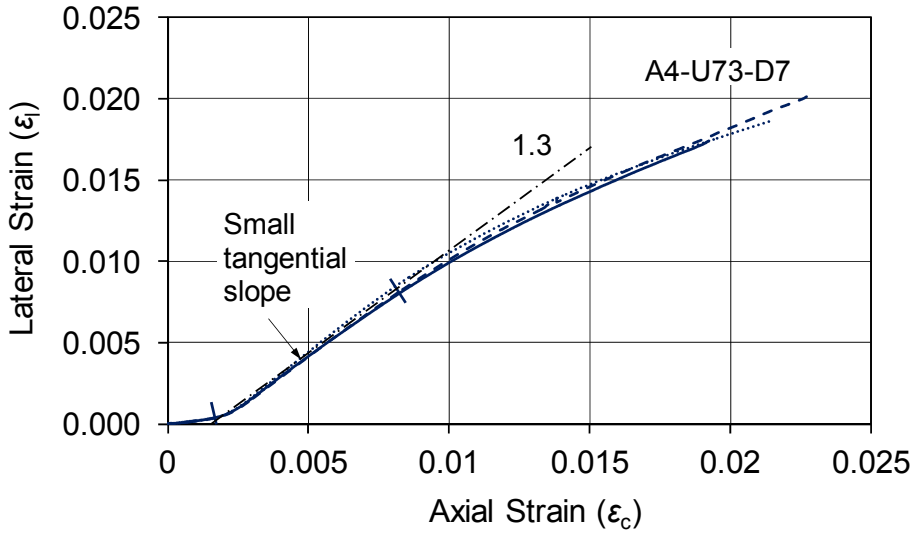

(a)

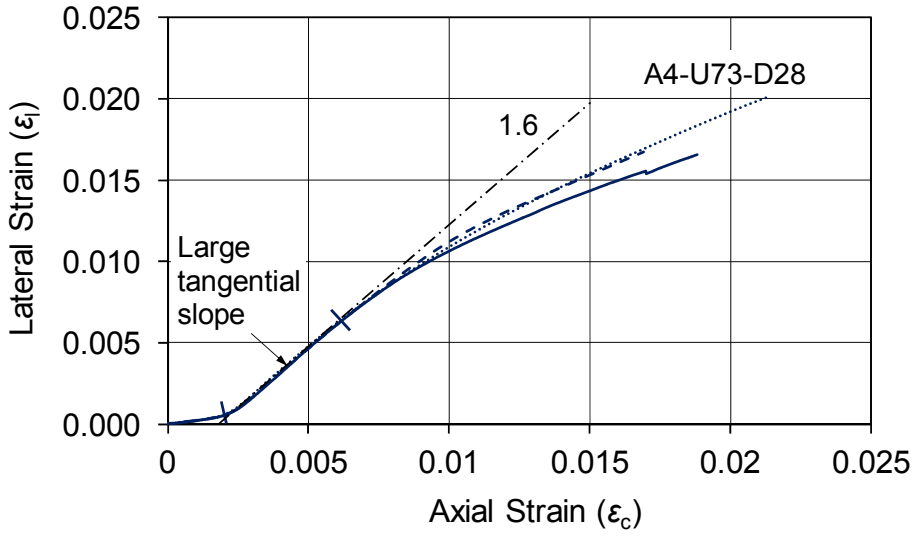

(b)

Figure 9. Lateral strain-axial strain curves of AFRP-confined HSC specimens tested at: a) 7 days; and b) 28 days

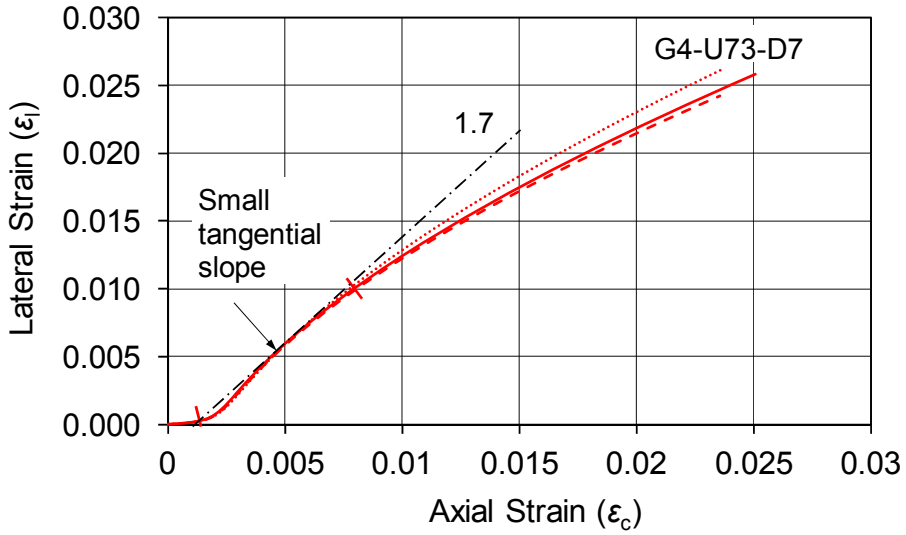

(a)

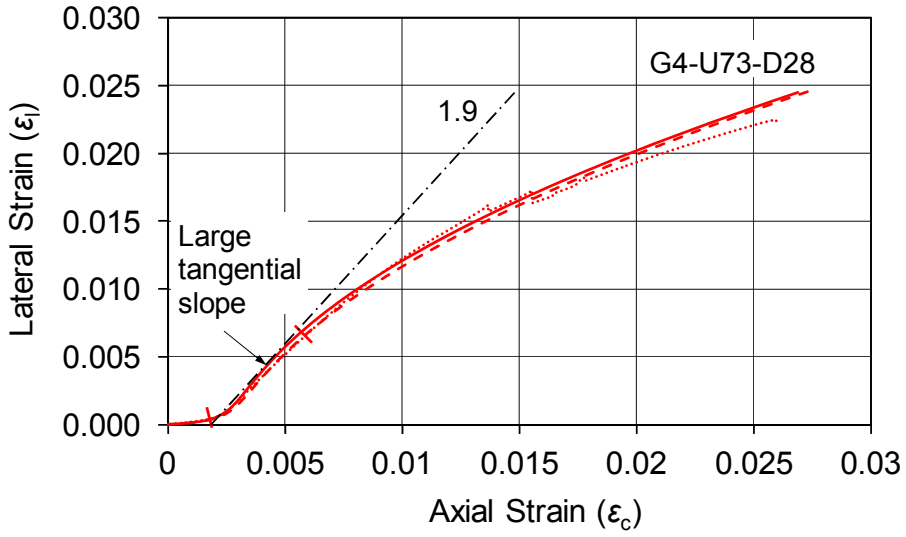

(b)

Figure 10. Lateral strain-axial strain curves of GFRP-confined HSC specimens tested at: a) 7 days; and b) 28 days

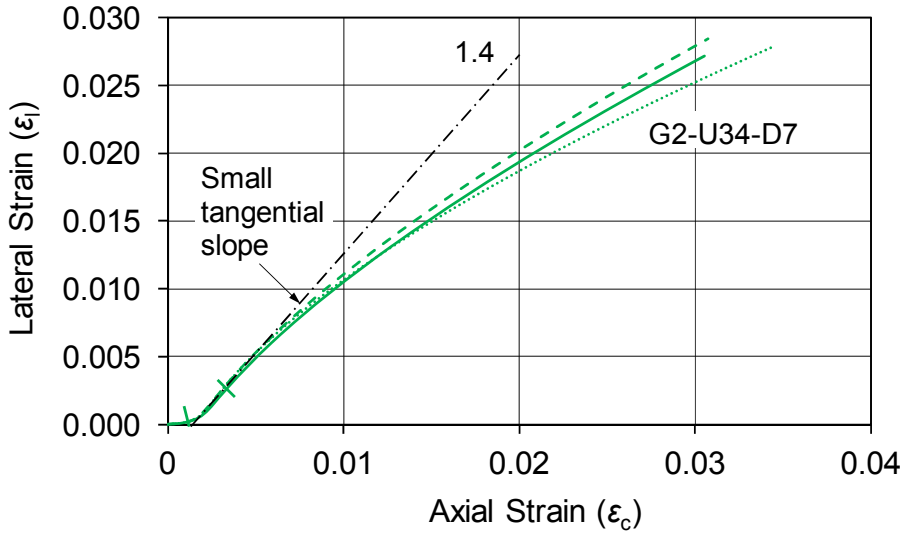

(a)

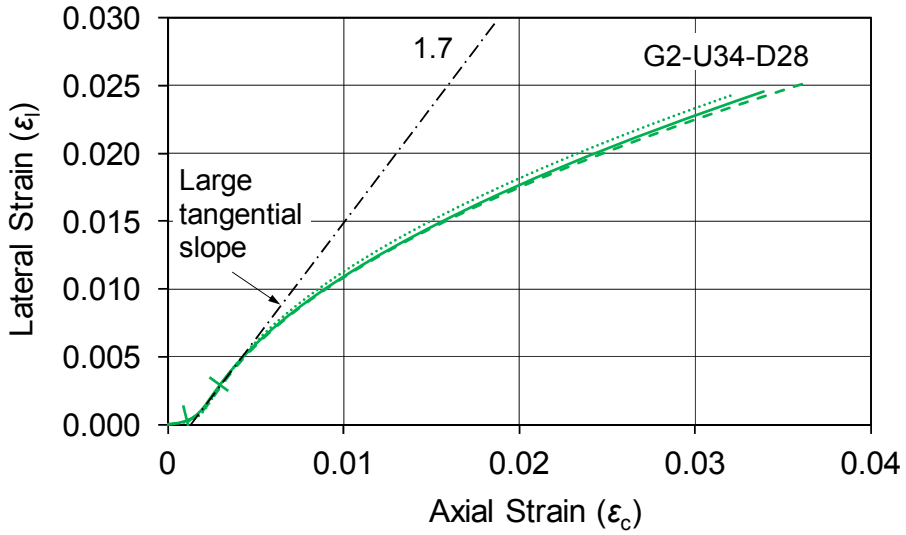

(b)

Figure 11. Lateral strain-axial strain curves of GFRP-confined NSC specimens tested at: a) 7 days; and b) 28 days

3.3 Ultimate conditions

The ultimate condition of FRP-confined concrete is often characterized as the ultimate axial stress and strain of concrete recorded at the rupture of the FRP jacket. This makes the relationship between the ultimate axial stress (f'_{cu}), ultimate axial strain (ε_{cu}) and hoop rupture strain ($\varepsilon_{h,rup}$) an important one. The test results of the FRP-confined specimens of the present study are given in Table 4, which include: the concrete age; compressive strength and ultimate axial strain of the specimens (f'_{cc} and ε_{cu}); hoop rupture strain ($\varepsilon_{h,rup}$); strength and strain enhancement ratios (f'_{cc}/f'_{co} and $\varepsilon_{cu}/\varepsilon_{co}$); and hoop strain reduction factor ($k_{\varepsilon,f}$). The hoop strain reduction factor ($k_{\varepsilon,f}$) of the confined specimens was calculated as the ratio of the hoop rupture strain ($\varepsilon_{h,rup}$) to ultimate tensile strain of the fiber (ε_f). The ultimate axial strain of confined concrete (ε_{cu}) reported in Table 4 was averaged from the four steel platen mounted LVDTs, with corrections supplied from the four mid-section LVDTs, as mentioned previously.

Table 4. Compression test results of confined specimens tested at different ages

Specimen	Concrete batch	Age (day)	f'_{cc} (MPa)	ε_{cu} (%)	$\varepsilon_{h,rup}$ (%)	f'_{cc}/f'_{co}	Avg. f'_{cc}/f'_{co}	$\varepsilon_{cu}/\varepsilon_{co}$	Avg. $\varepsilon_{cu}/\varepsilon_{co}$	$k_{\varepsilon,f}$	Avg. $k_{\varepsilon,f}$
A4-U73-D7-1			132.4	1.92	1.74	1.84		7.34		0.79	
A4-U73-D7-2	B1	7	145.1	2.30	2.04	2.02	1.94	8.79	8.11	0.93	0.86
A4-U73-D7-3			140.5	2.15	1.87	1.95		8.21		0.85	
A4-U73-D28-1			130.1	1.88	1.65	1.74		7.12		0.75	
A4-U73-D28-2	B2	28	130.5	1.69	1.67	1.74	1.78	6.40	7.21	0.76	0.81
A4-U73-D28-3			139.3	2.14	2.02	1.86		8.10		0.92	
G4-U73-D7-1			126.7	2.51	2.57	1.79		9.63		0.73	
G4-U73-D7-2	B3	7	128.4	2.36	2.44	1.81	1.77	9.05	9.25	0.70	0.72
G4-U73-D7-3			121.3	2.37	2.57	1.71		9.09		0.73	
G4-U73-D28-1			136.0	2.69	2.45	1.84		10.21		0.70	
G4-U73-D28-2	B4	28	138.7	2.74	2.46	1.87	1.85	10.40	10.17	0.70	0.68
G4-U73-D28-3			136.3	2.61	2.23	1.84		9.91		0.64	
G2-U34-D7-1			67.3	3.06	2.72	2.04		13.93		0.78	
G2-U34-D7-2	B5	7	68.7	3.08	2.97	2.08	2.07	14.02	14.54	0.85	0.80
G2-U34-D7-3			69.3	3.44	2.73	2.10		15.66		0.78	
G2-U34-D28-1			78.1	3.39	2.45	2.25		15.26		0.70	
G2-U34-D28-2	B6	28	76.3	3.63	2.48	2.20	2.20	16.34	15.38	0.71	0.71
G2-U34-D28-3			75.1	3.23	2.49	2.16		14.54		0.71	

Table 5. Summary of referenced specimen results in Figures 12-15

Group	Paper	Number of specimens	Concrete age (day)	f'_{co} (MPa)	Dimensions of cylinder (mm)	Details of FRP confinement
G6-U85-D28	Lim and Ozbakkaloglu [27]	3	28	84.5	152.5×305	6 layers of GFRP
G6-U85-D61	Lim and Ozbakkaloglu [27]	3	61	84.8		
C5-U103-D77	Vincent and Ozbakkaloglu [17]	3	77	102.5	152×305	5 layers of CFRP
C5-U103-D102	Vincent and Ozbakkaloglu [17]	3	102	102.5		
A6-U110-D48	Ozbakkaloglu and Vincent [16]	6	47-48	104.5	152.5×305	6 layers of AFRP
	& Lim and Ozbakkaloglu [27]	3	48	109.8		
A6-U110-D358	Lim and Ozbakkaloglu [27]	3	358	113.5		
C2-C41-D450	Saenz and Pantelides [1]	3	439-450	40.3	152×304	2 layers of CFRP
C2-C41-D900	Saenz and Pantelides [1]	3	886-900	41.7		
G1-C41-D450	Saenz and Pantelides [1]	3	439-450	40.3	152×304	1 layer of GFRP
G1-C41-D900	Saenz and Pantelides [1]	3	886-900	41.7		

3.3.1 Strength and strain enhancements

To illustrate the influence of concrete age on the ultimate condition of FRP-confined concrete, Figure 12(a) and 13(a) show the variation of the strength and strain enhancement ratios (f'_{cc}/f'_{co} and $\varepsilon_{cu}/\varepsilon_{co}$) with concrete age for specimens of the present study. Comparison of the first two groups of specimens in Figures 12(a) and 13(a) indicates that both the strength and strain enhancement ratios (f'_{cc}/f'_{co} and $\varepsilon_{cu}/\varepsilon_{co}$) of the 7-day old AFRP-confined HSC specimens were slightly higher than that of their 28-day old counterparts. As opposed to the AFRP-confined specimens, the 7-day old GFRP-confined HSC and NSC specimens had slightly lower strength and strain enhancement ratios (f'_{cc}/f'_{co} and $\varepsilon_{cu}/\varepsilon_{co}$) than their 28-day old counterparts, as evident from the comparison of the remaining four groups of specimens in Figures 12(a) and 13(a). To gain further insight into this influence, a large experimental test database that was assembled through an extensive review of the literature [18, 19] was also studied in the analysis. Specimen groups were prepared by sorting specimens in the database according to the specimen unconfined concrete strengths, geometrical dimensions, types of FRP material, amount of FRP confinement, and concrete age. These specimen groups, as summarized in Table 5, were sorted such that the concrete age was the only variable with the other parameters remaining nearly constant. The strength and strain enhancement ratios (f'_{cc}/f'_{co} and $\varepsilon_{cu}/\varepsilon_{co}$) of these specimen groups are presented in Figures 12(b-c) and 13(b-c), respectively. In Figure 12(b), a slight reduction in the strength enhancement ratios (f'_{cc}/f'_{co}) with concrete age can be seen in the specimen group tested at 77 and 102 days, but no notable change is evident in the specimen groups tested at 28 and 61 days and 48 and 358 days. Figure 13(b) illustrates that the strain enhancement ratios ($\varepsilon_{cu}/\varepsilon_{co}$) of all of these specimen groups decreased slightly with an increase in concrete age. Furthermore, as can be seen in Figures 12(c) and 13(c), both the strength and strain enhancement ratios (f'_{cc}/f'_{co} and $\varepsilon_{cu}/\varepsilon_{co}$) decreased with an increase in concrete age from 450 and 900 days. These observations indicate that, for specimens with up to 28 days of concrete age, the concrete age does not have a notable influence on the ultimate condition of FRP-confined concrete, and the slight differences observed in the test results appears to be mainly a margin of scatter among the results of different specimen groups. On the other hand, the results suggest that the strength and strain enhancements seen in FRP-confined concrete tends to decrease with an increase in concrete age for specimens with concrete ages of over 450 days. This effect is less pronounced for specimens with concrete ages between 28 to 450 days.

To validate the observed influence of concrete age on the ultimate condition of FRP-confined concrete the results in the large experimental test database [18, 19] was further studied. Out of 1063 available results, 339 and 329 datasets that were reported with concrete age details were used respectively to investigate the influence of concrete age on compressive strength (f'_{cc}) and ultimate axial strain (ε_{cu}). Figures 14(a) and 14(b), respectively, show the observed variations in the strength and strain enhancement coefficients (k_1 and k_2) with concrete age (d). The strength and strain enhancement coefficients (k_1 and k_2) shown in Fig. 14, which represent the level of increase in the compressive strength (f'_{cc}) and ultimate axial strain (ε_{cu}) with an increase in the level of confinement, were calculated using the model proposed by Ozbakkaloglu and Lim [18]. As can be seen in Fig. 14, both k_1 and k_2 exhibit trendlines with a very shallow descending slope. As a result, the ultimate condition of FRP-confined concrete

is not particularly sensitive to the variation in the concrete age in the short-term. However, the said trend results in slightly lower compressive strengths and ultimate axial strains of specimens with higher concrete ages when the longer term behavior is considered.

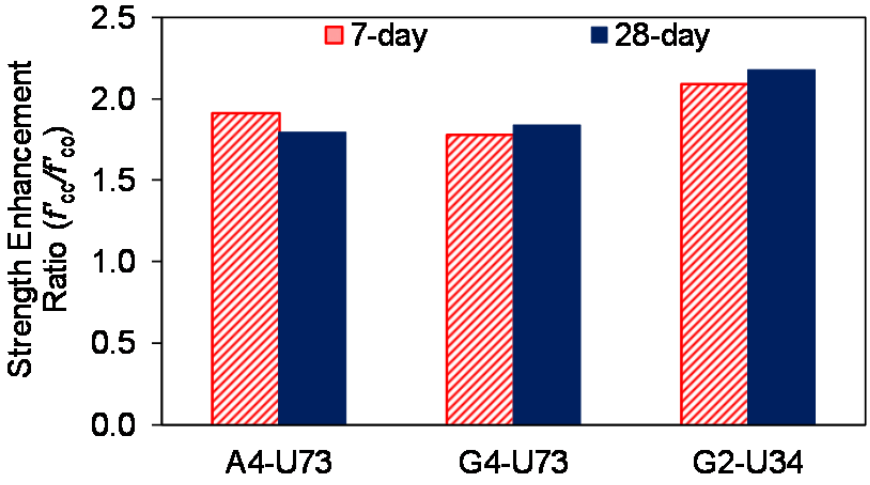

(a)

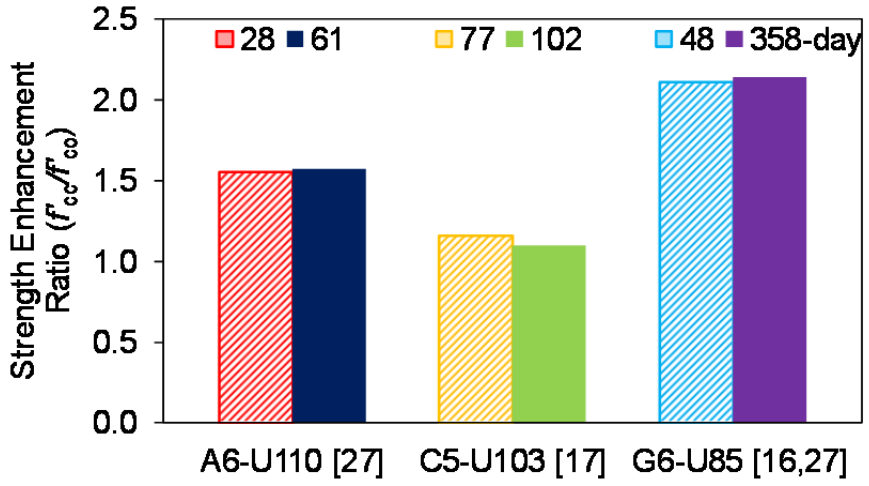

(b)

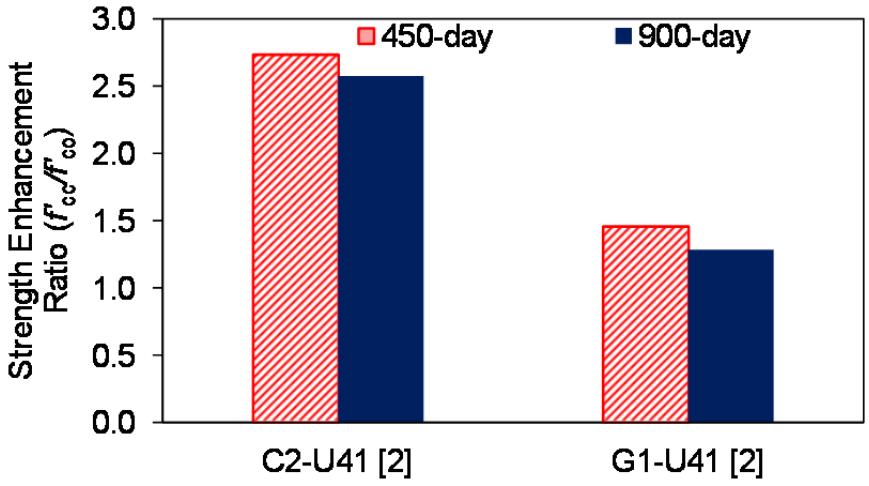

(c)

Figure 12. Variations of strength enhancement ratio (f'_{cc}/f'_{co}) with concrete age: (a) 7 to 28 days; (b) 28 to 358 days; and (c) 450 to 900 days

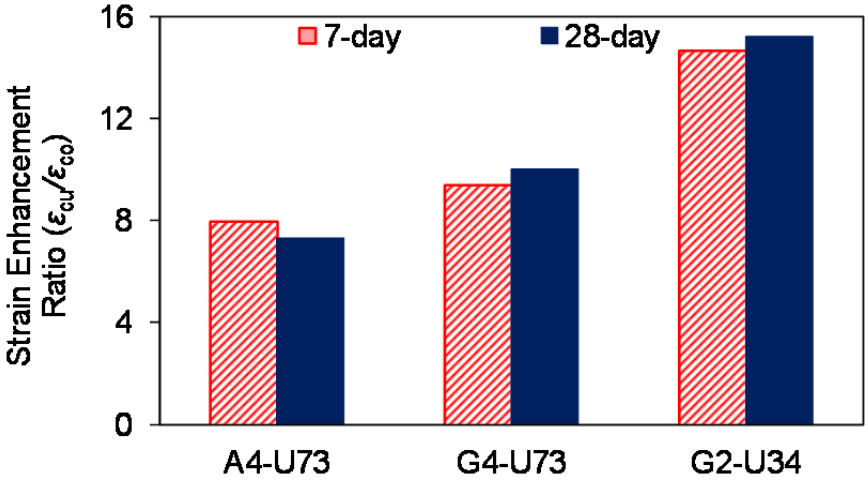

(a)

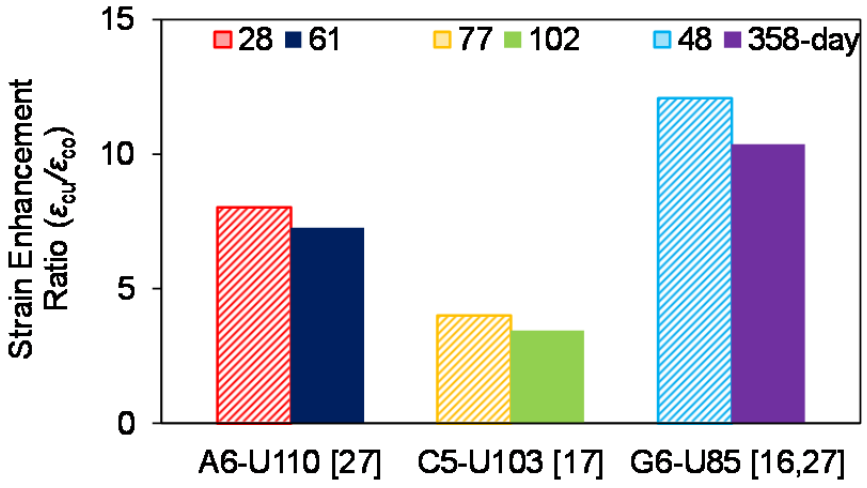

(b)

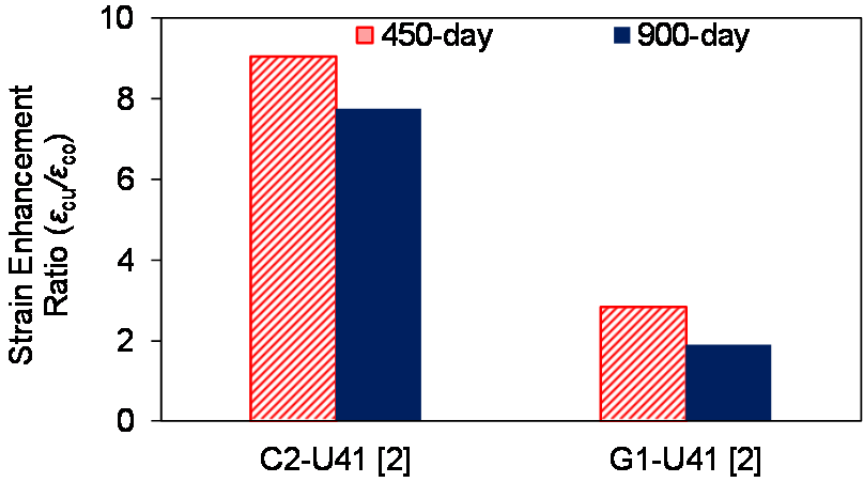

(c)

Figure 13. Variations of strain enhancement ratio ($\varepsilon_{cu}/\varepsilon_{co}$) with concrete age: (a) 7 to 28 days; (b) 28 to 358 days; and (c) 450 to 900 days

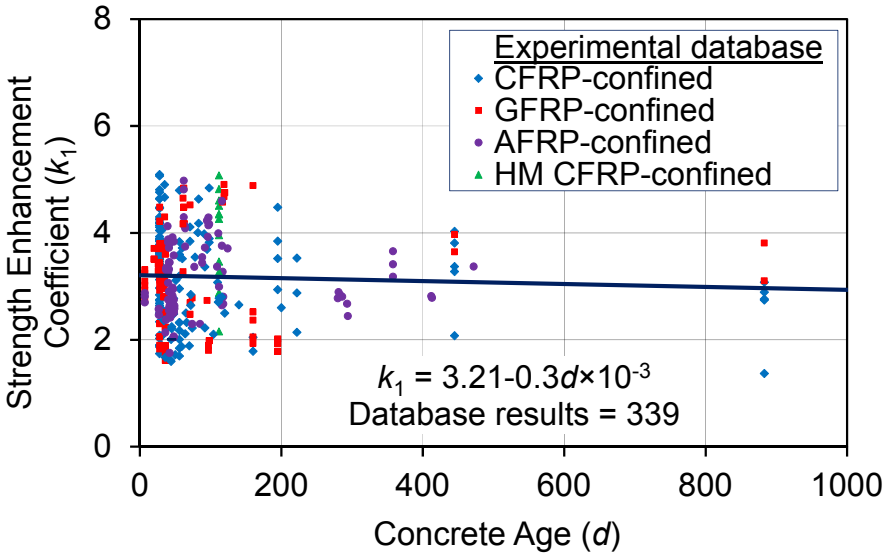

(a)

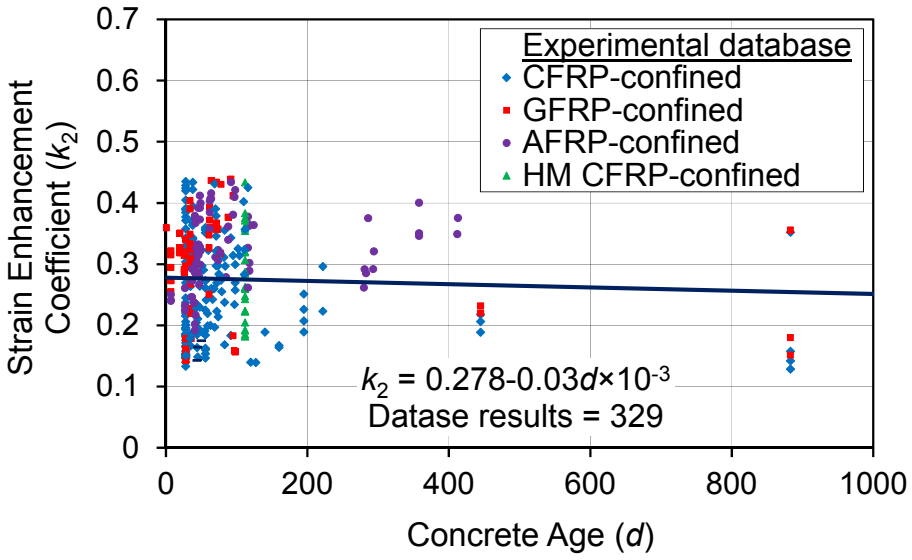

(b)

Figure 14. Variations of: (a) strength enhancement coefficient (k_1); and (b) strain enhancement coefficient (k_2) with concrete age (d)

3.3.2 Hoop strain reduction

It has been discussed previously in a number of studies [15-18, 20-25] that the ultimate hoop strain ($\varepsilon_{h,rup}$) reached in the FRP jacket is often smaller than the ultimate tensile strain of the fibers (ε_f), which necessitates the use of a strain reduction factor ($k_{\varepsilon,f}$) in the determination of the actual confining pressures. The recorded hoop rupture strains ($\varepsilon_{h,rup}$) and calculated strain reduction factors (i.e., $k_{\varepsilon,f} = \varepsilon_{h,rup}/\varepsilon_f$) of the specimens in the present study are provided in Table 4. It was recently demonstrated by the authors that the hoop rupture strain of FRP jacket reduces with an increase in the concrete strength [15, 18, 26]. A similar phenomenon was observed in

the specimens of the current study, which is evident from the comparison of the results of the 28-day old GFRP-confined HSC and NSC specimens (Batches B4 and B6) that shows a reduction in the recorded $k_{\varepsilon,f}$ values with an increase in unconfined concrete strength (f'_{co}).

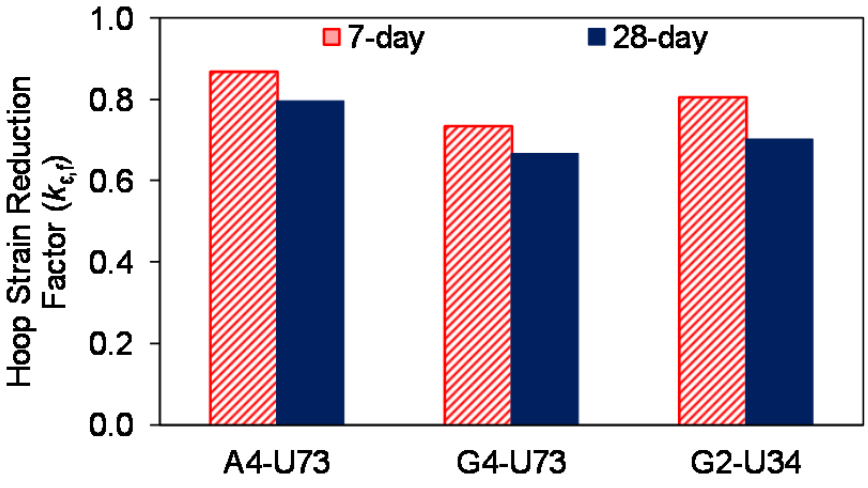

(a)

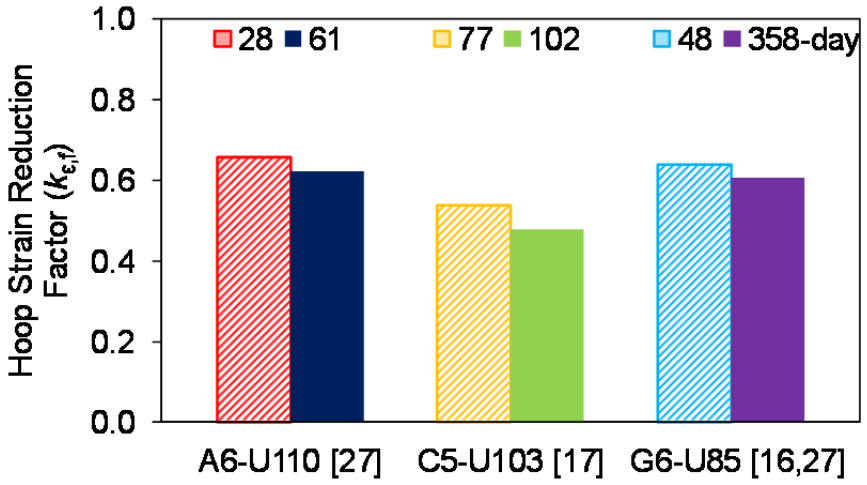

(b)

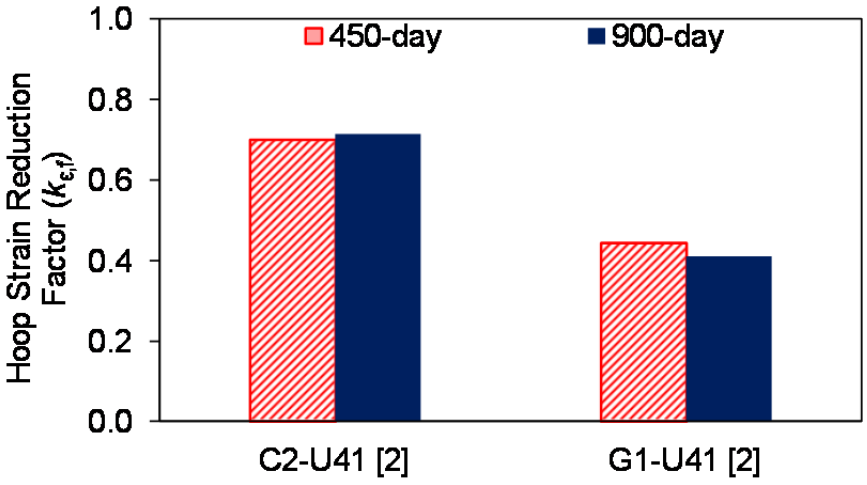

(c)

Figure 15. Variations of hoop rupture strain reduction factor ($k_{\varepsilon,f}$) with concrete age: (a) 7 to 28 days; (b) 28 to 358 days; and (c) 450 to 900 days

The results shown in Table 4 also indicate that the hoop rupture strain of FRP jacket is influenced by the age of concrete. Figure 15 shows the variation of $k_{\varepsilon,f}$ values with concrete age of the specimen groups tested in the present and the existing studies [2, 16, 17, 27]. As illustrated in Figure 15(a), the test results of the 7-day and 28-day old specimens with comparable unconfined concrete strength (f'_{co}) show that $k_{\varepsilon,f}$ decreased with an increase in concrete age. This reduction in $k_{\varepsilon,f}$ became less pronounced with a further increase in concrete age from 28 to 358 days, as illustrated in Figure 15(b). In Figure 15(c), no notable trend of the variation of $k_{\varepsilon,f}$ values can be seen from the change of concrete age from 450 to 900 days. These observations suggest that, for concretes of same strength, an increase in concrete age results in a reduction in the hoop rupture strain of FRP jackets. However, this effect becomes less pronounced when the concrete age reaches a certain threshold. This reduction can be attributed to the previously discussed influence of concrete age on concrete cracking pattern and resulting brittleness, as was illustrated in Figures 2 to 4. As a result of the change in the concrete cracking pattern from heterogenic microcracks to localized macrocracks, the hoop strain distribution in the circumference of the FRP jacket becomes less uniform, which results in a lower recorded average rupture strain. This change in the concrete cracking pattern, however, becomes less pronounced with a further increased concrete age, as can be seen from the more subtle changes in the $k_{\varepsilon,f}$ values of the higher age specimens in Figures 15(b) and 15(c), which suggests that concrete brittleness remains unchanged after a certain concrete age.

3.4 Axial strain measurement methods

As was previously discussed in Ozbakkaloglu and Lim [19], the recorded ultimate axial strains (ε_{cu}) are highly sensitive to the type of instrumentation used in their measurement. In the present study, factors causing difference between the axial strains obtained from LVDTs mounted at mid-height of the specimens (AML) and LVDTs mounted along the entire height of the specimens (AFL) were experimentally investigated. An example comparison is shown in Figure 16, which illustrates the typical stress-strain curves of the NSC and HSC specimens obtained using the two different measurement methods. As evident from the figure, for the NSC specimens, the difference between the strains obtained from the two measurement methods is minimal. On the other hand, this difference is significant for the HSC specimens. Table 6 presents the ultimate axial strains (ε_{cu}) of specimens recorded using the two measurement methods. Figure 17(a) shows the comparison of the difference between the axial strains obtained from LVDTs mounted at mid-height of the specimens (AML) and those mounted along the entire height of the specimens (AFL), defined as AML/AFL ratio, with a change in unconfined concrete strength (f'_{co}). As evident from the figure, the difference between AML and AFL increases with an increase in unconfined concrete strength (f'_{co}). This, once again, can be attributed to the change in the concrete cracking pattern from microcracks to macrocracks as a result of the increased concrete brittleness with an increase in concrete strength. Detailed discussions on this phenomenon can be found in Ozbakkaloglu and Lim [19] and Lim and Ozbakkaloglu [27].

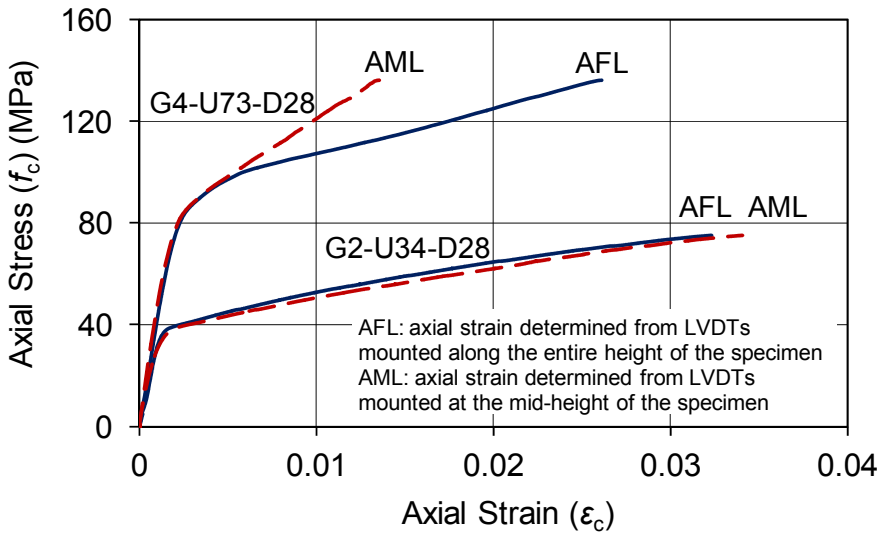

Figure 16. Influence of instrumentation arrangements on axial stress-strain curves

Table 6. Comparison of axial strains measured by different methods

Specimen	Concrete batch	Average f'_{co} (MPa)	Average ε_{cu} (%)		AML/ AFL
			AFL	AML	
A4-U73-D7	B1	70.0	2.12	1.65	0.78
A4-U73-D28	B2	74.9	1.90	1.15	0.61
G4-U73-D7	B3	69.5	2.41	1.33	0.55
G4-U73-D28	B4	74.1	2.68	1.39	0.52
G2-U34-D7	B5	32.3	3.19	3.23	1.01
G2-U34-D28	B6	34.7	3.42	3.53	1.03

AFL: axial strain determined from LVDTs mounted along the entire height of the specimen
AML: axial strain determined from LVDTs mounted at the mid-height of the specimen

Closer investigation of the result of the present study indicates that the AML/AFL ratio is also influenced by the age of concrete. This is evident from Figure 17(b), which shows that the AML/AFL ratio reduces slightly with an increase in the age of the HSC specimens. This variation in the AML/AFL ratio can also be attributed to the change in the concrete cracking pattern [19, 27], with larger crack formations observed in specimens with a higher age, as was previously shown in Figures 2 and 3. These observations indicate that both the unconfined concrete strength and concrete age of FRP-confined concrete influence the concrete cracking behavior, which in turn affect the relative measurements obtained from the two axial strain measurement method. Therefore, when reporting results of experimental studies it is important to specify the type of instrumentation used in the measurement of axial strains to allow an accurate interpretation of the reported strain data.

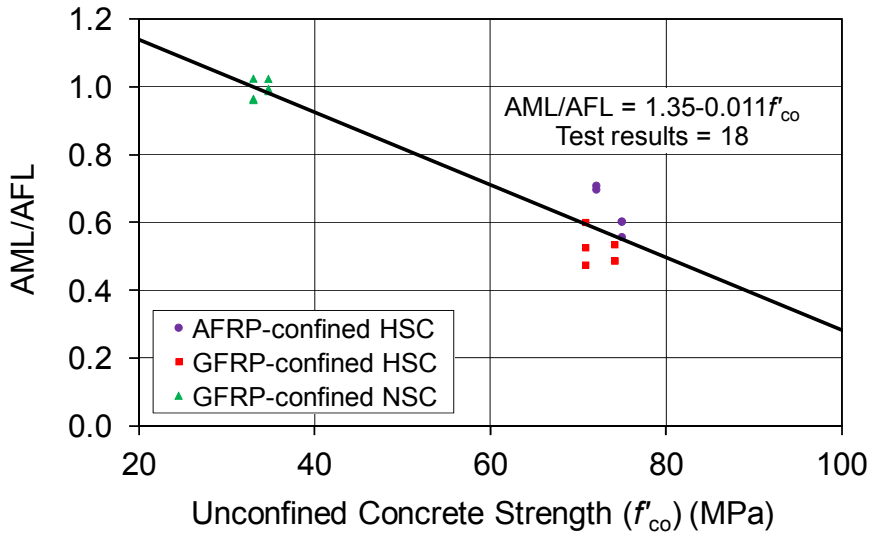

(a)

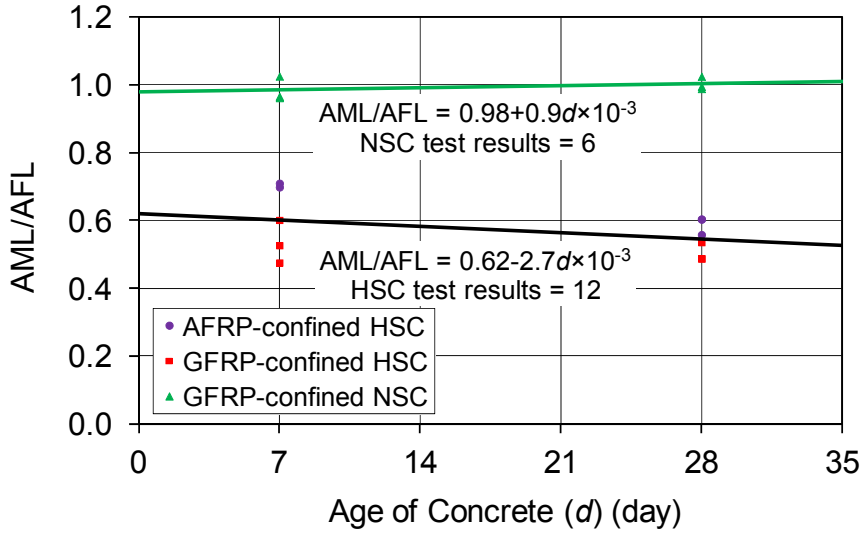

(b)

Figure 17. Variation of AML/AFL ratio with: (a) unconfined concrete strength (f'_{co}); and (b) age of concrete (d)

4. CONCLUSIONS

This paper has presented the results of an experimental study on the influence of concrete age on the axial compressive behavior of FRP-confined NSC and HSC. Based on the results and discussions presented in the paper, the following conclusions can be drawn:

1. For a given unconfined concrete strength, the change in concrete age does not significantly alter the ultimate condition of FRP-confined concrete with a concrete age up to 28 days. On the other hand, in the longer term, the compressive strength and the ultimate axial strain of FRP-confined concrete tend to decrease slightly with an increase in the concrete age.
2. The transition regions of stress-strain curves of FRP-confined concrete are observed to be sensitive to the change in concrete age, with specimens tested at a higher age exhibiting curves with smaller transition radii. This observed change has been shown to be a result of the change in the concrete cracking pattern, from microcrack to macrocrack formation,

as the concrete age increases. This change in the cracking pattern results in a more rapid concrete expansion and hence increases the concrete dilation rate at the transition region.

3. The hoop rupture strains of FRP jackets decrease with an increase in concrete strength. Furthermore, in specimens with similar unconfined concrete strengths, the hoop rupture strain of FRP also decreases with an increase in concrete age. However, this effect becomes less pronounced when the concrete age reaches a certain threshold.
4. The difference between the axial strains obtained from LVDTs mounted at mid-height of the specimen (AML) and those mounted along the entire specimen height (AFL) increases with an increase in the concrete strength. As a result, a significant difference exists between AML and AFL of HSC specimens. For the HSC specimens with similar unconfined concrete strengths, this difference tends to further increase with an increase in the concrete age. On the other hand, no notable difference exists in the axial strains of NSC specimens obtained from these two measurement methods.

REFERENCES

1. Toutanji, H.A., (1999). "Durability characteristics of concrete columns confined with advanced composite materials." *Composite Structures,* 44(2-3), 155-161.
2. Saenz, N. and Pantelides, C.P., (2006). "Short and medium term durability evaluation of FRP-confined circular concrete." *Journal of Composites for Construction,* 10(3), 244-153.
3. Walker, R.A. and Karbhari, V.M., (2007). "Durability based design of FRP jackets for seismic retrofit." *Composite structures,* 80(4), 553-568.
4. Erdil, B., Akyuz, U., and Yaman, I.O., (2012). "Mechanical behavior of CFRP confined low strength concretes subjected to simultaneous heating-cooling cycles and sustained loading." *Materials and Structures,* 45(1-2), 223-233.
5. Hadi, M.N.S. and Louk Fanggi, B.A., (2012). "Behaviour of FRP confined concrete cylinders under different temperature exposure." *Proceedings of the 6th International Conference on Bridge Maintenance, Safety and Management*, Stresa, Lake Maggiore, Italy.
6. Robert, M. and Fam, A., (2012). "Long-Term Performance of GFRP Tubes Filled with Concrete and Subjected to Salt Solution." *Journal of Composites for Construction,* 16(2), 217-224.
7. Naguib, W. and Mirmiran, A., (2002). "Time-dependent behavior of fiber-reinforced polymer-confined concrete columns under axial loads." *ACI Structural Journal,* 99(2), 142-148.
8. Theriault, M., Pelletier, M.A., Khayat, K., and Al Chami, G., (2003). "Creep performance of CFRP confined concrete cylinders." *Proceedings of the 6th International Symposium on FRP Reinforcement for Concrete Structures*, Singapore.
9. Berthet, J.F., Ferrier, E., Hamelin, P., Al Chami, G., Theriault, M., and Neale, K.W., (2006). "Modelling of the creep behavior of FRP-confined short concrete columns under compressive loading." *Materials and Structures,* 39(1), 53-62.
10. Kaul, R., Ravindrarajah, R.S., and Smith, S.T., (2006). "Deformational behavior of FRP confined concrete under sustained compression." *Proceedings of the 3rd International Conference on FRP Composites in Civil Engineering*, Miami, Florida.
11. Demir, C., Kolcu, K., and Ilki, A., (2010). "Effects of loading rate and duration on axial behavior of concrete confined by fiber-reinforced polymer sheets." *Journal of Composites for Construction,* 14(2), 146-151.
12. Wang, Y.F., Ma, Y.S., and Zhou, L., (2011). "Creep of FRP-wrapped concrete columns with or without fly ash under axial load." *Construction and Building Materials,* 25(2), 697-704.
13. Lim, J.C. and Ozbakkaloglu, T., (2014). "Stress-strain model for normal- and light-weight concretes under uniaxial and triaxial compression." *Construction and Building Materials*, 71, 492-509.
14. ASTM-D3039, (2008). "Standard test method for tensile properties of polymer matrix composite materials." *D3039/D3039M-08*, West Conshohocken, PA.
15. Ozbakkaloglu, T. and Akin, E., (2012). "Behavior of FRP-confined normal- and high-strength concrete under cyclic axial compression." *Journal of Composites for Construction, ASCE,* 16(4), 451-463.
16. Ozbakkaloglu, T. and Vincent, T., (2013). "Axial compressive behavior of circular high-strength concrete-filled FRP tubes." *Journal of Composites for Construction, ASCE,* 18(2), 04013037.

17. Vincent, T. and Ozbakkaloglu, T., (2013). "Influence of concrete strength and confinement method on axial compressive behavior of FRP-confined high- and ultra high-strength concrete." *Composites Part B,* 50, 413–428.
18. Lim, J.C. and Ozbakkaloglu, T., (2014). "Confinement model for FRP-confined high-strength concrete." *Journal of Composites for Construction, ASCE,* 17(5), 1-19.
19. Ozbakkaloglu, T. and Lim, J.C., (2013). "Axial compressive behavior of FRP-confined concrete: Experimental test database and a new design-oriented model." *Composites Part B,* 55, 607-634.
20. Harries, K.A. and Carey, S.A., (2003). "Shape and "gap" effects on the behavior of variably confined concrete." *Cement and Concrete Research,* 33(6), 881-890.
21. De Lorenzis, L. and Tepfers, R., (2003). "Comparative study of models on confinement of concrete cylinders with fiber-reinforced polymer composites." *Journal of Composites for Construction,* 7(3), 219-237.
22. Lam, L. and Teng, J.G., (2004). "Ultimate condition of fiber reinforced polymer-confined concrete." *Journal of Composites for Construction, ASCE,* 8(6), 539-548.
23. Ozbakkaloglu, T., Lim, J.C., and Vincent, T., (2013). "FRP-confined concrete in circular sections: Review and assessment of stress–strain models." *Engineering Structures,* 49, 1068–1088.
24. Vincent, T. and Ozbakkaloglu, T., (2013). "Influence of fiber orientation and specimen end condition on axial compressive behavior of FRP-confined concrete." *Construction and Building Materials,* 47, 814-826.
25. Lim, J.C. and Ozbakkaloglu, T., (2014). "Lateral strain-to-axial strain relationship of confined concrete." *Journal of Structural Engineering, ASCE,* Doi: 10.1061/(ASCE)ST.1943-541X.0001094.
26. Lim, J.C. and Ozbakkaloglu, T., (2014). "Hoop strains in FRP-confined concrete columns: Experimental observations." *Materials and Structures,* Doi: 10.1617/s11527-014-0358-8.
27. Lim, J.C. and Ozbakkaloglu, T., (2014). "Influence of silica fume on stress-strain behavior of FRP-confined HSC." *Construction and Building Materials,* 63, 11-24.

THIS PAGE HAS BEEN LEFT INTENTIONALLY BLANK

Statement of Authorship

Title of Paper	Design Model for FRP-Confined Normal- and High-Strength Concrete Square and Rectangular Columns
Publication Status	(•) Published ( ) Accepted for Publication ( ) Submitted for Publication ( ) Publication Style
Publication Details	Construction and Building Materials, Volume 60, Issue 22, Pages 1020-1035, Year 2014

Author Contributions

By signing the Statement of Authorship, each author certifies that their stated contribution to the publication is accurate and that permission is granted for the publication to be included in the candidate's thesis.

Name of Principal Author (Candidate)	Mr. Jian Chin Lim		
Contribution to the Paper	Preparation of experimental database, development of model, and preparation of manuscript		
Signature		Date	23/02/2015

Name of Co-Author	Dr. Togay Ozbakkaloglu		
Contribution to the Paper	Research supervision and review of manuscript		
Signature		Date	23/02/2015

THIS PAGE HAS BEEN LEFT INTENTIONALLY BLANK

DESIGN MODEL FOR FRP-CONFINED NORMAL- AND HIGH-STRENGTH CONCRETE SQUARE AND RECTANGULAR COLUMNS

Jian C. Lim, and Togay Ozbakkaloglu

ABSTRACT

It is well understood that the confinement of concrete with fiber reinforced polymer (FRP) composites can significantly enhance its strength and deformability. However, the effectiveness of FRP confinement on square and rectangular concrete sections, in which the concrete is non-uniformly confined, is much lower than the effective confinement of circular sections. To investigate the shape factors that influence the compressive behavior of FRP-confined concrete in square and rectangular sections, current theoretical models are reviewed and a database of existing test results was assembled. The database was then studied, together with a companion database consisting of the test results of FRP-confined concrete in circular sections, in order to capture the change in the effectiveness of confinement due to the change in the sectional shape. The combined database records the compression test results of 1547 specimens with unconfined concrete strengths ranging from 6.2 to 169.7 MPa. It provides a significantly extended parameter space, thereby allowing clearer observations of the important factors influencing the compressive behavior of FRP-confined concrete in various sections. The second half of the paper presents an assessment of the performance of existing models proposed to predict the ultimate conditions of the FRP-confined concrete in square and rectangular sections. Finally, a unified model for FRP-confined concrete in circular, square and rectangular sections was developed based on the observations from the databases.

Keywords
Columns; Composite structures; Concrete structures; Resins & plastics

1. INTRODUCTION

The axial compressive behavior of fiber reinforced polymer (FRP)-confined concrete has received significant attention over the last two decades, and it is now well understood that the confinement of concrete with FRP composites can substantially enhance concrete strength and deformability. As demonstrated in a recent a recent review by Ozbakkaloglu et al. (2013), it is clear that the behavior of FRP-confined concrete in circular sections has been extensively studied, resulting in the development of over 80 stress-strain models. On the other hand, the behavior of FRP-confined concrete in square and rectangular sections has received relatively less attention. A review of the literature revealed 27 models that are applicable to FRP-confined square or square and rectangular sections.

Based on the assessment of the existing models that was undertaken as part of the current study, some shortcomings of these models that require improvements have been identified. First, except for the model by Wang and Wu (2011), the test results used in the development of the existing models were limited to normal-strength concrete (NSC) with unconfined concrete strengths below 55 MPa. Second, the majority of the existing models are unable to predict the behavior of specimens with stress-strain curves exhibiting a descending type of second branch. To address these issues, an extensive database consisting of 484 test results of FRP-confined concrete in square and rectangular sections was first assembled from the published literature. The range of concrete strengths recorded in the database is extended to 110 MPa using additional results sourced from new tests undertaken at the University of Adelaide (Ozbakkaloglu and Oehlers 2008; Ozbakkaloglu 2013b,a). The additional results from high-strength concrete (HSC) specimens, a large number of which exhibited descending type second branches, allowed a closer investigation of the threshold confinement conditions that distinguish the ascending and descending types of stress-strain curves. In addition, a second, companion database, of FRP-confined concrete in circular sections covering 1063 test results (Ozbakkaloglu and Lim 2013; Lim and Ozbakkaloglu 2014) was employed. The inclusion of the second database allowed accurate shape factors to be established to describe the influences of geometric properties, as the specimen cross-section changed from circular to square and rectangular forms. Furthermore, the inclusion of the second database resulted in a combined database with a very wide parametric space, which allowed clearer observations to be made on the important factors influencing the compressive behavior of FRP-confined concrete. Based on these databases, a new model that is applicable to FRP-confined NSC and HSC in circular, square and rectangular sections was developed. This paper presents the test database of square and rectangular specimens and the new confinement model.

2. THE EXPERIMENTAL DATABASES

2.1 Database of FRP-confined concrete in square and rectangular sections

The initial database of FRP-confined concrete in square and rectangular sections was assembled through an extensive review of the literature that catalogued 3042 test results from 253 experimental studies published between 1991 and the middle of 2013. All specimens included in the database failed due to the rupture of their FRP jackets. The results included in the database were chosen using eight carefully considered selection criteria to ensure the reliability and consistency of the database. Assessment using these criteria resulted in a final

database of FRP-confined concrete in square and rectangular sections of 484 datasets from 37 sources. It is worthwhile noting that 63 of these test results were sourced from experimental studies conducted at the University of Adelaide (Ozbakkaloglu and Oehlers 2008; Ozbakkaloglu 2013b,a). The test results included in this database, which are summarized in Table 1 and presented in Tables A1 to A4 in Appendix, met the following criteria:

1) Only specimens with square and rectangular cross-sections were included in the database.
2) Only the specimens with unidirectional fibers orientated in the hoop direction were included.
3) Specimens with transverse and/or longitudinal steel or internal FRP reinforcement were excluded.
4) Only the specimens that were confined with continuous FRP shells were included. Specimens with partial wrapping (i.e., FRP strips) were excluded.
5) Specimens with height-to-width (H/b) ratio greater than four were excluded from the database to eliminate the influence of specimen slenderness.
6) Only the specimens that failed as a result of FRP rupture were included in the database. Specimens that failed prematurely owing to debonding of their FRP jackets at overlap regions were excluded.
7) Specimens for which the ultimate conditions were not recorded accurately because of inadequate testing equipment or instrumentation errors were excluded.
8) Specimens reported in insufficient detail with regards to material and geometric properties were excluded.

The specimens that satisfied the above conditions, and hence were included in the test database, were then subjected to an additional set of conditions to establish their suitability for their inclusion in the assessment of the existing models and development of the new model. The specimens with compressive strengths (f'_{cc}) and ultimate axial strains (ε_{cu}) that deviated significantly from the global trends of relevant strength and strain enhancement ratios (i.e., by limiting the variation of a given dataset from the trendline to maximum 40% for f'_{cc}/f'_{co} and 70% for $\varepsilon_{cu}/\varepsilon_{co}$) were identified and marked respectively with the superscripts '*s*' and '*a*' in Tables A1 to A4 in Appendix. In establishing these tolerances, the allowed limits for maximum scatter were reduced gradually, and the test results that fell outside these limits were identified. Details of these identified specimens were then carefully studied in the source document and the reasons causing significant deviation of their results from the global trends were established. The process was terminated when allowed variation tolerance reached the aforementioned limits (i.e., 40% of f'_{cc}/f'_{co} and 70% of $\varepsilon_{cu}/\varepsilon_{co}$), beyond which a clear cause of scatter could not be identified, and a further reduction in the limits would result in a significant increase in the number of excluded specimens due to the increased density of datasets within that segment of the database. Based on this approach, a small number of specimens (i.e., 8% of f'_{cc} and 18% of ε_{cu} of the combined database results) that exceed the limits were marked and excluded from the model development in order to ensure model reliability. The same approach was previously used in the development of the aforementioned companion database of circular specimens (Ozbakkaloglu and Lim 2013; Lim and Ozbakkaloglu 2014).

Table 1. Summary of test results included in the test database

Number	Researcher	Specimen number	Number of identical specimen per dataset	Confinement technique	Fiber type	Width	Depth	Height	Corner Radius	Unconfined concrete strength	Unconfined concrete strain	Ultimate axial stress ratio	Ultimate axial strain ratio
-	-	N	n	-	-	b (mm)	h (mm)	H (mm)	r (mm)	f'_{co} (MPa)	ε_{co}	f'_{cu}/f'_{co}	$\varepsilon_{cu}/\varepsilon_{co}$
1	Al-Salloum (2007)	8	1	CFRP	Wrapped	150	150	500	5 - 50	26.7 - 31.8	-	1.22 - 2.31	2.16 - 6.18
2	Benzaid et al. (2008)	6	1	GFRP	Wrapped	100	100	300	0 - 16	54.8	0.003	1.02 - 1.36	3.68 - 6.32
3	Campione (2006)	2	N/A	CFRP	Wrapped	150	150	450	3	13.0	-	1.08 - 1.46	0.85 - 1.71
4	Campione et al. (2001)	1	N/A	CFRP	Wrapped	152	152	200	3	20.1	0.002	-	1.23
5	Carrazedo (2002)	4	1	CFRP	Wrapped	150	150	450	10 - 30	33.5 - 36.5	0.003 - 0.003	0.83 - 1.43	2.31 - 4.41
6	Chaallal et al. (2003b)	24	1	CFRP	Wrapped	95.25 - 133.35	133.35 - 190.5	304.8	25.4	21.4 - 55.4	-	1.07 - 1.97	1.12 - 3.91
7	Demers and Neale (1994)	5	1	CFRP, GFRP	Wrapped	152	152	305 - 505	5	32.3 - 42.2	0.002	0.66 - 0.87	4.50 - 12.57
8	Erdil et al. (2012)	1	1	CFRP	Wrapped	150	150	300	25	10.0	0.005	2.58	5.20
9	Harajli et al. (2006)	9	1	CFRP	Wrapped	79 - 132	132 - 214	300	15	18.9 - 21.5	-	1.23 - 2.30	1.80 - 49.84
10	Harries and Carey (2003)	4	≥ 5	GFRP	Wrapped	152	152	305	11 - 25	31.2 - 32.4	0.002 - 0.003	0.86 - 1.15	1.26 - 7.81
11	Hosotani et al. (1997)	4	1	CFRP, HM CFRP	Wrapped	200	200	600	30	38.1	-	1.03 - 1.61	2.72 - 8.70
12	Ignatowski and Kaminska (2003)	3	1	CFRP	Wrapped	100 - 105	100 - 200	-	10	32.3	-	1.16 - 1.35	-
13	Ilki and Kumbasar (2003)	12	1	CFRP	Wrapped	150 - 250	250 - 300	500	40	32.8 - 34.0	0.003 - 0.003	0.98 - 1.73	2.86 - 11.07
14	Lam and Teng (2003)	12	1	CFRP	Wrapped	150	150 - 225	600	15 - 25	24.0 - 41.5	0.002	1.04 - 3.37	3.72 - 9.01
15	Masia et al. (2004)	15	1	CFRP	Wrapped	100 - 150	100 - 150	300 - 450	25	21.3 - 25.7	-	1.39 - 2.59	6.07 - 11.29
16	Mirmiran et al. (1998)	9	1	GFRP	Wrapped	152.5	152.5	305	6.35	40.6	-	0.56 - 0.93	3.71 - 7.88
17	Modarelli et al. (2005)	6	3	CFRP, GFRP	Wrapped	150	150 - 200	300 - 400	10 - 25	17.6 - 25.0	0.006 - 0.006	1.96	3.27 - 20.93
18	Ozbakkaloglu and Oehlers (2008)	15	1	CFRP	Tube-encased	150 - 200	200 - 300	600	10 - 40	24.0 - 35.5	0.002 - 0.002	0.46 - 1.77	6.70 - 16.67
19	Ozbakkaloglu (2013a)	24	1	CFRP	Tube-encased	112 - 150	150 - 224	300	15 - 30	76.6 - 79.6	0.003 - 0.003	0.53 - 1.48	3.95 - 11.39
20	Ozbakkaloglu (2013b)	24	1	CFRP	Tube-encased	112.5 - 150	150 - 225	300	15 - 30	105.2 - 110.8	0.003 - 0.004	0.55 - 1.32	4.10 - 11.10
21	Parvin and Wang (2001)	2	1	CFRP	Wrapped	108	108	105 - 305	8.26	22.6	-	1.54 - 2.00	7.79 - 11.98
22	Rochett and Labossiere (2000)	26	1	CFRP, AFRP	Wrapped	152	152 - 203	500	5 - 38	35.8 - 43.9	-	0.55 - 1.92	3.15 - 11.73
23	Rousakis et al. (2007)	15	1	CFRP, GFRP	Wrapped	200	200	320	30	33.0 - 39.9	-	0.91 - 1.68	2.14 - 11.41
24	Rousakis and Karabinis (2012)	4	1	CFRP, GFRP	Wrapped	200	200	320	30	25.5	-	1.06 - 2.19	2.50 - 6.10
25	Shehata et al. (2002)	8	9	CFRP	Wrapped	94 - 150	150 - 188	300	10	23.7 - 29.5	-	0.92 - 1.12	4.00 - 6.55
26	Suter and Pinzelli (2001)	16	≥ 1	CFRP, GFRP, AFRP, HM CFRP	Wrapped	150	150	300	5 - 25	33.9 - 36.7	-	-	-
27	Tao et al. (2008)	24	1	CFRP	Wrapped	150	150 - 300	450	20 - 50	19.5 - 49.5	-	1.07 - 3.48	5.41 - 23.53
28	Wang and Wu (2008)	60	1	CFRP	Wrapped	150	150	300	0 - 60	29.3 - 55.2	0.002	1.08 - 2.62	-
29	Wang and Wu (2010)	9	1	AFRP	Wrapped	100	100	300	10	46.4 - 101.2	0.003 - 0.005	0.99 - 1.90	0.84 - 7.57
30	Wang and Wu (2011)	15	1	AFRP	Wrapped	70 - 150	70 - 150	210 - 450	7 - 15	34.6 - 52.1	0.002 - 0.003	0.95 - 2.49	1.41 - 3.21
31	Wang et al. (2012a)	10	1	CFRP	Wrapped	100 - 400	100 - 400	300 - 1200	10 - 45	24.4	-	1.10 - 1.83	7.79 - 16.11
32	Wang et al. (2012b)	8	1	CFRP	Wrapped	204 - 305	204 - 305	612 - 915	20 - 30	25.5	-	0.67 - 1.26	4.44 - 17.85
34	Wu and Wei (2010)	30	1	CFRP	Wrapped	150	150 - 300	300 - 302	30	32.3 - 42.4	-	0.99 - 1.83	3.85 - 11.90
33	Yan et al. (2006)	2	1	CFRP, GFRP	Wrapped	279	279	914	19	15.2	0.002	1.45 - 1.72	5.00 - 10.00
35	Yeh and Chang (2012)	28	1	CFRP	Wrapped	150 - 450	150 - 600	300 - 1200	30	20.6	-	1.23 - 2.77	7.31 - 14.20
36	Youssef et al. (2007)	37	1	CFRP, GFRP	Wrapped	254 - 381	381	762	38	29.2 - 38.7	0.002	0.93 - 1.56	3.68 - 10.33
37	Zhang et al. (2010)	2	1	AFRP	Wrapped	150	150	400	15	45.0 - 50.0	-	0.94 - 0.97	8.94 - 9.42

The final database consisted of the following information for each specimen: specimen confinement methods (wrapped or tube-encased concrete); geometric properties (width b, depth h, corner radius r, and height H) (refer Fig. 1); unconfined concrete strength (f'_{co}) and strain (ε_{co}); material properties of FRP (elastic modulus E_{frp}, tensile strength f_{frp}, and total thickness t_{frp}); material properties of fiber (elastic modulus E_f, tensile strength f_f, and total thickness t_f); axial stress of confined concrete at initial peak of the stress-strain curve (f'_{c1}) and the corresponding axial strain (ε_{c1}); and ultimate axial stress (f'_{cu}) and strain (ε_{cu}) of confined concrete (refer Fig. 2). For some of the specimens included in the database, the elastic modulus (E_{frp}) and tensile strength (f_{frp}) of the FRP materials were established based on the total nominal thickness of the fiber sheets. These results are marked with the superscript 't' in Tables A1 to A4 in Appendix.

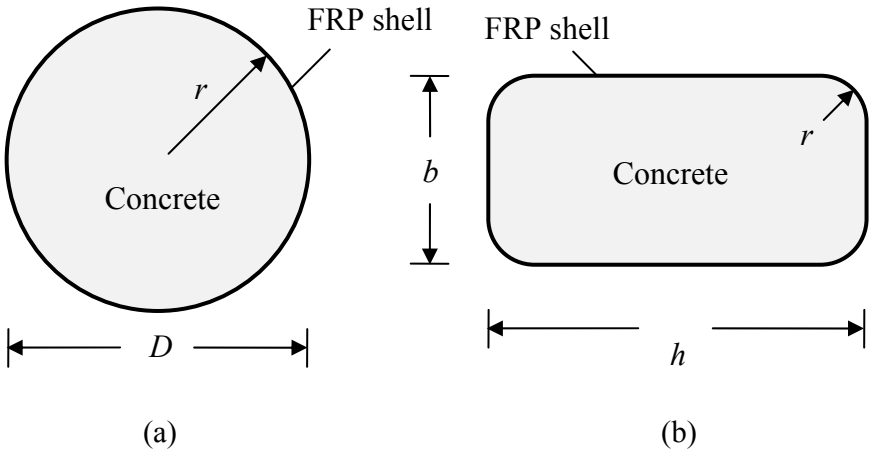

Figure 1. Sectional dimensions: (a) circular sections; (b) rectangular sections

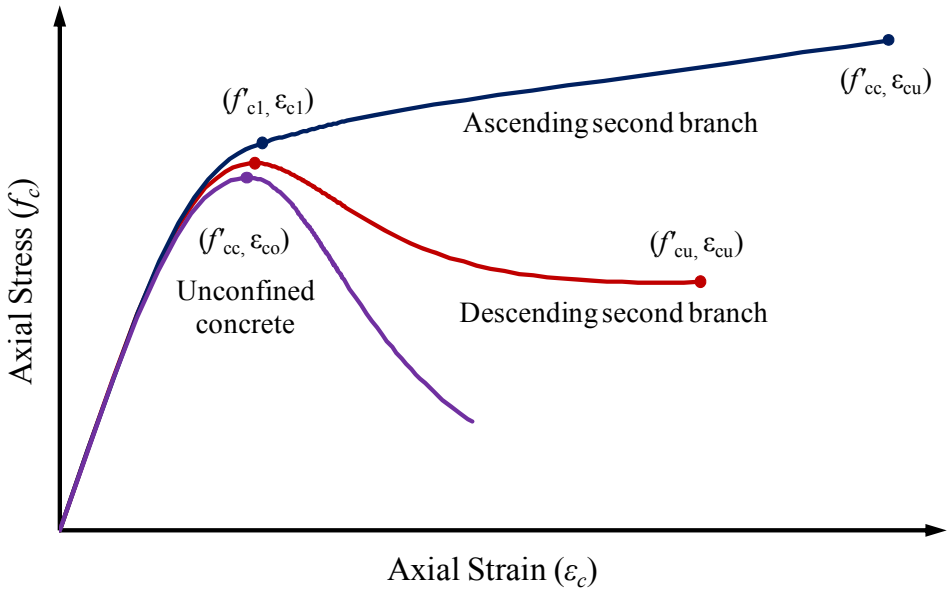

Figure 2. Axial stress-strain curves of unconfined concrete and FRP-confined concretes with ascending and descending second branches

The database consisted of specimens confined by five main types of FRP materials [carbon FRP (CFRP); high-modulus carbon FRP (HM CFRP); ultra high-modulus carbon FRP (UHM CFRP); S- or E-glass FRP (GFRP); and aramid FRP (AFRP)] and two confinement techniques (wraps and tubes). Carbon FRPs were categorized into three subgroups on the basis of their elastic modulus of fibers (E_f) (i.e., carbon FRP with $E_f \leq 270$ GPa is categorized as CFRP; with $270 < E_f \leq 440$ GPa as HM CFRP; and with $E_f > 440$ GPa as UHM CFRP). 421 specimens in the database were FRP-wrapped, whereas 63 specimens were confined by FRP tubes. 380 of the specimens were confined by CFRP, 55 by GFRP, 44 by AFRP, three by HM CFRP, and two by UHM CFRP. All of the specimens in the database were confined by FRP shells (i.e., wraps or tubes) manufactured using a manual hand lay-up technique.

The test results summarized in Table 1 are presented in the database supplied in Tables A1 to A4 in Appendix, where the results were categorized according to the confinement technique and fiber type. For some of the datasets, a single entry may represent the average results of more than one nominally identical specimen, as reported by the researchers of the original study. These datasets are marked in Table 1. As summarized in Table 1, the specimens included in the test database consisted of square and rectangular cross-sections with sectional dimensions that varied from 70 to 600 mm, with the majority of the specimens having sectional dimensions of 150 × 150 mm. 331 specimens in the database were square and 153 specimens were rectangular in cross-section. The sectional aspect ratio of the specimens varied from 1 to 3. The unconfined concrete strengths (f'_{co}) varied from 10.0 to 110.8 MPa. The unconfined concrete strengths (f'_{co}) varied from 10.0 to 110.8 MPa. Except for the specimens that were marked with the superscripts '*c*' in Tables A1 to A4 in Appendix, the reported unconfined concrete strengths (f'_{co}) were based on compressive tests of control specimens that had the same geometric dimensions as the corresponding confined specimens. For specimens marked with the superscripts '*c*', the reported unconfined concrete strengths (f'_{co}) were based on 152.5 × 305 mm concrete cylinder tests.

Care was taken to distinguish the results of specimens having stress-strain curves with descending second branches (i.e., $f'_{cu} < f'_{c1}$) and ascending second branches (i.e., $f'_{cu} > f'_{c1}$) (refer Fig. 2). The specimens that exhibit descending second branches are marked with superscript '*d*' in Tables A1 to A4 in Appendix. For the specimens with only a single compressive strength value reported in the original publication, this value was assigned to either f'_{c1} or f'_{cu} based on the observed shape of their stress-strain curves, or otherwise based on the authors' best knowledge.

2.2 Database of FRP-confined concrete in circular sections

Test results that satisfied the criteria used in the construction of the database of FRP-confined concrete, with Criterion 1 adjusted to only include the specimens with circular cross-sections, were collected to form another database. The details of the NSC and HSC components of the circular column database can be found in Ozbakkaloglu and Lim (2013) and Lim and Ozbakkaloglu (2014), respectively. The database of FRP-confined concrete in circular sections contained 1063 datasets assembled from 105 experimental studies. 910 specimens in the database were FRP wrapped, whereas 153 specimens were confined by FRP tubes. 619 of

the specimens were confined by CFRP, 246 by GFRP, 116 by AFRP, 64 by HM CFRP, and 18 by UHM CFRP. The diameters of the specimens (D) included in the test database varied between 47 and 600 mm. The peak unconfined concrete strength (f'_{co}) and strain (ε_{co}), as obtained from concrete cylinder tests, varied from 6.2 to 169.7 MPa and 0.14% to 0.70%, respectively. The confinement ratio, defined as the ratio of the actual ultimate confining pressure of the FRP shell to the peak strength of an unconfined concrete specimen ($f_{lu,a}/f'_{co}$), varied from 0.02 to 4.74.

3. EXISTING MODELS FOR FRP-CONFINED CONCRETE IN SQUARE AND RECTANGULAR SECTIONS

Out of the 27 existing models of FRP-confined concrete in square or square and rectangular sections (Restrepol and DeVino 1996; ACI-440 2002; Li et al. 2002; Shehata et al. 2002; Campione and Miraglia 2003; Chaallal et al. 2003a; Lam and Teng 2003; Ilki et al. 2004; Harajli 2005,2006; Harajli et al. 2006; Al-Salloum 2007; Kumutha et al. 2007; Wu et al. 2007; Yan and Pantelides 2007; Youssef et al. 2007; ACI-440 2008; Ilki et al. 2008; Wu and Wang 2009; Lee et al. 2010; Toutanji et al. 2010; Wang and Wu 2010; Wu and Zhou 2010; Wang and Wu 2011; Csuka and Kollar 2012; Wang et al. 2012a; Wei and Wu 2012) identified in this study (Table 2), 15 models are able to predict the ultimate conditions of square and rectangular sections confined by any type of FRP material and exhibit stress-strain curves with ascending second branches. The remaining 12 models are either limited in their applications to only square cross-sections (Campione and Miraglia 2003; Al-Salloum 2007; Wu and Wang 2009; Lee et al. 2010; Wu and Zhou 2010; Csuka and Kollar 2012) or to certain type of FRP confining materials (Li et al. 2002; Kumutha et al. 2007; Ilki et al. 2008; Wang and Wu 2010,2011; Wang et al. 2012a). In the assessment of model performances, the 15 models that are applicable to the entire range of the database (Restrepol and DeVino 1996; ACI-440 2002; Shehata et al. 2002; Chaallal et al. 2003a; Lam and Teng 2003; Ilki et al. 2004; Harajli 2005,2006; Harajli et al. 2006; Wu et al. 2007; Yan and Pantelides 2007; Youssef et al. 2007; ACI-440 2008; Toutanji et al. 2010; Wei and Wu 2012) were first compared using results of specimens having stress-strain curves with ascending second branches. Four of these 15 models (Wu et al. 2007; Yan and Pantelides 2007; Youssef et al. 2007; Wei and Wu 2012) that are also applicable to specimens having stress-strain curves with descending second branches were compared next.

Tables 3 and 4 present the statistics on performances of models in predictions of ultimate conditions of FRP-confined concrete in square and rectangular sections that exhibit stress-strain curves with ascending and descending type second branches, respectively. For the results presented in Table 3, only the specimens from the database with ascending second branches, for which the ultimate axial stress (f'_{cu}) was equal to the compressive strength (f'_{cc}), were used for model assessment. Not all the datasets included in the database contained all the relevant details required for the model assessments. Furthermore, the results that failed to satisfy the criteria outlined in Section 2.1 were excluded. As a result, out of the 484 FRP-confined concrete datasets, 300 were used in the assessment of the ultimate axial stress ratios (f'_{cc}/f'_{co}) and 166 were used in the assessment of the ultimate axial strain ratios ($\varepsilon_{cu}/\varepsilon_{co}$) in Table 3.

Table 2. Summary of existing models for FRP-confined concrete in square and rectangular sections

No.	Models	Applicability			
		Cross-sections	FRP materials	Post-peak stress-strain response	Ultimate condition
1	Restrepol and De Vino (1996)	Square and rectangular	Any	Ascending only	Stress only
2	ACI 440 (2002)	Square and rectangular	Any	Ascending only	Stress and strain
3	Li et al. (2002)	Square and rectangular	Any	Ascending only	Stress and strain
4	Shehata et al. (2002)	Square and rectangular	Any	Ascending only	Stress and strain
5	Campione and Miraglia (2003)	Square	Any	Ascending only	Stress and strain
6	Chaallal et al. (2003a)	Square and rectangular	Any	Ascending only	Stress and strain
7	Lam and Teng (2003)	Square and rectangular	Any	Ascending only	Stress and strain
8	Ilki et al. (2004)	Square and rectangular	Any	Ascending only	Stress and strain
9	Harajli (2005)	Square and rectangular	Any	Ascending only	Stress and strain
10	Harajli (2006)	Square and rectangular	Any	Ascending only	Stress and strain
11	Harajli et al. (2006)	Square and rectangular	Any	Ascending only	Stress and strain
12	Yan and Pantelides (2007)	Square and rectangular	Any	Ascending and descending	Stress and strain
13	Al-Salloum (2007)	Square	Any	Ascending only	Stress only
14	Kumutha et al. (2007)	Square and rectangular	GFRP	Ascending only	Stress only
15	Wu et al. (2007)	Square and rectangular	Any	Ascending and descending	Stress and strain
16	Youssef et al. (2007)	Square and rectangular	Any	Ascending and descending	Stress and strain
17	ACI 440 (2008)	Square and rectangular	Any	Ascending only	Stress and strain
18	Ilki et al. (2008)	Square and rectangular	CFRP	Ascending only	Stress and strain
19	Wu and Wang (2009)	Square	Any	Ascending only	Stress only
20	Lee et al. (2010)	Square	Any	Ascending only	Stress only
21	Toutanji et al. (2010)	Square and rectangular	Any	Ascending only	Stress only
22	Wang and Wu (2010)	Square and rectangular	AFRP	Ascending only	Stress and strain
23	Wu and Zhou (2010)	Square	Any	Ascending only	Stress only
24	Wang and Wu (2011)	Square and rectangular	AFRP	Ascending only	Stress only
25	Wei and Wu (2012)	Square and rectangular	Any	Ascending and descending	Stress and strain
26	Csuka and Kollar (2012)	Square	Any	Ascending only	Stress only
27	Wang et al. (2012a)	Square and rectangular	CFRP	Ascending only	Stress and strain

Table 3. Statistics on performances of models in predictions of ultimate conditions of FRP-confined square and rectangular concrete sections having stress-strain curves with ascending second branches

No.	Model	Prediction of f'_{cc}/f'_{co}			Prediction of $\varepsilon_{cu}/\varepsilon_{co}$		
		Average absolute error (%)	Mean (%)	Standard deviation (%)	Average absolute error (%)	Mean (%)	Standard deviation (%)
1	Restrepol and De Vino (1996)	89.6	189.6	43.0	-	-	-
2	ACI 440 (2002)	67.7	167.7	35.9	32.6	110.9	41.7
3	Shehata et al. (2002)	17.5	104.6	21.3	33.3	104.1	44.5
4	Chaallal et al. (2003a)	18.1	84.3	17.3	79.9	20.1	7.1
5	Lam and Teng (2003)	14.7	100.4	18.2	32.9	73.0	26.9
6	Ilki et al. (2004)	16.2	103.8	19.9	45.0	128.8	52.2
7	Harajli (2005)	95.7	191.7	69.5	67.7	32.3	13.9
8	Harajli (2006)	36.3	134.5	30.9	31.7	79.3	32.6
9	Harajli et al. (2006)	21.0	113.8	21.5	55.9	44.2	17.1
10	Yan and Pantelides (2007)	24.6	113.5	30.6	71.6	150.4	90.9
11	Wu et al. (2007)	21.6	97.7	31.7	33.9	105.9	45.4
12	Youssef et al. (2007)	21.3	81.2	16.2	87.2	183.2	78.7
13	ACI 440 (2008)	14.5	98.8	17.8	36.1	68.7	25.7
14	Toutanji et al. (2010)	17.5	110.0	20.2	-	-	-
15	Wei and Wu (2012)	14.3	104.8	17.3	22.8	92.4	25.6

Table 4. Statistics on performances of models in predictions of ultimate conditions of FRP-confined square and rectangular concrete sections having stress-strain curves with descending second branches

No.	Model	Prediction of f'_{cc}/f'_{co}			Prediction of $\varepsilon_{cu}/\varepsilon_{co}$		
		Average absolute error (%)	Mean (%)	Standard deviation (%)	Average absolute error (%)	Mean (%)	Standard deviation (%)
1	Yan and Pantelides (2007)	19.1	115.4	21.5	72.3	150.3	121.6
2	Wu et al. (2007)	27.0	97.8	39.1	33.4	97.6	46.3
3	Youssef et al. (2007)	26.2	119.4	29.4	46.1	128.8	67.2
4	Wei and Wu (2012)	39.9	134.7	39.6	31.0	88.1	38.2

In the assessment of model predictions on the ultimate condition of specimens having stress-strain curves with descending second branches presented in Table 4, 67 and 62 datasets were used to assess the performances of the four applicable models (Wu et al. 2007; Yan and Pantelides 2007; Youssef et al. 2007; Wei and Wu 2012) to predict the ultimate axial stress ratios (f'_{cu}/f'_{co}) and the ultimate axial strain ratios ($\varepsilon_{cu}/\varepsilon_{co}$), respectively.

In the comparison of model performances, average absolute error (*AAE*) was used to establish overall model accuracy; standard deviation (*SD*) was used to establish the magnitude of the associated scatter for each model; and mean (*M*) was used to describe the associated average overestimation or underestimation of the model, where an overestimation is represented by a mean value greater than 1. *AAE*, *SD*, and *M* are defined by Eq. 1 to 3, respectively. Based on a similar approach adopted by Wu and Zhou (2010), the accuracy of a model is classified into three categories: Category I (when AAE ≤ 15%), Category II (when 15% ≤ AAE ≤ 30%), and Category III (when AAE > 30%). In the assessment results of strength enhancement ratio predictions (f'_{cc}/f'_{co}) presented in Table 3, three models attain category I (Lam and Teng 2003; ACI-440 2008; Wei and Wu 2012), followed by eight models in Category II (Shehata et al. 2002; Chaallal et al. 2003a; Ilki et al. 2004; Harajli et al. 2006; Wu et al. 2007; Yan and Pantelides 2007; Youssef et al. 2007; Toutanji et al. 2010) and four models in Category III (Restrepol and DeVino 1996; ACI-440 2002; Harajli 2005,2006). In the assessment results of strain enhancement ratio predictions ($\varepsilon_{cu}/\varepsilon_{co}$) presented in Table 3, no model attains Category I. Only the model by Wei and Wu (2012) is found in Category II and the remaining 12 models fall in Category III (ACI-440 2002; Shehata et al. 2002; Chaallal et al. 2003a; Lam and Teng 2003; Ilki et al. 2004; Harajli 2005,2006; Harajli et al. 2006; Wu et al. 2007; Yan and Pantelides 2007; Youssef et al. 2007; ACI-440 2008).

$$AAE = \frac{\sum_{i=1}^{n}\left|\frac{mod_i - exp_i}{exp_i}\right|}{n} \quad (1)$$

$$M = \frac{\sum_{i=1}^{n}\frac{mod_i}{exp_i}}{n} \quad (2)$$

$$SD = \sqrt{\frac{\sum_{i=1}^{n}\left(\frac{mod_i}{exp_i} - M\right)^2}{n-1}} \quad (3)$$

In the assessment results of ultimate axial stress ratio predictions (f'_{cu}/f'_{co}) for specimens with descending second branches presented in Table 4, no model attains Category I, three models fall in Category II (Wu et al. 2007; Yan and Pantelides 2007; Youssef et al. 2007), and one model in Category III (Wei and Wu 2012). As illustrated in Table 4, all of these four models fall in Category III in their predictions of strain enhancement ratios ($\varepsilon_{cu}/\varepsilon_{co}$).

Based on the results of assessments presented in Tables 3 and 4, only a few of the models attain Category I in the predictions of the ultimate conditions of FRP-confined square and rectangular concrete sections. It is clear from the assessment that further modeling improvements are possible. The common modeling issues that compromised model accuracy,

identified from the results of model assessments, include the use of relatively small test databases in the development of the FRP-confined concrete models in square and rectangular sections, and the failure of the models to accurately capture the influence of important factors, such as the unconfined concrete strength and type of FRP material. A new confinement model that provides better predictions of the ultimate condition of FRP-confined square and rectangular concrete sections is, therefore, required. Such a model is presented in the following section.

4. A NEW MODEL FOR FRP-CONFINED SQUARE AND RECTANGULAR COLUMNS

This section presents a new design-oriented model to predict the ultimate condition of FRP-confined concrete. The new model contains simple closed-form expressions and was developed using the combined test databases of circular, square and rectangular FRP-confined concrete specimens. The model is applicable to both NSC and HSC columns of unconfined concrete strengths of up to 120 MPa.

Two sets of expressions are proposed for ultimate conditions of FRP-confined concretes. The first set was developed for specimens exhibiting stress-strain curves with ascending second branches and the second set was developed for specimens with descending second branches. To differentiate and properly categorize the specimens with ascending and descending second branches, a concept of threshold confinement level is introduced, which is discussed in the following section.

4.1 Threshold confinement level

The confinement stiffness threshold (K_{lo}) is the minimum stiffness of FRP confining shell required by the confined concrete to exhibit a stress-strain curve with an ascending second branch. It was previously shown that the confinement stiffness threshold (K_{lo}) changes with the unconfined concrete strength (f'_{co}) (Lim and Ozbakkaloglu 2014). Figure 3 illustrates the relationship between the threshold confinement stiffness (K_{lo}) and unconfined concrete strength (f'_{co}), which is defined by Eq. 4. This relationship was established based on the results from the database of circular specimens that exhibited stress-strain curves with near flat second branches.

$$K_{lo} = 73.7e^{0.027f'_{co}} \quad (4)$$

In square and rectangular concrete sections, the equivalent confinement stiffness provided by the FRP shell is defined as $k_{s1}K_l$, where k_{s1} is the strength efficiency factor as discussed in detail in Section 4.4, and K_l is the confinement stiffness calculated from Eq. 5. Figure 4 shows the variation of the ultimate stress ratio (f'_{cu}/f'_{co}) of the FRP-confined square and rectangular concrete specimens with the threshold confinement stiffness ratio ($k_{s1}K_l/K_{lo}$). A value of $k_{s1}K_l/K_{lo}$ greater than 1 represents a specimen having an equivalent stiffness above the minimum threshold, for which an ascending second branch is expected, and vice versa. In the proposed model, this boundary condition is used to distinguish and categorize the stress-strain curves of FRP-confined concrete.

$$K_l = \frac{2E_f t_f}{d_e} \quad (5)$$

In Eq. 5, d_e is the equivalent sectional dimension of square and rectangular sections, and it is defined by Eq. 6, where b and h are the width and depth of the section ($h \geq b$). For a circular section, d_e is equal to the diameter (D).

$$d_e = \sqrt{(h^2 + b^2)/2} \quad (6)$$

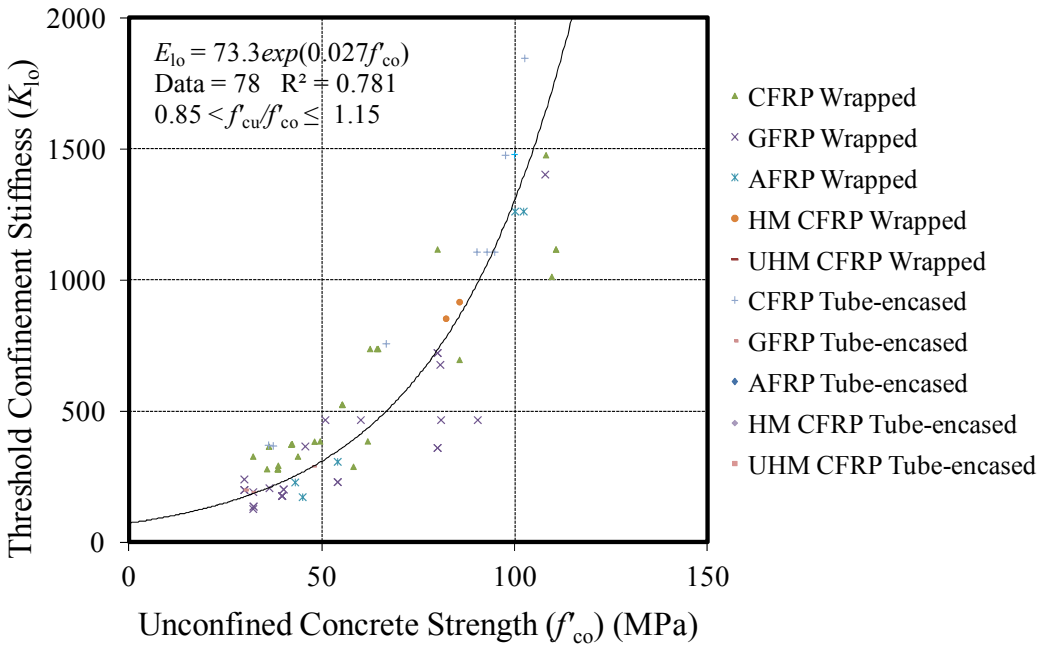

Figure 3. Variation of threshold confinement stiffness (K_{lo}) with unconfined concrete strength (f'_{co})

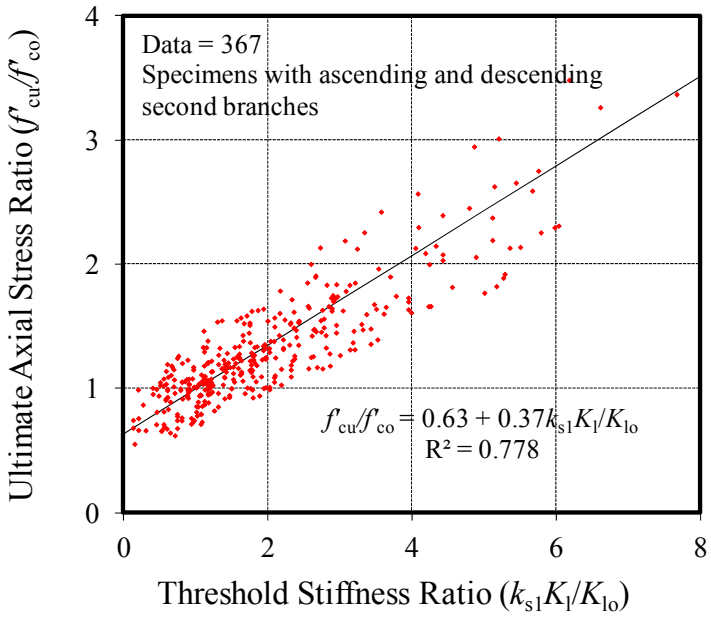

Figure 4. Variation of ultimate stress ratio (f'_{cu}/f'_{co}) with threshold stiffness ratio ($k_{s1}K_l/K_{lo}$)

4.2 General form of the proposed expressions

Eqs. 7 and 8 are proposed for the predictions of the compressive strength (f'_{cc}) and ultimate axial strain (ε_{cu}) of FRP-confined concretes that exhibit stress-strain curves with ascending second branches. Eqs. 9 and 10 are proposed for the predictions of the ultimate axial stress (f'_{cu}) and strain (ε_{cu}) of FRP-confined concretes that exhibit stress-strain curves with descending second branches. In Eqs. 7 and 9, the influence of the unconfined concrete strength (f'_{co}) is accounted for through the use of the confinement stiffness threshold (K_{lo}) given in Eq.4.

If $k_{s1}K_l/K_{lo} \geq 1$: Curves with Ascending Second Branches

$$f'_{cc} = f'_{co} + k_1(k_{s1}K_l - K_{lo})\varepsilon_{h,rup} \tag{7}$$

$$\varepsilon_{cu} = c_2\varepsilon_{co} + k_2 k_{s2}\left(\frac{K_l}{f'_{co}}\right)^{0.9}{\varepsilon_{h,rup}}^{1.35} \tag{8}$$

If $k_{s1}K_l/K_{lo} < 1$: Curves with Descending Second Branches

$$f'_{cu} = f'_{co} - k_{1,des}(K_{lo} - k_{s1,des}K_l)\varepsilon_{h,rup} \tag{9}$$

$$\varepsilon_{cu} = c_2\varepsilon_{co} + k_{2,des}k_{s2,des}\left(\frac{K_l}{f'_{co}}\right)^{0.9}{\varepsilon_{h,rup}}^{1.35} \tag{10}$$

In the expressions, f'_{co} is the unconfined concrete strength, K_{lo} is the threshold confinement stiffness calculated using Eq. 4, K_l is the confinement stiffness calculated using Eq. 5, k_1 and k_2 are the strength and strain enhancement coefficients discussed in Section 4.3, k_{s1} and k_{s2} are the strength and strain efficiency factors discussed in Section 4.4, and $\varepsilon_{h,rup}$ is the hoop rupture strain discussed in Section 4.5. In Eqs. 9 and 10, extra subscripts 'des' are assigned to $k_{1,des}$, $k_{2,des}$, $k_{s1,des}$, and $k_{s2,des}$ to make the distinction that these factors were established for specimens that exhibit stress-strain curves with descending second branches. Details of these factors are presented in Sections 4.3 and 4.4. In Eqs. 8 and 10, c_2 is the concrete strength factor and is calculated using Eq. 11 proposed by Lim and Ozbakkaloglu (2014), and the peak axial strain of unconfined concrete ε_{co} is determined using the expression proposed by Tasdemir et al. (1998) (Eq. 12).

$$c_2 = 2 - \left(\frac{f'_{co}-20}{100}\right) \quad \text{and} \quad c_2 \geq 1 \tag{11}$$

$$\varepsilon_{co} = \left(-0.067{f'_{co}}^2 + 29.9f'_{co} + 1053\right) \times 10^{-6} \tag{12}$$

4.3 Strength and strain enhancement coefficients

The strength and strain enhancement coefficients (k_1 and k_2) in Eqs. 7 and 8 were established from specimens that exhibit stress-strain curves with ascending second branches. These values were established from the database of circular specimens, specifically for each confinement method (i.e., FRP-wrapped or -tube encased concrete) and fiber type (e.g., carbon, glass or aramid), with average values recommended as $k_1 = 4.1$ and $k_2 = 0.27$.

The strength decay coefficient ($k_{1,des}$) and the strain enhancement coefficient ($k_{2,des}$) in Eqs. 9 and 10 were established using specimens from the database of circular specimens that exhibited stress-strain curves with descending second branches. The recommended average values are $k_{1,des} = 4.5$ and $k_{2,des} = 0.27$.

4.4 Strength and strain efficiency factors

The effectiveness of FRP confinement in square and rectangular concrete sections, in which the concrete is non-uniformly confined, is known to be significantly lower than the effectiveness of confinement in circular sections (Restrepol and DeVino 1996; Campione and Miraglia 2003; Lam and Teng 2003; Ozbakkaloglu and Oehlers 2008; Ozbakkaloglu 2013b,a). A number of early studies in FRP-confined square and rectangular concrete sections (Restrepol and DeVino 1996; ACI-440 2002; Campione and Miraglia 2003) attempted to capture the reduced confinement effectiveness resulted from the non-uniform confining pressure arising from the arching actions of confinement reinforcement using shape factors (k_s). In these studies, the shape factor (k_s) was directly related to the ratio between the concrete area effectively confined by the arching actions (A_e) and the gross concrete area of the cross-section (A_g). In more recent studies (Wu et al. 2007; Wei and Wu 2012), the shape factor (k_s) was established through direct statistical treatment of the test results, without the use of an effective confinement area ratio (A_e/A_g). In this approach, the shape factors (k_s) were determined using the differences between the test results of the confined square or rectangular sections and the circular sections for a given parameter. The model assessment results of the present study indicated that models established using this approach (Wu et al. 2007; Wei and Wu 2012) outperformed their counterparts that used the theoretical effective confinement area ratios (A_e/A_g). On the basis of this finding, the latter approach was adopted in the present study and the shape factors were used to establish the confinement effectiveness of a given section through its geometric properties, including the sectional aspect ratio and the corner radius. The shape factors were developed separately for specimens exhibiting stress-strain curves with ascending and descending second branches, as discussed in the following sections.

4.4.1 Curves with ascending second branches

Figure 5 shows the variation of the strength efficiency factor (k_{s1}) of square specimens with the corner radius ratio ($2r/d_e$). As expected, the value of k_{s1} increases asymptotically with an increase in the $2r/d_e$ ratio, until it reaches 1 in the case of a circular section (i.e., $2r/d_e = 1$). Figure 6 shows the variation of the strain efficiency factor (k_{s2}) of square specimens with the corner radius ratio ($2r/d_e$). As illustrated in the Fig. 6, k_{s2} also increases with an increase in the $2r/d_e$ ratio. An important observation, as shown by the test data having k_{s2} values that exceed 1 in the range of $2r/d_e$ ratio between 0.4 and 1.0, indicates that square and rectangular specimens with well-rounded corners can exhibit higher ultimate axial strains than companion specimens with circular cross-sections.

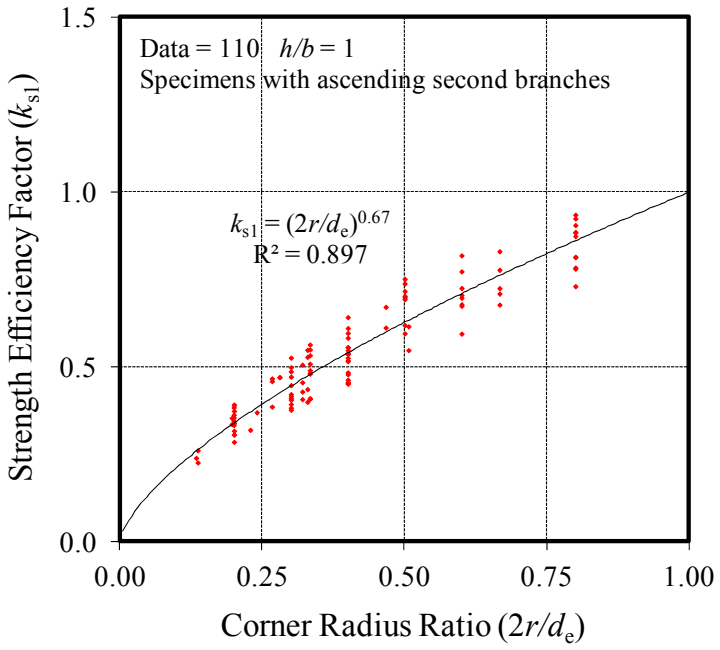

Figure 5. Variation of strength efficiency factor (k_{s1}) with corner radius ratio ($2r/d_e$) for specimens having stress-strain curves with ascending second branches

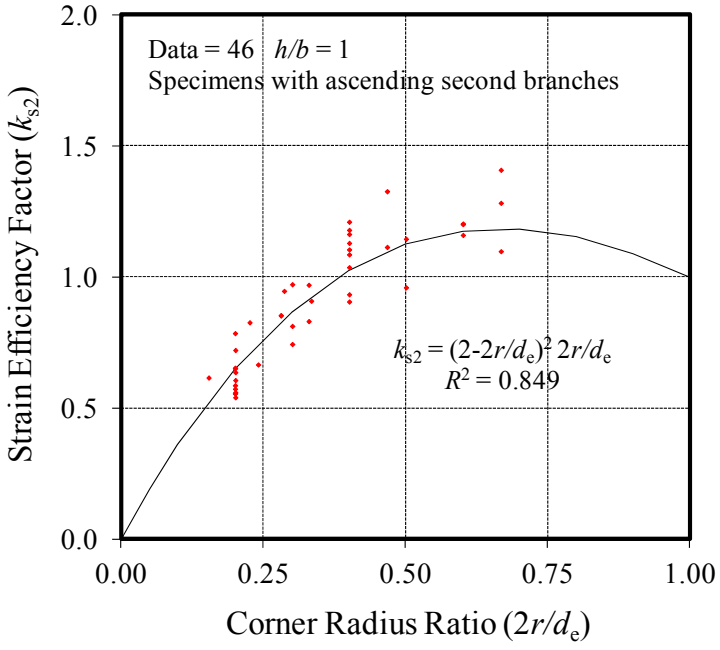

Figure 6. Variation of strain efficiency factor (k_{s2}) with corner radius ratio ($2r/d_e$) for specimens having stress-strain curves with ascending second branches

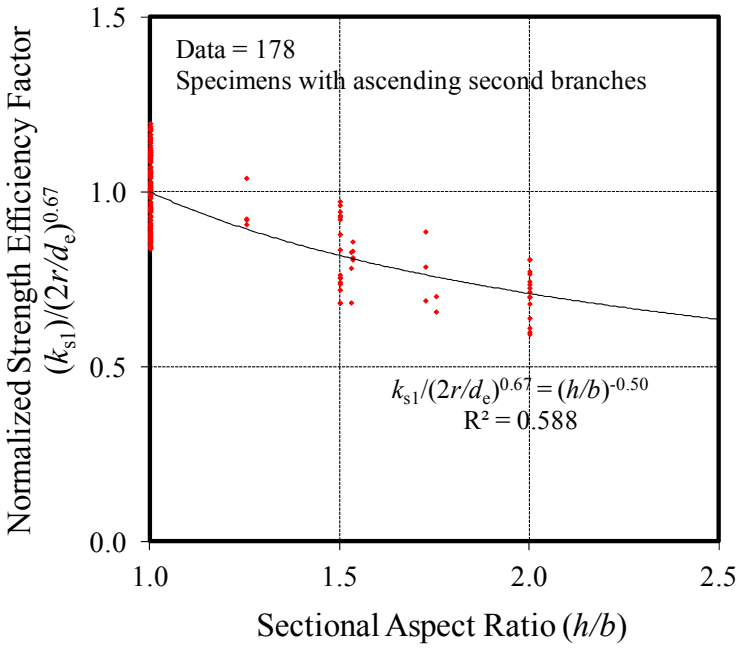

Figure 7. Variation of normalized strength efficiency factor $(k_{s1}/(2r/d_e)^{0.67})$ with sectional aspect ratio (h/b) for specimens having stress-strain curves with ascending second branches

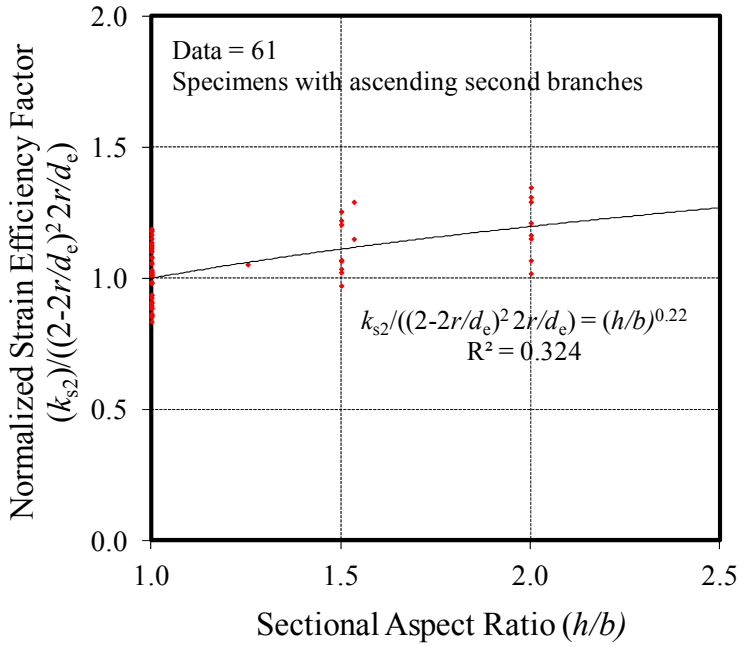

Figure 8. Variation of normalized strain efficiency factor $(k_{s2}/((2-2r/d_e)^2\, 2r/d_e))$ with sectional aspect ratio (h/b) for specimens having stress-strain curves with ascending second branches

After establishing the influence of the corner radius on strength efficiency factor based on the square specimens (i.e $k_{s1} = (2r/d_e)^{0.67}$), the influence of the sectional aspect ratio (h/b) was then established from the combined database of square and rectangular specimens. To capture the discrete influence of the sectional aspect ratio (h/b), the strength efficiency factor (k_{s1}) was normalized to eliminate the established influence of corner radius. Figure 7 shows the relationship between the normalized strength efficiency factor ($k_{s1}/(2r/d_e)^{0.67}$) and the sectional aspect ratio (h/b). As evident from Fig. 7, k_{s1} decreases with an increase in h/b ratio. Based on the relationships illustrated in Figs. 5 and 7, the following expression is proposed for the strength efficiency factor (k_{s1}):

$$k_{s1} = \left(\frac{2r}{d_e}\right)^{0.67} \left(\frac{h}{b}\right)^{-0.5} \tag{13}$$

Using a similar approach, the influence of the sectional aspect ratio (h/b) on the strain efficiency factor (k_{s2}) was then established. Figure 8 shows the relationship of between the normalized strain efficiency factor ($k_{s2}/((2-2r/d_e)^2 2r/d_e)$) and the sectional aspect ratio (h/b). The trend of Fig. 8 indicates that k_{s2} slightly increases with an increase in h/b ratio. Based on the relationships illustrated in Figs. 6 and 8, the strain efficiency factor is defined as:

$$k_{s2} = \left(2 - \frac{2r}{d_e}\right)^2 \left(\frac{2r}{d_e}\right) \left(\frac{h}{b}\right)^{0.22} \tag{14}$$

4.4.2 Curves with descending second branches

Following the approach outlined for specimens having stress-strain curves with ascending second branches, the expressions for strength and strain efficiency factors ($k_{s1,des}$ and $k_{s2,des}$) of specimens with descending second branches were also derived from the test database. Figure 9 shows the variations of the strength efficiency factor ($k_{s1,des}$) with the corner radius ratio ($2r/d_e$), and Figure 10 shows the variation of the normalized strength efficiency factor ($k_{s1,des}/(2r/d_e)^{0.68}$) with the sectional aspect ratio (h/b). As evident from Fig. 9, the variation of $k_{s1,des}$ with $2r/d_e$ ratio in specimens with descending second branches closely resembles that of k_{s1} with $2r/d_e$ ratio in specimens with ascending second branches, shown in Fig. 5. Likewise, similarity of the trendlines of specimens with ascending and descending second branches is evident from the comparison of Figs. 7 and 10, which illustrate the influence of sectional aspect ratio (h/b) on the strength efficiency factor. Based on the observed similarities in the comparisons of Figs. 5 and 9 (i.e., 0.606 probability associated with a Student's paired t-test, with a two-tailed distribution) and Figs. 7 and 10 (i.e., 0.439 probability associated with a Student's paired t-test, with a two-tailed distribution), it is proposed that the expression given for specimens with ascending second branches can also be adopted for specimens with descending second branches:

$$k_{s1,des} = k_{s1} \quad \text{for} \quad \frac{2r}{d_e} \geq 0.15 \tag{15}$$

Figure 11 shows the variation of the strain efficiency factor ($k_{s2,des}$) with a corner radius ratio ($2r/d_e$). The distinct trends observed from the comparison of Fig. 6 and Fig. 11 (i.e., probability <0.001 associated with a Student's paired t-test, with a two-tailed distribution) indicate that the strain efficiency factors for specimens with descending second branches

($k_{s2,des}$) are significantly different from those with ascending second branches. This observation indicates that Eq. 14 cannot be used for specimens exhibiting descending second branches and a new expression is required to predict the strain efficiency factor of these specimens.

To establish the discrete influence of the sectional aspect ratio (h/b), the strain efficiency factor ($k_{s2,des}$) was normalized to eliminate the established influence of the corner radius. Figure 12 shows the variation of the normalized strain efficiency factor ($k_{s2,des}/(2r/d_e)^{-0.26}$) with a sectional aspect ratio (h/b). The trendline of Fig. 12 illustrates that $k_{s2,des}$ increases slightly with an increase in h/b ratio, indicating that specimens with rectangular cross-sections exhibit slightly higher strain enhancements than the companion specimens with square cross-sections. Based on the relationships observed from Figs. 11 and 12, Eq. 16 is proposed to determine the strain efficiency factor of specimens with descending second branches ($k_{s2,des}$).

$$k_{s2,des} = \left(\frac{2r}{d_e}\right)^{-0.26}\left(\frac{h}{b}\right)^{0.22} \quad \text{for} \quad \frac{2r}{d_e} \geq 0.15 \tag{16}$$

It should be noted that Eqs. 15 and 16 are not applicable to specimens having $2r/d_e$ ratio lower than 0.15, as the failure modes of these specimens were found to be inconsistent, with both premature and progressive failures commonly observed. Among these specimens with sharp corners (i.e., $2r/d_e < 0.15$), prematurely failed specimens exhibited very low ultimate axial strains, whereas progressively failed specimens demonstrated extremely large ultimate axial strains. Therefore, to prevent inconsistencies, specimens having $2r/d_e$ ratio lower than 0.15 were excluded from the development of expressions presented in this section. It should also be noted that the trendlines in Figs. 9 to 12, along with Eqs. 15 and 16, are based on the limited number of test results available in the literature to date. Therefore, in future, these expressions can be further improved when additional test results from specimens exhibiting descending second branches become available.

4.5 Hoop rupture strain

To establish the relationship of the hoop rupture strain of the FRP shell ($\varepsilon_{h,rup}$) and the ultimate tensile strain of the fiber (ε_f), the hoop rupture strain $\varepsilon_{h,rup}$ is calculated through Eq. 17 using hoop strain reduction factor $k_{\varepsilon,f}$ given in Eq. 18. The $k_{\varepsilon,f}$ expression was developed by Ozbakkaloglu and Lim (2013) using a large experimental database of circular FRP-confined NSC and HSC specimens (Ozbakkaloglu and Lim 2013; Lim and Ozbakkaloglu 2014). The expression captures the observed reduction in the hoop strain reduction factor ($k_{\varepsilon,f}$) with an increase in compressive strength of concrete (f'_{co}) and elastic modulus of confining fibers (E_f), and it is applicable to concretes with f'_{co} up to 120 MPa and confined by any FRP type.

$$\varepsilon_{h,rup} = k_{\varepsilon,f}\varepsilon_f \tag{17}$$

$$k_{\varepsilon,f} = 0.9 - 2.3f'_{co} \times 10^{-3} - 0.75E_f \times 10^{-6} \tag{18}$$

where f'_{co} and E_f are in MPa, and 100,000 MPa $\leq E_f \leq$ 640,000 MPa.

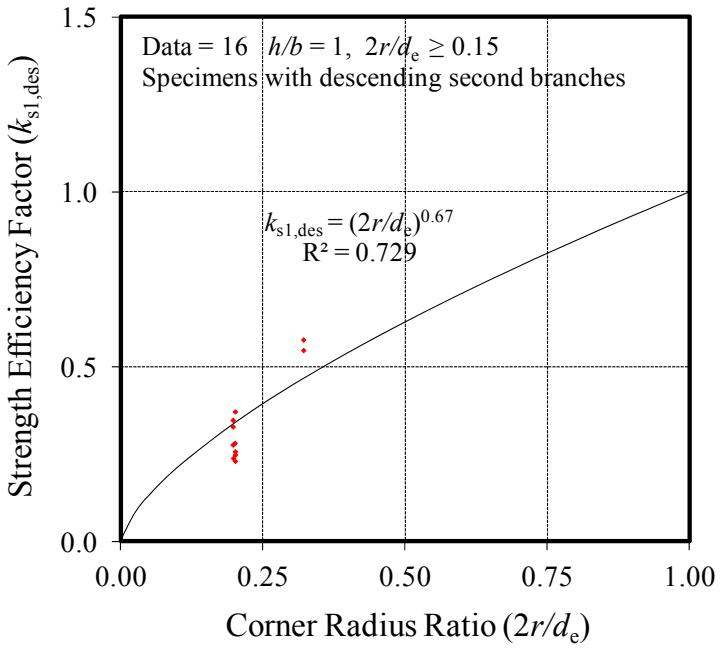

Figure 9. Variation of strength efficiency factor ($k_{s1,des}$) with corner radius ratio ($2r/d_e$) for specimens having stress-strain curves with descending second branches

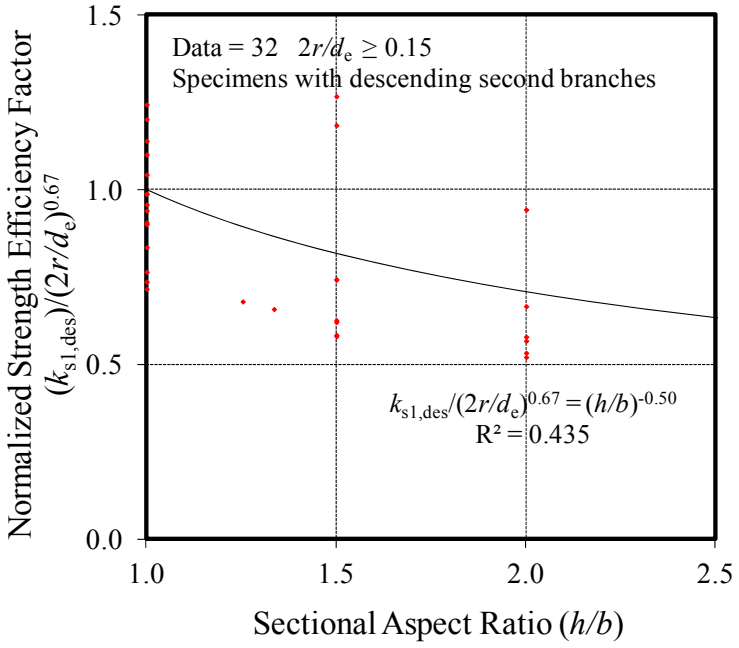

Figure 10. Variation of normalized strength efficiency factor ($k_{s1,des}/(2r/d_e)^{0.68}$) with sectional aspect ratio (h/b) for specimens having stress-strain curves with descending second branches

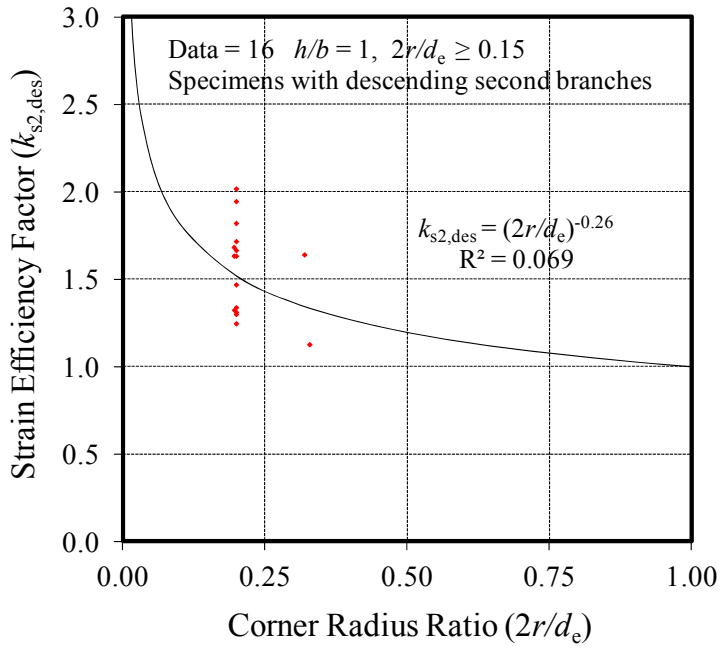

Figure 11. Variation of strain efficiency factor ($k_{s2,des}$) with corner radius ratio ($2r/d_e$) for specimens having stress-strain curves with descending second branches

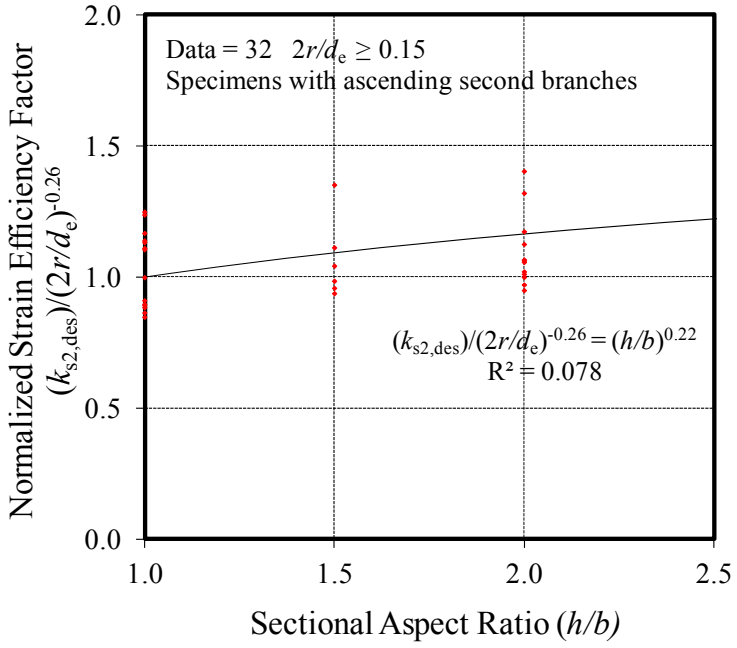

Figure 12. Variation of normalized strain efficiency factor ($k_{s2,des}/(2r/d_e)^{-0.26}$) with sectional aspect ratio (h/b) for specimens having stress-strain curves with descending second branches

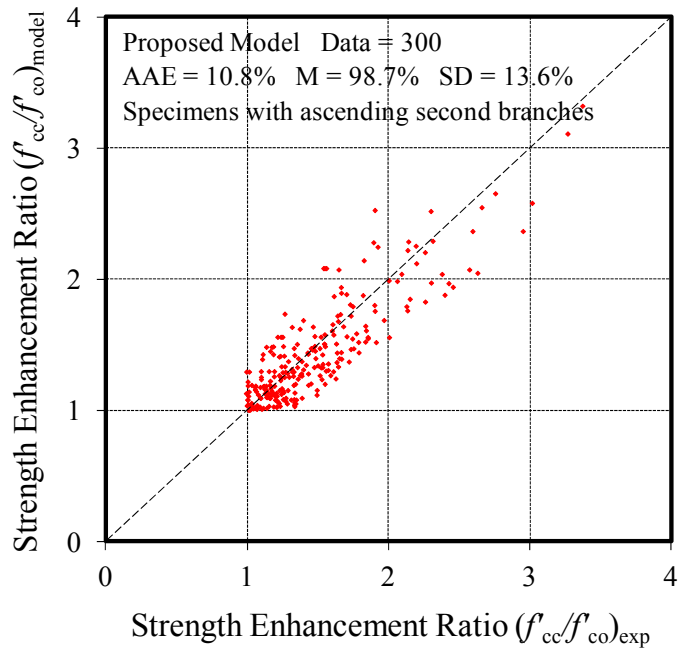

(a)

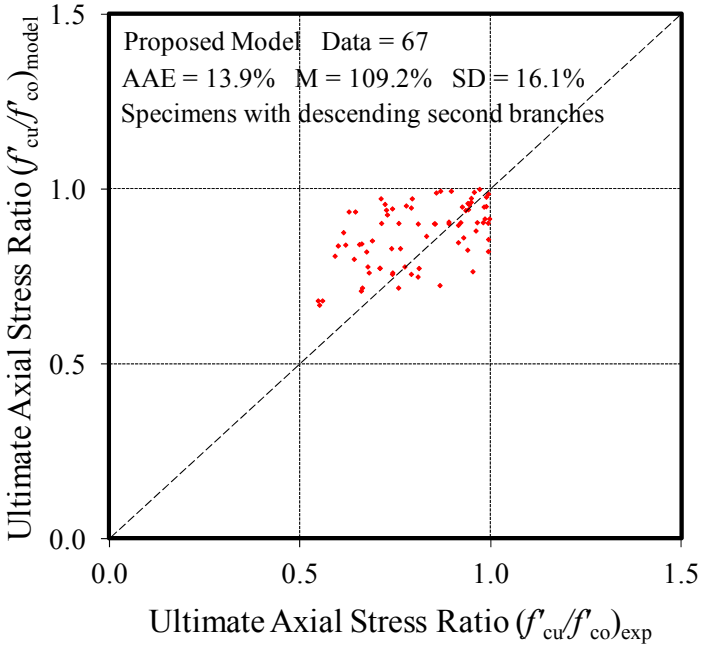

(b)

Figure 13. Comparison of model predictions of the ultimate axial stress ratios (f'_{cu}/f'_{co}) with experimental test data: (a) specimens with ascending second branches, (b) specimens with descending second branches

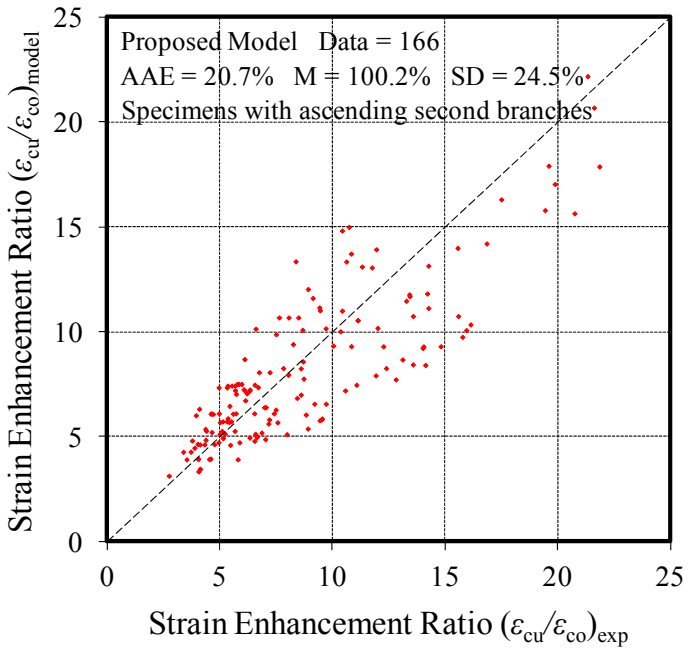

(a)

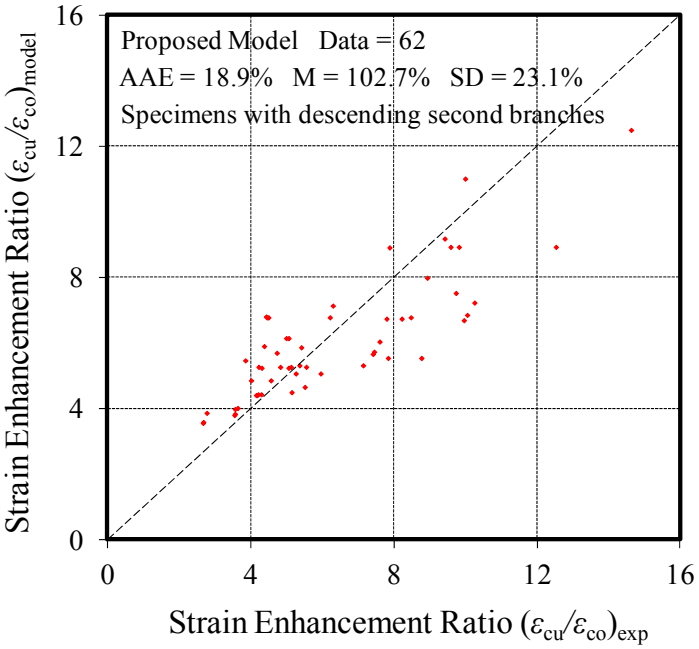

(b)

Figure 14. Comparison of model predictions of the ultimate axial strain ratios ($\varepsilon_{cu}/\varepsilon_{co}$) with experimental test data: (a) specimens with ascending second branches, (b) specimens with descending second branches

4.6 Comparisons with experimental results

Figures 13(a) and 14(a) compare the predictions of the proposed model with the experimental results of specimens exhibiting stress-strain curves with ascending second branches. Figures 13(b) and 14(b) compare the predictions of the proposed model with the experimental results of specimens exhibiting descending second branches. As shown in Figs. 13(a) and 14(a), the prediction of the proposed model is in close agreement with the test results, with AAEs of 10.8% and 20.7% for the strength enhancement ratio (f'_{cc}/f'_{co}) and strain enhancement ratio ($\varepsilon_{cu}/\varepsilon_{co}$), respectively. Figs. 13(b) and 14(b) illustrate that model predictions of the ultimate axial stress ratio (f'_{cu}/f'_{co}) and strain enhancement ratio ($\varepsilon_{cu}/\varepsilon_{co}$) are also in good agreement with the experimental results, with AAEs of the 13.9% and 18.9%, respectively.

5. CONCLUSIONS

This paper has presented the results of an investigation into the axial compressive behavior of FRP-confined NSC and HSC in square and rectangular sections. A large experimental test database consisting of 484 test results of FRP-confined concrete in square and rectangular sections has been presented. The database was augmented with another database of FRP-confined concrete in circular sections to create a combined database of 1547 axial compression test results for FRP-confined concrete specimens with unconfined concrete strengths ranging from 6.2 to 169.7 MPa. The combined databases provided a significantly extended parameter space, thereby allowing clearer observations to be made on the important factors that influence the behavior of FRP-confined concrete. A new design-oriented model, which was developed from these databases, was presented in the second half of the paper. The model is applicable to FRP-confined concrete in circular, square and rectangular sections with unconfined concrete strengths up to 120 MPa. It incorporates the influence of the change in concrete strength on the ultimate conditions, and other important factors identified from the close examination of the results recorded in the database. An important feature of the proposed model is its ability to accurately determine the threshold confinement conditions to distinguish ascending and descending types of stress-strain curves. In addition, the specific shape factors given by the model for different types of curves enable accurate prediction of the ultimate conditions of specimens exhibiting either ascending or descending types of stress-strain curves.

NOMENCLATURE

AAE Average absolute error
A_e Effectively confined concrete area of a cross-section (mm^2)
A_g gross concrete area of a cross-section (mm^2)
b width of a cross-section (mm)
c_2 Parameter in the ultimate strain expression
d_e Equivalent sectional dimension of square or rectangular section (mm)
D Diameter of a circular section (mm)
E_f Elastic modulus of fibers (MPa)
E_{frp} Elastic modulus of FRP material (MPa)
f'_{c1} Axial compressive stress of FRP-confined concrete at first peak (MPa)
f'_{cc} Peak axial compressive stress of FRP-confined concrete (MPa)
f'_{co} Peak axial compressive stress of unconfined concrete (MPa)
f'_{cu} Ultimate axial compressive stress of FRP-confined concrete (MPa)
f_f Ultimate tensile strength of fibers; $f_f = E_f \varepsilon_f$ (MPa)
f_{frp} Ultimate tensile strength of FRP material; $f_{frp} = E_{frp} \varepsilon_{frp}$ (MPa)
$f_{lu,a}$ Actual lateral confining pressure at ultimate; $f_{lu,a} = K_l \varepsilon_{h,rup}$ (MPa)
H Height of specimen (mm)
h Depth of a cross-section (mm)
K_l Lateral confinement stiffness; $K_l = 2 E_f t_f / d_e$ or $2 E_{frp} t_{frp} / d_e$ (MPa)
K_{lo} Lateral confinement stiffness threshold (MPa)
k_1 Axial strength enhancement coefficient for specimens with ascending second branch
$k_{1,des}$ Axial strength decay coefficient for specimens with descending second branch
k_2 Axial strain enhancement coefficient for specimens with ascending second branch
$k_{2,des}$ Axial strain enhancement coefficient for specimens with descending second branch
k_s Shape factor
k_{s1} Strength efficiency factor for specimens with ascending second branch
$k_{s1,des}$ Strain efficiency factor for specimens with descending second branch
k_{s2} Strain efficiency factor for specimens with ascending second branch
$k_{s2,des}$ Strength efficiency factor for specimens with descending second branch
$k_{\varepsilon,f}$ Hoop strain reduction factor of fibers
M Mean
r Corner radius of a square or rectangular section
SD Standard deviation
t_f Total nominal thickness of fibers (mm)
t_{frp} Total thickness of FRP material (mm)
ε_{co} Axial strain of unconfined concrete at f'_{co}
ε_{c1} Axial strain of concrete at f'_{c1}
ε_{cu} Ultimate axial strain of FRP-confined concrete
ε_f Ultimate tensile strain of fibers
ε_{frp} Ultimate tensile strain of FRP material
$\varepsilon_{h,rup}$ Hoop rupture strain of FRP shell

REFERENCES

ACI-440 (2002). Guide for the design and construction of externally bonded FRP systems for strengthening concrete structures (ACI 440.2R-02). *ACI Committee 440*, American Concrete Institute Farmington Hills, Michigan.

ACI-440 (2008). Guide for the design and construction of externally bonded FRP systems for strengthening concrete structures (ACI 440.2R-08). *ACI Committee 440*, American Concrete Institute Farmington Hills, Michigan.

Al-Salloum, Y. A. (2007). "Influence of edge sharpness on the strength of square concrete columns confined with FRP composite laminates." *Composites Part B-Engineering*, 38(5-6), 640-650.

Benzaid, R., Chikh, N. E. and Mesbah, H. (2008). "Behaviour of square concrete column confined with GFRP composite wrap." *Journal of Civil Engineering and Management*, 14(2), 115-120.

Campione, G. (2006). "Influence of FRP wrapping techniques on the compressive behavior of concrete prisms." *Cement and Concrete Composites*, 28(5), 497-505.

Campione, G. and Miraglia, N. (2003). "Strength and strain capacities of concrete compression members reinforced with FRP." *Cement and Concrete Composites*, 25(1), 31-41.

Campione, G., Miraglia, N. and Scibilia, N. (2001). "Compressive behaviour of RC members strengthened with carbon fibre reinforced plastic layers." *Advances in Earthquake Engineering*, 9, 397-406.

Carrazedo, R. (2002). "Mechanisms of confinement and its implication in strengthening of concrete columns with FRP jacketing." PhD dissertation, University of São Paulo.

Chaallal, O., Hassan, M. and Shahawy, M. (2003a). "Confinement model for axially loaded short rectangular columns strengthened with fiber-reinforced polymer wrapping." *ACI Structural Journal*, 100(2), 215-221.

Chaallal, O., Shahawy, M. and Hassan, M. (2003b). "Performance of axially loaded short rectangular columns strengthened with carbon fiber-reinforced polymer wrapping." *Journal of Composites for Construction*, 7(3), 200-208.

Csuka, B. and Kollar, L. P. (2012). "Fiber-reinforced plastic-confined rectangular columns subjected to axial loading." *Journal of Reinforced Plastics and Composites*, 31(7), 481-493.

Demers, M. and Neale, K. W. (1994). "Strengthening of concrete columns with unidirectional composite sheets." *Proceedings of Developments in Short and Medium Span Bridge Engineering*, Montreal, Que.

Erdil, B., Akyuz, U. and Yaman, I. O. (2012). "Mechanical behavior of CFRP confined low strength concretes subjected to simultaneous heating-cooling cycles and sustained loading." *Materials and Structures*, 45(1-2), 223-233.

Harajli, M. H. (2005). "Behavior of gravity load-designed rectangular concrete columns confined with fiber reinforced polymer sheets." *Journal of Composites for Construction*, 9(1), 4-14.

Harajli, M. H. (2006). "Axial stress-strain relationship for FRP confined circular and rectangular concrete columns." *Cement and Concrete Composites*, 28(10), 938-948.

Harajli, M. H., Hantouche, E. and Soudki, K. (2006). "Stress-strain model for fiber-reinforced polymer jacketed concrete columns." *ACI Structural Journal*, 103(5), 672-682.

Harries, K. A. and Carey, S. A. (2003). "Shape and "gap" effects on the behavior of variably confined concrete." *Cement and Concrete Research*, 33(6), 881-890.

Hosotani, K., Kawashima, K., and Hoshikuma, J. (1997). "A model for confinement effect for concrete cylinders confined by carbon fiber sheets." *NCEER-INCEDE Workshop on Earthquake Engineering Frontiers of Transportation Facilities*, State University of New York, Buffalo, New York.

Ignatowski, P. and Kamińska, M. E. (2003). "On behaviour of compressed concrete confined with CFRP composites." *Engineering and Building*, 4, 204-208.

Ilki, A. and Kumbasar, N. (2003). "Compressive behaviour of carbon fibre composite jacketed concrete with circular and non-circular cross-sections." *Journal of Earthquake Engineering*, 7(3), 381-406.

Ilki, A., Kumbasar, N. and Koc, V. (2004). "Low strength concrete members externally confined with FRP sheets." *Structural Engineering and Mechanics*, 18(2), 167-194.

Ilki, A., Peker, O., Karamuk, E., Demir, C. and Kumbasar, N. (2008). "FRP retrofit of low and medium strength circular and rectangular reinforced concrete columns." *Journal of Materials in Civil Engineering, ASCE*, 20(2), 169-188.

Kumutha, R., Vaidyanathan, R. and Palanichamy, M. S. (2007). "Behaviour of reinforced concrete rectangular columns strengthened using GFRP." *Cement and Concrete Composites*, 29(8), 609-615.

Lam, L. and Teng, J. G. (2003). "Design-oriented stress-strain model for FRP-confined concrete in rectangular columns." *Journal of Reinforced Plastics and Composites*, 22(13), 1149-1186.

Lee, C. S., Hegemier, G. A. and Phillippi, D. J. (2010). "Analytical model for fiber-reinforced polymer-jacketed square concrete columns in axial compression." *ACI Structural Journal*, 107(2), 208-217.

Li, J., Qian, J. R. and Jiang, J. B. (2002). "Experimental investigation on axial compressive behavior of FRP confined concrete columns." *Advances in Building Technology*, 1-2, 289-296.

Lim, J. C. and Ozbakkaloglu, T. (2014). "Confinement model for FRP-confined high-strength concrete." *Journal of Composites for Construction, ASCE*, 18(4), 04013058.

Masia, M. J., Gale, T. N. and Shrive, N. G. (2004). "Size effects in axially loaded square-section concrete prisms strengthened using carbon fibre reinforced polymer wrapping." *Canadian Journal of Civil Engineering*, 31(1), 1-13.

Mirmiran, A., Shahawy, M., Samaan, M., El Echary, H., Mastrapa, J. C. and Pico, O. (1998). "Effect of column parameters on FRP-confined concrete." *Journal of Composites for Construction*, 2(4), 175-185.

Modarelli, R., Micelli, F. and Manni, O. (2005). "FRP-confinement of hollow concrete cylinders and prisms." *Proceedings of the 7th International Symposium on Fiber Reinforced Polymer Reinforcement of Reinforced Concrete Structures*, 1029-1046.

Ozbakkaloglu, T. (2013a). "Axial compressive behavior of square and rectangular high-strength concrete-filled FRP tubes." *Journal of Composites for Construction*, 17(1), 151-161.

Ozbakkaloglu, T. (2013b). "Behavior of square and rectangular ultra high-strength concrete-filled FRP tubes under axial compression." *Composites Part B: Engineering.*, 54, 97-111.

Ozbakkaloglu, T. and Lim, J. C. (2013). "Axial compressive behavior of FRP-confined concrete: Experimental test database and a new design-oriented model." *Composites Part B: Engineering*, 55, 607-634.

Ozbakkaloglu, T., Lim, J. C. and Vincent, T. (2013). "FRP-confined concrete in circular sections: Review and assessment of stress–strain models." *Engineering Structures*, 49, 1068–1088.

Ozbakkaloglu, T. and Oehlers, D. J. (2008). "Concrete-filled square and rectangular FRP tubes under axial compression." *Journal of Composites for Construction*, 12(4), 469-477.

Parvin, A. and Wang, W. (2001). "Behavior of FRP jacketed concrete columns under eccentric loading." *Journal of Composites for Construction*, 5(3), 146-152.

Restrepol, J. I. and DeVino, B. (1996). "Enhancement of the axial load carrying capacity of reinforced concrete columns by means of fiberglass-epoxy jackets." *Proceedings of the 2nd International Conference on Advanced Composite Materials in Bridges and Structures*, Montreal, 547-553.

Rochette, P. and Labossiére, P. (2000). "Axial testing of rectangular column models confined with composites." *Journal of Composites for Construction*, 4(3), 129-136.

Rousakis, T. C. and Karabinis, A. I. (2012). "Adequately FRP confined reinforced concrete columns under axial compressive monotonic or cyclic loading." *Materials and Structures*, 45(7), 957-975.

Rousakis, T. C., Karabinis, A. I. and Kiousis, P. D. (2007). "FRP-confined concrete members: Axial compression experiments and plasticity modelling." *Engineering Structures*, 29(7), 1343-1353.

Shehata, I., Carneiro, L. A. V. and Shehata, L. C. D. (2002). "Strength of short concrete columns confined with CFRP sheets." *Materials and Structures*, 35(245), 50-58.

Suter, R. and Pinzelli, R. (2001). "Confinement of concrete columns with FRP sheets." *Proceedings of the 5th Symposuim on Fibre Reinforced Plastic Reinforcement for Concrete Structures*, London, 791-802.

Tao, Z., Yu, Q. and Zhong, Y. Z. (2008). "Compressive behaviour of CFRP-confined rectangular concrete columns." *Magazine of Concrete Research*, 60(10), 735-745.

Tasdemir, M. A., Tasdemir, C., Jefferson, A. D., Lydon, F. D. and Barr, B. I. G. (1998). "Evaluation of strains at peak stresses in concrete: A three-phase composite model approach." *Cement and Concrete Research*, 20(4), 301-318.

Toutanji, H., Han, M., Gilbert, J. and Matthys, S. (2010). "Behavior of large-scale rectangular columns confined with FRP composites." *Journal of Composites for Construction*, 14(1), 62-71.

Wang, L. M. and Wu, Y. F. (2008). "Effect of corner radius on the performance of CFRP-confined square concrete columns: Test." *Engineering Structures*, 30(2), 493-505.

Wang, Y. F. and Wu, H. L. (2010). "Experimental investigation on square high-strength concrete short columns confined with AFRP sheets." *Journal of Composites for Construction*, 14(3), 346-351.

Wang, Y. F. and Wu, H. L. (2011). "Size effect of concrete short columns confined with aramid FRP jackets." *Journal of Composites for Construction*, 15(4), 535-544.

Wang, Z., Wang, D. and Smith, S. T. (2012a). "Size effect of square concrete columns confined with CFRP wraps." *Proceedings of the Third Asia-Pacific Conference on FRP in Structures*, Hokkaido University, Japan, S1A01.

Wang, Z. Y., Wang, D. Y., Smith, S. T. and Lu, D. G. (2012b). "CFRP-confined square RC columns. I: experimental investigation." *Journal of Composites for Construction*, 16(2), 150-160.

Wei, Y. Y. and Wu, Y. F. (2012). "Unified stress-strain model of concrete for FRP-confined columns." *Construction and Building Materials*, 26(1), 381-392.

Wu, G., Wu, Z. S. and Lu, Z. T. (2007). "Design-oriented stress-strain model for concrete prisms confined with FRP composites." *Construction and Building Materials*, 21(5), 1107-1121.

Wu, Y. F. and Wang, L. M. (2009). "Unified strength model for square and circular concrete columns confined by external jacket." *Journal of Structural Engineering*, 135(3), 253-261.

Wu, Y. F. and Wei, Y. Y. (2010). "Effect of cross-sectional aspect ratio on the strength of CFRP-confined rectangular concrete columns." *Engineering Structures*, 32(1), 32-45.

Wu, Y. F. and Zhou, Y. W. (2010). "Unified strength model based on Hoek-Brown failure criterion for circular and square concrete columns confined by FRP." *Journal of Composites for Construction*, 14(2), 175-184.

Yan, Z. and Pantelides, C. P. (2007). "Design-oriented model for concrete columns confined with bonded FRP jackets or post-tensioned FRP shells." *Proceedings of the 8th International Symposium on Fiber Reinforced Polymer Reinforcement for Concrete Structures*, University of Patras, Patras, Greece.

Yan, Z. H., Pantelides, C. P. and Reaveley, L. D. (2006). "Fiber-reinforced polymer jacketed and shape-modified compression members: I - Experimental behavior." *ACI Structural Journal*, 103(6), 885-893.

Yeh, F. Y. and Chang, K. C. (2012). "Size and shape effects on strength and ultimate strain in FRP confined rectangular concrete columns." *Journal of Mechanics*, 28(4), 677-690.

Youssef, M. N., Feng, M. Q. and Mosallam, A. S. (2007). "Stress-strain model for concrete confined by FRP composites." *Composites Part B-Engineering*, 38(5-6), 614-628.

Zhang, D. J., Wang, Y. F. and Ma, Y. S. (2010). "Compressive behaviour of FRP-confined square concrete columns after creep." *Engineering Structures*, 32(8), 1957-1963.

APPENDIX

Table A1. Test database of CFRP-confined concrete specimens

Paper	Specimen Dimensions				Concrete Properties		FRP Properties			Fiber Properties			Measured Initial Peak Conditions		Measured Ultimate Conditions	
	b (mm)	h (mm)	H (mm)	r (mm)	f'_{co} (MPa)	ε_{co} (%)	E_{frp} (GPa)	f_{frp} (MPa)	t_{frp} (mm)	E_f (GPa)	f_f (MPa)	t_f (mm)	f'_{c1} (MPa)	ε_{c1} (%)	f'_{cu} (MPa)	ε_{cu} (%)
CFRP-wrapped specimens																
Demers and Neale (1994)	152	152	505	5	32.3					25.0	380	0.900	34.1	0.40	28.0[d]	2.45[a]
Demers and Neale (1994)	152	152	505	5	42.2					25.0	380	0.900	46.0	0.35	32.0[d]	1.40[a]
Demers and Neale (1994)	152	152	505	5	42.2					25.0	380	0.900	45.7	0.35	28.0[d]	2.50[a]
Hosotani et al. (1997)	200	200	600	30	38.1		252.0[t]	4433[t]	0.668	230.0	3481	0.668	42.2	1.82	56.1	1.82
Rochett and Labossiere (2000)	152	152	500	5	42.0					82.7	1265	0.900	39.5		25.2[d]	0.69
Rochett and Labossiere (2000)	152	152	500	25	42.0					82.7	1265	0.900	41.6		41.6[d]	0.94
Rochett and Labossiere (2000)	152	152	500	25	42.0					82.7	1265	0.900	43.3		42.4	0.89
Rochett and Labossiere (2000)	152	152	500	38	42.0					82.7	1265	0.900			47.5	1.08
Rochett and Labossiere (2000)	152	152	500	38	42.0					82.7	1265	0.900	50.4		49.1	1.16
Rochett and Labossiere (2000)	152	152	500	5	43.9					82.7	1265	1.500	43.9		32.0[d]	1.02
Rochett and Labossiere (2000)	152	152	500	25	43.9					82.7	1265	1.200			50.9	1.35
Rochett and Labossiere (2000)	152	152	500	25	43.9					82.7	1265	1.500	47.9		57.6	0.90[a]
Rochett and Labossiere (2000)	152	152	500	25	35.8					82.7	1265	1.200			52.3	2.04
Rochett and Labossiere (2000)	152	152	500	25	35.8					82.7	1265	1.500			57.6	2.12
Rochett and Labossiere (2000)	152	152	500	38	35.8					82.7	1265	1.200			59.4	1.92
Rochett and Labossiere (2000)	152	152	500	38	35.8					82.7	1265	1.500			68.7	2.39
Rochett and Labossiere (2000)	152	203	500	25	42.0					82.7	1265	0.900	42.0		29.4[d]	0.79[a]
Rochett and Labossiere (2000)	152	203	500	38	42.0					82.7	1265	0.900	43.7		42.0	0.85[a]
Rochett and Labossiere (2000)	152	203	500	5	43.9					82.7	1265	1.500	44.3		27.2[d]	0.98
Rochett and Labossiere (2000)	152	203	500	25	43.9					82.7	1265	1.200	44.3		42.1[d]	0.93[a]
Rochett and Labossiere (2000)	152	152	200	3	20.1	0.21				230.0	3430	0.165	31.2			0.26[a]
Parvin and Wang (2001)	108	108	305	8.26	22.6		188.9	3022	0.178						34.7	1.32
Parvin and Wang (2001)	108	108	105	8.26	22.6		188.9	3022	0.356						45.2	2.03
Suter and Pinzelli (2001)	150	150	300	5	33.9					240.0	3800	0.234	36.1			
Suter and Pinzelli (2001)	150	150	300	25	36.6					240.0	3800	0.234	41.4			
Shehata et al. (2002)	150	150	300	10	23.7					235.0	3550	0.165	27.4			
Shehata et al. (2002)	150	150	300	10	23.7					235.0	3550	0.330	36.5			
Shehata et al. (2002)	150	150	300	10	29.5					235.0	3550	0.165	40.4	0.30	27.0[d]	0.88
Shehata et al. (2002)	150	150	300	10	29.5					235.0	3550	0.330	43.7	0.50	33.0	1.23
Shehata et al. (2002)	94	188	300	10	23.7					235.0	3550	0.165	25.8			
Shehata et al. (2002)	94	188	300	10	23.7					235.0	3550	0.330	33.2			
Shehata et al. (2002)	94	188	300	10	29.5					235.0	3550	0.165	32.0	0.20	27.0[d]	0.79
Shehata et al. (2002)	94	188	300	10	29.5					235.0	3550	0.330	38.7	0.25	28.0[d]	0.75[a]
Ilki and Kumbasar (2003)	250	250	500	40	32.8[c]	0.30				230.0	3400	0.165			32.7[d]	
Ilki and Kumbasar (2003)	250	250	500	40	32.8[c]	0.30				230.0	3400	0.165			32.3[d]	1.01
Ilki and Kumbasar (2003)	250	250	500	40	32.8[c]	0.30				230.0	3400	0.495			41.4	1.90
Ilki and Kumbasar (2003)	250	250	500	40	32.8[c]	0.30				230.0	3400	0.495			40.6	1.80
Ilki and Kumbasar (2003)	250	250	500	40	32.8[c]	0.30				230.0	3400	0.825			56.7	2.90
Ilki and Kumbasar (2003)	250	250	500	40	32.8[c]	0.30				230.0	3400	0.825			53.6	2.40
Ilki and Kumbasar (2003)	150	300	500	40	34.0[c]	0.28				230.0	3400	0.165			35.2	0.91
Ilki and Kumbasar (2003)	150	300	500	40	34.0[c]	0.28				230.0	3400	0.165			38.7	0.80
Ilki and Kumbasar (2003)	150	300	500	40	34.0[c]	0.28				230.0	3400	0.495			40.4	2.20
Ilki and Kumbasar (2003)	150	300	500	40	34.0[c]	0.28				230.0	3400	0.495			38.4	1.30
Ilki and Kumbasar (2003)	150	300	500	40	34.0[c]	0.28				230.0	3400	0.825			49.2	2.70

Paper (continued)	b (mm)	h (mm)	H (mm)	r (mm)	f'_{co} (MPa)	ε_{co} (%)	E_{frp} (GPa)	f_{frp} (MPa)	t_{frp} (mm)	E_f (GPa)	f_f (MPa)	t_f (mm)	f'_{c1} (MPa)	ε_{c1} (%)	f'_{cu} (MPa)	ε_{cu} (%)
Ilki and Kumbasar (2003)	150	300	500	40	34.0[c]	0.28				230.0	3400	0.825			51.3	3.10
Carrazedo (2002)	150	150	450	10	36.5	0.31				71.0	872	0.500	38.8	0.39	30.4[d]	0.74[a]
Carrazedo (2002)	150	150	450	30	33.5	0.28				71.0	872	0.500	38.3	0.46	38.7	0.79
Carrazedo (2002)	150	150	450	10	36.5	0.31				71.0	872	1.000	39.1	0.43	37.4	0.72
Carrazedo (2002)	150	150	450	30	33.5	0.28				71.0	872	1.000	42.2	0.44	47.8	1.22
Chaallal et al. (2003b)	107.95	165.1	304.8	25.4	25.1					231.0	3650	0.170			29.2	0.38[a]
Chaallal et al. (2003b)	107.95	165.1	304.8	25.4	25.1					231.0	3650	0.340			34.3	0.50[a]
Chaallal et al. (2003b)	107.95	165.1	304.8	25.4	25.1					231.0	3650	0.510			41.2	0.60[a]
Chaallal et al. (2003b)	107.95	165.1	304.8	25.4	25.1					231.0	3650	0.680			47.6	0.60[a]
Chaallal et al. (2003b)	95.25	190.5	304.8	25.4	22.3					231.0	3650	0.170			28.3	0.36[a]
Chaallal et al. (2003b)	95.25	190.5	304.8	25.4	22.3					231.0	3650	0.340			32.9	0.40[a]
Chaallal et al. (2003b)	95.25	190.5	304.8	25.4	22.3					231.0	3650	0.510			37.9	0.65[a]
Chaallal et al. (2003b)	95.25	190.5	304.8	25.4	22.3					231.0	3650	0.680			42.2	0.60[a]
Chaallal et al. (2003b)	107.95	165.1	304.8	25.4	55.4					231.0	3650	0.170			59.2	0.28[a]
Chaallal et al. (2003b)	107.95	165.1	304.8	25.4	55.4					231.0	3650	0.340			66.2	0.32[a]
Chaallal et al. (2003b)	107.95	165.1	304.8	25.4	55.4					231.0	3650	0.510			69.0	0.38[a]
Chaallal et al. (2003b)	107.95	165.1	304.8	25.4	55.4					231.0	3650	0.680			73.4	0.38[a]
Chaallal et al. (2003b)	95.25	190.5	304.8	25.4	48.1					231.0	3650	0.170			53.2	0.28[a]
Chaallal et al. (2003b)	95.25	190.5	304.8	25.4	48.1					231.0	3650	0.340			57.4	0.30[a]
Chaallal et al. (2003b)	95.25	190.5	304.8	25.4	48.1					231.0	3650	0.510			59.4	0.31[a]
Chaallal et al. (2003b)	95.25	190.5	304.8	25.4	48.1					231.0	3650	0.680			60.4	0.31[a]
Chaallal et al. (2003b)	133.35	133.35	304.8	25.4	21.4					231.0	3650	0.170			26.2	0.35[a]
Chaallal et al. (2003b)	133.35	133.35	304.8	25.4	21.4					231.0	3650	0.340			30.8	0.42[a]
Chaallal et al. (2003b)	133.35	133.35	304.8	25.4	21.4					231.0	3650	0.510			36.4[s]	0.55[a]
Chaallal et al. (2003b)	133.35	133.35	304.8	25.4	21.4					231.0	3650	0.680			42.2[s]	0.65[a]
Chaallal et al. (2003b)	133.35	133.35	304.8	25.4	54.7					231.0	3650	0.170			59.0	0.28[a]
Chaallal et al. (2003b)	133.35	133.35	304.8	25.4	54.7					231.0	3650	0.340			59.8	0.32[a]
Chaallal et al. (2003b)	133.35	133.35	304.8	25.4	54.7					231.0	3650	0.510			64.5	0.38[a]
Chaallal et al. (2003b)	133.35	133.35	304.8	25.4	54.7					231.0	3650	0.680			68.9	0.40[a]
Ignatowski and Kaminska (2003)	100	100		10	32.3					230.0	3500	0.260			43.6	
Ignatowski and Kaminska (2003)	105	200		10	32.3					230.0	3500	0.130			37.5	
Ignatowski and Kaminska (2003)	105	200		10	32.3					230.0	3500	0.260			40.7	
Lam and Teng (2003)	150	150	600	15	33.7	0.20	257.0[t]	4519[t]	0.165				32.5	0.45	35.0	0.74
Lam and Teng (2003)	150	150	600	25	33.7	0.20	257.0[t]	4519[t]	0.165				39.8	0.93	39.4	0.93
Lam and Teng (2003)	150	150	600	15	33.7	0.20	257.0[t]	4519[t]	0.330					0.87	50.4	0.87[a]
Lam and Teng (2003)	150	150	600	25	33.7	0.20	257.0[t]	4519[t]	0.330					0.85	61.9	0.85[a]
Lam and Teng (2003)	150	150	600	15	24.0	0.20	257.0[t]	4519[t]	0.495					1.80	61.6	1.80
Lam and Teng (2003)	150	150	600	25	24.0	0.20	257.0[t]	4519[t]	0.495					1.52	66.0	1.52[a]
Lam and Teng (2003)	150	150	600	15	24.0	0.20	257.0[t]	4519[t]	0.660						63.7	
Lam and Teng (2003)	150	150	600	25	24.0	0.20	257.0[t]	4519[t]	0.660						80.8	
Lam and Teng (2003)	150	150	600	15	41.5	0.20	257.0[t]	4519[t]	0.825						82.9	
Lam and Teng (2003)	150	150	600	25	41.5	0.20	257.0[t]	4519[t]	0.825						95.2	
Lam and Teng (2003)	150	225	600	15	41.5	0.20	257.0[t]	4519[t]	0.660				50.7	0.33	49.2	1.23
Lam and Teng (2003)	150	225	600	25	41.5	0.20	257.0[t]	4519[t]	0.660				56.9	0.32	51.9	1.04[a]
Masia et al. (2004)	100	100	300	25	25.5					230.0	3500	0.260			55.9	2.00
Masia et al. (2004)	100	100	300	25	22.8					230.0	3500	0.260			48.7	1.82
Masia et al. (2004)	100	100	300	25	25.1					230.0	3500	0.260			45.7	1.47
Masia et al. (2004)	100	100	300	25	23.8					230.0	3500	0.260			50.7	

Paper (continued)	b (mm)	h (mm)	H (mm)	r (mm)	f'_{co} (MPa)	ε_{co} (%)	E_{frp} (GPa)	f_{frp} (MPa)	t_{frp} (mm)	E_f (GPa)	f_f (MPa)	t_f (mm)	f'_{c1} (MPa)	ε_{c1} (%)	f'_{cu} (MPa)	ε_{cu} (%)
Masia et al. (2004)	100	100	300	25	21.7					230.0	3500	0.260			56.2	
Masia et al. (2004)	125	125	375	25	23.7					230.0	3500	0.260			45.0	1.62
Masia et al. (2004)	125	125	375	25	22.9					230.0	3500	0.260			39.9	1.55
Masia et al. (2004)	125	125	375	25	25.7					230.0	3500	0.260			42.1	1.72
Masia et al. (2004)	125	125	375	25	25.5					230.0	3500	0.260			35.5	
Masia et al. (2004)	125	125	375	25	24.3					230.0	3500	0.260			40.2	
Masia et al. (2004)	150	150	450	25	24.5					230.0	3500	0.260			35.7	1.06
Masia et al. (2004)	150	150	450	25	21.3					230.0	3500	0.260			36.2	1.09
Masia et al. (2004)	150	150	450	25	24.8					230.0	3500	0.260			36.6	1.52
Masia et al. (2004)	150	150	450	25	23.6					230.0	3500	0.260			36.5	
Masia et al. (2004)	150	150	450	25	25.3					230.0	3500	0.260			36.0	
Modarelli et al. (2005)	150	200	400	10	17.6					221.0	3068	0.165	30.3[s]			2.36[a]
Modarelli et al. (2005)	150	200	400	10	17.6					221.0	3068	0.330	34.1[s]			3.26[a]
Modarelli et al. (2005)	150	150	300	10	25.0	0.63				221.0	3068	0.330	32.0			3.57[a]
Modarelli et al. (2005)	150	150	300	25	21.4	0.56				221.0	3068	0.165	36.2[s]			1.83
Modarelli et al. (2005)	150	150	300	25	21.4	0.56				221.0	3068	0.330			42.1	3.11
Campione (2006)	150	150	450	3	13.0					230.0	3430	0.165	16.0		14.0	0.12[a]
Campione (2006)	150	150	450	3	13.0					230.0	3430	0.330	17.0		19.0	0.24[a]
Harajli et al. (2006)	132	132	300	15	18.9					230.0	3500	0.130			29.2	0.90
Harajli et al. (2006)	132	132	300	15	18.9					230.0	3500	0.260			40.3[s]	
Harajli et al. (2006)	132	132	300	15	18.9					230.0	3500	0.390			43.4	1.90
Harajli et al. (2006)	102	176	300	15	19.3					230.0	3500	0.130			23.7	8.00[a]
Harajli et al. (2006)	102	176	300	15	19.3					230.0	3500	0.260			31.3	1.20
Harajli et al. (2006)	102	176	300	15	19.3					230.0	3500	0.390			36.8	1.70
Harajli et al. (2006)	79	214	300	15	21.5					230.0	3500	0.130			28.0	0.30[a]
Harajli et al. (2006)	79	214	300	15	21.5					230.0	3500	0.260			28.6	0.40[a]
Harajli et al. (2006)	79	214	300	15	21.5					230.0	3500	0.390			30.7	0.60[a]
Harajli et al. (2006)	79	214	300	15	21.5					230.0	3500	0.260			28.6	0.40[a]
Harajli et al. (2006)	79	214	300	15	21.5					230.0	3500	0.390			30.7	0.60[a]
Yan et al. (2006)	279	279	914	19	15.2	0.20	86.9	1220	2.000						26.2	1.00[a]
Al-Salloum (2007)	150	150	500	5	28.7					75.1	935	1.200	41.2	0.17	35.0	0.40[a]
Al-Salloum (2007)	150	150	500	5	30.9					75.1	935	1.200	42.5	0.17		
Al-Salloum (2007)	150	150	500	25	31.8					75.1	935	1.200			48.3	0.69[a]
Al-Salloum (2007)	150	150	500	25	28.5					75.1	935	1.200			45.6	0.69[a]
Al-Salloum (2007)	150	150	500	38	27.7					75.1	935	1.200			57.0	0.79[a]
Al-Salloum (2007)	150	150	500	38	30.3					75.1	935	1.200			55.0	0.79[a]
Al-Salloum (2007)	150	150	500	50	26.7					75.1	935	1.200			61.7	1.11[a]
Al-Salloum (2007)	150	150	500	50	28.3					75.1	935	1.200			63.7	1.11[a]
Rousakis et al. (2007)	200	200	320	30	33.0	0.17				240.0	3800	0.117	38.4[s]	4.50	38.0	4.79[a]
Rousakis et al. (2007)	200	200	320	30	33.0	0.17				240.0	3800	0.351	45.9	7.74	45.5	10.08[a]
Rousakis et al. (2007)	200	200	320	30	33.0	0.17				240.0	3800	0.585	55.6	11.04	55.4	11.11[a]
Rousakis et al. (2007)	200	200	320	30	34.2	0.19				240.0	3800	0.117	42.2[s]	2.86	40.1	4.04[a]
Rousakis et al. (2007)	200	200	320	30	34.2	0.19				240.0	3800	0.351	45.2	8.80	45.2	9.59[a]
Rousakis et al. (2007)	200	200	320	30	34.2	0.19				240.0	3800	0.585			54.6	14.04[a]
Youssef (2007)	381	381	762	38	34.2	0.20				103.8	1246	1.168			35.2	0.90
Youssef (2007)	381	381	762	38	34.2	0.20				103.8	1246	1.168			34.0	0.89
Youssef (2007)	381	381	762	38	34.2	0.20				103.8	1246	1.168			36.4	0.80
Youssef (2007)	381	381	762	38	34.2	0.20				103.8	1246	2.337			40.6	1.06
Youssef (2007)	381	381	762	38	34.2	0.20				103.8	1246	2.337			39.3	1.02
Youssef (2007)	381	381	762	38	34.2	0.20				103.8	1246	2.337			37.4	1.10

Paper (continued)	b (mm)	h (mm)	H (mm)	r (mm)	f'_{co} (MPa)	ε_{co} (%)	E_{frp} (GPa)	f_{frp} (MPa)	t_{frp} (mm)	E_f (GPa)	f_f (MPa)	t_f (mm)	f'_{c1} (MPa)	ε_{c1} (%)	f'_{cu} (MPa)	ε_{cu} (%)
Youssef (2007)	381	381	762	38	34.2	0.20				103.8	1246	3.505			42.6	1.06
Youssef (2007)	381	381	762	38	34.2	0.20				103.8	1246	3.505			41.4	1.10
Youssef (2007)	381	381	762	38	34.2	0.20				103.8	1246	3.505			42.2	1.13
Youssef (2007)	381	381	762	38	34.2	0.20				103.8	1246	5.842			53.2	1.69
Youssef (2007)	381	381	762	38	34.2	0.20				103.8	1246	5.842			52.5	1.60
Youssef (2007)	381	381	762	38	34.2	0.20				103.8	1246	5.842			52.8	1.52
Youssef (2007)	254	381	762	38	38.7	0.20				103.8	1246	1.168			40.0	0.78
Youssef (2007)	254	381	762	38	38.7	0.20				103.8	1246	1.753			41.0	0.91
Youssef (2007)	254	381	762	38	34.8	0.20				103.8	1246	1.753			36.7	0.79
Youssef (2007)	254	381	762	38	36.6	0.20				103.8	1246	2.921			40.5	1.65
Youssef (2007)	254	381	762	38	36.6	0.20				103.8	1246	2.921			43.2	1.65
Youssef (2007)	254	381	762	38	38.7	0.20				103.8	1246	4.674			45.6	1.62
Youssef (2007)	254	381	762	38	38.7	0.20				103.8	1246	4.674			46.0	1.69
Youssef (2007)	254	381	762	38	38.7	0.20				103.8	1246	4.674			47.2	1.58
Tao et al. (2008)	150	150	450	20	22.0					239.0	4470	0.170			33.5	2.53[a]
Tao et al. (2008)	150	150	450	20	22.0					239.0	4470	0.340			49.6	3.95[a]
Tao et al. (2008)	150	150	450	20	19.5					239.0	4470	0.340			47.2	3.34
Tao et al. (2008)	150	150	450	35	22.0					239.0	4470	0.340			64.8	3.66
Tao et al. (2008)	150	150	450	35	19.5					239.0	4470	0.340			58.7	3.48
Tao et al. (2008)	150	150	450	50	22.0					239.0	4470	0.340			76.6[s]	3.87
Tao et al. (2008)	150	150	450	50	19.5					239.0	4470	0.340			63.6	3.43
Tao et al. (2008)	150	230	450	20	22.0					239.0	4470	0.170			23.6	0.91
Tao et al. (2008)	150	230	450	20	22.0					239.0	4470	0.340			33.2	3.31[a]
Tao et al. (2008)	150	230	450	35	22.0					239.0	4470	0.340			40.7	2.82
Tao et al. (2008)	150	230	450	50	22.0					239.0	4470	0.340			46.7	2.93
Tao et al. (2008)	150	300	450	20	19.5					239.0	4470	0.170	21.8	0.38		
Tao et al. (2008)	150	300	450	20	19.5					239.0	4470	0.340			23.6	2.71[a]
Tao et al. (2008)	150	300	450	35	19.5					239.0	4470	0.340			30.9	2.99[a]
Tao et al. (2008)	150	300	450	50	19.5					239.0	4470	0.340			34.8	3.13
Tao et al. (2008)	150	150	450	20	49.5					241.0	4200	0.170	54.2	0.39		
Tao et al. (2008)	150	150	450	20	49.5					241.0	4200	0.340			61.4	1.66
Tao et al. (2008)	150	150	450	35	49.5					241.0	4200	0.340			84.9	2.08
Tao et al. (2008)	150	150	450	50	49.5					241.0	4200	0.340			86.1	1.65
Tao et al. (2008)	150	230	450	20	49.5					241.0	4200	0.170	50.0	0.31		
Tao et al. (2008)	150	230	450	20	49.5					241.0	4200	0.340	50.5	0.29		
Tao et al. (2008)	150	300	450	20	49.5					241.0	4200	0.340	52.4	0.31		
Tao et al. (2008)	150	300	450	35	49.5					241.0	4200	0.340	51.3	0.30		
Tao et al. (2008)	150	300	450	50	49.5					241.0	4200	0.340	54.1	0.30		
Wang and Wu (2008)	150	150	300	0	31.4	0.20	219.0[t]	4364[t]	0.165	230.5	3482	0.165	32.0			
Wang and Wu (2008)	150	150	300	0	31.2	0.20	219.0[t]	4364[t]	0.165	230.5	3482	0.165	32.0			
Wang and Wu (2008)	150	150	300	0	32.3	0.20	219.0[t]	4364[t]	0.165	230.5	3482	0.165	32.7			
Wang and Wu (2008)	150	150	300	0	31.4	0.20	219.0[t]	4364[t]	0.330	230.5	3482	0.330	32.1			
Wang and Wu (2008)	150	150	300	0	31.2	0.20	219.0[t]	4364[t]	0.330	230.5	3482	0.330	31.8			
Wang and Wu (2008)	150	150	300	0	32.3	0.20	219.0[t]	4364[t]	0.330	230.5	3482	0.330	32.7			
Wang and Wu (2008)	150	150	300	15	32.9	0.20	219.0[t]	4364[t]	0.165	230.5	3482	0.165			38.8	
Wang and Wu (2008)	150	150	300	15	32.2	0.20	219.0[t]	4364[t]	0.165	230.5	3482	0.165	31.0			
Wang and Wu (2008)	150	150	300	15	30.7	0.20	219.0[t]	4364[t]	0.165	230.5	3482	0.165	30.8			
Wang and Wu (2008)	150	150	300	15	32.9	0.20	219.0[t]	4364[t]	0.330	230.5	3482	0.330			40.5	
Wang and Wu (2008)	150	150	300	15	32.2	0.20	219.0[t]	4364[t]	0.330	230.5	3482	0.330			43.6	
Wang and Wu (2008)	150	150	300	15	30.7	0.20	219.0[t]	4364[t]	0.330	230.5	3482	0.330			42.4	

Paper (continued)	b (mm)	h (mm)	H (mm)	r (mm)	f'_{co} (MPa)	ε_{co} (%)	E_{frp} (GPa)	f_{frp} (MPa)	t_{frp} (mm)	E_f (GPa)	f_f (MPa)	t_f (mm)	f'_{c1} (MPa)	ε_{c1} (%)	f'_{cu} (MPa)	ε_{cu} (%)
Wang and Wu (2008)	150	150	300	30	32.6	0.20	219.0[t]	4364[t]	0.165	230.5	3482	0.165			43.4	
Wang and Wu (2008)	150	150	300	30	31.1	0.20	219.0[t]	4364[t]	0.165	230.5	3482	0.165			38.8	
Wang and Wu (2008)	150	150	300	30	33.1	0.20	219.0[t]	4364[t]	0.165	230.5	3482	0.165			37.1	
Wang and Wu (2008)	150	150	300	30	32.6	0.20	219.0[t]	4364[t]	0.330	230.5	3482	0.330			58.1	
Wang and Wu (2008)	150	150	300	30	31.1	0.20	219.0[t]	4364[t]	0.330	230.5	3482	0.330			57.5	
Wang and Wu (2008)	150	150	300	30	33.1	0.20	219.0[t]	4364[t]	0.330	230.5	3482	0.330			53.8	
Wang and Wu (2008)	150	150	300	45	30.1	0.20	219.0[t]	4364[t]	0.165	230.5	3482	0.165			48.3	
Wang and Wu (2008)	150	150	300	45	32.6	0.20	219.0[t]	4364[t]	0.165	230.5	3482	0.165			42.1	
Wang and Wu (2008)	150	150	300	45	29.3	0.20	219.0[t]	4364[t]	0.165	230.5	3482	0.165			40.8	
Wang and Wu (2008)	150	150	300	45	30.1	0.20	219.0[t]	4364[t]	0.330	230.5	3482	0.330			64.6	
Wang and Wu (2008)	150	150	300	45	32.6	0.20	219.0[t]	4364[t]	0.330	230.5	3482	0.330			69.4	
Wang and Wu (2008)	150	150	300	45	29.3	0.20	219.0[t]	4364[t]	0.330	230.5	3482	0.330			70.1	
Wang and Wu (2008)	150	150	300	60	30.9	0.20	219.0[t]	4364[t]	0.165	230.5	3482	0.165			50.9	
Wang and Wu (2008)	150	150	300	60	31.1	0.20	219.0[t]	4364[t]	0.165	230.5	3482	0.165			51.7	
Wang and Wu (2008)	150	150	300	60	33.5	0.20	219.0[t]	4364[t]	0.165	230.5	3482	0.165			47.3	
Wang and Wu (2008)	150	150	300	60	30.9	0.20	219.0[t]	4364[t]	0.330	230.5	3482	0.330			81.1	
Wang and Wu (2008)	150	150	300	60	31.1	0.20	219.0[t]	4364[t]	0.330	230.5	3482	0.330			73.8	
Wang and Wu (2008)	150	150	300	60	33.5	0.20	219.0[t]	4364[t]	0.330	230.5	3482	0.330			82.1	
Wang and Wu (2008)	150	150	300	0	51.2		225.7[t]	3788[t]	0.165	230.0	3500	0.165	52.4			
Wang and Wu (2008)	150	150	300	0	53.3		225.7[t]	3788[t]	0.165	230.0	3500	0.165	54.6			
Wang and Wu (2008)	150	150	300	0	52.0		225.7[t]	3788[t]	0.165	230.0	3500	0.165	54.1			
Wang and Wu (2008)	150	150	300	0	51.2		225.7[t]	3788[t]	0.330	230.0	3500	0.330	56.2			
Wang and Wu (2008)	150	150	300	0	53.3		225.7[t]	3788[t]	0.330	230.0	3500	0.330	55.0			
Wang and Wu (2008)	150	150	300	0	52.0		225.7[t]	3788[t]	0.330	230.0	3500	0.330	56.7			
Wang and Wu (2008)	150	150	300	15	54.7		225.7[t]	3788[t]	0.165	230.0	3500	0.165	55.0			
Wang and Wu (2008)	150	150	300	15	55.2		225.7[t]	3788[t]	0.165	230.0	3500	0.165	56.1			
Wang and Wu (2008)	150	150	300	15	52.5		225.7[t]	3788[t]	0.165	230.0	3500	0.165	56.2			
Wang and Wu (2008)	150	150	300	15	54.7		225.7[t]	3788[t]	0.330	230.0	3500	0.330			59.6	
Wang and Wu (2008)	150	150	300	15	55.2		225.7[t]	3788[t]	0.330	230.0	3500	0.330			59.6	
Wang and Wu (2008)	150	150	300	15	52.5		225.7[t]	3788[t]	0.330	230.0	3500	0.330			59.0	
Wang and Wu (2008)	150	150	300	30	53.5		225.7[t]	3788[t]	0.165	230.0	3500	0.165	56.2			
Wang and Wu (2008)	150	150	300	30	53.1		225.7[t]	3788[t]	0.165	230.0	3500	0.165	55.5			
Wang and Wu (2008)	150	150	300	30	49.4		225.7[t]	3788[t]	0.165	230.0	3500	0.165	56.0			
Wang and Wu (2008)	150	150	300	30	53.5		225.7[t]	3788[t]	0.330	230.0	3500	0.330	65.2			
Wang and Wu (2008)	150	150	300	30	53.1		225.7[t]	3788[t]	0.330	230.0	3500	0.330	61.4			
Wang and Wu (2008)	150	150	300	30	49.4		225.7[t]	3788[t]	0.330	230.0	3500	0.330	62.5			
Wang and Wu (2008)	150	150	300	45	53.2		225.7[t]	3788[t]	0.165	230.0	3500	0.165	56.4			
Wang and Wu (2008)	150	150	300	45	51.5		225.7[t]	3788[t]	0.165	230.0	3500	0.165	58.4			
Wang and Wu (2008)	150	150	300	45	53.5		225.7[t]	3788[t]	0.165	230.0	3500	0.165	57.9			
Wang and Wu (2008)	150	150	300	45	53.2		225.7[t]	3788[t]	0.330	230.0	3500	0.330			81.3	
Wang and Wu (2008)	150	150	300	45	51.5		225.7[t]	3788[t]	0.330	230.0	3500	0.330			78.8	
Wang and Wu (2008)	150	150	300	45	53.3		225.7[t]	3788[t]	0.330	230.0	3500	0.330			80.9	
Wang and Wu (2008)	150	150	300	60	53.9		225.7[t]	3788[t]	0.165	230.0	3500	0.165			62.4	
Wang and Wu (2008)	150	150	300	60	52.0		225.7[t]	3788[t]	0.165	230.0	3500	0.165			62.7	
Wang and Wu (2008)	150	150	300	60	52.3		225.7[t]	3788[t]	0.165	230.0	3500	0.165			62.8	
Wang and Wu (2008)	150	150	300	60	53.9		225.7[t]	3788[t]	0.330	230.0	3500	0.330			87.9	
Wang and Wu (2008)	150	150	300	60	52.0		225.7[t]	3788[t]	0.330	230.0	3500	0.330			90.9	
Wang and Wu (2008)	150	150	300	60	52.3		225.7[t]	3788[t]	0.330	230.0	3500	0.330			90.4	
Wu and Wei (2010)	150	150	300	30	32.3		229.0[t]	4192[t]	0.167	230.0	3400	0.167		1.54	40.5	1.55
Wu and Wei (2010)	150	150	300	30	35.9		229.0[t]	4192[t]	0.167	230.0	3400	0.167		1.10	40.7	1.11

Paper (continued)	b (mm)	h (mm)	H (mm)	r (mm)	f'_{co} (MPa)	ε_{co} (%)	E_{frp} (GPa)	f_{frp} (MPa)	t_{frp} (mm)	E_f (GPa)	f_f (MPa)	t_f (mm)	f'_{c1} (MPa)	ε_{c1} (%)	f'_{cu} (MPa)	ε_{cu} (%)
Wu and Wei (2010)	150	150	300	30	42.4		229.0[t]	4192[t]	0.167	230.0	3400	0.167		0.50	42.5	1.27
Wu and Wei (2010)	150	188	300	30	34.2		229.0[t]	4192[t]	0.167	230.0	3400	0.167		0.65	38.0	0.77
Wu and Wei (2010)	150	188	300	30	32.9		229.0[t]	4192[t]	0.167	230.0	3400	0.167		0.64	38.9	0.93
Wu and Wei (2010)	150	188	300	30	39.9		229.0[t]	4192[t]	0.167	230.0	3400	0.167		0.70	39.4[d]	1.18
Wu and Wei (2010)	150	225	300	30	35.8		229.0[t]	4192[t]	0.167	230.0	3400	0.167	37.6	0.56		1.44
Wu and Wei (2010)	150	225	300	30	36.6		229.0[t]	4192[t]	0.167	230.0	3400	0.167	35.6	0.40		0.86
Wu and Wei (2010)	150	225	300	30	39.7		229.0[t]	4192[t]	0.167	230.0	3400	0.167	39.2	0.56		1.16
Wu and Wei (2010)	150	263	300	30	36.5		229.0[t]	4192[t]	0.167	230.0	3400	0.167	35.2	0.44		0.96
Wu and Wei (2010)	150	263	300	30	38.1		229.0[t]	4192[t]	0.167	230.0	3400	0.167	37.8	0.42		0.84
Wu and Wei (2010)	150	263	300	30	38.9		229.0[t]	4192[t]	0.167	230.0	3400	0.167	37.6	0.43		0.95
Wu and Wei (2010)	150	300	300	30	33.9		229.0[t]	4192[t]	0.167	230.0	3400	0.167	36.6	0.47		0.77
Wu and Wei (2010)	150	300	300	30	36.8		229.0[t]	4192[t]	0.167	230.0	3400	0.167	37.7	0.44		0.82
Wu and Wei (2010)	150	300	300	30	39.9		229.0[t]	4192[t]	0.167	230.0	3400	0.167	38.0	0.38		0.88
Wu and Wei (2010)	150	150	300	30	32.3		229.0[t]	4192[t]	0.334	230.0	3400	0.334		2.32	59.2	2.32
Wu and Wei (2010)	150	150	300	30	35.9		229.0[t]	4192[t]	0.334	230.0	3400	0.334		1.74	59.6	1.75
Wu and Wei (2010)	150	150	300	30	42.4		229.0[t]	4192[t]	0.334	230.0	3400	0.334		2.07	62.3	2.07
Wu and Wei (2010)	150	188	300	30	34.2		229.0[t]	4192[t]	0.334	230.0	3400	0.334		1.22	48.8	1.22
Wu and Wei (2010)	150	188	300	30	32.9		229.0[t]	4192[t]	0.334	230.0	3400	0.334		1.12	51.1	1.12
Wu and Wei (2010)	150	188	300	30	39.9		229.0[t]	4192[t]	0.334	230.0	3400	0.334		2.09	53.3	2.23[a]
Wu and Wei (2010)	150	225	300	30	35.8		229.0[t]	4192[t]	0.334	230.0	3400	0.334		1.42	43.0	1.46
Wu and Wei (2010)	150	225	300	30	36.6		229.0[t]	4192[t]	0.334	230.0	3400	0.334		1.55	45.2	1.55
Wu and Wei (2010)	150	225	300	30	39.7		229.0[t]	4192[t]	0.334	230.0	3400	0.334		1.30	43.4	1.46
Wu and Wei (2010)	150	263	301	30	36.5		229.0[t]	4192[t]	0.334	230.0	3400	0.334		0.45	38.9	2.00[a]
Wu and Wei (2010)	150	263	301	30	38.1		229.0[t]	4192[t]	0.334	230.0	3400	0.334		0.56	41.4	1.32
Wu and Wei (2010)	150	263	301	30	38.9		229.0[t]	4192[t]	0.334	230.0	3400	0.334		0.45	41.3	0.92
Wu and Wei (2010)	150	300	302	30	33.9		229.0[t]	4192[t]	0.334	230.0	3400	0.334	38.6	0.44		1.07[a]
Wu and Wei (2010)	150	300	302	30	36.8		229.0[t]	4192[t]	0.334	230.0	3400	0.334	39.1	0.42		1.19
Wu and Wei (2010)	150	300	302	30	39.9		229.0[t]	4192[t]	0.334	230.0	3400	0.334	39.3	0.41		1.46
Erdil et al. (2012)	150	150	300	25	10.0	0.50				230.0	3430	0.165			25.8[s]	2.60
Rousakis and Karabinis (2012)	200	200	320	30	25.5	0.21				240.0	3720	0.117	27.5	3.63	26.9	5.30[a]
Rousakis and Karabinis (2012)	200	200	320	30	25.5	0.21				240.0	3720	0.585			42.4	6.25[a]
Wang et al. (2012a)	100	100	300	10	24.4		244.0[t]	4340[t]	0.167			0.167			40.0	2.28
Wang et al. (2012a)	200	200	600	28	24.4		244.0[t]	4340[t]	0.334			0.334			37.6	1.93
Wang et al. (2012a)	125	125	375	15	24.4		244.0[t]	4340[t]	0.167			0.167			29.8	1.36
Wang et al. (2012a)	250	250	750	30	24.4		244.0[t]	4340[t]	0.334			0.334			33.4	2.15
Wang et al. (2012a)	150	150	450	20	24.4		244.0[t]	4340[t]	0.167			0.167			37.7	2.23
Wang et al. (2012a)	300	300	900	35	24.4		244.0[t]	4340[t]	0.334			0.334			31.3	1.84
Wang et al. (2012a)	175	175	525	25	24.4		244.0[t]	4340[t]	0.334			0.334			44.7	2.33
Wang et al. (2012a)	350	350	1050	40	24.4		244.0[t]	4340[t]	0.668			0.668			32.9	2.81
Wang et al. (2012a)	200	200	600	28	24.4		244.0[t]	4340[t]	0.334			0.334			37.6	1.93
Wang et al. (2012a)	400	400	1200	45	24.4		244.0[t]	4340[t]	0.668			0.668			26.9	1.88
Wang et al. (2012a)	305	305	915	30	25.5		229.0[t]	4192[t]	0.167	240.0	4340	0.167	29.4	0.31	17.2[d]	0.79
Wang et al. (2012a)	305	305	915	30	25.5		229.0[t]	4192[t]	0.334	240.0	4340	0.334	32.3	0.39	24.4[d]	1.77
Wang et al. (2012a)	204	204	612	20	25.5		229.0[t]	4192[t]	0.167	240.0	4340	0.167	28.7	0.39	25.0[d]	1.74
Wang et al. (2012a)	204	204	612	20	25.5		229.0[t]	4192[t]	0.167	240.0	4340	0.167	28.8	0.31	24.6[d]	1.70
Wang et al. (2012a)	204	204	612	20	25.5		229.0[t]	4192[t]	0.167	240.0	4340	0.167	31.2	0.34	23.5[d]	2.22[a]
Wang et al. (2012a)	204	204	612	20	25.5		229.0[t]	4192[t]	0.334	240.0	4340	0.334	30.8	0.48	31.4	2.29[a]
Wang et al. (2012a)	204	204	612	20	25.5		229.0[t]	4192[t]	0.334	240.0	4340	0.334	31.9	0.45	27.9	2.81[a]
Wang et al. (2012a)	204	204	612	20	25.5		229.0[t]	4192[t]	0.334	240.0	4340	0.334	32.4	0.51	32.1	3.16[a]
Yeh and Chang (2012)	150	150	300	30	27.5					230.5	1153	0.220			44.4[s]	1.89[a]

Paper (continued)	b (mm)	h (mm)	H (mm)	r (mm)	f'_{co} (MPa)	ε_{co} (%)	E_{frp} (GPa)	f_{frp} (MPa)	t_{frp} (mm)	E_f (GPa)	f_f (MPa)	t_f (mm)	f'_{c1} (MPa)	ε_{c1} (%)	f'_{cu} (MPa)	ε_{cu} (%)
Yeh and Chang (2012)	150	150	300	30	27.5					230.5	1153	0.220			40.9	1.56[a]
Yeh and Chang (2012)	150	150	300	30	27.5					230.5	1153	0.413			55.8[s]	2.33[a]
Yeh and Chang (2012)	150	150	300	30	27.5					230.5	1153	0.413			57.0[s]	2.30[a]
Yeh and Chang (2012)	300	300	600	30	27.5					230.5	1153	0.413			31.6	1.20[a]
Yeh and Chang (2012)	300	300	600	30	27.5					230.5	1153	0.413			33.7	1.53[a]
Yeh and Chang (2012)	300	300	600	30	27.5					230.5	1153	0.825			42.8	1.78[a]
Yeh and Chang (2012)	300	300	600	30	27.5					230.5	1153	0.825			40.9	1.91[a]
Yeh and Chang (2012)	450	450	900	30	27.5					230.5	1153	0.660			30.2	1.31[a]
Yeh and Chang (2012)	450	450	900	30	27.5					230.5	1153	0.660			29.2	1.33[a]
Yeh and Chang (2012)	450	450	900	30	27.5					230.5	1153	1.155			34.3	1.53[a]
Yeh and Chang (2012)	450	450	900	30	27.5					230.5	1153	1.155			36.5	1.60[a]
Yeh and Chang (2012)	150	225	450	30	27.5					230.5	1153	0.275			36.8	1.65[a]
Yeh and Chang (2012)	150	225	450	30	27.5					230.5	1153	0.275			35.1	1.22[a]
Yeh and Chang (2012)	150	225	450	30	27.5					230.5	1153	0.495			45.1[s]	1.94[a]
Yeh and Chang (2012)	150	225	450	30	27.5					230.5	1153	0.495			44.6	2.00[a]
Yeh and Chang (2012)	300	450	900	30	27.5					230.5	1153	0.495			29.6	1.31[a]
Yeh and Chang (2012)	300	450	900	30	27.5					230.5	1153	0.495			28.5	1.37[a]
Yeh and Chang (2012)	300	450	900	30	27.5					230.5	1153	0.990			33.2	1.52[a]
Yeh and Chang (2012)	300	450	900	30	27.5					230.5	1153	0.990			34.8	1.56[a]
Yeh and Chang (2012)	150	300	600	30	27.5					230.5	1153	0.275			32.2	1.47[a]
Yeh and Chang (2012)	150	300	600	30	27.5					230.5	1153	0.275			31.6	1.43[a]
Yeh and Chang (2012)	150	300	600	30	27.5					230.5	1153	0.550			36.9	1.52[a]
Yeh and Chang (2012)	150	300	600	30	27.5					230.5	1153	0.550			35.9	1.76[a]
Yeh and Chang (2012)	300	600	1200	30	27.5					230.5	1153	0.550			27.0	1.20[a]
Yeh and Chang (2012)	300	600	1200	30	27.5					230.5	1153	0.550			25.4	1.26[a]
Yeh and Chang (2012)	300	600	1200	30	27.5					230.5	1153	1.100			31.2	1.43[a]
Yeh and Chang (2012)	300	600	1200	30	27.5					230.5	1153	1.100			28.8	1.60[a]
CFRP tube-encased specimens																
Ozbakkaloglu and Oehlers (2008)	150	300	600	10	24.0	0.21	36.2	386	2.040	240.0	3800	0.351	22.1		14.2[d]	1.44
Ozbakkaloglu and Oehlers (2008)	150	300	600	20	24.0	0.20	36.2	386	2.040	240.0	3800	0.351	22.7		19.0[d]	1.48
Ozbakkaloglu and Oehlers (2008)	150	300	600	40	24.0	0.21	36.2	386	2.040	240.0	3800	0.351			24.1	1.54
Ozbakkaloglu and Oehlers (2008)	150	300	600	10	24.0	0.21	36.2	386	3.400	240.0	3800	0.585	22.3		12.8[d]	2.77[a]
Ozbakkaloglu and Oehlers (2008)	150	300	600	20	24.0	0.20	36.2	386	3.400	240.0	3800	0.585	22.9		22.2[d]	2.93[a]
Ozbakkaloglu and Oehlers (2008)	150	300	600	40	24.0	0.21	36.2	386	3.400	240.0	3800	0.585			30.7	3.39[a]
Ozbakkaloglu and Oehlers (2008)	150	300	600	10	35.5	0.23	36.2	386	2.040	240.0	3800	0.351	33.1		16.2[d]	1.78
Ozbakkaloglu and Oehlers (2008)	150	300	600	20	35.5	0.23	36.2	386	2.040	240.0	3800	0.351	33.8		21.8[d]	1.60
Ozbakkaloglu and Oehlers (2008)	150	300	600	40	35.5	0.23	36.2	386	2.040	240.0	3800	0.351	33.2		29.1[d]	1.54
Ozbakkaloglu and Oehlers (2008)	200	200	600	10	26.7	0.21	47.4	750	1.779	240.0	3800	0.351	24.7		19.3[d]	1.75
Ozbakkaloglu and Oehlers (2008)	200	200	600	20	26.7	0.22	47.4	750	1.779	240.0	3800	0.351	25.9		25.1	2.12
Ozbakkaloglu and Oehlers (2008)	200	200	600	40	26.7	0.22	47.4	750	1.779	240.0	3800	0.351			33.8	2.39
Ozbakkaloglu and Oehlers (2008)	200	200	600	10	26.7	0.21	47.4	750	2.965	240.0	3800	0.585			26.9	3.50[a]
Ozbakkaloglu and Oehlers (2008)	200	200	600	20	26.7	0.22	47.4	750	2.965	240.0	3800	0.585			35.0	3.35[a]
Ozbakkaloglu and Oehlers (2008)	200	200	600	40	26.7	0.22	47.4	750	2.965	240.0	3800	0.585			47.2	3.58
Ozbakkaloglu (2013b)	150	150	300	15	105.2[c]	0.35				240.0	3800	1.175	98.6	0.54	89.9[d]	1.82[a]
Ozbakkaloglu (2013b)	150	150	300	15	105.2[c]	0.35				240.0	3800	1.175	104.5	1.88	85.2[d]	2.06[a]
Ozbakkaloglu (2013b)	150	150	300	30	107.3[c]	0.35				240.0	3800	1.175	110.5	0.70	125.8	1.50
Ozbakkaloglu (2013b)	150	150	300	30	107.3[c]	0.35				240.0	3800	1.175	104.1	0.80	115.1	1.43
Ozbakkaloglu (2013b)	150	150	300	15	110.5[c]	0.35				240.0	3800	1.880	110.2	0.56	120.1	3.93[a]
Ozbakkaloglu (2013b)	150	150	300	15	110.5[c]	0.35				240.0	3800	1.880	103.4	0.55	101.4[d]	1.74
Ozbakkaloglu (2013b)	150	150	300	30	110.8[c]	0.35				240.0	3800	1.880	118.3	2.00	146.8	1.62

Paper (continued)	b (mm)	h (mm)	H (mm)	r (mm)	f'_{co} (MPa)	ε_{co} (%)	E_{frp} (GPa)	f_{frp} (MPa)	t_{frp} (mm)	E_f (GPa)	f_f (MPa)	t_f (mm)	f'_{c1} (MPa)	ε_{c1} (%)	f'_{cu} (MPa)	ε_{cu} (%)
Ozbakkaloglu (2013b)	150	150	300	30	110.8[c]	0.35				240.0	3800	1.880	109.2	2.25	145.6	1.97
Ozbakkaloglu (2013b)	125	187.5	300	15	105.2[c]	0.35				240.0	3800	1.175	99.1	2.23	81.5[d]	1.92
Ozbakkaloglu (2013b)	125	187.5	300	15	105.2[c]	0.35				240.0	3800	1.175	102.0	2.14	71.3[d]	1.46
Ozbakkaloglu (2013b)	125	187.5	300	30	107.3[c]	0.35				240.0	3800	1.175	104.1	0.70	93.2[d]	1.50
Ozbakkaloglu (2013b)	125	187.5	300	30	107.3[c]	0.35				240.0	3800	1.175	107.2	0.67	96.2[d]	1.47
Ozbakkaloglu (2013b)	125	187.5	300	15	110.5[c]	0.35				240.0	3800	1.880	109.8	0.72	94.2[d]	2.20
Ozbakkaloglu (2013b)	125	187.5	300	15	110.5[c]	0.35				240.0	3800	1.880	105.5	0.60	98.4[d]	3.00[a]
Ozbakkaloglu (2013b)	125	187.5	300	30	110.8[c]	0.35				240.0	3800	1.880	119.6	0.56	135.7	1.75
Ozbakkaloglu (2013b)	125	187.5	300	30	110.8[c]	0.35				240.0	3800	1.880	112.9	0.60	125.5	1.63
Ozbakkaloglu (2013b)	112.5	225	300	15	105.2[c]	0.35				240.0	3800	1.175	101.5	0.50	57.6[d]	1.75
Ozbakkaloglu (2013b)	112.5	225	300	15	105.2[c]	0.35				240.0	3800	1.175	102.1	0.50	58.8[d]	1.49
Ozbakkaloglu (2013b)	112.5	225	300	30	107.3[c]	0.35				240.0	3800	1.175	109.6	1.74	81.9[d]	1.46
Ozbakkaloglu (2013b)	112.5	225	300	30	107.3[c]	0.35				240.0	3800	1.175	108.9	1.66	79.4[d]	1.45
Ozbakkaloglu (2013b)	112.5	225	300	15	110.5[c]	0.35				240.0	3800	1.880	106.4	0.60	87.5[d]	2.76
Ozbakkaloglu (2013b)	112.5	225	300	15	110.5[c]	0.35				240.0	3800	1.880	104.7	0.70	82.0[d]	2.91
Ozbakkaloglu (2013b)	112.5	225	300	30	110.8[c]	0.35				240.0	3800	1.880	115.3	0.70	106.7[d]	1.64
Ozbakkaloglu (2013b)	112.5	225	300	30	110.8[c]	0.35				240.0	3800	1.880	112.4	0.66	98.1[d]	1.55
Ozbakkaloglu (2013a)	150	150	300	15	76.6[c]	0.30				240.0	3800	0.705	78.0	0.42	73.6[d]	2.30[a]
Ozbakkaloglu (2013a)	150	150	300	15	76.6[c]	0.30				240.0	3800	0.705	77.5	0.42	65.2[d]	2.03[a]
Ozbakkaloglu (2013a)	150	150	300	30	76.6[c]	0.30				240.0	3800	0.705	86.7	0.46	83.3	1.59
Ozbakkaloglu (2013a)	150	150	300	30	76.6[c]	0.30				240.0	3800	0.705	84.4	0.44	80.5	1.47
Ozbakkaloglu (2013a)	150	150	300	15	76.6[c]	0.30				240.0	3800	1.175	79.4	0.44	88.5	3.36[a]
Ozbakkaloglu (2013a)	150	150	300	15	76.6[c]	0.30				240.0	3800	1.175	80.6	0.58	78.7	2.94[a]
Ozbakkaloglu (2013a)	150	150	300	30	77.2[c]	0.30				240.0	3800	1.175	94.6	0.72	114.2	2.13
Ozbakkaloglu (2013a)	150	150	300	30	77.2[c]	0.30				240.0	3800	1.175	86.4	0.69	104.7	1.99
Ozbakkaloglu (2013a)	126	189	300	15	77.2[c]	0.30				240.0	3800	0.705	80.7	0.59	55.1[d]	1.50
Ozbakkaloglu (2013a)	126	189	300	15	77.2[c]	0.30				240.0	3800	0.705	79.1	0.55	58.6[d]	1.48
Ozbakkaloglu (2013a)	126	189	300	30	77.2[c]	0.30				240.0	3800	0.705	85.5	0.65	77.1	1.33
Ozbakkaloglu (2013a)	126	189	300	30	77.2[c]	0.30				240.0	3800	0.705	74.9	0.49	77.1	1.17
Ozbakkaloglu (2013a)	126	189	300	15	79.6[c]	0.30				240.0	3800	1.175	85.5	0.53	73.9[d]	1.96
Ozbakkaloglu (2013a)	126	189	300	15	79.6[c]	0.30				240.0	3800	1.175	84.7	0.55	75.1[d]	2.55
Ozbakkaloglu (2013a)	126	189	300	30	79.6[c]	0.30				240.0	3800	0.585	92.7	0.56	95.9	1.48
Ozbakkaloglu (2013a)	126	189	300	30	79.6[c]	0.30				240.0	3800	0.585	90.1	0.67	95.7	1.76
Ozbakkaloglu (2013a)	112	224	300	15	79.6[c]	0.30				240.0	3800	0.705	76.3	0.44	42.3[d]	1.84
Ozbakkaloglu (2013a)	112	224	300	15	79.6[c]	0.30				240.0	3800	0.705	78.6	0.49	51.1[d]	1.63
Ozbakkaloglu (2013a)	112	224	300	30	78.2[c]	0.30				240.0	3800	0.705	74.4	0.44	55.7[d]	1.53
Ozbakkaloglu (2013a)	112	224	300	30	78.2[c]	0.30				240.0	3800	0.705	82.4	0.58	62.1[d]	1.44
Ozbakkaloglu (2013a)	112	224	300	15	78.2[c]	0.30				240.0	3800	0.585	77.5	0.44	63.5[d]	2.13
Ozbakkaloglu (2013a)	112	224	300	15	78.2[c]	0.30				240.0	3800	0.585	84.9	0.49	55.0[d]	1.60
Ozbakkaloglu (2013a)	112	224	300	30	78.2[c]	0.30				240.0	3800	1.175	85.7	0.46	89.6	1.99
Ozbakkaloglu (2013a)	112	224	300	30	78.2[c]	0.30				240.0	3800	1.175	79.0	0.46	77.3[d]	1.57

t *denotes FRP properties calculated based on total nominal ply thickness of fiber sheet*
c *denotes unconfined concrete strength obtained from 152.5 x 305 mm concrete cylinder tests*
s *denotes inconsistent axial strength when compared with overall trend in database*
a *denotes inconsistent axial strain when compared with overall trend in database*
d *denotes ultimate axial stress values that are lower than the unconfined concrete strength*

Table A2. Test database of GFRP-confined concrete specimens

Paper	Specimen Dimensions				Concrete Properties		FRP Properties			Fiber Properties			Measured Initial Peak Conditions		Measured Ultimate Conditions	
	b (mm)	h (mm)	H (mm)	r (mm)	f'_{co} (MPa)	ε_{co} (%)	E_{frp} (GPa)	f_{frp} (MPa)	t_{frp} (mm)	E_f (GPa)	f_f (MPa)	t_f (mm)	f'_{c1} (MPa)	ε_{c1} (%)	f'_{cu} (MPa)	ε_{cu} (%)
GFRP-wrapped specimens																
Demers and Neale (1994)	152	152	505	5	32.3	0.20				10.5	220	1.050	31.8	0.30	24.0[d]	1.05
Demers and Neale (1994)	152	152	505	5	32.3	0.20				10.5	220	1.050	33.0	0.30	22.0[d]	0.90
Mirmiran et al. (1998)	152.5	152.5	305	6.35	40.6[c]					69.6	2186	1.450	47.8		22.8[d]	0.80
Mirmiran et al. (1998)	152.5	152.5	305	6.35	40.6[c]					69.6	2186	1.450	40.2		25.5[d]	1.00
Mirmiran et al. (1998)	152.5	152.5	305	6.35	40.6[c]					69.6	2186	1.450	42.8		26.2[d]	0.80
Mirmiran et al. (1998)	152.5	152.5	305	6.35	40.6[c]					69.6	2186	2.417	45.2		26.9[d]	1.50
Mirmiran et al. (1998)	152.5	152.5	305	6.35	40.6[c]					69.6	2186	2.417	46.5		34.5[d]	1.70
Mirmiran et al. (1998)	152.5	152.5	305	6.35	40.6[c]					69.6	2186	2.417	43.3		34.5[d]	1.70
Mirmiran et al. (1998)	152.5	152.5	305	6.35	40.6[c]					69.6	2186	3.383	41.9		31.0[d]	1.10[a]
Mirmiran et al. (1998)	152.5	152.5	305	6.35	40.6[c]					69.6	2186	3.383	45.2		37.9[d]	0.90[a]
Mirmiran et al. (1998)	152.5	152.5	305	6.35	40.6[c]					69.6	2186	3.383	47.9		33.1[d]	1.10[a]
Suter and Pinzelli (2001)	150	150	300	5	33.9					73.0	2400	0.616	37.1			
Suter and Pinzelli (2001)	150	150	300	5	33.9					73.0	2400	1.232	37.9			
Suter and Pinzelli (2001)	150	150	300	25	36.7					73.0	2400	0.616	39.8			
Suter and Pinzelli (2001)	150	150	300	25	36.7					73.0	2400	1.232	42.2			
Harries and Carey (2003)	152	152	305	25	32.4	0.27	4.9	75	3[P]	10.3	154	3[P]	37.9	0.18	27.8[d]	0.34[a]
Harries and Carey (2003)	152	152	305	25	32.4	0.27	4.9	75	9[P]	10.3	154	9[P]	43.1	0.46	37.2	1.09
Harries and Carey (2003)	152	152	305	11	31.2	0.16	4.9	75	3[P]	10.3	154	3[P]	37.4	0.26	27.8[d]	0.63[a]
Harries and Carey (2003)	152	152	305	11	31.2	0.16	4.9	75	9[P]	10.3	154	9[P]	39.0	0.33	31.2	1.25
Modarelli et al. (2005)	150	200	400	10	17.6					86.0	1957	0.460	32.2[s]			1.58[a]
Yan et al. (2006)	279	279	914	19	15.2	0.20	16.9	228	9.600					0.30	22.1	2.00
Rousakis et al. (2007)	200	200	320	30	33.0	0.17				65.0	3000	0.414	42.6	4.22	39.0	5.98[a]
Rousakis et al. (2007)	200	200	320	30	33.0	0.17				65.0	3000	0.828	44.4	7.74	43.8	9.81[a]
Rousakis et al. (2007)	200	200	320	30	33.0	0.17				65.0	3000	1.242	51.9	10.38	51.0	11.24[a]
Rousakis et al. (2007)	200	200	320	30	38.0	0.22				65.0	3000	0.414	40.4	3.70	34.4[d]	5.79[a]
Rousakis et al. (2007)	200	200	320	30	38.0	0.22				65.0	3000	0.828	52.8	9.32	52.5	9.37[a]
Rousakis et al. (2007)	200	200	320	30	38.0	0.22				65.0	3000	1.242	59.8	20.57	58.0	22.12[a]
Rousakis et al. (2007)	200	200	320	30	39.9	0.15				65.0	3000	0.414	43.1	2.22	40.7	3.13[a]
Rousakis et al. (2007)	200	200	320	30	39.9	0.15				65.0	3000	0.828	54.2	4.42	53.1	8.15[a]
Rousakis et al. (2007)	200	200	320	30	39.9	0.15				65.0	3000	1.242	59.5	12.97	55.1	16.72[a]
Youssef et al. (2007)	381	381	762	38	34.2					18.5	425	8.001			40.3	1.19
Youssef et al. (2007)	381	381	762	38	34.2					18.5	425	8.001			39.8	1.16
Youssef et al. (2007)	381	381	762	38	34.2					18.5	425	8.001			40.7	1.15
Youssef et al. (2007)	381	381	762	38	34.2					18.5	425	4.572			36.0	1.13
Youssef et al. (2007)	381	381	762	38	34.2					18.5	425	4.572			35.9	1.01
Youssef et al. (2007)	381	381	762	38	34.2					18.5	425	3.429			34.0[d]	0.88
Youssef et al. (2007)	381	381	762	38	29.2					18.5	425	3.429			29.6	0.86
Youssef et al. (2007)	254	381	762	38	36.6					18.5	425	9.144			40.8	1.78
Youssef et al. (2007)	254	381	762	38	36.8					18.5	425	9.144			40.8	2.13
Youssef et al. (2007)	254	381	762	38	38.7					18.5	425	9.144			40.7	1.74
Youssef et al. (2007)	254	381	762	38	36.8					18.5	425	5.715			37.0	1.30
Youssef et al. (2007)	254	381	762	38	36.6					18.5	425	5.715			37.2	1.30
Youssef et al. (2007)	254	381	762	38	36.8					18.5	425	5.715			37.1	1.26

Paper (Continued)	b (mm)	h (mm)	H (mm)	r (mm)	f'_{co} (MPa)	ε_{co} (%)	E_{frp} (GPa)	f_{frp} (MPa)	t_{frp} (mm)	E_f (GPa)	f_f (MPa)	t_f (mm)	f'_{c1} (MPa)	ε_{c1} (%)	f'_{cu} (MPa)	ε_{cu} (%)
Youssef et al. (2007)	254	381	762	38	36.6					18.5	425	3.429			34.0[d]	0.81
Youssef et al. (2007)	254	381	762	38	31.0					18.5	425	3.429			29.8[d]	0.71[a]
Youssef et al. (2007)	254	381	762	38	32.3					18.5	425	2.286			32.1	0.73
Youssef et al. (2007)	254	381	762	38	29.8					18.5	425	2.286			28.0	0.73
Benzaid et al. (2008)	100	100	300	0	54.8	0.25				23.8	383	0.440			56.1	0.92[a]
Benzaid et al. (2008)	100	100	300	0	54.8	0.25				23.8	383	0.880			58.2[s]	1.46[a]
Benzaid et al. (2008)	100	100	300	8	54.8	0.25				23.8	383	0.440			59.7	0.99[a]
Benzaid et al. (2008)	100	100	300	8	54.8	0.25				23.8	383	0.880			65.7	1.53[a]
Benzaid et al. (2008)	100	100	300	16	54.8	0.25				23.8	383	0.440			63.6	1.04[a]
Benzaid et al. (2008)	100	100	300	16	54.8	0.25				23.8	383	0.880			74.5	1.58[a]
Rousakis and Karabinis (2012)	200	200	320	30	25.5	0.21				73.0	3285	0.462	41.3	3.41	38.9[s]	6.25[a]
Rousakis and Karabinis (2012)	200	200	320	30	25.5	0.21				73.0	3285	1.386			55.8	12.94[a]

c *denotes unconfined concrete strength obtained from 152.5 x 305 mm concrete cylinder tests*
p *denotes fiber tensile strength and elastic modulus are given in N/mm-ply*
s *denotes inconsistent axial strength when compared with overall trend in database*
a *denotes inconsistent axial strain when compared with overall trend in database*
d *denotes ultimate axial stress values that are lower than the unconfined concrete strength*

Table A3. Test database of AFRP-confined concrete specimens

Paper	Specimen Dimensions				Concrete Properties		FRP Properties			Fiber Properties			Measured Initial Peak Conditions		Measured Ultimate Conditions	
	b (mm)	h (mm)	H (mm)	r (mm)	f'_{co} (MPa)	ε_{co} (%)	E_{frp} (GPa)	f_{frp} (MPa)	t_{frp} (mm)	E_f (GPa)	f_f (MPa)	t_f (mm)	f'_{c1} (MPa)	ε_{c1} (%)	f'_{cu} (MPa)	ε_{cu} (%)
AFRP-wrapped specimens																
Rochett and Labossiere (2000)	152	152	500	5	43.0					13.6	230	1.260	50.7		23.7[d]	1.06
Rochett and Labossiere (2000)	152	152	500	5	43.0					13.6	230	2.520	51.6		28.4[d]	1.49
Rochett and Labossiere (2000)	152	152	500	5	43.0					13.6	230	3.780	53.8		34.8[d]	2.08
Rochett and Labossiere (2000)	152	152	500	5	43.0					13.6	230	5.040	54.2		46.9	1.24
Rochett and Labossiere (2000)	152	152	500	25	43.0					13.6	230	1.260	51.2		30.5[d]	0.79
Rochett and Labossiere (2000)	152	152	500	25	43.0					13.6	230	2.520	51.2		44.3	0.97
Rochett and Labossiere (2000)	152	152	500	25	43.0					13.6	230	3.780	53.3		49.9	1.10
Rochett and Labossiere (2000)	152	152	500	25	43.0					13.6	230	5.040	55.0		57.2	1.26
Rochett and Labossiere (2000)	152	152	500	38	43.0					13.6	230	2.520	50.7		43.9	0.96
Rochett and Labossiere (2000)	152	152	500	38	43.0					13.6	230	3.780	52.9		52.9	1.18
Suter and Pinzelli (2001)	150	150	300	5	33.9					125.0	2100	0.290	32.4			
Suter and Pinzelli (2001)	150	150	300	5	33.9					125.0	2100	0.580	37.3			
Suter and Pinzelli (2001)	150	150	300	5	34.9					125.0	2100	0.870	36.9			
Suter and Pinzelli (2001)	150	150	300	5	35.9					125.0	2100	1.160	38.4			
Suter and Pinzelli (2001)	150	150	300	25	36.6					125.0	2100	0.290	39.4			
Suter and Pinzelli (2001)	150	150	300	25	36.6					125.0	2100	0.580	43.7			
Suter and Pinzelli (2001)	150	150	300	25	36.6					125.0	2100	0.870	56.8			
Suter and Pinzelli (2001)	150	150	300	25	36.6					125.0	2100	1.160	64.9			
Wang and Wu (2010)	100	100	300	10	46.4	0.26				118.0	2060	0.286	55.1	0.22	46.1	0.59[a]
Wang and Wu (2010)	100	100	300	10	46.4	0.26				118.0	2060	0.572	62.0	0.30	59.7	1.00
Wang and Wu (2010)	100	100	300	10	46.4	0.26				118.0	2060	0.858	66.6	0.32	88.0	1.93
Wang and Wu (2010)	100	100	300	10	78.5	0.45				118.0	2060	0.286	96.1	0.40		
Wang and Wu (2010)	100	100	300	10	78.5	0.45				118.0	2060	0.572	95.7	0.32	97.6[s]	0.93
Wang and Wu (2010)	100	100	300	10	78.5	0.45				118.0	2060	0.858	106.0	0.47	101.6[s]	1.06
Wang and Wu (2010)	100	100	300	10	101.2	0.46				118.0	2060	0.286	103.5	0.35	100.0[s]	0.38[a]
Wang and Wu (2010)	100	100	300	10	101.2	0.46				118.0	2060	0.572	113.0	0.46	101.4[s]	0.52[a]
Wang and Wu (2010)	100	100	300	10	101.2	0.46				118.0	2060	0.858	121.5	0.50	120.8[s]	1.13[a]
Zhang et al. (2010)	150	150	400	15	45.0					118.0	2065	0.572	50.2	172.00	43.7[d]	2.13
Zhang et al. (2010)	150	150	400	15	50.0					118.0	2065	0.572	54.5	110.00	47.2[d]	2.13
Wang and Wu (2011)	70	70	210	7	34.6	0.22				118.0	2060	0.072	49.5	0.22	44.4[s]	0.63[a]
Wang and Wu (2011)	100	100	300	10	34.6	0.22				118.0	2060	0.095	42.8	0.23	41.0[s]	0.48[a]
Wang and Wu (2011)	150	150	450	15	34.6	0.22				118.0	2060	0.143	43.3	0.17	33.0[s]	0.59[a]
Wang and Wu (2011)	70	70	210	7	52.1	0.27				118.0	2060	0.143	76.7	0.33	70.4[s]	0.88[a]
Wang and Wu (2011)	100	100	300	10	52.1	0.27				118.0	2060	0.191	62.5	0.27	54.6[s]	0.61[a]
Wang and Wu (2011)	150	150	450	15	52.1	0.27				118.0	2060	0.286	56.3	0.25	53.4[s]	0.39[a]
Wang and Wu (2011)	70	70	210	7	34.6	0.22				118.0	2060	0.143	49.6	0.28	57.7[s]	0.44[a]
Wang and Wu (2011)	100	100	300	10	34.6	0.22				118.0	2060	0.191	49.0	0.22	51.0[s]	0.57[a]
Wang and Wu (2011)	150	150	450	15	34.6	0.22				118.0	2060	0.286	45.0	0.21	41.6[s]	0.53[a]
Wang and Wu (2011)	70	70	210	7	52.1	0.27				118.0	2060	0.286	100.9	0.25	95.1[s]	0.81[a]
Wang and Wu (2011)	100	100	300	10	52.1	0.27				118.0	2060	0.381	85.0	0.28	85.4[s]	0.56[a]
Wang and Wu (2011)	150	150	450	15	52.1	0.27				118.0	2060	0.572	80.2	0.31	80.7[s]	0.51[a]

Paper (Continued)	b (mm)	h (mm)	H (mm)	r (mm)	f'_{co} (MPa)	ε_{co} (%)	E_{frp} (GPa)	f_{frp} (MPa)	t_{frp} (mm)	E_f (GPa)	f_f (MPa)	t_f (mm)	f'_{c1} (MPa)	ε_{c1} (%)	f'_{cu} (MPa)	ε_{cu} (%)
Wang and Wu (2011)	70	70	210	7	34.6	0.22				118.0	2060	0.286	68.0	0.26	86.2[s]	0.66[a]
Wang and Wu (2011)	100	100	300	10	34.6	0.22				118.0	2060	0.381	62.3	0.23	76.3[s]	0.52[a]
Wang and Wu (2011)	150	150	450	15	34.6	0.22				118.0	2060	0.572	51.3	0.24	54.3[s]	0.54[a]

s *denotes inconsistent axial strength when compared with overall trend in database*
a *denotes inconsistent axial strain when compared with overall trend in database*
d *denotes ultimate axial stress values that are lower than the unconfined concrete strength*

Table A4. Test database of HM and UHM CFRP-confined concrete specimens

Paper	Specimen Dimensions				Concrete Properties		FRP Properties			Fiber Properties			Measured Initial Peak Conditions		Measured Ultimate Conditions	
	b (mm)	h (mm)	H (mm)	R (mm)	f'_{co} (MPa)	ε_{co} (%)	E_{frp} (GPa)	f_{frp} (MPa)	t_{frp} (mm)	E_f (GPa)	f_f (MPa)	t_f (mm)	f'_{c1} (MPa)	ε_{c1} (%)	f'_{cu} (MPa)	ε_{cu} (%)
HM CFRP-wrapped specimens																
Hosotani et al. (1997)	200	200	600	30	38.1		439.0[t]	3972[t]	0.169	392.0	2942	0.163		0.57	39.2	0.57
Hosotani et al. (1997)	200	200	600	30	38.1		439.0[t]	3972[t]	0.338	392.0	2942	0.326		0.70	44.1	0.70
Hosotani et al. (1997)	200	200	600	30	38.1		439.0[t]	3972[t]	0.676	392.0	2942	0.652		1.47	61.2	1.47
UHM CFRP-wrapped specimens																
Suter and Pinzelli (2001)	150	150	300	5	33.9					640.0	2650	0.380	39.9			
Suter and Pinzelli (2001)	150	150	300	25	36.6					640.0	2650	0.380	46.4			

t *denotes FRP properties calculated based on total nominal ply thickness of fiber sheet*

THIS PAGE HAS BEEN LEFT INTENTIONALLY BLANK

Statement of Authorship

Title of Paper	Lateral Strain-to-Axial Strain Relationship of Confined Concrete
Publication Status	(•) Published ( ) Accepted for Publication ( ) Submitted for Publication ( ) Publication Style
Publication Details	Journal of Structural Engineering, Doi: 10.1061/(ASCE)ST.1943-541X.0001094, Year 2014

Author Contributions

By signing the Statement of Authorship, each author certifies that their stated contribution to the publication is accurate and that permission is granted for the publication to be included in the candidate's thesis.

Name of Principal Author (Candidate)	Mr. Jian Chin Lim		
Contribution to the Paper	Preparation of experimental database, development of model, and preparation of manuscript		
Signature		Date	23/02/2015

Name of Co-Author	Dr. Togay Ozbakkaloglu		
Contribution to the Paper	Research supervision and review of manuscript		
Signature		Date	23/02/2015

THIS PAGE HAS BEEN LEFT INTENTIONALLY BLANK

LATERAL STRAIN-TO-AXIAL STRAIN RELATIONSHIP OF CONFINED CONCRETE

Jian C. Lim and Togay Ozbakkaloglu

ABSTRACT

The use of fiber reinforced polymers (FRP) has become widely accepted engineering practice for strengthening reinforced concrete members. It is well established that lateral confinement of concrete with FRP composites can significantly enhance its strength and ductility. As the confinement pressure generated by FRP on the confined concrete depends on the lateral expansion of concrete, the mechanism of concrete expansion inside the FRP shell is of significant interest. A review of the existing stress-strain models of FRP-confined concrete revealed the need for a model that accurately predicts the dilation characteristic of confined concrete as it provides the essential link between the response of the concrete core and the passive confinement mechanism of the FRP shell. It is also understood that knowledge established from the research area of actively confined concrete can be employed in the development of a model applicable for both FRP-confined and actively confined concretes. Based on a large number of experimental test results of both FRP-confined and actively confined concretes, a generic model is proposed to describe the lateral strain-to-axial strain relationship of confined concrete. The instrumentation arrangements of the tested specimens have allowed for the lateral strain-axial strain relationships of confined concrete to be captured throughout the tests. The trend of the lateral strain-to-axial strain relationship of confined concrete is shown to be a function of the confining pressure, type of confining material and concrete strength. Assessment of models with the experimental databases showed that the predictions of the proposed model are well above existing models and in good agreement with the test results of both FRP-confined and actively confined concretes.

KEYWORDS: Concrete; Fiber reinforced polymer (FRP); Confinement; Dilation; Lateral strain; Axial strain; Stress-strain models.

1. INTRODUCTION

It is well established that lateral confinement of concrete enhances its axial strength and deformability (Kent and Park 1971; Sheikh and Uzumeri 1980; Mander et al. 1988; Saatcioglu and Razvi 1992; Ozbakkaloglu and Saatcioglu 2006; Ozbakkaloglu et al. 2013). Traditionally, confinement was provided by means of steel tubes and hoop reinforcing steels. In recent years, external reinforcement using FRP material has become an increasingly popular method of confining columns due to superior mechanical properties offered by the material. A great number of studies have been conducted to understand and model the behavior of FRP-confined concrete. The studies have lead the development of a large number of stress–strain models, which have recently been reviewed in Ozbakkaloglu et al. (2013). These models were categorized into two categories: design-oriented models presented in closed-form expressions; and analysis-oriented models which predict stress–strain curves by an incremental procedure. Most design-oriented models do not fully capture the confinement mechanism as they focus mainly on the ultimate conditions. Analysis-oriented models on the other hand, consider the interaction between the external confining shell and internal concrete core and are capable of establishing the full axial stress-strain relationship and lateral strain-to-axial strain relationship (i.e. dilation behavior) of FRP-confined concrete. As was also previously stated by Teng et al. (2007) these features make analysis-oriented models more versatile and powerful than design-oriented models. All of the analysis-oriented models are built on the assumption that the axial stress and axial strain of FRP-confined concrete at a given lateral strain are the same as those in concrete actively confined with a constant confining pressure equal to that supplied by the FRP shell. It is therefore, the accuracy of the analysis-oriented models depends greatly on their prediction of the lateral strain-to-axial strain relationship of the FRP-confined concrete (Jiang and Teng 2007; Ozbakkaloglu et al. 2013). In the majority of existing analysis-oriented models, the lateral strain-to-axial strain expressions are given implicitly (e.g., (Spoelstra and Monti 1999; Fam and Rizkalla 2001; Chun and Park 2002; Marques et al. 2004; Binici 2005; Albanesi et al. 2007) through the modification of the expressions originally given by actively confined concrete models. Such modifications do not capture the realistic dilation behavior of FRP-confined concrete, as was also reported in Jiang and Teng (2007). On the other hand, there are only a few models that explicitly used the results of tests conducted on FRP-confined concrete in the development of their lateral strain-to-axial strain expressions (e.g., (Mirmiran and Shahawy 1997; Harries and Kharel 2002; Jiang and Teng 2007; Teng et al. 2007; Xiao et al. 2010). These explicit expressions were developed based on limited experimental test data, which were often obtained only from the tests performed by the originators of the models. It became evident from the results of the assessment reported in Ozbakkaloglu et al. (2013) and Jiang and Teng (2007) that the performances of these analysis-oriented models were not satisfactory when assessed against a large test database with a parametric range that is much wider than the databases used in the development of these models. As was also revealed in Ozbakkaloglu et al. (2013), none of the existing analysis-oriented models considered the influence of concrete strength as a parameter that influences the dilation behavior of confined concrete, although it has been well accepted that the concrete strength has significant influence on the brittleness and crack pattern of confined concrete which in turn alters its dilation behavior (Ozbakkaloglu and Akin 2012).

To address these research gaps, two large databases of experimental test results for FRP-confined and actively confined concretes having a wide range of concrete strengths were collected from the existing literature. Based on the test results, relationships between the dilation behaviors of FRP-confined and actively confined concretes were closely investigated. Due attention was given to the trend of the lateral strain-to-axial strain responses of both confinement types and the way they were influenced by the concrete strength. Finally, a model capable of predicting the lateral-strain-to-axial strain relationships of both passively and actively confined concretes was developed and is presented in this paper.

2. EXPERIMENTAL TEST DATABASES

In this section, two carefully prepared test databases of FRP-confined and actively-confined concretes used in the model development are summarized. The database of FRP-confined concrete was assembled through an extensive review of the literature that covered 2038 test results from 202 experimental studies. The suitability of these results for the database was then assessed using a set of carefully established selection criteria to ensure the reliability and consistency of the database. Only monotonically loaded circular specimens with unidirectional fibers orientated in the hoop direction and an aspect ratio (H/D) less than three were included in the database. Specimens containing internal steel reinforcement, partial FRP confinement were not included. This resulted in a final database size of 976 datasets collected from 116 experimental studies published between 1992 and the end of 2011. The details of the normal-strength concrete (NSC) and high-strength concrete (HSC) components of the FRP-confined concrete test database can be found in Ozbakkaloglu and Lim (2013) and Lim and Ozbakkaloglu (2014), respectively. The database consists of specimens confined by five main type of FRP materials [Carbon FRP (CFRP), high-modulus carbon FRP (HM CFRP), ultra high-modulus carbon (UHM CFRP), S- or E-glass FRP (GFRP), and aramid FRP (AFRP)] and two confinement techniques (wraps and tubes). It is worthwhile noting that carbon FRPs were categorized into three subgroups on the basis of their elastic modulus of fibers (E_f) (i.e., Carbon FRP with $E_f \leq 270$ GPa is categorized as CFRP; followed by $270 < E_f \leq 440$ GPa as HM CFRP; and $E_f > 440$ GPa as UHM CFRP). The diameters of the specimens (D) included in the test database varied between 47 and 600 mm. The peak unconfined concrete strength (f'_{co}) and strain (ε_{co}), as obtained from the tests of companion control cylinders, varied from 6.2 to 169.7 MPa and 0.14% to 0.70%, respectively. The actual confinement ratio, defined as the ratio of the actual ultimate confining pressure of FRP shell to the peak strength of unconfined concrete specimen ($f_{lu,a}/f'_{co}$), varied from 0.02 to 4.74. Figure 1 shows the relationship of the ultimate strain enhancement ratio ($\varepsilon_{cu}/\varepsilon_{co}$) versus the actual confinement ratio ($f_{lu,a}/f'_{co}$), established from the database for a range of actual confinement ratios between 0 to 1.0.

The database of actively confined concrete was assembled from 25 experimental studies and consists of 346 test results. Only triaxially loaded circular specimens with an aspect ratio (H/D) less than three were included in the database. Specimens containing internal steel or microfiber reinforcement in concrete were not included. The diameters of the specimens (D) included in the test database varied between 50 and 160 mm. The unconfined concrete strength (f'_{co}) and strain (ε_{co}), as obtained from concrete cylinder tests, varied from 7.2 to 132.0 MPa and 0.15%

to 0.40%, respectively. The active confinement ratio (f^*_l/f'_{co}), defined as the ratio of the hydrostatic confining pressure of the triaxial cell to the peak strength of the unconfined concrete specimen, varied from 0.004 to 21.67.

The details of the actively-confined concrete database are presented in Table 1 in Appendix. Figures 2 and 3, respectively, show the variations of peak strain enhancement ratio ($\varepsilon^*_{cc}/\varepsilon_{co}$) and the residual strain ratio ($\varepsilon_{c,res}/\varepsilon_{co}$) versus active confinement ratio (f^*_l/f'_{co}). In the database inputs, when the values of the peak confined concrete strength and strain (f^*_{cc}, ε^*_{cc}) and the values of the residual concrete strength and strain ($f_{c,res}$, $\varepsilon_{c,res}$) are not directly available in text in the original publication, such details were interpreted from the axial stress-strain curves given in the source documents. As illustrated in Fig. 4, the coordinates corresponding to the peak axial stress along the curve are referred to as the peak concrete strength and strain (f^*_{cc}, ε^*_{cc}). With the increase in deformation after the peak stress is reached, the interparticle cohesion in concrete continues to decrease and the remaining strength generated from frictional action in the confined concrete is known as the residual concrete strength (Imran and Pantazopoulou 2001). The coordinates corresponding to the beginning of the constant axial stress region along the stress-strain curve are referred to as the residual concrete strength and strain ($f_{c,res}$, $\varepsilon_{c,res}$). The ratio of the residual strain ($\varepsilon_{c,res}$) to the peak strain of unconfined concrete (ε_{co}) is defined as the residual strain ratio ($\varepsilon_{c,res}/\varepsilon_{co}$).

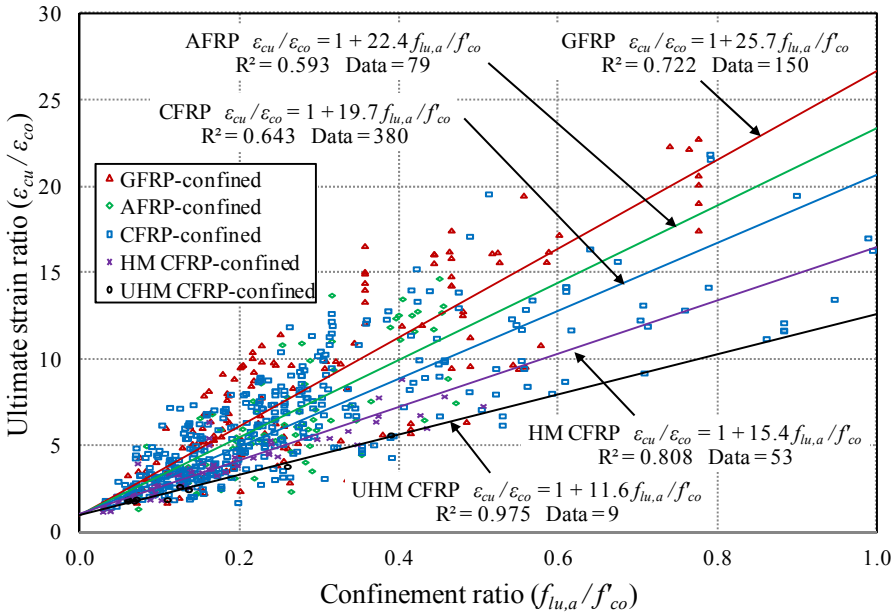

Figure 1. Variation of ultimate strain enhancement ratio ($\varepsilon_{cu}/\varepsilon_{co}$) of FRP-confined concrete with confinement ratio ($f_{lu,a}/f'_{co}$)

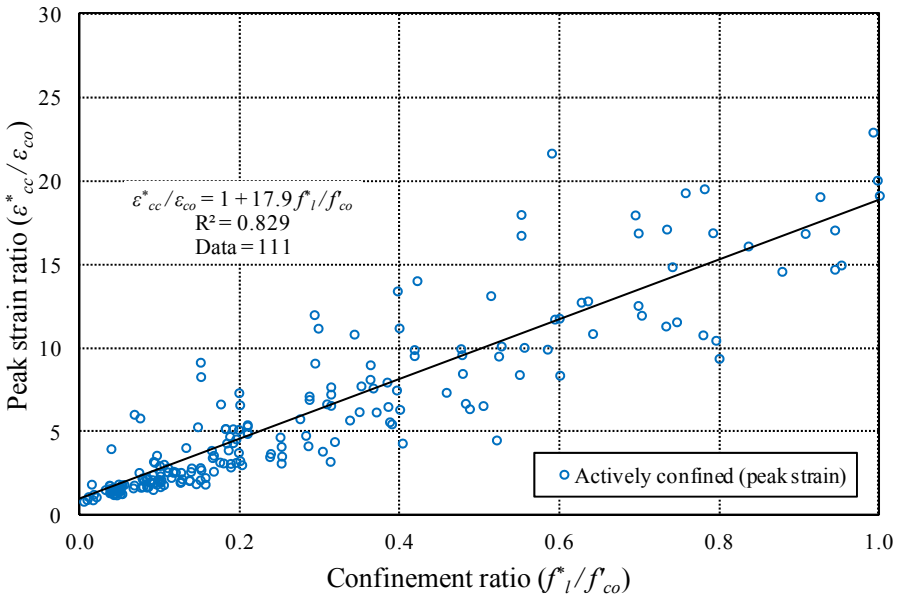

Figure 2. Variation of peak strain enhancement ratio ($\varepsilon^*_{cc}/\varepsilon_{co}$) of actively confined concrete with confinement ratio (f^*_l/f'_{co})

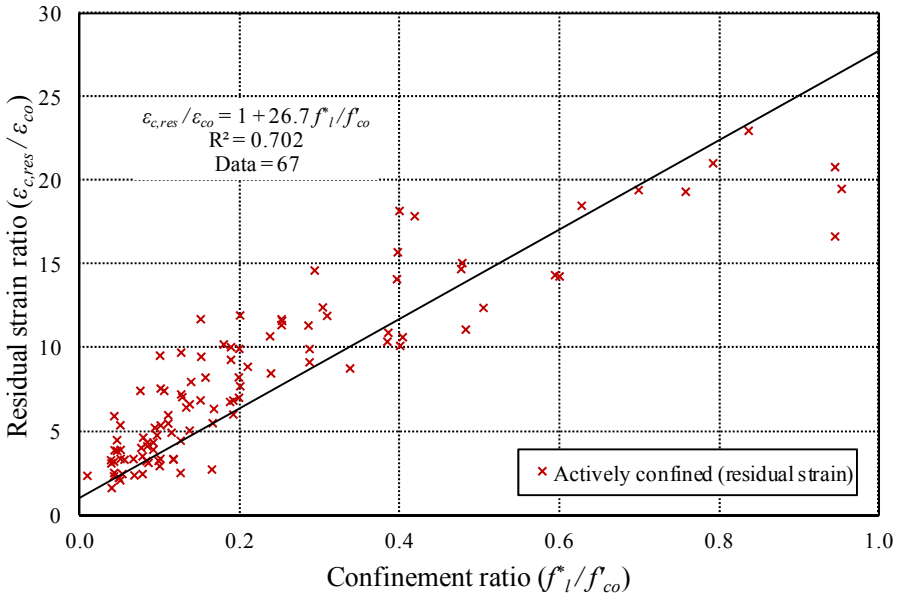

Figure 3. Variation of residual strain ratio ($\varepsilon_{c,res}/\varepsilon_{co}$) of actively confined concrete with confinement ratio (f^*_l/f'_{co})

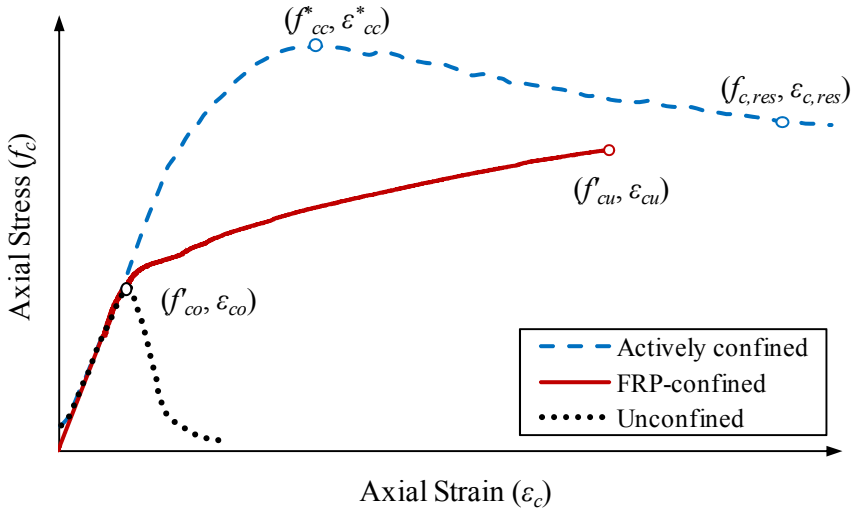

Figure 4. Axial stress-strain curves of actively-confined, FRP-confined and unconfined concretes

3. LATERAL STRAIN-TO-AXIAL STRAIN RELATIONSHIP OF CONFINED CONCRETE

Concrete confinement can be classified as active or passive, depending on the way the confining pressure is applied onto the concrete. Concrete tested in triaxial load cell is categorized as active confinement, as the constant confining pressure exerted from the load cell acts independently from the lateral expansion of concrete. Concrete confined by steel encasement, can be approximated as actively confined concrete, as the confining pressure remains almost constant beyond yielding of steel. Concrete confined with linear-elastic materials like FRP, is considered as passively confined concrete, as the level of confining pressure generated by the FRP confinement passively increases and is dependent on the lateral expansion of the concrete. Assuming a uniform confining pressure distribution for a circular concrete section confined by FRP shell, the confining pressure (f_l) can be expressed by Eq. 1, which satisfies the strain compatibility and force equilibrium conditions between the core and confining shell.

$$f_l = \frac{2E_f t_f \varepsilon_l}{D} = K_l \varepsilon_l \tag{1}$$

where E_f is the elastic modulus of fibers, t_f is the total thickness fibers, ε_l is the hoop strain of FRP shell, D is the diameter of concrete core, and K_l is the lateral confinement stiffness of FRP shell.

To compare the lateral strain-to-axial strain relationships of FRP-confined and actively confined concretes, a number of specimens in both categories that have a comparable range of unconfined concrete strengths (f'_{co}) were sorted into groups. Details of these specimens are summarized in Table 2. In the group notations, the numbers that follow the letter 'U' represent the nominal unconfined concrete strength (f'_{co}) of the first specimen of a given group.

Table 2. Summary of test results used in Figures 5 to 16

Group	Paper	Number of data	Dimensions of cylinder (mm)	Lateral confinement	$f_{lu,a}$ or f^*_l (MPa)	f'_{co} (MPa)
U21	Imram and Pantazopoulou (1996)	4	54 x 115	Active	2.1, 4.2, 8.4, 14.7	21.2
	Newman (1979)	4	100 x 250	Active	3.5, 6.8, 13.7, 22.6	23.2
U30	Ozbakkaloglu and Vincent (2013)	1	152 x 305	2 layers of CFRP	9.3	30.0
	Ozbakkaloglu and Akin (2012)	1	152 x 305	3 layers of AFRP	16.1	38.9
U35	Smith et al. (1989)	4	54 x 108	Active	6.9, 13.8, 20.7, 27.6	34.5
	Sfer et al. (2002)	6	150 x 300	Active	1.5, 4.5, 9.0	35.8
	Kotsovos and Newman (1978)	1	100 x 250	Active	24	31.7
	Ozbakkaloglu and Akin (2012)	1	152 x 305	3 layers of AFRP	15.7	38.9
U36	Ozbakkaloglu and Vincent (2013)	1	152 x 305	2 layers of CFRP	10.0	36.3
	Ozbakkaloglu and Vincent (2013)	1	152 x 305	3 layers of CFRP	12.0	59.0
	Vincent and Ozbakkaloglu (2013a)	1	152 x 305	5 layers of CFRP	16.1	102.5
U42	Candappa et al. (2001)	5	98 x 200	Active	4.0, 8.0, 12.0	41.9
	Kotsovos and Newman (1978)	2	100 x 250	Active	18.0, 35.0	46.9
	Lahlou et al. (1992)	1	52 x 104	Active	7.6	46.0
	Vincent and Ozbakkaloglu (2013b)	3	153 x 305	3 layers of AFRP	22.5	49.4
U64	Ozbakkaloglu and Vincent (2013)	4	152 x 305	1, 2, 3, 4 layers of CFRP	3.6, 8.0, 11.2, 15.2	64.2 – 65.8
U73	Candappa et al. (2001)	3	98 x 200	Active	4.0, 8.0	73.1
	Newman (1979)	4	100 x 250	Active	3.5, 6.8, 13.7, 34.9	73.3
	Lahlou et al. (1992)	2	52 x 104	Active	7.6, 22.0	78
	Ozbakkaloglu and Vincent (2013)	1	100 x 200	3 layers of AFRP	15.1	77.2
U103	Candappa et al. (2001)	6	98 x 200	Active	4.0, 8.0, 12.0	103.3
	Lahlou et al. (1992)	1	52 x 104	Active	22.0	113.0
	Vincent and Ozbakkaloglu (2013a)	3	152 x 305	4, 5, and 6 layers of CFRP	13.0, 16.1, 19.7	102.5

Figures 5 and 6 show the lateral strain-to-axial strain relationships of the unconfined, actively-confined, and FRP-confined concretes for two groups of specimens (i.e., U35 and U103). As illustrated in the figures, the initial responses of the unconfined, actively-confined, and FRP-confined concretes are similar and their initial slopes are in agreement with the Poisson's ratio of concrete within the elastic range. When the axial compressive stress in concrete reaches around 0.6 to 0.8 of the peak strength of unconfined concrete (f'_{co}), the unrestrained microcrack propagation occurs and results in a rapid increase in the lateral strain. In the unconfined concrete specimens, this unrestrained concrete expansion results in an exponential increase in the slope of the lateral strain-to-axial strain curves. Due to differences in the ways the confining pressures are applied to concrete, lateral strain-to-axial strain curves of actively confined and FRP-confined concretes exhibit different trends beyond the initial elastic range. In the actively confined concrete specimens, although the dilation curves exhibit high axial strains in the presence of confining pressure, the trend of the curves maintain an exponential form. In the FRP-confined concrete specimens, the curves also exhibit increased axial strains as a result of the passive confinement provided by FRP shells. However, the gradual increase in the confining pressure results in an asymptotic change in the second portion of lateral strain-to-axial strain curves of FRP-confined concrete. As illustrated in Figs. 5 and 6, the lateral strain-to-axial strain curves of the FRP-confined concrete specimens intersect the curves of the actively confined concrete sequentially in the order of increasing confining pressure. Figure 7 shows the comparison of the confinement ratios of the FRP-confined and the actively confined concretes at the intersecting points for four groups of specimens (i.e., U35, U42, U73, and U103). The figure illustrates that the confinement ratios at the intersecting points are close to each other and they yield a strong correlation. This observation suggests that the lateral strain-to-axial strain relationships of both FRP-confined and actively confined concretes depend on the instantaneous confining pressure at the corresponding axial strain.

The observation is further validated using the ultimate conditions of 182 datasets from the database of FRP-confined concrete that have comparable concrete strengths (f'_{co}) and confinement ratios ($f_{lu,a}/f'_{co}$) within 15% differences to that of the actively confined concrete specimens in either group U21, U35, U42, U73, or U103. The axial strain (ε_c) of the actively confined concrete specimen corresponding to the lateral strain (ε_l) that is equal to the hoop rupture strain ($\varepsilon_{h,rup}$) of the matching FRP-confined concrete dataset was recorded. Figure 8 shows the comparison of the recorded axial strains (ε_c) of the actively confined concrete specimens with the ultimate axial strains (ε_{cu}) of the companion FRP-confined concrete specimens. Figure 9 illustrates the range of nominal confinement ratios used for the FRP-confined and actively confined concrete specimens shown in Fig. 8. As evident from the good correlation in Fig. 8, the influence of confining pressure on the lateral strain-to-axial strain relationship of confined concrete is further validated for a confinement ratio (f_l/f'_{co}) range up to 0.8 and axial strains (ε_c) up to 3.5%. Using this as a premise, a generic lateral strain-to-axial strain model applicable to both confinement types was developed and presented later in the paper. It should be noted that the model presented in this paper is applicable within the aforementioned validation ranges of confinement ratio and axial strain. It was observed that

the relationship between the axial strains (ε_c) of FRP-confined and actively confined concretes starts to become nonlinear for heavily confined specimens at strain levels above 3.5%, with FRP-confined concretes starting to exhibit higher axial strains (ε_c) than actively confined concretes at given confinement ratios (f_l/f'_{co}). Additional tests on heavily confined companion FRP- and actively confined concrete specimens are required to be able to derive reliable observations on the relationship between the axial strains of FRP and actively confined concretes for the confinement ratio range above 0.8.

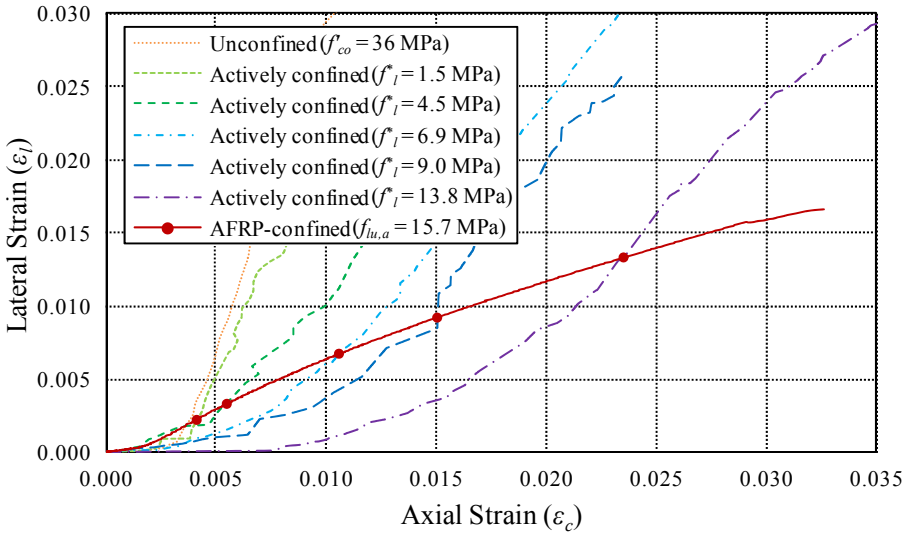

Figure 5. Lateral strain-to-axial strain relationships of actively confined and FRP-confined normal strength concrete (Group U35)

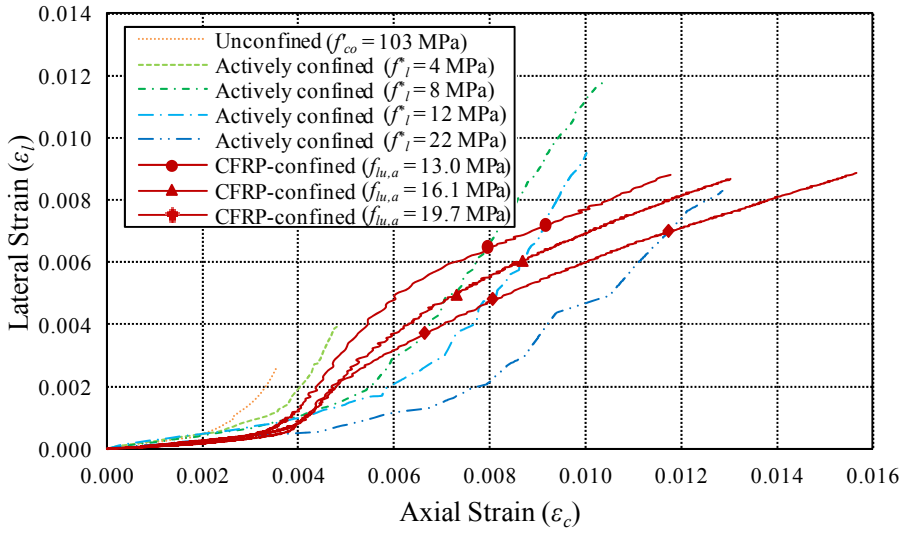

Figure 6. Lateral strain-to-axial strain relationships of actively confined and FRP-confined high strength concrete (Group U103)

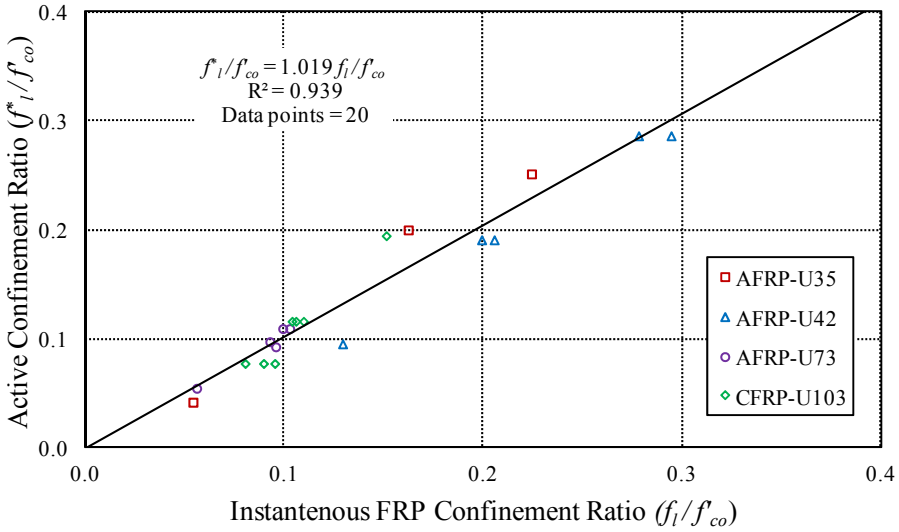

Figure 7. Instantantenous confinement ratios of FRP-confined concrete (f_l/f'_{co}) and actively confined concrete (f^*_l/f'_{co}) at points of intersection on lateral strain-to-axial strain curves

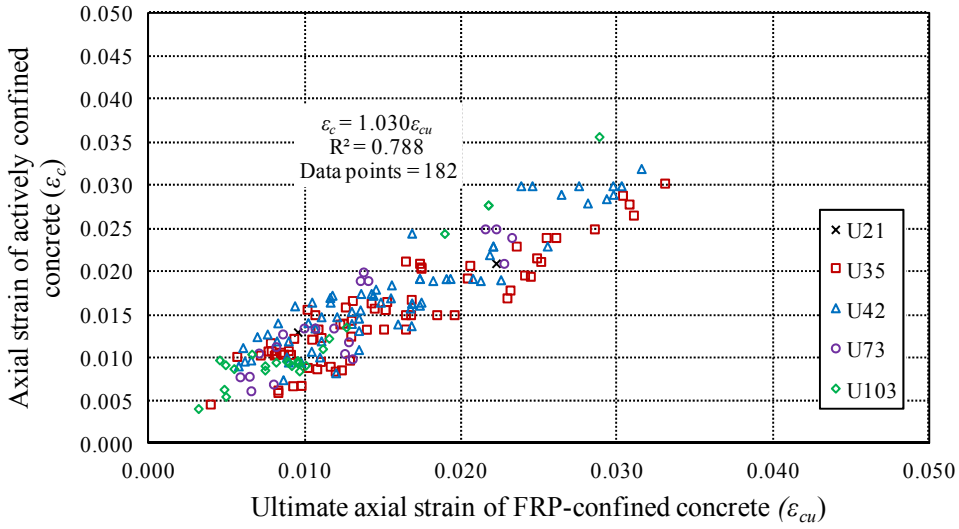

Figure 8. Comparison of axial strains of FRP-confined concrete and actively confined concrete specimens with comparable concrete strengths and confinement ratios

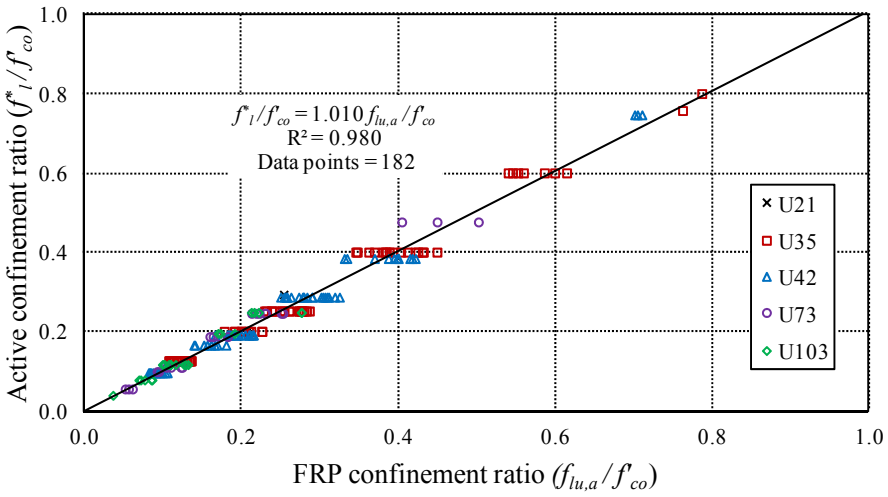

Figure 9. Comparison of confinement ratios of FRP-confined and actively confined concrete specimens shown in Figure 8

3.1 Parameters that influence lateral strain-to-axial strain relationship

A detailed discussion on the important parameters that influence the dilation behavior of confined concrete is provided in the following sections. The experimentally observed changes in dilation behaviors of FRP-confined and actively confined concretes caused by the variations in the identified parameters are presented in Figs. 10 to 16, together with the comparisons of the predictions of the proposed model, which is presented later in the paper. These figures indicate a close agreement between the test results and the model predictions.

3.1.1 Influence of lateral confining pressure

Figure 10 shows the experimentally obtained lateral strain-to-axial strain curves of FRP-confined concrete specimens tested by Ozbakkaloglu and Vincent (2013). The specimens shown in the figure all had unconfined concrete strengths of around 64 MPa, but they were confined with different amounts of FRP (i.e. 1 to 4 layers of CFRP sheets). As illustrated in Fig. 10, after the inflection points near the peak strain of unconfined concrete (ε_{co}), the slope of the lateral strain-to-axial curves changes, and the slope of the second part of the curves is strongly influenced by the level of confinement provided to the specimens. Figure 11 shows the corresponding dilation rate (μ_t) of the specimens shown in Fig. 10. The dilation rate (μ_t) represents the change in the slope of the lateral strain-to-axial strain curves and can be calculated by Eq. 2. As illustrated in Fig. 11, after the unrestrained crack propagation is stabilized by the FRP shell, the dilation rate is reversed and the peak dilation rate corresponds to the inflection point of the lateral strain-to-axial strain curve can be found. It is evident from the figure that the peak dilation rate reduces and the ultimate axial strain increases with the increase in the level of FRP confinement.

$$\mu_t = \frac{\Delta\varepsilon_l}{\Delta\varepsilon_c} \tag{2}$$

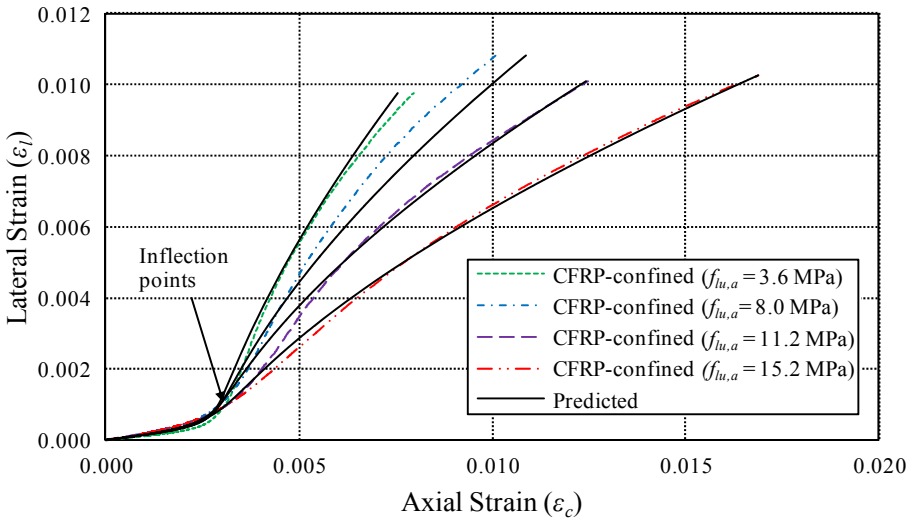

Figure 10. Variation of lateral strain-to-axial strain relationships of FRP-confined concrete specimens with amount of FRP confinement (Group U64)

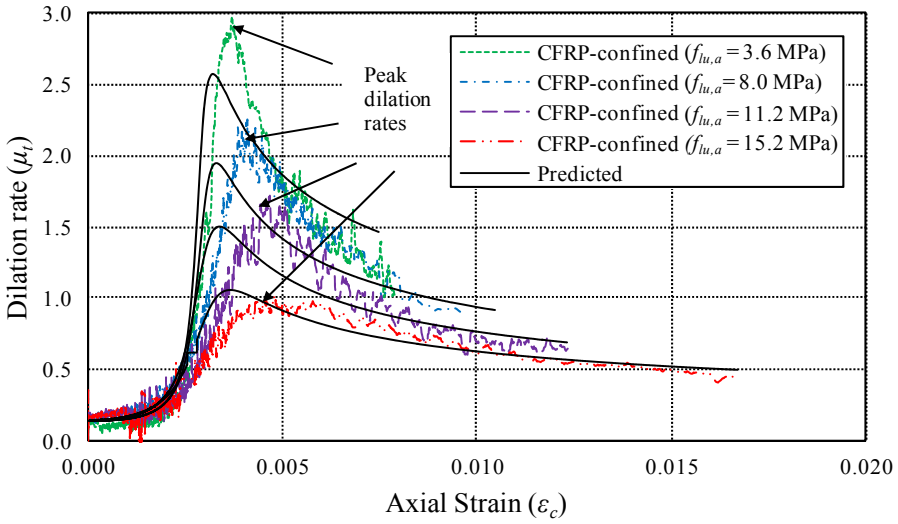

Figure 11. Influence of amount of confinement on dilation rates of FRP-confined concrete (Group U64)

Figure 12 shows the lateral strain-to-axial strain curves of actively confined concrete specimens for a group of specimens having different levels of lateral confining pressures. Under the active confinement, the specimens show exponential curves which exhibit higher axial strains with increasing level of confinement. Although the trend of the lateral strain-to-axial strain curves of the actively confined concrete is significantly different from that of FRP-confined concrete, as evident from Figs. 10 and 12, the proposed model is capable of predicting the trends of the both types of curves with good accuracy.

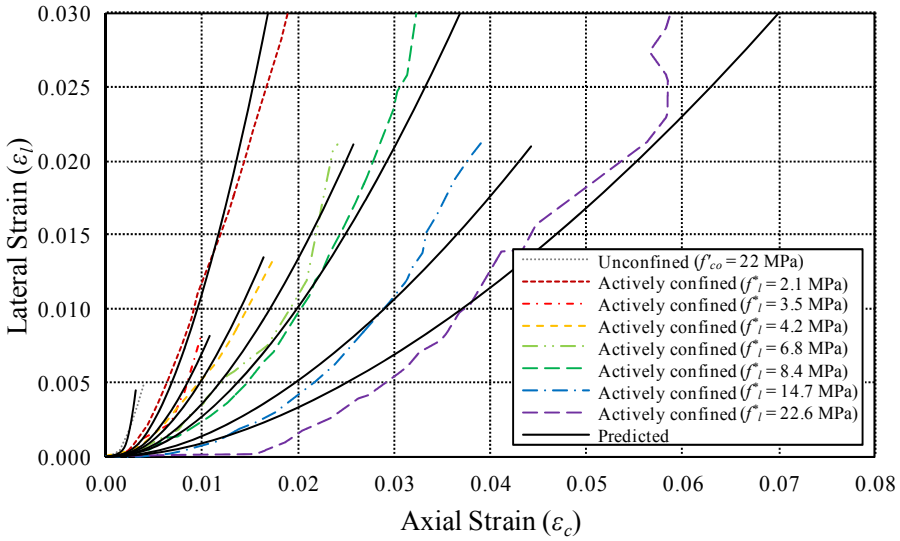

Figure 12. Variation of the lateral strain-to-axial strain relationships of actively confined concrete specimens with lateral confining pressure (Group U21)

3.1.2 Influence of confining materials

In addition to the level of confinement provided by the FRP shell, the mechanical properties of the confining material have a significant influence on the ultimate condition of the confined concrete. Figures 13 and 14 show the comparisons of test results of two specimens that were confined either with CFRP or AFRP. Both of the specimens had the same normalized confinement stiffness (K_l/f'_{co}). As shown in the figures, the specimens follow identical lateral strain- and dilation rate-to-axial strain curves but they have noticeable differences in their terminating coordinates, caused by the difference in hoop rupture strains of confining FRP materials.

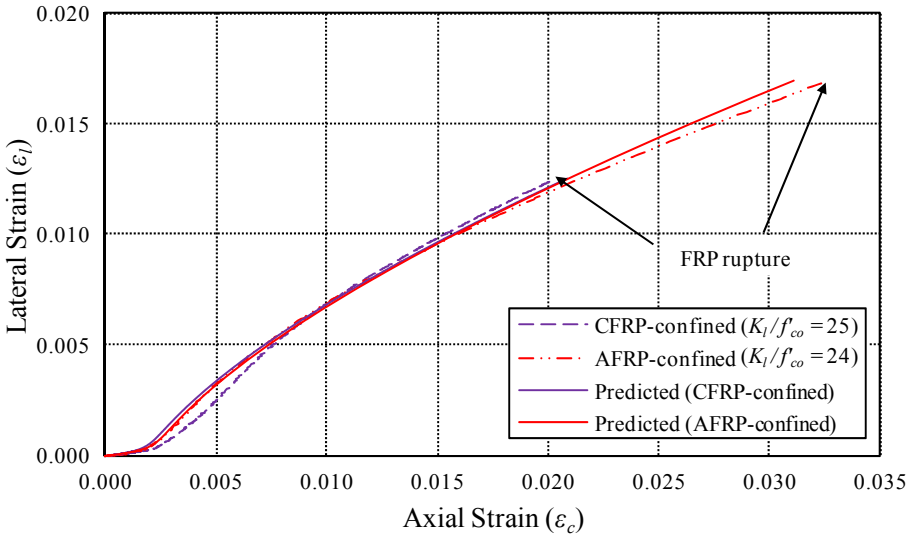

Figure 13. Lateral strain-to-axial strain relationships of FRP-confined concrete specimens confined by different FRP materials (Group U30)

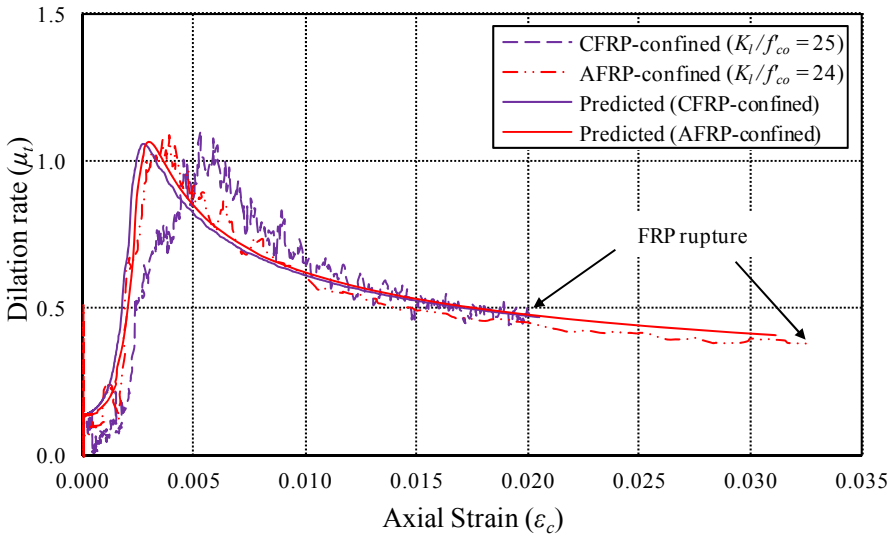

Figure 14. Dilation rates of FRP-confined concrete specimens confined by different FRP materials (Group U30)

It is now understood that the hoop rupture strain of the FRP shell is often smaller than the ultimate material tensile strain and it can be estimated from the material properties using a strain reduction factor (k_ε) (Eq. 3) (Pessiki et al. 2001). As was discussed in detail in Lim and Ozbakkaloglu (2014), the influences of the elastic modulus of fiber material (E_f) and unconfined concrete strength (f'_{co}) on the strain reduction factor ($k_{\varepsilon,f}$) can be expressed through Eq. 4.

$$k_{\varepsilon,f} = \frac{\varepsilon_{h,rup}}{\varepsilon_f} \tag{3}$$

$$k_{\varepsilon,f} = 0.9 - 2.3 f'_{co} \times 10^{-3} - 0.75 E_f \times 10^{-6} \tag{4}$$

where $\varepsilon_{h,rup}$ is the ultimate hoop rupture strain of FRP shell, ε_f is the ultimate material tensile strain of FRP material, f'_{co} is the peak unconfined concrete strength in MPa, and E_f is the elastic modulus of the fiber sheet in MPa.

3.1.3 Influence of unconfined concrete strength

Figure 15 shows the lateral strain-to-axial strain curves of CFRP-confined concrete specimens having comparable normalized confinement stiffness ratios (K_l/f'_{co}) but different unconfined concrete strengths (f'_{co}) of 36.3, 59.0 and 102.5 MPa. As illustrated in the figure, the lateral strain-to-axial strain curves have a similar pattern except for slight differences observed at the initial transition zones of specimens with different concrete strengths. In addition, the radius in the transition zone of the curves reduces with an increase in concrete strength as a result of the increased concrete brittleness. Although barely visible from Fig. 15, the difference in the radius of transition region of the three specimens is evident from the differences in the peak dilation rates shown in Fig. 16. The figure illustrates that both the peak dilation rate and the corresponding axial strain slightly increase with the increase in the

unconfined concrete strength. In the model proposed in the following section, the offset in the initial axial strain is captured as a function of the unconfined concrete strain (ε_{co}) and the change in the radius of the transition region is captured using the curve-shape parameter (n).

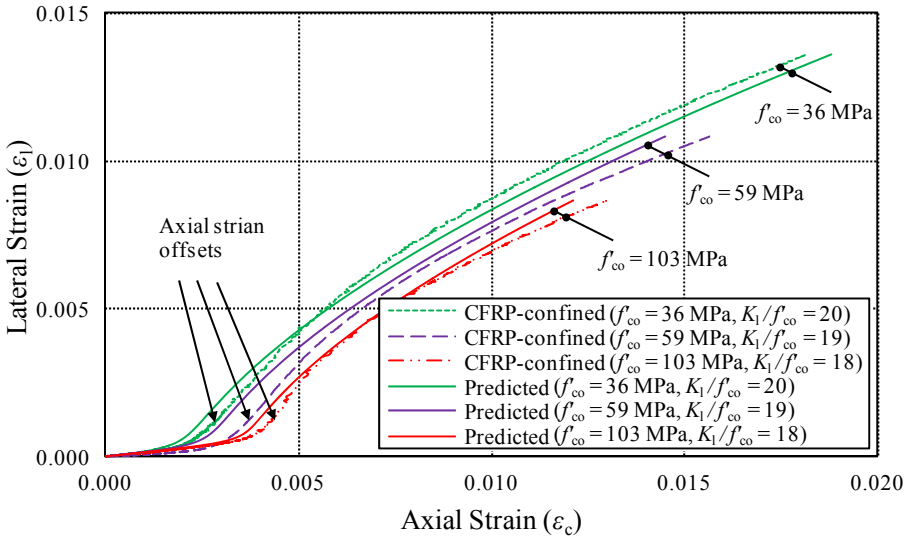

Figure 15. Lateral strain-to-axial strain relationships of FRP-confined concrete specimens having comparable confinement stiffness ratios and different unconfined concrete strengths (Group U36)

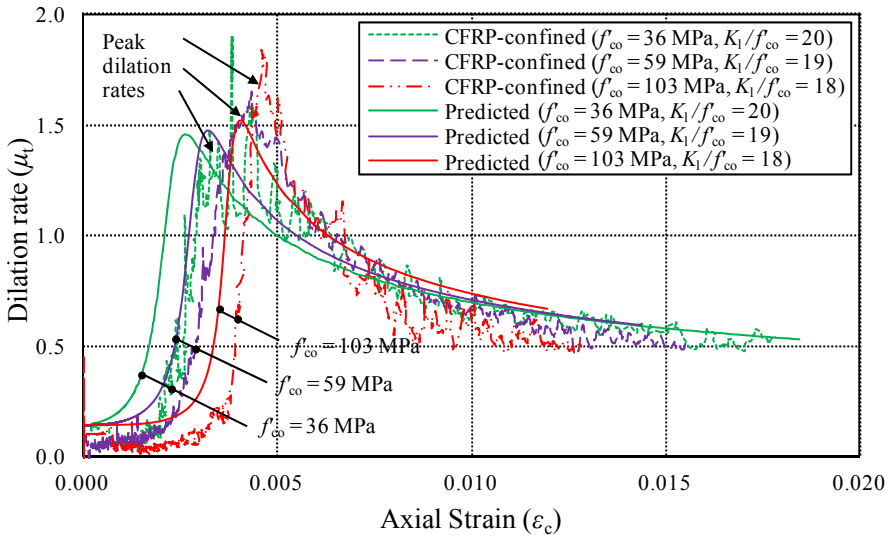

Figure 16. Dilation rates of FRP-confined concrete specimens having similar confinement stiffness ratios and different unconfined concrete strengths (Group U36)

3.2 Proposed model

In several of the existing studies, attempts have been made to quantify the lateral strain-to-axial strain relationship of FRP-confined concrete as a function of confinement stiffness of FRP shell (Mirmiran and Shahawy 1997; Xiao and Wu 2000; Harries and Kharel 2002; Moran and Pantelides 2002; Xiao and Wu 2003; Marques et al. 2004). Teng et al. (2007) on the other hand related the lateral strain-to-axial strain relationship of confined concrete to a function of lateral confining pressure (f_l). In a review study reported in Ozbakkaloglu et al. (2013) and Jiang and Teng (2007), it was found that Teng's (2007) approach yielded a better model performance compared to its counterparts.

The soundness of the previous approaches was thoroughly investigated and a model that predicts the lateral strain-to-axial strain relationships of both passively and actively confined concretes as functions of the concrete strength, properties of confining material and confining pressure is presented in Eq. 5. The model accurately predicts the trend of the lateral strain-to-axial strain curves and critical coordinates along the curves. These coordinates include: the peak axial and lateral strains (ε^*_{cc}, ε^*_{lc}); and residual axial and lateral strain ($\varepsilon_{c,res}$, $\varepsilon_{l,res}$) of actively confined concrete; and the ultimate axial and hoop rupture strains (ε_{cu}, $\varepsilon_{h,rup}$) of FRP-confined concrete. In establishing the trends given by the proposed expression, the results of 144 FRP-confined concrete specimens tested at the University of Adelaide (i.e., (Ozbakkaloglu and Akin 2012; Ozbakkaloglu and Vincent 2013; Vincent and Ozbakkaloglu 2013a,b)), together with the results of 159 actively confined concrete specimens assembled from published literature where complete lateral strain-to-axial strain curves were available (i.e., (Gardner 1969; Kotsovos and Newman 1978; Kotsovos 1979; Newman 1979; Smith et al. 1989; Bellotti and Rossi 1991; Lahlou et al. 1992; Imran and Pantazopoulou 1996; Candappa et al. 2001; Sfer et al. 2002; Lu and Hsu 2007; Gabet et al. 2008; Vu et al. 2009). For the calibration of the proposed expression for the prediction of the critical coordinates, two comprehensive databases, which consisted of 976 and 341 test results respectively of FRP-confined and actively confined concretes, were used. It should be noted that not all of the datasets included in the databases contained all the relevant details required for model development. Some test results that were inconsistent with the overall trends of the databases were also excluded from the model development. As a result, 671 and 213 carefully selected datasets from FRP-confined and actively confined concrete databases, respectively, were used in the model calibration. The model incorporates the important factors identified from the close examination of the results reported in the database, and is applicable to both FRP-confined and actively confined concretes in circular sections. It should be noted that the database used in the model development contained specimens with diameters ranging between 47 and 600 mm, with aspect ratios (H/D) less than three and unconfined concrete strengths less than 170 MPa. These ranges, therefore, should be considered as the application domain of the proposed model, and further validation of the model is recommended for its application outside the specified ranges.

$$\varepsilon_c = \frac{\varepsilon_l}{\upsilon_i\left(1+\left(\frac{\varepsilon_l}{\upsilon_i \varepsilon_{co}}\right)^n\right)^{\frac{1}{n}}} + 0.04\varepsilon_l^{0.7}\left(1+21\left(\frac{f_l}{f'_{co}}\right)^{0.8}\right) \quad (5)$$

$$\upsilon_i = 8\times10^{-6} f'^{2}_{co} + 0.0002 f'_{co} + 0.138 \quad (6)$$

$$\varepsilon_{co} = \left(-0.067 f'^{2}_{co} + 29.9 f'_{co} + 1053\right)\times10^{-6} \quad (7)$$

$$n = 1 + 0.03 f'_{co} \quad (8)$$

where ε_c is the axial strain, ε_l is the lateral strain, f_l is the corresponding confinement pressure for a given lateral strain, υ_i is the initial Poisson's ratio of concrete, to be calculated using Eq. 6 proposed by Candappa et al. (2001), f'_{co} is the peak unconfined concrete strength in MPa, ε_{co} is the peak unconfined concrete strain, to be calculated using Eq. 7 proposed by Tasdemir et al. (1998), n is the curve-shape parameter (Eq. 8) to adjust the initial transition radius of the predicted lateral strain-to-axial strain relationship curve, which was developed from test results of 144 FRP-confined concrete specimens tested at the University of Adelaide (i.e., (Ozbakkaloglu and Akin 2012; Ozbakkaloglu and Vincent 2013; Vincent and Ozbakkaloglu 2013a,b)). It should be noted that the confining pressure (f_l) in Eq. 5 is a constant for actively confined concrete and a variable for FRP-confined concrete. The variable confining pressure of FRP-confined concrete can be determined from Eq. 1 by gradually increasing the lateral strain (ε_l) until the hoop rupture strain of FRP shell ($\varepsilon_{h,rup}$) is reached.

3.2.1 Critical coordinates on lateral strain-to-axial strain curves

In addition to the trend of the lateral strain-to-axial strain curve, the accuracy of the proposed model also depends on its predictions of the critical coordinates along the curve. As mentioned earlier, these critical coordinates include the peak strains (ε^*_{cc}, ε^*_{lc}) and residual strains ($\varepsilon_{c,res}$, $\varepsilon_{l,res}$) of actively confined concrete, and ultimate strains (ε_{cu}, $\varepsilon_{h,rup}$) of FRP-confined concrete. In Figs. 17 to 18, the axial strain predictions of the critical coordinates are compared with the experimental values obtained from the two large databases used in the presented study. The axial strains of these critical coordinates (ε^*_{cc}, $\varepsilon_{c,res}$, and ε_{cu}) were calculated from Eq. 5 by substituting the lateral strain input (ε_l) with the corresponding lateral strains (ε^*_{lc}, $\varepsilon_{l,res}$, and $\varepsilon_{h,rup}$), and the confining pressure input (f_l) with the corresponding confining pressures (f^*_l, f^*_l, and $f_{lu,a}$). As evident from the values of coefficient of determination (R^2) in Fig. 17, the comparison of model predictions of the ultimate strain enhancement ratios ($\varepsilon_{cu}/\varepsilon_{co}$) with the experimental test results of FRP-confined concrete is in good agreement. Similarly, the peak strain enhancement ratios ($\varepsilon^*_{cc}/\varepsilon_{co}$) and residual strain ratios ($\varepsilon_{c,res}/\varepsilon_{co}$) of actively confined concrete specimens are estimated by the proposed model with good accuracy, as shown in Figs. 18 and 19.

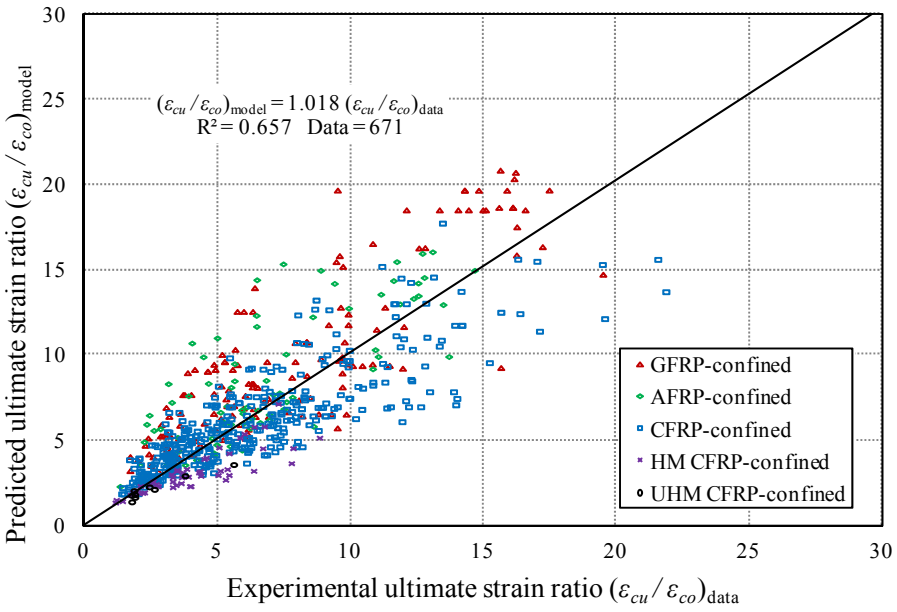

Figure 17. Comparison of model predictions of ultimate strain enhancement ratios ($\varepsilon_{cu}/\varepsilon_{co}$) of FRP-confined concrete with test results

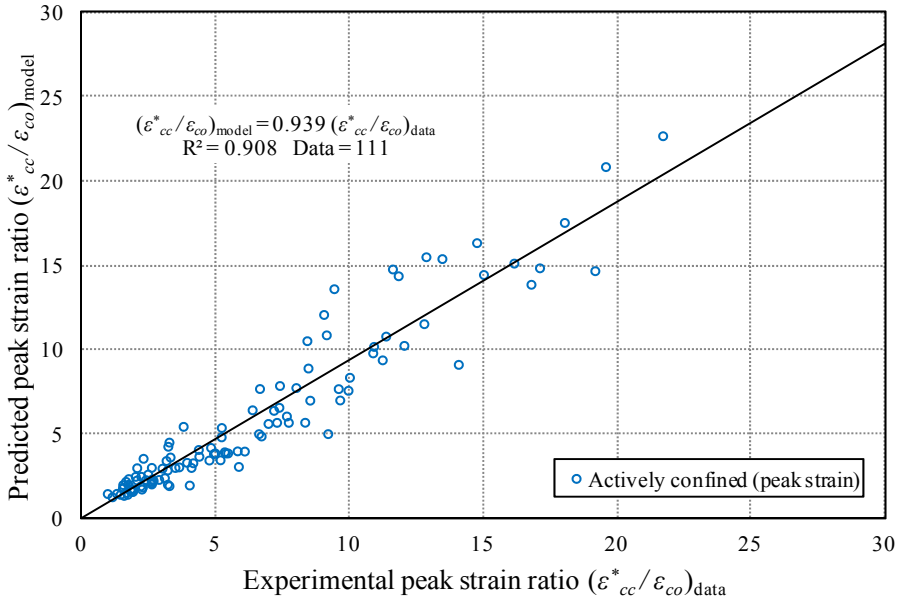

Figure 18. Comparison of model predictions of peak strain ratios ($\varepsilon^*_{cc}/\varepsilon_{co}$) of actively confined concrete with test results

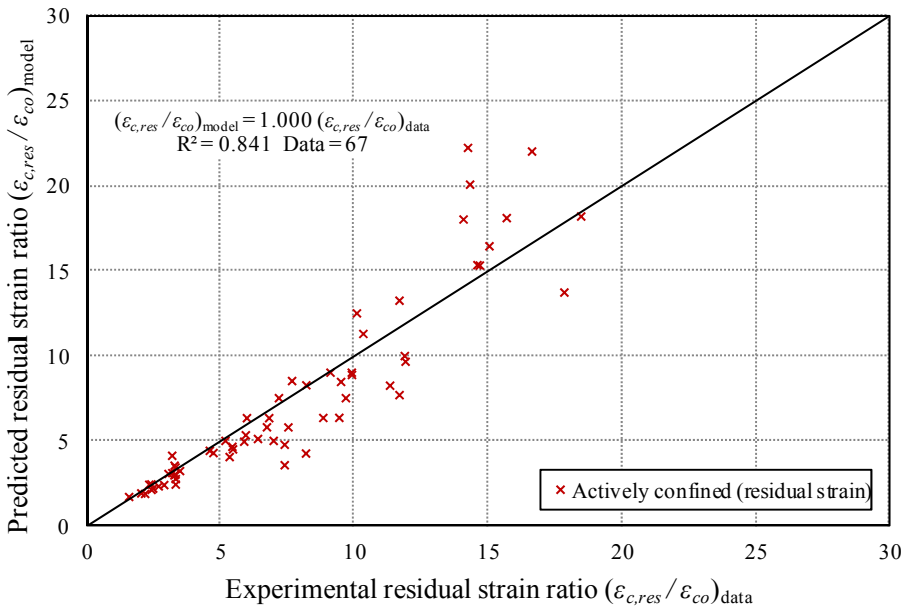

Figure 19. Comparison of model predictions of residual strain ratios ($\varepsilon_{c,res}/\varepsilon_{co}$) of actively confined concrete with test results

3.3 Comparison with test data

Table 3 presents the performance statistics of the proposed model, analysis-oriented models of FRP-confined concrete (Mirmiran and Shahawy 1997; Spoelstra and Monti 1999; Fam and Rizkalla 2001; Chun and Park 2002; Harries and Kharel 2002; Marques et al. 2004; Binici 2005; Albanesi et al. 2007; Teng et al. 2007) and actively confined concrete models (Elwi and Murray 1979; Imran and Pantazopoulou 1996; Lokuge et al. 2005; Montoya et al. 2006) in the prediction of the ultimate strain enhancement ratios ($\varepsilon_{cu}/\varepsilon_{co}$) of FRP-confined concrete and peak strain enhancement ratios ($\varepsilon^*_{cc}/\varepsilon_{co}$) of actively confined concrete. In the comparisons shown in Table 3, the mean square error (MSE), average absolute error (AAE), mean (M) and standard deviation (SD) were used as the statistical indicator to evaluate the accuracy and consistency of the model predictions. The comparisons of the statistics of model predictions shown in the table demonstrate the improved accuracy of the proposed model over the existing analysis-oriented models. The improvement on the predictions of both the ultimate strain enhancement ratio ($\varepsilon_{cu}/\varepsilon_{co}$) of FRP-confined concrete and the peak strain enhancement ratio ($\varepsilon^*_{cc}/\varepsilon_{co}$) of actively-confined concrete is achieved through accurate modeling of the dilation behavior of confined concrete, as influenced by the key parameters, including the level of confining pressure, type of confining materials, and concrete strength. The large and reliable databases used in the model development enabled accurate determination of relative influences of these key parameters.

It should be noted that in the evaluation of the model predictions of FRP-confined concrete, the experimentally recorded hoop rupture strains ($\varepsilon_{h,rup}$) were used rather than the values or expressions recommended by the original models for the calculation of $\varepsilon_{h,rup}$. Due to the improved accuracy provided by Eq. 4 in the calculation of the hoop strain reduction factor ($k_{\varepsilon,f}$) over that of the expressions reported previously, the proposed model would more

significantly outperform the other existing models if the hoop rupture strains were established using the model expressions. It is also worthwhile noting that in the assessment of model predictions of actively confined concrete, models proposed by Mirmiran and Shahawy (1997) and Harries and Kharel (2002), which were developed exclusively on the basis of FRP-confined concrete test results, were not included in the comparison. Similarly, actively confined concrete models (Elwi and Murray 1979; Imran and Pantazopoulou 1996; Lokuge et al. 2005; Montoya et al. 2006) were not used in the prediction of FRP-confined concrete test results. In addition, the models by Jiang and Teng (2007) and Xiao et al. (2010) had the same dilation expression as the one given in Teng et al. (2007), and they were not included in the comparisons due to their identical axial strain predictions to those of the model by Teng et al. (2007). A number of models that adopted alternative approaches for concrete deformability predictions, including concrete crack slip and separation approach (e.g.(Harmon et al. 1998; Harmon et al. 2002), non-linearity index approach (e.g. Candappa et al. (2001), octahedral stress-strain approach (e.g. (Becque et al. 2003; Lu and Hsu 2007), plasticity approach (e.g. (Karabinis and Rousakis 2002; Park and Kim 2005), and finite-element approach (e.g. (Grassl 2004; Yu et al. 2010a,b) were also excluded from the model comparisons due to the absence of all the input required for the direct comparison of the models with the test results.

The accuracy of models depends not only on their accuracy in predicting the critical coordinates but also their ability in capturing the shape of the lateral strain-to-axial strain curves. Figures 20(a) and 20(b) show the comparisons of the lateral strain-to-axial strain curves predicted by the assessed models with the experimental results from FRP-confined NSC and HSC specimens. As illustrated in Figs. 20(a) and 20(b), the lateral strain-to-axial strain relationship of FRP-confined concrete consists of a double-curvature curve with an inflection point where the curvature changes sign and terminates at the ultimate condition. These comparisons illustrate that the models that were developed on the basis of FRP-confined concrete test results (Mirmiran and Shahawy 1997; Harries and Kharel 2002; Teng et al. 2007), including the proposed model, capture the inflection point and ultimate point of the lateral strain-to-axial strain curve more accurately than the models that were based on expressions that were derived from the test results of actively confined concrete specimens (Spoelstra and Monti 1999; Fam and Rizkalla 2001; Chun and Park 2002; Marques et al. 2004; Binici 2005; Albanesi et al. 2007). The comparisons also illustrate that the proposed model provides an improved accuracy over the existing models in the prediction of the inflection point, ultimate point and the overall trend of the curves. Figures 20(c) and 20(d) show the comparisons of the model predictions of the lateral strain-to-axial strain curves with the experimental results from actively confined NSC and HSC specimens. It is evident from these comparisons that the proposed model provides improved predictions of the lateral strain-to-axial strain relationships of actively confined concrete.

Table 3. Model predictions of ultimate axial strain enhancement ratios ($\varepsilon_{cu}/\varepsilon_{co}$) of FRP-confined concrete and peak axial strain enhancement ratios ($\varepsilon^*_{cc}/\varepsilon_{co}$) of actively-confined concrete

Model	Prediction of $\varepsilon_{cu}/\varepsilon_{co}$				Prediction of $\varepsilon^*_{cc}/\varepsilon_{co}$			
	Mean Square Error	Average Absolute Error (%)	Mean (%)	Standard Deviation (%)	Mean Square Error	Average Absolute Error (%)	Mean (%)	Standard Deviation (%)
Albanesi et al. (2007)	7.5	50.4	138.8	58.4	3.8	27.8	114.7	32.5
Binici (2005)	10.9	43.8	96.3	56.2	15.9	72.1	104.9	105.0
Chun and Park (2002)	1,247.0	314.2	414.2	252.8	115.8	60.6	137.2	77.2
Elwi and Murray (1979)	-	-	-	-	21.0	40.1	60.8	19.5
Fam and Rizkalla (2001)	272.2	295.6	393.7	253.6	26.7	82.8	173.0	100.5
Harries and Kharel (2002)	1,208.4	81.4	110.1	533.9	-	-	-	-
Imran and Pantazopoulou (1996)	-	-	-	-	4.5	30.2	117.7	40.6
Lokuge et al. (2005)	-	-	-	-	5.5	24.4	92.5	28.5
Marques et al. (2004)	3,489.5	341.6	441.5	1,139.5	13.4	49.0	133.4	52.5
Mirmiran and Shahawy (1997)	24.0	51.4	49.1	18.3	-	-	-	-
Montoya et al. (2006)	-	-	-	-	10.0	32.8	81.2	31.8
Spoelstra and Monti (1999)	230.6	169.7	268.0	142.7	21.9	39.6	106.8	47.8
Teng et al. (2007)	8.1	34.0	124.4	40.5	5.3	22.2	107.1	28.8
Proposed model	6.2	29.1	113.1	38.1	2.9	19.9	98.5	22.8

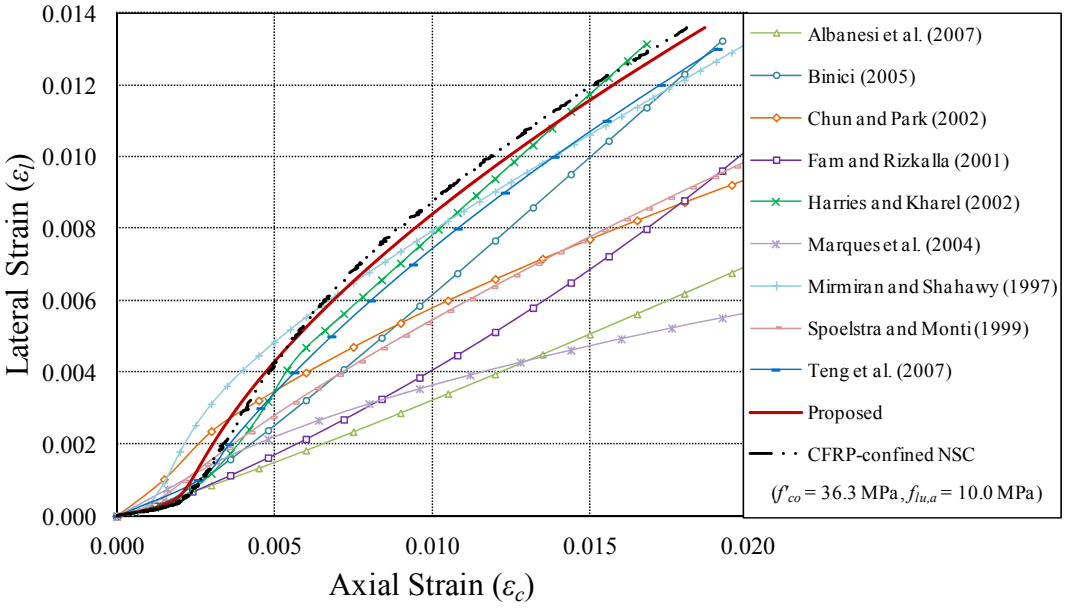
0.014
0.012
0.010
0.008
0.006
0.004
0.002
0.000
Lateral Strain (ε_l)
0.000
0.005
0.010
0.015
0.020
Axial Strain (ε_c)
Albanesi et al. (2007)
Binici (2005)
Chun and Park (2002)
Fam and Rizkalla (2001)
Harries and Kharel (2002)
Marques et al. (2004)
Mirmiran and Shahawy (1997)
Spoelstra and Monti (1999)
Teng et al. (2007)
Proposed
CFRP-confined NSC
(f'_{co} = 36.3 MPa, $f_{lu,a}$ = 10.0 MPa)

(a)

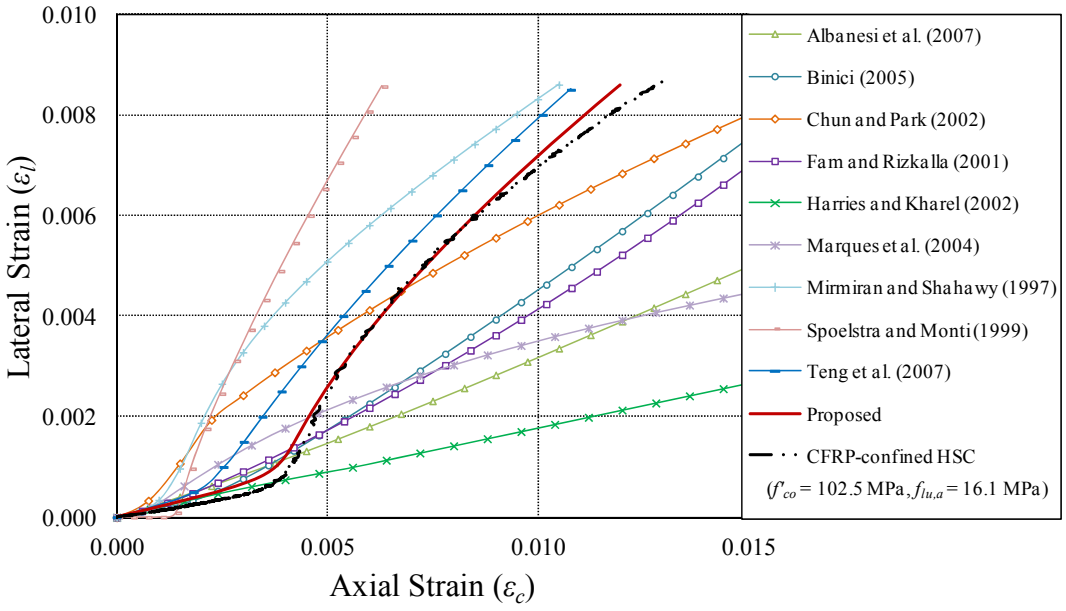
0.010
0.008
0.006
0.004
0.002
0.000
Lateral Strain (ε_l)
0.000
0.005
0.010
0.015
Axial Strain (ε_c)
Albanesi et al. (2007)
Binici (2005)
Chun and Park (2002)
Fam and Rizkalla (2001)
Harries and Kharel (2002)
Marques et al. (2004)
Mirmiran and Shahawy (1997)
Spoelstra and Monti (1999)
Teng et al. (2007)
Proposed
CFRP-confined HSC
(f'_{co} = 102.5 MPa, $f_{lu,a}$ = 16.1 MPa)

(b)

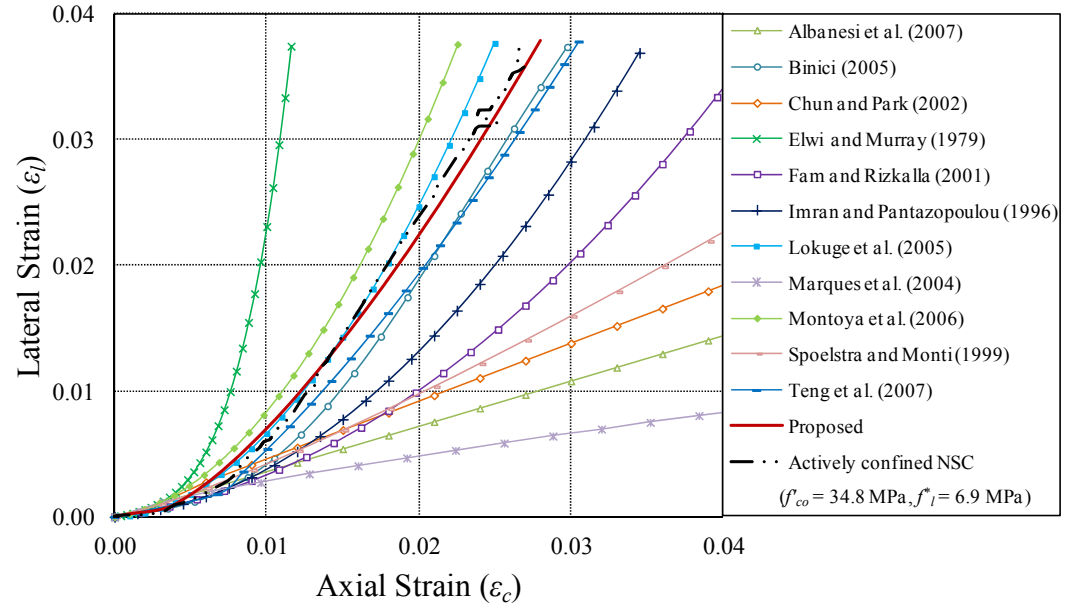

(c)

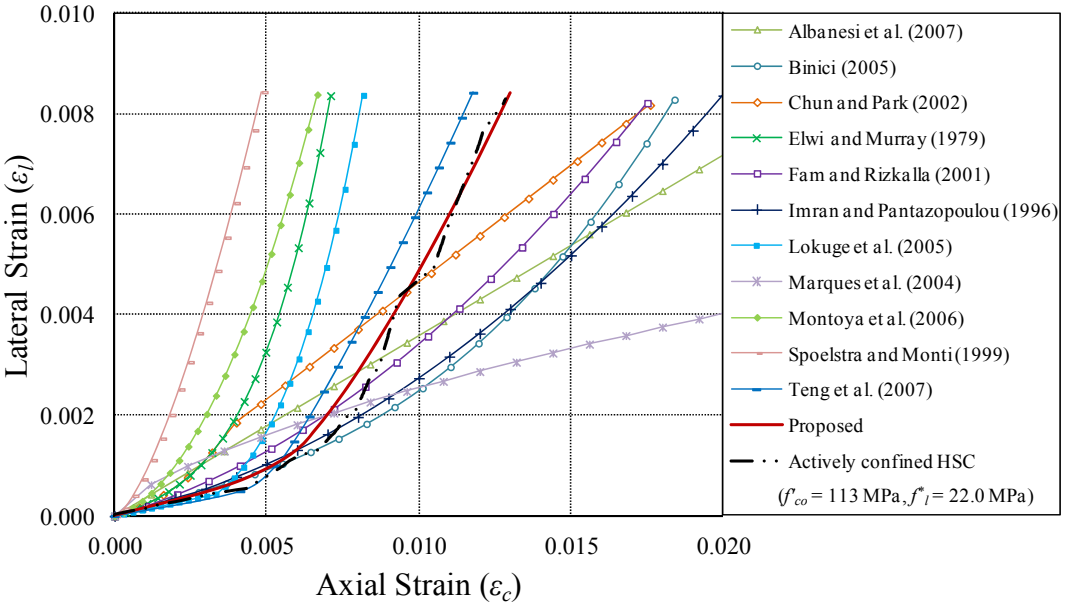

(d)

Figure 20. Comparison of model predictions with experimental lateral strain-to-axial strain curves: (a) CFRP-confined NSC specimen in Group U36; (b) CFRP-confined HSC specimen in Group U103; (c) Actively confined NSC specimen in Group U35; (d) Actively confined HSC specimen in Group U103

4. CONCLUSIONS

This paper has presented the results of an investigation on the dilation behavior of both FRP-confined and actively confined concretes. Two large experimental test databases that consist of 976 axial compression test results of FRP-confined concrete and 346 triaxial test results of actively confined concrete specimens have been assembled from the published literatures. The databases cover a wide range of parameters, thereby allowing clearer observations to be made on several important factors, including concrete strength, type of FRP material, and level of confining pressure, that influence the dilation behavior of confined concrete. In addition, a number of test results that contain complete records of dilation responses have been used to study the trend of the lateral strain-to-axial strain curves. On the basis of these databases, a new lateral strain-to-axial strain model has been developed and presented in this paper. The model is applicable to both passively and actively confined concretes, and it incorporates the important factors identified from the close examination of the results reported in the databases. The proposed model provides improved predictions of the ultimate axial strain of FRP-confined concrete and peak axial strain of actively confined concrete compared to the existing analysis-oriented models. Comparisons with experimental test results show that the model accurately predicts the trend and critical coordinates of the lateral strain-to-axial strain curves, including the ultimate strain of FRP-confined concrete and the peak and residual strains of actively confined concrete.

NOMENCLATURE

D	Diameter of concrete core (*mm*)
E_f	Elastic modulus of fibers (*MPa*)
f^*_{cc}	Peak axial compressive stress of actively confined concrete (*MPa*)
f^*_l	Active confining pressure (*MPa*)
f^*_l/f'_{co}	Confinement ratio of actively confined concrete
$f_{c,res}$	Residual compressive stress of actively confined concrete (*MPa*)
f'_{co}	Peak axial compressive stress of unconfined concrete (*MPa*)
f'_{cu}	Ultimate axial compressive stress of FRP-confined concrete (*MPa*)
f_l	Confining pressure (*MPa*)
$f_{lu,a}$	Actual confining pressure of FRP at ultimate condition; $f_{lu,a} = K_l\varepsilon_{h,rup}$ (*MPa*)
$f_{lu,a}/f'_{co}$	Confinement ratio of FRP-confined concrete
H	FRP confined concrete specimen height (mm)
K_l	Lateral confinement stiffness (*MPa*); $K_l = 2E_f t_f/D$
$k_{\varepsilon,f}$	Hoop strain reduction factor of fibers
n	Curve-shape parameter in dilation model
t_f	Total nominal thickness of fibers (*mm*)
ε^*_{cc}	Axial strain of actively confined concrete at f^*_{cc}
ε^*_{lc}	Lateral strain of actively confined concrete at f^*_{cc}
ε_c	Axial strain
$\varepsilon_{c,res}$	Axial strain of actively confined concrete at $f_{c,res}$
ε_{co}	Axial strain of unconfined concrete at f'_{co}
ε_{cu}	Ultimate axial strain of FRP-confined concrete at f'_{cu}
ε_f	Ultimate tensile strain of fibers
$\varepsilon_{h,rup}$	Hoop rupture strain of FRP shell
ε_l	Lateral strain
$\varepsilon_{l,res}$	Lateral strain of actively confined concrete at $f_{c,res}$
ε_{lo}	Lateral strain of unconfined concrete at f'_{co}
μ_t	Dilation rate of confined concrete
υ_i	Initial Poisson's ratio of concrete

REFERENCES

Albanesi, T., Nuti, C. and Vanzi, I. (2007). "Closed form constitutive relationship for concrete filled FRP tubes under compression." *Construction and Building Materials*, 21(2), 409-427.

Ansari, F. and Li, Q. B. (1998). "High-strength concrete subjected to triaxial compression." *ACI Materials Journal*, 95(6), 747-755.

Attard, M. M. and Setunge, S. (1996). "Stress-strain relationship of confined and unconfined concrete." *ACI Materials Journal*, 93(5), 432-442.

Balmer, G. G. (1949). "Shearing Strength of Concrete Under High Triaxial Stress-computation of Mohr's Envelope as a Curve." *Structural Research Laboratory Report No. SP-23*, Department of the Interior Bureau of Reclamation, Denver, Colorado, United States.

Becque, J., Patnaik, A. K. and Rizkalla, S. H. (2003). "Analytical models for concrete confined with FRP tubes." *Journal of Composites for Construction*, 7(1), 31-38.

Bellotti, R. and Rossi, P. (1991). "Cylinder tests: experimental technique and results." *Materials and Structures*, 24(1), 45-51.

Binici, B. (2005). "An analytical model for stress-strain behavior of confined concrete." *Engineering Structures*, 27(7), 1040-1051.

Candappa, D. C., Sanjayan, J. G. and Setunge, S. (2001). "Complete triaxial stress-strain curves of high-strength concrete." *Journal of Materials in Civil Engineering*, 13(3), 209-215.

Chun, S. S. and Park, H. C. (2002). "Load carrying capacity and ductility of RC columns confined by carbon fiber reinforced polymer." *Proceedings of the 3rd International Conference on Composites in Infrastructure*, San Francisco.

Elwi, A. A. and Murray, D. W. (1979). "A 3D hypoelastic concrete constitutive relationship." *Journal of the Engineering Mechanics Division*, 105(4), 623-641.

Fam, A. Z. and Rizkalla, S. H. (2001). "Confinement model for axially loaded concrete confined by circular fiber-reinforced polymer tubes." *ACI Structural Journal*, 98(4), 451-461.

Gabet, T., Malecot, Y. and Daudeville, L. (2008). "Triaxial behaviour of concrete under high stresses: Influence of the loading path on compaction and limit states." *Cement and Concrete Research*, 38(3), 403-412.

Gardner, N. J. (1969). "Triaxial behavior of concrete." *Journal of the American Concrete Institute*, 66(2), 136-146.

Grassl, P. (2004). "Modelling of dilation of concrete and its effect in triaxial compression." *Finite Elements in Analysis and Design*, 40(9-10), 1021-1033.

Hammons, M. I. and Neeley, B. D. (1993). "Triaxial characterization of high-strength Portland cement concrete." *Transportation Research Record*(1382), 73-77.

Harmon, T. G., Gould, N. C., Ramakrishnan, S. and Wang, E. H. (2002). "Confined concrete columns subjected to axial load, cyclic shear, and cyclic flexure - Part I: Analytical models." *Aci Structural Journal*, 99(1), 32-41.

Harmon, T. G., Ramakrishnan, S. and Wang, E. H. (1998). "Confined concrete subjected to uniaxial monotonic loading." *Journal of Engineering Mechanics*, 124(12), 1303-1309.

Harries, K. A. and Kharel, G. (2002). "Behavior and modeling of concrete subject to variable confining pressure." *ACI Materials Journal*, 99(2), 180-189.

Hurlbut, B. (1985). "Experimental and computational investigation of strain-softening in concrete." PhD Dissertation, University of Colorado.

Imran, I. (1994). "Applications of Nonassociated Plasticity in Modeling the Mechanical Response of Concrete." PhD, *Department of Civil Engineering*, University of Toronto, Toronto.

Imran, I. and Pantazopoulou, S. J. (1996). "Experimental study of plain concrete under triaxial stress." *ACI Materials Journal*, 93(6), 589-601.

Imran, I. and Pantazopoulou, S. J. (2001). "Plasticity model for concrete under triaxial compression." *Journal of Engineering Mechanics, ASCE*, 127(3), 281-290.

Jamet, P., Millard, A. and Nahas, G. (1984). "Triaxial behaviour of a micro-concrete complete stress-strain curves for confining pressures ranging from 0 to 100 MPa." *RILEM-CEB International Conference on Concrete Under Multiaxial Conditions*, France.

Jiang, T. and Teng, J. G. (2007). "Analysis-oriented stress-strain models for FRP-confined concrete." *Engineering Structures*, 29(11), 2968-2986.

Karabinis, A. I. and Rousakis, T. C. (2002). "Concrete confined by FRP material: a plasticity approach." *Engineering Structures*, 24(7), 923-932.

Kent, D. C. and Park, R. (1971). "Flexural members with confined concrete." *Journal of the Structural Division, ASCE*, 97(7), 1969-1990.

Kotsovos, M. D. (1979). "Effect of stress path on the behavior of concrete under triaxial stress states." *Journal of the American Concrete Institute*, 76(2), 213-223.

Kotsovos, M. D. and Newman, J. B. (1978). "Generalized stress-strain relations for concrete." *Journal of the Engineering Mechanics Division, ASCE*, 104(4), 845-856.

Lahlou, K., Aitcin, P. C. and Chaallal, O. (1992). "Behaviour of High-strength Concrete Under Confined Stresses." *Cement and Concrete Composites*, 14(3), 185-193.

Lim, J. C. and Ozbakkaloglu, T. (2014). "Confinement model for FRP-confined high-strength concrete." *Journal of Composites for Construction*, 18(4), 04013058.

Lokuge, W. P., Sanjayan, J. G. and Setunge, S. (2005). "Stress-strain model for laterally confined concrete." *Journal of Materials in Civil Engineering*, 17(6), 607-616.

Lu, X. B. and Hsu, C. T. T. (2007). "Stress-strain relations of high-strength concrete under triaxial compression." *Journal of Materials in Civil Engineering*, 19(3), 261-268.

Mander, J. B., Priestley, M. J. N. and Park, R. (1988). "Theoretical stress-strain model for confined concrete." *Journal of Structural Engineering, ASCE*, 114(8), 1804-1826.

Marques, S. P. C., Marques, D., da Silva, J. L. and Cavalcante, M. A. A. (2004). "Model for analysis of short columns of concrete confined by fiber-reinforced polymer." *Journal of Composites for Construction, ASCE*, 8(4), 332-340.

Mirmiran, A. and Shahawy, M. (1997). "Dilation characteristics of confined concrete." *Mechanics of Cohesive-Frictional Materials*, 2(3), 237-249.

Montoya, E., Vecchio, F. J. and Sheikh, S. A. (2006). "Compression field modeling of confined concrete: Constitutive models." *Journal of Materials in Civil Engineering*, 18(4), 510-517.

Moran, D. A. and Pantelides, C. P. (2002). "Stress-strain model for fiber-reinforced polymer-confined concrete." *Journal of Composites for Construction*, 6(4), 233-240.

Newman, J. B. (1979). "Concrete under complex stress." Department of Civil Engineering, Imperial College of Science and Technology, London, UK, London, UK.

Ozbakkaloglu, T. and Akin, E. (2012). "Behavior of FRP-confined normal- and high-strength concrete under cyclic axial compression." *Journal of Composites for Construction, ASCE*, 16(4), 451-463.

Ozbakkaloglu, T. and Lim, J. C. (2013). "Axial compressive behavior of FRP-confined concrete: Experimental test database and a new design-oriented model." *Composites Part B: Engineering*, 55, 607-634.

Ozbakkaloglu, T., Lim, J. C. and Vincent, T. (2013). "FRP-confined concrete in circular sections: Review and assessment of stress–strain models." *Engineering Structures*, 49, 1068–1088.

Ozbakkaloglu, T. and Saatcioglu, M. (2006). "Seismic behavior of high-strength concrete columns confined by fiber-reinforced polymer tubes." *Journal of Composites for Construction, ASCE*, 10(6), 538-549.

Ozbakkaloglu, T. and Vincent, T. (2013). "Axial compressive behavior of circular high-strength concrete-filled FRP tubes." *Journal of Composites for Construction, ASCE*, 18(2), 04013037.

Park, H. and Kim, J. Y. (2005). "Plasticity model using multiple failure criteria for concrete in compression." *International Journal of Solids and Structures*, 42(8), 2303-2322.

Pessiki, S., Harries, K. A., Kestner, J. T., Sause, R. and Ricles, J. M. (2001). "Axial behavior of reinforced concrete columns confined with FRP jackets." *Journal of Composites for Construction*, 5(4), 237-245.

Richart, F. E., Brandtzaeg, A. and Brown, R. L. (1928). "A study of the failure of concrete under combined compressive stresses." *Bulletin No. 185*, Engineering Experimental Station, University of Illinois, Champaign, Illinois.

Rutland, C. A. and Wang, M. L. (1997). "The effects of confinement on the failureorientation in cementitiousmaterialsexperimentalobservations." *Cement and Concrete Composites*, 19(2), 149-160.

Saatcioglu, M. and Razvi, S. R. (1992). "Strength and ductility of confined concrete." *Journal of Structural Engineering, ASCE*, 118(6), 1590-1607.

Setunge, S., Attard, M. M. and Darvall, P. L. (1993). "Ultimate strength of confined very high-strength concretes." *ACI Structural Journal*, 90(6), 632-641.

Sfer, D., Carol, I., Gettu, R. and Etse, G. (2002). "Study of the behavior of concrete under triaxial compression." *Journal of Engineering Mechanics*, 128(2), 156-163.

Sheikh, S. A. and Uzumeri, S. M. (1980). "Strength and Ductility of Tied Concrete Columns." *Journal of Structural Engineering, ASCE*, 106(5), 1079-1102.

Smith, S. S., Willam, K. J., Gerstle, K. H. and Sture, S. (1989). "Concrete Over The Top, Or: Is There Life After Peak?" *ACI Materials Journal*, 86(5), 491-497.

Spoelstra, M. R. and Monti, G. (1999). "FRP-confined concrete model." *Journal of Composites for Construction*, 3(3), 143-150.

Tan, K. H. and Sun, X. (2004). "Failure criteria of concrete under triaxial compression." *International Symposium on Confined Concrete*.

Tasdemir, M. A., Tasdemir, C., Jefferson, A. D., Lydon, F. D. and Barr, B. I. G. (1998). "Evaluation of strains at peak stresses in concrete: A three-phase composite model approach." *Cement and Concrete Research*, 20(4), 301-318.

Teng, J. G., Huang, Y. L., Lam, L. and Ye, L. P. (2007). "Theoretical model for fiber-reinforced polymer-confined concrete." *Journal of Composites for Construction, ASCE*, 11(2), 201-210.

Vincent, T. and Ozbakkaloglu, T. (2013a). "Influence of concrete strength and confinement method on axial compressive behavior of FRP-confined high- and ultra high-strength concrete." *Composites Part B*, 50, 413–428.

Vincent, T. and Ozbakkaloglu, T. (2013b). "Influence of fiber orientation and specimen end condition on axial compressive behavior of FRP-confined concrete." *Construction and Building Materials*, 47, 814-826.

Vu, X. H., Malecot, Y., Daudeville, L. and Buzaud, E. (2009). "Experimental analysis of concrete behavior under high confinement: Effect of the saturation ratio." *International Journal of Solids and Structures*, 46(5), 1105-1120.

Xiao, Q. G., Teng, J. G. and Yu, T. (2010). "Behavior and Modeling of Confined High-Strength Concrete." *Journal of Composites for Construction, ASCE*, 14(3), 249-259.

Xiao, Y. and Wu, H. (2000). "Compressive behavior of concrete confined by carbon fiber composite jackets." *Journal of Materials in Civil Engineering*, 12(2), 139-146.

Xiao, Y. and Wu, H. (2003). "Compressive behavior of concrete confined by various types of FRP composite jackets." *Journal of Reinforced Plastics and Composites*, 22(13), 1187-1201.

Xie, J., Elwi, A. E. and Macgregor, J. G. (1995). "Mechanical-properties of high-strength concretes containing silica fume." *ACI Materials Journal*, 92(2), 135-145.

Yu, T., Teng, J. G., Wong, Y. L. and Dong, S. L. (2010a). "Finite element modeling of confined concrete-I: Drucker-Prager type plasticity model." *Engineering Structures*, 32(3), 665-679.

Yu, T., Teng, J. G., Wong, Y. L. and Dong, S. L. (2010b). "Finite element modeling of confined concrete-II: Plastic-damage model." *Engineering Structures*, 32(3), 680-691.

APPENDIX

Table 1. Test database of actively confined concrete specimens

Paper	Number of specimen per data entry	Geometries		Concrete Properties			Peak Conditions				Residual Conditions		
		D (mm)	H (mm)	f'_{co} (MPa)	ε_{co} (%)	ε_{lo} (%)	f^*_l (MPa)	f^*_{cc} (MPa)	ε^*_{cc} (%)	ε^*_l (%)	$f_{c,res}$ (MPa)	$\varepsilon_{c,res}$ (%)	$\varepsilon_{l,res}$ (%)
		101	202	47.23	0.202		8.29	79.79	1.350				
Ansari and Li (1998)	2	101	202	47.23	0.202		16.59	109.74	1.568				
Ansari and Li (1998)	2	101	202	47.23	0.202		24.88	130.80	2.049				
Ansari and Li (1998)	6	101	202	47.23	0.202		33.17	144.30	2.420				
Ansari and Li (1998)	2	101	202	47.23	0.202		41.47	167.04	2.950				
Ansari and Li (1998)	4	101	202	71.08	0.203		13.16	129.13	0.798				
Ansari and Li (1998)	3	101	202	71.08	0.203		26.32	156.15	1.258				
Ansari and Li (1998)	2	101	202	71.08	0.203		39.48	185.38	2.042				
Ansari and Li (1998)	2	101	202	71.08	0.203		52.65	209.37	3.019				
Ansari and Li (1998)	2	101	202	71.08	0.203		65.80	224.77	3.868				
Ansari and Li (1998)	2	101	202	107.28	0.194		20.90	192.50	0.890				
Ansari and Li (1998)	3	101	202	107.28	0.194		41.80	232.97	1.065				
Ansari and Li (1998)	2	101	202	107.28	0.194		62.70	285.91	1.930				
Ansari and Li (1998)	2	101	202	107.28	0.194		83.59	314.95	2.096				
Attard and Setunge (1996)	1	100	200	120	0.3		0.5	125	0.26				
Attard and Setunge (1996)	1	100	200	120	0.3		1	128	0.29		33.7	0.70	
Attard and Setunge (1996)	1	100	200	120	0.3		5	165	0.38		110.3	0.69	
Attard and Setunge (1996)	1	100	200	120	0.3		10	192	0.53		99.3	1.23	
Attard and Setunge (1996)	1	100	200	120	0.3		15	220	0.60		136.3	1.33	
Attard and Setunge (1996)	1	100	200	120	0.3		20	234	0.80		130.9	1.90	
Attard and Setunge (1996)	1	100	200	120	0.28		5	168	0.42		83.2	0.89	
Attard and Setunge (1996)	1	100	200	120	0.28		10	187	0.48		101.2	1.21	
Attard and Setunge (1996)	1	100	200	120	0.28		15	211	0.57		199.6	0.70	
Attard and Setunge (1996)	1	100	200	110	0.28		5	150	0.35		63.0	1.25	
Attard and Setunge (1996)	1	100	200	110	0.28		10	175	0.44		104.7	1.21	
Attard and Setunge (1996)	1	100	200	110	0.28		15	192	0.60		126.9	1.41	
Attard and Setunge (1996)	1	100	200	100	0.27		1	106	0.31				
Attard and Setunge (1996)	1	100	200	100	0.27		5	121	0.36				
Attard and Setunge (1996)	1	100	200	100	0.27		10	144	0.47				
Attard and Setunge (1996)	1	100	200	100	0.27		15	165	0.58				
Attard and Setunge (1996)	1	100	200	132	0.34		5	180	0.50		82.5	1.11	
Attard and Setunge (1996)	1	100	200	132	0.34		10	200	0.58		101.4	1.36	
Attard and Setunge (1996)	1	100	200	132	0.34		15	222	0.78		123.0	1.67	
Attard and Setunge (1996)	1	100	200	126	0.34		5	162	0.50				
Attard and Setunge (1996)	1	100	200	126	0.34		10	186	0.71				
Attard and Setunge (1996)	1	100	200	126	0.34		15	211	0.89				
Attard and Setunge (1996)	1	100	200	118	0.28		5	154	0.38		79.4	1.08	
Attard and Setunge (1996)	1	100	200	118	0.28		10	173	0.49		76.2	0.87	
Attard and Setunge (1996)	1	100	200	118	0.28		15	201	0.62		107.5	1.97	
Attard and Setunge (1996)	1	100	200	110	0.28		5	153	0.41		80.3	1.07	
Attard and Setunge (1996)	1	100	200	110	0.28		10	164	0.55		104.9	1.09	
Attard and Setunge (1996)	1	100	200	110	0.28		15	185	0.59		123.1	1.85	
Attard and Setunge (1996)	1	100	200	100	0.26		5	127	0.39		76.4	1.01	
Attard and Setunge (1996)	1	100	200	100	0.26		10	153	0.52		102.9	1.39	
Attard and Setunge (1996)	1	100	200	100	0.26		15	169	0.75		127.4	1.78	
Attard and Setunge (1996)	1	100	200	96	0.28		5	119	0.37				
Attard and Setunge (1996)	1	100	200	96	0.28		10	147	0.52				
Attard and Setunge (1996)	1	100	200	96	0.28		15	157	0.53				
Attard and Setunge (1996)	1	100	200	60	0.21		1	67	0.27				
Attard and Setunge (1996)	1	100	200	60	0.21		5	98	0.48				
Attard and Setunge (1996)	1	100	200	60	0.21		10	122	0.76				
Attard and Setunge (1996)	1	100	200	60	0.21		15	145	0.99				
Balmer (1949)	9	152	305	24.6	0.36		172.37	535.21	4.140*				
Balmer (1949)	9	152	305	24.6	0.36		137.90	469.95	4.772*				
Balmer (1949)	9	152	305	24.6	0.36		103.42	369.05	4.651*				
Balmer (1949)	9	152	305	24.6	0.36		68.95	273.74	4.758*				
Balmer (1949)	9	152	305	24.6	0.36		34.47	168.06	3.051*				
Bellotti and Rossi (1991)	1	160	320	53.5	0.31	0.17	4.9	84.3	1.01	0.30			
Bellotti and Rossi (1991)	1	160	320	53.5	0.31	0.17	9.8	104.6	1.35	0.90			
Bellotti and Rossi (1991)	1	160	320	53.5	0.31	0.17	14.7	125.0	1.80	0.58			
Bellotti and Rossi (1991)	1	160	320	53.5	0.31	0.17	19.6	147.1	2.37	0.92			
Bellotti and Rossi (1991)	1	160	320	53.5	0.31	0.17	24.5	163.8	2.29	1.13			
Bellotti and Rossi (1991)	1	160	320	53.5	0.31	0.17	29.4	184.1	2.62	1.14			
Bellotti and Rossi (1991)	1	160	320	53.5	0.31	0.17	34.3	198.2	3.38	1.20			
Bellotti and Rossi (1991)	1	160	320	53.5	0.31	0.17	39.2	210.8	3.52	1.14			
Candappa et al. (2001)	1	98	200	41.9	0.24	0.13	4	66.6	0.87	0.63	63.6	1.14	1.26
Candappa et al. (2001)	1	98	200	41.9	0.24	0.13	8	85.1	1.25	0.82	82.7	1.44	1.33
Candappa et al. (2001)	1	98	200	41.9	0.24	0.13	8	85.4	1.05	0.49	83.1	1.64	1.33
Candappa et al. (2001)	1	98	200	41.9	0.24	0.13	12	102.4	1.72	0.9	99.2	2.19	1.59
Candappa et al. (2001)	1	98	200	41.9	0.24	0.13	12	105.1	1.67	0.72	101.7	2.38	1.59
Candappa et al. (2001)	1	98	200	60.6	0.24	0.1	4	78.2	0.40	0.12	62.4	0.80	0.86
Candappa et al. (2001)	1	98	200	60.6	0.24	0.1	5	81.8	0.53	0.45	69.9	0.77	1.33
Candappa et al. (2001)	1	98	200	60.6	0.24	0.1	8	97.8	0.98	0.46	89.2	1.54	1.30
Candappa et al. (2001)	1	98	200	60.6	0.24	0.1	12	115.5	1.24	0.42	113.8	1.68	0.85
Candappa et al. (2001)	1	98	200	73.1	0.24	0.21	4	102.6	0.45	0.16	79.0	0.79	0.96
Candappa et al. (2001)	1	98	200	73.1	0.24	0.21	8	121.5	0.63	0.30	92.1	1.31	1.30
Candappa et al. (2001)	1	98	200	73.1	0.24	0.21	8	122.3	0.69	0.29	100.3	1.43	1.66
Candappa et al. (2001)	1	98	200	73.1	0.24	0.21	12	138.1	0.94	0.46	131.1	0.65	0.21
Candappa et al. (2001)	1	98	200	103.3	0.3	0.12	4	133.1	0.43	0.17	126.7	0.48	0.39

Paper	n	D (mm)	H (mm)	f'_{co} (MPa)	ε_{co} (%)	ε_{lo} (%)	f^*_l (MPa)	f^*_{cc} (MPa)	ε^*_{cc} (%)	ε^*_l (%)	$f_{c,res}$ (MPa)	$\varepsilon_{c,res}$ (%)	$\varepsilon_{l,res}$ (%)
Candappa et al. (2001)	1	98	200	103.3	0.3	0.12	8	151.0	0.68	0.29	116.7	1.05	1.19
Candappa et al. (2001)	1	98	200	103.3	0.3	0.12	8	158.0	0.67	0.23	146.1	0.73	0.64
Candappa et al. (2001)	1	98	200	103.3	0.3	0.12	12	171.5	0.80	0.35	147.3	0.99	1.01
Candappa et al. (2001)	1	98	200	103.3	0.3	0.12	12	169.3	0.78	0.30	154.1	1.00	0.95
Gabet et al. (2008)	1	70	140	30			50	171.70	2.708*	0.842	168.44	3.229*	1.372
Gabet et al. (2008)	1	70	140	30			100	280.85	8.039*	3.192	278.14	8.039*	3.192
Gabet et al. (2008)	1	70	140	30			200	487.68	10.196*	3.192	487.68	10.196*	3.192
Gabet et al. (2008)	1	70	140	30			500	708.28	6.552*	1.594	708.16	6.552*	1.594
Gabet et al. (2008)	1	70	140	30			650	1002.99	9.476*	4.058	1000.57	9.476*	4.058
Gardner (1969)	3	76.2	152.4	28.96	0.4		8.62	72.39	0.70*				
Gardner (1969)	4	76.2	152.4	28.96	0.4		17.24	117.90	2.15*				
Gardner (1969)	5	76.2	152.4	28.96	0.4		25.86	144.79	2.60*				
Hammons and Neeley (1993)	1	53.6	88.9	96			50	257	1.5				
Hammons and Neeley (1993)	1	51	88.5	96			100	408	10.0*				
Hammons and Neeley (1993)	1	53.6	88.5	96			150	540	10.0*				
Hammons and Neeley (1993)	1	53.6	88.9	96			200	631	10.0*				
Hurlbut (1985)	1	54	108	19	0.18		0.69	26.2	0.33				
Hurlbut (1985)	1	54	108	19	0.18		3.45	33.3	0.94				
Hurlbut (1985)	1	54	108	19	0.18		6.89	51.8	1.47				
Hurlbut (1985)	1	54	108	19	0.18		13.76	78.3	1.57*				
Imran (1994)	1	54	115	43	0.24	0.09	14	106.6	3.29*	1.41			
Imran (1994)	1	54	115	43	0.24	0.09	43	182.3	4.60	0.91			
Imram and Pantazopoulou (1996)	1	54	115	73.35	0.325	0.31	3.2	96.1	0.495	0.445			
Imram and Pantazopoulou (1996)	1	54	115	73.35	0.325	0.31	6.4	108.7	0.650	0.660			
Imram and Pantazopoulou (1996)	1	54	115	73.35	0.325	0.31	12.8	125.6	1.045	1.100			
Imram and Pantazopoulou (1996)	1	54	115	73.35	0.325	0.31	25.6	168.6	2.025	2.465*			
Imram and Pantazopoulou (1996)	1	54	115	73.35	0.325	0.31	38.4	204.0	3.105	4.525*			
Imram and Pantazopoulou (1996)	1	54	115	73.35	0.325	0.31	51.2	240.5	4.090	3.920*			
Imram and Pantazopoulou (1996)	1	54	115	64.69	0.297	0.277	3.2	80.9	0.455	0.510	76.48	0.611	0.468
Imram and Pantazopoulou (1996)	1	54	115	64.69	0.297	0.277	6.4	96.8	0.61	0.800	91.59	0.864	0.493
Imram and Pantazopoulou (1996)	1	54	115	64.69	0.297	0.277	12.8	113.5	1.125	1.335	97.88	2.441	2.709
Imram and Pantazopoulou (1996)	1	54	115	64.69	0.297	0.277	25.6	153.9	2.235	2.585*	145.11	4.186	4.538
Imram and Pantazopoulou (1996)	1	54	115	64.69	0.297	0.277	38.4	190.6	3.495	3.110*	188.72	4.258	3.483
Imram and Pantazopoulou (1996)	1	54	115	64.69	0.297	0.277	51.2	230.5	5.03	5.390*	231.82	6.246	
Imram and Pantazopoulou (1996)	1	54	115	47.4	0.28	0.273	2.15	57.7	0.43	0.395			
Imram and Pantazopoulou (1996)	1	54	115	47.4	0.28	0.273	4.3	67.3	0.69	0.585			
Imram and Pantazopoulou (1996)	1	54	115	47.4	0.28	0.273	8.6	83.6	1.46	1.305			
Imram and Pantazopoulou (1996)	1	54	115	47.4	0.28	0.273	17.2	118.1	2.53	2.470			
Imram and Pantazopoulou (1996)	1	54	115	47.4	0.28	0.273	30.1	161.1	3.6	2.015			
Imram and Pantazopoulou (1996)	1	54	115	47.4	0.28	0.273	43	204.7	4.73	5.950*			
Imram and Pantazopoulou (1996)	1	54	115	43.11	0.25	0.295	2.15	46.0	0.43	0.405	41.33	0.836	0.692
Imram and Pantazopoulou (1996)	1	54	115	43.11	0.25	0.295	4.3	53.5	0.65	0.63	53.92	0.836	0.526
Imram and Pantazopoulou (1996)	1	54	115	43.11	0.25	0.295	8.6	73.0	1.66	1.86	67.85	2.982	2.695
Imram and Pantazopoulou (1996)	1	54	115	43.11	0.25	0.295	17.2	107.0	2.81	3.580*	102.96	4.544	
Imram and Pantazopoulou (1996)	1	54	115	43.11	0.25	0.295	30.1	149.3	4.23	5.410*	149.29	4.856	
Imram and Pantazopoulou (1996)	1	54	115	43.11	0.25	0.295	43	184.2	5.02	8.500*	184.59		
Imram and Pantazopoulou (1996)	1	54	115	28.62	0.26	0.24	1.05	33.6	0.47	0.315			
Imram and Pantazopoulou (1996)	1	54	115	28.62	0.26	0.24	2.1	36.4	0.675	0.405			
Imram and Pantazopoulou (1996)	1	54	115	28.62	0.26	0.24	4.2	48.1	1.385	0.810			
Imram and Pantazopoulou (1996)	1	54	115	28.62	0.26	0.24	8.4	65.2	2.375	2.340			
Imram and Pantazopoulou (1996)	1	54	115	28.62	0.26	0.24	14.7	92.3	3.425	3.570*			
Imram and Pantazopoulou (1996)	1	54	115	28.62	0.26	0.24	21	114.5	4.46	3.800*			
Imram and Pantazopoulou (1996)	1	54	115	21.17	0.22	0.26	1.05	25.9	0.36	0.430	21.51	1.178	1.706
Imram and Pantazopoulou (1996)	1	54	115	21.17	0.22	0.26	2.1	28.5	0.66	0.510	24.49	2.094	3.480
Imram and Pantazopoulou (1996)	1	54	115	21.17	0.22	0.26	4.2	38.0	1.62	1.200	37.43	2.184	1.974
Imram and Pantazopoulou (1996)	1	54	115	21.17	0.22	0.26	8.4	55.2	2.96	2.320	54.89	3.455	2.969
Imram and Pantazopoulou (1996)	1	54	115	21.17	0.22	0.26	14.7	79.4	3.96	3.930*	78.083		
Imram and Pantazopoulou (1996)	1	54	115	21.17	0.22	0.26	21	102.6	5.05	5.340*	102.32	5.51	
Jamet et al. (1984)	1	110	220	31.43	0.369		3	45.13	0.697				
Jamet et al. (1984)	1	110	220	31.43	0.369		10	62.71	1.639				
Jamet et al. (1984)	1	110	220	31.43	0.369		25	99.82	3.875				
Jamet et al. (1984)	1	110	220	31.43	0.369		50	142.96	10.177				
Kotsovos and Newman (1978)	1	100	250	31.7			19	99.15	2.286	1.125	98.09	2.757	2.177
Kotsovos and Newman (1978)	1	100	250	31.7			24	112.92	3.737	2.286	112.92	3.737	2.286
Kotsovos and Newman (1978)	1	100	250	31.7			44	175.64	4.934	1.524	163.98	7.039*	3.991
Kotsovos and Newman (1978)	1	100	250	46.9			18	121.72	1.846	0.869	120.13	2.389	1.593
Kotsovos and Newman (1978)	1	100	250	46.9			35	177.65	2.679	1.195	169.70	3.403	2.787
Kotsovos and Newman (1978)	1	100	250	46.9			51	227.54	3.910	1.195	220.55	5.140	3.077
Kotsovos and Newman (1978)	1	100	250	46.9			70	271.40	5.032	1.774	253.60	7.385	7.095*
Kotsovos and Newman (1979)	1	100	250	73.3	0.2		35	217.85	1.927	0.477	205.71	3.012	1.845
Kotsovos and Newman (1979)	1	100	250	73.3	0.2		69.8	322.68	3.001	0.722	315.86	3.900	1.996
Newman (1979)	1	100	250	91.19	0.147		3.5	110.34	0.591	0.216	104.45	0.452	0.657
Newman (1979)	1	100	250	91.19	0.147		6.8	126.75	0.861	0.394	119.45	1.091	0.544
Newman (1979)	1	100	250	91.19	0.147		13.7	147.49	1.352	0.55	140.33	1.722	1.148
Newman (1979)	1	100	250	91.19	0.147		22.6	179.80	2.154*	0.708	167.72	3.052*	1.688
Newman (1979)	1	100	250	91.19	0.147		34.9	208.54	3.369*	1.062	202.41	4.633*	1.656
Newman (1979)	1	100	250	91.19	0.147		69.2	287.49	6.106*	1.666	271.33	11.818*	6.924
Newman (1979)	1	100	250	91.19	0.147		138.2	461.03	12.76*	2.22	452.70	18.760*	5.942
Newman (1979)	1	100	250	91.19	0.147		138.2	480.41	11.152*	2.596	472.35	14.108*	4.536
Newman (1979)	1	100	250	73.3	0.2		3.5	97.40	0.38	0.14	92.01	0.44	0.260
Newman (1979)	1	100	250	73.3	0.2		6.8	115.04	0.64	0.18	90.51	1.04	1.320
Newman (1979)	1	100	250	73.3	0.2		13.7	147.19	0.95	0.34	133.43	1.35	0.900
Newman (1979)	1	100	250	73.3	0.2		22.6	187.82	1.34	0.4	165.79	2.38	1.340
Newman (1979)	1	100	250	73.3	0.2		34.9	220.89	2	0.64	206.92	2.94	1.660
Newman (1979)	1	100	250	73.3	0.2		69.2	312.92	3.42	0.76	306.09	4.16	1.780

Paper	n	D (mm)	H (mm)	f'_{co} (MPa)	ε_{co} (%)	ε_{lo} (%)	f^*_l (MPa)	f^*_{cc} (MPa)	ε^*_{cc} (%)	ε^*_l (%)	$f_{c,res}$ (MPa)	$\varepsilon_{c,res}$ (%)	$\varepsilon_{l,res}$ (%)
Newman (1979)	1	100	250	73.3	0.2		69.2	325.96	2.95	0.88	322.08	3.33	1.380
Newman (1979)	1	100	250	73.3	0.2		138.2	483.65	4.82*	0.46	478.71	5.08*	0.520
Newman (1979)	1	100	250	73.3	0.2		138.2	491.62	4.9*	0.48	480.92	6.25*	2.520
Newman (1979)	1	100	250	23.23	0.173		3.5	38.56	1.441	0.864	36.67	1.635	1.050
Newman (1979)	1	100	250	23.23	0.173		6.8	52.17	2.082	1.194	50.48	2.528	2.236
Newman (1979)	1	100	250	23.23	0.173		13.7	77.09	3.754	1.948	73.77	6.124*	4.330
Newman (1979)	1	100	250	23.23	0.173		22.6	114.31	5.635	2.132	109.49	6.465*	3.672
Newman (1979)	1	100	250	23.23	0.173		34.9	152.91	6.372	2.314	149.82	7.224*	3.910
Newman (1979)	1	100	250	23.23	0.173		69.2	261.16	8.977*	5.176	257.13	9.347*	5.716
Newman (1979)	1	100	250	23.23	0.173		138.2	462.20	11.705*	5.652	453.58	14.089*	7.502
Lahlou et al. (1992)	2	52	104	46	0.27	0.1	7.6	84	0.94	0.44	80.3	1.48	0.99
Lahlou et al. (1992)	2	52	104	46	0.27	0.1	22	133	2.3	0.73	132.4	2.34*	0.73
Lahlou et al. (1992)	2	52	104	78	0.32	0.23	7.6	119	0.7	0.29	110.7*	1.03	0.99
Lahlou et al. (1992)	2	52	104	78	0.32	0.23	22	169	1.54	0.65	168.5	1.3*	0.55
Lahlou et al. (1992)	2	52	104	113	0.31	0.26	7.6	156	0.57	0.29	147.1*	0.73	0.74
Lahlou et al. (1992)	2	52	104	113	0.31	0.26	22	211	0.99	0.41	199.4	1.29*	0.83
Lu and Hsu (2007)	1	100	200	67	0.251	0.1	3.5	84.9	0.466	0.217	78.71	0.613	0.474
Lu and Hsu (2007)	1	100	200	67	0.251	0.1	7	99.0	0.776	0.361	78.53	1.864	1.516
Lu and Hsu (2007)	1	100	200	67	0.251	0.1	14	130.7	1.237	0.521	120.86	2.226	1.306
Lu and Hsu (2007)	1	100	200	67	0.251	0.1	14	132.7	1.250	0.531			
Lu and Hsu (2007)	1	100	200	67	0.251	0.1	14	134.9	1.350	0.531			
Lu and Hsu (2007)	1	100	200	67	0.251	0.1	14	135.5	1.370	0.531			
Lu and Hsu (2007)	1	100	200	67	0.251	0.1	21	154.0	1.661	0.574			
Lu and Hsu (2007)	1	100	200	67	0.251	0.1	21	157.1	1.830	0.717			
Lu and Hsu (2007)	1	100	200	67	0.251	0.1	21	161.2	1.940	0.717			
Lu and Hsu (2007)	1	100	200	67	0.251	0.1	28	180.2	2.501	0.868	165.76	4.490	2.230
Lu and Hsu (2007)	1	100	200	67	0.251	0.1	28	179.9	2.409	0.887			
Lu and Hsu (2007)	1	100	200	67	0.251	0.1	42	229.1	3.213	1.108	221.65	4.648	2.234
Lu and Hsu (2007)	1	100	200	67	0.251	0.1	56	276.0	4.058	1.238	267.95	5.775	2.366
Richart et al. (1928)	1	101.6	203.2	17.8			2.1	30.7	1.71*	1.02			
Richart et al. (1928)	1	101.6	203.2	17.8			1.2	24.8	2.96*	1.07			
Richart et al. (1928)	1	101.6	203.2	17.8			1.2	22.3	0.95	0.79			
Richart et al. (1928)	1	101.6	203.2	17.8			1.2	19.6					
Richart et al. (1928)	1	101.6	203.2	17.8			3.8	34.3	2.61*	0.80			
Richart et al. (1928)	1	101.6	203.2	17.8			3.8	38.7	1.94*	2.08*			
Richart et al. (1928)	1	101.6	203.2	17.8			3.8	35.8	2.35*	1.56			
Richart et al. (1928)	1	101.6	203.2	17.8			3.8	33.9	4.40*	2.05			
Richart et al. (1928)	1	101.6	203.2	17.8			6.1	46.8	1.7	0.82			
Richart et al. (1928)	1	101.6	203.2	17.8			5.4	48.9	3.64*	1.64			
Richart et al. (1928)	1	101.6	203.2	17.8			5.4	42.4	3.17*	1.14			
Richart et al. (1928)	1	101.6	203.2	17.8			5.4	41.9	4.38*	1.61			
Richart et al. (1928)	1	101.6	203.2	17.8			7.5	52.8	2.2	0.59			
Richart et al. (1928)	1	101.6	203.2	17.8			7.5	52.7	3.48*	1.62			
Richart et al. (1928)	1	101.6	203.2	17.8			7.5	50.7	6.10*	2.46			
Richart et al. (1928)	1	101.6	203.2	17.8			7.5	49.4	5.38*	2.33			
Richart et al. (1928)	1	101.6	203.2	17.8			10.4	63.5	4.37*	1.25			
Richart et al. (1928)	1	101.6	203.2	17.8			10.4	61.4	5.12*	1.82			
Richart et al. (1928)	1	101.6	203.2	17.8			10.4	39.4*					
Richart et al. (1928)	1	101.6	203.2	17.8			10.4	61.2	6.5*	2.05			
Richart et al. (1928)	1	101.6	203.2	17.8			13.9	79.3	4.97*	2.00			
Richart et al. (1928)	1	101.6	203.2	17.8			13.9	71.0	3.06	1.10			
Richart et al. (1928)	1	101.6	203.2	17.8			13.9	73.4	5.32*	1.90			
Richart et al. (1928)	1	101.6	203.2	17.8			13.9	72.7	6.11*	1.85			
Richart et al. (1928)	1	101.6	203.2	17.8			20.8	87.6					
Richart et al. (1928)	1	101.6	203.2	17.8			20.8	100.7	5.22	1.60			
Richart et al. (1928)	1	101.6	203.2	17.8			20.8	97.2	5.26	2.02			
Richart et al. (1928)	1	101.6	203.2	17.8			20.8	97.1	5.22	1.90			
Richart et al. (1928)	1	101.6	203.2	17.8			25.9	119.3	4.46	1.54			
Richart et al. (1928)	1	101.6	203.2	17.8			28.2	122.4	5.28	1.69			
Richart et al. (1928)	1	101.6	203.2	17.8			28.2	121.7					
Richart et al. (1928)	1	101.6	203.2	17.8			28.2	121.3	7.12	2.02			
Richart et al. (1928)	1	101.6	203.2	25.2			3.8	46.9	3.15*	1.92			
Richart et al. (1928)	1	101.6	203.2	25.2			3.8	47.0	3.16*	1.69			
Richart et al. (1928)	1	101.6	203.2	25.2			3.8	47.1	2.78*	1.59			
Richart et al. (1928)	1	101.6	203.2	25.2			3.8	45.7	3.16*	1.37			
Richart et al. (1928)	1	101.6	203.2	25.2			7.5	58.4	1.98	1.05			
Richart et al. (1928)	1	101.6	203.2	25.2			7.5	57.2	2.77*	0.68			
Richart et al. (1928)	1	101.6	203.2	25.2			7.5	60.2	2.97*	1.23			
Richart et al. (1928)	1	101.6	203.2	25.2			7.5	62.0	5.97*	1.95			
Richart et al. (1928)	1	101.6	203.2	25.2			13.9	83.7	2.96	1.02			
Richart et al. (1928)	1	101.6	203.2	25.2			13.9	87.9	3.18	1.46			
Richart et al. (1928)	1	101.6	203.2	25.2			13.9	81.5	5.68*	1.85			
Richart et al. (1928)	1	101.6	203.2	25.2			13.9	82.0	4.75*	1.80			
Richart et al. (1928)	1	101.6	203.2	25.2			28.2	133.1					
Richart et al. (1928)	1	101.6	203.2	25.2			28.2	135.1	4.39	1.59			
Richart et al. (1928)	1	101.6	203.2	25.2			28.2	131.0	6.68	1.95			
Richart et al. (1928)	1	101.6	203.2	25.2			28.2	129.3	6.14	1.72			
Richart et al. (1928)	1	101.6	203.2	7.2			3.8	20.0					
Richart et al. (1928)	1	101.6	203.2	7.2			3.8	29.2	5.56*	2.30			
Richart et al. (1928)	1	101.6	203.2	7.2			3.8	27.4					
Richart et al. (1928)	1	101.6	203.2	7.2			3.8	26.5	6.20*	2.25			
Richart et al. (1928)	1	101.6	203.2	7.2			7.5	43.4	6.52*	1.41			
Richart et al. (1928)	1	101.6	203.2	7.2			7.5	43.6	3.56	1.64			
Richart et al. (1928)	1	101.6	203.2	7.2			7.5	43.4	6.58*	1.72			
Richart et al. (1928)	1	101.6	203.2	7.2			7.5	42.2	5.58*	1.23			

Paper	n	D (mm)	H (mm)	f'_{co} (MPa)	ε_{co} (%)	ε_{lo} (%)	f^*_l (MPa)	f^*_{cc} (MPa)	ε^*_{cc} (%)	ε^*_l (%)	$f_{c,res}$ (MPa)	$\varepsilon_{c,res}$ (%)	$\varepsilon_{l,res}$ (%)
Richart et al. (1928)	1	101.6	203.2	7.2			13.9	70.2	5.34*	1.98			
Richart et al. (1928)	1	101.6	203.2	7.2			13.9	69.3	5.94*	1.95			
Richart et al. (1928)	1	101.6	203.2	7.2			13.9	51.7					
Richart et al. (1928)	1	101.6	203.2	7.2			13.9	71.0					
Richart et al. (1928)	1	101.6	203.2	7.2			28.2	118.9					
Richart et al. (1928)	1	101.6	203.2	7.2			28.2	118.2	5.36*	2.02			
Richart et al. (1928)	1	101.6	203.2	7.2			28.2	123.1	6.96*	1.95			
Richart et al. (1928)	1	101.6	203.2	7.2			28.2	120.7					
Richart et al. (1928)	1	101.6	203.2	7.2			45.2	169.6	7.80*	2.00			
Rutland and Wang (1997)	1	50	100	39.4			1.7	56.6					
Rutland and Wang (1997)	1	50	100	39.4			1.7	61.9					
Rutland and Wang (1997)	1	50	100	39.4			3.5	56.6					
Rutland and Wang (1997)	1	50	100	39.4			3.5	60.2					
Rutland and Wang (1997)	1	50	100	39.4			3.5	78.3					
Rutland and Wang (1997)	1	50	100	39.4			3.5	81.0					
Rutland and Wang (1997)	1	50	100	39.4			3.5	83.6					
Rutland and Wang (1997)	1	50	100	39.4			7	73.9					
Rutland and Wang (1997)	1	50	100	39.4			7	95.6					
Rutland and Wang (1997)	1	50	100	39.4			7	98.2					
Rutland and Wang (1997)	1	50	100	39.4			14	119.0					
Rutland and Wang (1997)	1	50	100	39.4			14	120.8					
Rutland and Wang (1997)	1	50	100	39.4			14	131.0					
Rutland and Wang (1997)	1	50	100	39.4			28	141.6					
Rutland and Wang (1997)	1	50	100	39.4			28	161.5					
Rutland and Wang (1997)	1	50	100	39.4			28	167.3					
Rutland and Wang (1997)	1	50	100	39.4			28	188.1					
Rutland and Wang (1997)	1	50	100	39.4			42	206.6					
Rutland and Wang (1997)	1	50	100	39.4			42	211.1					
Rutland and Wang (1997)	1	50	100	39.4			42	213.7					
Rutland and Wang (1997)	1	50	100	39.4			42	219.5					
Rutland and Wang (1997)	1	50	100	39.4			56	248.7					
Rutland and Wang (1997)	1	50	100	39.4			56	267.7					
Rutland and Wang (1997)	1	50	100	39.4			1.7	59.7					
Rutland and Wang (1997)	1	50	100	39.4			3.5	74.3					
Rutland and Wang (1997)	1	50	100	39.4			3.5	77.0					
Rutland and Wang (1997)	1	50	100	39.4			3.5	61.9					
Rutland and Wang (1997)	1	50	100	39.4			3.5	70.8					
Rutland and Wang (1997)	1	50	100	39.4			7	79.6					
Rutland and Wang (1997)	1	50	100	39.4			7	96.9					
Rutland and Wang (1997)	1	50	100	39.4			14	61.1*					
Rutland and Wang (1997)	1	50	100	39.4			14	106.2					
Rutland and Wang (1997)	1	50	100	39.4			14	110.6					
Rutland and Wang (1997)	1	50	100	39.4			14	115.0					
Rutland and Wang (1997)	1	50	100	39.4			14	101.8					
Rutland and Wang (1997)	1	50	100	39.4			28	131.0					
Rutland and Wang (1997)	1	50	100	39.4			28	158.0					
Rutland and Wang (1997)	1	50	100	39.4			42	203.5					
Rutland and Wang (1997)	1	50	100	39.4			56	259.3					
Rutland and Wang (1997)	1	50	100	39.4			1.7	61.1					
Rutland and Wang (1997)	1	50	100	39.4			1.7	65.5					
Rutland and Wang (1997)	1	50	100	39.4			3.5	71.7					
Rutland and Wang (1997)	1	50	100	39.4			3.5	77.9					
Rutland and Wang (1997)	1	50	100	39.4			7	86.3					
Rutland and Wang (1997)	1	50	100	39.4			7	82.7					
Rutland and Wang (1997)	1	50	100	39.4			14	109.3					
Rutland and Wang (1997)	1	50	100	39.4			42	167.3					
Rutland and Wang (1997)	1	50	100	39.4			42	150.0					
Setunge et al. (1993)	1	100	200	108			5	144					
Setunge et al. (1993)	1	100	200	108			10	172					
Setunge et al. (1993)	1	100	200	108			15	194					
Setunge et al. (1993)	1	100	200	102			5	145					
Setunge et al. (1993)	1	100	200	102			10	158					
Setunge et al. (1993)	1	100	200	102			15	175					
Setunge et al. (1993)	1	100	200	96			5	125					
Setunge et al. (1993)	1	100	200	96			10	147					
Setunge et al. (1993)	1	100	200	96			15	163					
Setunge et al. (1993)	1	100	200	96			5	117					
Setunge et al. (1993)	1	100	200	96			10	144					
Setunge et al. (1993)	1	100	200	96			15	151					
Sfer et al. (2002)	1	150	300	35.8	0.2		1.5	45.5	0.26	0.11	33.7	0.50	0.44
Sfer et al. (2002)	1	150	300	35.8	0.2		1.5	47.8	0.34	0.09	30.1	1.18	2.44
Sfer et al. (2002)	1	150	300	35.8	0.2		4.5	55.3	0.41	0.19	38.8	1.44	2.02
Sfer et al. (2002)	1	150	300	35.8	0.2		4.5	58.2	0.52	0.14	41.9	1.94	2.02
Sfer et al. (2002)	1	150	300	35.8	0.2		9	65.7	0.83	0.23	57.8	2.27	1.21
Sfer et al. (2002)	1	150	300	35.8	0.2		9	66.5	0.63	0.25	57.2	2.34	2.56
Sfer et al. (2002)	1	150	300	35.8	0.2		30	124.5	7.00*	3.23	120.8	8.17*	3.98
Sfer et al. (2002)	1	150	300	35.8	0.2		30	129.3	10.90*		127.5	9.85*	
Sfer et al. (2002)	1	150	300	35.8	0.2		60	192.9	8.50	3.23	192.6	7.33	
Sfer et al. (2002)	1	150	300	35.8	0.2		60	205.1	8.30		202.9	8.75	
Smith et al. (1989)	1	54	108	22.1	0.339		0.69	28.08	0.531	0.182	13.68	3.953*	4.074
Smith et al. (1989)	1	54	108	22.1	0.339		3.45	36.11	2.085*	0.842	32.70	2.783	1.306
Smith et al. (1989)	1	54	108	22.1	0.339		13.79	85.44	2.864*	0.318	85.41	2.864*	0.318
Smith et al. (1989)	1	54	108	34.5	0.351		0.69	41.73	0.397	0.164	16.38	2.375*	3.064
Smith et al. (1989)	1	54	108	34.5	0.351		3.45	57.81	0.838	0.532	39.70	2.651	3.576
Smith et al. (1989)	1	54	108	34.5	0.351		6.89	78.21	1.158	0.788	56.05	2.698	3.578

Paper	n	D (mm)	H (mm)	f'_{co} (MPa)	ε_{co} (%)	ε_{lo} (%)	f^*_l (MPa)	f^*_{cc} (MPa)	ε^*_{cc} (%)	ε^*_l (%)	$f_{c,res}$ (MPa)	$\varepsilon_{c,res}$ (%)	$\varepsilon_{l,res}$ (%)
Smith et al. (1989)	1	54	108	34.5	0.351		13.79	107.58	2.234	1.110	90.51	3.548	3.256
Smith et al. (1989)	1	54	108	34.5	0.351		20.70	130.15	2.952	1.620	123.75	3.431*	2.582
Smith et al. (1989)	1	54	108	34.5	0.351		27.58	159.52	3.306	1.778	152.32	3.306*	1.778
Smith et al. (1989)	1	54	108	34.5	0.351		34.47	170.03	3.128*	0.870	166.30	3.128*	0.870
Smith et al. (1989)	1	54	108	44.1	0.354		0.69	57.39	0.338	0.436	24.20	1.284*	2.394
Smith et al. (1989)	1	54	108	44.1	0.354		3.45	88.04	0.616	0.714	54.59	1.634	2.756
Smith et al. (1989)	1	54	108	44.1	0.354		6.89	113.93	0.811	0.968	96.13	1.365*	2.542
Smith et al. (1989)	1	54	108	44.1	0.354		13.79	131.45	1.153	0.774	126.11	1.171*	0.804
Smith et al. (1989)	1	54	108	44.1	0.354		27.58	167.87	1.078*	0.400	165.94	1.078*	0.400
Smith et al. (1989)	1	54	108	44.1	0.354		34.47	167.87	1.078*	0.400	165.94	1.078*	0.400
Tan and Sun (2004)	1	100	300	51.8	0.24		1.9	64.8	0.33				
Tan and Sun (2004)	1	100	300	51.8	0.24		1.9	66.0	0.39				
Tan and Sun (2004)	1	100	300	51.8	0.24		7.5	86.6	0.46				
Tan and Sun (2004)	1	100	300	51.8	0.28		7.5	84.2	0.49*				
Tan and Sun (2004)	1	100	300	51.8	0.24		12.5	99.3	0.49*				
Tan and Sun (2004)	1	100	300	51.8	0.24		12.5	103.3	0.66*				
Vu et al. (2009)	1	70	140	41.15			50	174.90	2.544*	0.466	154.354	7.568*	3.366
Vu et al. (2009)	1	70	140	41.15			100	248.97	5.419*	0.908	246.927	5.675*	1.126
Vu et al. (2009)	1	70	140	41.15			200	446.50	8.498*	1.386	428.704	8.498*	1.384
Vu et al. (2009)	1	70	140	41.15			400	779.84	11.890*		779.835	11.890*	
Vu et al. (2009)	1	70	140	41.15			650	868.31	7.592*	2.486	868.171	7.592*	2.486
Xie et al. (1995)	1	55.5	110	60.2	0.37		0.84	58.39*	0.70		29.08	3.00*	
Xie et al. (1995)	1	55.5	110	60.2	0.37		2.29	80.61	0.53		42.32	2.54*	
Xie et al. (1995)	1	55.5	110	60.2	0.37		5.30	97.58	0.75		58.82	2.96*	
Xie et al. (1995)	1	55.5	110	60.2	0.37		8.31	107.64	0.98		78.20	2.94	
Xie et al. (1995)	1	55.5	110	60.2	0.37		11.32	121.60	1.08		95.42	3.43	
Xie et al. (1995)	1	55.5	110	60.2	0.37		14.33	136.83	1.38		111.91	3.13	
Xie et al. (1995)	1	55.5	110	60.2	0.37		20.29	156.88	2.12		141.11	3.24	
Xie et al. (1995)	1	55.5	110	60.2	0.37		23.30	172.05	2.08		153.51	3.18*	
Xie et al. (1995)	1	55.5	110	60.2	0.37		29.32	193.24	2.37		177.59	3.22*	
Xie et al. (1995)	1	55.5	110	92.21	0.37		3.78	129.36	0.62		60.58	3.45*	
Xie et al. (1995)	1	55.5	110	92.21	0.37		8.30	155.63	0.80		85.93	3.90*	
Xie et al. (1995)	1	55.5	110	92.21	0.37		12.82	181.17	1.06		111.10	3.80*	
Xie et al. (1995)	1	55.5	110	92.21	0.37		16.5	199.80	1.17		137.01	3.77	
Xie et al. (1995)	1	55.5	110	92.21	0.37		17.33	194.27	1.16		150.01	3.71	
Xie et al. (1995)	1	55.5	110	92.21	0.37		21.85	208.74	1.31		167.99	3.95	
Xie et al. (1995)	1	55.5	110	92.21	0.37		26.28	234.65	1.55		187.81	4.19	
Xie et al. (1995)	1	55.5	110	92.21	0.37		35.5	261.11	2.42		225.89	4.03	
Xie et al. (1995)	1	55.5	110	92.21	0.37		44.44	293.47	2.49		262.77	4.10	
Xie et al. (1995)	1	55.5	110	119	0.37		6.07	172.31	0.67		74.97	3.93*	
Xie et al. (1995)	1	55.5	110	119	0.37		12.02	212.18	0.79		113.76	4.02*	
Xie et al. (1995)	1	55.5	110	119	0.37		17.97	225.86	1.02		143.16	3.98*	
Xie et al. (1995)	1	55.5	110	119	0.37		24.04	250.97	1.13		173.26	4.28*	
Xie et al. (1995)	1	55.5	110	119	0.37		29.99	261.80	1.32		195.76	4.29	
Xie et al. (1995)	1	55.5	110	119	0.37		36.06	280.96	1.43		228.84	4.59	
Xie et al. (1995)	1	55.5	110	119	0.37		47.96	316.30	1.61		285.84	3.93	
Xie et al. (1995)	1	55.5	110	119	0.37		59.98	367.35	2.44		330.82	4.58	

* denotes inconsistent data when compared with overall trend in the database (data excluded from the calibration of the proposed model)

Statement of Authorship

Title of Paper	Hoop Strains in FRP-Confined Concrete Columns: Experimental Observations
Publication Status	◉ Published ○ Accepted for Publication ○ Submitted for Publication ○ Publication Style
Publication Details	Materials and Structures, Doi: 10.1617/s11527-014-0358-8, Year 2014

Author Contributions

By signing the Statement of Authorship, each author certifies that their stated contribution to the publication is accurate and that permission is granted for the publication to be included in the candidate's thesis.

Name of Principal Author (Candidate)	Mr. Jian Chin Lim		
Contribution to the Paper	Preparation of experiment, analysis of test results, and preparation of manuscript		
Signature		Date	23/02/2015

Name of Co-Author	Dr. Togay Ozbakkaloglu		
Contribution to the Paper	Research supervision and review of manuscript		
Signature		Date	23/02/2015

THIS PAGE HAS BEEN LEFT INTENTIONALLY BLANK

HOOP STRAINS IN FRP-CONFINED CONCRETE COLUMNS: EXPERIMENTAL OBSERVATIONS

Jian C. Lim and Togay Ozbakkaloglu

ABSTRACT

It is now well understood that the hoop rupture strain of fiber reinforced polymer (FRP) jackets confining concrete is often lower than the ultimate tensile strain of the component fibers. This paper presents the results of an experimental study designed specifically to investigate the two newly identified material dependent factors influencing the hoop strain efficiency of FRP jackets. 36 circular FRP-confined normal and high-strength concrete (NSC and HSC) specimens were tested under axial compression. The results indicate that the hoop rupture strains of FRP jackets decrease with either an increase in the strength of the unconfined concrete or the elastic modulus of the fiber material. These observations were verified by additional results from a large FRP-confined concrete test database assembled from the published literature. In addition, the hoop strain-axial strain relationship of FRP-confined concrete was studied and the influence of the test parameters on the behavior was established. The findings from these investigations are presented together with an expression for the prediction of the strain reduction factor and a model to describe the hoop strain-axial strain relationship.

KEYWORDS: Fiber reinforced polymer (FRP); Concrete; High-strength concrete (HSC); Confinement; Compression; Hoop rupture strain; Stress-strain relationships; Ultimate condition.

1. INTRODUCTION

As demonstrated in a recent review study [1], extensive research on the use of fiber reinforced polymer (FRP) composites as a confinement material for concrete columns has led to a good understanding of the compressive behavior of FRP-confined concrete [2-5]. It is now well established that accurate determination of the hoop rupture strain developed by the confining FRP jacket is essential for the accurate prediction of the ultimate axial stress and strain of FRP-confined concrete. Research has shown that the ultimate material tensile strain of fibers is unachievable in the in-situ form of an FRP jacket, and the lower observed efficiency has led to the development of a range of strain reduction factors to establish the actual hoop rupture strain of the FRP jacket [6-9].

A number of factors contributing to lower efficiency in FRP jackets have been identified in previous studies [3, 5, 6, 8, 10-20], which include: (i) the differences between FRP jackets and flat coupons as a result of differences in fabrication processes and in-situ forms; (ii) the differences in methods of measurement and testing; and (iii) other factors, such as the quality of workmanship, geometric imperfections, residual strains, presence of an overlap region, and curvature and multiaxial stress state of the FRP jacket. However, the attention of the majority of the previous studies focused on the influences relating to specimen fabrication and testing, and the material dependent influences, such as the strength of concrete and the type of FRP material, have been brought to attention by only a few recent studies [9, 21-27]. Indeed, as was reported in Wu and Jiang [5], the strain reduction factors recommended in the past vary substantially from 0.274 to 1.133 [5-8, 12, 14, 19, 20, 28-41], indicating that additional targeted investigations are required to gain clearer insights into the hoop rupture strain efficiency of FRP jackets.

To this end, this paper presents the results of the first-ever experimental study that was aimed at closely examining the influences of the concrete strength and type of FRP material on the hoop strain efficiency of FRP jackets. The results of the experimental study are presented together with additional 357 test results of FRP-confined concrete collated from the published literature and previously reported in Refs. [9, 27], which further reinforced the key observations of the present study.

2. EXPERIMENTAL PROGRAM

2.1 Test Specimens and Materials

Thirty-six FRP-confined concrete specimens were manufactured and tested under monotonic axial compression. All of the specimens were 152 mm in diameter and 305 mm in height. To fabricate the specimens, FRP tubes were first manufactured from either carbon, S-glass or aramid fiber sheets using manual wet-layup techniques, which involved wrapping epoxy resin impregnated fiber sheets around polystyrene forms in the hoop direction. The tubes were fabricated with 1 to 4 layers of fiber sheets, using a single continuous sheet which terminated with an overlap region of 150 mm. The top and bottom ends of the tubes were strengthened with one additional layer of 50 mm wide fiber sheets to constrain the location of FRP rupture to the middle section of the tubes.

The properties of the unidirectional fiber sheets used for tube fabrications are provided in Table 1. Flat coupon tests were used to determine the tensile properties of the FRP composite jackets, where the loading was applied in accordance with ASTM D 3039 [42]. For each type of fiber, three 1 mm thick and 25 mm wide FRP flat coupon specimens were made in a high-precision mould with three layers of fiber sheets using the wet layup technique. The nominal dry fiber thicknesses of the CFRP, GFRP, and AFRP coupons were 0.495, 0.600, and 0.600 mm, respectively. The coupons had a 138 mm clear span with each end bonded with two 0.5 mm by 85 mm long aluminum tabs for stress transfer during tensile tests. Each coupon was instrumented with two 20 mm strain gauges at mid-height, with one on each side, for the measurement of the longitudinal strains. The coupons were allowed to cure in the laboratory for at least seven days prior to testing. After curing, the unidirectional fiber configuration was confirmed through examination of the slopes of fibers. The coupon specimens were tested using a screw-driven tensile test machine with a peak capacity of 200 kN. The load was applied at a constant cross-head movement rate of 0.03 mm per second. The test results from the flat coupon specimens, calculated based on nominal dry fiber thicknesses and actual coupon widths, are reported in Table 1, together with the manufacturer supplied properties of fibers and epoxy. The average rupture strain obtained from the tensile coupon tests was slightly lower than that reported by the manufacturer.

The pre-fabricated FRP tubes were filled with four different concrete mixtures having target strengths of 25, 50, 75, and 100 MPa. Details of these mixtures are given in Table 2. Crushed bluestone gravel with a maximum nominal size of 10 mm and graded sand were used as the aggregate. Changes in the strength of unconfined concrete were monitored by compression tests of 100 mm cylinders conducted throughout the testing program.

Table 2. Concrete mix proportions

Batch	B25	B50	B75	B100
Cement (kg/m^3)	350	380	450	494
Silica fume (kg/m^3)	0	0	39	43
Sand (kg/m^3)	660	710	712	712
Gravel (kg/m^3)	1000	1065	1067	1067
Water (kg/m^3)	255	209	163	135
Superplasticiser (kg/m^3)	0	0	10	20
Water-binder ratio	0.67	0.55	0.35	0.28
28-day strength* (MPa)	27.5	44.0	65.2	93.1
Test-day strength (MPa)	29.6	49.6	74.1	98.0

* based on compression tests of 100 mm concrete cylinders

2.2 Specimen Designation

The details and the test results of the FRP-confined specimens are given in Table 3. In the specimen designations in Table 3, letters are used to represent the test parameters: B for concrete batch, FRP for type of FRP material, and L for number of FRP layers. Letters B and L were followed by a number that was used to represent the value of that particular parameter for a given specimen. Finally, the last number in the specimen designation (i.e. 1, 2, or 3) was used to make a distinction between the nominally identical specimens. For instance, B25-CFRP-L1-1 is the first of the three identical specimens that were cast from a concrete mix with 25 MPa target strength in an FRP jacket made of 1 layer of carbon fibers.

2.3 Instrumentation and Testing

Axial deformations of the specimens were measured with four linear variable displacement transducers (LVDTs), which were mounted at the corners between the loading and supporting steel plates of the compression test machine as shown in Figure 1. The recorded deformations were used in the calculation of the average axial strains along the height of the specimens. In addition, four LVDTs with a gauge length of 170 mm were placed at mid-height at 90° spacing along the circumference of the specimens. These mid-height LVDTs were used to correct the measurements of the platen-mounted full-height LVDTs at the early stages of loading, where additional displacements due to closure of the gaps in the setup were also recorded by the full-height LVDTs. As illustrated in Figure 2, the hoop strains were measured by 12 unidirectional strain gauges 5 mm in gauge length that were bonded to the FRP at mid-height at 30° equal spacing along the circumference. Three of these strain gauges were located on the 150 mm overlap region of FRP and the remaining nine were located outside the overlap region.

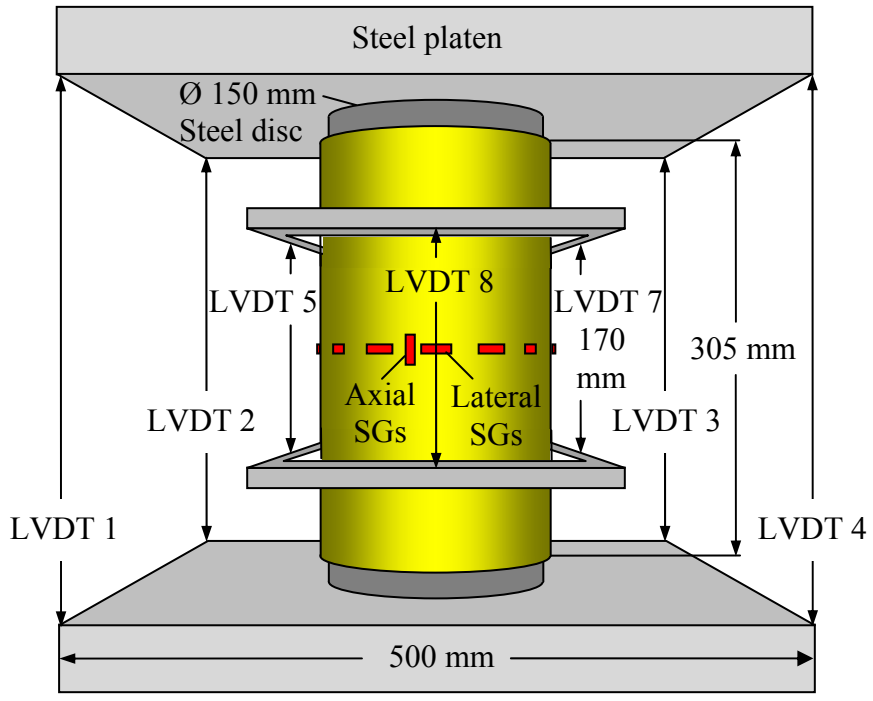

Figure 1. Test setup and instrumentation

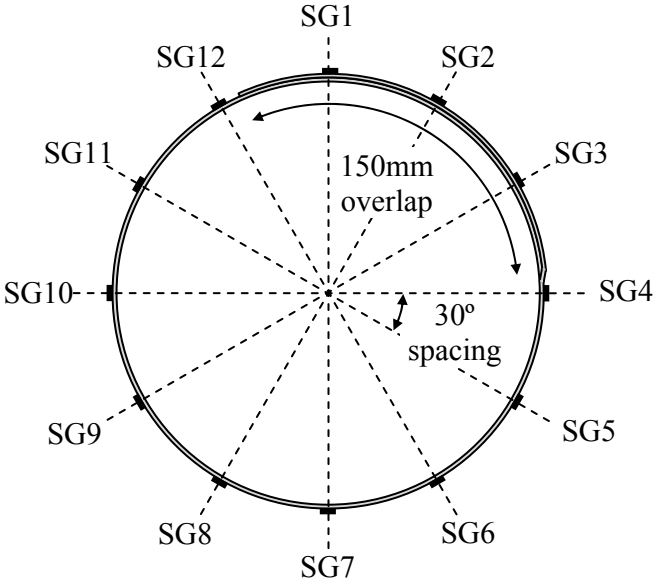

Figure 2. Strain gauge arrangement

The specimens were tested under axial compression using a 5000-kN capacity universal testing machine. During the initial elastic stage of specimen behavior, the loading was applied with a load control of 5 kN per second. Once initial softening had taken place, displacement control was used at approximately 0.003 mm per second until specimen failure. Prior to testing, the specimens were capped at both ends to ensure uniform distribution of the applied pressure, and the load was applied directly to the concrete core through the use of precision-cut high-strength steel discs.

3. TEST RESULTS AND DISCUSSIONS

Figures 3(a) to 3(c) show the axial stress-axial strain and axial stress-hoop strain curves of the AFRP, CFRP, and GFRP-confined specimens, respectively. The summary of the test results of the specimens is presented in Tables 3 and 4. Table 3 provides: the compressive strength of the unconfined concrete (f'_{co}); compressive strength and ultimate axial strain of confined concrete (f'_{cc} and ε_{cu}); maximum, minimum and average hoop strains recorded on the FRP jackets at ultimate ($\varepsilon_{h,max}$, $\varepsilon_{h,min}$, $\varepsilon_{h,ave}$); strain localization factor ($k_{\varepsilon 1}$); in-situ factor ($k_{\varepsilon 2}$); FRP-to-fiber strain ratio ($k_{\varepsilon 3}$); and strain reduction factor ($k_{\varepsilon,f}$). The compressive strengths of specimens (f'_{cc}) were calculated from the recorded axial loads at the ultimate condition. The full-height LVDTs were used in the calculation of ultimate axial strains (ε_{cu}). $\varepsilon_{h,max}$, $\varepsilon_{h,min}$ and $\varepsilon_{h,ave}$ were determined from the values recorded by the nine strain gauges located outside the overlap region of the FRP jackets. $k_{\varepsilon 1}$ was calculated as the ratio of $\varepsilon_{h,ave}/\varepsilon_{h,max}$, $k_{\varepsilon 2}$ as the ratio of $\varepsilon_{h,max}/\varepsilon_{frp}$, and $k_{\varepsilon 3}$ as the ratio of $\varepsilon_{frp}/\varepsilon_f$. The ultimate tensile strains of FRP (ε_{frp}) and fibers (ε_f) are supplied in Table 1, together with the calculated values of $k_{\varepsilon 3}$. The strain reduction factor ($k_{\varepsilon,f}$) is the product of the three individual components ($k_{\varepsilon 1}$, $k_{\varepsilon 2}$, $k_{\varepsilon 3}$) as defined by Eq. 2 later in the paper. Table 4 presents the maximum hoop strains recorded by the individual strain gauges that were placed within and outside the overlap region.

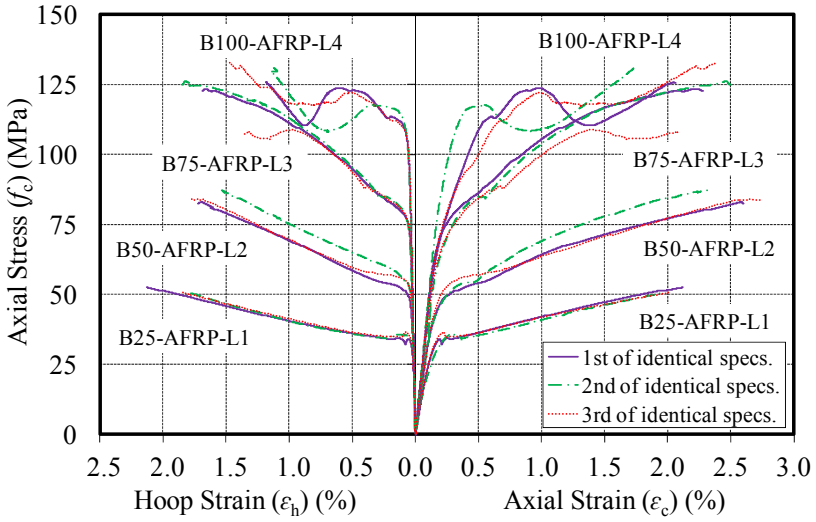

(a)

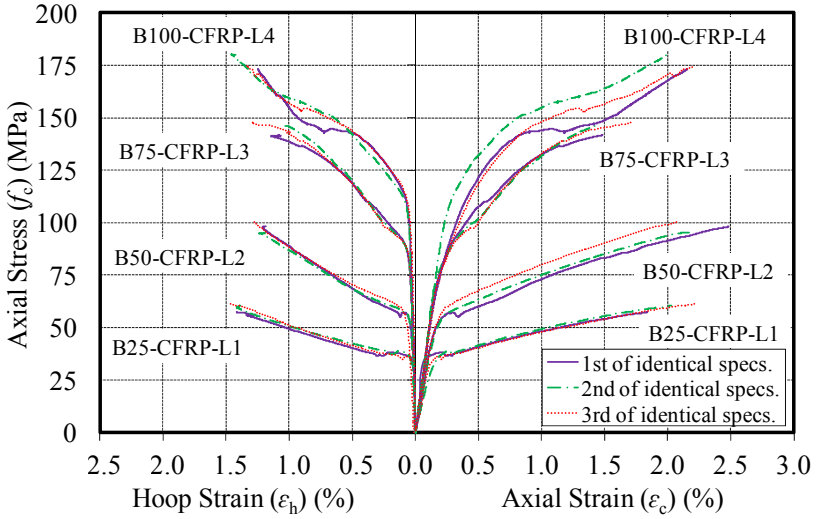

(b)

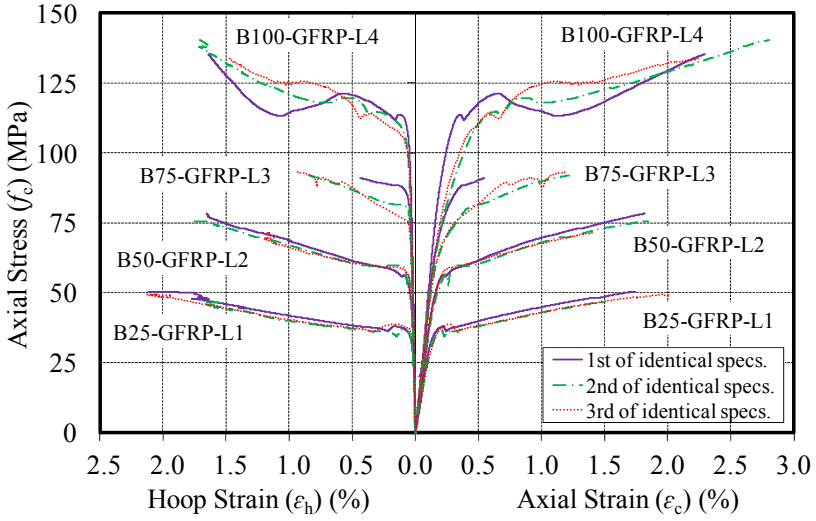

(c)

Figure 3. Stress-strain curves of: (a) AFRP-confined specimens, (b) CFRP-confined specimens, and (c) GFRP-confined specimens

Table 3. Results of compression tests

Specimen	Number of FRP layers	f'_{co} (MPa)	f'_{cc} (MPa)	ε_{cu} (%)	$\varepsilon_{h,max}$ (%)	$\varepsilon_{h,min}$ (%)	$\varepsilon_{h,ave}$ (%)	$k_{\varepsilon 1}$	$k_{\varepsilon 2}$	$k_{\varepsilon,f}$
B25-AFRP-L1-1	1	29.6	52.5	2.12	2.29	1.73	2.13	0.93	1.23	0.97
B25-AFRP-L1-2	1	29.6	50.3	1.95	2.34	1.01	1.88	0.80	1.26	0.85
B25-AFRP-L1-3	1	29.6	50.5	2.01	2.41	1.47	1.84	0.76	1.30	0.84
B25-CFRP-L1-1	1	29.6	57.3	1.84	1.80	0.80	1.52	0.93	0.84	0.85
B25-CFRP-L1-2	1	29.6	60.4	2.03	1.84	0.94	1.52	0.83	0.94	0.84
B25-CFRP-L1-3	1	29.6	61.2	2.23	1.87	0.86	1.50	0.80	0.95	0.83
B25-GFRP-L1-1	1	29.6	50.8	1.82	2.54	1.25	2.00	0.79	0.79	0.57
B25-GFRP-L1-2	1	29.6	46.6	1.51	2.18	0.98	1.89	0.87	0.68	0.54
B25-GFRP-L1-3	1	29.6	49.4	2.02	2.60	1.16	2.00	0.77	0.81	0.57
B50-AFRP-L2-1	2	49.6	83.1	2.60	1.97	1.18	1.80	0.92	1.06	0.82
B50-AFRP-L2-2	2	49.6	87.2	2.32	2.11	1.20	1.80	0.83	1.17	0.82
B50-AFRP-L2-3	2	49.6	84.0	2.75	2.05	0.91	1.77	0.86	1.10	0.81
B50-CFRP-L2-1	2	49.6	98.0	2.48	1.47	0.95	1.22	0.83	0.75	0.68
B50-CFRP-L2-2	2	49.6	95.3	2.17	1.66	0.98	1.33	0.80	0.85	0.74
B50-CFRP-L2-3	2	49.6	100.3	2.07	1.54	0.96	1.36	0.88	0.79	0.76
B50-GFRP-L2-1	2	49.6	78.3	1.82	2.00	1.10	1.59	0.79	0.62	0.45
B50-GFRP-L2-2	2	49.6	75.6	1.85	1.95	1.19	1.69	0.87	0.61	0.48
B50-GFRP-L2-3*	2	49.6	71.4	1.42	1.45	1.01	1.23	0.85	0.45	0.35

Table 3. (continued)

Specimen	Number of FRP layers	f'_{co} (MPa)	f'_{cc} (MPa)	ε_{cu} (%)	$\varepsilon_{h,max}$ (%)	$\varepsilon_{h,min}$ (%)	$\varepsilon_{h,ave}$ (%)	$k_{\varepsilon 1}$	$k_{\varepsilon 2}$	$k_{\varepsilon,f}$
B75-AFRP-L3-1	3	74.1	123.5	2.28	1.93	1.35	1.69	0.88	1.04	0.77
B75-AFRP-L3-2	3	74.1	126.4	2.51	2.12	1.49	1.80	0.85	1.14	0.82
B75-AFRP-L3-3*	3	74.1	108.8	2.09	1.86	0.98	1.35	0.73	1.00	0.61
B75-CFRP-L3-1	3	74.1	141.7	1.49	1.79	0.89	1.17	0.65	0.91	0.65
B75-CFRP-L3-2	3	74.1	146.1	1.47	1.24	0.84	1.03	0.83	0.63	0.57
B75-CFRP-L3-3	3	74.1	147.6	1.71	1.72	0.53	1.29	0.75	0.88	0.72
B75-GFRP-L3-1*	3	74.1	90.8	0.54	0.50	0.30	0.43	0.87	0.16	0.12
B75-GFRP-L3-2*	3	74.1	91.8	1.22	1.04	0.60	0.84	0.81	0.33	0.24
B75-GFRP-L3-3*	3	74.1	93.0	1.21	1.07	0.76	0.93	0.87	0.33	0.27
B100-AFRP-L4-1	4	98.0	125.8	2.06	1.49	0.79	1.19	0.80	0.80	0.54
B100-AFRP-L4-2	4	98.0	130.9	1.73	1.49	0.71	1.17	0.79	0.80	0.53
B100-AFRP-L4-3	4	98.0	132.8	2.39	1.84	0.76	1.47	0.80	0.99	0.67
B100-CFRP-L4-1	4	98.0	173.1	2.16	1.59	0.92	1.20	0.76	0.81	0.67
B100-CFRP-L4-2	4	98.0	180.3	2.03	1.74	1.20	1.48	0.85	0.89	0.82
B100-CFRP-L4-3	4	98.0	174.4	2.20	1.74	1.16	1.34	0.77	0.89	0.74
B100-GFRP-L4-1	4	98.0	135.2	2.29	1.77	1.43	1.64	0.93	0.55	0.47
B100-GFRP-L4-2	4	98.0	140.3	2.80	1.98	1.46	1.74	0.88	0.62	0.50
B100-GFRP-L4-3	4	98.0	133.9	2.40	1.84	1.05	1.54	0.84	0.57	0.44

* denotes prematurely failed specimens

Table 4. Hoop strain distribution at ultimate condition

Specimen	Hoop strain in overlap region (%)				Hoop strains in non-overlap region (%)									
	SG1	SG2	SG3	Average	SG4	SG5	SG6	SG7	SG8	SG9	SG10	SG11	SG12	Average
B25-AFRP-L1-1	1.00	1.07	1.18	1.08	1.73	2.20	2.17	2.26	2.06	2.06	2.29	2.22	2.14	2.13
B25-AFRP-L1-2	0.62	1.12	0.96	0.90	-	2.14	2.34	1.75	1.51	1.68	1.81	1.86	1.93	1.88
B25-AFRP-L1-3	0.97	1.00	1.09	1.02	1.49	1.84	2.22	2.41	2.14	1.53	1.68	1.81	1.47	1.84
B25-CFRP-L1-1	0.39	0.76	0.88	0.68	-	-	-	1.64	1.48	1.45	1.35	1.61	1.60	1.52
B25-CFRP-L1-2	0.36	0.83	0.81	0.67	-	1.44	1.41	1.39	1.57	1.16	1.67	1.84	1.67	1.52
B25-CFRP-L1-3	0.76	0.92	0.84	0.84	-	1.87	1.15	1.47	1.37	1.73	1.31	1.54	1.55	1.50
B25-GFRP-L1-1	1.18	0.93	1.75	1.29	-	-	2.20	1.80	2.07	1.48	2.02	1.89	2.54	2.00
B25-GFRP-L1-2	1.19	1.19	0.91	1.09	-	1.67	1.92	-	1.76	2.18	2.00	1.92	1.78	1.89
B25-GFRP-L1-3	1.45	1.28	1.20	1.31	1.54	2.22	1.66	2.13	2.10	1.16	2.60	2.16	2.41	2.00
B50-AFRP-L2-1	-	0.96	1.11	1.04	-	1.60	1.87	-	1.88	1.90	1.97	1.75	1.65	1.80
B50-AFRP-L2-2	1.25	1.36	1.20	1.27	1.83	2.17	1.79	1.90	1.70	1.31	2.11	1.56	-	1.80
B50-AFRP-L2-3	0.46	1.31	1.35	1.04	1.52	1.82	1.97	2.05	-	1.71	1.83	1.54	1.73	1.77
B50-CFRP-L2-1	0.44	0.94	0.91	0.76	-	1.24	1.47	1.17	1.25	0.95	0.97	1.47	1.20	1.22
B50-CFRP-L2-2	0.69	0.83	0.70	0.74	-	1.26	1.16	1.30	1.48	1.19	1.28	1.66	-	1.33
B50-CFRP-L2-3	0.54	0.79	0.84	0.72	-	-	1.37	1.50	1.54	1.33	1.25	1.28	1.26	1.36
B50-GFRP-L2-1	0.84	1.24	1.31	1.13	1.54	1.67	2.00	1.92	1.22	1.42	1.68	1.10	1.74	1.59
B50-GFRP-L2-2	0.70	1.28	1.11	1.03	1.32	1.72	1.81	1.83	1.87	1.95	1.79	1.19	1.71	1.69
B50-GFRP-L2-3*	0.54	0.88	0.92	0.78	1.01	1.45	1.28	1.28	1.06	1.09	1.38	1.20	1.29	1.23

Table 4. (continued)

Specimen	Hoop strain in overlap region (%)				Hoop strains in non-overlap region (%)									
	SG1	SG2	SG3	Average	SG4	SG5	SG6	SG7	SG8	SG9	SG10	SG11	SG12	Average
B75-AFRP-L3-1	0.56	1.16	1.46	1.06	1.74	1.78	1.85	1.35	1.67	1.93	1.66	1.50	1.70	1.69
B75-AFRP-L3-2	0.54	1.27	1.27	1.03	1.62	1.49	2.00	2.06	1.75	1.81	1.53	1.81	2.12	1.80
B75-AFRP-L3-3*	-	-	1.00	1.00	1.05	1.60	1.86	1.57	1.36	1.21	1.35	1.19	0.98	1.35
B75-CFRP-L3-1	-	0.94	0.87	0.90	0.89	1.79	1.43	1.04	0.94	1.15	1.00	1.20	1.07	1.17
B75-CFRP-L3-2	0.33	0.89	0.94	0.72	0.99	0.84	0.87	1.14	1.02	1.24	0.99	1.09	1.08	1.03
B75-CFRP-L3-3	0.49	0.77	0.87	0.71	-	0.96	1.18	1.36	1.25	1.24	1.32	1.72	1.29	1.29
B75-GFRP-L3-1*	0.23	0.30	0.33	0.28	0.30	0.43	0.47	0.43	0.45	0.47	0.40	0.47	0.50	0.43
B75-GFRP-L3-2*	0.71	0.70	0.65	0.69	0.60	0.92	0.75	0.94	0.85	0.80	0.84	0.86	1.04	0.84
B75-GFRP-L3-3*	0.36	0.79	0.62	0.59	0.76	1.07	0.97	0.98	0.78	0.95	0.88	1.03	0.95	0.93
B100-AFRP-L4-1	0.68	0.81	0.68	0.72	0.79	1.21	1.49	1.46	1.29	1.00	1.07	1.24	1.16	1.19
B100-AFRP-L4-2	0.83	0.77	0.95	0.85	0.71	1.47	-	1.18	1.11	0.99	1.27	-	1.49	1.17
B100-AFRP-L4-3	0.92	1.01	1.32	1.08	-	-	-	1.46	1.44	1.84	1.35	1.28	-	1.47
B100-CFRP-L4-1	0.66	0.68	0.78	0.70	0.94	1.54	-	1.21	1.06	1.17	0.92	1.59	-	1.20
B100-CFRP-L4-2	0.63	0.93	1.09	0.88	1.20	1.36	1.64	1.49	1.69	1.74	1.47	1.39	1.32	1.48
B100-CFRP-L4-3	-	1.02	1.10	1.06	1.16	1.34	1.18	1.27	1.35	1.74	1.35	1.27	1.36	1.34
B100-GFRP-L4-1	1.06	1.27	1.40	1.24	1.72	-	1.69	1.43	-	1.61	-	1.77	-	1.64
B100-GFRP-L4-2	0.81	1.23	1.08	1.04	1.50	1.69	1.91	1.98	1.63	-	1.46	1.93	1.78	1.74
B100-GFRP-L4-3	-	0.84	1.17	1.00	1.43	1.77	1.84	1.66	1.05	1.53	1.55	1.49	-	1.54

* denotes prematurely failed specimens

3.1 Failure modes

Unless noted otherwise in Table 3, all of the specimens failed due to the rupture of the FRP jackets at mid-height (Figure 4). The failures of the CFRP and AFRP-confined specimens involved a sudden rupture of the jacket, and were accompanied by instantaneous loss of applied axial load. The GFRP-confined specimens, on the other hand, exhibited progressive FRP jacket failures. In Table 3, the reported ultimate conditions of these specimens were established at the initiation of the progressive failure. As indicated in Table 2, the epoxy resin that was used in the fabrication of the FRP tubes had a lower yield strain (ε_{epoxy} = 2.5%) than the ultimate tensile strain of S-glass fibers (ε_f = 3.5%). The progressive failure observed in these specimens is believed to have been contributed by the yielding of the epoxy resin that left individual fiber strands susceptible to discrete failure. The yielding of the epoxy resin also caused measurement inconsistencies in strain gauges bonded to the epoxy coated surface of the jackets. Due to the difficulties faced in establishing the hoop rupture strains of GFRP-confined specimens, these specimens are excluded from discussions presented in the following sections on the hoop rupture strains. Based on these observations, it is recommended that epoxy resins with higher yield strains than the ultimate tensile strains of the fibers be used in future applications.

Four GFRP-confined specimens and an AFRP-confined specimen that are marked with an asterisk in Table 3 experienced premature failures, showing a partial debonding failure of the jackets prior to the ultimate conditions due to an incomplete impregnation that caused stress concentrations. The prematurely failed AFRP-confined specimen was also excluded from the discussions presented in the following sections.

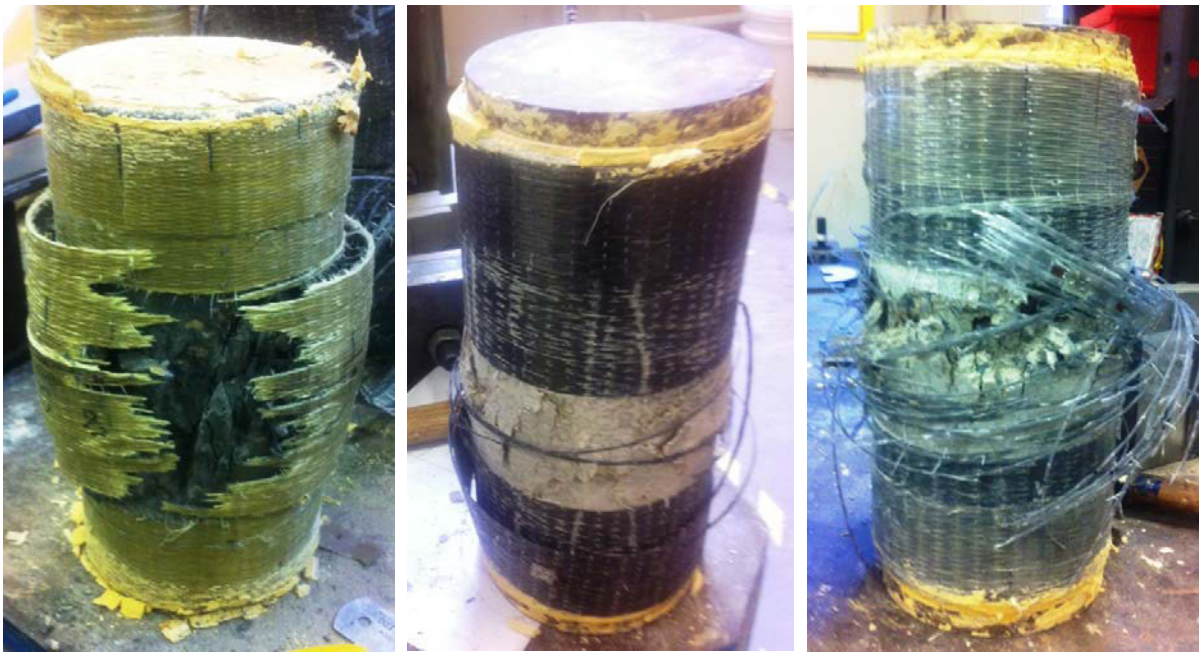

(a) (b) (c)

Figure 4. Failure modes of: (a) AFRP-confined specimen, (b) CFRP-confined specimen, and (c) GFRP-confined specimen

3.2 Hoop strain-axial strain relationships

Figure 5(a) shows the hoop strain-axial strain curves of specimens that had a same unconfined concrete strength (i.e. f'_{co} = 30 MPa) that were confined with different FRP materials (i.e. either with GFRP, AFRP or CFRP). Figure 5(b) shows the hoop strain-axial strain curves of specimens that had different unconfined concrete strengths (i.e. f'_{co} = 30, 50, 74, and 98 MPa) that were confined with a same FRP material with almost identical normalized confinement stiffness ratios (i.e. AFRP with K_l/f'_{co} = 10), with the lateral confinement stiffness of the FRP jacket (K_l) defined as:

$$K_l = 2E_f t_f / D \tag{1}$$

where E_f is the elastic modulus of fibers, t_f is the total nominal dry fiber thickness of the FRP jacket and D is the diameter of the concrete core.

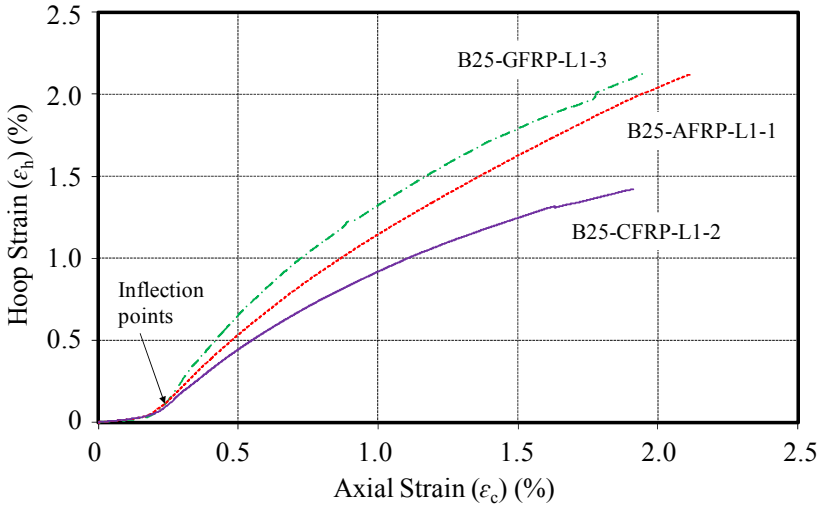

(a)

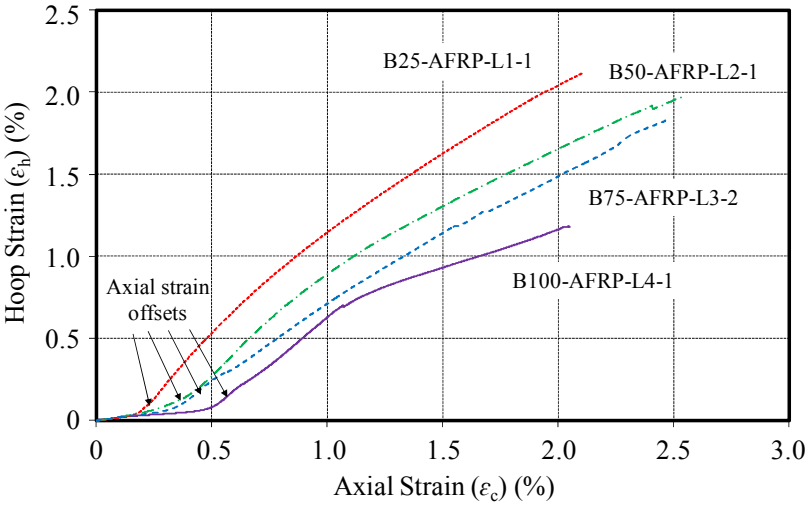

(b)

Figure 5. Hoop strain-axial strain curves of: (a) concretes of a same strength confined by different types of FRP materials, and (b) concretes with different strengths confined by a same type of FRP material

As demonstrated in Figs. 5(a) and 5(b), the initial slopes of the hoop strain-axial strain curves of the specimens follow Poisson's ratio (υ_i) of concrete within the elastic range. When the axial compressive stress in the concrete reaches around 60 to 80% of the compressive strength of unconfined concrete (f'_{co}), the lateral expansion of concrete increases rapidly due to the increased damage the concrete sustains. This expansion results in a progressive increase in the confining pressure of the FRP jacket, which alters the tangential slope of the second portion of hoop strain-axial strain curves that starts after the inflection point. As shown in Fig. 5(a), the secant slopes of these portions of the curves reduce with an increase in the normalized stiffness of the confining jackets (i.e. K_l/f'_{co} = 8, 10, 18 for GFRP, AFRP, and CFRP, respectively), but the coordinates of the inflection point is not significantly altered. Furthermore, the axial strains at the inflection points increase with the concrete strengths (f'_{co}), as evident from the initial axial strain offsets in the curves shown in Fig. 5(b). Important differences can be observed at the ultimate conditions of the specimens shown in Figs. 5(a) and 5(b). The figures indicate that hoop rupture strains ($\varepsilon_{h,ave}$) reduce with an increase in unconfined concrete strength (f'_{co}), and they vary with the type of FRP materials. These observed influences have been closely examined based on the results of the present study and those from two large test databases of FRP-confined concrete reported elsewhere [9, 27]. A detailed discussion on the findings of this investigation is presented in the following section.

3.3 Hoop strain reduction factors

To illustrate the typical hoop strain distributions of the specimens of the present study, Figures 6 and 7 show strain distributions of a group of selected specimens recorded by 12 strain gauges placed in the arrangement shown in Fig. 2. Strain distributions shown in Figs. 6 and 7 were established using hoop strains recorded at every 20% increment of axial strain to ultimate axial strain ratio ($\varepsilon_c/\varepsilon_{cu}$) up to the ultimate condition. As expected, the figures illustrate that the hoop strains are lower within the overlap region compared to the non-overlap region. This can be also observed from Table 4, which indicates that the ratios of the average overlap to non-overlap region strains were 0.54, 0.61, 0.64 and 0.68 for specimens with 1, 2, 3 and 4 layers of FRP, respectively. More importantly, Figs. 6 and 7 and Table 4 further illustrate that the hoop strain distributions outside the overlap regions were also non-uniform. One of the major reasons to these variations in strains is the non-homogeneity of concrete, which results in non-uniform deformations and crack formations. In the context of the discussion presented in this paper, the non-homogeneity of concrete is classified as a partial material dependent factor influencing efficiency of FRP jackets, as the crack formation of concrete is random in nature, whereas the pattern of the cracks changes with concrete strength [9, 21].

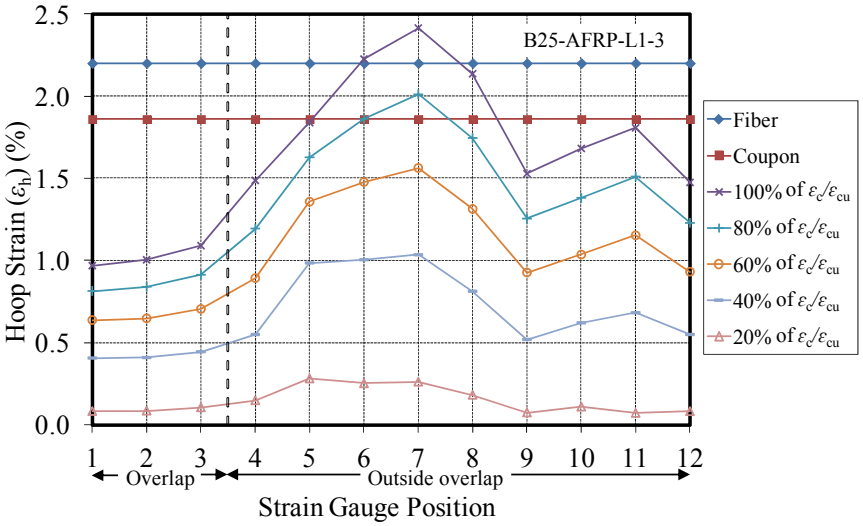

(a)

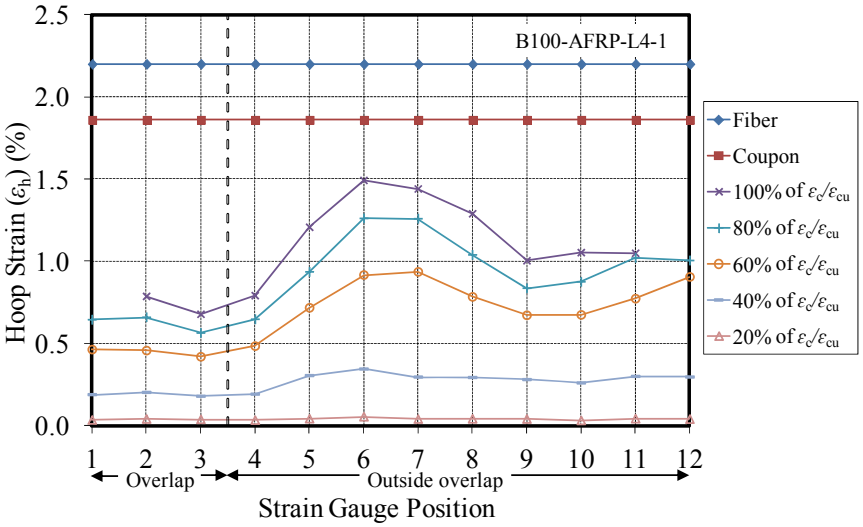

(b)

Figure 6. Distribution of hoop strains of (a) AFRP-confined NSC, and (b) AFRP-confined HSC

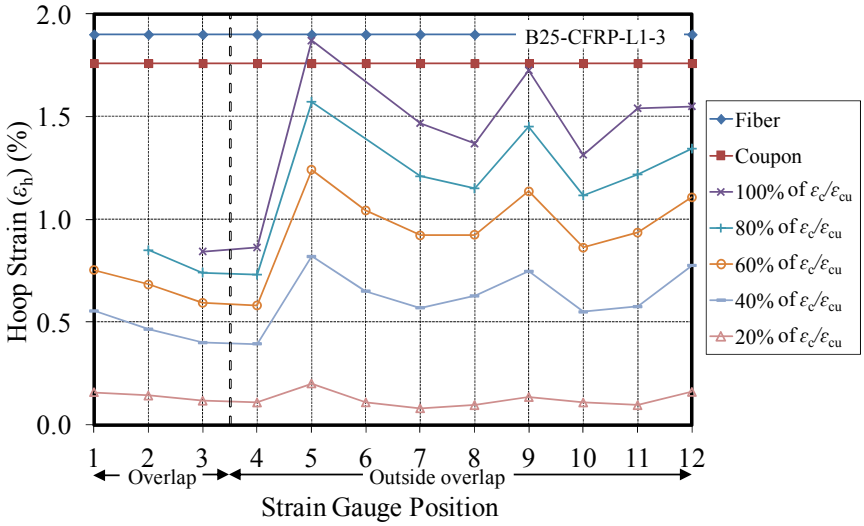

(a)

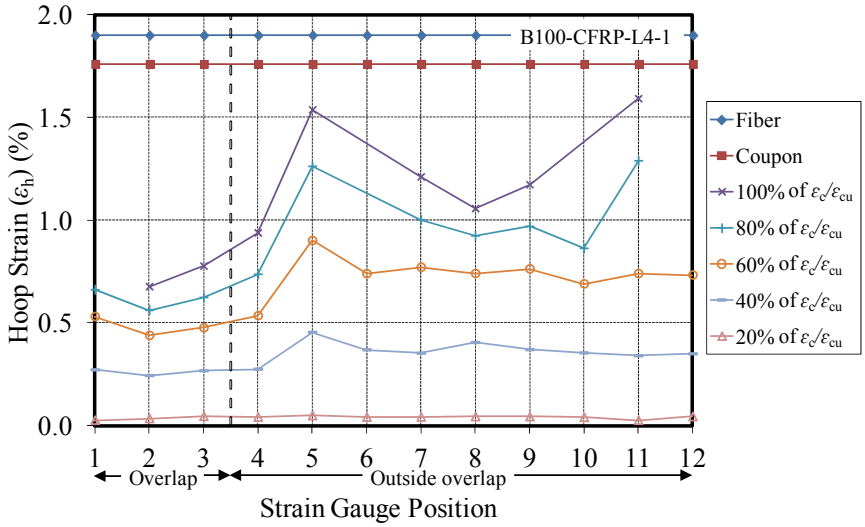

(b)

Figure 7. Distribution of hoop strains of: (a) CFRP-confined NSC, and (b) CFRP-confined HSC

The use of a strain reduction factor ($k_{\varepsilon,frp}$) is a common approach to quantify the lower hoop strains of FRP jackets to compared to the ultimate tensile strain of the FRP material. As was proposed by Pessiki et al. [6], the FRP strain reduction factor ($k_{\varepsilon,frp}$) can be seen as a product of the strain localization factor ($k_{\varepsilon1}$) and in-situ factor ($k_{\varepsilon2}$) (i.e. $k_{\varepsilon,frp} = k_{\varepsilon1}.k_{\varepsilon2}$). Using a similar approach that was adopted in a number of previous studies to allow for the use of the manufacturer specified fiber properties as reference material properties for the calculations of the FRP strain efficiency (e.g. [27, 43-45]), in the present study fiber strain reduction factor ($k_{\varepsilon,f}$) was defined through the incorporation of FRP-to-fiber strain ratio ($k_{\varepsilon3}$) into the strain reduction factor expression:

$$k_{\varepsilon,f} = k_{\varepsilon1}.k_{\varepsilon2}.k_{\varepsilon3} = \frac{\varepsilon_{h,ave}}{\varepsilon_{h,max}}.\frac{\varepsilon_{h,max}}{\varepsilon_{frp}}.\frac{\varepsilon_{frp}}{\varepsilon_f} = \frac{\varepsilon_{h,ave}}{\varepsilon_f} \quad (2)$$

where ε_{frp} is the ultimate strain of FRP composite obtained from flat coupon tests and ε_f is the ultimate tensile strain of fibers.

The strain localization factor ($k_{\varepsilon 1}$) accounts for the effect of a non-uniform strain distribution in the FRP jacket, whereas the in-situ factor ($k_{\varepsilon 2}$) accounts for the difference between the maximum strain measured on the FRP jacket and that obtained from a flat tension coupon specimen. The average $k_{\varepsilon 1}$ and $k_{\varepsilon 2}$ of the specimens of the present study are calculated as 0.826 and 0.948, respectively. The average values reported in previous studies [5, 8, 20] varied from 0.782 to 0.906 for $k_{\varepsilon 1}$ and from 0.710 to 0.893 for $k_{\varepsilon 2}$. The variation of $k_{\varepsilon 1}$ and $k_{\varepsilon 2}$ with concrete strength and FRP properties is discussed in detail in the following section.

The FRP-to-fiber strain ratio ($k_{\varepsilon 3}$) is a new factor introduced in this study to account for the difference in the strain capacities of FRP flat coupons and fiber material. The average $k_{\varepsilon 3}$ of the fibers used in the present study are established as 0.900, 0.917 and 0.845 for CFRP, GFRP and AFRP, respectively. The average values calculated from the results of the experimental databases reported in Lim and Ozbakkaloglu [9] and Ozbakkaloglu and Lim [27] were 0.954, 0.931, and 0.798 for CFRP, GFRP, and AFRP, respectively.

3.3.1. Influence of unconfined concrete strength

Figure 8 shows the variation of hoop strain reduction factors ($k_{\varepsilon,f}$) with unconfined concrete strengths (f'_{co}) both for the specimens of the present study and those obtained from the large experimental test database [9, 27]. Both the results of the present study and those from published literature indicate that the fiber strain reduction factor ($k_{\varepsilon,f}$) decreases with an increase in unconfined concrete strength (f'_{co}). This accords with Ozbakkaloglu and Akin [21], who observed that an increase in the compressive strength of concrete adversely affected the hoop rupture strain of FRP jackets. The reduction in FRP rupture strain with an increase in concrete strength can be explained by the increase in concrete brittleness, which alters the concrete crack patterns from heterogenic microcracks in normal-strength concrete (NSC) to localized macrocracks in high-strength concrete (HSC) [46, 47]. The changed cracking pattern reduces the in-situ capacity of the FRP jackets by causing localized stress concentrations. Excluding the GFRP-confined specimens, the average values of $k_{\varepsilon,f}$, calculated from the results given in Table 3, decrease from 0.841 to 0.643 as the unconfined concrete strength (f'_{co}) increases from 30 to 98 MPa.

To establish the relative influence of unconfined concrete strength (f'_{co}) on the strain localization factor ($k_{\varepsilon 1}$) and in-situ factor ($k_{\varepsilon 2}$), the results of the present study were further investigated. Figures 9(a) and 9(b) show the variation of the strain localization factors ($k_{\varepsilon 1}$) with the unconfined concrete strength (f'_{co}) for the AFRP and CFRP-confined specimens, respectively. The figures indicate that the strain localization factor ($k_{\varepsilon 1}$) decreases slightly with an increase in the unconfined concrete strength (f'_{co}). The variation of the in-situ factors ($k_{\varepsilon 2}$) with the unconfined concrete strength (f'_{co}) is illustrated in Figures 10(a) and 10(b). As shown in the figures, an increase in unconfined concrete strength (f'_{co}) also results in a decrease in the in-situ factors ($k_{\varepsilon 2}$). The reductions in the in-situ jacket capacities are also evident from Figs. 6 and 7, which demonstrate that the maximum hoop strains recorded in the HSC specimens are consistently lower than those observed in the companion NSC specimens.

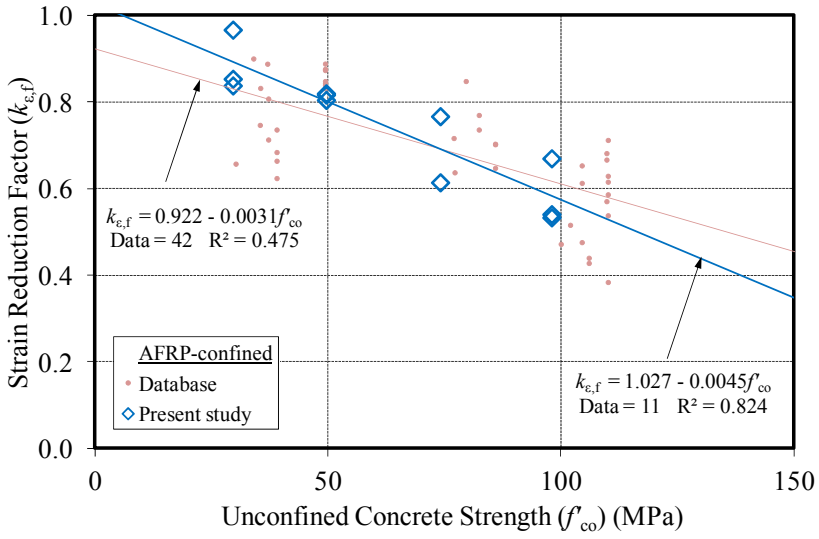

(a)

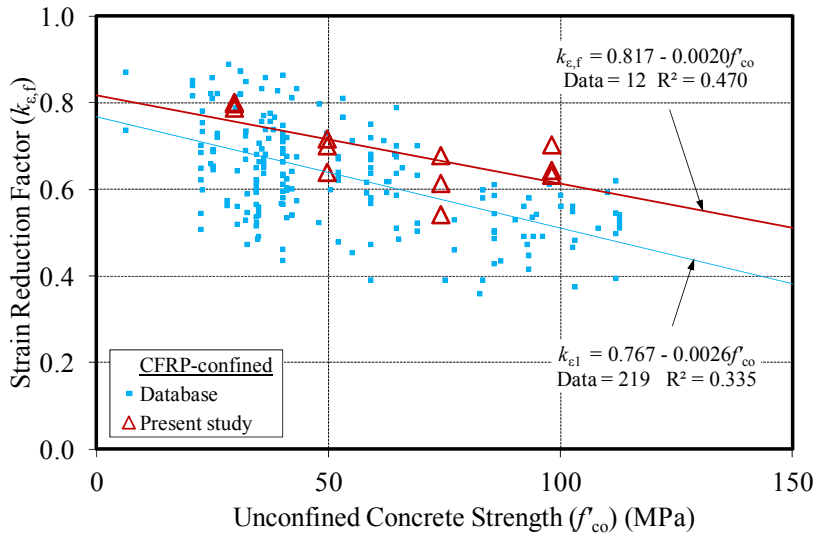

(b)

Figure 8. Variation of hoop strain reduction factors ($k_{\varepsilon,f}$) with concrete strength (f'_{co}): (a) AFRP-confined specimens, and (b) CFRP-confined specimens

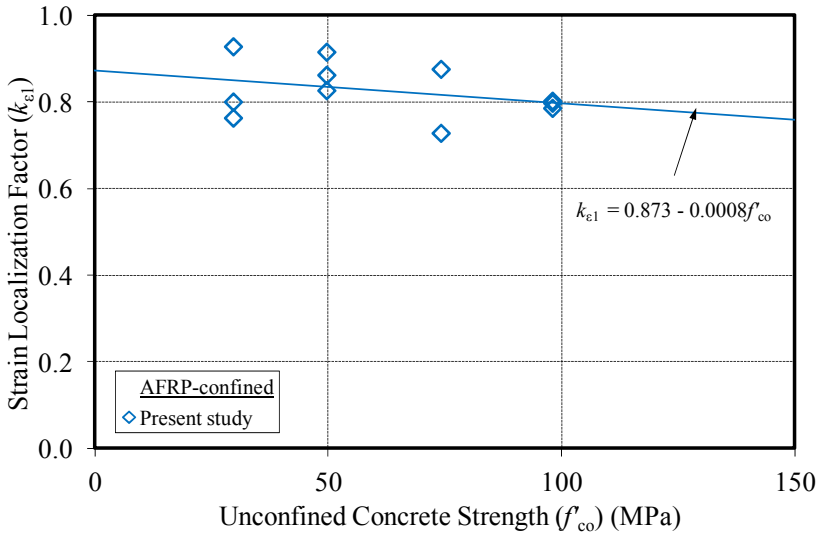

(a)

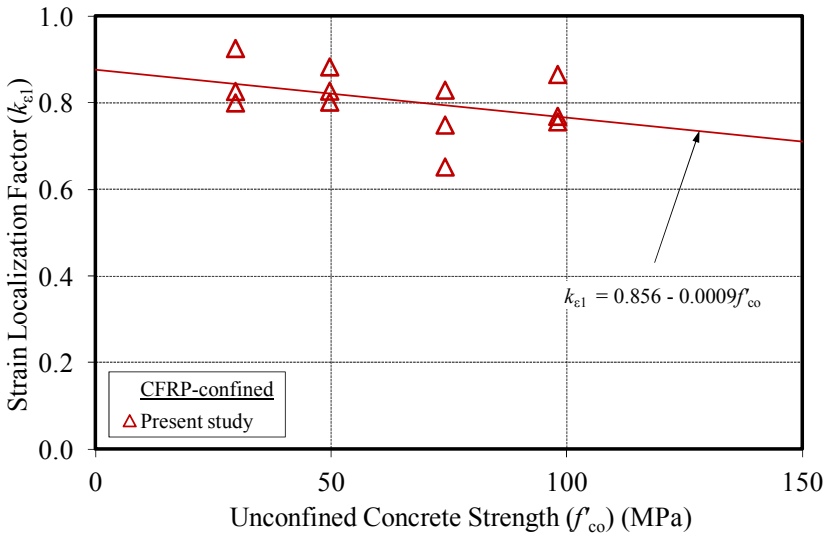

(b)

Figure 9. Variation of strain localization factors ($k_{\varepsilon 1}$) with concrete strength (f'_{co}): (a) AFRP-confined specimens, (b) CFRP-confined specimens

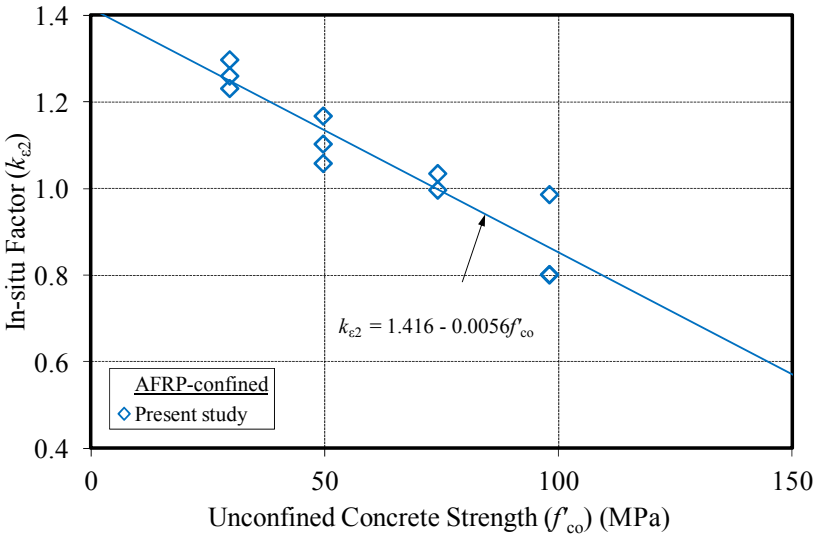

(a)

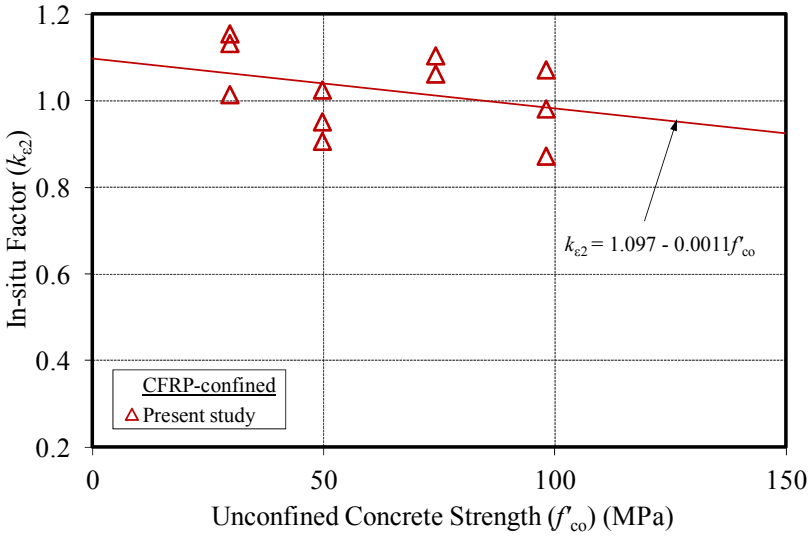

(b)

Figure 10. Variation of in-situ factors ($k_{\varepsilon 2}$) with concrete strength (f'_{co}): (a) AFRP-confined specimens, and (b) CFRP-confined specimens

3.3.2. Influence of type of FRP material

The observed dependence of the hoop rupture strain of the FRP jacket to the type of fiber materials was previously reported in Ozbakkaloglu and Akin [21] and Dai et al. [48]. To closely examine the material dependency of the hoop rupture strain of the FRP jacket, in the present study the relationship between the elastic modulus of the confining fibers (E_f) and the recorded hoop rupture strains ($\varepsilon_{h,ave}$) were investigated using the results of the present study and those from the aforementioned test databases [9, 27]. Figure 11 shows the variation of hoop strain reduction factors ($k_{\varepsilon,f}$) with the elastic modulus of fibers (E_f). As evident from trendline of the figure, an increase in the elastic modulus of fibers (E_f) results in a decrease in the hoop strain reduction factor ($k_{\varepsilon,f}$). Consistent trends were found between the results of the present study and those from the test database. Figures 12 and 13, respectively, show the

variations of the strain localization factor ($k_{\varepsilon 1}$) and in-situ factor ($k_{\varepsilon 2}$) with the elastic modulus of fibers (E_f). As illustrated in the figures, an increase in the elastic modulus of fibers (E_f) results in a slight decrease in both the strain localization factor ($k_{\varepsilon 1}$) and in-situ factor ($k_{\varepsilon 2}$).

It should be noted, Figures 11 to 13 contain specimens with a wide range of unconfined strengths (f'_{co}) (i.e. 6 to 170 MPa from the test database and 30 to 98 MPa in the present tests). Due to the change in the strain efficiency factor ($k_{\varepsilon,f}$) with unconfined concrete strength (f'_{co}), as discussed previously, the bandwidths of the trendlines in Figures 11 to 13 expand as the ranges of concrete strengths widen. The coefficient of determination (R^2) in Figure 11 and the dispersion of the results in Figures 12 and 13 improve significantly when the results are subdivided into smaller groups according to the unconfined concrete strengths of the specimens (i.e. 40-50 MPa, 50-60 MPa, etc). However, for brevity, these individual charts were not included in this paper.

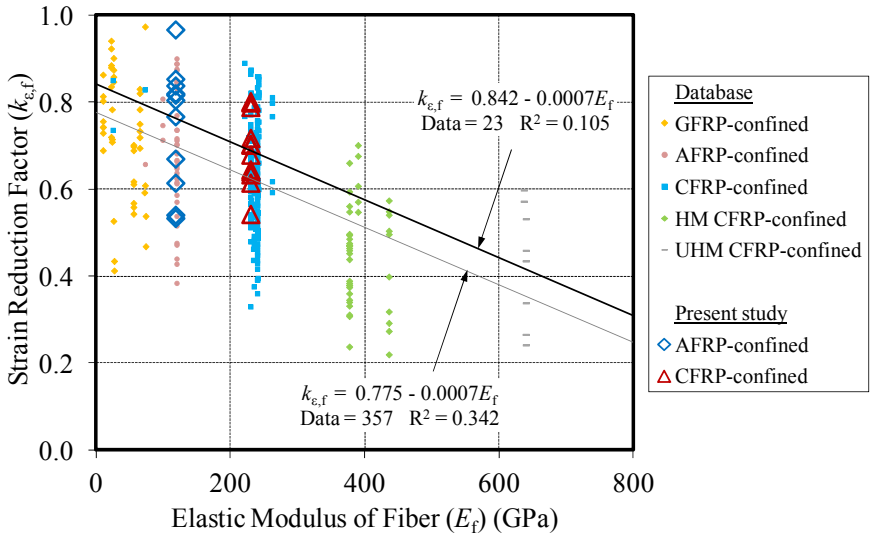

Figure 11. Variation of hoop strain reduction factors ($k_{\varepsilon,f}$) with elastic modulus of fibers (E_f)

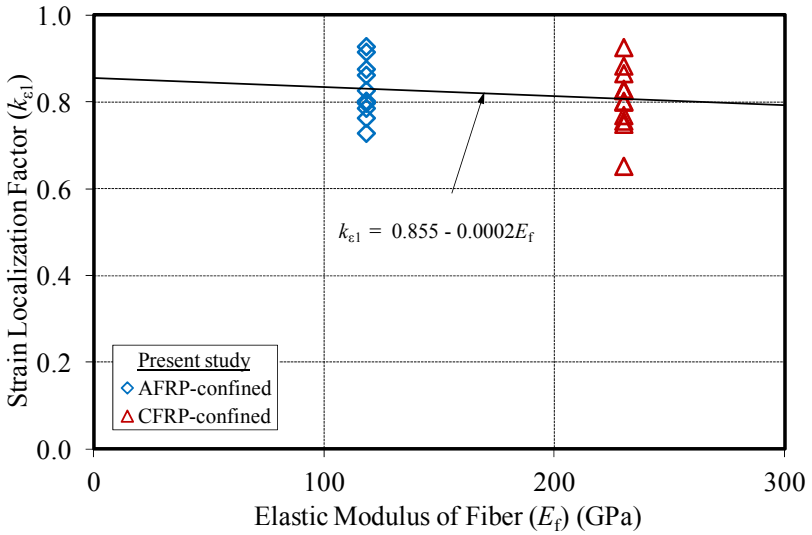

Figure 12. Variation of strain localization factors ($k_{\varepsilon 1}$) with elastic modulus of fibers (E_f)

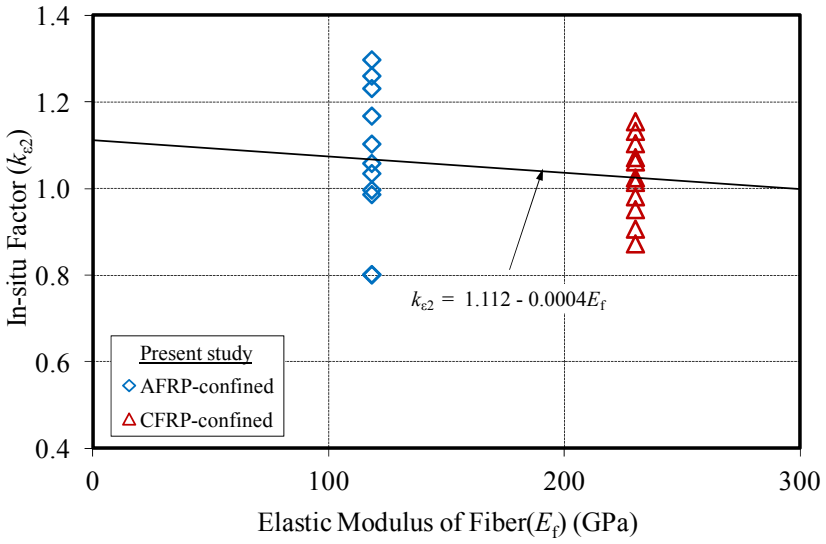

Figure 13. Variation of in-situ factors ($k_{\varepsilon 2}$) with elastic modulus of fibers (E_f)

4. THEORETICAL STRAIN REDUCTION FACTOR

Based on the analysis of a large database cataloguing 1063 test datasets, Eq. 3 was previously proposed in Lim and Ozbakkaloglu [9] to predict the strain reduction factor ($k_{\varepsilon,f}$) as a function of the unconfined concrete strengths (f'_{co}) and the elastic modulus of the fibers (E_f).

$$k_{\varepsilon,f} = 0.9 - 2.3f'_{co} \times 10^{-3} - 0.75E_f \times 10^{-6} \quad (3)$$

where E_f is in MPa and $100{,}000\text{MPa} \leq E_f \leq 640{,}000\text{MPa}$.

Figure 14 shows the comparison of the strain reduction factors ($k_{\varepsilon,f}$) predicted using Eq. 3 with the results of the present study. As evident from Fig. 14, Eq. 3 provides close and slightly conservative estimates of the experimentally obtained $k_{\varepsilon,f}$ values. The higher $k_{\varepsilon,f}$ values of the specimens of the present study are believed to have been contributed by the improved instrumentation arrangement used in the present study, which involved the use of large number of hoop strain gauges.

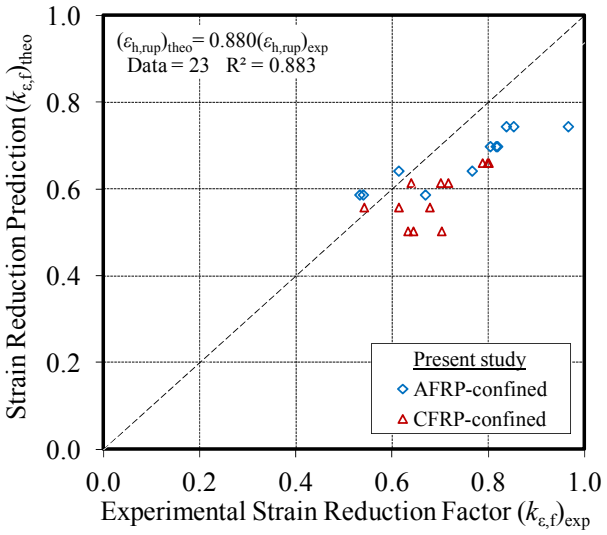

Figure 14. Comparison of predicted strain reduction factors ($k_{\varepsilon,f}$) with experimental results

5. HOOP STRAIN-AXIAL STRAIN MODEL

To establish the relationship between hoop and axial strain, a model that predicts the hoop strain-axial strain relationships of FRP and actively confined concretes as functions of the concrete strength, properties of confining material and confining pressure was proposed in Lim and Ozbakkaloglu [49] (Eq. 4). The shape of the predicted hoop strain-axial strain curves was established based on 144 FRP-confined and 159 actively confined concrete test results, and the important coordinates along the curves were calibrated using 671 FRP-confined and 213 actively confined concrete test results.

$$\varepsilon_c = \frac{\varepsilon_h}{\upsilon_i\left(1+\left(\frac{\varepsilon_h}{\upsilon_i\varepsilon_{co}}\right)^n\right)^{\frac{1}{n}}} + 0.04{\varepsilon_h}^{0.7}\left(1+21\left(\frac{f_l}{{f'}_{co}}\right)^{0.8}\right) \tag{4}$$

$$\upsilon_i = 8\times10^{-6}{f'_{co}}^2 + 0.0002f'_{co} + 0.138 \tag{5}$$

$$\varepsilon_{co} = \left(-0.067{f'_{co}}^2 + 29.9f'_{co} + 1053\right)\times10^{-6} \tag{6}$$

$$n = 1 + 0.03f'_{co} \tag{7}$$

where ε_c is the axial strain, ε_h is the hoop strain, f_l is the corresponding confinement pressure for a given hoop strain ($f_l = K_l.\ \varepsilon_h$), υ_i is the initial Poisson's ratio of concrete, to be calculated using Eq. 5 proposed by Candappa et al. [50], f'_{co} is the peak unconfined concrete strength in MPa, ε_{co} is the peak unconfined concrete strain, to be calculated using Eq. 6 proposed by Tasdemir et al. [51], n is the curve-shape parameter proposed by Lim and Ozbakkaloglu [49] (Eq. 7) to adjust the initial transition radius of the predicted hoop strain-axial strain relationship curve. The confining pressure (f_l) in Eq. 4 is a variable for FRP-confined concrete, which can be determined by gradually increasing the lateral strain (ε_h) until the hoop rupture strain of the FRP jacket ($\varepsilon_{h,ave}$) is reached. $\varepsilon_{h,ave}$ can be predicted by Eq. 2, with $k_{\varepsilon,f}$ calculated from Eq. 3.

Figure 15 shows the comparison of the hoop strain-axial strain curves predicted with Eq. 4 with the results of the CFRP-confined specimens of the current study. It is evident from these comparisons that the predicted shapes of the hoop strain-axial strain curves closely match the experimental results. Comparisons of the model predictions with the results from all the specimens of the present study are shown in Figures 16(a) to 16(c). In these figures, the model predictions of the hoop strains $(\varepsilon_h)_{theo}$ corresponding to the axial strains (ε_c) recorded at 20%, 40%, 60%, 80%, and 100% of the ultimate axial strain (ε_{cu}) are compared with the experimental recorded hoop strains $(\varepsilon_h)_{exp}$ at the corresponding axial strain intervals. As evident from the figures, the model predictions are in good agreement with the experimental results. It should be noted that the comparison at 100% $\varepsilon_c/\varepsilon_{cu}$ were not provided for the GFRP-confined specimens due to the difficulties encountered in the measurement of the hoop strains of these specimens at ultimate, as discussed previously.

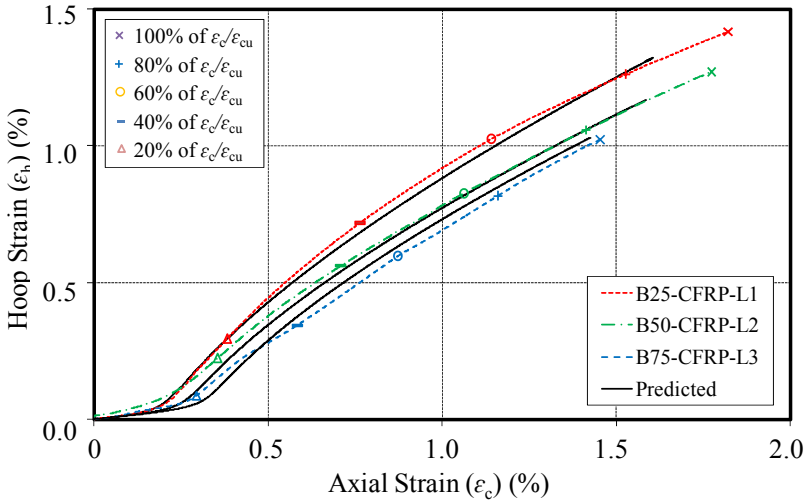

Figure 15. Comparison of model predictions with experimental hoop strain-axial strain curves

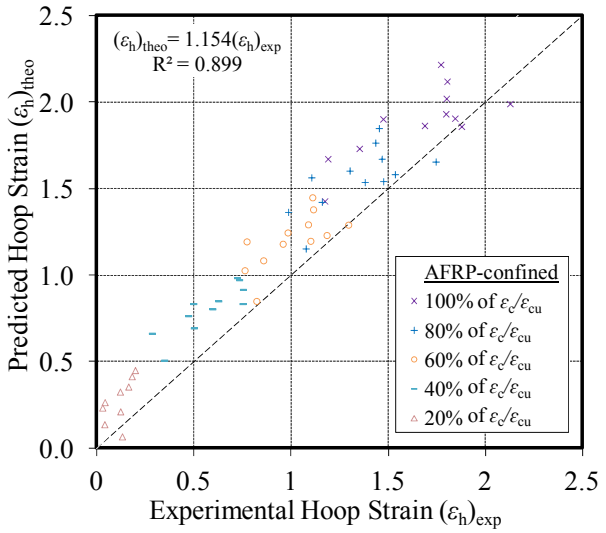

(a)

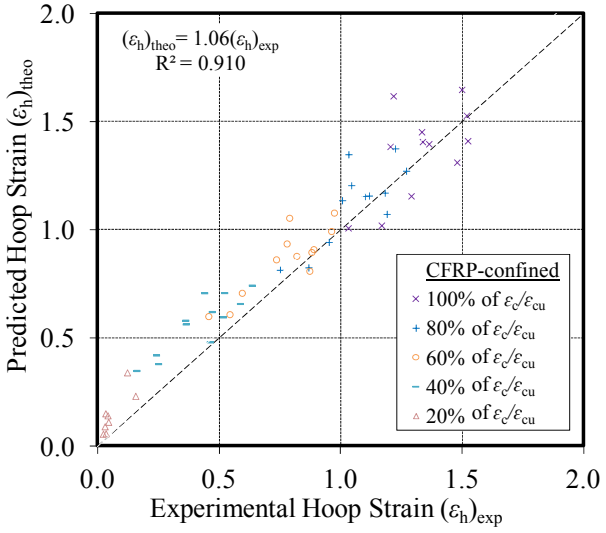

(b)

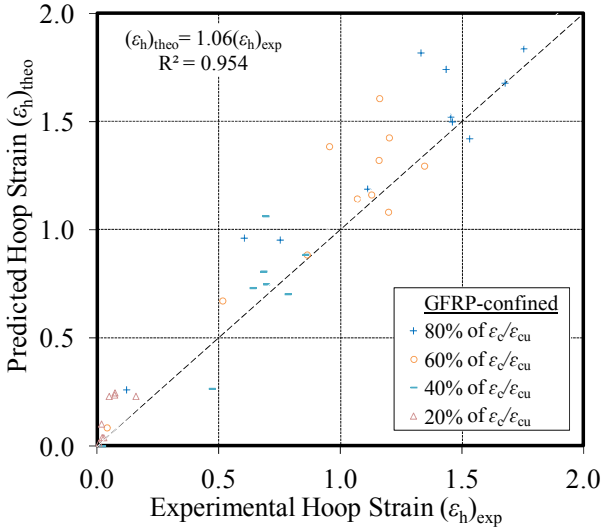

(c)

Figure 16. Comparison of predicted hoop strain (ε_h) with experimental results: (a) AFRP-confined specimens, (b) CFRP-confined specimens, and (c) GFRP-confined specimens

6. CONCLUSIONS

This paper has presented the results of an experimental study that closely examined factors influencing the hoop rupture strains and axial strains in FRP-confined concrete. It has been demonstrated in the paper that the average hoop rupture strains of FRP-confined concrete are significantly affected by two parameters investigated in the present study, namely: (a) concrete strength, and (b) type of FRP material. The hoop rupture strain reduction factor ($k_{\varepsilon,f}$) of FRP jackets has been observed to decrease with an increase in the unconfined concrete strength (f'_{co}) and elastic modulus of fiber material (E_f). Based on the results, it has been established that an increase in the elastic modulus of fibers (E_f) results in a slight decrease in the strain localization factor ($k_{\varepsilon 1}$) and in-situ factor ($k_{\varepsilon 2}$). Similarly, an increase in the unconfined concrete strength (f'_{co}) leads to a decrease in $k_{\varepsilon 1}$ and $k_{\varepsilon 2}$. Based on the observations on hoop strain-axial strain curves, the slope of the curves after the inflection points have been found to decrease with an increase in the normalized stiffness (K_l/f'_{co}) of the confining jackets. On the other hand, the axial strain at the inflection points of the curve increases with the concrete strength (f'_{co}).

The strain reduction factor expression previously proposed by Lim and Ozbakkaloglu [9] have been shown to be in good agreement with the results of the present study. The hoop strain-axial strain curves of the specimens of the present study have been compared with the predictions of the hoop strain-axial strain model proposed in Lim and Ozbakkaloglu [49], which also demonstrates good agreement.

REFERENCES

1. Ozbakkaloglu, T., Lim, J.C., and Vincent, T., (2013). "FRP-confined concrete in circular sections: Review and assessment of stress–strain models." *Engineering Structures,* 49, p. 1068–1088.
2. Ilki, A. and Kumbasar, N., (2003). "Compressive behaviour of carbon fibre composite jacketed concrete with circular and non-circular cross-sections." *Journal of Earthquake Engineering,* 7(3), p. 381-406.
3. Lam, L. and Teng, J.G., (2003). "Design-oriented stress-strain model for FRP-confined concrete." *Construction and Building Materials,* 17(6-7), p. 471-489.
4. Rousakis, T.C. and Karabinis, A.I., (2008). "Substandard reinforced concrete members subjected to compression: FRP confining effects." *Materials and Structures,* 41(9), p. 1595-1611.
5. Wu, Y.-F. and Jiang, J.-F., (2013). "Effective strain of FRP for confined circular concrete columns." *Composite Structures,* 95, p. 479–491.
6. Pessiki, S., Harries, K.A., Kestner, J.T., Sause, R., and Ricles, J.M., (2001). "Axial behavior of reinforced concrete columns confined with FRP jackets." *Journal of Composites for Construction,* 5(4), p. 237-245.
7. Harries, K.A. and Kharel, G., (2002). "Behavior and modeling of concrete subject to variable confining pressure." *ACI Materials Journal,* 99(2), p. 180-189.
8. Lam, L. and Teng, J.G., (2004). "Ultimate condition of fiber reinforced polymer-confined concrete." *Journal of Composites for Construction, ASCE,* 8(6), p. 539-548.
9. Lim, J.C. and Ozbakkaloglu, T., (2013). "Confinement model for FRP-confined high-strength concrete." *Journal of Composites for Construction,* 18(4), 04013058.
10. Matthys, S., Taerwe, L., and Audenaert, K., (1999). "Tests on axially loaded concrete columns confined by fiber reinforced polymer sheet wrapping." *ACI Special Publications 188*, p. 217-228.
11. Shahawy, M., Mirmiran, A., and Beitelman, T., (2000). "Tests and modeling of carbon-wrapped concrete columns." *Composites Part B-Engineering,* 31(6-7), p. 471-480.
12. Xiao, Y. and Wu, H., (2000). "Compressive behavior of concrete confined by carbon fiber composite jackets." *Journal of Materials in Civil Engineering,* 12(2), p. 139-146.
13. De Lorenzis, L. and Tepfers, R., (2003). "Comparative study of models on confinement of concrete cylinders with fiber-reinforced polymer composites." *Journal of Composites for Construction,* 7(3), p. 219-237.
14. Harries, K.A. and Carey, S.A., (2003). "Shape and "gap" effects on the behavior of variably confined concrete." *Cement and Concrete Research,* 33(6), p. 881-890.
15. Carey, S.A. and Harries, K.A., (2005). "Axial behavior and modeling of confined small-, medium-, and large-scale circular sections with carbon fiber-reinforced polymer jackets." *ACI Structural Journal,* 102(4), p. 596-604.
16. Lignola, G.P., Prota, A., Manfredi, G., and Cosenza, E., (2008). "Effective strain in FRP jackets on circular RC columns." *Proceedings of the 4th International Conference on FRP Composites in Civil Engineering*, Zurich, Switzerland. p. 6.
17. Ozbakkaloglu, T. and Oehlers, D.J., (2008). "Concrete-filled square and rectangular FRP tubes under axial compression." *Journal of Composites for Construction,* 12(4), p. 469-477.

18. Ozbakkaloglu, T. and Oehlers, D.J., (2008). "Manufacture and testing of a novel FRP tube confinement system." *Engineering Structures,* 30, p. 2448-2459.
19. Chen, J.F., Ai, J., and Stratford, T.J., (2010). "Effect of Geometric Discontinuities on Strains in FRP-Wrapped Columns." *Journal of Composites for Construction,* 14(2), p. 136-145.
20. Smith, S.T., Kim, S.J., and Zhang, H., (2010). "Behavior and Effectiveness of FRP Wrap in the Confinement of Large Concrete Cylinders." *Journal of Composites for Construction,* 14(5), p. 573-582.
21. Ozbakkaloglu, T. and Akin, E., (2012). "Behavior of FRP-confined normal- and high-strength concrete under cyclic axial compression." *Journal of Composites for Construction, ASCE,* 16(4), p. 451-463.
22. Rousakis, T.C., Rakitzis, T.D., and Karabinis, A.I., (2012). "Design-Oriented Strength Model for FRP-Confined Concrete Members." *Journal of Composites for Construction,* 16(6), p. 615-625.
23. Ozbakkaloglu, T., (2013). "Compressive behavior of concrete-filled FRP tube columns: Assessment of critical column parameters." *Engineering Structures,* 51, p. 188-199.
24. Ozbakkaloglu, T. and Vincent, T., (2013). "Axial compressive behavior of circular high-strength concrete-filled FRP tubes." *Journal of Composites for Construction, ASCE,* 18(2), p. 04013037.
25. Vincent, T. and Ozbakkaloglu, T., (2013). "Influence of concrete strength and confinement method on axial compressive behavior of FRP-confined high- and ultra high-strength concrete." *Composites Part B,* 50, p. 413–428.
26. Vincent, T. and Ozbakkaloglu, T., (2013). "Influence of fiber orientation and specimen end condition on axial compressive behavior of FRP-confined concrete." *Construction and Building Materials,* 47, p. 814-826.
27. Ozbakkaloglu, T. and Lim, J.C., (2013). "Axial compressive behavior of FRP-confined concrete: Experimental test database and a new design-oriented model." *Composites Part B: Engineering,* 55, p. 607-634.
28. Watanabe, K., Nakamura, R., Honda, Y., Toyoshima, M., Iso, M., Fujimaki, T., Kaneto, M., and Shirai, N., (1997). "Confinement effect of FRP sheet on strength and ductility of concrete cylinders under uniaxial compression." *Proceedings of the Non-metallic Reinforcement for Concrete Structures, Japan Concrete Institute*.
29. De Lorenzis, L., Micelli, F., and La Tegola, A. , (2002). "Influence of specimen size and resin type on the behavior of FRP-confined concrete cylinders." *Advanced Polymer Composites for Structural Applications in Construction: Proceedings of the First International Conference*, Southampton.
30. Bullo, S., (2003). "Experimental study of the effects of the ultimate strain of fiber reinforced plastic jackets on the behavior of confined concrete." *Proceedings of the International Conference of Composites in Construction*, Cosenza, Italy.
31. Tepfers, R., Rousakis, T., and You, C.S., (2003). "Concrete cylinders confined by carbon FRP sheets, subjected to monotonic and cyclic axial compressive load." *Proceedings of the 6th International Symposium on Fibre Reinforced Polymer (FRP) Reinforcement for Concrete Structures*, Singapore. p. 571-580.

32. Berthet, J.F., Ferrier, E., and Hamelin, P., (2005). "Compressive behavior of concrete externally confined by composite jackets. Part A: experimental study." *Construction and Building Materials,* 19(3), p. 223-232.
33. Lam, L., Teng, J.G., Cheung, C.H., and Xiao, Y., (2006). "FRP-confined concrete under axial cyclic compression." *Cement and Concrete Composites,* 28(10), p. 949-958.
34. Ciupala, M.A., Pilakoutas, K., and Mortazavi, A.A., (2007). "Effectiveness of FRP composites in confined concrete." *Proceedings of the 8th International Symposium on Fiber Reinforced Polymer Reinforcement for Concrete Structures*, University of Patras, Patras, Greece.
35. Jiang, T. and Teng, J.G., (2007). "Analysis-oriented stress-strain models for FRP-confined concrete." *Engineering Structures,* 29(11), p. 2968-2986.
36. Valdmanis, V., De Lorenzis, L., Rousakis, T., and Tepfers, R., (2007). "Behaviour and capacity of CFRP-confined concrete cylinders subjected to monotonic and cyclic axial compressive load." *Structural Concrete,* 8(4), p. 187-200.
37. Wang, L.M. and Wu, Y.F., (2008). "Effect of corner radius on the performance of CFRP-confined square concrete columns: Test." *Engineering Structures,* 30(2), p. 493-505.
38. Bisby, L.A. and Take, W.A., (2009). "Strain localisations in FRP-confined concrete: new insights." *Proceedings of the Institution of Civil Engineers-Structures and Buildings,* 162(5), p. 301-309.
39. Cui, C. and Sheikh, A., (2009). "Behaviour of normal- and high strength-concrete confined with fibre reinforced polymers (FRP)." Research Report No. CS-01-09, *Department of Civil Engineering*, University of Toronto, Toronto.
40. Benzaid, R., Mesbah, H., and Chikh, N.E., (2010). "FRP-confined Concrete Cylinders: Axial Compression Experiments and Strength Model." *Journal of Reinforced Plastics and Composites,* 29(16), p. 2469-2488.
41. Rousakis, T.C. and Karabinis, A.I., (2012). "Adequately FRP confined reinforced concrete columns under axial compressive monotonic or cyclic loading." *Materials and Structures,* 45(7), p. 957-975.
42. ASTM-D3039, (2008). "Standard test method for tensile properties of polymer matrix composite materials." *D3039/D3039M-08*, West Conshohocken, PA.
43. Ilki, A., Kumbasar, N., and Koc, V., (2004). "Low strength concrete members externally confined with FRP sheets." *Structural Engineering and Mechanics,* 18(2), p. 167-194.
44. Matthys, S., Toutanji, H., and Taerwe, L., (2006). "Stress-strain behavior of large-scale circular columns confined with FRP composites." *Journal of Structural Engineering,* 132(1), p. 123-133.
45. Rousakis, T.C., Karabinis, A.I., and Kiousis, P.D., (2007). "FRP-confined concrete members: Axial compression experiments and plasticity modelling." *Engineering Structures,* 29(7), p. 1343-1353.
46. Ozbakkaloglu, T., (2013). "Axial compressive behavior of square and rectangular high-strength concrete-filled FRP tubes." *Journal of Composites for Construction,* 17(1), p. 151-161.

47. Ozbakkaloglu, T., (2013). "Behavior of square and rectangular ultra high-strength concrete-filled FRP tubes under axial compression." *Composites Part B: Engineering.,* 54, p. 97-111.
48. Dai, J.G., Bai, Y. L., and Teng, J. G. , (2011). "Behavior and modeling of concrete confined with FRP composites of large deformability." *ASCE J. Compos. Constr.,* 15(6), p. 963–973.
49. Lim, J.C. and Ozbakkaloglu, T., (2014). "Lateral strain-to-axial strain relationship of confined concrete." *Journal of Structural Engineering, ASCE,* Doi: 10.1061/(ASCE)ST.1943-541X.0001094.
50. Candappa, D.C., Sanjayan, J.G., and Setunge, S., (2001). "Complete triaxial stress-strain curves of high-strength concrete." *Journal of Materials in Civil Engineering,* 13(3), p. 209-215.
51. Tasdemir, M.A., Tasdemir, C., Jefferson, A.D., Lydon, F.D., and Barr, B.I.G., (1998). "Evaluation of strains at peak stresses in concrete: A three-phase composite model approach." *Cement and Concrete Research,* 20(4), p. 301-318.

THIS PAGE HAS BEEN LEFT INTENTIONALLY BLANK

Statement of Authorship

Title of Paper	Investigation of the Influence of Application Path of Confining Pressure: Tests on Actively Confined and FRP-Confined Concretes
Publication Status	(•) Published ( ) Accepted for Publication ( ) Submitted for Publication ( ) Publication Style
Publication Details	Journal of Structural Engineering, Doi: 10.1061/(ASCE)ST.1943-541X.0001177, Year 2014

Author Contributions

By signing the Statement of Authorship, each author certifies that their stated contribution to the publication is accurate and that permission is granted for the publication to be included in the candidate's thesis.

Name of Principal Author (Candidate)	Mr. Jian Chin Lim		
Contribution to the Paper	Preparation of experiment, analysis of test results, and preparation of manuscript		
Signature		Date	23/02/2015

Name of Co-Author	Dr. Togay Ozbakkaloglu		
Contribution to the Paper	Research supervision and review of manuscript		
Signature		Date	23/02/2015

THIS PAGE HAS BEEN LEFT INTENTIONALLY BLANK

INVESTIGATION OF THE INFLUENCE OF APPLICATION PATH OF CONFINING PRESSURE: TESTS ON ACTIVELY CONFINED AND FRP-CONFINED CONCRETES

Jian C. Lim and Togay Ozbakkaloglu

ABSTRACT

It is often assumed that, at a given lateral strain, the axial compressive stress and strain of fiber reinforced polymer (FRP)-confined concrete are the same as those of the same concrete when it is actively confined under a confining pressure equal to that supplied by the FRP jacket. An experimental program was undertaken to assess the validity of this assumption, where 63 actively confined and FRP-confined normal- and high-strength concrete (NSC and HSC) specimens were tested under axial compression. The axial stress-strain and lateral strain-axial strain curves obtained from the two different confinement systems were assessed. The results indicate that, at a given axial strain, lateral strains of actively confined and FRP-confined concretes correspond, when they are subjected to the same lateral confining pressure. It is found that at the points of intersection on the lateral strain-axial strain curves, FRP-confined NSC exhibits only slightly lower axial compressive stresses compared to those of actively confined NSC. On the other hand, the difference between the axial stresses of actively confined and FRP-confined HSC is found to be significant, indicating that the compressive behavior of confined HSC is more sensitive to the application path of confining pressure than the behavior of confined NSC. Using the combined results of the present study and two comprehensive experimental databases of actively confined and FRP-confined concretes, an expression has been developed for the prediction of the difference in the confining pressures that results in differences in the axial stresses between actively confined and FRP-confined concretes.

KEYWORDS: Concrete; High-strength concrete (HSC); Fiber reinforced polymer (FRP); Confinement; Stress-strain relations; Active; Triaxial; Compression; Stress path; Lateral strain; Axial strain.

1. INTRODUCTION

It is well established that lateral confinement of concrete enhances its compressive strength and deformability (Kent and Park 1971; Sheikh and Uzumeri 1980; Mander et al. 1988; Saatcioglu and Razvi 1992; Pantazopoulou 1995; Imran and Pantazopoulou 2001; Ozbakkaloglu and Saatcioglu 2007; Ozbakkaloglu et al. 2013). Since the 1920s, a significant research effort has been dedicated to understanding the behavior of concrete under lateral confinement. More recently, research attention has turned to the potential applications of fiber reinforced polymer (FRP) composites as concrete confinement in retrofitting existing concrete columns (Lam and Teng 2004; Ilki et al. 2008; Rousakis and Karabinis 2012; Wu and Jiang 2013) and in the construction of new high-performance composite columns (Ozbakkaloglu 2013a,b; Ozbakkaloglu and Louk Fanggi 2013; Vincent and Ozbakkaloglu 2013a,b; Ozbakkaloglu and Idris 2014; Ozbakkaloglu and Louk Fanggi 2014). A comprehensive review of the literature that was undertaken as part of the current study and those previously reported in Ozbakkaloglu and Lim (2013), Ozbakkaloglu et al. (2013), and Lim and Ozbakkaloglu (2014a,b) revealed that over 500 experimental studies have been conducted on the axial compressive behavior of unconfined, actively confined and FRP-confined concretes, resulting in the development of over 110 stress-strain models. Among these models, the analysis-oriented models were found to be particularly versatile as they are applicable to both actively confined and FRP-confined concretes. Through the use of the stress-strain curves of actively confined concrete, these models are capable of establishing the complete axial stress-strain and lateral strain-axial strain curves of FRP-confined concrete on the basis of the interaction mechanism between the external confining jacket and the internal concrete core. Such models (e.g., (Fam and Rizkalla 2001; Harries and Kharel 2002; Marques et al. 2004; Binici 2005; Albanesi et al. 2007; Jiang and Teng 2007; Teng et al. 2007; Xiao et al. 2010)) are built on the assumption that the axial compressive stress and strain of FRP-confined concrete at a given lateral strain are the same as those of the concrete actively confined under a confining pressure equal to that supplied by the FRP jacket. However, this assumption, known as the stress path independency assumption, is yet to be validated experimentally through investigation of companion actively confined and FRP-confined specimens.

In the experimental study reported in this paper, axial compression tests were conducted on actively confined and FRP-confined normal-strength concrete (NSC) and high-strength concrete (HSC) specimens to study the influence of the application path of confining pressure, and thereby to assess the validity of the stress path independency assumption. An extensive review of the literature (Ozbakkaloglu and Lim 2013; Lim and Ozbakkaloglu 2014a,b) has revealed that the study reported in this paper is the first to investigate this influence through a carefully planned experimental program, which consisted of companion actively confined and FRP-confined concrete specimens with identical geometrical and material properties.

2. EXPERIMENTAL PROGRAM

2.1 Test Specimens

A total of 63 specimens were prepared from two batches of concretes. As shown in Table 1, 38 of the specimens were NSC, whereas 25 were HSC. Five of the specimens were unconfined, 31 were confined using a hydraulic Hoek cell, and 27 were confined using FRP jackets. A minimum of two up to a maximum of five nominally identical specimens were tested for each unique specimen configuration.

Table 1. Number and distribution of test specimens

Specimens	Concrete grade	
	NSC	HSC
Unconfined	3	2
Actively confined	17	14
AFRP-confined	6	3
CFRP-confined	7	3
GFRP-confined	5	3
Total	38	25

(a) (b)

Figure 1. (a) Concrete block after specimen coring; and (b) specimens cured in fog room

The dimensions of the specimens used in the study were prescribed by the geometry of the Hoek cell. To attain consistent geometric and material properties among the specimens tested under the different confinement conditions, each batch of concrete used to fabricate the companion actively confined and FRP-confined specimens was cast in a large block measuring 410 × 410 × 140 mm, from which cylindrical cores of 63 mm diameter were extracted. The cores were then ground to lengths of 126 mm using a surface grinding machine to remove irregularities and soft concrete from specimen ends, and to ensure that the specimen ends were orthogonal to the longitudinal axis. Figure 1(a) shows a concrete block with cores extracted, and Figure 1(b) shows the cored specimens being moist-cured in a fog room, where they remained for at least 28 days at 100% relative humidity.

2.2 Materials

The mix proportions of the NSC and HSC mixes are provided in Table 2. Crushed bluestones of 5 mm maximum size and graded sand were used as the coarse and fine aggregates. Carboxylic ether polymer based superplasticiser was used in both batches, which contained 80% water by weight. The average test-day compressive strengths of the NSC and HSC specimens were 51.6 and 128.0 MPa, respectively.

Table 2. Mix proportions of normal and high-strength concretes

Batch	NSC	HSC
Cement (kg/m^3)	410	490
Silica fume (kg/m^3)	35	45
Sand (kg/m^3)	710	710
Gravel (kg/m^3)	1060	1060
Water (kg/m^3)	235	110
Superplasticiser (kg/m^3)	15	30
Water-cementitious binder ratio	0.555	0.252
Maximum aggregate size (mm)	5	5
Slump height (mm)	240	160

The FRP composite materials of the confining jackets were fabricated from fiber sheet and epoxy adhesive. The two part FRP epoxy adhesive consisted of an epoxy resin binder (MBrace Saturant) and thixotropic epoxy adhesive (MBrace Laminate Adhesive), mixed in the ratio of 3:1. The material properties of the unidirectional fiber sheets are provided in Table 3. The table reports both the manufacturer supplied fiber properties and the tensile tested FRP composite properties. The tensile properties of the FRP composite were determined from flat coupon tests undertaken in accordance with ASTM D3039 (2008).

Table 3. Material properties of fibers and FRP composites

Type	Nominal thickness t_f (mm/ply)	Provided by manufacturers			Obtained from coupon tests*		
		Tensile strength f_{fu} (MPa)	Ultimate tensile strain ε_{fu} (%)	Elastic modulus E_f GPa)	Tensile strength f_{frp} (MPa)	Ultimate tensile strain ε_{frp} (%)	Elastic modulus E_{frp} (GPa)
Aramid	0.200	2600	2.20	118.2	2390	1.86	128.5
Carbon	0.111	4370	1.90	230.0	4152	1.76	236.0
S-Glass	0.200	3040	3.50	86.9	3055	3.21	95.3

* calculated based on nominal thickness of fibers

(a) (b)

Figure 2. (a) Hoek cell of actively confined specimen; and (b) jacketing of FRP-confined specimens

2.3 Concrete Confinement

As illustrated in Figures 2(a) and 2(b), two confinement systems, with one producing constant hydrostatic confining pressure using Hoek cell and the other producing passively increasing confining pressure using FRP jackets, were used to confine the test specimens. The actively confined specimens were subjected to 2.5, 5, 7.5, 10, 15, 20, or 25 MPa of applied hydrostatic pressures. The FRP-confined specimens were subjected to different levels of confining pressures resulting from different fiber type and layer arrangements of the FRP jackets. Out of the 27 FRP-confined specimens, nine were wrapped with Aramid FRP (AFRP) jackets, ten with Carbon FRP (CFRP) jackets, and the remaining eight with S-Glass FRP (GFRP) jackets. The specimens were wrapped in the hoop direction with either one or

two layers of epoxy resin impregnated fiber sheets using a manual wet lay-up process. Each specimen was wrapped with a continuous sheet and was provided with a 66-mm long overlap zone, which equates to one-third of the specimen perimeter. The required minimum overlap length to prevent debonding failure was determined from the results of a large number of trials with different overlap lengths.

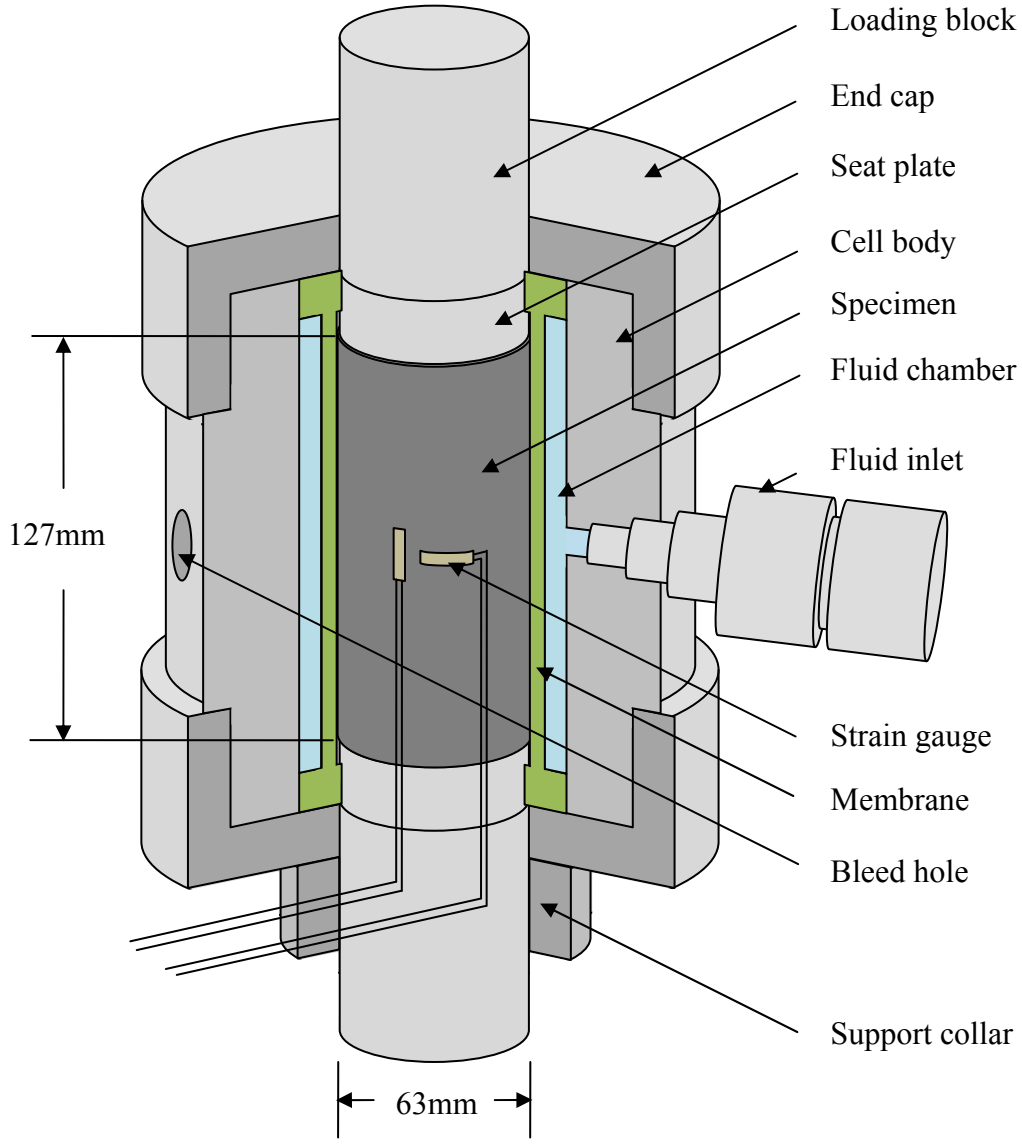

Figure 3. Schematic of the Hoek cell device

2.4 Instrumentation and Testing

The specimens were tested under axial compression using a 1000-kN capacity Instron testing machine that was connected to a computer for command signals and data acquisition. The axial load was applied with displacement control at a rate of 0.003 mm per second. For the actively confined specimens, a 30-MPa capacity Hoek cell was used to apply lateral pressure. The features of the Hoek cell are illustrated in Figure 3. A confining pressure intensifier was used to fill and pressurize the Hoek cell. Before the application of the axial load, the lateral pressure was applied at a load rate of 0.1 MPa per second until the required active confining pressure was achieved. The pressure was then monitored and manually controlled using a pressure gauge and a hand pump.

For the actively confined specimens, the axial load was applied onto the concrete core through the use of a pair of self-aligning spherical seat plates of 63.5-mm diameter placed at the specimen ends, as illustrated in Figure 3. No seat plates were used in the FRP-confined specimens. To avoid direct axial stress transfer from the steel platen onto the FRP jackets of the FRP-confined specimens, the FRP jackets were recessed by 1 mm at both ends of the specimens. As illustrated in Figure 2(b), the recesses were achieved through the use of timber blocks notched with 1 mm rebates and clamped on the specimen ends during FRP wrapping.

As illustrated in Figure 4, the lateral strain of the actively confined specimens was measured using four 10-mm unidirectional strain gauges placed at the mid-height of the specimens. To prevent shear damage and interference from friction caused by the Hoek cell membrane to the strain gauges, a thin coating of lubricating wax was smeared over the strain gauges and their wires prior to the insertion of the specimens into the membrane. These gauges were connected to their terminals outside the Hoek cell through the use of 0.25 mm enamel coated copper wires. The lateral strain on the FRP-confined specimens was measured using six 5-mm unidirectional strain gauges placed at the mid-height of the specimens. The axial strains of both the actively confined and FRP-confined specimens were measured using three types of instruments: (i) two linear variable displacement transformers (LVDTs) mounted at the steel loading platens with a gauge length of 127 mm; (ii) the in-built extensometer of the testing machine; (iii) two axial strain gauges placed at mid-height 180° apart.

2.5 Specimen Designation

The results of specimens in Tables 4 and 5 were labeled as follows: the first letter N or H stood for the concrete grade (i.e., normal or high-strength concretes), after which the unconfined concrete strength was given; the second letter T, A, C or G stood for the type of confinement (i.e. triaxial, AFRP, CFRP, or GFRP), after which the applied hydrostatic pressure or the number of FRP layers was supplied; the last number in the specimen designation (i.e., 1 to 5) was used to distinguish the nominally identical specimens.

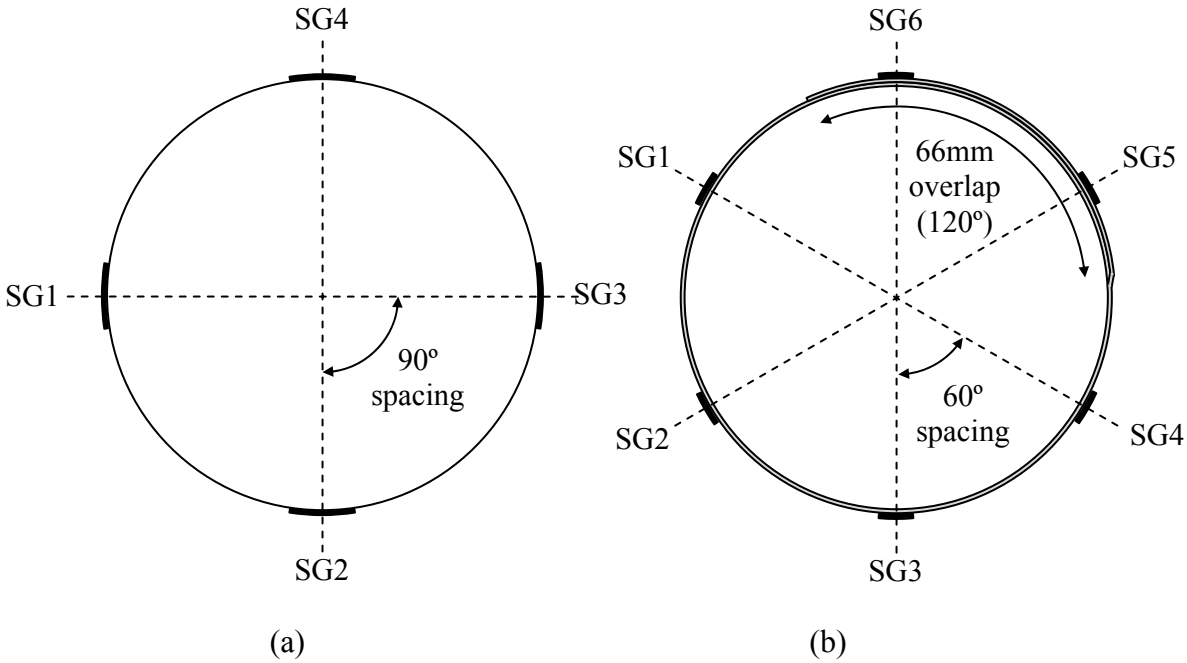

Figure 4. Lateral strain gauge arrangements of: (a) actively confined specimens; and (b) FRP-confined specimens

3. TEST RESULTS AND DISCUSSION

3.1 Failure Modes

Typical failure modes of the actively confined and FRP-confined specimens are shown in Figures 5(a) to 5(e). As illustrated in the figures, the actively confined specimens failed due to concrete crushing, whereas all of the FRP-confined specimens failed due to the ruptures of FRP jackets triggered by the expansion of concrete as a result of progressive crushing. As can be seen from Figures 5(b) to 5(d), the rupture of the FRP-confined NSC specimens occurred at mid-height. In these specimens, damage in the concrete was more evenly distributed, as evident from the large portion of the crushed concrete inside the rupture openings (Figures 5(b) to 5(d)). In the FRP-confined HSC specimens, on the other hand, damage to the concrete was localized around a few macrocracks, as illustrated in Figure 5(e).

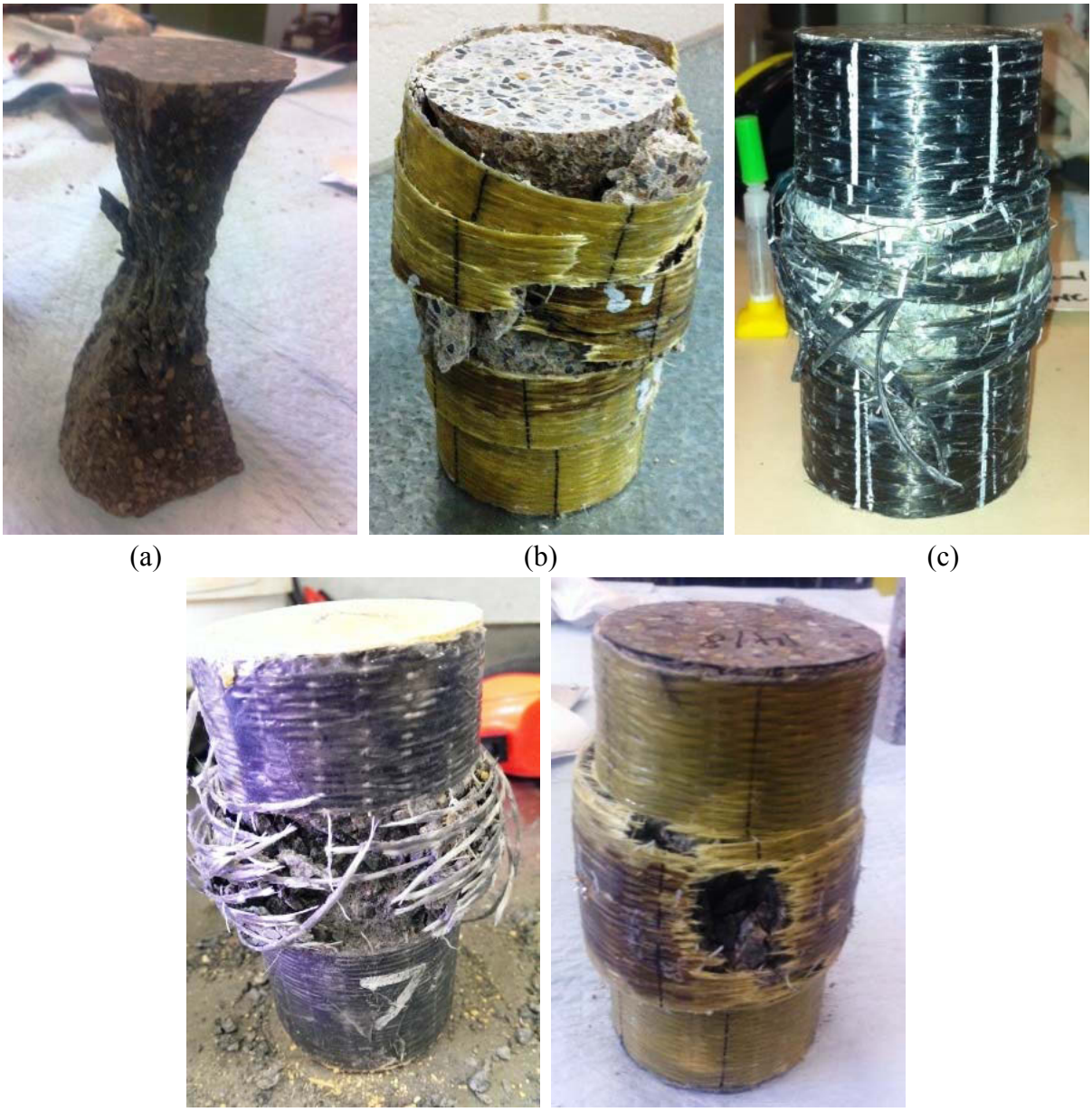

Figure 5. Failure modes of: (a) actively confined NSC; (b) AFRP-confined NSC; (c) CFRP-confined NSC; (d) GFRP-confined NSC; and (e) AFRP-confined HSC specimens

3.2 Peak, Residual and Ultimate Conditions

The representative stress-strain relationships of the unconfined, actively confined, and FRP-confined specimens are presented in Figure 6. The full sets of curves of all specimens are presented in Figures S1 to S8 in Appendix. As illustrated in Figure 6, the peak condition of actively confined concrete is characterized by the peak stress (f^*_{cc}), and the corresponding axial strain (ε^*_{cc}) and lateral strain (ε^*_{lc}). The residual condition is characterized by the residual stress ($f_{c,res}$), and the corresponding axial strain ($\varepsilon_{c,res}$). The test results summarizing the peak and residual conditions of the unconfined and actively confined specimens are given in Table 4. In Table 4, the lateral strain at peak stress (ε^*_{lc}) of the actively confined specimens were averaged from the measurements of four lateral strain gauges placed at mid-height of the specimens. The axial strain at peak stress (ε^*_{cc}) was obtained from the two steel platen mounted LVDTs that measured the displacements along the entire height of the specimens. It was not possible to obtain the residual conditions of the NSC specimens due to the termination of the tests at around 5% of lateral strain, in order to prevent the membrane of the Hoek cell from damage. As for the residual conditions of the HSC specimens, it was possible to obtain the axial stresses ($f_{c,res}$) and strains ($\varepsilon_{c,res}$) but not the lateral strains ($\varepsilon_{l,res}$) due to the exceedence of the strain capacity of the lateral strain gauges at that stage of testing.

The ultimate condition of the FRP-confined concrete is characterized by the compressive strength (f'_{cc}), and the corresponding axial strain (ε_{cu}) and lateral strain ($\varepsilon_{h,rup}$) recorded at the rupture of the FRP jacket (Figure 6). The test results summarizing the ultimate conditions of the FRP-confined specimens are provided in Table 5. In Table 5, the hoop rupture strains ($\varepsilon_{h,rup}$) of the FRP-confined specimens were averaged from the measurements of four lateral strain gauges placed outside the FRP overlap regions. The ultimate axial strain (ε_{cu}) was obtained from the two steel platen mounted LVDTs that measured the displacement along the entire height of the specimens.

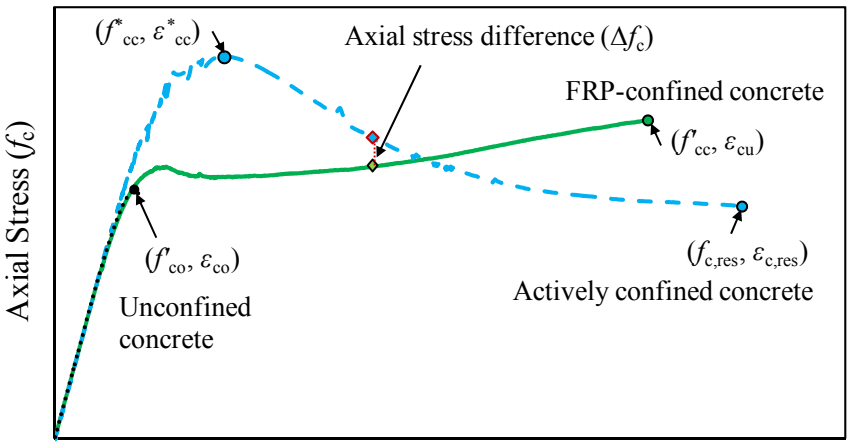

(a)

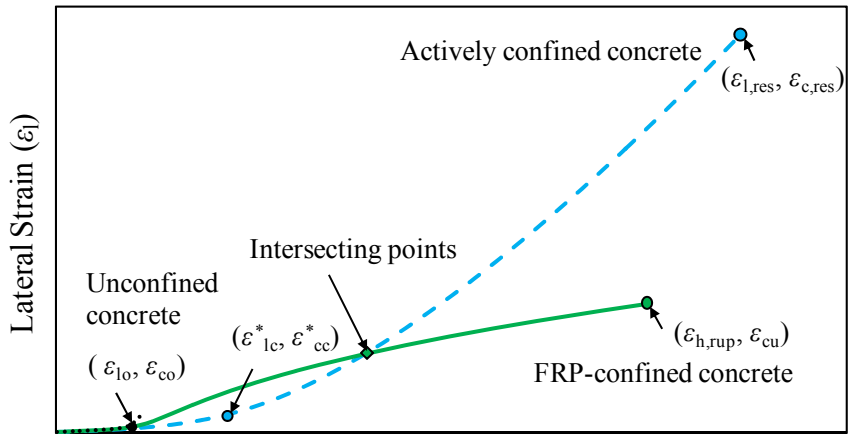

(b)

Figure 6. (a) Typical axial stress-strain curves; and (b) lateral strain-axial strain curves of actively-confined, FRP-confined and unconfined concretes

Table 4. Test results of unconfined and actively confined concrete specimens

Specimen	f'_{co} (MPa)	f^*_l (MPa)	f^*_{cc} (MPa)	ε^*_{cc} (%)	ε^*_{lc} (%)	$f_{c,res}$ (MPa)	$\varepsilon_{c,res}$ (%)
N52-T0-1		0	50.4	0.20	0.13	-	-
N52-T0-2		0	56.3	0.29	0.11	-	-
N52-T0-3		0	48.3	-	-	-	-
N52-T5-1		5	75.1	0.65	0.36	-	-
N52-T5-2		5	68.9	0.75	0.45	-	-
N52-T5-3		5	75.2	0.73	0.28	-	-
N52-T7.5-1		7.5	84.6	1.20	0.60	-	-
N52-T7.5-2		7.5	79.3	1.46	0.86	-	-
N52-T10-1		10	91.2	2.02	1.41	-	-
N52-T10-2	51.6	10	96.4	1.87	1.08	-	-
N52-T10-3		10	92.1	2.18	1.28	-	-
N52-T15-1		15	115.2	2.84	2.19	-	-
N52-T15-2		15	111.6	3.26	2.61	-	-
N52-T15-3		15	116.9	2.79	1.70	-	-
N52-T20-1		20	135.1	2.24	0.90	-	-
N52-T20-2		20	136.7	3.36	1.72	-	-
N52-T20-3		20	135.4	3.40	1.34	-	-
N52-T25-1		25	158.4	4.20	2.05	-	-
N52-T25-2		25	158.0	3.96	1.84	-	-
N52-T25-3		25	158.4	4.53	2.11	-	-
H128-T0-1		0	127.0	0.32	0.26	-	-
H128-T0-2		0	128.9	0.31	0.18	-	-
H128-T2.5-1		2.5	139.7	0.35	0.23	27.9	1.31
H128-T2.5-2		2.5	146.5	0.36	0.24	40.7	1.36
H128-T5-1		5	156.2	0.40	0.24	51.1	1.53
H128-T5-2		5	156.1	0.41	0.17	47.5	2.23
H128-T7.5-1		7.5	172.0	0.49	0.20	56.9	2.11
H128-T7.5-2	128.0	7.5	175.0	0.50	0.28	53.2	1.85
H128-T10-1		10	179.1	0.54	0.24	76.6	2.78
H128-T10-2		10	181.9	0.52	0.19	58.7	2.49
H128-T15-1		15	203.1	0.68	0.35	111.8	2.76
H128-T15-2		15	199.1	0.65	0.33	121.2	2.61
H128-T20-1		20	227.5	0.79	0.39	130.0	2.75
H128-T20-2		20	225.1	0.83	0.39	119.2	2.87
H128-T25-1		25	244.2	0.95	0.43	134.5	3.66
H128-T25-2		25	241.4	0.93	0.45	140.3	4.17

Table 5. Test results of FRP-confined concrete specimens

Specimen	f'_{co} (MPa)	FRP Type	Layer	f'_{cc} (MPa)	ε_{cu} (%)	$\varepsilon_{h,rup}$ (%)	$f_{lu,a}$ (MPa)
N52-A1-1		AFRP	1	103.3	2.68	1.71	12.8
N52-A1-2		AFRP	1	106.7	2.91	1.84	13.8
N52-A1-3		AFRP	1	103.2	3.02	1.87	14.0
N52-A2-1		AFRP	2	165.9	4.08	1.61	24.2
N52-A2-2		AFRP	2	170.3	4.61	1.72	25.8
N52-A2-3		AFRP	2	169.3	4.64	1.89	28.4
N52-C1-1		CFRP	1	97.4	2.61	1.50	12.2
N52-C1-2		CFRP	1	96.3	2.19	1.34	10.9
N52-C2-1	51.6	CFRP	2	153.6	3.68	1.47	23.8
N52-C2-2		CFRP	2	149.4	3.94	1.54	25.0
N52-C2-3		CFRP	2	150.6	3.57	1.45	23.5
N52-C2-4		CFRP	2	150.1	3.64	1.41	22.9
N52-C2-5		CFRP	2	157.1	3.90	1.98	32.1
N52-G1-1		GFRP	1	101.2	3.03	2.35	13.0
N52-G1-2^{p}		GFRP	1	81.7	2.32	1.64	9.0
N52-G2-1		GFRP	2	153.7	4.31	2.19	24.2
N52-G2-2		GFRP	2	152.9	4.50	2.25	24.8
N52-G2-3		GFRP	2	174.7	5.18	2.44	26.9
H128-A2-1		AFRP	2	161.0	1.74	1.77	26.5
H128-A2-2		AFRP	2	145.8	1.70	1.71	25.7
H128-A2-3		AFRP	2	138.9	1.65	1.62	24.3
H128-C2-1		CFRP	2	137.6	1.38	1.30	21.1
H128-C2-2	128.0	CFRP	2	129.4	1.50	1.22	19.8
H128-C2-3^{P}		CFRP	2	150.0	1.24	1.17	19.0
H128-G2-1		GFRP	2	161.8	2.15	2.34	25.8
H128-G2-2		GFRP	2	166.3	2.25	2.36	26.0
H128-G2-3		GFRP	2	151.9	1.98	2.13	23.5

p denotes prematurely failed specimens

3.4 Intersection Points of Lateral Strain-Axial Strain Curves

Figures 7 to 15 show the comparison of the axial stress-strain and lateral strain-axial strain curves of actively confined and FRP-confined specimens. As can be seen from Figures 7(a) to 15(a), the lateral strain-axial strain curves of the FRP-confined specimens intersect the curves of the actively confined specimens sequentially in the order of increasing confining pressure. To study the influence of the applied confining pressure on the lateral and axial strains of concretes in the two different types of confinement systems, the confinement ratios of actively confined and FRP-confined specimens at the intersecting points of their lateral strain-axial strain curves, as marked in Figures 7(a) to 15(a), were compared. Figures 16(a) and 16(b) show the comparison of the confinement ratios of FRP-confined (f_l/f'_{co}) and actively confined (f^*_l/f'_{co}) specimens at the points of intersection for NSC and HSC, respectively. As can be seen from Figures 16(a) and 16(b), the confinement ratios of the actively confined and FRP-confined specimens at the points of intersection are close to each other and yield a strong correlation. These observations suggest that the lateral strain-axial strain relationships of both actively confined and FRP-confined NSC and HSC depend only on the instantaneous confining pressure at the corresponding axial strain, and not on the application path of the confining pressure.

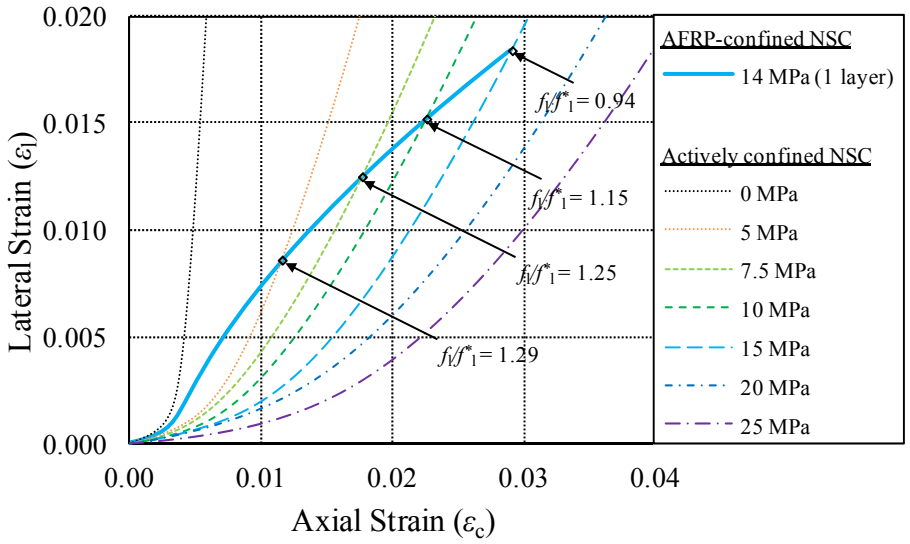

(a)

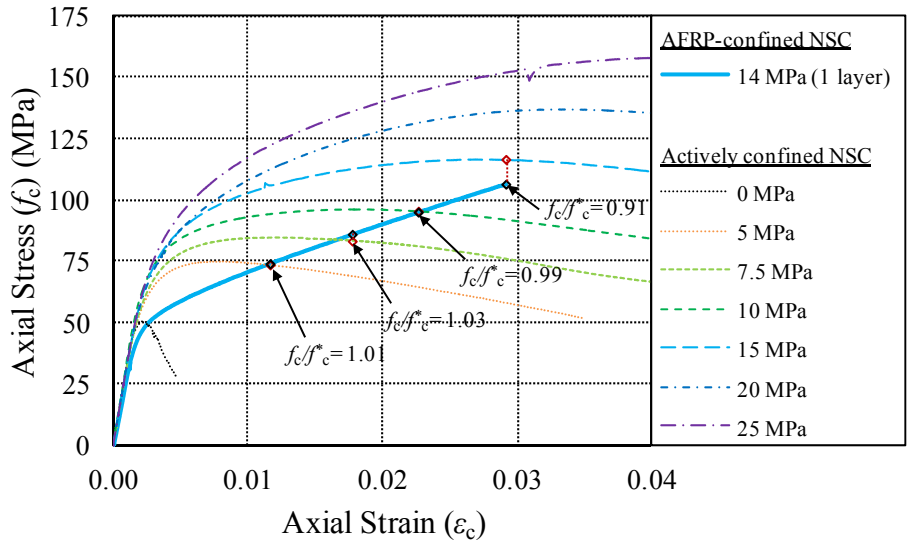

(b)

Figure 7. Comparison of actively confined and 1-layer-AFRP-confined NSC specimens: (a) lateral strain-axial strain curves; (b) axial stress-strain curves

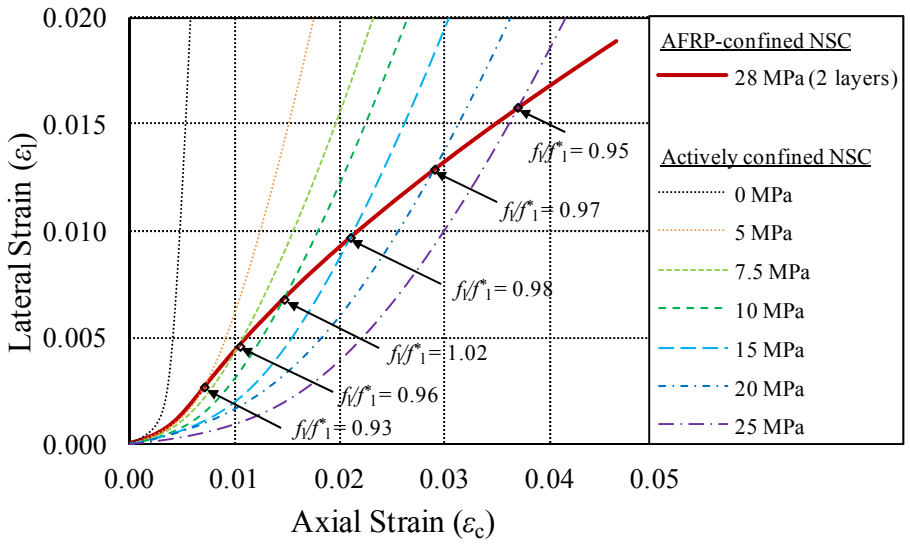

(a)

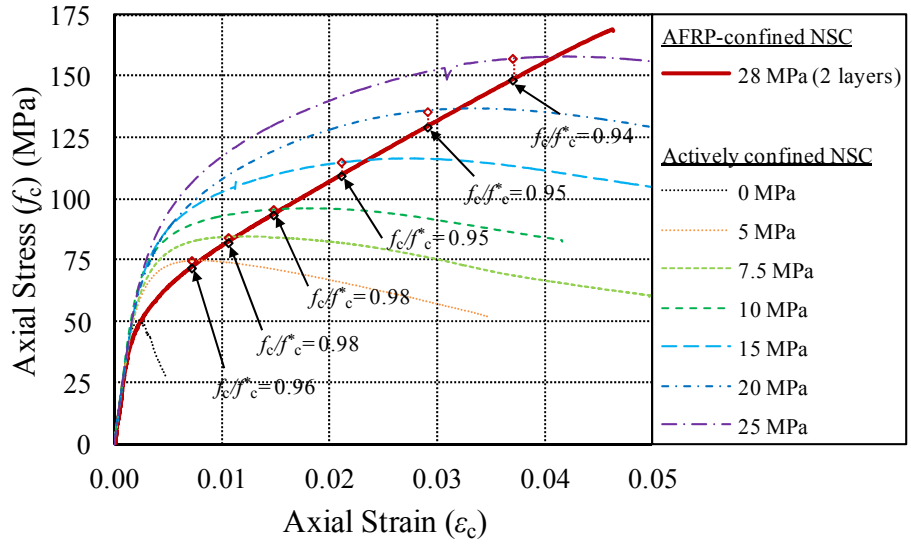

(b)

Figure 8. Comparison of actively confined and 2-layer-AFRP-confined NSC specimens: (a) lateral strain-axial strain curves; (b) axial stress-strain curves

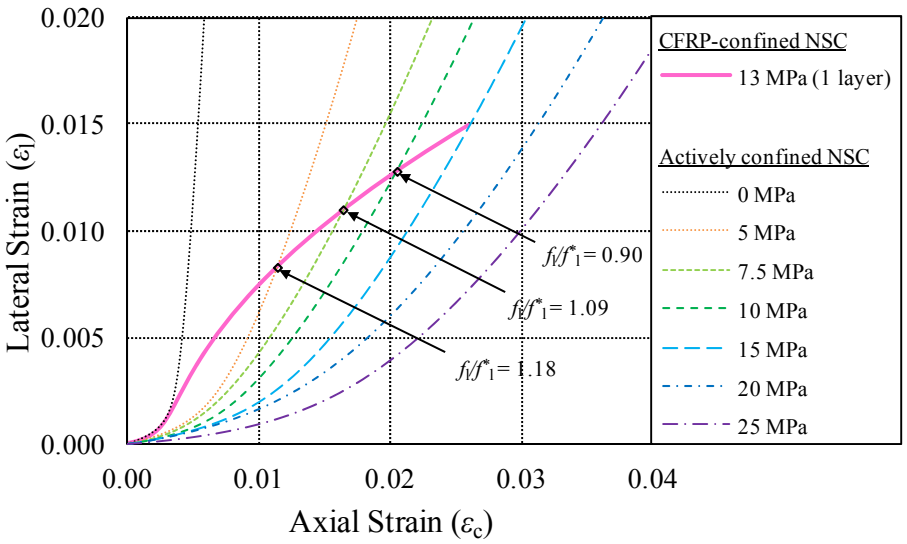

(a)

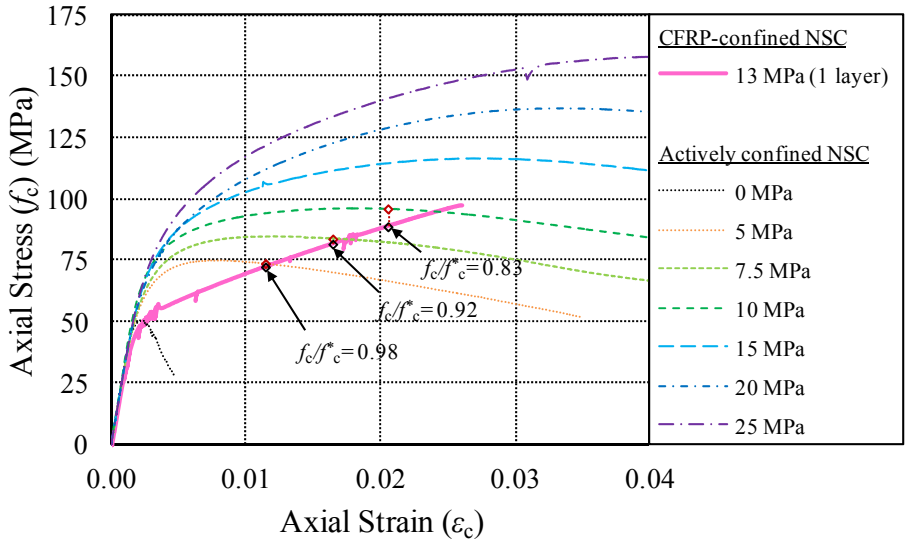

(b)

Figure 9. Comparison of actively confined and 1-layer-CFRP-confined NSC specimens: (a) lateral strain-axial strain curves; (b) axial stress-strain curves

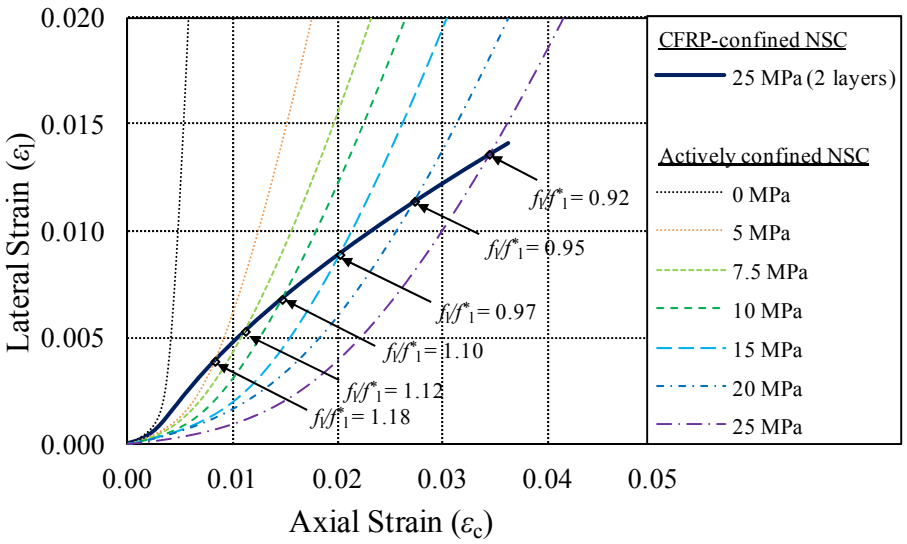

(a)

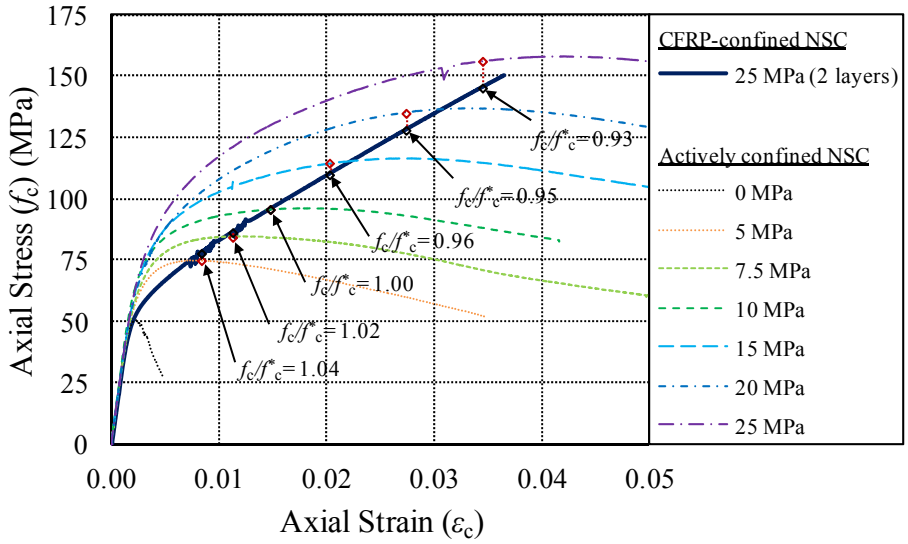

(b)

Figure 10. Comparison of actively confined and 2-layer-CFRP-confined NSC specimens: (a) lateral strain-axial strain curves; (b) axial stress-strain curves

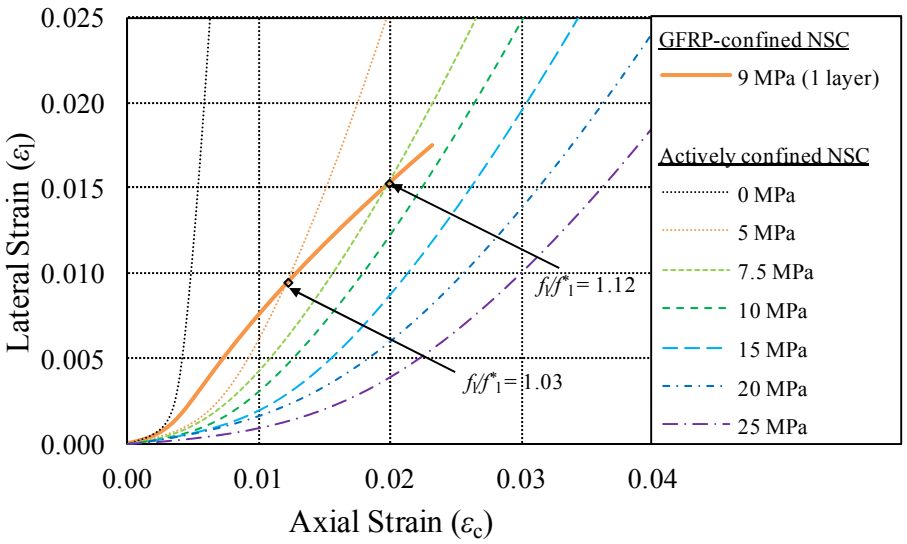

(a)

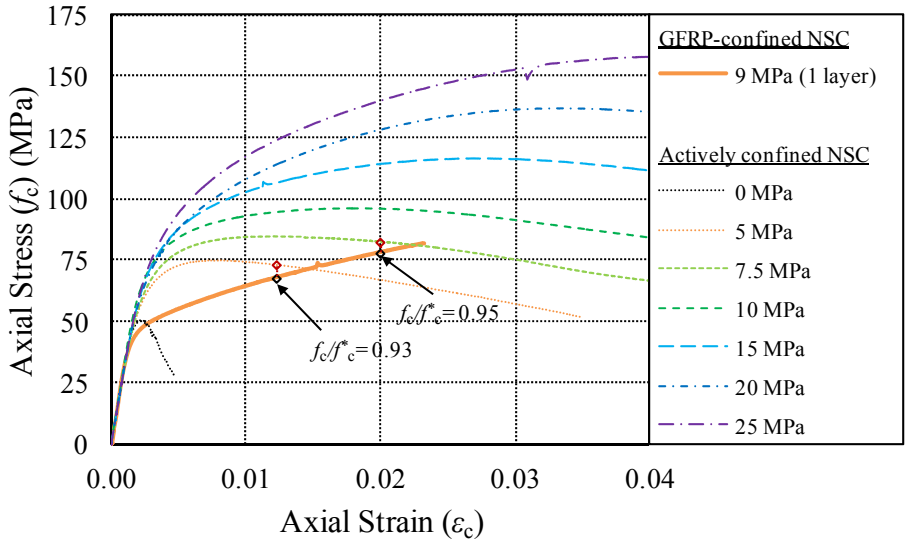

(b)

Figure 11. Comparison of actively confined and 1-layer-GFRP-confined NSC specimens: (a) lateral strain-axial strain curves; (b) axial stress-strain curves

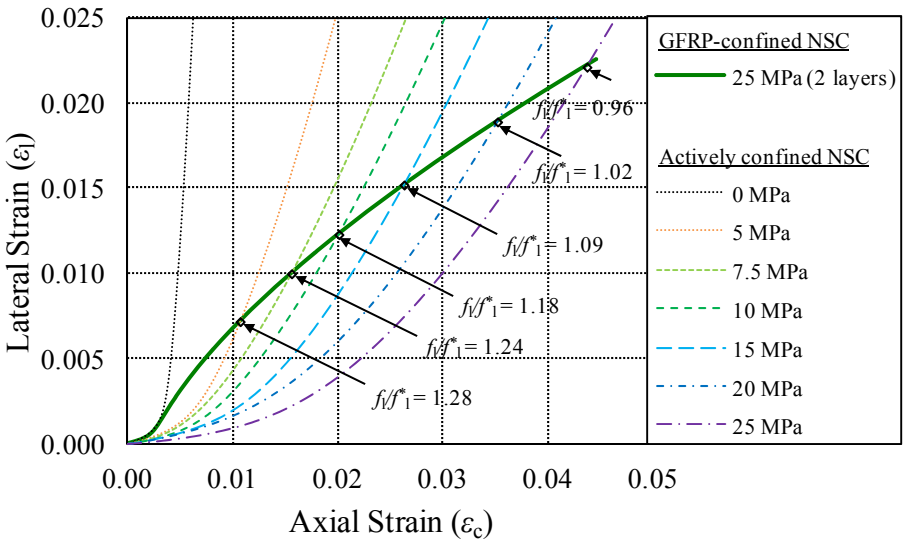

(a)

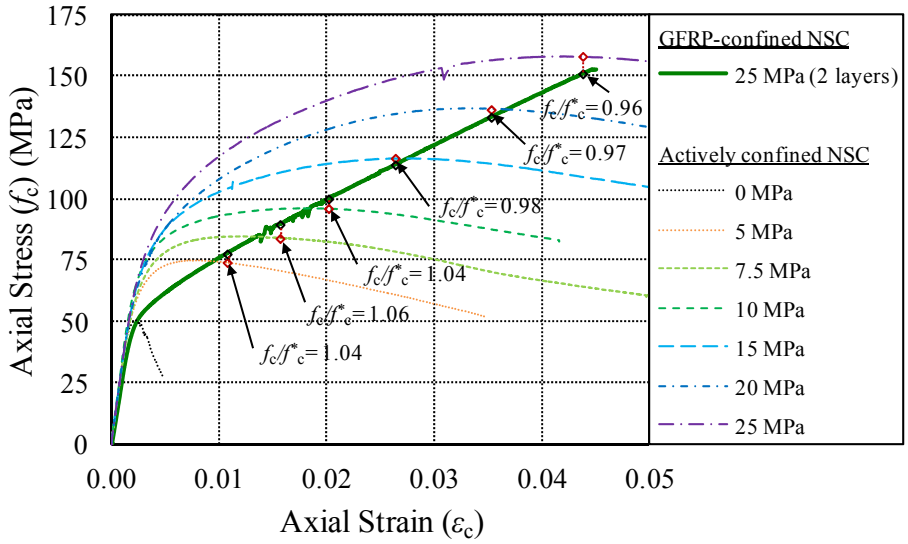

(b)

Figure 12. Comparison of actively confined and 2-layer-GFRP-confined NSC specimens: (a) lateral strain-axial strain curves; (b) axial stress-strain curves

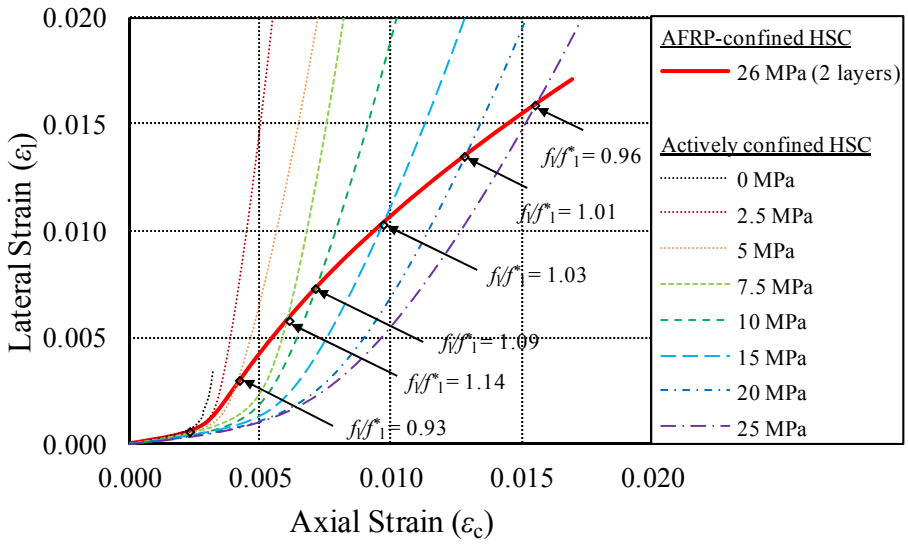

(a)

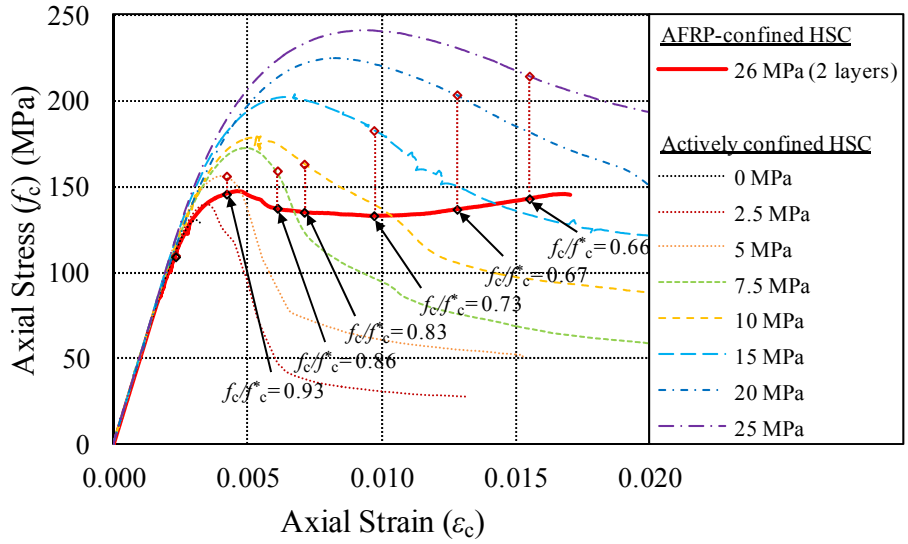

(b)

Figure 13. Comparison of actively confined and AFRP-confined HSC specimens: (a) lateral strain-axial strain curves; (b) axial stress-strain curves

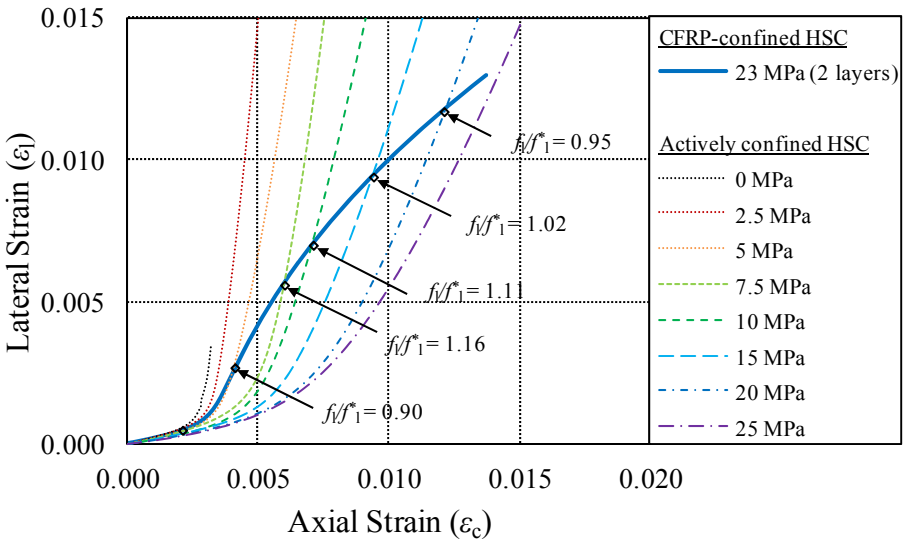

(a)

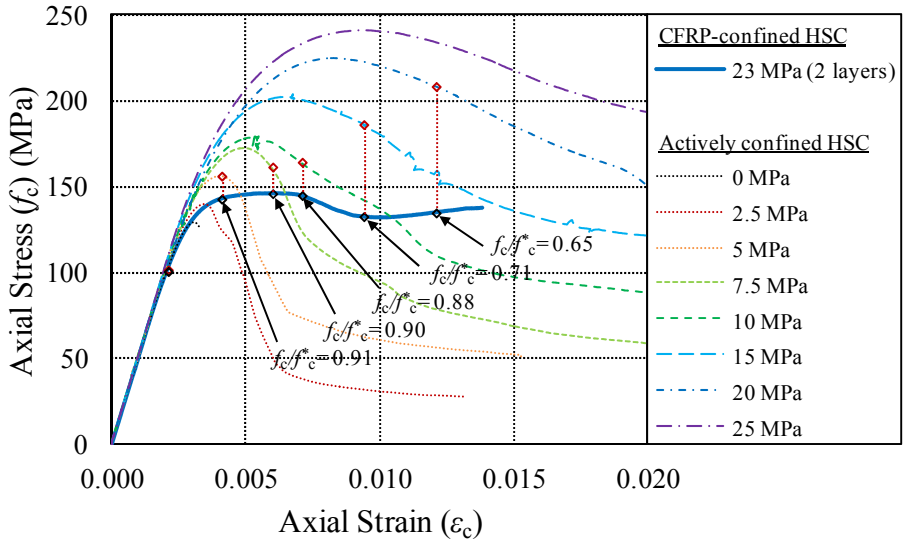

(b)

Figure 14. Comparison of actively confined and CFRP-confined HSC specimens: (a) lateral strain-axial strain curves; (b) axial stress-strain curves

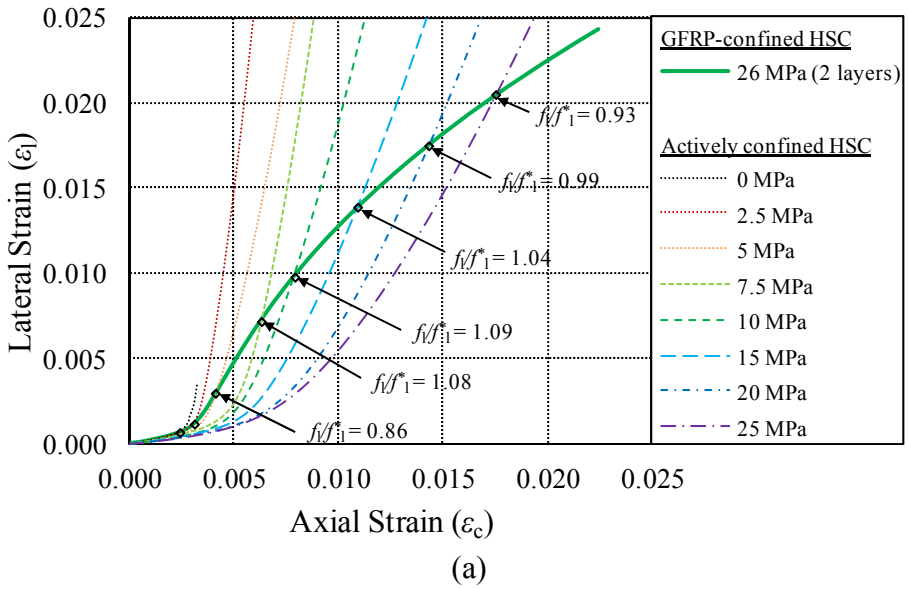

(a)

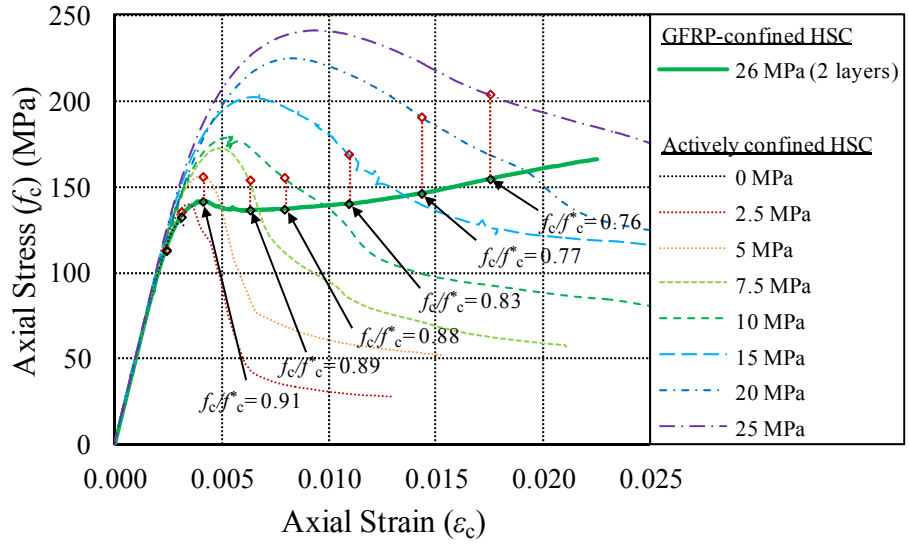

(b)

Figure 15. Comparison of actively confined and GFRP-confined HSC specimens: (a) lateral strain-axial strain curves; (b) axial stress-strain curves

3.5 Axial Stress Difference in Stress-Strain Curves of Active and FRP-Confined Concretes

To compare the levels of axial stresses achieved in specimens confined by the two different systems, the coordinates of the axial stresses and axial strains corresponding to the points of intersection in Figures 7(a) to 15(a) are marked in Figures 7(b) to 15(b). Figures 7(a) to 15(a) illustrate that the confinement ratios of actively confined (f^*_l/f'_{co}) and FRP-confined (f_l/f'_{co}) specimens are comparable at the points of intersections. The relationships between these confinement ratios are summarized in Figure 16 for all the specimens as discussed previously. Figures 7(b) to 12(b) show that, at a given axial and lateral strain and confining pressure, the axial stresses in FRP-confined NSC vary only slightly from those of the corresponding actively confined NSC. On the other hand, as illustrated in Figures 13(b) to 15(b), under the aforementioned conditions the FRP-confined HSC exhibit significantly

lower axial stresses than those of the companion actively confined HSC. These differences in the axial stresses (Δf_c) are clear evidence that, at a given axial and lateral strain and confining pressure, the magnitude of axial stresses on the axial stress-strain relationships of confined concrete is dependent on the application path of confining pressure, and hence varies from one confinement system to another.

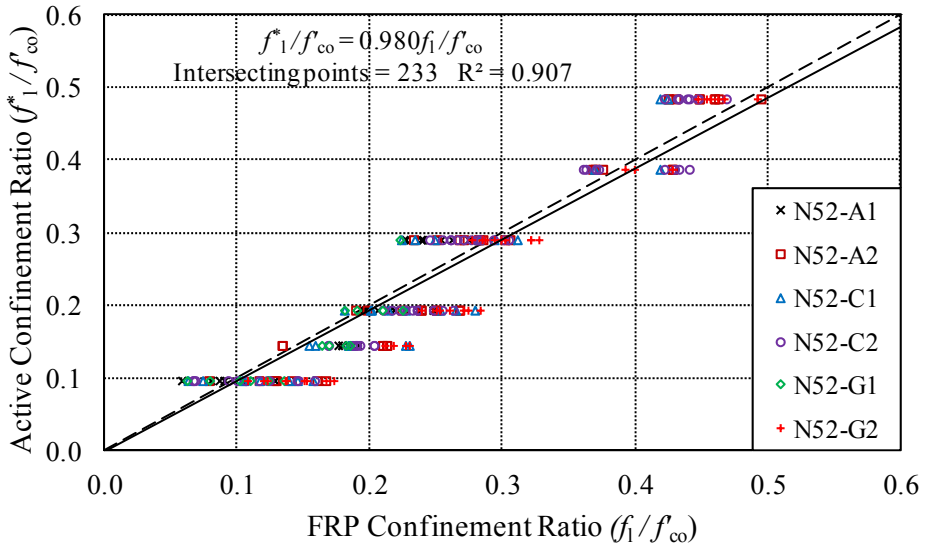

(a)

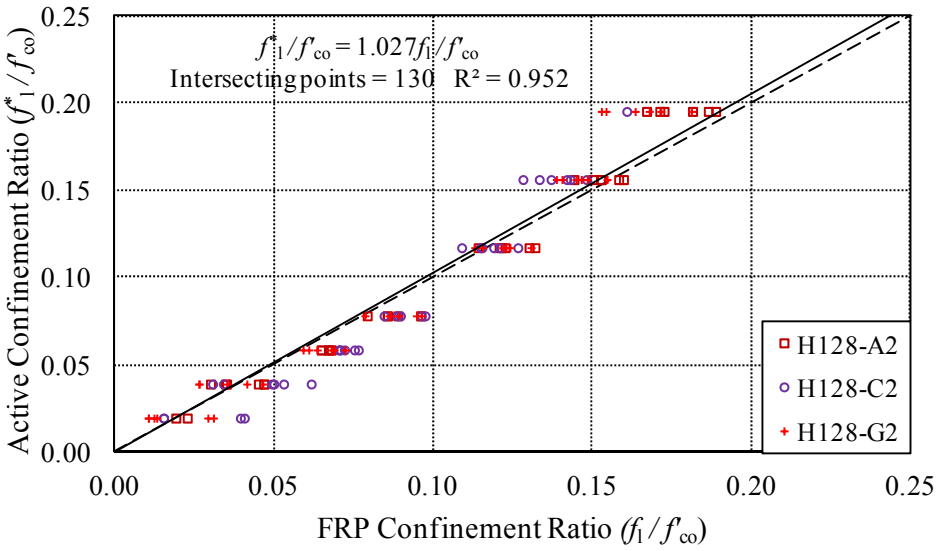

(b)

Figure 16. Confinement ratios of actively confined concrete (f^*_l/f'_{co}) and FRP-confined concrete (f_l/f'_{co}) at points of intersection on lateral strain-axial strain curves of: (a) NSC specimens; and (b) HSC specimens

The difference in the axial stresses between FRP-confined and actively confined concrete can be quantified in terms of an axial stress ratio (f_c/f^*_c). To study the change in the axial stress ratio of FRP-confined concrete-to-actively confined concrete (f_c/f^*_c) with the FRP confinement ratio (f_l/f'_{co}), companion FRP-confined and actively confined specimens having similar confinement ratios (i.e. $f_l/f'_{co} \approx f^*_l/f'_{co}$ with a difference no more than 20% from the average of the two values)

at the intersecting points of their lateral strain-axial strain curves were identified. Figures 17(a) and 17(b) illustrate the relationship between the axial stress ratio (f_c/f^*_c) and the confinement ratio (f_l/f'_{co}) for the NSC and HSC specimens, respectively. Figure 17(a) shows that, for the NSC specimens, the axial stress ratio (f_c/f^*_c) reduces slightly with an increase in the confinement ratio (f_l/f'_{co}). On the other hand, for the HSC specimens, the axial stress ratio (f_c/f^*_c) decreases significantly with an increase in the confinement ratio (f_l/f'_{co}), as illustrated in Figure 17(b).

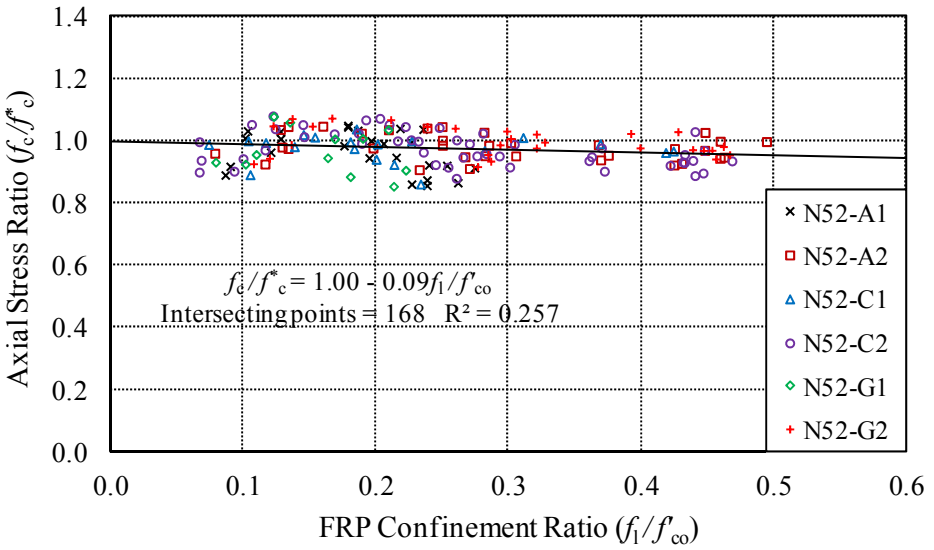

(a)

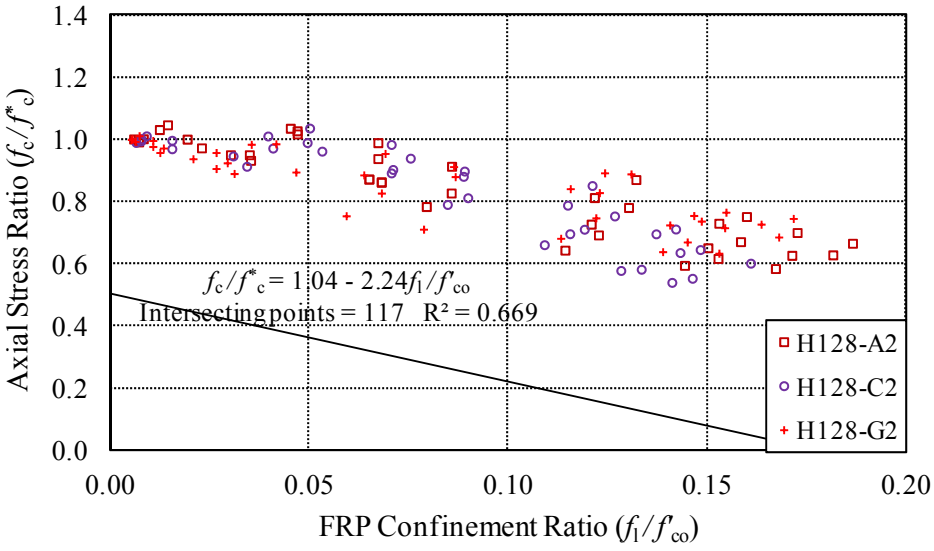

(b)

Figure 17. Variation of axial stress ratio of FRP-confined concrete-to-actively confined concrete (f_c/f^*_c) with FRP confinement ratio(f_l/f'_{co}) of: (a) NSC specimens; (b) HSC specimens

As evident from the difference in the trendlines of the relationships shown in Figures 17(a) and 17(b), the axial stress ratio (f_c/f^*_c) is influenced significantly by concrete strength (f'_{co}). This accords with the previous observations from Figures 7(b) to 15(b), where it was found that, at a given axial and lateral strain and confining pressure, the observed differences in axial stresses

(Δf_c) between actively confined and FRP-confined specimens were more pronounced in HSC compared to that of in NSC. This is an important observation indicating that the difference in strength enhancements observed in actively and passively confined concretes are dependent on the concrete strength and it becomes more significant as the concrete strength increases. This can be attributed to the difference in the cracking patterns of concrete, which varies with its strength (Lim and Ozbakkaloglu 2014a). In FRP-confined NSC, the microcracks formation results in a more uniform distribution of FRP confining pressure; whereas in FRP-confined HSC, the macrocrack formations results in strain localizations that results in a reduced confinement effectiveness and strength enhancement (Lim and Ozbakkaloglu 2014a). On the other hand, in the actively confined HSC the applied confining pressure is constant and is independent of the cracking pattern of concrete. As a result, when axial stresses of companion actively confined and FRP-confined concretes are compared, HSC exhibits a lower axial stress ratio (f_c/f^*_c) than that of NSC.

4. PROPOSED APPROACH FOR ESTIMATING CONFINING PRESSURE GRADIENT BETWEEN ACTIVELY CONFINED AND FRP-CONFINED CONCRETES

Factors influencing the differences in axial stresses between actively confined and FRP-confined concretes were discussed in the preceding section. This section introduces the proposed methodology for estimating the difference in confining pressures, at a given axial stress and axial strain, between actively confined and FRP-confined concretes of the same concrete strength. This difference in confining pressures of the companion actively confined and FRP-confined concretes is referred to in this paper as the confining pressure gradient (i.e. $\Delta f_l = f^*_l - f_l$). To accurately quantify the confining pressure gradient (Δf_l), the test results from two comprehensive experimental databases of actively confined and FRP-confined concretes (Ozbakkaloglu and Lim 2013; Lim and Ozbakkaloglu 2014a,b) were analyzed together with the test results from the present study.

4.1 Databases of actively confined and FRP-confined concretes

The database of actively confined concrete contained 346 datasets assembled from 25 experimental studies. The details of the database can be found in Lim and Ozbakkaloglu (2014b). The unconfined concrete strength (f'_{co}) and strain (ε_{co}), as obtained from concrete cylinder tests, varied from 7.2 MPa to 132.0 MPa and 0.15% to 0.40%, respectively. The active confinement ratio (f^*_l/f'_{co}) varied from 0.004 to 21.67. The database of FRP-confined concrete contained 1063 datasets assembled from 105 experimental studies. The details of the NSC and HSC components of the database can be found in Ozbakkaloglu and Lim (2013) and Lim and Ozbakkaloglu (2014a), respectively. The peak unconfined concrete strength (f'_{co}) and strain (ε_{co}), as obtained from concrete cylinder tests, varied from 6.2 MPa to 169.7 MPa and 0.14% to 0.70%, respectively. The confinement ratio, defined as the ratio of the actual ultimate confining pressure of the FRP jacket to the peak strength of an unconfined concrete specimen ($f_{lu,a}/f'_{co}$), varied from 0.02 to 4.74.

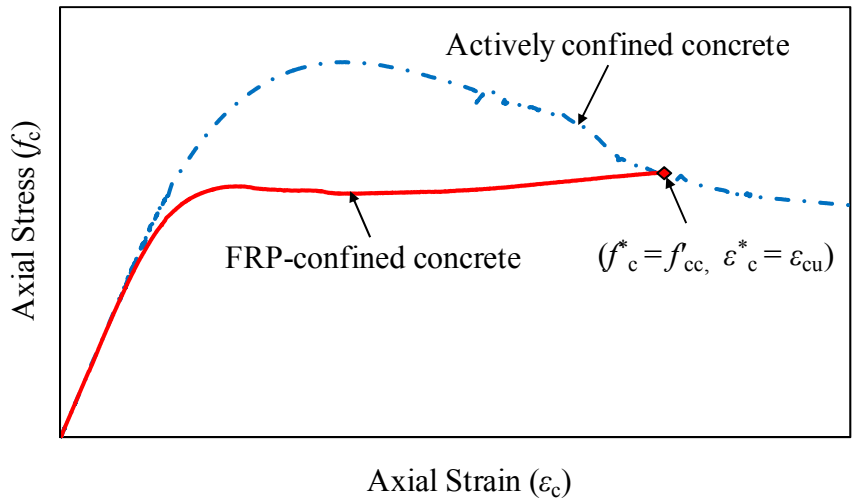

(a)

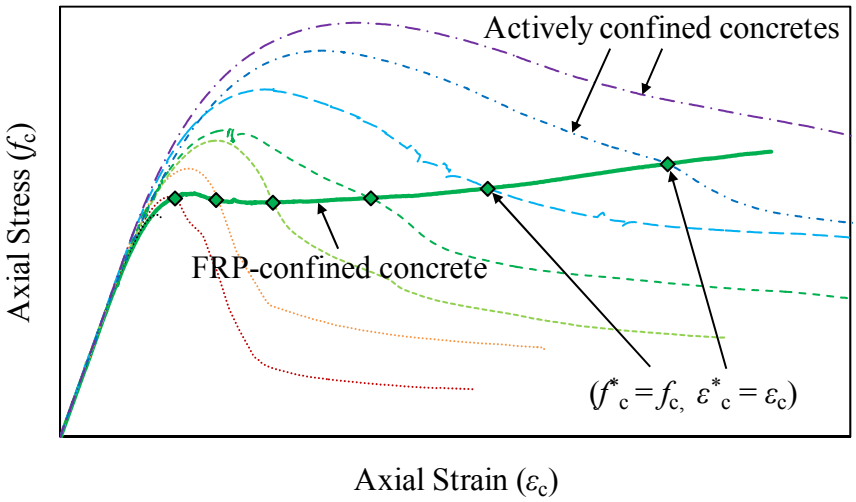

(b)

Figure 18. (a) Point of intersection of ultimate condition of FRP-confined concrete with axial stress-strain curve of actively confined concrete; (b) points of intersection of axial stress-strain curves of FRP-confined and actively confined concretes

4.2 Proposed Expression

Using the test results from the databases, FRP-confined specimens with compressive strengths and the corresponding strains that fall in close proximity to the axial stress-strain curves of actively confined specimens were identified. This process is illustrated in Figure 18(a) and it resulted in identification of 432 matches among 1063 FRP-confined specimens that were available from the database. In identifying these matches, the differences in unconfined concrete strengths (f'_{co}), ratios of axial stress-to-unconfined strength (f^*_c/f'_{co} and f'_{cc}/f'_{co}), and axial strains (ε^*_c and ε_{cu}) between the matching actively confined and FRP-confined specimens were limited to maximum 20%. The confining pressure gradient (Δf_l) between the active confining pressure (f^*_l) and the actual confining pressure of the matching actively confined and FRP-confined specimens ($f_{lu,a}$), calculated from Eq.1, was then established. In the calculation of the actual confining pressure ($f_{lu,a}$), the hoop rupture strains of FRP-confined concrete specimens ($\varepsilon_{h,rup}$) were calculated using Eq. 2 proposed by Lim and Ozbakkaloglu (2014a) for that purpose.

$$f_{lu,a} = K_l \varepsilon_{h,rup} \text{ , where } K_l = 2E_f t_f / D \quad (1)$$

$$\varepsilon_{h,rup} = (0.9 - 2.3 f'_{co} \times 10^{-3} - 0.75 E_f \times 10^{-6}) \varepsilon_{fu} \quad (2)$$

In Eq.1, K_l is the confinement stiffness of the FRP jacket, E_f is the elastic modulus of fibers, t_f is the total nonimal fiber thickness of the FRP jacket, and D is the diameter of the concrete core. In Eq.2, both f'_{co} and E_f are in MPa and ε_{fu} is the ultimate tensile strain of fibers.

In addition to the database results, the confining pressure gradients (Δf_l) were also established for the specimens of the present study through the use of the intersection points on the axial stress-strain curves. This process is illustrated in Figure 18(b), where the confining pressure gradient (Δf_l) were established based on the difference between the active confining pressure (f^*_l) and FRP confining pressure corresponding to the points of intersection (i.e., $f_l = K_l \varepsilon_l$). Using the results from both groups, the parameters affecting the confining pressure gradient (Δf_l) were identified and their relative influences were then established using regression analysis. Based on the results of the regression analysis shown in Figure 19, Eq. 3 is proposed for the prediction of the confining pressure gradient (Δf_l). In Eq. 3, the confining pressure gradient (Δf_l) is expressed as a function of unconfined concrete strength (f'_{co}) and confinement stiffness (K_l), which gradually increases with an increase in the lateral strain (ε_l) and terminates at the hoop rupture strain of FRP ($\varepsilon_{h,rup}$).

$$\Delta f_l = 0.13 {f'_{co}}^{0.24} K_l^{0.95} \varepsilon_l \quad (3)$$

In Eq. 3, both f'_{co} and K_l are in MPa.

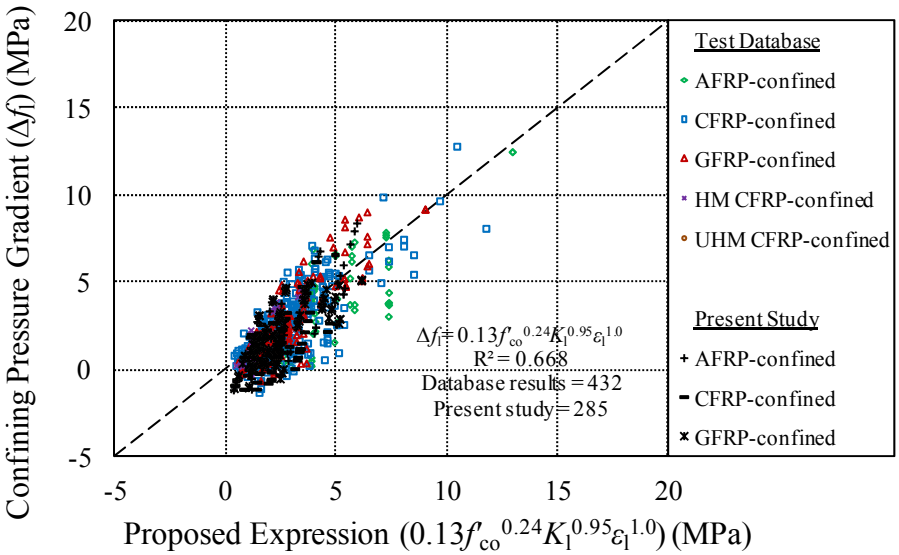

Figure 19. Comparison of confining pressure gradients (Δf_l) with predictions of the proposed expression

4.3 Generation of Axial Stress-Strain Curve of FRP-Confined Concrete using Curves of Actively Confined Concrete

To demonstrate the application of the proposed confining pressure gradient (Δf_l) given in Eq. 3, Figure 20 illustrates an example of axial stress-strain curve of FRP-confined HSC established using base curves of actively confined HSC having the same unconfined concrete strength. As illustrated in the figure, for a given axial strain (ε_c), there are significant differences in the axial stresses (Δf_c) of actively confined and FRP-confined concretes that are under the same confining pressure ($f^*_l = f_l$). On the other hand, as can be seen in Figure 20, after the adjustment of the curves of actively confined concrete with consideration of the confining pressure gradient ($f^*_l = f_l - \Delta f_l$), the axial stresses of actively confined and FRP-confined concretes show close agreement, confirming that the proposed approach is suitable for its intended purpose. Furthermore, through the use of the proposed approach the initial strength loss that occurs at the post-peak strength softening region on the stress-strain curve of FRP-confined HSC (Lim and Ozbakkaloglu 2014a) can also be estimated accurately, as illustrated in Figure 20.

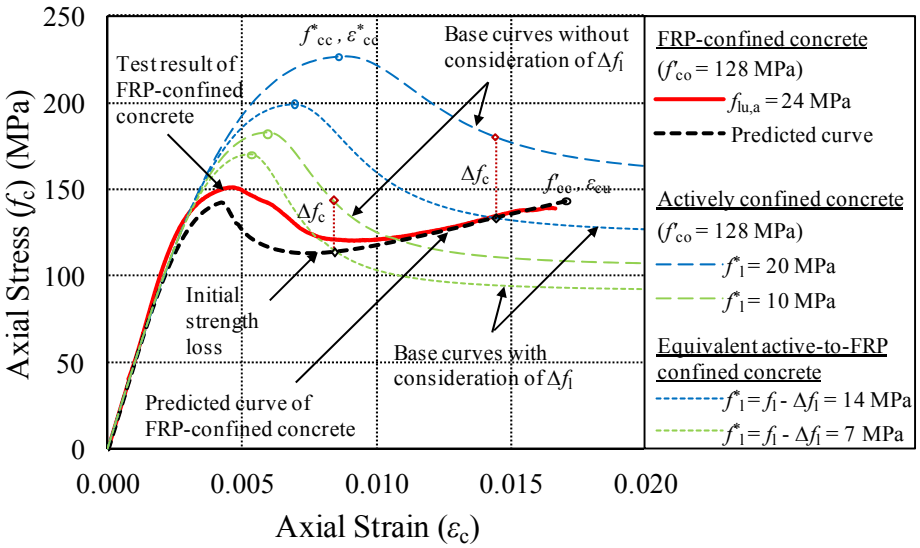

Figure 20. Generation of axial stress-strain curves of FRP-confined concrete using curves of actively confined concrete

5. CONCLUSIONS

An experimental program was undertaken to identify the changes in the axial stress-strain and lateral strain-axial strain behaviors of NSC and HSC subjected to two different confinement systems. The active confinement was provided by a Hoek cell, whereas the passive confinement was provided by FRP jacketing. Based on the experimental observations the following conclusions can be drawn:

1. At a given axial strain, the lateral strains of actively confined and FRP-confined concretes of the same concrete strength correspond, when they are subjected to the same lateral confining pressure. This finding suggests that the lateral strain-axial strain relationships of actively and FRP-confined confined NSC and HSC depend on the instantaneous confining pressure at the corresponding axial strain.
2. On the other hand, at a given axial and lateral strain and confining pressure, the FRP-confined NSC exhibits a slight difference in axial stress compared to actively confined NSC, whereas the FRP-confined HSC exhibits a significantly lower axial stress than actively confined HSC. The difference in the axial stresses becomes more significant with an increase in the level of confining pressure and concrete strength. These differences in the axial stresses are clear evidence that, at a given axial and lateral strain and confining pressure, the magnitude of axial stresses on the axial stress-strain relationships of confined concrete is dependent on the application path of confining pressure, and hence varies from one confinement system to the other.

Using the combined results of the present study and two comprehensive experimental databases of actively confined and FRP-confined concretes, an expression is established for the prediction of the confining pressure difference resulting in the axial stress difference between actively confined and FRP-confined concretes. Through this approach, the axial stress-strain curve of FRP-confined concrete can be accurately estimated based on the axial stress-strain curves of actively confined concrete.

REFERENCES

Albanesi, T., Nuti, C. and Vanzi, I. (2007). "Closed form constitutive relationship for concrete filled FRP tubes under compression." *Construction and Building Materials*, 21(2), 409-427.

ASTM-D3039 (2008). "Standard test method for tensile properties of polymer matrix composite materials." *D3039/D3039M-08*, West Conshohocken, PA.

Binici, B. (2005). "An analytical model for stress-strain behavior of confined concrete." *Engineering Structures*, 27(7), 1040-1051.

Fam, A. Z. and Rizkalla, S. H. (2001). "Confinement model for axially loaded concrete confined by circular fiber-reinforced polymer tubes." *ACI Structural Journal*, 98(4), 451-461.

Harries, K. A. and Kharel, G. (2002). "Behavior and modeling of concrete subject to variable confining pressure." *ACI Materials Journal*, 99(2), 180-189.

Ilki, A., Peker, O., Karamuk, E., Demir, C. and Kumbasar, N. (2008). "FRP retrofit of low and medium strength circular and rectangular reinforced concrete columns." *Journal of Materials in Civil Engineering, ASCE*, 20(2), 169-188.

Imran, I. and Pantazopoulou, S. J. (2001). "Plasticity model for concrete under triaxial compression." *Journal of Engineering Mechanics, ASCE*, 127(3), 281-290.

Jiang, T. and Teng, J. G. (2007). "Analysis-oriented stress-strain models for FRP-confined concrete." *Engineering Structures*, 29(11), 2968-2986.

Kent, D. C. and Park, R. (1971). "Flexural members with confined concrete." *Journal of the Structural Division, ASCE*, 97(7), 1969-1990.

Lam, L. and Teng, J. G. (2004). "Ultimate condition of fiber reinforced polymer-confined concrete." *Journal of Composites for Construction, ASCE*, 8(6), 539-548.

Lim, J. C. and Ozbakkaloglu, T. (2014a). "Confinement model for FRP-confined high-strength concrete." *Journal of Composites for Construction, ASCE*, 18(4), 04013058.

Lim, J. C. and Ozbakkaloglu, T. (2014b). "Lateral strain-to-axial strain relationship of confined concrete." *Journal of Structural Engineering, ASCE*, Doi: 10.1061/(ASCE)ST.1943-541X.0001094.

Mander, J. B., Priestley, M. J. N. and Park, R. (1988). "Theoretical stress-strain model for confined concrete." *Journal of Structural Engineering, ASCE*, 114(8), 1804-1826.

Marques, S. P. C., Marques, D., da Silva, J. L. and Cavalcante, M. A. A. (2004). "Model for analysis of short columns of concrete confined by fiber-reinforced polymer." *Journal of Composites for Construction, ASCE*, 8(4), 332-340.

Ozbakkaloglu, T. (2013a). "Behavior of square and rectangular ultra high-strength concrete-filled FRP tubes under axial compression." *Composites Part B*, 54, 97-111.

Ozbakkaloglu, T. (2013b). "Compressive behavior of concrete-filled FRP tube columns: Assessment of critical column parameters." *Engineering Structures*, 51, 188-199.

Ozbakkaloglu, T. and Idris, Y. (2014). "Seismic Behavior of FRP-High-Strength Concrete–Steel Double-Skin Tubular Columns." *Journal of Structural Engineering, ASCE*, 140(6), 04014019.

Ozbakkaloglu, T. and Lim, J. C. (2013). "Axial compressive behavior of FRP-confined concrete: Experimental test database and a new design-oriented model." *Composites Part B*, 55, 607-634.

Ozbakkaloglu, T., Lim, J. C. and Vincent, T. (2013). "FRP-confined concrete in circular sections: Review and assessment of stress–strain models." *Engineering Structures*, 49, 1068–1088.

Ozbakkaloglu, T. and Louk Fanggi, B. A. (2013). "FRP-HSC-steel composite columns: Behavior under monotonic and cyclic axial compression." *Materials and Structures*, Doi: 10.1617/s11527-013-0216-0.

Ozbakkaloglu, T. and Louk Fanggi, B. A. (2014). "Axial compressive behavior of FRP-concrete-steel double-skin tubular columns made of normal- and high-strength concrete." *Journal of Composites for Construction, ASCE*, 18(1), 04013027.

Ozbakkaloglu, T. and Saatcioglu, M. (2007). "Seismic performance of square high-strength concrete columns in FRP stay-in-place formwork." *Journal of Structural Engineering*, 133(1), 44-56.

Pantazopoulou, S. J. (1995). "Role of expansion on mechanical-behavior of concrete." *Journal of Structural Engineering, ASCE*, 121(12), 1795-1805.

Rousakis, T. C. and Karabinis, A. I. (2012). "Adequately FRP confined reinforced concrete columns under axial compressive monotonic or cyclic loading." *Materials and Structures*, 45(7), 957-975.

Saatcioglu, M. and Razvi, S. R. (1992). "Strength and ductility of confined concrete." *Journal of Structural Engineering, ASCE*, 118(6), 1590-1607.

Sheikh, S. A. and Uzumeri, S. M. (1980). "Strength and Ductility of Tied Concrete Columns." *Journal of Structural Engineering, ASCE*, 106(5), 1079-1102.

Teng, J. G., Huang, Y. L., Lam, L. and Ye, L. P. (2007). "Theoretical model for fiber-reinforced polymer-confined concrete." *Journal of Composites for Construction, ASCE*, 11(2), 201-210.

Vincent, T. and Ozbakkaloglu, T. (2013a). "Influence of concrete strength and confinement method on axial compressive behavior of FRP-confined high- and ultra high-strength concrete." *Composites Part B*, 50, 413–428.

Vincent, T. and Ozbakkaloglu, T. (2013b). "Influence of fiber orientation and specimen end condition on axial compressive behavior of FRP-confined concrete." *Construction and Building Materials*, 47, 814-826.

Wu, Y.-F. and Jiang, J.-F. (2013). "Effective strain of FRP for confined circular concrete columns." *Composite Structures*, 95, 479–491.

Xiao, Q. G., Teng, J. G. and Yu, T. (2010). "Behavior and Modeling of Confined High-Strength Concrete." *Journal of Composites for Construction, ASCE*, 14(3), 249-259.

APPENDIX

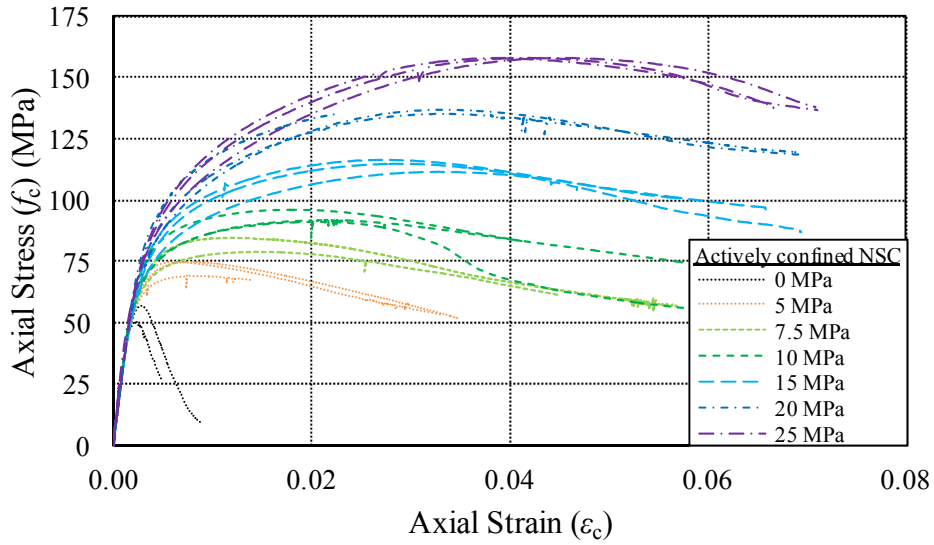

(a)

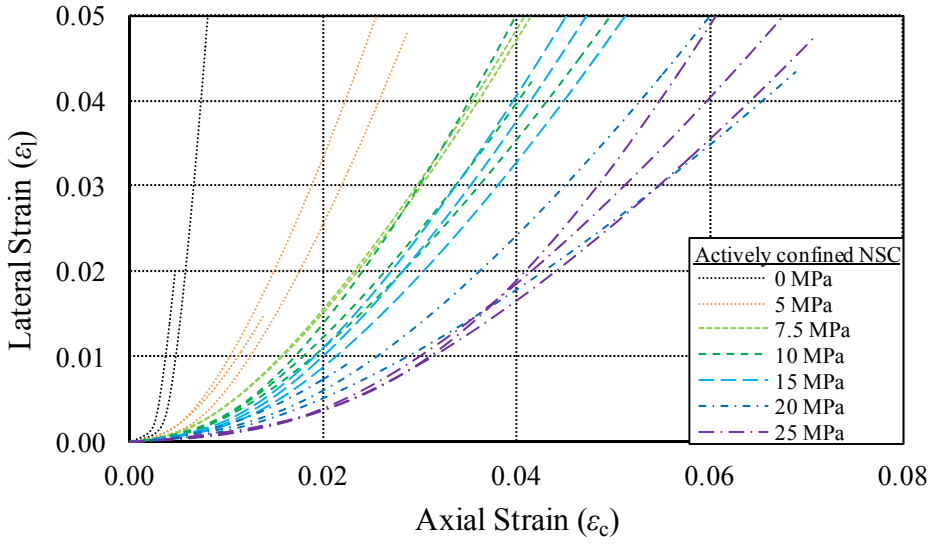

(b)

Figure S1. (a) Axial stress-strain curves; and (b) lateral strain-axial strain curves of actively confined NSC specimens

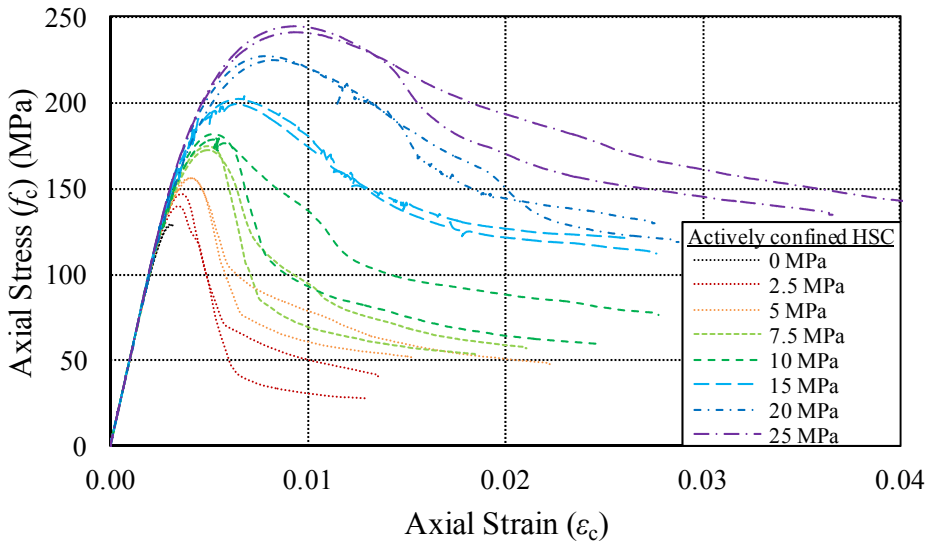

(a)

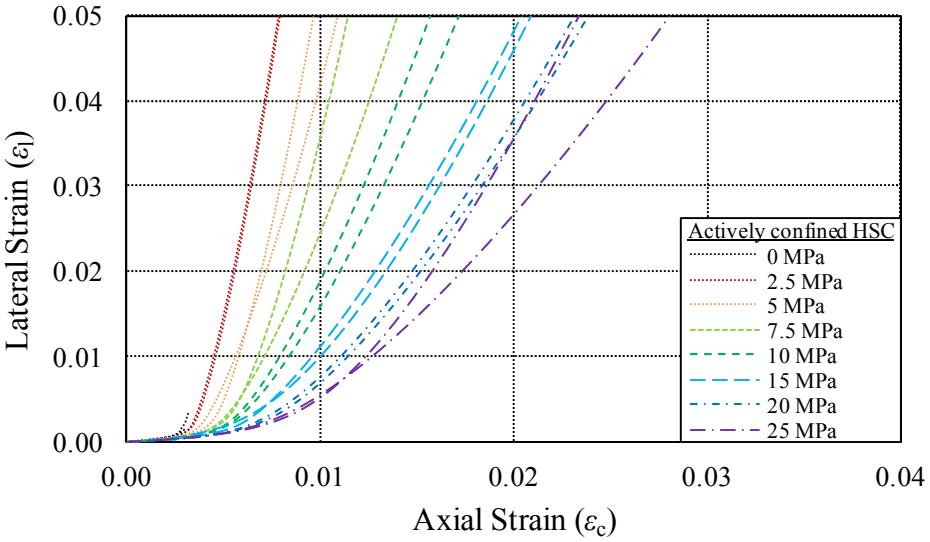

(b)

Figure S2. (a) Axial stress-strain curves; and (b) lateral strain-axial strain curves of actively confined HSC specimens

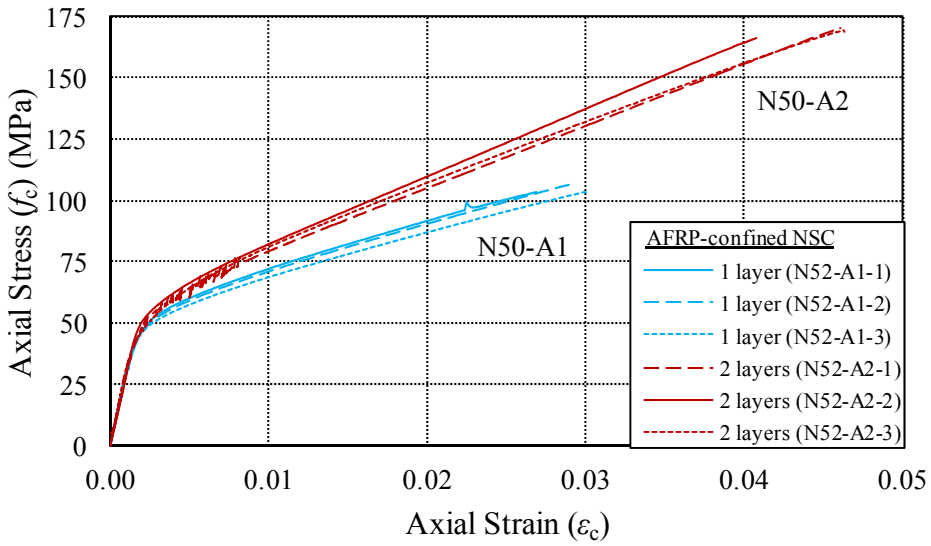

(a)

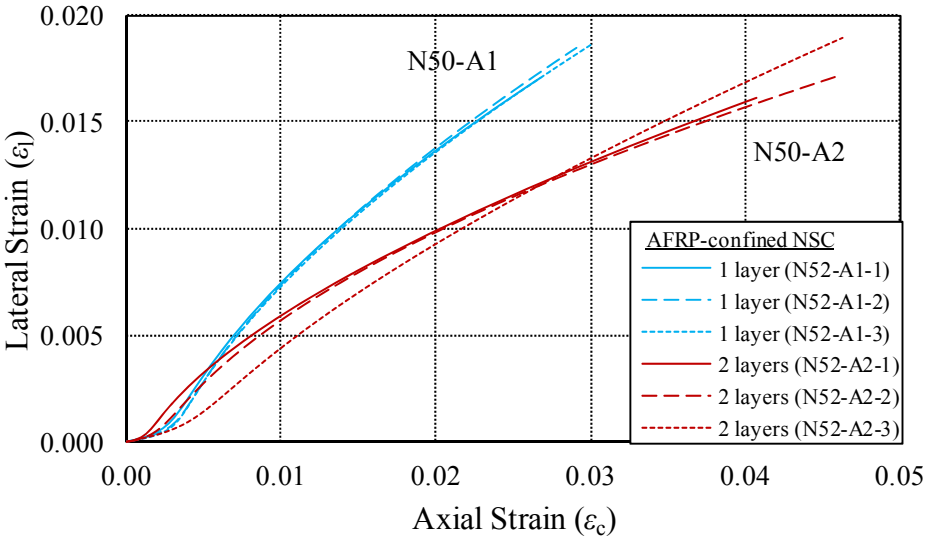

(b)

Figure S3. (a) Axial stress-strain curves; and (b) lateral strain-axial strain curves of AFRP-confined NSC specimens

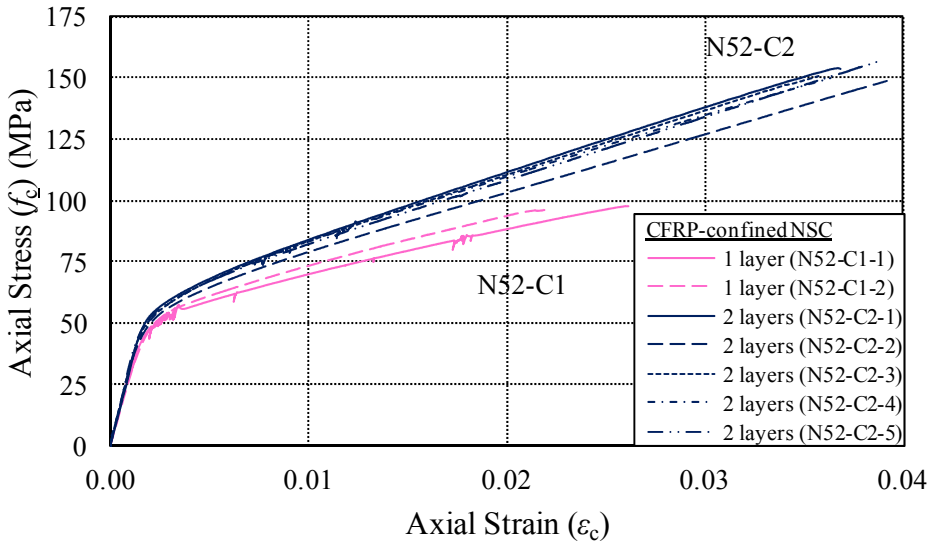

(a)

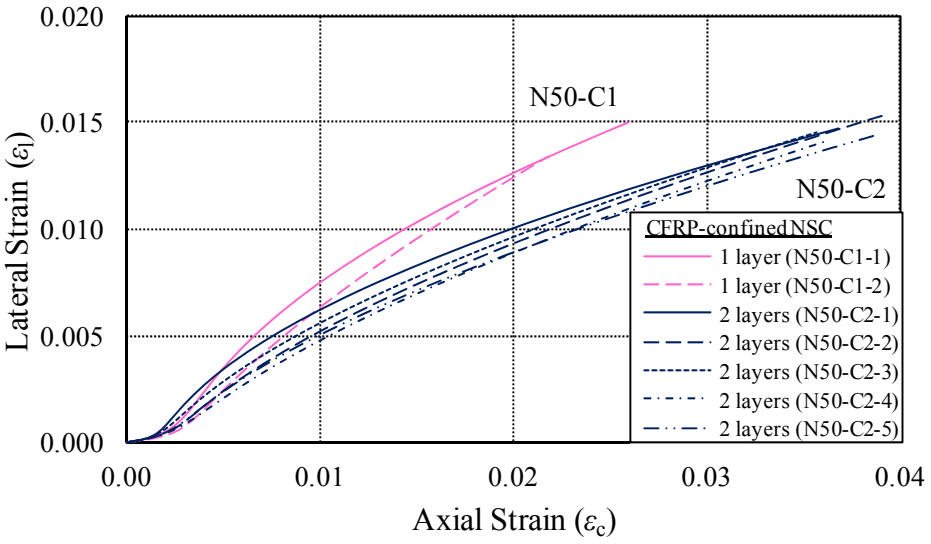

(b)

Figure S4. (a) Axial stress-strain curves; and (b) lateral strain-axial strain curves of CFRP-confined NSC specimens

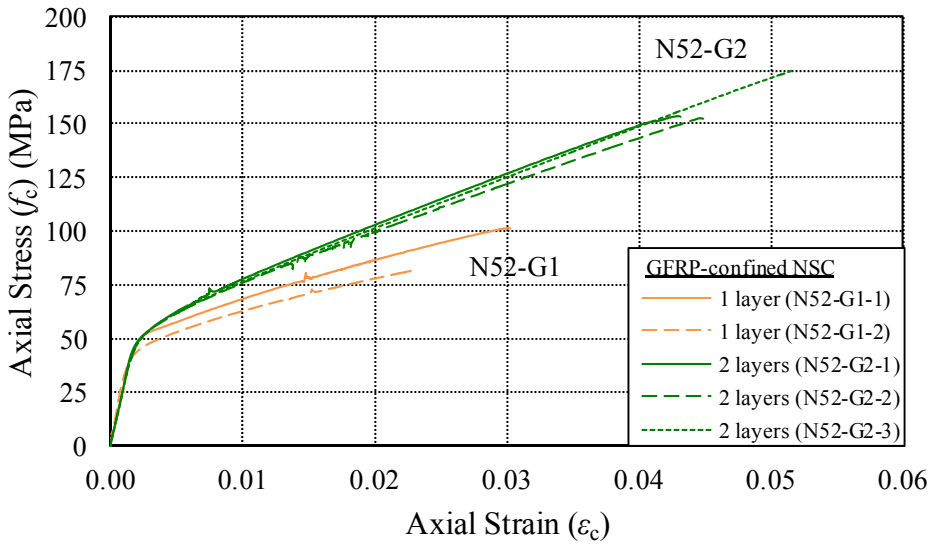

(a)

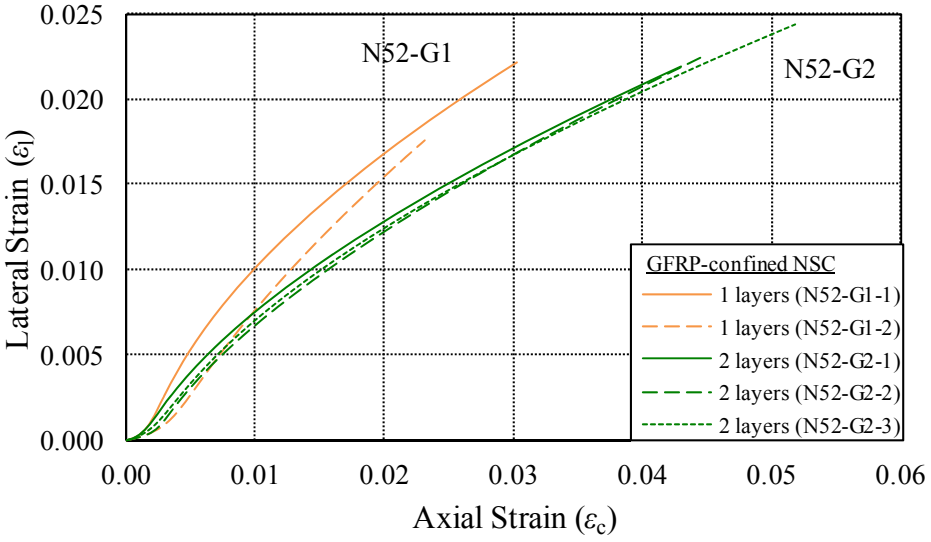

(b)

Figure S5. (a) Axial stress-strain curves; and (b) lateral strain-axial strain curves of GFRP-confined NSC specimens

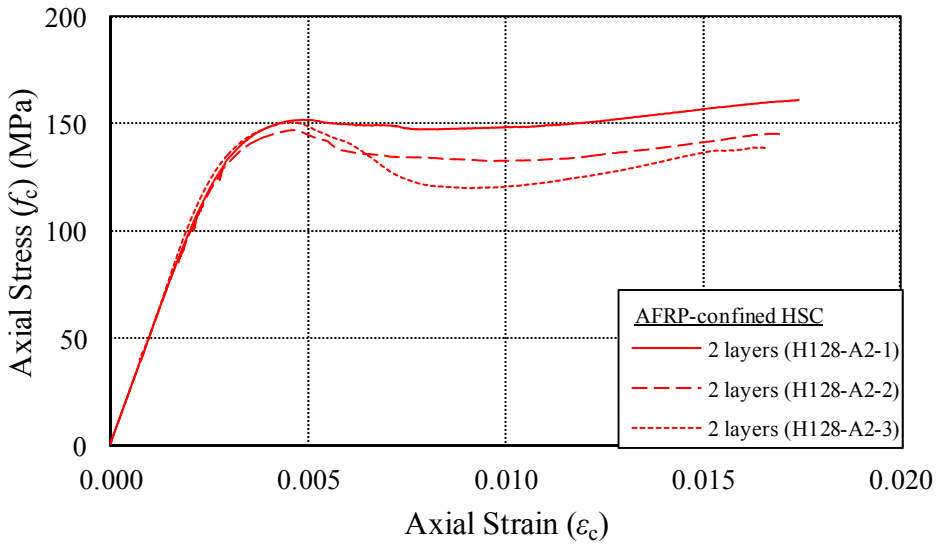

(a)

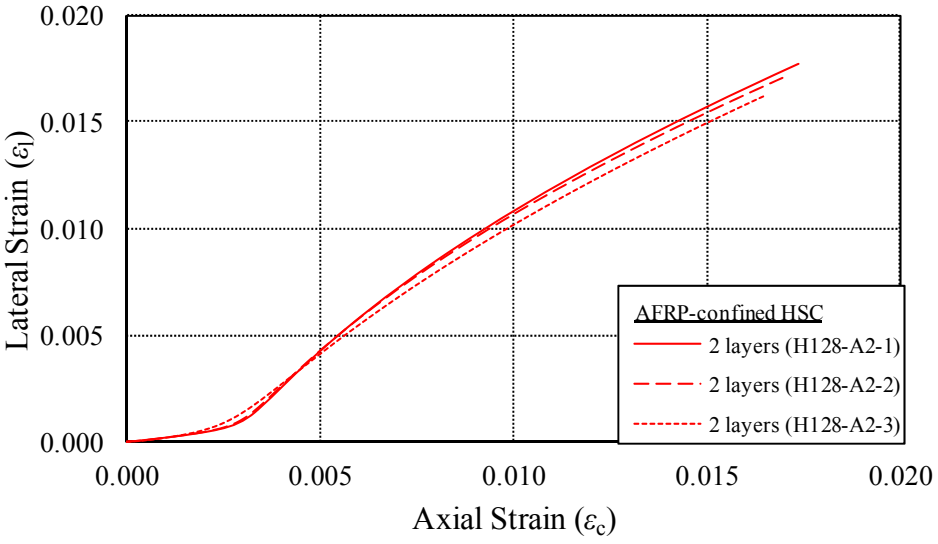

(b)

Figure S6. (a) Axial stress-strain curves; and (b) lateral strain-axial strain curves of AFRP-confined HSC specimens

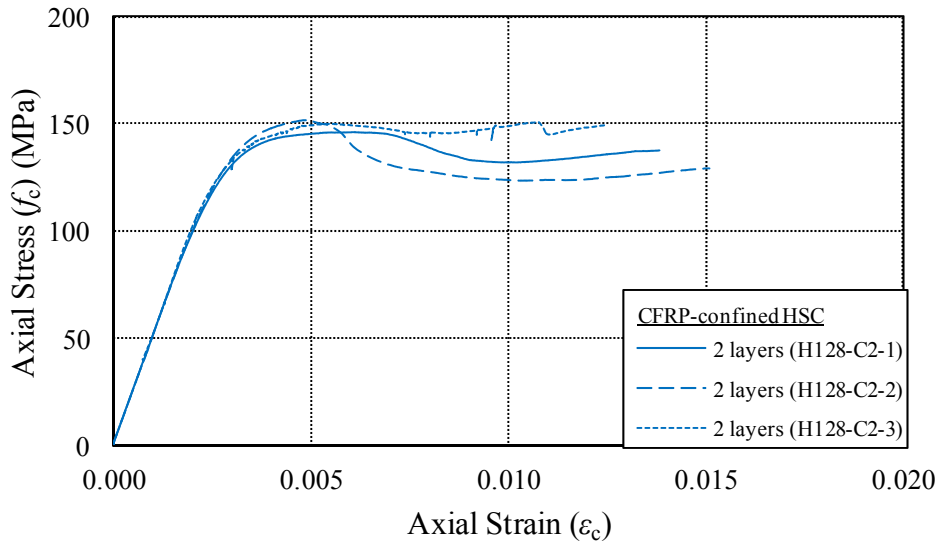

(a)

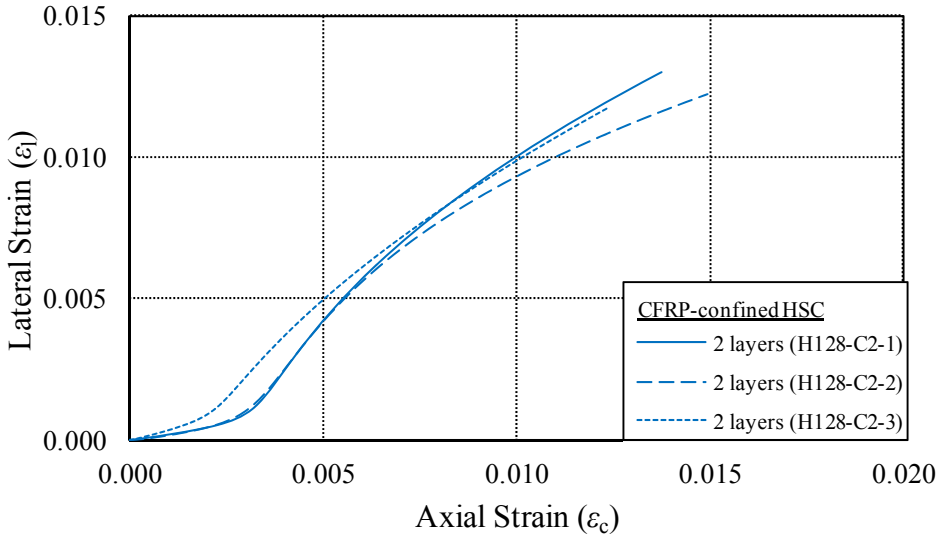

(b)

Figure S7. (a) Axial stress-strain curves; and (b) lateral strain-axial strain curves of CFRP-confined HSC specimens

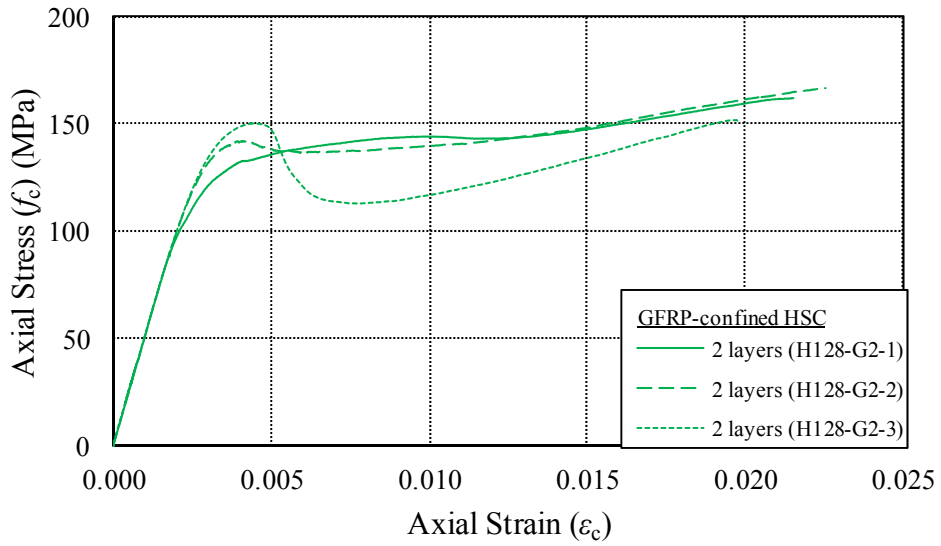

(a)

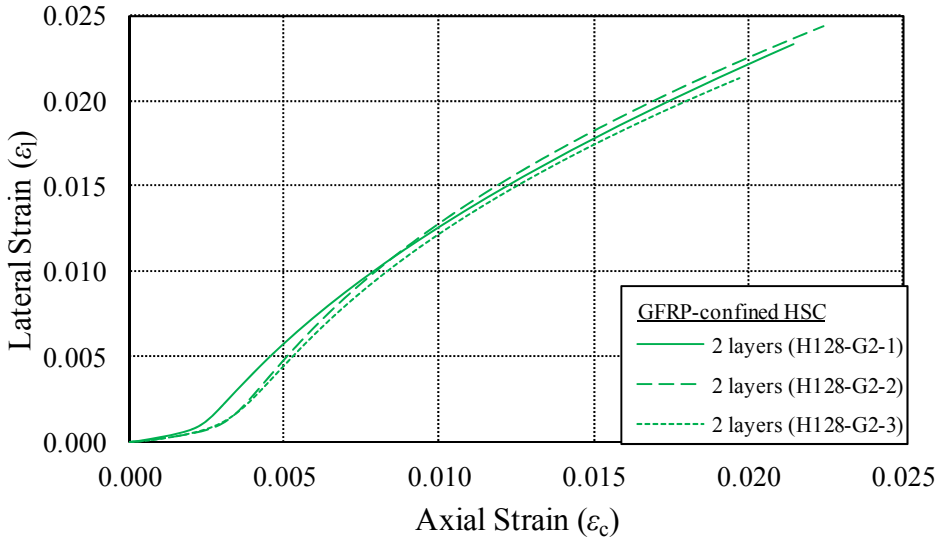

(b)

Figure S8. (a) Axial stress-strain curves; and (b) lateral strain-axial strain curves of GFRP-confined HSC specimens

THIS PAGE HAS BEEN LEFT INTENTIONALLY BLANK

Statement of Authorship

Title of Paper	Stress-Strain Model for Normal- and Light-Weight Concretes under Uniaxial and Triaxial Compression
Publication Status	◉ Published ○ Accepted for Publication ○ Submitted for Publication ○ Publication Style
Publication Details	Construction and Building Materials, Volume 71, Pages 492–509, Year 2014

Author Contributions

By signing the Statement of Authorship, each author certifies that their stated contribution to the publication is accurate and that permission is granted for the publication to be included in the candidate's thesis.

Name of Principal Author (Candidate)	Mr. Jian Chin Lim		
Contribution to the Paper	Preparation of experimental database, development of model, and preparation of manuscript		
Signature		Date	23/02/2015

Name of Co-Author	Dr. Togay Ozbakkaloglu		
Contribution to the Paper	Research supervision and review of manuscript		
Signature		Date	23/02/2015

THIS PAGE HAS BEEN LEFT INTENTIONALLY BLANK

STRESS-STRAIN MODEL FOR NORMAL- AND LIGHT-WEIGHT CONCRETES UNDER UNIAXIAL AND TRIAXIAL COMPRESSION

Jian C. Lim and Togay Ozbakkaloglu

ABSTRACT

Accurate prediction of stress-strain relationship of concrete is of vital importance to accurately predict the overall structural behavior of reinforced concrete members. The various types of concrete that are available in the construction industry today makes it essential that the models developed for the prediction of their behavior are of high versatility. Review of the existing literature revealed that existing stress-strain models for unconfined and confined concretes are limited in their application domains, defined by the parametric range of the experimental results considered in their development. The review also indicated that a unified model that is applicable to normal- and light-weight concretes is not yet available. The aim of the present study was to develop a unified confinement model that is applicable to various types of concrete, ranging from light-weight to high-strength. To this end, two large databases of experimental results of concrete specimens tested under uniaxial and triaxial compression were assembled through an extensive review of the literature. The databases covered a wide range of concrete properties, thereby allowing detailed observation of the important factors influencing the compressive behavior of concrete. The analysis of the unconfined concrete database resulted in the development of expressions for the prediction of elastic modulus, compressive strength and corresponding axial strain of various types of concrete. In addition, through a comprehensive analysis of the combined test database a unified stress-strain model was developed to predict the peak and residual conditions and the complete stress-strain behavior of unconfined and actively confined concretes.

KEYWORDS: Concrete; High-strength concrete (HSC); Confinement; Triaxial; Stress-strain; Water-cement ratio; Density; Slenderness; Size effect; Light-weight.

1. INTRODUCTION

It is well established that lateral confinement of concrete enhances its compressive strength and axial deformation capacity [1-6]. A comprehensive review of the literature that was undertaken as part of the current study and those previously reported in Refs. [6, 7] revealed that over 500 experimental studies have been conducted on the axial compressive behavior of unconfined, actively confined, and fiber reinforced polymer (FRP)-confined concretes, resulting in the development of over 110 stress-strain models. However, due to the limitations in the parametric ranges of the experimental results considered in their development, the applicability of the existing models are often restricted to specific specimens subsets. The current availability of variety of concrete confinement techniques and reinforcing materials [4, 8-21], and the abundance of concretes with different mechanical and material properties [9, 22-26] poses a challenge for engineers in finding a suitable model given the possible composite combinations of these materials.

The work presented in this paper was motivated by the need to develop a unified model applicable to various types of concrete under unconfined and confined conditions. To this end, firstly two extensive databases of unconfined and actively confined concrete test results, which covered various concrete types, were assembled. The database results indicated significant differences in the stress-strain behavior of different types of concrete, ranging from light-weight (LWC) to normal-weight (NWC), and normal-strength (NSC) to high-strength (HSC). Based on these results, changes in the compressive behavior of concrete with various test parameters were then investigated, and the influential parameters were established. Finally, through a comprehensive examination of the results in the databases, a unified stress-strain model that it is applicable to: i) both LWC and NWC, ii) both NSC and HSC, and iii) both unconfined and actively confined concretes was developed.

2. EXPERIMENTAL TEST DATABASES

2.1 Database of Unconfined Concrete

The database of unconfined concrete was assembled from 209 experimental studies and consisted of 4353 datasets. 1167 datasets from 161 studies that reported the specimen axial strain at peak compressive stress of concrete (ε_{co}) are presented in Tables A1 to A3 in Appendix, whereas the remaining datasets are presented in Tables A4 to A7. The results in Tables A1 to A3 and A4 to A7 were sorted into seven groups according to the type of concrete (NWC or LWC) and the cross-sectional shape of specimen (circular or square). Out of the 4353 datasets presented in Tables A1 to A7, 2279 of the datasets were NWC cylinders, 1167 were LWC cylinders, 864 were NWC prisms, 43 were LWC prisms. In Tables A1 to A7, the following information was available for each dataset in the database: the number of identical specimen; the geometric properties (cross-sectional dimension B and height H); the specimen age; the water-to-cementitious binder ratio (w/c); the density of concrete ($\rho_{c,f}$); the type and size of aggregates; the silica fume-to-cementitious binder percentage (sf/c); the mineral additive-to-cementitious binder percentage (ma/c); the elastic modulus of concrete (E_c); and the compressive strength of concrete (f'_{co}). In Tables A1 to A3, the axial strain corresponding to the peak compressive stress (ε_{co}) and its measurement method is available in the last two columns. It should be noted that in some of the datasets, details of the aggregate

type were not available from the source documents. Given the omission of such details, the aggregate types are noted as either normal-weight or light-weight aggregates in Tables A1 to A7, according to the type of concrete (NWC or LWC). Regarding the percentages of mineral additives in concrete mixes of specimens presented in Tables A1 to A7, except for silica fume that is presented in the 9th column, details of other mineral additives, such as fly-ash, slag, and hi-fi are presented in the same column in the 10th column. To distinguish their types in this column, these mineral additives are noted with superscripts *'f', 's', 'h'*, respectively.

In the database presented in Tables A1 to A7 in Appendix, the specimen cross-sectional dimensions (B) varied from 50 to 406 mm, the specimen heights (H) varied from 25 to 1016 mm and the specimen aspect ratios (H/B) varied from 0.25 to 8, the water-cementitious binder ratios (w/c) varied from 0.16 to 1.27, the concrete densities ($\rho_{c,f}$) varied from 666 to 2584 kg/m^3, the concrete elastic moduli (E_c) varied from 9620 to 57800 MPa, and the compressive strengths (f'_{co}) and the corresponding axial strains (ε_{co}) varied from 5.3 to 171.1 MPa and 0.07 to 0.53 %, respectively.

2.2 Database of Actively Confined Concrete

The database of actively confined concrete, presented in Ref. [7], was assembled from 25 experimental studies that consisted of 346 test datasets, and 31 additional datasets from tests recently undertaken at the University of Adelaide [27]. All of the specimens in the database had circular cross-sections, with cross-sectional dimensions (B) varying from 50 and 160 mm. The specimen heights (H) varied from 88 to 320 mm, the specimen aspect ratios (H/B) varied from 1 to 3, and the compressive strength (f'_{co}) and the corresponding axial strains (ε_{co}), obtained from unconfined concrete cylinder tests, varied from 7.2 to 132.0 MPa and 0.15% to 0.40%, respectively. Various instruments were used in existing studies to measure the axial strains (ε_{co}) of specimens, including in-built extensometers of compression machines, linear variable displacement transducers, and axial strain gauges. The unconfined concrete cylinders had the same geometric dimensions as the corresponding confined specimens. The active confinement ratio (f^*_l/f'_{co}), defined as the ratio of the hydrostatic confining pressure of the triaxial cell to the unconfined concrete strength, varied from 0.004 to 21.67.

It is worth noting that, given the limitation of the actively confined concrete database only to specimens with circular cross-sections, for a consistent treatment of the test results, only the specimens with circular cross-sections from both unconfined and actively confined concrete databases were included in the development of the models that are presented later in the paper. However, wherever possible, observations on the influences of the cross-sectional shape on the observed behavior are also supplied. Thereafter, the specimen cross-sectional dimension (B) is referred to as the specimen diameter (D).

3. ELASTIC MODULUS AND PEAK CONDITION OF UNCONFINED CONCRETE

Based on the observed difference in their compressive behavior, concretes with a density (ρ_c) greater than 2250 kg/m^3 were categorized as NWC, whereas concretes with a density below the limit were categorized as LWC. A same transition boundary between NWC and LWC at concrete density of 2250 kg/m^3 were previously reported in Tasdemir et al. [23] based on the

observed difference in concrete heterogeneity and material properties. In the database results, details of fresh concrete density ($\rho_{c,f}$) of specimens are commonly available from source documents, whereas the densities of air dried ($\rho_{c,a}$) and oven dried hardened concretes ($\rho_{c,o}$) are less commonly reported. Given the availability of information about the fresh densities of concrete ($\rho_{c,f}$), this parameter was therefore used in the analysis of the database results. Figure 1 shows the comparisons of the densities of air dried ($\rho_{c,a}$) and oven dried concretes ($\rho_{c,o}$) to fresh concrete ($\rho_{c,f}$). The slight variations between the densities of fresh ($\rho_{c,f}$), air dried ($\rho_{c,a}$) and oven dried ($\rho_{c,o}$) concretes can be accounted using the expressions given by the trendlines of Figure 1, of which $\rho_{c,f}$ is in unit kg/m^3.

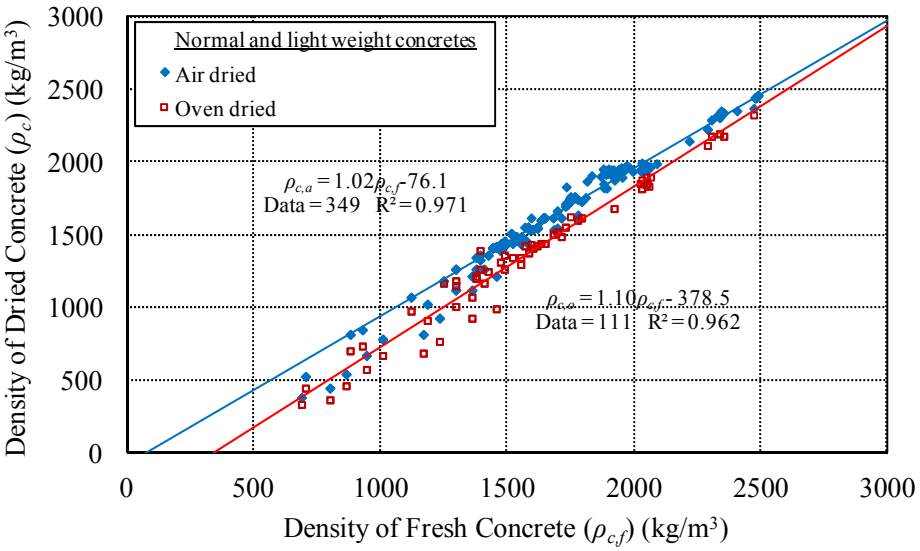

Figure 1. Variation of densities of air dried ($\rho_{c,a}$) and oven dried concretes ($\rho_{c,o}$) with fresh concrete density ($\rho_{c,f}$)

3.1 Influence of Water-Cementitious Binder Ratio, Silica Fume, and Concrete Density on Compressive Strength of Concrete

Several studies have been reported to date on the modelling of concrete compressive strength (Refs. [28-33]). However, a unified expression to estimate the compressive strength of different types of concrete is not yet available. To establish a unified expression for the prediction of the compressive strength of concrete, the mix designs of various types of concrete in the database were carefully studied, and important parameters identified to have prominent effect on the compressive strength of concrete were quantified. Figure 2 shows the variation in the compressive strength of concrete (f'_{co}) with the *w/c* ratio, for both NWC and LWC. It is generally understood that the compressive strength (f'_{co}) of both NWC and LWC increase with a reduction in the *w/c* ratio, as shown in Figure 2. However, the relative influences of the *w/c* ratio, concrete density ($\rho_{c,f}$), and silica fume-to-cementitious binder ratio (*sf/c*) on the compressive strength (f'_{co}) are much less understood. Figure 3 shows the change in the compressive strength of concrete (f'_{co}) with concrete density ($\rho_{c,f}$) and Figure 4 shows the change in the compressive strength of concrete (f'_{co}) with silica fume-to-cementitous binder ratio (*sf/c*), of several subgroups of specimens that fall within the selected ranges of *w/c* ratios for comparisons. As illustrated in the figures, the concrete compressive strength

(f'_{co}) increases with an increase in concrete density ($\rho_{c,f}$) or silica fume ratio (sf/c) for a given w/c ratio. Based on the observed trendlines of Figures 2 to 4, the relative influences of the w/c ratio, concrete density ($\rho_{c,f}$), and silica fume ratio (sf/c) on the compressive strength of concrete (f'_{co}) were statistically quantified through multivariable regression analysis, which resulted in the expression given in Eq. 1. The new expression proposed in this study is applicable for the prediction of the 28-day compressive strength (f'_{co}) of 152×305 mm concrete cylinder up to 120 MPa, for NWC and LWC with water-cementitious binder ratios (w/c) ranging from 0.2 to 1.3, concrete densities ($\rho_{c,f}$) ranging from 650 to 2550 kg/m^3, and silica fume-to-cementitious binder ratios (sf/c) ranging from 0 to 0.2. In Eq. 1, the average density of NWC ($\rho_{c,f}$) of 2400 kg/m^3 is adopted as the reference value in establishing the change in concrete compressive strength (f'_{co}) with concrete density ($\rho_{c,f}$). Figure 5 shows that the predictions of the proposed expression (Eq. 1) are in good agreement with the experimental results.

$$f'_{co} = \left(\frac{21}{w/c} + 32\sqrt{sf/c}\right)\left(\frac{\rho_{c,f}}{2400}\right)^{1.6} \quad (1)$$

where f'_{co} is in MPa and $\rho_{c,f}$ is in kg/m^3.

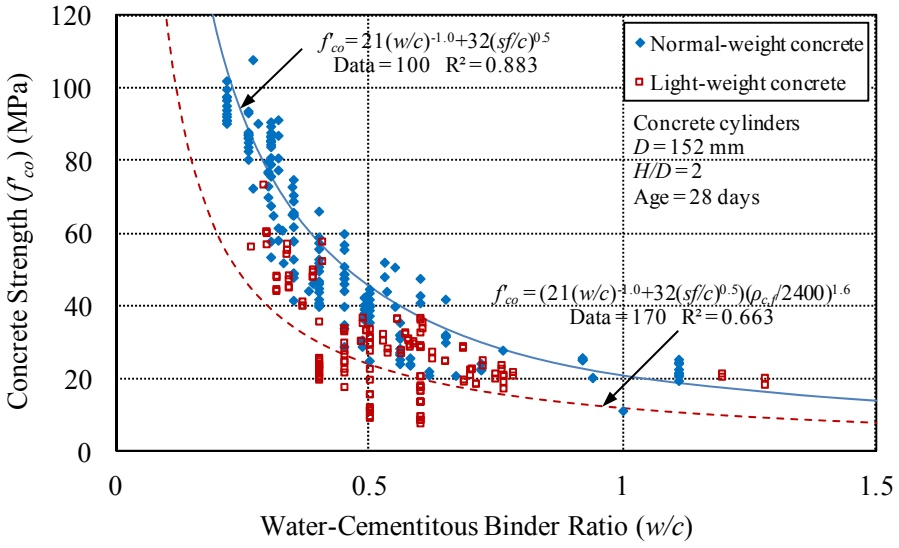

Figure 2. Variation of concrete compressive strength (f'_{co}) with water-cementitious binder ratio (w/c)

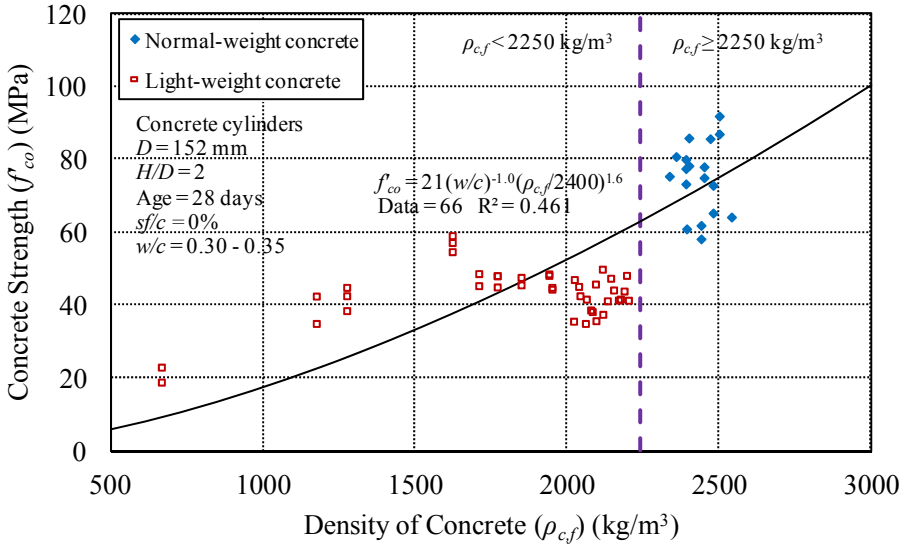

(a)

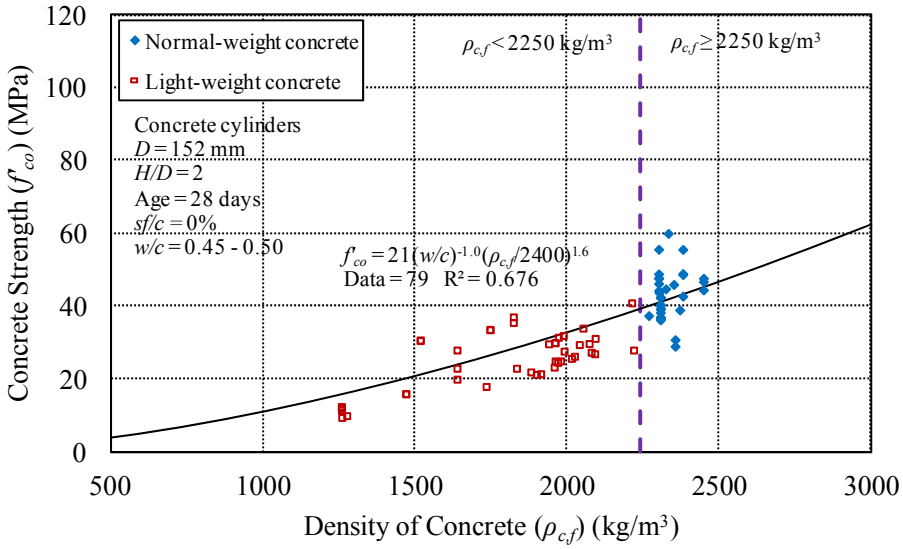

(b)

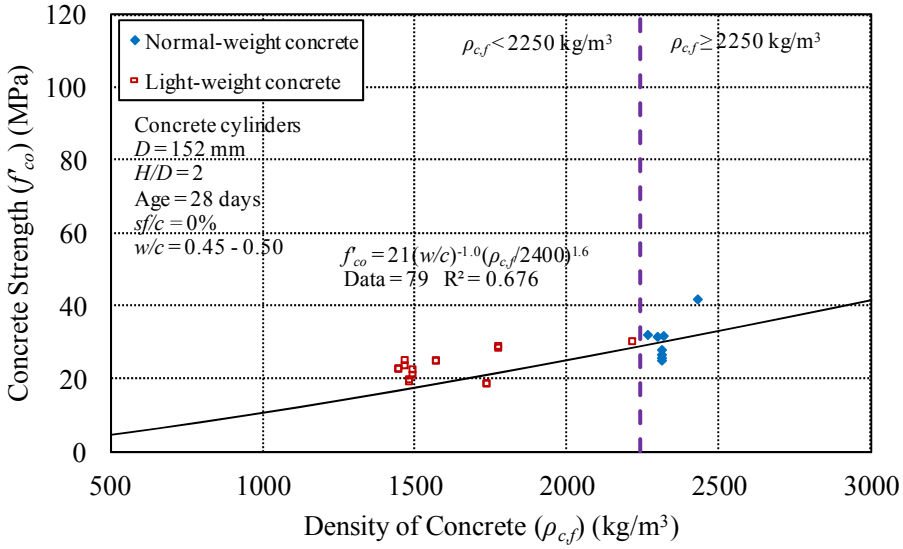

(c)

Figure 3. Variation of concrete compressive strength (f'_{co}) with concrete density ($\rho_{c,f}$): (a) w/c = 0.30 to 0.35; (b) w/c = 0.50 to 0.55; and (c) w/c = 0.70 to 0.75

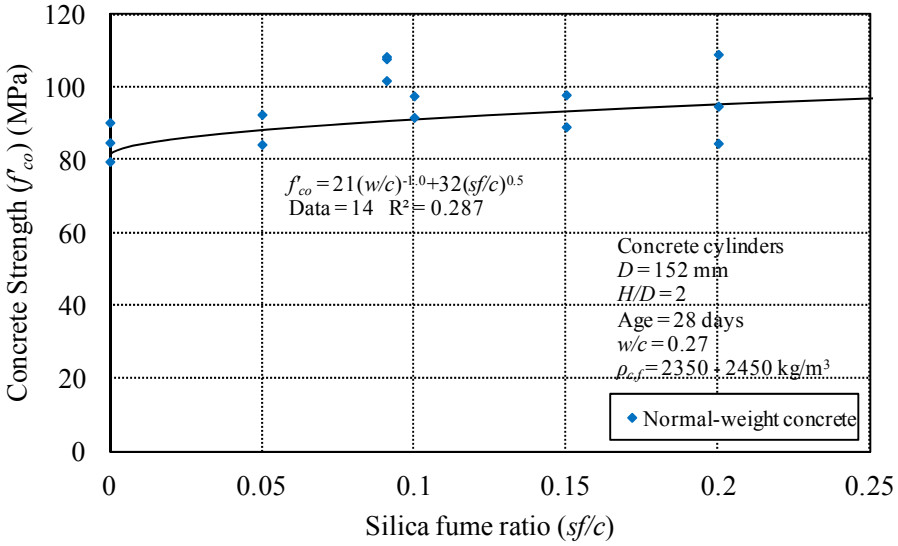

(a)

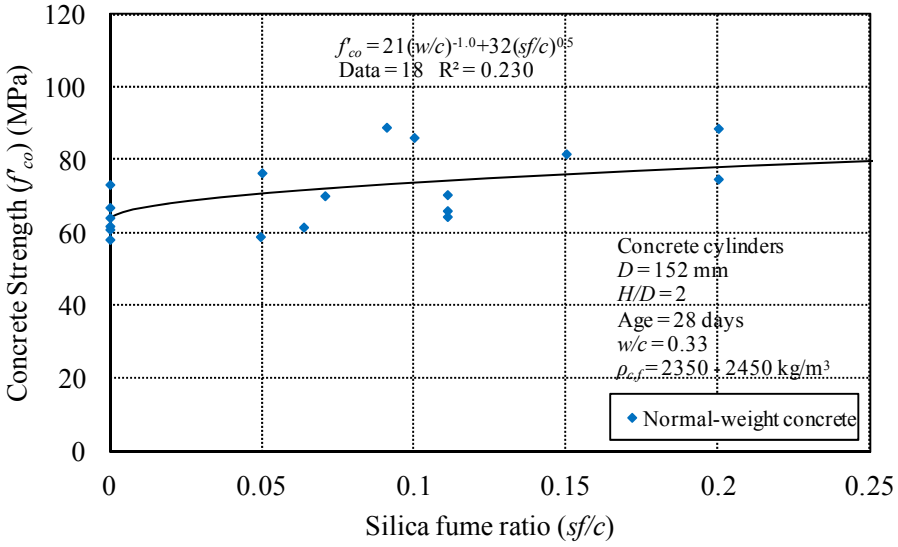

(b)

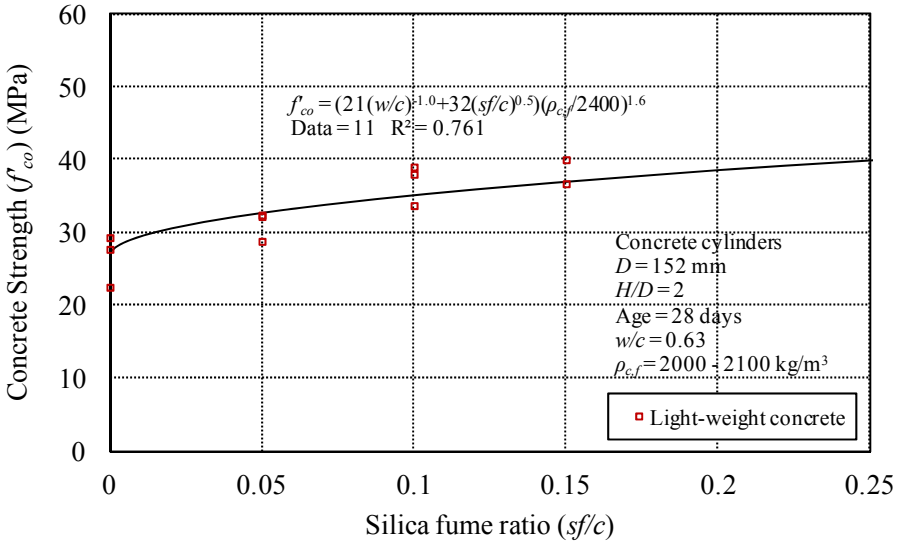

(b)

Figure 4. Variation of concrete compressive strength (f'_{co}) with silica fume ratio (sf/c): (a) w/c = 0.27, NWC; (b) w/c = 0.33; NWC; and (c) w/c = 0.63, LWC

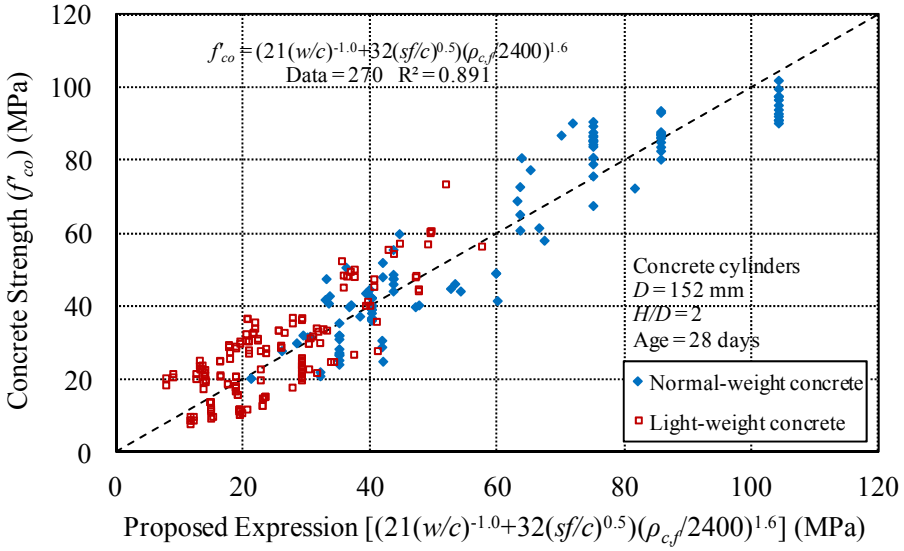

Figure 5. Comparison of concrete compressive strengths (f'_{co}) with model predictions

3.2 Influence of Compressive Strength and Concrete Density on Elastic Modulus of Concrete

Extensive research has been conducted to study the relationship between compressive strength of concrete (f'_{co}), its density ($\rho_{c,f}$) and elastic modulus (E_c) [34-48]. Table 1 presents the prediction statistics of the existing expressions proposed for the prediction of the elastic modulus of concrete (E_c) on the experimental results of the unconfined concrete database. It should be noted that not all the datasets included in the database contained all the relevant details required for model assessment. As a result, out of the 4353 datasets, 1471 test results of NWC cylinders and 739 test results of LWC cylinders from the experimental database were used in the assessment of the concrete elastic modulus (E_c). In the comparisons shown in Table 1, average absolute error (*AAE*) was used to establish overall model accuracy; standard deviation (*SD*) was used to establish the magnitude of the associated scatter for each model; and mean (*M*) was used to describe the associated average overestimation or underestimation of the model, where an overestimation was represented by a mean value greater than 1. Based on the prediction statistics in Table 1, it is clear that further improvement to prediction of concrete elastic modulus (E_c) is possible.

Figure 6 shows the typical stress-strain curves of unconfined NWC and LWC in compression. Figure 7 shows the variation of concrete elastic modulus (E_c) with the compressive strength (f'_{co}). As evident from Figure 7, the elastic moduli (E_c) of both NWC and LWC increase with an increase in the compressive strength of concrete (f'_{co}). Figure 8 shows the variation concrete elastic modulus (E_c) with the concrete density ($\rho_{c,f}$), for several subgroups of specimens that fall within the selected ranges of compressive strengths (f'_{co}) for comparisons. As illustrated Figure 8, the elastic modulus (E_c) of LWC is significantly lower than that of NWC, and varies with the concrete density ($\rho_{c,f}$) at a given compressive strength (f'_{co}). The influence of the concrete age was also investigated through the analysis of the results from specimens with concrete ages ranging from 28 to 1975 days, but no significant influence of the age on the concrete elastic modulus (E_c) was found. Likewise, the specimen cross-sectional shape (i.e. circular and square), which was studied through the use of additional test

results of the concrete prisms (Tables A3, A6 and A7), was found to have no significant on the elastic modulus (E_c). Based on the observed trendlines of Figures 7 and 8, the relative influences of the compressive strength (f'_{co}) and concrete density ($\rho_{c,f}$) on the elastic modulus of concrete (E_c) were statistically quantified using multivariable regression analysis, which resulted in the expression given in Eq. 2. The expression is applicable to concrete cylinders upto 120 MPa for NWC and LWC with concrete densities ($\rho_{c,f}$) ranging from 650 to 2550 kg/m^3. In Eq. 2, the average density of NWC ($\rho_{c,f}$) of 2400 kg/m^3 is treated as the reference value to establish the change in concrete elastic modulus (E_c) with concrete density ($\rho_{c,f}$). Figure 9 shows that the predictions of the proposed expression (Eq. 2) are in good agreement with the experimental results.

$$E_c = 4400\sqrt{f'_{co}}\left(\frac{\rho_{c,f}}{2400}\right)^{1.4} \quad (2)$$

where E_c and f'_{co} are in MPa and $\rho_{c,f}$ is in kg/m^3.

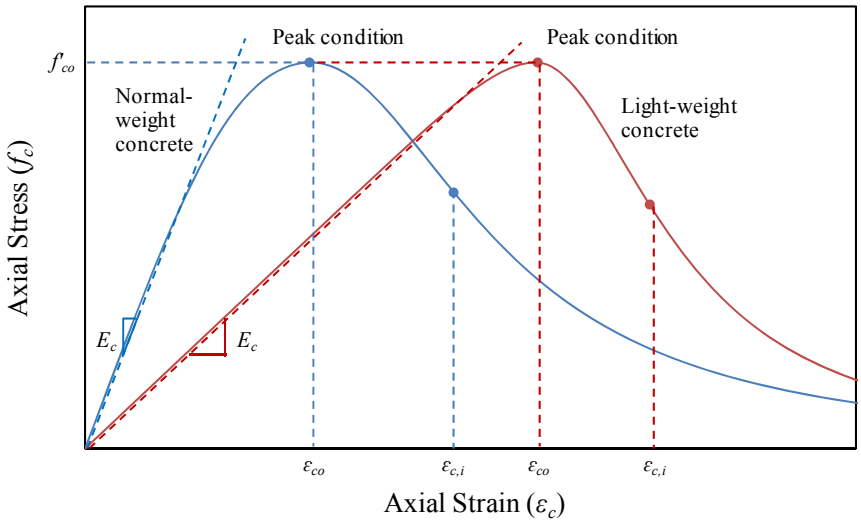

Figure 6. Typical stress-strain curves of normal and light-weight concretes

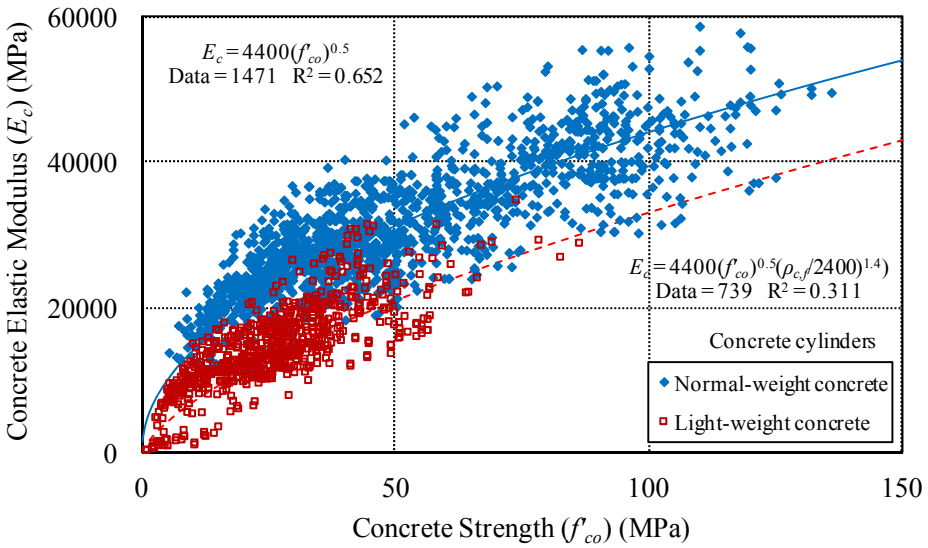

Figure 7. Variation of concrete elastic modulus (E_c) with concrete compressive strength (f'_{co})

Table 1. Statistics on performances of models in predictions of elastic modulus of concrete (E_c)

Model	Year of publication	Prediction of E_c of NWC			Prediction of E_c of LWC		
		Average Absolute Error (%)	Mean (%)	Standard Deviation (%)	Average Absolute Error (%)	Mean (%)	Standard Deviation (%)
Jensen [34]	1943	20.0	110.6	24.9	119.3	215.9	139.7
Ahmad and Shah [35]	1982	15.6	98.8	20.9	20.5	92.2	31.0
Oluokun et al. [36]	1991	20.5	113.9	22.8	20.6	106.3	34.5
ACI-363 [58]	1992	16.2	107.6	22.1	24.7	111.6	48.0
NS-3473 [37]	1992	15.6	103.5	20.3	24.9	111.3	46.4
CEB-FIP [38]	1993	36.9	135.0	28.3	226.1	319.5	402.1
ACI-318 [62]	1995	23.4	118.3	22.6	21.9	110.5	34.7
CSA [39]	1995	16.6	108.5	20.2	25.0	112.6	46.4
Iravani [40]	1996	21.0	81.6	15.1	50.2	145.1	97.2
Wee et al. [41]	1996	31.9	129.9	25.8	176.3	271.1	246.1
TS-500 [42]	2000	31.5	129.2	26.3	201.9	296.0	347.1
Fam and Rizkalla [43]	2001	24.4	120.9	22.4	118.4	215.0	143.9
Persson [44]	2001	15.9	90.7	19.9	64.1	161.2	111.0
Gesoglu [45]	2002	21.2	113.8	22.4	81.0	177.5	87.8
Kim et al. [46]	2002	56.5	45.1	10.1	52.5	105.1	115.6
Mesbah et al. [47]	2002	25.4	122.1	22.6	120.7	217.1	145.4
Nassif [48]	2005	15.7	99.7	21.1	20.3	93.0	31.3

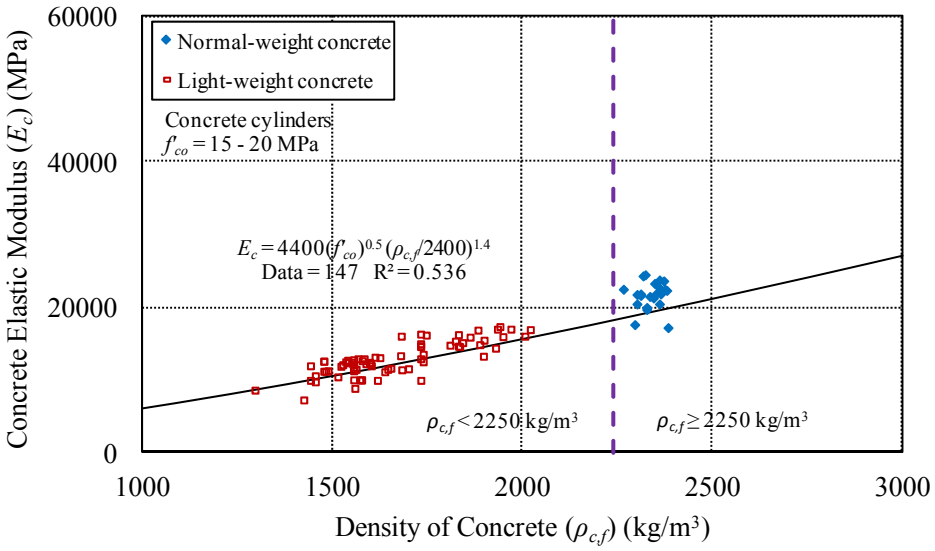

(a)

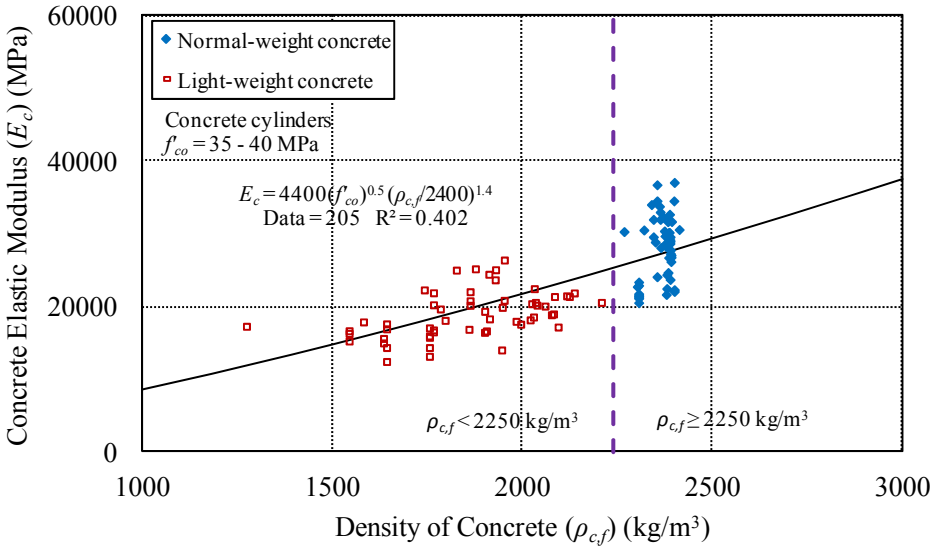

(b)

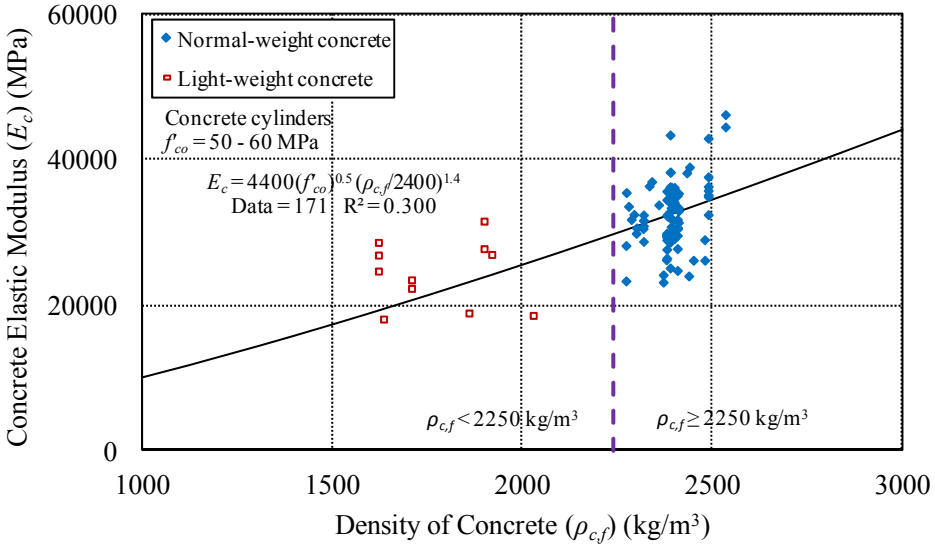

(c)

Figure 8. Variation of concrete elastic modulus (E_c) with concrete density ($\rho_{c,f}$): (a) low-strength concrete; (b) normal-strength concrete; and (c) high-strength concrete

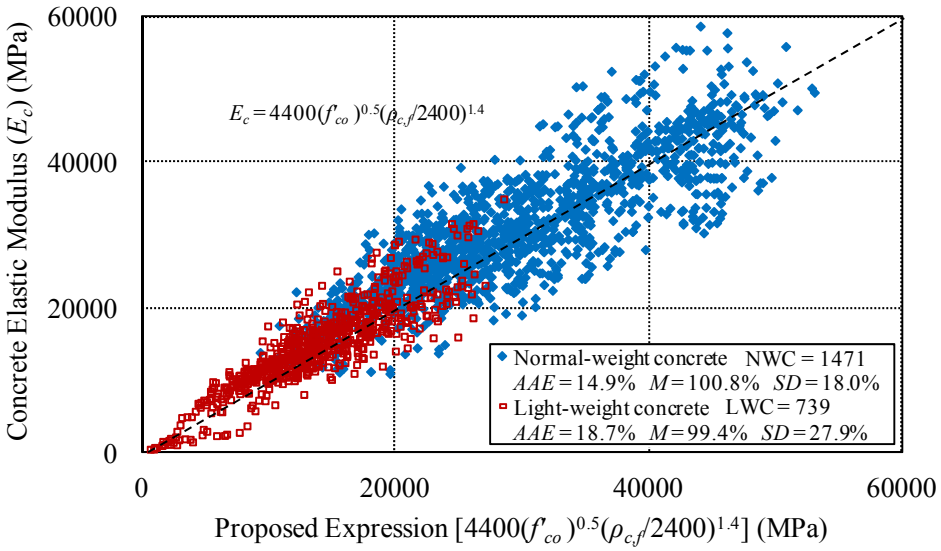

Figure 9. Comparison of concrete elastic moduli (E_c) with model predictions

3.3 Axial Strain at Peak Compressive Stress

Extensive research has been conducted to study the relationship between the compressive strength of concrete (f'_{co}) and the corresponding axial strain (ε_{co}) [22, 23, 41, 49-68]. Table 2 presents the prediction statistics of the existing expressions proposed for the prediction of the axial strain at peak compressive stress (ε_{co}) on the experimental results of the unconfined concrete database. Out of the 1167 datasets that reported the axial strains at peak compressive stress (ε_{co}), 810 test results from the experimental database that contain relevant information required for model assessment of ε_{co}. 663 of these results came from NWC cylinders and 147 came from LWC cylinders. In the existing expressions, the concrete compressive strength (f'_{co}) is often considered the sole parameter influencing the axial strain at peak compressive stress (ε_{co}). Based on the comparison statistics in Table 2, it is clear that the modelling accuracy for the axial strain prediction can be further improved through the incorporation of other influential factors.

Figure 10 shows the variation of the axial strain at peak compressive stress (ε_{co}) with compressive strength of concrete (f'_{co}). As can be seen from the figure, the axial strain at peak compressive stress (ε_{co}) of LWC and NWC are significantly different. Apart from the influence of concrete density ($\rho_{c,f}$), other parameters including specimen diameter (D) and aspect ratio (H/D) were also observed to have major influence on the axial strain at peak compressive stress (ε_{co}). To establish the relative influence of these parameters, 152×305-mm normal-weight concrete cylinders with concrete densities ($\rho_{c,f}$) ranging from 2250 to 2550 kg/m^3 (i.e., 2400 kg/m^3 ± 6%) were first selected as the reference specimens. The base expression ($f'_{co}{}^{0.225}/1000$) established from the axial strains at peak compressive stress (ε_{co}) of these reference specimens, as illustrated in Figure 11, were then used to quantify the relative changes in the axial strains at peak compressive stress (ε_{co}) in other specimens that have different geometric dimensions (H and D) and concrete densities ($\rho_{c,f}$) than the reference specimens. Figure 12 shows the variation of the axial strain at peak compressive stress (ε_{co}) with the concrete density ($\rho_{c,f}$), for several subgroups of specimens that fall within the

selected ranges of concrete compressive strengths (f'_{co}) for comparisons. As can be seen from the figure, for a given compressive strength (f'_{co}), the axial strain at peak compressive stress (ε_{co}) decreases with an increase in concrete density ($\rho_{c,f}$), and the reduction becomes more pronounced in the cases of higher strength concretes. As illustrated in the trendlines of Figure 12, the influence of concrete density ($\rho_{c,f}$) on the axial strain at peak compressive stress (ε_{co}) were related to the power of the base expression as a function of $(2400/\rho_{c,f})^{0.45}$. Apart from the concrete density ($\rho_{c,f}$), Figures 13 and 14 show that the specimen diameter (D) and aspect ratio (H/D) also slightly influence the axial strain at peak compressive stress (ε_{co}) of concrete. As illustrated in Figures 13 and 14, for a given compressive strength (f'_{co}), the axial strain at peak compressive stress (ε_{co}) decreases with either an increase in specimen diameter (D) or aspect ratio (H/D). Based on the observed trendlines in Figures 13 to 14, the relative influences of the specimen diameter (D), and aspect ratio (H/D) were incorporated into the base expression as multipliers $(152/D)^{0.1}$ and $(2D/H)^{0.13}$, respectively, which resulted in the final expression given in Eq. 3. The expression is applicable to concrete cylinders up to 120 MPa for NWC and LWC with concrete densities ($\rho_{c,f}$) ranging from 650 to 2550 kg/m^3. Figure 15 shows that the predictions of the proposed expression (Eq. 3) are in good agreement with the experimental results. It might be worth noting that the influence of the concrete age was also investigated through the analysis of the results from specimens with concrete ages ranging from 28 to 1975 days, but no significant influence of the age on the axial strain at peak compressive stress (ε_{co}) was found. Furthermore, investigation of the influence of specimen cross-sectional shape (i.e. circular and square) through the use of additional test results of the concrete prisms (Tables A3, A6 and A7) indicated no significant influence of specimen cross-sectional shape on the axial strain at peak (ε_{co}).

$$\varepsilon_{co} = \frac{f'^{\,0.225k_d}_{co}}{1000} k_s k_a \tag{3}$$

$$k_d = \left(\frac{2400}{\rho_{c,f}}\right)^{0.45} \tag{4}$$

$$k_s = \left(\frac{152}{D}\right)^{0.1} \tag{5}$$

$$k_a = \left(\frac{2D}{H}\right)^{0.13} \tag{6}$$

In Eqs. 3 to 6, f'_{co} is in MPa, $\rho_{c,f}$ is in kg/m^3, and D and H are in mm, and k_d, k_s, and k_a, respectively, are the coefficients to allow for concrete density, specimens size and specimen aspect ratio. Based on the geometric dimensions of the specimens used in the development of the model expressions, it is recommended that in Eqs. 5 and 6, the range of aspect ratios (H/D) be limited to 2-8, diameters (D) to 50-400 mm, and heights (H) to 100-850 mm.

Table 2. Statistics on performances of models in predictions of axial strain at peak compressive stress (ε_{co}) of unconfined concrete

Model	Year of publication	Prediction of ε_{co} of NWC			Prediction of ε_{co} of LWC		
		Average Absolute Error (%)	Mean (%)	Standard Deviation (%)	Average Absolute Error (%)	Mean (%)	Standard Deviation (%)
Ros [49]	1950	28.8	105.3	36.1	32.2	69.1	16.5
Saenz [50]	1964	17.1	85.1	14.7	21.4	80.2	16.7
Tadros [51]	1970	14.4	89.4	14.5	19.5	82.4	15.8
Popovics [52]	1973	13.1	103.4	15.3	15.5	91.7	15.2
Ahmad and Shah [53]	1979	15.1	105.8	17.6	14.5	92.4	14.9
Tomaszewicz [54]	1984	13.0	97.6	15.3	19.3	83.2	13.4
Carreira and Chu [55]	1985	16.1	86.3	12.9	19.8	82.4	16.0
Shah and Ahmad [56]	1985	19.0	114.9	17.8	15.2	103.7	17.8
Ali et al. [57]	1990	12.2	96.5	14.3	18.0	85.6	14.2
Taerwe [59]	1992	13.0	94.3	14.5	17.4	85.8	15.0
Collins et al. [60]	1993	13.5	96.3	16.0	17.3	88.4	17.1
De Nicolo et al. [22]	1994	15.0	99.8	18.2	21.6	79.8	14.0
Hsu and Hsu [61]	1994	20.3	117.4	17.7	17.4	108.5	19.6
Arioğlu [63]	1995	12.5	96.9	14.7	18.7	84.4	13.7
Attard and Setunge [64]	1996	16.0	108.2	17.9	13.7	100.7	15.4
Wee et al. [41]	1996	16.0	86.1	14.8	24.5	76.3	14.7
Tasdemir et al. [23]	1998	16.8	100.5	20.5	21.3	79.5	12.4
Mansur et al. [65]	1999	22.6	78.3	14.1	36.0	65.0	11.6
Lee [66]	2002	17.1	86.7	15.0	26.1	74.7	11.8
Wang et al. [67]	2006	27.6	73.2	14.7	35.6	65.4	14.1
Lu and Zhao [68]	2008	22.2	79.0	13.8	36.8	64.3	10.6
Chen et al. [83]	2013	12.8	100.0	15.9	18.4	99.3	21.0

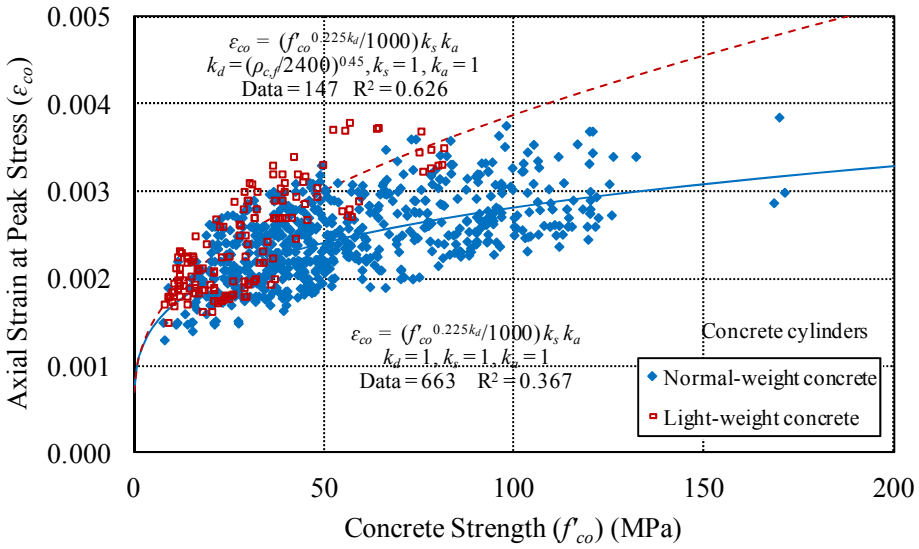

Figure 10. Variation of axial strain at peak compressive stress (ε_{co}) with compressive strength of concrete (f'_{co})

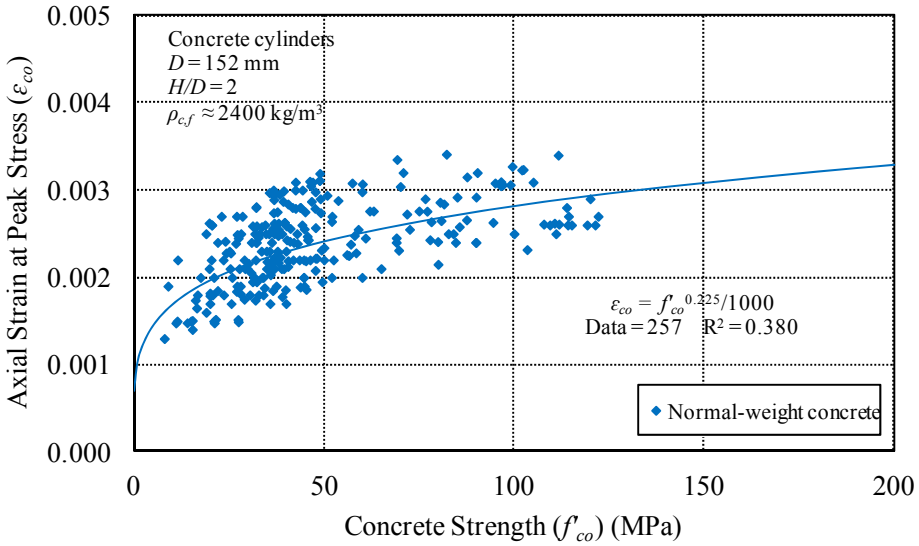

Figure 11. Variation of axial strain at peak compressive stress (ε_{co}) with compressive strength of concrete (f'_{co}) for 152×305-mm normal weight concrete cylinders

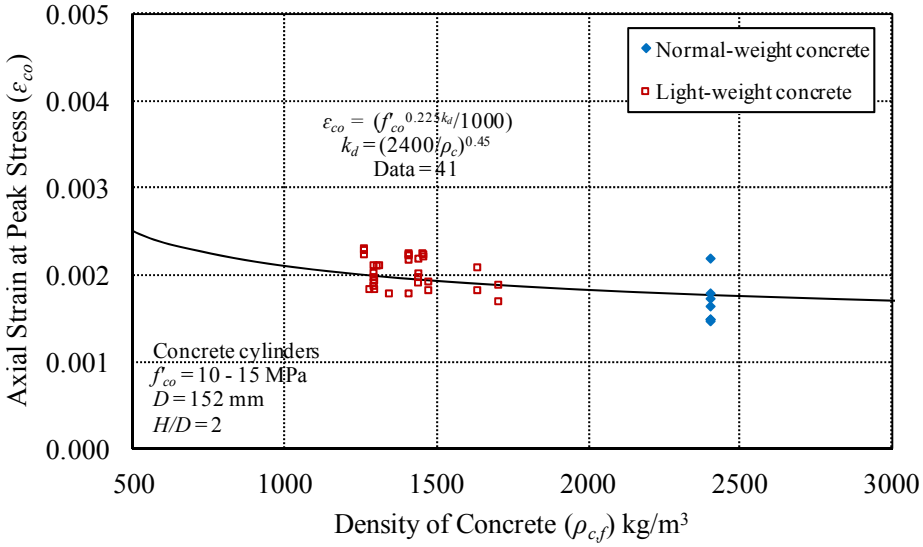

(a)

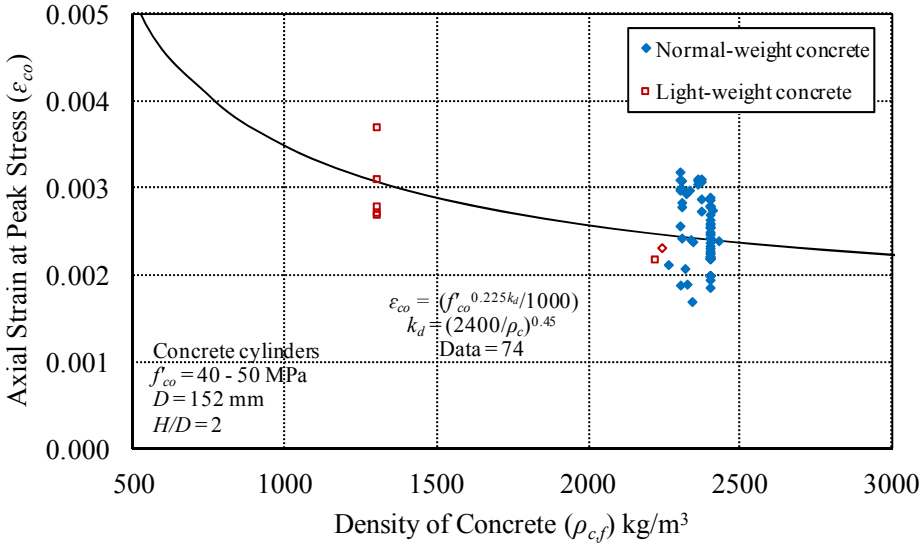

(b)

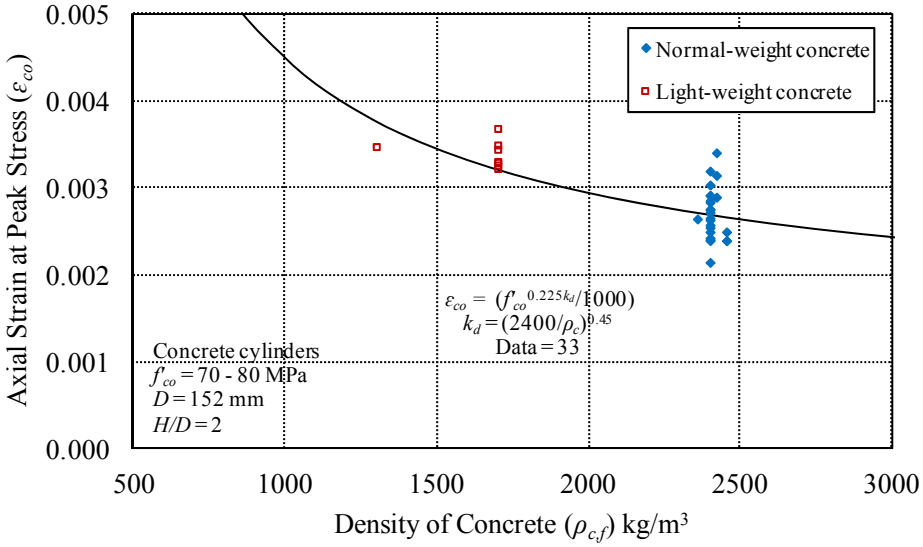

(c)

Figure 12. Variation of axial strain at peak compressive stress (ε_{co}) with concrete density ($\rho_{c,f}$): (a) low-strength concrete; (b) normal-strength concrete; and (c) high-strength concrete

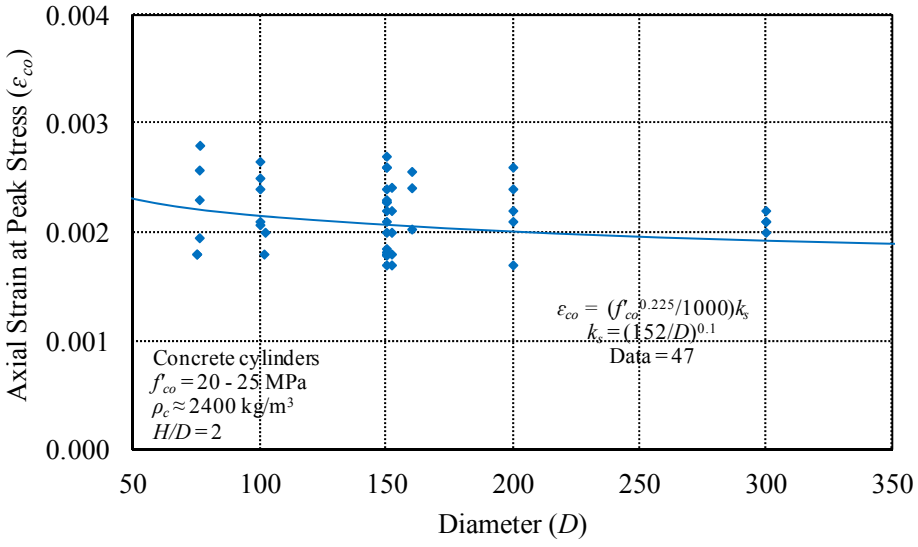

(a)

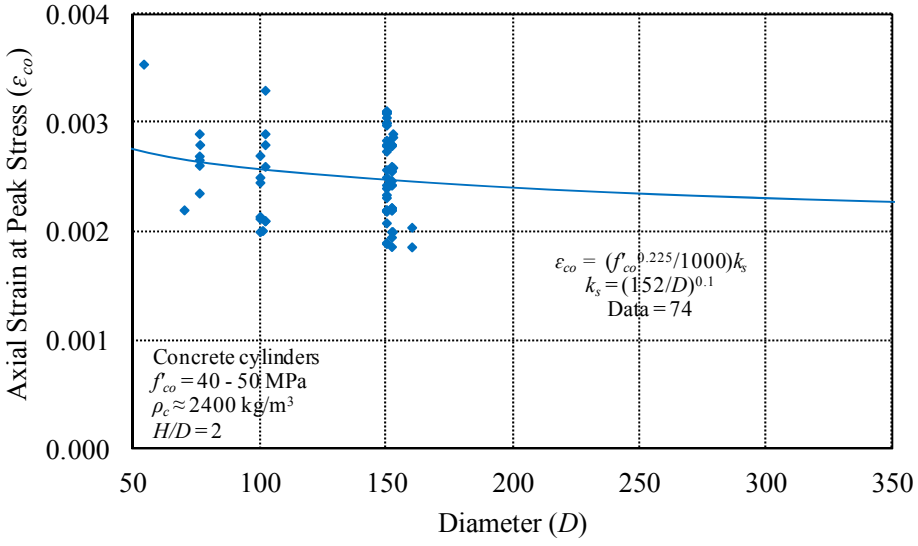

(b)

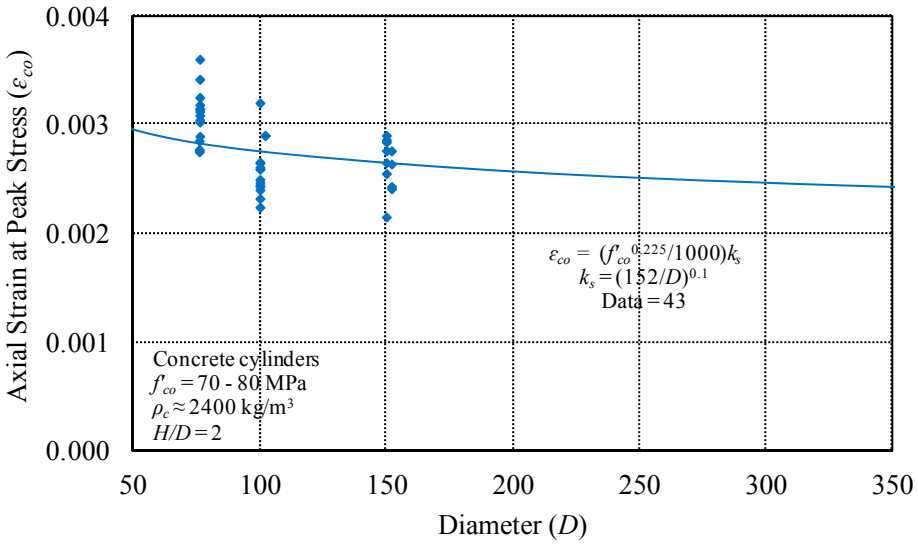

(c)

Figure 13. Variation of axial strain at peak compressive stress (ε_{co}) with specimen diameter (D): (a) low-strength concrete; (b) normal-strength concrete; and (c) high-strength concrete

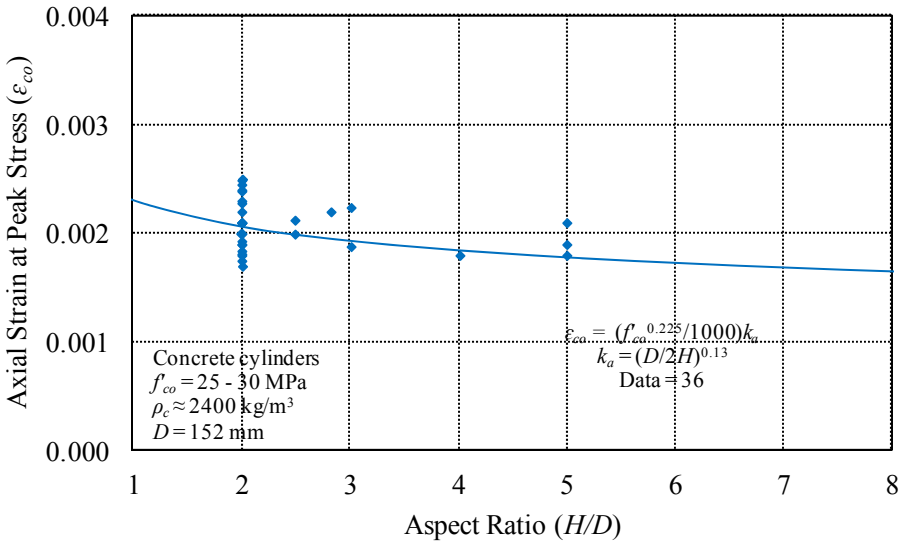

(a)

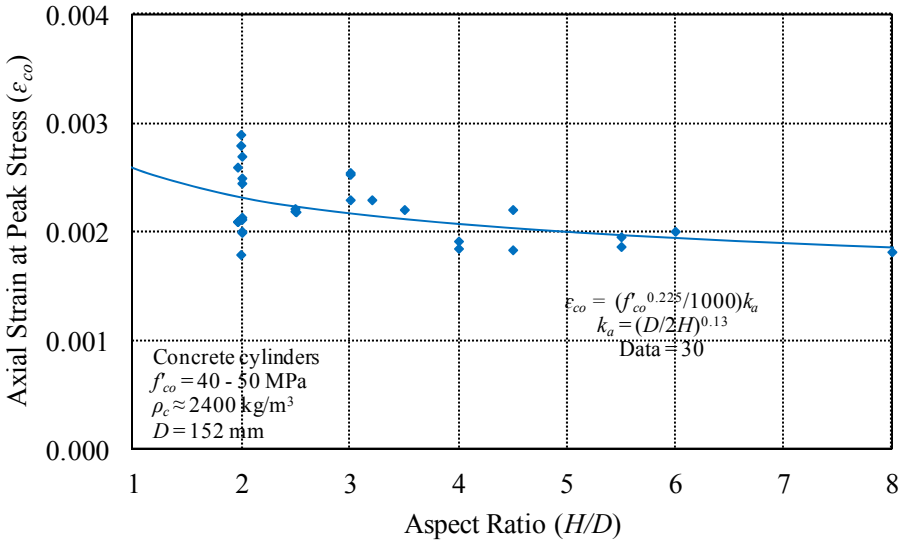

(b)

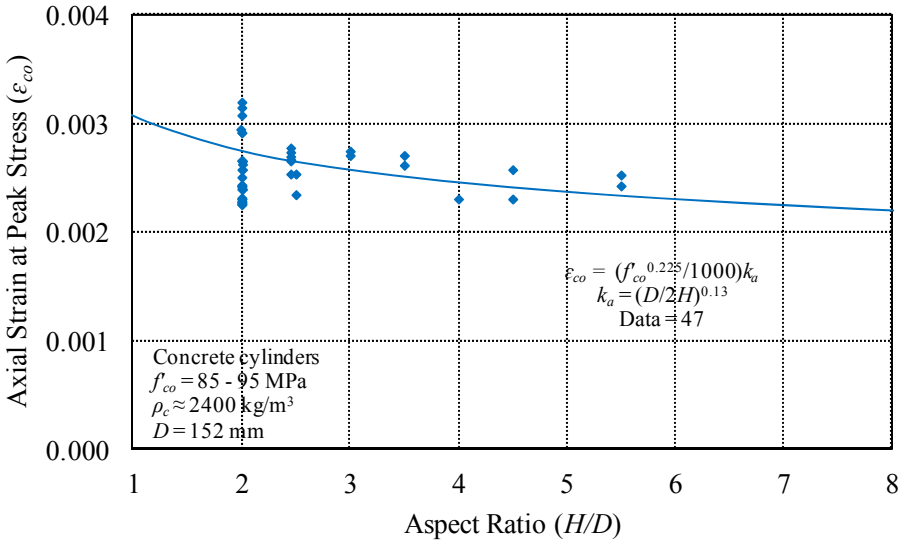

(c)

Figure 14. Variation of axial strain at peak compressive stress (ε_{co}) with specimen slenderness (H/D): (a) low-strength concrete; (b) normal-strength concrete; and (c) high-strength concrete

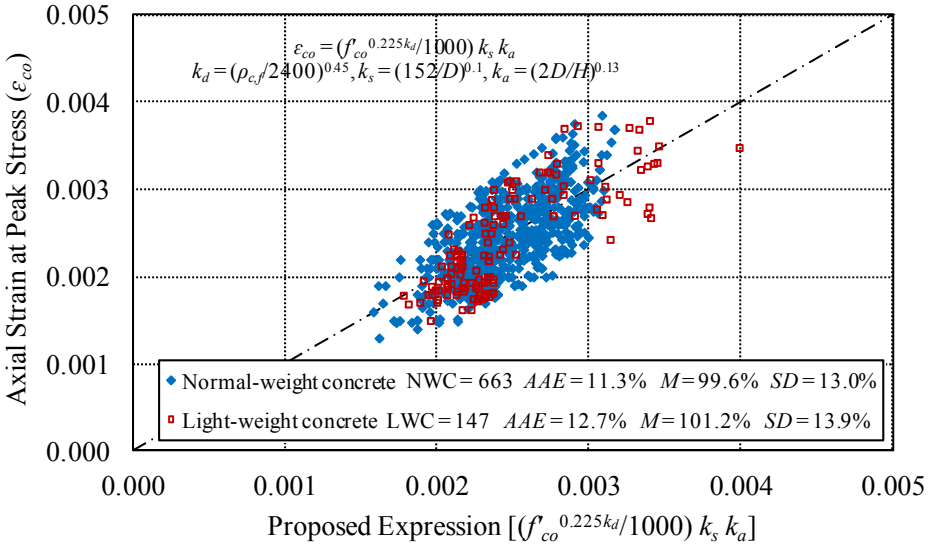

Figure 15. Comparison of axial strains at peak compressive stress (ε_{co}) with model predictions

4. PEAK AND RESIDUAL CONDITIONS OF ACTIVELY CONFINED CONCRETE

Since the 1920s [69, 70], a significant research effort has been dedicated to understanding the behavior of concrete under triaxial compression, resulting in the development of a number of stress-strain model for actively confined concrete [3, 24, 64, 70-79]. Figure 16 shows the typical stress-strain curves of unconfined and actively confined concretes, together with the important coordinates along the curves. As can be seen from the figure, the stress-strain curve of actively confined concrete consists of a linearly ascending initial segment followed by a parabolic curve forming the first branch that reaches the peak compressive stress (f^*_{cc}) and is followed by a gradually descending second branch. After the peak stress, interparticle cohesion in the concrete continues, and the remaining strength generated through frictional action that forms a stabilized plateau in the curve is known as the residual stress ($f_{c,res}$) [75]. The accuracy of models in the predictions of these important coordinates significantly affects the predicted shape of the stress-strain curve. To compare the performances of the existing actively confined concrete models, the predictions of the strength enhancement ratio (f^*_{cc}/f'_{co}), peak strain ratio ($\varepsilon^*_{cc}/\varepsilon_{co}$), and residual stress ratio ($f_{c,res}/f'_{co}$) of the existing models were assessed using the test results of the actively confined concrete database. In the calculations of the strength enhancement ratios (f^*_{cc}/f'_{co}) and the peak strain ratios ($\varepsilon^*_{cc}/\varepsilon_{co}$), the compressive strength (f'_{co}) and the corresponding axial strain (ε_{co}) of unconfined concrete were obtained from cylinder test results reported in the original studies. Out of the 377 datasets, 341, 243, and 173 test results from the experimental database were used in the assessment of the strength enhancement ratio (f^*_{cc}/f'_{co}), peak strain ratio ($\varepsilon^*_{cc}/\varepsilon_{co}$), and residual stress ratio ($f_{c,res}/f'_{co}$), respectively. Based on the prediction statistics in Table 3, a number of existing models were found to perform well in their predictions [24, 64, 75-77]. Nevertheless, the results suggest that, in the prediction of the peak stress and strain and residual stress of actively confined concrete, a further improvement in the modelling accuracy is possible.

Table 3. Statistics on performances of models in predictions of strength enhancement ratios (f^*_{cc}/f'_{co}), peak strain ratios ($\varepsilon^*_{cc}/\varepsilon_{co}$), and residual stress ratios ($f_{c,res}/f'_{co}$) of actively-confined concrete

Model	Year of publication	Prediction of f^*_{cc}/f'_{co}			Prediction of $\varepsilon^*_{cc}/\varepsilon_{co}$			Prediction of $f_{c,res}/f'_{co}$		
		Average Absolute Error (%)	Mean (%)	Standard Deviation (%)	Average Absolute Error (%)	Mean (%)	Standard Deviation (%)	Average Absolute Error (%)	Mean (%)	Standard Deviation (%)
Richart et al. [70]	1929	9.9	94.9	11.7	36.1	124.9	38.3	-	-	-
Mills and Zimmerman [71]	1970	29.7	83.8	33.4	-	-	-	-	-	-
Mander et al. [3]	1988	9.2	95.4	11.0	50.6	137.1	50.9	-	-	-
Xie et al. [72]	1995	9.4	105.3	10.8	-	-	-	-	-	-
Attard and Setunge [64]	1996	7.4	97.2	9.3	21.6	89.6	25.0	18.3	105.1	28.3
Ansari and Li [73]	1998	12.2	89.3	10.8	25.4	101.0	31.5	-	-	-
Candappa [74]	2001	13.5	107.7	17.1	-	-	-			
Imran and Pantazopoulou [75]	2001	7.7	97.7	9.9	-	-	-	20.4	113.4	28.9
Binici [76]	2005	8.0	96.3	9.7	45.1	134.4	44.9	24.1	76.8	16.3
Jiang and Teng [77]	2007	13.1	88.5	9.7	22.8	91.5	27.6	-	-	-
Teng et al. [78]	2007	Same as Jiang and Teng [77]			28.6	111.5	34.3	-	-	-
Xiao et al. [79]	2010	8.3	95.4	9.6	25.3	104.2	31.7	-	-	-
Samani and Attard [24]	2012	Same as Attard and Setunge [64]			24.7	96.4	30.1	14.4	93.9	18.5

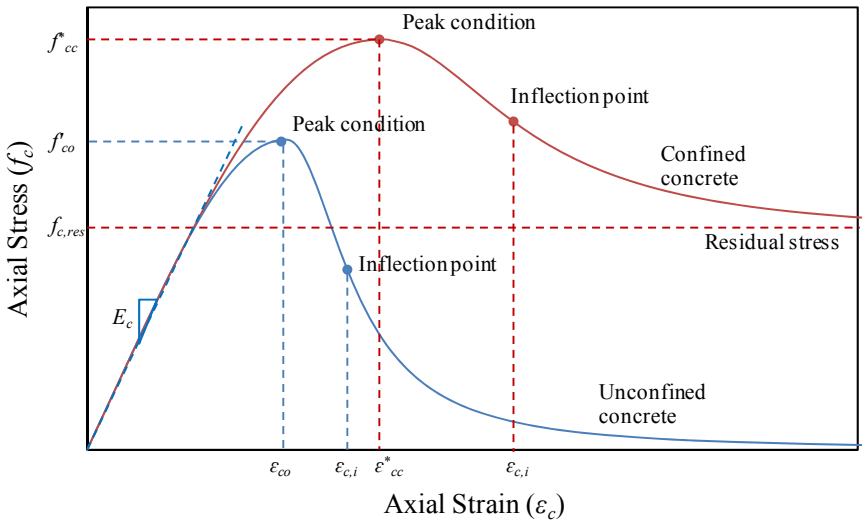

Figure 16. Typical stress-strain curves of unconfined and actively confined concretes

4.1 Peak Stress and Strain of Actively Confined Concrete

Based on the results from the test database of actively confined concrete [7], the expressions established for the predictions of the compressive strength (f^*_{cc}) and the corresponding axial strain (ε^*_{cc}) are given in Eqs. 7 and 8. In these equations, the active confinement ratio (f^*_l/f'_{co}) is expressed as the parameter influencing the compressive strength (f^*_{cc}) and the corresponding axial strain (ε^*_{cc}), whereas the unconfined concrete strength (f'_{co}) is considered a subsidiary parameter affecting the compressive strength (f^*_{cc}) of actively confined concrete. As illustrated in Figures 17 and 18, the trendlines of the proposed expressions (Eqs. 7 and 8) are in good agreement with the experimental results. In the calculations of the strength enhancement ratios (f^*_{cc}/f'_{co}) and the peak strain ratios ($\varepsilon^*_{cc}/\varepsilon_{co}$), the compressive strength (f'_{co}) and the corresponding axial strain (ε_{co}) of unconfined concrete were obtained from cylinder test results reported in the original studies. As can be seen from the comparison of the performance statistics (*AAE, M, SD*) of the proposed model in Figures 17 and 18 with those of the existing models shown in Table 3, the proposed model outperformes the existing models in the predictions of the strength enhancement ratios (f^*_{cc}/f'_{co}) and the peak strain ratios ($\varepsilon^*_{cc}/\varepsilon_{co}$). It might be worth noting that, in the prediction of the $\varepsilon^*_{cc}/\varepsilon_{co}$ ratios, the proposed model would have outperformed the existing models even more significantly, if in the model assessment ε_{co} values were established using the expressions proposed by the models as opposed to the experimental values.

$$f^*_{cc} = f'_{co} + 5.2 f'^{0.91}_{co} \left(\frac{f^*_l}{f'_{co}}\right)^a \qquad \text{where} \qquad a = f'^{-0.06}_{co} \tag{7}$$

$$\varepsilon^*_{cc} = \varepsilon_{co} + 0.045 \left(\frac{f^*_l}{f'_{co}}\right)^{1.15} \tag{8}$$

where f^*_l and f'_{co} are in MPa and ε_{co} is to be calculated using Eq. 3.

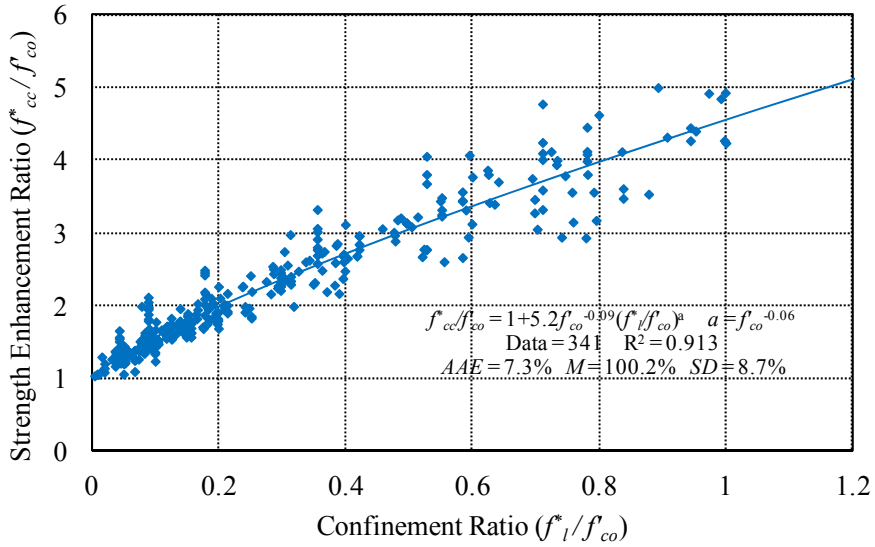

Figure 17. Variation of strength enhancement ratio (f^*_{cc}/f'_{co}) with confinement ratio (f^*_l/f'_{co})

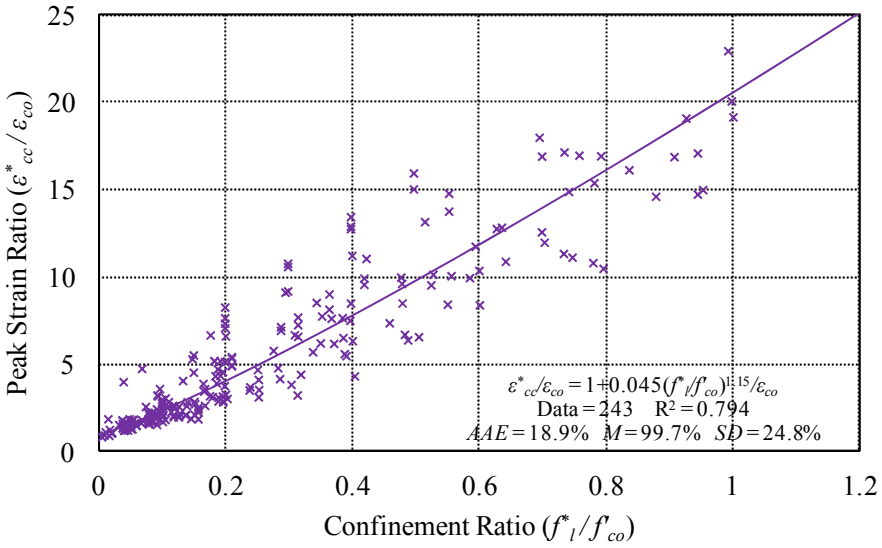

Figure 18. Variation of peak strain ratio ($\varepsilon^*_{cc}/\varepsilon_{co}$) with confinement ratio (f^*_l/f'_{co})

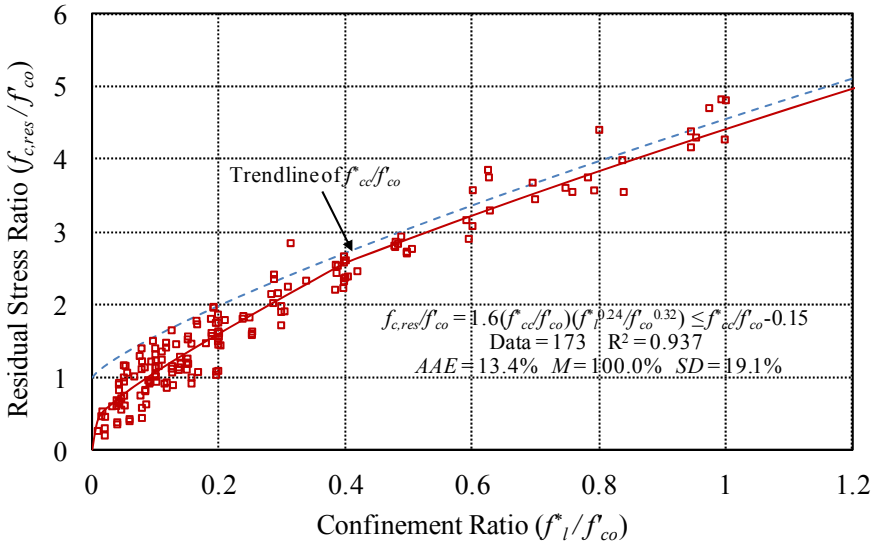

Figure 19. Variation of residual stress ratio ($f_{c,res}/f'_{co}$) with confinement ratio (f^*_l/f'_{co})

4.2 Residual Stress and Inflection Point of Post-Peak Relationship

Accurate determination of the residual stress ($f_{c,res}$) and the axial strain at the inflection point of descending branch ($\varepsilon_{c,i}$) is vital for the prediction of the post-peak stress-strain behavior of actively confined concrete. Based on the results from the test database of actively confined concrete [7], the expression established for the predictions of residual stress ($f_{c,res}$) is given in Eqs. 9. As illustrated in Figure 19, the residual stress ratio ($f_{c,res}/f'_{co}$) increases with the confinement reatio (f^*_l/f'_{co}) and nearly approaches the trendline of the peak stress ratio (f^*_{cc}/f'_{co}), as shown in dashed line in Figure 19, when the confinement ration (f^*_l/f'_{co}) approaches 0.4. In such condition, the residual stress ratio ($f_{c,res}/f'_{co}$) was observed to be slightly lower than the strength enhancement ratio at peak condition (i.e., $f^*_{cc}/f'_{co} - 0.15$), as evident from the comparison of trendlines in Figure 19. This condition is represented through the constraint assigned to the residual stress ($f_{c,res}$) in Eq. 9.

$$f_{c,res} = 1.6 f^*_{cc} \left(\frac{{f^*_l}^{0.24}}{{f'_{co}}^{0.32}} \right) \quad \text{and} \quad f_{c,res} \le f^*_{cc} - 0.15 f'_{co} \tag{9}$$

where f^*_{cc}, f^*_l, and f'_{co} are in MPa.

The inflection point ($\varepsilon_{c,i}$) is important for accurate modelling of the location where the change in shape of the descending branches of stress-strain curves occur. As illustrated in Figures 6 and 16, the inflection points ($\varepsilon_{c,i}$) mark to the locations of the change in the sign of curvature of the descending branches of axial stress-strain curves from negative to positive. Based on the descending branch results of unconfined and actively confined specimens in the databases that had complete axial stress-strain curves, the expression for predicting the inflection point ($\varepsilon_{c,i}$) was established as a function of the peak stress and strain (f^*_{cc}, ε^*_{cc}) and residual stress ($f_{c,res}$) and concrete density ($\rho_{c,f}$), as given in Eq. 10.

$$\varepsilon_{c,i} = \left(2.8 \varepsilon^*_{cc} \left(\frac{f_{c,res}}{f^*_{cc}} \right) {f'_{co}}^{-0.12} + 10 \varepsilon^*_{cc} \left(1 - \frac{f_{c,res}}{f^*_{cc}} \right) {f'_{co}}^{-0.47} \right) \left(\frac{\rho_{c,f}}{2400} \right)^{0.4} \tag{10}$$

where f^*_{cc}, $f_{c,res}$ and f'_{co} are in MPa, and $\rho_{c,f}$ is in kg/m^3.

5. PROPOSED AXIAL STRESS-STRAIN MODEL

A model applicable to both unconfined and actively confined concretes is presented in this section. The ascending branch of the stress-strain curve is to be predicted using the expression developed by Popovics [52] (Eq. 11), with the use of the concrete brittleness constant proposed by Carreira and Chu [55] (Eq. 12). To allow for the change in shape of the stress-strain curve at ascending branch for various types of concrete, the concrete elastic modulus (E_c), compressive strength (f^*_{cc}) and strain (ε^*_{cc}), are to be predicted using Eqs. 2, 7 and 8.

$$f_c = \frac{f^*_{cc} (\varepsilon_c / \varepsilon^*_{cc}) r}{r - 1 + (\varepsilon_c / \varepsilon^*_{cc})^r} \quad \text{if} \quad 0 \le \varepsilon_c \le \varepsilon^*_{cc} \tag{11}$$

$$r = \frac{E_c}{E_c - f^*_{cc} / \varepsilon^*_{cc}} \tag{12}$$

The descending branch of the stress-strain is to be predicted using a new expression developed in this study, which is given in Eq. 13 and was established using a large number of experimental stress-strain curves of unconfined and actively confined specimens in the databases covering various types of concrete. In Eq. 13, the residual stress of the confined concrete ($f_{c,res}$) is to be calculated using Eq. 9, and the inflection point ($\varepsilon_{c,i}$) of the descending branch is to be calculated using Eq. 10.

$$f_c = f^*_{cc} - \frac{f^*_{cc} - f_{c,res}}{1 + \left(\frac{\varepsilon_c - \varepsilon^*_{cc}}{\varepsilon_{c,i} - \varepsilon^*_{cc}}\right)^{-2}} \quad \text{if} \quad \varepsilon_c > \varepsilon^*_{cc} \tag{13}$$

For unconfined concrete, the f^*_{cc} and ε^*_{cc} in Eqs. 11 to 13 become f'_{co} and ε_{co}, respectively.

It should be noted that the proposed expression (Eq. 13) was developed based on the results from the reference specimens with a 152 mm diameter and 305 mm height. To account for the influences of the specimen size and slenderness on post-peak axial strains, an expression is given in the following section (i.e., Eq.14) for the adjustment of axial strains of specimens with geometric dimensions that differ from those of the reference specimens.

5.1 Post-peak Axial Strain Adjustment to Allow for Specimen Size and Slenderness

As was reported in a number of studies, the total deformation of concretes consists of elastic and inelastic components [24, 80-83]. The inelastic component is a displacement occurs in a compression damage zone (H_d) within a segment of the specimen height, whereas the elastic component is a strain occurs along the entire specimen height (H) [80, 81]. Due to the difference in the relative deformations of the elastic and inelastic components, the average axial strain (ε_c) varies with the change in heights (H), as evident from a number of test results [84-87]. To account for the relative contributions of the elastic and inelastic components in the average axial strain (ε_c), axial strain adjustments, which were based on the general concept established by Markeset and Hillerborg [81], were applied in a number of studies [24, 82, 83, 86, 87]. Based on the concept established by Markeset and Hillerborg [81], Eq. 14 was derived in the present study for the adjustment of the axial strains of specimens having diameters (D) and heights (H) different from those of the reference specimens of the proposed model (i.e., D_r = 152 mm, H_r = 305 mm). After the adjustment of the axial strain through Eq.14, the axial strain (ε_c) of the reference specimen in Eq.13 is to be replaced with the adjusted axial strain ($\varepsilon_{c,h}$) to establish the complete stress-train relationship of a specimen with given geometric properties.

$$\varepsilon_{c,h} = \varepsilon_c \quad \text{if} \quad 0 \le \varepsilon_c \le \varepsilon^*_{cc}$$

$$\varepsilon_{c,h} = \frac{\left(f_c - f^*_{cc}\right)}{E_c}\left(1 - \frac{H_r}{H}\right) + \varepsilon^*_{cc} + (\varepsilon_c - \varepsilon^*_{cc})\frac{H_r}{H} + \varepsilon_d \frac{(H_d - H_r)}{H} \quad \text{if} \quad \varepsilon_c > \varepsilon^*_{cc} \tag{14}$$

where $\varepsilon_{c,h}$ is the axial strain for a specimen of height H, H_r is the reference specimen height of 305 mm, H_d is the height of the compression damage zone, equal to twice the specimen diameter (i.e., $H_d = 2D$), and ε_d is the inelastic strain in the damage zone, to be calculated using a new expression (Eq. 15) developed in this study based on analysis of the results from the test databases.

$$\varepsilon_d = 0.02 {f'_{co}}^{-0.5} \left(\frac{f'_{co} - f_c}{f'_{co}} \right) \quad \text{for unconfined concrete}$$

$$\varepsilon_d = 0.02 {f'_{co}}^{-0.5} \left(\frac{f^*_{cc} - f_c}{f^*_{cc} - f_{c,res}} \right) \quad \text{for confined concrete} \tag{15}$$

where f'_{co} is in MPa.

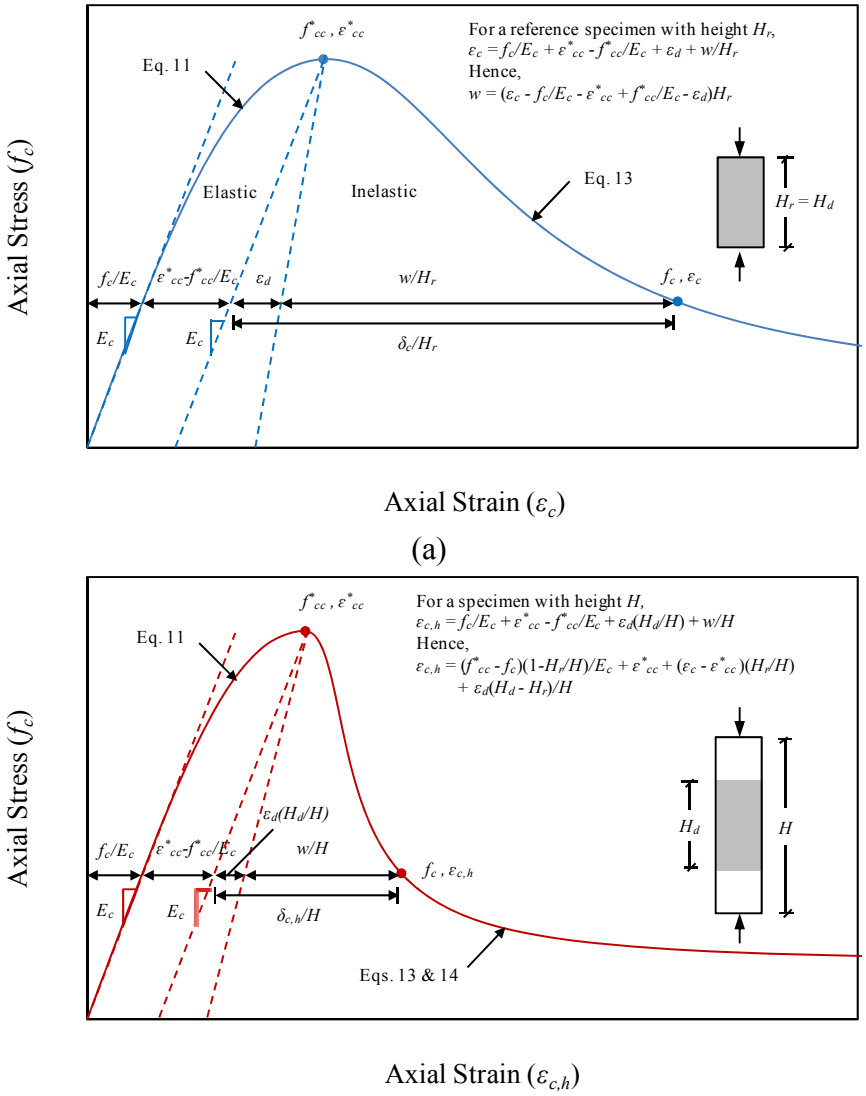

Figure 20. (a) Typical stress-strain curves of a reference specimen with height H_r; and (b) adjusted stress-strain curve of a specimen with height H

To illustrate the strain adjustment process, Figure 20(a) shows the stress-strain curve of a reference specimen (i.e., D_r = 152 mm, H_r = 305 mm), whereas Figure 20(b) shows the adjusted stress-strain curve of a specimen having different geometric dimensions from those of the reference specimen. As illustrated in Figure 20(a), the elastic component of the axial strain consists of a linear portion that follows a loading path equal to the concrete elastic modulus (E_c) and a parabolic portion that approaches the axial strain (ε^*_{cc}) corresponding to

the peak compressive stress (f^*_{cc}). After the peak condition is reached, a linear unloading path with a slope that is equal to the elastic modulus of concrete (E_c) is assumed for the elastic component of the axial strain, and the remaining strains are attributed to the inelastic displacement occurs in the damage zone ($\delta_{c,h}$) [81]. As illustrated in Figure 20(a), the inelastic displacement ($\delta_{c,h}$) consists of an inelastic strain (ε_d) occurs within the damage zone (H_d), and a localized displacement (w) that results from the formation of macrocracks (i.e., $\delta_{c,h} = \varepsilon_d H_d + w$) [81]. When the height of damage zone (H_d) is equal to the reference height (H_r), a typical stress-strain curve, as illustrated Figure 20(a), can be found. In the case of a specimen having a height (H) greater than the height of the damage zone (H_d) as shown in Figure 20(b), the axial strain adjustment to account for the relative contributions of each elastic and inelastic component becomes necessary. To this end, Eqs. 14 and 15, which were developed on the basis of the results from the test databases, are proposed in the present study. The proposed model is not recommended for specimens with a height (H) lower than 2D, where the effect of the frictional resistance supplied by the loading platens at specimen ends becomes evident on the compressive behavior of the specimen [88, 89]. It is recommended that the specimen aspect ratio (H/D), diameter (D), height (H) and concrete compressive strength (f'_{co}) in Eqs.14 and15 be limited to the experimental validation ranges previously noted in Section 3.3.

6. COMPARISON WITH EXPERIMENTAL RESULTS

Figure 21 compares the model predictions with experimental stress-strain curves of unconfined NWC of different compressive strengths (f'_{co}) [41, 59, 61, 87, 90-93]. Figure 22 compares of the model predictions with experimental stress-strain curves of unconfined LWC of different concrete density ($\rho_{c,f}$) [94-97]. Figure 23 compares the model predictions with experimental stress-strain curves of actively confined NWC with different confining pressures (f^*_l) [27, 64, 72, 74, 98-101]. Figure 24 compares of the model predictions with experimental stress-strain curves of unconfined NWC with different aspect ratio (H/D) [84, 86, 87, 102]. As evident from the comparisons, the predictions of the proposed model are in good agreement with the experimental results that consist of a wide range of compressive strengths (f'_{co}), concrete densities ($\rho_{c,f}$), specimen dimensions (H and D), and confining pressures (f^*_l). To complete the comparisons, the predictions of the proposed model is also compared with those of the existing models that are capable of generating complete stress-strain curves of unconfined and confined concretes [3, 24, 64, 76-79]. The results of this comparison are shown in Figure 25, which illustrate the improved accuracy of the proposed model in predicting the behavior of concretes under various levels of confinement.

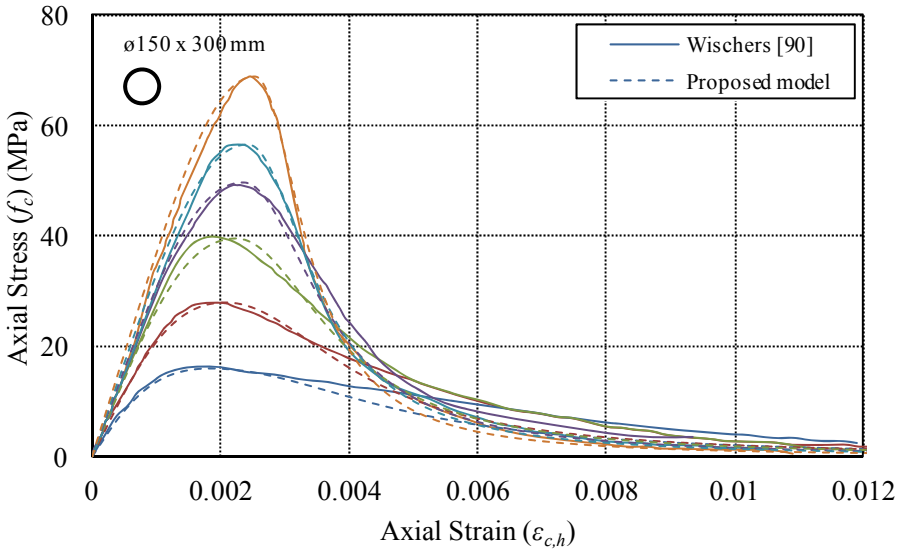
ø150 x 300 mm
Wischers [90]
Proposed model
Axial Stress (f_c) (MPa)
0
20
40
60
80
0
0.002
0.004
0.006
0.008
0.01
0.012
Axial Strain ($\varepsilon_{c,h}$)

(a)

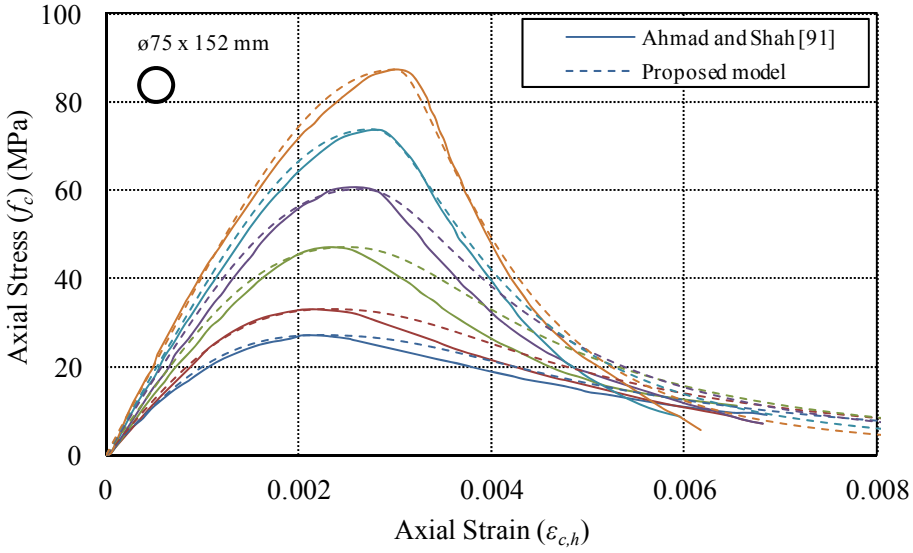
ø75 x 152 mm
Ahmad and Shah [91]
Proposed model
Axial Stress (f_c) (MPa)
0
20
40
60
80
100
0
0.002
0.004
0.006
0.008
Axial Strain ($\varepsilon_{c,h}$)

(b)

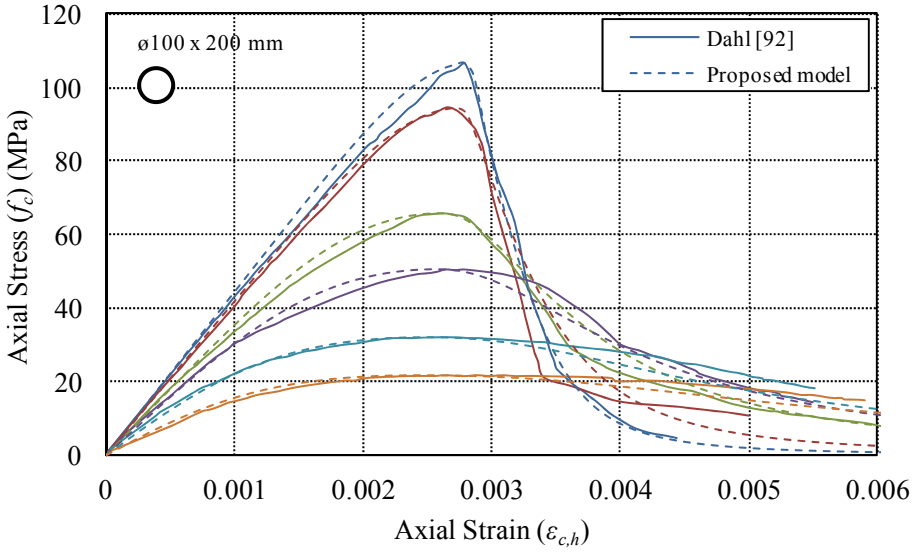
ø100 x 200 mm
Dahl [92]
Proposed model
Axial Stress (f_c) (MPa)
0
20
40
60
80
100
120
0
0.001
0.002
0.003
0.004
0.005
0.006
Axial Strain ($\varepsilon_{c,h}$)

(c)

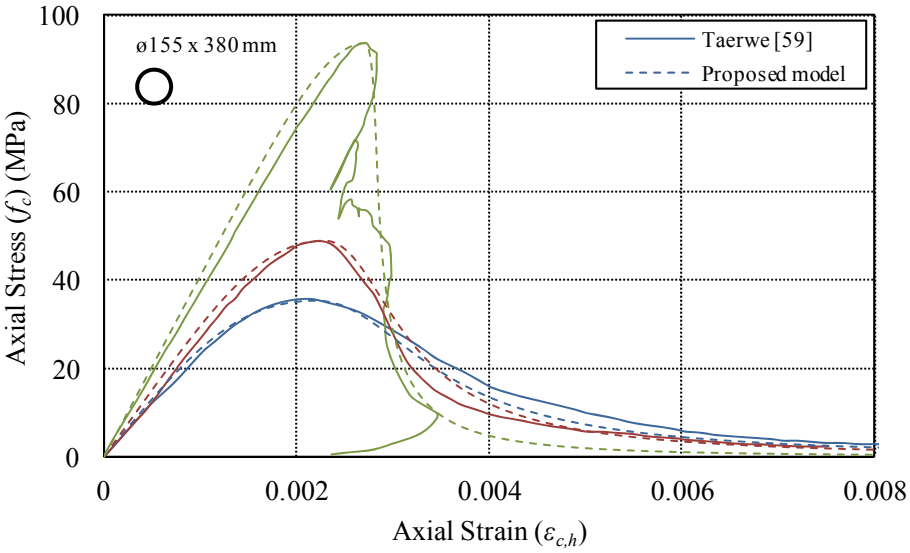
ø155 x 380 mm
Taerwe [59]
Proposed model
Axial Stress (f_c) (MPa)
Axial Strain ($\varepsilon_{c,h}$)
0
20
40
60
80
100
0
0.002
0.004
0.006
0.008

(d)

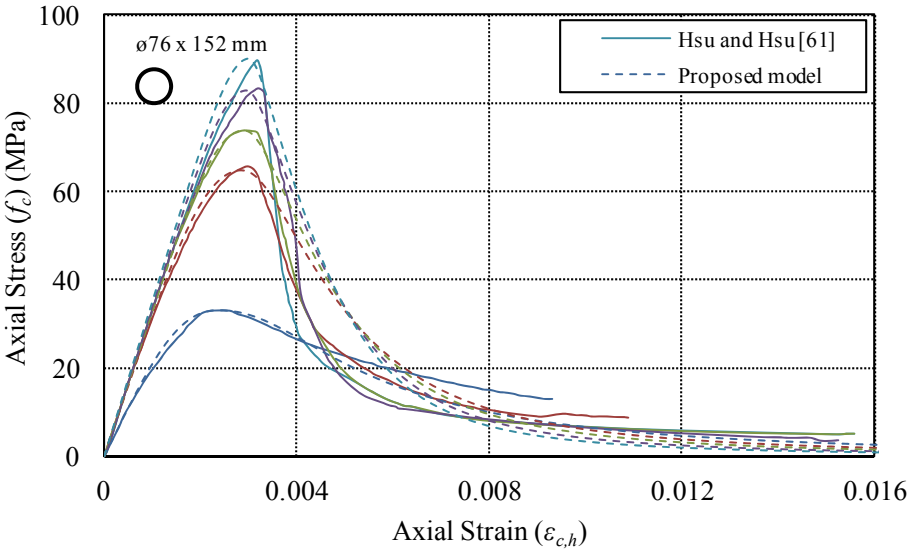
ø76 x 152 mm
Hsu and Hsu [61]
Proposed model
Axial Stress (f_c) (MPa)
Axial Strain ($\varepsilon_{c,h}$)
0
20
40
60
80
100
0
0.004
0.008
0.012
0.016

(e)

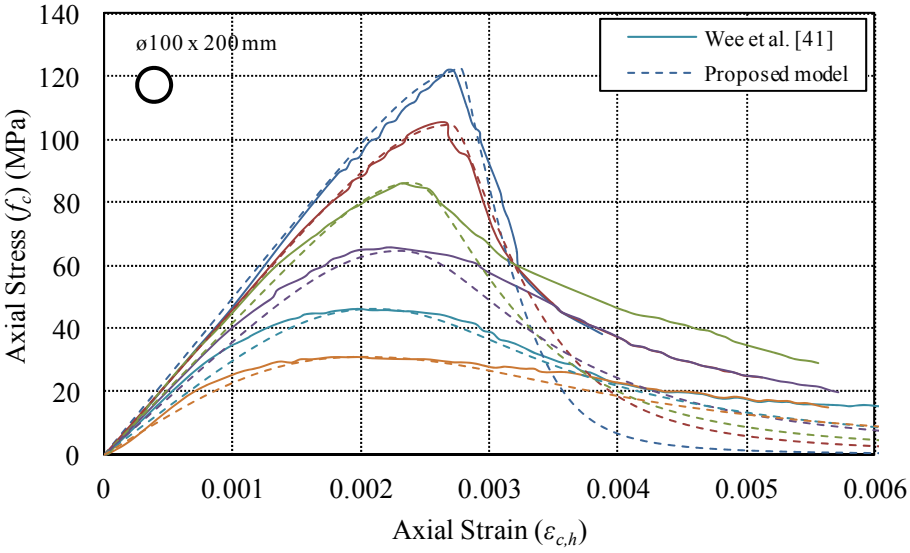
ø100 x 200 mm
Wee et al. [41]
Proposed model
Axial Stress (f_c) (MPa)
Axial Strain ($\varepsilon_{c,h}$)
0
20
40
60
80
100
120
140
0
0.001
0.002
0.003
0.004
0.005
0.006

(f)

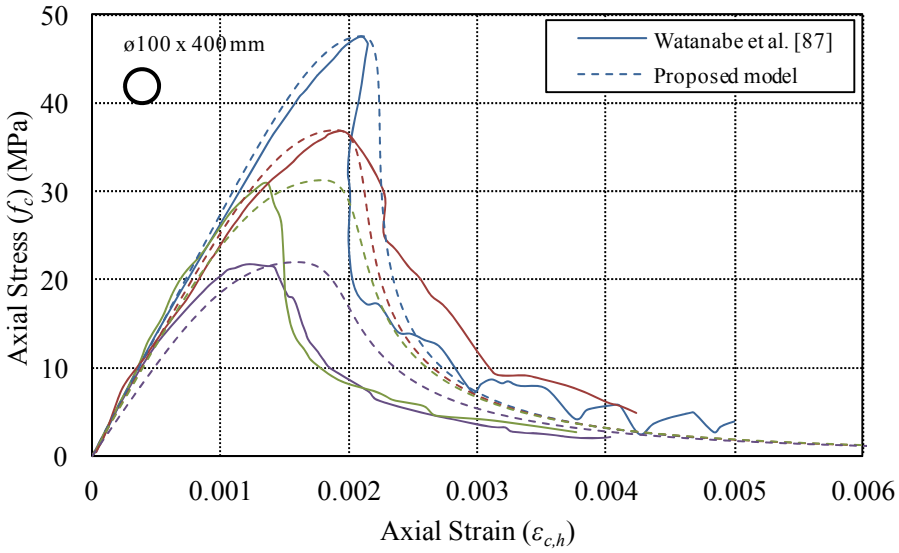

(g)

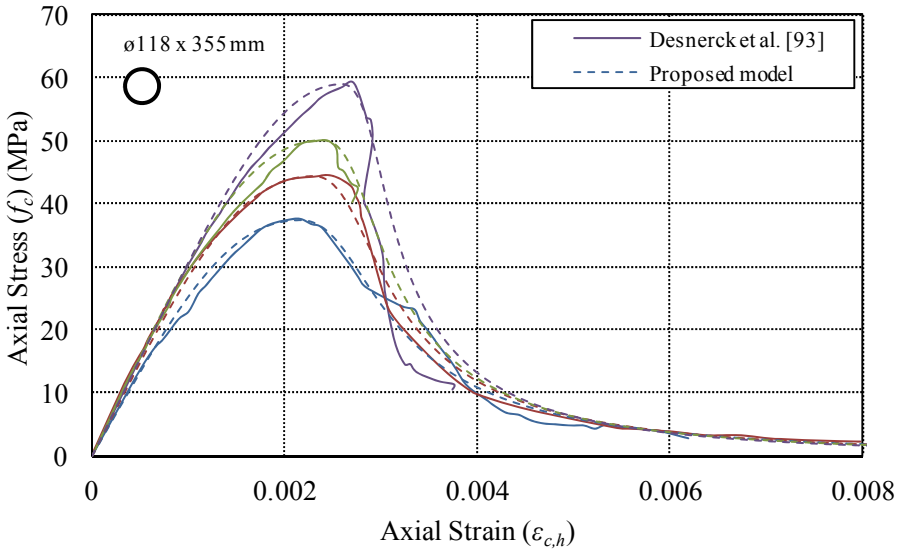

(h)

Figure 21. Comparison of the proposed model predictions with unconfined specimen results of different concrete strengths from: (a) Wischers [90]; (b) Ahmad and Shah [91]; (c) Dahl [92]; (d) Taerwe [59]; (e) Hsu and Hsu [61]; (f) Wee et al. [41]; (g) Watanabe et al. [87]; and (h) Desnerck et al. [93]

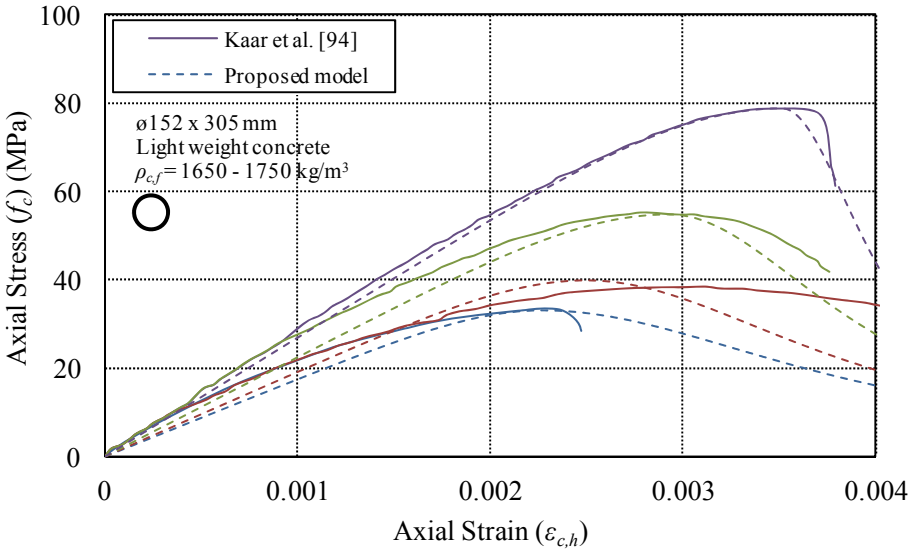
Kaar et al. [94]
Proposed model
ø152 x 305 mm
Light weight concrete
$\rho_{c,f}$ = 1650 - 1750 kg/m³
Axial Stress (f_c) (MPa)
Axial Strain ($\varepsilon_{c,h}$)
0
20
40
60
80
100
0.001
0.002
0.003
0.004

(a)

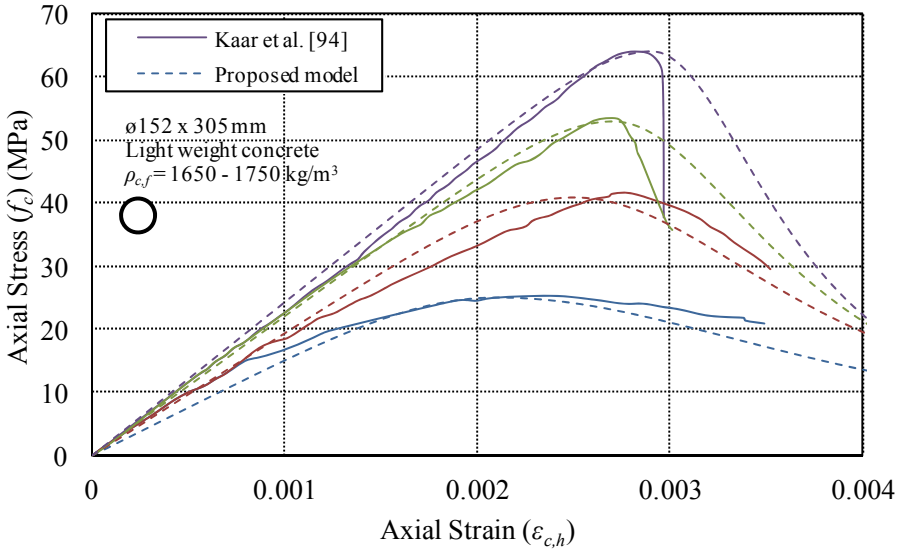
Kaar et al. [94]
Proposed model
ø152 x 305 mm
Light weight concrete
$\rho_{c,f}$ = 1650 - 1750 kg/m³
Axial Stress (f_c) (MPa)
Axial Strain ($\varepsilon_{c,h}$)
0
10
20
30
40
50
60
70
0.001
0.002
0.003
0.004

(b)

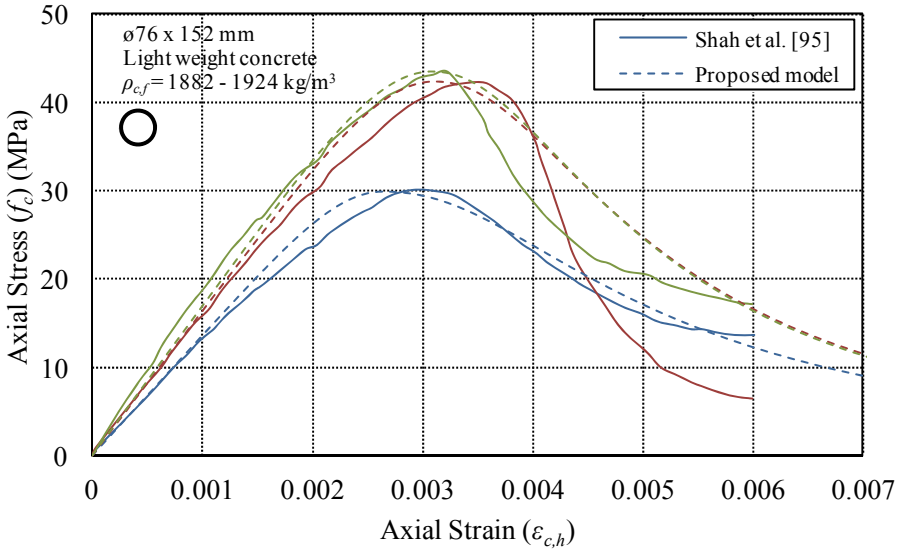
Shah et al. [95]
Proposed model
ø76 x 152 mm
Light weight concrete
$\rho_{c,f}$ = 1882 - 1924 kg/m³
Axial Stress (f_c) (MPa)
Axial Strain ($\varepsilon_{c,h}$)
0
10
20
30
40
50
0.001
0.002
0.003
0.004
0.005
0.006
0.007

(c)

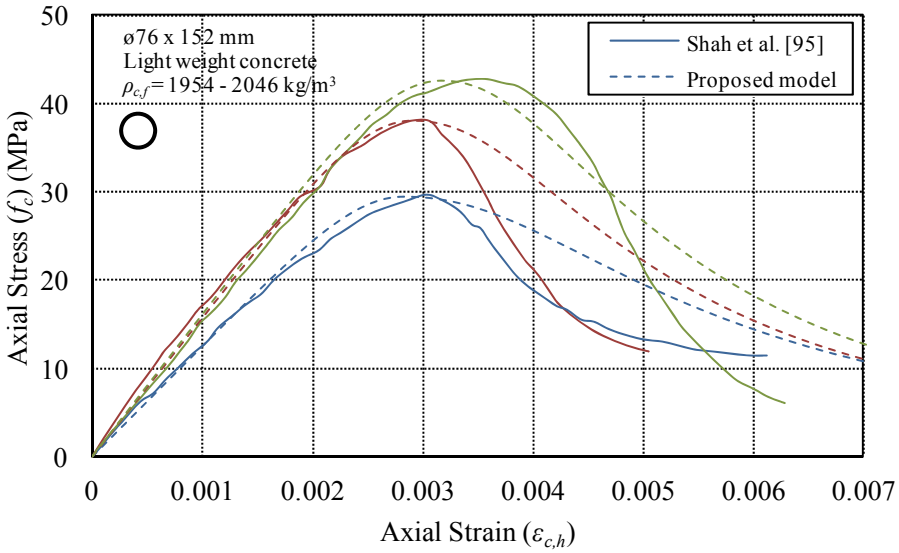
ø76 x 152 mm
Light weight concrete
$\rho_{c,f}$ = 1954 - 2046 kg/m³
Shah et al. [95]
Proposed model
Axial Stress (f_c) (MPa)
Axial Strain ($\varepsilon_{c,h}$)
0
10
20
30
40
50
0
0.001
0.002
0.003
0.004
0.005
0.006
0.007

(d)

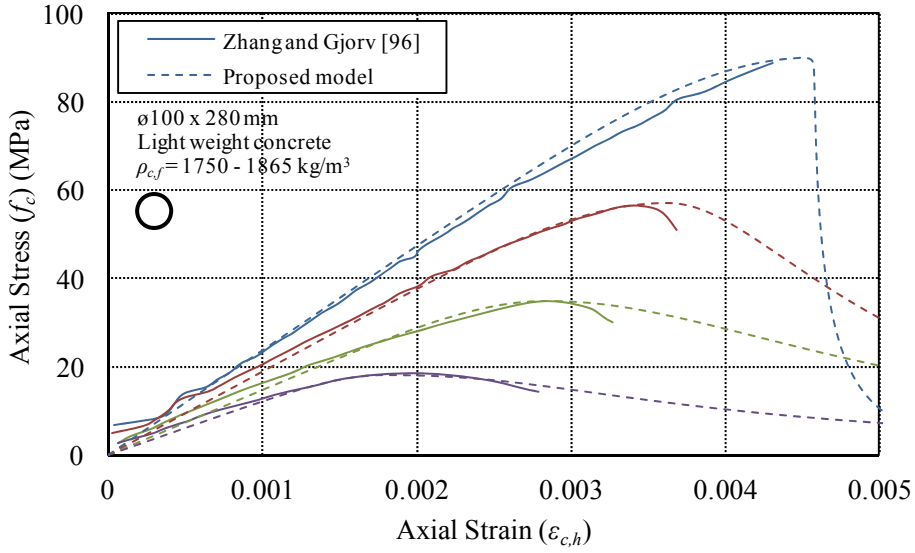
Zhang and Gjorv [96]
Proposed model
ø100 x 280 mm
Light weight concrete
$\rho_{c,f}$ = 1750 - 1865 kg/m³
Axial Stress (f_c) (MPa)
Axial Strain ($\varepsilon_{c,h}$)
0
20
40
60
80
100
0
0.001
0.002
0.003
0.004
0.005

(e)

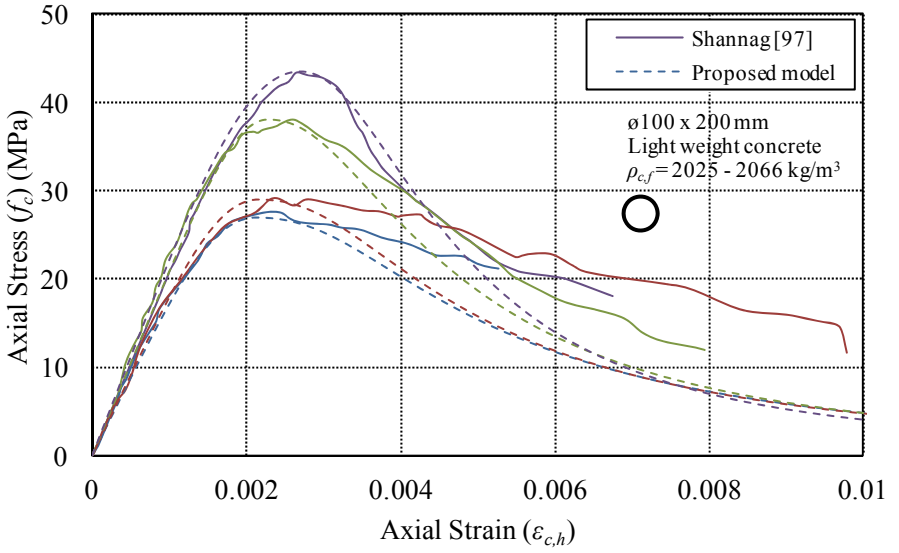
Shannag [97]
Proposed model
ø100 x 200 mm
Light weight concrete
$\rho_{c,f}$ = 2025 - 2066 kg/m³
Axial Stress (f_c) (MPa)
Axial Strain ($\varepsilon_{c,h}$)
0
10
20
30
40
50
0
0.002
0.004
0.006
0.008
0.01

(f)

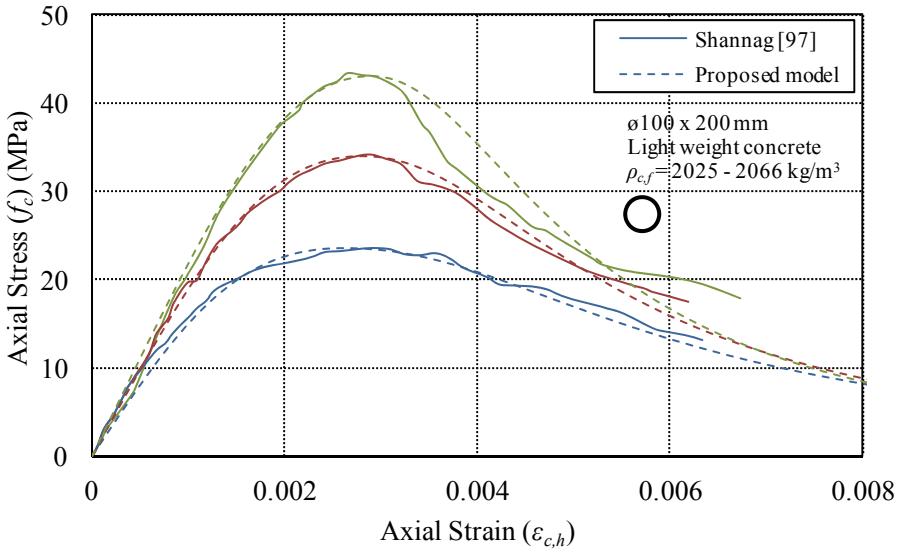

(g)

Figure 22. Comparison of the proposed model predictions with unconfined specimen results of light-weight concretes from: (a-b) Kaar et al. [94]; (c-d) Shah et al. [95]; (e) Zhang and Gjorv [96]; and (f-g) Shannag [97]

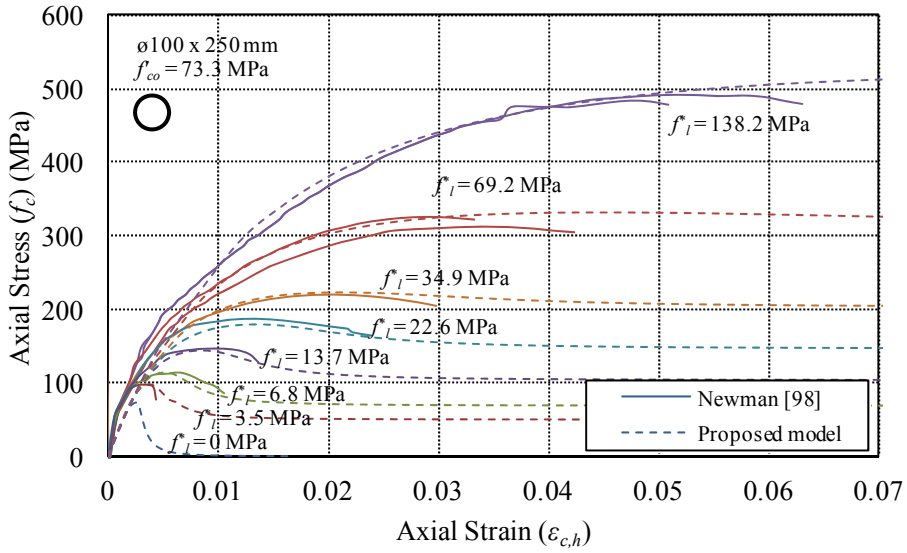

(a)

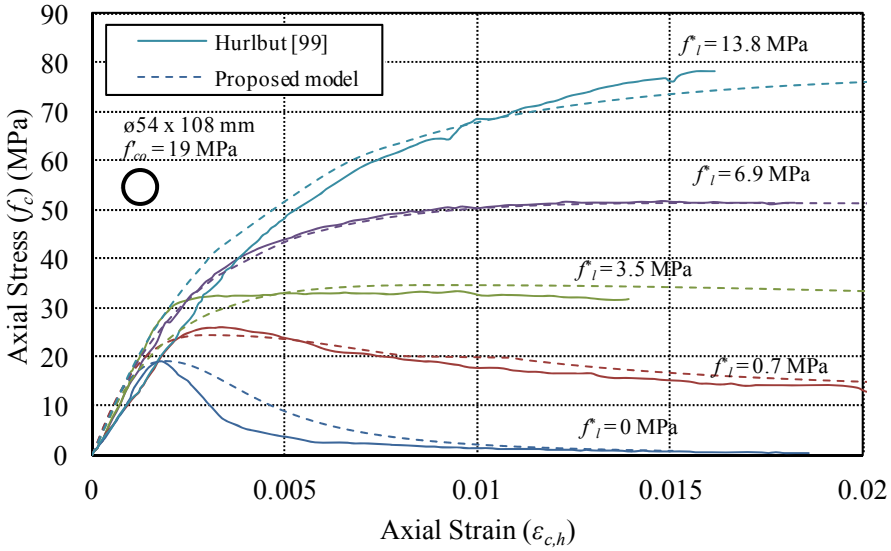
Hurlbut [99]
Proposed model
ø54 x 108 mm
f'_{co} = 19 MPa
f'_l = 13.8 MPa
f'_l = 6.9 MPa
f'_l = 3.5 MPa
f'_l = 0.7 MPa
f'_l = 0 MPa
Axial Stress (f_c) (MPa)
Axial Strain ($\varepsilon_{c,h}$)
0
10
20
30
40
50
60
70
80
90
0
0.005
0.01
0.015
0.02

(b)

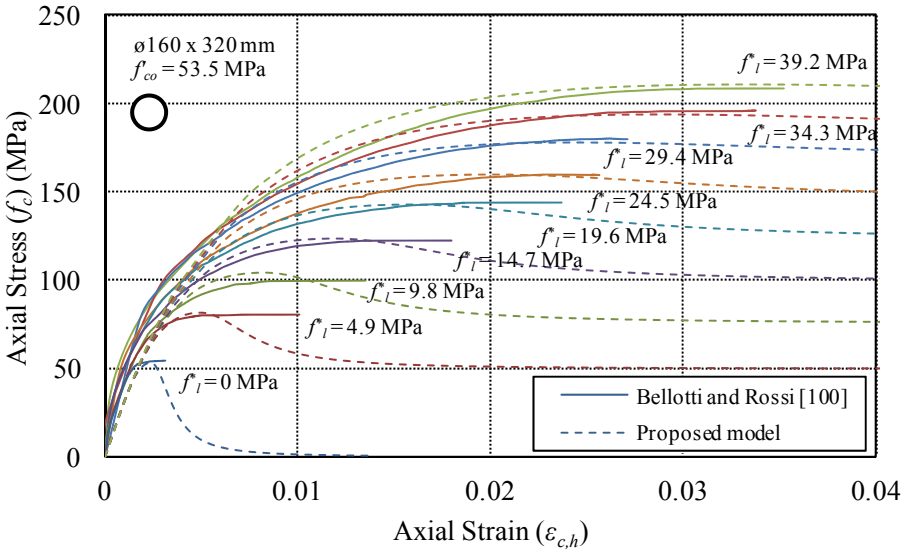
ø160 x 320 mm
f'_{co} = 53.5 MPa
f'_l = 39.2 MPa
f'_l = 34.3 MPa
f'_l = 29.4 MPa
f'_l = 24.5 MPa
f'_l = 19.6 MPa
f'_l = 14.7 MPa
f'_l = 9.8 MPa
f'_l = 4.9 MPa
f'_l = 0 MPa
Bellotti and Rossi [100]
Proposed model
Axial Stress (f_c) (MPa)
Axial Strain ($\varepsilon_{c,h}$)
0
50
100
150
200
250
0
0.01
0.02
0.03
0.04

(c)

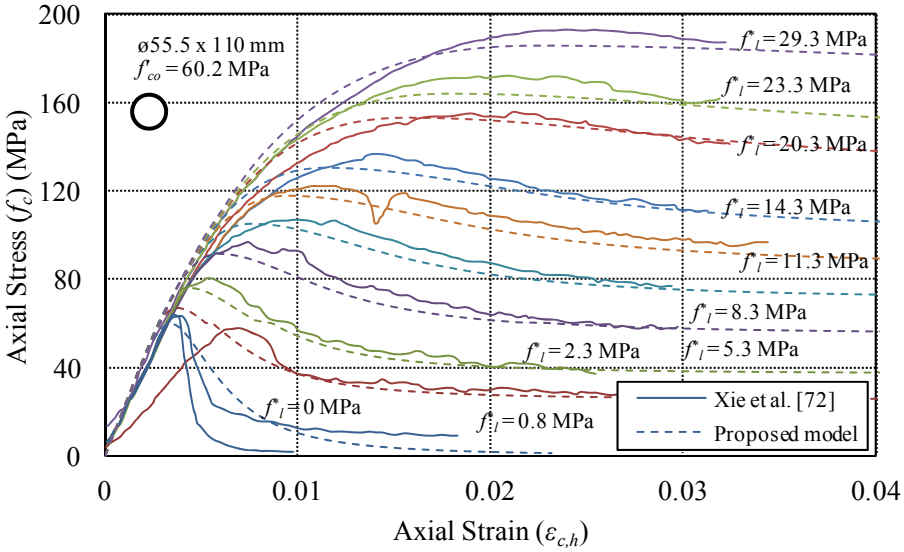
ø55.5 x 110 mm
f'_{co} = 60.2 MPa
f'_l = 29.3 MPa
f'_l = 23.3 MPa
f'_l = 20.3 MPa
f'_l = 14.3 MPa
f'_l = 11.3 MPa
f'_l = 8.3 MPa
f'_l = 5.3 MPa
f'_l = 2.3 MPa
f'_l = 0.8 MPa
f'_l = 0 MPa
Xie et al. [72]
Proposed model
Axial Stress (f_c) (MPa)
Axial Strain ($\varepsilon_{c,h}$)
0
40
80
120
160
200
0
0.01
0.02
0.03
0.04

(d)

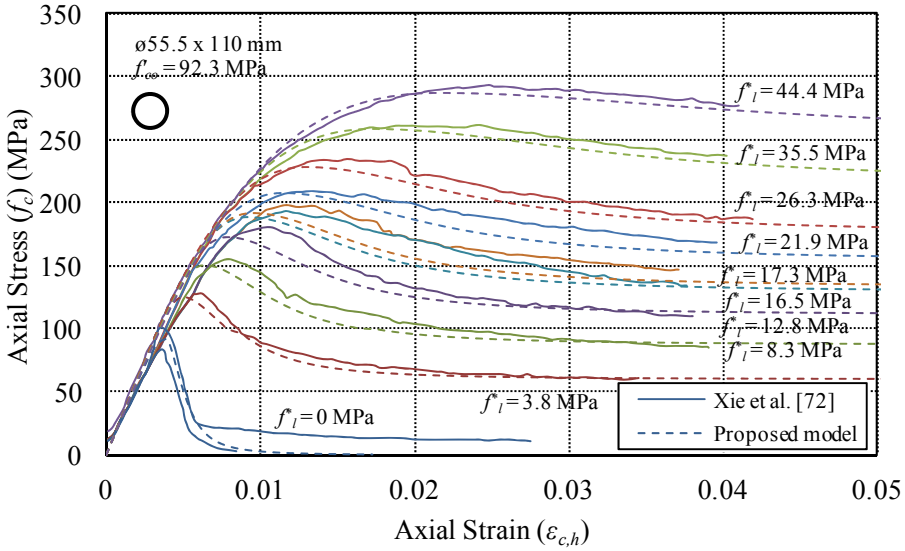
ø55.5 x 110 mm
f'_{co} = 92.3 MPa
f'_l = 44.4 MPa
f'_l = 35.5 MPa
f'_l = 26.3 MPa
f'_l = 21.9 MPa
f'_l = 17.3 MPa
f'_l = 16.5 MPa
f'_l = 12.8 MPa
f'_l = 8.3 MPa
f'_l = 3.8 MPa
f'_l = 0 MPa
Xie et al. [72]
Proposed model
Axial Stress (f_c) (MPa)
Axial Strain ($\varepsilon_{c,h}$)
0
50
100
150
200
250
300
350
0
0.01
0.02
0.03
0.04
0.05

(e)

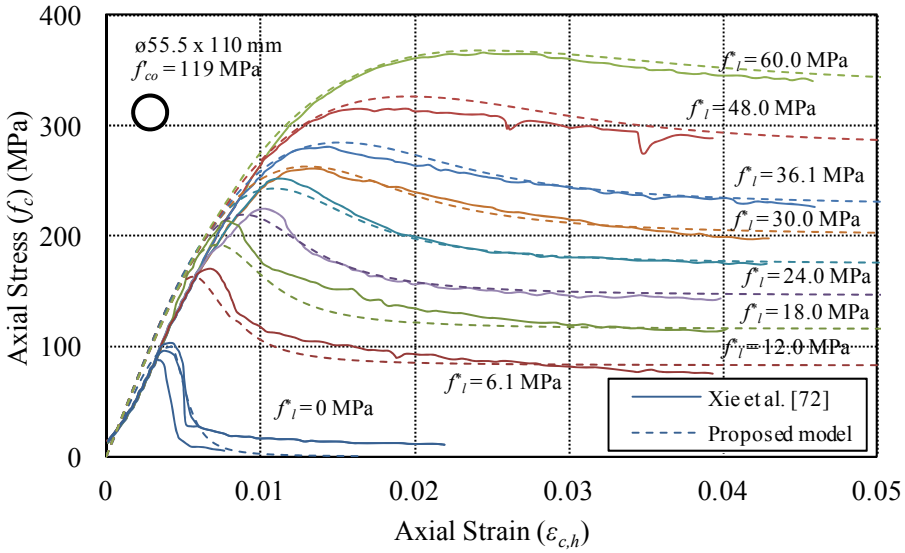
ø55.5 x 110 mm
f'_{co} = 119 MPa
f'_l = 60.0 MPa
f'_l = 48.0 MPa
f'_l = 36.1 MPa
f'_l = 30.0 MPa
f'_l = 24.0 MPa
f'_l = 18.0 MPa
f'_l = 12.0 MPa
f'_l = 6.1 MPa
f'_l = 0 MPa
Xie et al. [72]
Proposed model
Axial Stress (f_c) (MPa)
Axial Strain ($\varepsilon_{c,h}$)
0
100
200
300
400
0
0.01
0.02
0.03
0.04
0.05

(f)

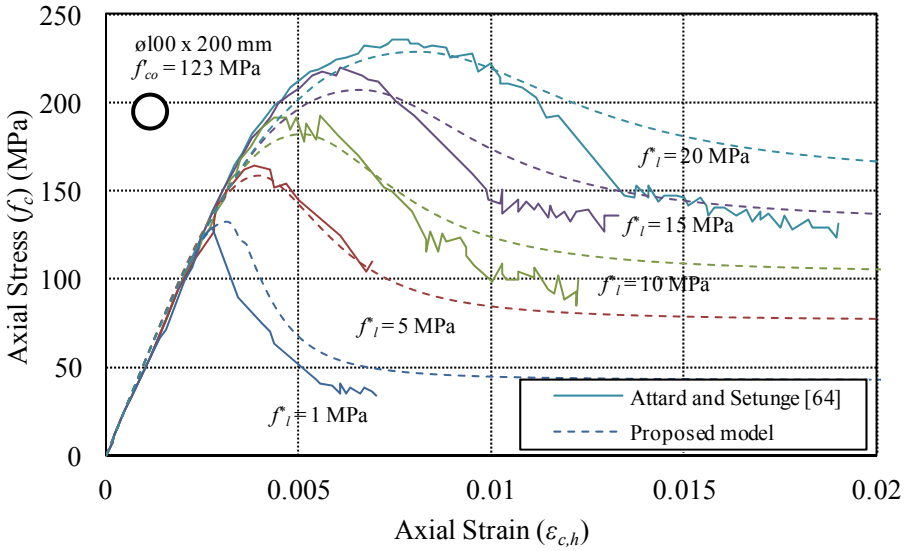
ø100 x 200 mm
f'_{co} = 123 MPa
f'_l = 20 MPa
f'_l = 15 MPa
f'_l = 10 MPa
f'_l = 5 MPa
f'_l = 1 MPa
Attard and Setunge [64]
Proposed model
Axial Stress (f_c) (MPa)
Axial Strain ($\varepsilon_{c,h}$)
0
50
100
150
200
250
0
0.005
0.01
0.015
0.02

(g)

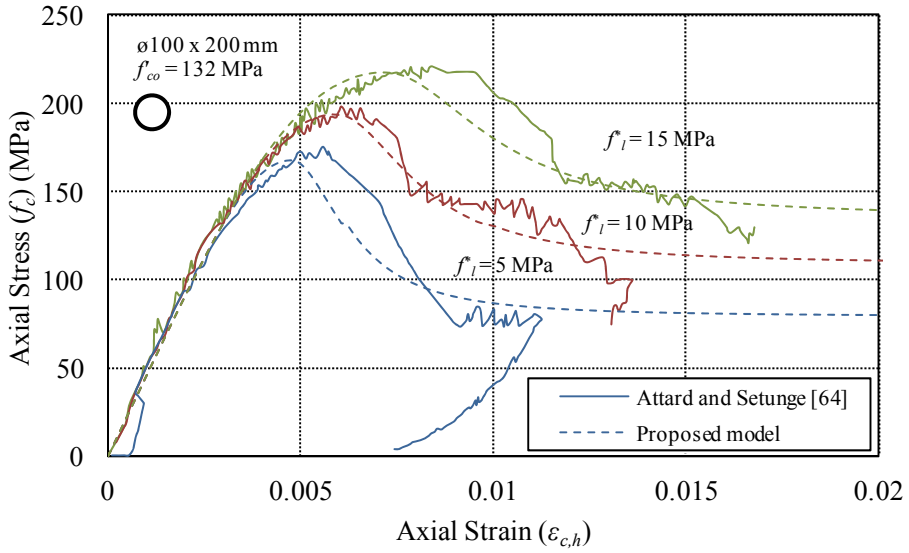
ø100 x 200 mm
f'_{co} = 132 MPa
f^*_l = 15 MPa
f^*_l = 10 MPa
f^*_l = 5 MPa
Attard and Setunge [64]
Proposed model
Axial Stress (f_c) (MPa)
Axial Strain ($\varepsilon_{c,h}$)
0
50
100
150
200
250
0.005
0.01
0.015
0.02

(h)

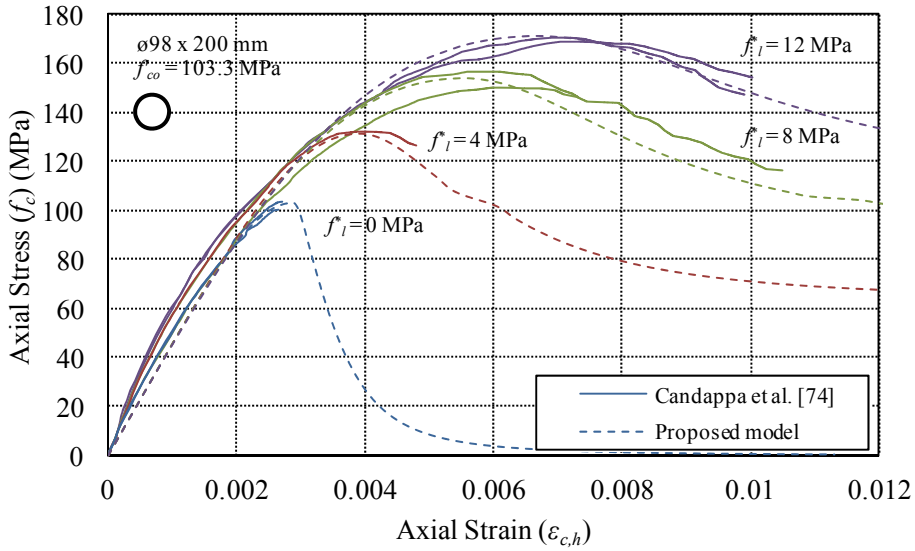
ø98 x 200 mm
f'_{co} = 103.3 MPa
f^*_l = 12 MPa
f^*_l = 8 MPa
f^*_l = 4 MPa
f^*_l = 0 MPa
Candappa et al. [74]
Proposed model
Axial Stress (f_c) (MPa)
Axial Strain ($\varepsilon_{c,h}$)
0
20
40
60
80
100
120
140
160
180
0.002
0.004
0.006
0.008
0.01
0.012

(i)

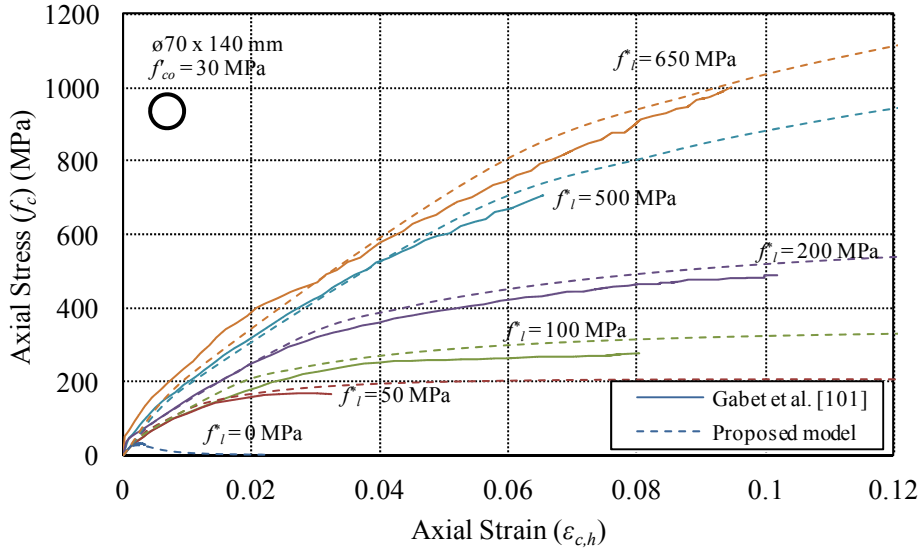
ø70 x 140 mm
f'_{co} = 30 MPa
f^*_l = 650 MPa
f^*_l = 500 MPa
f^*_l = 200 MPa
f^*_l = 100 MPa
f^*_l = 50 MPa
f^*_l = 0 MPa
Gabet et al. [101]
Proposed model
Axial Stress (f_c) (MPa)
Axial Strain ($\varepsilon_{c,h}$)
0
200
400
600
800
1000
1200
0.02
0.04
0.06
0.08
0.1
0.12

(j)

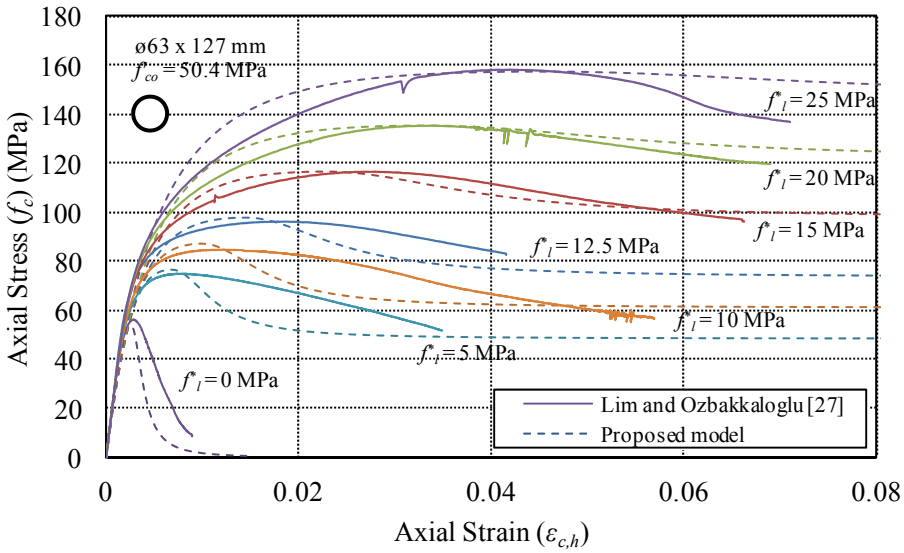

(k)

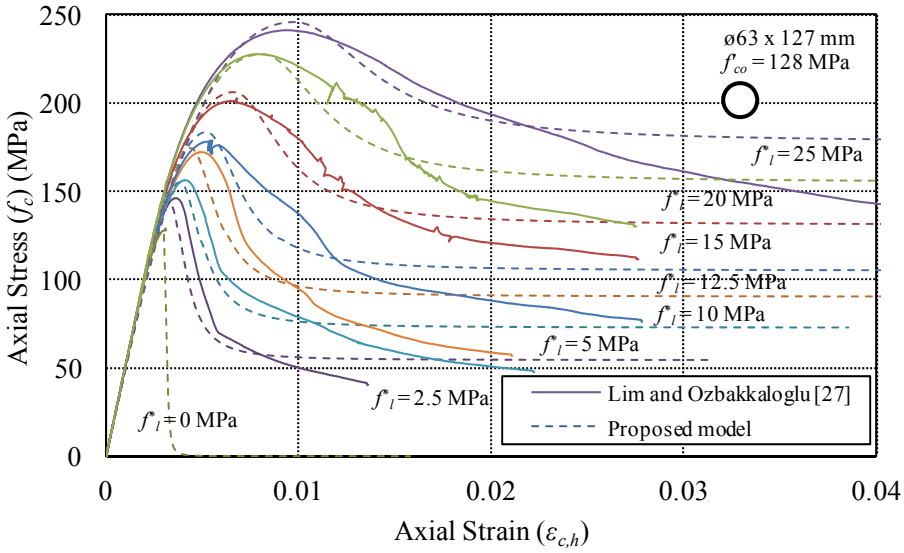

(l)

Figure 23. Comparison of the proposed model predictions with actively confined specimen results from: (a) Newman [98]; (b) Hurlbut [99]; (c) Bellotti and Rossi [100]; (d-f) Xie et al. [72]; (g-h) Attard and Setunge [64]; (i) Candappa et al. [74]; (j) Gabet et al. [101]; and (k-l) Lim and Ozbakkaloglu [27]

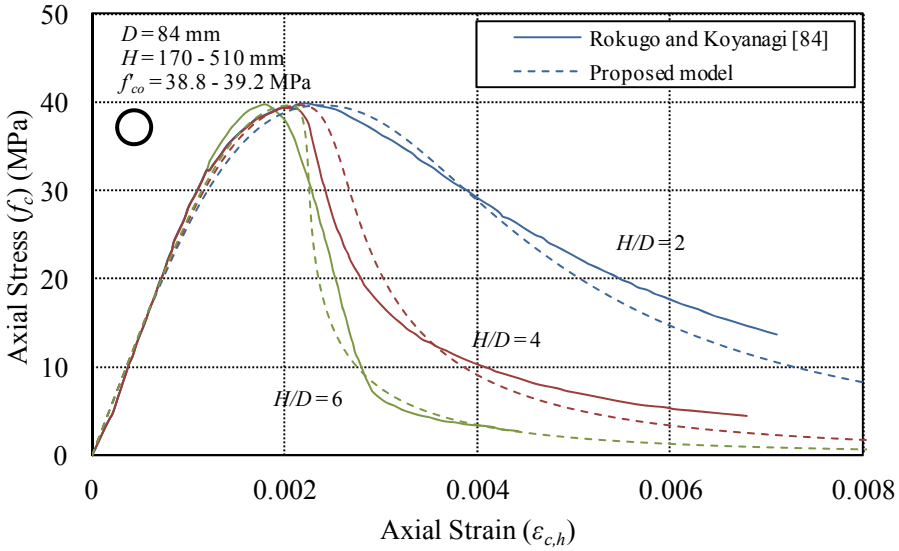
D = 84 mm
H = 170 - 510 mm
f'co = 38.8 - 39.2 MPa
Rokugo and Koyanagi [84]
Proposed model
H/D = 2
H/D = 4
H/D = 6
Axial Stress (fc) (MPa)
Axial Strain (εc,h)
0
10
20
30
40
50
0.002
0.004
0.006
0.008

(a)

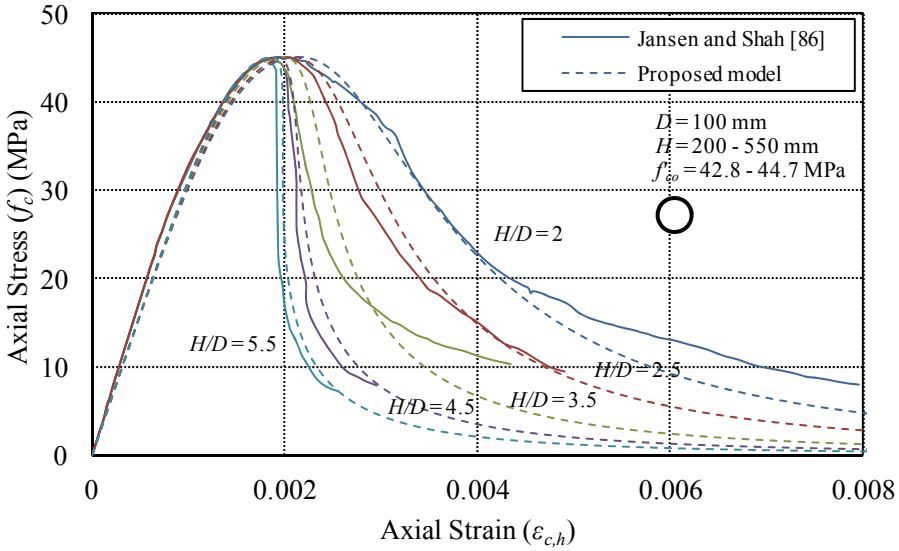
Jansen and Shah [86]
Proposed model
D = 100 mm
H = 200 - 550 mm
f'co = 42.8 - 44.7 MPa
H/D = 2
H/D = 2.5
H/D = 3.5
H/D = 4.5
H/D = 5.5
Axial Stress (fc) (MPa)
Axial Strain (εc,h)
0
10
20
30
40
50
0.002
0.004
0.006
0.008

(b)

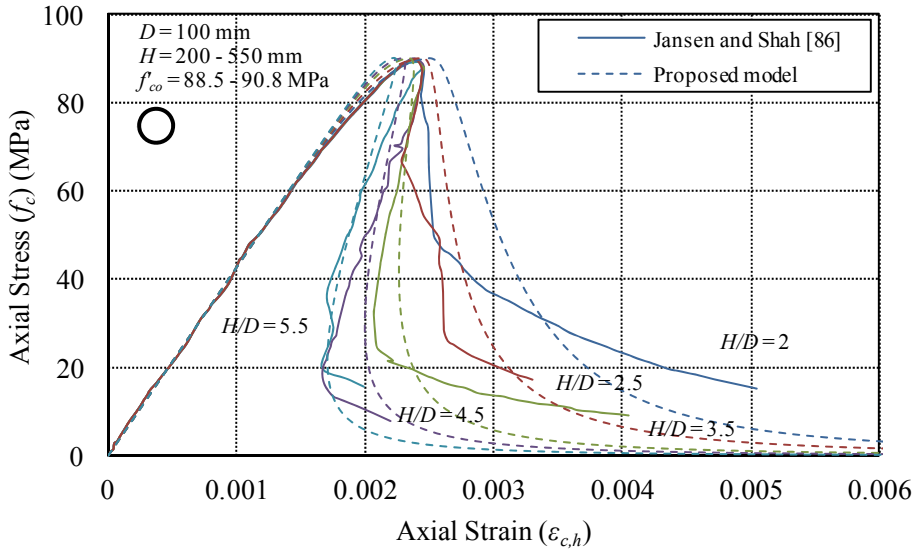
D = 100 mm
H = 200 - 550 mm
f'co = 88.5 - 90.8 MPa
Jansen and Shah [86]
Proposed model
H/D = 2
H/D = 2.5
H/D = 3.5
H/D = 4.5
H/D = 5.5
Axial Stress (fc) (MPa)
Axial Strain (εc,h)
0
20
40
60
80
100
0.001
0.002
0.003
0.004
0.005
0.006

(c)

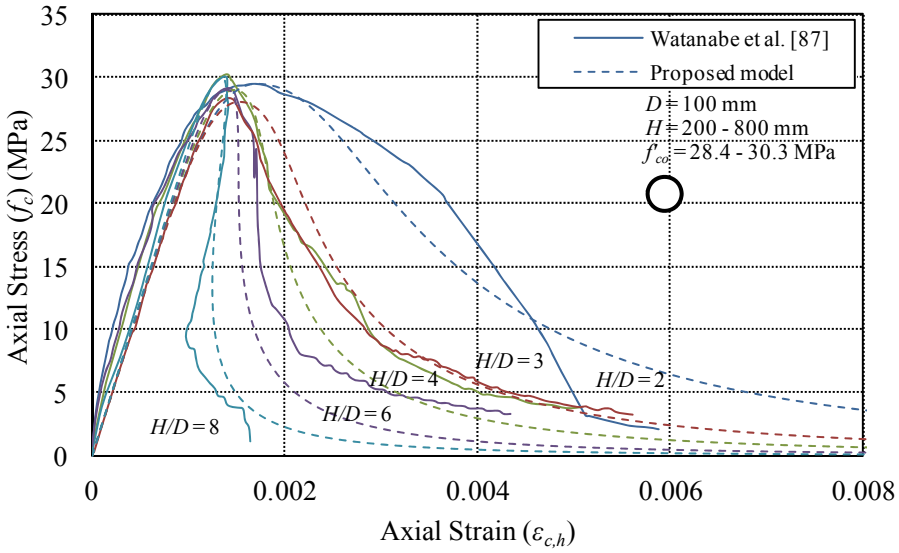

(d)

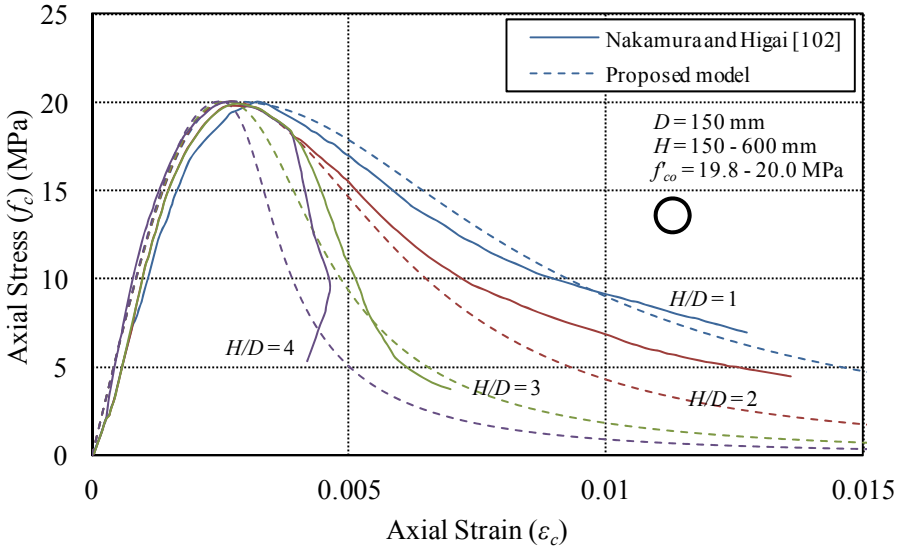

(e)

Figure 24. Comparison of the proposed model predictions with unconfined specimen results of different aspect ratios from: (a) Rokugo and Koyanagi [84]; (b-c) Jansen and Shah [86]; (d) Watanabe et al. [87]; and (e) Nakamura and Higai [102]

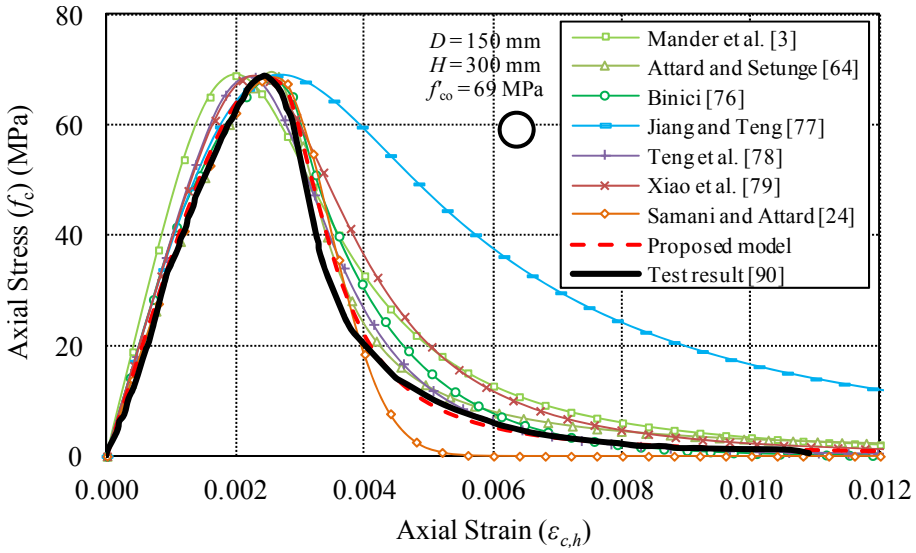

(a)

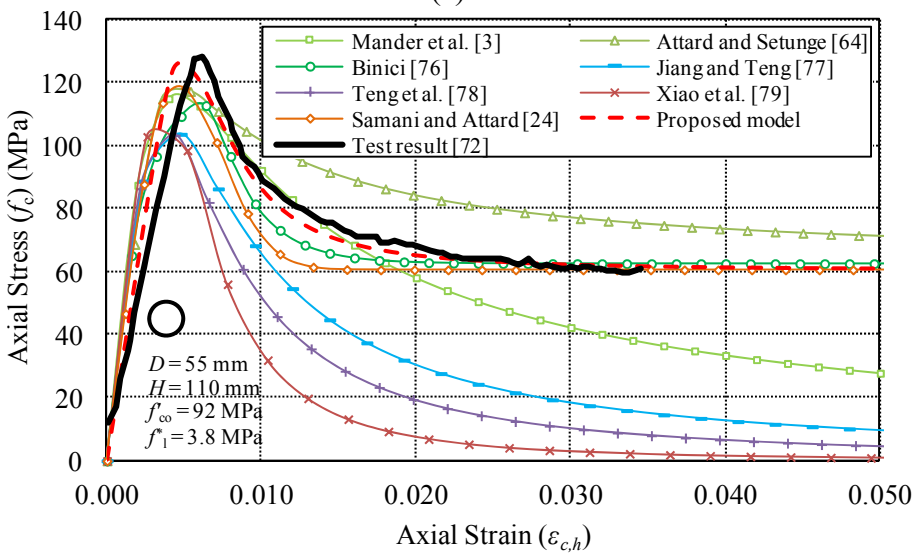

(b)

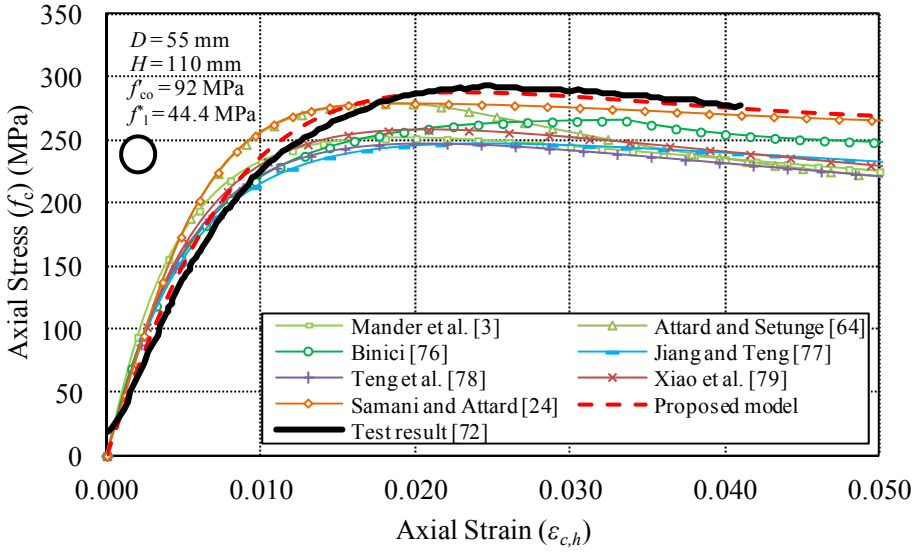

(c)

Figure 25. Comparison of stress-strain curves predicted by existing models: (a) unconfined concrete; (b) lightly-confined concrete; and (c) heavily-confined concrete

7. CONCLUSIONS

This paper has presented the results of an investigation into the stress-strain behavior of concrete in compression. Two large databases of experimental results of unconfined and actively confined specimens were assembled through an extensive review of the literature. Based on the unconfined concrete database, a wide range of parameters influencing the compressive behavior of various types of concrete ranging from light-weight to high-strength were carefully studied. This resulted in the development of unified expressions for the predictions of elastic modulus and compressive strength and the corresponding axial strain of various types of concrete. The database was then studied together with the companion actively confined concrete database, in order to capture the change in behavior of unconfined and confined concretes. A unified stress-strain model for the predictions of compressive behavior of unconfined and actively confined concretes was then developed and is presented. The model is applicable to normal and light-weight concretes with compressive strengths up to 120 MPa. The important features of the proposed stress-strain model include: i) applicability to concretes with various densities and strengths, ii) accurate prediction of the peak and residual stresses and strains of unconfined and confined concretes, iii) consideration of the change in shape of stress-strain curve with the type of concrete, and iv) consideration of specimen size and slenderness effects. The proposed model provides improved predictions of the peak stress and strain of unconfined and confined concretes compared to existing models. In addition, the model is capable of predicting the change in shapes of stress-strain curves of various types of concrete, including normal and light-weight concretes.

REFERENCES

1. Kent, D.C. and Park, R., (1971). "Flexural members with confined concrete." *Journal of the Structural Division, ASCE,* 97(7), 1969-1990.
2. Sheikh, S.A. and Uzumeri, S.M., (1980). "Strength and Ductility of Tied Concrete Columns." *Journal of Structural Engineering, ASCE,* 106(5), 1079-1102.
3. Mander, J.B., Priestley, M.J.N., and Park, R., (1988). "Theoretical stress-strain model for confined concrete." *Journal of Structural Engineering, ASCE,* 114(8), 1804-1826.
4. Saatcioglu, M. and Razvi, S.R., (1992). "Strength and ductility of confined concrete." *Journal of Structural Engineering, ASCE,* 118(6), 1590-607.
5. Ozbakkaloglu, T. and Saatcioglu, M., (2006). "Seismic behavior of high-strength concrete columns confined by fiber-reinforced polymer tubes." *Journal of Composites for Construction, ASCE,* 10(6), 538-549.
6. Ozbakkaloglu, T., Lim, J.C., and Vincent, T., (2013). "FRP-confined concrete in circular sections: Review and assessment of stress–strain models." *Engineering Structures,* 49, 1068–1088.
7. Lim, J.C. and Ozbakkaloglu, T., (2014). "Lateral strain-to-axial strain relationship of confined concrete." *Journal of Structural Engineering, ASCE,* Doi: 10.1061/(ASCE)ST.1943-541X.0001094.
8. Razvi, S. and Saatcioglu, M., (1999). "Confinement model for high-strength concrete." *Journal of Structural Engineering,* 125(3), 281-289.
9. Ilki, A., Peker, O., Karamuk, E., Demir, C., and Kumbasar, N., (2008). "FRP retrofit of low and medium strength circular and rectangular reinforced concrete columns." *Journal of Materials in Civil Engineering, ASCE,* 20(2), 169-188.
10. Wu, Y.F. and Wang, L.M., (2009). "Unified strength model for square and circular concrete columns confined by external jacket." *Journal of Structural Engineering,* 135(3), 253-261.
11. Saatcioglu, M., Ozbakkaloglu, T., and Elnabelsy, G., (2009). "Seismic behavior and design of reinforced concrete columns confined with FRP stay-in-place formwork." *ACI Special Publication SP-257*, 145-165.
12. Smith, S.T., Kim, S.J., and Zhang, H., (2010). "Behavior and Effectiveness of FRP Wrap in the Confinement of Large Concrete Cylinders." *Journal of Composites for Construction,* 14(5), 573-582.
13. Wang, Z.Y., Wang, D.Y., Smith, S.T., and Lu, D.G., (2012). "CFRP-confined square RC columns. I: experimental investigation." *Journal of Composites for Construction,* 16(2), 150-160.
14. Idris, Y. and Ozbakkaloglu, T., (2013). "Seismic behavior of high-strength concrete-filled FRP tube columns." *Journal of Composites for Construction, ASCE,* 17(6), 04013013.
15. Louk Fanggi, B.A. and Ozbakkaloglu, T., (2013). "Compressive behavior of aramid FRP-HSC-steel double-skin tubular columns." *Construction and Building Materials,* 48, 554-565.
16. Ozbakkaloglu, T., (2013). "Compressive behavior of concrete-filled FRP tube columns: Assessment of critical column parameters." *Engineering Structures,* 51, 188-199.

17. Ozbakkaloglu, T. and Louk Fanggi, B.A., (2013). "FRP-HSC-steel composite columns: Behavior under monotonic and cyclic axial compression." *Materials and Structures,* Doi: 10.1617/s11527-013-0216-0.
18. Ozbakkaloglu, T. and Vincent, T., (2013). "Axial compressive behavior of circular high-strength concrete-filled FRP tubes." *Journal of Composites for Construction, ASCE,* 18(2), 04013037.
19. Vincent, T. and Ozbakkaloglu, T., (2013). "Influence of concrete strength and confinement method on axial compressive behavior of FRP-confined high- and ultra high-strength concrete." *Composites Part B,* 50, 413–428.
20. Vincent, T. and Ozbakkaloglu, T., (2013). "Influence of fiber orientation and specimen end condition on axial compressive behavior of FRP-confined concrete." *Construction and Building Materials,* 47, 814-826.
21. Ozbakkaloglu, T. and Louk Fanggi, B.A., (2014). "Axial compressive behavior of FRP-concrete-steel double-skin tubular columns made of normal- and high-strength concrete." *Journal of Composites for Construction, ASCE,* 18(1), 04013027.
22. De Nicolo, B., Pani, L., and Pozzo, E., (1994). "Strain of concrete at peak compressive stress for a wide range of compressive strengths." *Materials and Structures,* 27(4), 206-210.
23. Tasdemir, M.A., Tasdemir, C., Jefferson, A.D., Lydon, F.D., and Barr, B.I.G., (1998). "Evaluation of strains at peak stresses in concrete: A three-phase composite model approach." *Cement and Concrete Research,* 20(4), 301-318.
24. Samani, A.K. and Attard, M.M., (2012). "A stress-strain model for uniaxial and confined concrete under compression." *Engineering Structures,* 41, 335-349.
25. Ozbakkaloglu, T. and Lim, J.C., (2013). "Axial compressive behavior of FRP-confined concrete: Experimental test database and a new design-oriented model." *Composites Part B,* 55, 607-634.
26. Lim, J.C. and Ozbakkaloglu, T., (2013). "Confinement model for FRP-confined high-strength concrete." *Journal of Composites for Construction,*18(4), 04013058.
27. Lim, J. C. and Ozbakkaloglu, T. (2014). "Investigation of the Influence of Application Path of Confining Pressure: Tests on Actively Confined and FRP-Confined Concretes." *Journal of Structural Engineering, ASCE*, Doi: 10.1061/(ASCE)ST.1943-541X.0001177.
28. Snell, L.M., Van Roekel, J., and Wallace, N.D., (1989). "Predicting early concrete strength." *Concrete International: Design and Construction,* 11(12), 43-47.
29. Popovics, S., (1990). "Analysis of concrete strength versus water-cement ratio relationship." *ACI Materials journal,* 87(5), 517-529.
30. Kronlöf, A., (1994). "Effect of very fine aggregate on concrete strength." *Materials and Structures,* 27(1), 15-25.
31. Kasperkiewicz, J., Racz, J., and Dubrawski, A., (1995). "HPC strength prediction using artificial neural network." *Journal of Computing in Civil Engineering,* 9(4), 279-284.
32. Popovics, S., (1998). "History of a mathematical model for strength development of Portland cement concrete." *ACI Materials Journal,* 95(5), 593-600.
33. Rashid, M.A., Mansur, M.A., and Paramasivam, P., (2002). "Correlations between mechanical properties of high-strength concrete." *Journal of Materials in Civil Engineering,* 14(3), 230-238.

34. Jensen, V.P., (1943). "The Plasticity Ratio of Concrete and It's Effect on the Ultimate Strength of Beamse." *ACI Journal Proceedings,* 39, 565-584.
35. Ahmad, S.H. and Shah, S.P., (1982). "Complete triaxial stress-strain curves for concrete." *Journal of the Structural Division,* 108(4), 728-742.
36. Oluokun, F.A., Burdette, E.G., and Deatherage, J.H., (1991). "Elastic modulus, Poisson's ratio, and compressive strength relationships at early ages." *ACI materials journal,* 88(1), 3-10.
37. NS-3473, (1992). "Norwegian Council for Building Standardization, Concrete Structures Design Rules NS 3473,." Norwegian Concrete Association, Stockholm.
38. CEB-FIB, (1993). "CEB-FIB Model Code 1990." Bulletins D'information CEB, No. 213/214, Lausanne.
39. CSA, (1995). "CSA A23.3-94, Design of Concrete Structures." Canadian Standard Association, Rexdale, Ontario.
40. Iravani, S., (1996). "Mechanical properties of high-performance concrete." *ACI Materials Journal,* 93(5), 416-425.
41. Wee, T.H., Chin, M.S., and Mansur, M.A., (1996). "Stress-strain relationship of high-strength concrete in compression." *Journal of Materials in civil Engineering,* 8(2), 70-76.
42. TS-500, (2000). "Requirements for Design and Construction of Reinforced Concrete Structures." Turkish Standardization Institute, Ankara.
43. Fam, A.Z. and Rizkalla, S.H., (2001). "Confinement model for axially loaded concrete confined by circular fiber-reinforced polymer tubes." *ACI Structural Journal,* 98(4), 451-461.
44. Persson, B., (2001). "A comparison between mechanical properties of self-compacting concrete and the corresponding properties of normal concrete." *Cement and Concrete Research,* 32(2), 193-198.
45. Gesoğlu, M., Güneyisi, E., and Özturan, T., (2002). "Effects of end conditions on compressive strength and static elastic modulus of very high strength concrete." *Cement and Concrete Research,* 32(10), 1545-1550.
46. Kim, J.K., Han, S.H., and Song, Y.C., (2002). "Effect of temperature and aging on the mechanical properties of concrete: Part I. Experimental results." *Cement and Concrete research,* 32(7), 1087-1094.
47. Mesbah, H.A., Lachemi, M., and Aitcin, P.C., (2002). "Determination of elastic properties of high-performance concrete at early ages." *ACI Materials Journal,* 99(1), 37-41.
48. Nassif, H.H., Najm, H., and Suksawang, N., (2005). "Effect of pozzolanic materials and curing methods on the elastic modulus of HPC." *Cement and Concrete Composites,* 27(6), 661-670.
49. Ros, M., (1950). "Material-technological foundation and problems of reinforced concrete." *Bericht No. 162*, Eidgenossische Materialprfifungs und Versuchsanstalt f/Jr Industrie, Bauwesen and Gewerbe, Zurich, Switzerland.
50. Saenz, L.P., (1964). "Discussion of a paper by P. Desayi and S. Krishnan - Equation for the stress strain curve of concrete." *ACI Journal,* 61(9), 1229-1235.
51. Tadros, G.S., (1970). "Plastic rotation of reinforced concrete members subjected to bending, axial load and shear." Ph.D. Thesis, University of Calgary.

52. Popovics, S., (1973). "A numerical approach to the complete stress-strain curves for concrete." *Cement and Concrete Research,* 3(5), 583-599.
53. Ahmad, S.H. and Shah, S.P., (1979). "Complete Stress-Strain Curves of Concrete and Nonlinear Design." *Progress Report, National Science Foundation Grant PFR 79-22878*, University of Illinois, Chicago Circle.
54. Tomaszewicz, A., (1984). "Betongens Arbeidsdiagram." *SINTEF Report No. STF 65A84065*, Trondheim, Norway.
55. Carreira, D.J. and Chu, K.H., (1985). "Stress-strain relationship for plain concrete in compression." *Journal of the American Concrete Institute,* 82(6), 797-804.
56. Shah, S.P. and Ahmad, S.H., (1985). "Structural properties of high strength concrete and its implication for precast pre-stressed concrete." *PCI Journal,* 30(6), 92-119.
57. Ali, A.M., Farid, B.J., and Al-Janabi, A.J.M., (1990). "Stress-strain relationship for concrete in compression made of local materials." *Engineering Sciences,* 2(1), 183-194.
58. ACI-363, (1992). "State-of-the-Art Report on High-Strength Concrete." *ACI Committee 363*, American Concrete Institute, Detroit, Michigan.
59. Taerwe, L.R., (1992). "Influence of steel fibers on strain-softening of high-strength concrete." *ACI Materials Journal,* 89(1), 54-60.
60. Collins, P.M., Mitchell, D., and MacGregor, J.G., (1993). "Structural design considerations for high-strength concrete." *Concrete International-Detroit,* 15, 27-34.
61. Hsu, L.S. and Hsu, C.T., (1994). "Complete stress-strain behaviour of high-strength concrete under compression." *Magazine of Concrete Research,* 46(169), 301-312.
62. ACI-318, (1995). "Building Code Requirement for Structural Concrete (ACI 318-95) and Commentary (318R-95)." *ACI Committee 318* American Concrete Institute, Farmington Hills, Michigan.
63. Arioğlu, E., (1995). "Discussion of 'Strain of concrete at peak compressive stress for a wide range of compressive strengths' by B. de Nicolo, L. Pani and E. Pozzo, Materials and Structures 1994, 27, 205–210." *Materials and Structures,* 28(10), 611-614.
64. Attard, M.M. and Setunge, S., (1996). "Stress-strain relationship of confined and unconfined concrete." *ACI Materials Journal,* 93(5), 432-442.
65. Mansur, M.A., Chin, M.S., and Wee, T.H., (1999). "Stress-strain relationship of confined high-strength plain and fiber concrete - Closure." *Journal of Materials in Civil Engineering,* 11(4), 364-364.
66. Lee, I., (2002). "Complete stress-strain characteristics of high performance concrete." *Department of civil and environmental engineering*, New Jersey Institute of Technology, Newark, NJ, USA.
67. Wang, Y.W., Pu, X.C., and Wang, Z.J., (2006). "A Numerical Stress-strain Response Model of All Grades of Concretes under Uniaxial Compression." *Journal of Wuhan University of Technology-Materials Science Edition,* 21(3), 149-152.
68. Lu, Z.H. and Zhao, Y.G., (2008). "An improved analytical constitutive relation for normal weight high-strength concrete." *International journal of modern physics B,* 22(31-32), 5425-5430.
69. Richart, F.E., Brandtzaeg, A., and Brown, R.L., (1928). "A study of the failure of concrete under combined compressive stresses." *Bulletin No. 185*, Engineering Experimental Station, University of Illinois, Champaign, Illinois.

70. Richart, F.E., Brandtzaeg, A., and Brown, R.L., (1929). "The failure of plain and spirally reinforced concrete in compression." *Bulletin No.190*, Engineering Experiment Station, University of Illinois, Urbana, USA.
71. Mills, L.L. and Zimmerman, R.M., (1970). "Compressive Strength of Plain Concrete Under Multiaxial Loading Conditions." *ACI Journal Proceedings,* 67(10), 802-807.
72. Xie, J., Elwi, A.E., and Macgregor, J.G., (1995). "Mechanical-properties of high-strength concretes containing silica fume." *ACI Materials Journal,* 92(2), 135-145.
73. Ansari, F. and Li, Q.B., (1998). "High-strength concrete subjected to triaxial compression." *ACI Materials Journal,* 95(6), 747-755.
74. Candappa, D.C., Sanjayan, J.G., and Setunge, S., (2001). "Complete triaxial stress-strain curves of high-strength concrete." *Journal of Materials in Civil Engineering,* 13(3), 209-215.
75. Imran, I. and Pantazopoulou, S.J., (2001). "Plasticity model for concrete under triaxial compression." *Journal of Engineering Mechanics, ASCE,* 127(3), 281-290.
76. Binici, B., (2005). "An analytical model for stress-strain behavior of confined concrete." *Engineering Structures,* 27(7), 1040-1051.
77. Jiang, T. and Teng, J.G., (2007). "Analysis-oriented stress-strain models for FRP-confined concrete." *Engineering Structures,* 29(11), 2968-2986.
78. Teng, J.G., Huang, Y.L., Lam, L., and Ye, L.P., (2007). "Theoretical model for fiber-reinforced polymer-confined concrete." *Journal of Composites for Construction, ASCE,* 11(2), 201-210.
79. Xiao, Q.G., Teng, J.G., and Yu, T., (2010). "Behavior and Modeling of Confined High-Strength Concrete." *Journal of Composites for Construction, ASCE,* 14(3), 249-259.
80. Bazant, Z.P., (1989). "Identification of Strain-Softening Constitutive Relation from Uniaxial Tests by Series Coupling Model for Localization." *Cement and Concrete Research,* 19, 973-977.
81. Markeset, G. and Hillerborg, A., (1995). "Softening of concrete in compression-localization and size effects." *Cement and Concrete Research,* 25(4), 702-708.
82. Carpinteri, A., Corrado, M., and Paggi, M., (2011). "An analytical model based on strain localisation for the study of size scale and slenderness effects in uniaxial compression tests." *Strain,* 47(4), 351-362.
83. Chen, Y., Visintin, P., Oehlers, D., and Alengaram, U., (2013). "Size Dependent Stress-Strain Model for Unconfined Concrete." *Journal of Structural Engineering,* 140(4), 04013088.
84. Rokugo, K. and Koyanagi, W., (1992). " Role of compressive fracture energy of concrete on the failure behaviour of reinforced concrete beams." *Applications of fracture mechanics to reinforced concrete*, 437-464.
85. Vonk, R., (1992). "Softening of concrete loaded in compression." PhD thesis, *Eindhoven University of Technology*, he Netherlands.
86. Jansen, D.C. and Shah, S.P., (1997). "Effect of length on compressive strain softening of concrete." *Journal of Engineering Mechanics,* 123(1), 25-35.
87. Watanabe, K., Niwa, J., Yokota, H., and Iwanami, M., (2004). "Experimental study on stress-strain curve of concrete considering localized failure in compression." *Journal of Advanced Concrete Technology,* 2(3), 395-407.

88. van Vliet, M.R. and van Mier, J.G., (1996). "Experimental investigation of concrete fracture under uniaxial compression." *Mechanics of Cohesive-frictional Materials,* 1(1), 115-127.
89. van Mier, J.G.M., Shah, S.P., Arnaud, M., Balayssac, J.P., Bascoul, A., Choi, S., Dasenbrock, D., Ferrara, G., French, C., Gobbi, M.E., Karihaloo, B.L., Konig, G., Kotsovos, M.D., Labuz, J., Lange-Kornbak, D., Markeset, G., Pavlovic, M.N., Simsch, G., Thiend, K.-C., Turatsinze, A., Ulmefl, M., Gee, H.J.G.M.v., Vliet, M.R.A.v., and Zissopoulos, D., (1997). "Strain-softening of concrete in uniaxial compression." *Materials and Structures,* 30(4), 195-209.
90. Wischers, G., (1979). "Application and Effects of Compressive Loads on Concrete." *Betonverlag GmbH, Dfisseldorf*, 31-56.
91. Ahmad, S.H. and Shah, S.P., (1985). "Behaviour of hoop confined concrete under high strain rates." *ACI Journal Proceedings,* 82, 634-647.
92. Dahl, K.K.B., (1992). "A constitutive model for normal and high strength concrete." *Project 5, Report 5.7*, American Concrete Institute, Detroit.
93. Desnerck, P., Schutter, G.D., and Taerwe, L., (2012). "Stress-strain behaviour of self-compacting concrete containing limestone fillers." *Structural Concrete,* 13(2), 95-101.
94. Kaar, P.H., Hanson, N.W., and Capell, H.T., (1977). "Stress-strain characteristic of high strength concrete." *Research and Development Bulletin RD051-01D*, Portland Cement Association, Skokie, Illinois.
95. Shah, S.P., Naaman, A.E., and Moreno, J., (1983). "Effect of confinement on the ductility of lightweight concrete." *International Journal of Cement Composites and Lightweight Concrete,* 5(1), 15-25.
96. Zhang, M.H. and Gjorv, O.E., (1991). "Mechanical properties of high-strength lightweight concrete." *ACI Materials Journal,* 88(3), 240-247.
97. Shannag, M.J., (2011). "Characteristics of lightweight concrete containing mineral admixtures." *Construction and Building Materials,* 25(2), 658-662.
98. Newman, J.B., (1979). "Concrete under complex stress." London, UK, Department of Civil Engineering, Imperial College of Science and Technology, London, UK.
99. Hurlbut, B., (1985). "Experimental and computational investigation of strain-softening in concrete." PhD Dissertation, University of Colorado.
100. Bellotti, R. and Rossi, P., (1991). "Cylinder tests: experimental technique and results." *Materials and Structures,* 24(1), 45-51.
101. Gabet, T., Malecot, Y., and Daudeville, L., (2008). "Triaxial behaviour of concrete under high stresses: Influence of the loading path on compaction and limit states." *Cement and Concrete Research,* 38(3), 403-412.
102. Nakamura, H. and Higai, T., (2001). "Compressive fracture energy and fracture zone length of concrete." *Modeling of inelastic behavior of RC structures under seismic loads*.

APPENDIX

Table A1. Test database of normal weight concrete cylinders

Source	*n*	*B (mm)*	*H (mm)*	*Age (d)*	*w/c*	$\rho_{c,f}$ *(kg/m³)*	*Aggregate properties*[p]	*sf/c (%)*	*ma/b (%)*	E_c *(MPa)*	f'_{co} *(MPa)*	ε_{co} *(%)*	*M**
Abdollahi et al. [1]	2	150	300		0.60	2400	n				14.8	0.24	fl
Abdollahi et al. [1]	2	150	300		0.50	2400	n				25.1	0.23	fl
Abdollahi et al. [1]	2	150	300		0.35	2400	n				41.7	0.28	fl
Ahmad and Shah [2]	1	76	152	>28			gv				48.0	0.190	fl
Ahmad and Shah [2]	1	76	152	>28			gv				61.0	0.245	fl
Ahmad and Shah [2]	1	76	152	>28			gv				74.0	0.276	fl
Ahmad and Shah [2]	1	76	152	>28			gv				81.0	0.285	fl
Ahmad and Shah [3]	3	76	305	114	0.45	2400	dl-12.7			13936	20.7	0.21	fl
Ahmad and Shah [3]	4	76	152	114	0.45	2400	dl-12.7			20064	26.2	0.21	fl
Ahmad and Shah [3]	4	76	152	114	0.45	2400	dl-12.7			37073	37.9	0.22	fl
Ahmad and Shah [3]	4	76	152	114	0.45	2400	dl-12.7			45291	51.7	0.25	fl
Ahmad and Shah [3]	4	76	152	114	0.45	2400	dl-12.7			38744	65.5	0.30	fl
Ahmad and Shah [3]	3	76	152	114	0.45	2400	dl-12.7			56518[m]	52.2	0.25	fl
Ahmad and Shah [4]	1	76	152			2400	n-12.7			22709	27.3	0.203	fl
Ahmad and Shah [4]	1	76	152			2400	n-12.7			23465	32.9	0.203	fl
Ahmad and Shah [4]	1	76	152			2400	n-12.7			27620	47.0	0.235	fl
Ahmad and Shah [4]	1	76	152			2400	n-12.7			30995	60.5	0.248	fl
Ahmad and Shah [4]	1	76	152			2400	n-12.7			36203	73.6	0.277	fl
Ahmad and Shah [4]	1	76	152			2400	n-12.7			41932	87.3	0.303	fl
Ahmad and Shah [4]	4	76	305	55	0.49	2400	n-12.7			28338	48.1	0.260	fl
Ahmad and Shah [4]	4	76	305	55	0.49	2400	n-12.7			29200	52.5	0.290	fl
Ahmad and Shah [4]	3	76	305	28	0.47	2400	n-12.7		11.7[f]	22340	37.3	0.23	fl
Ahmad and Shah [4]	2	152	610	28	0.47	2400	n-12.7		11.7[f]	22130	29.6	0.18	fl
Ahmad and Shah [4]	3	76	305	200	0.47	2400	n-12.7		11.7[f]	22100	37.9	0.23	fl
Ahmad and Shah [4]	3	76	305	200	0.47	2400	n-12.7		11.7[f]	22620	43.1	0.25	fl
Ahmad and Shah [4]	3	76	305	200	0.47	2400	n-12.7		11.7[f]	22440	43.8	0.28	fl
Ahmad and Shah [4]	1	76	305			2400	n-12.7		11.7[f]	31847	43.0	0.18	fl
Ahmad and Shah [4]	1	76	305			2400	n-12.7		11.7[f]	27196	43.0	0.21	fl
Ahmad and Shah [4]	1	76	305			2400	n-12.7		11.7[f]	51195[m]	56.2	0.23	fl
Ahmad and Shah [4]	1	76	305			2400	n-12.7		11.7[f]	33386	56.1	0.27	fl
Ahmad and Shah [4]	1	76	152			2400	n			17110	23.4	0.257	fl
Ahmad and Shah [4]	1	76	152			2400	n			40399	40.0	0.233	fl
Ahmad and Shah [4]	1	76	152			2400	n			48616[m]	49.5	0.270	fl
Ahmad et al. [5]	3	102	203	5	0.32	2540	n		10.4[f]		39.0	0.22	
Ahmad et al. [5]	3	102	203	14	0.32	2540	n		10.4[f]		50.5	0.24	
Ahmad et al. [5]	3	102	203	28	0.32	2540	n		10.4[f]		64.2	0.27	
Aire et al. [6]	3	150	300		0.65	2428	gv				42.0	0.24	fl
Aire et al. [6]	3	150	300		0.35	2477	gv	9.1			69.0	0.24	fl
Akogbe et al. [7]	4	100	200		0.71	2310	n				25.2	0.31[a]	ml
Akogbe et al. [7]	4	100	200		0.71	2310	n				25.9	0.21	ml
Akogbe et al. [7]	4	100	200		0.71	2310	n				28.1	0.33[a]	ml
Akogbe et al. [7]	4	100	200		0.71	2310	n				26.8	0.38[a]	ml
Akogbe et al. [7]	4	200	400		0.71	2310	n				21.8	0.26	ml
Akogbe et al. [7]	4	200	400		0.71	2310	n				20.6	0.17	ml
Akogbe et al. [7]	4	200	400		0.71	2310	n				23.6	0.21	ml
Akogbe et al. [7]	4	200	400		0.71	2310	n				20.6	0.24	ml
Akogbe et al. [7]	4	300	600		0.71	2310	n				25.3	0.21	ml
Akogbe et al. [7]	4	300	600		0.71	2310	n				24.0	0.21	ml
Akogbe et al. [7]	4	300	600		0.71	2310	n				23.7	0.20	ml
Akogbe et al. [7]	4	300	600		0.71	2310	n				25.0	0.26[a]	ml
Ali et al. [8]	1	150	300	28			gv				43.5	0.22	
Ali et al. [8]	1	150	300	28			gv				32.0	0.22	
Ali et al. [8]	1	150	300	28			gv				27.7	0.21	
Ali et al. [8]	1	150	300	28			gv				25.3	0.21	
Ali et al. [8]	1	150	300	28			gv				16.7	0.18	
Almusallam [9]	3	150	300		0.60	2317	n-19			31250	47.7	0.208	ml
Almusallam [9]	3	150	300		0.55	2321	n-19			65000[m]	50.8	0.294	ml
Almusallam [9]	3	150	300		0.45	2332	n-19			45000	60.0	0.298	ml
Almusallam [9]	3	150	300		0.32	2358	n-19			40000	80.8	0.265	ml
Almusallam [9]	3	150	300		0.28	2336	n-19			35200	90.3	0.320	ml
Almusallam [9]	3	150	300		0.27	2346	n-19	9.1		41940	107.8	0.261	ml
Almusallam and Alsayed [10]		150	300	28			dl-9.5			18170	28.0	0.190	
Almusallam and Alsayed [10]		150	300	28			dl-9.5			19650	34.9	0.230	
Almusallam and Alsayed [10]		150	300	28			dl-9.5			21200	42.9	0.250	
Almusallam and Alsayed [10]		150	300	28			dl-9.5			32580	70.1	0.304	
Almusallam and Alsayed [10]		150	300	28			dl-9.5			38170	84.0	0.250	
Ansari and Li [11]	3	101	202	40	0.46	2438	gv				45.0	0.201	ml
Ansari and Li [11]	3	101	202	40	0.32	2438	gv	11.7			71.0	0.202	ml
Ansari and Li [11]	3	101	202	40	0.19	2478	gv	7.1	12.8[f]		107.0	0.193[a]	ml
Arduini et al. [12]		150	300				n				36.9	0.25	
Assa et al. [13]	1	145	200	28			gv-12.7				25.0	0.325[a]	fl
Assa et al. [13]	1	145	200	28			gv-12.7				34.1	0.242	fl
Assa et al. [13]	1	145	200	28			gv-12.7				41.4	0.248	fl
Assa et al. [13]	1	145	200	28			gv-12.7				49.8	0.218	fl
Assa et al. [13]	1	145	200	28			gv-12.7				64.4	0.234	fl
Assa et al. [13]	1	145	200	28			gv-12.7				70.1	0.200	fl
Assa et al. [13]	1	145	200	28			gv-12.7				83.0	0.228	fl
Assa et al. [13]	1	145	200	28			gv-12.7				75.0	0.202	fl

Source	*n*	*B (mm)*	*H (mm)*	*Age (d)*	*w/c*	$\rho_{c,f}$ *(kg/m³)*	*Aggregate properties*[p]	*sf/c (%)*	*ma/b (%)*	E_c *(MPa)*	f'_{co} *(MPa)*	ε_{co} *(%)*	*M**
Assa et al. [13]	1	145	200	28			gv-12.7				75.0	0.191[a]	fl
Attard and Setunge [14]	1	100	200	90	0.26	2364	bs-cr			49400	126.0	0.34	fl
Attard and Setunge [14]	1	100	200	90	0.26	2346	rd			52900	100.0	0.27	fl
Attard and Setunge [14]	1	100	200	90	0.26	2359	hf			55800	96.0	0.28	fl
Attard and Setunge [14]	1	100	200	90	0.45	2257	rd			45100[m]	60.0	0.21	fl
Attard and Setunge [14]	1	100	200	90	0.26	2344	hf	8.3		49300	132.0	0.34	fl
Attard and Setunge [14]	1	100	200	90	0.26	2326	rd	8.3		55700	120.0	0.30	fl
Attard and Setunge [14]	1	100	200	90	0.26	2339	hf	8.3		57800	118.0	0.28	fl
Attard and Setunge [14]	1	100	200	90	0.30	2306	bs-cr	8.2		52800	120.0	0.28	fl
Attard and Setunge [14]	1	100	200	90	0.30	2319	rd	8.2		58700	110.0	0.28	fl
Attard and Setunge [14]	1	100	200	90	0.35	2275	hf	8.0		55400	110.0	0.28	fl
Attard and Setunge [14]	1	100	200	90	0.35	2288	hf	8.0		54600	100.0	0.26	fl
Au and Buyukozturk [15]	3	150	375	28		2438	n				24.2	0.36[a]	ml
Balmer [16]	1	152	305	28	0.58		n-38			41368[m]	23.9	0.4[a]	Fl
Balmer [16]	1	152	305	28	0.58		n-38			41368[m]	24.2	0.4[a]	Fl
Balmer [16]	1	152	305	28	0.58		n-38			41368[m]	25.9	0.4[a]	Fl
Balmer [16]	1	152	305	90	0.58		n-38			41368[m]	19.0	0.250	Fl
Balmer [16]	1	152	305	90	0.58		n-38			41368[m]	28.1	0.250	Fl
Balmer [16]	1	152	305	90	0.58		n-38			41368[m]	34.7	0.250	Fl
Barnard [17]	1	64	292	28			n				26.2	0.216	
Barnard [17]	1	64	292	28			n				23.9	0.279[a]	
Barnard [17]	1	64	292	28			n				24.6	0.273	
Barnard [17]	1	64	292	28			n				22.0	0.235	
Belén et al. [18]	1	150	300	28	0.65	2316	n			30645	31.9	0.174	ml
Belén et al. [18]	1	150	300	28	0.65	2296	n			29598	31.7	0.199	ml
Belén et al. [18]	1	150	300	28	0.65	2264	n			27459	32.3	0.195	ml
Belén et al. [18]	1	150	300	28	0.65	2215	n			25935	30.1	0.216	ml
Belén et al. [18]	1	150	300	28	0.50	2324	n			34374	44.8	0.190	ml
Belén et al. [18]	1	150	300	28	0.50	2302	n			33192	43.7	0.189	ml
Belén et al. [18]	1	150	300	28	0.50	2268	n			30321	37.5	0.190	ml
Belén et al. [18]	1	150	300	28	0.50	2216	n			24817	40.5	0.219	ml
Bellotti and Rossi [19]	1	160	320				n				53.5	0.310	
Benzaid et al [20]	1	160	320		0.46	2156	gv-cr-15.2				56.7	0.240	ml
Benzaid et al. [21]	2	160	320		0.64	2340	gv-cr-15.2				25.9	0.273	ml
Benzaid et al. [21]	2	160	320		0.46	2354	gv-cr-15.2				49.5	0.169[a]	ml
Benzaid et al. [21]	2	160	320		0.37	2389	gv-cr-15.2				61.8	0.284	ml
Berthet et al. [22]	1	160	320		0.54	2353	n-rd-10				24.3	0.241	ml
Berthet et al. [22]	1	160	320		0.54	2353	n-rd-10				25.5	0.203	ml
Berthet et al. [22]	1	160	320		0.54	2353	n-rd-10				25.2	0.256	ml
Berthet et al. [22]	1	160	320		0.53	2285	n-rd-10				40.3	0.186	ml
Berthet et al. [22]	1	160	320		0.53	2285	n-rd-10				39.3	0.211	ml
Berthet et al. [22]	1	160	320		0.53	2285	n-rd-10				40.6	0.204	ml
Berthet et al. [22]	1	160	320		0.33	2451	n-rd-10				51.4	0.248	ml
Berthet et al. [22]	1	160	320		0.33	2451	n-rd-10				52.7	0.201	ml
Berthet et al. [22]	1	160	320		0.33	2451	n-rd-10				51.8	0.231	ml
Berthet et al. [22]	1	70	140		0.30	2502	n-cr-12.7	10.0			112.7	0.251	ml
Berthet et al. [22]	1	70	140		0.30	2502	n-cr-12.7	10.0			113.2	0.211[a]	ml
Berthet et al. [22]	1	70	140		0.30	2502	n-cr-12.7	10.0			111.8	0.237	ml
Berthet et al. [22]	1	70	140		0.16	2500	qz-cr	24.5			169.7	0.385	ml
Berthet et al. [22]	1	70	140		0.16	2500	qz-cr	24.5			171.1	0.299	ml
Berthet et al. [22]	1	70	140		0.16	2500	qz-cr	24.5			168.3	0.287	ml
Bisby et al. [23]	1	150	300				n				33.3	0.36[a]	
Bisby et al. [23]	1	150	300				n				35.5	0.30[a]	
Bisby et al. [23]	1	150	300				n				34.4	0.33[a]	
Bisby et al. [24]	1	100	200				n				30.0	0.20	
Bisby et al. [24]	1	100	200				n				22.0	0.25	
Bisby et al. [24]	1	100	200				n				32.0	0.30	
Bisby et al. [24]	1	100	200				n				30.0	0.28	
Bisby et al. [24]	1	100	200				n				26.0	0.40[a]	
Bisby et al. [24]	1	100	200				n				25.0	0.65[a]	
Bischoff and Perry [25]	1	102	254	40	0.75		gv			29100	26.7	0.200	
Bischoff and Perry [25]	1	102	254	156	0.75		gv			29100	26.8	0.212	
Bischoff and Perry [25]	1	102	254	43	0.57		gv			33600	45.3	0.222	
Bischoff and Perry [25]	1	102	254	137	0.57		gv			33600	43.5	0.220	
Bullo [26]	1	150	300				n				32.5	0.247	fl
Bullo [26]	1	150	300				n				37.9	0.248	fl
Bullo [26]	1	150	300				n				27.2	0.249	fl
Campione et al. [27]	3	100	200				n				20.1	0.207	fl
Candappa et al. [28]	1	100	200	216	0.63	2500	n				39.4	0.239	fl
Candappa et al. [28]	1	100	200	216	0.63	2500	n				41.2	0.245	fl
Candappa et al. [28]	1	100	200	56	0.50	2500	n				58.1	0.224	fl
Candappa et al. [28]	1	100	200	56	0.50	2500	n				61.1	0.237	fl
Candappa et al. [28]	1	100	200	405	0.45	2522	n				73.7	0.245	fl
Candappa et al. [28]	1	100	200	405	0.45	2522	n				73.7	0.250	fl
Candappa et al. [28]	1	100	200	90	0.30	2584	n				100.7	0.273	fl
Candappa et al. [28]	1	100	200	90	0.30	2584	n				103.9	0.277	fl
Carey and Harries [29]	6	152	305				n				33.5	0.23	ml
Carey and Harries [29]	3	254	762				n				38.9	0.30[a]	ml
Carrasquillo et al. [30]	1	102	203	53	0.70		ls-cr			22339	33.8	0.26	
Carrasquillo et al. [30]	1	102	203	53	0.70		ls-cr			28613	32.5	0.23	

Source	*n*	*B (mm)*	*H (mm)*	*Age (d)*	*w/c*	$\rho_{c,f}$ *(kg/m³)*	*Aggregate properties*[p]	*sf/c (%)*	*ma/b (%)*	E_c *(MPa)*	f'_{co} *(MPa)*	ε_{co} *(%)*	*M**
Carrasquillo et al. [30]	1	102	203	53	0.70		ls-cr			20477	32.2	0.26	
Carrasquillo et al. [30]	1	102	203	53	0.47		ls-cr			29579	58.8	0.30	
Carrasquillo et al. [30]	1	102	203	53	0.47		ls-cr			29441	57.1	0.30	
Carrasquillo et al. [30]	1	102	203	53	0.47		ls-cr			29027	59.1	0.28	
Carrasquillo et al. [30]	1	102	203	53	0.32		ls-cr			34543	73.6	0.29	
Carrasquillo et al. [30]	1	102	203	53	0.32		ls-cr			36542	69.4	0.30	
Carrasquillo et al. [30]	1	102	203	53	0.32		ls-cr			36749	76.5	0.29	
Carrasquillo et al. [30]	1	102	203	53	0.70		gv			22063	33.8	0.31[a]	
Carrasquillo et al. [30]	1	102	203	53	0.70		gv			21098	32.0	0.31[a]	
Carrasquillo et al. [30]	1	102	203	53	0.70		gv			20822	31.5	0.29	
Carrasquillo et al. [30]	1	102	203	53	0.47		gv			22408	54.2	0.34[a]	
Carrasquillo et al. [30]	1	102	203	53	0.47		gv			23511	48.9	0.29	
Carrasquillo et al. [30]	1	102	203	53	0.47		gv			20822	49.3	0.33	
Carrasquillo et al. [30]	1	102	203	53	0.32		gv			27924	64.0	0.28	
Carrasquillo et al. [30]	1	102	203	53	0.32		gv			25235	65.6	0.31	
Carrasquillo et al. [30]	1	102	203	53	0.32		gv			25511	65.5	0.30	
Carrasquillo et al. [30]	1	102	203	53	0.32		gv			25649	72.9	0.36	
Chikh et al. [31]	2	160	320		0.38	2394	gv-cr-15.2				61.8	0.284	ml
Cui and Sheikh [32]	2	152	305				n				48.1	0.222	ml
Cui and Sheikh [32]	2	152	305				n				79.9	0.241	ml
Cui and Sheikh [32]	2	152	305				n				110.6	0.262	ml
Cui and Sheikh [32]	2	152	305				n				47.8	0.222	ml
Cui and Sheikh [32]	2	152	305				n				45.6	0.247	ml
Cui and Sheikh [32]	2	152	305				n				85.6	0.258	ml
Cui and Sheikh [32]	2	152	305				n				111.8	0.261	ml
Cui and Sheikh [32]	2	152	305				n				45.7	0.243	ml
Dahl [33]		100	200				n			43455	106.7	0.279	
Dahl [33]		100	200				n			40101	94.5	0.266	
Dahl [33]		100	200				n			35271	65.6	0.263	
Dahl [33]		100	200				n			31786	50.6	0.265	
Dahl [33]		100	200				n			27393	32.1	0.249	
Dahl [33]		100	200				n			15554	21.9	0.265	
Dahl and Brincker [34]		100	200				n			39829	109.1	0.303	
Dahl and Brincker [34]		100	200				n			55905	119.4	0.245	
De Stefano and Sabia [35]	1	150	300	28			n				38.0	0.255	
De Stefano and Sabia [35]	1	150	300	28			n				58.0	0.248	
Demers and Neale [36]		152	305				n				32.1	0.240	
Demers and Neale [36]		152	305				n				32.2	0.240	
Demers and Neale [36]		152	305				n				43.7	0.280	
Demers and Neale [36]		152	305				n				43.8	0.280	
Desnerck et al. [37]	1	118	355	3	0.46	2389	gv-12.7			28131	36.6	0.187	fl
Desnerck et al. [37]	1	118	355	7	0.46	2389	gv-12.7			29907	44.8	0.208	fl
Desnerck et al. [37]	1	118	355	14	0.46	2389	gv-12.7			28131	48.8	0.215	fl
Desnerck et al. [37]	1	118	355	28	0.46	2389	gv-12.7			28692	52.2	0.223	fl
Desnerck et al. [37]	1	118	355	90	0.46	2389	gv-12.7			32897	59.9	0.237	fl
Desnerck et al. [37]	1	118	355	3	0.46	2389	gv-12.7			17757	26.2	0.224	fl
Desnerck et al. [37]	1	118	355	7	0.46	2389	gv-12.7			23738	35.5	0.215	fl
Desnerck et al. [37]	1	118	355	14	0.46	2389	gv-12.7			25140	43.1	0.220	fl
Desnerck et al. [37]	1	118	355	28	0.46	2389	gv-12.7			25140	50.1	0.236	fl
Desnerck et al. [37]	1	118	355	90	0.46	2379	gv-12.7			26262	55.1	0.246	fl
Desnerck et al. [37]	1	118	355	3	0.55	2379	gv-12.7			18972	25.9	0.188	fl
Desnerck et al. [37]	1	118	355	7	0.55	2379	gv-12.7			22430	32.6	0.202	fl
Desnerck et al. [37]	1	118	355	14	0.55	2379	gv-12.7			21682	35.4	0.206	fl
Desnerck et al. [37]	1	118	355	28	0.55	2379	gv-12.7			28224	38.3	0.213	fl
Desnerck et al. [37]	1	118	355	90	0.55	2379	gv-12.7			27477	40.8	0.232	fl
Desnerck et al. [37]	1	118	355	3	0.46	2319	gv-12.7			28318	43.0	0.248	fl
Desnerck et al. [37]	1	118	355	7	0.46	2319	gv-12.7			31682	52.8	0.252	fl
Desnerck et al. [37]	1	118	355	14	0.46	2319	gv-12.7			31682	56.4	0.258	fl
Desnerck et al. [37]	1	118	355	28	0.46	2319	gv-12.7			32430	60.0	0.259	fl
Desnerck et al. [37]	1	118	355	90	0.46	2319	gv-12.7			34766	69.2	0.275	fl
Desnerck et al. [37]	1	118	355	3	0.55	2319	gv-12.7			27383	33.4	0.196	fl
Desnerck et al. [37]	1	118	355	7	0.55	2319	gv-12.7			27570	42.4	0.231	fl
Desnerck et al. [37]	1	118	355	14	0.55	2319	gv-12.7			30467	47.1	0.241	fl
Desnerck et al. [37]	1	118	355	28	0.55	2319	gv-12.7			28785	50.8	0.251	fl
Desnerck et al. [37]	1	118	355	90	0.55	2319	gv-12.7			30935	57.8	0.268	fl
Desnerck et al. [37]	1	118	355	3	0.55	2273	gv-12.7			21121	23.5	0.230	fl
Desnerck et al. [37]	1	118	355	7	0.55	2273	gv-12.7			22336	34.9	0.233	fl
Desnerck et al. [37]	1	118	355	14	0.55	2273	gv-12.7			22523	44.0	0.265	fl
Desnerck et al. [37]	1	118	355	28	0.55	2273	gv-12.7			23364	51.7	0.290	fl
Desnerck et al. [37]	1	118	355	90	0.55	2273	gv-12.7			28224	56.0	0.265	fl
Desnerck et al. [37]	1	118	355	3	0.66	2318	gv-12.7			24299	34.7	0.251	fl
Desnerck et al. [37]	1	118	355	7	0.66	2318	gv-12.7			24299	40.4	0.259	fl
Desnerck et al. [37]	1	118	355	14	0.66	2318	gv-12.7			28785	44.0	0.251	fl
Desnerck et al. [37]	1	118	355	28	0.66	2318	gv-12.7			32523	44.5	0.262	fl
Desnerck et al. [37]	1	118	355	90	0.66	2318	gv-12.7			30561	50.6	0.250	fl
Elsanadedy et al. [38]	4	50	100	35	0.50	2355	n-20				53.8	0.344[a]	ml
Elsanadedy et al. [38]	4	100	200	35	0.50	2355	n-20				49.1	0.361[a]	ml
Elsanadedy et al. [38]	5	150	300	35	0.50	2355	n-20				41.1	0.362[a]	ml
Erdil et al. [39]	1	150	300				n				11.1	0.30[a]	ml
Erdil et al. [39]	1	150	300				n				20.8	0.30[a]	ml

Source	*n*	*B (mm)*	*H (mm)*	*Age (d)*	*w/c*	*$\rho_{c,f}$ (kg/m^3)*	*Aggregate properties*[p]	*sf/c (%)*	*ma/b (%)*	*E_c (MPa)*	*f'_{co} (MPa)*	*ε_{co} (%)*	*M**
Galeota [40]	1	150	300	28			gv				19.0	0.160	
Galeota [40]	1	150	300	28			gv				20.0	0.170	
Galeota [40]	1	150	300	28			gv				20.0	0.179	
Galeota [40]	1	150	300	28			gv				21.0	0.150	
Galeota [40]	1	150	300	28			gv				35.0	0.218	
Galeota [40]	1	150	300	28			gv				36.0	0.215	
Galeota [40]	1	150	300	28			gv				36.5	0.220	
Galeota [40]	1	150	300	28			gv				37.0	0.223	
Galeota [40]	1	150	300	28			gv				35.5	0.250	
Galeota [40]	1	150	300	28			gv				22.0	0.185	
Galeota et al. [41]	1	150	300	28			gv				38.0	0.262	
Galeota et al. [41]	1	150	300	28			gv				52.0	0.264	
Gardner [42]	1	76	152	42			n				30.0	0.356[a]	fl
Gardner [42]	1	76	152	42			n				27.5	0.365[a]	fl
Gardner [42]	1	76	152	42			n				26.9	0.368[a]	fl
Güler et al. [43]	1	150	300				n			38005	60.0	0.200	
Güler et al. [43]	1	150	300				n			49058	65.0	0.210	
Güler et al. [43]	1	150	300				n			53242	80.0	0.215	
Güler et al. [43]	1	150	300				n			42277	90.0	0.240	
Güler et al. [43]	1	150	300				n			45479	100.0	0.250	
Güler et al. [43]	1	150	300				n			47890	120.0	0.290	
Hadi and Li [44]	1	205	910				n				71.2	0.555[a]	fl
Harries and Carey [45]	≥5	152	305				gv-38.1				31.8	0.25	ml
Harries and Kharel [46]	≥5	152	305				gv-38.1				32.1	0.28	ml
Hognestad et al. [47]	1	152	305	7	1.00		gv-38.1			13863	5.3	0.10[a]	
Hognestad et al. [47]	1	152	305	14	1.00		gv-38.1			13313	9.8	0.14	
Hognestad et al. [47]	1	152	305	28	1.00		gv-38.1			19034	11.4	0.15	
Hognestad et al. [47]	1	152	305	90	1.00		gv-38.1			23435	15.0	0.15	
Hognestad et al. [47]	1	152	305	7	0.67		gv-38.1			17054	11.5	0.22	
Hognestad et al. [47]	1	152	305	14	0.67		gv-38.1			19034	19.8	0.21	
Hognestad et al. [47]	1	152	305	28	0.67		gv-38.1			20794	21.0	0.20	
Hognestad et al. [47]	1	152	305	90	0.67		gv-38.1			30036	25.6	0.17	
Hognestad et al. [47]	1	152	305	7	0.50		gv-38.1			18704	20.3	0.22	
Hognestad et al. [47]	1	152	305	14	0.50		gv-38.1			22885	31.7	0.20	
Hognestad et al. [47]	1	152	305	28	0.50		gv-38.1			22005	35.6	0.23	
Hognestad et al. [47]	1	152	305	90	0.50		gv-38.1			29486	37.7	0.23	
Hognestad et al. [47]	1	152	305	7	0.40		gv-38.1			25965	36.9	0.21	
Hognestad et al. [47]	1	152	305	14	0.40		gv-38.1			24975	41.9	0.22	
Hognestad et al. [47]	1	152	305	28	0.40		gv-38.1			26625	46.3	0.22	
Hognestad et al. [47]	1	152	305	90	0.40		gv-38.1			30696	44.7	0.22	
Hognestad et al. [47]	1	152	305	7	0.33		gv-38.1			26736	39.4	0.21	
Hognestad et al. [47]	1	152	305	14	0.33		gv-38.1			26405	44.7	0.20	
Hognestad et al. [47]	1	152	305	28	0.33		n			32017	52.0	0.20	
Hognestad et al. [47]	1	152	305	90	0.33		gv-38.1			32897	52.5	0.22	
Hosotani et al. [48]	1	200	600				gv-38.1				41.7	0.34[a]	
Hsu and Hsu [49]		76.2	152.4	44	0.28	2544	bs	4.8		33241	89.8	0.317	fl
Hsu and Hsu [49]		76.2	152.4	31	0.28	2544	bs	4.8		33241	83.4	0.321	fl
Hsu and Hsu [49]		76.2	152.4	23	0.28	2544	bs	4.8		33241	80.0	0.304	fl
Hsu and Hsu [49]		76.2	152.4	18	0.28	2544	bs	4.8		33241	73.9	0.289	fl
Hsu and Hsu [49]		76.2	152.4	9	0.28	2544	bs	4.8		33241	65.9	0.298	fl
Hsu and Hsu [49]		76.2	152.4	28	0.28[w]	2544	bs	4.8		21864	33.0	0.248	fl
Hsu and Hsu [49]		76.2	152.4		0.28	2544	bs	4.8			65.8	0.308	fl
Hsu and Hsu [49]		76.2	152.4		0.28	2544	n	4.8			78.1	0.318	fl
Hsu and Hsu [49]		76.2	152.4		0.28	2544	n	4.8			78.4	0.309	fl
Hsu and Hsu [49]		76.2	152.4		0.28	2544	n	4.8			80.4	0.314	fl
Hsu and Hsu [49]		76.2	152.4		0.28	2544	n	4.8			81.9	0.312	fl
Hsu and Hsu [49]		76.2	152.4		0.28	2544	n	4.8			83.8	0.331	fl
Hsu and Hsu [49]		76.2	152.4		0.28	2544	bs	4.8			91.4	0.333	fl
Hsu and Hsu [49]		76.2	152.4		0.28	2544	bs	4.8		31000	65.8	0.304	fl
Hsu and Hsu [49]		76.2	152.4		0.28	2544	bs	4.8		32900	75.5	0.302	fl
Hsu and Hsu [49]		76.2	152.4		0.28	2544	bs	4.8		33400	80.4	0.314	fl
Hsu and Hsu [49]		76.2	152.4		0.28	2544	bs	4.8		32600	83.3	0.331	fl
Hsu and Hsu [49]		76.2	152.4		0.28	2544	bs	4.8		33000	92.4	0.333	fl
Hsu and Hsu [49]		76.2	152.4		0.28	2544	ls-cr	4.8		26700[m]	79.2	0.325	fl
Hsu and Hsu [49]		76.2	152.4		0.28	2544	ls-cr	4.8		25900[m]	80.5	0.342	fl
Hsu and Hsu [49]		76.2	152.4		0.28	2544	ls-cr	4.8		25300[m]	83.2	0.358	fl
Hurlbut [50]	1	54	108				n			16000	19.0	0.18	fl
Ilki et al. [51]	1	150	300	104	1.27	2347	gv				6.2	0.20[a]	fl
Imran and Pantazopoulou [52]	1	54	115	28	0.40	2398	n-10				73.4	0.325	fl
Imran and Pantazopoulou [52]	1	54	115	28	0.40	2398	n-10				64.7	0.297	fl
Imran and Pantazopoulou [52]	1	54	115	28	0.55	2404	n-10				47.4	0.280	fl
Imran and Pantazopoulou [52]	1	54	115	28	0.55	2404	n-10				43.1	0.250	fl
Imran and Pantazopoulou [52]	1	54	115	28	0.75	2348	n-10				28.6	0.260	fl
Imran and Pantazopoulou [52]	1	54	115	28	0.75	2348	n-10				21.2	0.220	fl
Iravani [53]	5	100	200	56	0.416	2374.5	st-14			29446	64.3	0.284	as
Iravani [53]	5	100	200	56	0.416	2374.5	st-14			29528	65.3	0.307	as
Iravani [53]	5	100	200	56	0.416	2374.5	st-14			24615	66.0	0.368	as
Iravani [53]	5	100	200	56	0.416	2374.5	st-14			29672	66.2	0.348	as
Iravani [53]	5	100	200	56	0.416	2374.5	st-14			28517	66.3	0.300	as
Iravani [53]	5	100	200	56	0.416	2374.5	st-14			31908	66.4	0.297	as

Source	*n*	*B (mm)*	*H (mm)*	*Age (d)*	*w/c*	$\rho_{c,f}$ *(kg/m³)*	*Aggregate properties*[p]	*sf/c (%)*	*ma/b (%)*	E_c *(MPa)*	f'_{co} *(MPa)*	ε_{co} *(%)*	*M**
Iravani [53]	5	100	200	56	0.416	2374.5	st-14			27195	66.4	0.314	as
Iravani [53]	5	100	200	56	0.416	2374.5	st-14			28933	67.1	0.298	as
Iravani [53]	5	100	200	56	0.272	2432.1	st-14			31479	90.9	0.320	as
Iravani [53]	5	100	200	56	0.272	2432.1	st-14			32094	94.2	0.334	as
Iravani [53]	5	100	200	56	0.272	2432.1	st-14			31900	95.9	0.364	as
Iravani [53]	5	100	200	56	0.272	2432.1	st-14			32456	97.5	0.351	as
Iravani [53]	5	100	200	56	0.272	2432.1	st-14			30293	97.9	0.375	as
Iravani [53]	5	100	200	56	0.289	2409.9	st-14	9.1		30065	103.5	0.345	as
Iravani [53]	5	100	200	56	0.289	2409.9	st-14	9.1		31448	102.4	0.332	as
Iravani [53]	5	100	200	56	0.289	2409.9	st-14	9.1		31683	105.1	0.354	as
Iravani [53]	5	100	200	56	0.289	2409.9	st-14	9.1		32333	106.2	0.335	as
Iravani [53]	5	100	200	56	0.289	2409.9	st-14	9.1		34353	106.5	0.328	as
Iravani [53]	5	100	200	56	0.234	2417	st-14	9.0		35151	106.1	0.288	as
Iravani [53]	5	100	200	56	0.234	2417	st-14	9.0		38816	115.5	0.290	as
Iravani [53]	5	100	200	56	0.234	2417	st-14	9.0		36163	119.7	0.332	as
Iravani [53]	5	100	200	56	0.234	2417	st-14	9.0		37181	120.6	0.344	as
Iravani [53]	5	100	200	56	0.234	2417	st-14	9.0		37188	121.6	0.294	as
Iravani [53]	5	100	200	56	0.234	2417	st-14	9.0		37922	125.0	0.309	as
Iyengar et al. [54]		152	305				n			36732	33.0	0.679[a]	
Iyengar et al. [54]		152	305				n			23858	24.0	0.241	
Iyengar et al. [54]		152	305				n			31710	33.7	0.200	
Iyengar et al. [54]		152	305				n				60.9	0.245	
Jamet et al. [55]	3	110	220		0.53		n				31.4	0.369[a]	
Jansen and Shah [56]	1	100	200	28	0.52	2380	gv-rd-9			27500	42.8	0.214	fl
Jansen and Shah [56]	1	100	200	28	0.52	2380	gv-rd-9			29400	55.6	0.243	fl
Jansen and Shah [56]	1	100	200	28	0.52	2380	gv-rd-9				49.0		fl
Jansen and Shah [56]	1	100	200	28	0.52	2380	gv-rd-9				48.7		fl
Jansen and Shah [56]	1	100	250	28	0.52	2380	gv-rd-9			28000	44.1	0.219	fl
Jansen and Shah [56]	1	100	250	28	0.52	2380	gv-rd-9			29900	55.4	0.235	fl
Jansen and Shah [56]	1	100	300	28	0.52	2380	gv-rd-9			29600	50.1	0.207	fl
Jansen and Shah [56]	1	100	300	28	0.52	2380	gv-rd-9			28800	45.7	0.230	fl
Jansen and Shah [56]	1	100	350	28	0.52	2380	gv-rd-9			29700	51.4	0.212	fl
Jansen and Shah [56]	1	100	350	28	0.52	2380	gv-rd-9			29800	43.1	0.221	fl
Jansen and Shah [56]	1	100	400	28	0.52	2380	gv-rd-9			30300	46.8	0.192	fl
Jansen and Shah [56]	1	100	450	28	0.52	2380	gv-rd-9			30900	46.7	0.184	fl
Jansen and Shah [56]	1	100	450	28	0.52	2380	gv-rd-9			30400	47.7	0.221	fl
Jansen and Shah [56]	1	100	550	28	0.52	2380	gv-rd-9			31100	45.8	0.196	fl
Jansen and Shah [56]	1	100	550	28	0.52	2380	gv-rd-9			30900	45.4	0.187	fl
Jansen and Shah [56]	1	100	200	56	0.33	2451	gv-rd-9	11.3		36800	90.9	0.258	fl
Jansen and Shah [56]	1	100	200	56	0.33	2451	gv-rd-9	11.3		35700	93.1	0.251	fl
Jansen and Shah [56]	1	100	250	56	0.33	2451	gv-rd-9	11.3		37300	88.5	0.235	fl
Jansen and Shah [56]	1	100	250	56	0.33	2451	gv-rd-9	11.3		37500	88.1	0.254	fl
Jansen and Shah [56]	1	100	300	56	0.33	2451	gv-rd-9	11.3		37500	93.2	0.271	fl
Jansen and Shah [56]	1	100	300	56	0.33	2451	gv-rd-9	11.3		37600	90.8	0.275	fl
Jansen and Shah [56]	1	100	350	56	0.33	2451	gv-rd-9	11.3		38700	90.1	0.271	fl
Jansen and Shah [56]	1	100	350	56	0.33	2451	gv-rd-9	11.3		38900	92.6	0.262	fl
Jansen and Shah [56]	1	100	400	56	0.33	2451	gv-rd-9	11.3		38900	88.2	0.231	fl
Jansen and Shah [56]	1	100	450	56	0.33	2451	gv-rd-9	11.3		38300	88.6	0.231	fl
Jansen and Shah [56]	1	100	450	56	0.33	2451	gv-rd-9	11.3		39600	91.0	0.258	fl
Jansen and Shah [56]	1	100	550	56	0.33	2451	gv-rd-9	11.3		39500	90.0	0.243	fl
Jansen and Shah [56]	1	100	550	56	0.33	2451	gv-rd-9	11.3		39700	90.1	0.253	fl
Jansen et al. [57]	3	102	203	56	0.49	2386	gv-rd-9			30214	38.3	0.184	fl
Jansen et al. [57]	3	102	203	56	0.49	2386	gv-rd-9			30214	39.4	0.180	fl
Jansen et al. [57]	3	102	203	56	0.49	2386	gv-rd-9			30214	40.5	0.180	fl
Jansen et al. [57]	3	76	152	56	0.49	2386	gv-rd-9			29373	34.5	0.177	fl
Jansen et al. [57]	3	152	305	56	0.49	2386	gv-rd-9			29766	34.5	0.158[a]	fl
Jansen et al. [57]	5	102	203	56	0.33	2400	gv-rd-9	2.2	5.5[f]	34144	59.0	0.222	fl
Jansen et al. [57]	3	102	203	56	0.33	2400	gv-rd-9	2.2	5.5[f]	34144	61.0	0.224	fl
Jansen et al. [57]	3	102	203	56	0.33	2400	gv-rd-9	2.2	5.5[f]	34144	64.0	0.226	fl
Jansen et al. [57]	3	102	203	56	0.27	2450	gv-rd-9	11.4	7.5[f]	35661	93.8	0.295	fl
Jansen et al. [57]	5	102	203	56	0.27	2450	gv-rd-9	11.4	7.5[f]	35661	96.7	0.298	fl
Jansen et al. [57]	3	102	203	56	0.27	2450	gv-rd-9	11.4	7.5[f]	35661	99.6	0.302	fl
Jansen et al. [57]	3	76	152	56	0.33	2400	gv-rd-9	2.2	5.5[f]	32910	62.1	0.224	fl
Jansen et al. [57]	2	152	305	56	0.33	2400	gv-rd-9	2.2	5.5[f]	35992	62.1	0.191	fl
Jansen et al. [57]	5	76	152	56	0.27	2450	gv-rd-9	11.4	7.5[f]	35316	103.4	0.299	fl
Jansen et al. [57]	4	152	305	56	0.27	2450	gv-rd-9	11.4	7.5[f]	39784	103.4	0.232	fl
Jensen [58]	1	152.4	304.8	28			n			18016	11.0	0.148	
Jensen [58]	1	152.4	304.8	28			n			19144	15.4	0.151	
Jensen [58]	1	152.4	304.8	28			n			21265	21.5	0.152	
Jensen [58]	1	152.4	304.8	28			n			23719	27.4	0.152	
Jensen [58]	1	152.4	304.8	28			n			25498	33.8	0.156	
Jiang and Teng [59]	1	152	305				n				37.7	0.275	ml
Jiang and Teng [59]	1	152	305				n				38.0	0.217	ml
Jiang and Teng [59]	1	152	305				n				44.2	0.260	ml
Jiang and Teng [59]	1	152	305				n				47.6	0.279	ml
Jiang and Teng [59]	1	152	305				n				33.1	0.309[a]	ml
Jiang and Teng [59]	1	152	305				n				45.9	0.243	ml
Kaar et al. [60]	3	152	305	28			gv			25648	44.8	0.256	fl
Kaar et al. [60]	3	152	305	28			gv			26338	47.6		fl
Kaar et al. [60]	3	152	305	28			gv			29441	58.4	0.228	fl

Source	*n*	*B (mm)*	*H (mm)*	*Age (d)*	*w/c*	$\rho_{c,f}$ *(kg/m³)*	*Aggregate properties*[p]	*sf/c (%)*	*ma/b (%)*	E_c *(MPa)*	f'_{co} *(MPa)*	ε_{co} *(%)*	*M**
Kaar et al. [60]	3	152	305	28			gv			32267	71.8	0.273	fl
Kaar et al. [60]	3	152	305	28			gv			31371	64.7		fl
Kaar et al. [60]	3	152	305	28			gv			36473	78.2	0.264	fl
Kaar et al. [60]	3	152	305	28			gv			40127	96.5	0.310	fl
Kaar et al. [60]	3	152	305	28			gv			38955	91.6		fl
Kaar et al. [60]	3	152	305	28			ls			35853	45.3	0.186	fl
Kaar et al. [60]	3	152	305	28			ls			32061	49.0		fl
Kaar et al. [60]	3	152	305	28			ls			36887	58.1	0.181[a]	fl
Kaar et al. [60]	3	152	305	28			ls			36197	67.6		fl
Kaar et al. [60]	3	152	305	28			ls			33440	69.6	0.231	fl
Kaar et al. [60]	3	152	305	28			ls			40886	77.1	0.276	fl
Kaar et al. [60]	3	152	305	28			ls			39714	88.7		fl
Kaar et al. [60]	3	152	305	28			ls			42885	102.4	0.323	fl
Kaar et al. [60]	3	152	305	28			tr			32474	77.8	0.243	fl
Kaar et al. [60]	3	152	305	28			tr			37645	87.5	0.266	fl
Kaar et al. [60]	3	152	305	28			tr			44195	94.5	0.263	fl
Karabinis and Rousakis [61]	2	200	320		0.51		gv-31.5				40.9	0.272	ml
Karabinis and Rousakis [61]	2	200	320		0.51		gv-31.5				38.5	0.280	ml
Karabinis and Rousakis [61]	2	200	320		0.58		gv-31.5				33.9	0.202	ml
Karabinis and Rousakis [61]	2	200	320		0.58		gv-31.5				35.7	0.180	ml
Karam and Tabbara [62]	2	150	300				n				12.8	0.47[a]	ml
Kawashima et al. [63]		200	600				n				39.0	0.200	
Kayali et al. [64]	4	150	300	28	0.27	2473	n	9.1		35000	72.5		
König et al. [65]	1	100	75				n			27028	83.5	0.530	fl
König et al. [65]	1	100	150				n			27833	58.0	0.377[a]	fl
König et al. [65]	1	100	300				n			28692	43.3	0.253	fl
König et al. [65]	1	100	75				n			27635	123.6	0.589[a]	fl
König et al. [65]	1	100	150				n			27537	83.1	0.380[a]	fl
König et al. [65]	1	100	300				n			27345	68.0	0.289	fl
Kotsovos and Newman [66]	1	100	250				n				73.3	0.200	fl
Kshirsagar et al. [67]	5	102	204	28			n				38.0	0.220	
Lahlou [68]	2	100	200	28	0.50	2350	n-10			25000	46.0	0.270	fl
Lahlou [68]	2	100	200	28	0.35	2450	n-10			34000	78.0	0.320	fl
Lahlou [68]	2	100	200	28	0.23	2520	n-10	10.1		43000	113.0	0.31	fl
Lam and Teng [69]	1	152	305				n			29828	34.3	0.188	ml
Lam and Teng [69]	1	152	305				n			27981	35.9	0.203	ml
Lam and Teng [69]	1	152	305				n			32270	38.5	0.223	ml
Lam et al. [70]	1	152	305				n				38.9	0.250	ml
Lam et al. [70]	1	152	305				n				41.1	0.256	ml
Lee [71]	1	100	200				gv				74.6	0.247	
Lee [71]	1	100	200				gv				76.3	0.259	
Lee [71]	1	100	200				gv				77.2	0.265	
Lee [71]	1	100	200				gv				77.4	0.261	
Lee [71]	1	100	200				gv				77.9	0.265	
Lee [71]	1	100	200				gv				76.6	0.259	
Lee et al. [72]	1	150	300	28			n				36.2	0.24	ml
Li et al. [73]	1	150	300	28	0.39		n				47.5	0.40	as
Li et al. [74]	1	100	300	28	0.50		gv			20100	22.9	0.25	
Li et al. [74]	1	100	300	28	0.50		gv			19300	21.2	0.26	
Li et al. [74]	1	100	300	28	0.50		gv			15500	16.3	0.22	
Li et al. [74]	1	100	300	28	0.50		gv			27000	34.8	0.23	
Liang et al. [75]	4	100	200				n				25.9	0.24	fl
Liang et al. [75]	4	200	400				n				22.7	0.22	fl
Liang et al. [75]	4	300	600				n				24.5	0.22	fl
Lim and Ozbakkaloglu [76]	1	152	305	280	0.27	2454	gv-10				89.9	0.24	fl
Lim and Ozbakkaloglu [76]	1	152	305	280	0.27	2454	gv-10				82.7	0.25	fl
Lim and Ozbakkaloglu [76]	1	152	305	280	0.27	2454	gv-10				84.6	0.24	fl
Lim and Ozbakkaloglu [76]	1	152	305	286	0.27	2454	gv-10	8.0		50000	114.1	0.26	fl
Lim and Ozbakkaloglu [76]	1	152	305	286	0.27	2454	gv-10	8.0		50000	113.8	0.28	fl
Lim and Ozbakkaloglu [76]	1	152	305	286	0.27	2454	gv-10	8.0		50000	109.4	0.26	fl
Lim and Ozbakkaloglu [76]	1	152	305	286	0.24	2438	gv-10	8.0		50000	122.1	0.27	fl
Lim and Ozbakkaloglu [76]	1	152	305	286	0.24	2438	gv-10	8.0		50000	119.2	0.26	fl
Lim and Ozbakkaloglu [76]	1	152	305	286	0.24	2438	gv-10	8.0		50000	121.3	0.26	fl
Lim and Ozbakkaloglu [76]	1	152	305	353	0.27	2454	gv-10	16.0		50000	115.1	0.26	fl
Lim and Ozbakkaloglu [76]	1	152	305	353	0.27	2454	gv-10	16.0		50000	114.3	0.27	fl
Lim and Ozbakkaloglu [76]	1	152	305	353	0.27	2454	gv-10	16.0		50000	111.0	0.25	fl
Lu et al. [77]	1	100	200		0.33		n				67.0	0.251	ml
Mandal et al. [78]	1	102	200	28	0.52	2448	gv				46.8	0.26	ml
Mandal et al. [78]	1	102	200	28	0.52	2448	gv				47.7	0.21	ml
Mandal et al. [78]	1	102	200	28	0.52	2448	gv				44.5	0.21	ml
Mandal et al. [78]	1	102	200	28	0.60	2336	gv				31.3	0.26	ml
Mandal et al. [78]	1	102	200	28	0.60	2336	gv				30.3	0.30	ml
Mandal et al. [78]	1	102	200	28	0.60	2336	gv				30.6	0.26	ml
Mandal et al. [78]	1	100	200	28	0.30	2574	gv	11.1			77.7	0.18[a]	ml
Mandal et al. [78]	1	100	200	28	0.30	2574	gv	11.1			81.5	0.24	ml
Mandal et al. [78]	1	100	200	28	0.30	2574	gv	11.1			82.6	0.25	ml
Mandal et al. [78]	1	100	200	28	0.32	2570	gv	11.1			70.5	0.25	ml
Mandal et al. [78]	1	100	200	28	0.32	2570	gv	11.1			66.1	0.19	ml
Mandal et al. [78]	1	100	200	28	0.32	2570	gv	11.1			64.5	0.21	ml
Mandal et al. [78]	1	102	200	28	0.46	2458	gv	9.1			54.3	0.25	ml

Source	*n*	*B (mm)*	*H (mm)*	*Age (d)*	*w/c*	$\rho_{c,f}$ *(kg/m³)*	*Aggregate properties*[p]	*sf/c (%)*	*ma/b (%)*	E_c *(MPa)*	f'_{co} *(MPa)*	ε_{co} *(%)*	*M**
Mandal et al. [78]	1	102	200	28	0.46	2458	gv	9.1			55.7	0.23	ml
Mandal et al. [78]	1	102	200	28	0.46	2458	gv	9.1			53.6	0.24	ml
Mansur et al. [79]	1	100	200	28	0.40	2336	gn-19	9.9		43000	70.2	0.211	ml
Mansur et al. [79]	1	100	200	28	0.35	2342	gn-19	9.9		45000	85.9	0.226	ml
Mansur et al. [79]	1	100	200	28	0.30	2361	gn-19	10.0		44300	85.9	0.231	ml
Mansur et al. [79]	1	100	200	28	0.25	2381	gn-19	10.0		47100	103.6	0.248	ml
Mansur et al. [79]	1	100	200	28	0.20	2412	gn-19	10.0		49100	119.9	0.275	ml
Matthys et al. [80]	1	150	300				n				34.9	0.21	as
Micelli et al. [81]	3	102	204				n				37.0	0.19	
Micelli et al. [81]	3	102	204				n				32.0	0.14[a]	
Mirmiran [82]	1	152	304				n				30.8	0.205	
Mirmiran [82]	1	152	304				n				32.7	0.246	
Miyauchi et al. [83]	1	150	300	28			n				31.2	0.195	as
Miyauchi et al. [83]	1	100	200	28			n				33.7	0.190	as
Miyauchi et al. [83]	1	150	300	28			n				45.2	0.219	as
Miyauchi et al. [83]	1	100	200	28			n				51.9	0.192	as
Miyauchi et al. [84]	1	150	300	35			n				23.6	0.180	as
Miyauchi et al. [84]	1	100	200	35			n				26.3	0.193	as
Miyauchi et al. [84]		100	200	35			n				109.5	0.287	as
Moral [85]	1	152	305	105			gv				11.0	0.125[a]	
Moral [85]	1	152	305	105			gv				12.0	0.107[a]	
Moral [85]	1	152	305	105			gv				14.0	0.130[a]	
Moral [85]	1	152	305	105			gv				17.5	0.137[a]	
Moral [85]	1	152	305	105			gv				18.0	0.126[a]	
Moral [85]	1	152	305	105			gv				26.5	0.131[a]	
Moral [85]	1	152	305	105			gv				35.0	0.137[a]	
Nakamura and Higai [86]		150	150				n				20.0	0.320[a]	
Nakamura and Higai [86]		150	300				n				19.8	0.262	
Nakamura and Higai [86]		150	450				n				19.9	0.276[a]	
Nakamura and Higai [86]		150	600				n				20.0	0.276[a]	
Newman [87]	3	100	250		0.38		n				91.2	0.147[a]	fl
Newman [87]	3	100	250		0.44		n-19				73.3	0.200	fl
Newman [87]	3	100	250		0.79		n-19				23.2	0.173	fl
Nilson and Slate [88]	1	150	300	>28			n				50.0	0.220	
Nilson and Slate [88]	1	150	300	>28			n				62.0	0.276	
Nilson and Slate [88]	1	150	300	>28			n				63.0	0.276	
Oktar [89]	1	152	305	180			gv				6.0	0.070	
Oktar [89]	1	152	305	180			gv				7.0	0.045[a]	
Oktar [89]	1	152	305	180			gv				10.0	0.090[a]	
Oktar [89]	1	152	305	180			gv				11.5	0.088[a]	
Oktar [89]	1	152	305	180			gv				14.0	0.101[a]	
Oktar [89]	1	152	305	180			gv				15.0	0.105[a]	
Oktar [89]	1	152	305	180			gv				15.5	0.077[a]	
Oktar [89]	1	152	305	180			gv				16.5	0.103[a]	
Oktar [89]	1	152	305	180			gv				18.0	0.085[a]	
Oktar [89]	1	152	305	180			gv				18.0	0.090[a]	
Oktar [89]	1	152	305	180			gv				18.0	0.103[a]	
Oktar [89]	1	152	305	180			gv				19.5	0.091[a]	
Oktar [89]	1	152	305	180			gv				20.0	0.118[a]	
Oktar [89]	1	152	305	180			gv				26.0	0.110[a]	
Oktar [89]	1	152	305	180			gv				27.0	0.100[a]	
Oktar [89]	1	152	305	180			gv				29.5	0.111[a]	
Oktar [89]	1	152	305	180			gv				32.5	0.120[a]	
Oktar [89]	1	152	305	180			gv				33.0	0.101[a]	
Oktar [89]	1	152	305	180			gv				33.0	0.102[a]	
Oktar [89]	1	152	305	180			gv				36.0	0.121[a]	
Oktar [89]	1	152	305	180			gv				37.0	0.110[a]	
Oktar [89]	1	152	305	180			gv				37.1	0.120[a]	
Oktar [89]	1	152	305	180			gv				38.0	0.102[a]	
Oktar [89]	1	152	305	180			gv				39.0	0.123[a]	
Oktar [89]	1	152	305	180			gv				39.5	0.110[a]	
Oktar [89]	1	152	305	180			gv				39.5	0.124[a]	
Oktar [89]	1	152	305	180			gv				41.5	0.120[a]	
Oktar [89]	1	152	305	180			gv				47.5	0.130[a]	
Osorio et al. [90]	8	100	200	7	0.60	2399	n-20			34535	37.3	0.19	fl
Osorio et al. [90]	8	100	200	7	0.50	2396	n-20			37718	45.9	0.20	fl
Osorio et al. [90]	7	100	200	7	0.40	2361	n-20			39561	61.0	0.22	fl
Osorio et al. [90]	8	100	200	7	0.30	2442	n-20			44606	84.3	0.23	fl
Park and Paulay [91]	1	150	300	28			n				8.0	0.130	
Park and Paulay [91]	1	150	300	28			n				14.0	0.148	
Park and Paulay [91]	1	150	300	28			n				20.0	0.182	
Park and Paulay [91]	1	150	300	28			n				27.0	0.184	
Park and Paulay [91]	1	150	300	28			n				34.0	0.180	
Park and Paulay [91]	1	150	300	28			n				39.0	0.178	
Ramaley and McHenry [92]		76	152	3			n				7.7	0.150	
Ramaley and McHenry [92]		76	152	15			n				15.2	0.220	
Ramaley and McHenry [92]		76	152	22			n				17.9	0.195	
Ramaley and McHenry [92]		76	152	42			n				24.6	0.195	
Ramaley and McHenry [92]		76	152	84			n				27.2	0.200	
Richart and Jensen [93]	3	152.4	304.8	28		2296	gv			26175	33.8	0.150	

Source	*n*	*B (mm)*	*H (mm)*	*Age (d)*	*w/c*	$\rho_{c,f}$ *(kg/m³)*	*Aggregate properties*[p]	*sf/c (%)*	*ma/b (%)*	E_c *(MPa)*	f'_{co} *(MPa)*	ε_{co} *(%)*	*M**
Richart and Jensen [93]	3	152.4	304.8	28		2296	gv			23584	27.5	0.149	
Richart and Jensen [93]	3	152.4	304.8	28		2296	gv			20698	21.2	0.148	
Richart and Jensen [93]	3	152.4	304.8	28		2296	gv			17645	15.4	0.140	
Richart and Jensen [93]	3	152.4	304.8	28		2296	gv			14688	10.7	0.107	
Richart et al. [94]	8	102	203	28			n			23580	17.8	0.21	fl
Richart et al. [94]	4	102	203	28			n			27648	25.2	0.18	fl
Richart et al. [94]	4	102	203	28			n			17582	7.2	0.22[a]	fl
Richart et al. [95]	1	254	1016	28			n			21650	15.8	0.17	ml
Richart et al. [95]	1	254	1016	28			n			20822	13.4	0.16	ml
Richart et al. [95]	1	254	1016	28			n			21098	14.6	0.19	ml
Richart et al. [95]	1	254	1016	28			n			20271	14.3	0.25[a]	ml
Richart et al. [95]	1	254	1016	28			n			22753	15.3	0.22[a]	ml
Rokugo and Koyanagi [96]	1	84	85				n			55692[m]	49.7	0.306	
Rokugo and Koyanagi [96]	1	84	170				n			36548	39.2	0.165[a]	
Rokugo and Koyanagi [96]	1	84	340				n			36589	39.2	0.159[a]	
Rokugo and Koyanagi [96]	1	84	510				n			36256	38.8	0.155[a]	
Rousakis [97]	1	150	300	105-119	0.94	2325	gv-16			18900	25.8	0.312[a]	ml
Rousakis [97]	1	150	300	105-119	0.94	2325	gv-16			13700	24.2	0.310[a]	ml
Rousakis [97]	1	150	300	105-119	0.94	2325	gv-16			19200	25.8	0.312[a]	ml
Rousakis [97]	1	150	300	105-119	0.55	2359	gv-16			22300	47.0	0.309	ml
Rousakis [97]	1	150	300	105-119	0.55	2359	gv-16			22100	46.5	0.305	ml
Rousakis [97]	1	150	300	105-119	0.55	2359	gv-16			23100	48.8	0.311	ml
Rousakis [97]	1	150	300	105-119	0.38	2371	gv-16			24200	57.4	0.308	ml
Rousakis [97]	1	150	300	105-119	0.38	2371	gv-16			25300	49.1	0.274	ml
Rousakis [97]	1	150	300	105-119	0.38	2371	gv-16			24200	48.8	0.311	ml
Rousakis [97]	1	150	300	105-119	0.38	2371	gv-16			27400	60.1	0.307	ml
Rousakis [97]	1	150	300	105-119	0.38	2371	gv-16			23200	53.7	0.288	ml
Rousakis [97]	1	150	300	105-119	0.35	2394	gv-16	3.2		27600	72.4	0.356[a]	ml
Rousakis [97]	1	150	300	105-119	0.35	2394	gv-16	3.2		25800	70.1	0.359[a]	ml
Rousakis [97]	1	150	300	105-119	0.35	2394	gv-16	3.2		28400	69.2	0.335	ml
Rousakis [97]	1	150	300	105-119	0.32	2421	gv-16	6.4		33700	87.6	0.315	ml
Rousakis [97]	1	150	300	105-119	0.32	2421	gv-16	6.4		31400	76.6	0.290	ml
Rousakis [97]	1	150	300	105-119	0.32	2421	gv-16	6.4		26500[m]	82.2	0.341	ml
Rousakis et al. [98]	1	150	300		0.94	2325	gv-16			24400	20.4	0.260	ml
Rousakis et al. [98]	1	150	300		0.35	2394	gv-16	3.2		36700	49.2	0.17[a]	ml
Saafi et al. [99]	12	152	434	28			n			30000	35.0	0.25	
Sangha [100]	2	50.8	50.8	28	0.5		n				50.8	0.643[a]	fl
Sangha [100]	2	50.8	76.2	28	0.5		n				42.2	0.496[a]	fl
Sangha [100]	2	50.8	101.6	28	0.5		n-9.5				41.6	0.406[a]	fl
Sangha [100]	2	50.8	127.0	28	0.5		n-9.5				41.0	0.385[a]	fl
Sangha [100]	2	50.8	152.4	28	0.5		n-9.5				40.9	0.374[a]	fl
Sangha [100]	2	50.8	50.8	28	0.5		n-9.5				58.0	0.672[a]	fl
Sangha [100]	2	50.8	50.8	28	0.5		n-9.5				57.8	0.636[a]	fl
Sangha [100]	2	50.8	127.0	28	0.5		n-9.5				47.8	0.402[a]	fl
Sangha [100]	2	50.8	127.0	28	0.5		n-9.5				47.8	0.396[a]	fl
Sangha [100]	2	50.8	50.8	28	0.5		n-9.5				58.9	0.641[a]	fl
Sangha [100]	2	101.6	101.6	28	0.5		n-9.5				57.8	0.619[a]	fl
Sangha [100]	2	50.8	127.0	28	0.5		n-9.5				47.9	0.374[a]	fl
Sangha [100]	2	101.6	254.0	28	0.5		n-9.5				46.6	0.391[a]	fl
Scott et al. [101]	1	75	150	42			n-9.5				25.3	0.18	ml
Scott et al. [101]	1	75	150	42			n-9.5				24.8	0.12[a]	ml
Scott et al. [101]	1	75	150	42			n-20				24.2	0.18	ml
Scott et al. [101]	1	75	150	42			n-20				24.2	0.10[a]	ml
Scott et al. [101]	1	75	150	42			n-20				24.2	0.06[a]	ml
Saenz [102]		69	140				n-20				43.0	0.392[a]	fl
Saenz [102]		69	140				n-20				20.3	0.360[a]	fl
Seffo and Hamcho [103]	3	150	300	28	0.29	2300	gv-cr			40529[m]	37.2	0.265	
Sfer et al. [104]	1	150	300	51	0.57		ls			27300	32.8	0.18	
Sfer et al. [104]	1	150	300	114	0.57		ls			28600	38.8	0.21	
Shah and Ahmad [105]	1	76	152	>28			gv				58.0	0.248	
Shah and Ahmad [105]	1	76	152	>28			gv				77.0	0.275	
Shah and Sankar [106]	1	76	152				n			22738	28.9	0.303	
Shah and Sankar [106]	1	76	152				n			16686	28.9	0.277	
Shah and Sankar [106]	1	76	152				n			24702	29.7	0.311[a]	
Shah and Sankar [106]	1	76	152				n			24702	29.6	0.279	
Shah et al. [107]	4	75	150	28-35	0.47	2407	n				46.0	0.29	fl
Shahawy et al. [108]	5	153	305				n			16376	19.4	0.33[a]	
Shahawy et al. [108]	5	153	305				n			22409	49.0	0.29	
Shehata et al. [109]	9	150	300				n				29.8	0.21	as
Shehata et al. [110]	9	225	450				n				34.0	0.20	as
Shehata et al. [110]	9	150	300				n				34.0	0.20	as
Shehata et al. [110]	9	150	300				n				61.7	0.18[a]	as
Silva and Rodrigues [111]	1	150	300	28			n				29.2	0.21	
Silva and Rodrigues [111]	1	150	300	28			n				27.1	0.19	
Silva and Rodrigues [111]	1	150	300	28			n				25.8	0.20	
Silva and Rodrigues [111]	1	150	750	241			n				26.6	0.19	
Silva and Rodrigues [111]	1	150	750	241			n				26.5	0.18	
Silva and Rodrigues [111]	1	150	750	248			n				26.4	0.21	
Silva and Rodrigues [111]	1	250	750	344			n				34.9	0.25	
Silva and Rodrigues [111]	1	250	750	345			n				29.4	0.22	

Source	*n*	*B (mm)*	*H (mm)*	*Age (d)*	*w/c*	$\rho_{c,f}$ *(kg/m³)*	*Aggregate properties*[p]	*sf/c (%)*	*ma/b (%)*	E_c *(MPa)*	f'_{co} *(MPa)*	ε_{co} *(%)*	*M**
Slate et al. [112]		102	203	28			n			17230	25.0	0.200	
Slate et al. [112]		102	203	28			n			22850	48.3	0.280	
Slate et al. [112]		102	203	28			n			31630	71.4	0.280	
Smeplass [113]	1	150	300	28			gv-cr				50.0	0.234	
Smeplass [113]	1	150	300	28			gv-cr				59.0	0.255	
Smeplass [113]	1	150	300	28			gv-cr				72.5	0.255	
Smeplass [113]	1	150	300	28			gv-cr				75.0	0.276	
Smeplass [113]	1	150	300	28			gv-cr				80.5	0.286	
Smeplass [113]	1	150	300	28			gv-cr				81.5	0.284	
Smeplass [113]	1	150	300	28			gv-cr				85.0	0.292	
Smeplass [113]	1	150	300	28			gv-cr				90.0	0.292	
Smeplass [113]	1	150	300	28			gv-cr				95.0	0.308	
Smeplass [113]	1	150	300	28			gv-cr				96.5	0.305	
Smeplass [113]	1	150	300	28			gv-cr				97.0	0.306	
Smeplass [113]	1	150	300	28			gv-cr				99.0	0.306	
Smeplass [113]	1	150	300	28			gv-cr				99.5	0.327	
Smeplass [113]	1	150	300	28			gv-cr				102.0	0.323	
Smeplass [113]	1	150	300	28			gv-cr				105.0	0.309	
Smith and Young [114]	1	150	300	28			n			14598	9.0	0.182	
Smith and Young [114]	1	150	300	28			n			26348	21.0	0.200	
Smith and Young [114]	1	150	300	28			n			32444	31.0	0.192	
Smith and Young [114]	1	150	300	28			n			36429	50.0	0.182	
Smith et al. [115]	1	54	108	240	0.83		gv				22.1	0.339[a]	fl
Smith et al. [115]	1	54	108	240	0.83		gv				34.5	0.351[a]	fl
Smith et al. [115]	1	54	108	240	0.833[w]		gv				44.1	0.354	fl
Taerwe [116]	1	155	380	30	0.55		gv-7.3			24521	34.7	0.206	fl
Taerwe [116]	1	155	380	30	0.55		gv-7.3			24521	34.0	0.196	fl
Taerwe [116]	1	155	380	30	0.55		gv-7.3			24521	35.6	0.204	fl
Taerwe [116]	1	155	380	30	0.55		gv-7.3			24521	34.5	0.205	fl
Taerwe [116]	1	155	380	30	0.55		gv-7.3			24521	37.5	0.218	fl
Taerwe [116]	1	155	380	45	0.49		gv-7.3			24521	49.7	0.222	fl
Taerwe [116]	1	155	380	45	0.49		gv-7.3			24521	49.7	0.214	fl
Taerwe [116]	1	155	380	45	0.49		gv-7.3			24521	49.1	0.224	fl
Taerwe [116]	1	155	380	45	0.49		gv-7.3			24521	48.0	0.210	fl
Taerwe [116]	1	155	380	45	0.49		gv-7.3			24521	53.0	0.233	fl
Taerwe [116]	1	155	380	30	0.32		gv-7.3			37836	87.5	0.267	fl
Taerwe [116]	1	155	380	30	0.32		gv-7.3			37836	89.7	0.254	fl
Taerwe [116]	1	155	380	120	0.32		gv-7.3			37836	93.0	0.266	fl
Taerwe [116]	1	155	380	120	0.32		gv-7.3			37836	93.0	0.278	fl
Taerwe [116]	1	192	483	120	0.32		gv-7.3			37836	96.6	0.276	fl
Taerwe [116]	1	192	483	120	0.32		gv-7.3			37836	96.6	0.271	fl
Taerwe [116]	1	192	483	120	0.32		gv-7.3			37836	94.8	0.277	fl
Taerwe [116]	1	155	380	120	0.32		gv-7.3			37836	90.9	0.267	fl
Taerwe [116]	1	155	380	120	0.32		gv-7.3			37836	95.2	0.282	fl
Taerwe [116]	1	155	380	120	0.32		gv-7.3			37836	94.1	0.270	fl
Taerwe [116]	1	155	380	120	0.32		gv-7.3			37836	94.1	0.274	fl
Tamuzs et al. [117]	1	150	300				n			20000	20.8	0.241	as
Tamuzs et al. [117]	1	150	300				n			33600	48.8	0.251	as
Tan and Sun [118]	1	100	300				n				51.8	0.24	
Tasdemir [119]	1	152	305	28	0.40	2262	pm,ls				40.5	0.170	
Tasdemir [119]	1	152	305	28	0.40	2246	pm,ls				40.0	0.184	
Tasdemir [119]	1	152	305	28	0.60	2337	pm,ls				41.0	0.193	
Tasdemir [119]	1	152	305	28	0.60	2343	pm,ls				43.0	0.191	
Tasdemir [119]	1	152	305	28	0.40	2408	pm,ls				45.0	0.220	
Tasnimi [120]	1	150	300	28	0.56	2303	qz			17760	24.3	0.228	
Tasnimi [120]	1	150	300	28	0.56	2303	qz			18800	25.5	0.228	
Tasnimi [120]	1	150	300	28	0.56	2303	qz			20180	26.8	0.239	
Tasnimi [120]	1	150	300	28	0.56	2303	qz			18570	27.0	0.270	
Tasnimi [120]	1	150	300	28	0.56	2303	qz			21280	27.4	0.245	
Tasnimi [120]	1	150	300	28	0.56	2303	qz			17530	28.5	0.270	
Tasnimi [120]	1	150	300	28	0.56	2303	qz			20210	31.2	0.259	
Tasnimi [120]	1	150	300	28	0.56	2303	qz			18640	32.2	0.281	
Tasnimi [120]	1	150	300	28	0.56	2303	qz			19460	32.3	0.259	
Tasnimi [120]	1	150	300	28	0.56	2303	qz			22760	35.6	0.297	
Tasnimi [120]	1	150	300	28	0.49	2306	qz			21650	36.3	0.311[a]	
Tasnimi [120]	1	150	300	28	0.49	2306	qz			22940	36.7	0.300	
Tasnimi [120]	1	150	300	28	0.49	2306	qz			21260	36.7	0.341[a]	
Tasnimi [120]	1	150	300	28	0.49	2306	qz			21800	36.7	0.310[a]	
Tasnimi [120]	1	150	300	28	0.49	2306	qz			20560	36.7	0.294	
Tasnimi [120]	1	150	300	28	0.49	2306	qz			21420	37.1	0.297	
Tasnimi [120]	1	150	300	28	0.49	2306	qz			23390	38.3	0.295	
Tasnimi [120]	1	150	300	28	0.49	2306	qz			21160	39.3	0.287	
Tasnimi [120]	1	150	300	28	0.49	2306	qz			21480	39.4	0.299	
Tasnimi [120]	1	150	300	28	0.49	2306	qz			20930	40.2	0.243	
Tasnimi [120]	1	150	300	28	0.49	2306	qz			20640	40.5	0.284	
Tasnimi [120]	1	150	300	28	0.49	2306	qz			22750	42.4	0.300	
Tasnimi [120]	1	150	300	28	0.49	2306	qz			25210	42.5	0.279	
Tasnimi [120]	1	150	300	28	0.49	2306	qz			22470	42.5	0.309	
Tasnimi [120]	1	150	300	28	0.45	2301	qz			22920	44.3	0.300	
Tasnimi [120]	1	150	300	28	0.45	2301	qz			28310	46.3	0.310	

Source	*n*	*B (mm)*	*H (mm)*	*Age (d)*	*w/c*	$\rho_{c,f}$ *(kg/m³)*	*Aggregate properties*[p]	*sf/c (%)*	*ma/b (%)*	E_c *(MPa)*	f'_{co} *(MPa)*	ε_{co} *(%)*	*M**
Tasnimi [120]	1	150	300	28	0.45	2301	qz			22810	47.7	0.298	
Tasnimi [120]	1	150	300	28	0.45	2301	qz			27260	47.8	0.257	
Tasnimi [120]	1	150	300	28	0.45	2301	qz			25030	48.9	0.319	
Tasnimi [120]	1	150	300	28	0.45	2301	qz			30640	55.7	0.337[a]	
Teng et al. [121]	1	152	305				n				39.6	0.263	ml
Tulin and Gerstle [122]		152	305	91			n				32.1	0.33[a]	
Valdmanis et al. [123]	1	150	300		0.94	2324	gv-16			24400	20.5	0.26	ml
Valdmanis et al. [123]	1	150	300		0.55	2340	gv-16			34030	40.0	0.17[a]	ml
Valdmanis et al. [123]	1	150	300		0.38	2371	gv-16			37830	44.3	0.17	ml
Valdmanis et al. [123]	1	150	300		0.35	2394	gv-16	3.2		36650	49.2	0.17[a]	ml
Valdmanis et al. [123]	1	150	300		0.32	2421	gv-16	6.4		39090	61.6	0.18[a]	ml
Vu et al. [124]	1	70	140	195		2278	n			24000	42.0	0.22	fl
Vu et al. [124]	1	110	210	163		2278	n			25000	34.0	0.22	fl
Vu et al. [124]	1	70	140	292		2278	n			25000	32.0	0.18	fl
Vu et al. [124]	1	70	140	292		2278	n			25000	32.0	0.18	fl
Wang and Wu [125]	3	150	300				n				30.9	0.24	
Wang and Wu [125]	3	150	300				n				52.1	0.27	
Wang and Wu [126]		70	210				n				51.6	0.248	
Wang and Wu [126]		105	315				n				50.6	0.244	
Wang and Wu [126]		194	582				n				44.9	0.260	
Wang and Wu [126]		70	210				n				29.4	0.203	
Wang and Wu [126]		105	315				n				28.8	0.202	
Wang and Wu [126]		194	582				n				24.0	0.207	
Wang et al. [127]	1	76.2	152.4	2-125	0.45	2390	n-9.5			10780[m]	20.7	0.280	fl
Wang et al. [127]	1	76.2	152.4	2-125	0.45	2390	n-9.5			18340	40.1	0.280	fl
Wang et al. [127]	1	76.2	152.4	2-125	0.45	2390	n-9.5			21310	50.3	0.299	fl
Wang et al. [127]	1	76.2	152.4	2-125	0.45	2390	n-9.5			27720	74.1	0.360	fl
Wang et al. [127]	1	76.2	152.4	2-125	0.45	2390	n-9.5			14959	29.8	0.286	fl
Wang et al. [127]	1	76.2	152.4	2-125	0.45	2390	n-9.5			20159	50.3	0.302	fl
Watanabe [128]	1	150	300				n				16.5	0.165	
Watanabe [128]	1	150	300				n				25.0	0.150[a]	
Watanabe [128]	1	150	300				n				29.0	0.175	
Watanabe [128]	1	150	300				n				35.8	0.170	
Watanabe [128]	1	150	300				n				36.5	0.185	
Watanabe [128]	1	150	300				n				17.5	0.200	
Watanabe [128]	1	150	300				n				22.0	0.240	
Watanabe [128]	1	150	300				n				29.0	0.220	
Watanabe [128]	1	150	300				n				33.0	0.250	
Watanabe [128]	1	150	300				n				34.5	0.260	
Watanabe et al. [129]		100	200		0.63		gv				30.2	0.230	
Watanabe et al. [130]		100	200		0.4	2359	n-20			33805	54.1	0.257	fl
Watanabe et al. [130]		100	200		0.6	2328	n-20				29.4		fl
Watanabe et al. [130]		100	300		0.4	2359	n-20			40320	48.1	0.154[a]	fl
Watanabe et al. [130]		100	300		0.6	2328	n-20				28.4		fl
Watanabe et al. [130]		100	400		0.4	2339	n-13			27824	48.6	0.158[a]	fl
Watanabe et al. [130]		100	400		0.5	2320	n-13			30550	39.3	0.164	fl
Watanabe et al. [130]		100	400		0.6	2307	n-13			28222	29.4	0.144[a]	fl
Watanabe et al. [130]		100	400		0.7	2292	n-13			26861	21.9	0.117[a]	fl
Watanabe et al. [130]		100	400		0.4	2359	n-20			49424[m]	47.5	0.185	fl
Watanabe et al. [130]		100	400		0.5	2342	n-20			30341	28.2	0.085[a]	fl
Watanabe et al. [130]		100	400		0.6	2328	n-20			30934	30.3	0.139[a]	fl
Watanabe et al. [130]		100	400		0.7	2317	n-20			35725[m]	22.5	0.118[a]	fl
Watanabe et al. [130]		100	600		0.4	2359	n-20			30570	48.4	0.201	fl
Watanabe et al. [130]		100	600		0.6	2328	n-20			45780[m]	29.3	0.110[a]	fl
Watanabe et al. [130]		100	800		0.4	2359	n-20			28257	44.7	0.182	fl
Watanabe et al. [130]		100	800		0.4	2359	n-20				16.6		fl
Watanabe et al. [130]		100	800		0.6	2328	n-20			28726	29.9	0.135	fl
Watstein [131]	3	76	152	28	0.90		n			20684	20.3	0.230	fl
Watstein [131]	3	76	152	28	0.90		n			20684	16.5	0.205	fl
Watstein [131]	3	76	152	28	0.90		n			21374	18.0	0.199	fl
Watstein [131]	3	76	152	28	0.50		n			26407	46.4	0.261	fl
Watstein [131]	3	76	152	28	0.50		n			26614	42.8	0.266	fl
Watstein [131]	3	76	152	28	0.44		n			35853	50.7	0.219	fl
Wee et al. [132]	12	100	200	5	0.40	2400	gn-19			37600	42.7	0.212	ml
Wee et al. [132]	5	100	200	28	0.40	2400	gn-19			41800	63.2	0.216	ml
Wee et al. [132]	5	100	200	28	0.30	2400	gn-19			44300	78.3	0.232	ml
Wee et al. [132]	5	100	200	28	0.33	2400	gn-19			44300	85.9	0.231	ml
Wee et al. [132]	5	100	200	28	0.25	2430	gn-19			45600	85.6	0.232	ml
Wee et al. [132]	5	100	200	28	0.44	2401	gn-19	2.5		43000	70.2	0.210	ml
Wee et al. [132]	5	100	200	28	0.553[w]	2401	gn-19		9.1[f]	41500	65.1	0.216	ml
Wee et al. [132]	3	100	200	56	0.553[w]	2401	gn-19		9.1[f]	40400	70.5	0.206	ml
Wee et al. [132]	5	100	200	28	0.797[w]	2400	gn-19		22.4[s]	41500	69.7	0.212	ml
Wee et al. [132]	3	100	200	56	0.797[w]	2400	gn-19		22.4[s]	41400	71.5	0.213	ml
Wee et al. [132]	5	100	200	28	0.47	2361	gn-19		5.4[h]	42600	63.6	0.228	ml
Wee et al. [132]	5	100	200	28	0.39	2400	gn-19	2.2		45000	85.9	0.226	ml
Wee et al. [132]	5	100	200	28	0.43	2400	gn-19	4.9		44400	90.2	0.243	ml
Wee et al. [132]	5	100	200	28	0.42	2400	gn-19		7.2[f]	43900	81.2	0.224	ml
Wee et al. [132]	3	100	200	56	0.42	2400	gn-19		7.2[f]	44500	88.1	0.227	ml
Wee et al. [132]	5	100	200	28	0.620[w]	2401	gn-19		18.2[s]	43800	81.6	0.211	ml
Wee et al. [132]	3	100	200	56	0.620[w]	2401	gn-19		18.2[s]	44200	82.6	0.216	ml

Source	*n*	*B (mm)*	*H (mm)*	*Age (d)*	*w/c*	$\rho_{c,f}$ *(kg/m³)*	*Aggregate properties*[p]	*sf/c (%)*	*ma/b (%)*	E_c *(MPa)*	f'_{co} *(MPa)*	ε_{co} *(%)*	*M**
Wee et al. [132]	5	100	200	28	0.36	2369	gn-19		4.0[h]	47200	84.8	0.252	ml
Wee et al. [132]	5	100	200	28	0.26	2430	gn-19	0.8		46600	96.2	0.237	ml
Wee et al. [132]	2	100	200	1	0.28	2430	gn-19	1.7		35200	46.4	0.250	ml
Wee et al. [132]	2	100	200	3	0.28	2430	gn-19	1.7		40800	65.8	0.237	ml
Wee et al. [132]	2	100	200	5	0.28	2430	gn-19	1.7		41600	73.9	0.243	ml
Wee et al. [132]	2	100	200	9	0.28	2430	gn-19	1.7		44500	87.6	0.243	ml
Wee et al. [132]	2	100	200	11	0.28	2430	gn-19	1.7		45400	93.1	0.244	ml
Wee et al. [132]	2	100	200	14	0.28	2430	gn-19	1.7		45200	95.3	0.242	ml
Wee et al. [132]	2	100	200	18	0.28	2430	gn-19	1.7		45800	100.6	0.258	ml
Wee et al. [132]	2	100	200	21	0.28	2430	gn-19	1.7		46100	102.1	0.256	ml
Wee et al. [132]	7	100	200	28	0.28	2430	gn-19	1.7		46700	102.8	0.247	ml
Wee et al. [132]	2	100	200	56	0.28	2430	gn-19	1.7		48400	106.3	0.251	ml
Wee et al. [132]	5	100	200	28	0.29	2430	gn-19	2.7		46300	104.2	0.249	ml
Wee et al. [132]	5	100	200	28	0.35	2430	gn-19		6.3[f]	45800	92.8	0.242	ml
Wee et al. [132]	3	100	200	56	0.35	2430	gn-19		6.3[f]	47300	94.6	0.228	ml
Wee et al. [132]	5	100	200	28	0.526[w]	2430	gn-19		16.0[s]	46300	94.4	0.229	ml
Wee et al. [132]	3	100	200	56	0.526[w]	2430	gn-19		16.0[s]	46500	96.6	0.232	ml
Wee et al. [132]	5	100	200	28	0.732[w]	2430	gn-19		26.7[s]	45900	91.5	0.228	ml
Wee et al. [132]	3	100	200	56	0.732[w]	2430	gn-19		26.7[s]	47100	93.6	0.219	ml
Wee et al. [132]	5	100	200	28	0.30	2580	gn-19		3.2[h]	46000	91.7	0.266	ml
Wee et al. [132]	5	100	200	28	0.22	2430	gn-19	1.5		49100	119.9	0.275	ml
Wee et al. [132]	5	100	200	170	0.22	2430	gn-19	1.5		50900	125.6	0.273	ml
Wischers [133]	1	150	300	>28			n			29705	69.0	0.245	
Wischers [133]	1	150	300	>28			n			29257	56.5	0.225	
Wischers [133]	1	150	300	>28			n			28900	49.3	0.231	
Wischers [133]	1	150	300	>28			n			20131	39.9	0.186	
Wischers [133]	1	150	300	>28			n			27894	28.0	0.181	
Wischers [133]	1	150	300	>28			n			19378	16.2	0.174	
Wischers [133]	1	150	300	>28			n				56.0	0.226	
Wischers [133]	1	150	300	>28			n				57.0	0.238	
Wong et al. [134]	3	153	305				n			30200	39.6	0.263	ml
Wong et al. [134]	3	153	305				n			29500	36.9	0.262	ml
Wong et al. [134]	3	153	305				n			28200	40.1	0.259	ml
Wong et al. [134]	3	153	305				n			30700	46.7	0.287	ml
Wong et al. [134]	3	153	305				n			27800	36.7	0.274	ml
Wong et al. [134]	3	153	305				n			30100	36.5	0.256	ml
Wong et al. [134]	3	153	305				n			27800	33.6	0.258	ml
Wong et al. [134]	3	153	305				n			27900	36.8	0.289	ml
Wu et al. [135]	1	150	300				n				23.5	0.22	fl
Wu et al. [135]	1	150	300				n				23.0	0.27	fl
Wu et al. [135]	1	150	300				n				22.7	0.31[a]	fl
Wu et al. [136]	1	100	300				n				46.4	0.255	ml
Wu et al. [136]	1	100	300				n				78.5	0.451[a]	ml
Wu et al. [136]	1	100	300				n				101.2	0.456[a]	ml
Xiao et al. [137]	4	152	305				n			39900	70.8	0.32	ml
Xiao et al. [137]	4	152	305				n			46400	111.6	0.34	ml
Xie et al. [138]	1	56	110	29	0.32	2438	gv-14	10.7		24050	59.6	0.293	fl
Xie et al. [138]	1	56	110	29	0.32	2438	gv-14	10.7		24050	60.6	0.298	fl
Xie et al. [138]	1	56	110	29	0.32	2438	gv-14	10.7		24050	60.4	0.298	fl
Xie et al. [138]	1	56	110	35	0.28	2241	gv-14	10.0		30491	90.4	0.311	fl
Xie et al. [138]	1	56	110	35	0.28	2241	gv-14	10.0		30491	93.2	0.323	fl
Xie et al. [138]	1	56	110	35	0.28	2241	gv-14	10.0		30491	93.0	0.323	fl
Xie et al. [138]	1	56	110	39	0.21	2371	gv-14	10.0		34072[m]	120.6	0.369	fl
Xie et al. [138]	1	56	110	39	0.21	2371	gv-14	10.0		34072[m]	116.6	0.354	fl
Xie et al. [138]	1	56	110	39	0.21	2371	gv-14	10.0		34072[m]	119.8	0.369	fl
Yan et al. [139]	1	305	610		0.72		gv-rd-10				15.2	0.20	ml
Youssef et al. [140]	3	406	813				n-9.5				29.4	0.24	ml
Youssef et al. [140]	3	152	305				n-9.5				44.6	0.20	ml

w Water-cementitious binder ratio that differ significantly from the reference values of the corresponding concrete strength
m Concrete elastic modulus that differ significantly from the reference values of the corresponding concrete strength
a Concrete strain at peak stress that differ significantly from the reference values of the corresponding concrete strength
f Fly-ash used as mineral admixture in concrete mix
s Blast-furnace slag used as mineral admixture in concrete mix
h Hi-fi (ettringite based material) used as mineral admixture in concrete mix
p Designation:- type-irregularity-size
Type:- n: normal weight aggregate, bs: basalt, dl: dolomitic limestone, gn: granite, gv: gravel, hf: hornfels, ls: limestone, qz: quartz, rd: rhyodacite, st: sandstone gravel, st: stone, tr: traprock
Irregularity:- cr: crushed, rd: round
Size:- maximum aggregate in mm
M Axial strain measurement method:- as: axial strain gauges attached on the surface of specimen
fl: linear variable displacement transducers mounted on loading platens to measure deformation along the full height of specimen
ml: linear variable displacement transducers mounted on specimen to measure deformation within a gauge length along the height of specimen

Table A2. Test database of light weight concrete cylinders

Source	*n*	*B (mm)*	*H (mm)*	*Age (d)*	*w/c*	$\rho_{c,f}$ *(kg/m³)*	*Aggregate properties*[p]	*sf/c (%)*	*ma/b (%)*	E_c *(MPa)*	f'_{co} *(MPa)*	ε_{co} *(%)*	*M**
Ahmad and Shah [3]	4	76	152	114	0.43	1860	es-12.7		12.8[f]		39.5	0.30	fl
Ahmad and Shah [3]	3	76	152	114	0.53	1545	ec-12.7		11.3[f]		31.6	0.27	fl
Ahmad and Shah [4]	4	76	305	58	0.53	1860	es		11.3[f]	16900	39.6	0.31	fl
Ahmad and Shah [4]	4	76	305	58	0.53	1860	es		11.3[f]	18960	51.7	0.35[a]	fl
Ahmad and Shah [4]	3	76	305	28	0.43	1545	ec		12.8[f]	15240	31.6	0.27	fl
Ahmad and Shah [4]	2	152	610	28	0.43	1545	ec		12.8[f]	16700	29.8	0.24	fl
Ahmad and Shah [4]	3	76	305	200	0.43	1545	ec		12.8[f]	15300	37.2	0.27	fl
Ahmad and Shah [4]	3	76	305	200	0.43	1545	ec		12.8[f]	16340	37.0	0.29	fl
Ahmad and Shah [4]	3	76	305	200	0.43	1545	ec		12.8[f]	16700	36.5	0.32	fl
Almusallam and Alsayed [10]		150	300	28		1300	ns-9.5			9620	16.6	0.212	
Almusallam and Alsayed [10]		150	300	28		1300	ns-9.5			16800	52.3	0.371	
Cui et al. [141]	1	100	200	28	0.35	666	l			21320[m]	30.4	0.186[a]	ml
Cui et al. [141]	1	100	200	28	0.35	666	l			17141	23.0	0.181[a]	ml
Cui et al. [141]	1	100	200	28	0.35	666	l			12459	18.9	0.184[a]	ml
Cui et al. [141]	1	100	200	28	0.35	1175	l			22247	45.5	0.268	ml
Cui et al. [141]	1	100	200	28	0.35	1175	l			21085	42.5	0.246	ml
Cui et al. [141]	1	100	200	28	0.35	1175	l			17512	35.0	0.243	ml
Cui et al. [141]	1	100	200	28	0.35	1275	l			22648	44.9	0.286	ml
Cui et al. [141]	1	100	200	28	0.35	1275	l			20526	42.6	0.294	ml
Cui et al. [141]	1	100	200	28	0.35	1275	l			17316	38.5	0.304	ml
Cui et al. [141]	1	100	200	28	0.35	1622	l			28657	59.1	0.289	ml
Cui et al. [141]	1	100	200	28	0.35	1622	l			26911	57.2	0.271	ml
Cui et al. [141]	1	100	200	28	0.35	1622	l			24711	54.7	0.278	ml
Cui et al. [141]	1	100	200	28	0.35	1770	l			24481	48.1	0.294	ml
Cui et al. [141]	1	100	200	28	0.35	1770	l			23588	48.1	0.304	ml
Cui et al. [141]	1	100	200	28	0.35	1770	l			20358	45.0	0.318	ml
Kaar et al. [60]	3	152	305	28			l			19374	29.2	0.226	fl
Kaar et al. [60]	3	152	305	28			l			21581	44.4	0.311	fl
Kaar et al. [60]	3	152	305	28			l			22960	56.6	0.280	fl
Kaar et al. [60]	3	152	305	28			l			24270	58.3		fl
Kaar et al. [60]	3	152	305	28			l			29441	78.1	0.348	fl
Kaar et al. [60]	3	152	305	28			l			29027	86.1		fl
Kaar et al. [60]	3	152	305	28			l			27096	82.4		fl
Kaar et al. [60]	3	152	305	28			l			17306	25.0	0.226	fl
Kaar et al. [60]	3	152	305	28			l			15651	24.5		fl
Kaar et al. [60]	3	152	305	28			l			19443	41.4	0.270	fl
Kaar et al. [60]	3	152	305	28			l			22684	56.6		fl
Kaar et al. [60]	3	152	305	28			l			21856	56.2	0.273	fl
Kaar et al. [60]	3	152	305	28			l			24270	66.0		fl
Kaar et al. [60]	3	152	305	28			l			28751	66.7		fl
Kaar et al. [60]	3	152	305	28			l			29165	68.9	0.281	fl
Kayali et al. [64]	4	150	300	28	0.31	1939[d]	l	9.1		24000	65.0	0.34[a]	
Richart and Jensen [93]	3	152.4	304.8	28		1856	es			26175	33.8	0.232	
Richart and Jensen [93]	3	152.4	304.8	28		1856	es			23672	27.7	0.263	
Richart and Jensen [93]	3	152.4	304.8	28		1856	es			20606	21.0	0.209	
Richart and Jensen [93]	3	152.4	304.8	28		1856	es			17159	14.5	0.189	
Richart and Jensen [93]	3	152.4	304.8	28		1856	es			14630	10.6	0.169	
Richart and Jensen [93]	3	152.4	304.8	28		1480	es			25065	31.0	0.309	
Richart and Jensen [93]	3	152.4	304.8	28		1480	es			23099	26.3	0.289	
Richart and Jensen [93]	3	152.4	304.8	28		1480	es			20894	21.6	0.268	
Richart and Jensen [93]	3	152.4	304.8	28		1480	es			18068	16.1	0.249	
Richart and Jensen [93]	3	152.4	304.8	28		1480	es			15464	11.8	0.196	
Shah et al. [107]	4	75	150	32	0.63	1882	et			13353	29.0	0.30	fl
Shah et al. [107]	4	75	150	32	0.50	1893	et			16100	42.0	0.34	fl
Shah et al. [107]	4	75	150	32	0.45	1924	et		7.6[f]	19593	43.0	0.32	fl
Shah et al. [107]	4	75	150	32	0.63	1954	es			13637	30.0	0.29	fl
Shah et al. [107]	4	75	150	32	0.50	1996	es			17605	39.0	0.29	fl
Shah et al. [107]	4	75	150	32	0.45	2046	es		7.6[f]	15888	42.0	0.35[a]	fl
Shannag [142]	6	100	200	28	0.63	2050	l			19788	29.3	0.25	ml
Shannag [142]	6	100	200	28	0.63	2040	l	5.0		19343	28.8	0.28	ml
Shannag [142]	6	100	200	28	0.63	2025	l	10.0		20413	38.0	0.27	ml
Shannag [142]	6	100	200	28	0.63	2032	l	15.0		22477	43.2	0.27	ml
Shannag [142]	6	100	200	28	0.63	2066	l		5.0[f]	20795	27.7	0.25	ml
Shannag [142]	6	100	200	28	0.63	2050	l		10.0[f]	19751	22.5	0.26	ml
Shannag [142]	6	100	200	28	0.63	2053	l	5.0	5.0[f]	18696	32.2	0.28	ml
Shannag [142]	6	100	200	28	0.63	2060	l	5.0	10.0[f]	17457	32.4	0.30	ml
Shannag [142]	6	100	200	28	0.63	2039	l	10.0	5.0[f]	20213	39.0	0.27	ml
Shannag [142]	6	100	200	28	0.63	2032	l	10.0	10.0[f]	18694	33.7	0.32	ml
Shannag [142]	6	100	200	28	0.63	2030	l	15.0	5.0[f]	18587	36.7	0.27	ml
Slate et al. [112]		102	203	28		1300	ns			10570	19.0	0.240	
Slate et al. [112]		102	203	28		1300	ns			14950	36.5	0.330	
Slate et al. [112]		102	203	28		1300	ns			19060	56.7	0.379	
Smeplass [143]	1	150	300	28		1750	ec				75.0	0.345	
Smeplass [143]	1	150	300	28		1750	ec				75.5	0.369	
Smeplass [143]	1	150	300	28		1750	ec				76.0	0.323	
Smeplass [143]	1	150	300	28		1750	ec				78.0	0.327	
Smeplass [143]	1	150	300	28		1750	ec				80.0	0.330	
Smeplass [143]	1	150	300	28		1750	ec				81.0	0.331	

Source	*n*	*B (mm)*	*H (mm)*	*Age (d)*	*w/c*	$\rho_{c,f}$ *(kg/m³)*	*Aggregate properties*[p]	*sf/c (%)*	*ma/b (%)*	E_c *(MPa)*	f'_{co} *(MPa)*	ε_{co} *(%)*	*M**
Smeplass [143]	1	150	300	28		1750	ec				81.5	0.350	
Tasdemir [119]	1	152	305	28	0.60	1211	pm,ls				9.0	0.141[a]	
Tasdemir [119]	1	152	305	28	0.60	1211	pm,ls				10.0	0.145[a]	
Tasdemir [119]	1	152	305	28	0.60	1211	pm,ls				9.0	0.150	
Tasdemir [119]	1	152	305	28	0.60	1211	pm,ls				8.0	0.171	
Tasdemir [119]	1	152	305	28	0.60	1243	pm,ls				10.0	0.174	
Tasdemir [119]	1	152	305	28	0.60	1243	pm,ls				9.0	0.180	
Tasdemir [119]	1	152	305	28	0.50	1259	pm,ls				9.5	0.180	
Tasdemir [119]	1	152	305	28	0.50	1275	pm,ls				10.0	0.185	
Tasdemir [119]	1	152	305	28	0.40	1291	pm,ls				10.5	0.185	
Tasdemir [119]	1	152	305	28	0.40	1291	pm,ls				10.5	0.195	
Tasdemir [119]	1	152	305	28	0.40	1308	pm,ls				11.0	0.213	
Tasdemir [119]	1	152	305	28	0.50	1258	pm,ls				11.5	0.225	
Tasdemir [119]	1	152	305	28	0.50	1258	pm,ls				12.5	0.230	
Tasdemir [119]	1	152	305	28	0.50	1258	pm,ls				12.0	0.232	
Tasdemir [119]	1	152	305	28	0.40	1340	pm,ls				12.0	0.180	
Tasdemir [119]	1	152	305	28	0.40	1289	pm,ls				11.5	0.151	
Tasdemir [119]	1	152	305	28	0.40	1289	pm,ls				11.5	0.159	
Tasdemir [119]	1	152	305	28	0.40	1289	pm,ls				12.0	0.154	
Tasdemir [119]	1	152	305	28	0.40	1289	pm,ls				12.0	0.163	
Tasdemir [119]	1	152	305	28	0.40	1436	pm,ls				13.0	0.159	
Tasdemir [119]	1	152	305	28	0.40	1436	pm,ls				13.0	0.154	
Tasdemir [119]	1	152	305	28	0.40	1289	pm,ls				12.0	0.170	
Tasdemir [119]	1	152	305	28	0.60	1405	pm,ls				14.0	0.175	
Tasdemir [119]	1	152	305	28	0.40	1437	pm,ls				15.0	0.176	
Tasdemir [119]	1	152	305	28	0.40	1453	pm,ls				15.5	0.178	
Tasdemir [119]	1	152	305	28	0.60	1405	pm,ls				14.0	0.179	
Tasdemir [119]	1	152	305	28	0.60	1405	pm,ls				14.0	0.180	
Tasdemir [119]	1	152	305	28	0.60	1405	pm,ls				14.0	0.181	
Tasdemir [119]	1	152	305	28	0.40	1453	pm,ls				15.5	0.180	
Tasdemir [119]	1	152	305	28	0.40	1450	pm,ls				15.4	0.181	
Tasdemir [119]	1	152	305	28	0.60	1405	pm,ls				14.0	0.144	
Tasdemir [119]	1	152	305	28	0.40	1437	pm,ls				15.0	0.163	
Tasdemir [119]	1	152	305	28	0.50	1469	pm,ls				16.0	0.155	
Tasdemir [119]	1	152	305	28	0.60	1631	pm,ls				17.0	0.168	
Tasdemir [119]	1	152	305	28	0.60	1631	pm,ls				18.0	0.170	
Tasdemir [119]	1	152	305	28	0.60	1631	pm,ls				21.0	0.166	
Tasdemir [119]	1	152	305	28	0.50	1638	pm,ls				23.0	0.180	
Tasdemir [119]	1	152	305	28	0.50	1638	pm,ls				28.0	0.209	
Tasdemir [119]	1	152	305	28	0.50	1469	pm,ls				16.0	0.147	
Tasdemir [119]	1	152	305	28	0.60	1631	pm,ls				17.0	0.147	
Tasdemir [119]	1	152	305	28	0.60	1631	pm,ls				18.0	0.150	
Tasdemir [119]	1	152	305	28	0.60	1631	pm,ls				18.5	0.150	
Tasdemir [119]	1	152	305	28	0.60	1631	pm,ls				18.0	0.130	
Tasdemir [119]	1	152	305	28	0.40	1666	pm,ls				20.0	0.122[a]	
Tasdemir [119]	1	152	305	28	0.40	1666	pm,ls				20.5	0.130	
Tasdemir [119]	1	152	305	28	0.40	1666	pm,ls				21.0	0.126[a]	
Tasdemir [119]	1	152	305	28	0.40	1666	pm,ls				23.0	0.130[a]	
Tasdemir [119]	1	152	305	28	0.40	1666	pm,ls				24.0	0.131[a]	
Tasdemir [119]	1	152	305	28	0.40	1666	pm,ls				25.0	0.142	
Tasdemir [119]	1	152	305	28	0.40	1666	pm,ls				25.5	0.145	
Tasdemir [119]	1	152	305	28	0.40	1666	pm,ls				26.0	0.146	
Tasdemir [119]	1	152	305	28	0.40	1666	pm,ls				24.0	0.128[a]	
Tasdemir [119]	1	152	305	28	0.40	1666	pm,ls				26.0	0.158	
Tasdemir [119]	1	152	305	28	0.40	1666	pm,ls				21.0	0.140	
Tasdemir [119]	1	152	305	28	0.40	1666	pm,ls				21.0	0.140	
Tasdemir [119]	1	152	305	28	0.40	1666	pm,ls				21.0	0.140	
Tasdemir [119]	1	152	305	28	0.40	1666	pm,ls				22.0	0.138	
Tasdemir [119]	1	152	305	28	0.40	1666	pm,ls				22.0	0.140	
Tasdemir [119]	1	152	305	28	0.40	1666	pm,ls				22.0	0.140	
Tasdemir [119]	1	152	305	28	0.40	1666	pm,ls				23.0	0.140	
Tasdemir [119]	1	152	305	28	0.40	1666	pm,ls				23.5	0.141	
Tasdemir [119]	1	152	305	28	0.40	1666	pm,ls				24.0	0.142	
Tasdemir [119]	1	152	305	28	0.40	1666	pm,ls				24.0	0.143	
Tasdemir [119]	1	152	305	28	0.40	1666	pm,ls				24.0	0.145	
Tasdemir [119]	1	152	305	28	0.60	1631	pm,ls				21.0	0.150	
Tasdemir [119]	1	152	305	28	0.60	1631	pm,ls				21.0	0.152	
Tasdemir [119]	1	152	305	28	0.50	1638	pm,ls				20.0	0.155	
Tasdemir [119]	1	152	305	28	0.60	1993	pm,ls				29.0	0.144	
Tasdemir [119]	1	152	305	28	0.60	1993	pm,ls				29.5	0.144	
Tasdemir [119]	1	152	305	28	0.60	1993	pm,ls				29.0	0.152	
Tasdemir [119]	1	152	305	28	0.60	1993	pm,ls				29.0	0.158	
Tasdemir [119]	1	152	305	28	0.50	1960	pm,ls				30.0	0.155	
Tasdemir [119]	1	152	305	28	0.50	1960	pm,ls				30.0	0.156	
Tasdemir [119]	1	152	305	28	0.50	1971	pm,ls				31.5	0.158	
Tasdemir [119]	1	152	305	28	0.50	1987	pm,ls				32.0	0.160	
Tasdemir [119]	1	152	305	28	0.60	2020	pm,ls				33.0	0.175	
Tasdemir [119]	1	152	305	28	0.50	2052	pm,ls				34.0	0.175	
Tasdemir [119]	1	152	305	28	0.40	2059	pm,ls				36.0	0.155	
Tasdemir [119]	1	152	305	28	0.60	2149	pm,ls				37.0	0.160	
Tasdemir [119]	1	152	305	28	0.60	2146	pm,ls				36.5	0.179	

Source	*n*	*B (mm)*	*H (mm)*	*Age (d)*	*w/c*	$\rho_{c,f}$ *(kg/m³)*	*Aggregate properties*[p]	*sf/c (%)*	*ma/b (%)*	E_c *(MPa)*	f'_{co} *(MPa)*	ε_{co} *(%)*	*M**
Wang et al. [127]	1	76.2	152.4	56	0.64	1869	es			11780	23.4	0.260	fl
Wang et al. [127]	1	76.2	152.4	56	0.56	1884	es			13040	30.3	0.310	fl
Wang et al. [127]	1	76.2	152.4	56	0.45	1901	es		13.6[f]	16490	39.0	0.320	fl
Wang et al. [127]	1	76.2	152.4	56	0.38	2029	es		11.3[f]	18640	55.5	0.37[a]	fl
Wang et al. [127]		76.2	152.4	56	0.56	1884	es			14488	29.8	0.290	fl
Wang et al. [127]		76.2	152.4	56	0.38	2029	es		11.3[f]	15984	50.5	0.405[a]	fl
Yildirim [144]	1	152	305	28		1700	pm,ls,gv				9.0	0.179	
Yildirim [144]	1	152	305	28		1700	pm,ls,gv				12.0	0.121[a]	
Yildirim [144]	1	152	305	28		1700	pm,ls,gv				14.0	0.171	
Yildirim [144]	1	152	305	28		1700	pm,ls,gv				16.0	0.190	
Yildirim [144]	1	152	305	28		1700	pm,ls,gv				22.0	0.139[a]	
Yildirim [144]	1	152	305	28		1700	pm,ls,gv				26.0	0.147[a]	
Zhang and Gjorv [145]	1	100	280	28	0.28[w]	1865	ec	9.1		25900	90.1	0.416	ml
Zhang and Gjorv [145]	1	100	280	28	0.34[w]	1835	ec	9.1		24700	89.3	0.442	ml
Zhang and Gjorv [145]	1	100	280	28	0.43[w]	1750	ec	9.1		24300	88.3	0.463	ml
Zhang and Gjorv [145]	1	100	280	28	0.36	1815	ec			22300	64.3	0.373	ml
Zhang and Gjorv [145]	1	100	280	28	0.36[w]	1800	ec	9.1		24300[m]	89.8	0.452	ml
Zhang and Gjorv [145]	1	100	280	28	0.37[w]	1710	ec	9.1		21600	69.1	0.355	ml
Zhang and Gjorv [145]	1	100	280	28	0.40	1595	ec	9.1		17800	49.7	0.331	ml
Zhang and Gjorv [145]	1	100	280	28	0.36	1750	ec	9.1		22200	63.8	0.372	ml
Zhang and Gjorv [145]	1	100	280	28	0.44[w]	1880	fa	9.1		24800	76.8	0.404	ml

w Water-cementitious binder ratio that differ significantly from the reference values of the corresponding concrete strength
d Fresh concrete density that is significantly higher than the reference values
m Concrete elastic modulus that differ significantly from the reference values of the corresponding concrete strength
a Concrete strain at peak stress that differ significantly from the reference values of the corresponding concrete strength
f Fly-ash used as mineral admixture in concrete mix
p Designation:- type-size
Type:- l: light weight aggregate, ec: expanded clay, es: expanded shale, et: expanded slate, fa: sintered fly-ash, ns: Normanskill shale
Size:- maximum aggregate in mm
M Axial strain measurement method:- fl: linear variable displacement transducers mounted on loading platens to measure deformation along the full height of specimen
ml: linear variable displacement transducers mounted on specimen to measure deformation within a gauge length along the height of specimen

Table A3. Test database of normal weight concrete prisms

Source	*n*	*B (mm)*	*H (mm)*	*Age (d)*	*w/c*	$\rho_{c,f}$ *(kg/m³)*	*Aggregate properties*[p]	*sf/c (%)*	*ma/b (%)*	E_c *(MPa)*	f'_{co} *(MPa)*	ε_{co} *(%)*	*M**
Benzaid et al [20]	1	100	300		0.46	2156	gv-cr-15.2				54.8	0.25	
Campione et al. [27]	3	152	200				n				20.1	0.207	
Carrazedo [146]		150	450				n				36.5	0.313[a]	
Carrazedo [146]		150	450				n				33.5	0.277	
Chaallal et al. [147]		133	305		0.68	2497	n-rd-19				21.4	0.20	
Chaallal et al. [147]		133	305		0.41	2526	n-rd-19				54.7	0.24	
Chikh et al. [31]	2	140	280		0.38	2394	gv-cr-15.2				59.5	0.356[a]	ml
Demers and Neale [36]		152	505				n				32.2	0.24	
Demers and Neale [36]		152	505				n				43.7	0.26	
Dilger et al. [148]	1	152	610	40	0.80	2319	n-12.7				30.2	0.166	fl
Dilger et al. [148]	1	152	610	40	0.80	2319	n-12.7				27.2	0.130[a]	fl
Dilger et al. [148]	1	152	610	40	0.80	2319	n-12.7				32.5	0.165	fl
Dilger et al. [148]	1	152	610	40	0.80	2319	n-12.7				34.6	0.165	fl
Dilger et al. [148]	1	152	610	40	0.80	2319	n-12.7				16.3	0.204	fl
Dilger et al. [148]	1	152	610	40	0.80	2319	n-12.7				28.5	0.191	fl
Dilger et al. [148]	1	152	610	40	0.80	2319	n-12.7				25.0	0.170	fl
Dilger et al. [148]	1	152	610	40	0.80	2319	n-12.7				30.7	0.167	fl
Dilger et al. [148]	1	152	610	40	0.80	2319	n-12.7				15.1	0.218	fl
Dilger et al. [148]	1	152	610	40	0.80	2319	n-12.7				14.9	0.216	fl
Dilger et al. [148]	1	152	610	40	0.80	2319	n-12.7				25.2	0.190	fl
Dilger et al. [148]	1	152	610	40	0.80	2319	n-12.7				26.5	0.180	fl
Dilger et al. [148]	1	152	610	40	0.80	2319	n-12.7				23.6	0.160	fl
Dilger et al. [148]	1	152	610	40	0.80	2319	n-12.7				13.8	0.224[a]	fl
Erdil et al. [39]	1	150	300				n				10.0	0.50[a]	ml
Haneef et al. [149]	1	100	100	7	0.44		gn-20				35.8	0.26	fl
Haneef et al. [149]	1	100	100	14	0.44		gn-20				44.5	0.27	fl
Haneef et al. [149]	1	100	100	28	0.44		gn-20				54.0	0.29	fl
Haneef et al. [149]	1	100	100	56	0.44		gn-20				59.1	0.30	fl
Haneef et al. [149]	1	100	100	7	0.44		gn-20		30.0[f]		26.7	0.280	fl
Haneef et al. [149]	1	100	100	14	0.44		gn-20		30.0[f]		38.5	0.290	fl
Haneef et al. [149]	1	100	100	28	0.44		gn-20		30.0[f]		48.3	0.300	fl
Haneef et al. [149]	1	100	100	56	0.44		gn-20		30.0[f]		59.5	0.320	fl
Harries and Carey [45]	≥ 5	152	305				n				32.4	0.27	ml
Harries and Carey [45]	≥ 5	152	305				n				31.2	0.16	ml
Ilki and Kumbasar [150]		250	500				n				32.8	0.295[a]	
Ilki et al. [51]	1	250	500	28-180	1.27	2357	gv				6.8	0.28[a]	
Karam and Tabbara [62]	3	200	400				n				11.6	0.76[a]	fl
Mansur et al. [79]	1	100	200	28	0.40	2336	gn-19	9.9		41600	64.1	0.191	ml
Mansur et al. [79]	1	100	200	28	0.35	2342	gn-19	9.9		41400	71.4	0.212	ml
Mansur et al. [79]	1	100	200	28	0.30	2361	gn-19	10.0		44200	85.3	0.231	ml
Mansur et al. [79]	1	100	200	28	0.25	2381	gn-19	10.0		45700	94.2	0.234	ml
Mansur et al. [79]	1	100	200	28	0.20	2412	gn-19	10.0		47900	113.5	0.258	ml
Mansur et al. [79]	1	100	200	28	0.40	2336	gn-19	9.9		40400	66.0	0.210	ml
Mansur et al. [79]	1	100	200	28	0.35	2342	gn-19	9.9		39600	72.9	0.226	ml
Mansur et al. [79]	1	100	200	28	0.30	2361	gn-19	10.0		42800	87.0	0.241	ml
Mansur et al. [79]	1	100	200	28	0.25	2381	gn-19	10.0		45900	99.3	0.266	ml
Mansur et al. [79]	1	100	200	28	0.20	2412	gn-19	10.0		46900	115.6	0.265	ml
Markeset and Hillerborg [151]	1	100	200	>28			n			34536	99.6	0.280	fl
Markeset and Hillerborg [151]	1	100	300	>28			n			34536	100.8	0.290	fl
Markeset and Hillerborg [151]	1	100	400	>28			n			34536	101.0	0.288	fl
Masia et al. [152]		100	300				n			31519[m]	25.5	0.26	ml
Masia et al. [152]		125	375				n			29528[m]	23.7	0.22	ml
Masia et al. [152]		125	375				n			32794[m]	22.9	0.27[a]	ml
Masia et al. [152]		150	450				n			30159[m]	24.8	0.25	ml
Masia et al. [152]		150	450				n			31700[m]	23.6	0.21	ml
Modarelli et al. [153]		150	300	60			n-9				25.0	0.63[a]	ml
Modarelli et al. [153]		150	300	60			n-9				21.4	0.56[a]	ml
Ozbakkaloglu and Oehlers [154]		200	600	50			n-10				26.6	0.21	fl
Ozbakkaloglu and Oehlers [154]		200	600	51			n-10				26.9	0.22	fl
Ozbakkaloglu and Oehlers [154]		200	600	51			n-10				26.6	0.22	fl
Rousakis et al. [155]		200	320				n				33.0	0.171	ml
Rousakis et al. [155]		200	320				n				34.2	0.186	ml
Rousakis et al. [155]		200	320				n				38.0	0.224	ml
Rousakis et al. [155]		200	320				n				39.9	0.147[a]	ml
Rousakis et al. [156]		200	320				n				25.5	0.212	ml
Shehata et al. [109]	9	150	300				n				29.5	0.16	as
Shehata et al. [110]	9	225	450				n				33.2	0.18	as
Van Geel [157]	1	100	75	>28			n			29530	72.7	0.643[a]	fl
Van Geel [157]	1	100	150	>28			n			30256	52.1	0.326	fl
Van Geel [157]	1	100	300	>28			n			30656	42.0	0.198	fl
Van Geel [157]	1	100	75	>28			n			33109	90.3	0.408[a]	fl
Van Geel [157]	1	100	150	>28			n			33076	71.0	0.315	fl
Van Geel [157]	1	100	300	>28			n			33133	59.8	0.207	fl
Van Vliet and Van Mier [158]	1	100	25	>28			n			24948[m]	93.2	0.897[a]	fl
Van Vliet and Van Mier [158]	1	100	50	>28			n			27665	64.6	0.387	fl
Van Vliet and Van Mier [158]	1	100	100	>28			n			27994	47.8	0.268	fl
Van Vliet and Van Mier [158]	1	100	200	>28			n			27833	40.1	0.180	fl
Van Vliet and Van Mier [158]	1	100	25	>28			n			32864[m]	161.9	0.799[a]	fl

Source	*n*	*B (mm)*	*H (mm)*	*Age (d)*	*w/c*	$\rho_{c,f}$ *(kg/m³)*	*Aggregate properties*[p]	*sf/c (%)*	*ma/b (%)*	E_c *(MPa)*	f'_{co} *(MPa)*	ε_{co} *(%)*	*M**
Van Vliet and Van Mier [158]	1	100	50	>28			n			32292	108.5	0.597[a]	fl
Van Vliet and Van Mier [158]	1	100	100	>28			n			31692	86.0	0.291	fl
Van Vliet and Van Mier [158]	1	100	200	>28			n			31304	71.0	0.240	fl
Vonk [159]		50	50		0.5	2350	n			45624[m]	48.6	0.195[a]	fl
Vonk [159]		50	100		0.5	2350	n			46830[m]	45.4	0.191[a]	fl
Vonk [159]		50	200		0.5	2350	n			45718[m]	41.9	0.159[a]	fl
Wang and Wu [160]		100	300				n				46.4	0.255	
Wang and Wu [160]		100	300				n				78.5	0.451[a]	
Wang and Wu [160]		100	300				n				101.2	0.456[a]	
Wang and Wu [126]		70	210				n				34.6	0.219	
Wang and Wu [126]		70	210				n				52.1	0.273	
Wang et al. [161]	1	100	300		0.50		ls				45.9	0.183	as
Wang et al. [161]	1	100	300		0.40		ls				63.1	0.191	as
Wang et al. [161]	1	100	300		0.30		ls				74.1	0.185[a]	as
Wang et al. [161]	1	100	300		0.25		ls				97.3	0.217	as
Wang et al. [161]	1	100	300		0.20		ls				96.7	0.299	as
Wang et al. [161]	1	100	300		0.18		ls				99.9	0.228	as
Wang et al. [161]	1	100	300		0.20		ls				99.9	0.279	as
Wang et al. [161]	1	100	300		0.20		ls				97.7	0.210	as
Wang et al. [161]	1	100	300		0.20		ls				117.5	0.259	as
Wang et al. [161]	1	100	300		0.18		ls				113.7	0.226	as
Wang et al. [161]	1	100	300		0.18		ls				102.9	0.220	as
Wang et al. [161]	1	100	300		0.18		ls				100.5	0.224	as
Wang et al. [161]	1	100	300		0.18		ls				116.3	0.242	as
Wang et al. [161]	1	100	300		0.18		ls				119.7	0.251	as
Wang et al. [161]	1	100	300		0.18		ls				114.1	0.241	as
Wang et al. [161]	1	100	300		0.18		ls				104.1	0.223	as
Wang et al. [161]	1	100	300		0.18		ls				111.3	0.230	as
Wang et al. [161]	1	100	300		0.18		ls				124.9	0.244	as
Wang et al. [161]	1	100	300		0.18		ls				117.6	0.236	as
Wang et al. [161]	1	100	300		0.18		ls				141.7	0.275	as
Wang et al. [161]	1	100	300		0.20		ls				137.3	0.259	as
Wang et al. [161]	1	100	100		0.50		ls				56.3	0.183	as
Wang et al. [161]	1	100	100		0.40		ls				76.6	0.191	as
Wang et al. [161]	1	100	100		0.30		ls				88.8	0.185	as
Wang et al. [161]	1	100	100		0.25		ls				107.5	0.217	as
Wang et al. [161]	1	100	100		0.20		ls				118.3	0.299	as
Wang et al. [161]	1	100	100		0.18		ls				131.9	0.228	as
Wang et al. [161]	1	100	100		0.20		ls				129.0	0.279	as
Wang et al. [161]	1	100	100		0.20		ls				118.6	0.210	as
Wang et al. [161]	1	100	100		0.20		ls				123.7	0.259	as
Wang et al. [161]	1	100	100		0.18		ls				124.4	0.226	as
Wang et al. [161]	1	100	100		0.18		ls				131.3	0.220	as
Wang et al. [161]	1	100	100		0.18		ls				126.2	0.224	as
Wang et al. [161]	1	100	100		0.18		ls				127.5	0.242	as
Wang et al. [161]	1	100	100		0.18		ls				125.4	0.251	as
Wang et al. [161]	1	100	100		0.18		ls				128.7	0.241	as
Wang et al. [161]	1	100	100		0.18		ls				126.9	0.223	as
Wang et al. [161]	1	100	100		0.18		ls				127.3	0.230	as
Wang et al. [161]	1	100	100		0.18		ls				135.0	0.244	as
Wang et al. [161]	1	100	100		0.18		ls				138.1	0.236	as
Wang et al. [161]	1	100	100		0.18		ls				164.9	0.275	as
Wang et al. [161]	1	100	100		0.20		ls				156.7	0.259	as
Youssef et al. [140]	3	381	762				n-9.5				34.2	0.24	ml

m Concrete elastic modulus that differ significantly from the reference values of the corresponding concrete strength
a Concrete strain at peak stress that differ significantly from the reference values of the corresponding concrete strength
f Fly-ash used as mineral admixture in concrete mix
p Designation:- type-irregularity-size
Type:- n: normal weight aggregate, gn: granite, gv: gravel, ls: limestone
Irregularity:- cr: crushed, rd: round
Size:- maximum aggregate in mm
M Axial strain measurement method:- as: axial strain gauges attached on the surface of specimen
fl: linear variable displacement transducers mounted on loading platens to measure deformation along the full height of specimen
ml: linear variable displacement transducers mounted on specimen to measure deformation within a gauge length along the height of specimen

Table A4. Test database of normal weight concrete cylinders (without ε_{co} values)

Source	*n*	*B (mm)*	*H (mm)*	*Age (d)*	*w/c*	$\rho_{c,f}$ *(kg/m³)*	*Aggregate properties*[p]	*sf/c (%)*	*ma/b (%)*	E_c *(MPa)*	f'_{co} *(MPa)*
Aitcin and Mehta [162]		101.6	203.2	1	0.27	2495	db-10	8.4			41.1
Aitcin and Mehta [162]		101.6	203.2	28	0.27	2495	db-10	8.4		36600	100.7
Aitcin and Mehta [162]		101.6	203.2	56	0.27	2495	db-10	8.4		37900	104.8
Aitcin and Mehta [162]		101.6	203.2	1	0.27	2495	ls-10	8.4			42.5
Aitcin and Mehta [162]		101.6	203.2	28	0.27	2495	ls-10	8.4		37900	97.3
Aitcin and Mehta [162]		101.6	203.2	56	0.27	2495	ls-10	8.4		40700	101.3
Aitcin and Mehta [162]		101.6	203.2	1	0.27	2495	gv-10	8.4			40.6
Aitcin and Mehta [162]		101.6	203.2	28	0.27	2495	gv-10	8.4		33800	92.1
Aitcin and Mehta [162]		101.6	203.2	56	0.27	2495	gv-10	8.4		35900	95.9
Aitcin and Mehta [162]		101.6	203.2	1	0.27	2495	gn-14	8.4			37.2
Aitcin and Mehta [162]		101.6	203.2	28	0.27	2495	gn-14	8.4		31700	84.8
Aitcin and Mehta [162]		101.6	203.2	56	0.27	2495	gn-14	8.4		33800	88.6
Baalbaki et al. [163]	4	100	200	1	0.28	2484	ls-10				59.4
Baalbaki et al. [163]	4	100	200	1	0.28	2484	qz-10				59.9
Baalbaki et al. [163]	4	100	200	1	0.28	2484	st-10				65.4
Baalbaki et al. [163]	4	100	200	7	0.28	2484	ls-10				70.5
Baalbaki et al. [163]	4	100	200	7	0.28	2484	qz-10				78.2
Baalbaki et al. [163]	4	100	200	7	0.28	2484	st-10				86.0
Baalbaki et al. [163]	4	100	200	28	0.28	2484	ls-10			42000	90.8
Baalbaki et al. [163]	4	100	200	28	0.28	2484	qz-10			40000	98.0
Baalbaki et al. [163]	4	100	200	28	0.28	2484	st-10			31000[m]	102.0
Baalbaki et al. [163]	4	100	200	28	0.28	2484	ls-10			45000	99.3
Baalbaki et al. [163]	4	100	200	28	0.28	2484	qz-10			44000	106.0
Baalbaki et al. [163]	4	100	200	28	0.28	2484	st-10			31000[m]	116.0
Baalbaki et al. [164]	2	101.6	203.2	28	0.28		ls-10			40000	95.3
Baalbaki et al. [164]	2	101.6	203.2	28	0.28		ls-10			40000	98.0
Baalbaki et al. [164]	2	101.6	203.2	28	0.28		st-10			24000[m]	101.0
Baalbaki et al. [164]	2	101.6	203.2	28	0.28		st-10			31000[m]	102.0
Baalbaki et al. [164]	2	101.6	203.2	28	0.28		gn-10			40000	103.0
Baalbaki et al. [164]	2	101.6	203.2	28	0.28		qz-10			42000	90.8
Baalbaki et al. [164]	2	101.6	203.2	28	0.28		qz-10			41000	89.2
Baalbaki et al. [164]	2	101.6	203.2	91	0.28		ls-10			42000	105.0
Baalbaki et al. [164]	2	101.6	203.2	91	0.28		ls-10			44000	106.0
Baalbaki et al. [164]	2	101.6	203.2	91	0.28		st-10			27000[m]	107.0
Baalbaki et al. [164]	2	101.6	203.2	91	0.28		st-10			31000[m]	116.0
Baalbaki et al. [164]	2	101.6	203.2	91	0.28		gn-10			41000	111.0
Baalbaki et al. [164]	2	101.6	203.2	91	0.28		qz-10			45000	99.3
Baalbaki et al. [164]	2	101.6	203.2	91	0.28		qz-10			42000	99.7
Bower and Viest [165]	4	152.4	304.8	29	1.11		gv-19.1			22891	22.8
Bower and Viest [165]	4	152.4	304.8	30	1.11		gv-19.1			29096	30.0
Bower and Viest [165]	4	152.4	304.8	30	1.11		gv-19.1			23925	24.8
Bower and Viest [165]	4	152.4	304.8	28	1.11		gv-19.1			23304	24.4
Bower and Viest [165]	4	152.4	304.8	30	1.11		gv-19.1			26752	27.7
Bower and Viest [165]	4	152.4	304.8	28	1.11		gv-19.1			24132	24.5
Bower and Viest [165]	4	152.4	304.8	30	1.11		gv-19.1			24270	22.8
Bower and Viest [165]	4	152.4	304.8	28	1.11		gv-19.1			20960	21.9
Bower and Viest [165]	4	152.4	304.8	30	1.11		gv-19.1			24132	23.9
Bower and Viest [165]	4	152.4	304.8	30	1.11		gv-19.1			20822	21.5
Bower and Viest [165]	4	152.4	304.8	30	1.11		gv-19.1			22270	24.1
Bower and Viest [165]	4	152.4	304.8	30	1.11		gv-19.1			22546	21.5
Bower and Viest [165]	4	152.4	304.8	25	1.11		gv-19.1			22960	21.5
Bower and Viest [165]	4	152.4	304.8	30	1.11		gv-19.1			22408	24.3
Bower and Viest [165]	4	152.4	304.8	27	1.11		gv-19.1			20684	21.2
Bower and Viest [165]	4	152.4	304.8	30	1.11		gv-19.1			24270	22.6
Bower and Viest [165]	4	152.4	304.8	30	1.11		gv-19.1			21098	22.2
Bower and Viest [165]	4	152.4	304.8	30	1.11		gv-19.1			20546	21.2
Bower and Viest [165]	4	152.4	304.8	33	1.11		gv-19.1			22063	22.8
Bower and Viest [165]	4	152.4	304.8	32	1.11		gv-19.1			23097	24.1
Bower and Viest [165]	4	152.4	304.8	31	1.11		gv-19.1			19926	22.8
Bower and Viest [165]	4	152.4	304.8	28	1.11		gv-19.1			26821	25.5
Bower and Viest [165]	4	152.4	304.8	29	1.11		gv-19.1			22201	21.6
Bower and Viest [165]	4	152.4	304.8	30	1.11		gv-19.1			22615	21.7
Bower and Viest [165]	4	152.4	304.8	30	1.11		gv-19.1			20822	20.0
Bower and Viest [165]	4	152.4	304.8	25	1.11		gv-19.1			23994	22.9
Bower and Viest [165]	4	152.4	304.8	30	1.11		gv-19.1			19719	18.4
Bower and Viest [165]	4	152.4	304.8	30	1.11		gv-19.1			22753	21.2
Bower and Viest [165]	4	152.4	304.8	30	1.11		gv-19.1			22960	23.6
Bower and Viest [165]	4	152.4	304.8	30	1.11		gv-19.1			23166	24.1
Bower and Viest [165]	4	152.4	304.8	30	1.11		gv-19.1			22960	23.8
Bower and Viest [165]	4	152.4	304.8	28	1.11		gv-19.1			21374	24.7
Bower and Viest [165]	4	152.4	304.8	28	1.11		gv-19.1			22201	20.9
Bower and Viest [165]	4	152.4	304.8	28	1.11		gv-19.1			19719	19.7
Cetin and Carrasquillo [166]		102	204	1	0.28		gv-cr-19			30250	25.5
Cetin and Carrasquillo [166]		102	204	1	0.28		gv-cr-19			29250	25.5
Cetin and Carrasquillo [166]		102	204	1	0.28		gv-cr-19			35875	33.0
Cetin and Carrasquillo [166]		102	204	7	0.28		gv-cr-19			41500	59.0
Cetin and Carrasquillo [166]		102	204	7	0.28		gv-cr-19			41750	60.0
Cetin and Carrasquillo [166]		102	204	7	0.28		gv-cr-19			45000	57.0
Cetin and Carrasquillo [166]		102	204	28	0.28		gv-cr-19			45500	68.0

Source	*n*	*B (mm)*	*H (mm)*	*Age (d)*	*w/c*	*$\rho_{c,f}$ (kg/m^3)*	*Aggregate properties*[p]	*sf/c (%)*	*ma/b (%)*	*E_c (MPa)*	*f'_{co} (MPa)*
Cetin and Carrasquillo [166]		102	204	28	0.28		gv-cr-19			43750	67.0
Cetin and Carrasquillo [166]		102	204	28	0.28		gv-cr-19			44875	61.5
Cetin and Carrasquillo [166]		102	204	56	0.28		gv-cr-19			47250	75.0
Cetin and Carrasquillo [166]		102	204	56	0.28		gv-cr-19			49000	76.0
Cetin and Carrasquillo [166]		102	204	56	0.28		gv-cr-19			50375	68.0
Cetin and Carrasquillo [166]		102	204	1	0.28		tr-19			33250	35.0
Cetin and Carrasquillo [166]		102	204	1	0.28		tr-19			30000	29.0
Cetin and Carrasquillo [166]		102	204	1	0.28		tr-19			26250	24.0
Cetin and Carrasquillo [166]		102	204	7	0.28		tr-19				71.5
Cetin and Carrasquillo [166]		102	204	7	0.28		tr-19			43250	68.0
Cetin and Carrasquillo [166]		102	204	7	0.28		tr-19			45000	67.0
Cetin and Carrasquillo [166]		102	204	28	0.28		tr-19			46250	78.5
Cetin and Carrasquillo [166]		102	204	28	0.28		tr-19			46000	77.0
Cetin and Carrasquillo [166]		102	204	28	0.28		tr-19			44875	76.5
Cetin and Carrasquillo [166]		102	204	56	0.28		tr-19			51250	89.5
Cetin and Carrasquillo [166]		102	204	56	0.28		tr-19			48750	84.5
Cetin and Carrasquillo [166]		102	204	56	0.28		tr-19			48500	78.0
Cetin and Carrasquillo [166]		102	204	1	0.28		dl-19				35.0
Cetin and Carrasquillo [166]		102	204	1	0.28		dl-19			30000	37.0
Cetin and Carrasquillo [166]		102	204	1	0.28		dl-19			26500	19.0
Cetin and Carrasquillo [166]		102	204	7	0.28		dl-19			43250	73.0
Cetin and Carrasquillo [166]		102	204	7	0.28		dl-19			48375	78.0
Cetin and Carrasquillo [166]		102	204	7	0.28		dl-19			46625	65.5
Cetin and Carrasquillo [166]		102	204	28	0.28		dl-19			48750	87.5
Cetin and Carrasquillo [166]		102	204	28	0.28		dl-19			49500	89.5
Cetin and Carrasquillo [166]		102	204	28	0.28		dl-19			50500	70.0
Cetin and Carrasquillo [166]		102	204	56	0.28		dl-19			49750	93.0
Cetin and Carrasquillo [166]		102	204	56	0.28		dl-19			49250	95.0
Cetin and Carrasquillo [166]		102	204	56	0.28		dl-19			52500	79.5
Cetin and Carrasquillo [166]		102	204	1	0.28		dl-13			34250	38.0
Cetin and Carrasquillo [166]		102	204	1	0.28		dl-13			30000	26.5
Cetin and Carrasquillo [166]		102	204	1	0.28		dl-13			22125	13.0
Cetin and Carrasquillo [166]		102	204	7	0.28		dl-13			45500	76.0
Cetin and Carrasquillo [166]		102	204	7	0.28		dl-13			47625	76.0
Cetin and Carrasquillo [166]		102	204	7	0.28		dl-13			46250	73.0
Cetin and Carrasquillo [166]		102	204	28	0.28		dl-13			47250	75.0
Cetin and Carrasquillo [166]		102	204	28	0.28		dl-13			51250	89.0
Cetin and Carrasquillo [166]		102	204	28	0.28		dl-13			51375	88.0
Cetin and Carrasquillo [166]		102	204	56	0.28		dl-13			49750	90.5
Cetin and Carrasquillo [166]		102	204	56	0.28		dl-13			50750	94.5
Cetin and Carrasquillo [166]		102	204	56	0.28		dl-13			52125	91.0
Cetin and Carrasquillo [166]		102	204	1	0.28		cl-19			24500	31.0
Cetin and Carrasquillo [166]		102	204	1	0.28		cl-19			20250	19.5
Cetin and Carrasquillo [166]		102	204	1	0.28		cl-19			22125	24.0
Cetin and Carrasquillo [166]		102	204	7	0.28		cl-19			35500	72.0
Cetin and Carrasquillo [166]		102	204	7	0.28		cl-19			35000	66.0
Cetin and Carrasquillo [166]		102	204	7	0.28		cl-19			34875	69.5
Cetin and Carrasquillo [166]		102	204	28	0.28		cl-19			39000	78.0
Cetin and Carrasquillo [166]		102	204	28	0.28		cl-19			36000	78.0
Cetin and Carrasquillo [166]		102	204	28	0.28		cl-19			35500	75.0
Cetin and Carrasquillo [166]		102	204	56	0.28		cl-19			38625	81.0
Cetin and Carrasquillo [166]		102	204	56	0.28		cl-19			39625	79.5
Cetin and Carrasquillo [166]		102	204	56	0.28		cl-19			43000	95.0
de Larrard and Belloc [167]	3	110	220	1	0.29	2443	ft-rd-2.5	9.1			56.9
de Larrard and Belloc [167]	3	110	220	1	0.30	2458	ft-rd-12.5	9.1			45.9
de Larrard and Belloc [167]	3	110	220	1	0.30	2471	ft-rd-20	9.1			47.5
de Larrard and Belloc [167]	3	110	220	1	0.28	2418	ls-cr-3.15	9.2			72.0
de Larrard and Belloc [167]	3	110	220	1	0.28	2482	ls-cr-12.5	9.1			72.4
de Larrard and Belloc [167]	3	110	220	1	0.28	2479	ls-cr-20	9.1			61.8
de Larrard and Belloc [167]	3	110	220	1	0.31	2370	ls-cr-2	9.1			56.3
de Larrard and Belloc [167]	3	110	220	1	0.33	2401	ls-cr-25	9.1			53.4
de Larrard and Belloc [167]	3	110	220	1	0.29	2486	bs-cr-5	9.1			61.4
de Larrard and Belloc [167]	3	110	220	1	0.30	2558	bs-cr-20	9.1			46.3
de Larrard and Belloc [167]	3	110	220	1	0.27	2353	qz-cr-2	9.1			71.8
de Larrard and Belloc [167]	3	110	220	1	0.28	2426	qz-cr-20	9.1			61.9
de Larrard and Belloc [167]	3	110	220	3	0.29	2443	ft-rd-2.5	9.1			76.4
de Larrard and Belloc [167]	3	110	220	3	0.30	2458	ft-rd-12.5	9.1			64.9
de Larrard and Belloc [167]	3	110	220	3	0.30	2471	ft-rd-20	9.1			62.7
de Larrard and Belloc [167]	3	110	220	3	0.28	2418	ls-cr-3.15	9.2			94.9
de Larrard and Belloc [167]	3	110	220	3	0.28	2482	ls-cr-12.5	9.1			90.7
de Larrard and Belloc [167]	3	110	220	3	0.28	2479	ls-cr-20	9.1			82.6
de Larrard and Belloc [167]	3	110	220	3	0.31	2370	ls-cr-2	9.1			79.2
de Larrard and Belloc [167]	3	110	220	3	0.33	2401	ls-cr-25	9.1			71.0
de Larrard and Belloc [167]	3	110	220	3	0.29	2486	bs-cr-5	9.1			76.9
de Larrard and Belloc [167]	3	110	220	3	0.30	2558	bs-cr-20	9.1			64.2
de Larrard and Belloc [167]	3	110	220	3	0.27	2353	qz-cr-2	9.1			87.0
de Larrard and Belloc [167]	3	110	220	3	0.28	2426	qz-cr-20	9.1			76.7
de Larrard and Belloc [167]	3	110	220	28	0.29	2443	ft-rd-2.5	9.1		45400	106.3
de Larrard and Belloc [167]	3	110	220	28	0.30	2458	ft-rd-12.5	9.1		55400	90.5
de Larrard and Belloc [167]	3	110	220	28	0.30	2471	ft-rd-20	9.1		55500	86.8

Source	*n*	*B (mm)*	*H (mm)*	*Age (d)*	*w/c*	$\rho_{c,f}$ *(kg/m^3)*	*Aggregate properties*[p]	*sf/c (%)*	*ma/b (%)*	E_c *(MPa)*	f'_{co} *(MPa)*
de Larrard and Belloc [167]	3	110	220	28	0.28	2418	ls-cr-3.15	9.2		44700	112.1
de Larrard and Belloc [167]	3	110	220	28	0.28	2482	ls-cr-12.5	9.1		52600	109.5
de Larrard and Belloc [167]	3	110	220	28	0.28	2479	ls-cr-20	9.1		53800	107.7
de Larrard and Belloc [167]	3	110	220	28	0.31	2370	ls-cr-2	9.1		37600	101.9
de Larrard and Belloc [167]	3	110	220	28	0.33	2401	ls-cr-25	9.1		42000	89.0
de Larrard and Belloc [167]	3	110	220	28	0.29	2486	bs-cr-5	9.1		45500	104.9
de Larrard and Belloc [167]	3	110	220	28	0.30	2558	bs-cr-20	9.1		52100	90.9
de Larrard and Belloc [167]	3	110	220	28	0.27	2353	qz-cr-2	9.1		38000	108.4
de Larrard and Belloc [167]	3	110	220	28	0.28	2426	qz-cr-20	9.1		42600	101.8
Gabet et al. [168]	1	70	140	28	0.64	2277	n-8				28.6
Gesoglu [169]	4	150	300	28	0.22[w]	2523	ls-cr-32	13.0		47100	77.2
Gesoglu [169]	4	150	300	28	0.22[w]	2523	ls-cr-32	13.0		48000	71.5
Gesoglu [169]	4	150	300	28	0.22[w]	2523	ls-cr-32	13.0		46800	66.5
Gesoglu [169]	4	150	300	28	0.22[w]	2523	ls-cr-32	13.0		47300	70.7
Gesoglu [169]	4	150	300	28	0.26	2496	ls-cr-32	13.0		45400	61.8
Gesoglu [169]	4	150	300	28	0.26	2496	ls-cr-32	13.0		47600	68.9
Gesoglu [169]	4	150	300	28	0.26	2496	ls-cr-32	13.0		40900	59.1
Gesoglu [169]	4	150	300	28	0.26	2496	ls-cr-32	13.0		45400	62.2
Gesoglu [169]	4	150	300	28	0.31	2535	ls-cr-32	13.0		43000	75.8
Gesoglu [169]	4	150	300	28	0.31	2535	ls-cr-32	13.0		48200	67.7
Gesoglu [169]	4	150	300	28	0.31	2535	ls-cr-32	13.0		46200	53.6
Gesoglu [169]	4	150	300	28	0.31	2535	ls-cr-32	13.0		44500	57.9
Gesoglu [169]	4	150	300	28	0.22	2523	ls-cr-32	13.0		46400	92.9
Gesoglu [169]	4	150	300	28	0.22	2523	ls-cr-32	13.0		48300	94.0
Gesoglu [169]	4	150	300	28	0.22	2523	ls-cr-32	13.0		47000	97.7
Gesoglu [169]	4	150	300	28	0.22	2523	ls-cr-32	13.0		48800	102.0
Gesoglu [169]	4	150	300	28	0.26	2496	ls-cr-32	13.0		50500	93.7
Gesoglu [169]	4	150	300	28	0.26	2496	ls-cr-32	13.0		47100	86.2
Gesoglu [169]	4	150	300	28	0.26	2496	ls-cr-32	13.0		43000	87.9
Gesoglu [169]	4	150	300	28	0.26	2496	ls-cr-32	13.0		45400	82.7
Gesoglu [169]	4	150	300	28	0.31	2535	ls-cr-32	13.0		44700	79.1
Gesoglu [169]	4	150	300	28	0.31	2535	ls-cr-32	13.0		45000	85.3
Gesoglu [169]	4	150	300	28	0.31	2535	ls-cr-32	13.0		46100	86.6
Gesoglu [169]	4	150	300	28	0.31	2535	ls-cr-32	13.0		44300	85.5
Gesoglu [169]	4	150	300	28	0.22	2523	ls-cr-32	13.0		46800	91.1
Gesoglu [169]	4	150	300	28	0.22	2523	ls-cr-32	13.0		53200	96.7
Gesoglu [169]	4	150	300	28	0.22	2523	ls-cr-32	13.0		47600	99.7
Gesoglu [169]	4	150	300	28	0.22	2523	ls-cr-32	13.0		49300	91.2
Gesoglu [169]	4	150	300	28	0.26	2496	ls-cr-32	13.0		45900	83.8
Gesoglu [169]	4	150	300	28	0.26	2496	ls-cr-32	13.0		47700	87.1
Gesoglu [169]	4	150	300	28	0.26	2496	ls-cr-32	13.0		46200	93.2
Gesoglu [169]	4	150	300	28	0.26	2496	ls-cr-32	13.0		44700	85.1
Gesoglu [169]	4	150	300	28	0.31	2535	ls-cr-32	13.0		46100	86.9
Gesoglu [169]	4	150	300	28	0.31	2535	ls-cr-32	13.0		48100	90.7
Gesoglu [169]	4	150	300	28	0.31	2535	ls-cr-32	13.0		47600	89.5
Gesoglu [169]	4	150	300	28	0.31	2535	ls-cr-32	13.0		45400	87.8
Gesoglu [169]	4	150	300	28	0.22	2523	ls-cr-32	13.0		45000	90.3
Gesoglu [169]	4	150	300	28	0.22	2523	ls-cr-32	13.0		50800	95.2
Gesoglu [169]	4	150	300	28	0.22	2523	ls-cr-32	13.0		50000	92.2
Gesoglu [169]	4	150	300	28	0.22	2523	ls-cr-32	13.0		49300	97.6
Gesoglu [169]	4	150	300	28	0.26	2496	ls-cr-32	13.0		48500	87.5
Gesoglu [169]	4	150	300	28	0.26	2496	ls-cr-32	13.0		41100	87.2
Gesoglu [169]	4	150	300	28	0.26	2496	ls-cr-32	13.0		43200	80.4
Gesoglu [169]	4	150	300	28	0.26	2496	ls-cr-32	13.0		44200	86.5
Gesoglu [169]	4	150	300	28	0.31	2535	ls-cr-32	13.0		45800	83.9
Gesoglu [169]	4	150	300	28	0.31	2535	ls-cr-32	13.0		44600	80.9
Gesoglu [169]	4	150	300	28	0.31	2535	ls-cr-32	13.0		45300	84.5
Gesoglu [169]	4	150	300	28	0.31	2535	ls-cr-32	13.0		45100	85.7
Giaccio et al. [170]		100	200	28	0.32	2500	bs-cr-19			55400	91.9
Giaccio et al. [170]		100	200	28	0.32	2390	gn-cr-19			42400	80.0
Giaccio et al. [170]		100	200	28	0.32	2440	ls-cr-19			46100	61.9
Giaccio et al. [170]		150	300	28	0.32	2500	bs-cr-19			46500	87.0
Giaccio et al. [170]		150	300	28	0.32	2390	gn-cr-19			38500	77.5
Giaccio et al. [170]		150	300	28	0.32	2440	ls-cr-19			39000	58.2
Hammons and Neeley [171]	1	53.6	88.9		0.24	2365	ls-9.5	9.8	16.4[f]	44000	105.0
Han and Kim [172]	1	100	200	1	0.4		gn-cr-19			20000	21.0
Han and Kim [172]	1	100	200	1	0.4		gn-cr-19			21000	22.0
Han and Kim [172]	1	100	200	1	0.4		gn-cr-19			20000	20.0
Han and Kim [172]	1	100	200	3	0.4		gn-cr-19			24000	31.0
Han and Kim [172]	1	100	200	3	0.4		gn-cr-19			24000	32.0
Han and Kim [172]	1	100	200	3	0.4		gn-cr-19			23000	32.0
Han and Kim [172]	1	100	200	7	0.4		gn-cr-19			26000	38.0
Han and Kim [172]	1	100	200	7	0.4		gn-cr-19			26000	37.0
Han and Kim [172]	1	100	200	7	0.4		gn-cr-19			26000	35.0
Han and Kim [172]	1	100	200	28	0.4		gn-cr-19			29000	43.0
Han and Kim [172]	1	100	200	28	0.4		gn-cr-19			31000	36.0
Han and Kim [172]	1	100	200	28	0.4		gn-cr-19			32000	35.0
Han and Kim [172]	1	100	200	1	0.5		gn-cr-19			17000	11.0
Han and Kim [172]	1	100	200	1	0.5		gn-cr-19			17000	12.0
Han and Kim [172]	1	100	200	1	0.5		gn-cr-19			16000	11.0

Source	*n*	*B (mm)*	*H (mm)*	*Age (d)*	*w/c*	$\rho_{c,f}$ *(kg/m^3)*	*Aggregate properties*[p]	*sf/c (%)*	*ma/b (%)*	E_c *(MPa)*	f'_{co} *(MPa)*
Han and Kim [172]	1	100	200	3	0.5		gn-cr-19			23000	22.0
Han and Kim [172]	1	100	200	3	0.5		gn-cr-19			22000	22.0
Han and Kim [172]	1	100	200	3	0.5		gn-cr-19			22000	21.0
Han and Kim [172]	1	100	200	7	0.5		gn-cr-19			24000	28.0
Han and Kim [172]	1	100	200	7	0.5		gn-cr-19			25000	25.0
Han and Kim [172]	1	100	200	7	0.5		gn-cr-19			24000	28.0
Han and Kim [172]	1	100	200	28	0.5		gn-cr-19			27000	35.0
Han and Kim [172]	1	100	200	28	0.5		gn-cr-19			28000	37.0
Han and Kim [172]	1	100	200	28	0.5		gn-cr-19			27000	36.0
Han and Kim [172]	1	100	200	1	0.4		gn-cr-19			6000	4.0
Han and Kim [172]	1	100	200	1	0.4		gn-cr-19			7000	3.0
Han and Kim [172]	1	100	200	1	0.4		gn-cr-19			7000	4.0
Han and Kim [172]	1	100	200	3	0.4		gn-cr-19			17000	16.0
Han and Kim [172]	1	100	200	3	0.4		gn-cr-19			18000	16.0
Han and Kim [172]	1	100	200	3	0.4		gn-cr-19			20000	17.0
Han and Kim [172]	1	100	200	7	0.4		gn-cr-19			25000	25.0
Han and Kim [172]	1	100	200	7	0.4		gn-cr-19			22000	24.0
Han and Kim [172]	1	100	200	7	0.4		gn-cr-19			23000	25.0
Han and Kim [172]	1	100	200	28	0.4		gn-cr-19			25000	32.0
Han and Kim [172]	1	100	200	28	0.4		gn-cr-19			26000	35.0
Han and Kim [172]	1	100	200	28	0.4		gn-cr-19			26000	33.0
Han and Kim [172]	1	100	200	1	0.4		gn-cr-19			15000	11.0
Han and Kim [172]	1	100	200	1	0.4		gn-cr-19			15000	12.0
Han and Kim [172]	1	100	200	1	0.4		gn-cr-19			17000	13.0
Han and Kim [172]	1	100	200	3	0.4		gn-cr-19			24000	22.0
Han and Kim [172]	1	100	200	3	0.4		gn-cr-19			23000	24.0
Han and Kim [172]	1	100	200	3	0.4		gn-cr-19			21000	25.0
Han and Kim [172]	1	100	200	7	0.4		gn-cr-19			26000	29.0
Han and Kim [172]	1	100	200	7	0.4		gn-cr-19			27000	29.0
Han and Kim [172]	1	100	200	7	0.4		gn-cr-19			28000	30.0
Han and Kim [172]	1	100	200	28	0.4		gn-cr-19			29000	38.0
Han and Kim [172]	1	100	200	28	0.4		gn-cr-19			29000	40.0
Han and Kim [172]	1	100	200	28	0.4		gn-cr-19			28000	38.0
Han and Kim [172]	1	100	200	1	0.4		gn-cr-19			21000	22.0
Han and Kim [172]	1	100	200	1	0.4		gn-cr-19			20000	20.0
Han and Kim [172]	1	100	200	1	0.4		gn-cr-19			21000	22.0
Han and Kim [172]	1	100	200	3	0.4		gn-cr-19			25000	30.0
Han and Kim [172]	1	100	200	3	0.4		gn-cr-19			25000	31.0
Han and Kim [172]	1	100	200	3	0.4		gn-cr-19			24000	32.0
Han and Kim [172]	1	100	200	7	0.4		gn-cr-19			25000	36.0
Han and Kim [172]	1	100	200	7	0.4		gn-cr-19			26000	37.0
Han and Kim [172]	1	100	200	7	0.4		gn-cr-19			26000	35.0
Han and Kim [172]	1	100	200	28	0.4		gn-cr-19			28000	45.0
Han and Kim [172]	1	100	200	28	0.4		gn-cr-19			27000	45.0
Han and Kim [172]	1	100	200	28	0.4		gn-cr-19			26000	45.0
Han and Kim [172]	1	100	200	1	0.5		gn-cr-19			2000	2.0
Han and Kim [172]	1	100	200	1	0.5		gn-cr-19			4000	2.0
Han and Kim [172]	1	100	200	1	0.5		gn-cr-19			5000	2.0
Han and Kim [172]	1	100	200	3	0.5		gn-cr-19			13000	10.0
Han and Kim [172]	1	100	200	3	0.5		gn-cr-19			14000	11.0
Han and Kim [172]	1	100	200	3	0.5		gn-cr-19			15000	12.0
Han and Kim [172]	1	100	200	7	0.5		gn-cr-19			19000	18.0
Han and Kim [172]	1	100	200	7	0.5		gn-cr-19			18000	18.0
Han and Kim [172]	1	100	200	7	0.5		gn-cr-19			18000	16.0
Han and Kim [172]	1	100	200	28	0.5		gn-cr-19			21000	22.0
Han and Kim [172]	1	100	200	28	0.5		gn-cr-19			23000	26.0
Han and Kim [172]	1	100	200	28	0.5		gn-cr-19			24000	26.0
Han and Kim [172]	1	100	200	1	0.5		gn-cr-19			13000	7.0
Han and Kim [172]	1	100	200	1	0.5		gn-cr-19			12000	7.0
Han and Kim [172]	1	100	200	1	0.5		gn-cr-19			12000	7.0
Han and Kim [172]	1	100	200	3	0.5		gn-cr-19			21000	17.0
Han and Kim [172]	1	100	200	3	0.5		gn-cr-19			19000	17.0
Han and Kim [172]	1	100	200	3	0.5		gn-cr-19			19000	17.0
Han and Kim [172]	1	100	200	7	0.5		gn-cr-19			23000	22.0
Han and Kim [172]	1	100	200	7	0.5		gn-cr-19			22000	22.0
Han and Kim [172]	1	100	200	7	0.5		gn-cr-19			24000	22.0
Han and Kim [172]	1	100	200	28	0.5		gn-cr-19			27000	29.0
Han and Kim [172]	1	100	200	28	0.5		gn-cr-19			27000	31.0
Han and Kim [172]	1	100	200	1	0.5		gn-cr-19			16000	10.0
Han and Kim [172]	1	100	200	1	0.5		gn-cr-19			15000	10.0
Han and Kim [172]	1	100	200	1	0.5		gn-cr-19			16000	11.0
Han and Kim [172]	1	100	200	3	0.5		gn-cr-19			18000	17.0
Han and Kim [172]	1	100	200	3	0.5		gn-cr-19			21000	17.0
Han and Kim [172]	1	100	200	3	0.5		gn-cr-19			19000	18.0
Han and Kim [172]	1	100	200	7	0.5		gn-cr-19			24000	21.0
Han and Kim [172]	1	100	200	7	0.5		gn-cr-19			22000	23.0
Han and Kim [172]	1	100	200	7	0.5		gn-cr-19			25000	24.0
Han and Kim [172]	1	100	200	28	0.5		gn-cr-19			24000	26.0
Han and Kim [172]	1	100	200	28	0.5		gn-cr-19			25000	28.0
Han and Kim [172]	1	100	200	1	0.4		gn-cr-19			24000	21.0

Source	*n*	*B (mm)*	*H (mm)*	*Age (d)*	*w/c*	*$\rho_{c,f}$ (kg/m^3)*	*Aggregate properties*[p]	*sf/c (%)*	*ma/b (%)*	*E_c (MPa)*	*f'_{co} (MPa)*
Han and Kim [172]	1	100	200	1	0.4		gn-cr-19			24000	22.0
Han and Kim [172]	1	100	200	1	0.4		gn-cr-19			24000	20.0
Han and Kim [172]	1	100	200	3	0.4		gn-cr-19			26000	31.0
Han and Kim [172]	1	100	200	3	0.4		gn-cr-19			28000	32.0
Han and Kim [172]	1	100	200	3	0.4		gn-cr-19			28000	32.0
Han and Kim [172]	1	100	200	7	0.4		gn-cr-19			32000	38.0
Han and Kim [172]	1	100	200	7	0.4		gn-cr-19			32000	37.0
Han and Kim [172]	1	100	200	7	0.4		gn-cr-19			28000	35.0
Han and Kim [172]	1	100	200	28	0.4		gn-cr-19			32000	43.0
Han and Kim [172]	1	100	200	28	0.4		gn-cr-19			36000	36.0
Han and Kim [172]	1	100	200	28	0.4		gn-cr-19			36000	35.0
Han and Kim [172]	1	100	200	1	0.5		gn-cr-19			18000	11.0
Han and Kim [172]	1	100	200	1	0.5		gn-cr-19			18000	12.0
Han and Kim [172]	1	100	200	1	0.5		gn-cr-19			20000	11.0
Han and Kim [172]	1	100	200	3	0.5		gn-cr-19			26000	22.0
Han and Kim [172]	1	100	200	3	0.5		gn-cr-19			27000	22.0
Han and Kim [172]	1	100	200	3	0.5		gn-cr-19			24000	21.0
Han and Kim [172]	1	100	200	7	0.5		gn-cr-19			28000	28.0
Han and Kim [172]	1	100	200	7	0.5		gn-cr-19			28000	25.0
Han and Kim [172]	1	100	200	7	0.5		gn-cr-19			28000	28.0
Han and Kim [172]	1	100	200	28	0.5		gn-cr-19			31000	35.0
Han and Kim [172]	1	100	200	28	0.5		gn-cr-19			32000	37.0
Han and Kim [172]	1	100	200	28	0.5		gn-cr-19			32000	36.0
Han and Kim [172]	1	100	200	1	0.4		gn-cr-19			10000	4.0
Han and Kim [172]	1	100	200	1	0.4		gn-cr-19			12000	3.0
Han and Kim [172]	1	100	200	1	0.4		gn-cr-19			12000	4.0
Han and Kim [172]	1	100	200	3	0.4		gn-cr-19			24000	16.0
Han and Kim [172]	1	100	200	3	0.4		gn-cr-19			24000	16.0
Han and Kim [172]	1	100	200	3	0.4		gn-cr-19			26000	17.0
Han and Kim [172]	1	100	200	7	0.4		gn-cr-19			31000	25.0
Han and Kim [172]	1	100	200	7	0.4		gn-cr-19			29000	24.0
Han and Kim [172]	1	100	200	7	0.4		gn-cr-19			30000	25.0
Han and Kim [172]	1	100	200	28	0.4		gn-cr-19			31000	32.0
Han and Kim [172]	1	100	200	28	0.4		gn-cr-19			32000	35.0
Han and Kim [172]	1	100	200	28	0.4		gn-cr-19			35000	33.0
Han and Kim [172]	1	100	200	1	0.4		gn-cr-19			22000	11.0
Han and Kim [172]	1	100	200	1	0.4		gn-cr-19			22000	12.0
Han and Kim [172]	1	100	200	1	0.4		gn-cr-19			23000	13.0
Han and Kim [172]	1	100	200	3	0.4		gn-cr-19			30000	22.0
Han and Kim [172]	1	100	200	3	0.4		gn-cr-19			27000	24.0
Han and Kim [172]	1	100	200	3	0.4		gn-cr-19			26000	25.0
Han and Kim [172]	1	100	200	7	0.4		gn-cr-19			30000	29.0
Han and Kim [172]	1	100	200	7	0.4		gn-cr-19			31000	29.0
Han and Kim [172]	1	100	200	7	0.4		gn-cr-19			33000	30.0
Han and Kim [172]	1	100	200	28	0.4		gn-cr-19			35000	38.0
Han and Kim [172]	1	100	200	28	0.4		gn-cr-19			35000	40.0
Han and Kim [172]	1	100	200	28	0.4		gn-cr-19			36000	38.0
Han and Kim [172]	1	100	200	1	0.4		gn-cr-19			29000	22.0
Han and Kim [172]	1	100	200	1	0.4		gn-cr-19			27000	20.0
Han and Kim [172]	1	100	200	1	0.4		gn-cr-19			26000	22.0
Han and Kim [172]	1	100	200	3	0.4		gn-cr-19			30000	30.0
Han and Kim [172]	1	100	200	3	0.4		gn-cr-19			33000	31.0
Han and Kim [172]	1	100	200	3	0.4		gn-cr-19			29000	32.0
Han and Kim [172]	1	100	200	7	0.4		gn-cr-19			30000	36.0
Han and Kim [172]	1	100	200	7	0.4		gn-cr-19			36000	37.0
Han and Kim [172]	1	100	200	7	0.4		gn-cr-19			35000	35.0
Han and Kim [172]	1	100	200	7	0.4		gn-cr-19			35000	45.0
Han and Kim [172]	1	100	200	28	0.4		gn-cr-19			36000	45.0
Han and Kim [172]	1	100	200	28	0.4		gn-cr-19			34000	45.0
Han and Kim [172]	1	100	200	1	0.5		gn-cr-19			5000	2.0
Han and Kim [172]	1	100	200	1	0.5		gn-cr-19			10000	2.0
Han and Kim [172]	1	100	200	1	0.5		gn-cr-19			8000	2.0
Han and Kim [172]	1	100	200	3	0.5		gn-cr-19			21000	10.0
Han and Kim [172]	1	100	200	3	0.5		gn-cr-19			22000	11.0
Han and Kim [172]	1	100	200	3	0.5		gn-cr-19			23000	12.0
Han and Kim [172]	1	100	200	7	0.5		gn-cr-19			28000	18.0
Han and Kim [172]	1	100	200	7	0.5		gn-cr-19			27000	18.0
Han and Kim [172]	1	100	200	7	0.5		gn-cr-19			26000	16.0
Han and Kim [172]	1	100	200	28	0.5		gn-cr-19			27000	22.0
Han and Kim [172]	1	100	200	28	0.5		gn-cr-19			32000	26.0
Han and Kim [172]	1	100	200	28	0.5		gn-cr-19			33000	26.0
Han and Kim [172]	1	100	200	1	0.5		gn-cr-19			16000	7.0
Han and Kim [172]	1	100	200	1	0.5		gn-cr-19			17000	7.0
Han and Kim [172]	1	100	200	1	0.5		gn-cr-19			18000	7.0
Han and Kim [172]	1	100	200	3	0.5		gn-cr-19			31000	17.0
Han and Kim [172]	1	100	200	3	0.5		gn-cr-19			28000	17.0
Han and Kim [172]	1	100	200	3	0.5		gn-cr-19			27000	17.0
Han and Kim [172]	1	100	200	7	0.5		gn-cr-19			29000	22.0
Han and Kim [172]	1	100	200	7	0.5		gn-cr-19			30000	22.0
Han and Kim [172]	1	100	200	7	0.5		gn-cr-19			31000	22.0

Source	*n*	*B (mm)*	*H (mm)*	*Age (d)*	*w/c*	$\rho_{c,f}$ *(kg/m³)*	*Aggregate properties*[p]	*sf/c (%)*	*ma/b (%)*	E_c *(MPa)*	f'_{co} *(MPa)*
Han and Kim [172]	1	100	200	28	0.5		gn-cr-19			34000	29.0
Han and Kim [172]	1	100	200	28	0.5		gn-cr-19			32000	31.0
Han and Kim [172]	1	100	200	1	0.5		gn-cr-19			21000	10.0
Han and Kim [172]	1	100	200	1	0.5		gn-cr-19			20000	10.0
Han and Kim [172]	1	100	200	1	0.5		gn-cr-19			23000	11.0
Han and Kim [172]	1	100	200	3	0.5		gn-cr-19			26000	17.0
Han and Kim [172]	1	100	200	3	0.5		gn-cr-19			30000	17.0
Han and Kim [172]	1	100	200	3	0.5		gn-cr-19			28000	18.0
Han and Kim [172]	1	100	200	7	0.5		gn-cr-19			29000	21.0
Han and Kim [172]	1	100	200	7	0.5		gn-cr-19			28000	23.0
Han and Kim [172]	1	100	200	7	0.5		gn-cr-19			30000	24.0
Han and Kim [172]	1	100	200	28	0.5		gn-cr-19			28000	26.0
Han and Kim [172]	1	100	200	28	0.5		gn-cr-19			31000	28.0
Hansen and Boegh [173]	5	100	200	47	0.40	2389	gv			43400	58.5
Hansen and Boegh [173]	5	100	200	47	0.70	2363	gv			38500[m]	33.2
Hansen and Boegh [173]	5	100	200	47	1.20	2329	gv			30800[m]	15.0
Hognestad [174]	1	152.4	304.8				n			18995	12.9
Hognestad [174]	1	152.4	304.8				n			17578	15.0
Hognestad [174]	1	152.4	304.8				n			19729	16.4
Hognestad [174]	1	152.4	304.8				n			21933	20.5
Hognestad [174]	1	152.4	304.8				n			21723	20.9
Hognestad [174]	1	152.4	304.8				n			23875	21.3
Hognestad [174]	1	152.4	304.8				n			22720	21.5
Hognestad [174]	1	152.4	304.8				n			27705	25.3
Hognestad [174]	1	152.4	304.8				n			23979	25.5
Hognestad [174]	1	152.4	304.8				n			27180	28.7
Hognestad [174]	1	152.4	304.8				n			29384	29.0
Hognestad [174]	1	152.4	304.8				n			29332	29.6
Hognestad [174]	1	152.4	304.8				n			25606	31.5
Hognestad [174]	1	152.4	304.8				n			27495	31.5
Hognestad [174]	1	152.4	304.8				n			26708	32.8
Hognestad [174]	1	152.4	304.8				n			28230	34.1
Hognestad [174]	1	152.4	304.8				n			28177	36.3
Hognestad [174]	1	152.4	304.8				n			29856	37.1
Hognestad [174]	1	152.4	304.8				n			30014	37.3
Hognestad [174]	1	152.4	304.8				n			31955	38.2
Hognestad [174]	1	152.4	304.8				n			30276	41.2
Hognestad [174]	1	152.4	304.8				n			22458	19.0
Hognestad [174]	1	152.4	304.8				n			20569	20.3
Hognestad [174]	1	152.4	304.8				n			20674	20.5
Hognestad [174]	1	152.4	304.8				n			23665	20.7
Hognestad [174]	1	152.4	304.8				n			22353	20.9
Hognestad [174]	1	152.4	304.8				n			21828	21.2
Hognestad [174]	1	152.4	304.8				n			21251	21.3
Hognestad [174]	1	152.4	304.8				n			23350	21.6
Hognestad [174]	1	152.4	304.8				n			21986	21.6
Hognestad [174]	1	152.4	304.8				n			20936	21.8
Hognestad [174]	1	152.4	304.8				n			23297	22.1
Hognestad [174]	1	152.4	304.8				n			25659	22.4
Hognestad [174]	1	152.4	304.8				n			23140	22.5
Hognestad [174]	1	152.4	304.8				n			21618	22.7
Hognestad [174]	1	152.4	304.8				n			19152	22.8
Hognestad [174]	1	152.4	304.8				n			22563	22.8
Hognestad [174]	1	152.4	304.8				n			23140	23.1
Hognestad [174]	1	152.4	304.8				n			22615	23.2
Hognestad [174]	1	152.4	304.8				n			23822	23.4
Hognestad [174]	1	152.4	304.8				n			22458	23.6
Hognestad [174]	1	152.4	304.8				n			21251	23.7
Hognestad [174]	1	152.4	304.8				n			20884	23.8
Hognestad [174]	1	152.4	304.8				n			21041	23.9
Hognestad [174]	1	152.4	304.8				n			24976	24.7
Hognestad [174]	1	152.4	304.8				n			25868	25.1
Hognestad [174]	1	152.4	304.8				n			23770	25.2
Hognestad [174]	1	152.4	304.8				n			24976	25.4
Hognestad [174]	1	152.4	304.8				n			26656	25.8
Hognestad [174]	1	152.4	304.8				n			26498	26.5
Hognestad [174]	1	152.4	304.8				n			29227	28.2
Hognestad [174]	1	152.4	304.8				n			28387	29.1
Hossain [175]		150	300	28	0.45	2711[d]	pm			21200	35.0
Hossain [175]		150	300	28	0.45	2694[d]	pm			20700	34.0
Kim et al. [176]	1	100	200	1	0.4		gn-cr-19			10700	5.4
Kim et al. [176]	1	100	200	1	0.4		gn-cr-19			20700	20.9
Kim et al. [176]	1	100	200	1	0.4		gn-cr-19			23700	22.8
Kim et al. [176]	1	100	200	1	0.4		gn-cr-19			25600	31.7
Kim et al. [176]	1	100	200	1	0.5		gn-cr-19			9100	3.5
Kim et al. [176]	1	100	200	1	0.5		gn-cr-19			16900	9.4
Kim et al. [176]	1	100	200	1	0.5		gn-cr-19			20700	17.1
Kim et al. [176]	1	100	200	1	0.5		gn-cr-19			22300	19.8
Kim et al. [176]	1	100	200	1	0.4		gn-cr-19			6900	3.4
Kim et al. [176]	1	100	200	1	0.4		gn-cr-19			15700	11.8

Source	*n*	*B (mm)*	*H (mm)*	*Age (d)*	*w/c*	*$\rho_{c,f}$ (kg/m^3)*	*Aggregate properties*[p]	*sf/c (%)*	*ma/b (%)*	*E_c (MPa)*	*f'_{co} (MPa)*
Kim et al. [176]	1	100	200	1	0.4		gn-cr-19			20500	17.9
Kim et al. [176]	1	100	200	1	0.4		gn-cr-19			20700	21.0
Kim et al. [176]	1	100	200	1	0.5		gn-cr-19			3500	2.3
Kim et al. [176]	1	100	200	1	0.5		gn-cr-19			12500	7.1
Kim et al. [176]	1	100	200	1	0.5		gn-cr-19			14200	10.2
Kim et al. [176]	1	100	200	1	0.5		gn-cr-19			16000	10.3
Kim et al. [176]	1	100	200	1	0.4		gn-cr-19			4000	2.2
Kim et al. [176]	1	100	200	1	0.4		gn-cr-19			11100	6.7
Kim et al. [176]	1	100	200	1	0.4		gn-cr-19			20600	16.5
Kim et al. [176]	1	100	200	1	0.4		gn-cr-19			21600	19.2
Kim et al. [176]	1	100	200	3	0.4		gn-cr-19			21200	22.1
Kim et al. [176]	1	100	200	3	0.4		gn-cr-19			23900	31.6
Kim et al. [176]	1	100	200	3	0.4		gn-cr-19			26200	34.6
Kim et al. [176]	1	100	200	3	0.4		gn-cr-19			26700	35.8
Kim et al. [176]	1	100	200	3	0.5		gn-cr-19			19200	14.3
Kim et al. [176]	1	100	200	3	0.5		gn-cr-19			25000	23.4
Kim et al. [176]	1	100	200	3	0.5		gn-cr-19			24500	24.2
Kim et al. [176]	1	100	200	3	0.5		gn-cr-19			24900	28.1
Kim et al. [176]	1	100	200	3	0.4		gn-cr-19			18200	16.4
Kim et al. [176]	1	100	200	3	0.4		gn-cr-19			21900	22.7
Kim et al. [176]	1	100	200	3	0.4		gn-cr-19			24600	29.4
Kim et al. [176]	1	100	200	3	0.4		gn-cr-19			24600	38.2
Kim et al. [176]	1	100	200	3	0.5		gn-cr-19			14100	10.9
Kim et al. [176]	1	100	200	3	0.5		gn-cr-19			19800	17.2
Kim et al. [176]	1	100	200	3	0.5		gn-cr-19			19900	17.3
Kim et al. [176]	1	100	200	3	0.5		gn-cr-19			19200	17.4
Kim et al. [176]	1	100	200	3	0.4		gn-cr-19			18600	18.2
Kim et al. [176]	1	100	200	3	0.4		gn-cr-19			21600	21.1
Kim et al. [176]	1	100	200	3	0.4		gn-cr-19			24300	24.1
Kim et al. [176]	1	100	200	3	0.4		gn-cr-19			24700	28.1
Kim et al. [176]	1	100	200	7	0.4		gn-cr-19			24400	36.0
Kim et al. [176]	1	100	200	7	0.4		gn-cr-19			27100	41.5
Kim et al. [176]	1	100	200	7	0.4		gn-cr-19			27600	39.2
Kim et al. [176]	1	100	200	7	0.4		gn-cr-19			29200	43.6
Kim et al. [176]	1	100	200	7	0.5		gn-cr-19			23400	24.7
Kim et al. [176]	1	100	200	7	0.5		gn-cr-19			26400	31.5
Kim et al. [176]	1	100	200	7	0.5		gn-cr-19			26500	33.1
Kim et al. [176]	1	100	200	7	0.5		gn-cr-19			27000	34.6
Kim et al. [176]	1	100	200	7	0.4		gn-cr-19			23400	24.5
Kim et al. [176]	1	100	200	7	0.4		gn-cr-19			24300	29.4
Kim et al. [176]	1	100	200	7	0.4		gn-cr-19			26500	32.7
Kim et al. [176]	1	100	200	7	0.4		gn-cr-19			25800	36.3
Kim et al. [176]	1	100	200	7	0.5		gn-cr-19			18400	17.2
Kim et al. [176]	1	100	200	7	0.5		gn-cr-19			23500	22.3
Kim et al. [176]	1	100	200	7	0.5		gn-cr-19			22300	21.9
Kim et al. [176]	1	100	200	7	0.5		gn-cr-19			22900	22.5
Kim et al. [176]	1	100	200	7	0.4		gn-cr-19			25300	28.2
Kim et al. [176]	1	100	200	7	0.4		gn-cr-19			25800	30.5
Kim et al. [176]	1	100	200	7	0.4		gn-cr-19			28000	31.0
Kim et al. [176]	1	100	200	7	0.4		gn-cr-19			27700	34.6
Kim et al. [176]	1	100	200	28	0.4		gn-cr-19			30000	51.3
Kim et al. [176]	1	100	200	28	0.4		gn-cr-19			30200	50.8
Kim et al. [176]	1	100	200	28	0.4		gn-cr-19			32100	49.4
Kim et al. [176]	1	100	200	28	0.4		gn-cr-19			29700	48.7
Kim et al. [176]	1	100	200	28	0.5		gn-cr-19			27600	36.9
Kim et al. [176]	1	100	200	28	0.5		gn-cr-19			28800	42.4
Kim et al. [176]	1	100	200	28	0.5		gn-cr-19			29100	41.3
Kim et al. [176]	1	100	200	28	0.5		gn-cr-19			30100	39.3
Kim et al. [176]	1	100	200	28	0.4		gn-cr-19			25600	33.8
Kim et al. [176]	1	100	200	28	0.4		gn-cr-19			28600	38.2
Kim et al. [176]	1	100	200	28	0.4		gn-cr-19			29900	38.5
Kim et al. [176]	1	100	200	28	0.4		gn-cr-19			27100	44.9
Kim et al. [176]	1	100	200	28	0.5		gn-cr-19			22500	24.7
Kim et al. [176]	1	100	200	28	0.5		gn-cr-19			26800	30.7
Kim et al. [176]	1	100	200	28	0.5		gn-cr-19			27900	28.6
Kim et al. [176]	1	100	200	28	0.5		gn-cr-19			24600	27.1
Kim et al. [176]	1	100	200	28	0.4		gn-cr-19			28300	39.9
Kim et al. [176]	1	100	200	28	0.4		gn-cr-19			28000	39.6
Kim et al. [176]	1	100	200	28	0.4		gn-cr-19			30500	41.2
Kim et al. [176]	1	100	200	28	0.4		gn-cr-19			30300	45.4
Klieger [177]		152.4	304.8	28			gv-38.1			24614	48.4
Klieger [177]		152.4	304.8	28			gv-38.1			21650	32.8
Klieger [177]		152.4	304.8	28			gv-38.1				50.8
Klieger [177]		152.4	304.8	28			gv-38.1				46.2
Klieger [177]		152.4	304.8	28			gv-38.1				40.3
Klieger [177]		152.4	304.8	28			gv-38.1				40.8
Klieger [177]		152.4	304.8	28			gv-38.1			27717	51.6
Klieger [177]		152.4	304.8	28			gv-38.1				46.7
Klieger [177]		152.4	304.8	28			gv-38.1				32.2
Klieger [177]		152.4	304.8	28			gv-38.1				46.5

Source	*n*	*B (mm)*	*H (mm)*	*Age (d)*	*w/c*	$\rho_{c,f}$ *(kg/m^3)*	*Aggregate properties*[p]	*sf/c (%)*	*ma/b (%)*	E_c *(MPa)*	f'_{co} *(MPa)*
Klieger [177]		152.4	304.8	28			gv-38.1				45.2
Klieger [177]		152.4	304.8	28			gv-38.1				40.0
Klieger [177]		152.4	304.8	28			gv-38.1			24270	29.8
Klieger [177]		152.4	304.8	28			gv-38.1			23925	39.4
Klieger [177]		152.4	304.8	28			gv-38.1			25373	43.6
Klieger [177]		152.4	304.8	28			gv-38.1			26131	41.4
Klieger [177]		152.4	304.8	28			gv-38.1			24063	33.6
Klieger [177]		152.4	304.8	28			gv-38.1				45.2
Klieger [177]		152.4	304.8	28			gv-38.1				41.2
Klieger [177]		152.4	304.8	28			gv-38.1				36.6
Klieger [177]		152.4	304.8	28			gv-38.1				39.4
Klieger [177]		152.4	304.8	28			gv-38.1			26062	45.2
Klieger [177]		152.4	304.8	28			gv-38.1				42.1
Klieger [177]		152.4	304.8	28			gv-38.1				39.0
Klieger [177]		152.4	304.8	28			gv-38.1			26752	40.7
Klieger [177]		152.4	304.8	28			gv-38.1				32.1
Klieger [177]		152.4	304.8	28			gv-38.1				39.3
Klieger [177]		152.4	304.8	28			gv-38.1				35.7
Klieger [177]		152.4	304.8	28			gv-38.1			25166	42.7
Klieger [177]		152.4	304.8	28			gv-38.1			22477	36.2
Klieger [177]		152.4	304.8	28			gv-38.1			20202	26.5
Klieger [177]		152.4	304.8	28			gv-38.1				38.0
Klieger [177]		152.4	304.8	28			gv-38.1				37.8
Klieger [177]		152.4	304.8	28			gv-38.1				27.5
Klieger [177]		152.4	304.8	28			gv-38.1				31.0
Klieger [177]		152.4	304.8	28			gv-38.1			25373	38.5
Klieger [177]		152.4	304.8	28			gv-38.1				34.5
Klieger [177]		152.4	304.8	28			gv-38.1				27.4
Klieger [177]		152.4	304.8	28			gv-38.1				33.9
Klieger [177]		152.4	304.8	28			gv-38.1				36.1
Klieger [177]		152.4	304.8	28			gv-38.1				34.8
Klieger [177]		152.4	304.8	28			gv-38.1			21581	19.0
Klieger [177]		152.4	304.8	28			gv-38.1			21787	26.3
Klieger [177]		152.4	304.8	28			gv-38.1			23373	32.5
Klieger [177]		152.4	304.8	28			gv-38.1			23787	29.8
Klieger [177]		152.4	304.8	28			gv-38.1			21305	27.7
Klieger [177]		152.4	304.8	28			gv-38.1				31.7
Klieger [177]		152.4	304.8	28			gv-38.1				32.3
Klieger [177]		152.4	304.8	28			gv-38.1				26.6
Klieger [177]		152.4	304.8	28			gv-38.1				24.7
Klieger [177]		152.4	304.8	28			gv-38.1			25442	37.5
Klieger [177]		152.4	304.8	28			gv-38.1				36.6
Klieger [177]		152.4	304.8	28			gv-38.1				33.0
Klieger [177]		152.4	304.8	28			gv-38.1			22063	23.5
Klieger [177]		152.4	304.8	28			gv-38.1				19.4
Klieger [177]		152.4	304.8	28			gv-38.1				27.2
Klieger [177]		152.4	304.8	28			gv-38.1				20.8
Klieger [177]		152.4	304.8	28			gv-38.1			22270	26.8
Klieger [177]		152.4	304.8	28			gv-38.1			20271	16.3
Klieger [177]		152.4	304.8	28			gv-38.1			19650	13.9
Klieger [177]		152.4	304.8	28			gv-38.1			18547	8.8
Kluge et al. [178]		152.4	304.8	28		2291	gv			16547	12.4
Kluge et al. [178]		152.4	304.8	28		2339	gv			25373	33.2
Kluge et al. [178]		152.4	304.8	28		2355	gv			24132	38.5
Kluge et al. [178]		152.4	304.8	28		2307	gv			24407	43.1
Kluge et al. [178]		152.4	304.8	7		2291	gv				7.2
Kluge et al. [178]		152.4	304.8	7		2339	gv				27.9
Kluge et al. [178]		152.4	304.8	7		2355	gv				31.3
Kluge et al. [178]		152.4	304.8	7		2307	gv				35.8
Martinez et al. [179]	1	101.6	406.4				ls-cr-19			19512	22.1
Martinez et al. [179]	1	101.6	406.4				ls-cr-19			21718	22.1
Martinez et al. [179]	1	101.6	406.4				ls-cr-19			23511	22.1
Martinez et al. [179]	1	101.6	406.4				ls-cr-19			20753	23.5
Martinez et al. [179]	1	101.6	406.4				ls-cr-19			21994	23.5
Martinez et al. [179]	1	101.6	406.4				ls-cr-19			19857	23.5
Martinez et al. [179]	1	101.6	406.4				ls-cr-19			20202	20.8
Martinez et al. [179]	1	101.6	406.4				ls-cr-19			17651	20.8
Martinez et al. [179]	1	101.6	406.4				ls-cr-19			18133	20.8
Martinez et al. [179]	1	101.6	406.4				ls-cr-19			24821	50.2
Martinez et al. [179]	1	101.6	406.4				ls-cr-19			23235	50.2
Martinez et al. [179]	1	101.6	406.4				ls-cr-19			23994	50.2
Martinez et al. [179]	1	101.6	406.4				ls-cr-19			17857[m]	46.6
Martinez et al. [179]	1	101.6	406.4				ls-cr-19			19236	46.6
Martinez et al. [179]	1	101.6	406.4				ls-cr-19			25717	46.6
Martinez et al. [179]	1	101.6	406.4				ls-cr-19			27372	50.2
Martinez et al. [179]	1	101.6	406.4				ls-cr-19			27234	50.2
Martinez et al. [179]	1	101.6	406.4				ls-cr-19			27648	50.2
Martinez et al. [179]	1	101.6	406.4				ls-cr-19			34336	67.4
Martinez et al. [179]	1	101.6	406.4				ls-cr-19			32819	67.4
Martinez et al. [179]	1	101.6	406.4				ls-cr-19			34405	67.4

Source	*n*	*B (mm)*	*H (mm)*	*Age (d)*	*w/c*	$\rho_{c,f}$ *(kg/m³)*	*Aggregate properties*[p]	*sf/c (%)*	*ma/b (%)*	E_c *(MPa)*	f'_{co} *(MPa)*
Martinez et al. [179]	1	101.6	406.4				ls-cr-19			35232	68.7
Martinez et al. [179]	1	101.6	406.4				ls-cr-19			22753[m]	68.7
Martinez et al. [179]	1	101.6	406.4				ls-cr-19			34405	68.7
Martinez et al. [179]	1	101.6	406.4				ls-cr-19			34060	68.1
Martinez et al. [179]	1	101.6	406.4				ls-cr-19			37094	68.1
Martinez et al. [179]	1	101.6	406.4				ls-cr-19			34681	68.1
Martinez et al. [179]	1	101.6	203.2				ls-cr-19			10963	21.7
Martinez et al. [179]	1	101.6	203.2				ls-cr-19			11514	21.7
Martinez et al. [179]	1	101.6	203.2				ls-cr-19			23235	42.7
Martinez et al. [179]	1	101.6	203.2				ls-cr-19			21374	42.7
Martinez et al. [179]	1	101.6	203.2				ls-cr-19			32267	58.2
Martinez et al. [179]	1	101.6	203.2				ls-cr-19			32061	58.2
Martinez et al. [179]	1	152.4	609.6				ls-cr-19			22063	22.1
Martinez et al. [179]	1	152.4	609.6				ls-cr-19			23097	22.1
Martinez et al. [179]	1	152.4	609.6				ls-cr-19			22684	22.1
Martinez et al. [179]	1	152.4	609.6				ls-cr-19			21236	37.7
Martinez et al. [179]	1	152.4	609.6				ls-cr-19			21443	37.7
Martinez et al. [179]	1	152.4	609.6				ls-cr-19			25855	53.3
Martinez et al. [179]	1	152.4	609.6				ls-cr-19			25855	53.3
Martinez et al. [179]	1	152.4	609.6				ls-cr-19			26131	53.3
Mesbah et al. [180]	3	100	200	7	0.30	2450	ml-cr-14			37077	62.0
Mesbah et al. [180]	3	100	200	7	0.36	2400	ml-cr-14			34697	42.0
Mesbah et al. [180]	3	100	200	7	0.45	2370	ml-cr-14			23925	29.0
Mesbah et al. [180]	3	100	200	28	0.30	2450	ml-cr-14			41336	75.0
Mesbah et al. [180]	3	100	200	28	0.36	2400	ml-cr-14			36200	56.0
Mesbah et al. [180]	3	100	200	28	0.45	2370	ml-cr-14			32317	39.0
Mostofinejad and Nozhati [181]	4	100	200	7	0.44	2354	ls-9.5			34000	45.5
Mostofinejad and Nozhati [181]	4	100	200	7	0.44	2348	ls-9.5	5.0		35300	49.7
Mostofinejad and Nozhati [181]	4	100	200	7	0.44	2341	ls-9.5	10.0		37000	54.2
Mostofinejad and Nozhati [181]	4	100	200	7	0.44	2334	ls-9.5	15.0		36400	50.8
Mostofinejad and Nozhati [181]	4	100	200	7	0.44	2328	ls-9.5	20.0		35200	48.5
Mostofinejad and Nozhati [181]	4	100	200	7	0.34	2390	ls-9.5			36100	58.7
Mostofinejad and Nozhati [181]	4	100	200	7	0.34	2376	ls-9.5	5.0		37500	61.2
Mostofinejad and Nozhati [181]	4	100	200	7	0.34	2373	ls-9.5	10.0		36800	70.7
Mostofinejad and Nozhati [181]	4	100	200	7	0.34	2360	ls-9.5	15.0		39000	65.3
Mostofinejad and Nozhati [181]	4	100	200	7	0.34	2355	ls-9.5	20.0		37100	61.4
Mostofinejad and Nozhati [181]	4	100	200	7	0.27	2420	ls-9.5			38800	67.2
Mostofinejad and Nozhati [181]	4	100	200	7	0.27	2410	ls-9.5	5.0		38500	70.8
Mostofinejad and Nozhati [181]	4	100	200	7	0.27	2400	ls-9.5	10.0		38600	79.6
Mostofinejad and Nozhati [181]	4	100	200	7	0.27	2390	ls-9.5	15.0		40100	75.2
Mostofinejad and Nozhati [181]	4	100	200	7	0.27	2380	ls-9.5	20.0		42100	72.6
Mostofinejad and Nozhati [181]	4	100	200	28	0.44	2354	ls-9.5			37000	61.4
Mostofinejad and Nozhati [181]	4	100	200	28	0.44	2348	ls-9.5	5.0		38500	67.8
Mostofinejad and Nozhati [181]	4	100	200	28	0.44	2341	ls-9.5	10.0		37100	72.7
Mostofinejad and Nozhati [181]	4	100	200	28	0.44	2334	ls-9.5	15.0		40200	68.9
Mostofinejad and Nozhati [181]	4	100	200	28	0.44	2328	ls-9.5	20.0		39200	65.6
Mostofinejad and Nozhati [181]	4	100	200	28	0.34	2390	ls-9.5			38600	73.3
Mostofinejad and Nozhati [181]	4	100	200	28	0.34	2376	ls-9.5	5.0		40300	76.5
Mostofinejad and Nozhati [181]	4	100	200	28	0.34	2373	ls-9.5	10.0		41500	86.2
Mostofinejad and Nozhati [181]	4	100	200	28	0.34	2360	ls-9.5	15.0		42300	81.7
Mostofinejad and Nozhati [181]	4	100	200	28	0.34	2355	ls-9.5	20.0		42000	74.8
Mostofinejad and Nozhati [181]	4	100	200	28	0.27	2420	ls-9.5			41600	79.6
Mostofinejad and Nozhati [181]	4	100	200	28	0.27	2410	ls-9.5	5.0		41500	84.3
Mostofinejad and Nozhati [181]	4	100	200	28	0.27	2400	ls-9.5	10.0		43200	91.7
Mostofinejad and Nozhati [181]	4	100	200	28	0.27	2390	ls-9.5	15.0		42600	89.1
Mostofinejad and Nozhati [181]	4	100	200	28	0.27	2380	ls-9.5	20.0		42000	84.6
Mostofinejad and Nozhati [181]	4	100	200	91	0.44	2354	ls-9.5			40400	74.6
Mostofinejad and Nozhati [181]	4	100	200	91	0.44	2348	ls-9.5	5.0		40800	78.8
Mostofinejad and Nozhati [181]	4	100	200	91	0.44	2341	ls-9.5	10.0		42100	86.0
Mostofinejad and Nozhati [181]	4	100	200	91	0.44	2334	ls-9.5	15.0		41000	81.7
Mostofinejad and Nozhati [181]	4	100	200	91	0.44	2328	ls-9.5	20.0		41800	77.4
Mostofinejad and Nozhati [181]	4	100	200	91	0.34	2390	ls-9.5			41600	81.0
Mostofinejad and Nozhati [181]	4	100	200	91	0.34	2376	ls-9.5	5.0		42800	84.5
Mostofinejad and Nozhati [181]	4	100	200	91	0.34	2373	ls-9.5	10.0		43100	95.4
Mostofinejad and Nozhati [181]	4	100	200	91	0.34	2360	ls-9.5	15.0		43300	98.1
Mostofinejad and Nozhati [181]	4	100	200	91	0.34	2355	ls-9.5	20.0		42700	82.8
Mostofinejad and Nozhati [181]	4	100	200	91	0.27	2420	ls-9.5			42200	87.3
Mostofinejad and Nozhati [181]	4	100	200	91	0.27	2410	ls-9.5	5.0		44400	91.7
Mostofinejad and Nozhati [181]	4	100	200	91	0.27	2400	ls-9.5	10.0		45400	105.0
Mostofinejad and Nozhati [181]	4	100	200	91	0.27	2390	ls-9.5	15.0		44700	116.0
Mostofinejad and Nozhati [181]	4	100	200	91	0.27	2380	ls-9.5	20.0		44900	110.0
Mostofinejad and Nozhati [181]	4	100	200	7	0.45	2300	ad-9.5			29900	50.6
Mostofinejad and Nozhati [181]	4	100	200	7	0.45	2294	ad-9.5	5.0		32500	55.9
Mostofinejad and Nozhati [181]	4	100	200	7	0.45	2287	ad-9.5	10.0		31800	58.7
Mostofinejad and Nozhati [181]	4	100	200	7	0.45	2280	ad-9.5	15.0		33600	56.8
Mostofinejad and Nozhati [181]	4	100	200	7	0.45	2274	ad-9.5	20.0		35500	55.2
Mostofinejad and Nozhati [181]	4	100	200	7	0.34	2336	ad-9.5			33700	61.5
Mostofinejad and Nozhati [181]	4	100	200	7	0.34	2322	ad-9.5	5.0		34300	66.8
Mostofinejad and Nozhati [181]	4	100	200	7	0.34	2319	ad-9.5	10.0		36300	70.9
Mostofinejad and Nozhati [181]	4	100	200	7	0.34	2306	ad-9.5	15.0		35400	68.2

Source	*n*	*B (mm)*	*H (mm)*	*Age (d)*	*w/c*	$\rho_{c,f}$ *(kg/m^3)*	*Aggregate properties*[p]	*sf/c (%)*	*ma/b (%)*	E_c *(MPa)*	f'_{co} *(MPa)*
Mostofinejad and Nozhati [181]	4	100	200	7	0.34	2301	ad-9.5	20.0		34400	66.3
Mostofinejad and Nozhati [181]	4	100	200	7	0.28	2367	ad-9.5			34200	71.9
Mostofinejad and Nozhati [181]	4	100	200	7	0.28	2357	ad-9.5	5.0		35800	78.2
Mostofinejad and Nozhati [181]	4	100	200	7	0.28	2347	ad-9.5	10.0		37000	83.5
Mostofinejad and Nozhati [181]	4	100	200	7	0.28	2337	ad-9.5	15.0		39300	80.9
Mostofinejad and Nozhati [181]	4	100	200	7	0.28	2327	ad-9.5	20.0		37200	79.7
Mostofinejad and Nozhati [181]	4	100	200	28	0.45	2300	ad-9.5			36200	64.4
Mostofinejad and Nozhati [181]	4	100	200	28	0.45	2294	ad-9.5	5.0		37600	71.1
Mostofinejad and Nozhati [181]	4	100	200	28	0.45	2287	ad-9.5	10.0		36300	74.0
Mostofinejad and Nozhati [181]	4	100	200	28	0.45	2280	ad-9.5	15.0		36700	72.0
Mostofinejad and Nozhati [181]	4	100	200	28	0.45	2274	ad-9.5	20.0		37300	70.0
Mostofinejad and Nozhati [181]	4	100	200	28	0.34	2336	ad-9.5			36700	75.4
Mostofinejad and Nozhati [181]	4	100	200	28	0.34	2322	ad-9.5	5.0		34400	81.8
Mostofinejad and Nozhati [181]	4	100	200	28	0.34	2319	ad-9.5	10.0		38200	86.8
Mostofinejad and Nozhati [181]	4	100	200	28	0.34	2306	ad-9.5	15.0		39600	84.3
Mostofinejad and Nozhati [181]	4	100	200	28	0.34	2301	ad-9.5	20.0		36200	81.1
Mostofinejad and Nozhati [181]	4	100	200	28	0.28	2367	ad-9.5			38500	84.8
Mostofinejad and Nozhati [181]	4	100	200	28	0.28	2357	ad-9.5	5.0		40100	92.5
Mostofinejad and Nozhati [181]	4	100	200	28	0.28	2347	ad-9.5	10.0		43000	97.6
Mostofinejad and Nozhati [181]	4	100	200	28	0.28	2337	ad-9.5	15.0		40800	97.9
Mostofinejad and Nozhati [181]	4	100	200	28	0.28	2327	ad-9.5	20.0		38900	94.8
Mostofinejad and Nozhati [181]	4	100	200	91	0.45	2300	ad-9.5			36800	76.7
Mostofinejad and Nozhati [181]	4	100	200	91	0.45	2294	ad-9.5	5.0		37200	83.1
Mostofinejad and Nozhati [181]	4	100	200	91	0.45	2287	ad-9.5	10.0		38400	86.2
Mostofinejad and Nozhati [181]	4	100	200	91	0.45	2280	ad-9.5	15.0		39000	86.6
Mostofinejad and Nozhati [181]	4	100	200	91	0.45	2274	ad-9.5	20.0		38100	82.8
Mostofinejad and Nozhati [181]	4	100	200	91	0.34	2336	ad-9.5			37900	90.2
Mostofinejad and Nozhati [181]	4	100	200	91	0.34	2322	ad-9.5	5.0		39500	98.8
Mostofinejad and Nozhati [181]	4	100	200	91	0.34	2319	ad-9.5	10.0		41600	102.0
Mostofinejad and Nozhati [181]	4	100	200	91	0.34	2306	ad-9.5	15.0		42000	104.0
Mostofinejad and Nozhati [181]	4	100	200	91	0.34	2301	ad-9.5	20.0		38900	98.5
Mostofinejad and Nozhati [181]	4	100	200	91	0.28	2367	ad-9.5			39500	100.9
Mostofinejad and Nozhati [181]	4	100	200	91	0.28	2357	ad-9.5	5.0		41500	109.5
Mostofinejad and Nozhati [181]	4	100	200	91	0.28	2347	ad-9.5	10.0		41600	114.2
Mostofinejad and Nozhati [181]	4	100	200	91	0.28	2337	ad-9.5	15.0		42600	119.3
Mostofinejad and Nozhati [181]	4	100	200	91	0.28	2327	ad-9.5	20.0		42200	116.2
Mostofinejad and Nozhati [181]	4	100	200	7	0.44	2433	qz-9.5			38200	57.9
Mostofinejad and Nozhati [181]	4	100	200	7	0.44	2427	qz-9.5	5.0		39200	63.6
Mostofinejad and Nozhati [181]	4	100	200	7	0.44	2420	qz-9.5	10.0		39800	70.5
Mostofinejad and Nozhati [181]	4	100	200	7	0.44	2413	qz-9.5	15.0		41200	65.5
Mostofinejad and Nozhati [181]	4	100	200	7	0.44	2407	qz-9.5	20.0		39200	61.2
Mostofinejad and Nozhati [181]	4	100	200	7	0.33	2470	qz-9.5			38300	70.8
Mostofinejad and Nozhati [181]	4	100	200	7	0.34	2456	qz-9.5	5.0		39400	75.4
Mostofinejad and Nozhati [181]	4	100	200	7	0.33	2453	qz-9.5	10.0		42000	83.7
Mostofinejad and Nozhati [181]	4	100	200	7	0.34	2440	qz-9.5	15.0		42100	77.2
Mostofinejad and Nozhati [181]	4	100	200	7	0.33	2435	qz-9.5	20.0		40900	72.9
Mostofinejad and Nozhati [181]	4	100	200	7	0.27	2500	qz-9.5			41000	86.1
Mostofinejad and Nozhati [181]	4	100	200	7	0.27	2490	qz-9.5	5.0		43900	92.2
Mostofinejad and Nozhati [181]	4	100	200	7	0.27	2480	qz-9.5	10.0		45100	105.0
Mostofinejad and Nozhati [181]	4	100	200	7	0.27	2470	qz-9.5	15.0		43900	98.2
Mostofinejad and Nozhati [181]	4	100	200	7	0.27	2460	qz-9.5	20.0		45700	95.4
Mostofinejad and Nozhati [181]	4	100	200	28	0.44	2433	qz-9.5			40900	75.7
Mostofinejad and Nozhati [181]	4	100	200	28	0.44	2427	qz-9.5	5.0		41600	82.5
Mostofinejad and Nozhati [181]	4	100	200	28	0.44	2420	qz-9.5	10.0		43500	89.2
Mostofinejad and Nozhati [181]	4	100	200	28	0.44	2413	qz-9.5	15.0		43000	84.3
Mostofinejad and Nozhati [181]	4	100	200	28	0.44	2407	qz-9.5	20.0		43500	79.4
Mostofinejad and Nozhati [181]	4	100	200	28	0.33	2470	qz-9.5			45000	85.7
Mostofinejad and Nozhati [181]	4	100	200	28	0.34	2456	qz-9.5	5.0		45200	90.9
Mostofinejad and Nozhati [181]	4	100	200	28	0.33	2453	qz-9.5	10.0		44400	102.0
Mostofinejad and Nozhati [181]	4	100	200	28	0.34	2440	qz-9.5	15.0		44500	95.9
Mostofinejad and Nozhati [181]	4	100	200	28	0.33	2435	qz-9.5	20.0		44300	88.7
Mostofinejad and Nozhati [181]	4	100	200	28	0.27	2500	qz-9.5			43700	95.3
Mostofinejad and Nozhati [181]	4	100	200	28	0.27	2490	qz-9.5	5.0		44800	102.0
Mostofinejad and Nozhati [181]	4	100	200	28	0.27	2480	qz-9.5	10.0		46400	115.0
Mostofinejad and Nozhati [181]	4	100	200	28	0.27	2470	qz-9.5	15.0		46600	117.0
Mostofinejad and Nozhati [181]	4	100	200	28	0.27	2460	qz-9.5	20.0		49100	109.0
Mostofinejad and Nozhati [181]	4	100	200	91	0.44	2433	qz-9.5			44400	89.1
Mostofinejad and Nozhati [181]	4	100	200	91	0.44	2427	qz-9.5	5.0		45600	94.0
Mostofinejad and Nozhati [181]	4	100	200	91	0.44	2420	qz-9.5	10.0		44300	99.8
Mostofinejad and Nozhati [181]	4	100	200	91	0.44	2413	qz-9.5	15.0		45400	103.0
Mostofinejad and Nozhati [181]	4	100	200	91	0.44	2407	qz-9.5	20.0		46100	92.7
Mostofinejad and Nozhati [181]	4	100	200	91	0.33	2470	qz-9.5			46600	107.0
Mostofinejad and Nozhati [181]	4	100	200	91	0.34	2456	qz-9.5	5.0		47500	117.0
Mostofinejad and Nozhati [181]	4	100	200	91	0.33	2453	qz-9.5	10.0		47100	121.0
Mostofinejad and Nozhati [181]	4	100	200	91	0.34	2440	qz-9.5	15.0		49000	126.0
Mostofinejad and Nozhati [181]	4	100	200	91	0.33	2435	qz-9.5	20.0		47900	116.0
Mostofinejad and Nozhati [181]	4	100	200	91	0.27	2500	qz-9.5			48300	118.0
Mostofinejad and Nozhati [181]	4	100	200	91	0.27	2490	qz-9.5	5.0		47200	125.0
Mostofinejad and Nozhati [181]	4	100	200	91	0.27	2480	qz-9.5	10.0		50200	132.0
Mostofinejad and Nozhati [181]	4	100	200	91	0.27	2470	qz-9.5	15.0		49700	143.0

Source	*n*	*B (mm)*	*H (mm)*	*Age (d)*	*w/c*	$\rho_{c,f}$ *(kg/m³)*	*Aggregate properties*[p]	*sf/c (%)*	*ma/b (%)*	E_c *(MPa)*	f'_{co} *(MPa)*
Mostofinejad and Nozhati [181]	4	100	200	91	0.27	2460	qz-9.5	20.0		49600	136.0
Nassif [182]	3	100	200	1	0.40	2390	gn-cr-9.5				19.8
Nassif [182]	3	100	200	1	0.40	2390	gn-cr-9.5		10.1[f]		21.4
Nassif [182]	3	100	200	1	0.40	2389	gn-cr-9.5		19.9[f]		19.4
Nassif [182]	3	100	200	1	0.40	2388	gn-cr-9.5		30.0[f]		15.0
Nassif [182]	3	100	200	1	0.40	2391	gn-cr-9.5	5.0			29.0
Nassif [182]	3	100	200	1	0.40	2392	gn-cr-9.5	10.1			30.5
Nassif [182]	3	100	200	1	0.40	2392	gn-cr-9.5	15.1			25.1
Nassif [182]	3	100	200	1	0.40	2392	gn-cr-9.5	5.0	10.1[f]		27.6
Nassif [182]	3	100	200	1	0.40	2391	gn-cr-9.5	5.0	19.9[f]		22.3
Nassif [182]	3	100	200	1	0.40	2391	gn-cr-9.5	10.1	19.9[f]		13.9
Nassif [182]	3	100	200	1	0.40	2392	gn-cr-9.5	15.1	19.9[f]		14.0
Nassif [182]	3	100	200	1	0.30	2408	gn-cr-9.5	10.0		29600	40.9
Nassif [182]	3	100	200	1	0.30	2408	gn-cr-9.5	10.0		32400	37.0
Nassif [182]	3	100	200	1	0.30	2408	gn-cr-9.5	10.0		29600	41.0
Nassif [182]	3	100	200	1	0.30	2408	gn-cr-9.5	10.0	20.1[f]	32600	26.9
Nassif [182]	3	100	200	1	0.30	2408	gn-cr-9.5	10.0	20.1[f]	29200	27.7
Nassif [182]	3	100	200	1	0.30	2408	gn-cr-9.5	10.0	20.1[f]	27600	26.1
Nassif [182]	3	100	200	1	0.30	2408	gn-cr-9.5	10.0	20.1[s]	32800	46.8
Nassif [182]	3	100	200	1	0.30	2408	gn-cr-9.5	10.0	20.1[s]	30100	40.1
Nassif [182]	3	100	200	1	0.30	2408	gn-cr-9.5	10.0	20.1[s]	29600	46.2
Nassif [182]	3	100	200	1	0.36	2383	gn-cr-9.5	10.0		28200	37.6
Nassif [182]	3	100	200	1	0.36	2383	gn-cr-9.5	10.0		25900	30.0
Nassif [182]	3	100	200	1	0.36	2383	gn-cr-9.5	10.0		28100	23.8
Nassif [182]	3	100	200	1	0.36	2380	gn-cr-9.5	10.0		29500	40.6
Nassif [182]	3	100	200	1	0.36	2380	gn-cr-9.5	10.0		29900	39.1
Nassif [182]	3	100	200	1	0.36	2380	gn-cr-9.5	10.0		29100	37.3
Nassif [182]	3	100	200	1	0.36	2380	gn-cr-9.5	10.0	20.0[f]	23500	24.3
Nassif [182]	3	100	200	1	0.36	2380	gn-cr-9.5	10.0	20.0[f]	22500	23.5
Nassif [182]	3	100	200	1	0.36	2380	gn-cr-9.5	10.0	20.0[f]	23100	23.0
Nassif [182]	3	100	200	1	0.36	2380	gn-cr-9.5	10.0	20.0[s]	30900	33.1
Nassif [182]	3	100	200	1	0.36	2380	gn-cr-9.5	10.0	20.0[s]	26300	40.6
Nassif [182]	3	100	200	1	0.36	2380	gn-cr-9.5	10.0	20.0[s]	29000	29.4
Nassif [182]	3	100	200	3	0.40	2390	gn-cr-9.5			24000	36.6
Nassif [182]	3	100	200	3	0.40	2390	gn-cr-9.5		10.1[f]	26200	32.3
Nassif [182]	3	100	200	3	0.40	2389	gn-cr-9.5		19.9[f]	26100	29.3
Nassif [182]	3	100	200	3	0.40	2388	gn-cr-9.5		30.0[f]	24300	26.8
Nassif [182]	3	100	200	3	0.40	2391	gn-cr-9.5	5.0		28600	39.6
Nassif [182]	3	100	200	3	0.40	2392	gn-cr-9.5	10.1		28500	39.6
Nassif [182]	3	100	200	3	0.40	2392	gn-cr-9.5	15.1		25800	39.2
Nassif [182]	3	100	200	3	0.40	2392	gn-cr-9.5	5.0	10.1[f]	27000	36.5
Nassif [182]	3	100	200	3	0.40	2391	gn-cr-9.5	5.0	19.9[f]	24000	29.3
Nassif [182]	3	100	200	3	0.40	2391	gn-cr-9.5	10.1	19.9[f]	22000	21.5
Nassif [182]	3	100	200	3	0.40	2392	gn-cr-9.5	15.1	19.9[f]	22600	24.9
Nassif [182]	3	100	200	3	0.44	2379	gn-cr-9.5	5.0	9.9[f]	24200	24.0
Nassif [182]	3	100	200	3	0.44	2378	gn-cr-9.5	5.0	14.9[f]	22800	22.3
Nassif [182]	3	100	200	3	0.40	2389	gn-cr-9.5	9.0	18.1[f]	28700	38.6
Nassif [182]	3	100	200	3	0.38	2394	gn-cr-9.5	5.0	10.0[f]	29900	39.1
Nassif [182]	3	100	200	3	0.38	2393	gn-cr-9.5	5.0	14.9[f]	25500	36.1
Nassif [182]	3	100	200	3	0.38	2396	gn-cr-9.5	5.0	14.9[f]	30500	43.1
Nassif [182]	3	100	200	3	0.38	2411	gn-cr-9.5	7.1	15.0[f]		47.3
Nassif [182]	3	100	200	3	0.38	2411	gn-cr-9.5	4.9	15.0[f]	28500	48.6
Nassif [182]	3	100	200	3	0.30	2446	gn-cr-9.5	7.5	14.9[f]	31900	49.4
Nassif [182]	3	100	200	3	0.32	2410	gn-cr-9.5	5.3	10.5[f]	31000	49.4
Nassif [182]	3	100	200	3	0.30	2408	gn-cr-9.5	10.0		35300	51.3
Nassif [182]	3	100	200	3	0.30	2408	gn-cr-9.5	10.0		32000	53.6
Nassif [182]	3	100	200	3	0.30	2408	gn-cr-9.5	10.0		31900	50.1
Nassif [182]	3	100	200	3	0.30	2408	gn-cr-9.5	10.0	20.1[f]	30500	40.6
Nassif [182]	3	100	200	3	0.30	2408	gn-cr-9.5	10.0	20.1[f]	27100	42.8
Nassif [182]	3	100	200	3	0.30	2408	gn-cr-9.5	10.0	20.1[f]	28400	38.6
Nassif [182]	3	100	200	3	0.30	2408	gn-cr-9.5	10.0	20.1[s]	34400	59.0
Nassif [182]	3	100	200	3	0.30	2408	gn-cr-9.5	10.0	20.1[s]	32700	54.6
Nassif [182]	3	100	200	3	0.30	2408	gn-cr-9.5	10.0	20.1[s]	27800	52.1
Nassif [182]	3	100	200	3	0.36	2383	gn-cr-9.5	10.0		29300	41.8
Nassif [182]	3	100	200	3	0.36	2383	gn-cr-9.5	10.0		28700	41.3
Nassif [182]	3	100	200	3	0.36	2383	gn-cr-9.5	10.0		27800	42.3
Nassif [182]	3	100	200	3	0.36	2380	gn-cr-9.5	10.0		32600	47.1
Nassif [182]	3	100	200	3	0.36	2380	gn-cr-9.5	10.0		33500	44.6
Nassif [182]	3	100	200	3	0.36	2380	gn-cr-9.5	10.0		31300	46.1
Nassif [182]	3	100	200	3	0.36	2380	gn-cr-9.5	10.0	20.0[f]	27100	30.5
Nassif [182]	3	100	200	3	0.36	2380	gn-cr-9.5	10.0	20.0[f]	25300	31.8
Nassif [182]	3	100	200	3	0.36	2380	gn-cr-9.5	10.0	20.0[f]	25400	30.5
Nassif [182]	3	100	200	3	0.36	2380	gn-cr-9.5	10.0	20.0[s]	28400	42.8
Nassif [182]	3	100	200	3	0.36	2380	gn-cr-9.5	10.0	20.0[s]	26800	42.0
Nassif [182]	3	100	200	3	0.36	2380	gn-cr-9.5	10.0	20.0[s]	29800	38.4
Nassif [182]	3	100	200	7	0.40	2390	gn-cr-9.5			27300	40.0
Nassif [182]	3	100	200	7	0.40	2390	gn-cr-9.5		10.1[f]	30800	40.1
Nassif [182]	3	100	200	7	0.39	2389	gn-cr-9.5		19.9[f]	29600	36.0
Nassif [182]	3	100	200	7	0.39	2388	gn-cr-9.5		30.0[f]	27700	30.8
Nassif [182]	3	100	200	7	0.40	2391	gn-cr-9.5	5.0		31200	45.9

Source	*n*	*B (mm)*	*H (mm)*	*Age (d)*	*w/c*	$\rho_{c,f}$ *(kg/m³)*	*Aggregate properties*[p]	*sf/c (%)*	*ma/b (%)*	E_c *(MPa)*	f'_{co} *(MPa)*
Nassif [182]	3	100	200	7	0.40	2392	gn-cr-9.5	10.1		30300	43.5
Nassif [182]	3	100	200	7	0.40	2392	gn-cr-9.5	15.1		26700	40.7
Nassif [182]	3	100	200	7	0.40	2392	gn-cr-9.5	5.0	10.1[f]	29400	43.9
Nassif [182]	3	100	200	7	0.40	2391	gn-cr-9.5	5.0	19.9[f]	25200	32.9
Nassif [182]	3	100	200	7	0.40	2391	gn-cr-9.5	10.1	19.9[f]	22400	29.4
Nassif [182]	3	100	200	7	0.40	2392	gn-cr-9.5	15.1	19.9[f]	24500	28.7
Nassif [182]	3	100	200	7	0.44	2379	gn-cr-9.5	5.0	9.9[f]	26600	27.9
Nassif [182]	3	100	200	7	0.44	2378	gn-cr-9.5	5.0	14.9[f]	22400	25.5
Nassif [182]	3	100	200	7	0.40	2388	gn-cr-9.5	6.9	14.9[f]	28000	33.5
Nassif [182]	3	100	200	7	0.40	2389	gn-cr-9.5	9.0	18.1[f]	28700	37.1
Nassif [182]	3	100	200	7	0.38	2394	gn-cr-9.5	5.0	10.0[f]	31200	42.8
Nassif [182]	3	100	200	7	0.38	2393	gn-cr-9.5	5.0	14.9[f]	31700	35.2
Nassif [182]	3	100	200	7	0.38	2396	gn-cr-9.5	5.0	14.9[f]	31700	50.7
Nassif [182]	3	100	200	7	0.34	2411	gn-cr-9.5	7.1	15.0[f]	33000	56.3
Nassif [182]	3	100	200	7	0.34	2411	gn-cr-9.5	4.9	15.0[f]	31400	53.9
Nassif [182]	3	100	200	7	0.30	2446	gn-cr-9.5	7.5	14.9[f]		60.5
Nassif [182]	3	100	200	7	0.32	2410	gn-cr-9.5	5.3	10.5[f]	34100	60.5
Nassif [182]	3	100	200	7	0.30	2408	gn-cr-9.5	10.0		30400	62.0
Nassif [182]	3	100	200	7	0.30	2408	gn-cr-9.5	10.0		31800	59.0
Nassif [182]	3	100	200	7	0.30	2408	gn-cr-9.5	10.0		27800	57.1
Nassif [182]	3	100	200	7	0.30	2408	gn-cr-9.5	10.0	20.1[f]	30500	46.8
Nassif [182]	3	100	200	7	0.30	2408	gn-cr-9.5	10.0	20.1[f]	27900	46.2
Nassif [182]	3	100	200	7	0.30	2408	gn-cr-9.5	10.0	20.1[f]	28400	41.3
Nassif [182]	3	100	200	7	0.30	2408	gn-cr-9.5	10.0	20.1[s]	35100	57.9
Nassif [182]	3	100	200	7	0.30	2408	gn-cr-9.5	10.0	20.1[s]	30500	57.6
Nassif [182]	3	100	200	7	0.30	2408	gn-cr-9.5	10.0	20.1[s]	30700	51.6
Nassif [182]	3	100	200	7	0.36	2383	gn-cr-9.5	10.0		30600	45.3
Nassif [182]	3	100	200	7	0.36	2383	gn-cr-9.5	10.0		28800	46.0
Nassif [182]	3	100	200	7	0.36	2383	gn-cr-9.5	10.0		25700	41.6
Nassif [182]	3	100	200	7	0.36	2380	gn-cr-9.5	10.0		35700	51.6
Nassif [182]	3	100	200	7	0.36	2380	gn-cr-9.5	10.0		30100	49.8
Nassif [182]	3	100	200	7	0.36	2380	gn-cr-9.5	10.0		29500	49.9
Nassif [182]	3	100	200	7	0.36	2380	gn-cr-9.5	10.0	20.0[f]	25600	34.0
Nassif [182]	3	100	200	7	0.36	2380	gn-cr-9.5	10.0	20.0[f]	23300	33.5
Nassif [182]	3	100	200	7	0.36	2380	gn-cr-9.5	10.0	20.0[f]	23700	33.5
Nassif [182]	3	100	200	7	0.36	2380	gn-cr-9.5	10.0	20.0[s]	32400	48.9
Nassif [182]	3	100	200	7	0.36	2380	gn-cr-9.5	10.0	20.0[s]	29300	49.4
Nassif [182]	3	100	200	7	0.36	2380	gn-cr-9.5	10.0	20.0[s]	29100	41.7
Nassif [182]	3	100	200	14	0.40	2390	gn-cr-9.5			27700	43.8
Nassif [182]	3	100	200	14	0.40	2390	gn-cr-9.5		10.1[f]	31900	41.6
Nassif [182]	3	100	200	14	0.39	2389	gn-cr-9.5		19.9[f]	29000	39.0
Nassif [182]	3	100	200	14	0.39	2388	gn-cr-9.5		30.0[f]	29200	35.5
Nassif [182]	3	100	200	14	0.40	2391	gn-cr-9.5	5.0		31800	44.2
Nassif [182]	3	100	200	14	0.40	2392	gn-cr-9.5	10.1		31500	46.9
Nassif [182]	3	100	200	14	0.40	2392	gn-cr-9.5	15.1		30400	46.6
Nassif [182]	3	100	200	14	0.40	2392	gn-cr-9.5	5.0	10.1[f]	30000	50.8
Nassif [182]	3	100	200	14	0.40	2391	gn-cr-9.5	5.0	19.9[f]	26700	41.1
Nassif [182]	3	100	200	14	0.40	2391	gn-cr-9.5	10.1	19.9[f]	22600	32.9
Nassif [182]	3	100	200	14	0.40	2392	gn-cr-9.5	15.1	19.9[f]	26800	36.8
Nassif [182]	3	100	200	14	0.44	2379	gn-cr-9.5	5.0	9.9[f]	28500	35.3
Nassif [182]	3	100	200	14	0.44	2378	gn-cr-9.5	5.0	14.9[f]	22900	28.9
Nassif [182]	3	100	200	14	0.40	2388	gn-cr-9.5	6.9	14.9[f]	32700	36.4
Nassif [182]	3	100	200	14	0.40	2389	gn-cr-9.5	9.0	18.1[f]	29800	44.2
Nassif [182]	3	100	200	14	0.38	2394	gn-cr-9.5	5.0	10.0[f]	34600	51.4
Nassif [182]	3	100	200	14	0.38	2393	gn-cr-9.5	5.0	14.9[f]	34900	49.6
Nassif [182]	3	100	200	14	0.38	2396	gn-cr-9.5	5.0	14.9[f]	34400	57.5
Nassif [182]	3	100	200	14	0.34	2411	gn-cr-9.5	7.1	15.0[f]	34600	62.8
Nassif [182]	3	100	200	14	0.34	2411	gn-cr-9.5	4.9	15.0[f]	33400	58.9
Nassif [182]	3	100	200	14	0.30	2446	gn-cr-9.5	7.5	14.9[f]		70.0
Nassif [182]	3	100	200	14	0.32	2410	gn-cr-9.5	5.3	10.5[f]	35900	70.0
Nassif [182]	3	100	200	14	0.30	2408	gn-cr-9.5	10.0		37100	68.7
Nassif [182]	3	100	200	14	0.30	2408	gn-cr-9.5	10.0		30700	60.8
Nassif [182]	3	100	200	14	0.30	2408	gn-cr-9.5	10.0		31600	60.1
Nassif [182]	3	100	200	14	0.30	2408	gn-cr-9.5	10.0	20.1[f]	30600	51.3
Nassif [182]	3	100	200	14	0.30	2408	gn-cr-9.5	10.0	20.1[f]	28500	47.7
Nassif [182]	3	100	200	14	0.30	2408	gn-cr-9.5	10.0	20.1[f]	29400	49.0
Nassif [182]	3	100	200	14	0.30	2408	gn-cr-9.5	10.0	20.1[s]	35600	66.9
Nassif [182]	3	100	200	14	0.30	2408	gn-cr-9.5	10.0	20.1[s]	32300	60.1
Nassif [182]	3	100	200	14	0.30	2408	gn-cr-9.5	10.0	20.1[s]	29600	51.7
Nassif [182]	3	100	200	14	0.36	2383	gn-cr-9.5	10.0		29000	46.1
Nassif [182]	3	100	200	14	0.36	2383	gn-cr-9.5	10.0		28100	48.3
Nassif [182]	3	100	200	14	0.36	2383	gn-cr-9.5	10.0		24700	38.4
Nassif [182]	3	100	200	14	0.36	2380	gn-cr-9.5	10.0		32400	56.5
Nassif [182]	3	100	200	14	0.36	2380	gn-cr-9.5	10.0		29600	52.9
Nassif [182]	3	100	200	14	0.36	2380	gn-cr-9.5	10.0		27700	53.1
Nassif [182]	3	100	200	14	0.36	2380	gn-cr-9.5	10.0	20.0[f]	30000	37.3
Nassif [182]	3	100	200	14	0.36	2380	gn-cr-9.5	10.0	20.0[f]	24400	36.2
Nassif [182]	3	100	200	14	0.36	2380	gn-cr-9.5	10.0	20.0[f]	22500	36.8
Nassif [182]	3	100	200	14	0.36	2380	gn-cr-9.5	10.0	20.0[s]	34500	54.3
Nassif [182]	3	100	200	14	0.36	2380	gn-cr-9.5	10.0	20.0[s]	29000	53.5

Source	*n*	*B (mm)*	*H (mm)*	*Age (d)*	*w/c*	$\rho_{c,f}$ *(kg/m³)*	*Aggregate properties*[p]	*sf/c (%)*	*ma/b (%)*	E_c *(MPa)*	f'_{co} *(MPa)*
Nassif [182]	3	100	200	14	0.36	2380	gn-cr-9.5	10.0	20.0[s]	26500	50.2
Nassif [182]	3	100	200	28	0.40	2390	gn-cr-9.5			31800	46.6
Nassif [182]	3	100	200	28	0.40	2390	gn-cr-9.5		10.1[f]	37100	49.4
Nassif [182]	3	100	200	28	0.39	2389	gn-cr-9.5		19.9[f]	31600	44.2
Nassif [182]	3	100	200	28	0.39	2388	gn-cr-9.5		30.0[f]	30700	42.7
Nassif [182]	3	100	200	28	0.40	2391	gn-cr-9.5	5.0		32000	52.4
Nassif [182]	3	100	200	28	0.40	2392	gn-cr-9.5	10.1		31900	53.4
Nassif [182]	3	100	200	28	0.40	2392	gn-cr-9.5	15.1		34300	50.1
Nassif [182]	3	100	200	28	0.40	2392	gn-cr-9.5	5.0	10.1[f]	30800	54.9
Nassif [182]	3	100	200	28	0.40	2391	gn-cr-9.5	5.0	19.9[f]	27700	46.0
Nassif [182]	3	100	200	28	0.40	2391	gn-cr-9.5	10.1	19.9[f]	26200	38.1
Nassif [182]	3	100	200	28	0.40	2392	gn-cr-9.5	15.1	19.9[f]	27100	39.8
Nassif [182]	3	100	200	28	0.44	2379	gn-cr-9.5	5.0	9.9[f]	29800	38.2
Nassif [182]	3	100	200	28	0.44	2378	gn-cr-9.5	5.0	14.9[f]	26500	33.8
Nassif [182]	3	100	200	28	0.40	2388	gn-cr-9.5	6.9	14.9[f]	30800	48.0
Nassif [182]	3	100	200	28	0.40	2389	gn-cr-9.5	9.0	18.1[f]	32100	46.6
Nassif [182]	3	100	200	28	0.38	2394	gn-cr-9.5	5.0	10.0[f]	35500	47.6
Nassif [182]	3	100	200	28	0.38	2393	gn-cr-9.5	5.0	14.9[f]	33900	53.4
Nassif [182]	3	100	200	28	0.38	2396	gn-cr-9.5	5.0	14.9[f]	33800	65.4
Nassif [182]	3	100	200	28	0.34	2411	gn-cr-9.5	7.1	15.0[f]		70.2
Nassif [182]	3	100	200	28	0.34	2411	gn-cr-9.5	4.9	15.0[f]	35400	59.0
Nassif [182]	3	100	200	28	0.30	2446	gn-cr-9.5	7.5	14.9[f]	37600	73.5
Nassif [182]	3	100	200	28	0.32	2410	gn-cr-9.5	5.3	10.5[f]	37900	73.5
Nassif [182]	3	100	200	28	0.30	2408	gn-cr-9.5	10.0		36200	70.3
Nassif [182]	3	100	200	28	0.30	2408	gn-cr-9.5	10.0		28000	67.5
Nassif [182]	3	100	200	28	0.30	2408	gn-cr-9.5	10.0		32600	62.8
Nassif [182]	3	100	200	28	0.30	2408	gn-cr-9.5	10.0	20.1	33500	59.8
Nassif [182]	3	100	200	28	0.30	2408	gn-cr-9.5	10.0	20.1	24800	51.0
Nassif [182]	3	100	200	28	0.30	2408	gn-cr-9.5	10.0	20.1	26300	49.9
Nassif [182]	3	100	200	28	0.30	2408	gn-cr-9.5	10.0	20.1[s]	37200	64.8
Nassif [182]	3	100	200	28	0.30	2408	gn-cr-9.5	10.0	20.1[s]	29600	61.5
Nassif [182]	3	100	200	28	0.30	2408	gn-cr-9.5	10.0	20.1[s]	28100	60.4
Nassif [182]	3	100	200	28	0.36	2383	gn-cr-9.5	10.0		32200	56.5
Nassif [182]	3	100	200	28	0.36	2383	gn-cr-9.5	10.0		26000	49.9
Nassif [182]	3	100	200	28	0.36	2383	gn-cr-9.5	10.0		24000	46.3
Nassif [182]	3	100	200	28	0.36	2380	gn-cr-9.5	10.0			60.1
Nassif [182]	3	100	200	28	0.36	2380	gn-cr-9.5	10.0			53.5
Nassif [182]	3	100	200	28	0.36	2380	gn-cr-9.5	10.0			59.2
Nassif [182]	3	100	200	28	0.36	2380	gn-cr-9.5	10.0	20.0[f]		45.2
Nassif [182]	3	100	200	28	0.36	2380	gn-cr-9.5	10.0	20.0[f]		38.4
Nassif [182]	3	100	200	28	0.36	2380	gn-cr-9.5	10.0	20.0[f]		39.1
Nassif [182]	3	100	200	28	0.36	2380	gn-cr-9.5	10.0	20.0[s]		63.8
Nassif [182]	3	100	200	28	0.36	2380	gn-cr-9.5	10.0	20.0[s]		51.0
Nassif [182]	3	100	200	28	0.36	2380	gn-cr-9.5	10.0	20.0[s]		54.1
Nassif [182]	3	100	200	56	0.40	2390	gn-cr-9.5			36000	52.2
Nassif [182]	3	100	200	56	0.40	2390	gn-cr-9.5		10.1[f]	38300	53.1
Nassif [182]	3	100	200	56	0.39	2389	gn-cr-9.5		19.9[f]	38300	51.0
Nassif [182]	3	100	200	56	0.39	2388	gn-cr-9.5		30.0[f]	37500	48.7
Nassif [182]	3	100	200	56	0.40	2391	gn-cr-9.5	5.0		34200	57.6
Nassif [182]	3	100	200	56	0.40	2392	gn-cr-9.5	10.1		35600	58.8
Nassif [182]	3	100	200	56	0.40	2392	gn-cr-9.5	15.1		34900	56.7
Nassif [182]	3	100	200	56	0.40	2392	gn-cr-9.5	5.0	10.1[f]	33400	57.8
Nassif [182]	3	100	200	56	0.40	2391	gn-cr-9.5	5.0	19.9[f]	30300	49.6
Nassif [182]	3	100	200	56	0.40	2391	gn-cr-9.5	10.1	19.9[f]	30100	42.5
Nassif [182]	3	100	200	56	0.40	2392	gn-cr-9.5	15.1	19.9[f]	30600	47.5
Nassif [182]	3	100	200	90	0.40	2390	gn-cr-9.5				54.6
Nassif [182]	3	100	200	90	0.40	2390	gn-cr-9.5		10.1[f]		57.1
Nassif [182]	3	100	200	90	0.39	2389	gn-cr-9.5		19.9[f]		56.1
Nassif [182]	3	100	200	90	0.39	2388	gn-cr-9.5		30.0[f]		52.1
Nassif [182]	3	100	200	90	0.40	2391	gn-cr-9.5	5.0			54.5
Nassif [182]	3	100	200	90	0.40	2392	gn-cr-9.5	10.1			57.3
Nassif [182]	3	100	200	90	0.40	2392	gn-cr-9.5	15.1			52.1
Nassif [182]	3	100	200	90	0.40	2392	gn-cr-9.5	5.0	10.1[f]		64.5
Nassif [182]	3	100	200	90	0.40	2391	gn-cr-9.5	5.0	19.9[f]		53.6
Nassif [182]	3	100	200	90	0.40	2391	gn-cr-9.5	10.1	19.9[f]		42.1
Nassif [182]	3	100	200	90	0.40	2392	gn-cr-9.5	15.1	19.9[f]		46.8
Oluokun et al. [183]	3	152.4	304.8	1	0.39	2383	st-cr-25.4			26196	24.8
Oluokun et al. [183]	3	152.4	304.8	2	0.39	2383	st-cr-25.4			27618	27.4
Oluokun et al. [183]	3	152.4	304.8	3	0.39	2383	st-cr-25.4			28848	29.9
Oluokun et al. [183]	3	152.4	304.8	7	0.39	2383	st-cr-25.4			31688	35.7
Oluokun et al. [183]	3	152.4	304.8	28	0.39	2383	st-cr-25.4			35381	46.3
Oluokun et al. [183]	3	152.4	304.8	1	0.76	2324	st-cr-25.4			16362	7.8
Oluokun et al. [183]	3	152.4	304.8	2	0.76	2324	st-cr-25.4			19405	12.2
Oluokun et al. [183]	3	152.4	304.8	3	0.76	2324	st-cr-25.4			21629	14.3
Oluokun et al. [183]	3	152.4	304.8	7	0.76	2324	st-cr-25.4			24495	18.6
Oluokun et al. [183]	3	152.4	304.8	28	0.76	2324	st-cr-25.4			31435	28.0
Oluokun et al. [183]	3	152.4	304.8	1	0.53	2413	st-cr-25.4			22309	18.7
Oluokun et al. [183]	3	152.4	304.8	2	0.53	2413	st-cr-25.4			25784	23.9
Oluokun et al. [183]	3	152.4	304.8	3	0.53	2413	st-cr-25.4			26509	26.5
Oluokun et al. [183]	3	152.4	304.8	7	0.53	2413	st-cr-25.4			30602	35.4

Source	*n*	*B (mm)*	*H (mm)*	*Age (d)*	*w/c*	$\rho_{c,f}$ *(kg/m³)*	*Aggregate properties*[p]	*sf/c (%)*	*ma/b (%)*	E_c *(MPa)*	f'_{co} *(MPa)*
Oluokun et al. [183]	3	152.4	304.8	28	0.53	2413	st-cr-25.4			34326	44.1
Oluokun et al. [183]	3	152.4	304.8	1	0.33	2393	st-cr-25.4			31194	35.9
Oluokun et al. [183]	3	152.4	304.8	2	0.33	2393	st-cr-25.4			35095	44.2
Oluokun et al. [183]	3	152.4	304.8	3	0.33	2393	st-cr-25.4			35417	46.2
Oluokun et al. [183]	3	152.4	304.8	7	0.33	2393	st-cr-25.4			36206	50.1
Oluokun et al. [183]	3	152.4	304.8	28	0.33	2393	st-cr-25.4			40293	61.0
Ozturan [184]		150	300				n			15600	14.0
Ozturan [184]		150	300				n			20500	16.9
Ozturan [184]		150	300				n			23300	16.2
Ozturan [184]		150	300				n			26300	17.1
Ozturan [184]		150	300				n			28800	18.0
Ozturan [184]		150	300				n			30100	18.5
Ozturan [184]		150	300				n			20900	21.8
Ozturan [184]		150	300				n			23900	23.2
Ozturan [184]		150	300				n			28600	25.8
Ozturan [184]		150	300				n			32900	27.3
Ozturan [184]		150	300				n			35900	30.3
Ozturan [184]		150	300				n			36800	29.6
Ozturan [184]		150	300				n			18000	17.9
Ozturan [184]		150	300				n			23100	19.6
Ozturan [184]		150	300				n			30300	19.4
Ozturan [184]		150	300				n			23900	20.9
Ozturan [184]		150	300				n			26500	21.2
Ozturan [184]		150	300				n			30500	23.9
Ozturan [184]		150	300				n			32100	23.6
Ozturan [184]		150	300				n			33600	24.2
Ozturan [184]		150	300				n			25500	31.8
Ozturan [184]		150	300				n			27400	32.2
Ozturan [184]		150	300				n			24700	27.1
Ozturan [184]		150	300				n			28600	30.6
Ozturan [184]		150	300				n			31600	29.6
Ozturan [184]		150	300				n			35600	35.0
Ozturan [184]		150	300				n			36700	32.8
Ozturan [184]		150	300				n			39300	36.6
Ozturan [184]		150	300				n			26600	38.4
Ozturan [184]		150	300				n			30100	35.7
Ozturan [184]		150	300				n			34100	42.7
Ozturan [184]		150	300				n			29300	36.8
Ozturan [184]		150	300				n			32600	37.5
Ozturan [184]		150	300				n			28400	40.1
Ozturan [184]		150	300				n			29600	47.7
Perenchio and Klieger [185]	3	152.4	304.8	28	0.30		gv-10			34198	76.9
Perenchio and Klieger [185]	3	152.4	304.8	28	0.30		tr-10			41162	79.8
Perenchio and Klieger [185]	3	152.4	304.8	28	0.30		ls-13			37025	77.1
Perenchio and Klieger [185]	3	152.4	304.8	28	0.30		gv-10			33509	70.1
Perenchio and Klieger [185]	3	152.4	304.8	28	0.30		tr-10			39645	76.7
Perenchio and Klieger [185]	3	152.4	304.8	28	0.30		ls-13			33164	73.1
Perenchio and Klieger [185]	3	152.4	304.8	28	0.35		gv-10			33922	65.8
Perenchio and Klieger [185]	3	152.4	304.8	28	0.35		tr-10			40265	74.9
Perenchio and Klieger [185]	3	152.4	304.8	28	0.35		ls-13			33233	65.4
Perenchio and Klieger [185]	3	152.4	304.8	28	0.35		gv-10			31026	61.9
Perenchio and Klieger [185]	3	152.4	304.8	28	0.35		tr-10			39231	70.6
Perenchio and Klieger [185]	3	152.4	304.8	28	0.35		ls-13			34750	65.1
Perenchio and Klieger [185]	3	152.4	304.8	28	0.40		gv-10			29923	55.8
Perenchio and Klieger [185]	3	152.4	304.8	28	0.40		tr-10			36680	66.2
Perenchio and Klieger [185]	3	152.4	304.8	28	0.40		ls-13			33095	59.1
Perenchio and Klieger [185]	3	152.4	304.8	28	0.40		gv-10			28406	49.8
Perenchio and Klieger [185]	3	152.4	304.8	28	0.40		tr-10			33784	57.5
Perenchio and Klieger [185]	3	152.4	304.8	28	0.40		ls-13			29923	51.0
Powers [186]		152.4	304.8	28			n				53.0
Powers [186]		152.4	304.8	28			n				47.0
Powers [186]		152.4	304.8	28			n				53.0
Powers [186]		152.4	304.8	28			n				46.0
Powers [186]		152.4	304.8	28			n				34.0
Powers [186]		152.4	304.8	28			n				24.0
Richart and Jensen [93]	3	152.4	304.8	7		2376	gv-12.7			23856	25.4
Richart and Jensen [93]	3	152.4	304.8	7		2376	gv-12.7			22477	17.9
Richart and Jensen [93]	3	152.4	304.8	7		2342	gv-12.7			18340	13.9
Richart and Jensen [93]	3	152.4	304.8	7		2364	gv-12.7			25166	25.0
Richart and Jensen [93]	3	152.4	304.8	7		2364	gv-12.7			21856	19.1
Richart and Jensen [93]	3	152.4	304.8	7		2372	gv-12.7			21718	14.8
Richart and Jensen [93]	3	152.4	304.8	7		2337	gv-12.7			24959	23.5
Richart and Jensen [93]	3	152.4	304.8	7		2311	gv-12.7			21856	19.7
Richart and Jensen [93]	3	152.4	304.8	7		2303	gv-12.7			19581	14.6
Richart and Jensen [93]	3	152.4	304.8	7		2372	gv-12.7			23649	19.9
Richart and Jensen [93]	3	152.4	304.8	7		2360	gv-12.7			22891	15.0
Richart and Jensen [93]	3	152.4	304.8	7		2376	gv-12.7			15927	11.4
Richart and Jensen [93]	3	152.4	304.8	7		2361	gv-12.7			22684	18.9
Richart and Jensen [93]	3	152.4	304.8	7		2384	gv-12.7			17237	15.3
Richart and Jensen [93]	3	152.4	304.8	7		2319	gv-12.7			16065	11.9

Source	*n*	*B (mm)*	*H (mm)*	*Age (d)*	*w/c*	$\rho_{c,f}$ *(kg/m^3)*	*Aggregate properties*[p]	*sf/c (%)*	*ma/b (%)*	E_c *(MPa)*	f'_{co} *(MPa)*
Richart and Jensen [93]	3	152.4	304.8	7		2327	gv-12.7			19719	15.2
Richart and Jensen [93]	3	152.4	304.8	7		2315	gv-12.7			18547	12.8
Richart and Jensen [93]	3	152.4	304.8	7		2302	gv-12.7			15100	9.8
Richart and Jensen [93]	3	152.4	304.8	7		2360	gv-12.7			19926	13.0
Richart and Jensen [93]	3	152.4	304.8	7		2361	gv-12.7			16272	8.9
Richart and Jensen [93]	3	152.4	304.8	7		2311	gv-12.7			13100	7.5
Richart and Jensen [93]	3	152.4	304.8	7		2366	gv-12.7			19926	12.7
Richart and Jensen [93]	3	152.4	304.8	7		2318	gv-12.7			17444	9.6
Richart and Jensen [93]	3	152.4	304.8	7		2327	gv-12.7			12755	7.6
Richart and Jensen [93]	3	152.4	304.8	7		2302	gv-12.7			16272	9.9
Richart and Jensen [93]	3	152.4	304.8	7		2307	gv-12.7			16892	8.3
Richart and Jensen [93]	3	152.4	304.8	7		2287	gv-12.7			13238	6.8
Richart and Jensen [93]	3	152.4	304.8	28		2376	gv-12.7			29716	37.2
Richart and Jensen [93]	3	152.4	304.8	28		2376	gv-12.7			26545	27.7
Richart and Jensen [93]	3	152.4	304.8	28		2342	gv-12.7			23856	24.7
Richart and Jensen [93]	3	152.4	304.8	28		2364	gv-12.7			28544	31.7
Richart and Jensen [93]	3	152.4	304.8	28		2364	gv-12.7			26821	30.5
Richart and Jensen [93]	3	152.4	304.8	28		2372	gv-12.7			25580	24.7
Richart and Jensen [93]	3	152.4	304.8	28		2337	gv-12.7			27579	30.9
Richart and Jensen [93]	3	152.4	304.8	28		2311	gv-12.7			25993	30.4
Richart and Jensen [93]	3	152.4	304.8	28		2303	gv-12.7			23649	24.8
Richart and Jensen [93]	3	152.4	304.8	28		2372	gv-12.7			27993	30.1
Richart and Jensen [93]	3	152.4	304.8	28		2360	gv-12.7			25649	26.1
Richart and Jensen [93]	3	152.4	304.8	28		2376	gv-12.7			22891	21.3
Richart and Jensen [93]	3	152.4	304.8	28		2361	gv-12.7			27234	21.3
Richart and Jensen [93]	3	152.4	304.8	28		2384	gv-12.7			27786	26.4
Richart and Jensen [93]	3	152.4	304.8	28		2319	gv-12.7			23718	22.0
Richart and Jensen [93]	3	152.4	304.8	28		2327	gv-12.7			25855	25.8
Richart and Jensen [93]	3	152.4	304.8	28		2315	gv-12.7			24132	26.8
Richart and Jensen [93]	3	152.4	304.8	28		2302	gv-12.7			20477	19.1
Richart and Jensen [93]	3	152.4	304.8	28		2360	gv-12.7			26200	21.2
Richart and Jensen [93]	3	152.4	304.8	28		2361	gv-12.7			23787	18.9
Richart and Jensen [93]	3	152.4	304.8	28		2311	gv-12.7			21650	15.8
Richart and Jensen [93]	3	152.4	304.8	28		2366	gv-12.7			21029	22.0
Richart and Jensen [93]	3	152.4	304.8	28		2318	gv-12.7			24338	18.7
Richart and Jensen [93]	3	152.4	304.8	28		2327	gv-12.7			19995	15.3
Richart and Jensen [93]	3	152.4	304.8	28		2302	gv-12.7			21787	17.7
Richart and Jensen [93]	3	152.4	304.8	28		2307	gv-12.7			19857	14.9
Richart and Jensen [93]	3	152.4	304.8	28		2287	gv-12.7			20477	13.9
Richart and Jensen [93]	3	152.4	304.8	7		2361	gv			20477	16.8
Richart and Jensen [93]	3	152.4	304.8	28		2361	gv			26959	27.4
Richart and Jensen [93]	3	152.4	304.8	90		2361	gv			31026	32.2
Richart and Jensen [93]	3	152.4	304.8	180		2361	gv			32130	32.6
Richart and Jensen [93]	3	152.4	304.8	365		2361	gv			33784	39.3
Richart and Jensen [93]	3	152.4	304.8	28		2335	gv-9.5			27027	33.0
Richart and Jensen [93]	3	152.4	304.8	28		2339	gv-9.5			27648	32.5
Richart and Jensen [93]	3	152.4	304.8	28		2331	gv-9.5			26959	32.3
Richart and Jensen [93]	3	152.4	304.8	28		2345	gv-9.5			26200	22.8
Richart and Jensen [93]	3	152.4	304.8	28		2345	gv-9.5			25442	28.3
Richart and Jensen [93]	3	152.4	304.8	28		2361	gv-9.5			28269	29.0
Richart and Jensen [93]	3	152.4	304.8	28		2352	gv-9.5			24063	20.6
Richart and Jensen [93]	3	152.4	304.8	28		2347	gv-9.5			25511	21.6
Richart and Jensen [93]	3	152.4	304.8	28		2339	gv-9.5			26959	22.8
Richart and Jensen [93]	3	152.4	304.8	28		2323	ls-9.5			23580	32.5
Richart and Jensen [93]	3	152.4	304.8	28		2318	ls-9.5			25649	32.5
Richart and Jensen [93]	3	152.4	304.8	28		2324	ls-9.5			25028	34.7
Richart and Jensen [93]	3	152.4	304.8	28		2305	ls-9.5			21236	25.6
Richart and Jensen [93]	3	152.4	304.8	28		2310	ls-9.5			25580	28.3
Richart and Jensen [93]	3	152.4	304.8	28		2331	ls-9.5			25786	26.8
Richart and Jensen [93]	3	152.4	304.8	28		2380	ls-9.5			22339	20.0
Richart and Jensen [93]	3	152.4	304.8	28		2335	ls-9.5			21512	19.9
Richart and Jensen [93]	3	152.4	304.8	28		2332	ls-9.5			25511	22.0
Richart and Jensen [93]	3	152.4	304.8	28		2366	gv-12.7			26062	27.9
Richart and Jensen [93]	3	152.4	304.8	28		2353	gv-12.7			25717	27.3
Richart and Jensen [93]	3	152.4	304.8	28		2334	gv-12.7			25235	21.9
Richart and Jensen [93]	3	152.4	304.8	28		2340	gv-12.7			25097	23.5
Richart and Jensen [93]	3	152.4	304.8	28		2334	gv-12.7			22408	20.6
Richart and Jensen [93]	3	152.4	304.8	28		2348	gv-12.7			23304	18.8
Richart and Jensen [93]	3	152.4	304.8	28		2366	gv-12.7			26200	32.8
Richart and Jensen [93]	3	152.4	304.8	28		2382	gv-12.7			28269	31.9
Richart and Jensen [93]	3	152.4	304.8	28		2380	gv-12.7			26407	29.6
Richart and Jensen [93]	3	152.4	304.8	28		2372	gv-12.7			24614	26.6
Richart and Jensen [93]	3	152.4	304.8	28		2345	gv-12.7			21305	15.4
Richart and Jensen [93]	3	152.4	304.8	28		2353	gv-12.7			21925	18.1
Richart and Jensen [93]	3	152.4	304.8	28		2384	es,gv-12.7			28062	35.0
Richart and Jensen [93]	3	152.4	304.8	28		2376	es,gv-12.7			28613	36.3
Richart and Jensen [93]	3	152.4	304.8	28		2361	es,gv-12.7			27855	34.6
Richart and Jensen [93]	3	152.4	304.8	28		2364	es,gv-12.7			28131	36.3
Richart and Jensen [93]	3	152.4	304.8	28		2385	es,gv-12.7			26752	36.5
Richart and Jensen [93]	3	152.4	304.8	28		2361	es,gv-12.7			28337	34.7

Source	*n*	*B (mm)*	*H (mm)*	*Age (d)*	*w/c*	$\rho_{c,f}$ *(kg/m³)*	*Aggregate properties*[p]	*sf/c (%)*	*ma/b (%)*	E_c *(MPa)*	f'_{co} *(MPa)*
Richart and Jensen [93]	3	152.4	304.8	28		2361	es,gv-12.7			28275	33.7
Richart and Jensen [93]	3	152.4	304.8	28		2374	es,gv-12.7			30406	37.2
Richart and Jensen [93]	3	152.4	304.8	28		2350	es,gv-12.7			28889	36.4
Richart and Jensen [93]	3	152.4	304.8	28		2390	gv			27786	38.2
Richart and Jensen [93]	3	152.4	304.8	28		2251	sd-4.75			25649	30.3
Richart and Jensen [93]	3	152.4	304.8	28		2289	gv-19.1			22201	8.7
Richart et al. [95]	1	152	305	28			n			21650	17.4
Richart et al. [95]	1	152	305	28			n			20822	17.6
Richart et al. [95]	1	152	305	28			n			21098	15.8
Richart et al. [95]	1	152	305	28			n			20271	15.7
Richart et al. [95]	1	152	305	28			n			22753	17.1
Richart et al. [187]	3	152.4	304.8	28			n			20684	13.4
Richart et al. [187]	3	152.4	304.8	28			n			18271	11.9
Richart et al. [187]	3	152.4	304.8	28			n			14065	13.9
Richart et al. [187]	3	152.4	304.8	28			n			19512	13.0
Richart et al. [187]	3	152.4	304.8	28			n			20064	11.2
Richart et al. [187]	3	152.4	304.8	28			n			18064	13.9
Richart et al. [187]	3	152.4	304.8	28			n			17168	13.6
Richart et al. [187]	3	152.4	304.8	28			n			18685	12.8
Richart et al. [187]	3	152.4	304.8	28			n			15858	11.9
Richart et al. [187]	3	152.4	304.8	28			n			21994	12.9
Richart et al. [187]	3	152.4	304.8	28			n			16203	11.7
Richart et al. [187]	3	152.4	304.8	28			n			20064	12.9
Richart et al. [187]	3	152.4	304.8	28			n			20615	13.7
Richart et al. [187]	3	152.4	304.8	28			n			16961	12.6
Richart et al. [187]	3	152.4	304.8	28			n			17857	12.7
Richart et al. [187]	3	152.4	304.8	28			n			18754	14.1
Richart et al. [187]	3	152.4	304.8	28			n			18685	13.7
Richart et al. [187]	3	152.4	304.8	28			n			18616	13.1
Richart et al. [187]	3	152.4	304.8	28			n			16410	11.3
Richart et al. [187]	3	152.4	304.8	28			n			18961	14.8
Richart et al. [187]	3	152.4	304.8	28			n			19236	14.5
Richart et al. [187]	3	152.4	304.8	28			n			19788	16.2
Richart et al. [187]	3	152.4	304.8	28			n			16272	13.0
Richart et al. [187]	3	152.4	304.8	28			n			18409	12.7
Richart et al. [187]	3	152.4	304.8	28			n			18478	13.3
Richart et al. [187]	3	152.4	304.8	28			n			18685	12.7
Richart et al. [187]	3	152.4	304.8	28			n			19443	14.1
Richart et al. [187]	3	152.4	304.8	28			n			19030	14.3
Richart et al. [187]	2	203.2	406.4	28			n			13376	9.7
Richart et al. [187]	2	203.2	406.4	28			n			16134	10.7
Richart et al. [187]	2	203.2	406.4	28			n			16478	11.8
Richart et al. [187]	2	203.2	406.4	28			n			16410	13.0
Richart et al. [187]	2	203.2	406.4	28			n			16754	12.3
Richart et al. [187]	2	203.2	406.4	28			n			15720	11.6
Richart et al. [187]	2	203.2	406.4	28			n			13583	13.5
Richart et al. [187]	2	203.2	406.4	28			n			12204	11.4
Richart et al. [187]	2	203.2	406.4	28			n			12342	14.5
Richart et al. [187]	2	203.2	406.4	28			n			11859	11.7
Richart et al. [187]	2	203.2	406.4	28			n			11652	13.7
Richart et al. [187]	2	203.2	406.4	28			n			12893	13.4
Richart et al. [187]	2	203.2	406.4	28			n			11652	14.6
Richart et al. [187]	2	203.2	406.4	28			n			11170	14.1
Richart et al. [187]	2	152.4	304.8	28			n			24270	16.9
Richart et al. [187]	2	152.4	304.8	28			n			30268	30.6
Richart et al. [187]	2	152.4	304.8	28			n			33509	39.8
Richart et al. [187]	2	152.4	304.8	28	0.92		fa			12893	25.9
Richart et al. [187]	1	152.4	304.8	28	0.92		fa			12893	25.5
Richart et al. [187]	2	152.4	304.8	28	0.92		fa			14341	25.4
Richart et al. [187]	1	152.4	304.8	28	0.92		fa			13790	25.3
Richart et al. [187]	2	152.4	304.8	28	0.72		gv			28303[m]	22.8
Richart et al. [187]	1	152.4	304.8	28	0.72		gv			24545	23.0
Richart et al. [187]	2	152.4	304.8	28	0.72		gv			23442	22.5
Richart et al. [187]	1	152.4	304.8	28	0.72		gv			29234	24.3
Richart et al. [187]	2	152.4	304.8	1975	0.92		fa			11893[m]	31.1
Richart et al. [187]	1	152.4	304.8	1975	0.92		fa			11893[m]	31.4
Richart et al. [187]	2	152.4	304.8	1975	0.92		fa			12893[m]	30.8
Richart et al. [187]	1	152.4	304.8	1975	0.92		fa			12514[m]	30.5
Richart et al. [187]	2	152.4	304.8	1975	0.72		gv			30509	29.8
Richart et al. [187]	1	152.4	304.8	1975	0.72		gv			31371	27.8
Richart et al. [187]	2	152.4	304.8	1975	0.72		gv			31544	28.6
Richart et al. [187]	1	152.4	304.8	1975	0.72		gv			29061	30.3
Rutland and Wang [188]	1	50	100				n				39.4
Shideler [189]	1	152.4	304.8	1	0.53	2489	gv-rd			11307[m]	9.7
Shideler [189]	1	152.4	304.8	1	0.35	2480	gv-rd			20546	28.1
Shideler [189]	1	152.4	304.8	3	0.49	2355	gv-rd			16754	14.0
Shideler [189]	1	152.4	304.8	3	0.53	2489	gv-rd			19374	24.0
Shideler [189]	1	152.4	304.8	3	0.35	2480	gv-rd			26752	48.1
Shideler [189]	1	152.4	304.8	7	0.62	2319	gv-rd			18202	14.1
Shideler [189]	1	152.4	304.8	7	0.49	2355	gv-rd			21098	21.2

Source	*n*	*B (mm)*	*H (mm)*	*Age (d)*	*w/c*	$\rho_{c,f}$ *(kg/m^3)*	*Aggregate properties*[p]	*sf/c (%)*	*ma/b (%)*	E_c *(MPa)*	f'_{co} *(MPa)*
Shideler [189]	1	152.4	304.8	7	0.53	2489	gv-rd			24270	35.6
Shideler [189]	1	152.4	304.8	7	0.35	2480	gv-rd			29027	58.1
Shideler [189]	1	152.4	304.8	28	0.62	2319	gv-rd			22063	21.1
Shideler [189]	1	152.4	304.8	28	0.62	2319	gv-rd			24338	22.2
Shideler [189]	1	152.4	304.8	28	0.49	2355	gv-rd			23649	29.0
Shideler [189]	1	152.4	304.8	28	0.49	2355	gv-rd			26476	30.8
Shideler [189]	1	152.4	304.8	28	0.53	2489	gv-rd			28889	48.2
Shideler [189]	1	152.4	304.8	28	0.53	2489	gv-rd			32474	52.1
Shideler [189]	1	152.4	304.8	28	0.35	2480	gv-rd			31992	65.3
Shideler [189]	1	152.4	304.8	28	0.35	2480	gv-rd			34612	72.9
Shideler [189]	1	152.4	304.8	90	0.62	2319	gv-rd			27579	24.4
Shideler [189]	1	152.4	304.8	90	0.49	2355	gv-rd			31578	34.0
Shideler [189]	1	152.4	304.8	90	0.49	2355	gv-rd			30268	34.5
Shideler [189]	1	152.4	304.8	90	0.53	2489	gv-rd			35163	53.1
Shideler [189]	1	152.4	304.8	90	0.53	2489	gv-rd			34956	58.1
Shideler [189]	1	152.4	304.8	90	0.35	2480	gv-rd			36887	72.6
Shideler [189]	1	152.4	304.8	90	0.35	2480	gv-rd			34750	70.9
Shideler [189]	1	152.4	304.8	180	0.62	2319	gv-rd			26269	25.2
Shideler [189]	1	152.4	304.8	180	0.49	2355	gv-rd			34543	36.0
Shideler [189]	1	152.4	304.8	180	0.49	2355	gv-rd			29303	32.8
Shideler [189]	1	152.4	304.8	180	0.53	2489	gv-rd			37645	58.4
Shideler [189]	1	152.4	304.8	180	0.53	2489	gv-rd			35784	57.2
Shideler [189]	1	152.4	304.8	180	0.35	2480	gv-rd			40472	78.3
Shideler [189]	1	152.4	304.8	180	0.35	2480	gv-rd			39852	82.7
Shideler [189]	1	152.4	304.8	365	0.49	2355	gv-rd			36749	36.8
Shideler [189]	1	152.4	304.8	365	0.49	2355	gv-rd			28820	32.4
Shideler [189]	1	152.4	304.8	365	0.53	2489	gv-rd			42954	59.5
Shideler [189]	1	152.4	304.8	365	0.53	2489	gv-rd			36335	58.1
Shideler [189]	1	152.4	304.8	365	0.35	2480	gv-rd			42885	77.4
Shideler [189]	1	152.4	304.8	365	0.35	2480	gv-rd			40610	80.3
Shkolnik [190]		150	300				n			28890	21.0
Shkolnik [190]		150	300				n			34820	28.0
Shkolnik [190]		150	300				n			39646[m]	34.0
Shkolnik [190]		150	300				n			43714[m]	41.0
Shkolnik [190]		150	300				n			47162[m]	48.0
Shkolnik [190]		150	300				n			50127[m]	55.0
Shkolnik and Aktan [191]		150	300		0.50		n			31000	40.0
Shkolnik and Aktan [191]		150	300		0.50		n			30500	42.0
Shkolnik and Aktan [191]		150	300		0.50		n			33800	39.0
Shkolnik and Aktan [191]		150	300		0.45		n			35800	57.0
Shkolnik and Aktan [191]		150	300		0.45		n			35500	40.0
Shkolnik and Aktan [191]		150	300		0.45		n			37700	51.0
Shkolnik and Aktan [191]		150	300		0.40		n			34800	52.0
Shkolnik and Aktan [191]		150	300		0.40		n			32000	53.0
Shkolnik and Aktan [191]		150	300		0.40		n			34000	41.0
Shkolnik and Aktan [191]		150	300		0.40		n			37500	42.0
Shkolnik and Aktan [191]		150	300		0.40		n			36800	44.0
Shkolnik and Aktan [191]		150	300		0.35		n			37400	49.0
Shkolnik and Aktan [191]		150	300		0.35		n			40800	58.0
Shkolnik and Aktan [191]		150	300		0.35		n			37500	48.0
Shkolnik and Aktan [191]		150	300		0.35		n			37700	58.0
Shkolnik and Aktan [191]		150	300		0.50		n			31768	40.0
Shkolnik and Aktan [191]		150	300		0.45		n			36340	49.0
Shkolnik and Aktan [191]		150	300		0.40		n			35020	47.0
Shkolnik and Aktan [191]		150	300		0.35		n			38335	53.0
Turan [192]		150	300				n			30400	31.4
Turan [192]		150	300				n			29100	27.8
Turan [192]		150	300				n			26800	28.5
Turan [192]		150	300				n			33000	29.4
Turan [192]		150	300				n			31500	29.4
Turan [192]		150	300				n			30000	26.4
Turan [192]		150	300				n			29000	28.5
Turan [192]		150	300				n			32400	32.6
Turan [192]		150	300				n			29000	28.8
Turan [192]		150	300				n			30200	29.9
Turan [192]		150	300				n			27500	29.8
Turan [192]		150	300				n			30800	28.0
Turan [192]		150	300				n			26500	27.3
Turan [192]		150	300				n			25600	27.7
Turan [192]		150	300				n			25200	27.5
Turan [192]		150	300				n			27200	27.0
Turan [192]		150	300				n			27300	28.5
Turan [192]		150	300				n			26500	26.4
Turan [192]		150	300				n			21800	22.1
Turan [192]		150	300				n			23900	27.1
Turan [192]		150	300				n			24000	26.3
Turan [192]		150	300				n			24900	26.1
Turan [192]		150	300				n			25300	27.8
Turan [192]		150	300				n			26800	28.9
Turan [192]		150	300				n			25700	25.7

Source	*n*	*B (mm)*	*H (mm)*	*Age (d)*	*w/c*	$\rho_{c,f}$ *(kg/m³)*	*Aggregate properties*[p]	*sf/c (%)*	*ma/b (%)*	E_c *(MPa)*	f'_{co} *(MPa)*
Turan [192]		150	300				n			26000	27.8
Turan [192]		150	300				n			27500	28.6
Turan [192]		150	300				n			26200	27.9
Turan [192]		150	300				n			23900	20.6
Turan [192]		150	300				n			21900	18.4
Turan [192]		150	300				n			26300	23.4
Turan [192]		150	300				n			30400	29.9
Turan [192]		150	300				n			26500	22.9
Turan [192]		150	300				n			28100	25.3
Turan [192]		150	300				n			27200	23.7
Turan [192]		150	300				n			27090	27.4
Wiegrink [193]	2	75	100	3	0.40	2450	gv-9				38.0
Wiegrink [193]	2	75	100	3	0.36	2420	gv-9	5.0		24000	40.9
Wiegrink [193]	2	75	100	3	0.36	2450	gv-9	5.0		23100	44.5
Wiegrink [193]	2	75	100	3	0.32	2480	gv-9	10.0		23500	49.7
Wiegrink [193]	2	75	100	3	0.29	2520	gv-9	15.0		26400	54.2
Wiegrink [193]	2	75	100	7	0.40	2450	gv-9			22600	40.5
Wiegrink [193]	2	75	100	7	0.36	2420	gv-9	5.0		23500	45.6
Wiegrink [193]	2	75	100	7	0.36	2450	gv-9	5.0		24800	48.1
Wiegrink [193]	2	75	100	7	0.32	2480	gv-9	10.0		26200	58.0
Wiegrink [193]	2	75	100	7	0.29	2520	gv-9	15.0		28000	63.0
Wiegrink [193]	2	75	100	28	0.40	2450	gv-9			26200	53.4
Wiegrink [193]	2	75	100	28	0.36	2420	gv-9	5.0		27700	65.4
Wiegrink [193]	2	75	100	28	0.36	2450	gv-9	5.0		26800	66.5
Wiegrink [193]	2	75	100	28	0.32	2480	gv-9	10.0		28000	74.6
Wiegrink [193]	2	75	100	28	0.29	2520	gv-9	15.0		31000	86.5
Yaman et al. [194]	4	100	200	31	0.35		n			40840	58.1
Yaman et al. [194]	4	100	200	31	0.35		n			40780	53.3
Yaman et al. [194]	4	100	200	31	0.35		n			38310	51.3
Yaman et al. [194]	4	100	200	31	0.35		n			37360	48.8
Yaman et al. [194]	4	100	200	31	0.35		n			37470	47.7
Yaman et al. [194]	4	100	200	31	0.40		n			36130	45.5
Yaman et al. [194]	4	100	200	31	0.40		n			37040	44.8
Yaman et al. [194]	4	100	200	31	0.40		n			36810	44.4
Yaman et al. [194]	4	100	200	31	0.40		n			37450	42.4
Yaman et al. [194]	4	100	200	31	0.40		n			35750	42.1
Yaman et al. [194]	4	100	200	31	0.45		n			33990	41.1
Yaman et al. [194]	4	100	200	31	0.45		n			35460	40.5
Yaman et al. [194]	4	100	200	31	0.45		n			32860	39.0
Yaman et al. [194]	4	100	200	31	0.45		n			33790	38.9
Yaman et al. [194]	4	100	200	31	0.50		n			32180	35.9
Yaman et al. [194]	4	100	200	31	0.35		n			38430	58.1
Yaman et al. [194]	4	100	200	31	0.35		n			35940	53.3
Yaman et al. [194]	4	100	200	31	0.35		n			33510	51.3
Yaman et al. [194]	4	100	200	31	0.35		n			32920	48.8
Yaman et al. [194]	4	100	200	31	0.35		n			35110	47.7
Zhang and Malhotra [195]	2	102	203	1	0.40	2345	ls-19				20.9
Zhang and Malhotra [195]	2	102	203	1	0.40	2345	ls-19		10.0[t]		25.0
Zhang and Malhotra [195]	2	102	203	1	0.40	2330	ls-19	10.0			23.2
Zhang and Malhotra [195]	2	102	203	3	0.40	2345	ls-19				25.5
Zhang and Malhotra [195]	2	102	203	3	0.40	2345	ls-19		10.0[t]		32.9
Zhang and Malhotra [195]	2	102	203	3	0.40	2330	ls-19	10.0			28.6
Zhang and Malhotra [195]	2	102	203	7	0.40	2345	ls-19				28.9
Zhang and Malhotra [195]	2	102	203	7	0.40	2345	ls-19		10.0[t]		37.9
Zhang and Malhotra [195]	2	102	203	7	0.40	2330	ls-19	10.0			34.1
Zhang and Malhotra [195]	2	102	203	28	0.40	2345	ls-19			29600	36.4
Zhang and Malhotra [195]	2	102	203	28	0.40	2345	ls-19		10.0[t]	32000	39.9
Zhang and Malhotra [195]	2	102	203	28	0.40	2330	ls-19	10.0		31100	44.4
Zhang and Malhotra [195]	2	102	203	90	0.40	2345	ls-19				42.5
Zhang and Malhotra [195]	2	102	203	90	0.40	2345	ls-19		10.0[t]		43.0
Zhang and Malhotra [195]	2	102	203	90	0.40	2330	ls-19	10.0			48.0
Zhang and Malhotra [195]	2	102	203	280	0.40	2345	ls-19				44.2
Zhang and Malhotra [195]	2	102	203	280	0.40	2345	ls-19		10.0[t]		46.2
Zhang and Malhotra [195]	2	102	203	280	0.40	2330	ls-19	10.0			50.2

w Water-cementitious binder ratio that differ significantly from the reference values of the corresponding concrete strength
d Fresh concrete density that is significantly higher than the reference values
m Concrete elastic modulus that differ significantly from the reference values of the corresponding concrete strength
f Fly-ash used as mineral admixture in concrete mix
s Blast-furnace slag used as mineral admixture in concrete mix
h Hi-fi (ettringite based material) used as mineral admixture in concrete mix
t thermally activated alumina-silicate
p Designation:- type-irregularity-size
Type:- n: normal weight aggregate, ad: andesite, bs: basalt, cl: calcitic limestone, db: diabase, dl: dolomitic limestone, fa: sintered fly-ash, ft: flint, gn: granite, gv: gravel, ls: limestone, ml: metamorphic limestone, pm: volcanic pumice, qz: quartz, sd: sand, st: sandstone gravel, tr: traprock
Irregularity:- ag: angular, cr: crushed, fn: fine, rd: round, sh: sharp
Size:- maximum aggregate in mm

Table A5. Test database of light weight concrete cylinders (without ε_{co} values)

Source	*n*	*B (mm)*	*H (mm)*	*Age (d)*	*w/c*	$\rho_{c,f}$ *(kg/m³)*	*Aggregate properties*[p]	*sf/c (%)*	*ma/b (%)*	E_c *(MPa)*	f'_{co} *(MPa)*
Balaguru and Foden [196]	3	150	300	28		1780	l			14800	22.4
Balaguru and Foden [196]	3	150	300	28		1698	l			18800	32.4
Balaguru and Foden [196]	3	150	300	28		1684	l			18000	33.4
Balaguru and Foden [196]	3	150	300	28		1785	l			19700	35.1
Balaguru and Foden [196]	3	150	300	28		1810	l			20100	34.1
Chi et al. [197]	5	100	200	28	0.30	2175	fa			22900	41.7
Chi et al. [197]	5	100	200	28	0.30	2117	fa			21500	37.5
Chi et al. [197]	5	100	200	28	0.30	2060	fa			20100	35.0
Chi et al. [197]	5	100	200	28	0.30	2002	fa			18700	31.8
Chi et al. [197]	5	100	200	28	0.40	2117	fa			20300	32.6
Chi et al. [197]	5	100	200	28	0.40	2059	fa			16500	29.5
Chi et al. [197]	5	100	200	28	0.40	2002	fa			16500	27.6
Chi et al. [197]	5	100	200	28	0.40	1944	fa			13800	23.0
Chi et al. [197]	5	100	200	28	0.50	2072	fa			18200	29.8
Chi et al. [197]	5	100	200	28	0.50	2014	fa			15500	25.7
Chi et al. [197]	5	100	200	28	0.50	1957	fa			14200	23.3
Chi et al. [197]	5	100	200	28	0.50	1899	fa			13300	21.3
Chi et al. [197]	5	100	200	28	0.30	2187	fa			22800	43.9
Chi et al. [197]	5	100	200	28	0.30	2132	fa			21700	41.2
Chi et al. [197]	5	100	200	28	0.30	2077	fa			18900	38.7
Chi et al. [197]	5	100	200	28	0.30	2021	fa			18200	35.6
Chi et al. [197]	5	100	200	28	0.40	2124	fa			21400	37.3
Chi et al. [197]	5	100	200	28	0.40	2069	fa			18200	33.4
Chi et al. [197]	5	100	200	28	0.40	2014	fa			17400	30.4
Chi et al. [197]	5	100	200	28	0.40	1958	fa			16100	28.4
Chi et al. [197]	5	100	200	28	0.50	2079	fa			17100	27.4
Chi et al. [197]	5	100	200	28	0.50	2024	fa			17000	26.3
Chi et al. [197]	5	100	200	28	0.50	1969	fa			15200	24.6
Chi et al. [197]	5	100	200	28	0.50	1913	fa			14800	21.5
Chi et al. [197]	5	100	200	28	0.30	2195	fa			23100	48.2
Chi et al. [197]	5	100	200	28	0.30	2143	fa			21900	47.4
Chi et al. [197]	5	100	200	28	0.30	2093	fa			20900	45.8
Chi et al. [197]	5	100	200	28	0.30	2042	fa			19800	42.6
Chi et al. [197]	5	100	200	28	0.40	2137	fa			21900	38.3
Chi et al. [197]	5	100	200	28	0.40	2085	fa			21400	37.6
Chi et al. [197]	5	100	200	28	0.40	2035	fa			20600	38.9
Chi et al. [197]	5	100	200	28	0.40	1984	fa			18000	37.5
Chi et al. [197]	5	100	200	28	0.50	2092	fa			19300	31.2
Chi et al. [197]	5	100	200	28	0.50	2040	fa			17900	29.5
Chi et al. [197]	5	100	200	28	0.50	1990	fa			16300	27.7
Chi et al. [197]	5	100	200	28	0.50	1939	fa			15400	29.7
Hanson [198]	1	152.4	304.8	28	0.72	1464	es-cr-4.75			11652	23.9
Hanson [198]	1	152.4	304.8	28	0.70	1490	es-rd			13376	21.3
Hanson [198]	1	152.4	304.8	28	1.28	1515	ec-cr			10480	18.6
Hanson [198]	1	152.4	304.8	28	0.76	1541	et-cr-4.75			14272	23.0
Hanson [198]	1	152.4	304.8	28	0.65	1567	eg-cr			19030	25.2
Hanson [198]	1	152.4	304.8	28	0.78	1592	ss-sh			16065	21.2
Hanson [198]	1	152.4	304.8	28	0.62	1618	gv-rd			22201	25.9
Hanson [198]	1	152.4	304.8	28	0.55	1643	es-cr-4.75			14410	36.7
Hanson [198]	1	152.4	304.8	28	0.56	1669	es-rd			14548	27.3
Hanson [198]	1	152.4	304.8	28	0.88	1695	ec-cr			13996	31.4
Hanson [198]	1	152.4	304.8	28	0.57	1720	et-cr-4.75			16134	32.7
Hanson [198]	1	152.4	304.8	28	0.49	1746	eg-cr			21236	33.6
Hanson [198]	1	152.4	304.8	28	0.68	1772	ss-sh			17168	28.8
Hanson [198]	1	152.4	304.8	28	0.60	1797	ss-sh			20340	34.1
Hanson [198]	1	152.4	304.8	28	0.49	1823	gv-rd			26821	35.6
Hanson [198]	1	152.4	304.8	28	0.34	1849	es-rd			21443	45.6
Hanson [198]	1	152.4	304.8	28	0.71	1874	ec-cr			14203	47.2
Hanson [198]	1	152.4	304.8	28	0.41	1900	gv-rd			27786	52.6
Hanson [198]	1	152.4	304.8	28	0.49	1925	ec-cr			16685	56.1
Hanson [198]	1	152.4	304.8	28	0.29	1951	gv-rd			32750	66.3
Hanson [198]	1	152.4	304.8	28	0.72	1464	es-cr-4.75			11032	25.4
Hanson [198]	1	152.4	304.8	28	0.70	1490	es-cr			13031	22.8
Hanson [198]	1	152.4	304.8	28	1.28	1515	ec-cr			11032	20.5
Hanson [198]	1	152.4	304.8	28	0.76	1541	et-cr-4.75			13790	24.1
Hanson [198]	1	152.4	304.8	28	0.65	1567	eg-cr			16823	25.3
Hanson [198]	1	152.4	304.8	28	0.78	1592	ss-sh			15100	22.1
Hanson [198]	1	152.4	304.8	28	0.62	1618	gv-rd			26338[m]	27.7
Hanson [198]	1	152.4	304.8	28	0.55	1643	es-cr-4.75			12480	36.9
Hanson [198]	1	152.4	304.8	28	0.56	1669	es-rd			13652	28.2
Hanson [198]	1	152.4	304.8	28	0.88	1695	ec-cr			12893	33.7
Hanson [198]	1	152.4	304.8	28	0.57	1720	et-cr-4.75			15375	33.0
Hanson [198]	1	152.4	304.8	28	0.49	1746	eg-cr			19098	33.6
Hanson [198]	1	152.4	304.8	28	0.68	1772	ss-sh			16065	29.2
Hanson [198]	1	152.4	304.8	28	0.60	1797	ss-sh			18133	35.9
Hanson [198]	1	152.4	304.8	28	0.49	1823	gv-rd			27648	37.1
Hanson [198]	1	152.4	304.8	28	0.34	1849	es-rd			20133	47.6
Hanson [198]	1	152.4	304.8	28	0.71	1874	ec-cr			13996	48.3
Hanson [198]	1	152.4	304.8	28	0.41	1900	gv-rd			31578	58.0

Source	*n*	*B (mm)*	*H (mm)*	*Age (d)*	*w/c*	$\rho_{c,f}$ *(kg/m³)*	*Aggregate properties*[p]	*sf/c (%)*	*ma/b (%)*	E_c *(MPa)*	f'_{co} *(MPa)*
Hanson [198]	1	152.4	304.8	28	0.49	1925	ec-cr			15444	56.3
Hanson [198]	1	152.4	304.8	28	0.29	1951	gv-rd			34956	73.6
Hossain [175]		150	300	28	0.45	1881	pm			10500	22.0
Hossain [175]		150	300	28	0.45	1961	pm			11000	25.0
Hossain [175]		150	300	28	0.45	2091	pm			12000	27.0
Hossain [175]		150	300	28	0.45	2291[d]	pm			14500	29.0
Hossain [175]		150	300	28	0.45	1734	pm			10000	18.0
Hossain [175]		150	300	28	0.45	1834	pm			11900	23.0
Hossain [175]		150	300	28	0.45	1979	pm			12200	25.0
Hossain [175]		150	300	28	0.45	2219	pm			14500	28.0
Ke et al. [199]	4	160	320	28		2071	es,ec			28845	40.3
Ke et al. [199]	4	160	320	28		1999	es,ec			27574	42.5
Ke et al. [199]	4	160	320	28		1949	es,ec			26477	42.5
Ke et al. [199]	4	160	320	28		1883	es,ec			25495	43.4
Ke et al. [199]	4	160	320	28		1865	es,ec			24513	43.0
Ke et al. [199]	4	160	320	28		1953	es,ec			26014	42.5
Ke et al. [199]	4	160	320	28		1877	es,ec			25206	36.9
Ke et al. [199]	4	160	320	28		1827	es,ec			25032	39.4
Ke et al. [199]	4	160	320	28		1792	es,ec			24801	43.6
Ke et al. [199]	4	160	320	28		1913	es,ec			24455	38.1
Ke et al. [199]	4	160	320	28		1743	es,ec			22318	35.3
Ke et al. [199]	4	160	320	28		1606	es,ec			20296	30.1
Ke et al. [199]	4	160	320	28		1542	es,ec			18448	29.0
Ke et al. [199]	4	160	320	28		1931	es,ec			25090	37.4
Ke et al. [199]	4	160	320	28		1757	es,ec			21625	32.5
Ke et al. [199]	4	160	320	28		1599	es,ec			17350	27.9
Ke et al. [199]	4	160	320	28		1513	es,ec			15791	25.8
Ke et al. [199]	4	160	320	28		1953	es,ec			26419	39.2
Ke et al. [199]	4	160	320	28		1804	es,ec			21798	34.2
Ke et al. [199]	4	160	320	28		1663	es,ec			17755	28.8
Ke et al. [199]	4	160	320	28		1599	es,ec			16715	28.0
Ke et al. [199]	4	160	320	28		1929	es,ec			23704	36.7
Ke et al. [199]	4	160	320	28		1805	es,ec			20816	30.9
Ke et al. [199]	4	160	320	28		1640	es,ec			16773	27.3
Ke et al. [199]	4	160	320	28		1561	es,ec			15733	24.6
Khayat et al. [200]		150	300	28			ls-9.5			45500	85.0
Kluge et al. [178]		152.4	304.8	28		801	vm-9.5			593	0.9
Kluge et al. [178]		152.4	304.8	28		865	vm-9.5			1089	2.0
Kluge et al. [178]		152.4	304.8	28		945	vm-9.5			1248	3.2
Kluge et al. [178]		152.4	304.8	28		1009	vm-9.5			1193	4.0
Kluge et al. [178]		152.4	304.8	28		1169	dt-9.5			1524	2.2
Kluge et al. [178]		152.4	304.8	28		1233	dt-9.5			1944	4.5
Kluge et al. [178]		152.4	304.8	28		1362	dt-9.5			2441	8.3
Kluge et al. [178]		152.4	304.8	28		1458	dt-9.5			2247[m]	11.2
Kluge et al. [178]		152.4	304.8	28		689	pl-7.1			579	0.7
Kluge et al. [178]		152.4	304.8	28		705	pl-7.1			827	1.9
Kluge et al. [178]		152.4	304.8	28		881	pl-7.1			1875	6.6
Kluge et al. [178]		152.4	304.8	28		929	pl-7.1			1999	7.7
Kluge et al. [178]		152.4	304.8	28		1554	eg-19.1			5054	2.6
Kluge et al. [178]		152.4	304.8	28		1586	eg-19.1			8860	4.9
Kluge et al. [178]		152.4	304.8	28		1650	eg-19.1			1234[m]	9.7
Kluge et al. [178]		152.4	304.8	28		1922	eg-19.1			18133	24.6
Kluge et al. [178]		152.4	304.8	28		1378	eg-19.1			5054	2.9
Kluge et al. [178]		152.4	304.8	28		1570	eg-19.1			10756	9.7
Kluge et al. [178]		152.4	304.8	28		1682	eg-19.1			16065	16.9
Kluge et al. [178]		152.4	304.8	28		1794	eg-19.1			16478	29.6
Kluge et al. [178]		152.4	304.8	28		1121	eg-19.1			4923	4.0
Kluge et al. [178]		152.4	304.8	28		1297	eg-19.1			9080	11.9
Kluge et al. [178]		152.4	304.8	28		1490	eg-19.1			11301	19.1
Kluge et al. [178]		152.4	304.8	28		1554	eg-19.1			9584	20.5
Kluge et al. [178]		152.4	304.8	28		1394	fa-19.1			7329	5.3
Kluge et al. [178]		152.4	304.8	28		1474	fa-19.1			10018	12.4
Kluge et al. [178]		152.4	304.8	28		1618	fa-19.1			12976	22.1
Kluge et al. [178]		152.4	304.8	28		1714	fa-19.1			13645	29.0
Kluge et al. [178]		152.4	304.8	28		1185	pm-25.4			3309	8.1
Kluge et al. [178]		152.4	304.8	28		1297	pm-25.4			2654	12.2
Kluge et al. [178]		152.4	304.8	28		1362	pm-25.4			2896	14.1
Kluge et al. [178]		152.4	304.8	28		1410	pm-25.4			3792	15.0
Kluge et al. [178]		152.4	304.8	28		1602	es-12.7			12528	10.2
Kluge et al. [178]		152.4	304.8	28		1698	es-12.7			17092	27.6
Kluge et al. [178]		152.4	304.8	28		1730	es-12.7			19354	42.8
Kluge et al. [178]		152.4	304.8	28		1778	es-12.7			18244	48.6
Kluge et al. [178]		152.4	304.8	28		1249	et-12.7			7557	9.0
Kluge et al. [178]		152.4	304.8	28		1297	et-12.7			8653	15.9
Kluge et al. [178]		152.4	304.8	28		1394	et-12.7			10377	23.8
Kluge et al. [178]		152.4	304.8	28		1490	et-12.7			11997	27.6
Kluge et al. [178]		152.4	304.8	28		1378	ec-19.1			5771	8.9
Kluge et al. [178]		152.4	304.8	28		1426	ec-19.1			7308	17.9
Kluge et al. [178]		152.4	304.8	28		1522	ec-19.1			8101	28.8
Kluge et al. [178]		152.4	304.8	28		1634	ec-19.1			10156	32.7

Source	*n*	*B (mm)*	*H (mm)*	*Age (d)*	*w/c*	$\rho_{c,f}$ *(kg/m³)*	*Aggregate properties*[p]	*sf/c (%)*	*ma/b (%)*	E_c *(MPa)*	f'_{co} *(MPa)*
Kluge et al. [178]		152.4	304.8	7		801	vm-9.5				0.6
Kluge et al. [178]		152.4	304.8	7		865	vm-9.5				1.3
Kluge et al. [178]		152.4	304.8	7		945	vm-9.5				2.2
Kluge et al. [178]		152.4	304.8	7		1009	vm-9.5				3.7
Kluge et al. [178]		152.4	304.8	7		1169	dt-9.5				1.6
Kluge et al. [178]		152.4	304.8	7		1233	dt-9.5				2.8
Kluge et al. [178]		152.4	304.8	7		1362	dt-9.5				6.5
Kluge et al. [178]		152.4	304.8	7		1458	dt-9.5				9.4
Kluge et al. [178]		152.4	304.8	7		689	pl-7.1				0.3
Kluge et al. [178]		152.4	304.8	7		705	pl-7.1				1.7
Kluge et al. [178]		152.4	304.8	7		881	pl-7.1				6.7
Kluge et al. [178]		152.4	304.8	7		929	pl-7.1				7.6
Kluge et al. [178]		152.4	304.8	7		1554	eg-19.1				1.4
Kluge et al. [178]		152.4	304.8	7		1586	eg-19.1				4.2
Kluge et al. [178]		152.4	304.8	7		1650	eg-19.1				9.0
Kluge et al. [178]		152.4	304.8	7		1922	eg-19.1				15.8
Kluge et al. [178]		152.4	304.8	7		1378	eg-12.7				1.1
Kluge et al. [178]		152.4	304.8	7		1570	eg-12.7				3.7
Kluge et al. [178]		152.4	304.8	7		1682	eg-12.7				11.7
Kluge et al. [178]		152.4	304.8	7		1794	eg-12.7				23.2
Kluge et al. [178]		152.4	304.8	7		1121	eg-12.7				2.0
Kluge et al. [178]		152.4	304.8	7		1297	eg-12.7				8.3
Kluge et al. [178]		152.4	304.8	7		1490	eg-12.7				16.5
Kluge et al. [178]		152.4	304.8	7		1554	eg-12.7				20.6
Kluge et al. [178]		152.4	304.8	7		1394	fa-19.1				2.8
Kluge et al. [178]		152.4	304.8	7		1474	fa-19.1				8.1
Kluge et al. [178]		152.4	304.8	7		1618	fa-19.1				18.1
Kluge et al. [178]		152.4	304.8	7		1714	fa-19.1				26.4
Kluge et al. [178]		152.4	304.8	7		1185	pm-25.4				6.6
Kluge et al. [178]		152.4	304.8	7		1297	pm-25.4				10.6
Kluge et al. [178]		152.4	304.8	7		1362	pm-25.4				14.7
Kluge et al. [178]		152.4	304.8	7		1410	pm-25.4				16.1
Kluge et al. [178]		152.4	304.8	7		1602	es-12.7				5.2
Kluge et al. [178]		152.4	304.8	7		1698	es-12.7				16.4
Kluge et al. [178]		152.4	304.8	7		1730	es-12.7				31.0
Kluge et al. [178]		152.4	304.8	7		1778	es-12.7				38.5
Kluge et al. [178]		152.4	304.8	7		1249	et-12.7				5.2
Kluge et al. [178]		152.4	304.8	7		1297	et-12.7				11.6
Kluge et al. [178]		152.4	304.8	7		1394	et-12.7				20.0
Kluge et al. [178]		152.4	304.8	7		1490	et-12.7				26.0
Kluge et al. [178]		152.4	304.8	7		1378	ec-19.1				4.3
Kluge et al. [178]		152.4	304.8	7		1426	ec-19.1				12.0
Kluge et al. [178]		152.4	304.8	7		1522	ec-19.1				22.4
Kluge et al. [178]		152.4	304.8	7		1634	ec-19.1				27.4
Martinez et al. [179]	1	101.6	406.4				es-10			10963	28.6
Martinez et al. [179]	1	101.6	406.4				es-10			11790	28.6
Martinez et al. [179]	1	101.6	406.4				es-10			11652	28.6
Martinez et al. [179]	1	101.6	406.4				es-10			11032	25.5
Martinez et al. [179]	1	101.6	406.4				es-10			11238	25.5
Martinez et al. [179]	1	101.6	406.4				es-10			10411	25.5
Martinez et al. [179]	1	101.6	406.4				es-10			11170	25.2
Martinez et al. [179]	1	101.6	406.4				es-10			10411	25.2
Martinez et al. [179]	1	101.6	406.4				es-10			11101	25.2
Martinez et al. [179]	1	101.6	406.4				es-10			13583	44.3
Martinez et al. [179]	1	101.6	406.4				es-10			13445	44.3
Martinez et al. [179]	1	101.6	406.4				es-10			13307	44.3
Martinez et al. [179]	1	101.6	406.4				es-10			15031	49.0
Martinez et al. [179]	1	101.6	406.4				es-10			13858	49.0
Martinez et al. [179]	1	101.6	406.4				es-10			14962	49.0
Martinez et al. [179]	1	101.6	406.4				es-10			15237	44.6
Martinez et al. [179]	1	101.6	406.4				es-10			15513	44.6
Martinez et al. [179]	1	101.6	406.4				es-10			15582	44.6
Martinez et al. [179]	1	101.6	406.4				es-10			16616	55.1
Martinez et al. [179]	1	101.6	406.4				es-10			17651	55.1
Martinez et al. [179]	1	101.6	406.4				es-10			17099	55.1
Martinez et al. [179]	1	101.6	406.4				es-10			16203	54.0
Martinez et al. [179]	1	101.6	406.4				es-10			17857	54.0
Martinez et al. [179]	1	101.6	406.4				es-10			17995	54.0
Martinez et al. [179]	1	101.6	406.4				es-10			17030	56.2
Martinez et al. [179]	1	101.6	406.4				es-10			18547	56.2
Martinez et al. [179]	1	101.6	406.4				es-10			17030	56.2
Martinez et al. [179]	1	101.6	203.2				es-10			12135	33.0
Martinez et al. [179]	1	101.6	203.2				es-10			11997	33.0
Martinez et al. [179]	1	101.6	203.2				es-10			12411	41.0
Martinez et al. [179]	1	101.6	203.2				es-10			12135	41.0
Martinez et al. [179]	1	101.6	203.2				es-10			17995	54.1
Martinez et al. [179]	1	101.6	203.2				es-10			17857	54.1
Martinez et al. [179]	1	152.4	609.6				es-10			12204	28.2
Martinez et al. [179]	1	152.4	609.6				es-10			11790	28.2
Martinez et al. [179]	1	152.4	609.6				es-10			13514	34.5

Source	*n*	*B (mm)*	*H (mm)*	*Age (d)*	*w/c*	$\rho_{c,f}$ *(kg/m³)*	*Aggregate properties*[p]	*sf/c (%)*	*ma/b (%)*	E_c *(MPa)*	f'_{co} *(MPa)*
Martinez et al. [179]	1	152.4	609.6				es-10			13376	34.5
Martinez et al. [179]	1	152.4	609.6				es-10			12480	34.5
Martinez et al. [179]	1	152.4	609.6				es-10			16616	50.7
Martinez et al. [179]	1	152.4	609.6				es-10			16065	50.7
Martinez et al. [179]	1	152.4	609.6				es-10			17237	50.7
Nassif [182]	23	100	200	1	0.30	1756	es-19	10.0		15300	23.1
Nassif [182]	24	100	200	1	0.30	1756	es-19	10.0		17400	23.9
Nassif [182]	25	100	200	1	0.30	1756	es-19	10.0		15000	22.6
Nassif [182]	68	100	200	3	0.30	1756	es-19	10.0		16000	37.9
Nassif [182]	69	100	200	3	0.30	1756	es-19	10.0		14800	32.9
Nassif [182]	70	100	200	3	0.30	1756	es-19	10.0		14900	34.0
Nassif [182]	114	100	200	7	0.30	1756	es-19	10.0		17100	35.7
Nassif [182]	115	100	200	7	0.30	1756	es-19	10.0		13200	36.2
Nassif [182]	116	100	200	7	0.30	1756	es-19	10.0		14700	34.9
Nassif [182]	160	100	200	14	0.30	1756	es-19	10.0		16000	38.4
Nassif [182]	161	100	200	14	0.30	1756	es-19	10.0		14400	36.5
Nassif [182]	162	100	200	14	0.30	1756	es-19	10.0		15800	35.4
Nassif [182]	206	100	200	28	0.30	1756	es-19	10.0			38.7
Nassif [182]	207	100	200	28	0.30	1756	es-19	10.0			38.4
Nassif [182]	208	100	200	28	0.30	1756	es-19	10.0			37.3
Price and Cordon [201]	1	152.4	304.8	7			es,ec				5.0
Price and Cordon [201]	1	152.4	304.8	7			es,ec				14.4
Price and Cordon [201]	1	152.4	304.8	7			es,ec				20.8
Price and Cordon [201]	1	152.4	304.8	7			es,ec				21.8
Price and Cordon [201]	1	152.4	304.8	7			es,ec				25.2
Price and Cordon [201]	1	152.4	304.8	7			es,ec				3.1
Price and Cordon [201]	1	152.4	304.8	7			es,ec				8.0
Price and Cordon [201]	1	152.4	304.8	7			es,ec				17.5
Price and Cordon [201]	1	152.4	304.8	7			es,ec				16.6
Price and Cordon [201]	1	152.4	304.8	7			es,ec				25.8
Price and Cordon [201]	1	152.4	304.8	7			eg				1.2
Price and Cordon [201]	1	152.4	304.8	7			eg				3.9
Price and Cordon [201]	1	152.4	304.8	7			eg				8.1
Price and Cordon [201]	1	152.4	304.8	7			eg				5.9
Price and Cordon [201]	1	152.4	304.8	7			eg				11.4
Price and Cordon [201]	1	152.4	304.8	7			eg				1.2
Price and Cordon [201]	1	152.4	304.8	7			eg				3.1
Price and Cordon [201]	1	152.4	304.8	7			eg				2.1
Price and Cordon [201]	1	152.4	304.8	7			eg				2.7
Price and Cordon [201]	1	152.4	304.8	7			sr				0.5
Price and Cordon [201]	1	152.4	304.8	7			sr				5.1
Price and Cordon [201]	1	152.4	304.8	7			sr				7.7
Price and Cordon [201]	1	152.4	304.8	7			sr				14.8
Price and Cordon [201]	1	152.4	304.8	7			pm				1.2
Price and Cordon [201]	1	152.4	304.8	7			pm				5.9
Price and Cordon [201]	1	152.4	304.8	7			pm				11.4
Price and Cordon [201]	1	152.4	304.8	7			pm				10.5
Price and Cordon [201]	1	152.4	304.8	7			pm				14.9
Price and Cordon [201]	1	152.4	304.8	7			pm				2.0
Price and Cordon [201]	1	152.4	304.8	7			pm				5.7
Price and Cordon [201]	1	152.4	304.8	7			pm				13.5
Price and Cordon [201]	1	152.4	304.8	7			pm				12.5
Price and Cordon [201]	1	152.4	304.8	7			pm				17.7
Price and Cordon [201]	1	152.4	304.8	7			pm				4.2
Price and Cordon [201]	1	152.4	304.8	7			pm				7.8
Price and Cordon [201]	1	152.4	304.8	7			pm				7.9
Price and Cordon [201]	1	152.4	304.8	7			pm				1.8
Price and Cordon [201]	1	152.4	304.8	7			pm				4.9
Price and Cordon [201]	1	152.4	304.8	7			pm				5.2
Price and Cordon [201]	1	152.4	304.8	7			pm				2.3
Price and Cordon [201]	1	152.4	304.8	7			pl				2.5
Price and Cordon [201]	1	152.4	304.8	7			pl				4.6
Price and Cordon [201]	1	152.4	304.8	7			pl				0.2
Price and Cordon [201]	1	152.4	304.8	7			pl				0.8
Price and Cordon [201]	1	152.4	304.8	7			pl				1.7
Price and Cordon [201]	1	152.4	304.8	7			pl				3.6
Price and Cordon [201]	1	152.4	304.8	7			pl				6.7
Price and Cordon [201]	1	152.4	304.8	7			pl				0.8
Price and Cordon [201]	1	152.4	304.8	7			pl				2.5
Price and Cordon [201]	1	152.4	304.8	7			pl				3.3
Price and Cordon [201]	1	152.4	304.8	7			pl				1.2
Price and Cordon [201]	1	152.4	304.8	7			pl				1.7
Price and Cordon [201]	1	152.4	304.8	7			pl				2.1
Price and Cordon [201]	1	152.4	304.8	7			pl				2.8
Price and Cordon [201]	1	152.4	304.8	7			pl				0.9
Price and Cordon [201]	1	152.4	304.8	7			vm				1.0
Price and Cordon [201]	1	152.4	304.8	7			vm				2.2
Price and Cordon [201]	1	152.4	304.8	7			vm				0.2
Price and Cordon [201]	1	152.4	304.8	7			vm				0.4
Price and Cordon [201]	1	152.4	304.8	7			vm				1.3

Source	*n*	*B (mm)*	*H (mm)*	*Age (d)*	*w/c*	$\rho_{c,f}$ *(kg/m³)*	*Aggregate properties*[p]	*sf/c (%)*	*ma/b (%)*	E_c *(MPa)*	f'_{co} *(MPa)*
Price and Cordon [201]	1	152.4	304.8	7			vm				2.6
Price and Cordon [201]	1	152.4	304.8	7			de				0.6
Price and Cordon [201]	1	152.4	304.8	7			de				1.5
Price and Cordon [201]	1	152.4	304.8	7			de				1.7
Price and Cordon [201]	1	152.4	304.8	7			de				2.8
Price and Cordon [201]	1	152.4	304.8	28			es,ec			9860	8.9
Price and Cordon [201]	1	152.4	304.8	28			es,ec			11514	22.5
Price and Cordon [201]	1	152.4	304.8	28			es,ec			12962	30.4
Price and Cordon [201]	1	152.4	304.8	28			es,ec			11238	30.0
Price and Cordon [201]	1	152.4	304.8	28			es,ec			11859	32.8
Price and Cordon [201]	1	152.4	304.8	28			es,ec			6826	7.1
Price and Cordon [201]	1	152.4	304.8	28			es,ec			11514	14.3
Price and Cordon [201]	1	152.4	304.8	28			es,ec			15100	27.6
Price and Cordon [201]	1	152.4	304.8	28			es,ec			12824	26.8
Price and Cordon [201]	1	152.4	304.8	28			es,ec			14134	34.3
Price and Cordon [201]	1	152.4	304.8	28			eg			3930	2.9
Price and Cordon [201]	1	152.4	304.8	28			eg			6412	7.8
Price and Cordon [201]	1	152.4	304.8	28			eg			9653	12.7
Price and Cordon [201]	1	152.4	304.8	28			eg			5585	9.8
Price and Cordon [201]	1	152.4	304.8	28			eg			9791	17.1
Price and Cordon [201]	1	152.4	304.8	28			eg				2.1
Price and Cordon [201]	1	152.4	304.8	28			eg				5.3
Price and Cordon [201]	1	152.4	304.8	28			eg				4.0
Price and Cordon [201]	1	152.4	304.8	28			eg				5.3
Price and Cordon [201]	1	152.4	304.8	28			sr				1.3
Price and Cordon [201]	1	152.4	304.8	28			sr				5.4
Price and Cordon [201]	1	152.4	304.8	28			sr			8274	12.9
Price and Cordon [201]	1	152.4	304.8	28			sr			7998	17.5
Price and Cordon [201]	1	152.4	304.8	28			pm				3.6
Price and Cordon [201]	1	152.4	304.8	28			pm			5723	11.7
Price and Cordon [201]	1	152.4	304.8	28			pm			6619	18.7
Price and Cordon [201]	1	152.4	304.8	28			pm			6274	18.9
Price and Cordon [201]	1	152.4	304.8	28			pm			7239	22.1
Price and Cordon [201]	1	152.4	304.8	28			pm				2.4
Price and Cordon [201]	1	152.4	304.8	28			pm			6964	9.2
Price and Cordon [201]	1	152.4	304.8	28			pm			5861	17.4
Price and Cordon [201]	1	152.4	304.8	28			pm				15.2
Price and Cordon [201]	1	152.4	304.8	28			pm			6688	21.9
Price and Cordon [201]	1	152.4	304.8	28			pm			2551	8.2
Price and Cordon [201]	1	152.4	304.8	28			pm			2482	12.4
Price and Cordon [201]	1	152.4	304.8	28			pm			3034	12.2
Price and Cordon [201]	1	152.4	304.8	28			pm				4.0
Price and Cordon [201]	1	152.4	304.8	28			pm			1310	10.2
Price and Cordon [201]	1	152.4	304.8	28			pm				10.3
Price and Cordon [201]	1	152.4	304.8	28			pm				6.2
Price and Cordon [201]	1	152.4	304.8	28			pl				3.7
Price and Cordon [201]	1	152.4	304.8	28			pl			2275	6.7
Price and Cordon [201]	1	152.4	304.8	28			pl				0.5
Price and Cordon [201]	1	152.4	304.8	28			pl				1.4
Price and Cordon [201]	1	152.4	304.8	28			pl			2068	4.8
Price and Cordon [201]	1	152.4	304.8	28			pl				5.8
Price and Cordon [201]	1	152.4	304.8	28			pl			1586	10.3
Price and Cordon [201]	1	152.4	304.8	28			pl				1.6
Price and Cordon [201]	1	152.4	304.8	28			pl			1241	4.4
Price and Cordon [201]	1	152.4	304.8	28			pl			1172	5.0
Price and Cordon [201]	1	152.4	304.8	28			pl				1.8
Price and Cordon [201]	1	152.4	304.8	28			pl			1793	3.0
Price and Cordon [201]	1	152.4	304.8	28			pl				3.4
Price and Cordon [201]	1	152.4	304.8	28			pl			3034	4.2
Price and Cordon [201]	1	152.4	304.8	28			pl			827	2.3
Price and Cordon [201]	1	152.4	304.8	28			vm				1.5
Price and Cordon [201]	1	152.4	304.8	28			vm			1655	2.8
Price and Cordon [201]	1	152.4	304.8	28			vm				0.9
Price and Cordon [201]	1	152.4	304.8	28			vm				1.8
Price and Cordon [201]	1	152.4	304.8	28			vm			1586	3.6
Price and Cordon [201]	1	152.4	304.8	28			de				1.0
Price and Cordon [201]	1	152.4	304.8	28			de				2.1
Price and Cordon [201]	1	152.4	304.8	28			de				2.3
Price and Cordon [201]	1	152.4	304.8	28			de				3.3
Price and Cordon [201]	1	152.4	304.8	42			es,ec				10.4
Price and Cordon [201]	1	152.4	304.8	42			es,ec				23.7
Price and Cordon [201]	1	152.4	304.8	42			es,ec				31.9
Price and Cordon [201]	1	152.4	304.8	42			es,ec				32.4
Price and Cordon [201]	1	152.4	304.8	42			es,ec				37.9
Price and Cordon [201]	1	152.4	304.8	42			es,ec				7.2
Price and Cordon [201]	1	152.4	304.8	42			es,ec				17.3
Price and Cordon [201]	1	152.4	304.8	42			es,ec				33.3
Price and Cordon [201]	1	152.4	304.8	42			es,ec				28.3
Price and Cordon [201]	1	152.4	304.8	42			es,ec				36.5
Price and Cordon [201]	1	152.4	304.8	42			eg				3.7

Source	*n*	*B (mm)*	*H (mm)*	*Age (d)*	*w/c*	$\rho_{c,f}$ *(kg/m³)*	*Aggregate properties*[p]	*sf/c (%)*	*ma/b (%)*	E_c *(MPa)*	f'_{co} *(MPa)*
Price and Cordon [201]	1	152.4	304.8	42			eg				8.4
Price and Cordon [201]	1	152.4	304.8	42			eg				15.4
Price and Cordon [201]	1	152.4	304.8	42			eg				9.8
Price and Cordon [201]	1	152.4	304.8	42			eg				16.5
Price and Cordon [201]	1	152.4	304.8	42			eg				1.8
Price and Cordon [201]	1	152.4	304.8	42			eg				4.3
Price and Cordon [201]	1	152.4	304.8	42			eg				4.0
Price and Cordon [201]	1	152.4	304.8	42			eg				4.5
Price and Cordon [201]	1	152.4	304.8	42			sr				1.5
Price and Cordon [201]	1	152.4	304.8	42			sr				5.7
Price and Cordon [201]	1	152.4	304.8	42			sr				12.4
Price and Cordon [201]	1	152.4	304.8	42			sr				20.5
Price and Cordon [201]	1	152.4	304.8	42			pm				3.5
Price and Cordon [201]	1	152.4	304.8	42			pm				11.7
Price and Cordon [201]	1	152.4	304.8	42			pm				19.6
Price and Cordon [201]	1	152.4	304.8	42			pm				17.7
Price and Cordon [201]	1	152.4	304.8	42			pm				22.2
Price and Cordon [201]	1	152.4	304.8	42			pm				4.9
Price and Cordon [201]	1	152.4	304.8	42			pm				12.1
Price and Cordon [201]	1	152.4	304.8	42			pm				19.8
Price and Cordon [201]	1	152.4	304.8	42			pm				15.0
Price and Cordon [201]	1	152.4	304.8	42			pm				22.5
Price and Cordon [201]	1	152.4	304.8	42			pm				8.9
Price and Cordon [201]	1	152.4	304.8	42			pm				11.1
Price and Cordon [201]	1	152.4	304.8	42			pm				10.3
Price and Cordon [201]	1	152.4	304.8	42			pm				4.3
Price and Cordon [201]	1	152.4	304.8	42			pm				11.1
Price and Cordon [201]	1	152.4	304.8	42			pm				11.0
Price and Cordon [201]	1	152.4	304.8	42			pm				5.4
Price and Cordon [201]	1	152.4	304.8	42			pl				4.0
Price and Cordon [201]	1	152.4	304.8	42			pl				6.0
Price and Cordon [201]	1	152.4	304.8	42			pl				0.6
Price and Cordon [201]	1	152.4	304.8	42			pl				1.6
Price and Cordon [201]	1	152.4	304.8	42			pl				4.8
Price and Cordon [201]	1	152.4	304.8	42			pl				5.6
Price and Cordon [201]	1	152.4	304.8	42			pl				9.1
Price and Cordon [201]	1	152.4	304.8	42			pl				0.8
Price and Cordon [201]	1	152.4	304.8	42			pl				4.2
Price and Cordon [201]	1	152.4	304.8	42			pl				4.8
Price and Cordon [201]	1	152.4	304.8	42			pl				1.6
Price and Cordon [201]	1	152.4	304.8	42			pl				3.2
Price and Cordon [201]	1	152.4	304.8	42			pl				3.4
Price and Cordon [201]	1	152.4	304.8	42			pl				5.6
Price and Cordon [201]	1	152.4	304.8	42			pl				2.0
Price and Cordon [201]	1	152.4	304.8	42			vm				1.9
Price and Cordon [201]	1	152.4	304.8	42			vm				3.2
Price and Cordon [201]	1	152.4	304.8	42			vm				0.3
Price and Cordon [201]	1	152.4	304.8	42			vm				1.0
Price and Cordon [201]	1	152.4	304.8	42			vm				2.3
Price and Cordon [201]	1	152.4	304.8	42			vm				4.3
Price and Cordon [201]	1	152.4	304.8	42			de				0.9
Price and Cordon [201]	1	152.4	304.8	42			de				2.2
Price and Cordon [201]	1	152.4	304.8	42			de				3.2
Richart and Jensen [93]	3	152.4	304.8	7		1836	es-12.7			14617	18.6
Richart and Jensen [93]	3	152.4	304.8	7		1820	es-12.7			12135	14.8
Richart and Jensen [93]	3	152.4	304.8	7		1805	es-12.7			12273	9.9
Richart and Jensen [93]	3	152.4	304.8	7		1941	es-12.7			17375	19.4
Richart and Jensen [93]	3	152.4	304.8	7		1930	es-12.7			14411	15.9
Richart and Jensen [93]	3	152.4	304.8	7		1762	es-12.7			13307	10.8
Richart and Jensen [93]	3	152.4	304.8	7		2022	es-12.7			16961	19.4
Richart and Jensen [93]	3	152.4	304.8	7		2007	es-12.7			16065	17.0
Richart and Jensen [93]	3	152.4	304.8	7		1999	es-12.7			14134	13.0
Richart and Jensen [93]	3	152.4	304.8	7		1815	es-12.7			13996	13.4
Richart and Jensen [93]	3	152.4	304.8	7		1825	es-12.7			11928	10.3
Richart and Jensen [93]	3	152.4	304.8	7		1810	es-12.7			11032	8.1
Richart and Jensen [93]	3	152.4	304.8	7		1906	es-12.7			15513	14.5
Richart and Jensen [93]	3	152.4	304.8	7		1898	es-12.7			12273	11.1
Richart and Jensen [93]	3	152.4	304.8	7		1863	es-12.7			12273	8.9
Richart and Jensen [93]	3	152.4	304.8	7		1959	es-12.7			14272	11.8
Richart and Jensen [93]	3	152.4	304.8	7		1970	es-12.7			12755	9.4
Richart and Jensen [93]	3	152.4	304.8	7		1949	es-12.7			11790	8.0
Richart and Jensen [93]	3	152.4	304.8	7		1825	es-12.7			10204	8.5
Richart and Jensen [93]	3	152.4	304.8	7		1794	es-12.7			9101	6.6
Richart and Jensen [93]	3	152.4	304.8	7		1799	es-12.7			7377	5.5
Richart and Jensen [93]	3	152.4	304.8	7		1884	es-12.7			11652	8.3
Richart and Jensen [93]	3	152.4	304.8	7		1881	es-12.7			10135	6.8
Richart and Jensen [93]	3	152.4	304.8	7		1877	es-12.7			9722	6.3
Richart and Jensen [93]	3	152.4	304.8	7		1935	es-12.7			10618	7.6
Richart and Jensen [93]	3	152.4	304.8	7		1935	es-12.7			8756	6.1
Richart and Jensen [93]	3	152.4	304.8	7		1941	es-12.7			9722	5.3

Source	*n*	*B (mm)*	*H (mm)*	*Age (d)*	*w/c*	$\rho_{c,f}$ *(kg/m³)*	*Aggregate properties*[p]	*sf/c (%)*	*ma/b (%)*	E_c *(MPa)*	f'_{co} *(MPa)*
Richart and Jensen [93]	3	152.4	304.8	28		1836	es-12.7			17995	29.6
Richart and Jensen [93]	3	152.4	304.8	28		1820	es-12.7			16823	26.3
Richart and Jensen [93]	3	152.4	304.8	28		1805	es-12.7			16341	20.3
Richart and Jensen [93]	3	152.4	304.8	28		1941	es-12.7			20753	30.1
Richart and Jensen [93]	3	152.4	304.8	28		1930	es-12.7			19167	27.3
Richart and Jensen [93]	3	152.4	304.8	28		1762	es-12.7			17926	21.4
Richart and Jensen [93]	3	152.4	304.8	28		2022	es-12.7			20960	28.6
Richart and Jensen [93]	3	152.4	304.8	28		2007	es-12.7			20822	27.8
Richart and Jensen [93]	3	152.4	304.8	28		1999	es-12.7			18340	23.6
Richart and Jensen [93]	3	152.4	304.8	28		1815	es-12.7			17926	25.1
Richart and Jensen [93]	3	152.4	304.8	28		1825	es-12.7			16341	21.4
Richart and Jensen [93]	3	152.4	304.8	28		1810	es-12.7			14824	17.4
Richart and Jensen [93]	3	152.4	304.8	28		1906	es-12.7			18478	23.4
Richart and Jensen [93]	3	152.4	304.8	28		1898	es-12.7			17444	20.9
Richart and Jensen [93]	3	152.4	304.8	28		1863	es-12.7			15927	18.6
Richart and Jensen [93]	3	152.4	304.8	28		1959	es-12.7			14272	21.4
Richart and Jensen [93]	3	152.4	304.8	28		1970	es-12.7			17030	17.9
Richart and Jensen [93]	3	152.4	304.8	28		1949	es-12.7			15996	16.3
Richart and Jensen [93]	3	152.4	304.8	28		1825	es-12.7			15375	17.4
Richart and Jensen [93]	3	152.4	304.8	28		1794	es-12.7			15237	14.1
Richart and Jensen [93]	3	152.4	304.8	28		1799	es-12.7			13790	12.8
Richart and Jensen [93]	3	152.4	304.8	28		1884	es-12.7			16892	18.1
Richart and Jensen [93]	3	152.4	304.8	28		1881	es-12.7			15306	14.5
Richart and Jensen [93]	3	152.4	304.8	28		1877	es-12.7			15375	13.2
Richart and Jensen [93]	3	152.4	304.8	28		1935	es-12.7			17030	15.0
Richart and Jensen [93]	3	152.4	304.8	28		1935	es-12.7			15996	13.0
Richart and Jensen [93]	3	152.4	304.8	28		1941	es-12.7			15237	9.9
Richart and Jensen [93]	3	152.4	304.8	7		1586	es-12.7			11307	13.7
Richart and Jensen [93]	3	152.4	304.8	7		1551	es-12.7			10342	10.3
Richart and Jensen [93]	3	152.4	304.8	7		1543	es-12.7			8343	8.0
Richart and Jensen [93]	3	152.4	304.8	7		1594	es-12.7			11032	13.0
Richart and Jensen [93]	3	152.4	304.8	7		1563	es-12.7			10204	10.1
Richart and Jensen [93]	3	152.4	304.8	7		1555	es-12.7			9156	8.3
Richart and Jensen [93]	3	152.4	304.8	7		1595	es-12.7			10549	12.8
Richart and Jensen [93]	3	152.4	304.8	7		1579	es-12.7			9653	10.1
Richart and Jensen [93]	3	152.4	304.8	7		1565	es-12.7			8963	7.3
Richart and Jensen [93]	3	152.4	304.8	7		1536	es-12.7			9722	9.4
Richart and Jensen [93]	3	152.4	304.8	7		1523	es-12.7			8963	8.0
Richart and Jensen [93]	3	152.4	304.8	7		1519	es-12.7			9722	6.0
Richart and Jensen [93]	3	152.4	304.8	7		1541	es-12.7			10273	8.6
Richart and Jensen [93]	3	152.4	304.8	7		1552	es-12.7			7998	7.4
Richart and Jensen [93]	3	152.4	304.8	7		1533	es-12.7			8274	6.2
Richart and Jensen [93]	3	152.4	304.8	7		1555	es-12.7			8481	7.7
Richart and Jensen [93]	3	152.4	304.8	7		1538	es-12.7			7860	6.0
Richart and Jensen [93]	3	152.4	304.8	7		1519	es-12.7			7102	4.6
Richart and Jensen [93]	3	152.4	304.8	7		1522	es-12.7			8550	5.2
Richart and Jensen [93]	3	152.4	304.8	7		1517	es-12.7			8205	5.2
Richart and Jensen [93]	3	152.4	304.8	7		1483	es-12.7			6895	3.7
Richart and Jensen [93]	3	152.4	304.8	7		1525	es-12.7			9101	5.7
Richart and Jensen [93]	3	152.4	304.8	7		1535	es-12.7			7446	4.9
Richart and Jensen [93]	3	152.4	304.8	7		1490	es-12.7			6688	3.7
Richart and Jensen [93]	3	152.4	304.8	7		1533	es-12.7			6688	4.4
Richart and Jensen [93]	3	152.4	304.8	7		1517	es-12.7			7033	3.9
Richart and Jensen [93]	3	152.4	304.8	7		1504	es-12.7			5792	3.2
Richart and Jensen [93]	3	152.4	304.8	28		1586	es-12.7			13858	25.5
Richart and Jensen [93]	3	152.4	304.8	28		1551	es-12.7			12824	21.1
Richart and Jensen [93]	3	152.4	304.8	28		1543	es-12.7			12411	16.8
Richart and Jensen [93]	3	152.4	304.8	28		1594	es-12.7			13445	23.9
Richart and Jensen [93]	3	152.4	304.8	28		1563	es-12.7			11514	19.9
Richart and Jensen [93]	3	152.4	304.8	28		1555	es-12.7			12204	16.5
Richart and Jensen [93]	3	152.4	304.8	28		1595	es-12.7			13031	22.9
Richart and Jensen [93]	3	152.4	304.8	28		1579	es-12.7			12686	19.1
Richart and Jensen [93]	3	152.4	304.8	28		1565	es-12.7			11445	14.8
Richart and Jensen [93]	3	152.4	304.8	28		1536	es-12.7			12548	17.4
Richart and Jensen [93]	3	152.4	304.8	28		1523	es-12.7			11928	15.9
Richart and Jensen [93]	3	152.4	304.8	28		1519	es-12.7			11514	13.2
Richart and Jensen [93]	3	152.4	304.8	28		1541	es-12.7			12755	18.1
Richart and Jensen [93]	3	152.4	304.8	28		1552	es-12.7			12480	15.9
Richart and Jensen [93]	3	152.4	304.8	28		1533	es-12.7			11238	14.2
Richart and Jensen [93]	3	152.4	304.8	28		1555	es-12.7			12204	16.2
Richart and Jensen [93]	3	152.4	304.8	28		1538	es-12.7			11445	13.5
Richart and Jensen [93]	3	152.4	304.8	28		1519	es-12.7			9997	9.0
Richart and Jensen [93]	3	152.4	304.8	28		1522	es-12.7			9170	10.9
Richart and Jensen [93]	3	152.4	304.8	28		1517	es-12.7			11170	11.6
Richart and Jensen [93]	3	152.4	304.8	28		1483	es-12.7			10618	9.0
Richart and Jensen [93]	3	152.4	304.8	28		1525	es-12.7			11032	12.1
Richart and Jensen [93]	3	152.4	304.8	28		1535	es-12.7			9032	11.2
Richart and Jensen [93]	3	152.4	304.8	28		1490	es-12.7			10825	8.8
Richart and Jensen [93]	3	152.4	304.8	28		1533	es-12.7			10687	10.1
Richart and Jensen [93]	3	152.4	304.8	28		1517	es-12.7			11238	8.4

Source	*n*	*B (mm)*	*H (mm)*	*Age (d)*	*w/c*	$\rho_{c,f}$ *(kg/m³)*	*Aggregate properties*[p]	*sf/c (%)*	*ma/b (%)*	E_c *(MPa)*	f'_{co} *(MPa)*
Richart and Jensen [93]	3	152.4	304.8	28		1504	es-12.7			9101	7.7
Richart and Jensen [93]	3	152.4	304.8	7		1680	es-12.7			13376	19.7
Richart and Jensen [93]	3	152.4	304.8	7		1655	es-12.7			11652	15.4
Richart and Jensen [93]	3	152.4	304.8	7		1599	es-12.7			8205	9.2
Richart and Jensen [93]	3	152.4	304.8	7		1695	es-12.7			13927	21.9
Richart and Jensen [93]	3	152.4	304.8	7		1684	es-12.7			11445	16.6
Richart and Jensen [93]	3	152.4	304.8	7		1626	es-12.7			9653	10.3
Richart and Jensen [93]	3	152.4	304.8	7		1703	es-12.7			13100	22.3
Richart and Jensen [93]	3	152.4	304.8	7		1701	es-12.7			11583	18.3
Richart and Jensen [93]	3	152.4	304.8	7		1660	es-12.7			10618	10.1
Richart and Jensen [93]	3	152.4	304.8	7		1632	es-12.7			11583	14.8
Richart and Jensen [93]	3	152.4	304.8	7		1626	es-12.7			10618	11.5
Richart and Jensen [93]	3	152.4	304.8	7		1602	es-12.7			9584	9.3
Richart and Jensen [93]	3	152.4	304.8	7		1647	es-12.7			11514	16.0
Richart and Jensen [93]	3	152.4	304.8	7		1648	es-12.7			11307	13.1
Richart and Jensen [93]	3	152.4	304.8	7		1619	es-12.7			10963	11.0
Richart and Jensen [93]	3	152.4	304.8	7		1663	es-12.7			10687	12.5
Richart and Jensen [93]	3	152.4	304.8	7		1650	es-12.7			11652	11.0
Richart and Jensen [93]	3	152.4	304.8	7		1639	es-12.7			9860	8.4
Richart and Jensen [93]	3	152.4	304.8	7		1584	es-12.7			9170	9.4
Richart and Jensen [93]	3	152.4	304.8	7		1591	es-12.7			9101	6.9
Richart and Jensen [93]	3	152.4	304.8	7		1587	es-12.7			7860	5.5
Richart and Jensen [93]	3	152.4	304.8	7		1613	es-12.7			10342	10.1
Richart and Jensen [93]	3	152.4	304.8	7		1589	es-12.7			8687	7.5
Richart and Jensen [93]	3	152.4	304.8	7		1599	es-12.7			8274	7.2
Richart and Jensen [93]	3	152.4	304.8	7		1599	es-12.7			9446	7.9
Richart and Jensen [93]	3	152.4	304.8	7		1605	es-12.7			7102	6.2
Richart and Jensen [93]	3	152.4	304.8	7		1616	es-12.7			7515	5.9
Richart and Jensen [93]	3	152.4	304.8	28		1680	es-12.7			14272	31.1
Richart and Jensen [93]	3	152.4	304.8	28		1655	es-12.7			13927	25.5
Richart and Jensen [93]	3	152.4	304.8	28		1599	es-12.7			12342	18.7
Richart and Jensen [93]	3	152.4	304.8	28		1695	es-12.7			14548	31.4
Richart and Jensen [93]	3	152.4	304.8	28		1684	es-12.7			14134	27.8
Richart and Jensen [93]	3	152.4	304.8	28		1626	es-12.7			13100	19.8
Richart and Jensen [93]	3	152.4	304.8	28		1703	es-12.7			15306	33.2
Richart and Jensen [93]	3	152.4	304.8	28		1701	es-12.7			15031	31.4
Richart and Jensen [93]	3	152.4	304.8	28		1660	es-12.7			12204	20.6
Richart and Jensen [93]	3	152.4	304.8	28		1632	es-12.7			13583	24.8
Richart and Jensen [93]	3	152.4	304.8	28		1626	es-12.7			13238	22.4
Richart and Jensen [93]	3	152.4	304.8	28		1602	es-12.7			12273	19.4
Richart and Jensen [93]	3	152.4	304.8	28		1647	es-12.7			13858	26.1
Richart and Jensen [93]	3	152.4	304.8	28		1648	es-12.7			14341	24.8
Richart and Jensen [93]	3	152.4	304.8	28		1619	es-12.7			13169	21.1
Richart and Jensen [93]	3	152.4	304.8	28		1663	es-12.7			13376	23.0
Richart and Jensen [93]	3	152.4	304.8	28		1650	es-12.7			12273	21.6
Richart and Jensen [93]	3	152.4	304.8	28		1639	es-12.7			11170	16.8
Richart and Jensen [93]	3	152.4	304.8	28		1584	es-12.7			12962	18.1
Richart and Jensen [93]	3	152.4	304.8	28		1591	es-12.7			11445	14.1
Richart and Jensen [93]	3	152.4	304.8	28		1587	es-12.7			10687	12.3
Richart and Jensen [93]	3	152.4	304.8	28		1613	es-12.7			13169	19.9
Richart and Jensen [93]	3	152.4	304.8	28		1589	es-12.7			12273	15.7
Richart and Jensen [93]	3	152.4	304.8	28		1599	es-12.7			10963	13.6
Richart and Jensen [93]	3	152.4	304.8	28		1599	es-12.7			12480	16.9
Richart and Jensen [93]	3	152.4	304.8	28		1605	es-12.7			11652	13.0
Richart and Jensen [93]	3	152.4	304.8	28		1616	es-12.7			10480	12.2
Richart and Jensen [93]	3	152.4	304.8	7		1849	es			12617	11.4
Richart and Jensen [93]	3	152.4	304.8	7		1635	es			13858	23.1
Richart and Jensen [93]	3	152.4	304.8	7		1863	es			14617	14.9
Richart and Jensen [93]	3	152.4	304.8	7		1863	es			13100	13.2
Richart and Jensen [93]	3	152.4	304.8	14		1635	es			14479	30.0
Richart and Jensen [93]	3	152.4	304.8	14		1863	es			15100	20.6
Richart and Jensen [93]	3	152.4	304.8	14		1863	es			16823	20.1
Richart and Jensen [93]	3	152.4	304.8	28		1849	es			17099	23.8
Richart and Jensen [93]	3	152.4	304.8	28		1635	es			15031	35.3
Richart and Jensen [93]	3	152.4	304.8	28		1863	es			18478	26.7
Richart and Jensen [93]	3	152.4	304.8	28		1863	es			18340	26.0
Richart and Jensen [93]	3	152.4	304.8	90		1849	es			18685	31.0
Richart and Jensen [93]	3	152.4	304.8	90		1635	es			15651	39.2
Richart and Jensen [93]	3	152.4	304.8	90		1863	es			19926	33.4
Richart and Jensen [93]	3	152.4	304.8	90		1863	es			19650	32.0
Richart and Jensen [93]	3	152.4	304.8	180		1849	es			17857	31.0
Richart and Jensen [93]	3	152.4	304.8	180		1635	es			18133	46.9
Richart and Jensen [93]	3	152.4	304.8	180		1863	es			20133	33.6
Richart and Jensen [93]	3	152.4	304.8	180		1863	es			20822	35.7
Richart and Jensen [93]	3	152.4	304.8	365		1849	es			19236	35.0
Richart and Jensen [93]	3	152.4	304.8	365		1635	es			18133	50.6
Richart and Jensen [93]	3	152.4	304.8	365		1863	es			20202	39.9
Richart and Jensen [93]	3	152.4	304.8	365		1863	es			22063	38.4
Richart and Jensen [93]	3	152.4	304.8	28		1876	es-2.4			18133	28.6
Richart and Jensen [93]	3	152.4	304.8	28		1881	es-2.4			18478	27.0

Source	*n*	*B (mm)*	*H (mm)*	*Age (d)*	*w/c*	$\rho_{c,f}$ *(kg/m³)*	*Aggregate properties*[p]	*sf/c (%)*	*ma/b (%)*	E_c *(MPa)*	f'_{co} *(MPa)*
Richart and Jensen [93]	3	152.4	304.8	28		1895	es-2.4			17582	30.3
Richart and Jensen [93]	3	152.4	304.8	28		1842	es-2.4			18064	24.1
Richart and Jensen [93]	3	152.4	304.8	28		1852	es-2.4			16065	24.3
Richart and Jensen [93]	3	152.4	304.8	28		1858	es-2.4			17720	22.0
Richart and Jensen [93]	3	152.4	304.8	28		1844	es-2.4			15168	17.9
Richart and Jensen [93]	3	152.4	304.8	28		1833	es-2.4			14686	18.8
Richart and Jensen [93]	3	152.4	304.8	28		1833	es-2.4			16272	17.5
Richart and Jensen [93]	3	152.4	304.8	28		1602	es-12.7			11928	22.8
Richart and Jensen [93]	3	152.4	304.8	28		1610	es-12.7			10894	22.1
Richart and Jensen [93]	3	152.4	304.8	28		1560	es-12.7			8894	16.5
Richart and Jensen [93]	3	152.4	304.8	28		1573	es-12.7			10066	16.4
Richart and Jensen [93]	3	152.4	304.8	28		1544	es-12.7			9584	11.7
Richart and Jensen [93]	3	152.4	304.8	28		1552	es-12.7			9928	12.3
Richart and Jensen [93]	3	152.4	304.8	28		1913	es-12.7			18409	27.4
Richart and Jensen [93]	3	152.4	304.8	28		1876	es-12.7			17237	26.8
Richart and Jensen [93]	3	152.4	304.8	28		1916	es-12.7			17237	23.4
Richart and Jensen [93]	3	152.4	304.8	28		1897	es-12.7			16892	23.4
Richart and Jensen [93]	3	152.4	304.8	28		1900	es-12.7			15513	17.7
Richart and Jensen [93]	3	152.4	304.8	28		1889	es-12.7			14893	17.4
Richart and Jensen [93]	3	152.4	304.8	28		1568	es-12.7			12962	19.4
Richart and Jensen [93]	3	152.4	304.8	28		1568	es-12.7			13721	20.1
Richart and Jensen [93]	3	152.4	304.8	28		1528	es-12.7			12135	17.8
Richart and Jensen [93]	3	152.4	304.8	28		1483	es-12.7			11238	15.5
Richart and Jensen [93]	3	152.4	304.8	28		1515	es-12.7			10273	12.1
Richart and Jensen [93]	3	152.4	304.8	28		1504	es-12.7			11307	11.9
Richart and Jensen [93]	3	152.4	304.8	28		1921	es-2.4			19650	31.4
Richart and Jensen [93]	3	152.4	304.8	28		1908	es-2.4			18133	27.1
Richart and Jensen [93]	3	152.4	304.8	28		1930	es-2.4			17306	25.7
Richart and Jensen [93]	3	152.4	304.8	28		1938	es-2.4			17582	23.9
Richart and Jensen [93]	3	152.4	304.8	28		1901	es-2.4			17237	24.0
Richart and Jensen [93]	3	152.4	304.8	28		1903	es-2.4			17375	26.7
Richart and Jensen [93]	3	152.4	304.8	28		1906	es-2.4			16478	25.1
Richart and Jensen [93]	3	152.4	304.8	28		1909	es-2.4			17237	24.0
Richart and Jensen [93]	3	152.4	304.8	28		1916	es-2.4			17237	24.5
Richart and Jensen [93]	3	152.4	304.8	28		1927	es-2.4			16065	23.4
Richart and Jensen [93]	3	152.4	304.8	28		1898	es-2.4			13307	16.7
Richart and Jensen [93]	3	152.4	304.8	28		1932	es-2.4			16754	22.6
Richart and Jensen [93]	3	152.4	304.8	28		1634	es-12.7			13445	23.4
Richart and Jensen [93]	3	152.4	304.8	28		1639	es-12.7			12755	21.3
Richart and Jensen [93]	3	152.4	304.8	28		1603	es-12.7			11997	16.9
Richart and Jensen [93]	3	152.4	304.8	28		1608	es-12.7			11376	20.6
Richart and Jensen [93]	3	152.4	304.8	28		1600	es-12.7			10411	12.3
Richart and Jensen [93]	3	152.4	304.8	28		1594	es-12.7			10066	12.4
Richart and Jensen [93]	3	152.4	304.8	28		2244	es-12.7			26683	29.6
Richart and Jensen [93]	3	152.4	304.8	28		1929	sd-4.75			20271	34.2
Richart and Jensen [93]	3	152.4	304.8	28		1892	sd-4.75			16616	33.7
Richart and Jensen [93]	3	152.4	304.8	28		1919	sd-4.75			16823	33.7
Richart and Jensen [93]	3	152.4	304.8	28		1901	sd-4.75			19374	35.0
Richart and Jensen [93]	3	152.4	304.8	28		1906	sd-4.75			16685	35.9
Richart and Jensen [93]	3	152.4	304.8	28		1914	sd-4.75			18340	35.9
Richart and Jensen [93]	3	152.4	304.8	28		1948	sd-4.75			19926	35.5
Richart and Jensen [93]	3	152.4	304.8	28		1943	sd-4.75			20684	34.8
Richart and Jensen [93]	3	152.4	304.8	28		1946	sd-4.75			14065	36.4
Richart and Jensen [93]	3	152.4	304.8	28		1953	sd-4.75			20891	36.4
Richart and Jensen [93]	3	152.4	304.8	28		1594	gv-19.1			12135	27.9
Richart and Jensen [93]	3	152.4	304.8	28		1586	gv-19.1			11859	26.8
Richart and Jensen [93]	3	152.4	304.8	28		1581	gv-19.1			12617	27.2
Richart and Jensen [93]	3	152.4	304.8	28		1591	gv-19.1			11721	28.4
Richart and Jensen [93]	3	152.4	304.8	28		1623	gv-19.1			12824	28.1
Richart and Jensen [93]	3	152.4	304.8	28		1594	gv-19.1			12273	25.9
Richart and Jensen [93]	3	152.4	304.8	28		1608	gv-19.1			13996	27.4
Richart and Jensen [93]	3	152.4	304.8	28		1621	gv-19.1			13583	26.9
Richart and Jensen [93]	3	152.4	304.8	28		1626	gv-19.1			14065	27.6
Richart and Jensen [93]	3	152.4	304.8	28		1615	gv-19.1			13790	30.1
Richart and Jensen [93]	3	152.4	304.8	28		1555	es-2.4			12824	22.5
Richart and Jensen [93]	3	152.4	304.8	28		1450	es-12.7			6343	4.3
Shideler [189]	1	152.4	304.8	1	0.58	1536	es-rd,cr			7308	7.9
Shideler [189]	1	152.4	304.8	1	0.53	1583	es-cr			9515	9.0
Shideler [189]	1	152.4	304.8	1	0.86	1619	ec-fn			5929	5.4
Shideler [189]	1	152.4	304.8	1	0.59	1643	et-ag			8205	6.9
Shideler [189]	1	152.4	304.8	1	0.54	1748	eg-cr			8205	6.0
Shideler [189]	1	152.4	304.8	1	0.58	1767	ss-cr			8550	7.2
Shideler [189]	1	152.4	304.8	1	0.34	1709	es-rd			16961	27.9
Shideler [189]	1	152.4	304.8	1	0.71	1748	ec-fn			7998	10.5
Shideler [189]	1	152.4	304.8	1	0.49	1831	ec-fn			11721	19.8
Shideler [189]	1	152.4	304.8	2	0.75	1456	es-rd,cr			7171	7.2
Shideler [189]	1	152.4	304.8	2	0.69	1479	es-cr			8687	6.6
Shideler [189]	1	152.4	304.8	2	1.20	1578	ec-fn			5723	5.9
Shideler [189]	1	152.4	304.8	2	0.76	1557	et-cr			7377	6.3
Shideler [189]	1	152.4	304.8	2	0.71	1733	eg-cr			7722	5.6

Source	*n*	*B (mm)*	*H (mm)*	*Age (d)*	*w/c*	$\rho_{c,f}$ *(kg/m³)*	*Aggregate properties*[p]	*sf/c (%)*	*ma/b (%)*	E_c *(MPa)*	f'_{co} *(MPa)*
Shideler [189]	1	152.4	304.8	2	0.76	1740	ss-cr			8550	6.7
Shideler [189]	1	152.4	304.8	2	0.48	1517	es-cr,rd			10756	16.6
Shideler [189]	1	152.4	304.8	2	0.58	1536	es-rd,cr			9239	12.8
Shideler [189]	1	152.4	304.8	2	0.53	1583	es-cr			12066	20.4
Shideler [189]	1	152.4	304.8	2	0.86	1619	ec-fn			8067	9.7
Shideler [189]	1	152.4	304.8	2	0.59	1643	et-ag			10480	12.5
Shideler [189]	1	152.4	304.8	2	0.34	1709	es-rd			18892	35.9
Shideler [189]	1	152.4	304.8	2	0.71	1748	ec-fn			10963	17.9
Shideler [189]	1	152.4	304.8	2	0.49	1831	ec-fn			13376	31.2
Shideler [189]	1	152.4	304.8	3	0.70	1443	es-cr,rd			9791	10.7
Shideler [189]	1	152.4	304.8	3	0.75	1456	es-rd,cr			7239	8.6
Shideler [189]	1	152.4	304.8	3	0.69	1479	es-cr			10411	8.9
Shideler [189]	1	152.4	304.8	3	1.20	1578	ec-ag			7377	7.5
Shideler [189]	1	152.4	304.8	3	0.76	1557	et-ag			9722	8.8
Shideler [189]	1	152.4	304.8	3	0.71	1733	eg-cr			10273	7.4
Shideler [189]	1	152.4	304.8	3	0.76	1740	ss-cr			9653	8.1
Shideler [189]	1	152.4	304.8	3	0.48	1517	es-cr,rd			11032	13.8
Shideler [189]	1	152.4	304.8	3	0.58	1536	es-rd,cr			9170	15.7
Shideler [189]	1	152.4	304.8	3	0.53	1583	es-cr			12204	19.0
Shideler [189]	1	152.4	304.8	3	0.86	1619	ec-fn			8687	13.1
Shideler [189]	1	152.4	304.8	3	0.59	1643	et-ag			10825	15.6
Shideler [189]	1	152.4	304.8	3	0.54	1748	eg-cr			13445	13.2
Shideler [189]	1	152.4	304.8	3	0.58	1767	ss-cr			13514	15.4
Shideler [189]	1	152.4	304.8	7	0.70	1443	es-cr,rd			9997	15.7
Shideler [189]	1	152.4	304.8	7	0.75	1456	es-rd,cr			9101	13.0
Shideler [189]	1	152.4	304.8	7	0.69	1479	es-cr			11445	12.9
Shideler [189]	1	152.4	304.8	7	1.19	1578	ec-fn			8343	11.2
Shideler [189]	1	152.4	304.8	7	0.76	1557	et-ag			11583	11.4
Shideler [189]	1	152.4	304.8	7	0.71	1733	eg-cr			13514	11.4
Shideler [189]	1	152.4	304.8	7	0.76	1740	ss-cr			12480	12.8
Shideler [189]	1	152.4	304.8	7	0.48	1517	es-cr,rd			12962	25.7
Shideler [189]	1	152.4	304.8	7	0.58	1536	es-rd,cr			11376	21.9
Shideler [189]	1	152.4	304.8	7	0.53	1583	es-cr			13652	24.8
Shideler [189]	1	152.4	304.8	7	0.86	1619	ec-fn			9997	19.9
Shideler [189]	1	152.4	304.8	7	0.59	1643	et-ag			13445	22.5
Shideler [189]	1	152.4	304.8	7	0.54	1748	eg-cr			16203	19.3
Shideler [189]	1	152.4	304.8	7	0.58	1767	ss-cr			15031	22.2
Shideler [189]	1	152.4	304.8	7	0.34	1709	es-rd			20753	42.9
Shideler [189]	1	152.4	304.8	7	0.71	1748	ec-fn			13100	34.3
Shideler [189]	1	152.4	304.8	7	0.49	1831	ec-fn			15651	48.0
Shideler [189]	1	152.4	304.8	14	0.70	1443	es-cr,rd			11997	19.9
Shideler [189]	1	152.4	304.8	14	0.70	1443	es-cr,rd			11721	20.1
Shideler [189]	1	152.4	304.8	14	0.75	1456	es-rd,cr			10618	17.7
Shideler [189]	1	152.4	304.8	14	0.75	1456	es-rd,cr			9791	16.1
Shideler [189]	1	152.4	304.8	14	0.69	1479	es-cr			12617	16.7
Shideler [189]	1	152.4	304.8	14	0.69	1479	es-cr			11238	16.4
Shideler [189]	1	152.4	304.8	14	1.19	1578	ec-fn			10066	15.3
Shideler [189]	1	152.4	304.8	14	1.19	1578	ec-fn			10066	15.6
Shideler [189]	1	152.4	304.8	14	0.76	1557	et-ag			11652	17.0
Shideler [189]	1	152.4	304.8	14	0.76	1557	et-ag			8205	14.8
Shideler [189]	1	152.4	304.8	14	0.71	1733	eg-cr			14755	15.1
Shideler [189]	1	152.4	304.8	14	0.71	1733	eg-cr			14410	14.9
Shideler [189]	1	152.4	304.8	14	0.76	1740	ss-cr			13583	16.9
Shideler [189]	1	152.4	304.8	14	0.76	1740	ss-cr			12548	16.4
Shideler [189]	1	152.4	304.8	14	0.48	1517	es-cr,rd			14479	28.6
Shideler [189]	1	152.4	304.8	14	0.48	1517	es-cr,rd			13652	28.6
Shideler [189]	1	152.4	304.8	14	0.58	1536	es-rd,cr			11997	25.9
Shideler [189]	1	152.4	304.8	14	0.58	1536	es-rd,cr			11859	27.5
Shideler [189]	1	152.4	304.8	14	0.53	1583	es-cr			14893	28.3
Shideler [189]	1	152.4	304.8	14	0.53	1583	es-cr			14686	30.1
Shideler [189]	1	152.4	304.8	14	0.86	1619	ec-fn			11238	25.6
Shideler [189]	1	152.4	304.8	14	0.86	1619	ec-fn			10756	25.4
Shideler [189]	1	152.4	304.8	14	0.59	1643	et-ag			14203	25.5
Shideler [189]	1	152.4	304.8	14	0.59	1643	et-ag			13858	26.3
Shideler [189]	1	152.4	304.8	14	0.54	1748	eg-cr			18202	25.2
Shideler [189]	1	152.4	304.8	14	0.54	1748	eg-cr			17099	24.4
Shideler [189]	1	152.4	304.8	14	0.58	1767	ss-cr			16892	25.6
Shideler [189]	1	152.4	304.8	14	0.58	1767	ss-cr			16685	26.8
Shideler [189]	1	152.4	304.8	28	0.70	1443	es-cr,rd			11652	23.1
Shideler [189]	1	152.4	304.8	28	0.70	1443	es-cr,rd			11032	23.0
Shideler [189]	1	152.4	304.8	28	0.75	1456	es-rd,cr			11721	21.7
Shideler [189]	1	152.4	304.8	28	0.75	1456	es-rd,cr			10204	20.3
Shideler [189]	1	152.4	304.8	28	0.69	1479	es-cr			13031	20.1
Shideler [189]	1	152.4	304.8	28	0.69	1479	es-cr			12617	19.5
Shideler [189]	1	152.4	304.8	28	1.19	1578	ec-fn			10480	20.8
Shideler [189]	1	152.4	304.8	28	1.19	1578	ec-fn			10687	21.7
Shideler [189]	1	152.4	304.8	28	0.76	1557	et-ag			12824	19.4
Shideler [189]	1	152.4	304.8	28	0.76	1557	et-ag			11307	17.6
Shideler [189]	1	152.4	304.8	28	0.71	1733	eg-cr			16341	19.0
Shideler [189]	1	152.4	304.8	28	0.71	1733	eg-cr			15031	18.9

Source	*n*	*B (mm)*	*H (mm)*	*Age (d)*	*w/c*	$\rho_{c,f}$ *(kg/m³)*	*Aggregate properties*[p]	*sf/c (%)*	*ma/b (%)*	E_c *(MPa)*	f'_{co} *(MPa)*
Shideler [189]	1	152.4	304.8	28	0.76	1740	ss-cr			15031	21.0
Shideler [189]	1	152.4	304.8	28	0.76	1740	ss-cr			14962	21.4
Shideler [189]	1	152.4	304.8	28	0.48	1517	es-cr,rd			14272	30.6
Shideler [189]	1	152.4	304.8	28	0.48	1517	es-cr,rd			13514	30.8
Shideler [189]	1	152.4	304.8	28	0.58	1536	es-rd,cr			13583	29.6
Shideler [189]	1	152.4	304.8	28	0.58	1536	es-rd,cr			11859	29.1
Shideler [189]	1	152.4	304.8	28	0.53	1583	es-cr			15306	30.8
Shideler [189]	1	152.4	304.8	28	0.53	1583	es-cr			14479	32.6
Shideler [189]	1	152.4	304.8	28	0.86	1619	ec-fn			12686	31.3
Shideler [189]	1	152.4	304.8	28	0.86	1619	ec-fn			12342	32.1
Shideler [189]	1	152.4	304.8	28	0.59	1643	et-ag			15100	30.0
Shideler [189]	1	152.4	304.8	28	0.59	1643	et-ag			14065	30.6
Shideler [189]	1	152.4	304.8	28	0.54	1748	eg-cr			19512	28.6
Shideler [189]	1	152.4	304.8	28	0.54	1748	eg-cr			17444	27.4
Shideler [189]	1	152.4	304.8	28	0.58	1767	ss-cr			18064	30.9
Shideler [189]	1	152.4	304.8	28	0.58	1767	ss-cr			16892	31.4
Shideler [189]	1	152.4	304.8	28	0.34	1709	es-rd			20822	45.4
Shideler [189]	1	152.4	304.8	28	0.34	1709	es-rd			20064	48.7
Shideler [189]	1	152.4	304.8	28	0.71	1748	ec-fn			14686	46.1
Shideler [189]	1	152.4	304.8	28	0.71	1748	ec-fn			13652	49.0
Shideler [189]	1	152.4	304.8	28	0.49	1831	ec-fn			17306	57.6
Shideler [189]	1	152.4	304.8	28	0.49	1831	ec-fn			15720	57.7
Shideler [189]	1	152.4	304.8	90	0.70	1443	es-cr,rd			13238	26.1
Shideler [189]	1	152.4	304.8	90	0.70	1443	es-cr,rd			10342	23.3
Shideler [189]	1	152.4	304.8	90	0.75	1456	es-rd,cr			12962	25.5
Shideler [189]	1	152.4	304.8	90	0.75	1456	es-rd,cr			10342	24.5
Shideler [189]	1	152.4	304.8	90	0.69	1479	es-cr			13996	23.5
Shideler [189]	1	152.4	304.8	90	0.69	1479	es-cr			12686	22.2
Shideler [189]	1	152.4	304.8	90	1.19	1578	ec-fn			12480	26.3
Shideler [189]	1	152.4	304.8	90	1.19	1578	ec-fn			10618	24.1
Shideler [189]	1	152.4	304.8	90	0.76	1557	et-ag			15237	23.6
Shideler [189]	1	152.4	304.8	90	0.76	1557	et-ag			11790	18.2
Shideler [189]	1	152.4	304.8	90	0.71	1733	eg-cr			18478	23.9
Shideler [189]	1	152.4	304.8	90	0.71	1733	eg-cr			14617	19.9
Shideler [189]	1	152.4	304.8	90	0.76	1740	ss-cr			17651	27.2
Shideler [189]	1	152.4	304.8	90	0.76	1740	ss-cr			13514	25.6
Shideler [189]	1	152.4	304.8	90	0.48	1517	es-cr,rd			15031	33.5
Shideler [189]	1	152.4	304.8	90	0.48	1517	es-cr,rd			12686	31.9
Shideler [189]	1	152.4	304.8	90	0.58	1536	es-rd,cr			13996	33.4
Shideler [189]	1	152.4	304.8	90	0.58	1536	es-rd,cr			11997	32.4
Shideler [189]	1	152.4	304.8	90	0.53	1583	es-cr			16616	34.8
Shideler [189]	1	152.4	304.8	90	0.53	1583	es-cr			15513	34.3
Shideler [189]	1	152.4	304.8	90	0.86	1619	ec-fn			13790	34.4
Shideler [189]	1	152.4	304.8	90	0.86	1619	ec-fn			13031	36.5
Shideler [189]	1	152.4	304.8	90	0.59	1643	et-ag			16961	32.3
Shideler [189]	1	152.4	304.8	90	0.54	1748	eg-cr			21374	32.8
Shideler [189]	1	152.4	304.8	90	0.54	1748	eg-cr			17237	30.2
Shideler [189]	1	152.4	304.8	90	0.58	1767	ss-cr			20271	35.5
Shideler [189]	1	152.4	304.8	90	0.58	1767	ss-cr			16547	35.7
Shideler [189]	1	152.4	304.8	90	0.34	1709	es-rd			21374	49.0
Shideler [189]	1	152.4	304.8	90	0.34	1709	es-rd			19857	47.7
Shideler [189]	1	152.4	304.8	90	0.71	1748	ec-fn			16616	53.1
Shideler [189]	1	152.4	304.8	90	0.71	1748	ec-fn			16547	56.3
Shideler [189]	1	152.4	304.8	90	0.49	1831	ec-fn			17513	60.8
Shideler [189]	1	152.4	304.8	90	0.49	1831	ec-fn			14824	60.5
Shideler [189]	1	152.4	304.8	180	0.70	1443	es-cr,rd			14617	27.2
Shideler [189]	1	152.4	304.8	180	0.70	1443	es-cr,rd			10756	22.6
Shideler [189]	1	152.4	304.8	180	0.75	1456	es-cr,rd			15168	27.0
Shideler [189]	1	152.4	304.8	180	0.75	1456	es-rd,cr			10687	23.4
Shideler [189]	1	152.4	304.8	180	0.69	1479	es-cr			15031	25.4
Shideler [189]	1	152.4	304.8	180	0.69	1479	es-cr			12548	22.1
Shideler [189]	1	152.4	304.8	180	1.19	1578	ec-fn			13307	27.4
Shideler [189]	1	152.4	304.8	180	1.19	1578	ec-fn			10894	22.7
Shideler [189]	1	152.4	304.8	180	0.76	1557	et-ag			15306	25.5
Shideler [189]	1	152.4	304.8	180	0.76	1557	et-ag			11376	19.1
Shideler [189]	1	152.4	304.8	180	0.71	1733	eg-cr			19650	25.9
Shideler [189]	1	152.4	304.8	180	0.71	1733	eg-cr			13583	20.1
Shideler [189]	1	152.4	304.8	180	0.76	1740	ss-cr			18892	28.9
Shideler [189]	1	152.4	304.8	180	0.76	1740	ss-cr			12893	24.4
Shideler [189]	1	152.4	304.8	180	0.48	1517	es-cr,rd			15582	34.9
Shideler [189]	1	152.4	304.8	180	0.48	1517	es-cr,rd			12135	29.9
Shideler [189]	1	152.4	304.8	180	0.58	1536	es-rd,cr			15789	31.7
Shideler [189]	1	152.4	304.8	180	0.58	1536	es-rd,cr			11997	30.6
Shideler [189]	1	152.4	304.8	180	0.53	1583	es-cr			17513	34.7
Shideler [189]	1	152.4	304.8	180	0.53	1583	es-cr			14893	34.6
Shideler [189]	1	152.4	304.8	180	0.86	1619	ec-fn			15237	37.1
Shideler [189]	1	152.4	304.8	180	0.86	1619	ec-fn			13169	36.1
Shideler [189]	1	152.4	304.8	180	0.59	1643	et-ag			16961	36.2
Shideler [189]	1	152.4	304.8	180	0.59	1643	et-ag			15168	32.4
Shideler [189]	1	152.4	304.8	180	0.54	1748	eg-cr			21443	33.0

Source	*n*	*B (mm)*	*H (mm)*	*Age (d)*	*w/c*	$\rho_{c,f}$ *(kg/m³)*	*Aggregate properties*[p]	*sf/c (%)*	*ma/b (%)*	E_c *(MPa)*	f'_{co} *(MPa)*
Shideler [189]	1	152.4	304.8	180	0.54	1748	eg-cr			16547	28.3
Shideler [189]	1	152.4	304.8	180	0.58	1767	ss-cr			21925	37.2
Shideler [189]	1	152.4	304.8	180	0.58	1767	ss-cr			16823	35.5
Shideler [189]	1	152.4	304.8	180	0.34	1709	es-rd			22339	50.3
Shideler [189]	1	152.4	304.8	180	0.34	1709	es-rd			19512	49.6
Shideler [189]	1	152.4	304.8	180	0.71	1748	ec-fn			16410	55.2
Shideler [189]	1	152.4	304.8	180	0.71	1748	ec-fn			15582	57.5
Shideler [189]	1	152.4	304.8	180	0.49	1831	ec-fn			18892	60.7
Shideler [189]	1	152.4	304.8	180	0.49	1831	ec-fn			17099	59.4
Shideler [189]	1	152.4	304.8	365	0.70	1443	es-cr,rd			14893	27.6
Shideler [189]	1	152.4	304.8	365	0.70	1443	es-cr,rd			10618	22.6
Shideler [189]	1	152.4	304.8	365	0.75	1456	es-rd,cr			14272	29.6
Shideler [189]	1	152.4	304.8	365	0.75	1456	es-rd,cr			9791	22.9
Shideler [189]	1	152.4	304.8	365	0.69	1479	es-cr			15651	25.6
Shideler [189]	1	152.4	304.8	365	0.69	1479	es-cr			12962	22.1
Shideler [189]	1	152.4	304.8	365	1.19	1578	ec-fn			13376	28.0
Shideler [189]	1	152.4	304.8	365	1.19	1578	ec-fn			10756	24.1
Shideler [189]	1	152.4	304.8	365	0.76	1557	et-ag			15582	27.2
Shideler [189]	1	152.4	304.8	365	0.76	1557	et-ag			10066	17.7
Shideler [189]	1	152.4	304.8	365	0.71	1733	eg-cr			20202	27.9
Shideler [189]	1	152.4	304.8	365	0.71	1733	eg-cr			12962	19.7
Shideler [189]	1	152.4	304.8	365	0.76	1740	ss-cr			19443	31.5
Shideler [189]	1	152.4	304.8	365	0.76	1740	ss-cr			12342	23.9
Shideler [189]	1	152.4	304.8	365	0.48	1517	es-cr,rd			16685	34.7
Shideler [189]	1	152.4	304.8	365	0.48	1517	es-cr,rd			13100	32.0
Shideler [189]	1	152.4	304.8	365	0.58	1536	es-rd,cr			15927	34.8
Shideler [189]	1	152.4	304.8	365	0.58	1536	es-rd,cr			11307	32.1
Shideler [189]	1	152.4	304.8	365	0.53	1583	es-cr			17926	35.4
Shideler [189]	1	152.4	304.8	365	0.53	1583	es-cr			15031	33.9
Shideler [189]	1	152.4	304.8	365	0.86	1619	ec-fn			14962	37.2
Shideler [189]	1	152.4	304.8	365	0.86	1619	ec-fn			12893	37.5
Shideler [189]	1	152.4	304.8	365	0.59	1643	et-ag			17651	36.4
Shideler [189]	1	152.4	304.8	365	0.59	1643	et-ag			14203	31.0
Shideler [189]	1	152.4	304.8	365	0.54	1748	eg-cr			21305	34.3
Shideler [189]	1	152.4	304.8	365	0.54	1748	eg-cr			16134	27.0
Shideler [189]	1	152.4	304.8	365	0.58	1767	ss-cr			21512	42.1
Shideler [189]	1	152.4	304.8	365	0.58	1767	ss-cr			15031	34.1
Shideler [189]	1	152.4	304.8	365	0.34	1709	es-rd			23511	51.5
Shideler [189]	1	152.4	304.8	365	0.34	1709	es-rd			20340	49.4
Shideler [189]	1	152.4	304.8	365	0.71	1748	ec-fn			17444	57.3
Shideler [189]	1	152.4	304.8	365	0.71	1748	ec-fn			15720	60.3
Shideler [189]	1	152.4	304.8	365	0.49	1831	ec-fn			18823	63.4
Shideler [189]	1	152.4	304.8	365	0.49	1831	ec-fn			15996	63.6
Wilson and Malhotra [202]	2	152	305	7	0.27	1970	es-19				49.2
Wilson and Malhotra [202]	2	152	305	28	0.27	1970	es-19				56.6
Wilson and Malhotra [202]	2	152	305	91	0.27	1970	es-19				50.3
Wilson and Malhotra [202]	2	152	305	365	0.27	1970	es-19				65.3
Wilson and Malhotra [202]	4	152	305	28	0.32	1950	es-19			25500	44.9
Wilson and Malhotra [202]	2	152	305	28	0.32	1940	es-19				48.6
Wilson and Malhotra [202]	2	152	305	28	0.32	1950	es-19				44.4
Wilson and Malhotra [202]	2	152	305	7	0.32	1940	es-19				39.9
Wilson and Malhotra [202]	2	152	305	28	0.32	1940	es-19				48.2
Wilson and Malhotra [202]	2	152	305	91	0.32	1940	es-19				51.9
Wilson and Malhotra [202]	2	152	305	365	0.32	1940	es-19				58.2
Wilson and Malhotra [202]	4	152	305	28	0.30	1920	es-19	5.5	15.7[f]	26100	60.8
Wilson and Malhotra [202]	2	152	305	28	0.30	1920	es-19	5.5	15.7[f]		60.3
Wilson and Malhotra [202]	2	152	305	28	0.30	1910	es-19	5.5	15.8[f]		57.2
Wilson and Malhotra [202]	2	152	305	7	0.30	1920	es-19	5.5	15.7[f]		50.7
Wilson and Malhotra [202]	2	152	305	28	0.30	1920	es-19	5.5	15.7[f]		60.7
Wilson and Malhotra [202]	2	152	305	91	0.30	1920	es-19	5.5	15.7[f]		63.4
Wilson and Malhotra [202]	2	152	305	365	0.30	1920	es-19	5.5	15.7[f]		66.5
Wilson and Malhotra [202]	4	152	305	28	0.37	1920	es-19			25800	40.4
Wilson and Malhotra [202]	2	152	305	28	0.37	1910	es-19				41.5
Wilson and Malhotra [202]	2	152	305	7	0.37	1900	es-19				34.7
Wilson and Malhotra [202]	2	152	305	28	0.37	1900	es-19				40.4
Wilson and Malhotra [202]	2	152	305	91	0.37	1900	es-19				46.7
Wilson and Malhotra [202]	2	152	305	365	0.37	1900	es-19				52.7
Wilson and Malhotra [202]	4	152	305	28	0.34	1920	es-19	5.5	15.8[f]	27000	54.6
Wilson and Malhotra [202]	2	152	305	28	0.34	1950	es-19	5.7	15.9[f]		57.4
Wilson and Malhotra [202]	2	152	305	7	0.34	1900	es-19	5.5	15.8[f]		44.8
Wilson and Malhotra [202]	2	152	305	28	0.34	1900	es-19	5.5	15.8[f]		55.7
Wilson and Malhotra [202]	2	152	305	91	0.34	1900	es-19	5.5	15.8[f]		59.1
Wilson and Malhotra [202]	2	152	305	365	0.34	1900	es-19	5.5	15.8[f]		58.8
Wilson and Malhotra [202]	4	152	305	28	0.45	1940	es-19			23800	33.6
Wilson and Malhotra [202]	2	152	305	28	0.45	1900	es-19				30.2
Wilson and Malhotra [202]	2	152	305	28	0.45	1890	es-19				33.3
Wilson and Malhotra [202]	2	152	305	7	0.45	1880	es-19				26.2
Wilson and Malhotra [202]	2	152	305	28	0.45	1880	es-19				34.2
Wilson and Malhotra [202]	2	152	305	91	0.45	1880	es-19				38.5
Wilson and Malhotra [202]	2	152	305	365	0.45	1880	es-19				44.4

Source	*n*	*B (mm)*	*H (mm)*	*Age (d)*	*w/c*	$\rho_{c,f}$ *(kg/m³)*	*Aggregate properties*[p]	*sf/c (%)*	*ma/b (%)*	E_c *(MPa)*	f'_{co} *(MPa)*
Wilson and Malhotra [202]	4	152	305	28	0.39	1870	es-19	5.4	15.7[f]	26200	48.4
Wilson and Malhotra [202]	2	152	305	28	0.39	1910	es-19	5.6	15.6[f]		50.3
Wilson and Malhotra [202]	2	152	305	28	0.39	1890	es-19	5.6	15.8[f]		49.7
Wilson and Malhotra [202]	2	152	305	7	0.39	1910	es-19	5.6	15.6[f]		36.5
Wilson and Malhotra [202]	2	152	305	28	0.39	1910	es-19	5.6	15.6[f]		48.3
Wilson and Malhotra [202]	2	152	305	91	0.39	1910	es-19	5.6	15.6[f]		52.2
Wilson and Malhotra [202]	2	152	305	365	0.39	1910	es-19	5.6	15.6[f]		53.0
Yaman et al. [194]	4	100	200	31	0.40		n			31370	45.5
Yaman et al. [194]	4	100	200	31	0.40		n			30610	44.8
Yaman et al. [194]	4	100	200	31	0.40		n			31570	44.4
Yaman et al. [194]	4	100	200	31	0.40		n			29760	42.4
Yaman et al. [194]	4	100	200	31	0.40		n			30930	42.1
Yaman et al. [194]	4	100	200	31	0.45		n			30930	41.1
Yaman et al. [194]	4	100	200	31	0.45		n			29990	40.5
Yaman et al. [194]	4	100	200	31	0.45		n			27100	39.0
Yaman et al. [194]	4	100	200	31	0.45		n			26880	38.9
Yaman et al. [194]	4	100	200	31	0.50		n			27330	35.9
Yang and Huang [203]	5-7	100	200	28	0.30	2201	l			23020	41.4
Yang and Huang [203]	5-7	100	200	28	0.30	2208	l			20600	37.3
Yang and Huang [203]	5-7	100	200	28	0.30	2221	l			18210	34.6
Yang and Huang [203]	5-7	100	200	28	0.30	2142	l			15800	31.5
Yang and Huang [203]	5-7	100	200	28	0.30	2152	l			23790	44.2
Yang and Huang [203]	5-7	100	200	28	0.30	2168	l			21530	41.4
Yang and Huang [203]	5-7	100	200	28	0.30	2083	l			19010	38.3
Yang and Huang [203]	5-7	100	200	28	0.30	2095	l			17220	35.7
Yang and Huang [203]	5-7	100	200	28	0.30	2116	l			24660	49.9
Yang and Huang [203]	5-7	100	200	28	0.30	2023	l			22580	47.1
Yang and Huang [203]	5-7	100	200	28	0.30	2038	l			20320	45.2
Yang and Huang [203]	5-7	100	200	28	0.30	2063	l			18650	41.7

d Fresh concrete density that is significantly higher than the reference values

m Concrete elastic modulus that differ significantly from the reference values of the corresponding concrete strength

f Fly-ash used as mineral admixture in concrete mix

p Designation:- type-irregularity-size

Type:- n: normal weight aggregate, l: light weight aggregate, de: diatomaceous earth, dt: sintered diatomite, ec: expanded clay, eg: expanded slag, es: expanded shale, et: expanded slate, fa: sintered fly-ash, gv: gravel, ls: limestone, pl: perlite, pm: volcanic pumice, sd: sand, sr: volcanic scoria, ss: sintered shale, vm: exfoliated vermiculite,

Irregularity:- ag: angular, cr: crushed, fn: fine, rd: round, sh: sharp

Size:- maximum aggregate in mm

Table A6. Test database of normal weight concrete prisms (without ε_{co} values)

Source	*n*	*B (mm)*	*H (mm)*	*Age (d)*	*w/c*	$\rho_{c,f}$ *(kg/m³)*	*Aggregate properties*[p]	*sf/c (%)*	*ma/b (%)*	E_c *(MPa)*	f'_{co} *(MPa)*
Alexander and Milne [204]		100	100	4	0.43		gn-19			21400	34.7
Alexander and Milne [204]		100	100	8	0.43		gn-19			20700	50.2
Alexander and Milne [204]		100	100	28	0.43		gn-19			31300	63.0
Alexander and Milne [204]		100	100	90	0.43		gn-19			37700	78.3
Alexander and Milne [204]		100	100	189	0.43		gn-19			41500	83.3
Alexander and Milne [204]		100	100	4	0.51		gn-19			17600	23.8
Alexander and Milne [204]		100	100	8	0.51		gn-19			21600	32.8
Alexander and Milne [204]		100	100	28	0.51		gn-19			29400	48.7
Alexander and Milne [204]		100	100	90	0.51		gn-19			34800	63.3
Alexander and Milne [204]		100	100	189	0.51		gn-19			38900	78.7
Alexander and Milne [204]		100	100	3	0.61		gn-19			16400	16.5
Alexander and Milne [204]		100	100	7	0.61		gn-19			16600	23.2
Alexander and Milne [204]		100	100	29	0.61		gn-19			27600	35.6
Alexander and Milne [204]		100	100	90	0.61		gn-19			36500	45.7
Alexander and Milne [204]		100	100	189	0.61		gn-19			40800	65.5
Alexander and Milne [204]		100	100	4	0.43		gn-19		50.0[s]	13000	19.1
Alexander and Milne [204]		100	100	7	0.43		gn-19		50.0[s]	13800	25.5
Alexander and Milne [204]		100	100	27	0.43		gn-19		50.0[s]	23500	52.2
Alexander and Milne [204]		100	100	90	0.43		gn-19		50.0[s]	31000	69.3
Alexander and Milne [204]		100	100	182	0.43		gn-19		50.0[s]	35500	73.7
Alexander and Milne [204]		100	100	4	0.51		gn-19		50.0[s]	16200	16.5
Alexander and Milne [204]		100	100	7	0.51		gn-19		50.0[s]	18600	20.7
Alexander and Milne [204]		100	100	27	0.51		gn-19		50.0[s]	23600	44.2
Alexander and Milne [204]		100	100	90	0.51		gn-19		50.0[s]	33500	60.5
Alexander and Milne [204]		100	100	182	0.51		gn-19		50.0[s]	37800	63.3
Alexander and Milne [204]		100	100	4	0.61		gn-19		50.0[s]	13300	13.2
Alexander and Milne [204]		100	100	7	0.61		gn-19		50.0[s]	14300	17.0
Alexander and Milne [204]		100	100	27	0.61		gn-19		50.0[s]	25400	36.0
Alexander and Milne [204]		100	100	90	0.61		gn-19		50.0[s]	31700	48.0
Alexander and Milne [204]		100	100	182	0.61		gn-19		50.0[s]	35500	51.5
Alexander and Milne [204]		100	100	4	0.43		gn-19		30.0[f]	20800	21.2
Alexander and Milne [204]		100	100	8	0.43		gn-19		30.0 [f]	20500	27.8
Alexander and Milne [204]		100	100	30	0.43		gn-19		30.0[f]	26000	48.4
Alexander and Milne [204]		100	100	90	0.43		gn-19		30.0[f]	33000	68.7
Alexander and Milne [204]		100	100	182	0.43		gn-19		30.0[f]	37900	79.0
Alexander and Milne [204]		100	100	4	0.51		gn-19		30.0[f]	20000	16.5
Alexander and Milne [204]		100	100	8	0.51		gn-19		30.0[f]	20100	21.8
Alexander and Milne [204]		100	100	30	0.51		gn-19		30.0[f]	25200	36.6
Alexander and Milne [204]		100	100	90	0.51		gn-19		30.0[f]	34100	53.7
Alexander and Milne [204]		100	100	182	0.51		gn-19		30.0[f]	40400	59.3
Alexander and Milne [204]		100	100	3	0.61		gn-19		30.0[f]	14600	13.6
Alexander and Milne [204]		100	100	7	0.61		gn-19		30.0[f]	14200	17.7
Alexander and Milne [204]		100	100	30	0.61		gn-19		30.0[f]	14800	27.0
Alexander and Milne [204]		100	100	90	0.61		gn-19		30.0[f]	27300	41.8
Alexander and Milne [204]		100	100	182	0.61		gn-19		30.0[f]	35500	49.2
Alexander and Milne [204]		100	100	4	0.43		gn-19	7.0		30200	33.1
Alexander and Milne [204]		100	100	7	0.43		gn-19	7.0		31200	43.5
Alexander and Milne [204]		100	100	29	0.43		gn-19	7.0		36100	67.8
Alexander and Milne [204]		100	100	90	0.43		gn-19	7.0		38000	73.7
Alexander and Milne [204]		100	100	182	0.43		gn-19	7.0		40100	78.7
Alexander and Milne [204]		100	100	4	0.51		gn-19	7.0		29100	22.9
Alexander and Milne [204]		100	100	7	0.51		gn-19	7.0		29400	29.3
Alexander and Milne [204]		100	100	29	0.51		gn-19	7.0		34700	53.2
Alexander and Milne [204]		100	100	90	0.51		gn-19	7.0		37700	59.0
Alexander and Milne [204]		100	100	182	0.51		gn-19	7.0		40100	63.0
Alexander and Milne [204]		100	100	4	0.61		gn-19	7.0		24900	14.8
Alexander and Milne [204]		100	100	7	0.61		gn-19	7.0		24600	19.8
Alexander and Milne [204]		100	100	29	0.61		gn-19	7.0		31400	37.8
Alexander and Milne [204]		100	100	90	0.61		gn-19	7.0		33900	42.5
Alexander and Milne [204]		100	100	182	0.61		gn-19	7.0		37300	45.3
Alexander and Milne [204]		100	100	4	0.43		dl-19			46900[m]	39.3
Alexander and Milne [204]		100	100	8	0.43		dl-19			44500	47.3
Alexander and Milne [204]		100	100	28	0.43		dl-19			55600	61.8
Alexander and Milne [204]		100	100	90	0.43		dl-19			59500	73.8
Alexander and Milne [204]		100	100	181	0.43		dl-19			61000	90.0
Alexander and Milne [204]		100	100	4	0.51		dl-19			39400	30.8
Alexander and Milne [204]		100	100	8	0.51		dl-19			40900	35.3
Alexander and Milne [204]		100	100	28	0.51		dl-19			49000	47.8
Alexander and Milne [204]		100	100	90	0.51		dl-19			56100	63.0
Alexander and Milne [204]		100	100	181	0.51		dl-19			59600	72.5
Alexander and Milne [204]		100	100	4	0.61		dl-19			39000[m]	25.5
Alexander and Milne [204]		100	100	8	0.61		dl-19			40000	30.0
Alexander and Milne [204]		100	100	28	0.61		dl-19			47700[m]	38.2
Alexander and Milne [204]		100	100	90	0.61		dl-19			54800[m]	47.7
Alexander and Milne [204]		100	100	181	0.61		dl-19			57600[m]	55.5
Alexander and Milne [204]		100	100	4	0.43		dl-19		50.0[s]	28200	23.7
Alexander and Milne [204]		100	100	7	0.43		dl-19		50.0[s]	33300	30.6
Alexander and Milne [204]		100	100	29	0.43		dl-19		50.0[s]	47200	53.5
Alexander and Milne [204]		100	100	90	0.43		dl-19		50.0[s]	53600	65.2

Source	*n*	*B (mm)*	*H (mm)*	*Age (d)*	*w/c*	$\rho_{c,f}$ *(kg/m^3)*	*Aggregate properties*[p]	*sf/c (%)*	*ma/b (%)*	E_c *(MPa)*	f'_{co} *(MPa)*
Alexander and Milne [204]		100	100	181	0.43		dl-19		50.0[s]	53600	70.8
Alexander and Milne [204]		100	100	4	0.51		dl-19		50.0[s]	29300	18.8
Alexander and Milne [204]		100	100	7	0.51		dl-19		50.0[s]	34200	25.4
Alexander and Milne [204]		100	100	29	0.51		dl-19		50.0[s]	46300	45.2
Alexander and Milne [204]		100	100	90	0.51		dl-19		50.0[s]	53200	53.0
Alexander and Milne [204]		100	100	181	0.51		dl-19		50.0[s]	55200	58.3
Alexander and Milne [204]		100	100	4	0.61		dl-19		50.0[s]	18600	14.4
Alexander and Milne [204]		100	100	7	0.61		dl-19		50.0[s]	21500	18.9
Alexander and Milne [204]		100	100	29	0.61		dl-19		50.0[s]	37500	31.5
Alexander and Milne [204]		100	100	90	0.61		dl-19		50.0[s]	45900	40.0
Alexander and Milne [204]		100	100	181	0.61		dl-19		50.0[s]	51600[m]	40.8
Alexander and Milne [204]		100	100	4	0.43		dl-19		30.0[f]	37800[m]	25.3
Alexander and Milne [204]		100	100	8	0.43		dl-19		30.0[f]	39200	30.7
Alexander and Milne [204]		100	100	30	0.43		dl-19		30.0[f]	45700	50.7
Alexander and Milne [204]		100	100	90	0.43		dl-19		30.0[f]	54100	74.7
Alexander and Milne [204]		100	100	181	0.43		dl-19		30.0[f]	57500	76.8
Alexander and Milne [204]		100	100	4	0.51		dl-19		30.0[f]	31900	19.8
Alexander and Milne [204]		100	100	8	0.51		dl-19		30.0[f]	35100	24.0
Alexander and Milne [204]		100	100	30	0.51		dl-19		30.0[f]	38900	37.7
Alexander and Milne [204]		100	100	90	0.51		dl-19		30.0[f]	50900	55.5
Alexander and Milne [204]		100	100	181	0.51		dl-19		30.0[f]	54800	61.3
Alexander and Milne [204]		100	100	4	0.61		dl-19		30.0[f]	27800	16.3
Alexander and Milne [204]		100	100	8	0.61		dl-19		30.0[f]	27900	20.4
Alexander and Milne [204]		100	100	30	0.61		dl-19		30.0[f]	30100	29.5
Alexander and Milne [204]		100	100	90	0.61		dl-19		30.0[f]	42400	43.7
Alexander and Milne [204]		100	100	181	0.61		dl-19		30.0[f]	50100	46.6
Alexander and Milne [204]		100	100	4	0.43		dl-19	7.0		47100[m]	34.2
Alexander and Milne [204]		100	100	7	0.43		dl-19	7.0		49600	47.8
Alexander and Milne [204]		100	100	28	0.43		dl-19	7.0		57400	62.2
Alexander and Milne [204]		100	100	90	0.43		dl-19	7.0		59500	73.5
Alexander and Milne [204]		100	100	182	0.43		dl-19	7.0		59700	75.5
Alexander and Milne [204]		100	100	4	0.51		dl-19	7.0		43700[m]	26.7
Alexander and Milne [204]		100	100	7	0.51		dl-19	7.0		45700[m]	36.5
Alexander and Milne [204]		100	100	28	0.51		dl-19	7.0		53300[m]	50.5
Alexander and Milne [204]		100	100	90	0.51		dl-19	7.0		59100[m]	61.0
Alexander and Milne [204]		100	100	182	0.51		dl-19	7.0		57000	63.7
Alexander and Milne [204]		100	100	4	0.61		dl-19	7.0		41300[m]	20.6
Alexander and Milne [204]		100	100	7	0.61		dl-19	7.0		44400[m]	27.7
Alexander and Milne [204]		100	100	28	0.61		dl-19	7.0		55000[m]	40.7
Alexander and Milne [204]		100	100	90	0.61		dl-19	7.0		58900[m]	49.3
Alexander and Milne [204]		100	100	182	0.61		dl-19	7.0		56300[m]	52.2
Alexander and Milne [204]		100	100	4	0.43		qz-19			28400	29.4
Alexander and Milne [204]		100	100	8	0.43		qz-19			27600	39.6
Alexander and Milne [204]		100	100	29	0.43		qz-19			33400	49.7
Alexander and Milne [204]		100	100	86	0.43		qz-19			38500	64.3
Alexander and Milne [204]		100	100	180	0.43		qz-19			41700	68.5
Alexander and Milne [204]		100	100	4	0.51		qz-19			30000	23.3
Alexander and Milne [204]		100	100	8	0.51		qz-19			29000	29.6
Alexander and Milne [204]		100	100	29	0.51		qz-19			31900	38.5
Alexander and Milne [204]		100	100	86	0.51		qz-19			37500	54.7
Alexander and Milne [204]		100	100	180	0.51		qz-19			41100	54.7
Alexander and Milne [204]		100	100	4	0.61		qz-19			21900	16.5
Alexander and Milne [204]		100	100	8	0.61		qz-19			20300	21.6
Alexander and Milne [204]		100	100	29	0.61		qz-19			26800	29.2
Alexander and Milne [204]		100	100	86	0.61		qz-19			34300	40.9
Alexander and Milne [204]		100	100	180	0.61		qz-19			37100	40.8
Alexander and Milne [204]		100	100	4	0.43		qz-19		50.0[s]	23800	18.5
Alexander and Milne [204]		100	100	7	0.43		qz-19		50.0[s]	24100	24.6
Alexander and Milne [204]		100	100	28	0.43		qz-19		50.0[s]	29000	46.0
Alexander and Milne [204]		100	100	90	0.43		qz-19		50.0[s]	35800	62.7
Alexander and Milne [204]		100	100	181	0.43		qz-19		50.0[s]	38700	60.7
Alexander and Milne [204]		100	100	4	0.51		qz-19		50.0[s]	20600	15.8
Alexander and Milne [204]		100	100	7	0.51		qz-19		50.0[s]	22900	19.4
Alexander and Milne [204]		100	100	28	0.51		qz-19		50.0[s]	26100	38.0
Alexander and Milne [204]		100	100	90	0.51		qz-19		50.0[s]	31000	51.0
Alexander and Milne [204]		100	100	181	0.51		qz-19		50.0[s]	36200	52.3
Alexander and Milne [204]		100	100	4	0.61		qz-19		50.0[s]	20300	12.6
Alexander and Milne [204]		100	100	7	0.61		qz-19		50.0[s]	22100	16.1
Alexander and Milne [204]		100	100	28	0.61		qz-19		50.0[s]	27300	31.9
Alexander and Milne [204]		100	100	90	0.61		qz-19		50.0[s]	34400	44.5
Alexander and Milne [204]		100	100	181	0.61		qz-19		50.0[s]	37900	44.0
Alexander and Milne [204]		100	100	4	0.43		qz-19		30.0[f]	23700	18.5
Alexander and Milne [204]		100	100	8	0.43		qz-19		30.0[f]	23000	24.2
Alexander and Milne [204]		100	100	30	0.43		qz-19		30.0[f]	26200	37.5
Alexander and Milne [204]		100	100	90	0.43		qz-19		30.0[f]	35300	55.7
Alexander and Milne [204]		100	100	181	0.43		qz-19		30.0[f]	38900	66.3
Alexander and Milne [204]		100	100	4	0.51		qz-19		30.0[f]	21800	15.3
Alexander and Milne [204]		100	100	8	0.51		qz-19		30.0[f]	23000	19.9
Alexander and Milne [204]		100	100	30	0.51		qz-19		30.0[f]	28300	30.3
Alexander and Milne [204]		100	100	90	0.51		qz-19		30.0[f]	34100	48.3

Source	*n*	*B (mm)*	*H (mm)*	*Age (d)*	*w/c*	$\rho_{c,f}$ *(kg/m³)*	*Aggregate properties*[p]	*sf/c (%)*	*ma/b (%)*	E_c *(MPa)*	f'_{co} *(MPa)*
Alexander and Milne [204]		100	100	181	0.51		qz-19		30.0[f]	37300	56.2
Alexander and Milne [204]		100	100	4	0.61		qz-19		30.0[f]	19300	12.6
Alexander and Milne [204]		100	100	8	0.61		qz-19		30.0[f]	18900	15.6
Alexander and Milne [204]		100	100	30	0.61		qz-19		30.0[f]	20500	22.7
Alexander and Milne [204]		100	100	90	0.61		qz-19		30.0[f]	34000	36.3
Alexander and Milne [204]		100	100	181	0.61		qz-19		30.0[f]	36900	44.7
Alexander and Milne [204]		100	100	4	0.43		qz-19	7.0		31600	31.5
Alexander and Milne [204]		100	100	7	0.43		qz-19	7.0		33300	40.0
Alexander and Milne [204]		100	100	29	0.43		qz-19	7.0		36900	58.7
Alexander and Milne [204]		100	100	90	0.43		qz-19	7.0		39700	65.8
Alexander and Milne [204]		100	100	181	0.43		qz-19	7.0		42800	74.2
Alexander and Milne [204]		100	100	4	0.51		qz-19	7.0		30200	23.2
Alexander and Milne [204]		100	100	7	0.51		qz-19	7.0		32300	29.5
Alexander and Milne [204]		100	100	29	0.51		qz-19	7.0		34500	47.0
Alexander and Milne [204]		100	100	90	0.51		qz-19	7.0		38500	52.0
Alexander and Milne [204]		100	100	181	0.51		qz-19	7.0		41200	58.2
Alexander and Milne [204]		100	100	4	0.61		qz-19	7.0		27500	18.0
Alexander and Milne [204]		100	100	7	0.61		qz-19	7.0		30500	20.5
Alexander and Milne [204]		100	100	29	0.61		qz-19	7.0		32500	33.5
Alexander and Milne [204]		100	100	90	0.61		qz-19	7.0		40000	40.0
Alexander and Milne [204]		100	100	181	0.61		qz-19	7.0		39700	43.7
Alexander and Milne [204]		100	100	4	0.43		ad-19			44300	40.3
Alexander and Milne [204]		100	100	8	0.43		ad-19			43800	51.5
Alexander and Milne [204]		100	100	29	0.43		ad-19			46900	70.2
Alexander and Milne [204]		100	100	90	0.43		ad-19			49000	84.3
Alexander and Milne [204]		100	100	182	0.43		ad-19			51700	81.8
Alexander and Milne [204]		100	100	4	0.51		ad-19			39000	31.9
Alexander and Milne [204]		100	100	8	0.51		ad-19			42400	41.7
Alexander and Milne [204]		100	100	29	0.51		ad-19			46600	56.8
Alexander and Milne [204]		100	100	90	0.51		ad-19			49700	67.3
Alexander and Milne [204]		100	100	182	0.51		ad-19			51800	67.0
Alexander and Milne [204]		100	100	4	0.61		ad-19			37800	26.6
Alexander and Milne [204]		100	100	8	0.61		ad-19			40000	35.0
Alexander and Milne [204]		100	100	29	0.61		ad-19			45400	48.7
Alexander and Milne [204]		100	100	90	0.61		ad-19			48900	58.8
Alexander and Milne [204]		100	100	182	0.61		ad-19			48700	58.8
Alexander and Milne [204]		100	100	4	0.43		ad-19		50.0[s]	32200	21.2
Alexander and Milne [204]		100	100	7	0.43		ad-19		50.0[s]	32500	29.9
Alexander and Milne [204]		100	100	27	0.43		ad-19		50.0[s]	40600	53.2
Alexander and Milne [204]		100	100	90	0.43		ad-19		50.0[s]	45800	65.3
Alexander and Milne [204]		100	100	181	0.43		ad-19		50.0[s]	51000	75.0
Alexander and Milne [204]		100	100	4	0.51		ad-19		50.0[s]	32800[m]	18.0
Alexander and Milne [204]		100	100	7	0.51		ad-19		50.0[s]	36200	26.4
Alexander and Milne [204]		100	100	27	0.51		ad-19		50.0[s]	42200	47.9
Alexander and Milne [204]		100	100	90	0.51		ad-19		50.0[s]	47100	58.8
Alexander and Milne [204]		100	100	181	0.51		ad-19		50.0[s]	52400	65.3
Alexander and Milne [204]		100	100	4	0.61		ad-19		50.0[s]	24200	12.8
Alexander and Milne [204]		100	100	7	0.61		ad-19		50.0[s]	24700	18.1
Alexander and Milne [204]		100	100	27	0.61		ad-19		50.0[s]	38400	35.2
Alexander and Milne [204]		100	100	90	0.61		ad-19		50.0[s]	42900	46.3
Alexander and Milne [204]		100	100	181	0.61		ad-19		50.0[s]	48200	52.2
Alexander and Milne [204]		100	100	4	0.43		ad-19		30.0[f]	36400	24.5
Alexander and Milne [204]		100	100	8	0.43		ad-19		30.0[f]	31900	30.5
Alexander and Milne [204]		100	100	30	0.43		ad-19		30.0[f]	37400	45.5
Alexander and Milne [204]		100	100	90	0.43		ad-19		30.0[f]	45300	73.3
Alexander and Milne [204]		100	100	177	0.43		ad-19		30.0[f]	49200	77.8
Alexander and Milne [204]		100	100	4	0.51		ad-19		30.0[f]	34300[m]	20.3
Alexander and Milne [204]		100	100	8	0.51		ad-19		30.0[f]	31200	23.6
Alexander and Milne [204]		100	100	30	0.51		ad-19		30.0[f]	35700	35.0
Alexander and Milne [204]		100	100	90	0.51		ad-19		30.0[f]	46700	60.3
Alexander and Milne [204]		100	100	177	0.51		ad-19		30.0[f]	50900	66.8
Alexander and Milne [204]		100	100	4	0.61		ad-19		30.0[f]	29600[m]	14.9
Alexander and Milne [204]		100	100	8	0.61		ad-19		30.0[f]	24700	17.9
Alexander and Milne [204]		100	100	30	0.61		ad-19		30.0[f]	27000	27.6
Alexander and Milne [204]		100	100	90	0.61		ad-19		30.0[f]	40000	44.0
Alexander and Milne [204]		100	100	177	0.61		ad-19		30.0[f]	46100	48.8
Alexander and Milne [204]		100	100	5	0.43		ad-19	7.0		43200	47.7
Alexander and Milne [204]		100	100	7	0.43		ad-19	7.0		44100	50.3
Alexander and Milne [204]		100	100	29	0.43		ad-19	7.0		50100	78.0
Alexander and Milne [204]		100	100	90	0.43		ad-19	7.0		54000	84.3
Alexander and Milne [204]		100	100	182	0.43		ad-19	7.0		53700	82.2
Alexander and Milne [204]		100	100	5	0.51		ad-19	7.0		43700	35.7
Alexander and Milne [204]		100	100	7	0.51		ad-19	7.0		43000	38.7
Alexander and Milne [204]		100	100	29	0.51		ad-19	7.0		49700	58.4
Alexander and Milne [204]		100	100	90	0.51		ad-19	7.0		51700	70.6
Alexander and Milne [204]		100	100	182	0.51		ad-19	7.0		53400	71.0
Alexander and Milne [204]		100	100	5	0.61		ad-19	7.0		45200[m]	25.9
Alexander and Milne [204]		100	100	7	0.61		ad-19	7.0		41700[m]	29.9
Alexander and Milne [204]		100	100	29	0.61		ad-19	7.0		50400	50.7
Alexander and Milne [204]		100	100	90	0.61		ad-19	7.0		50600	59.3

Source	*n*	*B (mm)*	*H (mm)*	*Age (d)*	*w/c*	$\rho_{c,f}$ *(kg/m^3)*	*Aggregate properties*[p]	*sf/c (%)*	*ma/b (%)*	E_c *(MPa)*	f'_{co} *(MPa)*
Alexander and Milne [204]		100	100	182	0.61		ad-19	7.0		53700	59.2
Corinaldesi [205]	15	100	100	28	0.40		gv-22			37300	58.6
Corinaldesi [205]	15	100	100	28	0.45		gv-22			36900	56.1
Corinaldesi [205]	15	100	100	28	0.50		gv-22			35600	51.2
Corinaldesi [205]	15	100	100	28	0.55		gv-22				47.1
Corinaldesi [205]	15	100	100	28	0.60		gv-22			33900	43.9
Hossain [175]		100	100	28	0.45	2711[d]	pm			21200	40.0
Hossain [175]		100	100	28	0.45	2694[d]	pm			20700	40.0
Klieger [177]		152.4	152.4	1			gv-38.1				10.7
Klieger [177]		152.4	152.4	1			gv-38.1				6.1
Klieger [177]		152.4	152.4	1			gv-38.1				7.7
Klieger [177]		152.4	152.4	1			gv-38.1				5.9
Klieger [177]		152.4	152.4	1			gv-38.1				10.5
Klieger [177]		152.4	152.4	1			gv-38.1				10.3
Klieger [177]		152.4	152.4	1			gv-38.1				15.4
Klieger [177]		152.4	152.4	1			gv-38.1				12.5
Klieger [177]		152.4	152.4	1			gv-38.1				8.6
Klieger [177]		152.4	152.4	1			gv-38.1				9.2
Klieger [177]		152.4	152.4	1			gv-38.1				8.4
Klieger [177]		152.4	152.4	1			gv-38.1				5.0
Klieger [177]		152.4	152.4	1			gv-38.1				5.3
Klieger [177]		152.4	152.4	1			gv-38.1				7.7
Klieger [177]		152.4	152.4	1			gv-38.1				10.6
Klieger [177]		152.4	152.4	1			gv-38.1				5.9
Klieger [177]		152.4	152.4	1			gv-38.1				5.3
Klieger [177]		152.4	152.4	1			gv-38.1				7.3
Klieger [177]		152.4	152.4	1			gv-38.1				9.8
Klieger [177]		152.4	152.4	1			gv-38.1				8.8
Klieger [177]		152.4	152.4	1			gv-38.1				9.0
Klieger [177]		152.4	152.4	1			gv-38.1				14.5
Klieger [177]		152.4	152.4	1			gv-38.1				25.4
Klieger [177]		152.4	152.4	1			gv-38.1				17.8
Klieger [177]		152.4	152.4	1			gv-38.1				6.7
Klieger [177]		152.4	152.4	1			gv-38.1				5.5
Klieger [177]		152.4	152.4	1			gv-38.1				4.6
Klieger [177]		152.4	152.4	1			gv-38.1				6.1
Klieger [177]		152.4	152.4	1			gv-38.1				9.8
Klieger [177]		152.4	152.4	7			gv-38.1				39.2
Klieger [177]		152.4	152.4	7			gv-38.1				25.4
Klieger [177]		152.4	152.4	7			gv-38.1				40.8
Klieger [177]		152.4	152.4	7			gv-38.1				34.0
Klieger [177]		152.4	152.4	7			gv-38.1				29.8
Klieger [177]		152.4	152.4	7			gv-38.1				34.6
Klieger [177]		152.4	152.4	7			gv-38.1				41.9
Klieger [177]		152.4	152.4	7			gv-38.1				41.6
Klieger [177]		152.4	152.4	7			gv-38.1				26.5
Klieger [177]		152.4	152.4	7			gv-38.1				36.0
Klieger [177]		152.4	152.4	7			gv-38.1				36.5
Klieger [177]		152.4	152.4	7			gv-38.1				32.8
Klieger [177]		152.4	152.4	7			gv-38.1				21.3
Klieger [177]		152.4	152.4	7			gv-38.1				30.0
Klieger [177]		152.4	152.4	7			gv-38.1				37.0
Klieger [177]		152.4	152.4	7			gv-38.1				28.3
Klieger [177]		152.4	152.4	7			gv-38.1				24.8
Klieger [177]		152.4	152.4	7			gv-38.1				34.7
Klieger [177]		152.4	152.4	7			gv-38.1				31.2
Klieger [177]		152.4	152.4	7			gv-38.1				30.3
Klieger [177]		152.4	152.4	7			gv-38.1				25.8
Klieger [177]		152.4	152.4	7			gv-38.1				39.5
Klieger [177]		152.4	152.4	7			gv-38.1				45.4
Klieger [177]		152.4	152.4	7			gv-38.1				36.7
Klieger [177]		152.4	152.4	7			gv-38.1				22.7
Klieger [177]		152.4	152.4	7			gv-38.1				17.0
Klieger [177]		152.4	152.4	7			gv-38.1				23.0
Klieger [177]		152.4	152.4	7			gv-38.1				17.8
Klieger [177]		152.4	152.4	7			gv-38.1				30.3
Klieger [177]		152.4	152.4	28			gv-38.1			24614	51.0
Klieger [177]		152.4	152.4	28			gv-38.1			21650	34.7
Klieger [177]		152.4	152.4	28			gv-38.1				51.6
Klieger [177]		152.4	152.4	28			gv-38.1				47.7
Klieger [177]		152.4	152.4	28			gv-38.1				43.3
Klieger [177]		152.4	152.4	28			gv-38.1				44.5
Klieger [177]		152.4	152.4	28			gv-38.1			27717	49.5
Klieger [177]		152.4	152.4	28			gv-38.1				49.8
Klieger [177]		152.4	152.4	28			gv-38.1				34.8
Klieger [177]		152.4	152.4	28			gv-38.1				48.5
Klieger [177]		152.4	152.4	28			gv-38.1				48.3
Klieger [177]		152.4	152.4	28			gv-38.1				43.5
Klieger [177]		152.4	152.4	28			gv-38.1			24270	33.2
Klieger [177]		152.4	152.4	28			gv-38.1			23925	45.2

Source	*n*	*B (mm)*	*H (mm)*	*Age (d)*	*w/c*	$\rho_{c,f}$ *(kg/m^3)*	*Aggregate properties*[p]	*sf/c (%)*	*ma/b (%)*	E_c *(MPa)*	f'_{co} *(MPa)*
Klieger [177]		152.4	152.4	28			gv-38.1			25373	47.3
Klieger [177]		152.4	152.4	28			gv-38.1			26131	44.9
Klieger [177]		152.4	152.4	28			gv-38.1			24063	39.9
Klieger [177]		152.4	152.4	28			gv-38.1				52.0
Klieger [177]		152.4	152.4	28			gv-38.1				46.2
Klieger [177]		152.4	152.4	28			gv-38.1				38.1
Klieger [177]		152.4	152.4	28			gv-38.1				40.7
Klieger [177]		152.4	152.4	28			gv-38.1			26062	45.1
Klieger [177]		152.4	152.4	28			gv-38.1				50.7
Klieger [177]		152.4	152.4	28			gv-38.1				0.6
Klieger [177]		152.4	152.4	28			gv-38.1			26752	41.0
Klieger [177]		152.4	152.4	28			gv-38.1				33.6
Klieger [177]		152.4	152.4	28			gv-38.1				37.7
Klieger [177]		152.4	152.4	28			gv-38.1				37.7
Klieger [177]		152.4	152.4	28			gv-38.1			25166	44.8
Klieger [177]		152.4	152.4	90			gv-38.1				52.5
Klieger [177]		152.4	152.4	90			gv-38.1				37.1
Klieger [177]		152.4	152.4	90			gv-38.1				60.5
Klieger [177]		152.4	152.4	90			gv-38.1				53.4
Klieger [177]		152.4	152.4	90			gv-38.1				52.1
Klieger [177]		152.4	152.4	90			gv-38.1				49.4
Klieger [177]		152.4	152.4	90			gv-38.1				53.9
Klieger [177]		152.4	152.4	90			gv-38.1				55.7
Klieger [177]		152.4	152.4	90			gv-38.1				25.6
Klieger [177]		152.4	152.4	90			gv-38.1				52.1
Klieger [177]		152.4	152.4	90			gv-38.1				52.4
Klieger [177]		152.4	152.4	90			gv-38.1				44.8
Klieger [177]		152.4	152.4	90			gv-38.1				45.5
Klieger [177]		152.4	152.4	90			gv-38.1				51.4
Klieger [177]		152.4	152.4	90			gv-38.1				51.0
Klieger [177]		152.4	152.4	90			gv-38.1				56.3
Klieger [177]		152.4	152.4	90			gv-38.1				47.9
Klieger [177]		152.4	152.4	90			gv-38.1				57.5
Klieger [177]		152.4	152.4	90			gv-38.1				52.1
Klieger [177]		152.4	152.4	90			gv-38.1				47.7
Klieger [177]		152.4	152.4	90			gv-38.1				53.2
Klieger [177]		152.4	152.4	90			gv-38.1				50.7
Klieger [177]		152.4	152.4	90			gv-38.1				56.1
Klieger [177]		152.4	152.4	90			gv-38.1				44.1
Klieger [177]		152.4	152.4	90			gv-38.1				53.3
Klieger [177]		152.4	152.4	90			gv-38.1				53.2
Klieger [177]		152.4	152.4	90			gv-38.1				50.2
Klieger [177]		152.4	152.4	90			gv-38.1				52.5
Klieger [177]		152.4	152.4	90			gv-38.1				57.2
Klieger [177]		152.4	152.4	365			gv-38.1			37783	63.2
Klieger [177]		152.4	152.4	365			gv-38.1			33509	39.6
Klieger [177]		152.4	152.4	365			gv-38.1				63.2
Klieger [177]		152.4	152.4	365			gv-38.1				60.1
Klieger [177]		152.4	152.4	365			gv-38.1				57.1
Klieger [177]		152.4	152.4	365			gv-38.1				60.2
Klieger [177]		152.4	152.4	365			gv-38.1			38404	58.8
Klieger [177]		152.4	152.4	365			gv-38.1				65.8
Klieger [177]		152.4	152.4	365			gv-38.1				44.0
Klieger [177]		152.4	152.4	365			gv-38.1				60.0
Klieger [177]		152.4	152.4	365			gv-38.1				57.6
Klieger [177]		152.4	152.4	365			gv-38.1				51.4
Klieger [177]		152.4	152.4	365			gv-38.1				51.4
Klieger [177]		152.4	152.4	365			gv-38.1			37852	50.7
Klieger [177]		152.4	152.4	365			gv-38.1			38335	53.4
Klieger [177]		152.4	152.4	365			gv-38.1			39438	54.9
Klieger [177]		152.4	152.4	365			gv-38.1			41575	66.5
Klieger [177]		152.4	152.4	365			gv-38.1			38473	57.6
Klieger [177]		152.4	152.4	365			gv-38.1				63.7
Klieger [177]		152.4	152.4	365			gv-38.1				63.5
Klieger [177]		152.4	152.4	365			gv-38.1				56.3
Klieger [177]		152.4	152.4	365			gv-38.1				59.0
Klieger [177]		152.4	152.4	365			gv-38.1			36404	53.8
Klieger [177]		152.4	152.4	365			gv-38.1				60.9
Klieger [177]		152.4	152.4	365			gv-38.1				50.5
Klieger [177]		152.4	152.4	365			gv-38.1			39093	63.0
Klieger [177]		152.4	152.4	365			gv-38.1				65.3
Klieger [177]		152.4	152.4	365			gv-38.1				58.5
Klieger [177]		152.4	152.4	365			gv-38.1				68.4
Klieger [177]		152.4	152.4	365			gv-38.1			44195	59.4
Klieger [177]		152.4	152.4	1095			gv-38.1			40265	67.6
Klieger [177]		152.4	152.4	1095			gv-38.1			34474	44.1
Klieger [177]		152.4	152.4	1095			gv-38.1			32750	66.9
Klieger [177]		152.4	152.4	1095			gv-38.1				64.3
Klieger [177]		152.4	152.4	1095			gv-38.1				59.4
Klieger [177]		152.4	152.4	1095			gv-38.1				64.0
Klieger [177]		152.4	152.4	1095			gv-38.1			40403	64.1

Source	*n*	*B (mm)*	*H (mm)*	*Age (d)*	*w/c*	$\rho_{c,f}$ *(kg/m^3)*	*Aggregate properties*[p]	*sf/c (%)*	*ma/b (%)*	E_c *(MPa)*	f'_{co} *(MPa)*
Klieger [177]		152.4	152.4	1095			gv-38.1				70.1
Klieger [177]		152.4	152.4	1095			gv-38.1				51.0
Klieger [177]		152.4	152.4	1095			gv-38.1				64.2
Klieger [177]		152.4	152.4	1095			gv-38.1				62.8
Klieger [177]		152.4	152.4	1095			gv-38.1				55.7
Klieger [177]		152.4	152.4	1095			gv-38.1			39369	54.7
Klieger [177]		152.4	152.4	1095			gv-38.1			38886	61.0
Klieger [177]		152.4	152.4	1095			gv-38.1			40127	62.1
Klieger [177]		152.4	152.4	1095			gv-38.1			41024	66.1
Klieger [177]		152.4	152.4	1095			gv-38.1			40265	65.2
Klieger [177]		152.4	152.4	1095			gv-38.1				68.5
Klieger [177]		152.4	152.4	1095			gv-38.1			33233	65.8
Klieger [177]		152.4	152.4	1095			gv-38.1				56.3
Klieger [177]		152.4	152.4	1095			gv-38.1				64.1
Klieger [177]		152.4	152.4	1095			gv-38.1			36473	55.0
Klieger [177]		152.4	152.4	1095			gv-38.1				64.4
Klieger [177]		152.4	152.4	1095			gv-38.1				54.3
Klieger [177]		152.4	152.4	1095			gv-38.1			40196	62.3
Klieger [177]		152.4	152.4	1095			gv-38.1				66.5
Klieger [177]		152.4	152.4	1095			gv-38.1				65.5
Klieger [177]		152.4	152.4	1095			gv-38.1			35853	68.2
Klieger [177]		152.4	152.4	1095			gv-38.1			44816	68.9
Klieger [177]		152.4	152.4	1			gv-38.1				5.4
Klieger [177]		152.4	152.4	1			gv-38.1				4.1
Klieger [177]		152.4	152.4	1			gv-38.1				4.0
Klieger [177]		152.4	152.4	1			gv-38.1				2.9
Klieger [177]		152.4	152.4	1			gv-38.1				6.1
Klieger [177]		152.4	152.4	1			gv-38.1				5.5
Klieger [177]		152.4	152.4	1			gv-38.1				8.7
Klieger [177]		152.4	152.4	1			gv-38.1				7.0
Klieger [177]		152.4	152.4	1			gv-38.1				5.5
Klieger [177]		152.4	152.4	1			gv-38.1				5.1
Klieger [177]		152.4	152.4	1			gv-38.1				4.6
Klieger [177]		152.4	152.4	1			gv-38.1				3.4
Klieger [177]		152.4	152.4	1			gv-38.1				2.8
Klieger [177]		152.4	152.4	1			gv-38.1				3.9
Klieger [177]		152.4	152.4	1			gv-38.1				6.1
Klieger [177]		152.4	152.4	1			gv-38.1				3.7
Klieger [177]		152.4	152.4	1			gv-38.1				3.1
Klieger [177]		152.4	152.4	1			gv-38.1				3.9
Klieger [177]		152.4	152.4	1			gv-38.1				5.7
Klieger [177]		152.4	152.4	1			gv-38.1				4.7
Klieger [177]		152.4	152.4	1			gv-38.1				4.3
Klieger [177]		152.4	152.4	1			gv-38.1				10.2
Klieger [177]		152.4	152.4	1			gv-38.1				15.8
Klieger [177]		152.4	152.4	1			gv-38.1				12.8
Klieger [177]		152.4	152.4	1			gv-38.1				3.5
Klieger [177]		152.4	152.4	1			gv-38.1				3.2
Klieger [177]		152.4	152.4	1			gv-38.1				2.3
Klieger [177]		152.4	152.4	1			gv-38.1				3.2
Klieger [177]		152.4	152.4	1			gv-38.1				5.4
Klieger [177]		152.4	152.4	7			gv-38.1				29.0
Klieger [177]		152.4	152.4	7			gv-38.1				20.8
Klieger [177]		152.4	152.4	7			gv-38.1				26.2
Klieger [177]		152.4	152.4	7			gv-38.1				25.4
Klieger [177]		152.4	152.4	7			gv-38.1				18.9
Klieger [177]		152.4	152.4	7			gv-38.1				24.0
Klieger [177]		152.4	152.4	7			gv-38.1				32.6
Klieger [177]		152.4	152.4	7			gv-38.1				27.6
Klieger [177]		152.4	152.4	7			gv-38.1				20.3
Klieger [177]		152.4	152.4	7			gv-38.1				24.0
Klieger [177]		152.4	152.4	7			gv-38.1				24.8
Klieger [177]		152.4	152.4	7			gv-38.1				27.4
Klieger [177]		152.4	152.4	7			gv-38.1				11.8
Klieger [177]		152.4	152.4	7			gv-38.1				18.2
Klieger [177]		152.4	152.4	7			gv-38.1				27.0
Klieger [177]		152.4	152.4	7			gv-38.1				17.9
Klieger [177]		152.4	152.4	7			gv-38.1				18.3
Klieger [177]		152.4	152.4	7			gv-38.1				19.3
Klieger [177]		152.4	152.4	7			gv-38.1				22.2
Klieger [177]		152.4	152.4	7			gv-38.1				19.3
Klieger [177]		152.4	152.4	7			gv-38.1				13.7
Klieger [177]		152.4	152.4	7			gv-38.1				33.2
Klieger [177]		152.4	152.4	7			gv-38.1				33.8
Klieger [177]		152.4	152.4	7			gv-38.1				29.8
Klieger [177]		152.4	152.4	7			gv-38.1				12.1
Klieger [177]		152.4	152.4	7			gv-38.1				10.3
Klieger [177]		152.4	152.4	7			gv-38.1				12.3
Klieger [177]		152.4	152.4	7			gv-38.1				10.3
Klieger [177]		152.4	152.4	7			gv-38.1				17.9

Source	*n*	*B (mm)*	*H (mm)*	*Age (d)*	*w/c*	$\rho_{c,f}$ *(kg/m^3)*	*Aggregate properties*[p]	*sf/c (%)*	*ma/b (%)*	E_c *(MPa)*	f'_{co} *(MPa)*
Klieger [177]		152.4	152.4	28			gv-38.1			22477	40.5
Klieger [177]		152.4	152.4	28			gv-38.1			20202	28.9
Klieger [177]		152.4	152.4	28			gv-38.1				39.4
Klieger [177]		152.4	152.4	28			gv-38.1				41.6
Klieger [177]		152.4	152.4	28			gv-38.1				32.6
Klieger [177]		152.4	152.4	28			gv-38.1				35.8
Klieger [177]		152.4	152.4	28			gv-38.1			25373	40.2
Klieger [177]		152.4	152.4	28			gv-38.1				40.1
Klieger [177]		152.4	152.4	28			gv-38.1				28.6
Klieger [177]		152.4	152.4	28			gv-38.1				39.8
Klieger [177]		152.4	152.4	28			gv-38.1				38.6
Klieger [177]		152.4	152.4	28			gv-38.1				37.6
Klieger [177]		152.4	152.4	28			gv-38.1			21581	21.4
Klieger [177]		152.4	152.4	28			gv-38.1			21787	29.4
Klieger [177]		152.4	152.4	28			gv-38.1			23373	38.1
Klieger [177]		152.4	152.4	28			gv-38.1			23787	31.9
Klieger [177]		152.4	152.4	28			gv-38.1			21305	31.6
Klieger [177]		152.4	152.4	28			gv-38.1				35.5
Klieger [177]		152.4	152.4	28			gv-38.1				34.7
Klieger [177]		152.4	152.4	28			gv-38.1				29.6
Klieger [177]		152.4	152.4	28			gv-38.1				27.6
Klieger [177]		152.4	152.4	28			gv-38.1			25442	40.1
Klieger [177]		152.4	152.4	28			gv-38.1				38.3
Klieger [177]		152.4	152.4	28			gv-38.1				34.1
Klieger [177]		152.4	152.4	28			gv-38.1			22063	26.6
Klieger [177]		152.4	152.4	28			gv-38.1				22.1
Klieger [177]		152.4	152.4	28			gv-38.1				26.3
Klieger [177]		152.4	152.4	28			gv-38.1				23.8
Klieger [177]		152.4	152.4	28			gv-38.1			22270	29.1
Klieger [177]		152.4	152.4	90			gv-38.1				44.1
Klieger [177]		152.4	152.4	90			gv-38.1				30.8
Klieger [177]		152.4	152.4	90			gv-38.1				45.9
Klieger [177]		152.4	152.4	90			gv-38.1				45.4
Klieger [177]		152.4	152.4	90			gv-38.1				39.7
Klieger [177]		152.4	152.4	90			gv-38.1				39.3
Klieger [177]		152.4	152.4	90			gv-38.1				43.3
Klieger [177]		152.4	152.4	90			gv-38.1				45.0
Klieger [177]		152.4	152.4	90			gv-38.1				30.9
Klieger [177]		152.4	152.4	90			gv-38.1				44.2
Klieger [177]		152.4	152.4	90			gv-38.1				43.0
Klieger [177]		152.4	152.4	90			gv-38.1				39.8
Klieger [177]		152.4	152.4	90			gv-38.1				29.5
Klieger [177]		152.4	152.4	90			gv-38.1				35.4
Klieger [177]		152.4	152.4	90			gv-38.1				42.7
Klieger [177]		152.4	152.4	90			gv-38.1				41.9
Klieger [177]		152.4	152.4	90			gv-38.1				40.7
Klieger [177]		152.4	152.4	90			gv-38.1				41.4
Klieger [177]		152.4	152.4	90			gv-38.1				42.7
Klieger [177]		152.4	152.4	90			gv-38.1				37.0
Klieger [177]		152.4	152.4	90			gv-38.1				38.8
Klieger [177]		152.4	152.4	90			gv-38.1				44.7
Klieger [177]		152.4	152.4	90			gv-38.1				43.7
Klieger [177]		152.4	152.4	90			gv-38.1				37.0
Klieger [177]		152.4	152.4	90			gv-38.1				40.8
Klieger [177]		152.4	152.4	90			gv-38.1				40.9
Klieger [177]		152.4	152.4	90			gv-38.1				38.3
Klieger [177]		152.4	152.4	90			gv-38.1				39.3
Klieger [177]		152.4	152.4	90			gv-38.1				44.4
Klieger [177]		152.4	152.4	365			gv-38.1			36473	48.4
Klieger [177]		152.4	152.4	365			gv-38.1			30337	33.0
Klieger [177]		152.4	152.4	365			gv-38.1				48.3
Klieger [177]		152.4	152.4	365			gv-38.1				49.9
Klieger [177]		152.4	152.4	365			gv-38.1				44.1
Klieger [177]		152.4	152.4	365			gv-38.1				45.1
Klieger [177]		152.4	152.4	365			gv-38.1			36749	44.4
Klieger [177]		152.4	152.4	365			gv-38.1				48.7
Klieger [177]		152.4	152.4	365			gv-38.1				32.9
Klieger [177]		152.4	152.4	365			gv-38.1				45.2
Klieger [177]		152.4	152.4	365			gv-38.1				45.1
Klieger [177]		152.4	152.4	365			gv-38.1				43.2
Klieger [177]		152.4	152.4	365			gv-38.1			37714	34.9
Klieger [177]		152.4	152.4	365			gv-38.1			37301	37.4
Klieger [177]		152.4	152.4	365			gv-38.1			38128	45.4
Klieger [177]		152.4	152.4	365			gv-38.1			39921	51.1
Klieger [177]		152.4	152.4	365			gv-38.1			36611	47.7
Klieger [177]		152.4	152.4	365			gv-38.1				45.6
Klieger [177]		152.4	152.4	365			gv-38.1				46.8
Klieger [177]		152.4	152.4	365			gv-38.1				41.0
Klieger [177]		152.4	152.4	365			gv-38.1				45.4
Klieger [177]		152.4	152.4	365			gv-38.1			36404	43.2

Source	*n*	*B (mm)*	*H (mm)*	*Age (d)*	*w/c*	$\rho_{c,f}$ *(kg/m^3)*	*Aggregate properties*[p]	*sf/c (%)*	*ma/b (%)*	E_c *(MPa)*	f'_{co} *(MPa)*
Klieger [177]		152.4	152.4	365			gv-38.1				45.5
Klieger [177]		152.4	152.4	365			gv-38.1				38.3
Klieger [177]		152.4	152.4	365			gv-38.1			37163	47.8
Klieger [177]		152.4	152.4	365			gv-38.1				49.2
Klieger [177]		152.4	152.4	365			gv-38.1				46.5
Klieger [177]		152.4	152.4	365			gv-38.1				47.0
Klieger [177]		152.4	152.4	365			gv-38.1			42954	47.2
Klieger [177]		152.4	152.4	1095			gv-38.1			37714	47.6
Klieger [177]		152.4	152.4	1095			gv-38.1			30406	35.0
Klieger [177]		152.4	152.4	1095			gv-38.1				50.9
Klieger [177]		152.4	152.4	1095			gv-38.1				52.1
Klieger [177]		152.4	152.4	1095			gv-38.1				46.5
Klieger [177]		152.4	152.4	1095			gv-38.1				48.5
Klieger [177]		152.4	152.4	1095			gv-38.1			35853	43.9
Klieger [177]		152.4	152.4	1095			gv-38.1				52.7
Klieger [177]		152.4	152.4	1095			gv-38.1				37.9
Klieger [177]		152.4	152.4	1095			gv-38.1				47.5
Klieger [177]		152.4	152.4	1095			gv-38.1				47.0
Klieger [177]		152.4	152.4	1095			gv-38.1				45.3
Klieger [177]		152.4	152.4	1095			gv-38.1			38542	41.0
Klieger [177]		152.4	152.4	1095			gv-38.1			37507	41.4
Klieger [177]		152.4	152.4	1095			gv-38.1			36129	48.1
Klieger [177]		152.4	152.4	1095			gv-38.1			39990	52.6
Klieger [177]		152.4	152.4	1095			gv-38.1			37025	48.8
Klieger [177]		152.4	152.4	1095			gv-38.1				49.4
Klieger [177]		152.4	152.4	1095			gv-38.1				49.0
Klieger [177]		152.4	152.4	1095			gv-38.1				41.8
Klieger [177]		152.4	152.4	1095			gv-38.1				47.0
Klieger [177]		152.4	152.4	1095			gv-38.1			34474	43.9
Klieger [177]		152.4	152.4	1095			gv-38.1				46.8
Klieger [177]		152.4	152.4	1095			gv-38.1				40.5
Klieger [177]		152.4	152.4	1095			gv-38.1			37025	47.1
Klieger [177]		152.4	152.4	1095			gv-38.1				54.1
Klieger [177]		152.4	152.4	1095			gv-38.1				48.7
Klieger [177]		152.4	152.4	1095			gv-38.1				50.9
Klieger [177]		152.4	152.4	1095			gv-38.1			43299	52.2
Klieger [177]		152.4	152.4	1			gv-38.1				1.2
Klieger [177]		152.4	152.4	1			gv-38.1				1.9
Klieger [177]		152.4	152.4	1			gv-38.1				1.1
Klieger [177]		152.4	152.4	7			gv-38.1				8.5
Klieger [177]		152.4	152.4	7			gv-38.1				8.8
Klieger [177]		152.4	152.4	7			gv-38.1				4.1
Klieger [177]		152.4	152.4	28			gv-38.1			20271	17.6
Klieger [177]		152.4	152.4	28			gv-38.1			19650	15.4
Klieger [177]		152.4	152.4	28			gv-38.1			18547	9.7
Klieger [177]		152.4	152.4	90			gv-38.1				19.4
Klieger [177]		152.4	152.4	90			gv-38.1				18.5
Klieger [177]		152.4	152.4	90			gv-38.1				18.1
Klieger [177]		152.4	152.4	365			gv-38.1			31164	19.2
Klieger [177]		152.4	152.4	365			gv-38.1			30820	19.7
Klieger [177]		152.4	152.4	365			gv-38.1			35646	21.7
Klieger [177]		152.4	152.4	1095			gv-38.1			32750	20.6
Klieger [177]		152.4	152.4	1095			gv-38.1			33233	20.3
Klieger [177]		152.4	152.4	1095			gv-38.1			35853	25.2
Persson [206]	3	100	100			2270	qz-16			16832	13.8
Persson [206]	3	100	100			2270	qz-16			14590	23.2
Persson [206]	3	100	100			2270	qz-16			21407	23.8
Persson [206]	3	100	100			2270	qz-16			16566	27.1
Persson [206]	3	100	100			2270	qz-16			25694	28.1
Persson [206]	3	100	100			2270	qz-16			16400	29.7
Persson [206]	3	100	100			2270	qz-16			22036	32.0
Persson [206]	3	100	100			2270	qz-16			23842	34.4
Persson [206]	3	100	100			2270	qz-16			25761	37.9
Persson [206]	3	100	100			2270	qz-16			27287	42.2
Persson [206]	3	100	100			2270	qz-16			28245	42.8
Persson [206]	3	100	100			2270	qz-16			19234	44.9
Persson [206]	3	100	100			2270	qz-16			25602	46.4
Persson [206]	3	100	100			2270	qz-16			27859	50.0
Persson [206]	3	100	100			2270	qz-16			28209	60.2
Persson [206]	3	100	100			2270	qz-16			39815	61.0
Persson [206]	3	100	100			2270	qz-16			16213	14.1
Persson [206]	3	100	100			2270	qz-16			14082	23.0
Persson [206]	3	100	100			2270	qz-16			22083	24.0
Persson [206]	3	100	100			2270	qz-16			19607	26.2
Persson [206]	3	100	100			2270	qz-16			14650	26.9
Persson [206]	3	100	100			2270	qz-16			23780	30.1
Persson [206]	3	100	100			2270	qz-16			15053	34.9
Persson [206]	3	100	100			2270	qz-16			22097	35.7
Persson [206]	3	100	100			2270	qz-16			20860	37.9
Persson [206]	3	100	100			2270	qz-16			19798	46.0

Source	*n*	*B (mm)*	*H (mm)*	*Age (d)*	*w/c*	$\rho_{c,f}$ *(kg/m^3)*	*Aggregate properties*[p]	*sf/c (%)*	*ma/b (%)*	E_c *(MPa)*	f'_{co} *(MPa)*
Persson [206]	3	100	100			2270	qz-16			25211	50.1
Persson [206]	3	100	100			2270	qz-16			33610	54.1
Persson [206]	3	100	100			2270	qz-16			24429	55.9
Persson [206]	3	100	100			2270	qz-16			29955	59.8
Persson [206]	3	100	100			2270	qz-16			28885	60.7
Persson [206]	3	100	100			2270	qz-16			38579	64.0
Persson [206]	3	100	100			2293	qz-16			15992	18.0
Persson [206]	3	100	100			2293	qz-16			20790	26.4
Persson [206]	3	100	100			2293	qz-16			28121	32.0
Persson [206]	3	100	100			2293	qz-16			29644	34.1
Persson [206]	3	100	100			2293	qz-16			23175	42.9
Persson [206]	3	100	100			2293	qz-16			27356	53.1
Persson [206]	3	100	100			2293	qz-16			35083	61.0
Persson [206]	3	100	100			2293	qz-16			28889	63.7
Persson [206]	3	100	100			2293	qz-16			27425	65.0
Persson [206]	3	100	100			2293	qz-16			35540	67.1
Persson [206]	3	100	100			2293	qz-16			29692	76.3
Persson [206]	3	100	100			2293	qz-16			38548	86.2
Persson [206]	3	100	100			2293	qz-16			39801	98.2
Persson [206]	3	100	100			2293	qz-16			40547	110.3
Persson [206]	3	100	100			2293	qz-16			45257	140.7
Persson [206]	3	100	100			2293	qz-16			47079	157.9
Persson [206]	3	100	100			2293	qz-16			14527	18.0
Persson [206]	3	100	100			2293	qz-16			18594	27.1
Persson [206]	3	100	100			2293	qz-16			25303	31.8
Persson [206]	3	100	100			2293	qz-16			25251	35.1
Persson [206]	3	100	100			2293	qz-16			22499	42.9
Persson [206]	3	100	100			2293	qz-16			26513	55.0
Persson [206]	3	100	100			2293	qz-16			32606	63.0
Persson [206]	3	100	100			2293	qz-16			27423	63.1
Persson [206]	3	100	100			2293	qz-16			28327	65.0
Persson [206]	3	100	100			2293	qz-16			32216	67.1
Persson [206]	3	100	100			2293	qz-16			31610	79.1
Persson [206]	3	100	100			2293	qz-16			37364	86.0
Persson [206]	3	100	100			2293	qz-16			36360	94.5
Persson [206]	3	100	100			2293	qz-16			38623	103.2
Persson [206]	3	100	100			2293	qz-16			43661	124.0
Persson [206]	3	100	100			2293	qz-16			43954	134.0
Shannag [207]	3	100	100	7	0.41	2390	ls-cr-10		15.0[v]		57.0
Shannag [207]	3	100	100	7	0.37	2310	ls-cr-10		13.5[v]		63.0
Shannag [207]	3	100	100	7	0.37	2270	ls-cr-10	4.8	14.3[v]		67.0
Shannag [207]	3	100	100	7	0.36	2230	ls-cr-10	9.1	13.6[v]		68.5
Shannag [207]	3	100	100	7	0.36	2250	ls-cr-10	13.0	13.0[v]		69.5
Shannag [207]	3	100	100	7	0.36	2260	ls-cr-10	16.7	12.5[v]		72.5
Shannag [207]	3	100	100	14	0.41	2390	ls-cr-10		15.0[v]		59.0
Shannag [207]	3	100	100	14	0.37	2310	ls-cr-10		13.5[v]		66.0
Shannag [207]	3	100	100	14	0.37	2270	ls-cr-10	4.8	14.3[v]		74.5
Shannag [207]	3	100	100	14	0.36	2230	ls-cr-10	9.1	13.6[v]		75.5
Shannag [207]	3	100	100	14	0.36	2250	ls-cr-10	13.0	13.0[v]		77.0
Shannag [207]	3	100	100	14	0.36	2260	ls-cr-10	16.7	12.5[v]		79.5
Shannag [207]	3	100	100	28	0.41	2390	ls-cr-10		15.0[v]		64.0
Shannag [207]	3	100	100	28	0.37	2310	ls-cr-10		13.5[v]		72.5
Shannag [207]	3	100	100	28	0.37	2270	ls-cr-10	4.8	14.3[v]		78.0
Shannag [207]	3	100	100	28	0.36	2230	ls-cr-10	9.1	13.6[v]		78.5
Shannag [207]	3	100	100	28	0.36	2250	ls-cr-10	13.0	13.0[v]		82.0
Shannag [207]	3	100	100	28	0.36	2260	ls-cr-10	16.7	12.5[v]		85.0
Shannag [207]	3	100	100	56	0.41	2390	ls-cr-10		15.0[v]	38500	68.0
Shannag [207]	3	100	100	56	0.37	2310	ls-cr-10		13.5[v]	47200	77.0
Shannag [207]	3	100	100	56	0.37	2270	ls-cr-10	4.8	14.3[v]	43800	86.0
Shannag [207]	3	100	100	56	0.36	2230	ls-cr-10	9.1	13.6[v]	42300	86.0
Shannag [207]	3	100	100	56	0.36	2250	ls-cr-10	13.0	13.0[v]	38600	89.5
Shannag [207]	3	100	100	56	0.36	2260	ls-cr-10	16.7	12.5[v]	36200	90.5
Topçu and Uygunoglu [208]	3	150	150	28	0.38	2324	n-cr			39283	51.2
Topçu and Uygunoglu [208]	3	150	150	28	0.42	2322	n-cr			33012	49.1
Topçu and Uygunoglu [208]	3	150	150	28	0.45	2299	n-cr			26926	48.9
Topçu and Uygunoglu [208]	3	150	150	28	0.47	2297	n-cr			25820	45.5
Topçu and Uygunoglu [208]	3	150	150	28	0.49	2282	n-cr			23607	42.3
Valdmanis et al. [123]	1	150	150		0.94	2324	gv-16			24400	34.2
Valdmanis et al. [123]	1	150	150		0.55	2340	gv-16			34030	60.5
Valdmanis et al. [123]	1	150	150		0.38	2371	gv-16			37830[m]	76.2
Valdmanis et al. [123]	1	150	150		0.35	2394	gv-16	3.2		36650	81.4
Valdmanis et al. [123]	1	150	150		0.32	2421	gv-16	6.4		39090	104.1
Wang et al. [161]	1	100	100		0.50		ls				56.3
Wang et al. [161]	1	100	100		0.40		ls				76.6
Wang et al. [161]	1	100	100		0.30		ls				88.8
Wang et al. [161]	1	100	100		0.25		ls				107.5
Wang et al. [161]	1	100	100		0.20		ls				118.3
Wang et al. [161]	1	100	100		0.18		ls				131.9
Wang et al. [161]	1	100	100		0.20		ls				129.0
Wang et al. [161]	1	100	100		0.20		ls				118.6

Source	*n*	*B (mm)*	*H (mm)*	*Age (d)*	*w/c*	$\rho_{c,f}$ *(kg/m^3)*	*Aggregate properties*[p]	*sf/c (%)*	*ma/b (%)*	E_c *(MPa)*	f'_{co} *(MPa)*
Wang et al. [161]	1	100	100		0.20		ls				123.7
Wang et al. [161]	1	100	100		0.18		ls				124.4
Wang et al. [161]	1	100	100		0.18		ls				131.3
Wang et al. [161]	1	100	100		0.18		ls				126.2
Wang et al. [161]	1	100	100		0.18		ls				127.5
Wang et al. [161]	1	100	100		0.18		ls				125.4
Wang et al. [161]	1	100	100		0.18		ls				128.7
Wang et al. [161]	1	100	100		0.18		ls				126.9
Wang et al. [161]	1	100	100		0.18		ls				127.3
Wang et al. [161]	1	100	100		0.18		ls				135.0
Wang et al. [161]	1	100	100		0.18		ls				138.1
Wang et al. [161]	1	100	100		0.18		ls				164.9
Wang et al. [161]	1	100	100		0.20		ls				156.7

d Fresh concrete density that is significantly higher than the reference values
m Concrete elastic modulus that differ significantly from the reference values of the corresponding concrete strength
f Fly-ash used as mineral admixture in concrete mix
s Blast-furnace slag used as mineral admixture in concrete mix
p Designation:- type-irregularity-size
Type:- n: normal weight aggregate, ad: andesite, dm: dolomite, gn: granite, gv: gravel, ls: limestone, pm: volcanic pumice, qz: quartz
Irregularity:- cr: crushed
Size:- maximum aggregate in mm

Table A7. Test database of light weight concrete prisms (without ε_{co} values)

Source	*n*	*B (mm)*	*H (mm)*	*Age (d)*	*w/c*	$\rho_{c,f}$ *(kg/m³)*	*Aggregate properties*[p]	*sf/c (%)*	*ma/b (%)*	E_c *(MPa)*	f'_{co} *(MPa)*
Haque et al. [209]	3	100	100	28	0.64	1775	fa-12.7	9.1		23782	38.0
Haque et al. [209]	3	100	100	28	0.64	1775	fa-12.7	9.1		21991	40.0
Haque et al. [209]	3	100	100	28	0.64	1775	fa-12.7	9.1		24003	42.5
Haque et al. [209]	3	100	100	365	0.64	1775	fa-12.7	9.1		26120	48.0
Haque et al. [209]	3	100	100	365	0.64	1775	fa-12.7	9.1		23030	41.0
Haque et al. [209]	3	100	100	365	0.64	1775	fa-12.7	9.1		25240	47.0
Haque et al. [209]	3	100	100	28	0.39	1800	fa-12.7	9.1		26648	49.5
Haque et al. [209]	3	100	100	28	0.39	1800	fa-12.7	9.1		27058	49.5
Haque et al. [209]	3	100	100	28	0.39	1800	fa-12.7	9.1		28198	57.0
Haque et al. [209]	3	100	100	365	0.39	1800	fa-12.7	9.1		29040	64.5
Haque et al. [209]	3	100	100	365	0.39	1800	fa-12.7	9.1		27190	52.5
Haque et al. [209]	3	100	100	365	0.39	1800	fa-12.7	9.1		29000	62.5
Hossain [175]		100	100	28	0.45	1881	pm			10500	28.0
Hossain [175]		100	100	28	0.45	1961	pm			11000	30.0
Hossain [175]		100	100	28	0.45	2091	pm			12000	32.0
Hossain [175]		100	100	28	0.45	2291[d]	pm			14500	36.0
Hossain [175]		100	100	28	0.45	1734	pm			10000	24.0
Hossain [175]		100	100	28	0.45	1834	pm			11900	25.0
Hossain [175]		100	100	28	0.45	1979	pm			12200	28.0
Hossain [175]		100	100	28	0.45	2219	pm			14500	36.0
Topçu and Uygunoglu [208]	3	150	150	28	0.39	1808	pm			18258	24.6
Topçu and Uygunoglu [208]	3	150	150	28	0.42	1759	pm			17152	21.3
Topçu and Uygunoglu [208]	3	150	150	28	0.45	1752	pm			9590	19.4
Topçu and Uygunoglu [208]	3	150	150	28	0.47	1741	pm			9221	18.7
Topçu and Uygunoglu [208]	3	150	150	28	0.49	1711	pm			8299	16.3
Topçu and Uygunoglu [208]	3	150	150	28	0.38	1877	tf			11066	22.4
Topçu and Uygunoglu [208]	3	150	150	28	0.42	1873	tf			10881	21.1
Topçu and Uygunoglu [208]	3	150	150	28	0.45	1812	tf			8115	17.5
Topçu and Uygunoglu [208]	3	150	150	28	0.47	1783	tf			11434	18.3
Topçu and Uygunoglu [208]	3	150	150	28	0.50	1780	tf			6639	15.9
Topçu and Uygunoglu [208]	3	150	150	28	0.39	1800	dt			12541	19.5
Topçu and Uygunoglu [208]	3	150	150	28	0.42	1778	dt			5164	16.9
Topçu and Uygunoglu [208]	3	150	150	28	0.45	1731	dt			5533	14.6
Topçu and Uygunoglu [208]	3	150	150	28	0.47	1712	dt			4426	13.7
Topçu and Uygunoglu [208]	3	150	150	28	0.49	1695	dt			4057	12.9
Zhang and Gjorv [145]	1	100	100	28	0.34	1835	ec	9.1			91.8
Zhang and Gjorv [145]	1	100	100	28	0.43	1750	ec	9.1			93.4
Zhang and Gjorv [145]	1	100	100	28	0.36	1815	ec				84.5
Zhang and Gjorv [145]	1	100	100	28	0.36	1800	ec	9.1			98.0
Zhang and Gjorv [145]	1	100	100	28	0.37	1710	ec	9.1			74.4
Zhang and Gjorv [145]	1	100	100	28	0.40	1595	ec	9.1			57.3
Zhang and Gjorv [145]	1	100	100	28	0.36	1750	ec	9.1			81.5
Zhang and Gjorv [145]	1	100	100	28	0.44	1880	fa	9.1			88.4

d Fresh concrete density that is significantly higher than the reference values

p Designation:- type-size

Type:- dt: sintered diatomite, ec: expanded clay, fa: sintered fly-ash, pm: volcanic pumice, tf: tuff

Size:- maximum aggregate in mm

REFERENCES

1. Abdollahi, B., Bakhshi, M., Motavalli, M., and Shekarchi, M., (2007). "Experimental modeling of GFRP confined concrete cylinders subjected to axial loads." *Proceedings of the 8th International Symposium on Fiber Reinforced Polymer Reinforcement for Concrete Structures*, University of Patras, Patras, Greece.
2. Ahmad, S.H. and Shah, S.P., (1979). "Complete Stress-Strain Curves of Concrete and Nonlinear Design." *Progress Report, National Science Foundation Grant PFR 79-22878*, University of Illinois, Chicago Circle.
3. Ahmad, S.H. and Shah, S.P., (1982). "Complete triaxial stress-strain curves for concrete." *Journal of the Structural Division,* 108(4), p. 728-742.
4. Ahmad, S.H. and Shah, S.P., (1985). "Behaviour of hoop confined concrete under high strain rates. ." *ACI Journal Proceedings,* 82, p. 634-647.
5. Ahmad, S.M., Khaloo, A.R., and Irshaid, A., (1991). "Behaviour of concrete spirally confined by fiberglass filaments." *Magazine of Concrete Research,* 43(56), p. 143-148.
6. Aire, C., Gettu, R., Casas, J.R., Marques, S., and Marques, D., (2010). "Concrete laterally confined with fibre-reinforced polymers (FRP): experimental study and theoretical model." *Materiales De Construccion,* 60(297), p. 19-31.
7. Akogbe, R.-K., Liang, M., and Wu., Z.-M., (2011). "Size effect of axial compressive strength of CFRP confined concrete cylinders." *International Journal of Concrete Structures and Materials,* 5(1), p. 49-55.
8. Ali, A.M., Farid, B.J., and Al-Janabi, A.J.M., (1990). "Stress-strain relationship for concrete in compression made of local materials." *Engineering Sciences,* 2(1), p. 183-194.
9. Almusallam, T.H., (2007). "Behavior of normal and high-strength concrete cylinders confined with E-glass/epoxy composite laminates." *Composites Part B-Engineering,* 38(5-6), p. 629-639.
10. Almusallam, T.H. and Alsayed, H., (1995). "Stress–strain relationship of normal, high-strength and lightweight concrete." *Magazine of Concrete Research,* 47(170), p. 39-44.
11. Ansari, F. and Li, Q.B., (1998). "High-strength concrete subjected to triaxial compression." *ACI Materials Journal,* 95(6), p. 747-755.
12. Arduini, M., Di Tommaso, A., Manfroni, O., Ferrari, S., and Romagnolo, M. II (1999). "Confinamento assive di elementi compressi in calcestruzzo con fogli di materiale composito." *Industria Italiana del Cemento,* 11, p. 836-841.
13. Assa, B., Nishiyama, M., and Watanabe, F., (2001). "New approach for modeling confined concrete. I: Circular columns." *Journal of Structural Engineering,* 127(7), p. 743-750.
14. Attard, M.M. and Setunge, S., (1996). "Stress-strain relationship of confined and unconfined concrete." *ACI Materials Journal,* 93(5), p. 432-442.
15. Au, C. and Buyukozturk, O., (2005). "Effect of fiber orientation and ply mix on fiber reinforced polymer-confined concrete." *Journal of Composites for Construction,* 9(5), p. 397-407.
16. Balmer, G.G., (1949). "Shearing Strength of Concrete Under High Triaxial Stress-computation of Mohr's Envelope as a Curve." *Structural Research Laboratory Report No. SP-23*, Department of the Interior Bureau of Reclamation, Denver, Colorado, United States.
17. Barnard, P.R., (1964). "Researches into the complete stress-strain curve for concrete." *Magazine of Concrete Research,* 16(49), p. 203-210.
18. Belén, G.F., Fernando, M.A., Diego, C.L., and Sindy, S.P., (2011). "Stress–strain relationship in axial compression for concrete using recycled saturated coarse aggregate." *Construction and Building Materials,* 25(5), p. 2335-2342.
19. Bellotti, R. and Rossi, P., (1991). "Cylinder tests: experimental technique and results." *Materials and Structures,* 24(1), p. 45-51.
20. Benzaid, R., Chikh, N.E., and Mesbah, H., (2009). "Study of the Compressive Behavior of Short Concrete Columns Confined by Fiber Reinforced Composite." *Arabian Journal for Science and Engineering,* 34(1B), p. 15-26.
21. Benzaid, R., Mesbah, H., and Chikh, N.E., (2010). "FRP-confined Concrete Cylinders: Axial Compression Experiments and Strength Model." *Journal of Reinforced Plastics and Composites,* 29(16), p. 2469-2488.
22. Berthet, J.F., Ferrier, E., and Hamelin, P., (2005). "Compressive behavior of concrete externally confined by composite jackets. Part A: experimental study." *Construction and Building Materials,* 19(3), p. 223-232.
23. Bisby, L., Take, W.A., and Caspary, A., (2007). "Quantifying strain variation FRP confined using digital image correlation: proof-of-concept and initial results." *Asia-Pacific Conference on FRP in Structures*.
24. Bisby, L.A., Chen, J.F., Li, S.Q., Stratford, T.J., Cueva, N., and Crossling, K., (2011). "Strengthening fire-damaged concrete by confinement with fibre-reinforced polymer wraps." *Engineering Structures,* 33(12), p. 3381-3391.
25. Bischoff, P.H. and Perry, S.H., (1995). "Impact behaviour of plain concrete loaded in uniaxial compression." *Journal of Engineering Mechanics, ASCE,* 121, p. 685-693.
26. Bullo, S., (2003). "Experimental study of the effects of the ultimate strain of fiber reinforced plastic jackets on the behavior of confined concrete." *Proceedings of the International Conference of Composites in Construction*, Cosenza, Italy.
27. Campione, G., Miraglia, N., and Scibilia, N., (2001). "Compressive behaviour of RC members strengthened with carbon fibre reinforced plastic layers." *Advances in Earthquake Engineering,* 9, p. 397-406.
28. Candappa, D.C., Sanjayan, J.G., and Setunge, S., (2001). "Complete triaxial stress-strain curves of high-strength concrete." *Journal of Materials in Civil Engineering,* 13(3), p. 209-215.
29. Carey, S.A. and Harries, K.A., (2005). "Axial behavior and modeling of confined small-, medium-, and large-scale circular sections with carbon fiber-reinforced polymer jackets." *ACI Structural Journal,* 102(4), p. 596-604.
30. Carrasquillo, R.L., Nilson, A.H., and Slate, F.O., (1981). "Properties of high strength concrete subject to short-term loads." *ACI Journal,* 78, p. 171-177.
31. Chikh, N., Benzaid, R., and Mesbah, H., (2012). "An Experimental Investigation of Circular RC Columns with Various Slenderness Confined with CFRP Sheets." *Arabian Journal for Science and Engineering,* 37(2), p. 315-323.
32. Cui, C. and Sheikh, S.A., (2010). "Experimental Study of Normal- and High-Strength Concrete Confined with Fiber-Reinforced Polymers." *Journal of Composites for Construction,* 14(5), p. 553-561.
33. Dahl, K.K.B., (1992). "Uniaxial Stress-Strain Curves for Normal and High-Strength Concrete." *ABK Report No. R282*, Department of Structural Engineering, Technical University of Denmark.

34. Dahl, H. and Brincker, R., (1989). "Fracture Energy of High-Strength Concrete in Compression." Institute of Building Technology Structural Engineering, Aalborg University Center.
35. De Stefano, A. and Sabia, D., (1991). "Effetti della cerchiatura elicoidale sui comportamento meccanico di cilindri di calcestruzzo ad alta resistenza." Atti del Dipartimento di Ingegneria Strutturale, Politecnico di Torino, Levrotto e Bella.
36. Demers, M. and Neale, K.W., (1994). "Strengthening of concrete columns with unidirectional composite sheets." *Proceedings of Developments in Short and Medium Span Bridge Engineering*, Montreal, Que.
37. Desnerck, P., Schutter, G.D., and Taerwe, L., (2012). "Stress-strain behaviour of self-compacting concrete containing limestone fillers." *Structural Concrete,* 13(2), p. 95-101.
38. Elsanadedy, H.M., Al-Salloum, Y.A., Alsayed, S.H., and Iqbal, R.A., (2012). "Experimental and numerical investigation of size effects in FRP-wrapped concrete columns." *Construction and Building Materials,* 29, p. 56-72.
39. Erdil, B., Akyuz, U., and Yaman, I.O., (2012). "Mechanical behavior of CFRP confined low strength concretes subjected to simultaneous heating-cooling cycles and sustained loading." *Materials and Structures,* 45(1-2), p. 223-233.
40. Galeota, l., (1988). "Legame costitutivo di calcestruzzi confinati normali a leggeri, sottoposti a compressione assiale." *Seminario A.I.C.A.P. sui Calcestruzzi Speciali*, L'Aquila, Italy.
41. Galeota, D., Giammateo, M.M., and Grillo, F., (1984). "Calestruzzi leggeri e normali - Legame costitutivo per elementi non confinati sottoposti a carico assiale monotono." *Giorn. Genio Civile,* 10(11-12), p. 387-400.
42. Gardner, N.J., (1969). "Triaxial behavior of concrete." *Journal of the American Concrete Institute,* 66(2), p. 136-146.
43. Güler, K., Demir, F., and Pakdamar, F., (2012). "Stress-strain modelling of high strength concrete by fuzzy logic approach." *Construction and Building Materials* 37, p. 680-684.
44. Hadi, M.N.S. and Li, J., (2004). "External reinforcement of high strength concrete columns." *Composite Structures,* 65(3-4), p. 279–287.
45. Harries, K.A. and Carey, S.A., (2003). "Shape and "gap" effects on the behavior of variably confined concrete." *Cement and Concrete Research,* 33(6), p. 881-890.
46. Harries, K.A. and Kharel, G., (2002). "Behavior and modeling of concrete subject to variable confining pressure." *ACI Materials Journal,* 99(2), p. 180-189.
47. Hognestad, E., Hanson, N.W., and McHenry, D., (1955). "Concrete stress distribution in ultimate strength design." *ACI Journal Proceedings* 52(4), p. 455-480.
48. Hosotani, K., Kawashima, K., and Hoshikuma, J. , (1997). "A model for confinement effect for concrete cylinders confined by carbon fiber sheets." *NCEER-INCEDE Workshop on Earthquake Engineering Frontiers of Transportation Facilities*, State University of New York, Buffalo, New York.
49. Hsu, L.S. and Hsu, C.T., (1994). "Complete stress-strain behaviour of high-strength concrete under compression." *Magazine of Concrete Research,* 46(169), p. 301-312.
50. Hurlbut, B., (1985). "Experimental and computational investigation of strain-softening in concrete." PhD Dissertation, University of Colorado.
51. Ilki, A., Kumbasar, N., and Koc, V., (2004). "Low strength concrete members externally confined with FRP sheets." *Structural Engineering and Mechanics,* 18(2), p. 167-194.
52. Imran, I. and Pantazopoulou, S.J., (1996). "Experimental study of plain concrete under triaxial stress." *ACI Materials Journal,* 93(6), p. 589-601.
53. Iravani, S., (1996). "Mechanical properties of high-performance concrete." *ACI Materials Journal,* 93(5), p. 416-425.
54. Iyengar, S.R., Desayi, P., and Reddy, K.N., (1970). "Stress-strain characteristics of concrete confined in steel binders." *Magazine of Concrete Research,* 22(72), p. 173-184.
55. Jamet, P., Millard, A., and Nahas, G., (1984). "Triaxial behaviour of a micro-concrete complete stress-strain curves for confining pressures ranging from 0 to 100 MPa." *RILEM-CEB International Conference on Concrete Under Multiaxial Conditions*, INSA Toulouse, France. p. 133-140.
56. Jansen, D.C. and Shah, S.P., (1997). "Effect of length on compressive strain softening of concrete." *Journal of Engineering Mechanics,* 123(1), p. 25-35.
57. Jansen, D.C., Shah, S., and Rossow, E., C., (1995). "Stress-strain results of concrete from circumferential strain feedback control testing." *ACI Material journal,* 92(4), p. 419-428.
58. Jensen, V.P., (1943). "The Plasticity Ratio of Concrete and It's Effect on the Ultimate Strength of Beamse." *ACI Journal Proceedings,* 39, p. 565-584.
59. Jiang, T. and Teng, J.G., (2007). "Analysis-oriented stress-strain models for FRP-confined concrete." *Engineering Structures,* 29(11), p. 2968-2986.
60. Kaar, P.H., Hanson, N.W., and Capell, H.T., (1977). "Stress-strain characteristic of high strength concrete." *Research and Development Bulletin RD051-01D*, Portland Cement Association, Skokie, Illinois.
61. Karabinis, A.I. and Rousakis, T.C., (2002). "Concrete confined by FRP material: a plasticity approach." *Engineering Structures,* 24(7), p. 923-932.
62. Karam, G.N. and Tabbara, M., (2004). "Corner effects in CFRP wrapped square columns." *Magazine of Concrete Research,* 56(8), p. 461-464.
63. Kawashima, K., Hosotani, M., and Hoshikuma, J., (1997). "A model for confinement effect for concrete cylinders confined by carbon fiber sheets." *NCEER-INCEDE Workshop on Earthquake Engineering Frontiers of Transportation Facilities*, State University of New York, Buffalo, New York.
64. Kayali, O., Haque, M.N., and Zhu, B., (2003). "Some characteristics of high strength fiber reinforced lightweight aggregate concrete." *Cement and Concrete Composites,* 25(2), p. 207-213.
65. König, G., Simsch, G., and Ulmer, M., (1994). "Strain Softening of Concrete." *Report*, Technical University of Darmstadt. p. 67.
66. Kotsovos, M.D. and Newman, J.B., (1978). "Generalized stress-strain relations for concrete." *Journal of the Engineering Mechanics Division, ASCE,* 104(4), p. 845-856.

67. Kshirsagar, S., Lopez-Anido, R.A., and Gupta, R.K., (2000). "Environmental aging of fiber-reinforced polymer-wrapped concrete cylinders." *ACI Materials Journal,* 97(6), p. 703-712.
68. Lahlou, K., Aitcin, P.C., and Chaallal, O., (1992). "Behaviour of High-strength Concrete Under Confined Stresses." *Cement and Concrete Composites,* 14(3), p. 185-193.
69. Lam, L. and Teng, J.G., (2004). "Ultimate condition of fiber reinforced polymer-confined concrete." *Journal of Composites for Construction, ASCE,* 8(6), p. 539-548.
70. Lam, L., Teng, J.G., Cheung, C.H., and Xiao, Y., (2006). "FRP-confined concrete under axial cyclic compression." *Cement and Concrete Composites,* 28(10), p. 949-958.
71. Lee, I., (2002). "Complete stress-strain characteristics of high performance concrete." *Department of civil and environmental engineering*, New Jersey Institute of Technology, Newark, NJ, USA.
72. Lee, J.Y., Yi, C.K., Jeong, H.S., Kim, S.W., and Kim, J.K., (2010). "Compressive Response of Concrete Confined with Steel Spirals and FRP Composites." *Journal of Composite Materials,* 44(4), p. 481-504.
73. Li, Y., Yan, X., and Ou, J.P., (2007). "Compressive behavior and nonlinear analysis of selfsensing concrete-filled frp tubes and frp-steel composite tubes." *Proceedings of the 8th international symposium on fiber reinforced polymer reinforcement for concrete structures*, Patras, Greece.
74. Li, G.Q., Pang, S.S., and Ibekwe, S.I., (2011). "FRP tube encased rubberized concrete cylinders." *Materials and Structures,* 44(1), p. 233-243.
75. Liang, M., Wu, Z.M., Ueda, T., Zheng, J.J., and Akogbe, R., (2012). "Experiment and modeling on axial behavior of carbon fiber reinforced polymer confined concrete cylinders with different sizes." *Journal of Reinforced Plastics and Composites,* 31(6), p. 389-403.
76. Lim, J.C. and Ozbakkaloglu, T., (2013). "Influence of silica fume on stress-strain behavior of FRP-confined HSC." *Proceedings of the 4th Asia-Pacific Conference on FRP in Structures*, Melbourne, Australia.
77. Lu, X.B. and Hsu, C.T.T., (2007). "Stress-strain relations of high-strength concrete under triaxial compression." *Journal of Materials in Civil Engineering,* 19(3), p. 261-268.
78. Mandal, S. and Fam, A., (2004). "Axial loading tests on FRP confined concrete of different compressive strengths." *Proceedings of the 4th International Conference of Advanced Composite Materials in Bridges and Structures*, Calgary, Alberta.
79. Mansur, M.A., Chin, M.S., and Wee, T.H., (1999). "Stress-strain relationship of confined high-strength plain and fiber concrete - Closure." *Journal of Materials in Civil Engineering,* 11(4), p. 364-364.
80. Matthys, S., Taerwe, L., and Audenaert, K., (1999). "Tests on axially loaded concrete columns confined by fiber reinforced polymer sheet wrapping." *ACI Special Publications 188*, p. 217-228.
81. Micelli, F., Myers, J.J., and Murthy, S., (2001). "Effect of environmental cycles on concrete cylinders confined with FRP." *Composites in Construction*, ed. J. Figueiras, L. Juvanders, and R. Faria. 317-322.
82. Mirmiran, A., (1996). "Analytical and experimental investigation of reinforced concrete columns encased in fibre glass tubular jackets and use of fiber jacket for pile splicing." *Final Report, Contract no. B-9135*, Florida Department of Transport, Tallahassee, FL.
83. Miyauchi, K., Nishibayashi, S., and Inoue, S., (1997). "Estimation of strengthening effects with carbon fiber sheet for concrete column." *Proceedings of the 3rd International Symposium of Non-Metallic Reinforcement for Concrete Structures*.
84. Miyauchi, K., Inoue, S., Kuroda, T., and Kobayashi, A., (1999). "Strengthening effects with carbon fiber sheet for concrete column." *Proceedings of Japan Concrete Institution*.
85. Moral, H., (1979). "Effects of the structure of binding cement paste on the inelastic behaviour of concrete and mortars under short-term compressive loading." M.S. Thesis, *Faculty of Civil Engineering*, Istanbul Technical University, Istanbul, Turkey.
86. Nakamura, H. and Higai, T., (2001). "Compressive fracture energy and fracture zone length of concrete." *Modeling of inelastic behavior of RC structures under seismic loads*.
87. Newman, J.B., (1979). "Concrete under complex stress." London, UK, Department of Civil Engineering, Imperial College of Science and Technology, London, UK.
88. Nilson, H. and Slate, O., (1979). "Structural design properties of very high strength concrete." *Second Progress Report, NSF Grant ENG 7805124*, School of Civil and Environ Environmental Engineering, Cornell University, Ithaca, NY.
89. Oktar, O.N., (1977). "Role of structure of binding cement paste on the inelastic behaviour of concrete under short-term compressive loading." Ph.D. Thesis, *Faculty of Civil Engineering*, Istanbul Technical University, Istanbul, Turkey.
90. Osorio, E., Bairán, J.M., and Marí, A.R., (2013). "Lateral behavior of concrete under uniaxial compressive cyclic loading." *Materials and Structures,* 46(5), p. 709-724.
91. Park, R. and Paulay, T., (1975). "Reinforced Concrete Structures." Department of Civil Engineering, University of Canterbury, Canterbury, New Zealand. p. 11-43.
92. Ramaley, D. and McHenry, D., (1947). "Stress-Strain Curves for Concrete Strained Beyond Ultimate Load." *Laboratory Report No. SP-12*, U.S. Bureau of Reclamation, Denver. p. 23.
93. Richart, F.E. and Jensen, V.P., (1931). "Tests of Plain and Reinforced Concrete Made with Haydite Aggregates." *Bulletin 237, University of Illinois Experiment Station*, p. 7-79.
94. Richart, F.E., Brandtzaeg, A., and Brown, R.L., (1928). "A study of the failure of concrete under combined compressive stresses." *Bulletin No. 185*, Engineering Experimental Station, University of Illinois, Champaign, Illinois.
95. Richart, F.E., Brandtzaeg, A., and Brown, R.L., (1929). "The failure of plain and spirally reinforced concrete in compression." *Bulletin No.190*, Engineering Experiment Station, University of Illinois, Urbana, USA.
96. Rokugo, K. and Koyanagi, W., (1992). " Role of compressive fracture energy of concrete on the failure behaviour of reinforced concrete beams." *Applications of fracture mechanics to reinforced concrete*, p. 437-464.
97. Rousakis, T., (2001). "Experimental investigation of concrete cylinders confined by carbon FRP sheets under monotonic and cyclic axial compressive load." Masters, *Department of Civil Engineering*, Demokritus University of Thrace, Greece.
98. Rousakis, T., You, C., De Lorenzis, L., and Tamuzs, V., (2003). "Concrete cylinders confined by carbon FRP sheets subjected to monotonic and cyclic axial compressive loads." *Proceedings of the 6th International Symposium on FRP Reinforcement for Concrete Structures*.

99. Saafi, M., Toutanji, H.A., and Li, Z.J., (1999). "Behavior of concrete columns confined with fiber reinforced polymer tubes." *Aci Materials Journal,* 96(4), p. 500-509.
100. Sangha, C.M., (1972). "Strength, Deformation and Fracture Properties of Rock and Concrete." Phd thesis, *Department of Civil Engineering*, University of Dundee, Nethergate, Dundee, United Kingdom.
101. Scott, B.D., Park, R., and Priestley, M.J.N., (1982). "Stress-strain behavior of concrete confined by overlapping hoop at low and high strain rates." *ACI Journal Proceedings,* 79(1), p. 13-27.
102. Saenz, L.P., (1964). "Discussion of a paper by P. Desayi and S. Krishnan - Equation for the stress strain curve of concrete." *ACI Journal,* 61(9), p. 1229-1235.
103. Seffo, M. and Hamcho, M., (2012). "Strength of Concrete Cylinder Confined by Composite Materials (CFRP)." *Energy Procedia,* 19, p. 276–285.
104. Sfer, D., Carol, I., Gettu, R., and Etse, G., (2002). "Study of the behavior of concrete under triaxial compression." *Journal of Engineering Mechanics,* 128(2), p. 156-163.
105. Shah, S.P. and Ahmad, S.H., (1985). "Structural properties of high strength concrete and its implication for precast pre-stressed concrete." *PCI Journal,* 30(6), p. 92-119.
106. Shah, S.P. and Sankar, R., (1987). "Internal cracking and strain softening response of concrete under uniaxial compression." *ACI Materials Journal,* 84(3), p. 200-212.
107. Shah, S.P., Naaman, A.E., and Moreno, J., (1983). "Effect of confinement on the ductility of lightweight concrete." *International Journal of Cement Composites and Lightweight Concrete,* 5(1), p. 15-25.
108. Shahawy, M., Mirmiran, A., and Beitelman, T., (2000). "Tests and modeling of carbon-wrapped concrete columns." *Composites Part B-Engineering,* 31(6-7), p. 471-480.
109. Shehata, I., Carneiro, L.A.V., and Shehata, L.C.D., (2002). "Strength of short concrete columns confined with CFRP sheets." *Materials and Structures,* 35(245), p. 50-58.
110. Shehata, I.A.E.M., Carneiro, L.A.V., and Shehata, L.C.D., (2007). "Strength of confined short concrete columns." *Proceedings of the 8th International Symposium on Fiber Reinforced Polymer Reinforcement for Concrete Structures*, University of Patras, Patras, Greece.
111. Silva, M.A.G. and Rodrigues, C.C., (2006). "Size and relative stiffness effects on compressive failure of concrete columns wrapped with glass FRP." *Journal of Materials in Civil Engineering,* 18(3), p. 334-342.
112. Slate, F.O., Nilson, A.H., and Martinez, S., (1986). "Mechanical properties of high-strength lightweight concrete." *ACI Journal Proceedings,* 83(4), p. 606–613.
113. Smeplass, S., (1992). "High Strength Concrete: Mechanical Properties - Normal Density Concretes." *SPC Materials Design, Report 4.4, SINTEF*, Trondheim, Norway.
114. Smith, G.M. and Young, L.E., (1956). "Ultimate flexural analysis based on stress-strain curves of cylinders." *ACI Journal Proceedings,* 53(6), p. 597-609.
115. Smith, S.S., Willam, K.J., Gerstle, K.H., and Sture, S., (1989). "Concrete Over The Top, Or: Is There Life After Peak?" *ACI Materials Journal,* 86(5), p. 491-497.
116. Taerwe, L.R., (1992). "Influence of steel fibers on strain-softening of high-strength concrete." *ACI Materials Journal,* 89(1), p. 54-60.
117. Tamuzs, V., Valdmanis, V., Tepfers, R., and Gylltoft, K., (2008). "Stability analysis of CFRP-wrapped concrete columns strengthened with external longitudinal CFRP sheets." *Mechanics of Composite Materials,* 44(3), p. 199-208.
118. Tan, K.H. and Sun, X., (2006). "Failure criteria of concrete under triaxial compression." *ACI Special Publication,* 238.
119. Tasdemir, M.A., (1982). "Elastic and inelastic behaviour of structural lightweight aggregate concretes." Ph.D. Thesis, *Faculty of Civil Engineering*, Istanbul Technical University, Istanbul, Turkey.
120. Tasnimi, A.A., (2004). "Mathematical model for complete stress–strain curve prediction of normal, light-weight and high-strength concretes." *Magazine of concrete research,* 56(1), p. 23-34.
121. Teng, J.G., Yu, T., Wong, Y.L., and Dong, S.L., (2007). "Hybrid FRP-concrete-steel tubular columns: Concept and behavior." *Construction and Building Materials,* 21(4), p. 846-854.
122. Tulin, L.G. and Gerstle, K.H., (1964). "Discussion of "Equation for the Stress-Strain Curve of Concrete" by Prakash Desayi and S. Krishnan." *ACI Journal Proceedings,* 61(9), p. 1236-1238.
123. Valdmanis, V., De Lorenzis, L., Rousakis, T., and Tepfers, R., (2007). "Behaviour and capacity of CFRP-confined concrete cylinders subjected to monotonic and cyclic axial compressive load." *Structural Concrete,* 8(4), p. 187-200.
124. Vu, X.H., Malecot, Y., Daudeville, L., and Buzaud, E., (2009). "Experimental analysis of concrete behavior under high confinement: Effect of the saturation ratio." *International Journal of Solids and Structures,* 46(5), p. 1105-1120.
125. Wang, L.M. and Wu, Y.F., (2008). "Effect of corner radius on the performance of CFRP-confined square concrete columns: Test." *Engineering Structures,* 30(2), p. 493-505.
126. Wang, Y.F. and Wu, H.L., (2011). "Size effect of concrete short columns confined with aramid FRP jackets." *Journal of Composites for Construction,* 15(4), p. 535-544.
127. Wang, P.T., Shah, S.P., and Naaman, A.E., (1978). "Stress-strain curves of normal and lightweight concrete in compression." *ACI Journal Proceedings,* 75(11), p. 603-611.
128. Watanabe, F., (1972). "Mechanical behaviour of materials." *Proceeding of the international conference on mechanical behaviour of materials*. p. 153 – 161.
129. Watanabe, K., Nakamura, R., Honda, Y., Toyoshima, M., Iso, M., Fujimaki, T., Kaneto, M., and Shirai, N., (1997). "Confinement effect of FRP sheet on strength and ductility of concrete cylinders under uniaxial compression." *Proceedings of the Non-metallic Reinforcement for Concrete Structures, Japan Concrete Institute*.
130. Watanabe, K., Niwa, J., Yokota, H., and Iwanami, M., (2004). "Experimental study on stress-strain curve of concrete considering localized failure in compression." *Journal of Advanced Concrete Technology,* 2(3), p. 395-407.
131. Watstein, D., (1953). "Effect of straining rate on the compressive strength and elastic properties of concrete." *ACI Journal Proceedings,* 49(4).

132. Wee, T.H., Chin, M.S., and Mansur, M.A., (1996). "Stress-strain relationship of high-strength concrete in compression." *Journal of Materials in civil Engineering,* 8(2), p. 70-76.
133. Wischers, G., (1979). "Application and Effects of Compressive Loads on Concrete." *Betonverlag GmbH, Dfisseldorf*, p. 31-56.
134. Wong, Y.L., Yu, T., Teng, J.G., and Dong, S.L., (2008). "Behavior of FRP-confined concrete in annular section columns." *Composites Part B-Engineering,* 39(3), p. 451-466.
135. Wu, G., Wu, Z.S., Lu, Z.T., and Ando, Y.B., (2008). "Structural performance of concrete confined with hybrid FRP composites." *Journal of Reinforced Plastics and Composites,* 27(12), p. 1323-1348.
136. Wu, H.L., Wang, Y.F., Yu, L., and Li, X.R., (2009). "Experimental and Computational Studies on High-Strength Concrete Circular Columns Confined by Aramid Fiber-Reinforced Polymer Sheets." *Journal of Composites for Construction,* 13(2), p. 125-134.
137. Xiao, Q.G., Teng, J.G., and Yu, T., (2010). "Behavior and Modeling of Confined High-Strength Concrete." *Journal of Composites for Construction, ASCE,* 14(3), p. 249-259.
138. Xie, J., Elwi, A.E., and Macgregor, J.G., (1995). "Mechanical-properties of high-strength concretes containing silica fume." *ACI Materials Journal,* 92(2), p. 135-145.
139. Yan, Z.H., Pantelides, C.P., and Reaveley, L.D., (2006). "Fiber-reinforced polymer jacketed and shape-modified compression members: I - Experimental behavior." *ACI Structural Journal,* 103(6), p. 885-893.
140. Youssef, M.N., Feng, M.Q., and Mosallam, A.S., (2007). "Stress-strain model for concrete confined by FRP composites." *Composites Part B-Engineering,* 38(5-6), p. 614-628.
141. Cui, H.Z., Lo, T.Y., Memon, S.A., Xing, F., and Shi, X., (2012). "Experimental investigation and development of analytical model for pre-peak stress-strain curve of structural lightweight aggregate concrete." *Construction and Building Materials,* 36, p. 845-859.
142. Shannag, M.J., (2011). "Characteristics of lightweight concrete containing mineral admixtures." *Construction and Building Materials,* 25(2), p. 658-662.
143. Smeplass, S., (1992). "High Strength Concrete: Mechanical Properties - Iwa Concretes." *SPC Materials Design, Report 4.5., SINTEF*, Trondheim, Norway.
144. Yildirim, H., (1989). "Effects of composition on the mechani behaviour of semi-lightweight concretes under cyclic loading conditions." M.S. Thesis, *Faculty of Civil Engineering*, Istanbul Technical University, Istanbul, Turkey.
145. Zhang, M.H. and Gjorv, O.E., (1991). "Mechanical properties of high-strength lightweight concrete." *ACI Materials Journal,* 88(3), p. 240-247.
146. Carrazedo, R., (2002). "Mechanisms of confinement and its implication in strengthening of concrete columns with FRP jacketing." PhD dissertation, University of São Paulo.
147. Chaallal, O., Shahawy, M., and Hassan, M., (2003). "Performance of axially loaded short rectangular columns strengthened with carbon fiber-reinforced polymer wrapping." *Journal of Composites for Construction,* 7(3), p. 200-208.
148. Dilger, W.H., Koch, R., and Kowalczyk, R., (1984). "Ductility of plain and confined concrete under different strain rates." *ACI Journal Proceedings,* 81(1), p. 73-81.
149. Haneef, T.K., Kumari, K., Mukhopadhyay, C.K., Rao, B., and Jayakumar, T., (2013). "Influence of fly ash and curing on cracking behavior of concrete by acoustic emission technique." *Construction and Building Materials,* 44, p. 342 -350.
150. Ilki, A. and Kumbasar, N., (2003). "Compressive behaviour of carbon fibre composite jacketed concrete with circular and non-circular cross-sections." *Journal of Earthquake Engineering,* 7(3), p. 381-406.
151. Markeset, G. and Hillerborg, A., (1995). "Softening of concrete in compression-localization and size effects." *Cement and Concrete Research,* 25(4), p. 702-708.
152. Masia, M.J., Gale, T.N., and Shrive, N.G., (2004). "Size effects in axially loaded square-section concrete prisms strengthened using carbon fibre reinforced polymer wrapping." *Canadian Journal of Civil Engineering,* 31(1), p. 1-13.
153. Modarelli, R., Micelli, F., and Manni, O., (2005). "FRP-confinement of hollow concrete cylinders and prisms." *Proceedings of the 7th International Symposium on Fiber Reinforced Polymer Reinforcement of Reinforced Concrete Structures*.
154. Ozbakkaloglu, T. and Oehlers, D.J., (2008). "Concrete-filled square and rectangular FRP tubes under axial compression." *Journal of Composites for Construction,* 12(4), p. 469-477.
155. Rousakis, T.C., Karabinis, A.I., and Kiousis, P.D., (2007). "FRP-confined concrete members: Axial compression experiments and plasticity modelling." *Engineering Structures,* 29(7), p. 1343-1353.
156. Rousakis, T.C., Rakitzis, T.D., and Karabinis, A.I., (2012). "Design-Oriented Strength Model for FRP-Confined Concrete Members." *Journal of Composites for Construction,* 16(6), p. 615-625.
157. Van Gee, H.J.G.M., (1994). "Uniaxial Strain Softening of Concrete - Influence of Specimen Size and Boundary Shear." *Report BKO94.09*, Eindhoven University of Technology. p. 34.
158. Van Vliet, M.R.A. and Van Mier, J.G.M., (1995). "Strain-Softening Behaviour of Concrete in Uniaxial Compression." *Report no. 25.5-95-9*, Department of Civil Engineering, Delft University of Technology. p. 87.
159. Vonk, R., (1992). "Softening of concrete loaded in compression." PhD thesis, *Eindhoven University of Technology*, he Netherlands.
160. Wang, Y.F. and Wu, H.L., (2010). "Experimental investigation on square high-strength concrete short columns confined with AFRP sheets." *Journal of Composites for Construction,* 14(3), p. 346-351.
161. Wang, Y.W., Pu, X.C., and Wang, Z.J., (2006). "A Numerical Stress-strain Response Model of All Grades of Concretes under Uniaxial Compression." *Journal of Wuhan University of Technology-Materials Science Edition,* 21(3), p. 149-152.
162. Aïtcin, P.C. and Mehta, P.K., (1990). "Effect of coarse aggregate characteristics on mechanical properties of high-strength concrete." *ACI Materials Journal, 87(2).* 87(2), p. 103-107.
163. Baalbaki, W., Benmokrane, B., and Chaallal, O.A., P. C., (1991). "Influence of coarse aggregate on elastic properties of high-performance concrete." *ACI Materials Journal,* 88(5), p. 499-503.
164. Baalbaki, W., Aicin, P.C., and Ballivy, G., (1992). "On Predicting Modulus of Elasticity inHigh-Strength Concrete." *On Predicting Modulus of Elasticity inHigh-Strength Concrete,* 89(5), p. 517-520.
165. Bower, J.E. and Viest, I.M., (1960). "Shear strength of restrained concrete beams without web reinforcement." *ACI Journal Proceedings,* 57(7), p. 73-98.

166. Cetin, A. and Carrasquillo, R.L., (1998). "High-performance concrete: Influence of coarse aggregates on mechanical properties." *ACI Materials Journal,* 95(3), p. 252-259.
167. de Larrard, F. and Belloc, A., (1997). "The influence of aggregate on the compressive strength of normal and high-strength concrete." *ACI materials journal,* 94(5), p. 417-425.
168. Gabet, T., Malecot, Y., and Daudeville, L., (2008). "Triaxial behaviour of concrete under high stresses: Influence of the loading path on compaction and limit states." *Cement and Concrete Research,* 38(3), p. 403-412.
169. Gesoğlu, M., Güneyisi, E., and Özturan, T., (2002). "Effects of end conditions on compressive strength and static elastic modulus of very high strength concrete." *Cement and Concrete Research,* 32(10), p. 1545-1550.
170. Giaccio, G., Rocco, C., Violini, D., Zappitelli, J., and Zerbino, R., (1992). "High-strength concretes incorporating different coarse aggregates." *ACI Materials Journal,* 89(3), p. 242-246.
171. Hammons, M.I. and Neeley, B.D., (1993). "Triaxial characterization of high-strength Portland cement concrete." *Transportation Research Record,* (1382), p. 73-77.
172. Han, S.H. and Kim, J.K., (2004). "Effect of temperature and age on the relationship between dynamic and static elastic modulus of concrete." *Cement and Concrete Research,* 34(7), p. 1219-1227.
173. Hansen, T.C. and Boegh, E., (1985). "Elasticity and Drying Shrinkage Concrete of Recycled-Aggregate." *ACI Journal Proceedings,* 82(5), p. 648-652.
174. Hognestad, E., (1951). "A study of combined bending and axial load in reinforced concrete members." *Bulletin No. 399, University of Illinois, Engineering Experimental Station, Champaign*.
175. Hossain, A.K.M., (2004). "Properties of volcanic pumice based cement and lightweight concrete." *Cement and Concrete Research,* 34(2), p. 283-291.
176. Kim, J.K., Han, S.H., and Song, Y.C., (2002). "Effect of temperature and aging on the mechanical properties of concrete: Part I. Experimental results." *Cement and Concrete research,* 32(7), p. 1087-1094.
177. Klieger, P., (1957). "Long-Time Study of Cement Performance in Concrete Chapter 10-Progress Report on Strength and Elastic Properties of Concrete." *ACI Journal Proceedings,* 54(12), p. 481-507.
178. Kluge, R.W., Sparks, M.M., and Tuma, E.C., (1949). "Lightweight aggregate concrete." *ACI Journal Proceedings,* 45(5), p. 625-642.
179. Martinez, S. and Nilson, A.H., (1984). "Spirally reinforced high-strength concrete columns." *ACI Journal Proceedings,* 81(5), p. 431-442.
180. Mesbah, H.A., Lachemi, M., and Aitcin, P.C., (2002). "Determination of elastic properties of high-performance concrete at early ages." *ACI Materials Journal,* 99(1), p. 37-41.
181. Mostofinejad, D. and Nozhati, M., (2005). "Prediction of the modulus of elasticity of high strength concrete." *Iranian Journal of Science & Technology, Transaction B, Engineering,* 29(B3), p. 311-321.
182. Nassif, H.H., Najm, H., and Suksawang, N., (2005). "Effect of pozzolanic materials and curing methods on the elastic modulus of HPC." *Cement and Concrete Composites,* 27(6), p. 661-670.
183. Oluokun, F.A., Burdette, E.G., and Deatherage, J.H., (1991). "Elastic modulus, Poisson's ratio, and compressive strength relationships at early ages." *ACI materials journal,* 88(1), p. 3-10.
184. Ozturan, T., (1984). "An investigation of concrete abrasion as two phase material." PhD thesis, *Faculty of Civil Engineering, I*, Istanbul Technical University, Istanbul.
185. Perenchio, W.F. and Klieger, P., (1978). "Some physical properties of high-strength concrete." *Portland Cement Association,* 56.
186. Powers, T.C., (1938). "Measuring Youngs modulus of elasticity by means of sonic vibrations." *Proceedings of the forty first annual meeting of the american society for testing materials,* 38(2), p. 460–470.
187. Richart, F.E., Draffin, J. O., & Olson, T. A., (1948). "Effect of eccentric loading, protective shells, slenderness ratios, and other variables in reinforced concrete columns." *Bulletin No. 368*, Engineering Experiment Station, University of Illinois, Urbana.
188. Rutland, C.A. and Wang, M.L., (1997). "The effects of confinement on the failureorientation in cementitiousmaterialsexperimentalobservations." *Cement and Concrete Composites,* 19(2), p. 149-160.
189. Shideler, J.J., (1957). "Lightweight-aggregate concrete for structural use." *ACI Journal Proceedings,* 54(10), p. 299-328.
190. Shkolnik, I.E., (2005). "Effect of nonlinear response of concrete on its elastic modulus and strength." *Cement and Concrete Composites,* 27(7), p. 747-757.
191. Shkolnik, I.E. and Aktan, H.M., (2003). "Nonlinear nondestructive methods for evaluating strength of concrete." *Proc of international symposium Non-Destructive Testing in Civil Engineering*
192. Turan, M. and Iren, M., (1997). "Strain stress relationship of concrete." *Journal of Engineering and Architecture, Faculty of Selcuk University,* 12(1), p. 76-81.
193. Wiegrink, K., Marikunte, S., and Shah, S.P., (1996). "Shrinkage cracking of high-strength concrete." *ACI Materials Journal,* 93(5), p. 409-415.
194. Yaman, I.O., Hearn, N., and Aktan, H.M., (2002). "Active and non-active porosity in concrete part I: experimental evidence." *Materials and Structures,* 35(2), p. 102-109.
195. Zhang, M.H. and Malhotra, V.M., (1995). "Characteristics of a thermally activated alumino-silicate pozzolanic material and its use in concrete." *Cement and Concrete Research,* 25(8), p. 1713-1725.
196. Balaguru, P. and Foden, A., (1996). "Properties of fiber reinforced structural lightweight concrete." *ACI Structural Journal,* 93, p. 1.
197. Chi, J.M., Huang, R., Yang, C.C., and Chang, J.J., (2003). "Effect of aggregate properties on the strength and stiffness of lightweight concrete." *Cement and Concrete Composites,* 25(2), p. 197-205.
198. Hanson, J.A., (1958). "Shear Strength of Lightweight Reinforced Concrete Beams." *ACI Journal Proceedings,* 55(9), p. 387-403.
199. Ke, Y., Beaucour, A.L., Ortola, S., Dumontet, H., and Cabrillac, R., (2009). "Influence of volume fraction and characteristics of lightweight aggregates on the mechanical properties of concrete." *Construction and Building Materials,* 23(8), p. 2821-2828.
200. Khayat, K.H., Bickley, J.A., and Hooton, R.D., (1995). "High-strength concrete properties derived from compressive strength values." *Cement, Concrete and Aggregates,* 17(2).
201. Price, W.H. and Cordon, W.A., (1949). "Tests of lightweight-aggregate concrete designed for monolithic construction." *ACI Journal Proceedings,* 45(4), p. 581-600.

202. Wilson, H.S. and Malhotra, V.M., (1988). "Development of high strength lightweight concrete for structural applications." *International Journal of Cement Composites and Lightweight Concrete,* 10(2), p. 79-90.
203. Yang, C.C. and Huang, R., (1998). "Approximate strength of lightweight aggregate using micromechanics method." *Advanced Cement Based Materials,* 7(3), p. 133-138.
204. Alexander, M.G. and Milne, T.I., (1995). "Influence of Cement Blend and Aggregate Type on the Stress-Strain Behavior and Elastic Modulus of Concrete." *ACI Materials Journal,* 92(3), p. 227-235.
205. Corinaldesi, V., (2010). "Mechanical and elastic behaviour of concretes made of recycled-concrete coarse aggregates." *Construction and Building Materials,* 24(9).
206. Persson, B., (2001). "A comparison between mechanical properties of self-compacting concrete and the corresponding properties of normal concrete." *Cement and Concrete Research,* 32(2), p. 193-198.
207. Shannag, M.J., (2000). "High strength concrete containing natural pozzolan and silica fume." *Cement and Concrete Composites,* 22(6), p. 399-406.
208. Topçu, İ.B. and Uygunoğlu, T., (2010). "Effect of aggregate type on properties of hardened self-consolidating lightweight concrete (SCLC)." *Construction and Building Materials,* 24(7), p. 1286-1295.
209. Haque, M.N., Al-Khaiat, H., and Kayali, O., (2004). "Strength and durability of lightweight concrete." *Cement and Concrete Composites,* 26(4), p. 307-314.

THIS PAGE HAS BEEN LEFT INTENTIONALLY BLANK

Statement of Authorship

Title of Paper	Influence of Size and Slenderness on Compressive Strain Softening of Confined and Unconfined Concrete
Publication Status	○ Published ○ Accepted for Publication ◉ Submitted for Publication ○ Publication Style
Publication Details	Journal of Materials in Civil Engineering, Manuscript MTENG-3153,Year 2014

Author Contributions

By signing the Statement of Authorship, each author certifies that their stated contribution to the publication is accurate and that permission is granted for the publication to be included in the candidate's thesis.

Name of Principal Author (Candidate)	Mr. Jian Chin Lim		
Contribution to the Paper	Preparation of experimental database, development of model, and preparation of manuscript		
Signature		Date	23/02/2015

Name of Co-Author	Dr. Togay Ozbakkaloglu		
Contribution to the Paper	Research supervision and review of manuscript		
Signature		Date	23/02/2015

THIS PAGE HAS BEEN LEFT INTENTIONALLY BLANK

INFLUENCE OF SIZE AND SLENDERNESS ON COMPRESSIVE STRAIN SOFTENING OF CONFINED AND UNCONFINED CONCRETE

Jian C. Lim and Togay Ozbakkaloglu

ABSTRACT

It is generally accepted that the post-peak strain softening behavior of concrete in compression is a localized phenomenon which occurs mainly in the compression damage zone. Accurate quantification of the size and slenderness effects on the post-peak behavior of concrete, therefore, depends on the accurate quantification of the inelastic deformations that occur in the compression damage zone. In this study, a novel approach is proposed to separate the two inelastic deformation components, known as the localized crack deformation and the deformation caused by the inelastic strain in the compression damage zone, from experimental stress-strain curves. This new approach allows the utilization of existing test results in the published literature in the model development. Based on two comprehensive experimental databases of confined and unconfined concretes covering a wide range of concrete strengths, a constitutive model for predicting the strain softening behavior of confined and unconfined concretes is proposed.

KEYWORDS: Concrete; Confinement; Stress-strain; Compression damage zone; Post-peak; Softening, Slenderness; Size effect; Deformation localization.

1. INTRODUCTION

It is well understood that deformability of concrete structures subjected to excessive loads depends heavily on the post-peak strain softening behavior of concrete (Bazant 1989; Vonk 1992). A number of existing studies reported that the post-peak strain softening of concrete is a localized phenomenon (Bazant 1989; Markeset and Hillerborg 1995; Jansen and Shah 1997). This implies that if this localization of concrete deformation can be quantified, the influence of specimen size and slenderness on the post-peak behavior of concrete can be determined. The localized zone in which the inelastic deformation occurs is referred to as the compression damage zone. Within the damage zone, the inelastic deformation can be separated into two components, including the localized crack deformation and the deformation caused by the inelastic strain (Markeset and Hillerborg 1995). Accurate quantification of these two inelastic components play an instrumental role in accounting for both the size and slenderness effects on the post-peak softening behavior of concrete. However, separating the two inelastic components from experimentally recorded stress-strain curves is no easy task. This paper presents a novel approach that was developed to separate the inelastic component of deformation from the total deformation. This new approach is applicable to confined and unconfined concretes of various strengths and geometries, and is therefore able to utilize the results in the comprehensive experimental test databases presented in Lim and Ozbakkaloglu (2014b; 2014c).

2. POST-PEAK BEHAVIOR OF CONCRETE

2.1 Compressive Damage Zone Concept

Figure 1 illustrates the compressive damage zone model proposed by Markeset and Hillerborg (1995). As illustrated in the figure, the model takes into account the elastic strain (ε_{ce}) that occurs along the entire specimen height (H), the inelastic strain (ε_d) that occurs in the compression damage zone (H_d), and the inelastic localized crack deformation (w) that occurs along the shear plane of the macrocrack. The combination of these three components results in the post-peak strain softening behavior commonly observed in the descending branches of stress-strain curves. It should be noted that the single shear-plane macrocrack illustrated in Figure 1 is only a hypothetical representation of a more random macrocrack formation typically observed in actual tests.

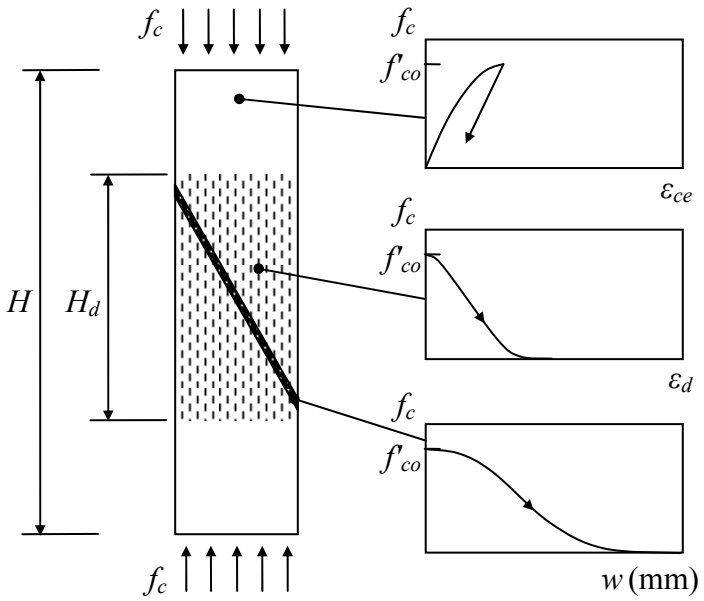

Figure 1. The compression damage zone model by Markeset and Hillerborg (1995)

2.2 Post-peak Axial Strain Adjustment to Allow for Specimen Size and Slenderness

A model describing the stress-strain relationship of concrete has recently been established by Lim and Ozbakkaloglu (2014c), based on two large test databases of unconfined and actively confined concretes previously reported in Lim and Ozbakkaloglu (2014b; 2014c). The model was developed on the basis of the results from the reference specimens with a 152 mm diameter and 305 mm height. To enable the application of the model in predicting the axial strains of specimens with sizes or slenderness ratios different than those of the reference specimen, an axial strain adjustments expression given in Eq. 1 was established in the present study. This expression accounts for the relative contributions of the elastic strain and the strains caused by two inelastic deformation components in determining the average axial strain ($\varepsilon_{c,h}$), and it was based on the concept originally proposed by Markeset and Hillerborg (1995). Through this adjustment, the axial strain of a specimen with a diameter (D) and height (H) different than those of the reference specimens of the proposed model (i.e., D_r = 152 mm, H_r = 305 mm) can be estimated as

$$\varepsilon_{c,h} = \frac{(f_c - f^*_{cc})}{E_c}\left(1 - \frac{H_r}{H}\right) + \varepsilon^*_{cc} + (\varepsilon_c - \varepsilon^*_{cc})\frac{H_r}{H} + \varepsilon_d \frac{(H_d - H_r)}{H} \quad \text{if} \quad \varepsilon_c > \varepsilon^*_{cc} \qquad (1)$$

In Eq. 1, $\varepsilon_{c,h}$ is the axial strain for a specimen of height H, E_c is the elastic modulus of concrete, f^*_{cc} is the peak compressive stress of concrete, ε^*_{cc} is the axial strain corresponding to the peak compressive stress, H_d is the height of compression damage zone, and ε_d is the inelastic strain in the damage zone.

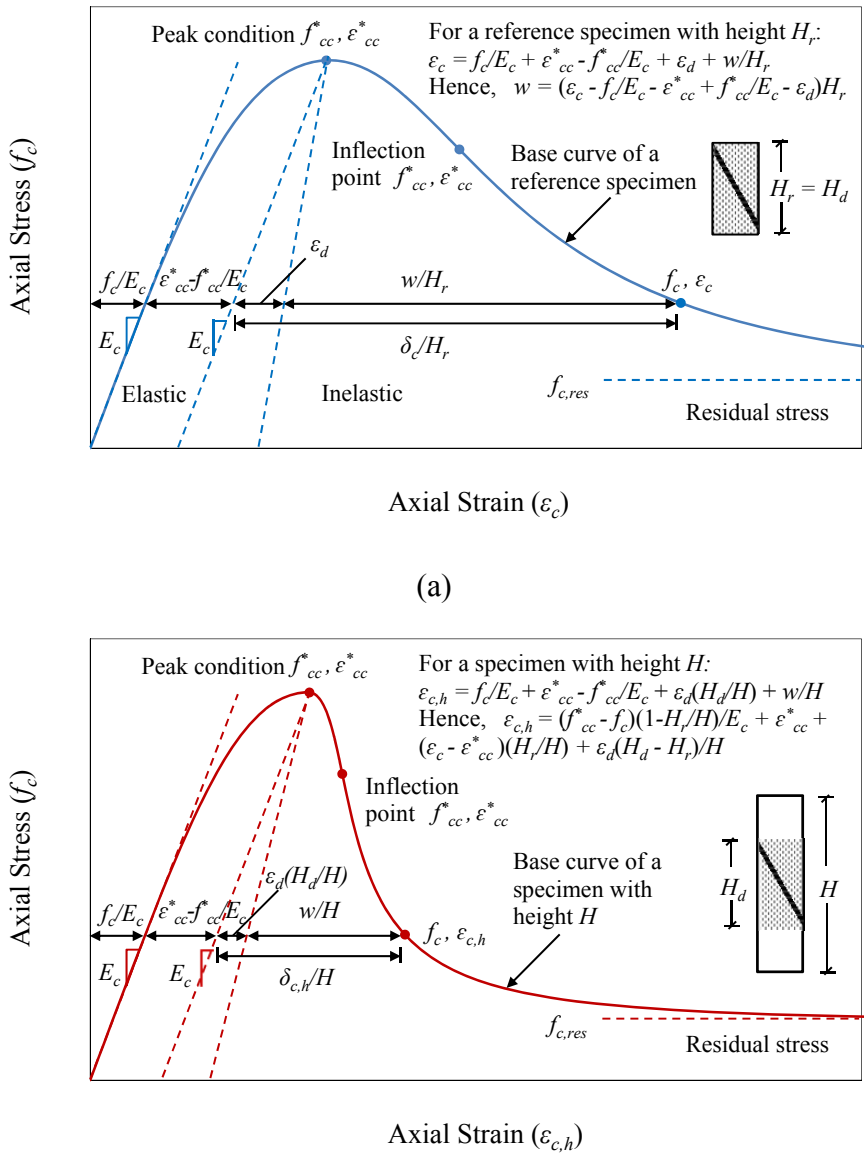

Figure 2. (a) Typical stress-strain curves of a reference specimen with height H_r; (b) adjusted stress-strain curve of a specimen with height H

To demonstrate the strain adjustment process, Figure 2(a) shows the stress-strain curve of a reference specimen (i.e., D_r = 152 mm, H_r = 305 mm), whereas Figure 2(b) shows the adjusted stress-strain curve of a specimen having different geometrical dimensions from those of the reference specimen. In a stress-strain curve, the formation of microcracks initiates when the path of the stress-strain curve deviates from the line defining the elastic modulus of concrete (E_c) to form a parabolic curve that connects the path to the peak condition. When the peak condition is reached, the formation of the shear plane of a macrocrack is complete and the subsequent inelastic deformations results in a post-peak strain softening phenomenon. As illustrated in Figure 2(a), after the peak condition is reached, a linear unloading path with a slope that is equal to the elastic modulus of concrete (E_c) is assumed for the elastic component of the axial strain, and the remaining strains are attributed to the inelastic

deformation ($\delta_{c,h}$) (Markeset and Hillerborg 1995). As shown in Figure 1, the inelastic deformation ($\delta_{c,h}$) consists of the deformation caused by the inelastic strain in damage zone (ε_d) and the localized crack deformation along the shear plane (w) (i.e., $\delta_{c,h} = \varepsilon_d H_d + w$). When the height of damage zone (H_d) is equal to the reference height (H_r), a typical stress-strain curve, as illustrated Figure 2(a), can be defined. For a slender specimen as illustrated in Figure 2(b), the damage zone (H_d) which depends on the specimen diameter (D) becomes a localized segment within the specimen height (H). In this case, the axial strain adjustment to account for the relative contributions of each elastic and inelastic component can be made using the approach illustrated in Figure 2(b). As shown in Figure 2(a), the localized deformation in shear plane can be rearranged as $w = (\varepsilon_c - f_c/E_c - \varepsilon^*_{cc} + f^*_{cc}/E_c - \varepsilon_d)H_r$. As this deformation component is independent of the specimen size, its substitution into the expression for the adjusted axial strain ($\varepsilon_{c,h}$), as shown in Figure 2(b), results in Eq. 1.

2.3 A New Approach to Separate Inelastic Strain in Damage Zone from Total Inelastic Deformation

The previous section illustrated the concept of strain adjustment introduced to relate the axial strain obtained from a reference specimen to that of another specimen with different geometrical dimensions. To complete this adjustment, quantifications of the damage zone height (H_d) and the inelastic strain in the damage zone (ε_d) are necessary. To this end, a novel approach that is used in the present study to separate and quantify the inelastic strain within the damage zone (ε_d) from an experimental stress-strain curve is presented in this section. Table 1 shows the details of the specimen groups used later in the paper to demonstrate the application of the proposed approach.

Table 1. Summary of test results used in Figures 3, 5-7, and 9

Group	Paper	Specimen	D (mm)	H (mm)	Coarse aggregate properties	f'_{co} (MPa)	f^*_l (MPa)
U22-107	Dahl (1992)	6	100	200	Crushed granite 4 to 16 mm	21.9 - 106.7	-
U27-87	Ahmad and Shah (1985)	6	76	152	Dolomitic limestone 12.7 mm	27.3 - 87.3	-
U28-30	Watanabe et al. (2004)	5	100	200 - 800	Crushed greywacke 13 and 20 mm	28.4 - 30.3	-
U43-60	Lim and Ozbakkaloglu (2014a)	1	63	127	Crushed bluestone 5 mm	51.6	-
	Rokugo and Koyanagi (1992)	1	84	170	Crushed stone 15 mm	46.4	-
	Jansen and Shah (1997)	1	100	200	Graded river pea gravel 9 mm	42.8	-
	Wischers (1979)	1	150	300	Gravel	49.3	-
U60	Xie et al. (1995)	11	55.5	110	Gravel 14 mm	60.2	0 - 29.3
U89-91	Jansen and Shah (1997)	5	100	200 - 550	Graded river pea gravel 9 mm	88.5 - 90.8	-
U119	Xie et al. (1995)	11	55.5	110	Gravel 14 mm	119.0	0 - 60.0
U123	Attard and Setunge (1996)	5	100	200	Crushed rhyodacite	123.0	1 - 20

2.3.1 Determining the height of the damage zone

Figure 3(a) shows the axial stress-strain curves of concrete specimens with the same diameter (D) but different heights (H). As can be seen from the curves of slender specimens with $H/D \geq 4.5$ in Figure 3(a), the snap-back phenomenon (Crisfield 1986) occurs in the descending branches of the stress-strain curves when the reversal of the elastic strain at post-peak condition exceeds the inelastic strain accumulated in the damage zone. Feedback-control testing method is commonly used to obtain these experimental curves (Jansen and Shah 1997). This method uses the inelastic deformation as a feedback signal, and therefore is able to provide a stable axial deformation measurement along the post-peak portion of the behavior.

To analyze the inelastic deformation that occurs in the damage zone, the approach illustrated in Figure 2 was used. Figure 3(b) shows the variation of the relative stress ratio (f_c/f'_{co}) with the inelastic deformation ($\delta_{c,h}$) of the specimen group. As illustrated in Figure 3(b), the inelastic deformations ($\delta_{c,h}$) of the specimens with different heights (H) are in close agreement. This accords with the findings of Bazant (1989) and Markeset and Hillerborg (1995) that the post-peak inelastic deformation ($\delta_{c,h}$) is in fact a localized phenomenon that occurs in the compressive damage zone (H_d) regardless of the total specimen height (H). The height of this localized damage zone (H_d), established based on the minimum specimen height of the observed group, is no greater than twice the specimen diameter (i.e., $H_d \leq 2D$). A review of previous studies that investigated specimens with heights less than $2D$ indicates that the effect of the frictional resistance supplied by the loading platens at specimen ends becomes evident on the compressive behavior of the specimens (van Vliet and van Mier 1996). Due to the presence of the additional frictional effects, which depend largely on the surface roughness of loading platens (van Mier et al. 1997), the damage zone height (H_d) of specimens with a height (H) less than $2D$ could not be quantified based on the available test results in a unified manner. Therefore, the proposed model is not intended for the specimens in that category, and, for the purpose of the axial strain adjustment, the model assumes the damage zone height to be equal to twice the specimen diameter (i.e., $H_d = 2D$).

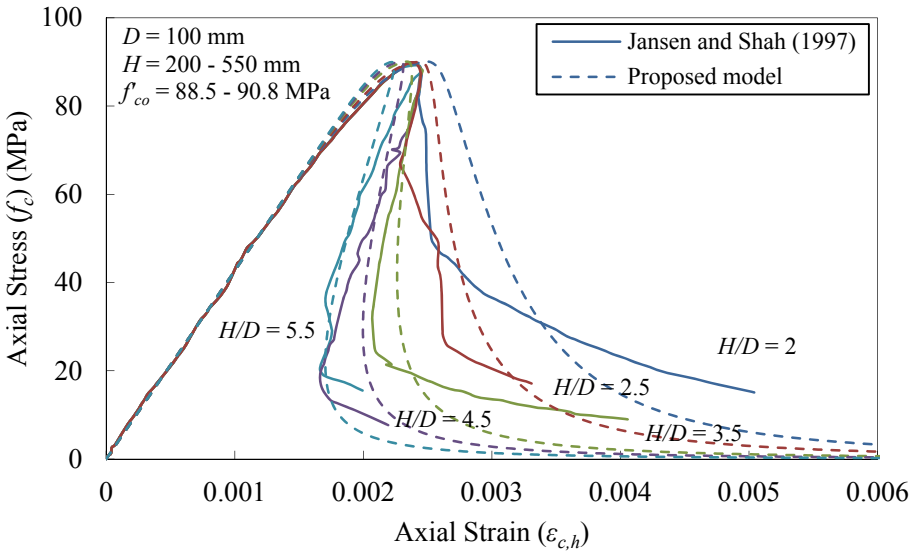

(a)

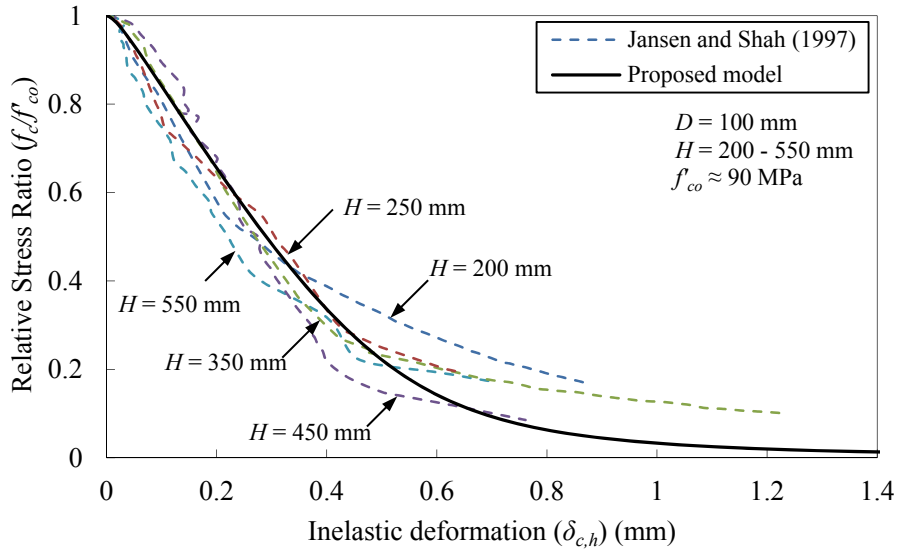

(b)

Figure 3. High-strength concrete specimens with different heights: (a) axial stress-strain curves; and (b) relative stress ratio-inelastic deformation curves (Group U89-91)

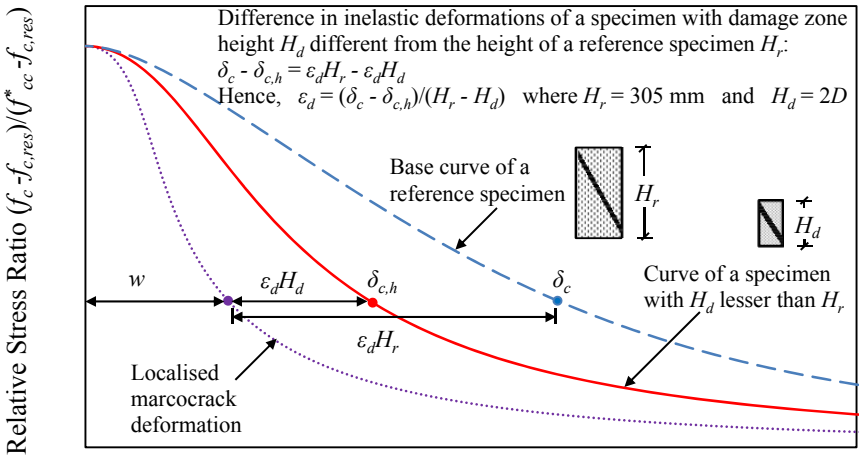

(a)

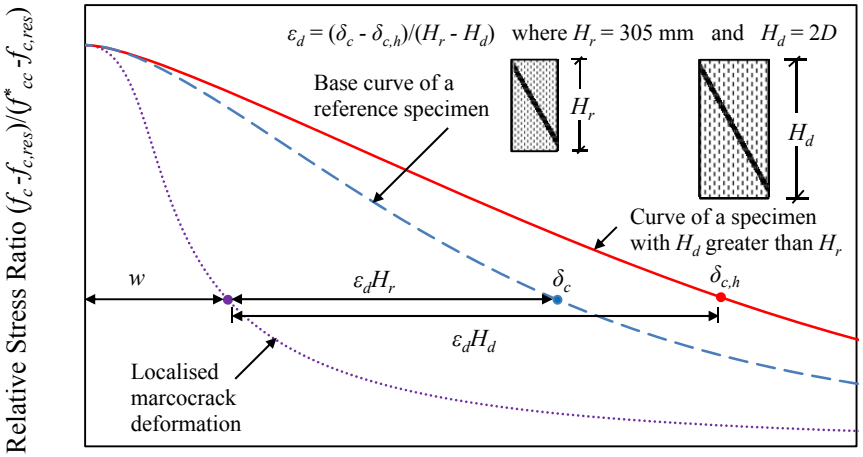

(b)

Figure 4. Differences in inelastic deformations of specimens with damage zone heights H_d: (a) lesser than; and (b) greater than the reference specimen height H_r

2.3.2 Determining the inelastic strain in damage zone

To quantify the inelastic strain in damage zone (ε_d), a novel approach, illustrated in Figure 4, is applied to analyze the inelastic deformation ($\delta_{c,h}$) calculated from the experimental test results. To explain the basis of this approach, Figure 4 shows two sets of theoretical curves; one for a reference specimen (i.e., D_r = 152 mm, H_r = 305 mm) represented by a dashed line, and one for a specimen with a height less than that of the reference specimen (i.e. $H < H_r$) represented by a solid line. As demonstrated in the figure, once the base stress-strain curves of a reference specimen has been established from the database results, the inelastic strain (ε_d) of specimens with damage zone heights (H_d) different from the reference specimen height (H_r) can be obtained. To demonstrate the application of the approach in quantifying the inelastic strain (ε_d) in concrete damage zone, examples from test results of specimens having different diameters (D), unconfined concrete strengths (f'_{co}), and confining pressures (f^*_l) are shown in Figures 5 to 7, respectively. Figures 5(a) and 5(b) show the axial stress-strain curves of the specimens with different diameters (D) but the same aspect ratio (H/D) and identical concrete strengths (f'_{co}). As illustrated in Figures 5(a) and 5(b), the smaller scale specimens exhibited larger axial strains compared to their larger scale counterparts, indicating that the small-scale specimens are influenced more heavily by the axial strains resulting from localized crack deformations along the shear plane (w) due to their smaller damage zone heights (H_d). Figure 5(c) shows the variation of relative stress ratio (f_c/f'_{co}) with inelastic deformation ($\delta_{c,h}$) of the specimen group. As evident from Figure 5(c), at a given aspect ratio (H/D), specimens with smaller diameters (D) exhibited lower inelastic deformations ($\delta_{c,h}$). This observation indicates that, as the specimen diameter (D) reduces, the deformation contributed by the inelastic strain ($\varepsilon_d H_d$) reduces as a result of a decrease in the damage zone height (i.e., H_d = 2D). Figure 5(d) shows the variation of the inelastic strain (ε_d) with the relative stress ratio (f_c/f'_{co}) of the specimen group. As evident from the figure, the specimens having the same aspect ratio (i.e., H/D = 2) but different diameters (D) exhibit very similar curves. This observation indicates that the specimen size has no influence on the inelastic strain (ε_d) of concrete.

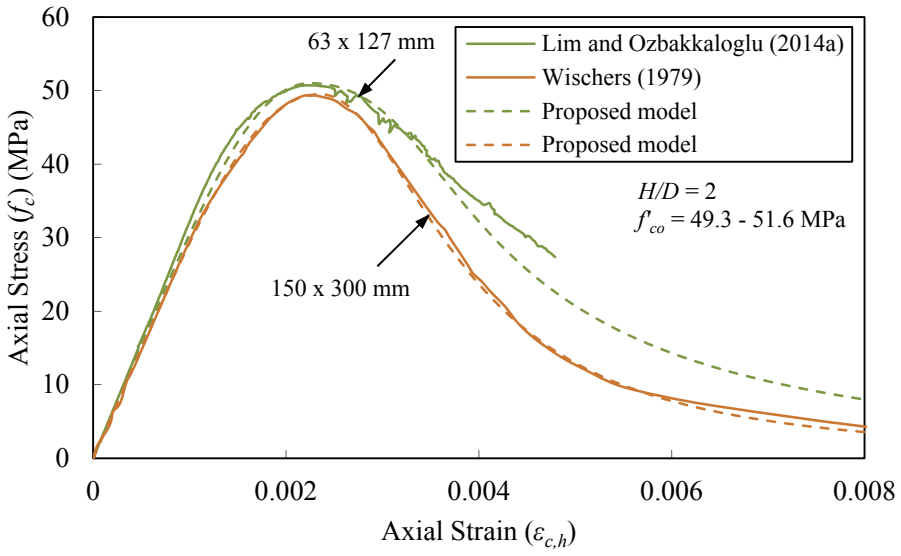

(a)

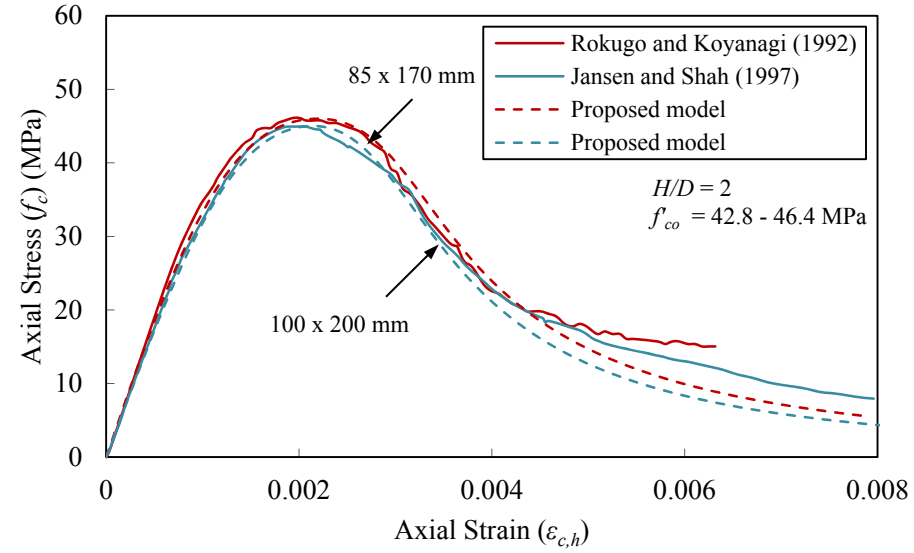

(b)

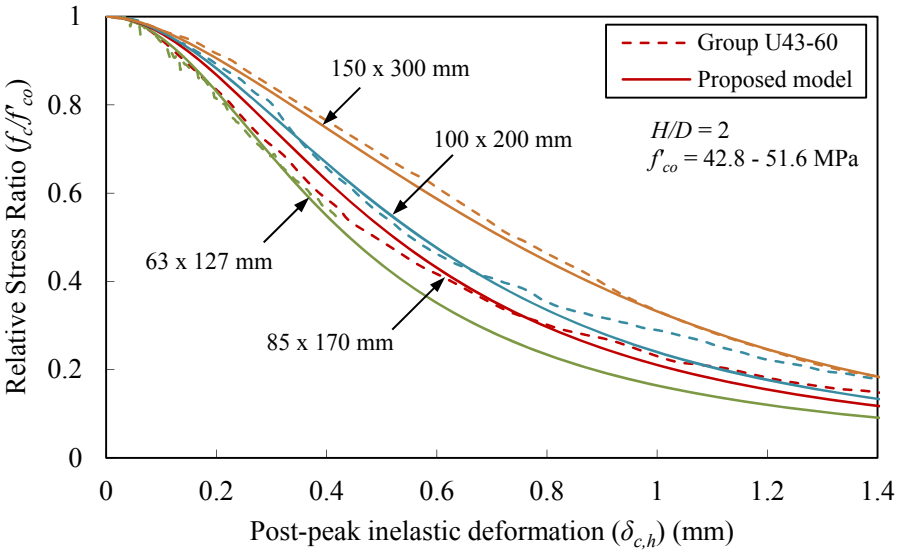

(c)

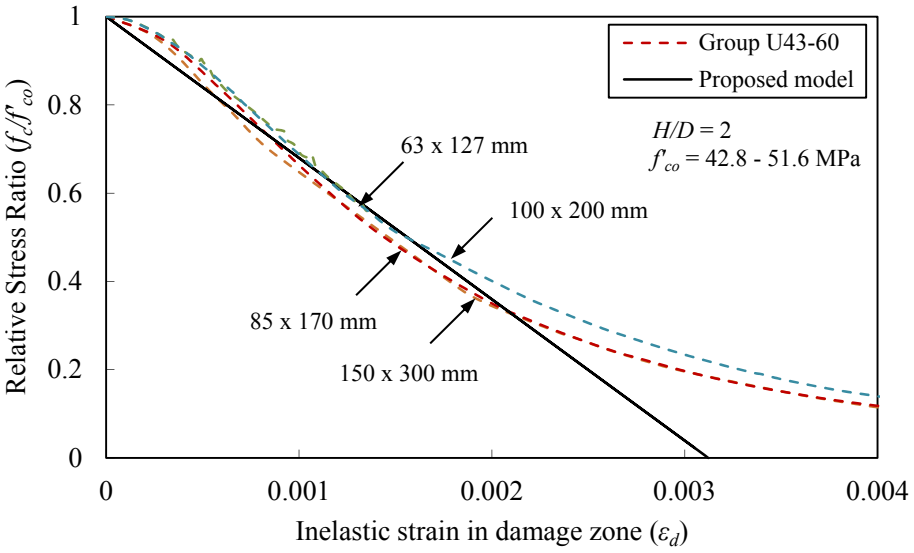

(d)

Figure 5. Specimens with a same aspect ratio but different diameters: (a-b) axial stress-strain curves; (c) relative stress ratio-inelastic deformation curves; and (d) relative stress ratio-inelastic strain curves (Group U43-60)

To illustrate the change in the inelastic strain in damage zone (ε_d) with the variation of unconfined concrete strength (f'_{co}), the axial stress-strain curves of specimens with the same geometrical dimensions (H and D) but different unconfined concrete strengths (f'_{co}) are shown in Figure 6(a). Figures 6(b) and 6(c) show the variations of the relative stress ratios (f_c/f'_{co}) of the specimens with the inelastic deformations ($\delta_{c,h}$) and the inelastic strains in damage zone (ε_d), respectively. As illustrated in Figures 6(a) and 6(b), the higher strength specimens exhibited steeper slopes in their descending curves compared to their lower strength counterparts. The inelastic strains of these specimens (ε_d) decreased with an increase in their unconfined concrete strength (f'_{co}), as evident from Figure 6(c).

To illustrate the influence of confining pressure (f^*_l) on the inelastic strains (ε_d) of confined concrete, the axial stress-strain curves of specimens that had the same geometrical dimensions (H and D) and unconfined concrete strengths (f'_{co}), but were subjected to different confining pressures (f^*_l) are shown in Figure 7(a). Figures 7(b) and 7(c) show the variations of the relative stress ratios (f_c-$f_{c,res}$)/(f^*_{cc}-$f_{c,res}$) of the specimens with the inelastic deformations ($\delta_{c,h}$) and the inelastic strains in damage zone (ε_d), respectively. As illustrated in Figures 7(a) and 7(b), the shapes of the axial stress-strain curves and the relative stress ratio-inelastic deformation curves vary with the change in the confining pressure (f^*_l). However, Figure 7(c) shows that the shapes of the relative stress ratio-inelastic strain curves are not affected by the magnitude of applied confining pressure. On the basis of observations shown in Figures 5 to 7, Eq. 2 which was established from the results of the comprehensive experimental databases (Lim and Ozbakkaloglu 2014b; 2014c), is proposed to determine the inelastic strains (ε_d) of both confined and unconfined concretes.

$$\varepsilon_d = 0.02{f'_{co}}^{-0.5}\left(\frac{f^*_{cc} - f_c}{f^*_{cc} - f_{c,res}}\right) \quad (2)$$

where f'_{co} is in MPa.

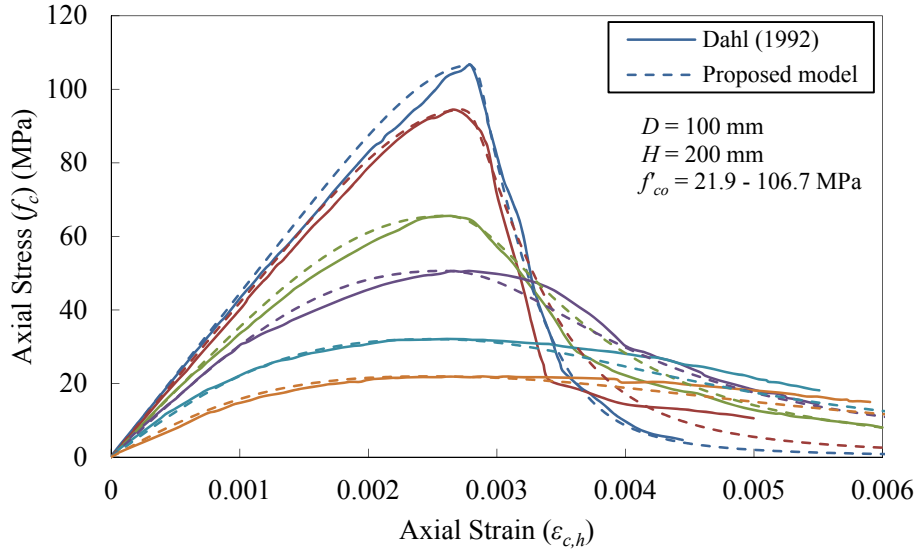

(a)

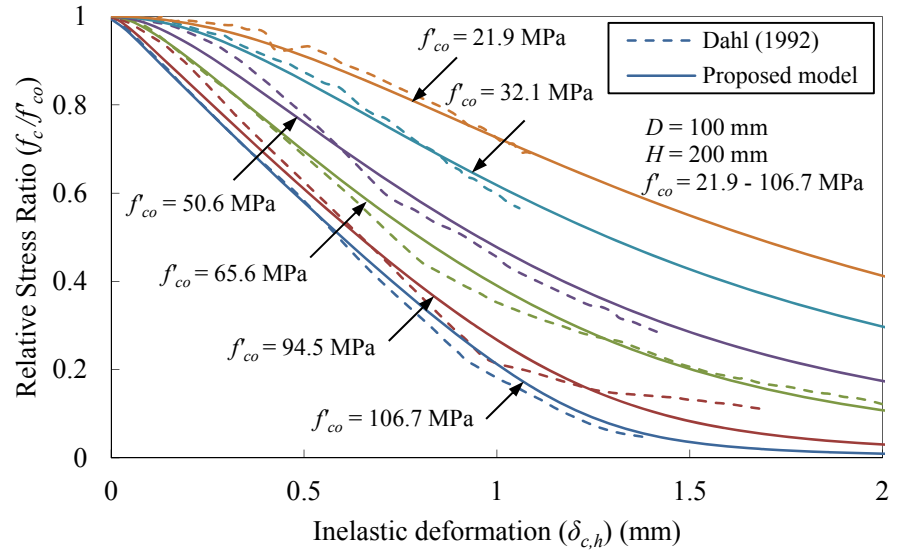

(b)

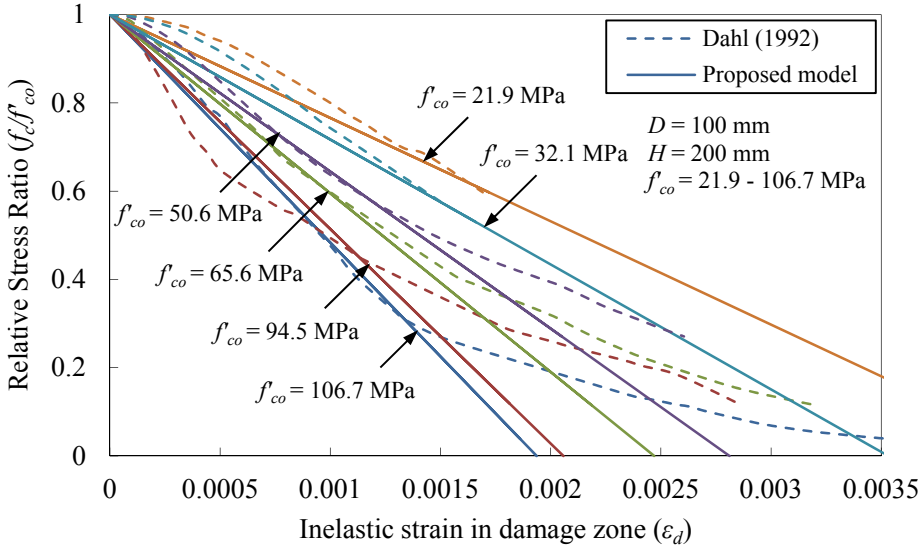

(c)

Figure 6. Specimens with same geometrical dimensions but different unconfined concrete strengths: (a) axial stress-strain curves; (b) relative stress ratio-inelastic deformation curves; and (c) relative stress ratio-inelastic strain curves (Group U22-107)

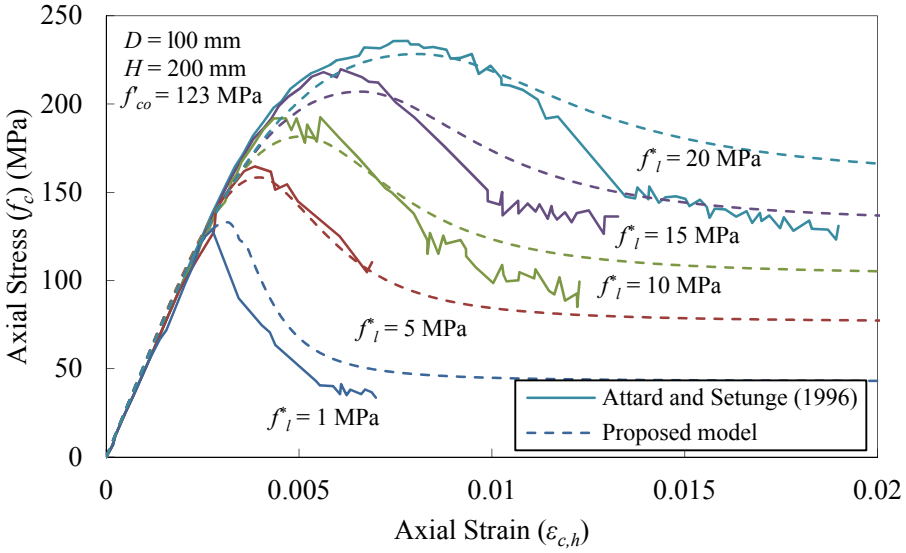

(a)

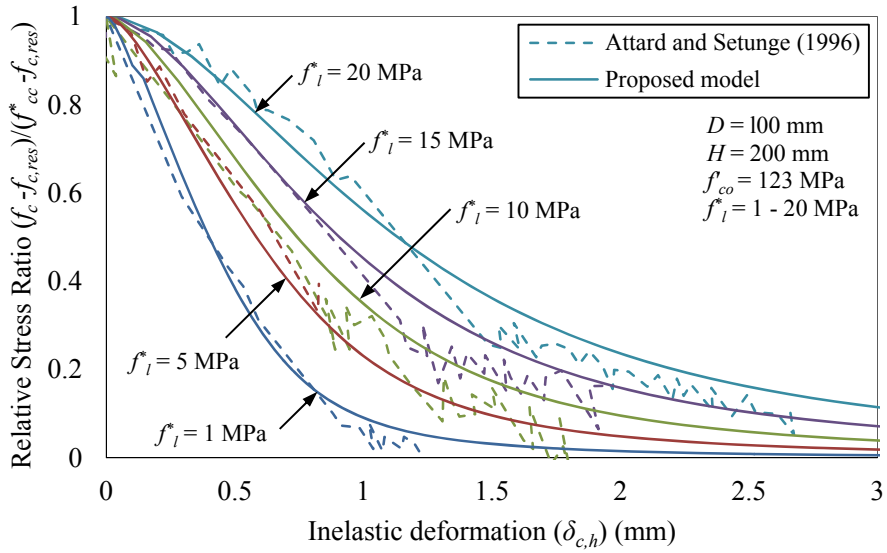

(b)

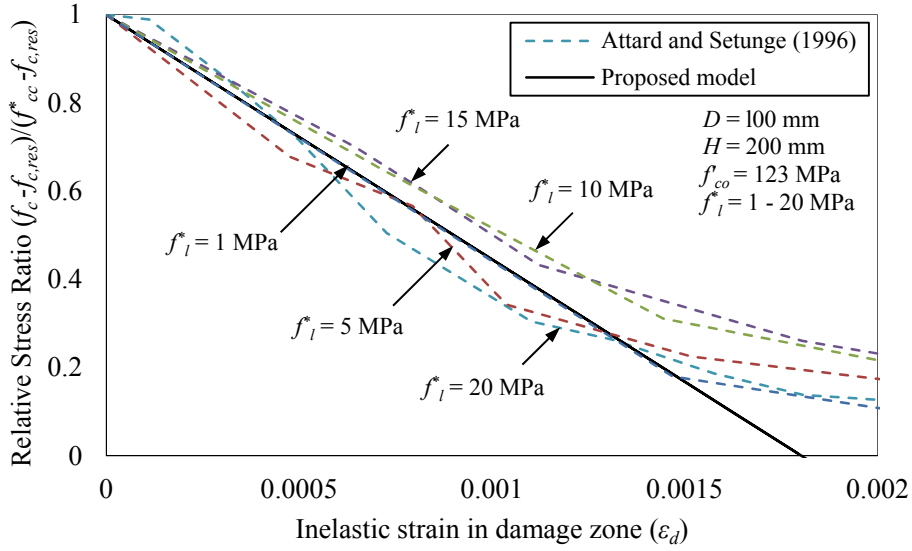

(c)

Figure 7. Specimens with different confining pressures: (a) axial stress-strain curves; (b) relative stress ratio-inelastic deformation curves; and (c) relative stress ratio-inelastic strain curves (Group U123)

2.3.3 Influence of coarse aggregate size

The coarse aggregate size of concrete is another parameter commonly reported to have influence on the crack localization and height of compression damage zone, and hence on the strain softening behavior of concrete. Although a number of studies have reported on this influence (Vonk 1992; Lertsrisakulrat et al. 2001; Akçaoğlu et al. 2004), their findings, which were based on limited test databases, have often been controversial. Vonk (1992) found that aggregate size altered the cracking pattern of concrete, whereas Lertsrisakulrat et al. (2001) tested specimens with different aggregate sizes and concluded that there was no significant difference in cracking pattern of concretes manufactured using different size aggregates. Akçaoğlu et al. (2004), found that the aggregate size influenced the cracking pattern of normal and high-strength concretes differently. In the present study, influences of size and volumetric ratio of coarse aggregates on the axial strains at peak compressive stress (ε_{co}) and post-peak inflection point ($\varepsilon_{c,i}$) were investigated based on the results of the large experimental database. Details of the coarse aggregates of the specimens included the database were provided in Lim and Ozbakkaloglu (2014c). Figure 8(a) shows the variation of the axial strain at peak compressive stress (ε_{co}) with compressive strength of concrete (f'_{co}), whereas Figure 8(b) shows the variation of the normalized axial strain at inflection point ($\varepsilon_{c,i}/\varepsilon_{co}$) with compressive strength of concrete (f'_{co}). As evident from the figures, the trends of test results are significantly influenced by the compressive strength of concrete (f'_{co}), with this influence successfully captured by the proposed model. To investigate the potential influence of the aggregate size-to-damage zone width ratio on the strain softening behavior of concrete, test results given in Figure 8 were sorted into groups based on specimen diameter-to-aggregate size ratios. Although variations of ε_{co} with specimen diameter-to-aggregate size ratio can be seen in Figure 8(a), these variations do not indicate a clear trend as to the influence of the aggregate size on ε_{co}. Similarly, in Figure 8(b), variations in the axial strains at inflection points ($\varepsilon_{c,i}$) with the aggregate size do not exhibit a clear pattern. With the aim of gaining additional insight into the influence of aggregate size, the test results were further analyzed after dividing them into smaller subgroups based on the aggregate volume ratios of the concrete mixes. However, even after this detailed analysis it was still not possible to obtain a clear pattern on the influence of aggregate size on concrete softening behavior. Therefore, a definitive conclusion cannot be derived as to the influence of the aggregate size based on the results that are currently available in the literature. It is clear from the above summary of the findings of the existing studies and the observations of the present study further research is needed to better understand the influence of aggregate size on the compressive behavior of concrete. Therefore, the model proposed in the present study makes no effort to formulate the individual influence of the aggregate size on the stress-strain behavior.

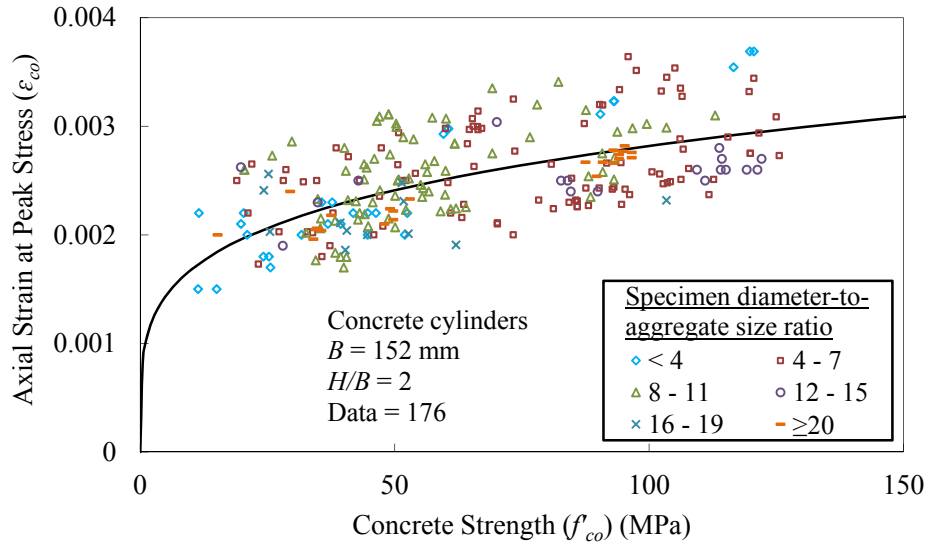

(a)

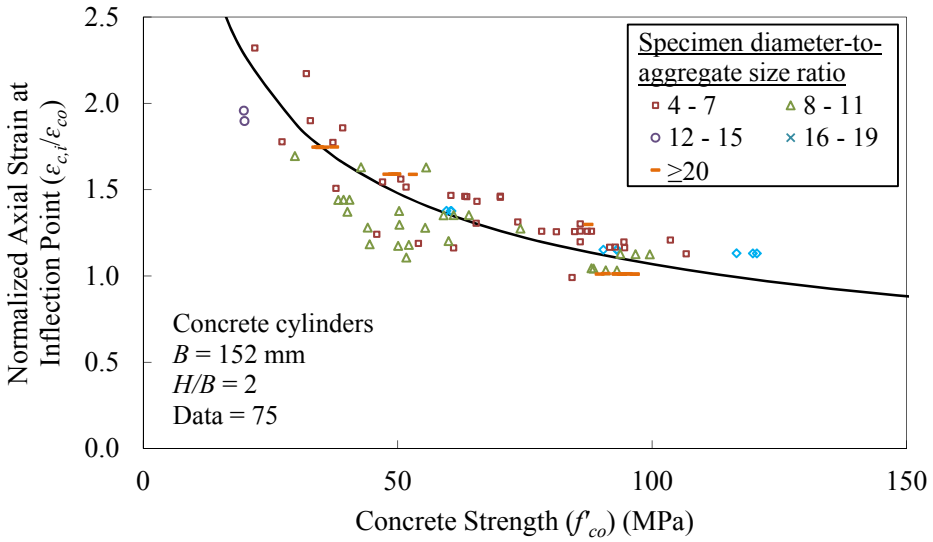

(b)

Figure 8. Variations of: (a) axial strain at peak compressive stress and; (b) normalized axial strain at inflection point with compressive strength of concrete and specimen diameter to-aggregate size ratio

3. COMPARISON WITH EXPERIMENTAL RESULTS

Figures 9(a) to 9(c), respectively, show the comparisons of the proposed model predictions with test results of unconfined specimens with different compressive strengths, unconfined specimens with different aspect ratios, and confined specimens with different confining pressures. As evident from the comparisons, the predictions of the proposed model are in good agreement with the experimental results that consist of a wide range of compressive strengths (f'_{co}), specimen geometrical dimensions (H and D), and confining pressures (f^*_l).

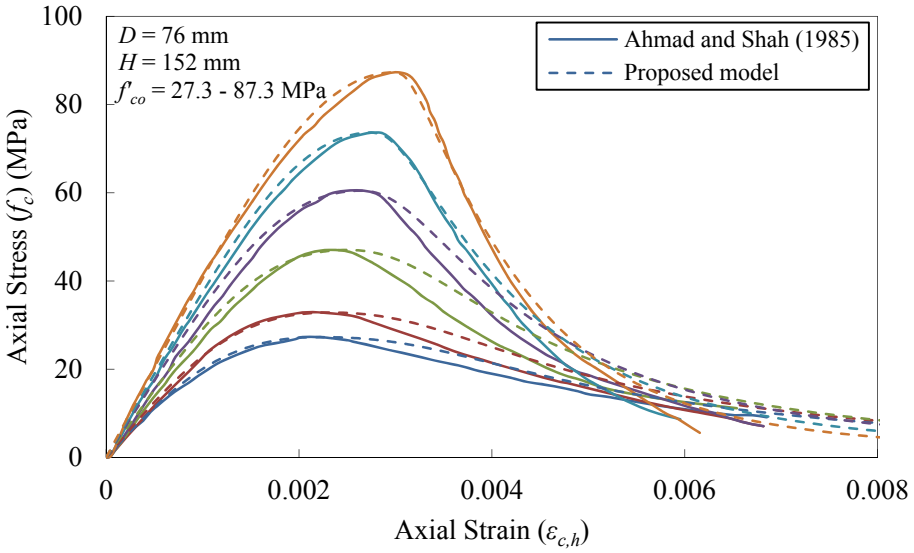

(a)

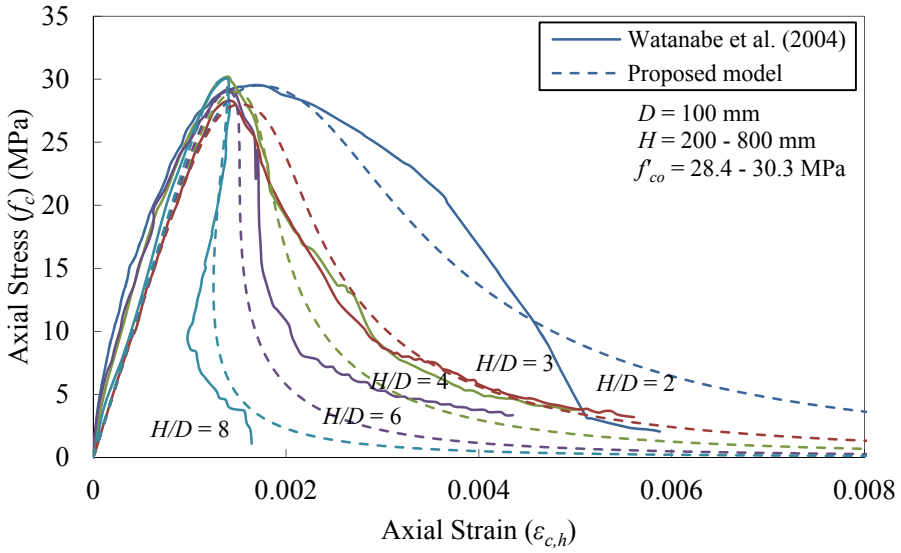

(b)

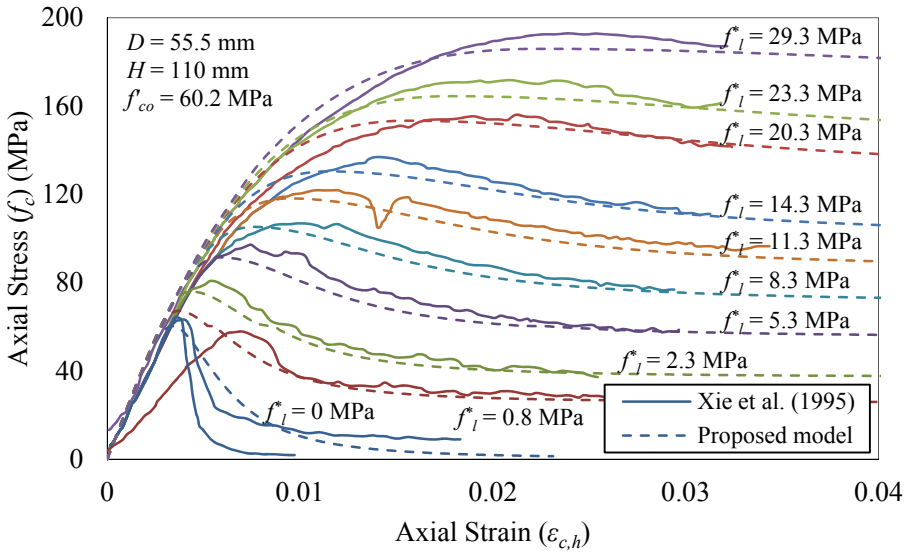

(c)

Figure 9. Comparisons of the proposed model predictions with test results of: (a) unconfined specimens with different compressive strengths (Group U27-87); (b) unconfined specimens with different aspect ratios (Group U28-30); (c) confined specimens with different confining pressures (Group U60)

4. CONCLUSIONS

This paper has presented a constitutive model for predicting the strain softening behavior of concrete in compression. The model was based on the concept of inelastic strain and crack localization that occur in the compression damage zone of softening concrete. A novel approach is proposed to separate and quantify the inelastic strain and the localized crack deformation from experimental stress-strain curves. Using the experimental databases of confined and unconfined concretes covering a wide range of concrete strengths, the inelastic strain in damage zone of various specimens were systematically quantified and a constitutive model for predicting the strain softening behavior of confined and unconfined concretes is proposed. The predictions of the proposed model are shown to be in good agreement with the test results of both unconfined and actively confined concretes.

REFERENCES

Ahmad, S. H., and Shah, S. P. (1985). "Behaviour of hoop confined concrete under high strain rates." *ACI Journal Proceedings*, 82, 634-647.

Akçaoğlu, T., Tokyay, M., and Çelik, T. (2004). "Effect of coarse aggregate size and matrix quality on ITZ and failure behavior of concrete under uniaxial compression." *Cement and Concrete Composites*, 26(6), 633-638.

Attard, M. M., and Setunge, S. (1996). "Stress-strain relationship of confined and unconfined concrete." *ACI Materials Journal*, 93(5), 432-442.

Bazant, Z. P. (1989). "Identification of Strain-Softening Constitutive Relation from Uniaxial Tests by Series Coupling Model for Localization." *Cement and Concrete Research*, 19, 973-977.

Crisfield, M. A. (1986). "Snap-through and snap-back response in concrete structures and the dangers of under-integration." *International Journal for Numerical Methods in Engineering*, 22(3), 751-767.

Dahl, K. K. B. (1992). "Uniaxial Stress-Strain Curves for Normal and High-Strength Concrete." *ABK Report No. R282*, Department of Structural Engineering, Technical University of Denmark.

Jansen, D. C., and Shah, S. P. (1997). "Effect of length on compressive strain softening of concrete." *Journal of Engineering Mechanics*, 123(1), 25-35.

Lertsrisakulrat, T., Watanabe, K., Matsuo, M., and Niwa, J. (2001). "Experimental study on parameters in localization of concrete subjected to compression." *Journal of Materials, Concrete Structures and Pavement, JSCE*, 669(50), 309-321.

Lim, J. C., and Ozbakkaloglu, T. (2014a). "Investigation of the Influence of Application Path of Confining Pressure: Tests on Actively Confined and FRP-Confined Concretes." *Journal of Structural Engineering, ASCE*, Doi: 10.1061/(ASCE)ST.1943-541X.0001177.

Lim, J. C., and Ozbakkaloglu, T. (2014b). "Lateral strain-to-axial strain relationship of confined concrete." *Journal of Structural Engineering, ASCE*, Doi: 10.1061/(ASCE)ST.1943-541X.0001094.

Lim, J. C., and Ozbakkaloglu, T. (2014c). "Stress-strain model for normal- and light-weight concretes under uniaxial and triaxial compression." *Construction and Building Materials*, 71, 492-509.

Markeset, G., and Hillerborg, A. (1995). "Softening of concrete in compression-localization and size effects." *Cement and Concrete Research*, 25(4), 702-708.

Rokugo, K., and Koyanagi, W. (1992). " Role of compressive fracture energy of concrete on the failure behaviour of reinforced concrete beams." *Applications of fracture mechanics to reinforced concrete*, 437-464.

van Mier, J. G. M., Shah, S. P., Arnaud, M., Balayssac, J. P., Bascoul, A., Choi, S., Dasenbrock, D., Ferrara, G., French, C., Gobbi, M. E., Karihaloo, B. L., Konig, G., Kotsovos, M. D., Labuz, J., Lange-Kornbak, D., Markeset, G., Pavlovic, M. N., Simsch, G., Thiend, K.-C., Turatsinze, A., Ulmefl, M., Gee, H. J. G. M. v., Vliet, M. R. A. v., and Zissopoulos, D. (1997). "Strain-softening of concrete in uniaxial compression." *Materials and Structures*, 30(4), 195-209.

van Vliet, M. R., and van Mier, J. G. (1996). "Experimental investigation of concrete fracture under uniaxial compression." *Mechanics of Cohesive-frictional Materials*, 1(1), 115-127.

Vonk, R. (1992). "Softening of concrete loaded in compression." PhD thesis, he Netherlands.
Watanabe, K., Niwa, J., Yokota, H., and Iwanami, M. (2004). "Experimental study on stress-strain curve of concrete considering localized failure in compression." *Journal of Advanced Concrete Technology*, 2(3), 395-407.
Wischers, G. (1979). "Application and Effects of Compressive Loads on Concrete." *Betonverlag GmbH, Dfisseldorf*, 31-56.
Xie, J., Elwi, A. E., and Macgregor, J. G. (1995). "Mechanical-properties of high-strength concretes containing silica fume." *ACI Materials Journal*, 92(2), 135-145.

Statement of Authorship

Title of Paper	Unified Stress-Strain Model for FRP and Actively Confined Normal-Strength and High-Strength Concrete
Publication Status	(•) Published ( ) Accepted for Publication ( ) Submitted for Publication ( ) Publication Style
Publication Details	Journal of Composites for Construction, Doi: 10.1061/(ASCE)CC.1943-5614.0000536,Year 2014

Author Contributions

By signing the Statement of Authorship, each author certifies that their stated contribution to the publication is accurate and that permission is granted for the publication to be included in the candidate's thesis.

Name of Principal Author (Candidate)	Mr. Jian Chin Lim		
Contribution to the Paper	Preparation of experimental database, development of model, and preparation of manuscript		
Signature		Date	23/02/2015

Name of Co-Author	Dr. Togay Ozbakkaloglu		
Contribution to the Paper	Research supervision and review of manuscript		
Signature		Date	23/02/2015

THIS PAGE HAS BEEN LEFT INTENTIONALLY BLANK

UNIFIED STRESS-STRAIN MODEL FOR FRP AND ACTIVELY CONFINED NORMAL-STRENGTH AND HIGH-STRENGTH CONCRETE

Jian C. Lim and Togay Ozbakkaloglu

ABSTRACT

Accurate modeling of the complete stress-strain relationship of confined and unconfined concrete is of vital importance in predicting the overall flexural behavior of reinforced concrete structures. The analysis-oriented models, which utilize the dilation characteristics of confined concretes for stress-strain relationship prediction, are well recognized for their versatility in such modeling applications. These models assume that, at a given lateral strain, the axial compressive stress and strain of FRP-confined concrete are the same as those of the same concrete when it is actively confined under a confining pressure equal to that supplied by the FRP jacket. However, this assumption has recently been demonstrated experimentally to be inaccurate for high-strength concrete (HSC). It was shown that, at a given axial strain, lateral strains of actively confined and FRP-confined concretes of the same concrete strength correspond when they are subjected to the same lateral confining pressure. However, it was also shown that, under the same condition, concrete confined by FRP exhibits a lower strength enhancement compared to that seen in companion actively confined concrete. To develop an accurate model that can describe the experimentally observed behavior, two large test databases were assembled for actively confined and FRP-confined concretes through an extensive review of the literature. Based on the analysis of the databases, a new approach is developed to establish the axial stress difference between the actively confined and FRP-confined concretes. Finally, a unified model is proposed to describe the stress-strain relationships of actively confined and FRP-confined concrete. Comparisons with experimental test results show that the predictions of the proposed model are in good agreement with the test results of both actively confined and FRP-confined concrete, and the model provides improved predictions compared to the existing models.

KEYWORDS: Concrete; High-strength concrete (HSC); Fiber reinforced polymer (FRP); Confinement; Stress-strain relations; Active; Triaxial; Compression; Stress-path.

1. INTRODUCTION

Since the 1920s, a significant research effort has been dedicated to understanding the improved compressive behavior of concrete under lateral confinement. More recently, research attention has turned to the potential applications of fiber reinforced polymer (FRP) composites, as concrete confinement in retrofitting existing concrete columns (e.g. (Lam and Teng 2004; Ilki et al. 2008; Smith et al. 2010; Ozbakkaloglu and Akin 2012; Rousakis and Karabinis 2012; Wu and Jiang 2013)) and in the construction of new high-performance composite columns (e.g. (Ozbakkaloglu 2013; Ozbakkaloglu and Vincent 2013; Vincent and Ozbakkaloglu 2013a,b)). A recent comprehensive review (Ozbakkaloglu et al. 2013) revealed that over 200 experimental studies have been conducted over the last two decades on the compressive behavior of FRP-confined concrete, resulting in the development of over 80 axial stress-strain models. These models have been categorized into two categories: design-oriented models presented in closed-form expressions; and analysis-oriented models, which predict stress-strain curves by an incremental procedure.

The majority of design-oriented models focus on the prediction of the ultimate condition of FRP-confined concrete and they are not able to provide a complete stress-strain relationship. Analysis-oriented models, on the other hand, are capable of establishing the full axial stress-strain and lateral strain-axial strain relationships of the FRP-confined concrete on the basis of the interaction mechanism between the external confining jacket and the internal concrete core. As was also previously discussed in detail in Teng et al. (2007), Ozbakkaloglu et al. (2013), and Lim and Ozbakkaloglu (2014e) these features make analysis-oriented models more versatile and powerful than design-oriented models. Such models are built on an assumption, known as the stress path independency, that the axial compressive stress and strain of FRP-confined concrete at a given lateral strain are the same as those of the same concrete when it is actively confined under a confining pressure equal to that supplied by the FRP jacket. The relationship between the axial strain, lateral strain, and confining pressure have been well established in a number of studies using experimental test results from both actively confined and FRP-confined normal-strength concrete (NSC) (Teng et al. 2007; Lim and Ozbakkaloglu 2014e) and high-strength concrete (HSC) (Lim and Ozbakkaloglu 2014e). However, the relationship between the axial stresses of the actively confined and FRP-confined concretes has been less understood. It was recently reported in Lim and Ozbakkaloglu (2014d) that a concrete confined by FRP exhibits a lower strength enhancement compared to that seen when the same concrete is actively confined under the same confining pressure.

Two large test databases assembled for actively confined and FRP-confined concretes were used to investigate the experimentally observed behavior. The results of this investigation confirms the finding of Lim and Ozbakkaloglu (2014d) that FRP confinement is unable to match the strength enhancement provided by active confinement at the same level of confining pressure. Based on these observations, a confining pressure gradient was established to quantify the reduction in the axial stress observed in FRP-confined concrete compared to that of actively confined concrete. Following this, a generic model was developed to describe the stress-strain relationships of actively confined and FRP-confined

concretes. Comparisons with experimental test results show that the predictions of the proposed model are in good agreement with the test results of both actively confined and FRP-confined concretes, and the model provides improved predictions compared to the existing models.

2. EXPERIMENTAL TEST DATABASES

The two carefully prepared test databases of actively confined and FRP-confined concretes used in the model development are summarized in this section. The database of FRP-confined concrete was assembled through an extensive review of the literature that covered 3042 test results from 253 experimental studies published between 1991 and 2013. The suitability of the results was then assessed using a set of carefully established selection criteria to ensure the reliability and consistency of the database. Only monotonically loaded circular specimens with unidirectional fibers orientated in the hoop direction and an aspect ratio (*H/D*) of less than three were included in the database. Specimens containing internal steel reinforcement or partial FRP confinement were not included. This resulted in a selected database that contained 1063 datasets collected from 105 experimental studies. The details of the NSC and HSC components of the circular column database can be found in Ozbakkaloglu and Lim (2013) and Lim and Ozbakkaloglu (2014a), respectively. In addition, 93 FRP-confined specimen results from tests recently conducted at the University of Adelaide (Lim and Ozbakkaloglu 2014b; Lim and Ozbakkaloglu 2014c,d) were included to the database.

The final database consisted of specimens confined by five main types of FRP materials (carbon FRP (CFRP), high-modulus carbon FRP (HM CFRP), ultra high-modulus carbon FRP (UHM CFRP), S- or E-glass FRP (GFRP), and aramid FRP (AFRP)) and two confinement techniques (wraps and tubes). The diameters of the specimens (D) included in the test database varied between 47 and 600 mm. The unconfined concrete strength (f'_{co}) and the corresponding axial strain (ε_{co}), as obtained from concrete cylinder tests, varied from 6.2 to 169.7 MPa and 0.14% to 0.70%, respectively. The unconfined concrete cylinders had the same geometric dimensions as the corresponding confined specimens. The actual confinement ratio, defined as the ratio of the ultimate confining pressure of the FRP jacket at rupture to the compressive strength of an unconfined concrete specimen ($f_{lu,a}/f'_{co}$), varied from 0.02 to 4.74.

The database of actively confined concretes (Lim and Ozbakkaloglu 2014e) was assembled from 25 published studies and consisted of 346 test datasets and 31 actively confined specimen results from tests conducted at the University of Adelaide (Lim and Ozbakkaloglu 2014d). Only triaxially loaded circular specimens with an aspect ratio (*H/D*) of less than three were included in the database. Specimens containing internal steel or microfiber reinforcement in the concrete were excluded. The diameters of the specimens (D) varied between 50 and 160 mm. The unconfined concrete strength (f'_{co}) and the corresponding axial strain (ε_{co}), as obtained from concrete cylinder tests, varied from 7.2 to 132.0 MPa and 0.15% to 0.40%, respectively. The active confinement ratio, defined as the ratio of the hydrostatic confining pressure of the triaxial cell to the compressive strength of the unconfined concrete specimen (f^*_l/f'_{co}), varied from 0.004 to 21.67.

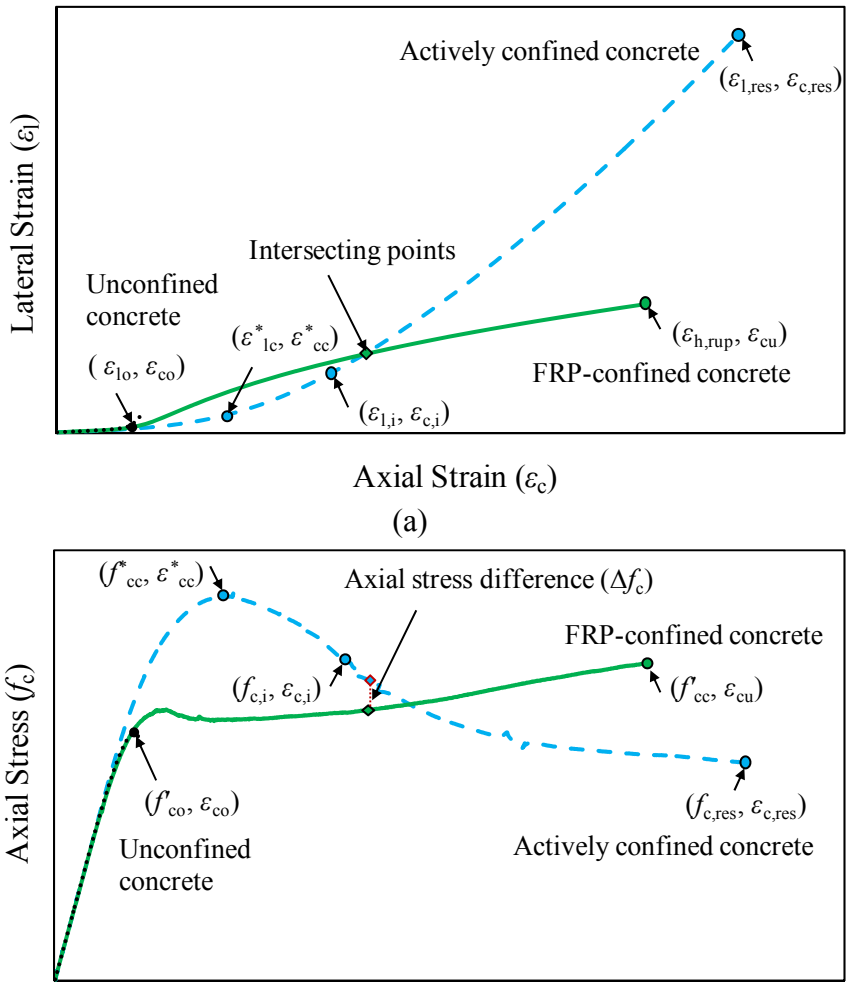

Figure 1. (a) Typical lateral strain-axial strain curves; and (b) axial stress-strain curves of actively-confined, FRP-confined and unconfined concretes

3. STRESS-STRAIN RELATIONSHIP OF CONFINED CONCRETE

Figures 1(a) and 1(b) show the typical lateral strain-axial strain and axial stress-strain curves of actively confined, FRP-confined and unconfined concretes. As illustrated in Figure 1, the peak condition of actively confined concrete is characterized by the peak stress (f^*_{cc}), and the corresponding axial strain (ε^*_{cc}) and lateral strain (ε^*_{lc}); the residual condition is characterized by the residual stress ($f_{c,res}$), and the corresponding axial strain ($\varepsilon_{c,res}$) and lateral strain ($\varepsilon_{l,res}$); and the ultimate condition of the FRP-confined concrete is characterized by the compressive strength (f'_{cc}), and the corresponding axial strain (ε_{cu}) and lateral strain ($\varepsilon_{h,rup}$) recorded at the rupture of the FRP jacket. As can be seen from the figure, the differences in the shapes of the stress-strain curves are highly dependent on the way the confining pressure is applied to the concrete. In actively confined concrete, the constant confining pressure exerted from the triaxial load cell results in a linearly ascending initial segment followed by a parabolic curve forming the first branch, which transitions into a gradually descending second branch after the peak compressive stress (f^*_{cc}) is reached. After peak stress, the interparticle cohesion in the concrete continues to decrease and the remaining strength generated from frictional action

forms a stabilized plateau in the curve, referred to as the residual stress ($f_{c,res}$) (Imran and Pantazopoulou 2001). In FRP-confined concrete, the gradually increasing confining pressure generated by the FRP jacket results in a stress-strain curve, which consists of an initial ascending branch that resembles that of the actively confined concrete followed by a nearly straight-line second branch that can either be ascending or descending. Assuming a uniform confining pressure distribution for a circular concrete section confined by an FRP jacket, the confining pressure (f_l) can be expressed by Eq. 1, which satisfies the strain compatibility and force equilibrium conditions between the core and the jacket.

$$f_l = \frac{2E_f t_f \varepsilon_l}{D} = K_l \varepsilon_l \quad (1)$$

In Eq.1, K_l is the confinement stiffness of the FRP jacket, E_f is the elastic modulus of fibers, t_f is the total nonimal fiber thickness of the FRP jacket, D is the diameter of the concrete specimen, and ε_l is the lateral strain of FRP jacket which gradually increase with the dilation of concrete and terminates at the hoop rupture strain of FRP ($\varepsilon_{h,rup}$).

3.1 Comparisons of actively confined and FRP-confined concrete curves

To compare the stress-strain behaviors of concretes with similar properties that were subjected to either active or FRP confinement, specimen groups were prepared by sorting the specimens according to their unconfined concrete strengths (f'_{co}). Details of these specimen groups are summarized in Table 1. In addition, Table 1 also contains groups of FRP-confined specimens that had comparable confinement stiffness ratio (K_l/f'_{co}) used subsequently in the paper to evaluate model predictions for specimens with different unconfined concrete strengths (f'_{co}). In the group notations, the numbers that follow the letter 'U' represent the nominal unconfined concrete strength (f'_{co}) of the first specimen in a given group. Figures 2 to 5 show the comparison of the lateral strain-axial strain and axial stress-strain curves of actively confined and FRP-confined specimens in Groups U35, U52, U103, and U128, respectively. As can be seen from Figures 2(a) to 5(a), the lateral strain-axial strain curves of the FRP-confined specimens intersect the curves of the actively confined specimens sequentially in the order of increasing confining pressure.

As discussed previously, the existing analysis-oriented models are built on the assumption that the axial compressive stress and strain of FRP-confined concrete at a given lateral strain are the same as those in the same concrete actively confined with a confining pressure equal to that supplied by the FRP jacket. To evaluate this assumption, the confinement ratios of actively confined and FRP-confined specimens at the intersecting points of their lateral strain-axial strain curves, as marked in Figures 2(a) to 5(a), were compared. The procedure was subsequently repeated for another two groups of specimens (i.e. U42 and U73). Figure 6 shows the comparison of the confinement ratios of actively confined (f^*_l/f'_{co}) and FRP-confined specimens (f_l/f'_{co}) at the points of intersection for all of the companion specimen groups. As can be seen from Figure 6, the confinement ratios of the actively confined and FRP-confined specimens at the points of intersection are close to each other and exhibit a strong correlation. These observations indicate that the lateral strain-axial strain relationships of both actively

confined and FRP-confined concretes depend only on the instantaneous confining pressure at the corresponding axial strain, and not on the application path of the confining pressure.

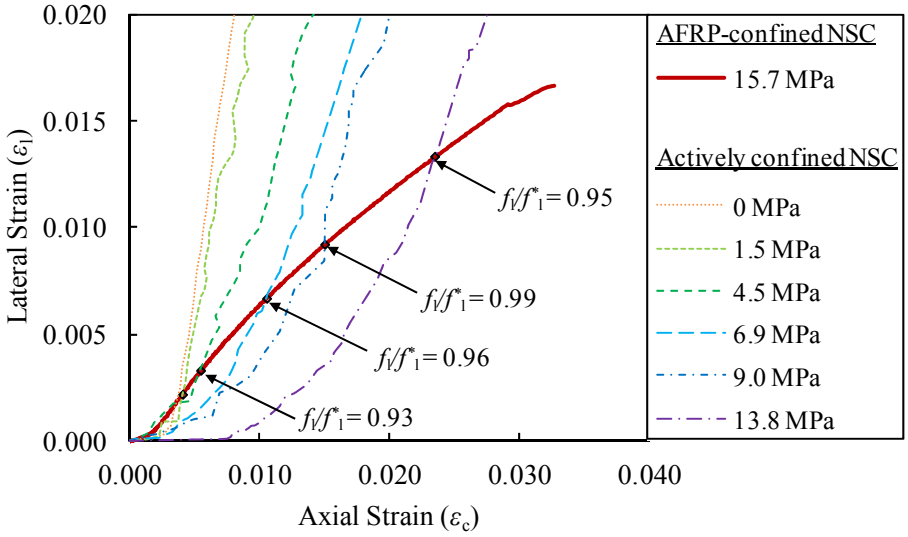

(a)

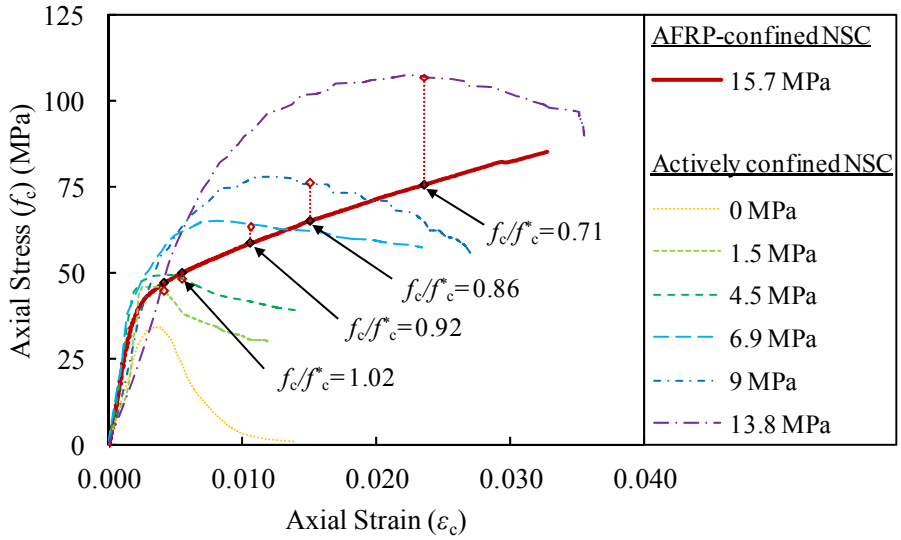

(b)

Figure 2. Comparison of actively confined and AFRP-confined NSC specimens: (a) lateral strain-axial strain curves; (b) axial stress-strain curves (Group U35)

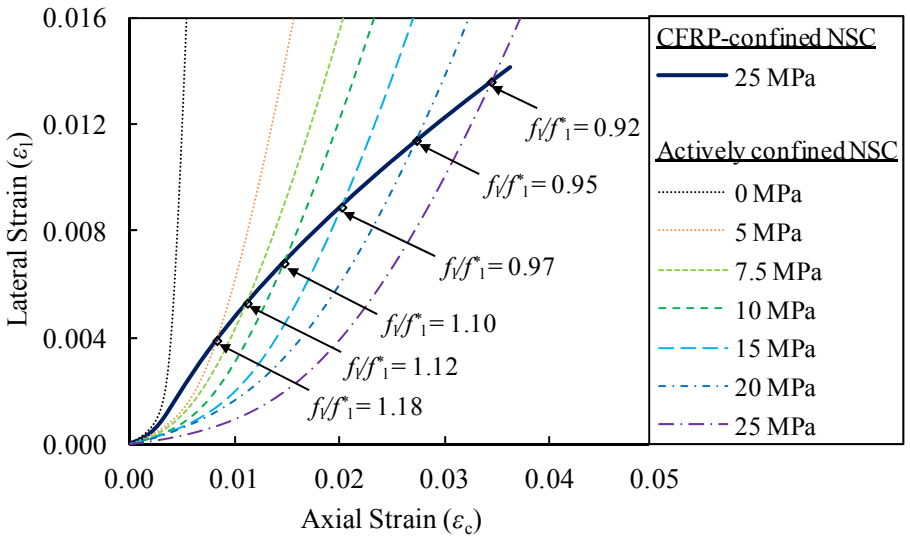

(a)

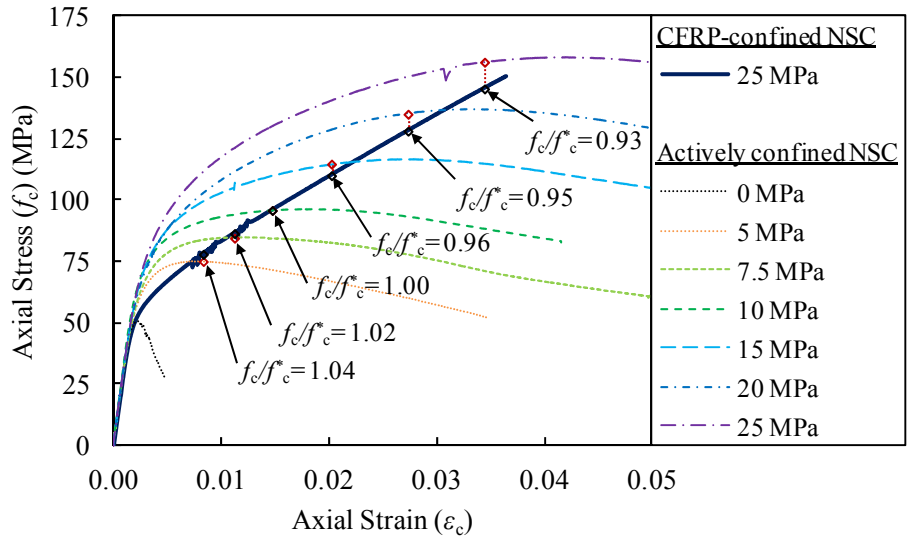

(b)

Figure 3. Comparison of actively confined and CFRP-confined NSC specimens: (a) lateral strain-axial strain curves; (b) axial stress-strain curves (Group U52)

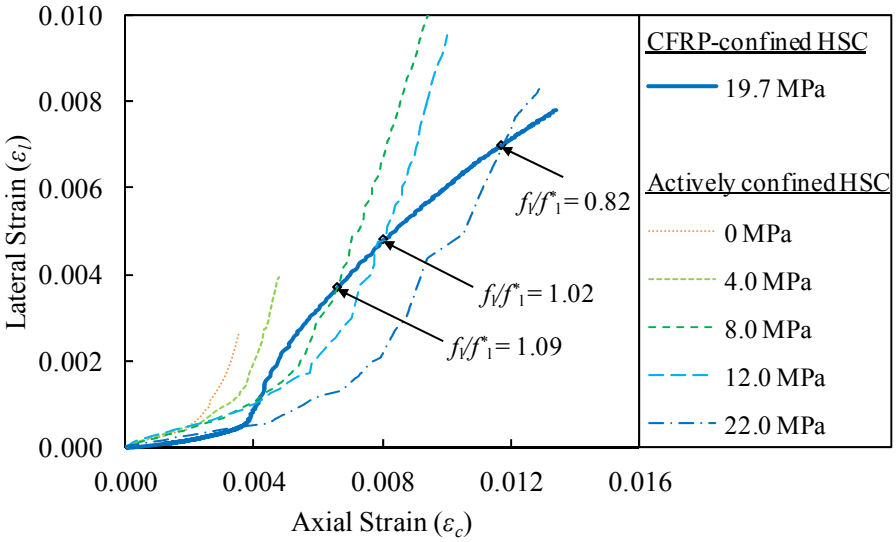

(a)

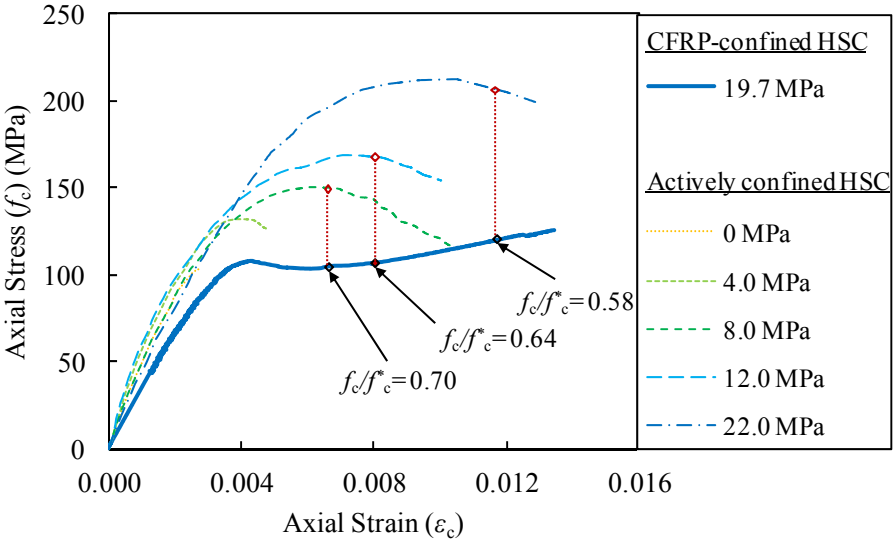

(b)

Figure 4. Comparison of actively confined and CFRP-confined HSC specimens: (a) lateral strain-axial strain curves; (b) axial stress-strain curves (Group U103)

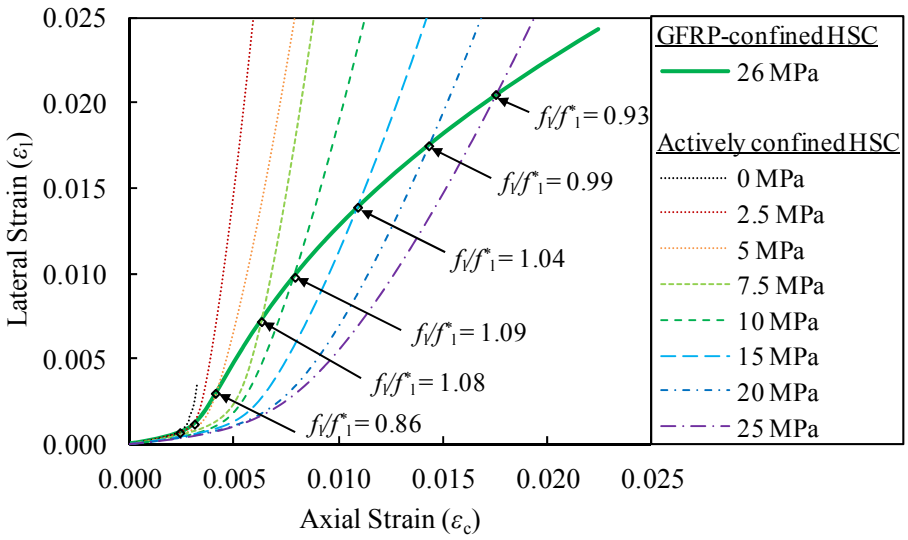

(a)

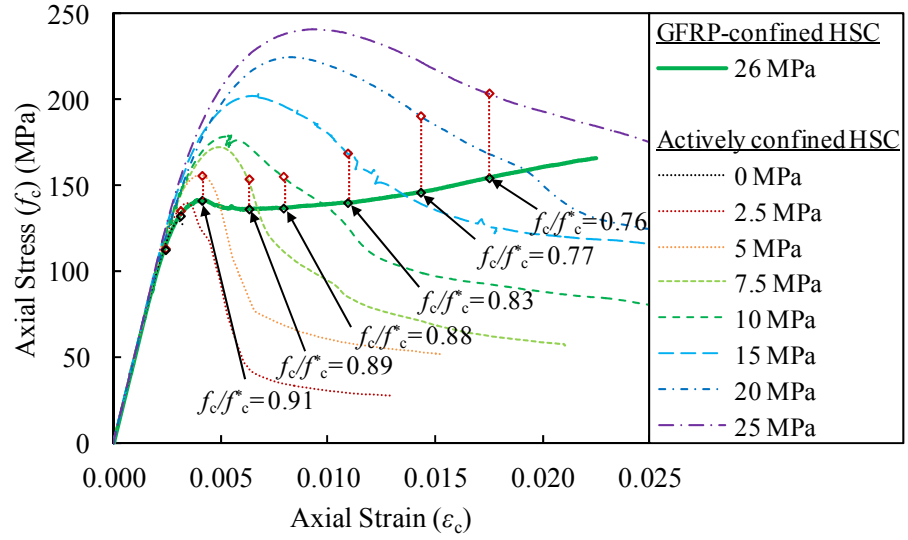

(b)

Figure 5. Comparison of actively confined and GFRP-confined HSC specimens: (a) lateral strain-axial strain curves; (b) axial stress-strain curves (Group U128)

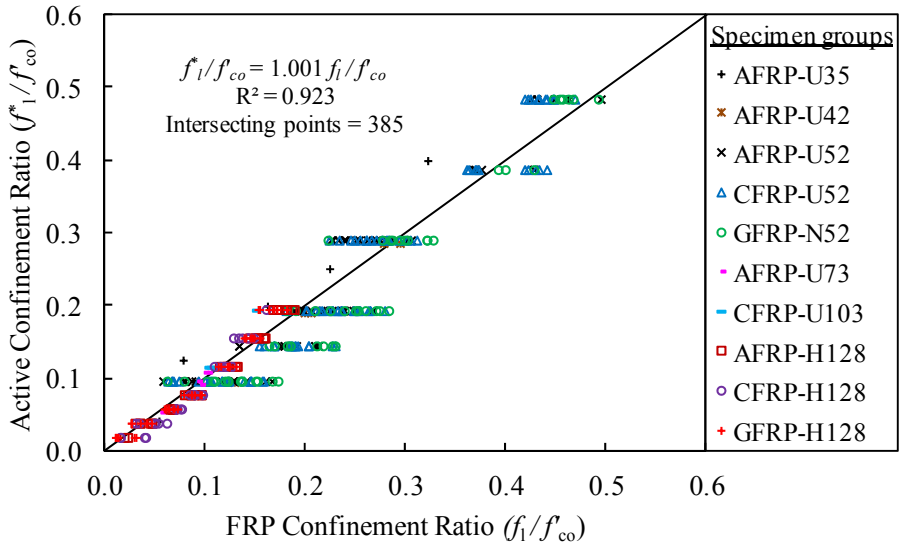

Figure 6. Confinement ratios of actively confined concrete (f^*_l/f'_{co}) and FRP-confined concrete (f_l/f'_{co})

To establish the relative axial stress levels of actively confined and FRP-confined specimens, the coordinates of the axial stresses and axial strains corresponding to the points of intersection in Figures 2(a) to 5(a) are marked in Figures 2(b) to 5(b). As evident from Figures 2(b) to 5(b), at a given axial and lateral strain and confining pressure, the FRP-confined concrete exhibits lower axial stress than that of the companion actively confined concrete. These differences in the axial stresses (Δf_c) indicate that, at a given axial and lateral strains and confining pressure, the magnitude of axial stresses on the axial stress-strain relationships of confined concrete is dependent on the application path of confining pressure, and hence varies from one confinement system to another. This observation also indicates that the path independency assumption used by the existing analysis-oriented models is not entirely correct.

The difference in the axial stresses between FRP-confined and actively confined concrete can be quantified in terms of an axial stress ratio (f_c/f^*_c). To study the factors influencing the axial stress ratio of FRP-confined concrete-to-actively confined concrete (f_c/f^*_c), companion FRP-confined and actively confined specimens having similar confinement ratios (i.e. $f_l/f'_{co} \approx f^*_l/f'_{co}$ with no more than 20% variation) at the intersecting points of their lateral strain-axial strain curves were identified. Figure 7(a) illustrates the relationship between the axial stress ratio (f_c/f^*_c) and the unconfined concrete strength (f'_{co}) for a given range of confinement ratios (f_l/f'_{co}), whereas Figure 7(b) illustrates the relationship between the axial stress ratio (f_c/f^*_c) and confinement ratio (f_l/f'_{co}) for a given unconfined concrete strength (f'_{co}). As evident from Figures 7(a) and 7(b), the axial stress ratio (f_c/f^*_c) reduces with either an increase in the unconfined concrete strength (f'_{co}) or the confinement ratio (f_l/f'_{co}). This accords with the previous observations from Figures 2(b) to 5(b), where it was found that, at a given axial strain, lateral strain, and confining pressure, the observed differences in axial stresses (Δf_c) between actively confined and FRP-confined specimens increase with an increase in the level of confining pressure and were more pronounced in specimens with higher concrete strengths.

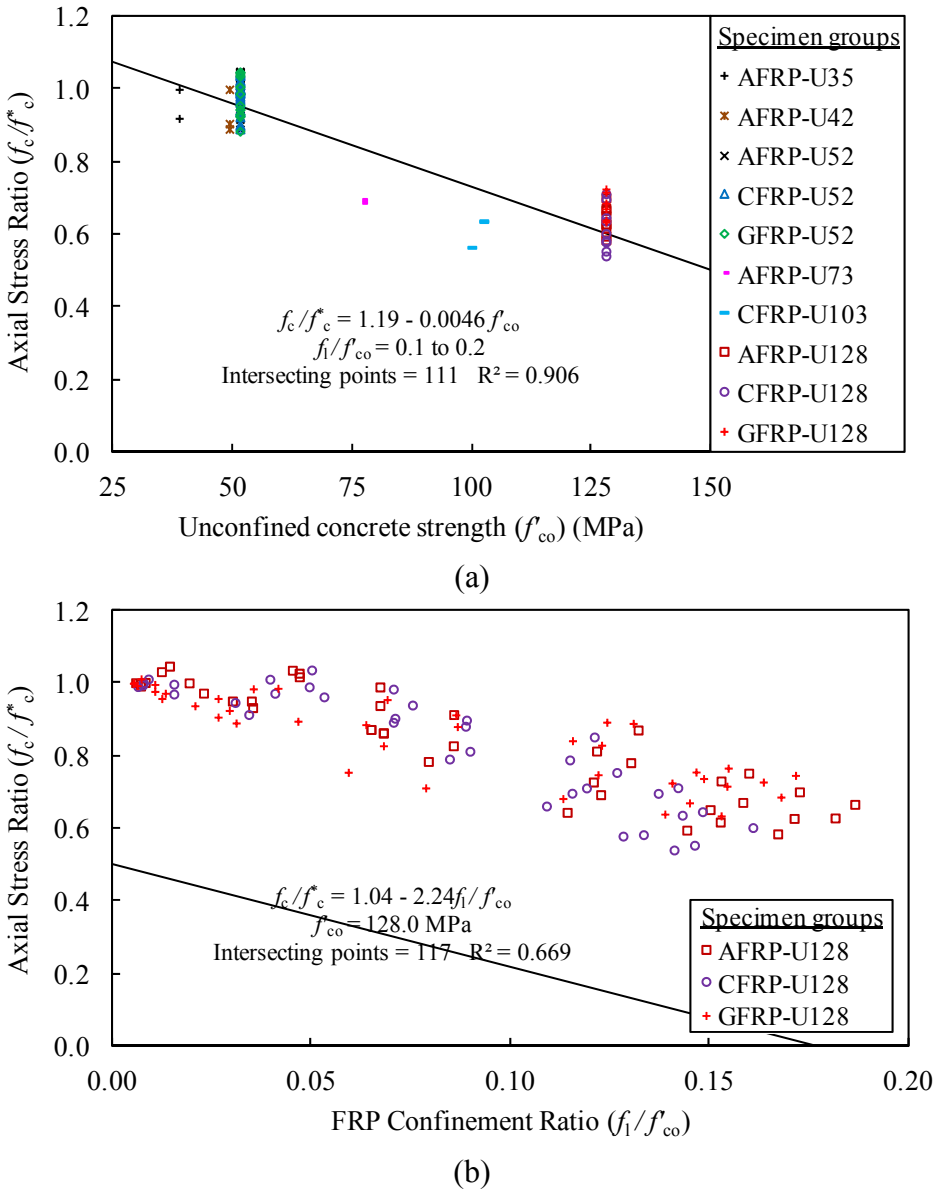

Figure 7. Variation of axial stress ratio of FRP-confined concrete-to-actively confined concrete (f_c/f^*_c) with: (a) unconfined concrete strength (f'_{co}); (b) FRP confinement ratio(f_l/f'_{co})

3.2 Confining pressure gradient between actively confined and FRP-confined concretes

Factors influencing the differences in axial stresses (Δf_c) between actively confined and FRP-confined concretes were discussed in the preceding section. This section presents a new approach for estimating the difference in confining pressures, at a given axial stress and axial strain, between actively confined and FRP-confined concretes. This difference in confining pressures of the companion actively confined and FRP-confined concretes is referred to in this paper as the confining pressure gradient (i.e. $\Delta f_l = f_l - f^*_l$). Using the test results from the databases (Ozbakkaloglu and Lim 2013; Lim and Ozbakkaloglu 2014a,e) and the specimen groups investigated in this study (i.e. U35, U42, U52, U72, U103, and U128), companion actively confined and FRP-confined specimens that attained the same axial stress ($f^*_c = f_c$) at a given axial strain ($\varepsilon^*_c = \varepsilon_c$) were compared and their difference in confining pressures (i.e. $\Delta f_l = f_l - f^*_l$) were recorded. Using the recorded results from both groups, Eq. 2 is proposed for the prediction of the confining pressure gradient (Δf_l).

$$\Delta f_l = 0.13 {f'_{co}}^{0.24} K_l^{0.95} \varepsilon_l \quad (2)$$

where Δf_l, f'_{co}, K_l are in MPa.

Figure 8 shows the comparison of the confining pressure gradients (Δf_l) predicted using Eq. 2 with the experimental results. As evident from the figure, the predicted values are in good agreement with the test results obtained from the database results as well as the results obtained from the specimen groups investigated in this study. The confining pressure gradient (Δf_l) determined from Eq. 2 is to be used to establish the equivalent confining pressure of FRP-confined concrete (f_l) by subtracting Δf_l from the corresponding confining pressure in actively confined concrete (f^*_l). To illustrate the application of this procedure in the prediction of the axial stress-strain curves of FRP-confined concrete, two examples are provided subsequently in the paper in Figure 13.

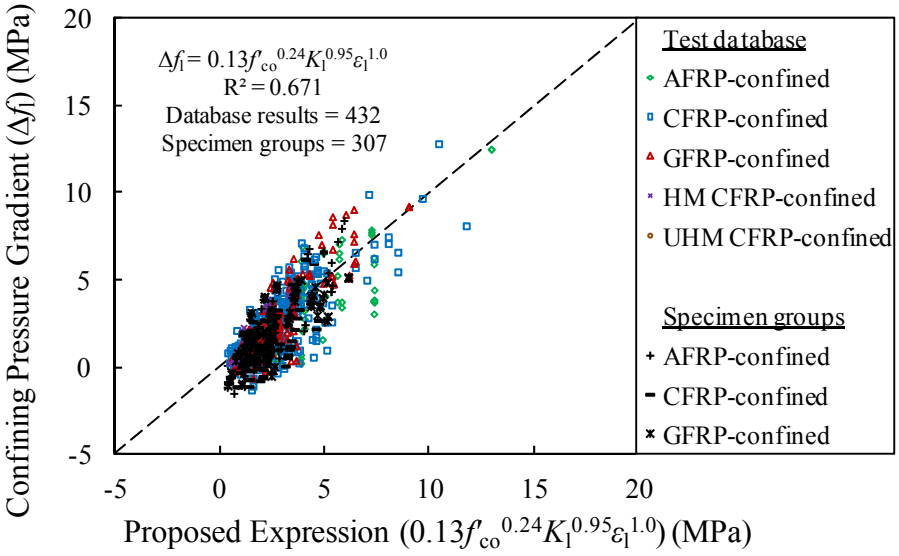

Figure 8. Comparison of confining pressure gradient (Δf_l) with proposed expression

4. ACTIVELY CONFINED AND FRP-CONFINED CONCRETE MODELS

As discussed previously, models that establish the stress-strain relationship of FRP-confined concrete on the basis of actively confined concrete are classified as analysis-oriented FRP-confined concrete models. The key to an accurate analysis-oriented FRP-confined concrete model is the accuracy of the estimated: i) lateral strain-axial strain relationship, and ii) stress-strain base curves of the actively confined concrete. The first issue has been addressed in a number of studies using experimental test results for both actively confined and FRP-confined NSC (Teng et al. 2007; Lim and Ozbakkaloglu 2014e), as well as HSC (Lim and Ozbakkaloglu 2014e). The second issue in regard to the stress-strain base curve is discussed in detail in the following sections, together with possible improvements identified from the assessment of existing models. In these sections, the performance of the existing actively confined concrete models in establishing the stress-strain base curves were first assessed. Following this the performance of the existing analysis-oriented models, which use such base curves to establish the stress-strain curve of FRP-confined concrete, were evaluated.

4.1 Performance of existing actively confined concrete models

Table 2 presents a summary of the existing analysis-oriented FRP-confined concrete models. As shown in the table, all of the analysis-oriented FRP-confined concrete models rely on other actively confined concrete models for the stress-strain base curve predictions. Except Albanesi et al. (2007), all of the models summarized in Table 2 adopted Popovics's expression (1973) or the modified version of the expression to establish the stress-strain base curves for generating the full stress-strain curve of FRP-confined concrete. Carreira and Chu's brittleness constant (1985) is used by the models to predict the curvature of transition of the stress-strain base curves. Figure 9 illustrates the comparison of Popovics's stress-strain base curves established using Xiao's model (2010) with the experimental results of actively confined concrete specimens in Groups U119 and U123. As clearly evident from the figure, the three major sources of inaccuracy in the predicted stress-strain base curves include: i) inaccurate prediction of the peak condition of actively confined concrete, ii) lack of consideration of the residual stress, and iii) inaccurate slope of the predicted descending branch of the stress-strain curve. The first issue results from the use of inaccurate peak condition expressions, whereas the second and third issues result from the use of Popovics's model, which is often unable to accurately predict the post-peak stress-strain behavior. These deficiencies in turn undermine the accuracy of the stress-strain curves of FRP-confined concrete predicted by the existing analysis-oriented models.

To investigate the first and second issues in regard to the peak and residual conditions, the performances of nine existing actively confined concrete models (Richart et al. 1929; Mills and Zimmerman 1970; Mander et al. 1988; Xie et al. 1995; Attard and Setunge 1996; Ansari and Li 1998; Candappa et al. 2001; Imran and Pantazopoulou 2001; Samani and Attard 2012) and four analysis-oriented models that are applicable to both actively confined and FRP-confined concrete (Binici 2005; Jiang and Teng 2007; Teng et al. 2007; Xiao et al. 2010) were assessed. The experimental values used for the model assessments were based on the specimen results of the actively confined concrete database (Lim and Ozbakkaloglu 2014e). Out of the total 377 datasets available in the experimental database, 341, 243, and 173 datasets were used in the assessment of the peak stress ratio (f^*_{cc}/f'_{co}), peak strain ratio ($\varepsilon^*_{cc}/\varepsilon_{co}$), and residual stress ratio ($f_{c,res}/f'_{co}$), respectively. In the calculations of the experimental values, the compressive strength (f'_{co}) and the corresponding axial strain (ε_{co}) of unconfined concrete were based on the test results of the unconfined cylinders. In calculating model predictions of the peak strain ratios ($\varepsilon^*_{cc}/\varepsilon_{co}$), ε_{co} values were determined using the expressions given in the original publication when available. If an expression was not specified in the original publication, the ε_{co} values were then based on the experimental values obtained from cylinder tests. The prediction statistics of the existing models are given in Table 3. In the statistics shown in the table, average absolute error (*AAE*) was used to establish overall model accuracy; standard deviation (*SD*) was used to establish the magnitude of the associated scatter for each model; and mean (*M*) was used to describe the associated average overestimation or underestimation of the model, where an overestimation is represented by a mean value greater than 1. In addition to the results shown in Table 3, the variation of the model predictions of peak stress, peak strain, and residual stress ratios (f^*_{cc}/f'_{co}, $\varepsilon^*_{cc}/\varepsilon_{co}$, $f_{c,res}/f'_{co}$) with the confinement ratio (f^*_l/f'_{co}) are presented in Figures 10(a) to

10(c). It is worth noting that, as shown in Table 3 and Figure 10(c), only four of the existing models are capable of predicting the residual stress ratios ($f_{c,res}/f'_{co}$) (Attard and Setunge 1996; Imran and Pantazopoulou 2001; Binici 2005; Samani and Attard 2012). The results shown in Table 3 and Figure 10 indicate that a further improvement in the predictions of the peak stress, peak strain, and residual stress ratios (f^*_{cc}/f'_{co}, $\varepsilon^*_{cc}/\varepsilon_{co}$, $f_{c,res}/f'_{co}$) is possible. This is also evidenced by the improved predictions of the new model proposed in this study, which is also shown in Figure 10 and is presented in detail later in the paper.

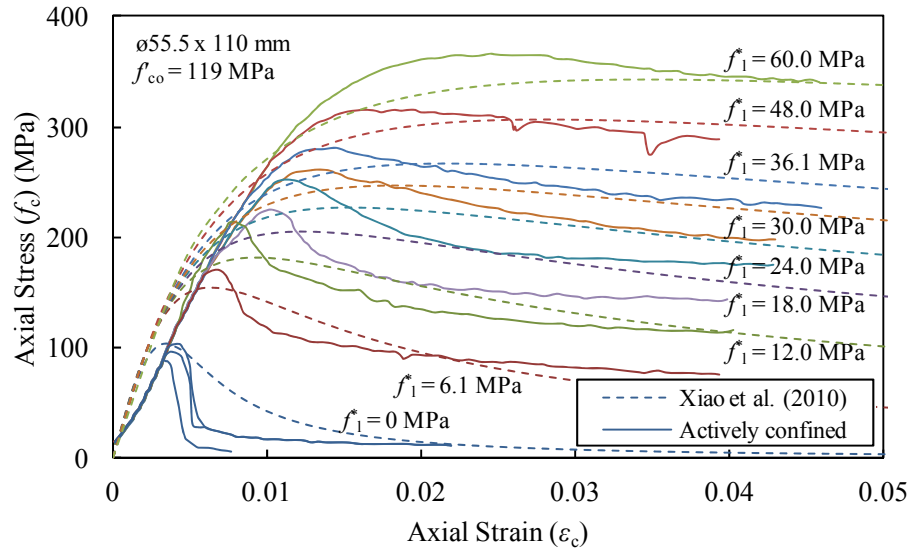

(a)

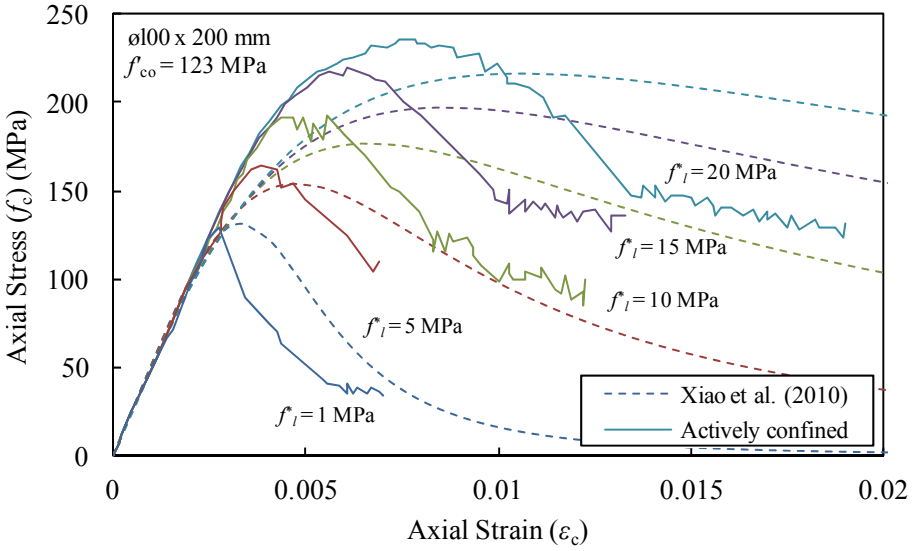

(b)

Figure 9. Stress-strain base curves of actively confined concretes predicted using Xiao's model (2010): (a) Specimen Group U119; and (b) Specimen Group U123

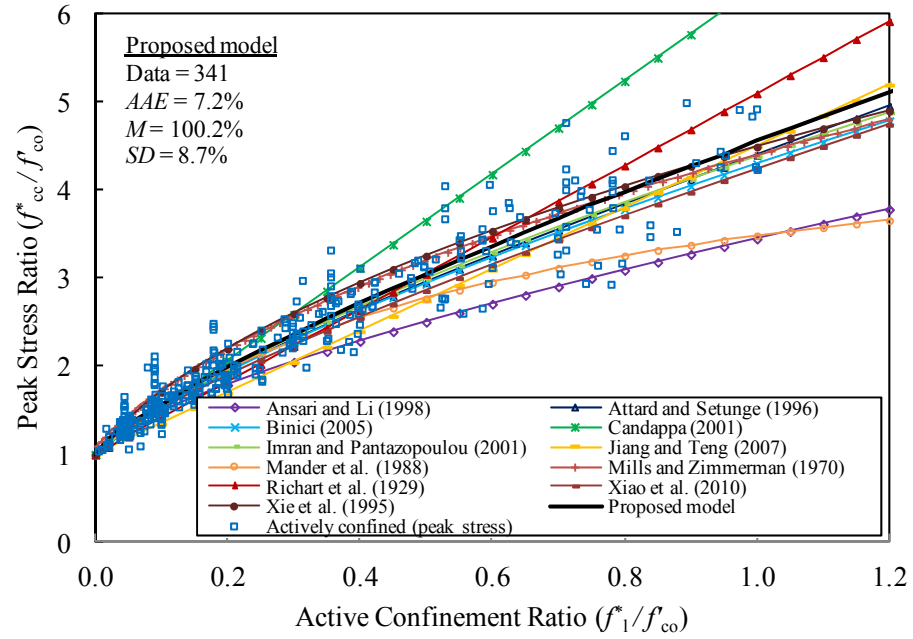
Proposed model
Data = 341
AAE = 7.2%
M = 100.2%
SD = 8.7%
Ansari and Li (1998)
Attard and Setunge (1996)
Binici (2005)
Candappa (2001)
Imran and Pantazopoulou (2001)
Jiang and Teng (2007)
Mander et al. (1988)
Mills and Zimmerman (1970)
Richart et al. (1929)
Xiao et al. (2010)
Xie et al. (1995)
Proposed model
Actively confined (peak stress)
Peak Stress Ratio (f^*_{cc}/f'_{co})
Active Confinement Ratio (f^*_l/f'_{co})
0
1
2
3
4
5
6
0.0
0.2
0.4
0.6
0.8
1.0
1.2

(a)

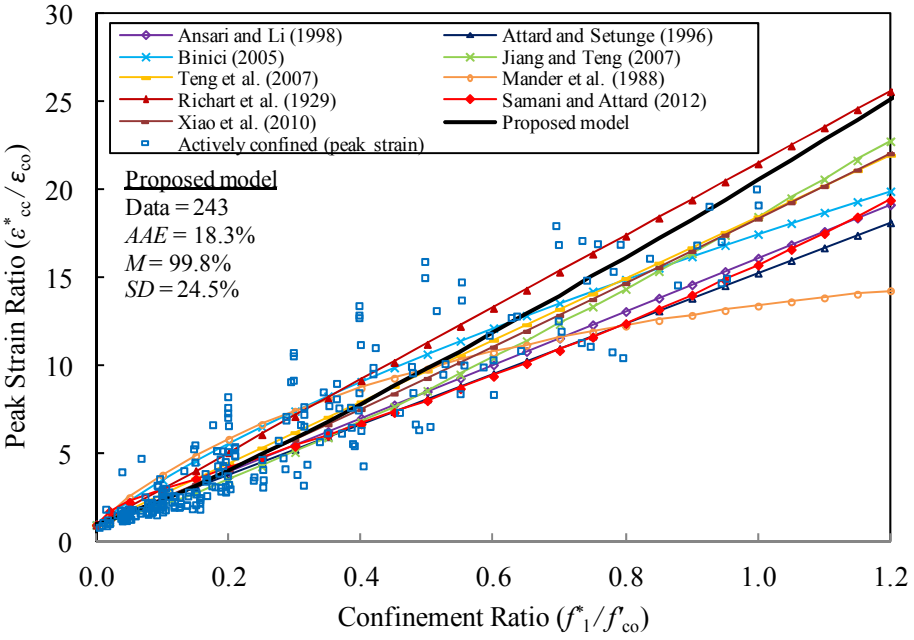
Ansari and Li (1998)
Attard and Setunge (1996)
Binici (2005)
Jiang and Teng (2007)
Teng et al. (2007)
Mander et al. (1988)
Richart et al. (1929)
Samani and Attard (2012)
Xiao et al. (2010)
Proposed model
Actively confined (peak strain)
Proposed model
Data = 243
AAE = 18.3%
M = 99.8%
SD = 24.5%
Peak Strain Ratio ($\varepsilon^*_{cc}/\varepsilon_{co}$)
Confinement Ratio (f^*_l/f'_{co})
0
5
10
15
20
25
30
0.0
0.2
0.4
0.6
0.8
1.0
1.2

(b)

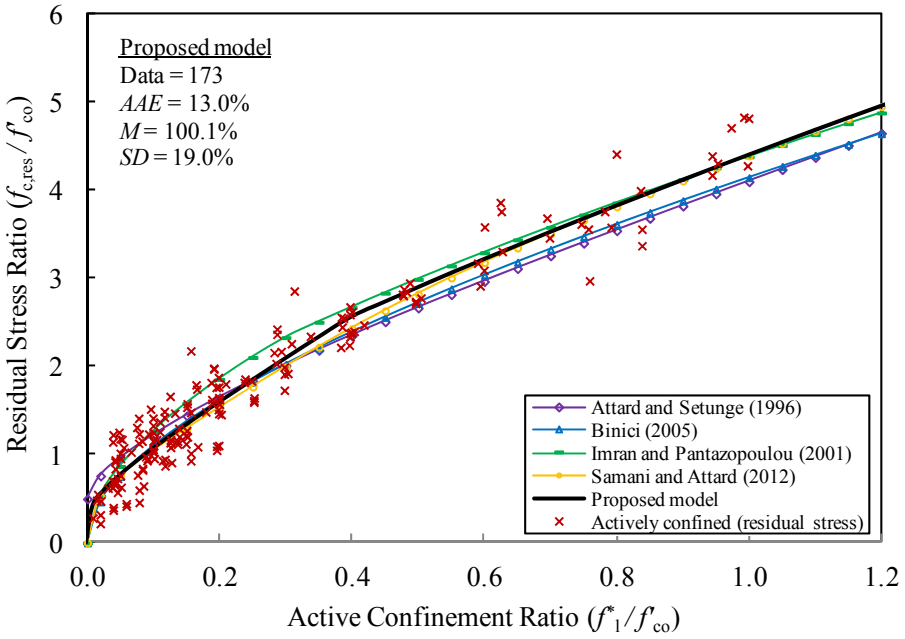

(c)

Figure 10. Comparison of model predictions of: (a) peak stress ratios (f^*_{cc}/f'_{co}); (b) peak strain ratios ($\varepsilon^*_{cc}/\varepsilon_{co}$); and (c) residual stress ratios ($f_{c,res}/f'_{co}$) of actively confined concretes with experimental results

4.2 Performance of existing analysis-oriented FRP-confined concrete models

As summarized in Table 2, the existing analysis-oriented FRP-confined concrete models are divided into three categories according to the basis of the model development, whether it was either: (1) based on expressions of other actively confined concrete models (Spoelstra and Monti 1999; Fam and Rizkalla 2001; Chun and Park 2002; Marques et al. 2004; Binici 2005; Albanesi et al. 2007; Aire et al. 2010); (2) based on the test results of FRP-confined concrete (Mirmiran and Shahawy 1997a,b; Harries and Kharel 2002; Moran and Pantelides 2002a); or (3) based on the test results of both actively confined and FRP-confined concretes (Jiang and Teng 2007; Teng et al. 2007; Xiao et al. 2010). As discussed previously, all of the existing analysis-oriented models were based on the stress path dependency assumption. To illustrate the implications of this assumption, Figures 11(a) and 11(b) show the comparison of the stress-strain predictions of the existing models with the test results of the NSC and HSC specimens in Groups U42 and U110, respectively. As evident from Figure 11(a), most of the existing models significantly overestimate the axial stress (f_c) of FRP-confined NSC for a given axial strain (ε_c). This overestimation becomes even more pronounced when the models are applied to FRP-confined HSC, as shown in Figure 11(b).

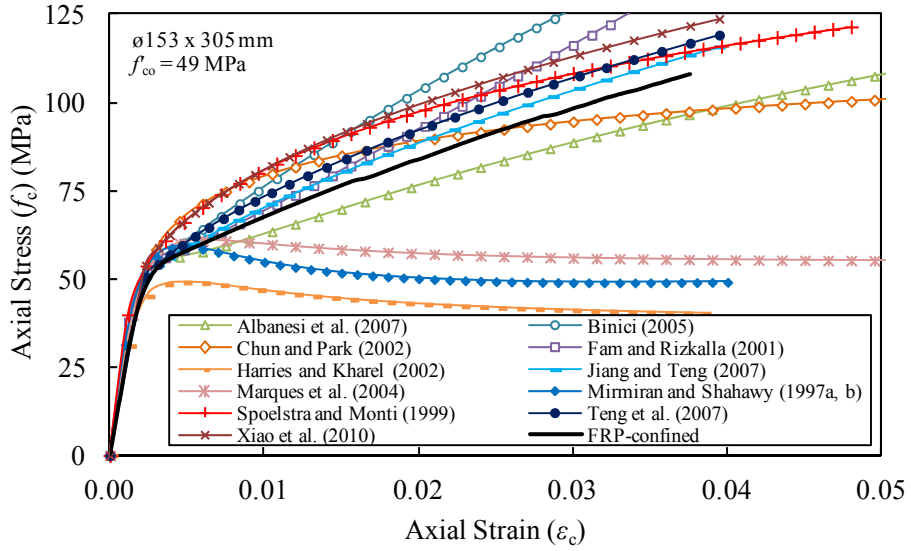

(a)

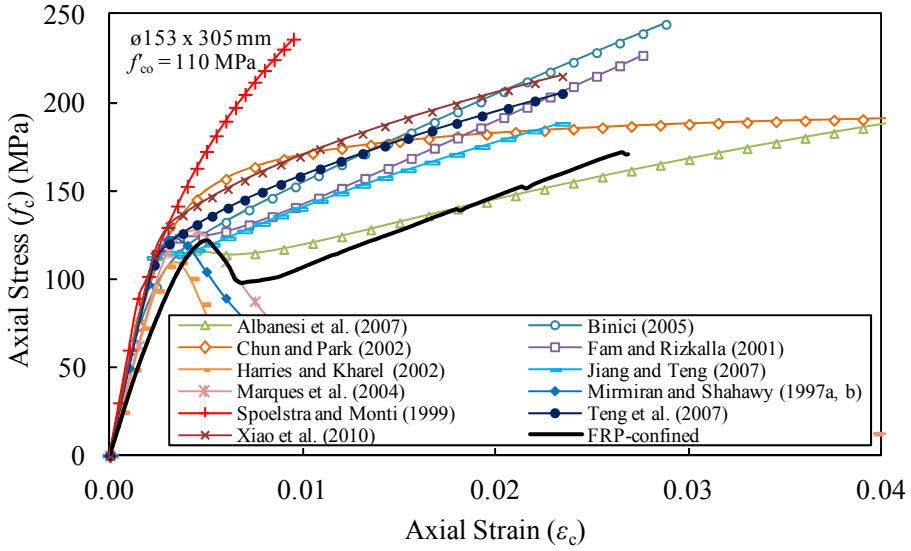

(b)

Figure 11. Comparison of model predictions of axial stress-strain curves of: (a) FRP-confined NSC (Group U42); and (b) FRP-confined HSC (Group U110) with experimental results

To complete the assessment, the ultimate condition of FRP-confined concrete predicted by the existing analysis-oriented models were compared with the experimental results of the FRP-confined concrete database (Ozbakkaloglu and Lim 2013; Lim and Ozbakkaloglu 2014a). Table 4 presents the prediction statistics of the existing analysis-oriented models. Out of the 1156 datasets, 961 and 683 datasets from the experimental database were used in the assessment of the strength and strain enhancement ratios (f'_{cc}/f'_{co} and $\varepsilon_{cu}/\varepsilon_{co}$), respectively. It should be noted that, only the models that had sufficiently defined parameters and test results that had sufficient detail to allow for numerical calculations were used in the assessment (Mirmiran and Shahawy 1997a,b; Spoelstra and Monti 1999; Fam and Rizkalla 2001; Chun and Park 2002; Harries and Kharel 2002; Marques et al. 2004; Binici 2005; Albanesi et al. 2007; Jiang and Teng 2007; Teng et al. 2007; Xiao et al. 2010).

As evident from the statistics presented in Table 4, the models in Category 3 that were developed on the basis of both actively confined and FRP-confined concrete (i.e. (Jiang and Teng 2007; Teng et al. 2007; Xiao et al. 2010)) outperformed the other models in the prediction of strength and strain enhancement ratios of FRP-confined concrete (f'_{cc}/f'_{co} and $\varepsilon_{cu}/\varepsilon_{co}$). Given these models' applicability to both types of confinement systems, understanding their relative performance when applied to these two confinement systems is of significant interest. As shown by the comparison of the mean values of the peak stress ratios (f^*_{cc}/f'_{co}) in Table 3 and the strength enhancement ratios (f'_{cc}/f'_{co}) in Table 4, these models either accurately estimate the mean of f^*_{cc}/f'_{co} and overestimate the mean of f'_{cc}/f'_{co}, or accurately estimate the mean of f'_{cc}/f'_{co} and underestimate the mean of f^*_{cc}/f'_{co}. The difference between the mean values of f'_{cc}/f'_{co} and f^*_{cc}/f'_{co} estimated by these models was found to be no less than 8%, indicating that a unified model that can predict both f'_{cc}/f'_{co} and f^*_{cc}/f'_{co} needs to take into account the axial stress difference (Δf_c) between the two confinement systems.

The performance statistics shown in Tables 3 and 4 support the previously discussed observations on identified areas for improvement, indicating that the modeling accuracy for both actively confined and FRP-confined concretes can be further improved. To this end, using the most complete databases to date (Ozbakkaloglu and Lim 2013; Lim and Ozbakkaloglu 2014a,e), a new stress-strain model that is applicable to both actively confined and FRP-confined concretes is developed and it is presented in the following section.

5. UNIFIED MODEL FOR CONFINED CONCRETE

This section presents a unified model applicable to both actively confined and FRP-confined concretes that is developed in the present study. The model accurately establishes: i) the stress-strain curve of actively confined concrete, ii) the lateral strain-axial strain relationship of concrete under active or FRP confinement, and iii) a relationship between compressive behaviors of actively confined and FRP-confined through a novel approach. These three main components of the proposed model are presented in the following sections.

5.1 Actively confined concrete

5.1.1 Peak and post-peak conditions of actively confined concrete

The peak and residual conditions are the two previously identified benchmarks in characterizing the stress-strain relationship of actively confined concrete. In this study, a third condition, referred to as the inflection point, is considered to accurately describe the descending branch of stress-strain relationship connecting the peak and residual conditions. As illustrated in Figure 1, the inflection point ($\varepsilon_{c,i}$) corresponds to the change in the sign of curvature of the descending branch of the stress-strain curve from negative to positive.

For the prediction of the peak stress (f^*_{cc}) and strain (ε^*_{cc}) of actively confined concrete, Eqs. 3 and 4 proposed by Lim and Ozbakkaloglu (2014f) based on the results of the actively confined concrete database (Lim and Ozbakkaloglu 2014e), are adopted.

$$f^*_{cc} = f'_{co} + 5.2 f'^{0.91}_{co} \left(\frac{f^*_l}{f'_{co}}\right)^a \quad \text{where} \quad a = f'^{-0.06}_{co} \tag{3}$$

$$\varepsilon^*_{cc} = \varepsilon_{co} + 0.045 \left(\frac{f^*_l}{f'_{co}}\right)^{1.15} \tag{4}$$

where f^*_{cc}, f^*_l, f'_{co} are in MPa; and ε_{co} is to be calculated using Eq. 5.

$$\varepsilon_{co} = \frac{f'^{0.225}_{co}}{1000} \left(\frac{152}{D}\right)^{0.1} \left(\frac{2D}{H}\right)^{0.13} \tag{5}$$

where f'_{co} is in MPa, D and H are the specimen diameter and height in mm.

The residual stress ($f_{c,res}$) and the axial strain corresponding to the inflection point of the descending branch of stress-strain curve ($\varepsilon_{c,i}$) are to be predicted using Eqs. 6 and 7, respectively.

$$f_{c,res} = 1.6 f^*_{cc} \left(\frac{f^{*0.24}_l}{f'^{0.32}_{co}}\right) \quad \text{and} \quad f_{c,res} \le f^*_{cc} - 0.15 f'_{co} \tag{6}$$

$$\varepsilon_{c,i} = 2.8 \varepsilon^*_{cc} \left(\frac{f_{c,res}}{f^*_{cc}}\right) f'^{-0.12}_{co} + 10 \varepsilon^*_{cc} \left(1 - \frac{f_{c,res}}{f^*_{cc}}\right) f'^{-0.47}_{co} \tag{7}$$

where $f^*_{cc}, f^*_l, f_{c,res}, f'_{co}$ are in MPa

5.1.2 Stress-strain curve of actively confined concrete

The proposed stress-strain curve for actively confined concrete is presented in this section. The ascending and descending portions of the curve are based on two separate expressions. For the ascending branch, the shape of the curve is based on Eq. 8 originally proposed by Popovics (1973). For the descending branch, the shape of the curve is based on a new expression, given in Eq. 9, which overcomes the previously discussed deficiencies of Popovics's expression.

$$f_c = \frac{f^*_{cc} (\varepsilon_c / \varepsilon^*_{cc}) r}{r - 1 + (\varepsilon_c / \varepsilon^*_{cc})^r} \quad \text{if} \quad 0 \le \varepsilon_c \le \varepsilon^*_{cc} \tag{8}$$

$$f_c = f^*_{cc} - \frac{f^*_{cc} - f_{c,res}}{1 + \left(\frac{\varepsilon_c - \varepsilon^*_{cc}}{\varepsilon_{c,i} - \varepsilon^*_{cc}}\right)^{-2}} \quad \text{if} \quad \varepsilon_c > \varepsilon^*_{cc} \tag{9}$$

where $f_c, f^*_{cc}, f_{c,res}, f'_{co}$ and E_c are in MPa; ε_c is the axial strain variable; r is the expression for concrete brittleness, to be calculated using Eq. 10 proposed by Carreira and Chu (1985); E_c is the elastic modulus of concrete, to be calculated using Eq. 11.

$$r = \frac{E_c}{E_c - f^*_{cc} / \varepsilon^*_{cc}} \tag{10}$$

$$E_c = 4400\sqrt{f'_{co}} \tag{11}$$

where E_c and f'_{co} are in MPa.

Figure 12 illustrates the comparison of the stress-strain curves established using the proposed model with the test results of the actively confined concrete specimens in Groups U119 and U123. As evident from the accurately predicted stress-strain curves shown in the figure, the proposed model has overcome the aforementioned modeling issues (Figure 9) and is in good agreement with the experimental results.

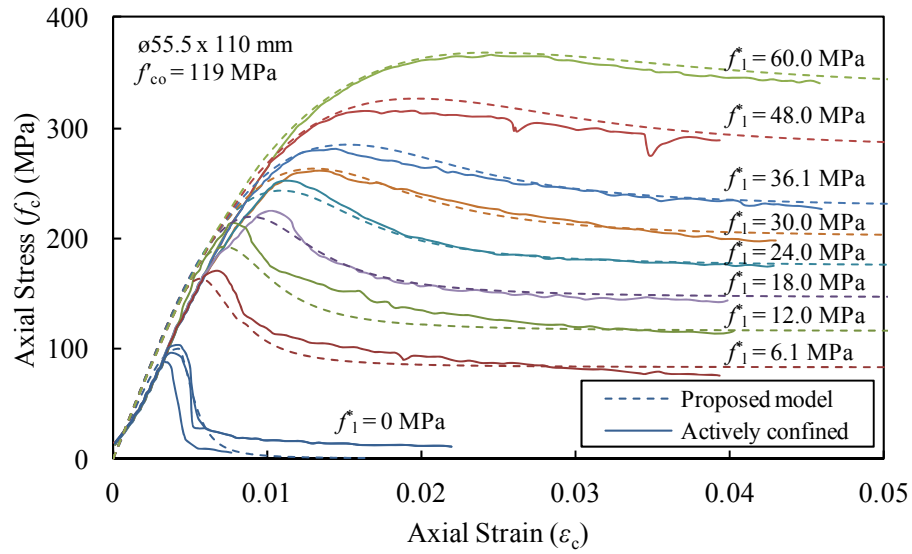

(a)

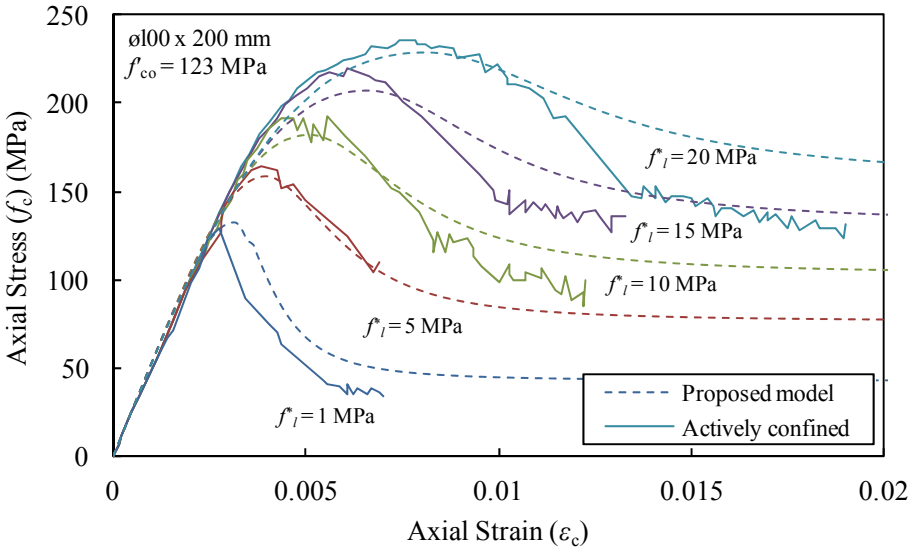

(b)

Figure 12. Stress-strain base curves of actively confined concretes predicted using the proposed model: (a) Specimen Group U119; and (b) Specimen Group U123

5.2 Lateral strain-axial strain curves of actively confined and FRP-confined concretes

As was previously illustrated in Figures 2(a) to 5(a) and Figure 6, at a given axial strain, lateral strains of actively confined and FRP-confined concretes correspond, when they are subjected to the same lateral confining pressure. This premise allows the development of a unified expression to describe the dilation behavior of confined concrete, which is applicable to both actively confined and FRP-confined concretes. The expression given in Eq. 12, which was proposed by Lim and Ozbakkaloglu (2014e) to predict the lateral strain-axial strain relationship of both actively confined and FRP-confined concretes, is adopted for this purpose in the present study. The shape and the important coordinates (ε^*_{cc}, ε^*_{lc}, and $\varepsilon_{c,res}$, $\varepsilon_{l,res}$, and ε_{cu}, $\varepsilon_{h,rup}$) of the lateral strain-axial strain curves predicted by the expression was established and validated using the database results of actively confined (Lim and Ozbakkaloglu 2014e) and FRP-confined concretes (Ozbakkaloglu and Lim 2013; Lim and Ozbakkaloglu 2014a).

$$\varepsilon_c = \frac{\varepsilon_l}{\upsilon_i\left(1+\left(\frac{\varepsilon_l}{\upsilon_i\varepsilon_{co}}\right)^n\right)^{\frac{1}{n}}} + 0.04{\varepsilon_l}^{0.7}\left(1+21\left(\frac{f_l}{f'_{co}}\right)^{0.8}\right) \tag{12}$$

$$\upsilon_i = 8\times10^{-6}{f'_{co}}^2 + 0.0002f'_{co} + 0.138 \tag{13}$$

$$n = 1 + 0.03f'_{co} \tag{14}$$

where υ_i is the initial Poisson's ratio of concrete, to be calculated using Eq. 13 as proposed by Candappa et al . (2001); ε_{co} is the axial strain corresponding to the compressive strength of unconfined concrete, to be calculated using Eq. 5; and n is the curve shape parameter, to be calculated using Eq. 14. It should also be noted that the confining pressure (f_l) in Eq. 12 is a variable for FRP-confined concrete, which can be determined from Eq. 1 by gradually increasing the lateral strain (ε_l) until the hoop rupture strain of the FRP jacket ($\varepsilon_{h,rup}$) is reached. The hoop rupture strain of the FRP jacket can be predicted using Eq. 15 proposed by Lim and Ozbakkaloglu (2014a).

$$\varepsilon_{h,rup} = (0.9 - 2.3f'_{co}\times10^{-3} - 0.75E_f\times10^{-6}\ )\varepsilon_f \tag{15}$$

where f'_{co} and E_f are in MPa.

5.3 Generation of axial stress-strain curves of FRP-confined concrete

To illustrate the application of the proposed model, Figures 13(a) and 13(b) show examples of axial stress-strain curves of FRP-confined NSC and HSC established using the parameters of specimens in Groups U42 and U110, respectively. To obtain the complete stress-strain curve of FRP-confined concrete, shown with dashed-dotted lines in Figure 13, the iterative procedure illustrated in Figure 14 is to be followed. As shown in Figure 14, the confining pressure of FRP jacket (f_l), which increases with the lateral expansion of concrete, will be calculated first from Eq. 1 by gradually increasing the lateral strain (ε_l). Next, the axial strain (ε_c) that corresponds to each increment of the lateral strain (ε_l) and the confining pressure (f_l) will be calculated from the lateral strain-axial strain expression given in Eq. 12. The axial stress (f_c) of FRP-confined concrete that corresponds to the axial strain (ε_c) will then be

calculated from the stress-strain base curve expression of actively confined concrete given in Eqs. 8 and 9, after considering the confining pressure gradient (Eq. 2) between the two confinement systems ($f^*_l = f_l - \Delta f_l$). The incremental procedure will be terminated when the hoop rupture strain of FRP is reached (Eq. 15).

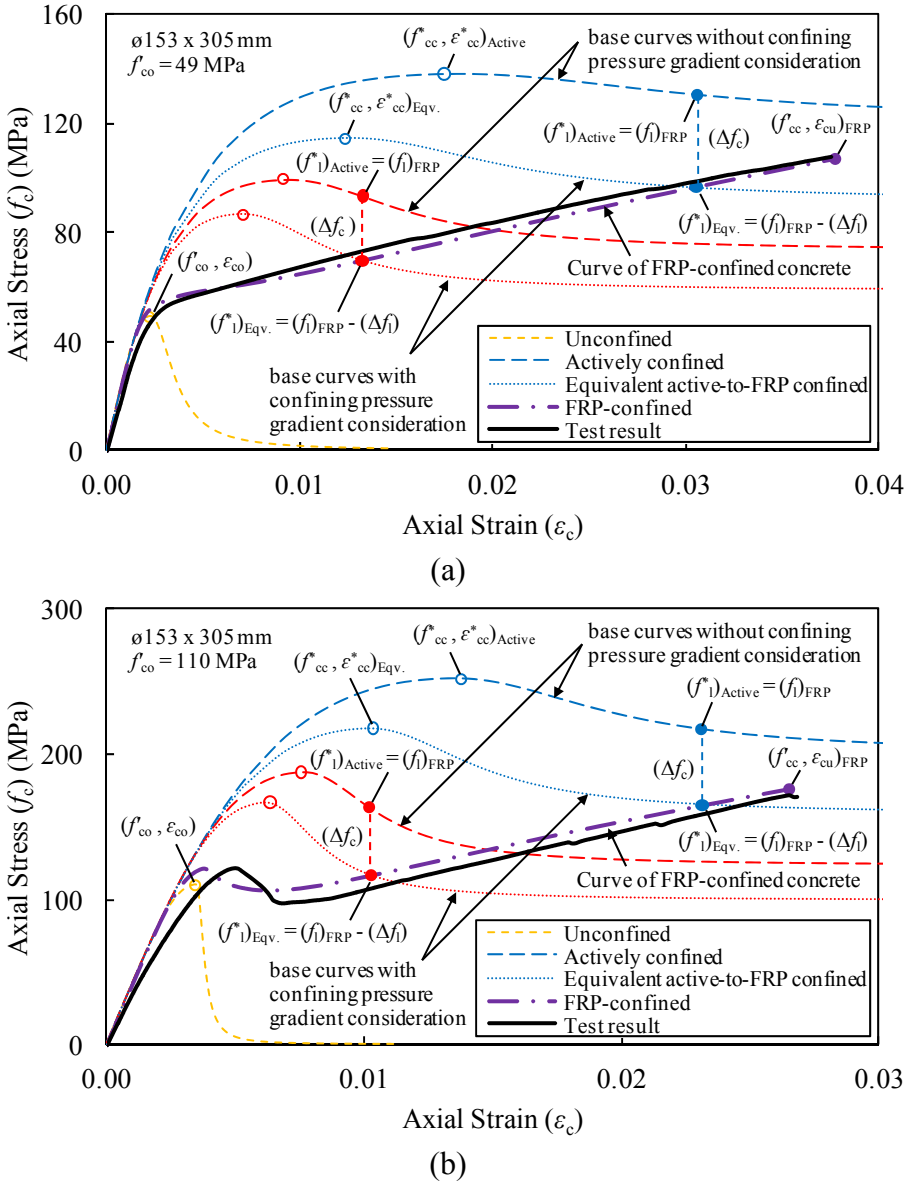

Figure 13. Generation of axial stress-strain curves of FRP-confined concrete using actively confined concrete model: (a) NSC; and (b) HSC

To illustrate the influence of the consideration of the confining pressure gradient in the generation of the stress-strain curves of FRP-confined concrete, two sets of stress-strain base curves are shown in Figures 13(a) and 13(b). The first set of curves, shown with dashed lines, was generated using the proposed expressions given in Eqs. 8 and 9 without the consideration of a confining pressure gradient between actively confined and FRP-confined concretes (i.e. $f^*_l = f_l$). The second set of curves, shown with dotted lines in Figure 13, was obtained after allowing for the confining pressure gradient (i.e. $f^*_l = f_l - \Delta f_l$), and hence they reflect the lower axial stress in FRP-confined concrete subjected to the same condition as the companion

actively confined concrete. As illustrated in the figures, for a given axial strain (ε_c), there are significant differences in the axial stresses (Δf_c) of actively confined and FRP-confined concretes that are under the same confining pressure (i.e. $f^*_l = f_l$). On the other hand, as can be seen in Figures 13(a) and 13(b), after the adjustment of the curves of actively confined concrete through consideration of the confining pressure gradient (i.e. $f^*_l = f_l - \Delta f_l$), the axial stresses of the corrected base curve and the FRP-confined concrete curve show close agreement, confirming that the proposed approach is suitable for its intended purpose. It is also evident from Figures 13(a) and 13(b) that the predicted stress-strain curves of the FRP-confined NSC and HSC (dashed-dotted lines) closely follow the experimental curves (full lines). Furthermore, as illustrated in Figure 13(b), through the use of the proposed approach the initial strength loss that that occurs at the post-peak strength softening region on the stress-strain curve of FRP-confined HSC can also be estimated accurately.

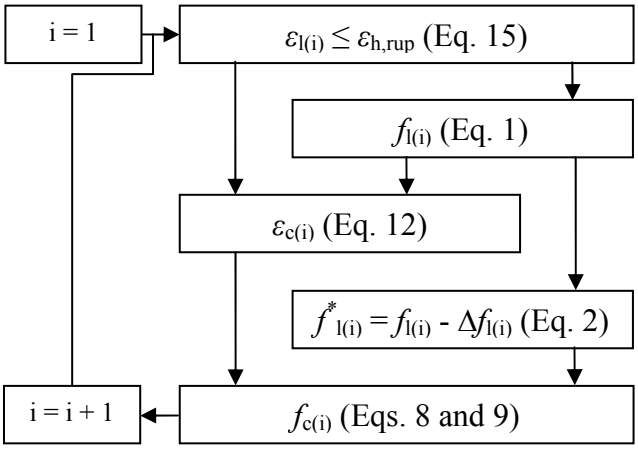

Figure 14. Incremental procedure to determine axial stress-strain curve of FRP-confined concrete

6. COMPARISON WITH EXPERIMENTAL RESULTS

The results of several groups of specimens in Table 1 were used to compare the model predictions with the experimental stress-strain curves obtained from FRP-confined concrete specimens that had different unconfined concrete strengths and were under different levels of confinement supplied by various FRP materials. These comparisons are shown in Figures 15 to 19. As evident from the figures, the predictions of the proposed model are in good agreement with the experimental results. To complete the assessment, Figure 20 presents comparisons of the model predictions of the peak stress ratios (f^*_{cc}/f'_{co}), peak strain ratios ($\varepsilon^*_{cc}/\varepsilon_{co}$), and residual stress ratio ($f_{c,res}/f'_{co}$) of actively confined concrete with the results from the experimental test database (Lim and Ozbakkaloglu 2014e). Figure 21 presents comparisons of the model predictions of the strength and strain enhancement ratios (f'_{cc}/f'_{co} and $\varepsilon_{cu}/\varepsilon_{co}$) of FRP-confined concrete with the results from the experimental test database (Ozbakkaloglu and Lim 2013; Lim and Ozbakkaloglu 2014a). The prediction statistics (*AAE*, *M*, and *SD*) of the proposed model shown in Figures 20 and 21 illustrate the improved accuracy of the proposed model over the existing actively confined and analysis-oriented FRP-confined concrete models summarized in Tables 3 and 4. The improvements in the f^*_{cc}/f'_{co} and $\varepsilon^*_{cc}/\varepsilon_{co}$ predictions of actively confined concrete and the f'_{cc}/f'_{co} and $\varepsilon_{cu}/\varepsilon_{co}$

predictions of FRP-confined concrete were achieved through the accurate modeling of: i) the axial stress-train relationship of actively confined concrete, ii) the lateral strain-axial strain for both actively confined and FRP-confined concretes, and iii) the confining pressure gradient between actively confined and FRP-confined concretes. As noted previously the databases used in the model development contained specimens with diameters ranging between 47 and 600 mm, aspect ratios (*H/D*) of less than three and unconfined concrete strengths of less than 170 MPa. These ranges, therefore, should be considered as the application domain of the proposed model, and further validation of the model is recommended for its application outside the specified ranges.

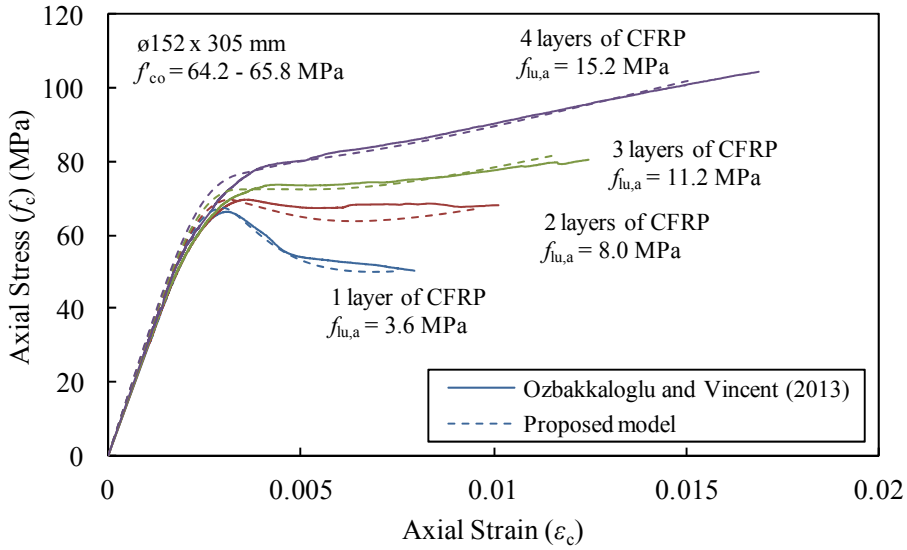

Figure 15. Comparison of proposed model predictions with axial stress-strain curves of FRP-confined concrete specimens with different amount of FRP confinement (Group U64)

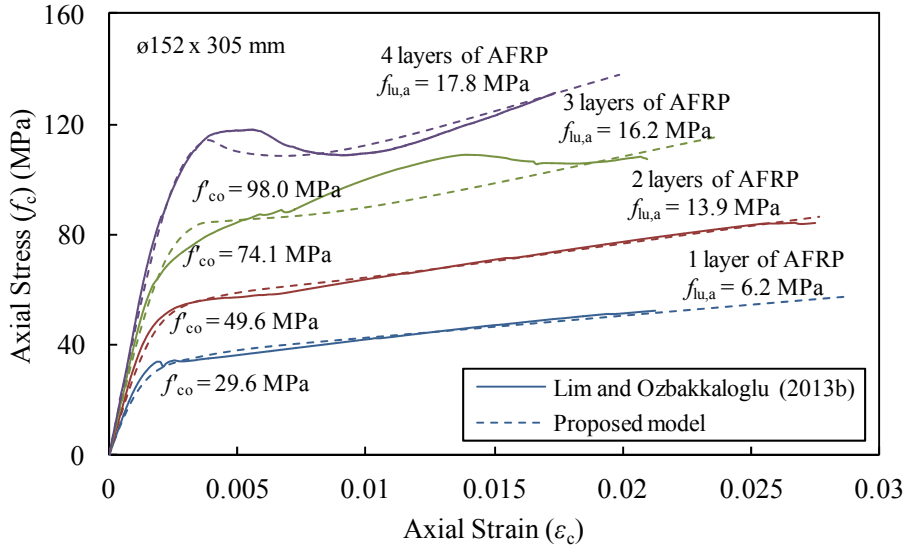

Figure 16. Comparison of the proposed model predictions with the axial stress-strain curves of AFRP-confined concrete specimens with different concrete strengths (Group U30)

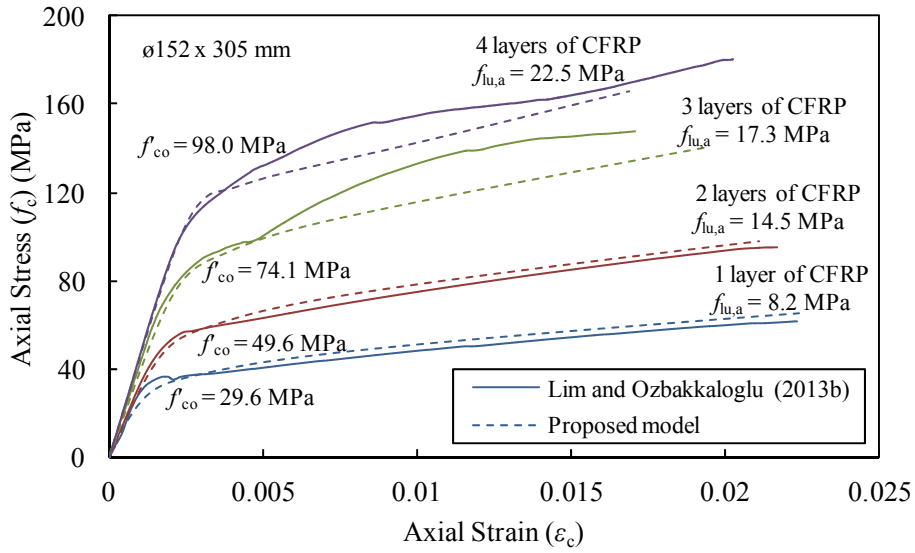

Figure 17. Comparison of the proposed model predictions with the axial stress-strain curves of CFRP-confined concrete specimens with different concrete strengths (Group U30)

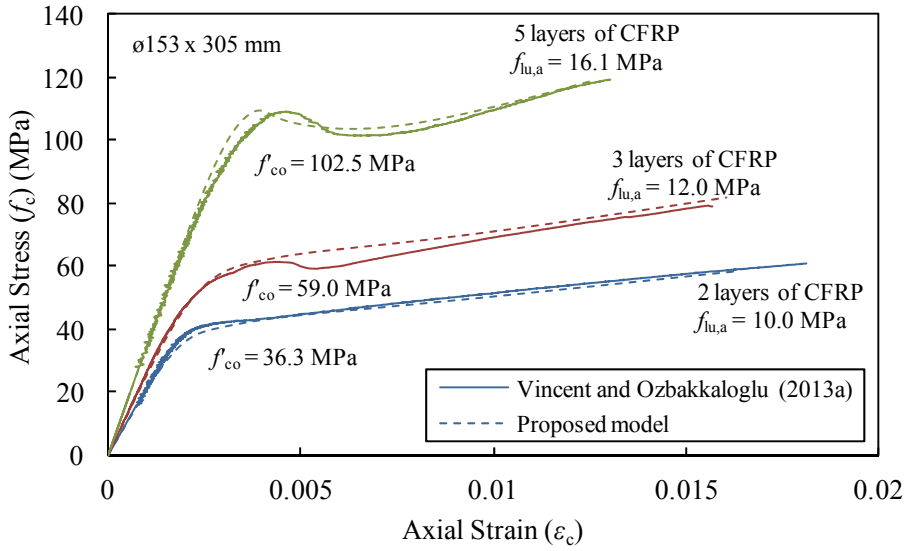

Figure 18. Comparison of the proposed model predictions with the axial stress-strain curves of CFRP-confined concrete specimens with different concrete strengths (Group U36)

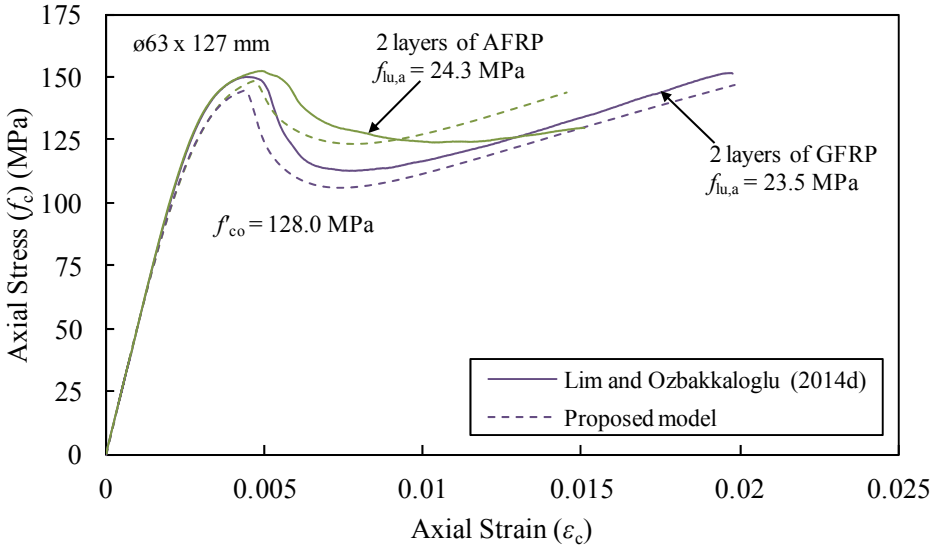

Figure 19. Comparison of the proposed model predictions with the axial stress-strain curves of FRP-confined HSC specimens with different types of FRP materials (Group U128)

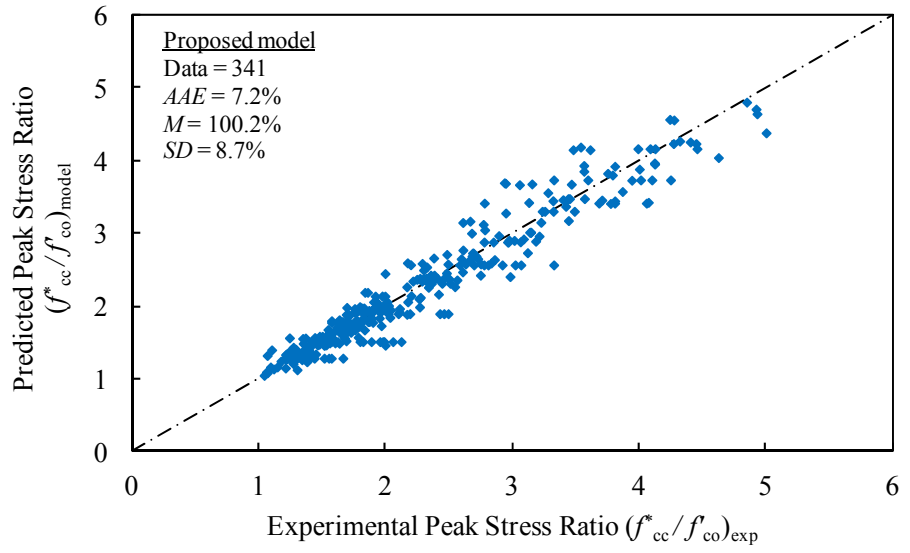

(a)

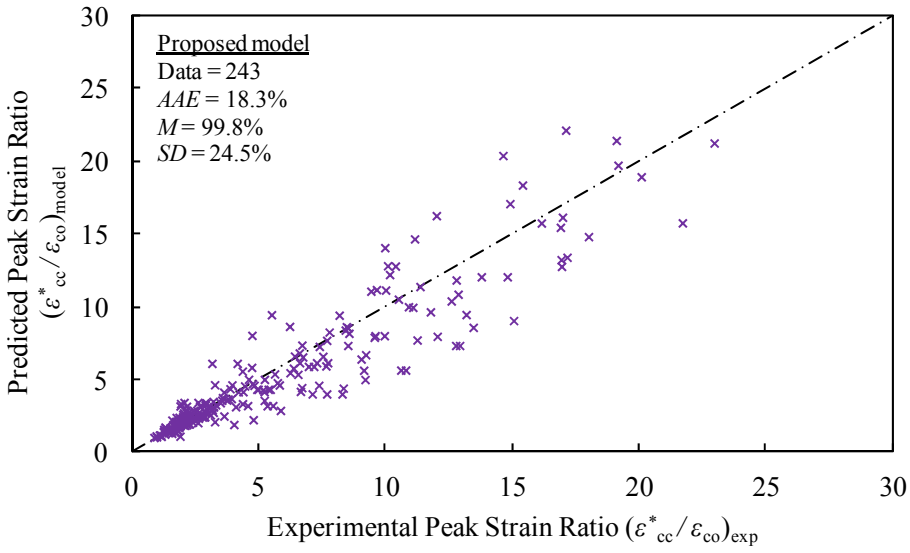

(b)

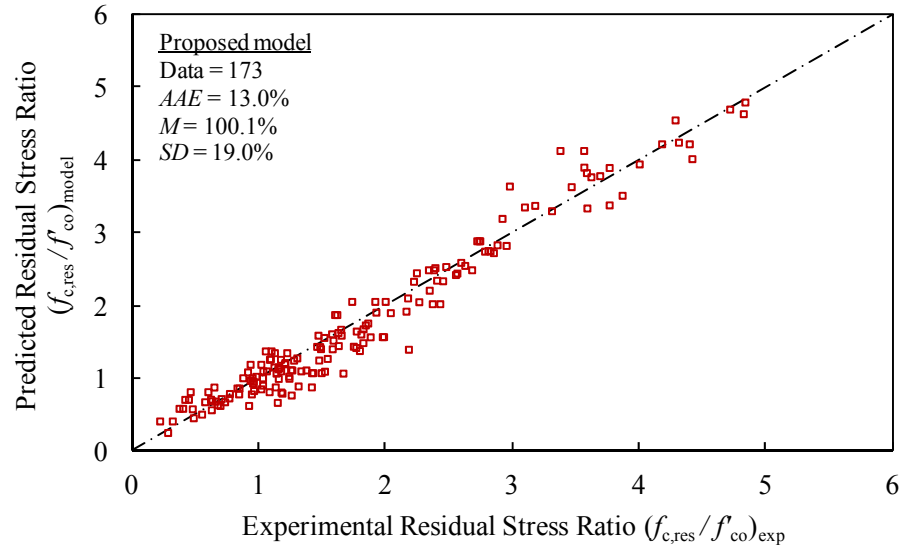

(c)

Figure 20. Comparison of model predictions of: (a) peak stress ratios (f^*_{cc}/f'_{co}); (b) peak strain ratios ($\varepsilon^*_{cc}/\varepsilon_{co}$); and residual stress ratios ($f_{c,res}/f'_{co}$) of actively-confined concrete with test results

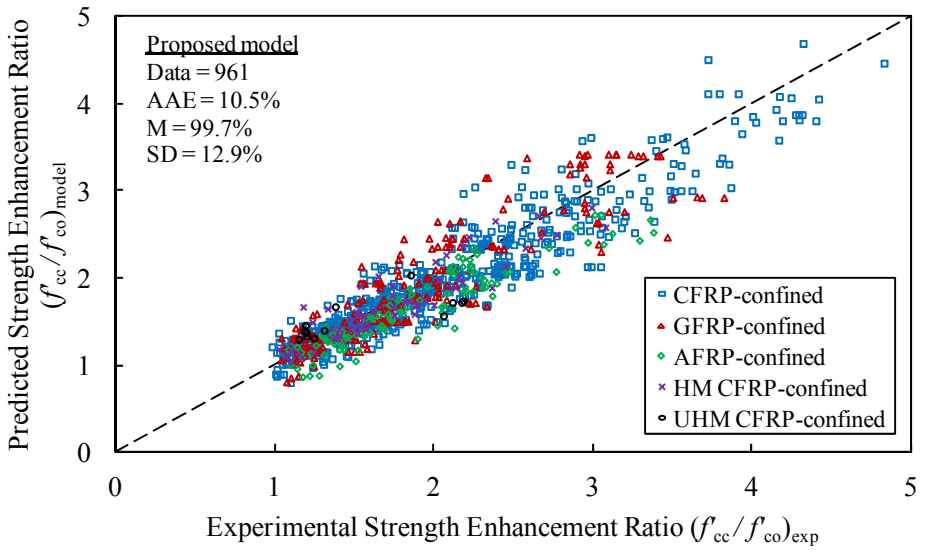

(a)

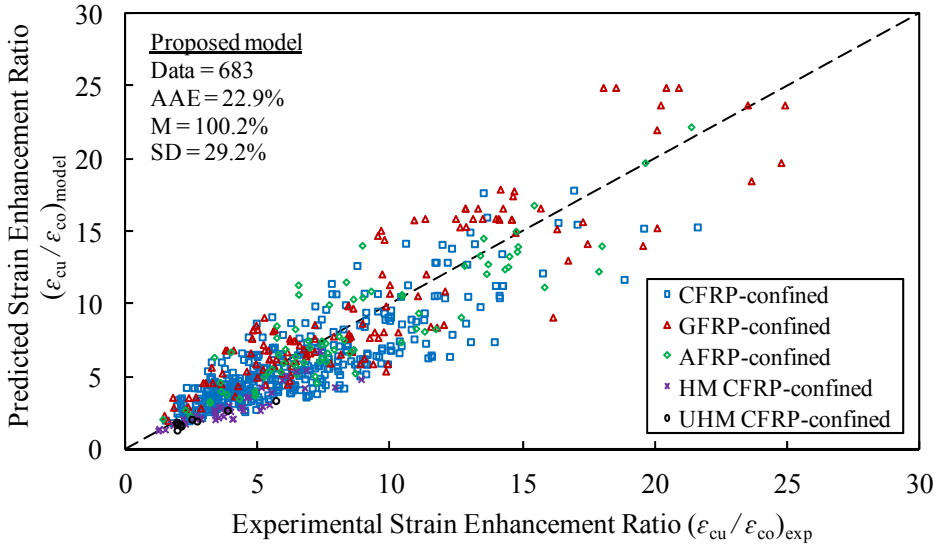

(b)

Figure 21. Comparison of model predictions of: (a) strength enhancement ratios (f'_{cc}/f'_{co}); and (b) strain enhancement ratios ($\varepsilon_{cu}/\varepsilon_{co}$) of FRP-confined concrete with test results

7. CONCLUSIONS

This paper has presented the results of an investigation on the confinement mechanisms of both actively confined and FRP-confined concretes, carefully establishing the important links between the two confinement systems using large experimental databases. The test databases consisted of 1156 axial compression test results of FRP-confined concrete and 377 triaxial test results of actively confined concrete specimens. A large number of actively confined and FRP-confined specimen results that contained complete records of axial stress-strain and lateral strain-axial strain curves were also compared. The results of this investigation indicate that the confining pressures of actively confined and FRP-confined concretes correspond at the points of intersection on their lateral strain-axial strain curves. However, it is found that the axial stresses of the FRP-confined concrete are lower than those of the actively confined concrete at these points of intersection. On the basis of these observations, a novel approach

that incorporates the confining pressure gradient between the two confinement systems has been proposed to enable the development of a unified model. Finally, a unified, analysis-oriented confinement model that incorporates this approach and other important factors identified from the close examination of the results in the databases has been presented. The model provides improved predictions of the ultimate condition of FRP-confined concrete and the peak and residual conditions of actively confined concrete compared to the existing actively confined and analysis-oriented FRP-confined concrete models. In addition, the accurate modeling of the residual stress and the inflection point of descending branch allows the accurate prediction of the stress-strain base curve of actively confined concrete. This accurate prediction of the base curve in turn results in the accurate prediction of the stress-strain curve of FRP-confined concrete, when the confining pressure gradient between the two confinement systems is considered. As revealed by the results of the model performance assessment, the proposed model is more accurate than any of the existing models in predicting the stress-strain curves of both actively confined and FRP-confined concretes.

REFERENCES

Aire, C., Gettu, R., Casas, J. R., Marques, S. and Marques, D. (2010). "Concrete laterally confined with fibre-reinforced polymers (FRP): experimental study and theoretical model." *Materiales De Construccion*, 60(297), 19-31.

Albanesi, T., Nuti, C. and Vanzi, I. (2007). "Closed form constitutive relationship for concrete filled FRP tubes under compression." *Construction and Building Materials*, 21(2), 409-427.

Ansari, F. and Li, Q. B. (1998). "High-strength concrete subjected to triaxial compression." *ACI Materials Journal*, 95(6), 747-755.

Attard, M. M. and Setunge, S. (1996). "Stress-strain relationship of confined and unconfined concrete." *ACI Materials Journal*, 93(5), 432-442.

Binici, B. (2005). "An analytical model for stress-strain behavior of confined concrete." *Engineering Structures*, 27(7), 1040-1051.

Candappa, D. C., Sanjayan, J. G. and Setunge, S. (2001). "Complete triaxial stress-strain curves of high-strength concrete." *Journal of Materials in Civil Engineering*, 13(3), 209-215.

Carreira, D. J. and Chu, K. H. (1985). "Stress-strain relationship for plain concrete in compression." *Journal of the American Concrete Institute*, 82(6), 797-804.

Cheek, J., Formichella, N., Graetz, D. and Varasteh, S. (2011). "The behaviour of ultra high strength concrete in FRP confined concrete systems under axial compression." Honours Bachelor's thesis, *The School of Civil, Environmental and Mining Engineering*, The University of Adelaide, Adelaide.

Chun, S. S. and Park, H. C. (2002). "Load carrying capacity and ductility of RC columns confined by carbon fiber reinforced polymer." *Proceedings of the 3rd International Conference on Composites in Infrastructure*, San Francisco.

Elwi, A. A. and Murray, D. W. (1979). "A 3D hypoelastic concrete constitutive relationship." *Journal of the Engineering Mechanics Division*, 105(4), 623-641.

Fam, A. Z. and Rizkalla, S. H. (2001). "Confinement model for axially loaded concrete confined by circular fiber-reinforced polymer tubes." *ACI Structural Journal*, 98(4), 451-461.

Harries, K. A. and Kharel, G. (2002). "Behavior and modeling of concrete subject to variable confining pressure." *ACI Materials Journal*, 99(2), 180-189.

Ilki, A., Peker, O., Karamuk, E., Demir, C. and Kumbasar, N. (2008). "FRP retrofit of low and medium strength circular and rectangular reinforced concrete columns." *Journal of Materials in Civil Engineering, ASCE*, 20(2), 169-188.

Imran, I. and Pantazopoulou, S. J. (2001). "Plasticity model for concrete under triaxial compression." *Journal of Engineering Mechanics, ASCE*, 127(3), 281-290.

Jiang, T. and Teng, J. G. (2007). "Analysis-oriented stress-strain models for FRP-confined concrete." *Engineering Structures*, 29(11), 2968-2986.

Kotsovos, M. D. and Newman, J. B. (1978). "Generalized stress-strain relations for concrete." *Journal of the Engineering Mechanics Division, ASCE*, 104(4), 845-856.

Lahlou, K., Aitcin, P. C. and Chaallal, O. (1992). "Behaviour of High-strength Concrete Under Confined Stresses." *Cement and Concrete Composites*, 14(3), 185-193.

Lam, L. and Teng, J. G. (2004). "Ultimate condition of fiber reinforced polymer-confined concrete." *Journal of Composites for Construction, ASCE*, 8(6), 539-548.

Lim, J. C. and Ozbakkaloglu, T. (2014a). "Confinement model for FRP-confined high-strength concrete." *Journal of Composites for Construction, ASCE*, 18(4), 04013058.

Lim, J. C. and Ozbakkaloglu, T. (2014b). "Hoop strains in FRP-confined concrete columns: Experimental observations." *Materials and Structures*, Doi: 10.1617/s11527-014-0358-8.

Lim, J. C. and Ozbakkaloglu, T. (2014c). "Influence of silica fume on stress-strain behavior of FRP-confined HSC." *Construction and Building Materials*, 63, 11-24.

Lim, J. C. and Ozbakkaloglu, T. (2014d). "Investigation of the Influence of Application Path of Confining Pressure: Tests on Actively Confined and FRP-Confined Concretes." *Journal of Structural Engineering, ASCE*, Doi: 10.1061/(ASCE)ST.1943-541X.0001177.

Lim, J. C. and Ozbakkaloglu, T. (2014e). "Lateral strain-to-axial strain relationship of confined concrete." *Journal of Structural Engineering, ASCE*, Doi: 10.1061/(ASCE)ST.1943-541X.0001094.

Lim, J. C. and Ozbakkaloglu, T. (2014f). "Stress-strain model for normal- and light-weight concretes under uniaxial and triaxial compression." *Construction and Building Materials*, Doi: 10.1016/j.conbuildmat.2014.08.050.

Mander, J. B., Priestley, M. J. N. and Park, R. (1988). "Theoretical stress-strain model for confined concrete." *Journal of Structural Engineering, ASCE*, 114(8), 1804-1826.

Marques, S. P. C., Marques, D., da Silva, J. L. and Cavalcante, M. A. A. (2004). "Model for analysis of short columns of concrete confined by fiber-reinforced polymer." *Journal of Composites for Construction, ASCE*, 8(4), 332-340.

Mills, L. L. and Zimmerman, R. M. (1970). "Compressive Strength of Plain Concrete Under Multiaxial Loading Conditions." *ACI Journal Proceedings*, 67(10), 802-807.

Mirmiran, A. and Shahawy, M. (1997a). "Behavior of concrete columns confined by fiber composites." *Journal of Structural Engineering*, 123(5), 583-590.

Mirmiran, A. and Shahawy, M. (1997b). "Dilation characteristics of confined concrete." *Mechanics of Cohesive-Frictional Materials*, 2(3), 237-249.

Moran, D. A. and Pantelides, C. P. (2002a). "Stress-strain model for fiber-reinforced polymer-confined concrete." *Journal of Composites for Construction*, 6(4), 233-240.

Moran, D. A. and Pantelides, C. P. (2002b). "Variable strain ductility ratio for fiber-reinforced polymer-confined concrete." *Journal of Composites for Construction*, 6(4), 224-232.

Newman, J. B. (1979). "Concrete under complex stress." Department of Civil Engineering, Imperial College of Science and Technology, London, UK, London, UK.

Ozbakkaloglu, T. (2013). "Behavior of square and rectangular ultra high-strength concrete-filled FRP tubes under axial compression." *Composites Part B*, 54, 97-111.

Ozbakkaloglu, T. and Akin, E. (2012). "Behavior of FRP-confined normal- and high-strength concrete under cyclic axial compression." *Journal of Composites for Construction, ASCE*, 16(4), 451-463.

Ozbakkaloglu, T. and Lim, J. C. (2013). "Axial compressive behavior of FRP-confined concrete: Experimental test database and a new design-oriented model." *Composites Part B*, 55, 607-634.

Ozbakkaloglu, T., Lim, J. C. and Vincent, T. (2013). "FRP-confined concrete in circular sections: Review and assessment of stress–strain models." *Engineering Structures*, 49, 1068–1088.

Ozbakkaloglu, T. and Vincent, T. (2013). "Axial compressive behavior of circular high-strength concrete-filled FRP tubes." *Journal of Composites for Construction, ASCE*, 18(2), 04013037.

Pantazopoulou, S. J. and Mills, R. H. (1995). "Microstructural aspects mechanical response of plain concrete." *ACI Materials Journal*, 92(6), 605-616.

Popovics, S. (1973). "A numerical approach to the complete stress-strain curves for concrete." *Cement and Concrete Research*, 3(5), 583-599.

Razvi, S. and Saatcioglu, M. (1999). "Confinement model for high-strength concrete." *Journal of Structural Engineering*, 125(3), 281-289.

Richard, R. M. and Abbottt, B. J. (1975). "Versatile elastic-plastic stress-strain formula." *Journal of the Engineering Mechanics Division*, 101(4), 511-515.

Richart, F. E., Brandtzaeg, A. and Brown, R. L. (1929). "The failure of plain and spirally reinforced concrete in compression." *Bulletin No.190*, Engineering Experiment Station, University of Illinois, Urbana, USA.

Rousakis, T. C. and Karabinis, A. I. (2012). "Adequately FRP confined reinforced concrete columns under axial compressive monotonic or cyclic loading." *Materials and Structures*, 45(7), 957-975.

Samani, A. K. and Attard, M. M. (2012). "A stress-strain model for uniaxial and confined concrete under compression." *Engineering Structures*, 41, 335-349.

Sfer, D., Carol, I., Gettu, R. and Etse, G. (2002). "Study of the behavior of concrete under triaxial compression." *Journal of Engineering Mechanics*, 128(2), 156-163.

Smith, S. S., Willam, K. J., Gerstle, K. H. and Sture, S. (1989). "Concrete Over The Top, Or: Is There Life After Peak?" *ACI Materials Journal*, 86(5), 491-497.

Smith, S. T., Kim, S. J. and Zhang, H. (2010). "Behavior and Effectiveness of FRP Wrap in the Confinement of Large Concrete Cylinders." *Journal of Composites for Construction*, 14(5), 573-582.

Spoelstra, M. R. and Monti, G. (1999). "FRP-confined concrete model." *Journal of Composites for Construction*, 3(3), 143-150.

Teng, J. G., Huang, Y. L., Lam, L. and Ye, L. P. (2007). "Theoretical model for fiber-reinforced polymer-confined concrete." *Journal of Composites for Construction, ASCE*, 11(2), 201-210.

Vincent, T. and Ozbakkaloglu, T. (2013a). "Influence of concrete strength and confinement method on axial compressive behavior of FRP-confined high- and ultra high-strength concrete." *Composites Part B*, 50, 413–428.

Vincent, T. and Ozbakkaloglu, T. (2013b). "Influence of fiber orientation and specimen end condition on axial compressive behavior of FRP-confined concrete." *Construction and Building Materials*, 47, 814-826.

Wu, Y.-F. and Jiang, J.-F. (2013). "Effective strain of FRP for confined circular concrete columns." *Composite Structures*, 95, 479–491.

Xiao, Q. G., Teng, J. G. and Yu, T. (2010). "Behavior and Modeling of Confined High-Strength Concrete." *Journal of Composites for Construction, ASCE*, 14(3), 249-259.

Xie, J., Elwi, A. E. and Macgregor, J. G. (1995). "Mechanical-properties of high-strength concretes containing silica fume." *ACI Materials Journal*, 92(2), 135-145.

THIS PAGE HAS BEEN LEFT INTENTIONALLY BLANK

Statement of Authorship

Title of Paper	Evaluation of Ultimate Conditions of FRP-Confined Concrete Columns Using Genetic Programming
Publication Status	○ Published ○ Accepted for Publication ◉ Submitted for Publication ○ Publication Style
Publication Details	Computers and Structures, Manuscript CAS-D-15-00127, Year 2015

Author Contributions

By signing the Statement of Authorship, each author certifies that their stated contribution to the publication is accurate and that permission is granted for the publication to be included in the candidate's thesis.

Name of Principal Author (Candidate)	Mr. Jian Chin Lim		
Contribution to the Paper	Preparation of experimental database, development of model, and preparation of manuscript		
Signature		Date	23/02/2015

Name of Co-Author	Dr. Murat Karakus		
Contribution to the Paper	Analysis of database results and development of model		
Signature		Date	23/02/2015

Name of Co-Author	Dr. Togay Ozbakkaloglu		
Contribution to the Paper	Research supervision and review of manuscript		
Signature		Date	23/02/2015

THIS PAGE HAS BEEN LEFT INTENTIONALLY BLANK

EVALUATION OF ULTIMATE CONDITIONS OF FRP-CONFINED CONCRETE COLUMNS USING GENETIC PROGRAMMING

Jian C. Lim, Murat Karakus and Togay Ozbakkaloglu

ABSTRACT

A large experimental test database that consists of 832 axial compression tests results of fiber reinforced polymer (FRP)-confined concrete specimens was assembled. Using the test database, existing conventional and evolutionary algorithm models developed for FRP-confined concrete were then assessed. The assessment results have led to important findings regarding the performances of models in each category. To this end, a new evolutionary algorithm model for predicting the ultimate condition of FRP-confined concrete was developed on the basis of genetic programming (GP) using the experimental database. The predictions of the proposed model which are in good agreement with the experimental results, suggest that more accurate results can be achieved in explaining and formulating the ultimate condition of FRP confined concretes by genetic programming. The model assessment that has been presented herein clearly illustrates the important influences of the size of the test databases and the selected test parameters used in the development of artificial intelligence models on their overall performances.

KEYWORDS: Genetic programming (GP); Fiber reinforced polymer (FRP); Confinement; Concrete; Compressive strength; Ultimate axial strain.

1. INTRODUCTION

It is now well understood that the confinement of concrete with fiber reinforced polymer (FRP) composites can substantially enhance concrete strength and deformability. A large number of studies undertaken to date have produced over 3000 test results on FRP-confined concrete and resulted in the development of over 90 models. The conventional models that were developed using regression analysis can be classified into two broad categories namely the design-oriented models and the analysis-oriented models. In predictions of the ultimate condition of FRP-confined concrete, the design-oriented model use closed-form empirical expressions that were derived directly from database results. The analysis-oriented models, on the other hand, use a combination of empirical and theoretical expressions through an incremental procedure to consider the interaction mechanism between the external FRP jacket and the internal concrete core. These analysis-oriented models are built on the assumption of stress path independence, which assumes that the axial stress and axial strain of FRP-confined concrete at a given lateral strain are the same as those of the same concrete actively confined with a constant confining pressure equal to that supplied by the FRP shell.

As indicated by the assessment results of these models using a comprehensive experimental database, the performances of a large proportion of the conventional models were compromised when they were assessed against a large database covering parametric ranges that are much wider than the original databases used to develop these models [1, 2]. This can be attributed to the limited capability of the design-oriented models in handling uncertainties in complex experimental database, whereas the assumption adopted by the analysis-oriented models has recently been shown to be inaccurate [3, 4]. In addition, the development of these existing conventional models are often based on the expressions proposed by Richart et al. [5], with refinement subsequently applied to those earlier expressions to incorporate new research findings. Given the dependencies of the conventional models on the base expressions and the gradual refinement process, an efficient alternative approach is therefore required. Recently, a new category of models has emerged through use of soft computing techniques involving artificial intelligence (AI) and advanced optimization algoritims, such as artificial neural network, genetic programming, stepwise regression, and fuzzy logic [6-18]. Models in this category could handle complex databases containing large number of independent variables, identify the sensitivity of input parameters, and provide mathematical solutions between dependent and independent variables. However, the complexity of modeling frameworks and the dependency of these models on computers have significantly reduces their versatility in design applications. The computer generated statistical solutions have also compromised the physical significance unfolding the structural behavior of FRP-confined concrete. In addition, several common modeling issues identified from the assessment of these models include: i) limited size of database results, ii) overfitted with redundant test parameters that cause unreliable prediction beyond their original observation range, and iii) lack of consideration of important test parameters, including the ultimate rupture strain of FRP jacket.

With proper treatments given to the aforementioned modeling issues, genetic programming (GP) can be a potential candidate to address these shortcomings. GP is an evolutionary

algorithm attempting to find key variables for a problem in a given search space, and generates mathematical expressions to explain the relations between the variables. By using GP based on the principles of symbolic regression (SR) analysis, the relationships between the dependent and independent variables of a complex database involving uncertainties and variability can be solved. SR is a process of finding a mathematical expression by minimizing the errors between given finite data set as well as providing a method of function identification [19]. Symbolic regression, as opposed to other regression techniques, discovers both the form of the model and its parameters from the search space. In other words, a measured dataset is fitted to an appropriate mathematical formula by a fitness function. Determination or identification of key variables and variable combinations, providing comprehension of developed models are among the benefits of symbolic regression analysis. In this research, SR analysis was conducted using GP approach, which is well suited to wide range of engineering based problems.

In the recent years, the use of GP for optimum solution and function identification of engineering problems has been gaining acceleration as the approach is capable of dealing with complex database that contain a large number of parameters. It gradually refines solution while maintaining the versatility of the model in closed-form expressions (e.g. [20-25]). For example, Johari et al. [26] has successfully applied GP for the prediction of soil-water characteristic curve. Baykasoglu et al. [27] applied multi expression programming (MEP), gene expression programming (GEP) and linear genetic programming (LGP) to estimate compressive and tensile strength of limestone for the first time with good predictions. Javadi et al. [28] introduced a new technique based on GP for the determination of liquefaction induced lateral spreading. Cabalar and Cevik [29] applied GP for the prediction of peak ground acceleration using strong-ground-motion data from Turkey. The use of GP for the prediction of axial compressive strength of FRP-confined concrete has also been demonstrated by Cevik 3 [11], Cevik and Cabalar [6], and Cevik et al. 1 [8]. These studies have demonstrated the use of GP in the formulation of highly accurate models.

In the present study, the GP approach was used to establish models to predict the ultimate conditions of FRP-confined concrete columns under concentric compression. Based on a comprehensive experimental database that was carefully assembled using a set of selection criteria to ensure the reliability and consistency of the database, three closed-form expressions are proposed for the predictions of the compressive strength, ultimate axial strain and hoop rupture strain of FRP-confined concrete. This is the first study in the literature to establish expressions for the ultimate axial strain and hoop rupture strain of FRP-confined concrete on the basis of evolutionary algorithms. Details of the adopted approach are discussed in Section 2. A summary of the experimental database is provided in Section 3. The selection process of independent variables, functions and fitness rule, together with the proposed expressions are presented in Section 4. The predictions statistics of the proposed and the existing models with experimental results are presented in Section 5.

2. OVERVIEW OF GENETIC PROGRAMMING

In this section, the GP paradigm is discussed and the essentials of GP are highlighted. Further concepts and terminology behind GP can be found from the inventor of this paradigm [19]. However, it is advised that the genetic algorithm concept developed in 1975 by Holland [30] and work from his student, Goldberg [31], can also be visited for further insight.

2.1. Basic concepts of GP

Genetic programming is an extension of the conventional genetic algorithm (GA), generating novel solutions to complex problems, developed by Koza [19]. Unlike GA which uses a string of numbers to represent the solution, the GP automatically creates several computer programs (CP) with a parse tree structure to solve the problem considered. The process of solving the problems with GP is equivalent to searching a space of possible computer programs for the fittest individual computer program [19]. The generated CP is based on Darwinian concept of survival and reproduction of the fittest as well as appropriate mating of CPs. As illustrated in the flow chart in Figure 1, the problem will be solved using the Darwinian genetic operators such as reproduction, crossover, and mutation. Initial population consists of randomly generated CPs, which are composed of functions and terminals appropriate to the characteristics of the problem. If the functions and terminals selected are not appropriate for the problem, the desired solution cannot be achieved. A basic flow chart of the genetic programming paradigm is shown in Figure 1.

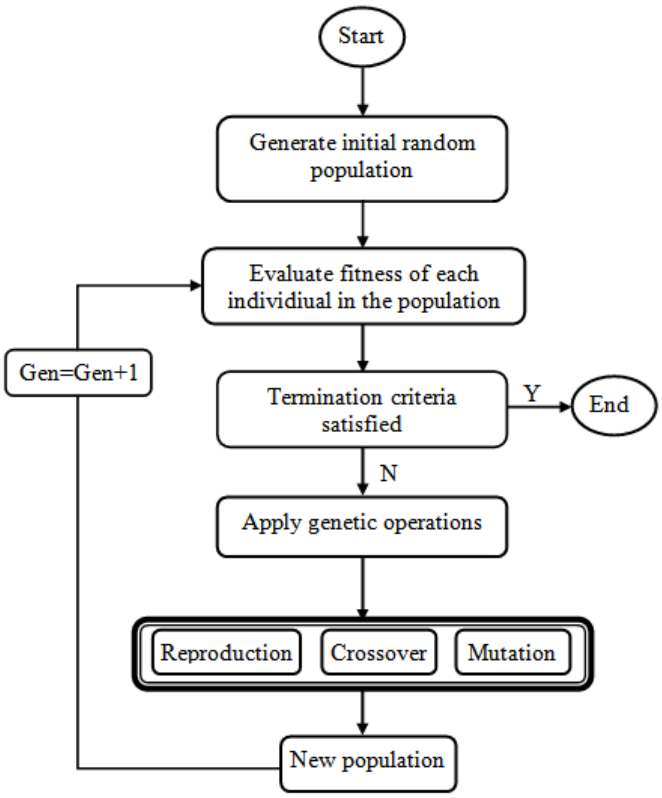

Figure 1. Flow chart of genetic programming [19]

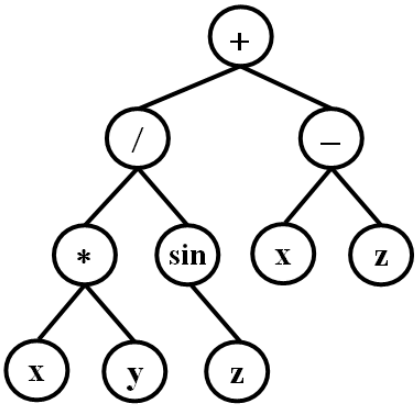

Figure 2. A typical expression tree

As stated earlier, CP is composed of functions and terminals. The functions can be standard arithmetic operators, trigonometric logarithmic or power, e.g. $f = \{/,\times,+,-,\sin,\cos,\log 2, power,...\}$ and/or any mathematical functions, logical functions, as well as user-defined operators. Depending on the nature of the problem investigated, the computer program might be Boolean-valued, integer-valued, real-valued, complex-valued, vector-valued, symbolic-valued, or multiple-valued [19]. A typical expression tree, representing the computer program is shown in Figure 2. In this example, the function set (*F*) is composed of multiplication, division, addition, subtraction and the sine function, $F = \{\times, /, -, \sin\}$. The terminal set (*T*) is composed of $N = 3$ variable as $T = \{x, y, z\}$. The functions and terminals must fulfil two important properties in order to solve the problem with an appropriate representation [19]. These parameters are *closure property* and *sufficiency property*. The *closure property* includes protection of the function set and the terminal set against all possible argument values, e.g. protection of negative square root. *Sufficiency property* is the selection of the appropriate functions and terminals to the solve problem.

2.2. Genetic Operations

Genetic operations used in GP are composed of; *reproduction*, *crossover*, and *mutation*. *Reproduction* operation involves selecting, in proportion to fitness, a computer program from the current population of programs, and allowing it to survive by copying it into the new population [19]. Several different types of reproduction operations such as fitness proportionate reproduction or roulette wheel algorithm, tournament selection and lexicographic parsimony pressure selection are commonly used in GP. In this study Lexicographic parsimony pressure selection was used, which is a multi-objective method similar to tournament selection. This particular method optimizes both fitness and parse tree size. The shortest individual, the tree with fewer nodes, is selected as the fittest when two individuals are equally fit. Silva and Almeida [32] reported that this technique is effective in controlling the bloat which is a phenomenon consisting of an excessive code growth without the corresponding improvement in fitness. The theory of Parsimony Pressure are discussed in detail by Poli and McPhee [33]. The standard method of controlling bloat is to set up a maximum depth on trees in the proposed GP model.

Crossover operation involves choosing random nodes in two parent trees and swapping respective branches creating two new offspring. Figure 3 illustrates the crossover operation. Mathematical expressions for parent I and parent II are as follows before crossover;

$$Parent\quad I: \frac{xy}{\sin(z)} + (x - z) \qquad Parent\quad II: \frac{x}{2} + e^{y} - z^{2}$$

Resulting offspring after crossover operation are:

$$Offspring\quad I: \frac{x}{2} + (x - z) \qquad Offspring\quad II: \frac{xy}{\sin(z)} + e^{y} - z^{2}$$

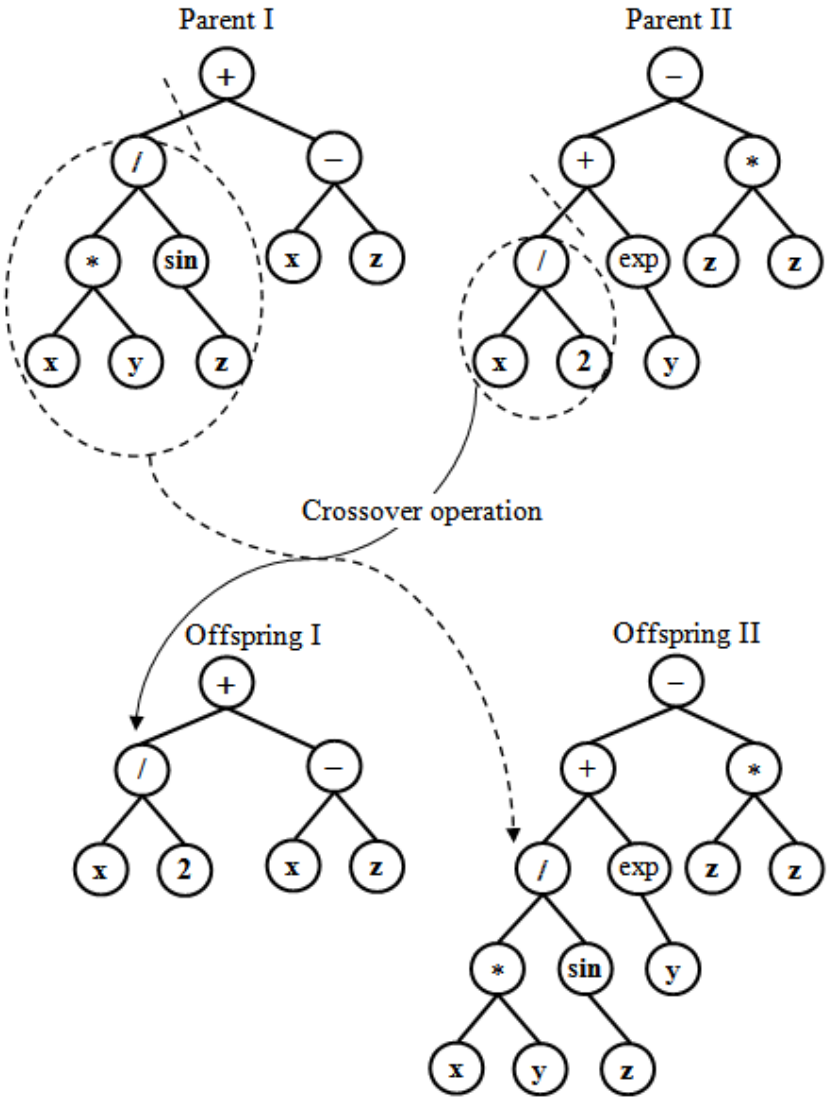

Figure 3. Crossover operation in genetic programming

As can be seen from the above expressions, crossover between S-expressions consists of swapping the randomly selected sub S-expressions.

Mutation operation includes selecting a random node from the parent tree and substitutes with a newly generated random tree having terminals and functions available. However, Koza [19] stated that mutation plays a minor role in GP. Therefore, it can be disregarded in most cases.

3. DATABASE OF FRP-CONFINED CONCRETE

The database of FRP-confined concrete was assembled through an extensive review of the literature that covered 3042 test results from 253 experimental studies published between 1991 and 2013. The suitability of the results was then assessed using a set of carefully established selection criteria to ensure the reliability and consistency of the database. Only monotonically loaded circular specimens with unidirectional fibers orientated in the hoop direction and an aspect ratio (H/D) of less than three were included in the database. Specimens containing internal steel reinforcement or partial FRP confinement were not included. This resulted in a final database size of 832 datasets collected from 99 experimental studies. The complete database of experimental results used in the present study can be found in Ozbakkaloglu and Lim [34]. The database consists of specimens confined by five main types of FRP materials (carbon FRP (CFRP), high-modulus carbon FRP (HM CFRP), ultra-high-modulus carbon FRP (UHM CFRP), S- or E-glass FRP (GFRP), and aramid FRP (AFRP)) and two confinement techniques (wraps and tubes). The carbon FRPs were categorized into three subgroups on the basis of their elastic modulus of fibers (E_f) (i.e., carbon FRP with $E_f \leq 270$ GPa is categorized as CFRP; followed by $270 < E_f \leq 440$ GPa as HM CFRP; and $E_f > 440$ GPa as UHM CFRP). 755 specimens in the database were FRP-wrapped, whereas 77 specimens were confined by FRP tubes. 495 of the specimens were confined by CFRP; 206 by GFRP; 79 by AFRP; 40 by HM CFRP; and 12 by UHM CFRP. The unconfined concrete strength (f'_{co}) and strain (ε_{co}), as obtained from concrete cylinder tests, varied from 6.2 to 55.2 MPa and 0.14% to 0.70%, respectively. The diameters of the specimens (D) included in the test database varied between 47 and 600 mm, with the majority of the specimens having a diameter of 150 mm. The hoop rupture strain ($\varepsilon_{h,rup}$) of the FRP-confined concrete specimens varied from 0.09 to 3.21%. The actual confinement ratio, defined as the ratio of the ultimate confining pressure of the FRP jacket at rupture to the compressive strength of an unconfined concrete specimen ($f_{lu,a}/f'_{co}$), varied from 0.02 to 4.74. Figures 4 and 5, respectively, show the relationship of the strength enhancement ratio (f'_{cc}/f'_{co}) and strain enhancement ratio ($\varepsilon_{cu}/\varepsilon_{co}$) versus the actual confinement ratio ($f_{lu,a}/f'_{co}$), established from the database.

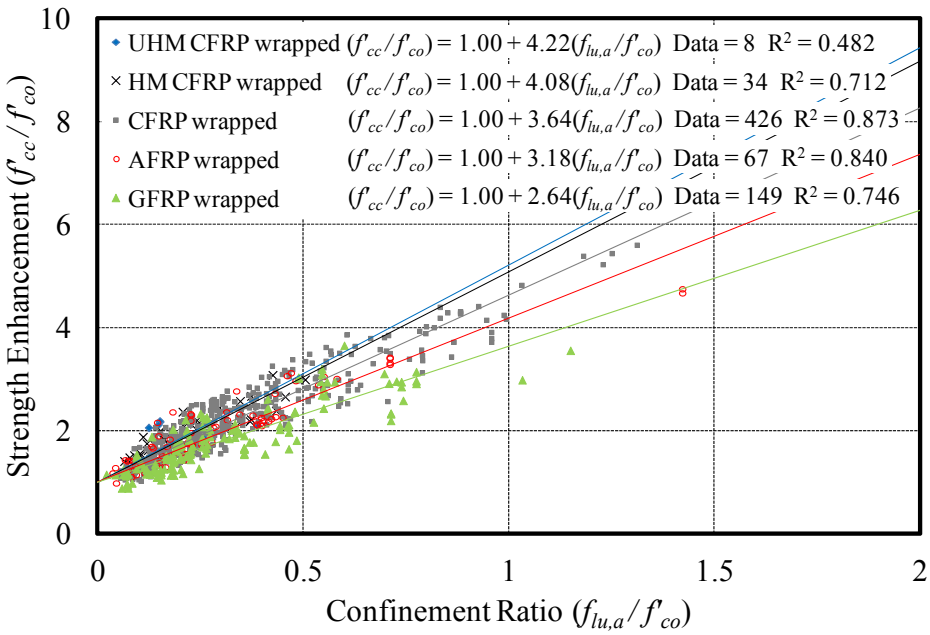

Figure 4. Variation of strength enhancement ratio (f'_{cc}/f'_{co}) of FRP-confined concrete with confinement ratio ($f_{lu,a}/f'_{co}$)

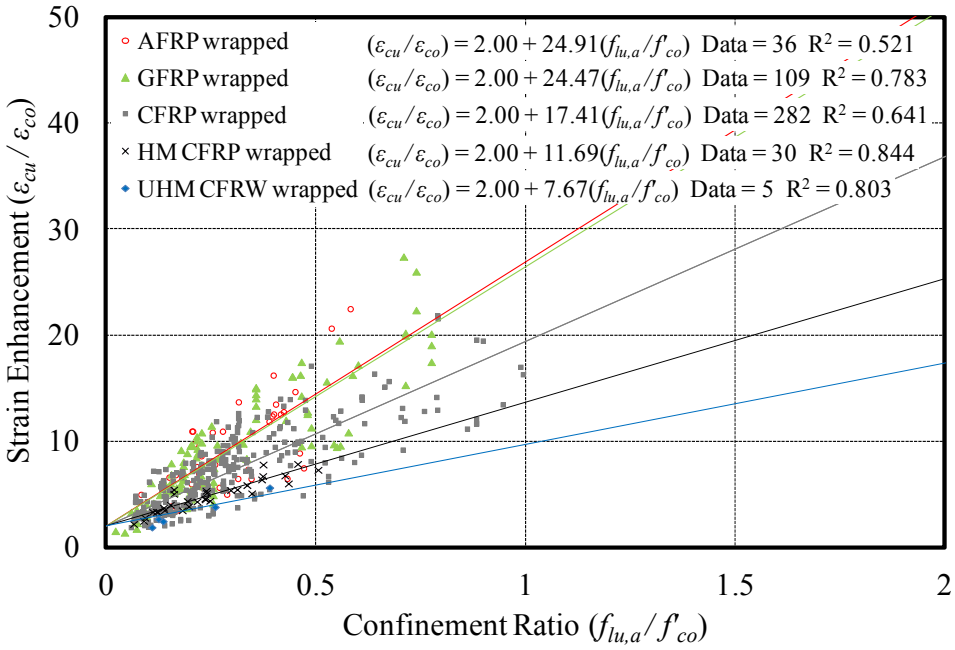

Figure 5. Variation of strain enhancement ratio ($\varepsilon_{cu}/\varepsilon_{co}$) of FRP-confined concrete with confinement ratio ($f_{lu,a}/f'_{co}$)

3.1 Parameter Selection

The GP analysis is based on three main stages. Firstly, the terminal sets are selected. The term *terminal* refers to independent variables used to approximate dependent variables. Parameters that were identified to be non influential were either eliminated or combined with several other parameters until a strong trend of influence was observed. One of such input parameter that combines several other input parameters is the confinement stiffness of FRP jacket (K_l), defined by Eq. 2 presented later in Section 4.1. In the experimental database [34], it has already been observed that strong exponential or power relations exist between the independent variable K_l and the dependent variables f'_{cc} and ε_{cu}. With the use of K_l as an independent variable, GP also generated similar exponential and/or power formulations which underscore the experimental observations. Other influential independent parameters selected for the GP analyses include the unconfined strength of concrete (f'_{co}), elastic modulus of fiber (E_f), hoop rupture strain of FRP jacket ($\varepsilon_{h,rup}$), and ultimate tensile strength of fibre (ε_f). A summary of the selected input parameters related to FRP-Confined concerte and GP parameters are given in Table 1.

In the second stage, a set of function believed to represent the nature of the problem or data set was determined. As can be seen from the Table 1, additional to the basic aithmatic operations (+, –, /, ×), *exponential (exp)*, *square root (sqrt)* and *power* functions are also included. We have also included logarithmic functions which did not improve the fitness. Therefore it was removed from the function set.

In the third stage, a symbolic expression (S-expression), a list or an atom in LISP, was generated by GP in terms of the fitness function adopted. The S-expression is the only syntactic form of the LISP programming language. For example, (+(- 3 4) 5) is a LISP S-expression. In this S-expression the atoms or individuals (3 and 4) are subtracted first and the result (-1) is added to 5 yielding in value 4. S-expressions were chosen according to the lower fitness value. The lower the fitness value, the better the model is. According to the selected fitness (AAE), the lowest value indicates a small error between the measured and predicted data. The genetic programming will run until the termination criterion (stopping condition) is satisfied. This can be done either by determining a maximum generation limit or a tolerated error limit. The program can also be terminated by the variation in fitness observed during the run. We used maximum generation limit as the termination criterion for the all GP runs. Some of the mathematical functions included in the GP are protected against zero division or negative square root. In the division operation, if the denominator is equal to zero then the results returns to the numerator. In the power operation $x_1^{x_2}$ returns zero if $x_1^{x_2}$ is not a number (NaN) or infinity (∞), or has an imaginary part, otherwise it returns $x_1^{x_2}$. In the function square root, $\sqrt{x}$ returns zero if $x \leq 0$ and $\sqrt{x}$ otherwise. Table 1 summarises the parameters adopted in GP analysis.

4. PROPOSED MODEL FOR ULTIMATE CONDITION OF FRP-CONFINED CONCRETE

The ultimate condition of FRP-confined concrete is often characterized as the compressive strength and the corresponding axial strain of concrete and hoop strain recorded at the rupture of the FRP jacket. This makes the relationship between the ultimate axial stress (f'_{cc}), ultimate axial strain (ε_{cu}) and hoop rupture strain ($\varepsilon_{h,rup}$) an important one. Using the comprehensive experimental database [34], a model consisting of three expressions for the predictions of the compressive strength (f'_{cc}), ultimate axial strain (ε_{cu}) and hoop rupture strain ($\varepsilon_{h,rup}$) was developed using GP and is presented in this section. The model is applicable to FRP-confined concrete with unconfined concrete strength up to 55 MPa. Table 1 summarizes the parameters that were used in GP analysis. As GP analysis does not directly reveal the underlying physical relationships of a given dataset, the search of a physically meaningful model structure relies on users' engineering knowledge of FRP-confined concrete systems. This is no easy task since both the structure and parameters of the physical model must be determined [35]. With the help of GP approach, a large number of potential model components and structures can be tested, while the best parts of these structures and combinations can be retained to produce new and possibly better expressions. In addition, the expressions resulting from GP formulation process is often useful in revealing pertinent aspects that are physically meaningful. Hence, with a carefully selection of functions for these pertinent aspects, an accurate and physically meaningful model can be established. In our trial run of this approach, larger population size up to 1500 was used. However, the use of the large population size tends to create bloated/large number of nodes leading to extremely complex formulation. Therefore, smaller population size of 300 was chosen in the actual analysis. Mutation and crossover probabilities are not fixed but random. In tree crossover, random nodes are chosen from both parent trees, and the respective branches are swapped creating two offspring. It should be noted that not all the datasets included in the database contained all the relevant details required for the model development. As a result, out of 832 results, 753, 511, and 325 were used in the development of the expressions of the compressive strength (f'_{cc}), ultimate axial strain (ε_{cu}), and hoop rupture strain ($\varepsilon_{h,rup}$), respectively. The experimental values of the compressive strength (f'_{co}) and the corresponding axial strain (ε_{co}) of unconfined concrete were based on the test results of the unconfined cylinders. In order to avoid overfitting random data division method was used, in which 70% of the total data were randomly selected for training and the remaining 30% were used for testing purposes. This approach was previously used by a number of existing studies [23, 36, 37].

Table 1. Parameters used in genetic programming

Parameters		Values
Terminal sets (**T**) for	f'_{cc}	f'_{co}, K_l, $\varepsilon_{h,rup}$
	ε_{cu}	f'_{co}, E_f, ε_f
	$\varepsilon_{h,rup}$	f'_{co}, E_f, ε_f
Function set (**F**)		+, –, /, ×, *exp*, *sqrt*, *power*
Population size		300
Maximum generation		50
Maximum tree depth		17
Selection method		Lexictour
Termination criterion		Maximum generation
Type of elitism		Half elitism
Mutation probability		Random
Crossover probability		Random

4.1 Compressive strength of FRP-confined concrete

As was discussed earlier, the majority of the conventional models are based on the expression forms proposed by Richart et al. [5]. GP, on the other hand, initiates the formulation of expressions from a few random seeds, of which the evolution took place artificially and terminated when a robust solution was found. In the GP formulation process, the selection of independent variables, functions and model structure for a given terminal set relies significantly on the users' knowledge of the FRP-confined concrete systems. Overfitting of model with redundant independent variables and functions results in a complex mathematical solution rather than a physically meaningful model structure, whereas underfitting reduces the model accuracy. In this process, finding the potential combination of several input parameter to form a single representative input parameter, such as the confinement stiffness of FRP jacket (K_l) used in this study, is important. As presented in Table 1, only parameters that had been observed experimentally to influence the terminal sets [2] were selected as independent variables for GP formulation. In addition, only simple model structure yielding practical close-formed expressions suitable for engineering application were adopted by the authors. The converged expression for the prediction of the compressive strength of FRP-confined concrete (f'_{cc}) is presented in Eq. 1.

$$f'_{cc} = f'_{co} + K_l\varepsilon_{h,rup} + K_l^{1.5}\varepsilon_{h,rup}^2 + a \quad \text{where} \quad a = \sqrt{K_l - \frac{f'_{co}}{\sqrt{\varepsilon_{h,rup}}}} \geq 0 \tag{1}$$

where f'_{co} is the unconfined concrete strength, K_l is the confinement stiffness of the FRP jacket, to be calculated using Eq. 2, and $\varepsilon_{h,rup}$ is the hoop rupture strain of the FRP jacket to be calculated using Eq. 8 presented later in Section 4.3. K_l and f'_{co} are in MPa.

$$K_l = \frac{2E_f t_f}{D} \quad (2)$$

E_f is the elastic modulus of fibers, t_f is the total nominal fiber thickness of the FRP jacket, D is the diameter of the concrete specimen.

To demonstrate an example of the GP formulation process, Figure 6 shows the relationship between accuracy and complexity of the GP formulation of the compressive strength expression. As illustrated by the figure, the fitness or accuracy of the expression improves significantly after the first few generations. After which, the complexity of the expression represented by the level and nodes in Figure 6 continue to increase with marginal improvements in its fitness in the proceeding generations. At the 28th generation, where a low level and a small number of nodes were found at lower fitness, the final expression is selected and presented as Eq. 1. Level is the depth of parse tree which controls the number of nodes. It is used to avoid bloating, an excessive code growth without corresponding improvement in fitness.

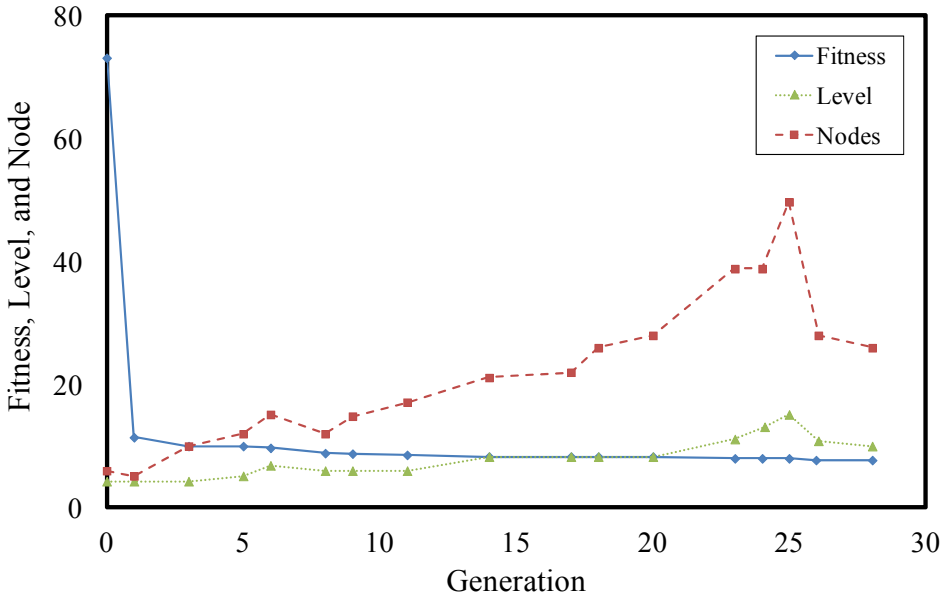

Figure 6. Fitness, level, and nodes versus generation of the compressive strength expression

Figure 7 shows the comparison of the strength enhancement ratio predictions (f'_{cc}/f'_{co}) of the proposed expression (Eq. 1) with the 30% testing datasets of the experimental database. The comparison indicates that the model predictions are in close agreement with the test results, which are quantified through the use of statistical indicators: average absolute error (*AAE*) to establish overall model accuracy; mean (*M*) to establish average overestimation or underestimation of the model; and standard deviation (*SD*) to establish the magnitude of the associated scatter of the model prediction. These indicators are defined by Eqs. 3 to 5. As evident from the figure, an *AAE*, *M*, and *SD* of 10.5%, 100.9%, and 13.5%, respectively, was achieved.

$$AAE = \frac{\sum_{i=1}^{n} \left| \frac{model_i - exp_i}{exp_i} \right|}{n} \tag{3}$$

$$M = \frac{\sum_{i=1}^{n} \frac{model_i}{exp_i}}{n} \tag{4}$$

$$SD = \sqrt{\frac{\sum_{i=1}^{n} \left(\frac{model_i}{exp_i} - M \right)^2}{n-1}} \tag{5}$$

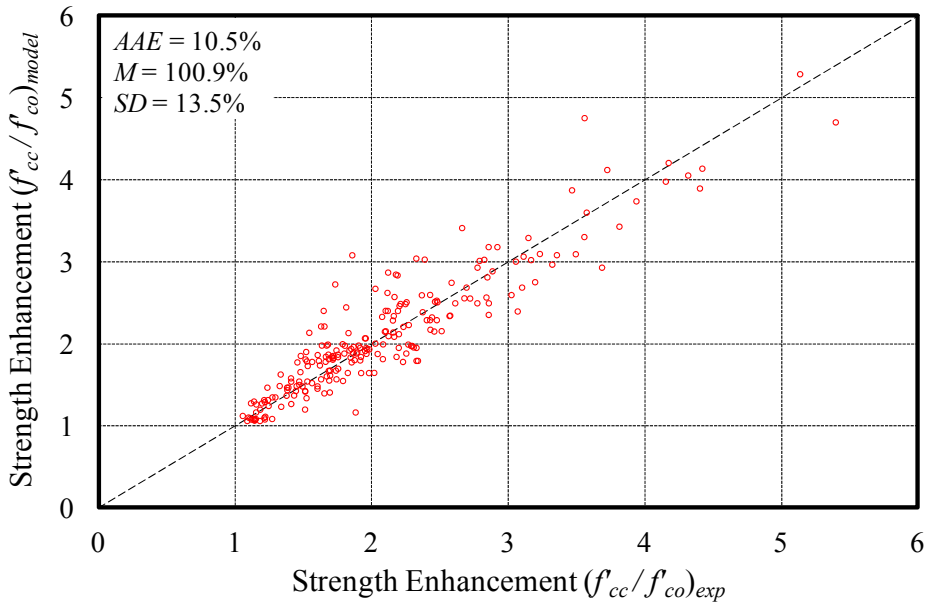

Figure 7. Comparison of model predictions of strength enhancement ratios (f'_{cc}/f'_{co}) with experimental results

4.2 Ultimate Axial Strain of FRP-confined concrete

Based on the GP formulation process discussed earlier, the expression for the prediction of the ultimate axial strain (ε_{cu}) of FRP-confined concrete is established and presented in Eq. 6.

$$\varepsilon_{cu} = (\varepsilon_{co} + b)\left(\varepsilon_{co}{}^{c} + \frac{K_l}{f'_{co}}(2\varepsilon_{co} + b)\right) \tag{6}$$

$$\text{where} \quad b = \varepsilon_{h,rup} - \varepsilon_{h,rup}{}^{\frac{K_l}{f'_{co}}} \quad and \quad c = \frac{f'_{co}\left(\varepsilon_{co} + \varepsilon_{h,rup} + e^{\varepsilon_{h,rup}}\right)}{K_l}$$

where ε_{co} is the axial strain corresponding to the compressive strength of unconfined concrete, to be calculated using Eq. 7 proposed by Lim and Ozbakkaloglu [38], $\varepsilon_{h,rup}$ is the hoop rupture strain of the FRP jacket, to be calculated using Eq. 8 presented in the next section, and K_l is the confinement stiffness of the FRP jacket, to be calculated using Eq. 2.

$$\varepsilon_{co} = \frac{f'_{co}{}^{0.225}}{1000} k_s k_a \tag{7}$$

$$\text{where} \quad k_s = \left(\frac{152}{D}\right)^{0.1} \quad \text{and} \quad k_a = \left(\frac{2D}{H}\right)^{0.13}$$

where, f'_{co} is in MPa, and k_s and k_a, respectively, are the coefficients to allow for the specimens size and specimen aspect ratio.

Figure 8 shows comparisons of the strain enhancement ratio predictions ($\varepsilon_{cu}/\varepsilon_{co}$) of the proposed model with testing datasets of the experimental database. The comparison indicates that the model predictions are in close agreement with the test results, of which an *AAE*, *M*, and *SD* of 25.7%, 101.1%, and 33.1%, respectively, was achieved.

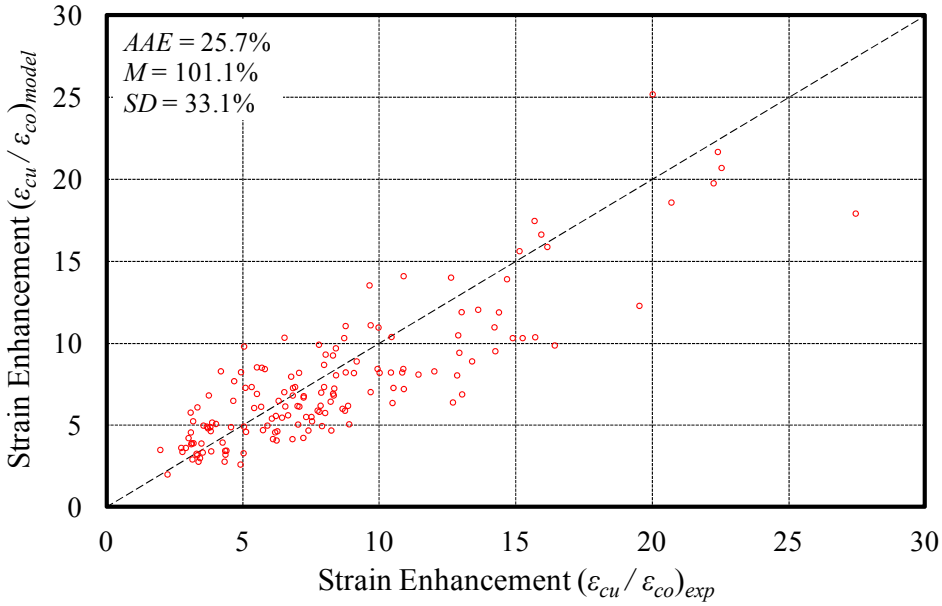

Figure 8. Comparison of model predictions of strain enhancement ratios ($\varepsilon_{cu}/\varepsilon_{co}$) with experimental results

4.3 Hoop rupture strain of FRP jacket

The hoop rupture strains ($\varepsilon_{h,rup}$) of FRP jackets are commonly reported to be lower than the ultimate tensile strain of the fiber material (ε_f) [39-43]. As previously reported in Ozbakkaloglu and Akin [44], an increase in the compressive strength of concrete, which alters the concrete cracking pattern from heterogenic mircrocracks to localized macrocracks, has an adverse influence on the hoop rupture strain ($\varepsilon_{h,rup}$) of the FRP jacket. An increase in the elastic modulus of fibers (E_f) of the FRP jacket was also reported to decrease the hoop rupture strain ($\varepsilon_{h,rup}$) [45]. To account for such dependencies of the hoop rupture strain on the FRP and concrete materials, the elastic modulus of fibers (E_f), ultimate tensile strain of fibers (ε_f), and unconfined concrete strength (f'_{co}) were considered as separate input variables for the development of the hoop rupture strain expression ($\varepsilon_{h,rup}$). The expression established using the GP formulation process for the prediction of the hoop rupture strain of FRP ($\varepsilon_{h,rup}$) is presented as Eq. 8.

$$\varepsilon_{h,rup} = \frac{\varepsilon_f}{f'^{\,0.125}_{co}} \tag{8}$$

To demonstrate an example of overfitted expression, the GP formulation process was allowed to continue until a next expression (Eq. 9) with a slightly higher accuracy is found. Figures 9(a) and 9(b) show the comparisons of testing dataset results with the hoop rupture strains ($\varepsilon_{h,rup}$) predicted using Eqs. 8 and 9, respectively. The comparison indicates that the model predictions are in close agreement with the test results, of which *AAE*, *M*, and *SD* of 22.7%, 109.6%, and 34.2% were achieved in the first expression, while 22.5%, 112.2%, and 33.1% were achieved in the second expression. With only a small margin of improvement achieved, the form of the expression of Eq. 9 became relatively complex in comparison to the earlier form shown in Eq. 8. On this basis, Eq. 8 is recommended for its simplicity. In addition, as Eq. 9 was overfitted for the current size of test database, its performance is likely to degrade at out-of-range prediction, due to its increased sensitivity to the parametric ranges of the current database.

$$\varepsilon_{h,rup} = \left(\frac{\varepsilon_f}{E_f + f'_{co}}\right)^{0.5\varepsilon_f{}^d} \quad \text{where} \quad d = \frac{\varepsilon_f}{f'^{\left(\frac{f'_{co}\varepsilon_f}{\varepsilon_f + f'_{co}}\right)}_{co}} \tag{9}$$

where E_f and f'_{co} are in MPa.

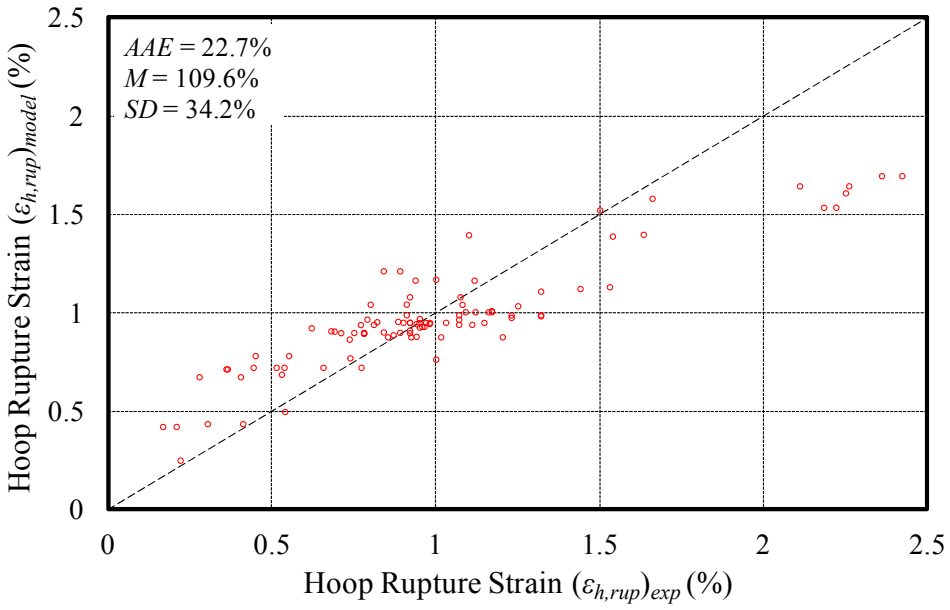

(a)

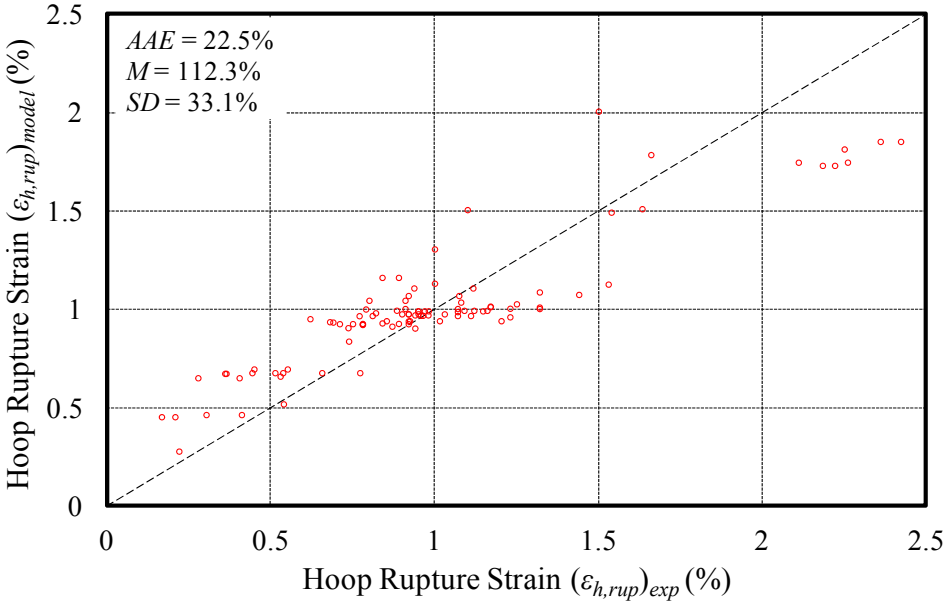

(b)

Figure 9. Comparison of model predictions of hoop rupture strains ($\varepsilon_{h,rup}$) with experimental results: (a) simplified function, (b) complex function

5. MODEL VALIDATION AND COMPARISONS WITH EXISTING MODELS

To establish the relative performance of the proposed model, its prediction statistics were compared with those of the 10 best performing conventional models identified in a recent comprehensive review study reported in Ozbakkaloglu et al. [34]. In addition, the model was also compared with seven artificial intelligence (AI) models currently available in the literature that were developed using evolutionary programming techniques, including neural network (NN) [7, 9, 11, 13, 14], genetic programming (GP) [6, 8, 11], and stepwise regression (SW) [8, 11]. It should be noted that a number model proposed in studies that only reported the architecture of their modeling framework without complete expressions for the prediction of the ultimate condition of FRP-confined concrete were not assessed (e.g., [10, 12, 15, 17, 18]). The prediction statistics for the strength and strain enhancement ratios (f'_{cc}/f'_{co} and $\varepsilon_{cu}/\varepsilon_{co}$) are given in Tables 2 and 3, respectively. In addition to the results shown in Tables 2 and 3, the graphical comparison the AAEs of the conventional and the AI models are given in Figures 10 and 11, respectively. In calculating model predictions of the peak strain ratios ($\varepsilon_{cu}/\varepsilon_{co}$), the ε_{co} values were determined using the expressions given in the original publication when available. If an expression was not specified in the original publication, the ε_{co} values were then based on the experimental values obtained from cylinder tests. If an experimental ε_{co} value was not available from a given dataset, Eq. 7 proposed by Tasdemir et al. [46] is used to determine the ε_{co} value. For the proposed model, two sets of prediction statistics are presented in Tables 2 and 3. The first set were based on the full datasets of 753 and 511 results in the experimental database for strength and strain enhancement ratios (f'_{cc}/f'_{co} and $\varepsilon_{cu}/\varepsilon_{co}$), while the second set were based the 30% testing datasets.

As evident from Tables 2 and 3 and Figures 10 and 11, the proposed model provides improved predictions of the strength enhancement ratios (f'_{cc}/f'_{co}) compared to all of the existing models. On the other hand, the predictions of the strain enhancement ratios ($\varepsilon_{cu}/\varepsilon_{co}$) of the model proposed by Ozbakkaloglu and Lim [34] are slightly better than that of the proposed model, given that the influence of axial strain instrumentation methods was considered in Ozbakkaloglu and Lim's model [34]. For such consideration, a numerical input such as the gauge length of the instrument is necessary for GP, however, was not available from the experimental database [34]. As a result, the minimum AAE of the predicted strain enhancement ratios ($\varepsilon_{cu}/\varepsilon_{co}$) by the proposed model is closer to the natural scatter of the database of 23%. It is also worthwhile noting that, none of the reviewed AI models proposed an expression for the prediction of the ultimate axial strain (ε_{cu}) of FRP-confined concrete. This paper presents the first expression established for the prediction of the ultimate axial strain (ε_{cu}) on the basis of GP (Eq. 6). As evident from Figure 8 and Table 3, the proposed expression provides reasonable predictions of the test results, which can be further improved in the future through accurate modelling of the specimen instrumentation methods.

Table 2. Statistics of strength enhancement ratio (f'_{cc}/f'_{co}) predictions of existing models

Model	Model Category*	Prediction of f'_{cc}/f'_{co}			
		Test data	Average Absolute Error (%)	Mean (%)	Standard Deviation (%)
Proposed model	GP	753	10.8	102.1	14.4
Proposed model (30% testing dataset)	GP	226	10.5	100.9	13.5
Ozbakkaloglu and Lim [31]	DO	753	11.2	99.6	13.7
Teng et al. [43]	AO	753	11.8	98.8	14.5
Lam and Teng [44]	DO	753	12.4	99.4	15.3
Wu and Zhou [45]	DO	753	12.4	102.1	15.5
Wu and Wang [46]	DO	753	12.7	101.4	15.7
Al-Salloum and Siddiqui [47]	DO	753	12.7	101.7	15.8
Wei and Wu [48]	DO	753	12.7	101.5	15.7
Realfonzo and Napoli [49]	DO	753	12.7	103.2	15.8
Bisby et al. [50]	DO	753	12.8	101.9	15.8
Jiang and Teng [1]	AO	753	12.9	93.9	14.6
Cevik 1 [9]	NN	753	15.6	96.2	18.5
Elsanadedy et al. [11]	NN	753	18.4	100.4	31.0
Cevik and Cabalar [4]	GP	753	19.6	115.1	22.6
Cevik 2 [9]	SW	753	20.1	95.7	29.9
Cevik 3 [9]	GP	753	21.0	116.1	23.2
Cevik et al. 1 [6]	GP	753	23.9	108.0	33.7
Cevik et al. 2 [6]	SW	753	33.3	108.8	42.2
Naderpour et al. [7]	NN	753	40.2	127.6	50.5
Cevik and Guzelbey [5]	NN	753	75.6	154.3	110.7
Jalal and Ramezanianpour [12]	NN	753	79.2	178.3	79.1

*Conventional models:-
AO: Analysis-oriented model
DO: Design-oriented model

Artificial Intelligence models:-
GP: Genetic programming model
NN: Neural network model
SW: Stepwise regression model

Table 3. Statistics of strain enhancement ratio ($\varepsilon_{cu}/\varepsilon_{co}$) predictions of existing models

Model	Model Category*	Prediction of $\varepsilon_{cu}/\varepsilon_{co}$			
		Test data	Average Absolute Error (%)	Mean (%)	Standard Deviation (%)
Ozbakkaloglu and Lim [31]	DO	511	21.7	100.5	27.2
Proposed model	GP	511	23.8	98.5	30.1
Proposed model (30% testing dataset)	GP	153	25.7	101.1	33.1
Tamuzs et al. [51]	DO	511	26.3	108.4	35.0
Wei and Wu [48]	DO	511	28.7	98.0	35.8
Binici [52]	AO	511	29.2	92.3	34.8
Jiang and Teng [53]	DO	511	29.5	116.1	38.5
Youssef et al. [54]	DO	511	30.0	112.5	39.0
Teng et al. [55]	DO	511	30.2	117.6	39.0
Fahmy and Wu [56]	DO	511	30.5	99.5	38.9
Teng et al. [43]	AO	511	30.5	117.0	39.3
De Lorenzis and Tepfers [57]	DO	511	31.3	77.9	27.9

*Conventional models:-
AO: Analysis-oriented model
DO: Design-oriented model

Artificial Intelligance models:-
GP: Genetic programming model
NN: Neural network model
SW: Stepwise regression model

A close examination of the assessment results has led to a number of important findings on factors influencing the performances of existing models, including the size of database, parameters considered, ability to handle uncertainties, dependency on assumptions, and the architecture of their modeling frameworks. For the conventional models, only the statistics of the model performances are presented in Tables 2 and 3 of this paper as a detailed review of factors influencing the performances of these models was previously discussed in Ozbakkaloglu et al. [2]. In this section, the factors influencing the performances of AI models are discussed. As evident from Figure 11, the proposed model outperformed existing AI models by a significant margin. This improvement was achieved through consideration of a wide range of parameters that was covered by the comprehensive experimental database and careful selection of influential input parameters in model development. In the better performing models illustrated in Figure 11, including the NN models proposed by Cevik [11] and Elsanadedy et al. [13], and the GP model proposed by Cevik and Cabalar [6], it was found that the sizes of the databases used in their development were generally larger than those of their underperforming counterparts, but the architecture of their modeling frameworks were not necessarily more complex. On the other hand, excessive complexity of modeling framework due to overfitting of models with redundant test parameters, as evident from some of the underperforming models (e.g., [9, 14]), significantly undermined the

modelling accuracy. On these bases, it is recommended that comprehensive experimental databases be used and selection of key test parameters be carefully implemented in the future development of AI models for FRP-confined concrete.

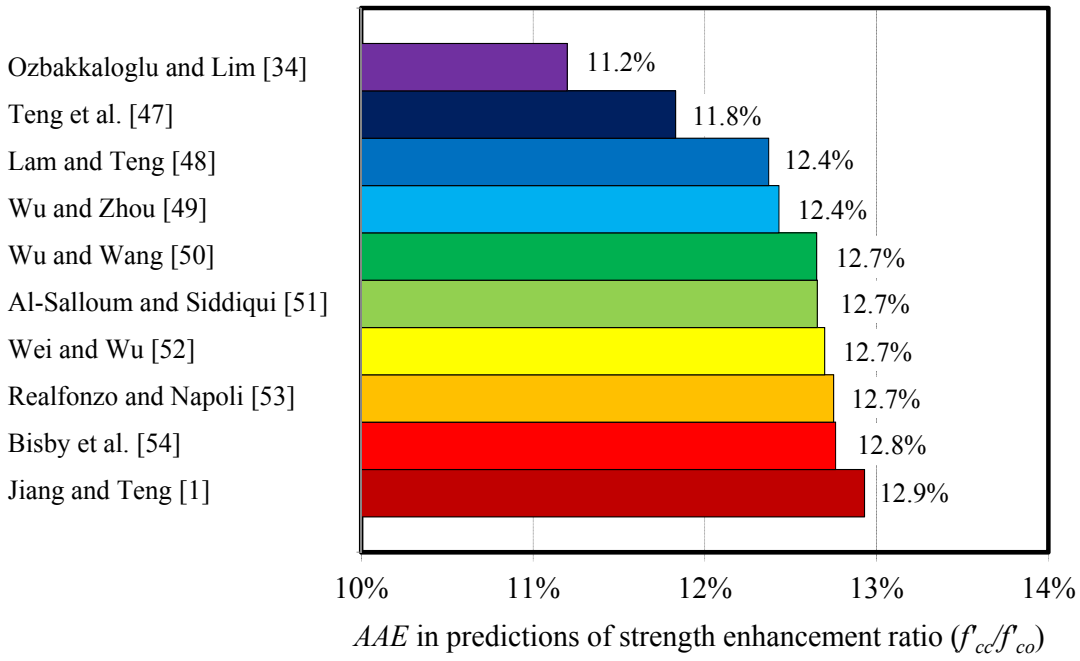

(a)

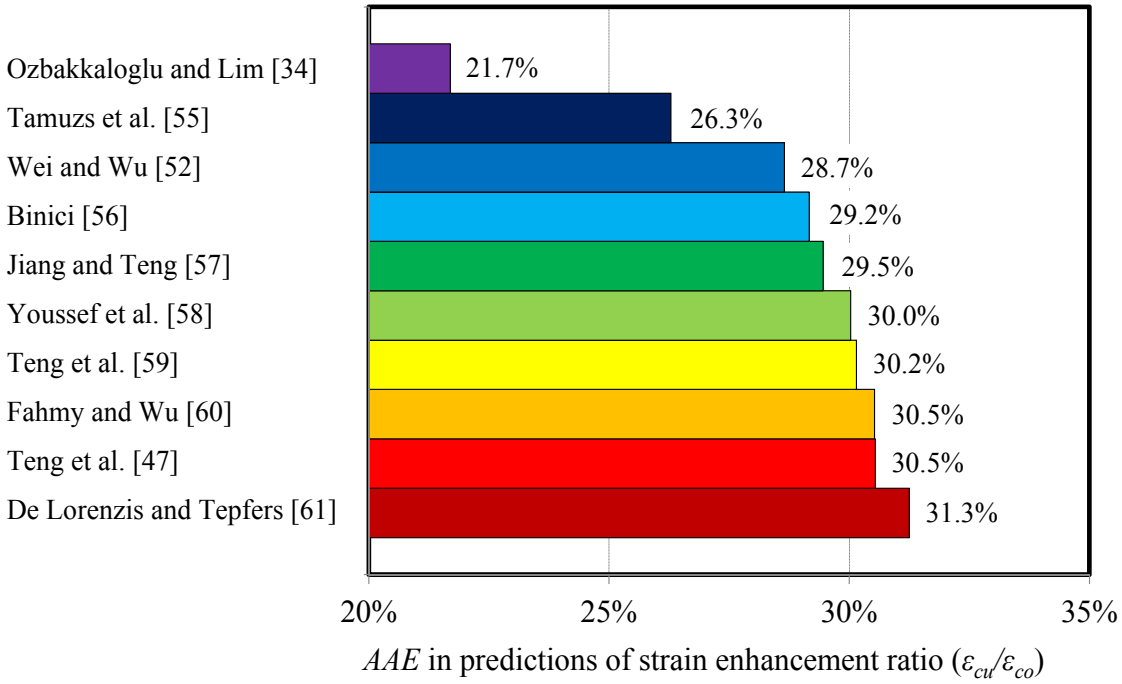

(b)

Figure 10. Average absolute error in predictions of conventional models: (a) strength enhancement ratios (f'_{cc}/f'_{co}), (b) strain enhancement ratios ($\varepsilon_{cu}/\varepsilon_{co}$)

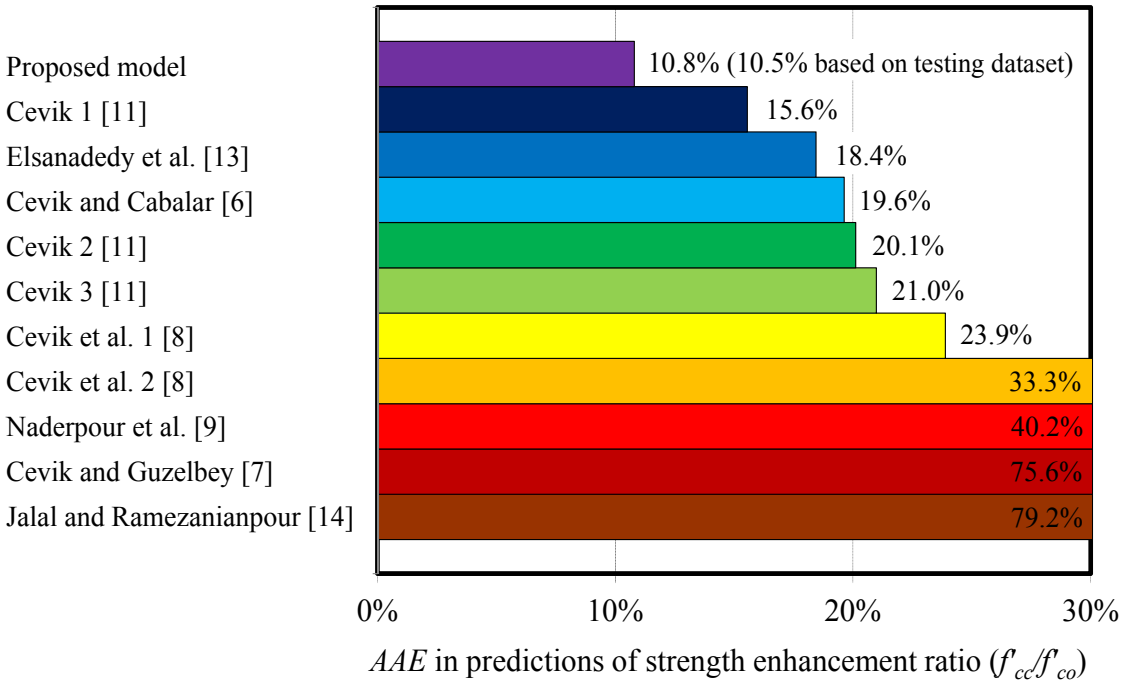

Figure 11. Average absolute error in strength enhancement ratios (f'_{cc}/f'_{co}) predictions of artificial intelligence models

6. CONCLUSIONS

A comprehensive experimental test database that consisted of 832 test results of FRP-confined concrete has been assembled from the published literature. Using the test database, the performances of a number of existing empirical, theoretical, and artificial intelligence models developed for FRP-confined concrete were then assessed. A close examination of the results of the model assessment has led to a number of important findings on factors influencing the strengths and weaknesses of models in each category. These findings have been summarized and discussed in detail in this paper. On the basis of the experimental database, a new model for evaluating the ultimate condition of FRP-confined concrete was developed using genetic programming and has been presented in this paper. The model is the first to establish the ultimate axial strain and hoop rupture strain expressions for FRP-confined concrete on the basis of evolutionary algorithms. Comparisons with experimental test results show that the predictions of the proposed model are in good agreement with the test results of the database, and provide improved predictions compared to the existing artificial intelligence models. Genetic programming proved that more accurate results can be achieved in explaining and formulating the ultimate condition of FRP confined concretes. The model assessment that has been presented herein clearly illustrates the important influences of the size of the test databases and the selected test parameters used in the development of artificial intelligence models on their overall performances.

REFERENCES

[1] Jiang T, Teng JG. Analysis-oriented stress-strain models for FRP-confined concrete. Engineering Structures. 2007;29:2968-86.

[2] Ozbakkaloglu T, Lim JC, Vincent T. FRP-confined concrete in circular sections: Review and assessment of stress–strain models. Engineering Structures. 2013;49:1068–88.

[3] Lim JC, Ozbakkaloglu T. Investigation of the Influence of Application Path of Confining Pressure: Tests on Actively Confined and FRP-Confined Concretes. Journal of Structural Engineering, ASCE. 2014;Doi: 10.1061/(ASCE)ST.1943-541X.0001177.

[4] Lim JC, Ozbakkaloglu T. Unified stress-strain model for FRP and actively confined normal-strength and high-strength concrete. Journal of Composites for Construction. 2014;Doi: 10.1061/(ASCE)CC.1943-5614.0000536.

[5] Richart FE, Brandtzaeg A, Brown RL. A study of the failure of concrete under combined compressive stresses. Bulletin No 185. Champaign, Illinois: Engineering Experimental Station, University of Illinois; 1928.

[6] Cevik A, Cabalar AF. A Genetic-Programming-Based Formulation for the Strength Enhancement of Fiber-Reinforced-Polymer-Confined Concrete Cylinders. Journal of Applied Polymer Science. 2008;110:3087-95.

[7] Cevik A, Guzelbey IH. Neural network modeling of strength enhancement for CFRP confined concrete cylinders. Building and Environment. 2008;43:751-63.

[8] Cevik A, Gogus MT, Guzelbey IH, Filiz H. Soft computing based formulation for strength enhancement of CFRP confined concrete cylinders. Advances in Engineering Software. 2010;41:527-36.

[9] Naderpour H, Kheyroddin A, Amiri GG. Prediction of FRP-confined compressive strength of concrete using artificial neural networks. Composite Structures. 2010;92:2817-29.

[10] Wu Y-b, Jin G-f, Ding T, Meng D. Modeling Confinement Efficiency of FRP-Confined Concrete Column Using Radial Basis Function Neural Network. 2nd International Workshop on Intelligent Systems and Applications (ISA). Wuhan, China; 2010.

[11] Cevik A. Modeling strength enhancement of FRP confined concrete cylinders using soft computing. Expert Systems with applications. 2011;38:5662-73.

[12] Oreta AWC, Ongpeng JMC. Modeling the confined compressive strength of hybrid circular concrete columns using neural networks. Computers and Concrete. 2011;8:597-616.

[13] Elsanadedy HM, Al-Salloum YA, Abbas H, Alsayed SH. Prediction of strength parameters of FRP-confined concrete. Composites Part B. 2012;43:228-39.

[14] Jalal M, Ramezanianpour AA. Strength enhancement modeling of concrete cylinders confined with CFRP composites using artificial neural networks. Composites Part B. 2012;43:2990-3000.

[15] Jalal M, Ramezanianpour AA, Pouladkhan AR, Tedro P. Application of genetic programming (GP) and ANFIS for strength enhancement modeling of CFRP-retrofitted concrete cylinders. Neural Computing and Applications. 2013;23:455-70.

[16] Mashrei MA, Seracino R, Rahman MS. Application of artificial neural networks to predict the bond strength of FRP-to-concrete joints. Construction and Building Materials. 2013;40:812-21.

[17] Yousif DST. New Model of CFRP-Confined Circular Concrete Columns: Ann Approach. International Journal of Civil Engineering and Technology. 2013;4:98-110.

[18] Pham TM, Hadi MN. Predicting Stress and Strain of FRP-Confined Square/Rectangular Columns Using Artificial Neural Networks. Journal of Composites for Construction. 2014;Doi: 10.1061/(ASCE)CC.1943-5614.0000477.
[19] Koza JR. Genetic programming: on the programming of computers by means of natural selection. Cambridge, MA: MIT press; 1992.
[20] Yang Y, Soh CK. Automated optimum design of structures using genetic programming. Computers and Structures. 2002;80:1537-46.
[21] Karakus M. Function identification for the intrinsic strength and elastic properties of granitic rocks via genetic programming (GP). Computers and Geosciences. 2011;37:1318-23.
[22] Shen J, Karakus M, Xu C. Direct expressions for linearization of shear strength envelopes given by the Generalized Hoek–Brown criterion using genetic programming. Computers and Geotechnics. 2012;44:139-46.
[23] Castelli M, Vanneschi L, Silva S. Prediction of high performance concrete strength using Genetic Programming with geometric semantic genetic operators. Expert Systems with applications. 2013;40:6856-62.
[24] Babanajad SK, Gandomi AH, Mohammadzadeh S D, Alavi AH. Numerical modeling of concrete strength under multiaxial confinement pressures using linear genetic programming. Automation in Construction. 2013;36:136-44.
[25] Vassilopoulos AP, Georgopoulos EF, Keller T. Comparison of genetic programming with conventional methods for fatigue life modeling of FRP composite materials. International Journal of Fatigue. 2008;30:1634-45.
[26] Johari A, Habibagahi G, Ghahramani A. Prediction of soil–water characteristic curve using genetic programming. Journal of Geotechnical and Geoenvironmental Engineering. 2006;132:661-5.
[27] Baykasoğlu A, Güllü H, Çanakçı H, Özbakır L. Prediction of compressive and tensile strength of limestone via genetic programming. Expert Systems with applications. 2008;35:111-23.
[28] Javadi AA, Rezania M, Nezhad MM. Evaluation of liquefaction induced lateral displacements using genetic programming. Computers and Geotechnics. 2006;33:222-33.
[29] Cabalar AF, Cevik A. Genetic programming-based attenuation relationship: An application of recent earthquakes in turkey. Computers and Geosciences. 2009;35:1884-96.
[30] Holland JH. Adaptation in natural and artificial systems: An introductory analysis with applications to biology, control, and artificial intelligence: University of Michigan Press; 1975.
[31] Goldberg DE. Genetic algorithms in search, optimization, and machine learning. 1st ed. Massachusetts: Reading Menlo Park: Addison-Wesley Professional; 1989.
[32] Silva S, Almeida J. GPLAB-a genetic programming toolbox for MATLAB. The Nordic MATLAB conference. Copenhagen, Denmark. 2003. p. 273-8.
[33] Poli R, McPhee NF. Parsimony Pressure Made Easy: Solving the Problem of Bloat in GP in Theory and Principled Methods for the Design of Metaheuristics: Springer-Verlag Berlin and Heidelberg GmbH & Co. KG; 2013.
[34] Ozbakkaloglu T, Lim JC. Axial compressive behavior of FRP-confined concrete: Experimental test database and a new design-oriented model. Composites Part B. 2013;55:607-34.

[35] Gray GJ, Murray-Smith DJL, Y., Sharman KC, Weinbrenner T. Nonlinear model structure identification using genetic programming. Control Engineering Practice. 1998;6:1341-52.
[36] Güllü H. Function finding via genetic expression programming for strength and elastic properties of clay treated with bottom ash. Engineering Applications of Artificial Intelligence. 2014;35:143-57.
[37] Roushangar K, Mouaze D, Shiri J. Evaluation of genetic programming-based models for simulating friction factor in alluvial channels. Journal of Hydrology. 2014;517:1154-61.
[38] Lim JC, Ozbakkaloglu T. Stress-strain model for normal- and light-weight concretes under uniaxial and triaxial compression. Construction and Building Materials. 2014;71:492-509.
[39] Shahawy M, Mirmiran A, Beitelman T. Tests and modeling of carbon-wrapped concrete columns. Composites Part B. 2000;31:471-80.
[40] Xiao Y, Wu H. Compressive behavior of concrete confined by carbon fiber composite jackets. Journal of Materials in Civil Engineering. 2000;12:139-46.
[41] Pessiki S, Harries KA, Kestner JT, Sause R, Ricles JM. Axial behavior of reinforced concrete columns confined with FRP jackets. Journal of Composites for Construction. 2001;5:237-45.
[42] Harries KA, Carey SA. Shape and "gap" effects on the behavior of variably confined concrete. Cement and Concrete Research. 2003;33:881-90.
[43] Lam L, Teng JG. Ultimate condition of fiber reinforced polymer-confined concrete. Journal of Composites for Construction, ASCE. 2004;8:539-48.
[44] Ozbakkaloglu T, Akin E. Behavior of FRP-confined normal- and high-strength concrete under cyclic axial compression. Journal of Composites for Construction, ASCE. 2012;16:451-63.
[45] Lim JC, Ozbakkaloglu T. Confinement model for FRP-confined high-strength concrete. Journal of Composites for Construction, ASCE. 2014;18:04013058.
[46] Tasdemir MA, Tasdemir C, Jefferson AD, Lydon FD, Barr BIG. Evaluation of strains at peak stresses in concrete: A three-phase composite model approach. Cement and Concrete Research. 1998;20:301-18.
[47] Teng JG, Huang YL, Lam L, Ye LP. Theoretical model for fiber-reinforced polymer-confined concrete. Journal of Composites for Construction, ASCE. 2007;11:201-10.
[48] Lam L, Teng JG. Design-oriented stress-strain model for FRP-confined concrete. Construction and Building Materials. 2003;17:471-89.
[49] Wu YF, Zhou YW. Unified strength model based on Hoek-Brown failure criterion for circular and square concrete columns confined by FRP. Journal of Composites for Construction. 2010;14:175-84.
[50] Wu YF, Wang LM. Unified strength model for square and circular concrete columns confined by external jacket. Journal of Structural Engineering. 2009;135:253-61.
[51] Al-Salloum Y, Siddiqui N. Compressive strength prediction model for FRP-confined concrete. 9th International Symposium on Fiber Reinforced Polymer Reinforcement for Concrete Structures. Sydney, Australia; 2009.
[52] Wei YY, Wu YF. Unified stress-strain model of concrete for FRP-confined columns. Construction and Building Materials. 2012;26:381-92.

[53] Realfonzo R, Napoli A. Concrete confined by FRP systems: Confinement efficiency and design strength models. Composites Part B. 2011;42:736-55.
[54] Bisby LA, Green MF, Kodur VKR. Modeling the behavior of fiber reinforced polymer-confined concrete columns exposed to fire. Journal of Composites for Construction. 2005;9:15-24.
[55] Tamuzs V, Tepfers R, Zile E, Ladnova O. Behavior of concrete cylinders confined by a carbon composite - 3. Deformability and the ultimate axial strain. Mechanics of Composite Materials. 2006;42:303-14.
[56] Binici B. An analytical model for stress-strain behavior of confined concrete. Engineering Structures. 2005;27:1040-51.
[57] Jiang T, Teng JG. Strengthening of short circular RC columns with FRP jackets: a design proposal. 3rd International Conference on FRP Composites in Civil Engineering. Miami, Florida, USA; 2006.
[58] Youssef MN, Feng MQ, Mosallam AS. Stress-strain model for concrete confined by FRP composites. Composites Part B. 2007;38:614-28.
[59] Teng JG, Jiang T, Lam L, Luo Y. Refinement of a design-oriented stress-strain model for FRP-confined concrete. Journal of Composites for Construction. 2009;13:269-78.
[60] Fahmy MFM, Wu ZS. Evaluating and proposing models of circular concrete columns confined with different FRP composites. Composites Part B. 2010;41:199-213.
[61] De Lorenzis L, Tepfers R. Comparative study of models on confinement of concrete cylinders with fiber-reinforced polymer composites. Journal of Composites for Construction. 2003;7:219-37.

THIS PAGE HAS BEEN LEFT INTENTIONALLY BLANK

Statement of Authorship

Title of Paper	Finite Element Modeling of Normal- and High-Strength Concrete Confined under Uni-, Bi-, and Triaxial Compression
Publication Status	○ Published ○ Accepted for Publication ○ Submitted for Publication ◉ Publication Style
Publication Details	Prepared for submission

Author Contributions

By signing the Statement of Authorship, each author certifies that their stated contribution to the publication is accurate and that permission is granted for the publication to be included in the candidate's thesis.

Name of Principal Author (Candidate)	Mr. Jian Chin Lim		
Contribution to the Paper	Preparation of experimental database, analysis of database results and development of model		
Signature		Date	23/02/2015

Name of Co-Author	Mr. Reza Sadeghi		
Contribution to the Paper	Analysis of experiment results and development of model		
Signature		Date	23/02/2015

Name of Co-Author	Dr. Terry Bennett		
Contribution to the Paper	Review of manuscript		
Signature		Date	23/02/2015

Name of Co-Author	Dr. Togay Ozbakkaloglu		
Contribution to the Paper	Research supervision and review of manuscript		
Signature		Date	23/02/2015

THIS PAGE HAS BEEN LEFT INTENTIONALLY BLANK

FINITE ELEMENT MODELING OF NORMAL- AND HIGH-STRENGTH CONCRETE UNDER UNI-, BI- AND TRIAXIAL COMPRESSION

Jian C. Lim, Reza Sadeghi, Terry Bennett and Togay Ozbakkaloglu

ABSTRACT

A concrete strength-sensitive finite element (FE) model applicable to concrete subjected to various confining pressure levels and conditions is presented. This study focuses mainly on the failure surface and flow rule of concrete in multiaxial compression, which were experimentally observed to vary with the unconfined concrete strength and level of confining pressure. To this end, a large experimental database, which consists of more than 1700 results of concrete specimens tested under biaxial and triaxial compression, was assembled through an extensive review of the literature. This database was augmented with another test database of concrete in uniaxial compression that consists of more than 4000 test results. Based on the test database results, it was observed that the tangential slope of the failure surface reduces with an increase in the unconfined concrete strength and confining pressure. The concrete dilation angle considered in the flow rule was observed to be is non-linear throughout loading history. To incorporate the observed changes in the failure surface and flow rule of concrete subjected to uni-, bi- and triaxial compression, an extension of Lubliner's (1989) concrete-damage plasticity model was proposed and presented in this paper. Comparisons with experimental test results show that the predictions of the extended model are in good agreement with the test results of both normal-strength (NSC) and high-strength concretes (HSC).

KEYWORDS: Concrete; High-strength concrete (HSC); Confinement; Stress-strain relations; Uniaxial; Triaxial; Compression; Plasticity; Finite element (FE).

1. INTRODUCTION

It is well established that lateral confinement of concrete enhances its compressive strength and axial deformation capacity (Kent and Park 1971; Sheikh and Uzumeri 1980; Mander et al. 1988; Saatcioglu and Razvi 1992; Ozbakkaloglu and Saatcioglu 2006; Ozbakkaloglu et al. 2013). A comprehensive review of the literature that was undertaken as part of the current study and those previously reported in Ozbakkaloglu et al. (2013) and Lim and Ozbakkaloglu (2014b) revealed that over 500 experimental studies have been conducted on the axial compressive behavior of unconfined, actively confined, and fiber reinforced polymer (FRP)-confined concretes, resulting in the development of over 120 stress-strain models. These models have been categorized into four main categories: i) design-oriented models presented in closed-form expressions; ii) analysis-oriented models, which predict stress-strain curves by an incremental procedure; iii) soft computing-based models, which utilizes evolutionary algorithms and computer programming to perform predictions; and iv) finite element (FE) models, which predict the constitutive stress-strain behavior of confined concrete by considering continuum material properties and interactions of individual elements. Among the large variety of modeling approaches available, finite element (FE) analysis is well known for its versatility in predicting the constitutive behavior of structural members. The use of FE approach is particularly advantageous in the modeling of non-uniformly confined concrete as it is capable of capturing complex stress variations in the concrete. In attempts to model the plasticity characteristics of confined concrete, most of the existing FE models use either on Drucker-Prager plasticity (Drucker and Prager 1952) or concrete-damage plasticity approach (Lubliner et al. 1989; Lee and Fenves 1998). While the majority of these models adopted the Drucker-Prager plasticity approach, comparisons with the test database results of concrete in triaxial and biaxial compressions indicate that the failure surface described using concrete-damage plasticity is more accurate. A review of the existing literature revealed that existing FE models for confined concretes are limited in their application domains, defined by the parametric range of the experimental results considered in their development. As a result of this limitation, the dependency of the stress-strain behavior and volumetric dilation behavior of confined concrete on the level of confining pressure and unconfined concrete strength has not been yet been established accurately. Furthermore, in the modeling of the stress-strain relationship and volumetric dilation behavior of concrete, most of the existing models focus on normal strength concrete (NSC) without much attention given to high strength concrete (HSC). A FE model suitable for a wide range of applications of conf ned concrete should consider the variations in concrete strength, confining pressure and includes non-associative f ow rule and strain hardening/softening rule. In this paper, an FE model satisfying these criteria is presented. The model utilizes failure surface and flow rule that were carefully established using comprehensive and up-to-date experimental databases.

2. EXPERIMENTAL TEST DATABASES

The two carefully prepared test databases of unconfined and confined concretes used in the model development are summarized in this section. The database of unconfined concrete, presented in Lim and Ozbakkaloglu (2014c), was assembled from 209 experimental studies and consisted of 4353 test results of concrete specimens subjected to uniaxial compression. 3446 of these datasets came from specimens that had circular cross-sections, with diameters (D) varied from 50 to 406 mm, heights (H) varied from 25 to 1016 mm, and aspect ratios (H/D) varied from 1 to 8. The unconfined compressive strengths (f'_{co}) and the corresponding axial strains (ε_{co}) of the circular specimens varied from 5.3 to 171.1 MPa and 0.07 to 0.53 %, respectively.

The second database that consists of test results of concrete subjected to biaxial and triaxial compressions are summarized in Table 1. The database was assembled from 64 published studies and consisted of 1752 test datasets, including 31 specimen results from tests conducted at the University of Adelaide (Lim and Ozbakkaloglu 2014a). As indicated in Table 1, specimen tests under triaxial compressions are subcategorized into true triaxial tests and triaxial pressure vessel tests. In true triaxial tests, cubical concrete specimens were tested in conventional triaxial compression test machines through multi-axial loading platens. In triaxial pressure vessel tests, cylindrical concrete specimens were tested in Hoek cells by subjecting specimens to fluid pressure through pressurized membrane. For specimens tested by triaxial pressure vessels, only specimens with an aspect ratio (H/D) of less than three were included in the database. The part of the database related to the triaxial pressure vessel tests can be found in Lim and Ozbakkaloglu (2014b). The cross-sectional dimensions of the specimens (D) varied between 50 and 200 mm. The unconfined concrete strength (f'_{co}) and the corresponding axial strain (ε_{co}), as obtained from concrete cylinder tests, varied from 7.2 to 132.0 MPa and 0.15% to 0.40%, respectively. The active confinement ratio, defined as the ratio of the lateral confining pressure of the triaxial cell to the compressive strength of the unconfined concrete specimen (f^*_l/f'_{co}), varied from 0.004 to 21.67.

Figure 1 shows the typical axial stress-strain curves of unconfined and actively confined concretes under different levels of confining pressure. As illustrated in the figure, the peak condition of unconfined concrete is characterized by the uniaxial compressive strength (f'_{co}) and the corresponding axial strain (ε_{co}); while the peak condition of actively confined concrete is characterized by the confined compressive strength (f^*_{cc}) and the corresponding axial strain (ε^*_{cc}); the residual condition is characterized by the residual stress ($f_{c,res}$) and the corresponding axial strain ($\varepsilon_{c,res}$). As can be seen from the figure, the differences in the shapes of the stress-strain curves are highly dependent on the level of confining pressure applied to the concrete. In both unconfined and confined concretes, the curves exhibit parabolic ascending branches that reach the compressive strengths (f'_{co} or f^*_{cc}) followed by gradually descending second branches. In confined concrete, after compressive strength is reached, the interparticle cohesion in the concrete continues to decrease and the remaining strength generated from frictional action forms a stabilized plateau in the curve, referred to as the residual stress ($f_{c,res}$) (Imran and Pantazopoulou 2001). Throughout this paper, compressive stresses (f_c) and strains (ε_c) are defined to be positive.

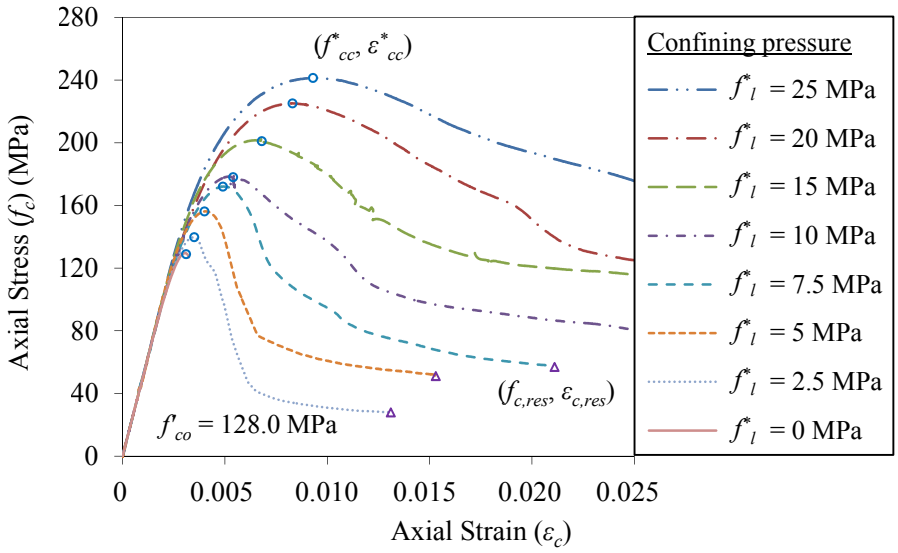

Figure 1. Axial stress-strain curves of concrete subjected to different levels of confining pressure (Group U128)

3. EXTENDED CONCRETE-DAMAGE PLASTICITY MODEL FOR UNCONFINED AND ACTIVELY CONFINED CONCRETE

In the developments of constitutive models, many researchers have used plasticity theory alone to characterize the stress-strain response of concrete (Chen and Chen 1975; Willam and Warnke 1975; Karabinis and Kiousis 1994; Grassl et al. 2002; Li and Crouch 2010; Yu et al. 2010), whereas others have relied solely on the continuum damage theory to model the nonlinear material behavior (Loland 1980; Ortiz and Popov 1982; Pijaudier-Cabot and Bazant 1987; Mazars and Pijaudier-Cabot 1989; Lubarda et al. 1994). These two approaches are complementary in a way the plasticity theory offers a good representation of ductile behavior under multiaxial compression whereas the continuum damage theory captures the damage mechanics and stiffness degradation in the concrete material. As a result, a constitutive model that covers both plasticity and concrete-damage approaches, proposed by Lubliner et al. (1989) and later modif ed by Lee and Fenves (1998) was adopted in this study for the proposed extensions. This model, which is readily available in the well-known finite element software ABAQUS (2012), was selected for implementation of the failure surface and flow rule carefully established from the up-to-date experimental databases. Although this implementation can also be applied to other concrete-damage plasticity models (Jefferson 1998; Crouch and Tahar 2000; Hansen et al. 2001; Grassl and Jirasek 2006; Jason et al. 2006; Wu et al. 2006), Lubliner's model (1989) was selected due to the versatility of ABAQUS software for implementing the intended modifications and the availability of other in-built features for finite-element modelling purposes. The proposed modifications to improve the concrete-damage plasticity model are discussed in detail in the following sections.

Table 1. Summary of expermemtal test database of concrete in biaxial and triaxial compressions

No.	Paper	Number of data	Dimensions of specimen D x B x H (mm)	Confinement type	f'_{co} (MPa)	f^*_l/f'_{co}
1	Ansari and Li (1998), Li and Ansari (1999)	14	ø101 x 202	Triaxial vessel	47.2 – 107.3	0.18 – 0.93
2	Balmer (1949)	51	ø152.4 x 304.8	Triaxial vessel	24.6	7.0 – 21.0
3	Bellamy (1961)	6	ø152.4 x 304.8	Triaxial vessel	29.5 – 33.8	0.28 – 1.29
4	Belloti and Ronzoni (1984)	3		Triaxial vessel	59.5	0.33 – 0.66
5	Bellotti and Rossi (1991)	8	ø160 x 320	Triaxial vessel	53.5	0.09 – 0.73
6	Calixto (2002)	5	127.0 x 127.0 x 12.7	Biaxial	74.5	0.05 – 0.30
7	Candappa et al. (1999) , Candappa et al. (2001)	22	ø98 x 200	Triaxial vessel	41.9 – 103.3	0.04 – 0.29
8	Chern et al. (1992)	12	ø54 x 108	Triaxial vessel	20.5	0.49 – 3.41
9	Chinn and Zimmerman (1965)	41	ø152.4 x 304.8	Triaxial vessel	32.4 – 70.0	0.49 – 17.14
10	Cordon and Gillespie (1963)	71	ø152.4 x 304.8	Triaxial vessel	12.2 – 51.0	0.05 – 1.13
11	Dahl (1992)	207	ø100 x 200	Triaxial vessel	9.8 – 108.8	0.20 – 13.85
12	Duke and Davis (1944)	16	ø76.2 x 152.4	Triaxial vessel	39.2 – 45.6	0.02 – 0.16
13	Endebrock and Traina (1972)	1		Biaxial	18.6	1.15
14	Farnam et al. (2010)	3	ø75 x 150	Triaxial vessel	76.0	0.07 – 0.28
15	Ferrara (1967)	2		Triaxial vessel	56.9	0.35 – 0.70
16	Gabet et al. (2008)	6	ø70 x 140	Triaxial vessel	30.0	1.67 – 21.67
17	Gardner (1969)	3	ø76.2 x 152.4	Triaxial vessel	29.0	0.30 – 0.89
18	Guo and Wang (1991)	218	70.7 x 70.7 x 70.7	Biaxial, True triaxial	7.6 – 38.3	
19	Hammons and Neeley (1993)	4	ø53.6 x 88.9	Triaxial vessel	96.0	0.52 – 2.08
20	Hobbs (1974)	4		Triaxial vessel	31.8 – 46.4	0.11 – 0.47

21	Hurlbut (1985)	4	ø54 x 108	Triaxial vessel	19.0	0.04 – 0.72
22	Hussein and Marzouk (2000)	24	150 x 150 x 40	Biaxial	38.1 – 96.0	0.20 – 1.19
23	Imran and Pantazopoulou (1996)	36	ø54 x 115	Triaxial vessel	21.2 – 73.4	0.04 – 1.00
24	Imran (1994)	2	ø54 x 115	Triaxial vessel	43.0	0.33 – 1.00
25	Jamet et al. (1984)	6	ø110 x 220	Triaxial vessel	26.0	0.12 – 3.85
26	Kotsovos (1979)	8	ø100 x 250	Triaxial vessel	21.7	0.25 – 1.70
27	Kotsovos and Newman (1978), Kotsovos and Newman (1980)	12	ø100 x 250	Triaxial vessel	31.7 – 62.1	0.23 – 1.49
28	Kupfer et al. (1969), Kupfer and Gerstle (1973)	39	200 x 200 x 50	Biaxial, True triaxial	19.3 – 59.3	0.26 – 1.18
29	Lahlou et al. (1992)	6	ø52 x 104	Triaxial vessel	46.0 – 113.0	0.07 – 0.49
30	Lan and Guo (1997)	47	70.7 x 70.7 x 70.7	Biaxial, True triaxial	24.0	0.30 – 3.50
31	Lan and Guo (1999)	13	100 x 100 x 40	Biaxial	24.0	0.25 – 1.46
32	Launay and Gachon (1972b), Launay and Gachon (1972a),	61	70.1 x 70.1 x 70.1	Biaxial, True triaxial	35.9	0.20 – 5.64
33	Lee et al. (2004)	24	200 x 200 x 60	Biaxial	30.3 – 39.0	0.25 – 1.33
34	Li and Ansari (2000)	11	ø76.2 x 152.4	Triaxial vessel	69.9 – 103.5	0.07 – 0.99
35	Lim and Ozbakkaloglu (2014a)	31	ø63 x 127	Triaxial vessel	50.4 – 128.0	0.02 – 0.50
36	Linse and Aschl (1976)	17	10.0 x 10.0 x 10.0	True Triaxial	26.5 – 34.7	0.41 – 1.48
37	Liu et al. (1972)	30	127.0 x 127.0 x x12.7	Biaxial	20.7 – 34.5	0.20 – 1.26
38	Lu and Hsu (2007)	13	ø100 x 200	Triaxial vessel	67.0	0.05 – 0.84
39	Mills and Zimmerman (1970)	107	57.2 x 57.2 x 57.2	Biaxial, True triaxial	23.0 – 36.1	0.04 – 3.14
40	Nawy et al. (2003)	1		Biaxial	73.6	1.00
41	Nelissen (1972)	10		Biaxial	34.2	0.11 – 1.28
42	Newman (1979)	24	ø100 x 250	Triaxial vessel	23.2 – 91.2	0.04 – 5.95

43	Newman and Newman (1972)	2	ø100 x 250	Triaxial vessel	73.3	0.91 – 1.84
44	Ottosen (1977)	41		Triaxial		
45	Palaniswamy and Shah (1974)	15	ø76 x 230	Triaxial vessel	22.1 – 54.1	0.25 – 2.50
46	Ren et al. (2008)	4	150 x 150 x 50	Biaxial	52.3	0.20 – 1.40
47	Richart et al. (1928)	77	ø101.6 x 203.2 ø101.6 x 558.8	Biaxial, Triaxial vessel	7.2 – 25.2	0.07 – 5.71
48	Rutland and Wang (1997)	48	ø50 x 100	Triaxial vessel	39.4	0.04 – 1.42
49	Schickert and Winkler (1977)	7				
50	Scholz et al. (1995)	42				0.05 – 1.50
51	Setunge et al. (1993), Attard and Setunge (1996)	60	ø100 x 200	Triaxial vessel	60.0 – 132.0	0.004 – 0.25
52	Sfer et al. (2002)	11	ø152 x 305	Triaxial vessel	35.8	0.04 – 1.68
53	Smith et al. (1989)	16	ø54 x 108	Triaxial vessel	22.1 – 44.1	0.02 – 1.00
54	Su and Hsu (1988)	4	152 x 152 x 38	Biaxial	42.9	0.20 - 1.30
55	Tan and Sun (2006)	6	ø100 x 300	Triaxial vessel	51.8	0.04 – 0.24
56	Tasuji et al. (1978)	10	127.0 x 127.0 x x12.7	Biaxial	33.3	0.23 – 1.23
57	Traina (1983)	1		Biaxial	11.8	1.33
58	Traina and Mansour (1991)	3	76 x 76 x 76	Biaxial	40.2	0.50 – 1.17
59	Untiveros (2002)	9	ø150 x 300	Triaxial vessel	33.2 – 67.0	0.10 – 1.05
60	Van Mier (1984)		101.6 x 101.6 x 101.6	True triaxial	40.0 – 51.0	0.03 – 0.33
61	Vu et al. (2009)	6	ø70 x 140	Triaxial vessel	41.2	1.21 – 15.79
62	Wang et al. (1987)	151	101.6 x 101.6 x 101.6	Biaxial, True triaxial	7.6 – 14.3	0.06 – 4.20
63	Xie et al. (1995)	26	ø55.5 x 110	Triaxial vessel	60.2 – 119.0	0.01 – 0.50
64	Yin et al. (1989)	4	152 x 152 x 38	Biaxial	37.6	0.20 - 1.43

3.1 Influence of unconfined concrete strength on failure surface of confined concrete

Failure of a concrete material is usually defined through its ultimate load-carrying capacity. Hence the influence of unconfined concrete strength directly affects the shape of the failure surface. In this paper, failure surface are presented in the meridional and deviatoric stress planes, which are def ned by the cylindrical coordinates of equivalent pressure (q), Mises equivalent stress (p) and Lode angle (θ) (refer Appendix for definitions). Figure 2 illustrates the failure surface of concrete in the meridional plane, whereas Figures 3 and 4 illustrate the cross-sectional shapes of the failure surface in the deviatoric plane and in the biaxial stress plane, respectively. Figure 5 shows the residual surface in meridional plane. As shown in Figure 6, the failure surface encloses all the loading surfaces and serves as a bounding surface. During strain hardening the initial loading surface expands and the subsequent loading surface are then obtained by the uniform expansion of the initial one. After the failure surface is reached, strain-softening occurs and the loading surface contracts towards the residual surface. For confined concrete, the strain hardening/softening rule is dependent on the level of confining pressure (Karabinis and Kiousis 1994; Chen and Lan 2006; Yu et al. 2010).

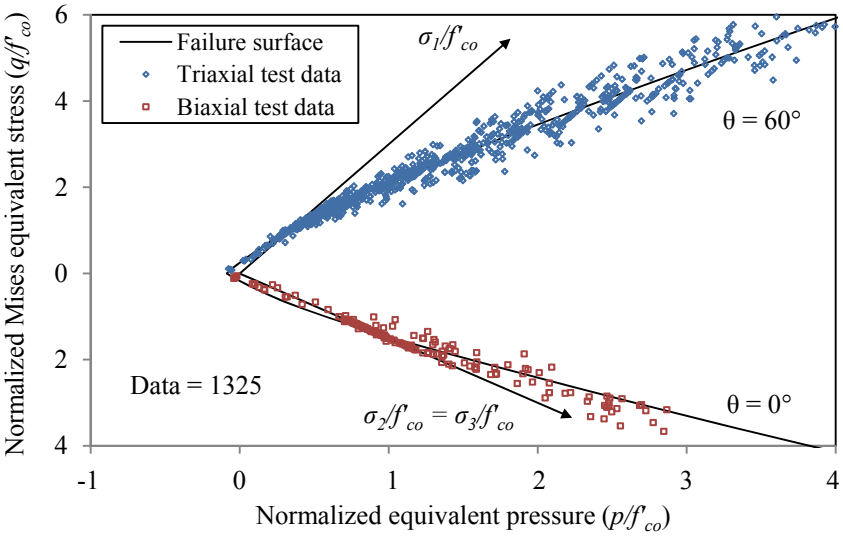

Figure 2. Failure surface of concrete in meridional plane

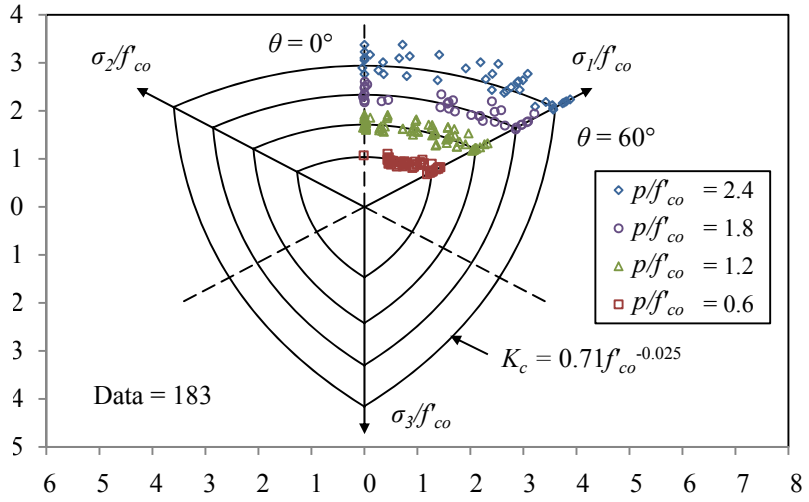

Figure 3. Failure surface of concrete in deviatoric plane

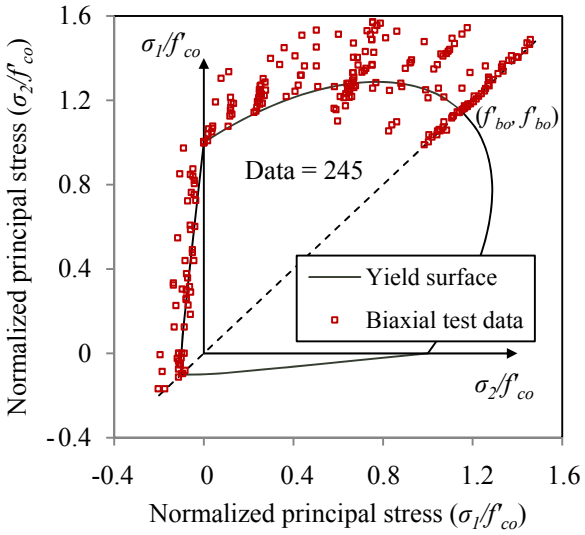

Figure 4. Failure surface of concrete in biaxial stress plane

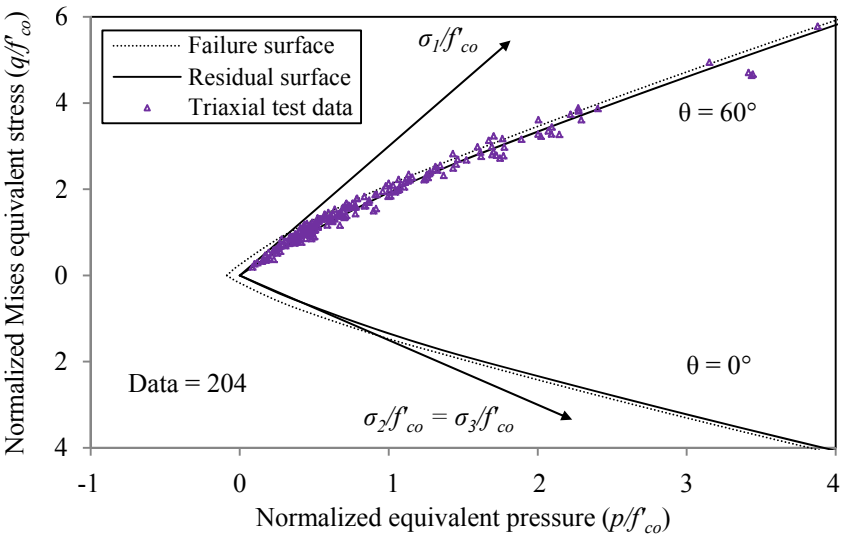

Figure 5. Residual surface of concrete in meridional plane

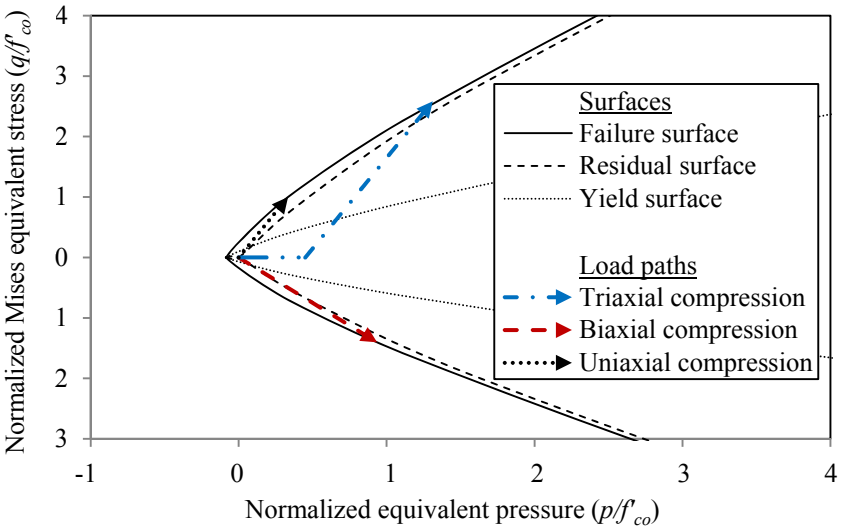

(a)

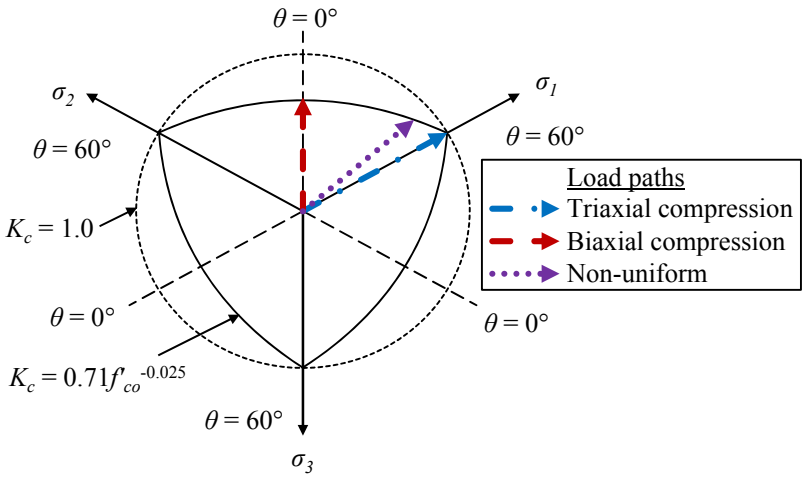

(b)

Figure 6. Load paths of concrete subjected to different confined conditions: (a) in meridional plane and (b) in deviatoric plane

To describe the plasticity of concrete subjected to these strain hardening/softening rule and failure criterion, the concrete-damage plasticity concrete model proposed by Lubliner et al. (1989) and later modified by Lee and Fenves (1998) is adopted (refer Appendix for the original model expressions). It should however be noted that the original model assumes linear trendlines for the compression and tensile meridians, which do not match the curve-shape meridians obtained from test database results, as evident in Figure 2. As can be seen from the figure, the tangential slope of the normalized Mises equivalent stress (q/f'_{co}) reduces with an increase in the normalized equivalent pressure (p/f'_{co}). This can be attributed to the reduction in strength enhancement efficiency with the increased level of confinement (Lim

and Ozbakkaloglu 2014c). In Figure 7, sorting the test database results into different concrete strength groups reveals that the meridians are also influenced by the unconfined concrete strength. It is evident from the figure that the tangential slope of the normalized Mises equivalent stress (q/f'_{co}) reduces with the increase in unconfined concrete strength (f'_{co}). To enable accurate prediction of changes in the compression and tensile meridians, modifications of the original failure criterion to account for the influences of the confining pressure and unconfined concrete strength are necessary.

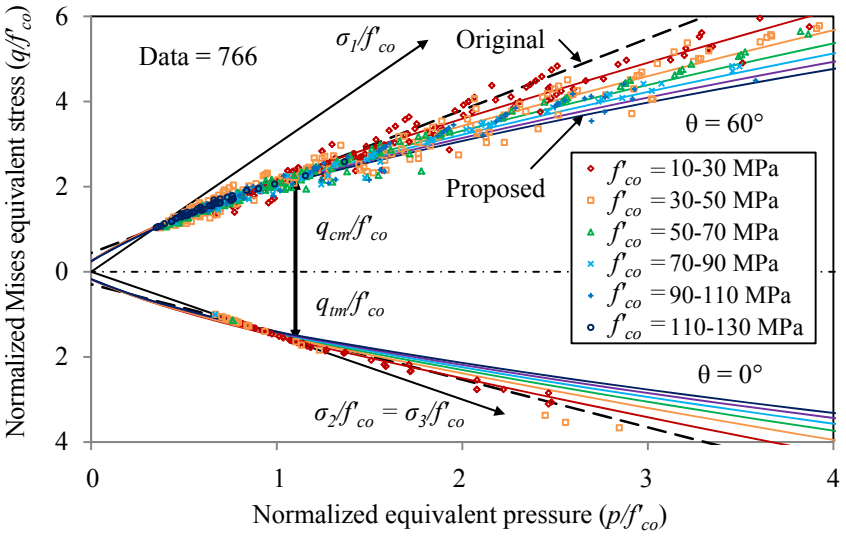

Figure 7. Variation of failure surafaces with unconfined concrete strength in meridional plane

The experimental values of biaxial-to-uniaxial compressive strength ratio (f'_{bo}/f'_{co}), as illustrated in Figure 8, change with the unconfined concrete strength (f'_{co}). This ratio affects the intersecting point of the tensile meridian with the biaxial stress plane. The tensile-to-compression meridian stress ratio (K_c), on the other hand, affects the shape of the cross-section of failure surface in the deviatoric stress plane (Figure 3) and can take values from 0.5 (triangular shape) to unity (circular shape). Based on the observed trend of the test results in Figure 8, the relationship between biaxial-to-uniaxial compressive strength ratio (f'_{bo}/f'_{co}) and unconfined concrete strength (f'_{co}) was established as Eq. 1. This in turn resulted in the tensile-to-compression meridian stress ratio (K_c) given in Eq. 2. As is evident from Eqs. 1 and 2, the f'_{bo}/f'_{co} and K_c ratios are influenced mainly by the unconfined concrete strength (f'_{co}). It is recommended that the f'_{co} values applied to these expressions be limited to the experimental validation ranges of 5 and 100 MPa.

$$\frac{f'_{bo}}{f'_{co}} = 1.57 {f'_{co}}^{-0.09} \tag{1}$$

$$K_c = 0.71 {f'_{co}}^{-0.025} \tag{2}$$

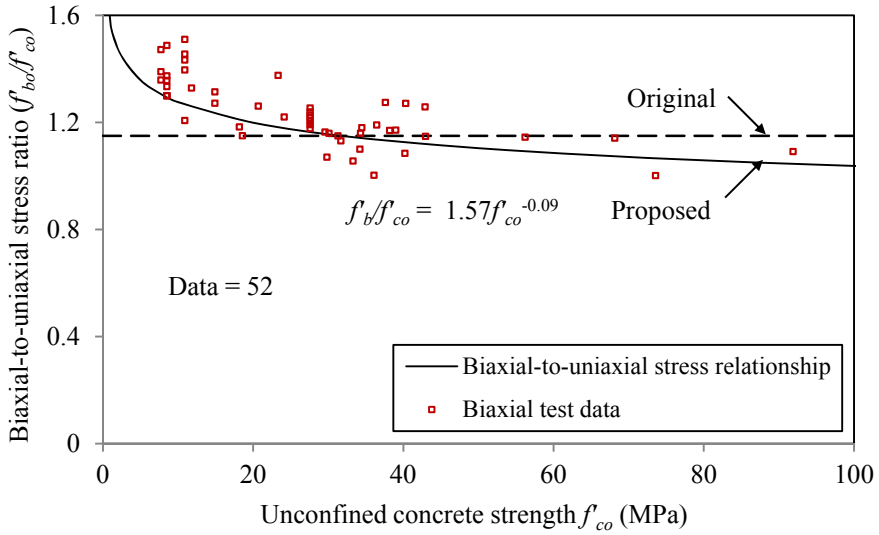

Figure 8. Variation of biaxial-to-uniaxial compressive strengh ratio with uniaxial compressive strength

Figure 2 shows the meridians define the failure surface in the meridional plane that correspond to Lode angle (θ) of 60º and 0º, respectively. To allow for the definition of curve-shape compression and tensile meridians while satisfying the original condition of f'_{bo}/f'_{co} ratio defined by Eq. A5 in Lubliner's model (1989) (i.e. when the tensile meridian intersect the biaxial stress plane), the following change is proposed to Lubliner's (1989) dimensionless parameter α in the present study:

$$\alpha = \frac{k_1 - 1}{2 + k_1}\left(\frac{\gamma}{3} + 1\right) - \frac{\gamma}{3} \tag{3}$$

which is obtained by rearranging the following equation, which defines the secant slope of the compression meridian (φ):

$$\tan\varphi = 3\frac{k_1 - 1}{2 + k_1} = \frac{\gamma + 3\alpha}{\frac{\gamma}{3} + 1} \tag{4}$$

where γ is a dimensionless parameter in Lubliner's model (1989). k_1 is the enhancement ratio of axial compressive stress (f^*_{cc}) of concrete under uniform lateral pressure ($\sigma_2 = \sigma_3 = f^*_l$), expressed as:

$$k_1 = \frac{f^*_{cc} - f'_{co}}{f^*_l} \tag{5}$$

To allow for the change in curvature of the compression meridian, the expression given in Eq. 6, which was proposed by Lim and Ozbakkaloglu (2014c) based on the database results of unconfined and actively confined concrete, can be used in establishing the relationship between the principal stresses f^*_{cc} and f^*_l in Eq. 5. This expression allows for a change in the strength enhancement ratio (k_1) with confining pressure (f^*_l) and unconfined concrete strength

(f'_{co}), which in turn accounts for the curvature of the compression meridian when substituted in Eqs. 3 and 5.

$$f^*_{cc} = f'_{co} + 5.2 f'^{0.91}_{co} \left(\frac{f^*_l}{f'_{co}}\right)^a \tag{6}$$

where $a = f'^{-0.06}_{co}$ and f^*_l and f'_{co} are in MPa.

3.2 Influence of confining pressure on plastic dilation angle of flow rule

For granular materials including concrete, the f ow rule is non-associated, that is, the plastic potential surface (G) is different from the yield surface (F). The consideration of this non-associated flow is important for realistic modeling of the volumetric expansion of concrete under compression. As the plastic strain vector ($d\varepsilon_p$), which represents a measure of the fraction of plastic volume change, governs the accumulation of the plastic volumetric strain it eventually controls the overall dilatancy characteristic of confined concrete. To relate the experimentally observed dilatancy characteristic of confined concrete to the flow rule of the present model, a hyperbolic Drucker-Prager plastic potential function (G) is adopted (refer Appendix for definition). Based on Jiang and Wu (2012), the plastic dilation angle (ψ) of the plastic potential function (G) in the case of uniformly confined concrete can be related to the axial and lateral components of the plastic strain vector ($d\varepsilon_{c,p}$ and $d\varepsilon_{l,p}$) as follow:

$$\tan\psi = -\frac{3\left(d\varepsilon_{c,p} + 2d\varepsilon_{l,p}\right)}{2\left(d\varepsilon_{c,p} - d\varepsilon_{l,p}\right)} \tag{7}$$

Based on this approach, the plastic dilation angle (ψ) can be experimentally measured from test results. In Figures 9(c) to 11(c) presented later in the paper, the experimentally measured changes in plastic dilation angles (ψ) of several groups of specimens are illustrated. It can be seen from the figures that the plastic dilation angles (ψ) do not remain constant but varies throughout the loading history. This accords with the observations reported in several studies that the dilatancy characteristic of confined concrete is non-linear with axial strain increments (Nemat-Nasser and Shokooh 1980; Dorris and Nemat-Nasser 1982; Vermeer and de Borst 1984; Mirmiran et al. 2000; Yu et al. 2010; Jiang and Wu 2012; Lim and Ozbakkaloglu 2014b).

To estimate the change in dilatancy characteristic of confined concrete, the lateral strain-axial strain relationship of concrete proposed by Lim and Ozbakkaloglu (2014b) based on the database results of unconfined and actively confined concrete can be used. In the calculation of the plastic dilation angle (ψ) (Eq. 7), the axial and lateral components of the plastic strain vector ($d\varepsilon_{c,p}$ and $d\varepsilon_{l,p}$) can be estimated from the relationship between axial strain (ε_c) and lateral strain (ε_l) of concrete given in Eq. 8 (see Appendix for strain decompositions). For detailed discussions on the parameters influencing concrete dilatancy characteristic, the reader is referred to Lim and Ozbakkaloglu (2014b).

$$\varepsilon_c = \frac{-\varepsilon_l}{v_i\left(1+\left(\frac{-\varepsilon_l}{v\varepsilon_{co}}\right)^n\right)^{\frac{1}{n}}} - 0.04{\varepsilon_l}^{0.7}\left(1+21\left(\frac{{f^*}_l}{{f'}_{co}}\right)^{0.8}\right) \quad (8)$$

$$v = 8\times10^{-6}{f'_{co}}^2 + 0.0002f'_{co} + 0.138 \quad (9)$$

$$\varepsilon_{co} = \frac{{f'_{co}}^{0.225}}{1000}\left(\frac{152}{D}\right)^{0.1}\left(\frac{2D}{H}\right)^{0.13} \quad (10)$$

$$n = 1 + 0.03f'_{co} \quad (11)$$

where v is the initial Poisson's ratio of concrete, to be calculated using Eq. 9 as proposed by Candappa et al. (2001); ε_{co} is the axial strain corresponding to the compressive strength of unconfined concrete, to be calculated using Eq. 10; and n is the curve shape parameter, to be calculated using Eq. 11. In Eqs. 9-11 f'_{co} is in MPa.

4. COMPARISON OF MODEL PREDICTIONS WITH EXPERIMENTAL RESULTS

The stress-strain curves and dilatancy characteristic of concrete predicted using the Lubliner's model (1989) and the extended version proposed in this study were compared with experimental results. Details of the specimen groups use in the comparisons are summarised in Table 2. Figures 9(a) to 11(a) show the predictions of the variation in axial stress-strain relationships of actively confined concrete with confining pressure using the Lubliner's model (1989). The predictions of the corresponding plastic volumetric strain-axial plastic strain relationships of these specimens groups are shown in Figures 9(b) to 11(b). As can be seen from Figure 9(a) to 11(a), the predicted axial stress-strain curves overestimate the axial stresses and underestimate the axial strains of confined concrete at the peak conditions. This can be attributed to the lack of consideration of the dependency of hardening/softening rule and flow rule on the level of confining pressure in the original Lubliner's model (1989). In addition, the significant overestimation of the peak axial stresses of confined HSC, seen in Figure 11(a), is caused by the lack of consideration of unconfined concrete strength influence on failure surface of confined concrete. In Figures 9(b) to 11(b), the experimental test results show that the change in the dilatancy characteristic of the specimens from plastic volumetric contraction to plastic volumetric expansion is influenced significantly by the level of confining pressure. However, the original Lubliner's model (1989) is unable to the predict the plastic volumetric contraction in confined concrete with an assumption of a constant positive plastic dilation angle (ψ).

Table 2. Summary of test results used in Figures 1 and 9 to 11

Group	Paper	Number of data	Dimensions of cylinder (mm)	Lateral confinement	$f_{lu,a}$ or f^*_1 (MPa)	f'_{co} (MPa)
U21	Imran and Pantazopoulou (1996)	4	ø54 x 115	Triaxial vessel	2.1, 4.2, 8.4, 14.7	21.2
	Newman (1979)	1	ø100 x 250	Triaxial vessel	22.6	23.2
U35	Smith et al. (1989)	2	ø54 x 108	Triaxial vessel	6.9, 13.8	34.5
	Sfer et al. (2002)	3	ø150 x 300	Triaxial vessel	1.5, 4.5, 9.0	35.8
U103	Candappa et al. (2001)	1	ø98 x 200	Triaxial vessel	12.0	103.3
	Li and Ansari (2000)	5	ø76.2 x 152.4	Triaxial vessel	6.8, 20.6, 41.1, 61.7, 80.2	103.5
U128	Lim and Ozbakkaloglu (2014a)	8	ø63 x 127	Triaxial vessel	0, 2.5, 5.0, 7.5, 10.0, 15.0, 20.0, 25.0	128.0

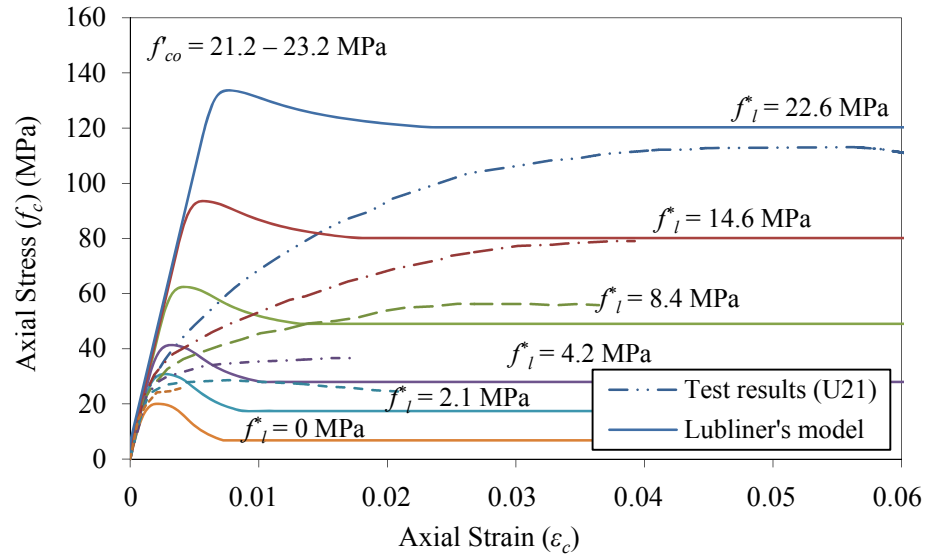

(a)

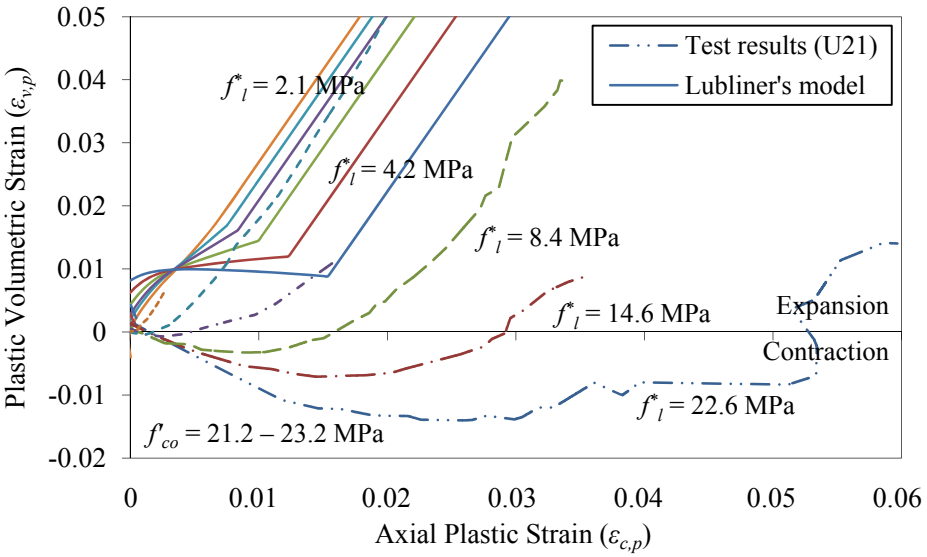

(b)

Figure 9. Predictions of: (a) axial stress-strain; and (b) plastic volumetric strain-axial plastic strain relationships of actively confined concrete specimens (Group U21) by Lubliner's model (1989)

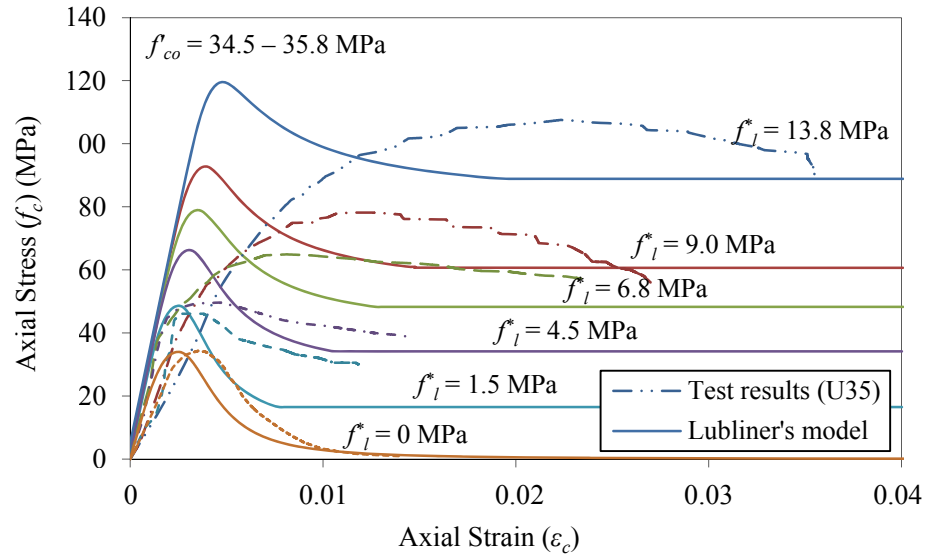

(a)

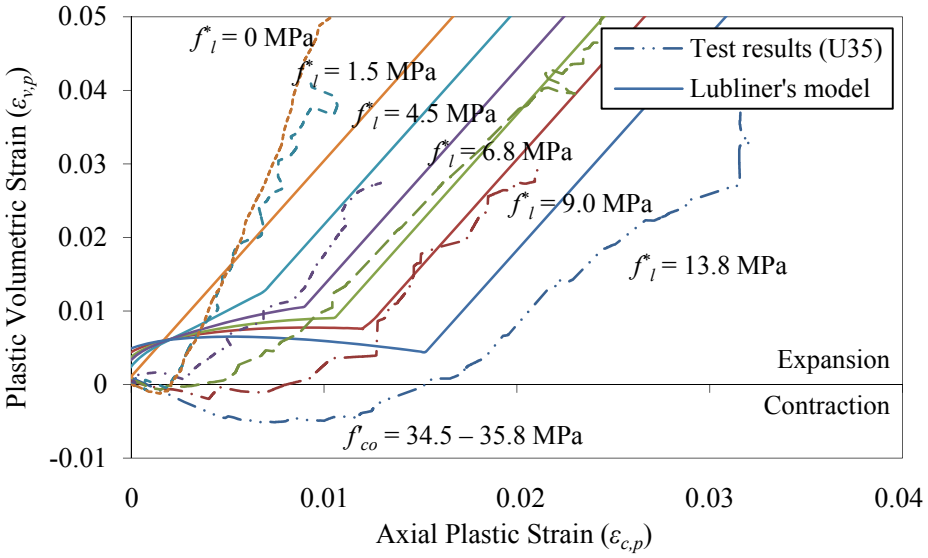

(b)

Figure 10.. Predictions of: (a) axial stress-strain; and (b) plastic volumetric strain-axial plastic strain relationships of actively confined concrete specimens (Group U35) by Lubliner's model (1989)

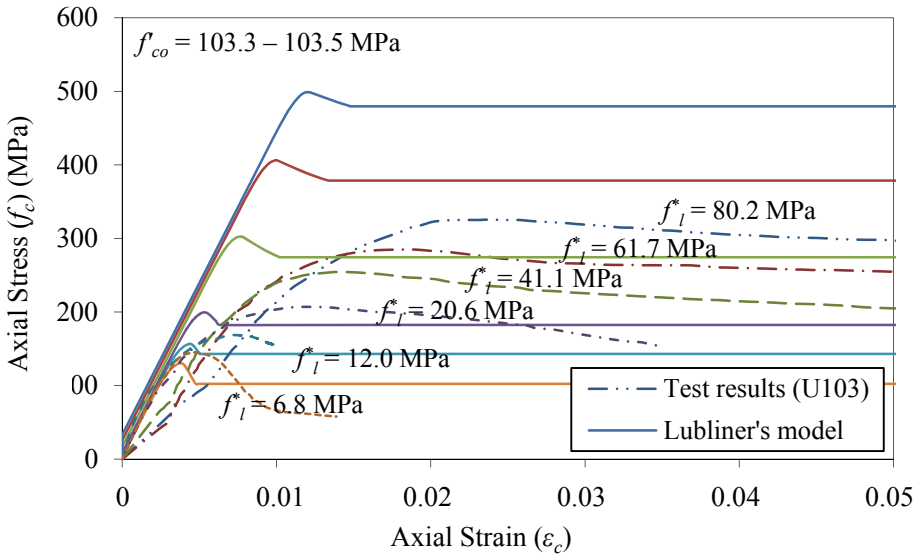

(a)

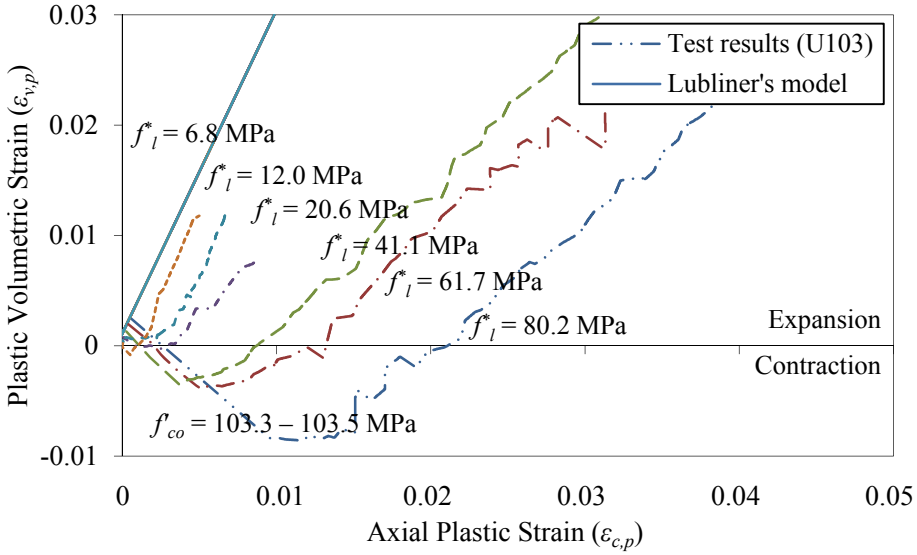

(b)

Figure 11. Predictions of: (a) axial stress-strain; and (b) plastic volumetric strain-axial plastic strain relationships of actively confined concrete specimens (Group U103) by Lubliner's model (1989)

For the same specimen groups, the companion predictions using the extended Lubliner's model (1989) proposed in this study are shown in Figures 12 to 14. As evident from the figures, the model predictions are in good agreement with the test results. In addition to the axial stress-strain and plastic volumetric strain-axial plastic strain relationships shown in Figures 12(a) to 14(a) and Figures 12(b) to 14(b), respectively, the plastic dilation angle-axial plastic strain relationships of these specimen groups are shown in Figures 12(c) to 14(c) to demonstrate the importance of considering the change in the plastic dilation angle throughout the loading history of confined concrete. The tangential slope of these plastic volumetric strain-axial plastic strain curves represents the plastic dilation angle (ψ) at the given strain. As can be seen from Figures 12(c) to 14(c), the plastic dilation angle (ψ) change sign from negative to positive and it correspond to the change in plastic volumetric strain from contraction to expansion in Figures 12(b) to 14(b). Based on the proposed extension to the concrete-damage plasticity model, this non-linear dilatancy characteristic can be estimated accurately as seen in the comparison of model predictions with experimental results in Figures 9(c) to 11(c). This accurate estimation of plastic dilation angle (ψ), in turn, results in the accurate prediction of the dilation characteristics of confined concrete seen in Figures 12(b) to 14(b).

It should be noted that the flow rule of the proposed model is based test results of specimens subjected to axial compression and uniform lateral confining pressure in triaxial compression (i.e., Lode angle $\theta = 60^{o}$). For confined concrete subjected to non-uniform lateral confinement (i.e., Lode angle $\theta \neq 60^{o}$), a further validation/modification of the flow rule is necessary. Further research in these areas is recommended in future studies.

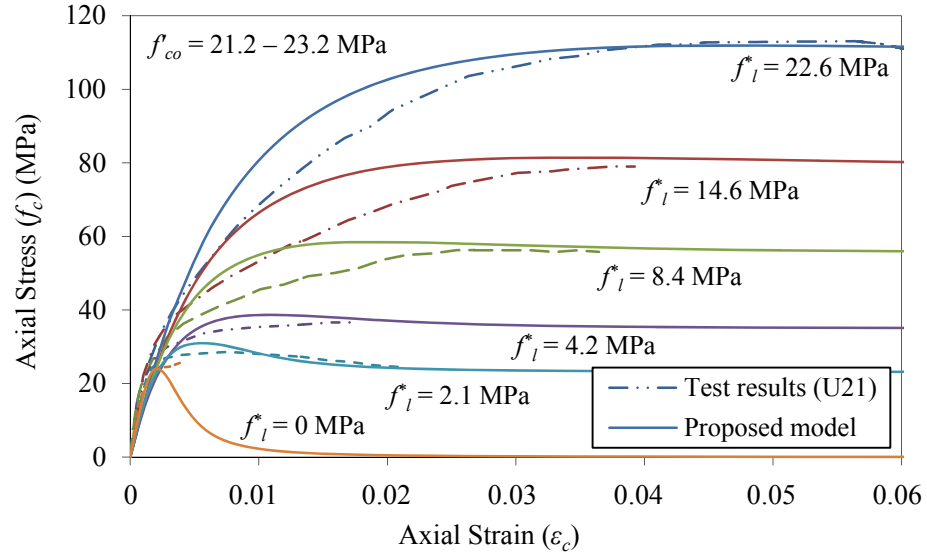

(a)

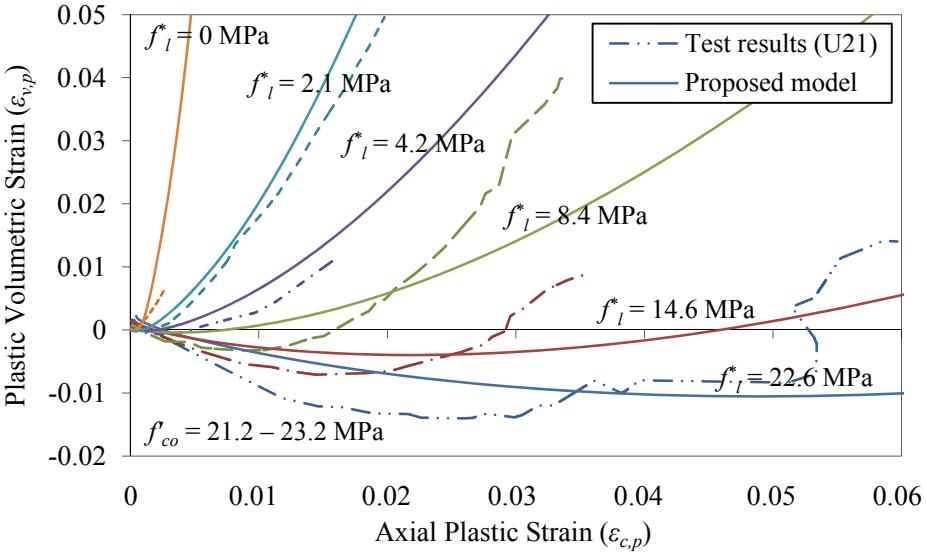

(b)

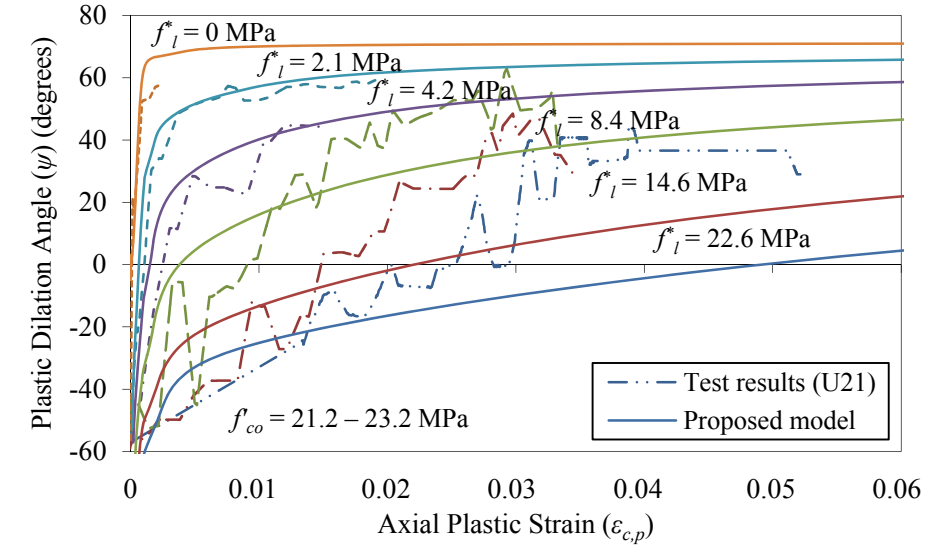

(c)

Figure 12. Predictions of: (a) axial stress-strain; (b) plastic volumetric strain-axial plastic strain; and (c) plastic dilation angle-axial plastic strain relationships of actively confined concrete specimens (Group U21) by proposed model

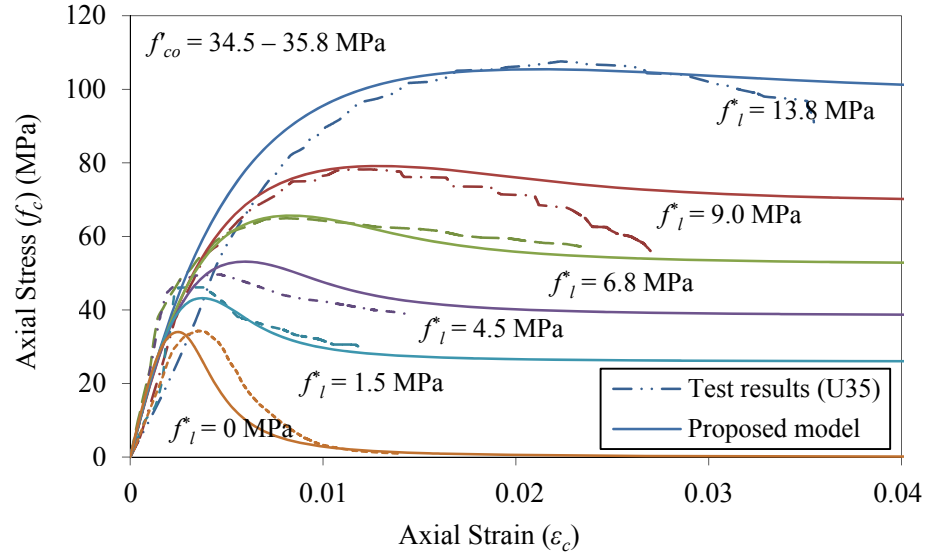

(a)

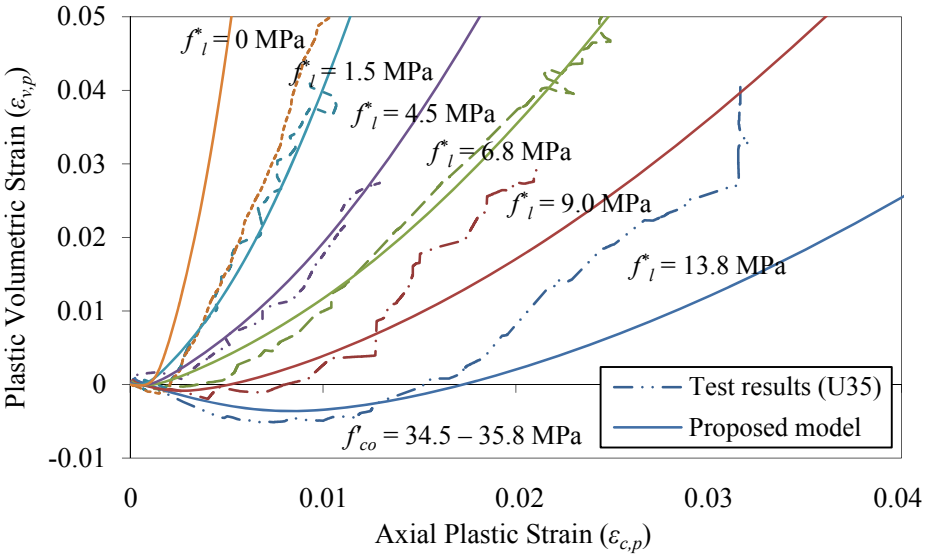

(c)

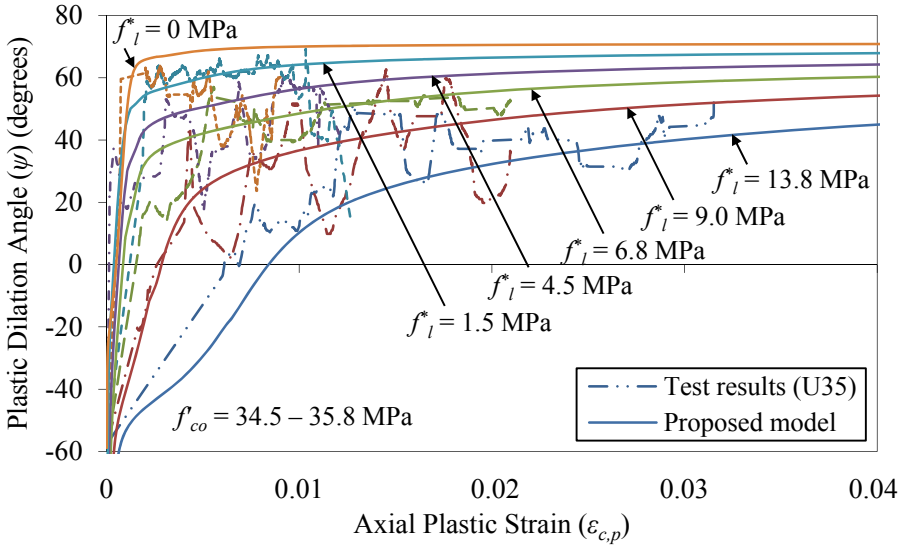

(d)

Figure 13. Predictions of: (a) axial stress-strain; (b) plastic volumetric strain-axial plastic strain; and (c) plastic dilation angle-axial plastic strain relationships of actively confined concrete specimens (Group U35) by proposed model

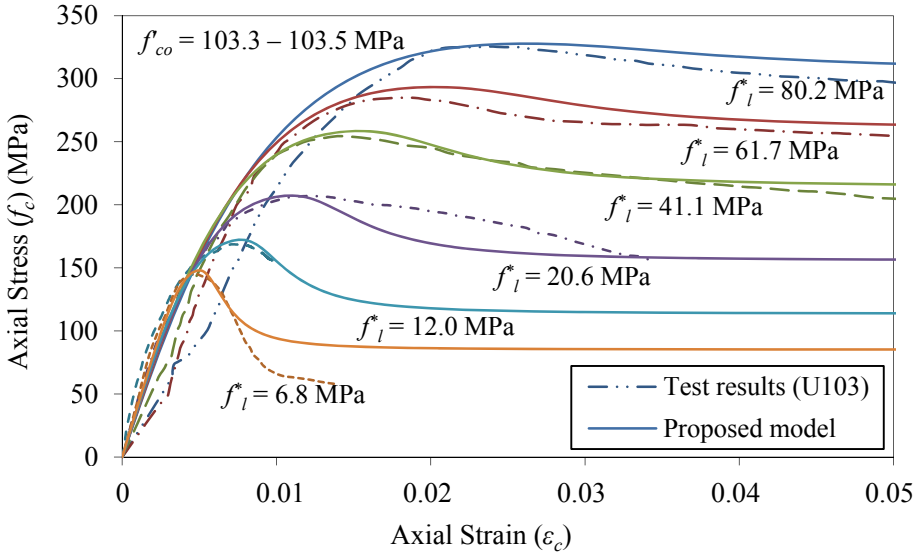

(a)

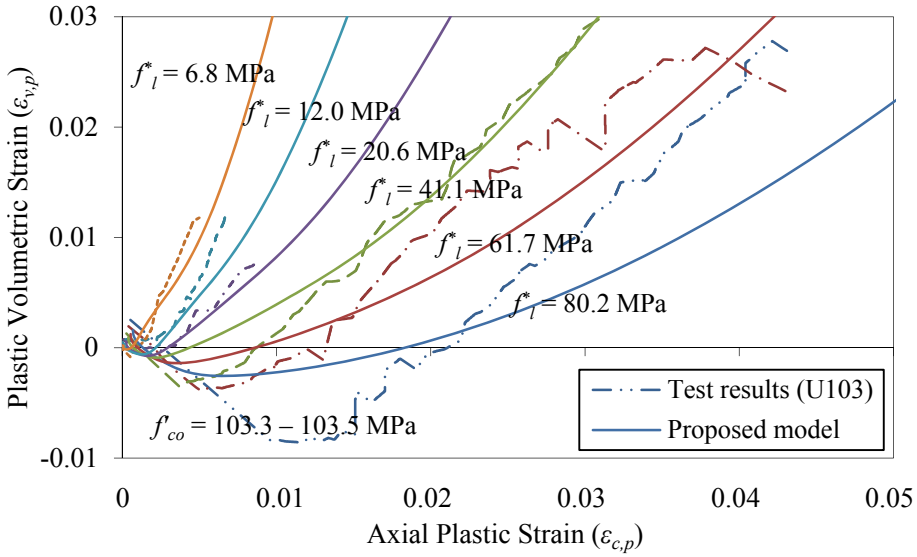

(b)

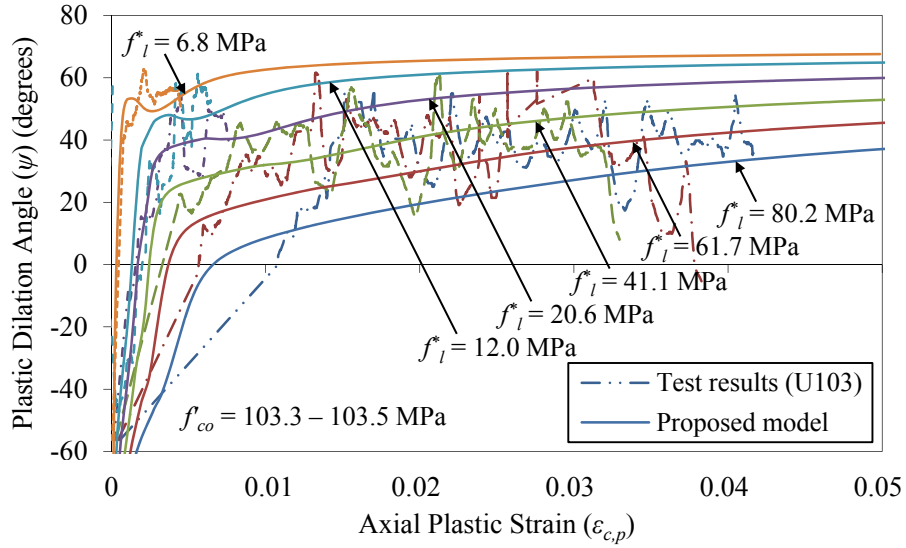

(c)

Figure 14. Predictions of: (a) axial stress-strain; (b) plastic volumetric strain-axial plastic strain; and (c) plastic dilation angle-axial plastic strain relationships of actively confined concrete specimens (Group U103) by proposed model

5. CONCLUSIONS

This paper has presented the results of an investigation on the confinement mechanisms of both unconfined and actively confined concretes using finite element modeling approach. Two large experimental test databases consisting of 4353 test results of unconfined concrete specimens under uniaxial compression and 1752 test results of concrete specimens subjected to biaxial or triaxial compression have been assembled from the published literature. Based on the test database results, the failure surface and flow rule of concrete in multiaxial compression were observed to vary with the unconfined concrete strength and level of confining pressure. To incorporate the observed changes in the failure surface and flow rule, an extension to the concrete-damage plasticity model originally developed by Lubliner's (1989) concrete-damage plasticity model was proposed. This extension enables the influence of concrete strength on the failure surface and the influence of confining pressure on the dilation angle of flow rule to be estimated accurately, and hence improving the overall model stress-strain and dilatancy predictions. Comparisons with experimental test results show that the predictions of the extended model are in good agreement with the test results of both unconfined and actively confined concretes.

REFERENCES

ABAQUS (2012). "ABAQUS Analysis User's Manual." *version 6.12*, Dassault Systèmes Simulia Corp., Providence, RI, USA.

Ansari, F., and Li, Q. B. (1998). "High-strength concrete subjected to triaxial compression." *ACI Materials Journal*, 95(6), 747-755.

Attard, M. M., and Setunge, S. (1996). "Stress-strain relationship of confined and unconfined concrete." *ACI Materials Journal*, 93(5), 432-442.

Balmer, G. G. (1949). "Shearing Strength of Concrete Under High Triaxial Stress-computation of Mohr's Envelope as a Curve." *Structural Research Laboratory Report No. SP-23*, Department of the Interior Bureau of Reclamation, Denver, Colorado, United States.

Bellamy, C. J. (1961). "Strength of concrete under combined stress." *ACI Journal Proceedings*, 58(4), 367-380.

Bellotti, R., and Ronzoni, E. (1984). "Results of tests carried out on cylindrical concrete specimens subjected to complex stress states: a critical analysis." *International Conference on Concrete under Multiaxial Conditions, RILEM*, Press de l'Universite Paul Sabatier, Toulouse, 9- 19.

Bellotti, R., and Rossi, P. (1991). "Cylinder tests: experimental technique and results." *Materials and Structures*, 24(1), 45-51.

Calixto, J. M. (2002). "Behavior of high-performance concrete subjected to biaxial tension-compression stresses." *ACI Special Publication*, 207, 1-14.

Candappa, D. C., Sanjayan, J. G., and Setunge, S. (2001). "Complete triaxial stress-strain curves of high-strength concrete." *Journal of Materials in Civil Engineering*, 13(3), 209-215.

Candappa, D. P., Setunge, S., and Sanjayan, J. G. (1999). "Stress versus strain relationship of high strength concrete under high lateral confinement." *Cement and Concrete Research*, 29(12), 1977-1982.

Chen, A. C. T., and Chen, W. F. (1975). "Constitutive relations for concrete." *Journal of the Engineering Mechanical Division, ASCE*, 101, 465-481.

Chen, W.-F., and Lan, Y.-M. (2006). "Finite element study of confined concrete." *ACI Special Publication 238*

Chern, J. C., Yang, H. J., and Chen, H. W. (1992). "Behavior of steel fiber reinforced concrete in multiaxial loading." *ACI Materials Journal*, 89(1), 32-40.

Chinn, J., and Zimmerman, R. M. (1965). "Behavior of plain concrete under various high triaxial compression loading conditions." *Technical Report WL TR 64-163*, Air Force Weapons Laboratory, University of Colorado, Boulder.

Cordon, W. A., and Gillespie, H. A. (1963). "Variables in concrete aggregates and portland cement paste which influence the strength of concrete." *ACI Journal Proceedings*, 60(8), 1029-1050.

Crouch, R. S., and Tahar, B. (2000). "Application of a stress return algorithm for elasto-plastic hardening-softening models with high yield surface curvature." *Proceedings of European Congress on computational methods in Applied Sciences and Engineering.*Barcelona.

Dahl, K. B. (1992). "A failure criterion for normal and high strength concrete." *Research Report, Series no. 286*, Department of Structural Engineering, Technical University of Denmark, Lyngby, Denmark.

Dorris, J. F., and Nemat-Nasser, S. (1982). "A plasticity model for flow of granular materials under triaxial stress states." *lnternational Journal of Solids and Structures*, 18(6), 497-531.

Drucker, D. C., and Prager, W. (1952). "Soil mechanics and plastic analysis or limit design." *Quarterly of Applied Mathematics*, 10(2), 157-165.

Duke, C. M., and Davis, H. E. (1944). "Some properties of concrete under sustained combined stresses." *Proceedings of American Society for Testing and Materials*, 888–896.

Endebrock, E. G., and Traiana, L. A. (1972). "Static concrete constitutive relations based on cubical specimens." *Technical Report No. AFWL-TR-72-59*, Air Force Weapon Lab,Kirtland Air Force Base, New Mexico.

Farnam, Y., Moosavi, M., Shekarchi, M., Babanajad, S. K., and Bagherzadeh, A. (2010). "Behaviour of slurry infiltrated fibre concrete (SIFCON) under triaxial compression." *Cement and Concrete Research*, 40(11), 1571-1581.

Ferrara, G. (1967). "Dispositivi di prova per l'analisi sperimentale del comportamento do conglomerati cementizi sottoposti a stati triassaili di sollecitazione." *4th Associazione Italiana Annalisi Sollecitazione Congress*Rome, Italy.

Gabet, T., Malecot, Y., and Daudeville, L. (2008). "Triaxial behaviour of concrete under high stresses: Influence of the loading path on compaction and limit states." *Cement and Concrete Research*, 38(3), 403-412.

Gardner, N. J. (1969). "Triaxial behavior of concrete." *Journal of the American Concrete Institute*, 66(2), 136-146.

Grassl, P., and Jirasek, M. (2006). "Damage-plastic model for concrete failure." *International Journal of Solids and Structures*, 43(22-23), 7166-7196.

Grassl, P., Lundgren, K., and Gylltoft, K. (2002). "Concrete in compression: a plasticity theory with a novel hardening law." *International Journal of Solids and Structures*, 39(20), 5205-5223.

Guo, Z., and Wang, C. (1991). "Experimental Investigation of Failure Criterion under Multiaxial Stress." *China Civil Engineering Journal*, 24(3), 1-24.

Hammons, M. I., and Neeley, B. D. (1993). "Triaxial characterization of high-strength Portland cement concrete." *Transportation Research Record*(1382), 73-77.

Hansen, E., Willam, K., and Carol, I. (2001). "A two-surface anisotropic damage/plasticity model for plain concrete." *Proc., Fourth International Conference on Fracture Mechanics of Concrete and Concrete Structures*, Balkema, 549-556.

Hobbs, D. W. (1974). "Strength and deformation properties of plain concrete subject to combined stress. Part 3: results obtained on a range of flint gravel aggregate concretes." *Report 42.497*, Cement and Concrete Association.

Hurlbut, B. (1985). "Experimental and computational investigation of strain-softening in concrete." PhD Dissertation, University of Colorado.

Hussein, A., and Marzouk, H. (2000). "Behavior of high-strength concrete under biaxial stress." *ACI Materials Journal*, 97(1), 27-36.

Imran, I. (1994). "Applications of Nonassociated Plasticity in Modeling the Mechanical Response of Concrete." PhD, University of Toronto, Toronto, Canada.

Imran, I., and Pantazopoulou, S. J. (1996). "Experimental study of plain concrete under triaxial stress." *ACI Materials Journal*, 93(6), 589-601.

Imran, I., and Pantazopoulou, S. J. (2001). "Plasticity model for concrete under triaxial compression." *Journal of Engineering Mechanics, ASCE*, 127(3), 281-290.

Jamet, P., Millard, A., and Nahas, G. (1984). "Triaxial behaviour of a micro-concrete complete stress-strain curves for confining pressures ranging from 0 to 100 MPa." *RILEM-CEB International Conference on Concrete Under Multiaxial Conditions*, INSA Toulouse, France, 133-140.

Jason, L., Huerta, A., Pijaudier-Cabot, G., and Ghavamian, S. (2006). "An elastic plastic damage formulation for concrete: Application to elementary tests and comparison with an isotropic damage model." *Computer methods in applied mechanics and engineering*, 195(52), 7077-7092.

Jefferson, A. D. (1998). "Plastic-damage model for interfaces in cementitious materials." *Journal of engineering mechanics*, 124(7), 775-782.

Jiang, J. F., and Wu, Y. F. (2012). "Identification of material parameters for Drucker-Prager plasticity model for FRP confined circular concrete columns." *International Journal of Solids and Structures*, 49(3-4), 445-456.

Karabinis, A. I., and Kiousis, P. D. (1994). "Effects of confinement on concrete columns: a plasticity theory approach." *Journal of Structural Engineering, ASCE*, 120, 2747-2767.

Kent, D. C., and Park, R. (1971). "Flexural members with confined concrete." *Journal of the Structural Division, ASCE*, 97(7), 1969-1990.

Kotsovos, M. D. (1979). "Effect of stress path on the behavior of concrete under triaxial stress states." *Journal of the American Concrete Institute*, 76(2), 213-223.

Kotsovos, M. D., and Newman, J. B. (1978). "Generalized stress-strain relations for concrete." *Journal of the Engineering Mechanics Division, ASCE*, 104(4), 845-856.

Kotsovos, M. D., and Newman, J. B. (1980). "Mathematical description of deformational behavior of concrete under generalized stress beyond ultimate strength." *ACI Journal*, 77(5), 340-346.

Kupfer, H., Hilsdorf, H. K., and Rusch, H. (1969). "Behavior of concrete under biaxial stresses." *ACI Journal Proceedings*, 66(8), 656-666.

Kupfer, H. B., and Gerstle, K. H. (1973). "Behavior of concrete under biaxial stresses." *Journal of the Engineering Mechanics Division*, 99(4), 853-866.

Lahlou, K., Aitcin, P. C., and Chaallal, O. (1992). "Behaviour of High-strength Concrete Under Confined Stresses." *Cement and Concrete Composites*, 14(3), 185-193.

Lan, S., and Guo, Z. (1999). "Biaxial compression behavior of concrete under repeated loading." *Journal of Materials in Civil Engineering*, 11(2), 105-115.

Lan, S. G., and Guo, Z. H. (1997). "Experimental investigation of multiaxial compressive strength of concrete under different stress paths." *ACI Materials Journal*, 94(5), 427-434.

Launay, P., and Gachon, H. (1972a). "Strain and ultimate strength of concrete under triaxial stress." *Proceedings of the First International Conference on Structural Mechanics in Reactor Technology*Berlin, Germany, 23-34.

Launay, P., and Gachon, H. (1972b). "Strain and ultimate strength of concrete under triaxial stress." *ACI Special Publication*, 34, 269-282.

Lee, J., and Fenves, G. L. (1998). "Plastic-damage model for cyclic loading of concrete structures." *Journal of Engineering Mechanics*, 124(8), 892-900.

Lee, S. K., Song, Y. C., and Han, S. H. (2004). "Biaxial behavior of plain concrete of nuclear containment building." *Nuclear Engineering and Design*, 227(2), 143-153.

Li, Q. B., and Ansari, F. (1999). "Mechanics of damage and constitutive relationships for high-strength concrete in triaxial compression." *Journal of Engineering Mechanics*, 125(1), 1-10.

Li, Q. B., and Ansari, F. (2000). "High-strength concrete in triaxial compression by different sites of specimens." *ACI Materials Journal*, 97(6), 684-689.

Li, T., and Crouch, R. (2010). " A C_2 plasticity model for structural concrete." *Computers and Structures*, 88(23-24), 1322-1332.

Lim, J. C., and Ozbakkaloglu, T. (2014a). "Investigation of the Influence of Application Path of Confining Pressure: Tests on Actively Confined and FRP-Confined Concretes." *Journal of Structural Engineering, ASCE*, Doi: 10.1061/(ASCE)ST.1943-541X.0001177.

Lim, J. C., and Ozbakkaloglu, T. (2014b). "Lateral strain-to-axial strain relationship of confined concrete." *Journal of Structural Engineering, ASCE*, Doi: 10.1061/(ASCE)ST.1943-541X.0001094.

Lim, J. C., and Ozbakkaloglu, T. (2014c). "Stress-strain model for normal- and light-weight concretes under uniaxial and triaxial compression." *Construction and Building Materials*, 71, 492-509.

Linse, D., and Aschl, H. (1976). "Versuche zum Verhalten von Beton unter mehrachsiger Beanspruchung." *In Munchen durchgefuhrtes Teilprojekt eines internationalen Vergleichsprogrammes, Versuchsbericht*, Lehrstuhl fur Massivbau, Technische Universitat Munchen.

Liu, T. C. Y., Nilson, A. H., and Slate, F. O. (1972). "Stress–strain response and fracture of concrete in uniaxial and biaxial compression." *ACI Journal*, 69(5), 291-295.

Loland, K. E. (1980). "Continuous damage model for load-response estimation of concrete." *Cement and Concrete Research*, 10, 395–402.

Lu, X. B., and Hsu, C. T. T. (2007). "Stress-strain relations of high-strength concrete under triaxial compression." *Journal of Materials in Civil Engineering*, 19(3), 261-268.

Lubarda, V. A., Kracjinvovic, D., and Mastilovic, S. (1994). "Damage model for brittle elastic solids with unequal tensile and compressive strength." *Engineering Fracture Mechanics*, 49, 681-697.

Lubliner, J., Oliver, J., Oller, S., and Onate, E. (1989). "A plastic-damage model for concrete." *International Journal of Solids and Structures*, 25(3), 299-326.

Mander, J. B., Priestley, M. J. N., and Park, R. (1988). "Theoretical stress-strain model for confined concrete." *Journal of Structural Engineering, ASCE*, 114(8), 1804-1826.

Mazars, J., and Pijaudier-Cabot, G. (1989). "Continuum damage theory-application to concrete." *Journal of Engineering Mechanics*, 115(2), 345-365.

Mills, L. L., and Zimmerman, R. M. (1970). "Compressive Strength of Plain Concrete Under Multiaxial Loading Conditions." *ACI Journal Proceedings*, 67(10), 802-807.

Mirmiran, A., Zagers, K., and Yuan, W. Q. (2000). "Nonlinear finite element modeling of concrete confined by fiber composites." *Finite Elements in Analysis and Design*, 35(1), 79-96.

Nawy, E. G., Lim, D. H., and McPherson, K. L. (2003). "Compressive behavior of high-strength high-performance concrete under biaxial loading." *ACI Special Publication*, 213, 43-60.

Nelissen, L. J. M. (1972). "Biaxial testing of normal concrete." *Heron*, 18(1), 90.

Nemat-Nasser, S., and Shokooh, A. (1980). "On finite plastic flows of compressible materials with internal friction." *International Journal of Solids and Structures*, 16(6), 495-514.

Newman, J. B. (1979). *Concrete under complex stress*, Department of Civil Engineering, Imperial College of Science and Technology, London, UK, London, UK.

Newman, J. B., and Newman, K. (1972). "The cracking and failure of concrete under combined stresses and its implications for structural design." *The Deformations and Rupture of Solids Subjected to Multiaxial Stresses, RILEM international symposium*Cannes.

Ortiz, M., and Popov, E. P. (1982). "Plain concrete as a composite material." *Mechanics of Material*, 1, 139–150.

Ottosen, N. S. (1977). "A failure criterion for concrete." *Journal of the Engineering Mechanics Division*, 103(4), 527-535.

Ozbakkaloglu, T., Lim, J. C., and Vincent, T. (2013). "FRP-confined concrete in circular sections: Review and assessment of stress–strain models." *Engineering Structures*, 49, 1068–1088.

Ozbakkaloglu, T., and Saatcioglu, M. (2006). "Seismic behavior of high-strength concrete columns confined by fiber-reinforced polymer tubes." *Journal of Composites for Construction, ASCE*, 10(6), 538-549.

Palaniswamy, R., and Shah, S. P. (1974). "Fracture and stress-strain relationship of concrete under triaxial compression." *Journal of the Structural Division*, 100(5), 901-916.

Pijaudier-Cabot, G., and Bazant, Z. P. (1987). "Nonlocal damage theory." *Journal of Engineering Mechanics*, 113(10), 1512-1533.

Ren, X., Yang, W., Zhou, Y., and Li, J. (2008). "Behavior of high-performance concrete under uniaxial and biaxial loading." *ACI Materials Journal*, 105(6), 548-577.

Richart, F. E., Brandtzaeg, A., and Brown, R. L. (1928). "A study of the failure of concrete under combined compressive stresses." *Bulletin No. 185*, Engineering Experimental Station, University of Illinois, Champaign, Illinois.

Rutland, C. A., and Wang, M. L. (1997). "The effects of confinement on the failureorientation in cementitiousmaterialsexperimentalobservations." *Cement and Concrete Composites*, 19(2), 149-160.

Saatcioglu, M., and Razvi, S. R. (1992). "Strength and ductility of confined concrete." *Journal of Structural Engineering, ASCE*, 118(6), 1590-1607.

Schickert, G., and Winkler, H. (1977). "Results of test concerning strength and strain of concrete subjected to multiaxial compressive stresses." Deutscher Ausschuss fur Stahlbeton, Berlin, West Germany.

Scholz, U., Nechvatal, D., Aschl, H., Linse, D., Stockl, S., Grasser, E., and Kupfer, H. (1995). "Versuche zum Verhalten von Beton unter dreiachsiger Kurzeitbeanspruchung." *Heft 447*, Deutscher Ausschuss fur Stahlbeton, Berlin, 64.

Setunge, S., Attard, M. M., and Darvall, P. L. (1993). "Ultimate strength of confined very high-strength concretes." *ACI Structural Journal*, 90(6), 632-641.

Sfer, D., Carol, I., Gettu, R., and Etse, G. (2002). "Study of the behavior of concrete under triaxial compression." *Journal of Engineering Mechanics*, 128(2), 156-163.

Sheikh, S. A., and Uzumeri, S. M. (1980). "Strength and Ductility of Tied Concrete Columns." *Journal of Structural Engineering, ASCE*, 106(5), 1079-1102.

Smith, S. S., Willam, K. J., Gerstle, K. H., and Sture, S. (1989). "Concrete Over The Top, Or: Is There Life After Peak?" *ACI Materials Journal*, 86(5), 491-497.

Su, E. C. M., and Hsu, T. T. C. (1988). "Biaxial compression fatigue and discontinuity of concrete." *ACI Materials Journal*, 85(3), 178-188.

Tan, K. H., and Sun, X. (2006). "Failure criteria of concrete under triaxial compression." *ACI Special Publication*, 238, 235-248.

Tasuji, M. E., Slate, F. O., and Nilson, A. H. (1978). "Stress–strain response and fracture of concrete in biaxial loading." *ACI Journal Proceedings*, 75(7), 306-312.

Traina, L. A. (1983). "Experimental stress–strain behavior of a low strength concrete under multiaxial states of stress." *Technical Report No. AFWL-TR-72-59*, Air Force Weapon Lab, Kirtland Air Force Base, New Mexico.

Traina, L. A., and Mansour, S. A. (1991). "Biaxial strength and deformational behavior of plain and steel fiber concrete." *ACI Materials Journal*, 88(4), 354-362.

Untiveros, C. A. (2002). "Estudio experimental del comportamiento del hormigón confinado sometido a compresión." Ph.D. Thesis, Universitat Politècnica de Catalunya, Barcelona, Spain.

van Mier, J. G. M. (1984). "strain-softening of concrete under multiaxial loading conditions." PhD thesis, Eindhoven University of Technology, The Netherlands.

Vermeer, P. A., and de Borst, R. (1984). "Non-associated plasticity for soils, concrete and rock." *Heron*, 29(1–64).

Vu, X. H., Malecot, Y., Daudeville, L., and Buzaud, E. (2009). "Experimental analysis of concrete behavior under high confinement: Effect of the saturation ratio." *International Journal of Solids and Structures*, 46(5), 1105-1120.

Wang, C. Z., Guo, Z. H., and Zhang, X. Q. (1987). "Experimental investigation of biaxial and triaxial compressive concrete strength." *ACI Materials Journal*, 84(2), 92-100.

Willam, K. J., and Warnke, E. P. (1975). "Constitutive model for the triaxial behaviour of concrete." *Proceedings of the International Association for Bridge and Structural Engineering*, 1-30.

Wu, J. Y., Li, J., and Faria, R. (2006). "An energy release rate-based plastic-damage model for concrete." *International Journal of Solids and Structures*, 43(3), 583-612.

Xie, J., Elwi, A. E., and Macgregor, J. G. (1995). "Mechanical-properties of high-strength concretes containing silica fume." *ACI Materials Journal*, 92(2), 135-145.

Yin, W. S., Su, E. C. M., Mansur, M. A., and Hsu, T. T. C. (1989). "Biaxial tests of plain and fiber concrete." *ACI Materials Journal*, 86(3), 236-243.

Yu, T., Teng, J. G., Wong, Y. L., and Dong, S. L. (2010). "Finite element modeling of confined concrete-I: Drucker-Prager type plasticity model." *Engineering Structures*, 32(3), 665-679.

APPENDIX

Definitions of equivalent pressure (q), Mises equivalent stress (p) and Lode angle (θ):

$$p = \frac{-I_1}{3} \quad \text{where} \quad I_1 = \sigma_1 + \sigma_2 + \sigma_3 \tag{A1}$$

$$q = \sqrt{3J_2} \quad \text{where} \quad J_2 = \frac{(\sigma_1 - \sigma_2)^2 + (\sigma_2 - \sigma_3)^2 + (\sigma_3 - \sigma_1)^2}{6} \tag{A2}$$

$$\theta = \frac{1}{3}\cos^{-1}\left(\frac{3\sqrt{3}}{2}\frac{J_3}{{J_2}^{3/2}}\right) \quad \text{where} \quad J_3 = \left(\sigma_1 - \frac{I_1}{3}\right)\left(\sigma_2 - \frac{I_1}{3}\right)\left(\sigma_3 - \frac{I_1}{3}\right) \tag{A3}$$

where I_1, J_2, J_3 are invariants of the principal stress tensor components and σ_1, σ_2, σ_3 are principal stresses.

Failure criterion (F) proposed by Lubliner et al. (1989) and modified by Lee and Fenves (1998):

$$F = \frac{1}{1-\alpha}\left(q - 3\alpha p + \beta\left(\bar{\varepsilon}_p\right)\langle -\bar{\sigma}_{min}\rangle - \gamma\langle\bar{\sigma}_{min}\rangle\right) - \bar{\sigma}_c\left(\bar{\varepsilon}_{c,p}\right) \leq 0 \tag{A4}$$

where $\overline{\sigma}_{min}$ is the minimum principal effective stress. The parameters α, $\beta(\overline{\varepsilon}_p)$, and γ are dimensionless parameters which are def ned in Eqs. A5 to A7. For more details on the derivation of the failure criterion, the reader is referred to Lubliner et al. (1989) and Lee and Fenves (1998).

$$\alpha = \frac{f'_{bo} - f'_{co}}{2f'_{bo} - f'_{co}} \tag{A5}$$

$$\beta\left(\bar{\varepsilon}_p\right) = \frac{\bar{\sigma}_c\left(\bar{\varepsilon}_{c,p}\right)}{\bar{\sigma}_t\left(\bar{\varepsilon}_{t,p}\right)}(1-\alpha) - (1+\alpha) \tag{A6}$$

$$\gamma = \frac{3(1-K_c)}{2K_c - 1} \quad \text{where} \quad K_c = \frac{q_{tm}}{q_{cm}} \tag{A7}$$

where f'_{bo} and f'_{co} are the biaxial and uniaxial compressive strengths; $\overline{\sigma}_c$ and $\overline{\sigma}_t$ are the effective compressive and tensile cohesion stresses; $\overline{\varepsilon}_{c,p}$ and $\overline{\varepsilon}_{t,p}$ are the equivalent compressive and tensile plastic strains, respectively. K_c is the ratio of the second stress invariants on the tensile meridian (q_{tm}) to that of the compression meridians (q_{cm}).

In the case of biaxial and triaxial compression under uniform lateral pressure ($\sigma_2 = \sigma_3$), the failure surface along the tensile and compressive meridians reduce to Eqs. A8 and A9, respectively. These meridians define the failure surface in the meridional plane that correspond to Lode angle (θ) of 60º and 0º, respectively.

$$\left(\frac{2}{3}\gamma + 1\right) q - (\gamma + 3\alpha)p = (1 - \alpha)\bar{\sigma}_c, \quad \text{for tensile meridian } (tm) \tag{A8}$$

$$\left(\frac{1}{3}\gamma + 1\right) q - (\gamma + 3\alpha)p = (1 - \alpha)\bar{\sigma}_c, \quad \text{for compression meridian } (cm) \tag{A9}$$

Definitions of plastic potential function (G) and the plastic strain vector ($d\varepsilon_p$):

$$G = \sqrt{(\epsilon f'_t \tan\psi)^2 + q^2} - p\tan\psi \tag{A10}$$

$$d\varepsilon_p = \lambda \frac{\partial G}{\partial \sigma} \tag{A11}$$

where ψ is the plastic dilation angle; f'_t is the uniaxial tensile strength; and ϵ is the eccentricity parameter that defines the rate at which the function approaches the asymptote. The flow potential tends to approach a straight line as the eccentricity approaches to zero.

Definitions of strain decompositions under uniform confinement and monotonic loading:

$$\varepsilon_c = \varepsilon_{c,e} + \varepsilon_{c,p} \quad \text{where} \quad \varepsilon_{c,p} = \varepsilon_c - \frac{1}{E}(\sigma_c - 2\nu\sigma_l) \tag{A12}$$

$$\varepsilon_l = \varepsilon_{l,e} + \varepsilon_{l,p} \quad \text{where} \quad \varepsilon_{l,p} = \varepsilon_l - \frac{1}{E}[(1 - \nu)\sigma_l - \nu\sigma_c] \tag{A13}$$

$$\varepsilon_v = \varepsilon_c + 2\varepsilon_l \quad \text{and} \quad \varepsilon_{v.p} = \varepsilon_{c,p} + 2\varepsilon_{l,p} \tag{A14}$$

where ε_c, ε_l, ε_v are the axial, lateral and volumetric strain, ε_c, ε_c, ε_c are the plastic axial, lateral and volumetric strain, E is the concrete elastic modulus, and v is the Poisson's ratio of concrete.

THIS PAGE HAS BEEN LEFT INTENTIONALLY BLANK

CONCLUSIONS

In the past few decades, a great deal of research effort has been devoted to the understanding of the improved compressive behavior of concrete under lateral confinement. To that end, over 110 models have been developed to predict the axial compressive behavior of unconfined, actively confined and FRP-confined concretes. Based on a systematic review and assessment, the key features and theoretical basis of each model have been carefully studied. A close examination of results of the model assessment has led to a number of important findings on factors influencing the performances of the existing models, including the size of database, test parameters considered, ability to handle uncertainties, dependency on theoretical assumptions, and architecture of their modeling frameworks. Gaps in test parameters of these existing models have been covered with new tests conducted at the University of Adelaide in a series of experimental programs. The identified new parameters include the: i) influence of silica fume on FRP-confined concrete, ii) influence of unconfined concrete strength and elastic modulus of fiber material on hoop rupture strain of FRP jacket, iii) influence of concrete age on FRP-confined concrete, and iv) confining pressure gradient between actively confined and FRP-confined concretes. To establish a reliable framework for model developments, these experimental test results have been augmented with published test data to form comprehensive experimental databases. Based on these test databases, four types of model, including the: i) design-oriented, ii) analysis-oriented, iii) evolutionary algorithm, and iv) finite element models, have been developed and presented in a series of publications. Comparisons with experimental test results show that the predictions of the proposed models are in good agreement with the test results, and the models provide improved predictions compared to the existing models reviewed in this study. The performances of model by category generally improved with the increased complexity of modeling framework, while the choice of models depends mainly on their end use.

Research contributions

The overall contribution of this research is the development of accurate models for the prediction of the compressive behavior of actively confined and FRP-confined concretes. Specifically, in meeting the objectives of this research mentioned earlier in the introduction, the research contributions of each of the publication [1-14] are summarized in Table 1. In addition to the journal publications, the work resulted from this research have been shared with other researchers in the field through a number of refereed conference papers [15-24].

Table 1. Summary of publications and research contributions

Publication	Contributions
Ozbakkaloglu et al. [1]	A systematic performance assessment of existing design-oriented and analysis-oriented models for FRP-confined concrete using an up-to-date database has been presented in this paper. Based on the review study, factors influencing the performances of exiting models and recommendations for modeling improvements have been outlined.
Ozbakkaloglu and Lim [2]	A comprehensive experimental test database of FRP-confined normal strength concrete assembled from the published literature has been presented in this paper. The database will serve as a valuable reference document for future model development efforts. Key issues affecting model accuracy has been discussed and a design-oriented model for predicting the ultimate conditions of FRP-confined concrete has been developed using the database.
Lim and Ozbakkaloglu [3]	To allow for an extension of the design-oriented model for high-strength concrete application, a companion experimental test database of FRP-confined HSC was assembled and presented in this paper. The analysis of the combined normal- and high-strength concrete database indicates that the confinement requirement increases significantly with an increase in concrete strength. To account for such effect, a novel feature referred to as the threshold confinement condition is introduced to the proposed model to distinguish ascending and descending types of stress-strain curves for FRP-confined concrete. In addition, the observed reduction in the hoop rupture strain of the FRP shell with an increase in the unconfined concrete strength has been quantified and incorporated into the proposed design-oriented model.
Lim and Ozbakkaloglu [4]	This paper has presented the results of an experimental study on the influence of silica fume on the axial compressive behavior of FRP-confined concrete. Several important findings of the observed influence of silica fume on the ultimate condition and the transition region of the stress-strain curve of FRP-confined concrete has been reported.
Lim and Ozbakkaloglu [5]	This paper has presented the results of an experimental study on the influence of concrete age on the axial compressive behavior of FRP-confined concrete. Findings on the influence of concrete age on the ultimate condition and the stress-strain behavior of FRP-confined concrete have been reported.
Lim and Ozbakkaloglu [6]	To extend the application of the design-oriented model from circular cross-section to square and rectangular cross-sections, another companion experimental test database of FRP-confined concrete in square and rectangular cross-sections was assembled and presented in this paper. The important feature of the proposed model is its incorporation of the threshold confinement conditions of FRP-confined concrete in square and rectangular cross-

	sections in order to distinguish the ascending and descending types of stress-strain curves of the square and rectangular specimens.
Lim and Ozbakkaloglu [7]	This paper has presented the results of an investigation on the dilation behavior of both FRP-confined and actively confined concretes. A large experimental database of actively confined concrete assembled form the published literature has been presented in this paper. On the basis of the combined database of actively confined and FRP-confined concretes, a new lateral strain-to-axial strain model has been developed and presented.
Lim and Ozbakkaloglu [8]	This paper has presented the results of an experimental study that closely examined factors influencing the hoop rupture strains and axial strains in FRP-confined concrete. The hoop rupture strain of FRP jackets has been observed to decrease with an increase in the unconfined concrete strength and elastic modulus of fiber material.
Lim and Ozbakkaloglu [9]	This paper has presented the results of an experimental study that examined the difference in the axial stress-strain and lateral strain-axial strain behaviors of NSC and HSC subjected to two different confinement systems. From the conducted tests, it was shown that, at a given axial strain, lateral strains of actively confined and FRP-confined concretes of the same concrete strength correspond when they are subjected to the same lateral confining pressure. However, under the same condition, concrete confined by FRP exhibits a lower strength enhancement compared to that seen in companion actively confined concrete. To describe the experimentally observed behavior, a novel concept, known as confining pressure gradient, has been developed to establish the axial stress difference between the actively confined and FRP-confined concretes.
Lim and Ozbakkaloglu [10]	On the basis of two large databases of unconfined and actively concrete concretes, a unified model applicable to confined and unconfined concretes ranging from light-weight to high-strength has been developed and presented in this paper. The important features of the proposed stress-strain model include the applicability to concretes with various densities and strengths, accurate prediction of the peak and residual conditions of unconfined and confined concretes, consideration of the change in shape of stress-strain curve with the type of concrete, and consideration of specimen size and slenderness effects.
Lim and Ozbakkaloglu [11]	This paper has presented a constitutive model for predicting the strain softening behavior of concrete in compression. The model was based on the concept of inelastic strain and crack localization that occur in the compression damage zone of softening concrete. A novel approach is proposed to separate and quantify the inelastic strain and the localized crack deformation from experimental stress-strain curves. Using the experimental databases of unconfined and confined concretes covering a wide range of test parameters, the inelastic strain component of various specimens were systematically quantified.

Lim and Ozbakkaloglu [12]	This paper has presented the results of an investigation on the confinement mechanisms of both actively confined and FRP-confined concretes, carefully establishing the important links between the two confinement systems using large experimental databases. A novel approach that incorporates the confining pressure gradient between the two confinement systems has been proposed to enable the development of a unified model presented in this paper.
Lim et al. [13]	To improve predictions of the ultimate condition of FRP-confined concrete using genetic algorithm and programming techniques, an evolutionary algorithm model has been developed and presented in this paper. This paper demonstrated a new approach to improve reliability of predictions while maintaining the simplicity of the proposed closed-form expressions.
Lim et al. [14]	This paper has presented a finite element model that is applicable to concrete subjected to uni-, bi-, and triaxial compression. Based on the comprehensive experimental databases assembled, an extension has been proposed to improve the failure criterion and flow rule of concrete-damage plasticity model for finite element modelling applications.

REFERENCES

Journal papers

[1] Ozbakkaloglu T, Lim JC, Vincent T. FRP-confined concrete in circular sections: Review and assessment of stress–strain models. Engineering Structures. 2013;49:1068–88.

[2] Ozbakkaloglu T, Lim JC. Axial compressive behavior of FRP-confined concrete: Experimental test database and a new design-oriented model. Composites Part B. 2013;55:607-34.

[3] Lim JC, Ozbakkaloglu T. Confinement model for FRP-confined high-strength concrete. Journal of Composites for Construction, ASCE. 2014;18(4):04013058.

[4] Lim JC, Ozbakkaloglu T. Influence of silica fume on stress-strain behavior of FRP-confined HSC. Construction and Building Materials. 2014;63:11-24.

[5] Lim JC, Ozbakkaloglu T. Influence of concrete age on stress–strain behavior of FRP-confined normal- and high-strength concrete. Construction and Building Materials. 2014; (Accepted).

[6] Lim JC, Ozbakkaloglu T. Design model for FRP-confined normal- and high-strength concrete square and rectangular columns. Magazine of Concrete Research. 2014;66(20):1020-35.

[7] Lim JC, Ozbakkaloglu T. Lateral strain-to-axial strain relationship of confined concrete. Journal of Structural Engineering, ASCE. 2014;Doi: 10.1061/(ASCE)ST.1943-541X.0001094.

[8] Lim JC, Ozbakkaloglu T. Hoop strains in FRP-confined concrete columns: Experimental observations. Materials and Structures. 2014;Doi: 10.1617/s11527-014-0358-8.

[9] Lim JC, Ozbakkaloglu T. Investigation of the Influence of Application Path of Confining Pressure: Tests on Actively Confined and FRP-Confined Concretes. Journal of Structural Engineering, ASCE. 2014;Doi: 10.1061/(ASCE)ST.1943-541X.0001177.

[10] Lim JC, Ozbakkaloglu T. Stress-strain model for normal- and light-weight concretes under uniaxial and triaxial compression. Construction and Building Materials. 2014;71:492-509.

[11] Lim JC, Ozbakkaloglu T. Influence of size and slenderness on compressive strain softening of confined and unconfined concrete. Journal of Materials in Civil Engineering. 2014; (Submitted).

[12] Lim JC, Ozbakkaloglu T. Unified stress-strain model for FRP and actively confined normal-strength and high-strength concrete. Journal of Composites for Construction. 2014;Doi: 10.1061/(ASCE)CC.1943-5614.0000536.

[13] Lim JC, Karakus M, Ozbakkaloglu T. Evaluation of ultimate conditions of FRP-confined concrete columns using genetic programming. Computers and Structures. 2014; (Submitted).

[14] Lim JC, Sadeghi R, Bennett T, Ozbakkaloglu T. Finite element modeling of normal- and high-strength concrete under uni-, bi-, and triaxial Compression International Journal of Plasticity. 2014; (To be submitted).

Conference papers

[15] Lim JC, Ozbakkaloglu T. FRP-confined high-strength concrete in circular sections: Summary of test database and a new design-oriented model. Proceedings of the 11th International Symposium on Fiber Reinforced Polymers for Reinforced Concrete Structures. Guimarães, Portugal; 2013.

[16] Lim JC, Ozbakkaloglu T. A simple design-oriented model for FRP-confined high-strength concrete. Proceedings of the 2nd International Conference on Building Materials and Structural Engineering. Beijing, China; 2013.

[17] Lim JC, Ozbakkaloglu T. Influence of silica fume on stress-strain behavior of FRP-confined HSC. Proceedings of the 4th Asia-Pacific Conference on FRP in Structures. Melbourne, Australia; 2013.

[18] Lim JC, Ozbakkaloglu T. Dilation behavior of FRP-confined concrete. Proceedings of the 11th International Symposium on Fiber Reinforced Polymers for Reinforced Concrete Structures. Guimarães, Portugal; 2013.

[19] Lim JC, Ozbakkaloglu T. A confinement model for FRP-confined normal and high-strength concrete in square and rectangular sections. Proceedings of the 4th Asia-Pacific Conference on FRP in Structures. Melbourne, Australia; 2013.

[20] Lim JC, Ozbakkaloglu T. Factors influencing hoop rupture strains of FRP-confined concrete. The 5th International Conference on Computer Engineering and Technology Vancouver, Canada; 2013.

[21] Lim JC, Ozbakkaloglu T. Comparison of stress-strain relationships of FRP and actively confined high-strength concretes: Experimental observations. Advanced Materials Research. 2014;919:29-34.

[22] Lim JC, Ozbakkaloglu T. Unified Stress-Strain Model for Unconfined and Actively Confined Concrete. Proceedings of the 13th International Symposium on Structural Engineering. Hefei, China; 2014.

[23] Lim JC, Ozbakkaloglu T. An accurate stress-strain model for FRP-confined concrete based on a novel approach. Proceedings of the 23rd Australasian Conference on the Mechanics of Structures and Materials. Byron Bay, Australia; 2014.

[24] Lim JC. Influence of concrete age on compressive behavior of FRP-confined concrete. Proceedings of the 4th International Conference on Civil Engineering and Transportation. Xiamen, China; 2014.